Acid-Catalyzed Condensation of Indole with Cyclic Ketones

&

Synthesis and Crystallographic Study of 2,6-Dihalobenzonitriles and Isocyanobenzenes

A THESIS
SUBMITTED TO THE FACULTY OF THE GRADUATE SCHOOL
OF THE UNIVERSITY OF MINNESOTA
BY

Kenneth James Tritch

IN PARTIAL FULFILLMENT OF THE REQUIREMENTS
FOR THE DEGREE
DOCTOR OF PHILOSOPHY

Adviser: Professor Wayland E. Noland

June, 2017

Acknowledgements

Matt Kappel was my 10th grade chemistry teacher. I am thankful for his inspiration. Before his class, chemistry was not a path I had considered for study beyond high school.

Wayland E. Noland has 64 years of faculty experience, enough passion for sharing chemistry to lend a lab coat to a high schooler roaming Smith Hall in search of a prop for a senior photo (me, 1999), the generosity to personally fund my entire graduate school career, great fishing, railroad, and scavenging stories, and the steady countenance to redirect me when my temper would have taken away my best. It is difficult to imagine a better doctoral adviser.

Doyle Britton (1930–2015) initiated the work described in Part II of this dissertation. Doyle co-authored a large percentage of the existing crystallographic publications regarding halogenated benzonitriles and isocyanides. He provided preliminary crystallographic data for iodo compounds **204da**,**db** and **209da**,**db**. He provided the idea to search for polytypism among the trihalo compounds, and some of the initial and final data for tribromo compounds **204ca** and **209ca**. He also provided preliminary data for cyano ester **204cd**. He is missed.

Victor G. Young, Jr. retrieved data from Doyle Britton's computers and finalized all CIF and structure files as needed for the crystallographic data to be ready for publication.

Part II was planned as a collaboration in which I would perform the synthetic portion and Doyle would perform the crystallographic portion. About 30% of the way through, Doyle retired for medical reasons. I had no crystallographic experience. Doyle and Victor kindly gave enough of their time to teach me all that I needed to know about crystallography to publish my first 5 research papers, and to prepare the crystallographic portions of this dissertation.

Stephen Philson and **Letitia Yao**, whose expertise with NMR instrumentation and interpretation made my structure determinations possible. They always knew the right instrument settings to suit my quirky samples.

Sean Murray, **Joe Dalluge**, **Kyle Kalstabakken**, and **Sarah Gruba** collectively obtained about half of the MS data. Sean and Joe were especially helpful with getting excellent signals from molecular ions that otherwise "wouldn't fly, even if thrown across the room."

Professor Tom Hoye provided use of IR and GC-MS instrumentation and data processing software. IR data collected on his instrument account for about 25% of those reported herein. Although none of those MS data are directly reported in this dissertation, they saved countless hours and materials during the optimization of synthetic work in Part II.

Professor Chris Douglas provided consultation on a moment's notice, and attained a perfect score at helping me to clear roadblocks in my synthetic routes. Chris suggested the use of lithium iodide for the demethylation of cyano esters, giving access to cyano acids **204bc**,**cc**, and **204dc**.

George Dirks taught me the basics of machining, which was helpful in keeping aging lab equipment operational, and thus made the IR data and the vacuum drying possible.

Hannah Leverentz performed the computational experiments in § 1.7.

Gregory Sutton and I were undergraduates together in the Noland Group in 2004. Greg performed the initial round of synthetic work for iodo compounds **204da**,**db** and **209da**,**db**, including the preparation of the crystals that were used to obtain the X-ray data.

Rozalin Dickson, **Cheng Lu**, **Glen Gullickson**, **Paul Erdman**, **Leah Groess**, **Srinu Narina**, **Matt Huisenga**, and **Vijay Kumar**, senior Noland Group members who 'walked' before me. They showed me the ropes and on countless occasions helped me to navigate the labyrinth of wet and dry chemistry that led to this dissertation. This group also includes **Nicholas Lanzatella**, who encouraged me to apply for grad school.

Those whom I had the privilege to mentor as undergraduates, and performed experiments for

Part I: **Sarah Dix** is a ranger for the National Park Service, **Siming Gao** is a process engineer at Corning Environmental Technologies, **Matt Worth** is a Ph.D. student in the Jiang group at UW Madison, **Julia Plewa** is a high school chemistry teacher and cheers for the Chicago

Blackhawks, **Courtney Paal** is an extraction technologist at Medtox Laboratories, and **Ashley Midtling** is an emergency medicine physician assistant somewhere in Wisconsin.

Part II: **Abby Engwall** is in surgery residency and had the courage to ask me where I go to church, **Nathan Klein** is a graduate student working with lasers at MIT and can stay on a unicycle for more than 10 seconds, **Jessica Shudy** works in quality control, **Ryan Herzig** is pursuing a career in pharmaceutical design and/or sales, **Zoe Tu** is studying chemistry at Princeton and might start a baked desserts business, and **Mark Jimenez** is a chemical engineering student in Duluth.

Parts I and II: **Renee Jensen** is a broadcast meteorologist, **Jacob Capek** recently completed pharmacy school at Creighton, **Andrew Schneerer** has recently completed his MS with the Noland group, **Janel Rieger** works at a distillery and can lead-climb a 5.12, and **Chris Brown** is a researcher in the Noland group.

Other manuscripts: **Kathryn Schneider** is a senior chemist at Ecolab, **Bee Kian Ong** is a paint chemist and aspiring rheology specialist in Malaysia, **Simon Lang** is a postdoctoral researcher at the University of Pennsylvania, **Corey LaSalle** is a scientist at St. Jude Medical, and **Nicholas O'Brian** is an engineer at 3M. I have unfortunately lost contact with **Ji-Eon Lee**, who is probably still generously giving her time to serve the community.

With humility, I admit that I did not always offer my best behavior to some of my early students, especially Ji-Eon, Bee, and Renee. I am thankful for your patience and dedication, which have left their marks on me, and will benefit those around you everywhere you go.

Eve Zabronsky, **Jeanette Voelz**, and **Brooke Jackson** were each willing to freely proofread 738 pages.

Gramma Irene (1923–1995) and **Grampa Bill (1919–1999)**, in whose home I lived for 8 childhood years. Together with **Gramma Marge** and **Grampa Ken**, they rendered in me hues of the wisdom and character of the greatest generation.

Mom, for providing the right insight at the right moments.

Dad, who has lived more years with his son living in his basement than any human should.

Abstract

I. As an extension of ongoing indole-ketone research, one-pot condensation reactions were performed between indole (**1**) and cyclic ketones with ring sizes n = 4–12 (**2d–l**) in the presence of boric, phosphoric, acetic, trifluoroacetic, hydrochloric, and toluene-4-sulfonic acids (Scheme 1). From fastest to slowest, the rate of condensation with indole was n = 6, 4, 5, 7, 12, 8, 11, 10, and 9. In addition to oligomerized indole, seven different types of products were isolated and identified. An eighth type of product was obtained from cyclododecanone, but it was not identified. The optimal catalyst for 2:1 condensation varied by ring size. CF_3COOH or HCl were the best catalysts for one-pot preparation of all other products.

II. Eleven 2,6-dihalobenzonitriles (**204**) and six corresponding isocyanobenzenes (**209**) were prepared (Scheme 2). To minimize radical-derived byproducts, it was important to perform cyanation in the presence of excess $NaHCO_3$. Six nitriles and five isocyanides were analyzed by X-ray diffraction to study substituent effects on cyano-halo short contacts and the resulting ribbon or layer structures. All crystals exhibited such contacts. Polytypism of tribromo analogs **204ca** and **209ca**; and 2:1 anthracene co-crystals of cyano acids **204bc**,**cc** were observed.

Numbering. The introduction and discussion material is separated into two parts. Compound numbering begins at **1** and **201**, for Part I and Part II, respectively. Main starting materials, intermediates, and products are given the lowest numbers. Entries in Part III and the appendices are given in numerical order, although Part III is also sorted by type of chemical reaction. Thus, several compounds in Part III are given more than one entry because they were prepared by more than one method.

Graphical Abstract

Scheme 1. Summary of the synthetic results of Part I. The yields given are from the best catalyst for each case.

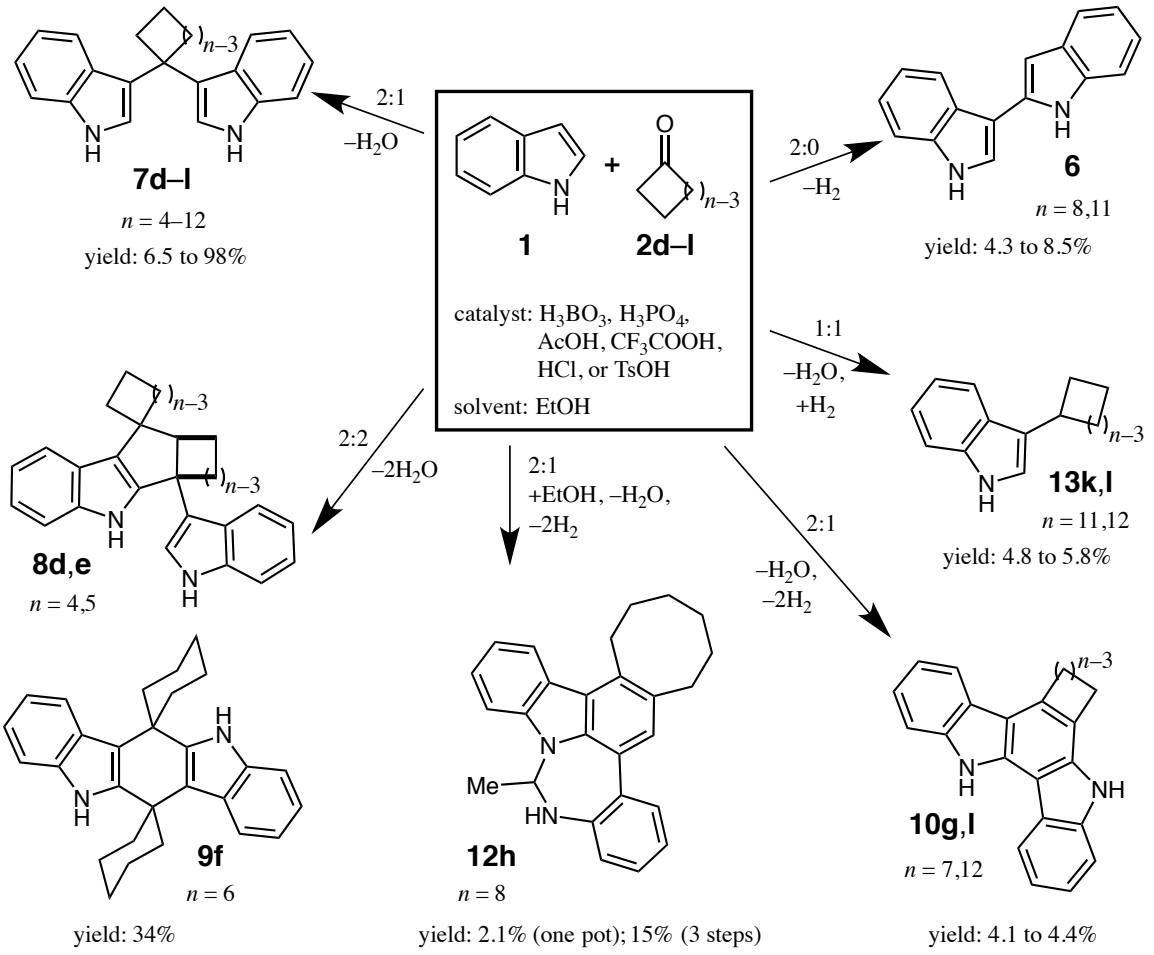

Scheme 2. Summary of the results from Part II.

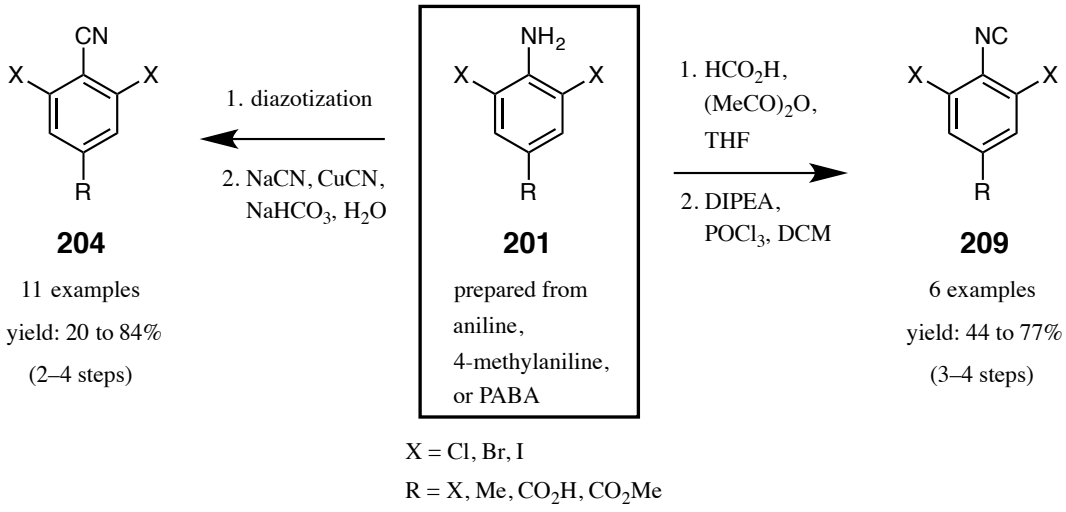

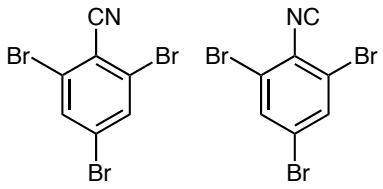

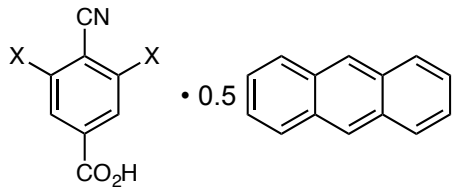

Table of Contents

Acknowledgements ----------i

Abstract ----------iv

Abstract iv

Graphical Abstract v

Contents ----------vii

Table of Contents vii

List of Tables xi

List of Figures....xiv

List of Schemes....xviii

List of Abbreviations xxiii

Part I. Acid-Catalyzed Condensation of Indole with Cyclic Ketones----------1
1.1 Background: Indole and Cyclic Ketones
1.1.1 Preparation of Indoles....1
1.1.2 Simple Reactions of Indoles with Electrophiles and Acids....6
1.1.3 Indole-Ketone 2:1 Condensation....12
1.1.4 Indole-Ketone 2:2 Condensation and Related Products....15
1.1.5 *In Situ* Indole-Ketone 1:1 Condensation and Diels-Alder Reactions....20
1.1.6 Summary of Reaction Conditions and Product Types....23
1.1.7 Preparation of Cyclic Ketones....25
1.2 Scope of the Present Work....31
1.3 Results: Preparation of Cyclic Ketones....33
1.4 Results: Preparation of Bisindoles....36
1.5 Results: Preparation of 2:2 and Related Products
1.5.1 Preliminary Work....47
1.5.2 Cyclohexanone....48
1.5.3 Cyclopentanone....49
1.5.4 Cyclobutanone....51
1.5.5 Cycloheptanone....51
1.5.6 Cyclododecanone....52
1.5.7 Cyclooctanone....56
1.5.8 Cycloundecanone....60
1.5.9 Other Experiments....60
1.5.10 Proposed Mechanisms....62
1.6 Selected NMR Analysis....69
1.7 Progress Toward Indolo[2,3-*b*]carbazoles....82
1.8 Conclusions....89
1.9 Prospective Future Work....95

Part II. Synthesis and Crystallographic Study of 2,6-Dihalobenzonitriles and Isocyanobenzenes ----------98
2.1 Background: Crystallography of 2,6-Dihalobenzonitriles and Isocyanobenzenes
2.1.1 Nitriles 98
2.1.2 Isocyanides 107
2.2 Background: Synthesis of 2,6-Dihalobenzonitriles and Isocyanobenzenes
2.2.1 Benzonitriles (General) 109
2.2.2 Benzonitriles (2,6-Dihalo)....112
2.2.3 Isocyanides 117
2.2.4 Halogenation of Anilines....119
2.3 Scope of the Present Work 123
2.4 Synthetic Results
2.4.1 Initial Survey: Brominated PABA Derivatives 125
2.4.2 Halogenation Results....130
2.4.3 Sandmeyer Cyanation Results....132
2.4.4 De-esterification Results 137
2.4.5 *N*-Formylation Results....138
2.4.6 Isocyanide Preparation Results 141
2.4.7 Overall Multi-Step Yields....144
2.5 Crystallographic Results
2.5.1 Trihalo Nitriles and Isocyanides 146
2.5.2 4-Methyl Nitriles and Isocyanides 150
2.5.3 4-Carboxy Derivatives....155
2.5.4 Short Contact Geometry 167
2.6 Conclusions....171
2.7 Prospective Future Work....173

Part III. Experimental Procedures ----------177
3.1 General
3.1.1 Reagents, Packings, and Other Basics.....177
3.1.2 Instrumentation, Elemental Analyses, and Sample Purity 177
3.1.3 Data Processing, Reporting, and Plotting 178
3.2 Indole and Cyclic Ketones
3.2.1 Cyclic Ketones 179
3.2.2 Indole Dimer and Trimer, and Biindolyl 182
3.2.3 Indole-Ketone Condensation Methodology (Methods A–F) 184
3.2.4 Bisindoles (2:1 Condensation Products).....186
3.2.5 Other Condensation-Derived Products 192
3.3 Progress Toward Indolo[2,3-*b*]carbazoles
3.3.1 Synthesis and Alkylations of Cyclohexane-1,3-diones.....200
3.3.2 Syntheses (Method G) and Indolization of Phenylhydrazones 203
3.4 Syntheses of Nitriles and Isocyanides
3.4.1 Esterification and Halogenations (Methods H & I) of Anilines.....206
3.4.2 Sandmeyer Cyanations (Methods J & K).....215
3.4.3 Hydrolyses of Esters (Method L).....222
3.4.4 *N*-Formylations of Anilines (Method M).....225
3.4.5 Isocyanide Syntheses (Method N) 229
3.5 Preparation and Analyses of Crystallographic Samples 232
Part IV. References and Notes ----------235
Appendix I. NMR Data for Products in Part I and §§ 3.2–3.3 ----------249
Appendix II. NMR Data for Products in Part II and § 3.4 ----------467
Appendix III. Crystallographic Data for Compounds 8d, 11h, and 12h----------555
Appendix IV. Crystallographic Data for Selected Products from Part II----------598
Appendix V. Index of References Found Within CIFs ----------713

List of Tables

Table 1. Selected cyclic-ketone-derived Diels-Alder products reported by Noland and coworkers 22

Table 2. Summary of the overall economic viability of common synthetic approaches to cyclic ketones 25

Table 3. The reported scope of study of condensation of indoles with cyclic ketones 31

Table 4. The preparation of bisindoles by Method A and Method B 37

Table 5. The preparation of bisindoles by Method C 39

Table 6. The preparation of bisindoles by Method D 41

Table 7. The preparation of bisindoles by Method E 43

Table 8. The R_f values, melting points, air sensitivities, and physical appearances of bisindoles **7a–l** 45

Table 9. The preparation of phenylhydrazones **18a–d** 87

Table 10. The recommended conditions for preparing bisindoles **7a–l** 90

Table 11. A summary of the 2:2 and related condensation products that were obtained from one-pot reactions with indole and cyclic ketones 92

Table 12. Type 1 CN...X contact features, polymorphism, and frequency of disorder reported in selected 2,6-dihalobenzonitriles in the Cambridge Structural Database 102

Table 13. In Type 3 sheets, a comparison of the sum of N and X atomic contact radii with the observed (**204bc**) and predicted (**204cc**,**dc**) gaps between N and X atoms 106

Table 14. Type 1 NC...X contact features observed in selected 2,6-dihalo-1-isocyanobenzenes in the CSD 107

Table 15. Halogenation yields. The highest-yielding conditions are listed 131

Table 16. Sandmeyer cyanation yields. The highest-yielding conditions are listed 133

Table 17. *N*-Formylation of 2,6-dihaloanilines with acetic formic anhydride (AFA) solution. The highest-yielding conditions are listed 139

Table 18. The overall yields of nitriles **204ba**–**204dc**, prepared from anilines **201aa**–**201ac**.....144

Table 19. The overall yields of isocyanides **209ba**–**209db**, prepared from anilines **201aa**–**201ac**.....145

Table 20. The novelty and crystallization solvents for polytypes of tribromo nitrile **204ca** and isocyanide **209ca**.....146

Table 21. A comparison of crystallographic features observed in **204db**, **209db**, and **209cb**.....152

Table 22. A comparison of the N...X contact gaps in cyano acids **204bc**–**dc**.....156

Table 23. The geometry of the isocyano-methoxy (C7...C9) contacts observed in a crystal of **209cd**. The molecules are viewed along {a, 0, 0}.....162

Table 24. A comparison of selected bond and torsion angles (º) in **204cd** and **209cd**.....163

Table 25. Cyano-halo, isocyano-halo, and halo-halo short contact geometry in all applicable crystals surveyed in § 2 167

Table 26. Mean C≡N bond lengths (Å).....168

Table 27. Comparison of *ipso*-cyano/isocyano distances with and without halo contacts. The legend is not to scale 169

Table 28. The mean cyano-halo and isocyano-halo contact angles (Z≡Y...X) in crystals that formed Type 2 sheets.....170

Table 29. The solvents that were used to prepare crystallographic samples, and the person that performed each analysis 233

Table 30. The CCDC deposition number or literature reference for each crystal structure.....234

Table 31. The contents of Appendix I 249

Table 32. Proton NMR summary for **8d**.....335

Table 33. Carbon NMR summary for **8d**.....337

Table 34. Proton NMR summary for **8e**.....359

Table 35. Carbon NMR summary for **8e**.....361

Table 36. Carbon NMR summary for **9f**.....369

Table 37. Proton NMR summary for **10g**.....387

Table 38. Carbon NMR summary for **10g**.....388

Table 39. Proton NMR summary for **12h**.....419

Table 40. Carbon NMR summary for **12h**.....421

Table 41. Nitrogen NMR summary for **12h**.....423

Table 42. The contents of Appendix II 467

Table 43. The contents of Appendix III 555

Table 44. The contents of Appendix IV.....599

Table 45. The corresponding reference numbers for references found in CIFs.....713

List of Figures

Fig. 1. Indole (**1**), with atom numbering 1

Fig. 2. A generic enamine (**38**), indole (**1**), and naphthalene (**39**), arranged by decreasing nucleophilicity. The preferred sites of electrophilic and nucleophilic attack are shown for the free (**38**, **1**) and protonated (**38H**, **1H**) forms, respectively 6

Fig. 3. Three reported acetone-derived 2:2 condensation products.....16

Fig. 4. Four products obtained from condensation of indole with acetone in the presence of strong acids.....20

Fig. 5. A summary of the types of products observed from condensation of indole with various carbonyl derivatives 23

Fig. 6. An ORTEP drawing of crystalline **8e**, with crystallographic atom labeling, viewed along {–10a, b, –2c}. This crystal was a *p*-xylene hemisolvate. Only the major conformer is shown.....50

Fig. 7. Four of the structures considered for product **14**. Based on the NMR data, none of these structures is correct.....55

Fig. 8. An ORTEP drawing of crystalline **12h**, with crystallographic atom labeling of skeletal atoms, viewed along {4a, –b, 3c} 59

Fig. 9. An ORTEP drawing of crystalline **11h**, with crystallographic atom labeling of skeletal atoms, viewed along {a, 4b, –c} 59

Fig. 10. The aromatic region of the ^{1}H NMR spectrum of indole (**1**) 69

Fig. 11. The alkyl region of the ^{1}H NMR spectrum of dimer **4** 70

Fig. 12. The alkyl region of the ^{1}H NMR spectrum of trimer **5** 71

Fig. 13. The aromatic region of the ^{1}H NMR spectrum of biindolyl **6**. The N–H signals (not shown) are farther downfield 72

Fig. 14. The (a) aromatic and (b) alkyl regions of the ^{1}H NMR spectrum of bisindole **7j**.....73

Fig. 15. The (a) aromatic and (b) alkyl regions of the ^{1}H NMR spectrum of product **8e**. The locations of low-*J*-value doublets in products **6**, **7**, and **13** are shown for comparison 74

Fig. 16. The (a) aromatic and (b) alkyl regions of the ^{1}H NMR spectrum of product **9f**. The N–H signal (not shown) is farther downfield.....75

Fig. 17. The alkyl region of the ^{13}C NMR spectrum of product **9f**. Compound **68f** is shown for comparison 76

Fig. 18. The (a) aromatic and (b) alkyl regions of the ^{1}H NMR spectrum of product **10g**. The N–H signals (not shown) are farther downfield 77

Fig. 19. The (a) aromatic and (b) alkyl regions of the ^{1}H NMR spectrum of product **11h**. The aromatic N–H signal (not shown) is farther downfield 78

Fig. 20. The (a) aromatic and (b) alkyl regions of the ^{1}H NMR spectrum of product **12h** 79

Fig. 21. The (a) aromatic and (b) alkyl regions of the ^{1}H NMR spectrum of product **13k**. The N–H signal (not shown) is farther downfield 80

Fig. 22. The alkyl region of the $^{1}H/^{13}C$ DEPT-135 spectrum of product **13k** 81

Fig. 23. A summary of the major products that can be obtained from the given conditions. Entries in parentheses are reported in the literature [37, 38, 39] 94

Fig. 24. Compounds **19b**–**d**, which were not obtained, were the main synthetic targets in the project described in § 1.7. One of the goals was to determine whether **68f** is a synthetic intermediate to **9f** 95

Fig. 25. (a) Hydrogen bonding between two molecules of methanol; (b) pseudo-hydrogen bonding between two molecules of a 2-halobenzonitrile. Dashed lines depict the hydrogen and pseudo-hydrogen bonds 98

Fig. 26. Examples of Type 1 crystallographic features: (a) A Type 1 ring formed by nitrile **204ba**, viewed along {4a, 0, c}; (b) a Type 1 ribbon formed by nitrile **214d**, viewed along {a, 0, –2c}; (c) a Type 1 sheet formed by dinitrile **210**, viewed along {4a, b, c}. CN...X contacts are shown as blue lines. In the sheet, ribbons are parallel to the purple arrow 99

Fig. 27. The Type 2 sheets that were observed in a crystal of **204ca**, viewed along {a, 0, –c}. CN...Br contacts are shown as blue lines 100

Fig. 28. (a) The Type 3 sheets observed in a 2:1 co-crystal of **204bc** with **215a**, viewed along {2a, 8b, –c}; (b) the envisioned Type 3 sheets with two Type 1 rings per N atom; (c) naphthalene (**39**), for comparison 104

Fig. 29. (Pseudo)translational and (pseudo)centric stacking of Type 2 layers. (T) Translational stacking between all adjacent layers of nitrile **204ca**, viewed along {2a, 0, –c}. (C) Pseudocentric stacking observed between alternating adjacent layer pairs of isocyanide **209ca**, viewed along {a, 0, 0} 108

Fig. 30. Translational (TT) stacking in the $Z = 2$ polytype of nitrile **204ca**, viewed along {a, b, 0} 147

Fig. 31. Pseudotranslational, pseudocentric (TC) stacking in the $Z = 8$ polytype of nitrile **204ca**, viewed along {a, 12b, 0}.....147

Fig. 32. TCT stacking in the $Z = 12$ polytype of nitrile **204ca**, viewed along {a, 11b, 0}.....148

Fig. 33. The $Z = 4$ unit cell of triiodo nitrile **204da**, with centric (CC) stacking, viewed along {a, 5b, 0}. The top and bottom layers are bisected by the *bc* face of the unit cell.....149

Fig. 34. The layer structure in dibromo 4-methyl nitrile **204cb**, viewed along {0, 0, c}. Two unit cells and two conformers of the methyl groups are shown. A, B, C, and D are the same cyano-methyl clusters shown in Fig. 35.....150

Fig. 35. One unit cell of dibromo 4-methyl nitrile **204cb**, viewed along {a, b, 0}. Two conformers of the methyl groups are shown. A, B, C, and D are the same cyano-methyl clusters shown in Fig. 34.....151

Fig. 36. The $Z = 4$ unit cell of diiodo 4-methyl nitrile **204db**, with centric (CC) stacking, viewed along {a, 4b, 0}. The top and bottom layers are bisected by the *bc* face of the unit cell.....152

Fig. 37. One layer of the sheet structure in **209db**, viewed along {a, 0, 0}.....153

Fig. 38. One layer of the sheet structure in **209db**, viewed along {a, 0, c}.....154

Fig. 39. (a) the Type 3 sheet structure observed in **209db**, viewed along {a, 0, c}; (b) The Type 3 sheet structure envisioned by Dr. Britton.....155

Fig. 40. The approximate contact dimensions of anthracene (**215a**) and pyromellitic diimide (**215b**).....157

Fig. 41. The envisioned Type 3 sheet containing pyromellitic diimide (**215b**). Blue lines show the prospective alignment of donor and acceptor groups. Dioxa analog **215c** is shown for comparison.....158

Fig. 42. The sheet structure in a crystal of dibromo cyano ester **204cd**, viewed along {a, 0, –c}.....159

Fig. 43. The sheet structure in a crystal of dibromo cyano ester **204cd**, viewed along {2a, 0, c}.....160

Fig. 44. One unit cell of the observed crystal of dibromo isocyano ester **209cd**, translated by {–0.5a, 0, 0} and viewed along {a, 0, 0}.....161

Fig. 45. Five molecules of carbamoyl acid **207** are shown, to illustrate the 3 main packing interactions, viewed along {–a, 3b, 0}. (a) Head-to-tail dimerization; (b) Tail-to-tail dimerization; (c) Carboxyl-hydroxyl-carbamoyl chains. The atoms in these interactions and one extra H3A atom are labeled. The major disorder component of 2-propanol is shown. 164

Fig. 46. Substituted benzamides, in their crystals, viewed along the carbamoyl *ipso* bonds. The angles listed (ω) are torsions between the planes of the benzene rings and the axes of the carbamoyl C=O bonds....165

Fig. 47. The four compounds prepared in the present study for which a polymorph search is suggested as future work 173

Fig. 48. The ribbon structure reported in a crystal of **241**....174

Fig. 49. Vapor-fed halogenation apparatus 208

List of Schemes

Scheme 1. Summary of the synthetic results of Part I. The yields given are from the best catalyst for each case iv

Scheme 2. Summary of the results from Part II v

Scheme 3. Summary of a common indole-based biosynthetic pathway 2

Scheme 4. Several key steps in the Fischer indole synthesis. This process is often carried out in one pot, although some intermediates, such as phenylhydrazone **18**, can be isolable 3

Scheme 5. The modified Fischer indole synthesis developed by Miyata and coworkers 4

Scheme 6. A modified Madelung indole synthesis, using *n*-butyllithium 5

Scheme 7. Indole syntheses involving the construction of both rings. (a) A Kanematsu indole synthesis; (b) a gold-catalyzed transannulation of alkynylaminoethylfuran **36** 5

Scheme 8. Acetylation of (a) indole at the 1-position; (b) indole at the 1- and 3-positions; (c) 3-methylindole at the 2-position; (d) indole on the benzene ring, which is not reported....8

Scheme 9. The preparation of 2,3-dimethylindole (**48**), *via* 3,3-dimethyl intermediate **47** 9

Scheme 10. An example of the Plancher rearrangement....10

Scheme 11. A 3-brominated indole (**54**) participating in a Suzuki-Miyaura cross-coupling reaction....11

Scheme 12. (a) The initial 1:1 indole-ketone condensation that takes place in acid; (b) the formation of 2:1 bisindoles (**7**) resulting from the addition of **1** to **57H** 12

Scheme 13. The proposed mechanism for the formation of 2,2'-bisindole **62** 13

Scheme 14. The preparation of trisindole leuco dye **64** and oxidation to colored acetate salt **65** 14

Scheme 15. A summary of the formation of 2:2 indole-acetone condensate **8b** from bisindole **7b** and leftover acetone (**2b**) 15

Scheme 16. The formation of indolo[3,2-*b*]carbazole **9b** *via* (a) condensation and cyclization at the indole-2-positions followed by a Plancher rearrangement; (b) condensation and cyclization at the indole-3-positions, each followed by a half-Plancher rearrangement. 17

Scheme 17. The formation of indolo[3,2-*b*]carbazole (**9a**) during attempted syntheses of mixed 2:2 products (**72**).....18

Scheme 18. The preparation of cyclohexanone-derived indolo[3,2-*b*]carbazole **9f**. Isomer **68f** may have also been obtained 19

Scheme 19. The preparation of **78** *via* a Diels-Alder reaction between maleic acid and **57f**.....21

Scheme 20. The preparation of cyclododecanone (**2l**) by Pd-catalyzed oxidation of cyclododecene (**80**) 26

Scheme 21. The preparation of C_n cyclic ketones (**2e**–**g**) *via* the Dieckmann cyclization of C_{n+1} linear diesters (**81**).....27

Scheme 22. The *in situ* preparation of diazomethane (**85**) from Diazald (**84**).....27

Scheme 23. The preparation of (a) cyclobutanone (**2d**) *via* ketene (**86**); (b) cyclooctanone (**2h**) from cycloheptanone (**2g**). Both preparations use diazomethane (**85**) that is generated *in situ* 28

Scheme 24. The preparation of cyclononanone (**2i**) from cycloheptanone (**2g**) 29

Scheme 25. The preparation of cycloundecanone (**2k**) by ring contraction. Cyclodecanone (**2j**) can be prepared by using **2k** as the starting material 30

Scheme 26. The preparation of (a) cyclononanone (**2i**); (b) cyclodecanone (**2j**) in the present study 33

Scheme 27. The autoxidation of cycloundecanone (**2k**) to diacid **3**.....35

Scheme 28. The preparation of indole dimer (**4**) and trimer (**5**) 47

Scheme 29. The preparation of cyclohexanone-derived 2:2 product **9f**.....49

Scheme 30. The preparation of cyclopentanone-derived 2:2 product **8e**.....49

Scheme 31. The preparation of cyclobutanone-derived 2:2 product **8d** 51

Scheme 32. The preparation of cycloheptanone-derived indolocarbazole **10g** 52

Scheme 33. The preparation of cyclododecanone-derived indolocarbazole **10l**.....52

Scheme 34. The preparation of cyclododecanone-derived products **13l**, **57l**, and **14**.....53

Scheme 35. The one-pot preparation of diazepine derivative **12h** and biindolyl **6** from cyclooctanone.....57

Scheme 36. The preparation of biindolyl **6** from dimer **4** *via* dehydrogenation 57

Scheme 37. The two-step preparation of diazepine **12h** *via* carbazolylaniline **11h** 58

Scheme 38. The preparation of cycloundecanone-derived condensation product **13k**. Biindolyl **6** was also obtained 60

Scheme 39. The attempted cross-condensation of ketones with bisindoles.....61

Scheme 40. Summary of the formation of products **7**, **8**, **9f**, and **67**.....62

Scheme 41. (a) The oligomerization of indole; (b) the autoxidation of dimer **4** to biindolyl **6**.....63

Scheme 42. The formation of cycloalkylindoles **13k** and **13l** *via* a hydride transfer from dimer **4** 64

Scheme 43. The formation of key intermediate **109g** from cycloheptanone (**2f**) and biindolyl **6**.....65

Scheme 44. The conversion of key intermediates of type **109** into products of type **10** and **11** 66

Scheme 45. The preparation of indolocarbazole **114** from biindolyl **6**, reported by Janosik & Bergman.....67

Scheme 46. The proposed pathway for the one-pot formation of diazepine **12h** from carbazolylaniline **11h**: (a) The conversion of ethanol into acetal **109**; (b) cyclizative condensation of **11h** with **106** *via* iminium species **115** 68

Scheme 47. Two of the possible routes for the formation of **9f**: (a) *via* **68f**, and then a Plancher rearrangement; (b) *via* **70f**, by a pathway similar to the formation of 2,2'-bisindoles.....82

Scheme 48. The computationally estimated free energy difference between compounds **9e** and **68e**. The estimated equilibrium mole percentages are shown 83

Scheme 49. The computationally estimated free energy difference between compounds **19d**, **117**, and **118**. The estimated equilibrium mole percentages are shown 84

Scheme 50. The retrosynthesis of **19d** to diketone **17d** and phenylhydrazine (**23**) 84

Scheme 51. The preparation of diketone **17d** from cyclopentanone (**2e**) 85

Scheme 52. (a) The preparation of diketones **17b** and **17c**; (b) the use of other alkyl halides favors *O*-alkylation; (c) **17d** could not be prepared by alkylation of **121b**....86

Scheme 53. (a) The preparation of 1,2,3,4-tetrahydrocarbazole (**19a**); (b) indolo[2,3-*b*]carbazoles **19b**–**d** were not observed 88

Scheme 54. A proposed project that primarily explores cyclizative condensation reactions between ketones (**2a**–**n**) and biindolyl **6** 96

Scheme 55. The conversion of aniline (**201aa**) into benzonitrile (**204aa**) is an example of the Sandmeyer reaction 109

Scheme 56. A proposed mechanism for the aqueous-phase diazotization of aniline 110

Scheme 57. A proposed mechanism for the Sandmeyer cyanation of diazonium salt **203aa** 111

Scheme 58. A general mechanism for the formation of the radical-derived products reported by Giumanini, *et al.* [114], from their attempted cyanation of diazonium-derived complex **220ca**. Their yields are also shown 112

Scheme 59. The preparation of nitrile **225**, performed by Toya, *et al.* [120]....114

Scheme 60. (a) The postulated preparation of SBDC, performed by Toya, *et al.*; (b) A possible mechanism for the synthesis of nitrile **204ca**, with SBDC regenerated by the addition of NaCN 115

Scheme 61. The two common preparations of organic isocyanides (**209**) from the corresponding amines (**201**): (a) The Hofmann carbylamine reaction; (b) Synthesis and dehydration of the corresponding formamides. Aniline derivatives are shown; alkyl examples are also reported 117

Scheme 62. The chlorination of aniline (**201aa**) with sulfuryl chloride 119

Scheme 63. The bromination of aniline (**201aa**) in hydrochloric acid....120

Scheme 64. The preparation of 4-fluoroaniline (**232**) by hydrogenation of 4-nitrofluorobenzene (**231**) 121

Scheme 65. (a) The preparation of 4-bromoaniline (**235**) by Sandmeyer bromination of 4-nitroaniline (**233**) and subsequent hydrogenation; (b) the preparation of 3,5-dibromoaniline (**238**) by bromination of **233**, followed by diazotization-reduction and then hydrogenation 122

Scheme 66. The original scope of proposed synthetic work for Part II 123

Scheme 67. Bromination of PABA (**201ac**) in (a) acidic and (b) alkaline conditions 125

Scheme 68. Attempted Sandmeyer cyanation of dibromo acid **201cc** 126

Scheme 69. (a) Synthesis of dibromo ester **201cd** for subsequent cyanation; (b) The preparation of dibromo acid **201cc** by 1- and 3-step routes 127

Scheme 70. The preparation of reduction product **206**, upon attempted Sandmeyer cyantion of **201cd** with NaCN and CuCN 128

Scheme 71. The preparation of dibromo cyano ester **204cd**, and subsequent hydrolysis transformations 129

Scheme 72. The products obtained from the Sandmeyer cyanation of **201ca**. The compounds shown inside of the box were obtained as a mixture 135

Scheme 73. The preparation of methyl 3,5-dibromobenzoate (**206**) 136

Scheme 74. De-esterification of cyano esters with lithium iodide 137

Scheme 75. *N*-Formylation of aniline with formic acid in a Dean-Stark trap. Subsequent bromination was not successful 140

Scheme 76. The attempted formylation of 2,4,6-trichloroaniline (**201ba**) with formic acid and $TsOH \cdot H_2O$ in refluxing mixed xylenes 141

Scheme 77. Dehydration of formanilides with DIPEA and $POCl_3$ to give 2,6-dihaloisocyanobenzenes 142

Scheme 78. The attempted selective hydrolysis of dibromo isocyano ester **209cd** 143

Scheme 79. The base-promoted hydrolysis of cyano ester **204cd** to **207**, which was not observed to continue to diacid **240** 166

Scheme 80. The proposed synthesis of 3,5-dibromobenzonitrile (**242**) 175

Scheme 81. The proposed synthesis of tetrabromo biscarbonitrile **245**. Iodinated nitrile **204dd** is shown for comparison 176

List of Abbreviations

AcOH	Glacial acetic acid
AFA	Acetic formic anhydride
a. k. a.	Also known as
AM400	Bruker Avance III 400 MHz NMR instrument, in the LeClaire-Dow Instrumentation Facility
AML	Atlantic Microlab
Anal.	Elemental analysis
App.	Appendix
aq.	Aqueous
AV500	Bruker Avance III 500 MHz NMR instrument, in the LeClaire-Dow Instrumentation Facility
Bn	Benzyl, (C_6H_5–CH_2–)
Bu	Butyl (C_4H_9–)
calcd	Calculated
cat.	Catalytic (less than one stoichiometric equivalent)
CC	Centric, or pseudocentric stacking between crystallographic layers
COSY	Correlation spectroscopy
CSD	Cambridge Structural Database
CIF	Crystallographic information file
compd.	Compound (generally referred by number)
d	Day(s)
DCE	1,2-Dichloroethane
DCM	Dichloromethane
dec.	Decomposes
DEPT	Distortionless enhancement by polarization transfer
diglyme	Di(2-methoxyethyl)ether; di(ethylene glycol) dimethyl ether
DIPEA	*N*-Ethyldiisopropylamine; diisopropylethylamine
DMAP	4-Dimethylaminopyridine
DMF	*N*,*N*-Dimethylformamide

DMSO	Dimethyl sulfoxide
DNPH	A solution of 2,4-dinitrophenylhydrazine in ethanol, water, and sulfuric acid
ESI	Electrospray ionization
Et	Ethyl, (C_2H_5–)
EtOAc	Ethyl acetate
freq.	Frequency
GC	Gas chromatography
G_{rel}	Relative Gibbs free energy
h	Hour(s)
HD500	Bruker Avance III HD 500 MHz NMR instrument
HFS	Hydrated ferric sulfate; [$Fe_2(SO_4)_3 \bullet xH_2O$]
HMBC	Heteronuclear multiple-bond correlation
HMIM	*N*-(*n*-hexyl)-*N*'-methylimidazolium, [1-(C_6H_{13})-3-(CH_3)-[1,3]$C_3H_3N_2$]$^+$
HMQC	Heteronuclear multiple-quantum correlation
HRMS-EI	High-resolution mass spectra, electron ionization
HRMS-ESI	High-resolution mass spectra, electrospray ionization
IAN	3-Methylbutyl nitrite, isoamyl nitrite, $(CH_3)_2CHC_2H_4$–ONO
lit.	Literature
mCPBA	*meta*-Chloroperoxybenzoic acid, 3-chloroperoxybenzoic acid
Me	Methyl (CH_3–)
MHW	M-H-W Laboratories
min	Minute(s)
M.p.	Melting point
m/*z*	Mass-to-charge ratio
NMR	Nuclear magnetic resonance (spectroscopy)
NOE	Nuclear Overhauser effect
n.r.	No reaction was observed
ORTEP	Oak Ridge thermal ellipsoid plot
PABA	4-Aminobenzoic acid; *p*-aminobenzoic acid
P/N	Part number
PFG	Pulsed field gradient
ppm	Parts per million

Pr	Propyl (C_3H_7–)
Q-TOF	Quadrupole-time-of-flight
ref.	Reference (numbers refer to entries in § 4)
RT	Room temperature (17–22 ºC)
sat.	Saturated
SBDC	Disodium aqua(carboxyloxy)dicyanocuprate(I), sodium bicarbonate dicyanocuprate, $Na_2[Cu(H_2O)(HCO_3)(CN)_2]$
TCD	Thermal conductivity detector
TC	Alternating (pseudo)translational and (pseudo)centric stacking between crystallographic layers
temp.	Temperature
TFA	Trifluoroacetic acid
TFAA	Trifluoroacetic anhydride
THF	Tetrahydrofuran
TLC	Thin-layer chromatography
TOF	Time of flight
Ts	Toluene-4-sulfonyl [4-CH_3–C_6H_4–$S(O_2)$–]
TsOH•H_2O	Toluene-4-sulfonic acid monohydrate
TT	Translational or pseudotranslational stacking between crystallographic layers
TCT	(Pseudo)translational stacking between crystallographic layers, with each third layer interface being (pseudo)centric
UV_{254}	A dye that glows green under 254 nm ultraviolet light
VI300	Varian Inova 300 MHz NMR instrument, in the LeClaire-Dow Instrumentation Facility
VI500	Varian Inova 500 MHz NMR instrument, in the LeClaire-Dow Instrumentation Facility
XCL	The University of Minnesota Department of Chemistry X-ray Crystallography Laboratory, in the LeClaire-Dow Instrumentation Facility
Z	The number of molecules in a crystallographic unit cell

Part I. Acid-Catalyzed Condensation of Indole with Cyclic Ketones

1.1. Background: Indole and Cyclic Ketones

1.1.1. Preparation of Indoles

Indole (**1**) is a 10 π-electron, electron-rich, bicyclic nitrogen heterocycle (Fig. 1). The importance of indole-related chemistry is well known to many members of chemical, biological, and pharmaceutical fields. Numerous indole-related drugs have been commercialized [1]. Scientific reports of indole-related syntheses date back roughly 150 years, and indole-related peer-reviewed articles have been published at a rate of approximately 2,500 per year during the past decade [2]. Thus, indole is not only among the oldest topics of modern organic chemistry, but the study of the chemistry and applications of indole derivatives is practical and continues to grow.

Fig 1. Indole (**1**), with atom numbering.

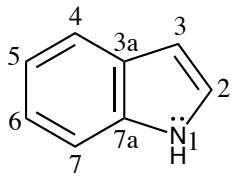

1

Indole is found in many microbes and plants as a biosynthetic intermediate of numerous proteins and alkaloids. A common pathway begins with the transformation of anthranilic acid (**20**) into indole, followed by conversion to tryptophan (**21**), and then indole-3-acetic acid (**22**, a. k. a. auxin, Scheme 3) [3]. Indole is found in jasmine oil at concentrations of roughly 2.5%, a feedstock commonly used in perfumes. Indole can be obtained at somewhat higher concentrations from the pyrolysis of rapeseed oil cake [4]. Currently the primary industrial source of indole is separation from coal tar [5].

Scheme 3. Summary of a common indole-based biosynthetic pathway.

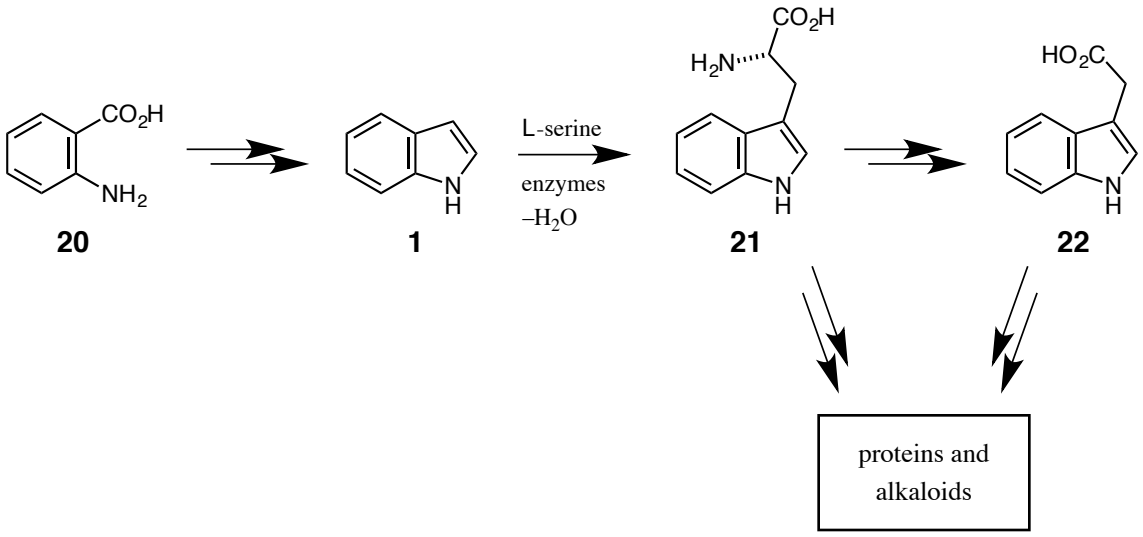

Many synthetic strategies for the preparation of indoles are based on closure of the pyrrolo ring, with the benzene ring already intact in the synthetic precursor [6]. The Fischer indole synthesis is the archetypal method. The mechanism is summarized in Scheme 4, and is included in a review article by D. L. Hughes [7].

Scheme 4. Several key steps in the Fischer indole synthesis. This process is often carried out in one pot, although some intermediates, such as phenylhydrazone **18**, can be isolable.

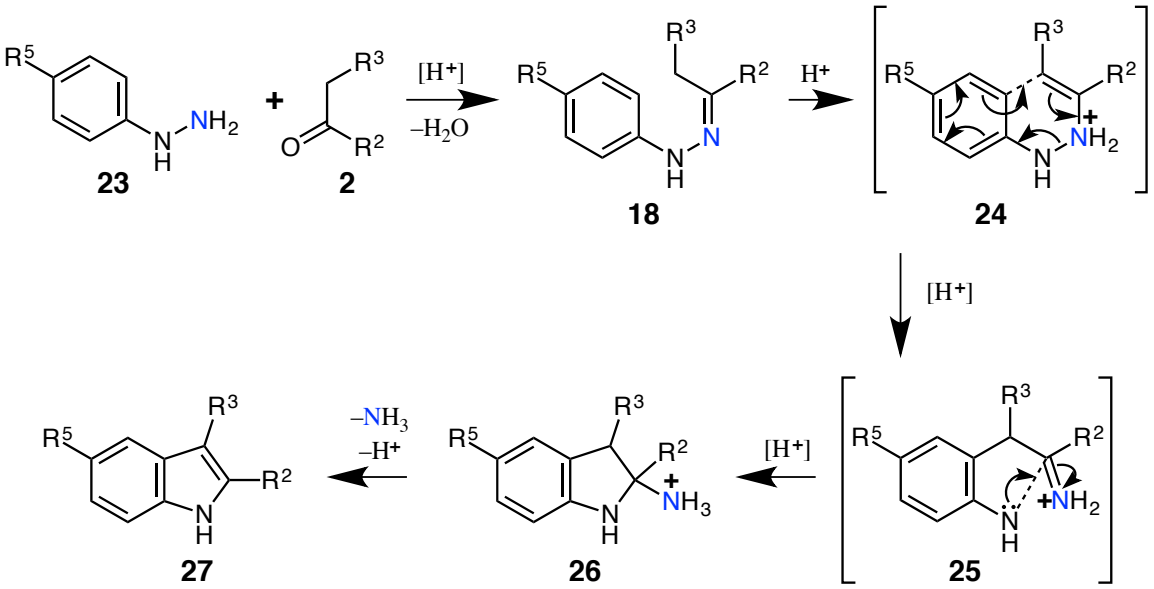

The benzene ring of phenylhydrazine **23** is symmetrical. Although this is not a requirement, the use of non-symmetrical phenylhydrazines results in regioisomeric product mixtures. This strategy is effective for making 7-substituted indoles, since annulation can only occur at the indole-3a-position in those cases. Similar symmetry considerations apply to carbonyl component **2**. The requirement of strongly acidic conditions is another limitation of the Fischer indole synthesis. This makes it difficult to prepare many 2- or 3-unsubstituted indoles by this method, because of the tendency of the products to undergo acid-catalyzed polymerization or rearrangements. Furthermore, it restricts the scope of functional groups that can be present.

Miyata and coworkers developed a modification in which the rearrangement-annulation sequence takes place in the absence of acid (Scheme 5) [8]. This approach removes most of the problems associated with strongly acidic conditions. The initial condensation of **23** with **2** usually takes place in the presence of a catalytic amount of acid and a drying agent.

Scheme 5. The modified Fischer indole synthesis developed by Miyata and coworkers.

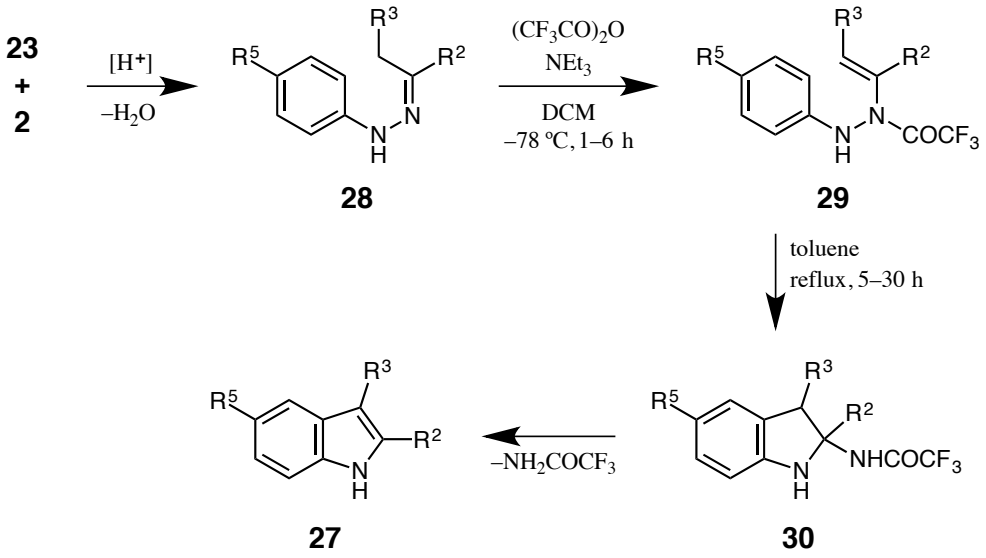

The Madelung indole synthesis allows access to 3-unsubstituted indoles (R^3 = H) that can be variously substituted on the benzene ring. There should be no substituent at the prospective 7-position that would compete with the desired annulation, and no acidic substituents. Within these boundaries, the limiting factor is usually preparation of the corresponding *o*-alkylanilide (**31**, Scheme 6). Historically, the Madelung indole synthesis was performed at temperatures of 200–400 °C with sodium amide or an alkoxide base. It has become increasingly popular to use two equivalents of *n*-butyllithium [9], which removes many of the problems associated with higher temperatures.

Scheme 6. A modified Madelung indole synthesis, using *n*-butyllithium.

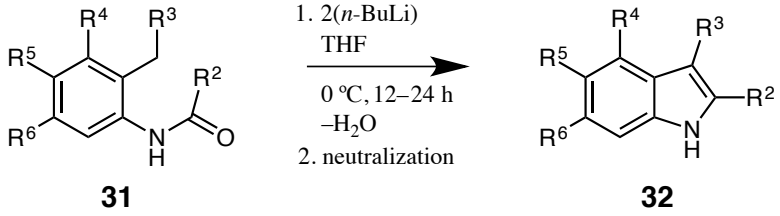

31 **32**

Preparations of indoles involving construction of the benzene ring are becoming increasingly common, as new developments are made in cycloaddition and transition metal catalysis. The Kanematsu indole synthesis involves an intramolecular Diels-Alder reaction of a 4-(dienamino)allene (**33**, Scheme 7a) [10]. In this strategy, both rings are simultaneously formed. The resulting tetrahydroindole (**34**) is dehydrogenated, giving the corresponding indole (**35**). This approach is particularly good for preparing 2,7-disubstituted indoles.

Scheme 7. Indole syntheses involving the construction of both rings. (a) A Kanematsu indole synthesis; (b) a gold-catalyzed transannulation of alkynylaminoethylfuran **36**.

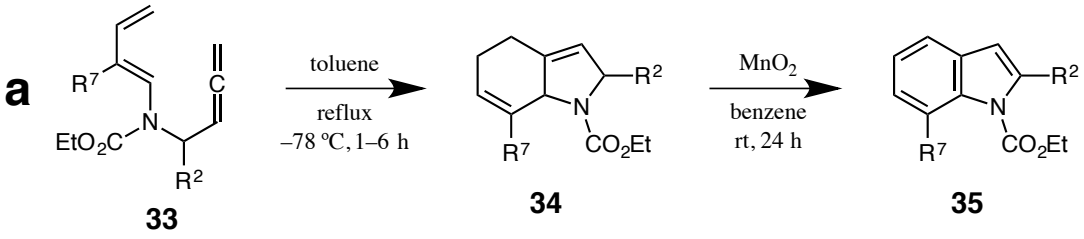

33 **34** **35**

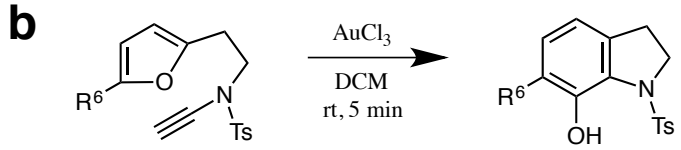

36 **37**

By a similar sequence, 2-(alkynylaminoethyl)furans (**36**) undergo gold-catalyzed transannulation to give 7-hydroxyindolines (**37**). This example is tailored toward the preparation of 6-substituted-7-hydroxyindoles, which is a small niche application. However, the two routes shown in Scheme 7 are illustrative of many emerging examples of preparing indoles by formation of the benzene ring.

1.1.2. Simple Reactions of Indoles with Electrophiles and Acids

Indole can be loosely thought of as a hybrid between an enamine (**38**) and naphthalene (**39**, Fig. 2). As with enamines, the most prominent reactivity of indole is the ease of electrophilic substitution at the β-C atom (the 3-position). The protonated forms of enamines (**38H**) and indole (**1H**) both readily undergo nucleophilic substitution at the α-C atom (the 2-position of **1H**).

Fig 2. A generic enamine (**38**), indole (**1**), and naphthalene (**39**), arranged by decreasing nucleophilicity. The preferred sites of electrophilic and nucleophilic attack are shown for the free (**38**, **1**) and protonated (**38H**, **1H**) forms, respectively.

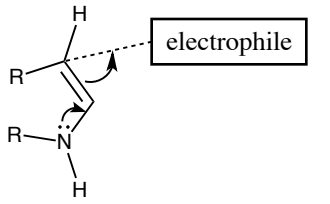

38

most nucleophilic

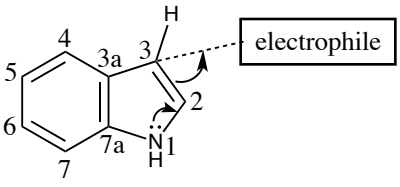

1

intermediate nucleophilicity

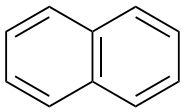

39

least nucleophilic

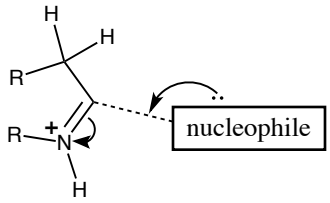

38H

electrophilic

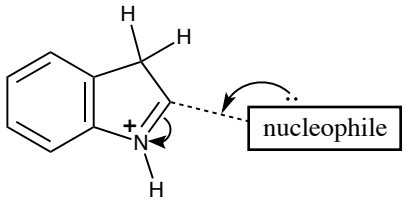

1H

electrophilic

Acylation is a suitable reaction for demonstrating the relative nucleophilic activity of the positions on the indole rings (Scheme 8). Conditions a–c are increasingly harsh. In the presence of base, acylation of the 1-position proceeds readily at room temperature to give **40** (Scheme 8a) [11]. The 1- and 3-positions both undergo acylation by acetic anhydride in refluxing acetic acid, with the 1-position reacting somewhat more rapidly (**40**–**42**, Scheme 8b) [12]. The conditions required to acylate the 2-position are more typical of a Friedel-Crafts acylation, and the 3-position must be occupied by an acid-stable substituent. 2-Acetylindole (**43**) is not directly accessible by acetylation of 1, but 3-methylindole (**44**) can be converted into **45** (Scheme 8c) [13]. Acylation at positions 4–7 is not easily accomplished. These regioisomers of acetylindoles (**46**) are not reported in the literature, with any combination of protecting groups or simple alkyl substituents (Scheme 8d). One noteworthy exception is that intramolecular acylation can take place on the benzene ring when favorable ring closure geometry is possible, and the pyrrolo ring is blocked [14]. Overall, the relative nucleophilicity of indole positions in the presence of acylating agents is 1 > 3 >> 2 >> 4–7.

Scheme 8. Acetylation of (a) indole at the 1-position; (b) indole at the 1- and 3-positions; (c) 3-methylindole at the 2-position; (d) indole on the benzene ring, which is not reported.

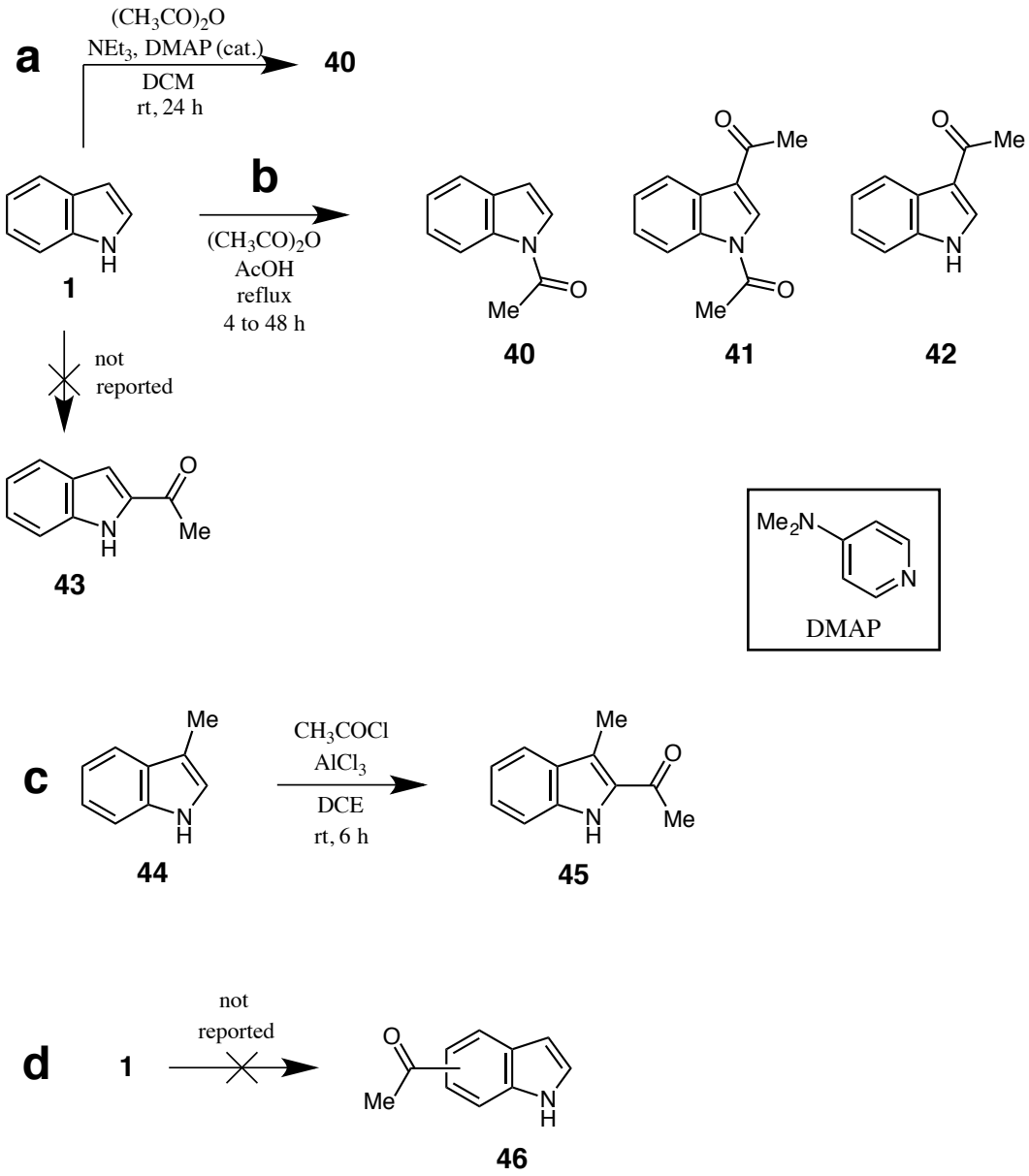

Alkylation of indole follows a trend similar to acylation. Alkylation at the 1-position is preferred in the presence of base. However, the alkylation is preferred at the 3-position in neutral or acidic conditions. In order for alkylation to proceed at the 2-position, the 3-position must be occupied. Unlike acylation, the 1-position can be open in some cases. There is considerable evidence that many preparations of 2,3-dialkylindoles proceed via two successive alkylations at the 3-position, followed by a 10-electron [1,2]-shift (**47**, Scheme 9) [15]. This is in contrast to the intuitive pathway, which would be 3-alkylation, followed by 2-alkylation.

Scheme 9. The preparation of 2,3-dimethylindole (**48**), *via* 3,3-dimethyl intermediate **47**.

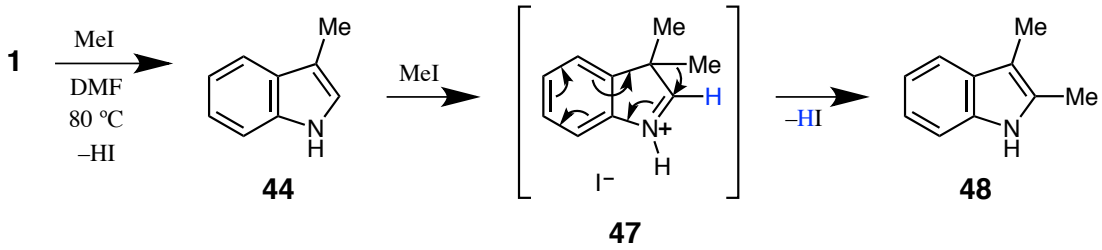

The acid-catalyzed transposition of the 2- and 3-substituents of an indole derivative is known as the Plancher rearrangement [16]. The key intermediates are 2,2- or 3,3-disubstituted indolenium cations. Methylation intermediate **47** is an example of this type of ion, thus, the dimethylation pathway in Scheme 9 invokes one half of the Plancher rearrangement. Note that the aforementioned acetylation of 3-methylindole (Scheme 8c) and the classical Fischer indole synthesis (Scheme 4) are also susceptible to the Plancher arrangement taking place *in situ*. When the two substituents in question are inequivalent, generally it is the softer substituent, the substituent better capable of stabilizing a positive charge, or the one providing better secondary orbital overlap, that migrates to the 2-position. For ring-fused indoles, the corresponding Plancher rearrangements favor the isomer that minimizes steric congestion by aligning the largest portion of the fused moiety away from the indole 4-position (Scheme 10) [17]. In this example, the Plancher rearrangement of **49** to **52** removes the 1,7-steric interaction.

Scheme 10. An example of the Plancher rearrangement.

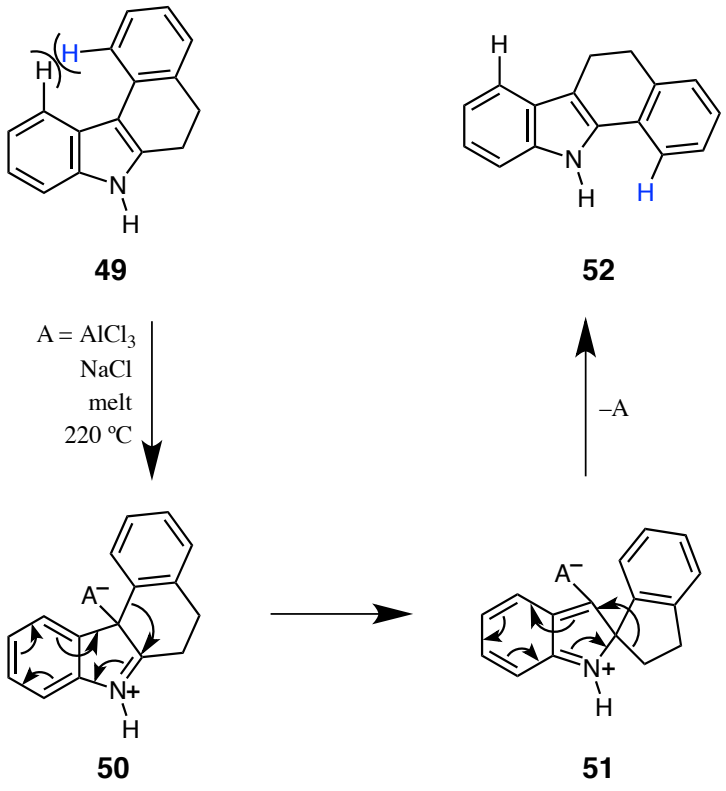

Substituted indoles can behave as analogs of electron-rich benzenes in other types of reactions, such as transition-metal-catalyzed coupling [18]. However, the indole 1-position often needs to be protected for the desired reaction to proceed (Scheme 11). In this example, 3-brominated indole **54** was the electron-rich halide component.

Scheme 11. A 3-brominated indole (**54**) participating in a Suzuki-Miyaura cross-coupling reaction.

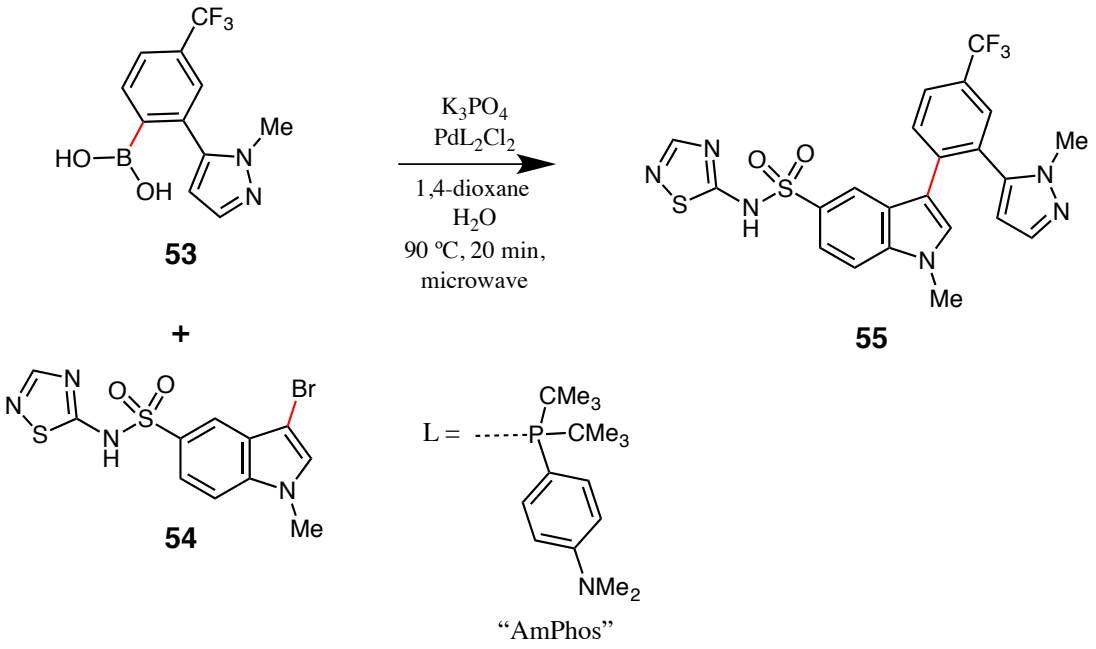

1.1.3. Indole-Ketone 2:1 Condensation

The performance of ketones and aldehydes (2) [19] reacting as electrophiles with indole is generally intermediate between acylating and alkylating agents, with respect to the required concentration, temperature, and acidity, as well as the resulting regioselectivity. In the presence of an acid, a ketone will add to the 3-position of indole (Scheme 12a). The resulting indole-3-carbinol (**56**) rapidly dehydrates. The resulting vinylogous iminium ion (**57H**) is more electrophilic than 2.

Scheme 12. (a) The initial 1:1 indole-ketone condensation that takes place in acid; (b) the formation of 2:1 bisindoles (**7**) resulting from the addition of **1** to **57H**.

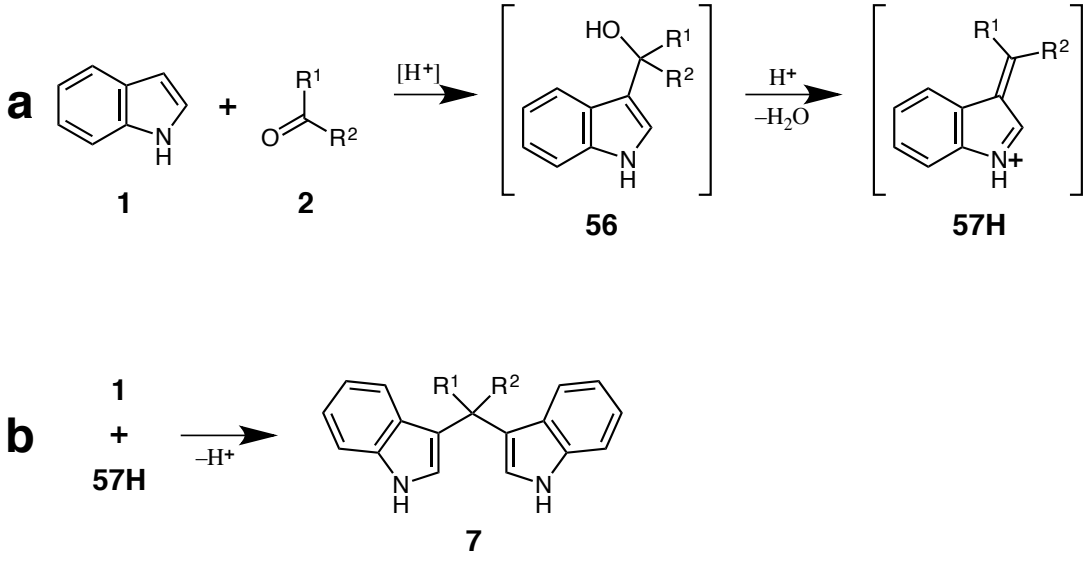

Provided that reaction conditions are mild enough that additional pathways are not activated, the major product of an acid-catalyzed condensation of indole with a ketone is the corresponding 3,3'-bisindole (**7**), a 2:1 ($-H_2O$) [20] product (Scheme 12b) [21]. When equimolar quantities of indole (**1**) and ketone (**2**) are used, most of the indole is recovered as bisindole **7**, and roughly half of the ketone will not react. The high electrophilicity of **57H** results in consumption of the available indole faster than it can react with **2**.

3,3'-Bisindoles were first reported by Fischer in 1887 [22]. The first examples were precipitates obtained when indoles and benzaldehydes were mixed in acetic acid. For decades, bisindoles garnered little attention because of their unassuming structure, but many examples were reported over the years while various indole-ketone condensation conditions were explored. These include fairly comprehensive coverage of 3,3'-bisindoles derived from simple indoles and aldehydes, alkyl ketones, and acetophenones. At the onset of the present study, cyclopentanone [23] and cyclohexanone [24] were the only cyclic ketones reported in bisindole preparations. A bisindole derived from cycloheptanone and indole [25], and one from cyclobutanone and 1-methylindole [26], were reported during the present study. There has been a surge of interest in bisindoles, mainly because several examples have shown promising anti-cancer activity [27].

During this renaissance, some work has also been devoted to the study of 2,2'-bisindoles [28], and 3,3',3"-trisindoles [29]. Some 2,2'-Bisindoles have shown promising pharmacological activity, similar to 3,3'-bisindoles [30]. There is considerable evidence that the mechanism of the formation of 2,2'-bisindoles includes two half-Plancher rearrangements (**58** and **61**, Scheme 13) of the same type reported for the preparation of 2,3-dimethylindole (Scheme 9) [31]. This pathway is in contrast to direct addition of the indole-2-position to a ketone.

Scheme 13. The proposed mechanism for the formation of 2,2'-bisindole **62**.

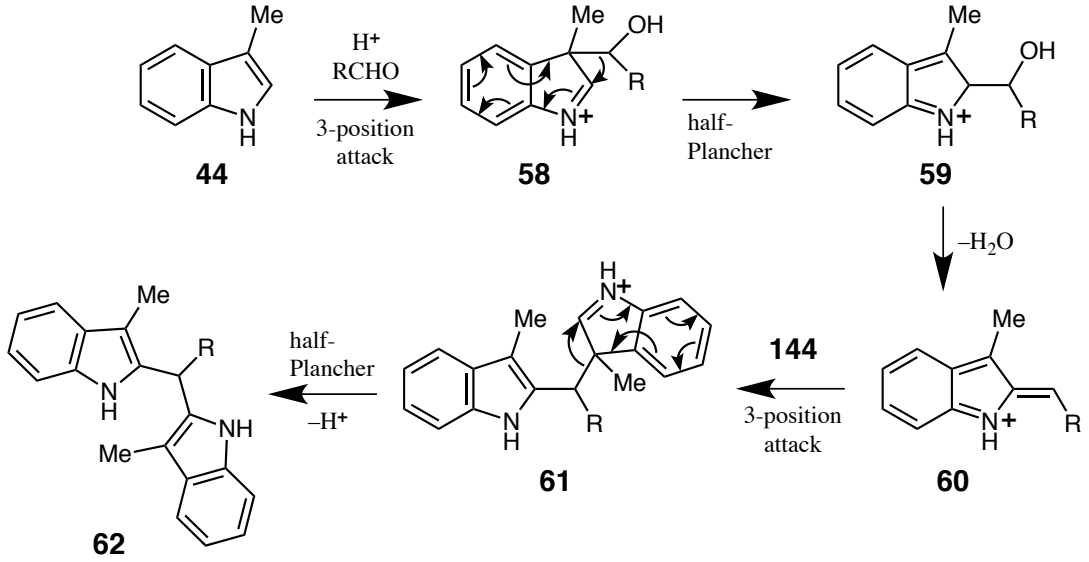

Symmetrical 3,3',3"-trisindoles are commonly prepared by 3:1 condensation of indoles with orthoformate esters. Unsymmetrical trisindoles can be prepared by 2:1 condensation of an indole (*e.g.*, **1**) with an indole-3-carbaldehyde (*e.g.*, **63**, Scheme 14) [29]. Trisindoles are primarily of interest because of their potential material applications by analogy to the more thoroughly studied alkyltris(oligothiophene) family of compounds [32]. Many trisindoles are also good hydride donors and leuco dyes; the parents are nearly colorless and the corresponding methylium cations are potently colored [33]. Trisindoles (*e.g.*, **64**) can be oxidized to tris(indolyl)methylium salts (*e.g.*, **65**) by chloranil, iron(III) salts, air, or by hydride donation to triphenylmethylium salts [34].

Scheme 14. The preparation of trisindole leuco dye **64** and oxidation to colored acetate salt **65**.

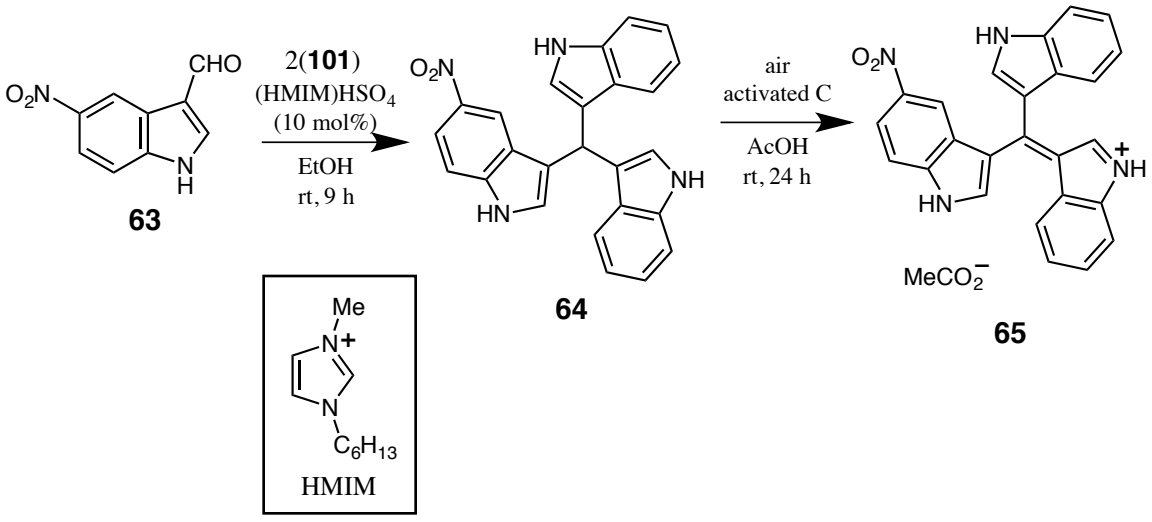

1.1.4. Indole-Ketone 2:2 Condensation and Related Products

If the temperature and acidity of indole-ketone condensation reaction conditions are increased, the scope of products expands. Acetone (**2b**) is the ketone in this example (Scheme 15). As with milder conditions, bisindole **7b** initially forms, *via* 2:1 condensation. Bisindoles can eliminate indole (**1**) upon protonation. The liberated indole can condense with acetone left over from the initial bisindole formation, generating additional **57bH**. The 1:1 condensation intermediates (**57b** and **57bH**) can combine, leading to 2:2 products (*e.g.*, **8b**), often with annulation [35]. This class of reactions is known as cyclizative condensation.

Scheme 15. A summary of the formation of 2:2 indole-acetone condensate **8b** from bisindole **7b** and leftover acetone (**2b**).

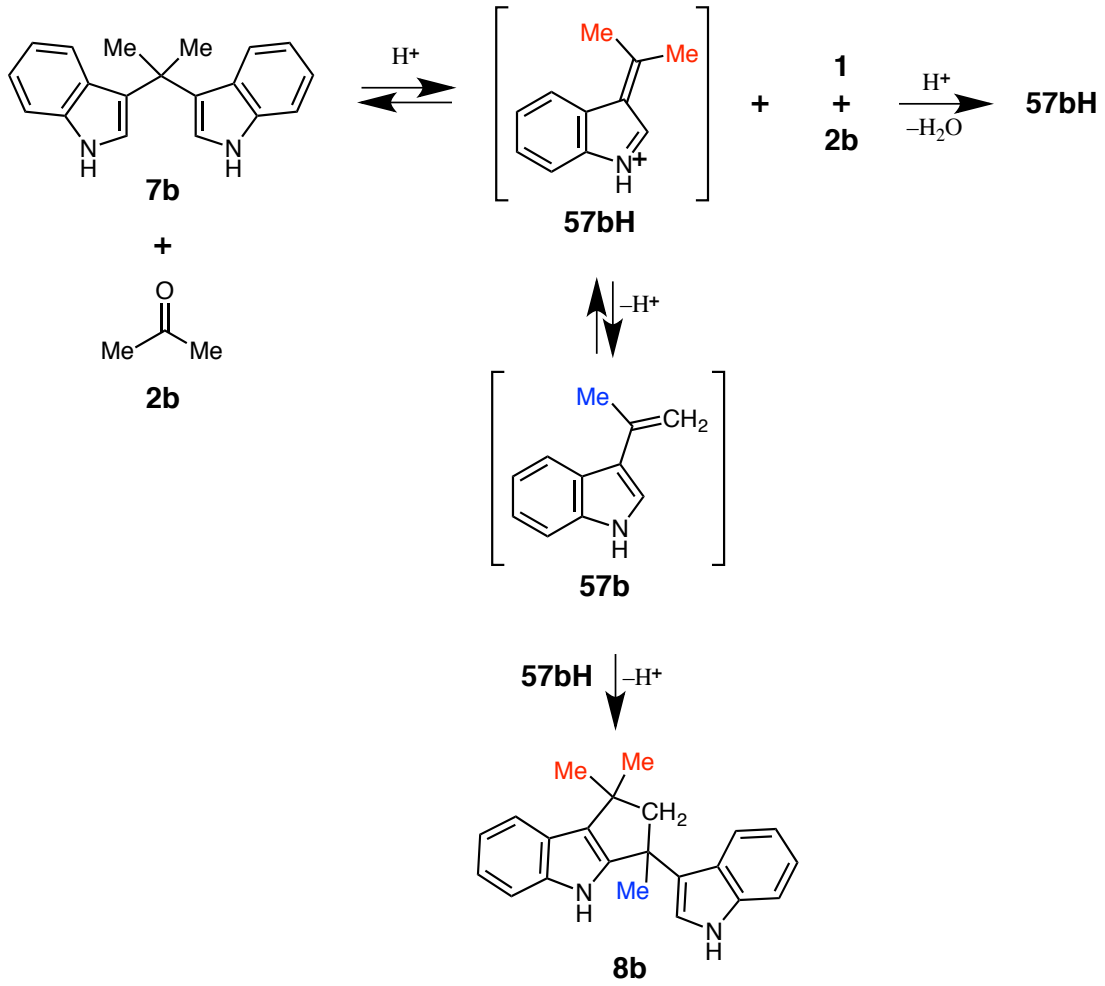

The first 2:2 ($-2H_2O$) [20] indole-ketone condensation was reported in 1913, as a precipitate obtained after adding hydrochloric acid to a solution of indole in acetone [36]. The product was initially thought to have structure **66b**, but was later determined by Noland and coworkers to be **67b** [37] (Fig. 3). Several other isomers of 2:2 condensation have also been reported. Products of type **8b** are the most commonly reported, and have been prepared from methyl ketones [35] and substituted acetophenones [38]. Both **67b** and **8b** form via a dimerization of 1:1 product **57b**, but from different modes of cyclization. Indoline **67b** is monobasic and precipitates as its hydrochloride salt when HCl is used as the catalyst.

Fig. 3. Three reported acetone-derived 2:2 condensation products.

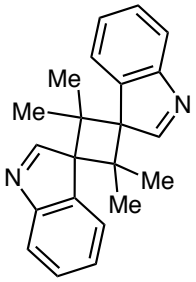

66b

originally proposed structure (not obs.)

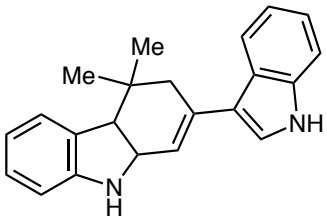

67b

correct structure of basic 2:2 product

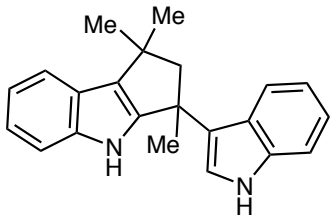

8b

most common non-basic 2:2 product

A fourth type of 2:2 product, indolo[2,3-*b*]carbazoles (*e.g.*, **68b**) was sought, based on the idea of condensing a second molecule of ketone (*e.g.*, **2b**) across the 2-positions of the corresponding bisindole (*e.g.*, **7b**, Scheme 16) [21, 39]. Some products of this type (**68b**) were reported. However, all reported examples that have been investigated with detailed NMR analysis have turned out to be other isomers. Many examples turned out to be analogs of **8b**. The other examples have been of type **9b**, which would be the result of **68b** undergoing a Plancher rearrangement (Scheme 16a). It is also possible that this reaction proceeds *via* a pathway that is similar to the formation of 2,2'-bisindoles (Scheme 16b), with addition and cyclization both taking place at indole-3-positions, each followed by a half-Plancher-type rearrangement. Either way, the net result is a rearrangement that follows the theme of rotating fused rings to minimize steric congestion at indole-4-positions.

Scheme 16. The formation of indolo[3,2-*b*]carbazole **9b** *via* (a) condensation and cyclization at the indole-2-positions followed by a Plancher rearrangement; (b) condensation and cyclization at the indole-3-positions, each followed by a half-Plancher rearrangement.

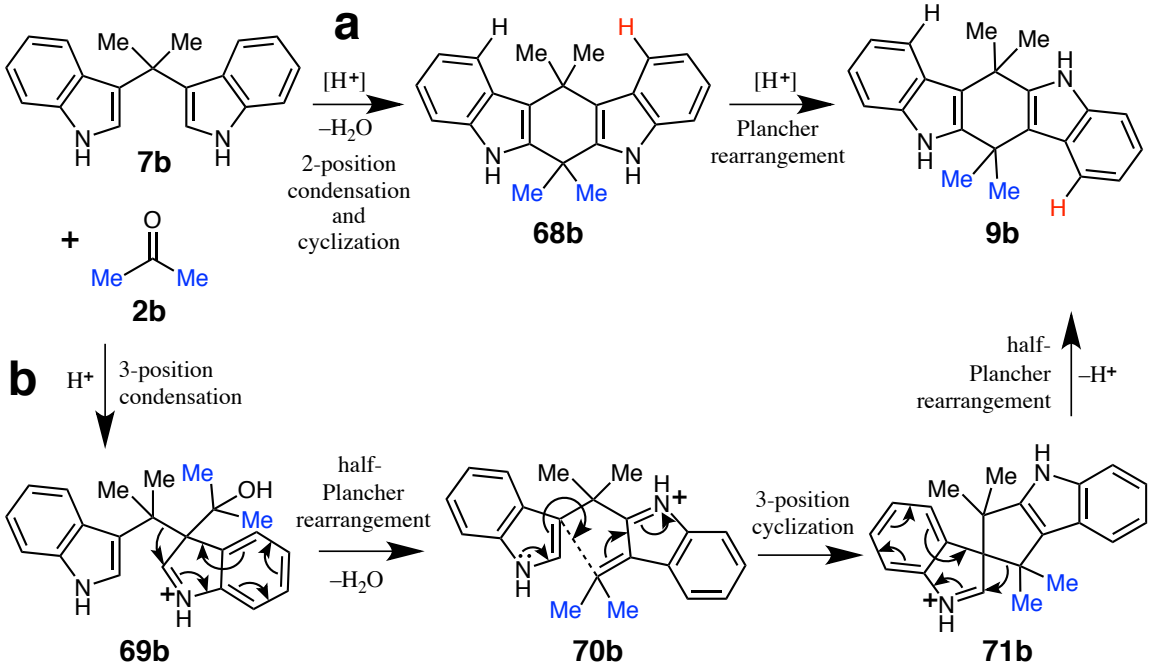

When attempts were made to prepare mixed 2:2 condensation products from formaldehyde and aromatic ketones, the only isolated product was indolo[3,2-*b*]carbazole **9a** (Scheme 17) [40]. This is another example of a bisindole fragmenting into a 1:1 product that then undergoes dimerization. It is interesting that ketone incorporation (**72**) was not observed. This is probably a result of the large difference in steric hindrance of a methylene group (from formaldehyde) and an aromatic ketone. One equivalent of H_2 has also been lost, probably *via* air-promoted autoxidation. Aromatization of the central ring is only possible for aldehyde-derived examples.

Scheme 17. The formation of indolo[3,2-*b*]carbazole (**9a**) during attempted syntheses of mixed 2:2 products (**72**).

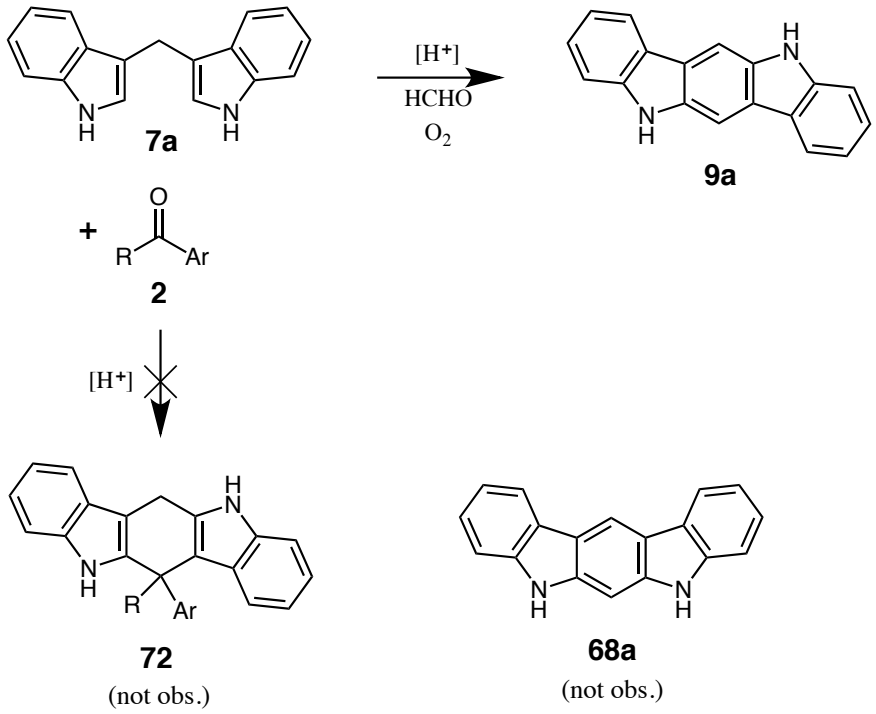

No traces of **68a** were observed during an investigation of the intermediates of this reaction [40]. Apparently, either the Plancher rearrangement takes place extremely quickly, or the pathway shown in Scheme 16b is preferred.

In the early 1990's, Eric Codner was an undergraduate in the Noland research group. He performed experiments with mixtures of indole, cyclohexanone (**2f**), and hydrochloric acid (Scheme 18). A white precipitate was obtained. It was too insoluble to be comprehensively characterized, but it was identified as **9f**, based on ^{1}H NMR, MS, and elemental analyses. Isomer **68f** might have been also obtained, however, there are no supporting data. As of the onset of the present study, this was the only known example of a 2:2 condensation of indole with a cyclic ketone. During the course of the present study, Eric Codner, currently a faculty member at the University of Wisconsin at Madison, co-authored a paper in which he confirmed the structure of **9f** by X-ray crystallographic analysis [41].

Scheme 18. The preparation of cyclohexanone-derived indolo[3,2-*b*]carbazole **9f**. Isomer **68f** may have also been obtained.

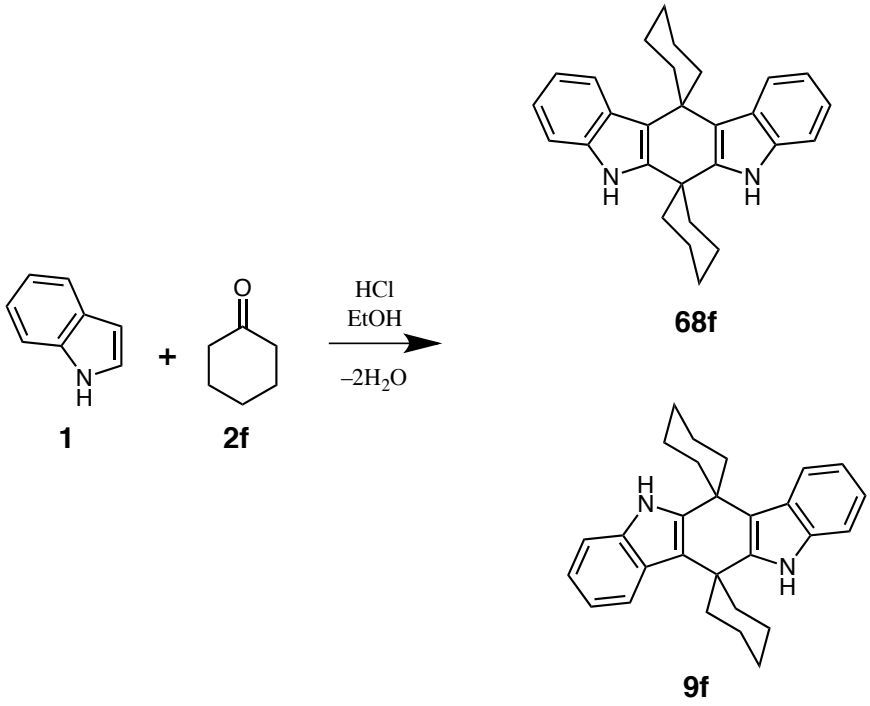

Overall, three types of 2:2 indole-ketone condensation products have been confirmed to be isolable from hydrochloric acid mixtures (non-basic **8**, **9**, and monobasic **67**). There is not yet an obvious means of confidently predicting which isomer is most likely to arise from a given novel experiment.

When the reaction acidity and temperature is further increased, the scope of observed products expands, including those derived from 3:2 condensation and indole ring-opening (Fig. 4). There is an increased occurrence of electrophilic attack at the indole-1-position [42], and various autoxidation-rearrangement cascades have also been reported [43]. A large portion of this work has been reported by Banerji and coworkers in a series of 24 papers [44].

Fig. **4**. Four products obtained from condensation of indole with acetone in the presence of strong acids.

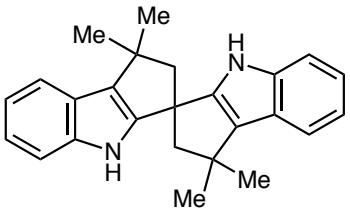

73

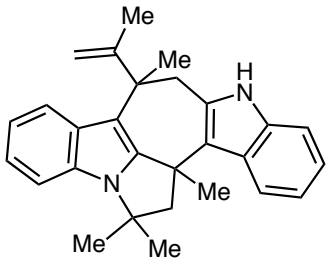

74

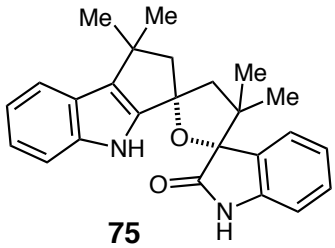

75

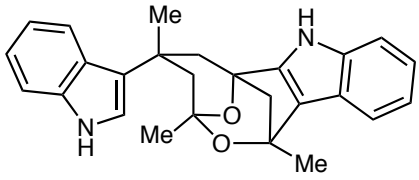

76

1.1.5. *In Situ* Indole-Ketone 1:1 Condensation and Diels-Alder Reactions

During the late 1980's, the Noland research group continued to study indole-ketone condensations. The ability to predict detailed outcomes of 2:2 or higher-order condensation remained elusive. However, a prevailing trend was quite clear. The use of acetic acid (pKa ≈ 4.8) favored bisindole products, and the use of hydrochloric acid (pKa ≈ –6.3) favored 2:2 or similar products. There was interest in trying a catalyst of intermediate acidity. Maleic acid (**77a**, pKa_1 ≈ 1.9) was an attractive option. When a mixture of indole, cyclohexanone, and maleic acid were heated to 100 ºC until no more indole was observed by TLC analysis (approx. 5 h), compound **78** was obtained (Scheme 19) [45]. This product is the result of a Diels-Alder reaction of **57f** with **77a**, followed by a tautomerism to re-aromatize the indole system.

Scheme 19. The preparation of **78** *via* a Diels-Alder reaction between maleic acid and **57f**.

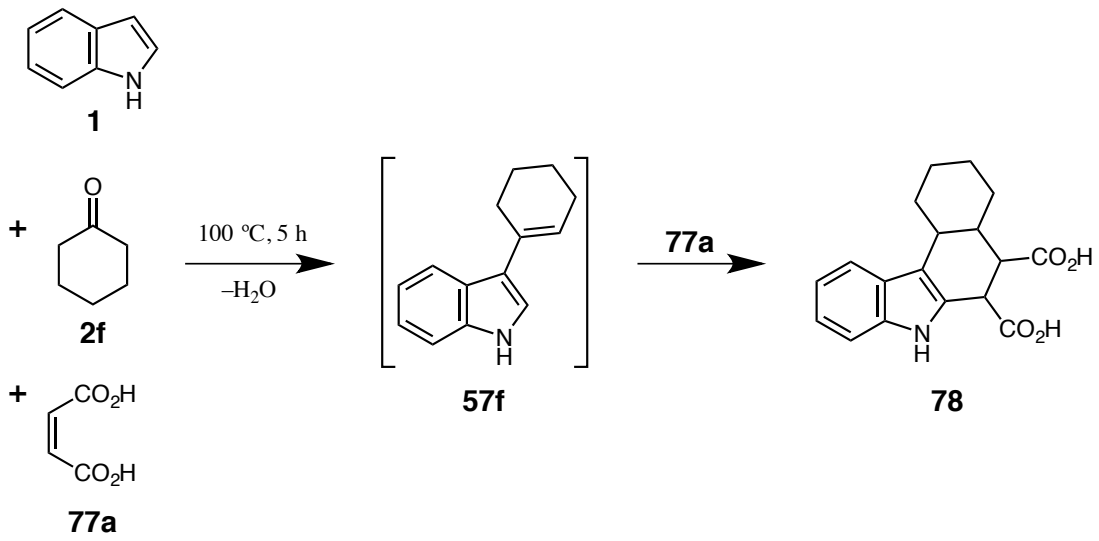

Roughly 200 products have been reported by Noland and coworkers using this *in situ* vinylheterocycle strategy, with various indoles and 2-substituted pyrroles as parents, and a series of dienophiles that mainly consisted of maleimides and quinones [46]. These reactions were mainly carried out in ethanolic HCl. The scope of ketones included alkyl, aromatic, and cyclic ketones. The cyclic ketone scope ranged from cyclobutanone to cyclododecanone, and several substituted cyclohexanones were also explored. Diels-Alder-derived products were obtained from cyclic ketones of every attempted ring size (Table 1) [47].

Table 1. Selected cyclic-ketone-derived Diels-Alder products reported by Noland and coworkers.

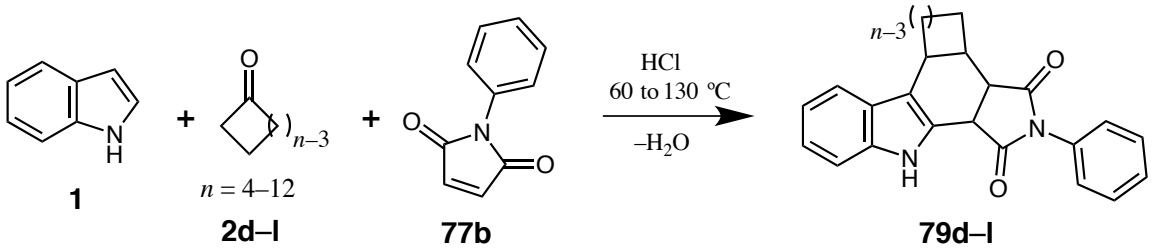

1 **2d–l** **77b** **79d–l**

ring size *n*	yield %
4	3
5	76
6	68
7	66
8	65
9	7
10	6
11	22
12	53

1.1.6. Summary of Reaction Conditions and Product Types

As with the majority of chemical reactions, indole-ketone condensations follow a pattern where minimal reaction progress is observed in sufficiently mild conditions, and impractically complicated mixtures are obtained from sufficiently harsh conditions. In Fig. 5, the reaction conditions introduced in §§ 1.1.3–1.1.5 are arranged within a spectrum that is increasingly harsh from left to right. Along this spectrum, the boxes illustrate the approximate window where each type of condensation reaction is the dominant pathway.

Fig. 5. A summary of the types of products observed from condensation of indole with various carbonyl derivatives.

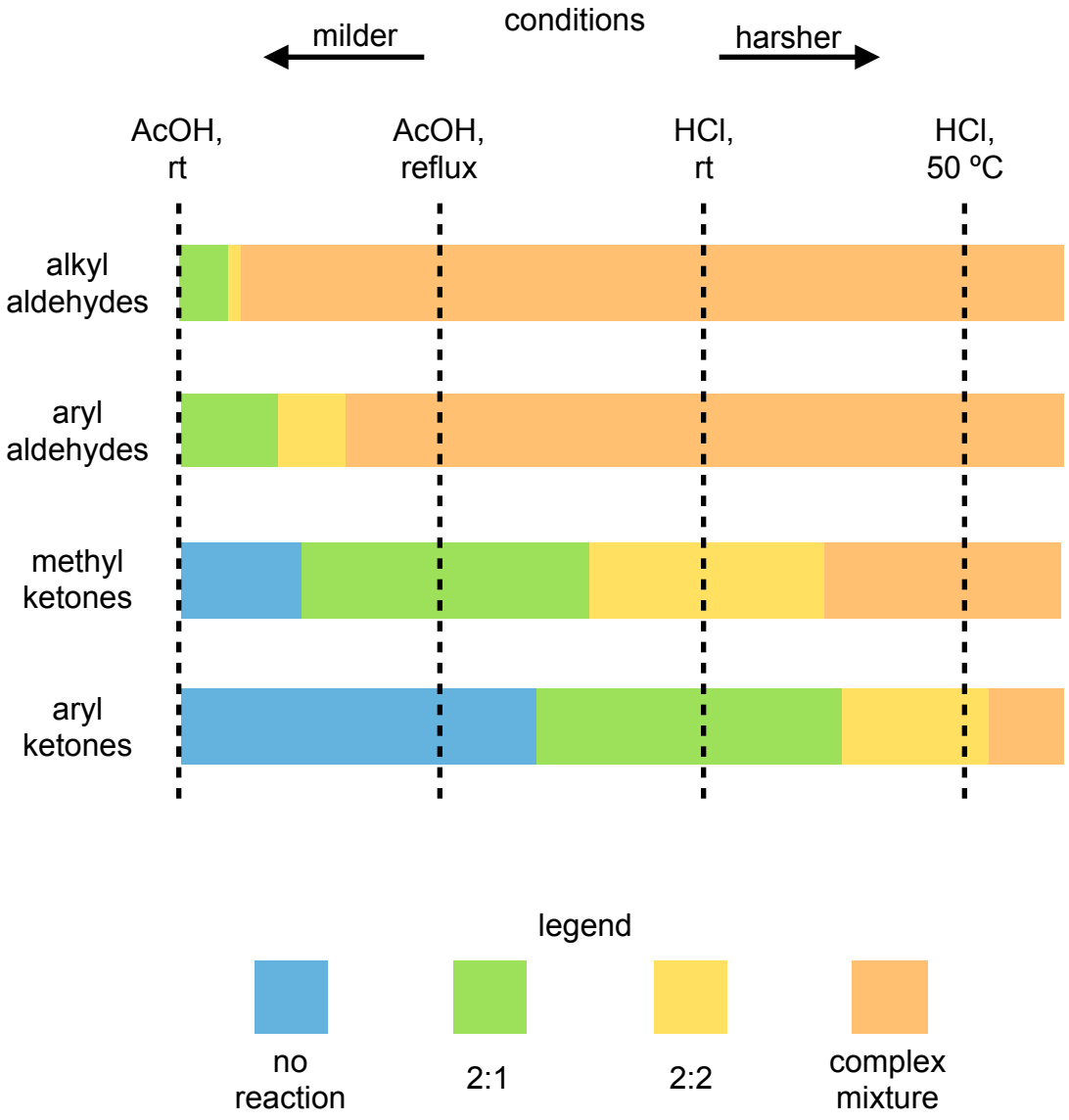

This diagram is a general guide that highlights prevailing trends, and is not comprehensive. There are many nuances. For example, there are cases where a cold hydrochloric acid solution will result in a simpler product mixture than refluxing acetic acid. Also, there are cases when products can be isolated from very complicated reaction mixtures, as is illustrated by the results reported by Banerji and coworkers using BF_3. In other cases, it may be extremely difficult to separate mixtures where there are multiple principal components, which is especially likely when one or both starting materials has a long alkyl chain.

Overall, alkyl aldehydes tend to have a very small window (or no window) where 2:2 condensation is activated without the formation of complex tarry mixtures. Aryl aldehydes have a slightly higher activation barrier to 2:2 condensation, and a somewhat wider window of viable preparation of 2:2 products, although they are often difficult to isolate. Methyl ketones offer the widest windows of 2:1 and 2:2 condensation. The viable window of 2:2 condensation with aryl ketones tends to be narrower. The best conditions for obtaining Diels-Alder-derived products *via* the *in situ* vinylindole strategy are usually within the 2:1 condensation window [48].

1.1.7. Preparation of Cyclic Ketones

Five common strategies for the preparation of cyclic ketones with ring sizes ranging from 4 to 12 are compared in Table 2. These qualitative comparisons are based on preparation in a general-purpose synthetic laboratory. Many variations of these strategies have also been reported.

Table 2. Summary of the overall economic viability of common synthetic approaches to cyclic ketones.

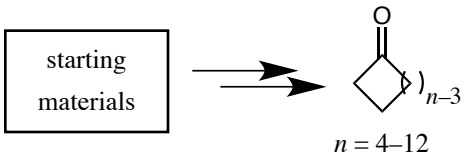

n = 4–12

2d–l

ring size n	oxidation of alkane or alkene	Dieckmann cyclization	diazomethane 1-carbon expansion	propiolate 2-carbon expansion	1-carbon contraction
4	x	x	**best**	x	x
5	poor	**best**	poor	x	x
6	good	**best**	poor	x	x
7	good	**best**	poor	x	x
8	good	x	**best**	x	x
9	poor	x	poor	**best**	x
10	poor	x	poor	**best**	good
11	poor	x	poor	poor	**best**
12	**best**	x	x	poor	x

With the exception of cyclobutanone and cyclopentanone, cyclic ketones that are produced industrially are usually prepared by catalytic oxidation of the corresponding cycloalkanes or cycloalkenes, which is generally the most economical approach [49]. New developments in catalytic methodology are making smaller-scale alkane or alkene oxidation increasingly competitive with the other approaches to cyclic ketones [50]. The geometry of cyclooctane makes it especially active among the listed cycloalkanes, followed by C_7, C_6, and C_{12} cycloalkanes [51]. However, cyclododecanone (**2l**) is the only ketone that is currently best prepared by catalytic alkane or alkene oxidation in the laboratory (Scheme 20). Note, however, that **80** and **2l** can be purchased at similar prices.

Scheme 20. The preparation of cyclododecanone (**2l**) by Pd-catalyzed oxidation of cyclododecene (**80**).

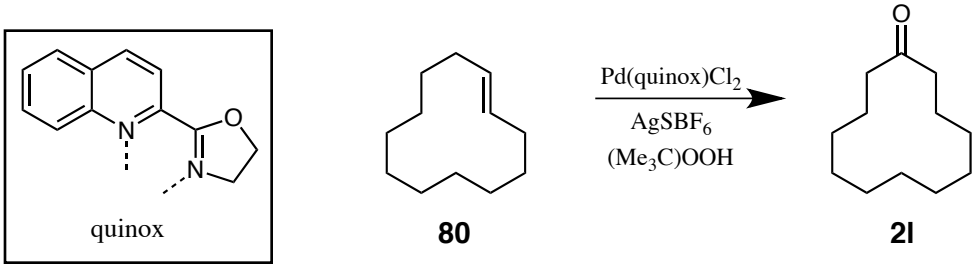

On a laboratory scale, Dieckmann cyclization [52] is the long-standing preparation of choice for cyclopentanone, cyclohexanone, and cycloheptanone (**2e**–**g**, Scheme 21). Cyclic ketones of other sizes are difficult to produce by this method, because intermolecular condensation kinetically competes with annulation. Because of the widespread use of adipic acid (**83**) in polymers, it is available at a low cost and the Dieckmann cyclization is the preferred preparation of **2e** on any scale.

Scheme 21. The preparation of C_n cyclic ketones (**2e**–**g**) *via* the Dieckmann cyclization of C_{n+1} linear diesters (**81**).

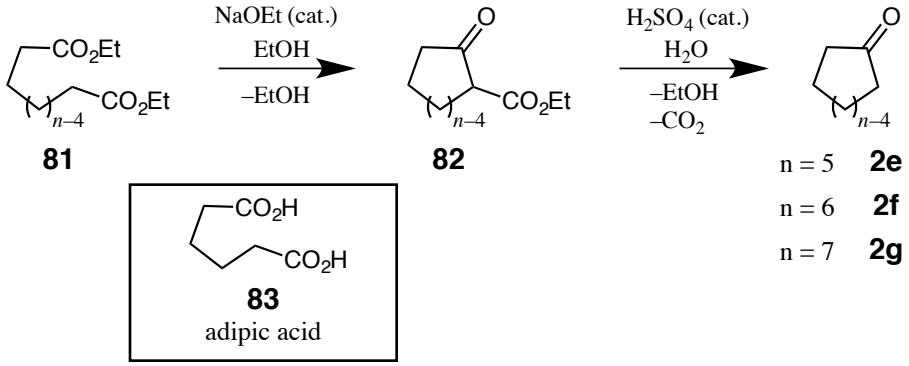

The ring size of cyclic ketones can be expanded by the insertion of a methylene unit between the C1 and C2 atoms. Diazomethane (**85**) is the most widely used reagent for this purpose, and is commonly used *in situ* to decrease the risk of detonation (Scheme 22) [53].

Scheme 22. The *in situ* preparation of diazomethane (**85**) from Diazald (**84**).

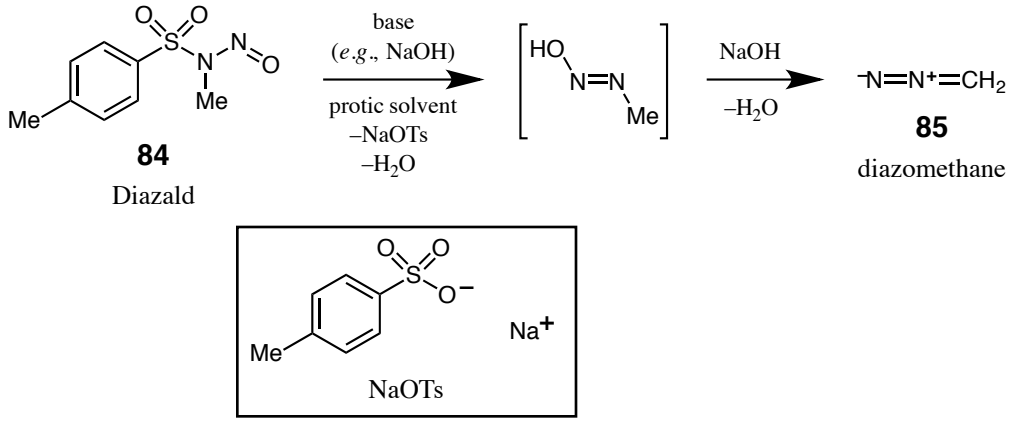

Cyclobutanone (**2d**) is prepared by the addition of two successive molecules of diazomethane to ketene (**86**, Scheme 23a) [54]. Cyclopropanone (**87**) is too reactive to be isolable under these conditions. Ketene (**86**) can be generated *in situ* by pyrolysis of acetone vapor or the cracking of diketene [55]. Because of the low cost of cycloheptanone (**2g**), diazomethane-promoted ring expansion is a popular preparation of cyclooctanone (**2h**, Scheme 23b) [53]. The release of N_2 and rearrangement of the resulting epoxide (*e.g.*, **88**) provides sufficient free energy to overcome the higher strain energy as the ring size increases to 8 and 9. However, ring sizes of 10 and larger tend to have progressively less strain, leading to runaway ring expansion when attempting to make cyclononanone or larger cyclic ketones. The resulting mixtures include the desired product, unreacted starting ketone, and several larger cyclic ketones. Such mixtures are not easily separated, but ketones as large as cycloundecanone can be isolated by rigorous vacuum distillation.

Scheme 23. The preparation of (a) cyclobutanone (**2d**) *via* ketene (**86**); (b) cyclooctanone (**2h**) from cycloheptanone (**2g**). Both preparations use diazomethane (**85**) that is generated *in situ*.

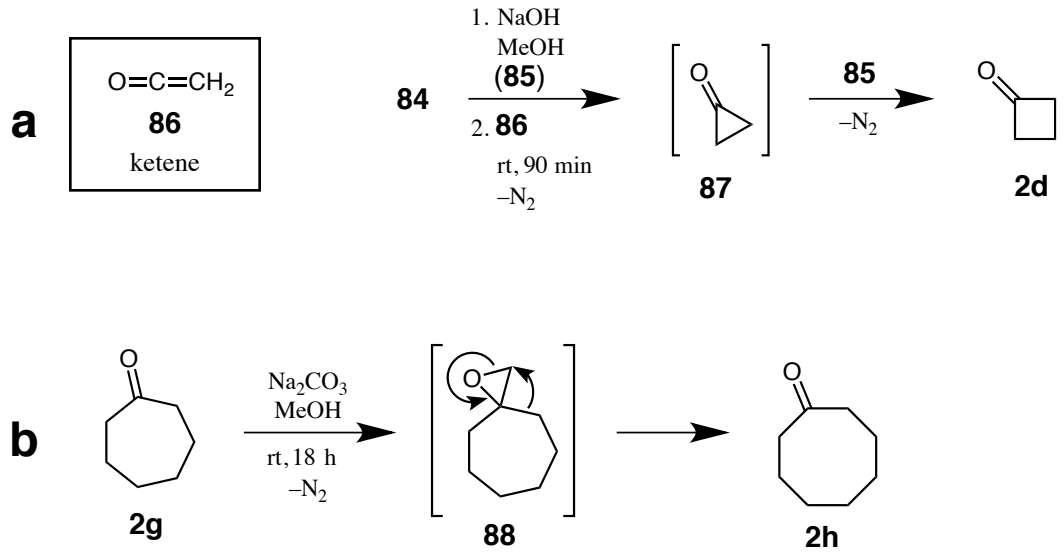

Cyclononanone (**2i**) and cyclodecanone (**2j**) can be prepared by a different strategy. The key step is the ring opening of a fused cyclobutene (**90g**) that forms after conjugate addition of a propiolate ester to the corresponding cyclic enamine (**89g**, Scheme 24) [56, 57]. The preparation of **2j** differs slightly, and is discussed in § 1.3.1 (p 33). This route is not a good approach to cyclic ketones of other sizes, because the analogs of **90g** undergo different rearrangements than the type shown in Scheme 24 [56].

Scheme 24. The preparation of cyclononanone (**2i**) from cycloheptanone (**2g**).

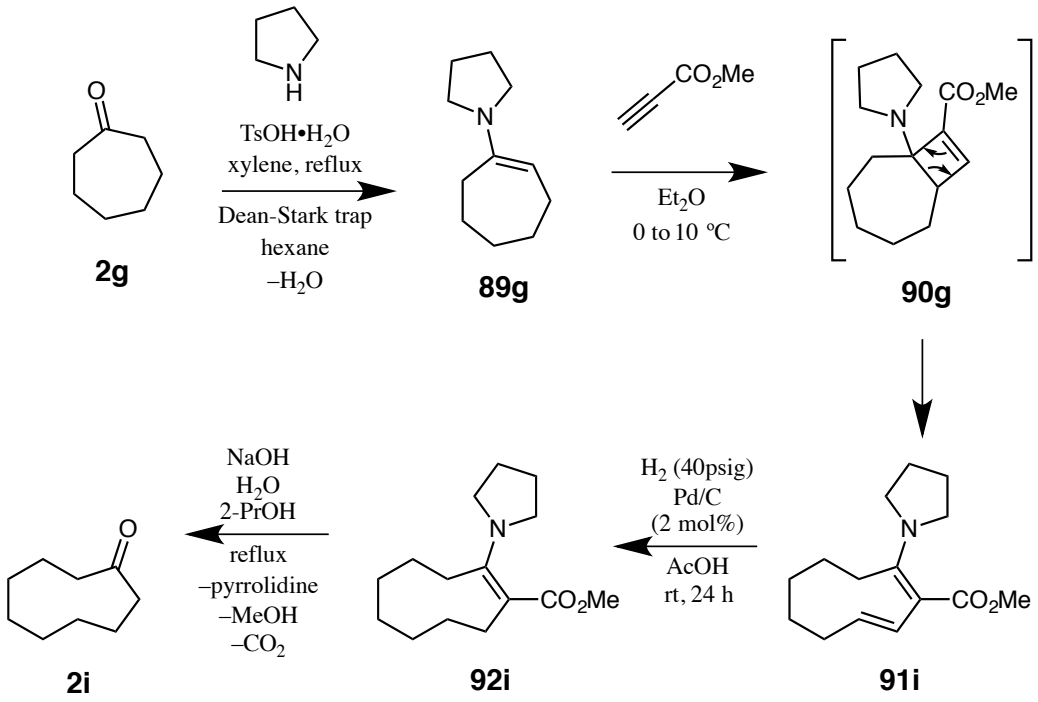

During the first step, the Dean-Stark trap is initially charged with hexane (b.p. 69 °C), and a packed column is installed between the boiler and the condenser. This configuration allows xylene (b.p. 138–145 °C) to be used in the reaction vessel, maintaining a suitable reaction temperature, while minimizing the loss of pyrrolidine (b.p. 87 °C, water-miscible) during the water removal process. Substitution of piperidine or morpholine for pyrrolidine gave unsatisfactory results. The second step is highly exothermic, but it proceeds slowly at temperatures below 0 °C. It is important to keep the reaction temperature between 0 and 10 °C during the addition of methyl propiolate so that it proceeds smoothly. If it is allowed to warm to above 20 °C, polymerization can occur if methyl propiolate and **90g** are still present.

Cycloundecanone (**2k**) and cyclodecanone (**2j**) can be prepared by ring contraction (Scheme 25) [58]. This sequence begins with α,ω-dibromination (**93**), followed by a Favorskii rearrangement [59]. The resulting α,β-unsaturated ester is (**95**) hydrolyzed and then converted into the corresponding isocyanate (**96**, *via* a Schmidt reaction) [60], followed by two more iterations of hydrolysis. It is not specified whether this strategy can be applied to make smaller cyclic ketones, but the increasing strain in smaller analogs of **94** could be problematic.

Scheme 25. The preparation of cycloundecanone (**2k**) by ring contraction. Cyclodecanone (**2j**) can be prepared by using **2k** as the starting material.

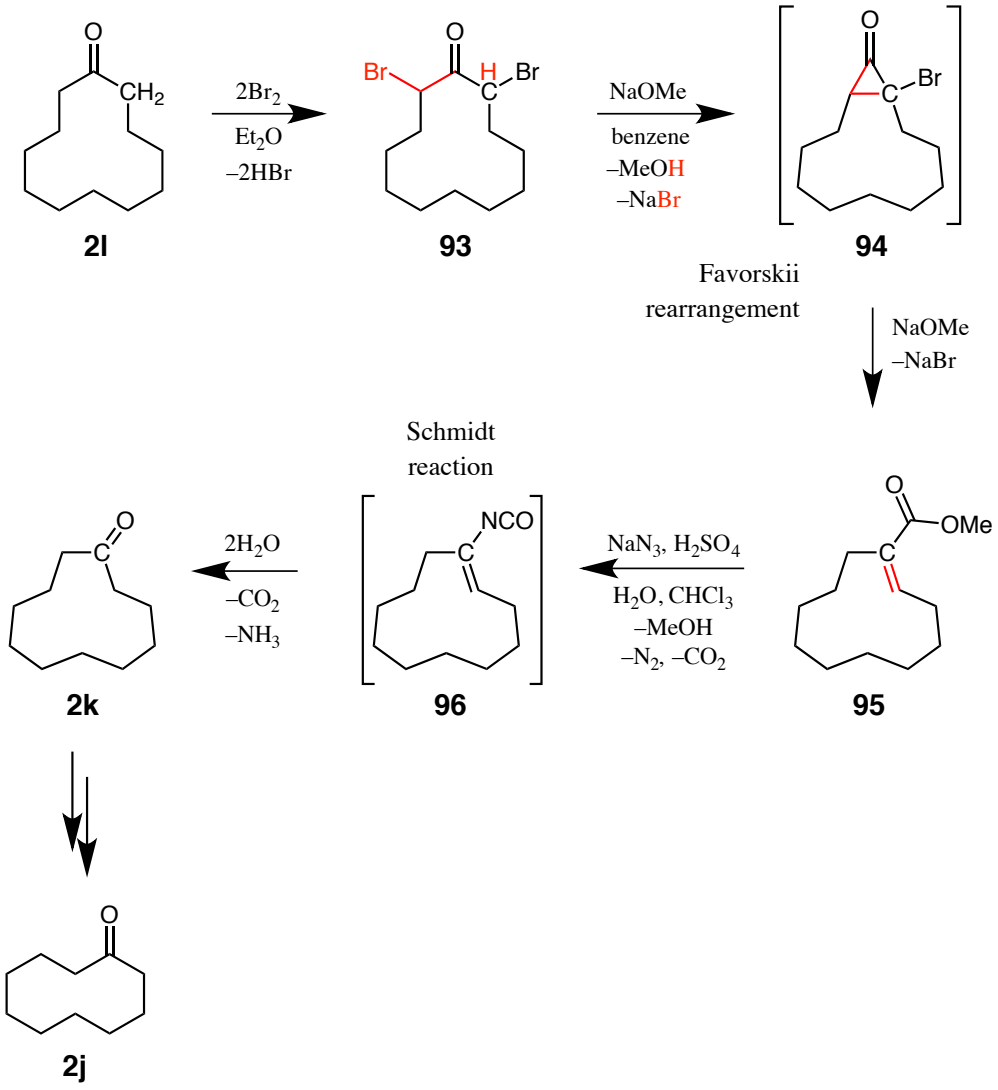

1.2. Scope of the Present Work

Condensation of indole with open-chain ketones has been widely studied with and without dienophiles present, using mild and strong acids. However, the corresponding reports using cyclic ketones are much more limited (Table 3). Mild condensation conditions were only reported for indole with ring sizes 4–7. Strong condensation conditions were only reported for indole with cyclohexanone, giving a different type of 2:2 condensation product (**9f**) than had been obtained from most other ketones. Screening of indole condensing with a series of cyclic ketones has only been reported in the presence of strong acid and dienophiles. It was desirable to expand the scope of dienophile-free conditions (boldface entries) to match that of the Diels-Alder study.

Table 3. The reported scope of study of condensation of indoles with cyclic ketones.

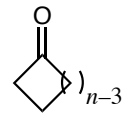

n = 4–12

2d–l

conditions	cyclic ketones	products
mild acid	***n* = 4[a], 5, 6, 7[a]**	bisindoles
strong acid	***n* = 6**	novel type of 2:2 product
strong acid, dienophile	n = 4–12	Diels-Alder adducts

[a]Reported during the course of the present study

Two of the most intriguing questions were:

(a) What conditions can be used to prepare a series of cyclic-ketone-derived bisindoles?

(b) What types of 2:2 condensation products, or related products, can be obtained from indole and cyclic ketones?

With desires to fill information gaps on the subject of indole-ketone condensation, and to provide undergraduate research opportunities in our laboratory, these questions merited performing a study with the following objectives:

1. Prepare cyclononanone and cyclodecanone using the propiolate ring-expansion method, completing the desired inventory of cyclic ketones. An ample supply of cycloundecanone was still in inventory from prior research. The remaining cyclic ketones were commercially available at favorable prices and were purchased.

2. Prepare bisindoles using indole and cyclic ketones with ring sizes ranging from 4 to 12. Use inexpensive, non-oxidizing acids of increasing strength as catalysts, with acetic acid as the starting point. Compare the results based on ring size. Use formaldehyde, and acetone and acetophenone as benchmark ketones [19].

3. Working in sequence from highest to lowest bisindole-yielding ring sizes, isolate and characterize at least one additional condensation-derived product per cyclic ketone.

4. As a secondary objective, provide mechanistic insight into the formation of the previously reported indole-cyclohexanone 2:2 condensation product **9f**.

5. Serve as a research mentor to 8–10 undergraduates during the course of this work (roughly one per cyclic ketone). Elevate each of them, within this work and their personal goals, to the level where they earn co-authorship on a publication derived from their results.

1.3. Results: Preparation of Cyclic Ketones

Cyclononanone (**2i**) was prepared from cycloheptanone (**2g**) according to the 4-step process described in § 1.1.6 (p 29) [57]. The best overall yield (18%) was obtained when all 4 steps were performed consecutively, without isolating or storing intermediates (Scheme 26a). The overall yield decreased to 10% or lower when any such attempts were made.

Scheme 26. The preparation of (a) cyclononanone (**2i**); (b) cyclodecanone (**2j**) in the present study.

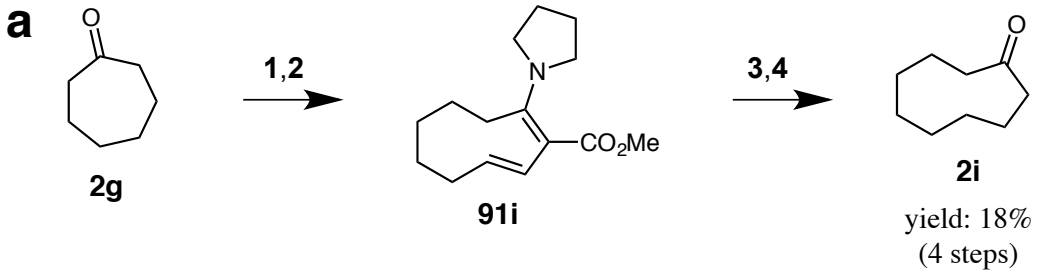

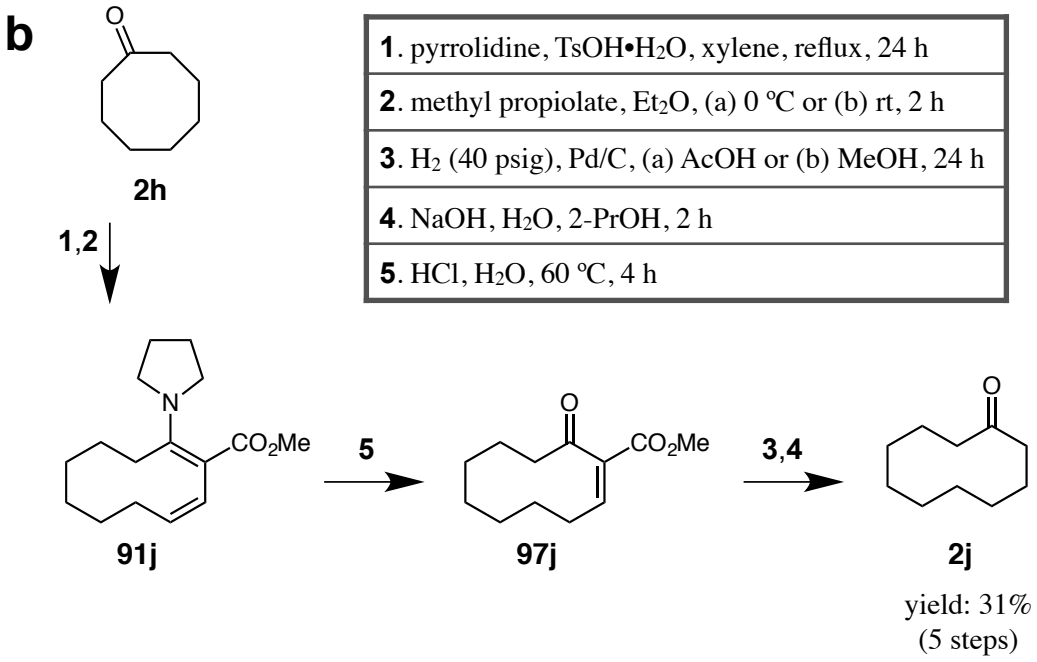

The preparation of cyclodecanone (**2j**) included the same 4 steps, but the methyl propiolate addition was maintained between 25 and 30 ºC by intermittent cooling in an ice bath, and methanol was the hydrogenation solvent. Also, a fifth step was inserted before hydrogenation (Scheme 26b) [56]. Acid-catalyzed hydrolysis of the enamine unit in **91j** gave unsaturated keto ester **97j**. This allowed the hydrogenation of **97j** to take place in the absence of amino groups, which was probably a factor in improving the overall yield to 31%. In agreement with the reported procedure [57], this strategy could not be applied to the synthesis of **2i** because dienamine **91i** polymerized upon attempted hydrolysis, whereas **91j** had no such issue. This is a good example of the need to be wary of nuances when planning to perform similar transformations that differ by the size of rings.

The cycloundecanone (**2k**) that was used for this project was taken from a batch that was probably prepared from cyclododecanone by ring contraction (*circa* 1960). A solid, white precipitate had formed that constituted roughly 20% of the remaining organic material. Cyclic ketones are known to undergo autoxidation to the corresponding α,ω-dioic acids [61]. After NMR and MS analyses, the precipitate was confirmed to be undecane-1,11-dioic acid (**3**, Scheme 27). This transformation is typically performed over several hours with an alkoxide base, an oxygen bubbler, and at reduced temperature. However, it is reasonable that an autocatalytic pathway could proceed to the observed extent during 50 years on the shelf. There are several plausible mechanistic pathways for this transformation, but it is likely that α-hydroperoxyketone **98** and 1,2-diketone **99** are intermediates.

Scheme 27. The autoxidation of cycloundecanone (**2k**) to diacid **3**.

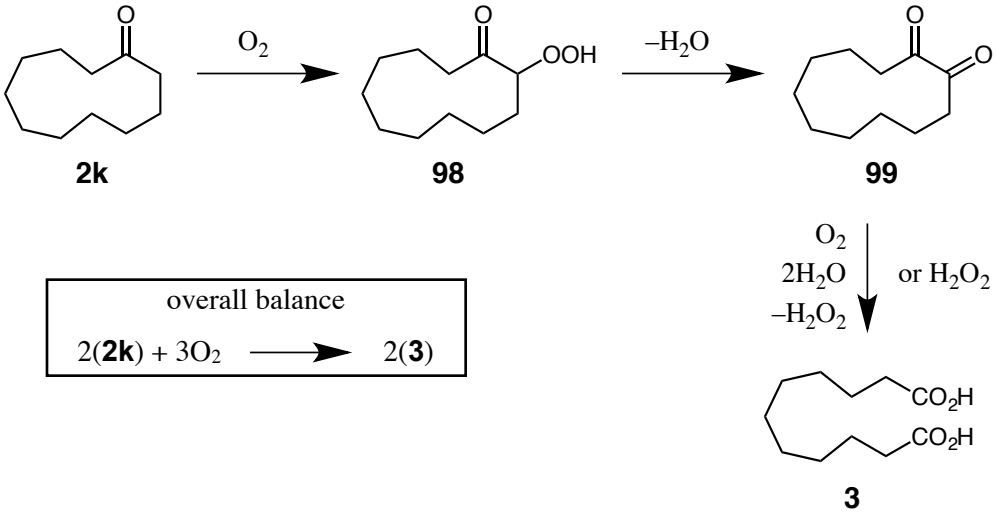

Following additional ^{1}H NMR analysis, the liquid phase in the bottle was estimated to be 96.5 mol% cycloundecanone (**2k**) and 3.5 mol% diacid **3**. It was assumed that this amount of **3** would not be problematic, so this batch of **2k** was used as found.

1.4. Results: Preparation of Bisindoles

A preliminary set of experiments was performed using indole, C_5–C_8 and C_{12} cyclic ketones, several common Brønsted acids, and several common protic and aprotic solvents. The initial goals were to find a suitable scope of acids for the study, to choose a good solvent for use with each acid, and to establish approximate boundaries for temperature and concentrations to be used with each acid. Experiments with the expensive cyclic ketones ($C_{9–11}$) would not be performed until results had been obtained from the other ketones, and suitable conditions could be predicted. In the preliminary experiments, TLC, ^{1}H NMR, and MS analyses were performed on neutralized samples taken from the reaction mixtures. Preparative separation of the product mixtures was not performed.

The scope of initially tested acids was acetic, trichloroacetic, trifluoroacetic, boric, phosphoric, hydrochloric, and sulfuric acids. The change in performance between acetic and trichloroacetic acids was small. Trifluoroacetic acid (TFA) was found to be a better intermediate acid to use between acetic and hydrochloric acids. Sulfuric acid gave dark, tarry mixtures under every attempted condition, probably due to oxidative degradation of indole and other reaction components. Toluene-4-sulfonic acid monohydrate (TsOH•H_2O) was used in place of sulfuric acid. The product mixtures that were observed to form from TsOH•H_2O were similar in composition to mixtures obtained from HCl, although TsOH•H_2O generally produced larger amounts of tar. Thus, no further study was performed using trichloroacetic or sulfuric acids. Ethanol performed well as the solvent for most acids. The use of aprotic solvents decreased the reaction rates, and aqueous reactions performed very poorly.

Phosphoric and boric acids were the exceptions to the superior performance of ethanol (Table 4). For these acids, the best results were obtained when multiphasic reactions were performed using an aromatic hydrocarbon as the solvent.

Table 4. The preparation of bisindoles by Method A and Method B.

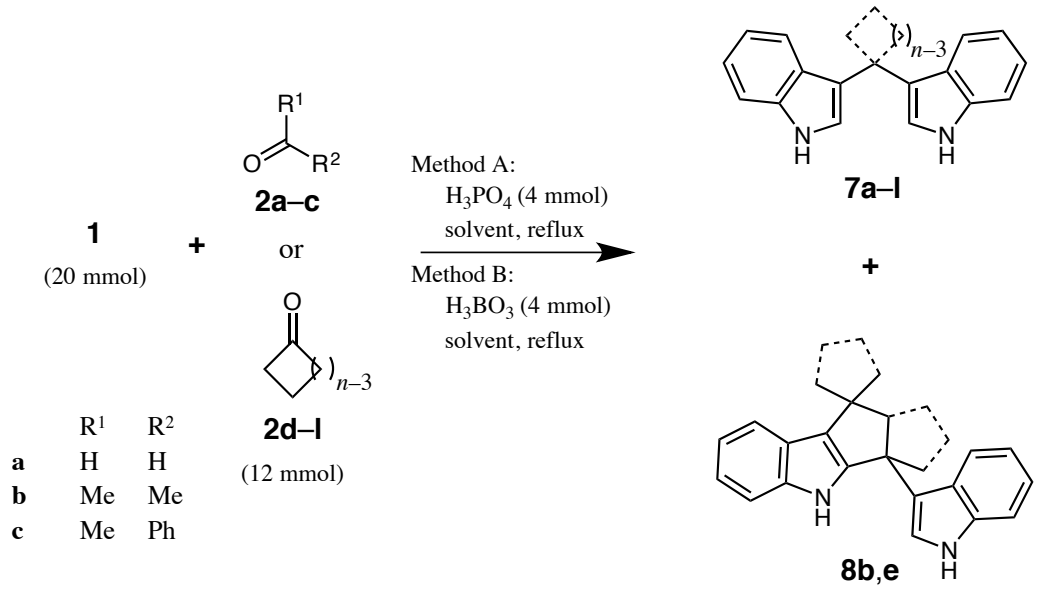

	R1	R2
a	H	H
b	Me	Me
c	Me	Ph

ketone	Method A			Method B		
	condition	product	yield %	condition	product	yield %
formaldehyde (**2a**)	toluene, 1 h	**7a**	27	toluene, 2 h	**7a**	63
acetone (**2b**)	toluene, 4 h	**7b**	79	acetone, 24 h	**7b**	66
acetophenone (**2c**)	xylenes, 6 h	**7c**	(tar)	xylenes, 3 d	**7c**	19
n = 4 (**2d**)	-	**7d**	-	toluene, 24 h	**7d**	2
n = 5 (**2e**)	xylenes, 2 h	**7e**	(tar)	toluene, 5 d	**7e**	29
n = 6 (**2f**)	benzene, 2 h	**7f**	65	toluene, 24 h	**7f**	80
n = 7 (**2g**)	xylenes, 18 h	**7g**	24	xylenes, 3 d	**7g**	21
n = 8 (**2h**)	xylenes, 18 h	**7h**	(tar)	toluene, 2 d	**7h**	(n.r.)
n = 9 (**2i**)	-	**7i**	-	-	**7i**	-
n = 10 (**2j**)	-	**7j**	-	-	**7j**	-
n = 11 (**2k**)	xylenes, 18 h	**7k**	(tar)	toluene, 2 d	**7k**	(n.r.)
n = 12 (**2l**)	xylenes, 18 h	**7l**	3	toluene, 2 d	**7l**	2

The best results from phosphoric acid were obtained using a 20:12:4 stoichiometric ratio of indole:ketone:acid in 1 mL of refluxing solvent. The use of phosphoric acid produced dark tar from all ketones. Tar formation outpaced bisindole formation from all ketones except formaldehyde (**2a**), acetone (**2b**), and cyclohexanone (**2f**). Formaldehyde-derived bisindole **7a** degraded quickly in these conditions. Bisindoles **7b** and **7f** had much longer lifetimes, but acetone-derived 2:2 product **8b** was observed by ^{1}H NMR analysis to form with **7b**. Although phosphoric acid gave the highest yield of **7b**, the formation of tar and **8b** made the separation process cumbersome. Thus, phosphoric acid is not recommended for use as the catalyst for preparing any of the bisindoles in the present study.

For boric acid, the best results were obtained using the same stoichiometry and solvents, except that acetone (**2b**) was used as its own solvent. Whereas the main problem with phosphoric acid was overreaction and tar formation, the main drawback of boric acid was very long reaction times. For most cyclic ketones, the reaction progress was impractically slow. However, the mild nature of boric acid was advantageous for the preparation of bisindole **7e**. With all stronger acids, **7e** was found to react with leftover **2e** to form the corresponding 2:2 product (**8e**).

Acetic acid, the classical catalyst for the preparation of ketone-derived bisindoles, had the best overall performance in the present study (Table 5). Acetic acid was the highest-yielding catalyst for bisindoles **7a**, **7d**, and **7g–i**. Plain acetic acid was effective for ketones **2a–g**. Although TsOH•H_2O was problematic as a stand-alone catalyst, the addition of 20 μmol (0.1 mol %) to an acetic acid mixture promoted the desired reaction between indole (**1**) and ketones **2h–l**, which was otherwise unacceptably slow. For bisindoles **7a**, **7e**, and all TsOH•H_2O-promoted entries (**7h–l**), the yield was limited by loss of material to side reactions, and minimal starting material was leftover. For the remaining bisindoles (**7b–d**, **7f**, and **7g**), the yield was limited by leftover starting material. These reactions could not be easily driven further without the onset of side product formation. Thus, they were stopped after the indicated reaction times, simplifying the purification process. The progress of the reaction between indole and acetone (**2b**) was anomalously slow. This may have been caused by a portion of the acetone (b.p. 56 ºC) being trapped in the vapor phase during the course of refluxing the acetic acid (b.p. 117 ºC). The formation of **7b** was very slow at room temperature.

Table 5. The preparation of bisindoles by Method C.

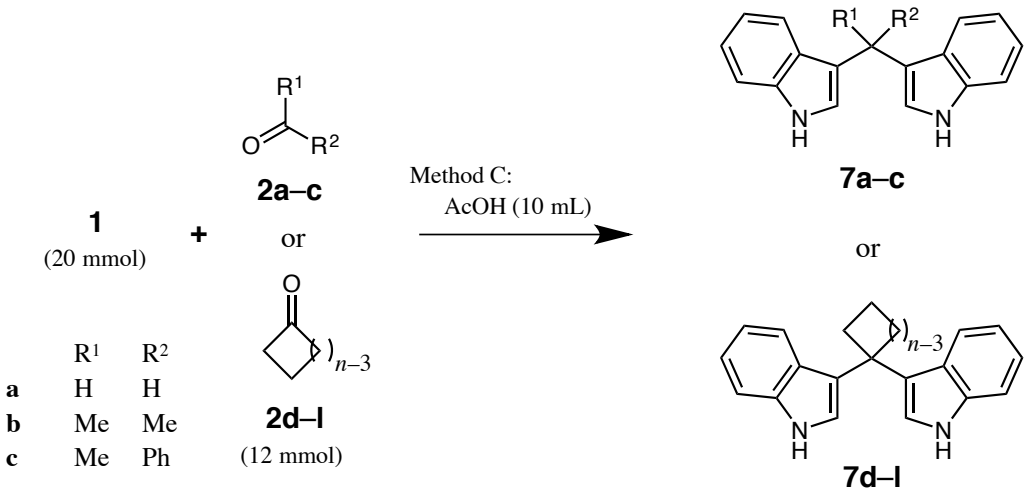

ketone	condition	product	yield %
formaldehyde (**2a**)	rt, 3 d	**7a**	96
acetone (**2b**)	reflux, 5 d	**7b**	72
acetophenone (**2c**)	reflux, 3 d	**7c**	67
n = 4 (**2d**)	60 ºC, 24 h	**7d**	64
n = 5 (**2e**)	reflux, 5 d	**7e**	14
n = 6 (**2f**)	50 ºC, 1.5 d	**7f**	87
n = 7 (**2g**)	reflux, 2 d	**7g**	70
n = 8 (**2h**)	20 μmol TsOH•H_2O, 50 ºC, 5 d	**7h**	39
n = 9 (**2i**)	20 μmol TsOH•H_2O, reflux, 7 d	**7i**	7
n = 10 (**2j**)	20 μmol TsOH•H_2O, reflux, 7 d	**7j**	4
n = 11 (**2k**)	20 μmol TsOH•H_2O, reflux, 3 d	**7k**	8
n = 12 (**2l**)	20 μmol TsOH•H_2O, reflux, 2 d	**7l**	30

As expected, trifluoroacetic acid (TFA) had an increased tendency to form side products. For ketones **2a–g**, dilution of the reaction mixture with a solvent was required to prevent excessive formation of tar (Table 6), although side product formation remained prominent. Cyclooctanone (**2h**) was a borderline case. The use of added solvent slowed the reaction progress, but a lack of solvent produced a complex reaction mixture that was not easily separated. The yield of cyclononanone-derived **7i** was nearly identical from acetic acid or TFA, although the mixture resulting from acetic acid was easier to process. The remaining bisindoles (**7j–l**) were best prepared using TFA, with no added solvent. The reaction times were long (3 to 14 d), and the yields were modest (11 to 37%), but no better conditions were found.

Table 6. The preparation of bisindoles by Method D.

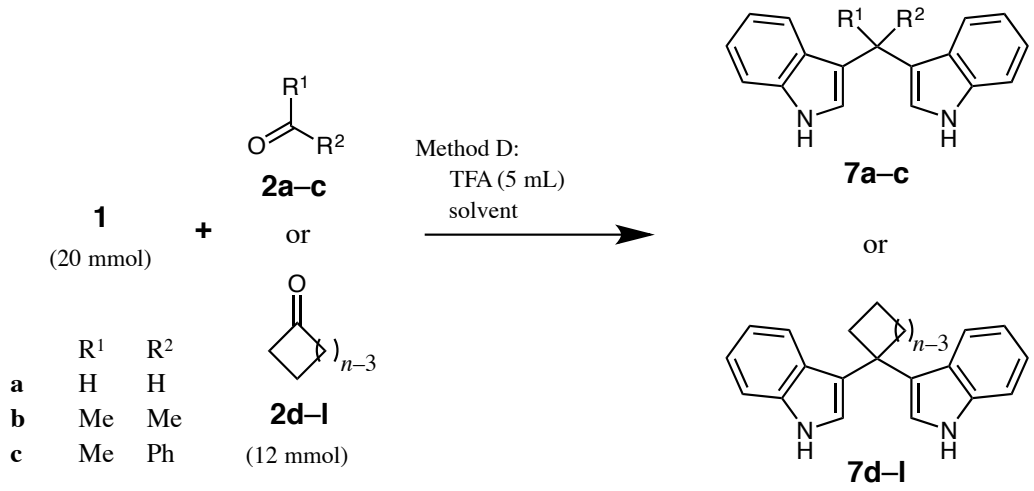

ketone	solvent	condition	product	yield %
formaldehyde (**2a**)	EtOH (5 mL)	reflux, 1 h	**7a**	20
acetone (**2b**)	acetone (10 mL)	rt, 6 h	**7b**	76
acetophenone (**2c**)	EtOH (5 mL)	reflux, 3 d	**7c**	72
n = 4 (**2d**)	EtOH (5 mL)	reflux, 18 h	**7d**	35
n = 5 (**2e**)	EtOH (5 mL)	reflux, 24 h	**7e**	25
n = 6 (**2f**)	EtOH (5 mL)	50 ºC, 1.5 d	**7f**	59
n = 7 (**2g**)	EtOH (5 mL)	reflux, 5 d	**7g**	33
n = 8 (**2h**)	EtOH (5 mL)	reflux, 5 d	**7h**	10
n = 9 (**2i**)	-	reflux, 14 d	**7i**	6
n = 10 (**2j**)	-	reflux, 14 d	**7j**	12
n = 11 (**2k**)	-	reflux, 14 d	**7k**	11
n = 12 (**2l**)	-	reflux, 3 d	**7l**	37

Lastly, attempts were made to prepare bisindoles **7a–l** using hydrochloric acid (Table 7). Each experiment was started in an ice bath, and the temperature was increased slowly until product formation was observed by TLC analysis. With formaldehyde, the reaction mixture rapidly became complex, even when additional solvent was used. Ketones **2b–2f** performed fairly well, although the formation of side products was observed. This method worked exceptionally well with cyclohexanone (**2f**), because the formation of bisindole **7f** was exceptionally rapid. Furthermore, the cyclohexanone-derived 2:2 product precipitated, whereas the side products formed from other ketones remained in solution. At room temperature, the formation of bisindole **7g** was clean but very slow. Heating the reaction mixture gave side products. For all larger ketones, the use of hydrocloric acid gave no condensation products at or below room temperature, and raising the temperature gave tarry mixtures. Experiments were not performed with cyclononanone or cyclodecanone because of the poor results obtained from the less expensive large ketones.

Table 7. The preparation of bisindoles by Method E.

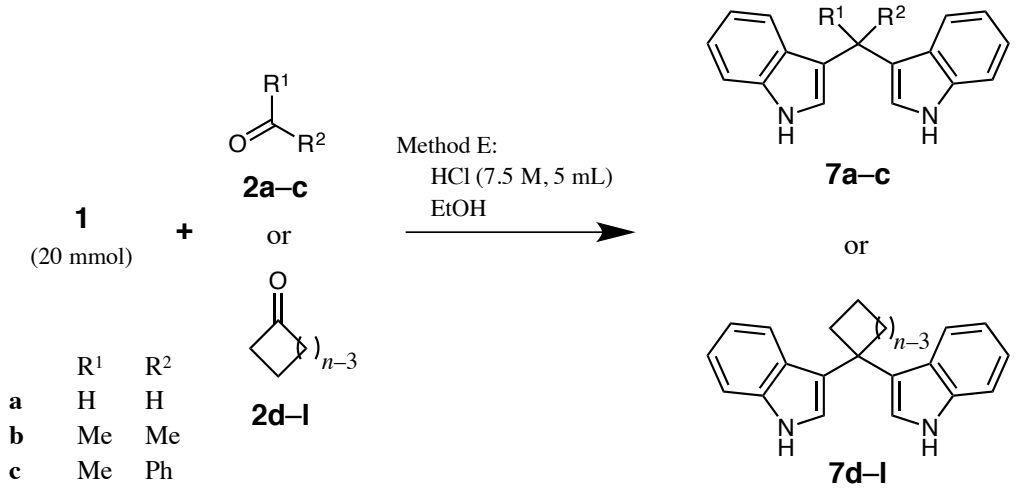

	R^1	R^2
a	H	H
b	Me	Me
c	Me	Ph

ketone	ketone mmol	EtOH mL	condition	product	yield %
formaldehyde (**2a**)	10	100	0 ºC, 1 h	**7a**	(tar)
acetone (**2b**)	10	60	0 ºC, 2 d	**7b**	60
acetophenone (**2c**)	10	60	rt, 2 d	**7c**	50
n = 4 (**2d**)	10	25	0 ºC, 4 h	**7d**	35
n = 5 (**2e**)	30	25	rt, 18 h	**7e**	17
n = 6 (**2f**)	10	25	0 ºC, 10 min	**7f**	98
n = 7 (**2g**)	12	0	rt, 8 d	**7g**	46
n = 8 (**2h**)	12	25	0 to 50 ºC, 2 d	**7h**	(tar)
n = 9 (**2i**)	-	-	-	**7i**	-
n = 10 (**2j**)	-	-	-	**7j**	-
n = 11 (**2k**)	12	25	0 to 50 ºC, 2 d	**7k**	(tar)
n = 12 (**2l**)	12	25	0 to 50 ºC, 2 d	**7l**	(tar)

With TLC analysis on the reaction mixtures, the spot arising from the bisindole is usually immediately below indole on the TLC plate. The retention factors (R_f) follow a trend of increasing as the size of the ketones increases (Table 8). Conversely, leftover ketone tends to elute from a column more slowly as its molecular weight increases. Thus, the R_f values of leftover indole and ketone, and the bisindole, tend to squeeze together as larger ketones are used, rendering the chromatographic separations increasingly challenging. Bisindoles **7a**–**g** are fairly easy to separate from their respective reaction components. Bisindoles **7h**–**l** are much more difficult to resolve. Bisindole **7l** will precipitate over the course of several days if an indole- or ketone-contaminated column fraction is allowed to slowly evaporate. Unfortunately, this feature is unique to **7l**. Bisindoles **7h**–**k** were not separable from leftover indole and ketone by fractional crystallization.

Table 8. The R_f values, melting points, air sensitivities, and physical appearances of bisindoles **7a–l**.

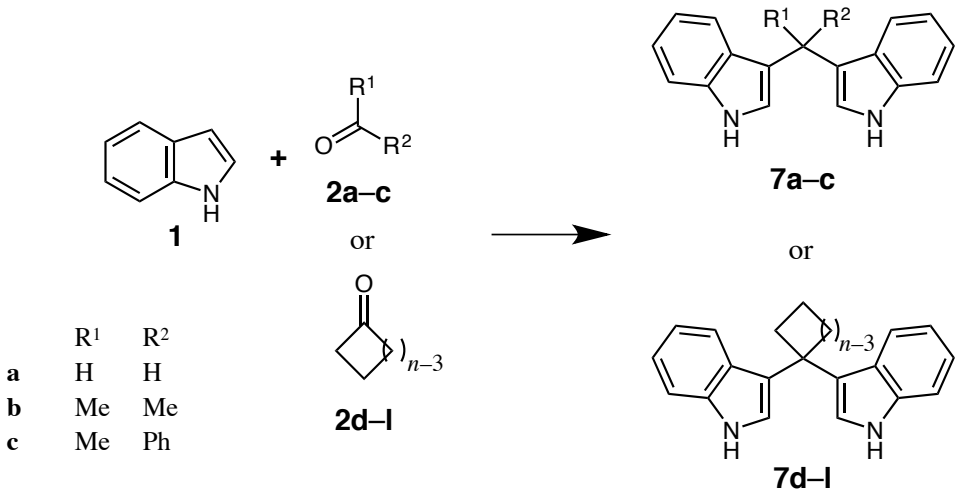

	R^1	R^2
a	H	H
b	Me	Me
c	Me	Ph

compound	ring size *n*	R_f[a]	m.p. °C	air sensitivity	appearance
1	-	0.47	49–52	low	flakes
7a	-	0.33	162–165	low	powder
7b	-	0.38	156–157	-	powder
7c	-	0.37	153–156	-	powder
7d	4	0.37	101–107	high	glassy
7e	5	0.38	164–167	-	powder
7f	6	0.39	164–168	-	crystals
7g	7	0.40	176–178	-	powder
7h	8	0.42	190–192	-	powder
7i	9	0.42	82–83	high	glassy
7j	10	0.42	190–191	low	powder
7k	11	0.45	197–198	-	powder
7l	12	0.46	210–213	-	crystals

[a]In 1:2 EtOAc:hexane on SiO_2.

The melting points of bisindoles **7d–l** tend to increase with increasing ring size. The exception is **7i**, which was not purified above 77 mass %. In spite of its low purity and depressed melting point, this sample of **7i** changed from a glassy solid to an oil over a narrow temperature range. Bisindole **7d** was also obtained as a glassy solid, and had a lower melting point than might be expected, based on the other bisindoles. ^{1}H NMR analysis showed that this sample contained roughly 1 mass% DCM, which was not removable by solvent-assisted vacuum drying. In addition to being glassy, bisindoles **7d** and **7i** were air-sensitive. If samples were exposed to air overnight, their color changed from white or beige to brown. Bisindoles **7a** and **7j** were slightly air-sensitive. Samples darkened over the course of several weeks. The air sensitivity of **7a** is justified by its ability to lose hydride to produce a conjugated system. Ketone-derived bisindoles cannot undergo this transformation. Instead, it is possible that the bisindoles with ring sizes 4, 9, and 10 do not pack well in the solid phase, allowing a high effective surface area to be exposed to molecular oxygen. Poor molecular packing would also explain the difficulty of solvent removal. The remaining bisindoles were stable white powders or colorless crystals.

1.5. Results: Preparation of 2:2 and Related Products

1.5.1. Preliminary Work

When performing ^{1}H NMR analysis on the bisindole reaction mixtures, several signals were observed in all of the experiments that lasted longer than 24 hours and used TFA or hydrochloric acid. To simplify the search for 2:2 condensation products, the compounds that were producing these NMR signals were characterized. Initially, it seemed likely that these compounds were indole oligomers, because the NMR signals did not change with different ketones. Indole can dimerize and trimerize in the presence of acid, and the most common dimer and trimer isomers are **4** [62] and **5** [63], respectively. Thus, compounds **4** and **5** were prepared according to the literature (Scheme 28). NMR and MS analyses confirmed that these were the two compounds that formed during the bisindole experiments.

Scheme 28. The preparation of indole dimer (**4**) and trimer (**5**).

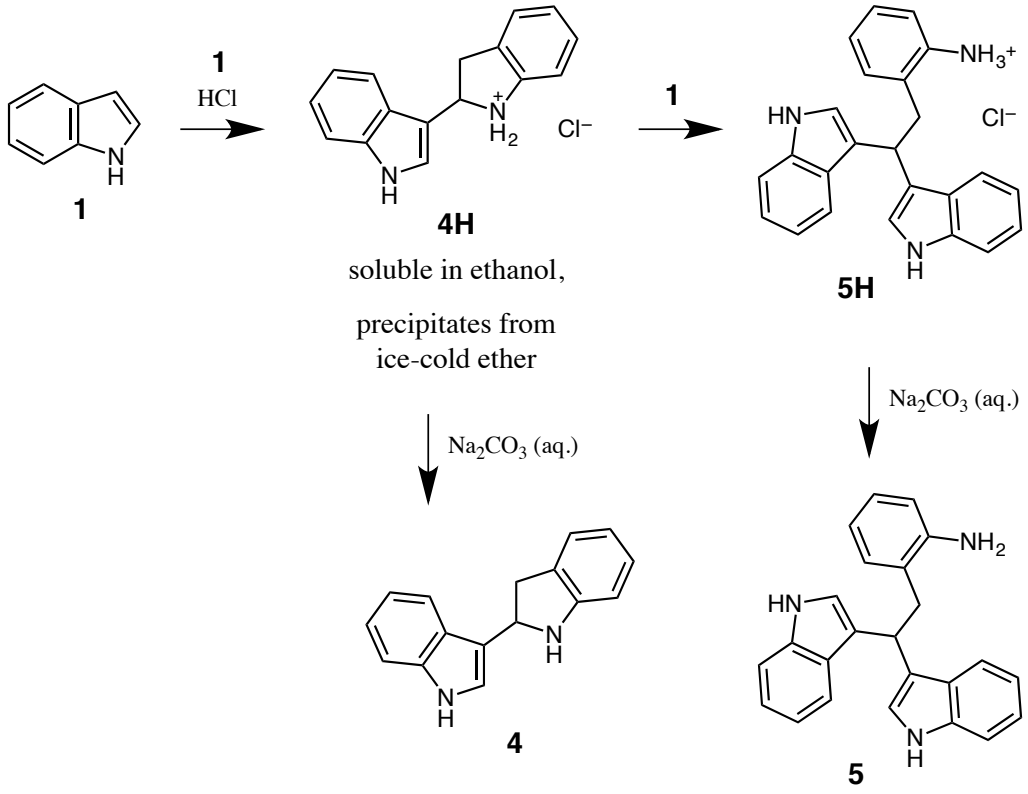

Blank reactions were then performed, in which indole (**1**) was exposed to TFA or hydrochloric acid in the absence of a ketone. This was done to assess the transient behavior of indole in experiments performed according to Method D or E. These reactions gave mixtures of **1**, **4**, and **5** in roughly a 2:1:2 molar ratio within 48 hours, although the reaction rates and molar ratios varied between batches. Salt **5H** was obtained as a white precipitate from some reaction mixtures (blank or regular experiments) that were not yet neutralized. Salt **4H** usually does not precipitate from protic solvents, but it is easily obtained as a precipitate from ether or benzene [62]. Thus, this synthetic sequence will stop at **4H** if the oligomerization solvent is ice-cold ether, and it will proceed to **5H** if the solvent is ethanol.

Now that the NMR, MS, and TLC signals were known for indole (**1**), dimer **4**, trimer **5**, and bisindoles **7d–l**, a search for 2:2 or related products could be performed more efficiently. In order to decide which ketones to try first, the bisindole yield data were reviewed, along with the minor NMR signals observed during the course of those experiments. For 2:2 and related reactions, the cyclic ketones were explored in the following order, by ring size: n = 6, 5, 4, 7, 12, 8, and then 11. This is roughly the order, from mildest to harshest, of the reaction conditions that were required to produce the respective bisindoles. No further study was done using cyclononanone or cyclodecanone because of their high costs, low bisindole yields, complex product mixtures, and time constraints.

1.5.2. Cyclohexanone

During the course of the present study, Guzei, *et al*. published the crystal structure of **9f**, although no other characterization data were presented [41]. They reported that acetonitrile performed well as the solvent. In the present work, both TFA and hydrochloric acid were used, and ethanol, acetonitrile, and cyclohexanone were tried as solvents. The reaction temperature was varied from 0 to 82 ºC, and various concentrations were used, in the hope of finding other condensation products. The best results were obtained from hydrochloric acid in refluxing acetonitrile (Scheme 29). No products were observed other than dimer **4**, trimer **5**, bisindole **7f**, and **9f**.

Scheme 29. The preparation of cyclohexanone-derived 2:2 product **9f**.

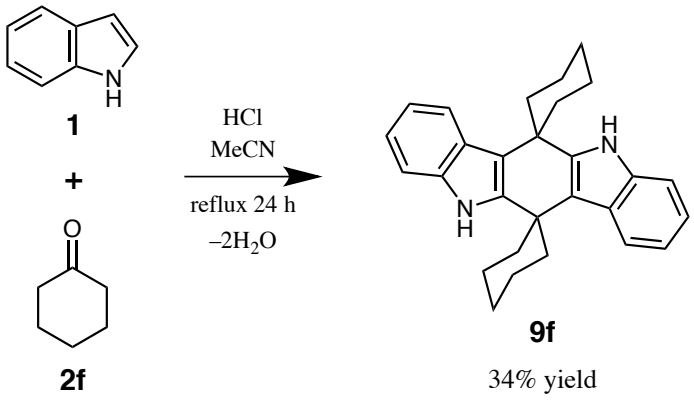

1.5.3. Cyclopentanone

A similar scope of reaction conditions was explored with cyclopentanone (**2e**). As with **2f**, **2e** only gave one 2:2 condensation product, but it was a different isomer (**8e**, Scheme 30). It was surprising to find that there was no overlap in the type of 2:2 condensation products that were obtained from **2e** and **2f**, given that these two ketones only differ by one methylene unit. The best results were obtained from hydrochloric acid, with excess cyclopentanone as the solvent.

Scheme 30. The preparation of cyclopentanone-derived 2:2 product **8e**.

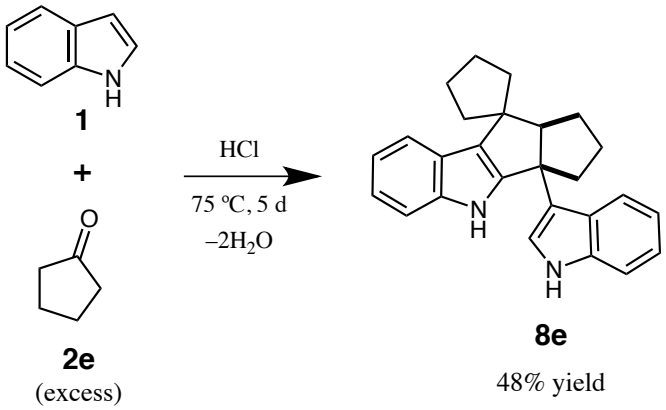

To confirm the molecular structure of **8e**, X-ray crystallographic analysis was performed on a crystal that was grown in *p*-xylene (Fig. 6) [64]. A previous batch of crystals was grown from toluene, which was on inversion centers and disordered into two components. Replacing toluene with *p*-xylene, which has inversion symmetry, removed disorder arising from the solvent, although the C16–C19 ring was still disordered into two envelope conformations.

Fig 6. An ORTEP drawing of crystalline **8e**, with crystallographic atom labeling, viewed along {–10a, b, –2c}. This crystal was a *p*-xylene hemisolvate. Only the major conformer is shown.

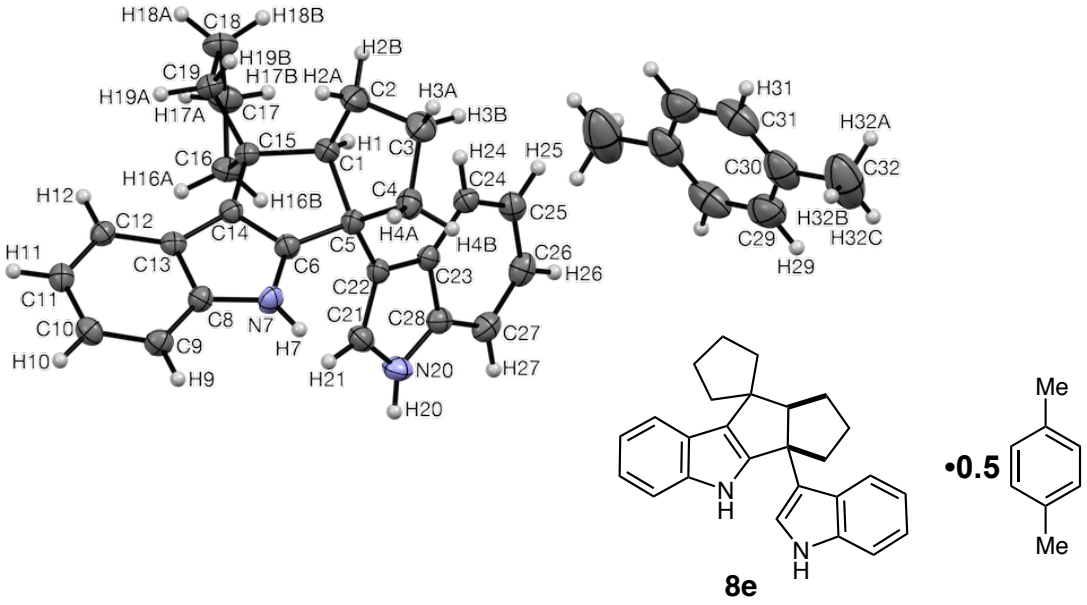

The NMR analysis of **8e** was a particularly instructive exercise. The NMR experiments included ^{1}H, ^{13}C, ^{1}H-COSY, ^{1}H-NOE, ^{1}H/^{13}C DEPT-90 and DEPT-135, ^{1}H/^{13}C-HMQC, and ^{1}H/^{13}C-HMBC [65]. Collectively, these NMR signals allowed every interatomic connection except one to be made. The final connection, C17–C18, was made by the process of elimination. This exercise has been used as an examination question in a graduate-level course at the University of Minnesota. The students were given a general description of the chemical reaction (Scheme 31), and the MS and IR results. The reader may use the spectra (App. I, p 339) and experimental data (p 193) for similar purposes.

1.5.4. Cyclobutanone

A similar scope of reaction conditions was used with cyclobutanone (**2d**). Once again, only one new product was observed (**8d**, Scheme 31). The best results were obtained from hydrochloric acid in ethanol at room temperature. As with bisindole **7d**, product **8d** was obtained as a glassy solid, was moderately air-sensitive, and could not be dried using solvent-assisted vacuum drying. The structure of product **8d** was determined using NMR analysis. Crystallographic analysis was not performed, because of the high similarity of the NMR signals of **8d** and **8e**. Furthermore, **8d** has two fewer methylene units, so the alkyl region of the various NMR spectra was easier to interpret.

Scheme 31. The preparation of cyclobutanone-derived 2:2 product **8d**.

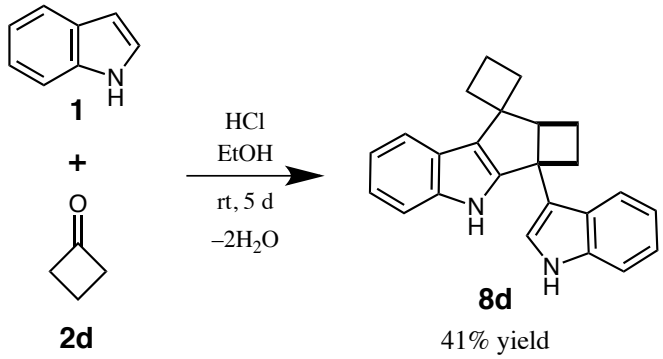

1.5.5. Cycloheptanone

Exposure of indole (**1**) and cycloheptanone (**2g**) to TFA gave indolo[2,3-*a*]carbazole derivative **10g** as the only condensation-derived product beside bisindole **7g** (Scheme 32). Most of the indole was converted into bisindole **7g** and a tarry mixture. The empirical formula of **10g** is $C_{23}H_{20}N_2$, which corresponds to 2:1 ($–H_2O$, $–H_2$) condensation. Based on the results obtained from the remaining ketones (n = 12, 8, and 11), the loss of hydrogen is probably affected by autoxidation, followed by an elimination of hydrogen peroxide. It is interesting that the two indole units are directly connected. This feature was not previously reported in cyclizative condensation products prepared from indole and a ketone in one pot.

Scheme 32. The preparation of cycloheptanone-derived indolocarbazole **10g**.

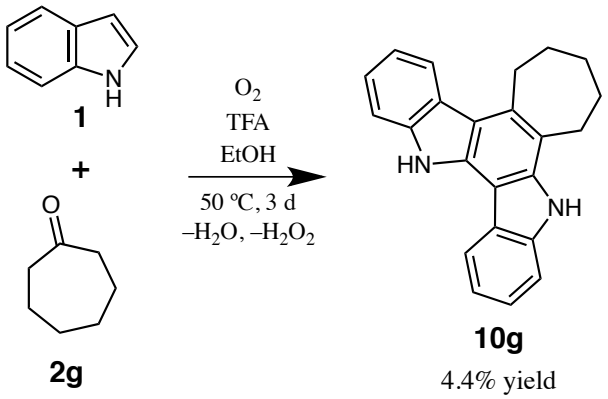

1.5.6. Cyclododecanone

Cyclododecanone (**2l**) was the first ketone that gave multiple condensation products in addition to the bisindole (**7l**). Indolocarbazole **10l** was obtained, and many of its properties were very similar to those of cycloheptanone-derived analog **10g**. Compound **10l** had a high melting point, very low solubility in most common solvents, and could not be dried by solvent-assisted vacuum drying. Other than removal of water and residual solvents, **10l** was easy to purify by trituration. The highest yield of **10l** was obtained from TFA (Scheme 33).

Scheme 33. The preparation of cyclododecanone-derived indolocarbazole **10l**.

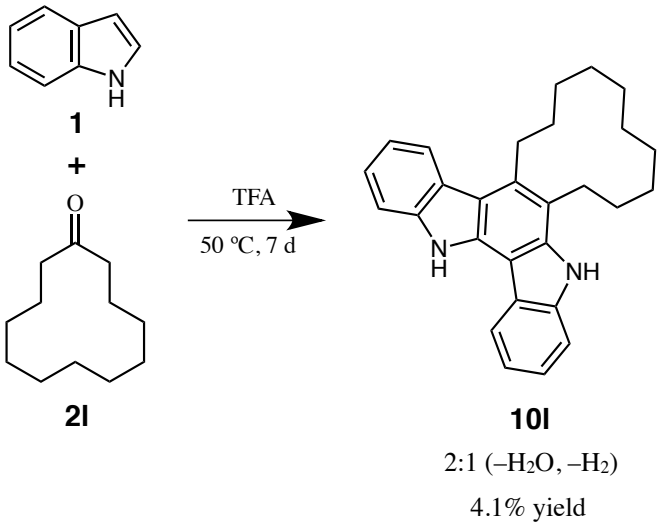

The remaining three products had higher solubilities and similar R_f values to indole and **2l**. Leftover **2l** was difficult to remove. Samples of the other products were enriched as much as possible by chromatography and trituration, but the major component of the product fractions was still **2l**. Nonetheless, two of the three products were identified by NMR analysis. Because of the high abundance of **2l** in the samples, MS and IR analyses gave very little meaningful data. The highest yields of products **13l**, **57l**, and **14** were obtained from acetic acid, with 5 mol% of added TsOH•H_2O (Scheme 34).

Scheme 34. The preparation of cyclododecanone-derived products **13l**, **57l**, and **14**.

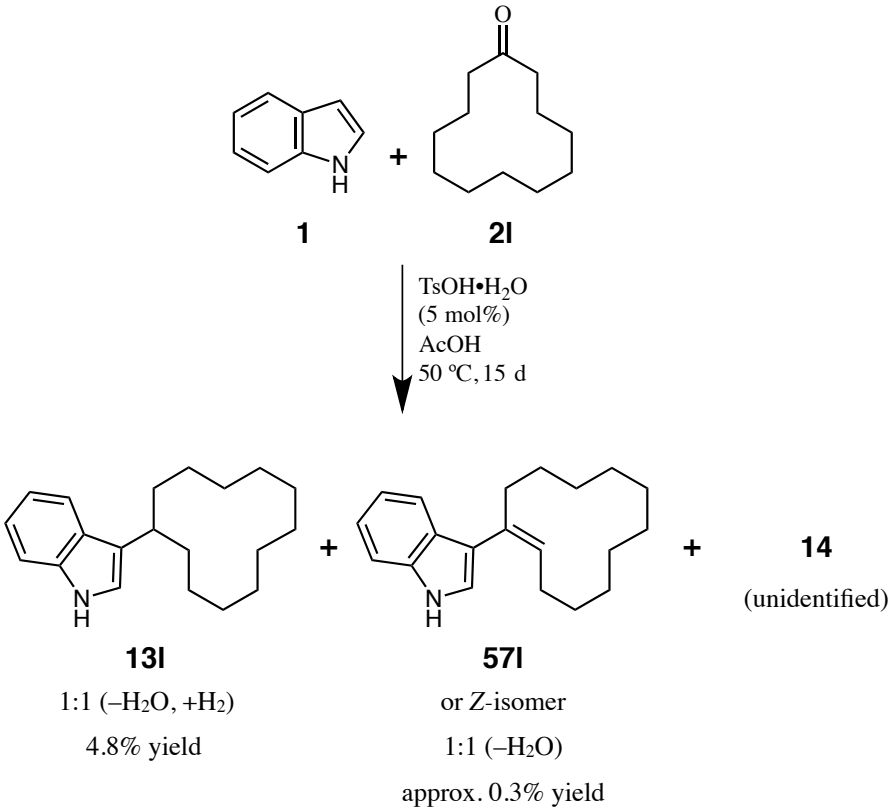

Compound **13l** is the result of a 1:1 ($-H_2O$, $+H_2$) condensation. NMR signals were observed from this sample that are consistent with **57l**, the result of a 1:1 ($-H_2O$) condensation. Because **57l** is known to be a precursor to almost all known types of indole-ketone condensation products, it is likely that **57l** is also the precursor to **13l**. Because the formation of **10l** requires an oxidation, and the conversion of **57l** into **13l** requires a reduction, it is possible that a hydride transfer is taking place during the course of this reaction.

The last product that was observed from this reaction mixture (**14**) was not identified. Aromatic ^{1}H and ^{13}C NMR signals were observed that are consistent with one 2,3-disubstituted indole unit, or possibly two that are chemically equivalent. This could not be reconciled with the alkyl NMR signals, which were consistent with two non-equivalent twelve-membered rings, or a similar combination of hydrocarbon components. There were two alkyl quaternary carbons, eleven alkyl CH_2 units, and no alkyl CH units. It is possible that a fourteenth carbon signal was present, and it was obscured by signals from **2l**. The number of signals present is consistent with symmetrical fusion of each alkyl ring. The three most downfield carbon signals are a CH_2 unit at 60 ppm, and two quaternary carbons at 49 and 47 ppm. HMBC analysis showed that the two most downfield alkyl protons (doublets, one proton each, per indolyl proton) are in close proximity to both the indole-2- and 3-positions, although it is not clear whether these two protons are geminal. No molecular structure has been devised that can simultaneously account for all of these NMR results. Several of the structures considered for **14** are shown in Fig. 7.

Fig. 7. Four of the structures considered for product **14**. Based on the NMR data, none of these structures is correct.

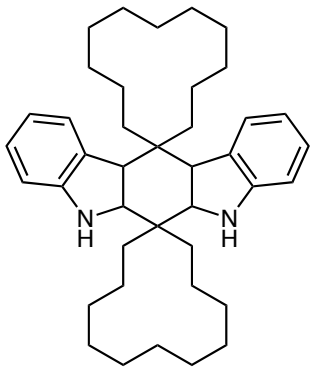

102

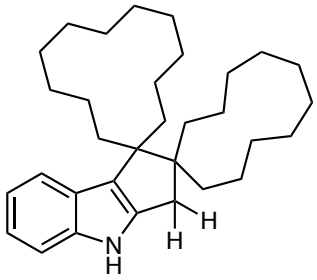

103

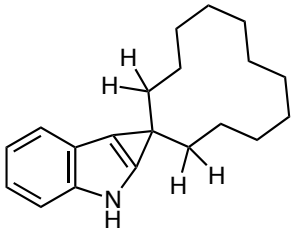

104

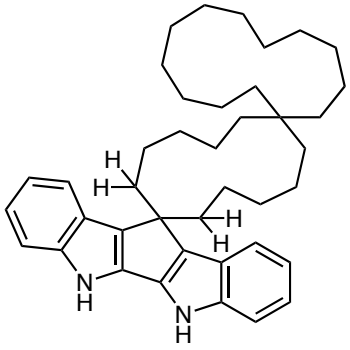

105

Many other structures were considered, regardless of their mechanistic implications. These four (**102**–**105**) illustrate most of the problems encountered when reviewing the NMR data. Structure **102** has too many protons that are vicinal to the bridgeheads, and they would have the wrong splitting pattern and HMBC crosspeaks. Structure **103** has the right number of every type of atoms and the right HMBC crosspeaks. The only discrepancy is that the methylene group indicated in **103** would have equivalent protons, whereas the two protons in **14** that correlate with the indolyl 2- and 3-carbons are inequivalent. Structure **104** has too many bridgehead-vicinal protons, not enough quaternary carbons, and not enough carbon signals. Structure **105** has the right number of each type of atom, but would have the wrong HMBC crosspeaks and alkyl splitting patterns.

Even though the identification of **14** could provide useful insight into the chemistry of these condensation reactions, no further analysis was performed due to time limitations. Structure **103** illustrates the most perplexing paradox with the structure of **14**: The indole unit(s) and rings

should be symmetrically connected, but one pair of alkyl protons should be inequivalent. Because of the difficulty of reconciling a structure with these aspects of the NMR data, it is possible that one or more spurious NMR signals was used. It is essential to prepare a sample of **14** in higher purity if the structure is to be determined.

1.5.7. Cyclooctanone

Cyclooctanone (**2h**) gave the most surprising and insightful results of any cyclic ketone. Diazepine derivative **12h** (Scheme 35) was obtained from the separation of the product mixture of one of the batches of bisindole **7h** from TFA in ethanol. Numerous attempts were made to reproduce this result, but all subsequent one-pot preparations of **12h** were unsuccessful. The empirical formula of **12h** is $C_{26}H_{26}N_2$, which would hypothetically come from 2:1 ($-H_2O$, $+C_2$) condensation. Direct transformations of this type are impractical, so is was postulated that ethanol was the source of the two added carbon atoms. If 2:1:1 ($-2H_2O$) condensation were to take place between **1**, **2h**, and ethanol, the result would be $C_{26}H_{30}N_2$. Because autoxidation-derived products had already been observed in this study, it seemed reasonable that the preparation of diazepine **12h** followed a 2:1:1 ($-2H_2O$, $-2H_2$) pathway.

Scheme 35. The one-pot preparation of diazepine derivative **12h** and biindolyl **6** from cyclooctanone.

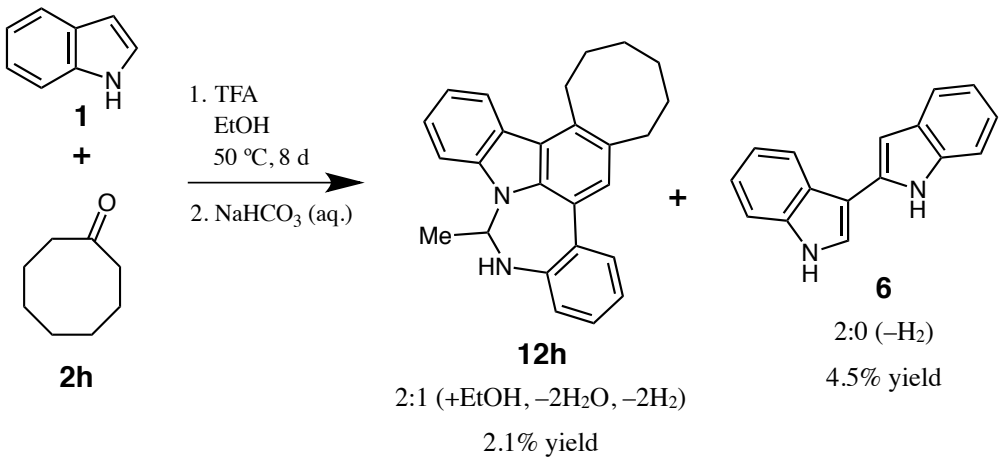

Further analysis of the product mixture revealed that 2,3'-biindolyl (**6**) also formed. The presence of **6** explained many of the mechanistic aspects of the formation of products **10**–**13** that were obtained from cycloheptanone and larger cyclic ketones (mechanisms are discussed in § 1.5.10). This finding also provided an explanation of redox reactions that were taking place. Biindolyl **6** can be prepared by the dehydrogenation of indole dimer **4** (Scheme 36), a transformation driven by the aromatization of the indoline system [60]. In the present study, **6** was prepared from **4** in 70% yield. Because **4** dehydrogenates so readily, **4** is probably the *in situ* source of hydride for the formation of reduction product **13l**.

Scheme 36. The preparation of biindolyl **6** from dimer **4** *via* dehydrogenation.

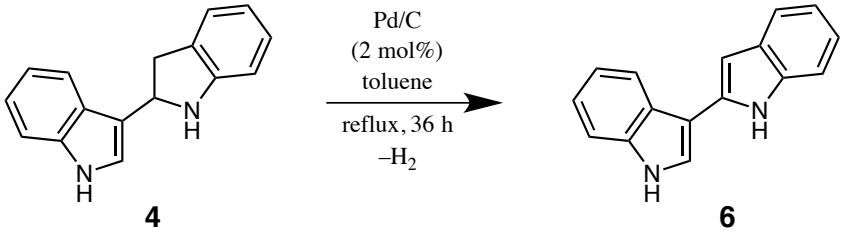

No palladium was present during the indole-ketone condensation reactions. Instead, dimer **4** was oxidized by air, producing **6** and a molecule of H_2O_2, which then oxidized ethanol to acetaldehyde. Aniline **11h** formed by a cyclizative condensation of **2h** with **6**, followed by opening of the 3-pyrrolyl ring (Scheme 37). A second cyclizative condensation, between

carbazolylaniline **11h** and acetaldehyde, gave **12h**. Although **11h** was not observed in any of the one-pot trials, this is the proposed pathway by which the first one-pot batch of **12h** formed. 1,1-Diethoxyethane (**106**) was the acetaldehyde synthon in the second step of the two-step preparation. The use of cesium carbonate gave a cleaner reaction mixture that was easier to separate, and a slightly higher yield of **12h**. The use of TFA demonstrates the plausibility of the proposed pathway for the formation of **12h** by the one-pot method, as each step was catalyzed by a strong acid.

Scheme 37. The two-step preparation of diazepine **12h** *via* carbazolylaniline **11h**.

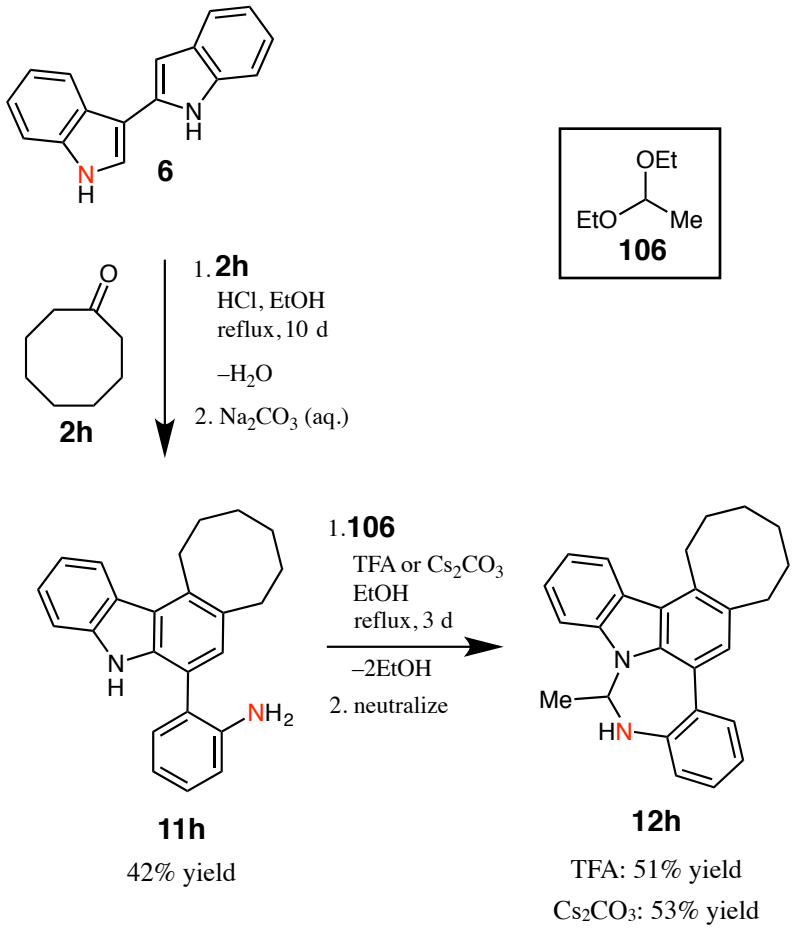

The structure of **12h** was initially solved by NMR analysis because crystals were difficult to obtain. A $^{1}H/^{15}N$ HMBC experiment was needed to determine the connectivity of the nitrogen atoms. After several months of trying different conditions, suitable crystals were prepared, and the structure of **12h** was confirmed by X-ray diffraction analysis (Fig. 8). The structure of **11h** was also confirmed by X-ray diffraction analysis (Fig. 9).

Fig 8. An ORTEP drawing of crystalline **12h**, with crystallographic atom labeling of skeletal atoms, viewed along {4a, –b, 3c}.

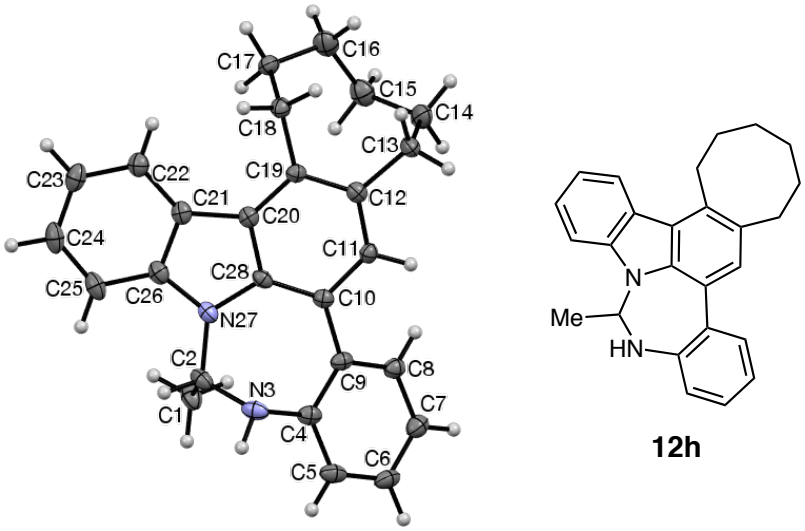

12h

Fig 9. An ORTEP drawing of crystalline **11h**, with crystallographic atom labeling of skeletal atoms, viewed along {a, 4b, –c}.

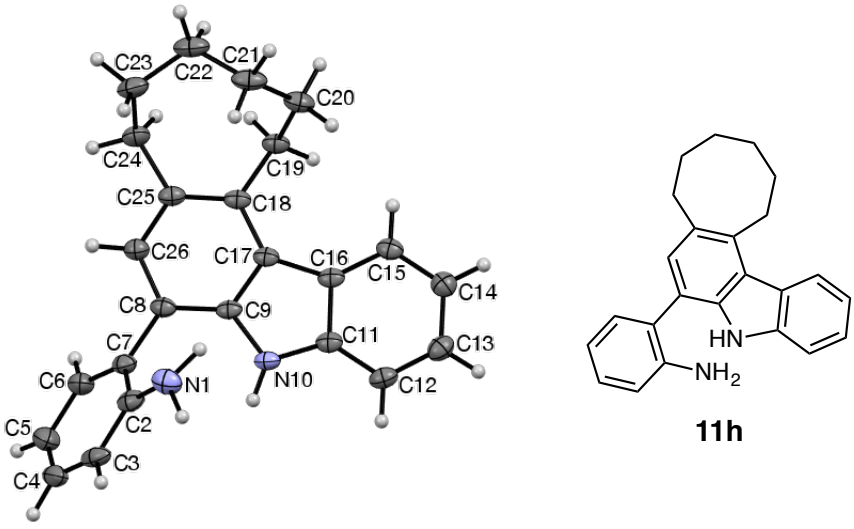

11h

1.5.8. Cycloundecanone

Following the diverse results obtained from cyclododecanone and cyclooctanone, the peformance of cycloundecanone (**2k**) was anticlimactic. Aside from bisindole **7k**, the only condensation products obtained were 3-cycloundecylindole (**13k**) and biindolyl (**6**, Scheme 38). The highest yields were obtained when TFA was the catalyst and the solvent.

Scheme 38. The preparation of cycloundecanone-derived condensation product **13k**. Biindolyl **6** was also obtained.

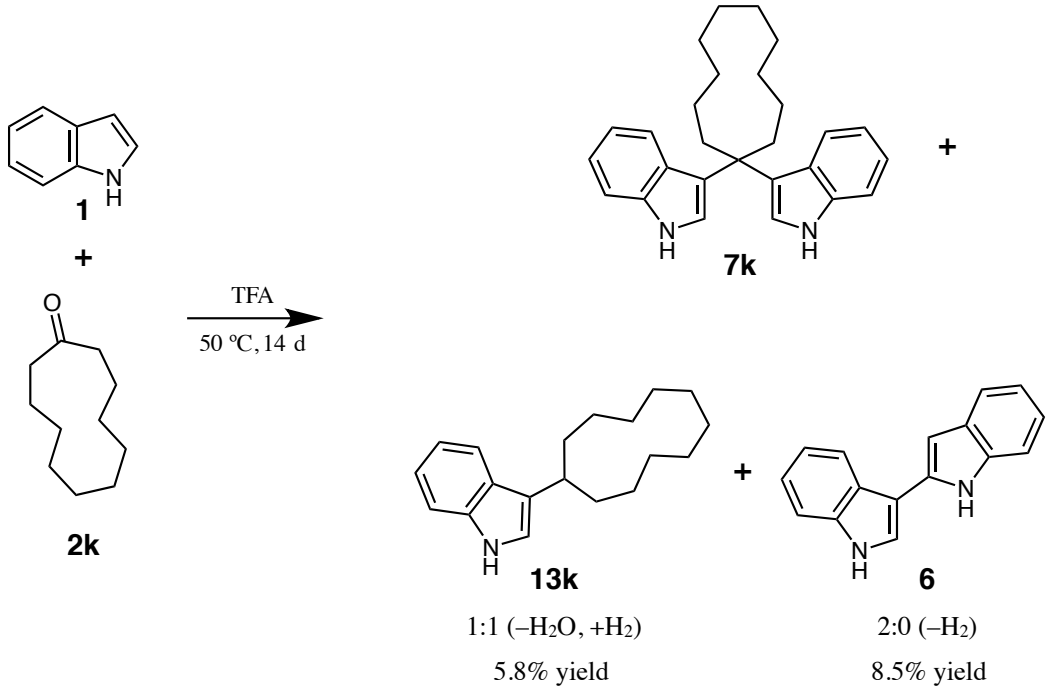

1.5.9. Other Experiments

During the course of studies with indole and cyclic ketones in Diels-Alder reactions [47], minimal solvent was used and the reaction temperatures were steadily increased until product formation was observed. This strategy gave products within several hours, which would be preferred to the long reaction times that were required with Methods D and E. In the present study, these experiments were largely duplicated, in the absence of dienophiles. It was also hoped that different products might be obtained than had been found using Methods D and E. Instead, no new products were observed, and the yields were considerably lower. Most of the indole was converted into tarry mixtures.

Experiments were also performed in which bisindoles **7d–g** were used as the starting material, and they were exposed to additional ketone in the presence of acid. The same products were observed as had been obtained using indole as the starting material.

Attempts to form cross-condensation products were unsuccessful (Scheme 39). This strategy was reported by Noland & Venkiteswaran with methyl ketones [21]. In the present study, sticky mixtures were obtained, and no novel products were identified. This result is unfortunate, because a wide scope of interesting products would be accessible. It is possible that this method would work for one or more combinations of ketones **2a–l** and bisindoles **7a–l**, but no additional attempts were made.

Scheme 39. The attempted cross-condensation of ketones with bisindoles.

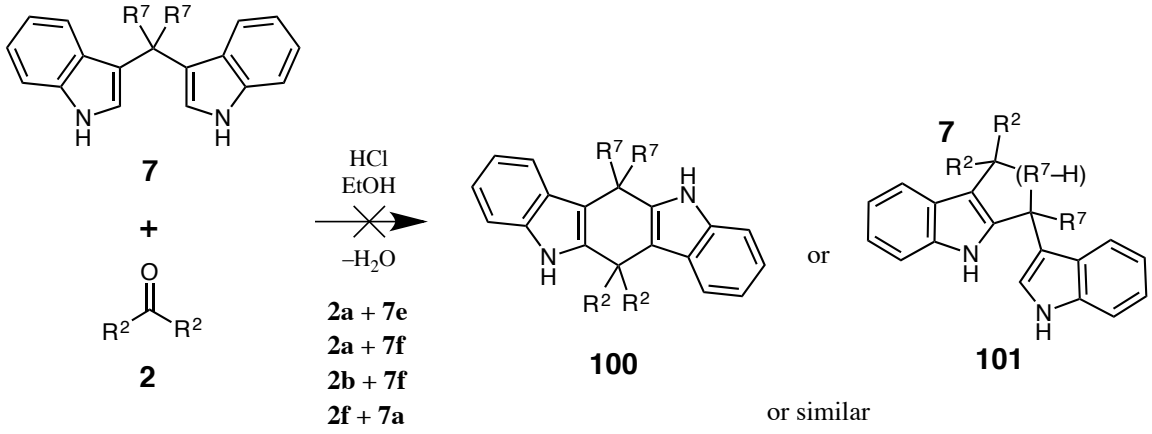

	R
a	H
b	Me
e	–[CH$_2$]$_4$–
f	–[CH$_2$]$_5$–

1.5.10. Proposed Mechanisms

An overall mechanism can be proposed based on the findings in the present work and the literature. The pathways discussed in this section were postulated to be simultaneously available during the one-pot reactions, based on the data discussed in §§ 1.1–1.3.9. The formation of 1:1, 2:1, and 2:2 condensation products is summarized in Scheme 40. The formation of bisindoles (**7**) was outlined in Scheme 12 (p 12). The formation of 2:2 products of type **8** was outlined in Scheme 15 (p 15). Detailed mechanisms for formation of these three products are given by Bergman *et al*. [35]. The formation of type **9** products was given in Scheme 16 (p 17).

Scheme 40. Summary of the formation of products **7**, **8**, **9f**, and **67**.

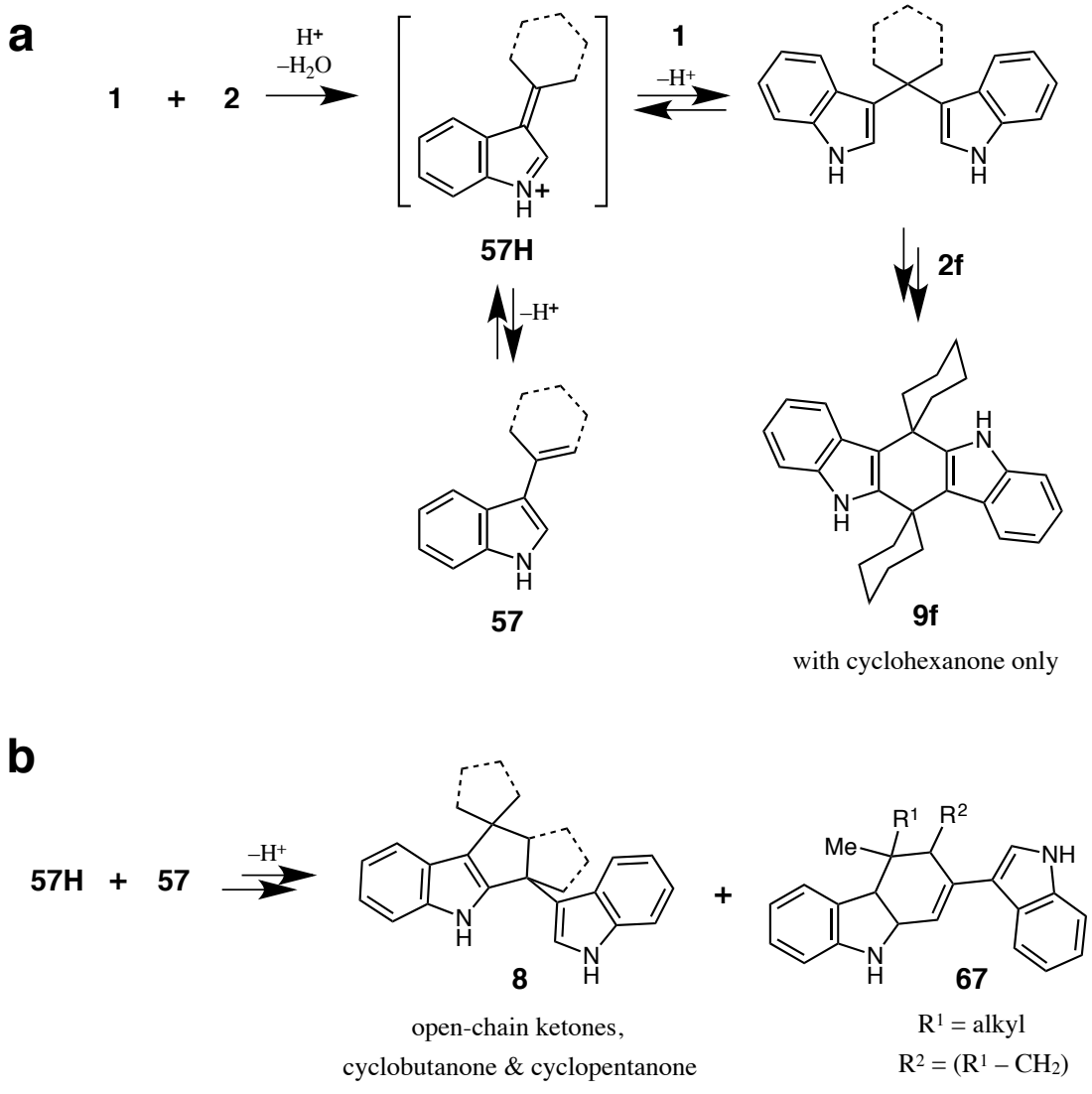

Among cyclic ketones, condensation of ketone (**2**) with bisindole (**7**) is only favored for cyclohexanone (**2f**), for reasons that are not yet understood. Cyclizative addition of **57** to **57H** is favored for cyclobutanone (**2d**) and cyclopentanone (**2e**). For these three ketones (**2d–f**), formation of 2:2 condensation products happens quickly enough that indole dimer (**4**) does not have enough time to appreciably oxidize to biindolyl (**6**, Scheme 41).

Scheme 41. (a) The oligomerization of indole; (b) the autoxidation of dimer **4** to biindolyl **6**.

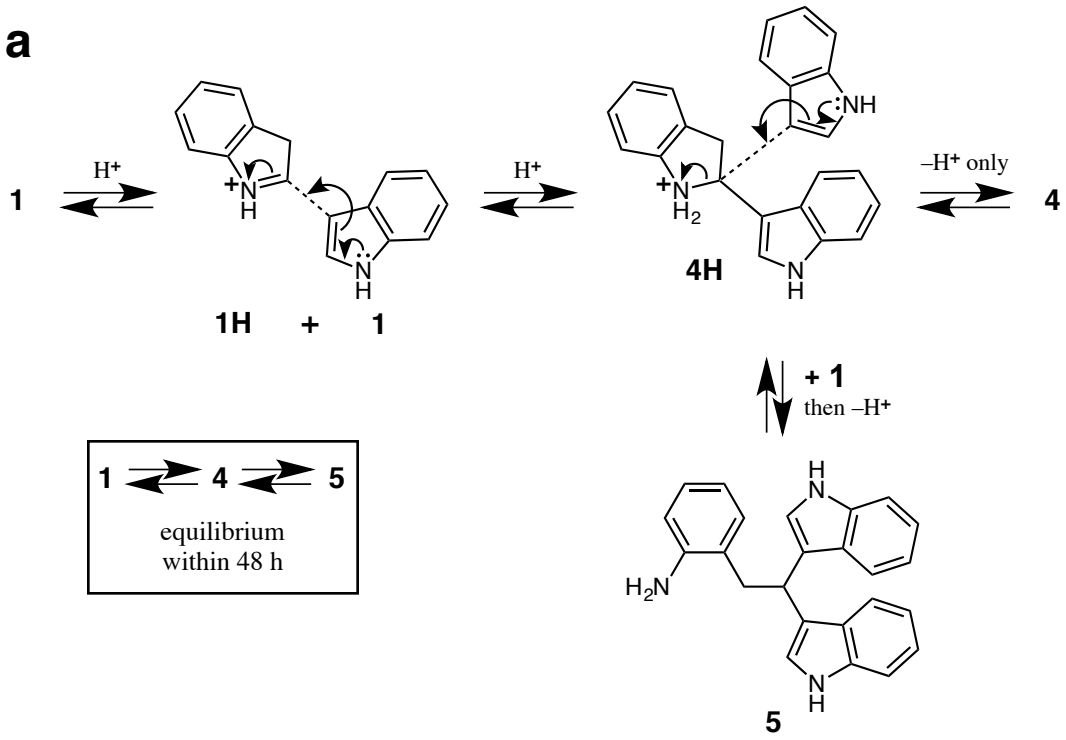

Conversely, the formation and combination of analogs of **57** and **7** from the larger cyclic ketones (**2g–l**) is much slower. Thus, formation of biindolyl **6** takes place to a significant extent. Biindolyl **6** can form *via* autoxidation (Scheme 41b), generating hydrogen peroxide. Alternatively, biindolyl **6** can form *via* a hydride transfer from dimer **4** to protonated vinylindole **57H** (Scheme 42). This explains the formation of cycloundecanone- and cyclododecanone-derived cycloalkylindoles **13k** and **13l**.

Scheme 42. The formation of cycloalkylindoles **13k** and **13l** *via* a hydride transfer from dimer **4**.

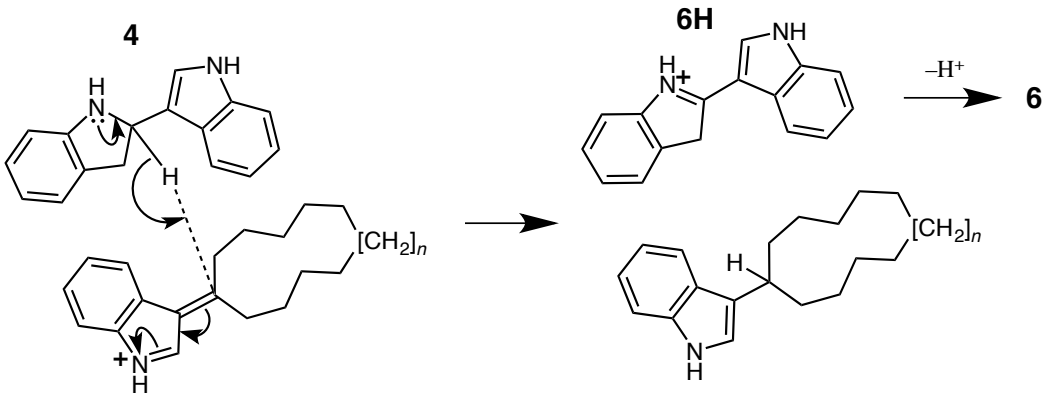

$n = 1$ **57kH** $n = 1$ **13k**

$n = 2$ **57lH** $n = 2$ **13l**

The 3'-position of biindolyl **6** is resonance-activated by both N atoms. Therefore, **6** is more nucleophilic than indole. Biindolyl **6** can undergo cyclizative condensation with ketones to give key intermediate **109** (**109g** is shown as an example, Scheme 43).

Scheme 43. The formation of key intermediate **109g** from cycloheptanone (**2f**) and biindolyl **6**.

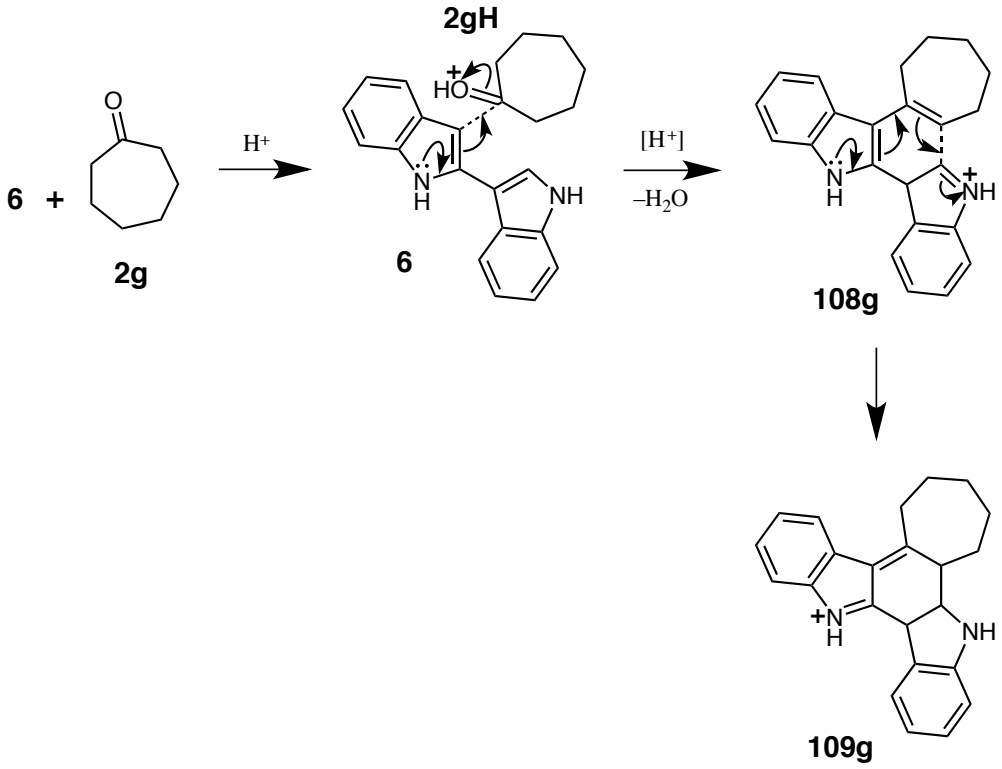

Key intermediates of type **109** are at a fork in the synthetic pathway (Scheme 44). For **109g** and **109l**, the proposed pathway is autoxidation at the indoline-2-position (analogous to the conversion of dimer **4** into biindolyl **6**), followed by elimination of hydrogen peroxide. The result is indolocarbazole **10g** or **10l**. By contrast, **109h** appears to have undergone a proton transfer to the indoline N atom, followed by ring opening (analogous to the conversion of dimer **4** into trimer **5**). It is not yet clear what factors influence the direction that this pathway follows, which is a subject of proposed future work (§ 1.9).

Scheme 44. The conversion of key intermediates of type **109** into products of type **10** and **11**.

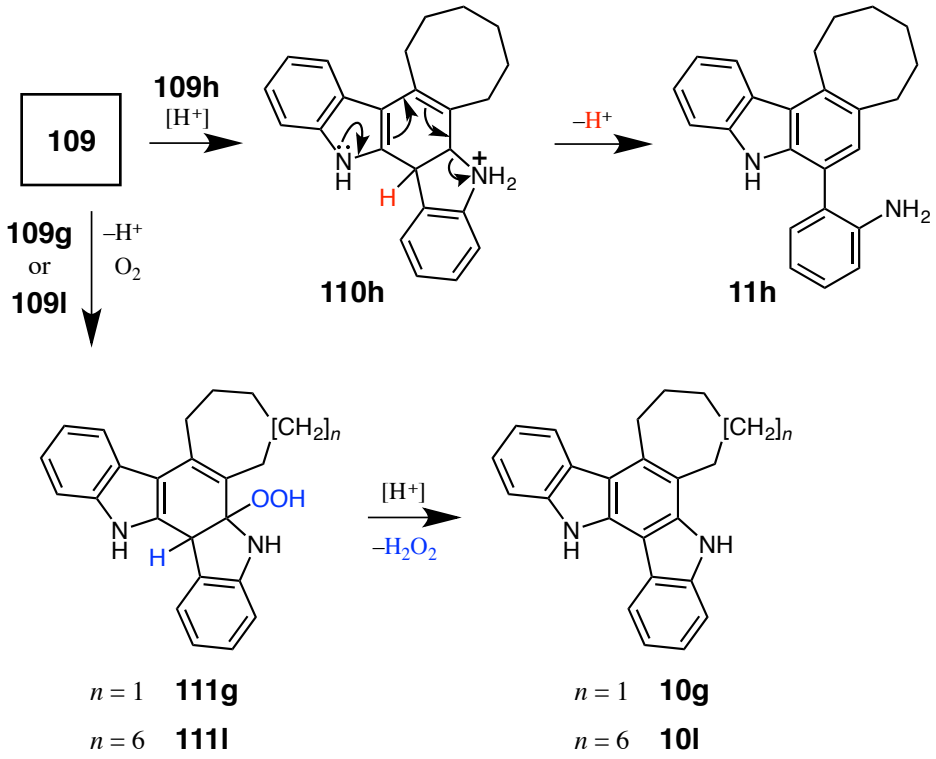

The cyclizative condensation, ring-opening sequence that gave **11h** was not found in the literature, nor were other examples of this type of carbazolylaniline. A search of the literature located an example of the reaction sequence that gave **10g** and **10l**. Janosik & Bergman reported that cyclizative condensation of **6** with dimethylaminoacetal (**112**) gave **114** (Scheme 45) [66]. In this sequence, **113** is a postulated intermediate. In compound **113**, the dimethylamino group serves as a built-in leaving group, facilitating aromatization of the newly-formed ring. This is analogous to to the aromatization of compounds **111g** and **111l** in the present work, although the leaving group (hydroperoxy) was added *in situ*, and the site of elimination was shifted by two atoms.

Scheme 45. The preparation of indolocarbazole **114** from biindolyl **6**, reported by Janosik & Bergman.

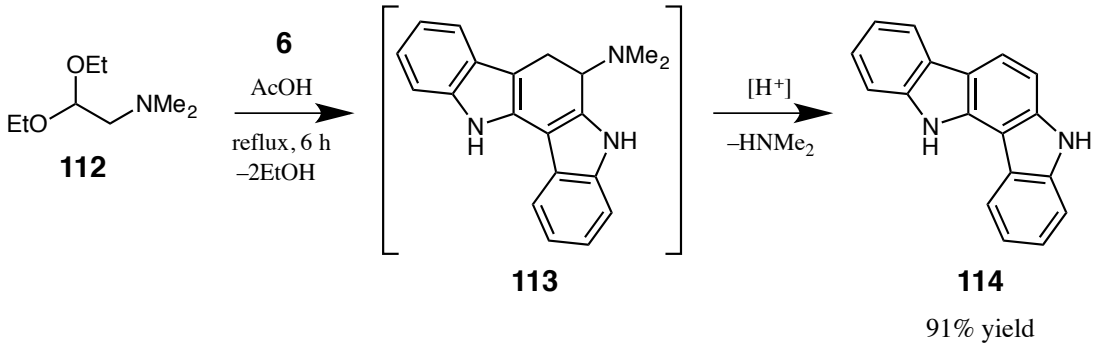

As introduced in § 1.5.7 (p 56), the one-pot formation of diazepine **12h** can be explained by the cyclizative condensation of an acetaldehyde synthon (**106**) with compound **11h** (Scheme 46). Compound **106** is generated *in situ* by hydrogen peroxide, a byproduct of the formation of biindolyl **6**.

Scheme 46. The proposed pathway for the one-pot formation of diazepine **12h** from carbazolylaniline **11h**: (a) The conversion of ethanol into acetal **109**; (b) cyclizative condensation of **11h** with **106** *via* iminium species **115**.

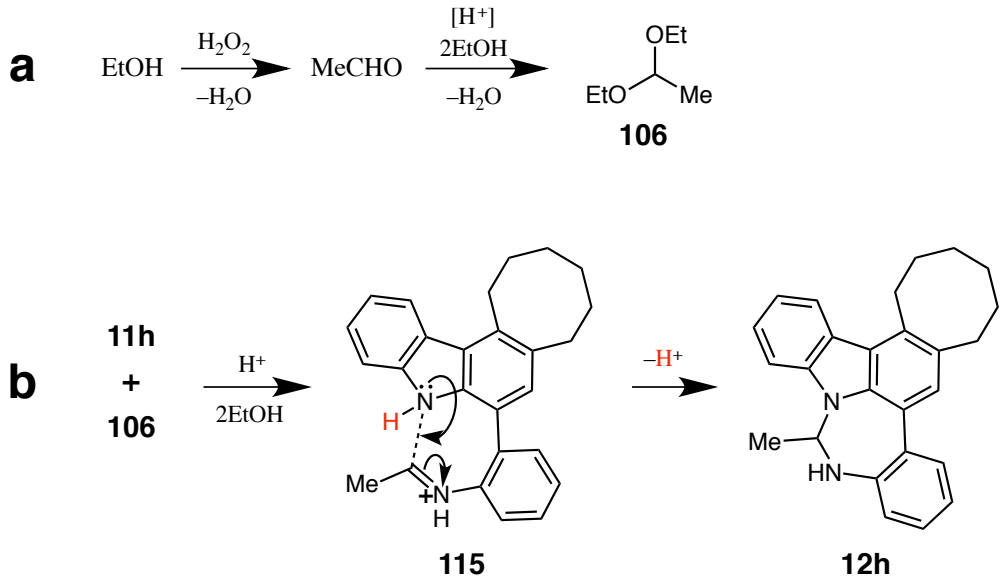

1.6. Selected NMR Analysis

Complete lists of ^{1}H and ^{13}C NMR signals are given for each product in §§ 3.2–3.4. At least one example of each product of types **8** through **13** was analyzed by two-dimensional or heteronuclear NMR experiments, generally including ^{1}H-COSY, ^{1}H-NOE, $^{1}H/^{13}C$-DEPT-90 and -135, and $^{1}H/^{13}C$-HMQC and -HMBC. Those data are presented in Appendix I. The figures presented in this section are intended to be practical guides that highlight a selection of particularly diagnostic NMR signals. NMR analysis of indole-ketone product mixtures is greatly simplified by first identifying and integrating these NMR signals, and then accounting for the remaining signals from each mixture component. In each figure, one or more signals are labeled that are most likely to be usable for quantitative integration.

Of the seven possible signals, leftover indole (**1**) is most easily identified by the C-3 proton (H_a, Fig. 10). This multiplet is usually the most upfield (lowest δ) signal in the aromatic (6–9 ppm) region of a given NMR spectrum. This signal usually consists of seven peaks, with a sharp, tall central peak. This signal can usually be cleanly integrated, even in tarry mixtures.

Fig. 10. The aromatic region of the ^{1}H NMR spectrum of indole (**1**).

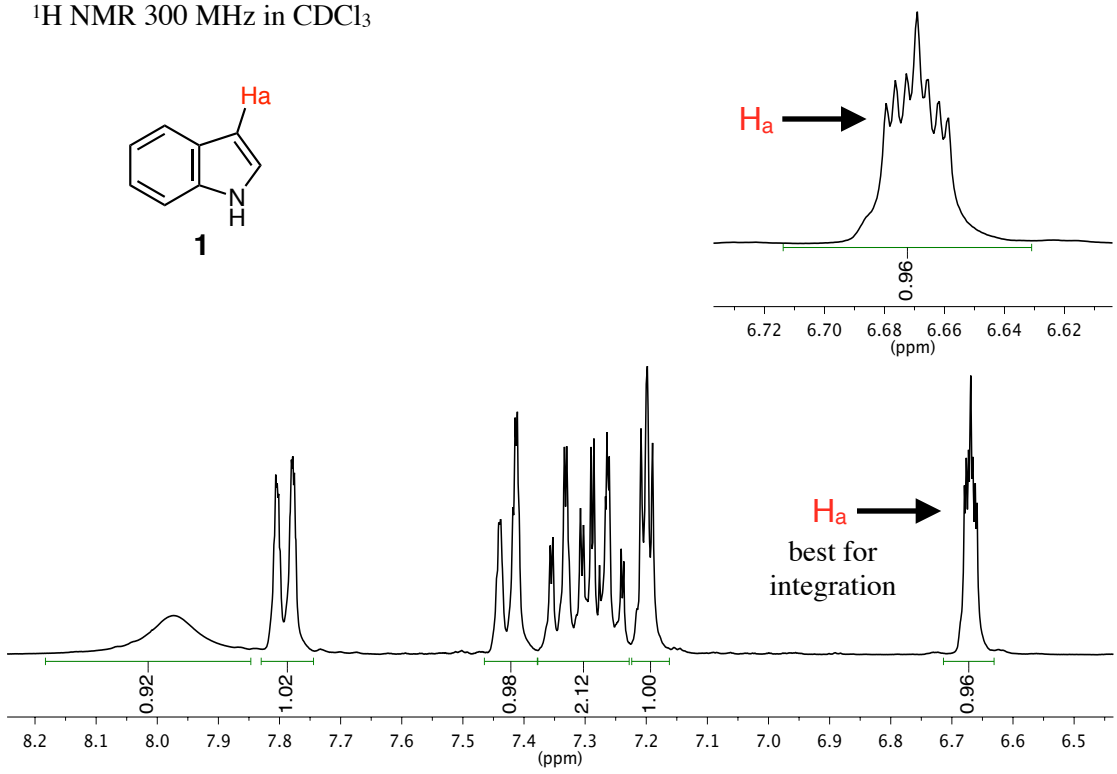

Dimer **4** can be quickly identified by its alkyl protons ($H_{b–d}$, Fig. 11). These signals are a triplet and two doublets of doublets, at 5.24, 3.46, and 3.15 ppm, respectively. These three signals should have equal integration. Hb can almost always be cleanly integrated. The aromatic NMR signals of **4** are usually difficult to discern from other mixture components.

Fig. 11. The alkyl region of the ^{1}H NMR spectrum of dimer **4**.

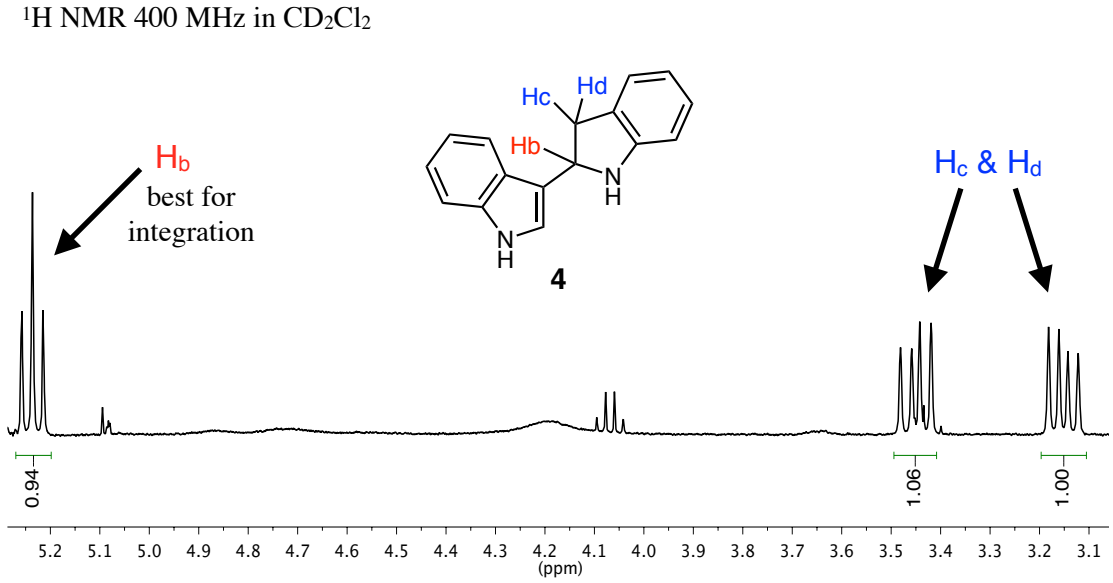

Similarly, trimer **5** is best identified by its alkyl protons (H_e and H_f, Fig. 12). These signals are a triplet at 4.85 ppm and a doublet at 3.42 ppm. These signals should have a 1:2 integration ratio. The aniline N–H_2 signal is usually broad and its chemical shift is variable.

Fig. 12. The alkyl region of the ^{1}H NMR spectrum of trimer **5**.

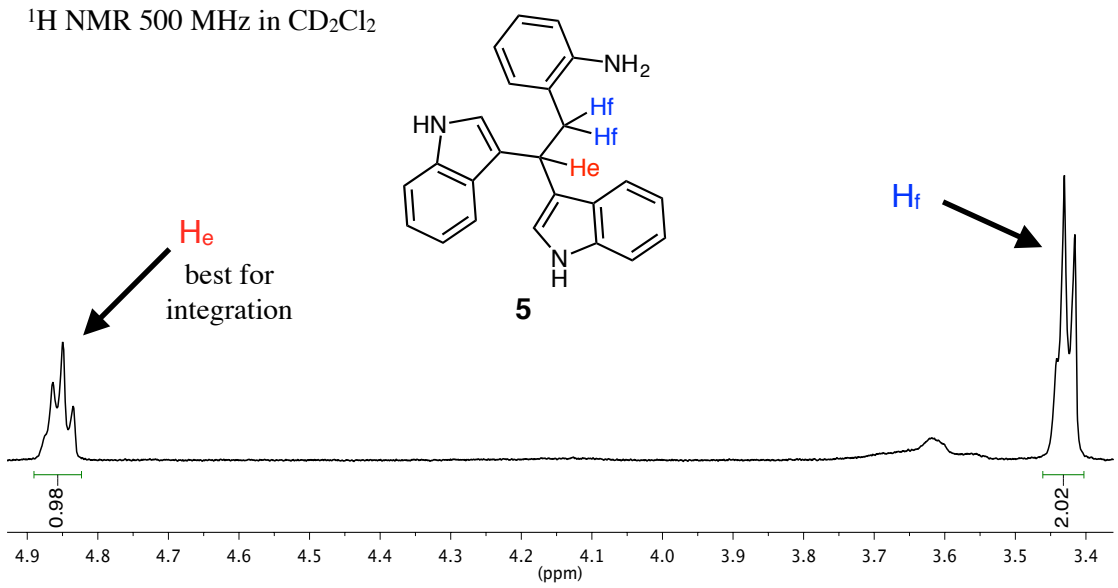

Biindolyl **6** has a low solubility in halogenated solvents. The use of polar, aprotic solvents tends to move the doublets downfield such that the most deshielded doublet is visible among the most downfield C–H signals in a given mixture (Fig. 13). The two low-*J*-value doublets (H_g and H_h) differentiate biindolyl **6** from other biindolyl derivatives (*i.e.*, products of types **10** or **11**), in which the corresponding protons have been lost to substitution.

Fig. 13. The aromatic region of the ^{1}H NMR spectrum of biindolyl **6**. The N–H signals (not shown) are farther downfield.

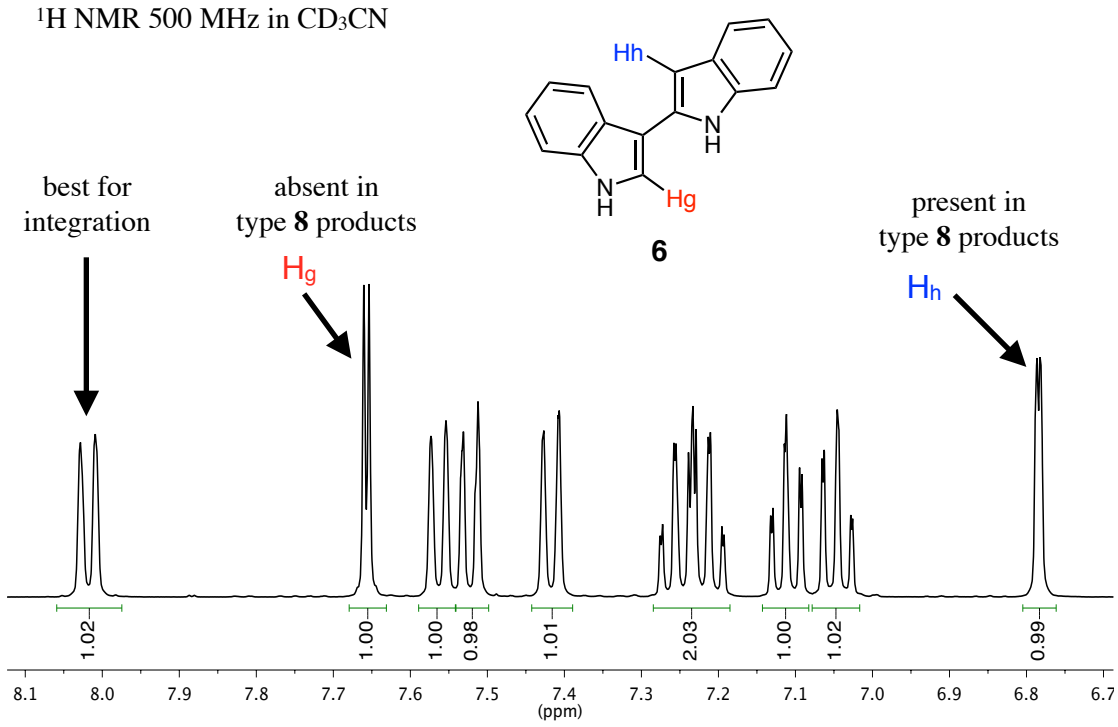

Bisindoles (*e.g.*, **7j**) can be quickly identified based on having only one N–H signal, with integrations corresponding to two N–H protons and four alkyl α-protons (H_b, Fig. 14). The other 2:1 condensation derivatives give two N–H signals, which are best resolved in a polar solvent. If a mixture is too complex for this strategy to be used, bisindoles can be identified by a low-*J*-value doublet at 7.2–7.4 ppm (H_a). This doublet is among or slightly downfield from the high-*J*-value doublets. H_b is usually a triplet between 2.3 and 2.6 ppm, but its position relative to the α-protons of leftover ketone is difficult to predict.

Fig. 14. The (a) aromatic and (b) alkyl regions of the ^{1}H NMR spectrum of bisindole **7j**.

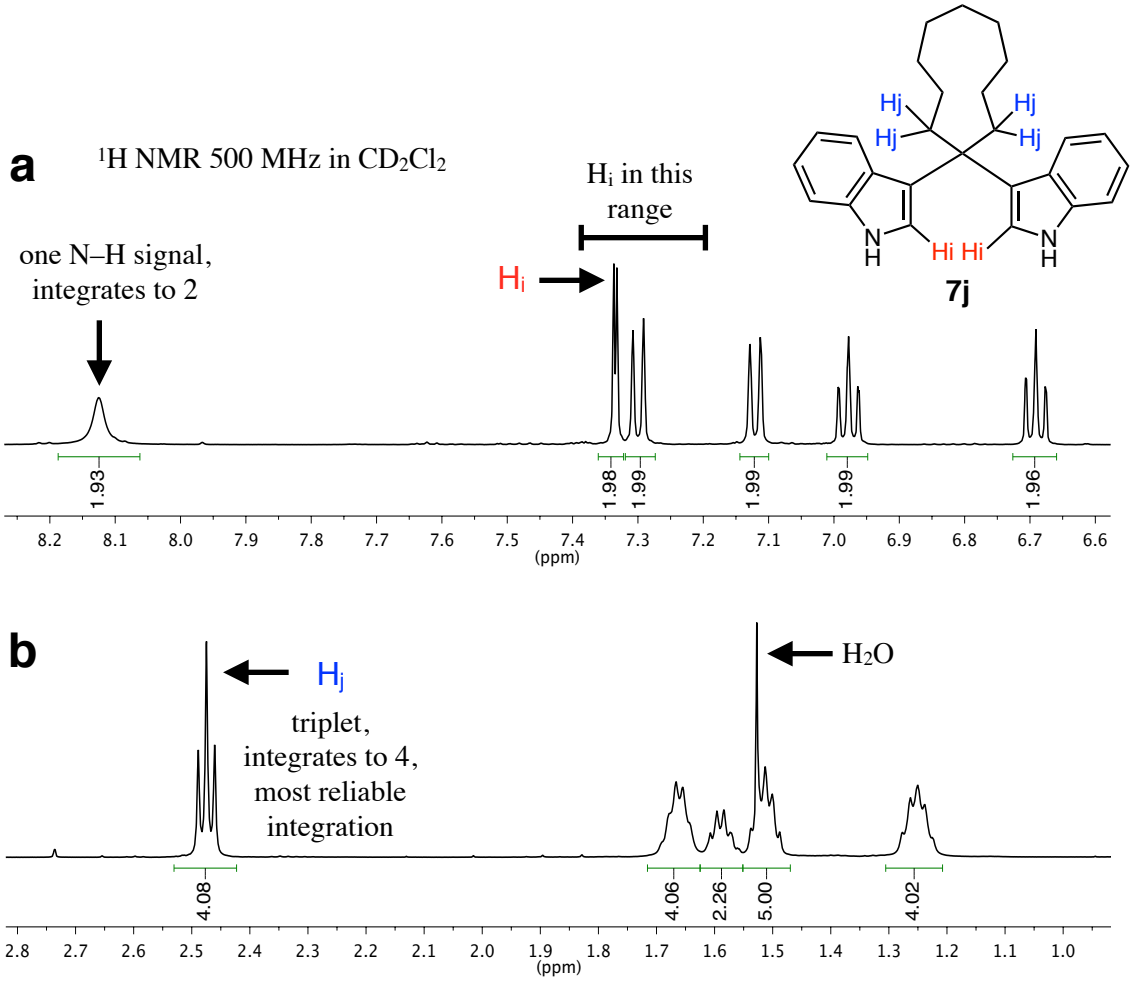

Products of type **8** (*e.g.*, **8e**, Fig. 15) have the highest number of inequivalent protons among product types that were obtained in the present work. Thus, they are easy to differentiate from products of types **9**–**13** based on all resolved signals having equal integration and a large enough number of signals that the absolute integration value must be 1. Products of type **8** give one low-*J*-value doublet at 6.8–7.1 ppm (H_k), which is upfield from the corresponding signal from the corresponding bisindole (*e.g.*, H_i, Fig. 14). H_k is in the same region as one of the two doublets given by biindolyl **6** (H_h, Fig. 13), but **6** and **8** are distinguishable because **8** does not give the more downfield of these two signals (H_g, Fig. 13). H_L is slightly downfield from the α-protons of leftover ketone, and it can be an apparent triplet or quartet.

Fig. 15. The (a) aromatic and (b) alkyl regions of the ^{1}H NMR spectrum of product **8e**. The locations of low-*J*-value doublets in products **6**, **7**, and **13** are shown for comparison.

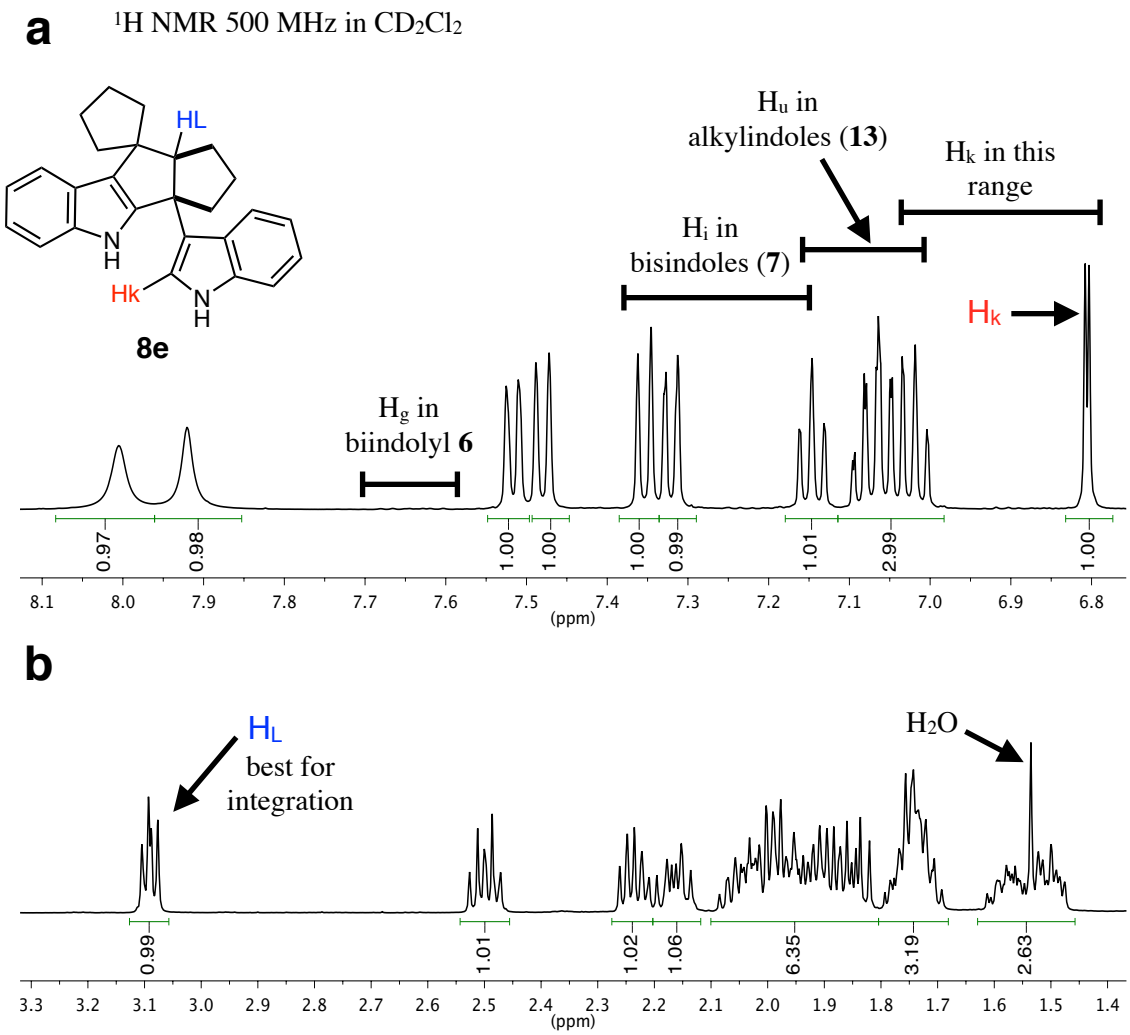

Conversely, product **9f** is centrosymmetric, and can be recognized by its MS analysis having the *m*/*z* ratio of a 2:2 product, while it has surprisingly few NMR signals. The shapes of the alkyl signals in the ^{1}H NMR spectrum are not very telling, but the aromatic region consists of two doublets and two triplets (in this example, the triplets are overlapping, Fig. 16). This aromatic fingerprint resembles that of bisindoles (**7**), without the low-*J*-value doublet (H_i, Fig. 14).

Fig. 16. The (a) aromatic and (b) alkyl regions of the ^{1}H NMR spectrum of product **9f**. The N–H signal (not shown) is farther downfield.

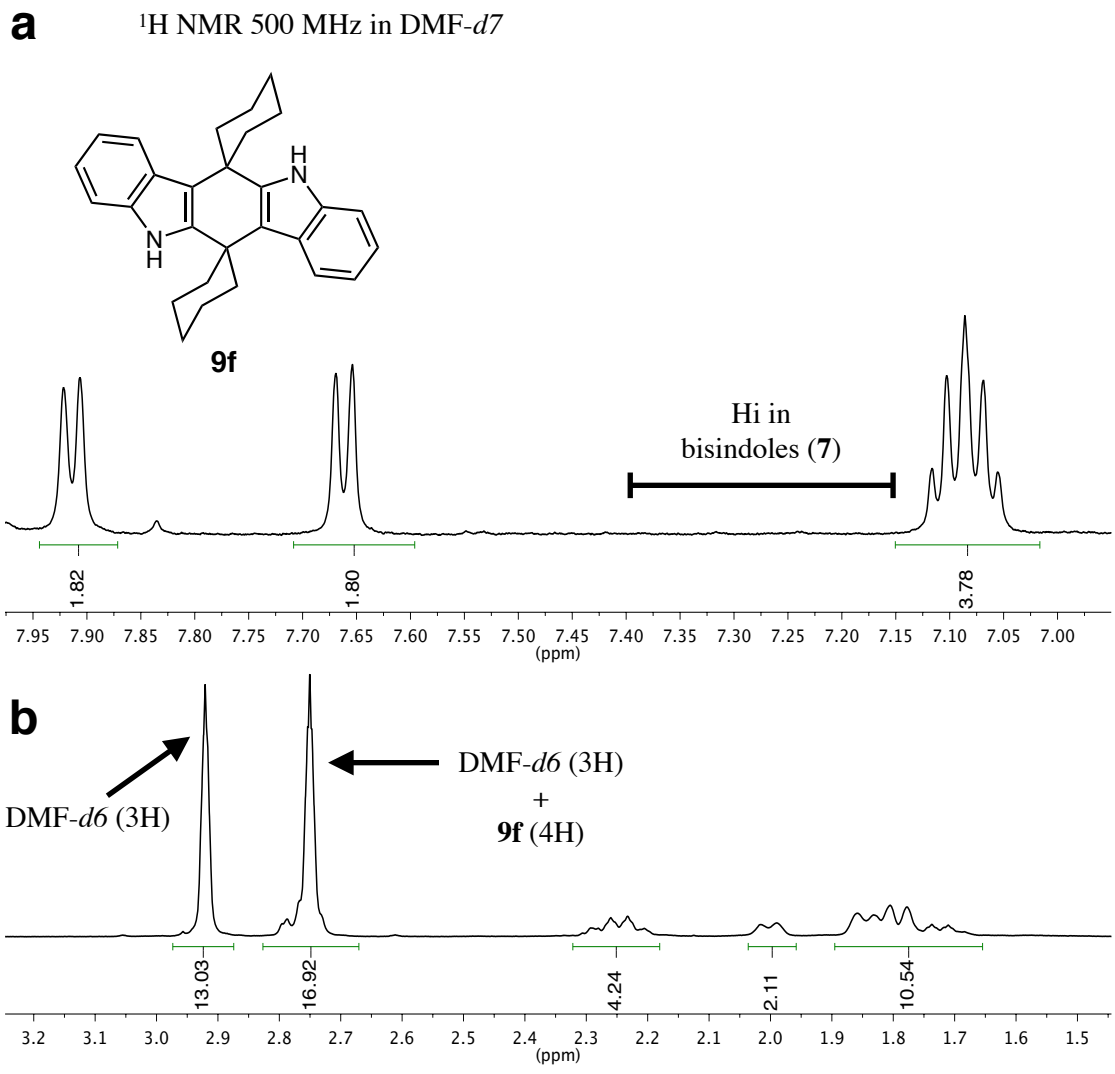

The solubility of **9f** is very low in most solvents, including hot DMSO. Fortunately, hot DMF can dissolve just enough **9f** for ^{13}C NMR analysis to be viable within roughly one hour per NMR experiment. Product **9f** can be differentiated from hypothetical isomer **68f** by inspection of the alkyl region of the ^{13}C NMR spectrum (Fig. 17). Compound **9f** gives four such signals (supported by HMBC analysis), whereas **68f** should give eight.

Fig. 17. The alkyl region of the ^{13}C NMR spectrum of product **9f**. Compound **68f** is shown for comparison.

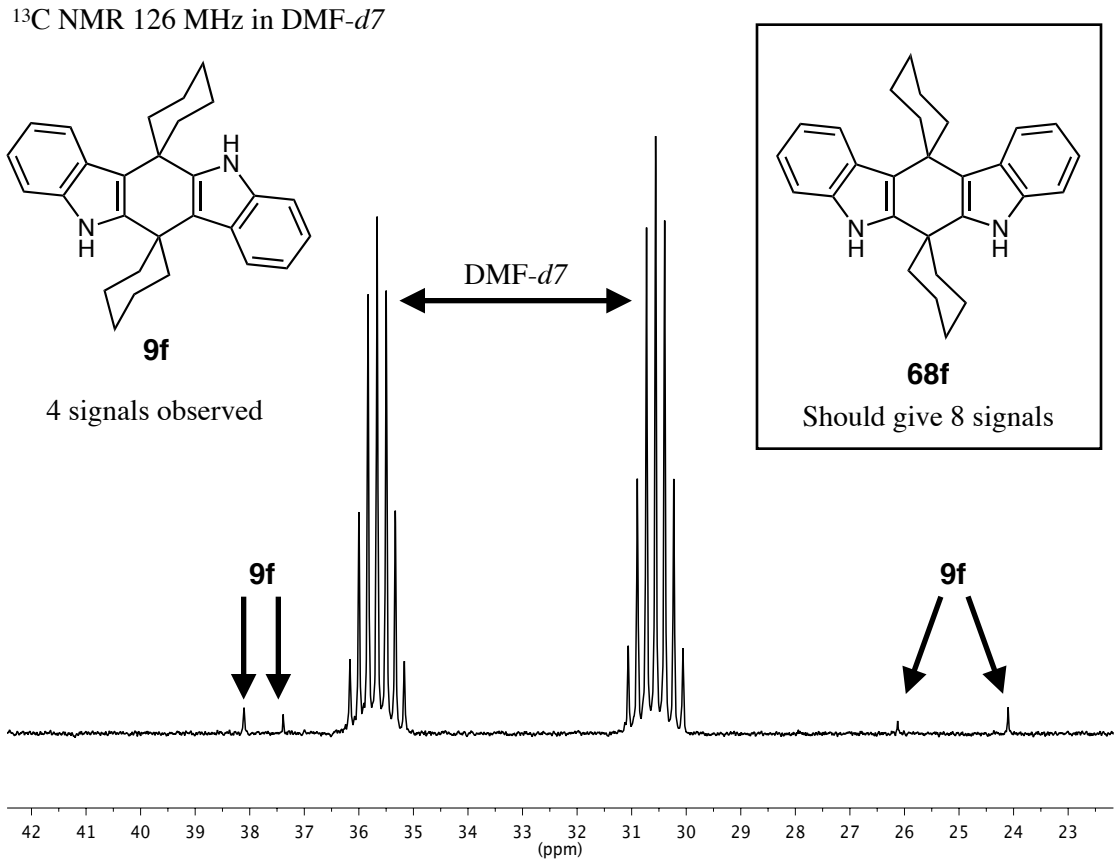

Although these ^{1}H and ^{13}C NMR signals from **9f** make for easy identification of samples with medium to high purity, there is no obvious shortcut NMR strategy to identifying small amounts of type **9** products in a mixture. The shapes and locations of all NMR signals are too similar to those of other mixture components. An effective approach might be trituration of the product sample, subsequent NMR analysis, and comparison of the changes of intensities of

groups of NMR signals. Fortunately, product **9f** was easily purified by several triturations in acetonitrile. It is uncertain whether other products of type **9** would cooperate in this fashion.

The aromatic region of the ^{1}H NMR spectrum of product **10g** (Fig. 18a) resembles that of biindolyl **6**, without both low-*J*-value doublets. In the alkyl region (Fig. 18b), the methylene groups adjacent to the central benzene ring are both shifted downfield from the α-protons of leftover ketone. Product **10l** gave similar NMR results.

Fig. 18. The (a) aromatic and (b) alkyl regions of the ^{1}H NMR spectrum of product **10g**. The N–H signals (not shown) are farther downfield.

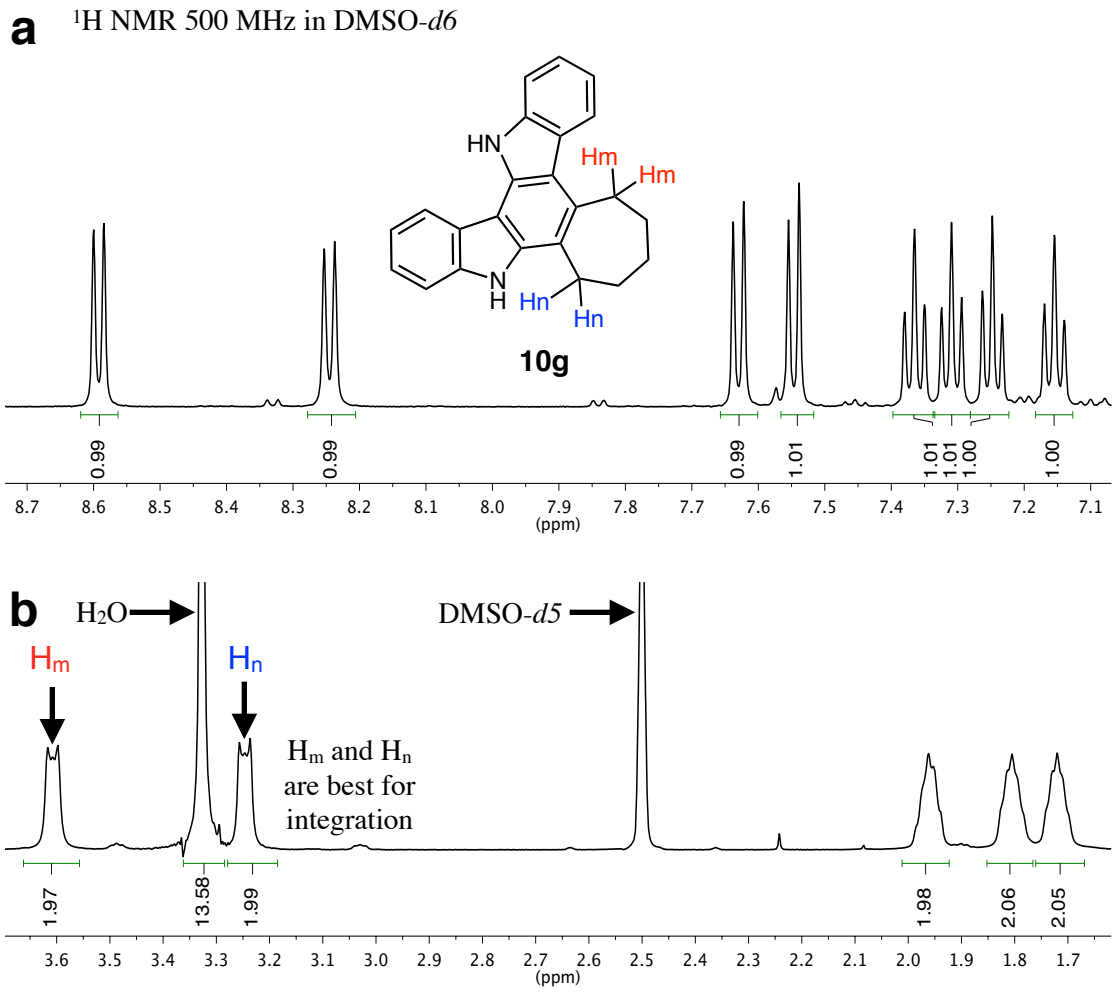

The aromatic region of the ^{1}H NMR spectrum of ring-opened product **11h** (Fig. 19a) differs in many ways from that of **10g**. The most prominent change is the addition of a singlet (H_o). Product **11h** has only one N–H signal (not shown), whereas **10g** has two. The alkyl region of **11h** (Fig. 19b) is nearly identical to that of **10g**, but the amino group (H_p) has been added. Compounds **11h** and **12h** are the only condensation-derived products in the present study (§§ 1.3–1.5) that give NMR signals in the 4–6 ppm range. The only other signals in this range are the triplets from dimer **4** (H_b, Fig. 11) and trimer **5** (H_e, Fig. 12), making the 4–6 ppm range very diagnostic for ^{1}H NMR analysis of these reaction mixtures.

Fig. 19. The (a) aromatic and (b) alkyl regions of the ^{1}H NMR spectrum of product **11h**. The aromatic N–H signal (not shown) is farther downfield.

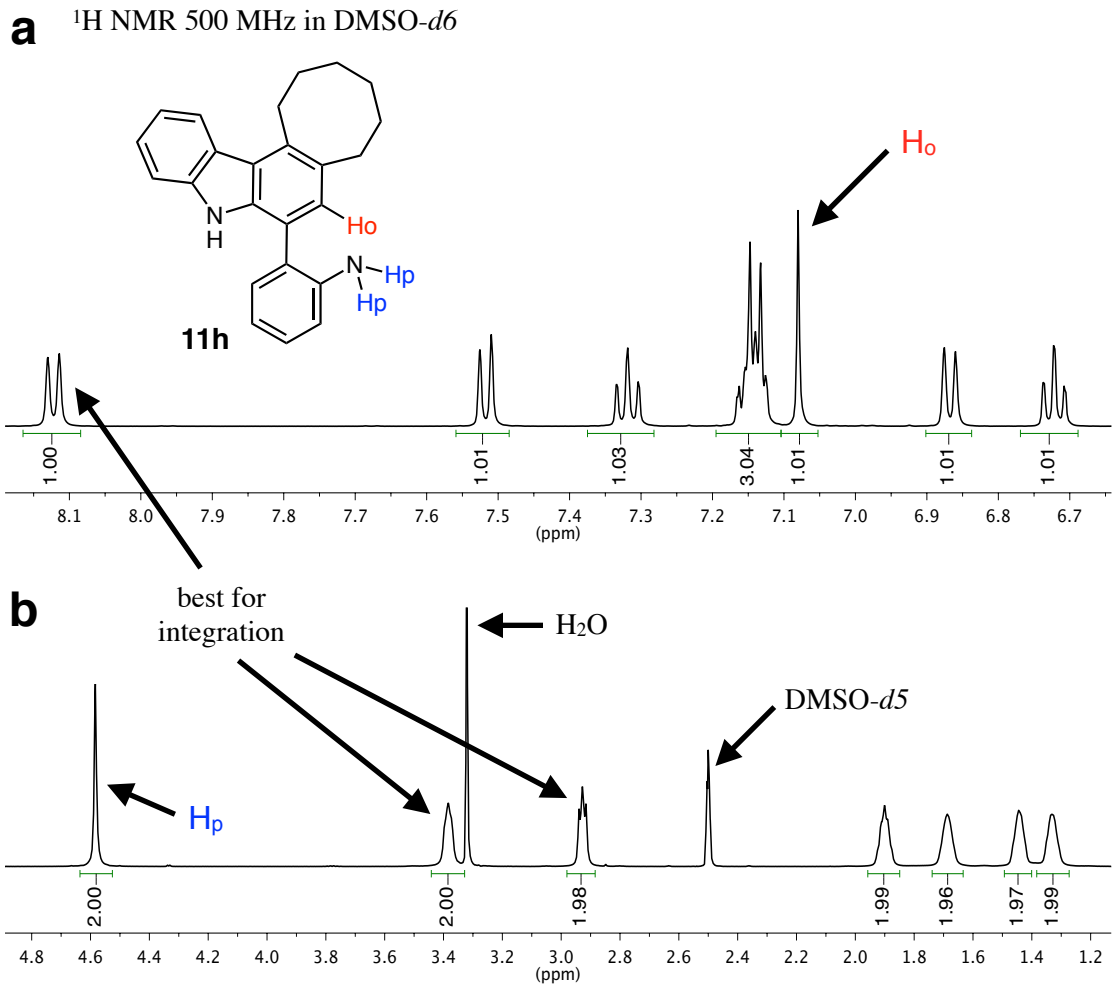

The aromatic region of the ^{1}H NMR spectrum of diazepine **12h** (Fig. 20a) is similar to that of **11h**. The two main changes are the lack of an N–H signal and the addition of H_r. In the alkyl region (Fig. 20b), the integration of the amino proton (H_s) has decreased to 1, and the methyl group (H_t) is the strongest signal. Additionally, the methylene groups have become diastereotopic, and some of them resolved into geminal pairs (*i.e.*, at 3.5 and 1.8 ppm).

Fig. 20. The (a) aromatic and (b) alkyl regions of the ^{1}H NMR spectrum of product **12h**.

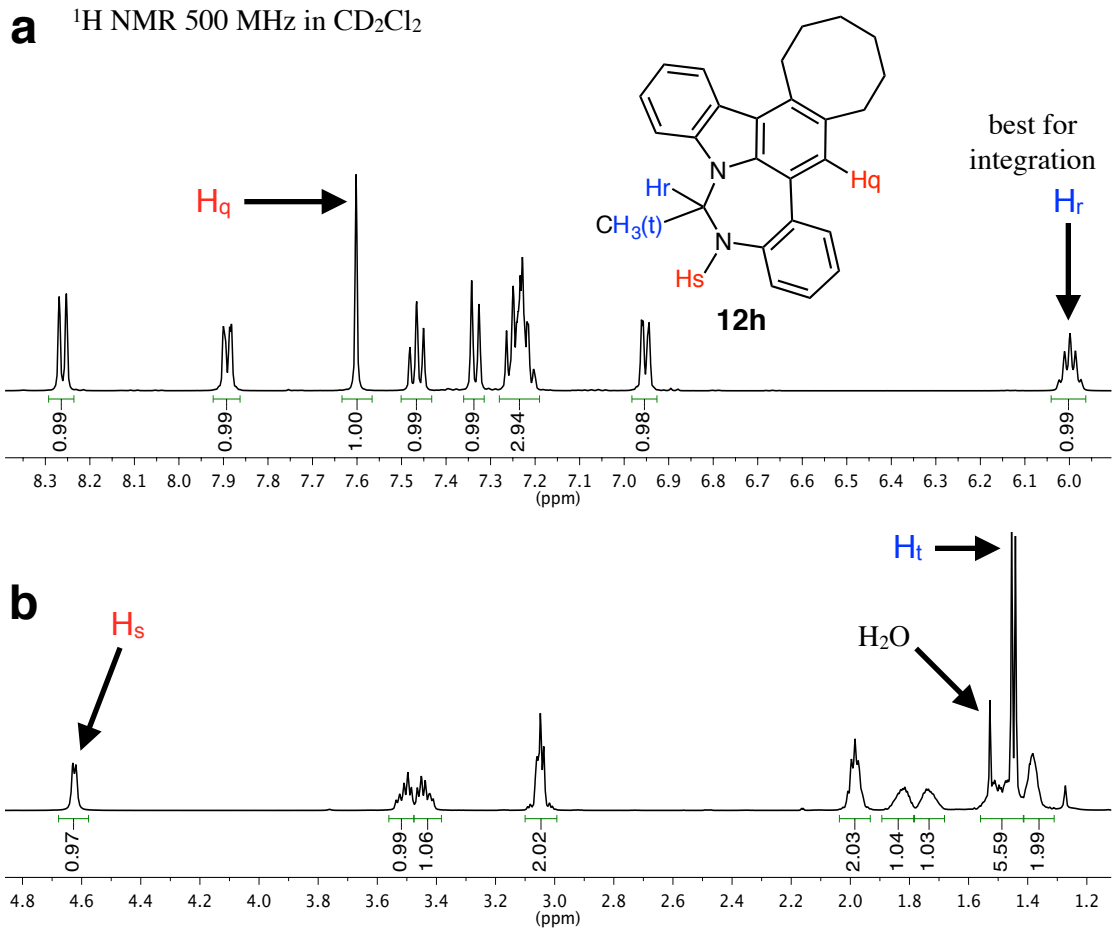

The aromatic region of the ^{1}H NMR spectrum of 3-cycloundecylindole (**13k**, Fig. 21a) is practically identical to that of a bisindole (**7**), although low-*J*-value doublet H_u is slightly upfield from the corresponding signal in **7** (H_i, Figs. 14 and 15). To distinguish products of type **13** from type **7** or other products, the alkyl region (Fig. 21b) must be investigated. In **13k**, the downfield alkyl proton (H_v) integrates to 1 relative to indole, whereas the downfield alkyl CH_2 signal in bisindoles (**7**) integrates to 2. Other products have more than one outlying downfield alkyl signal.

Fig. 21. The (a) aromatic and (b) alkyl regions of the ^{1}H NMR spectrum of product **13k**. The N–H signal (not shown) is farther downfield.

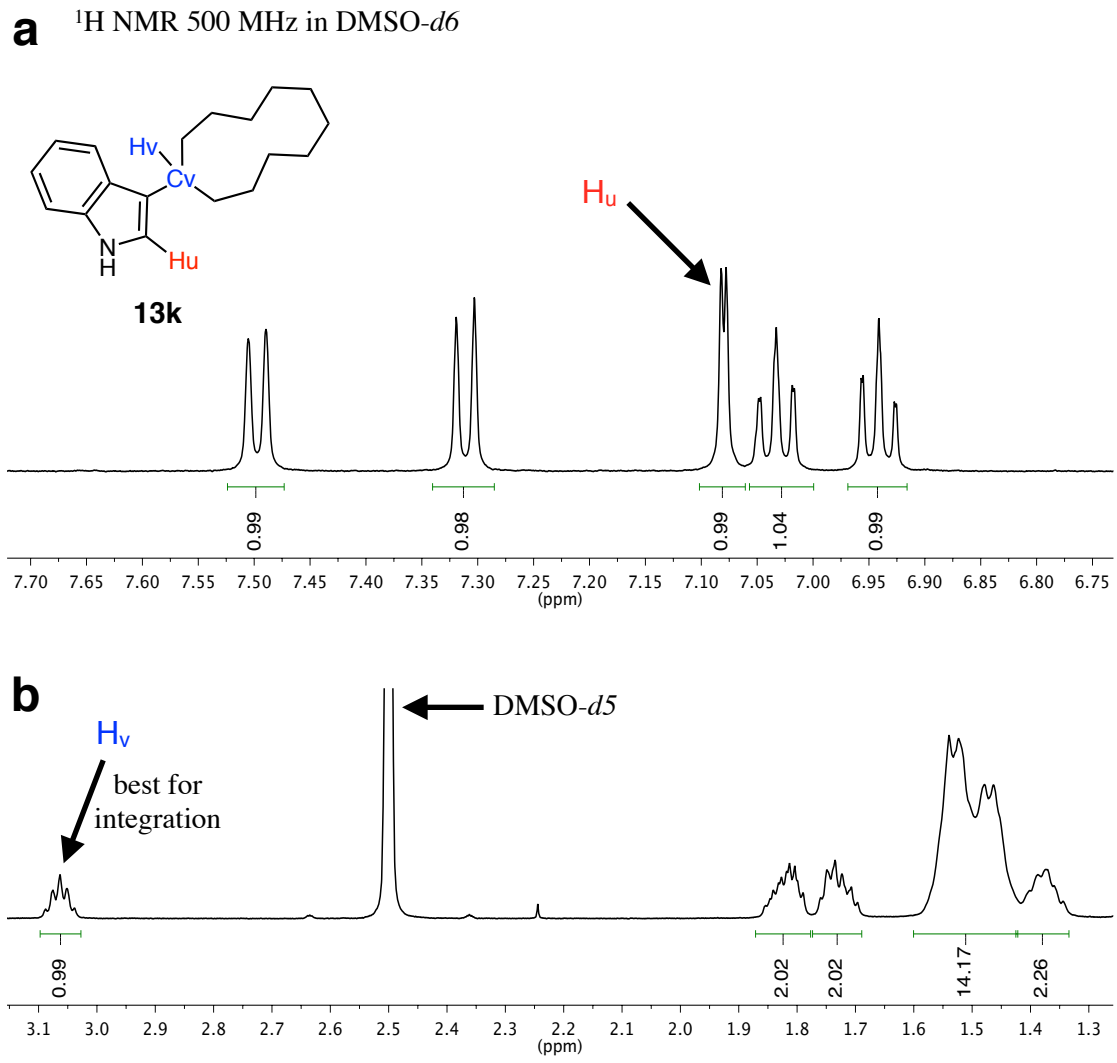

In cases where there are too many overlapping proton signals, $^{1}H/^{13}C$ DEPT-135 analysis can be performed. Carbon atom C_v (Fig. 22) is the only C–H signal (positive peak) that will appear near 20 ppm, from product types characterized in the present study. The remaining signals in this part of the spectrum are CH_2 (negative peaks) or quaternary (null). The C–H carbon signals from products of type **4**, **5**, **8** or **12** appear in the 40–70 ppm range.

Fig. 22. The alkyl region of the $^{1}H/^{13}C$ DEPT-135 spectrum of product **13k**.

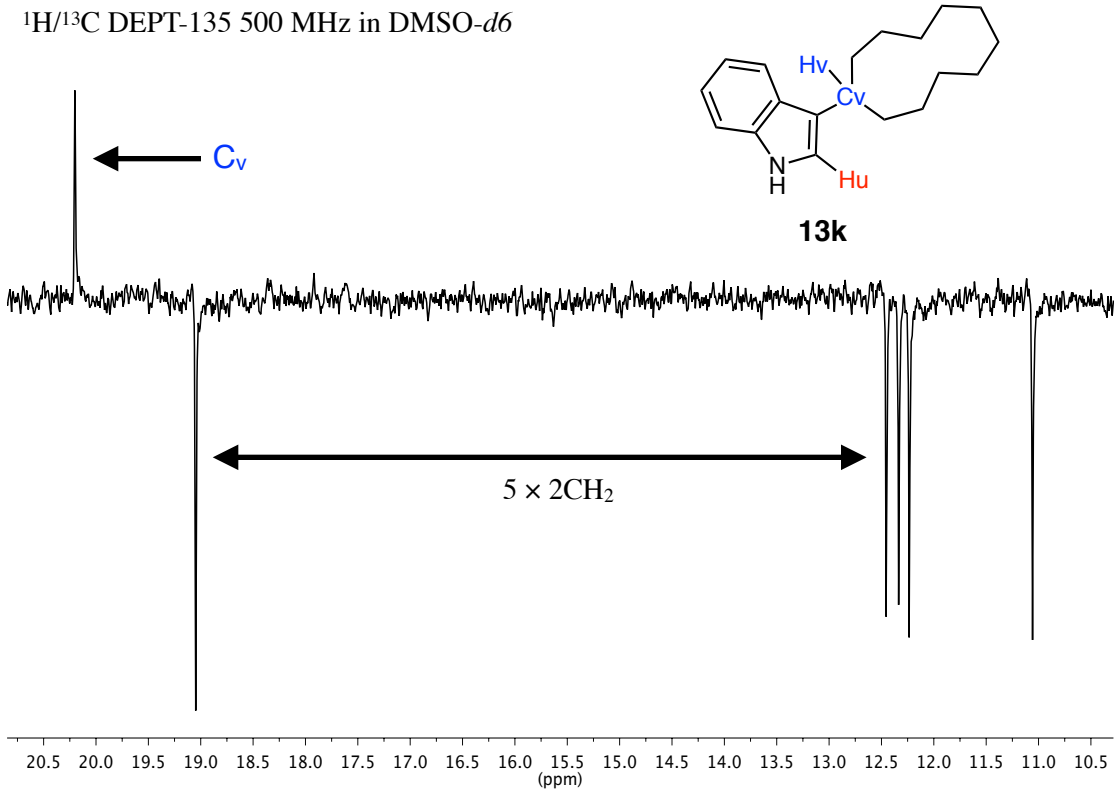

1.7. Progress Toward Indolo[2,3-*b*]carbazoles

As described in Scheme 16 (p 17), it is unknown whether indolo[3,2-*b*]carbazole derivative **9f** forms *via* a Plancher rearrangement of indolo[2,3-*b*]carbazole isomer **68f** (Scheme 47a), or by a different pathway (Scheme 47b, or otherwise).

Scheme 47. Two of the possible routes for the formation of **9f**: (a) *via* **68f**, and then a Plancher rearrangement; (b) *via* **70f**, by a pathway similar to the formation of 2,2'-bisindoles.

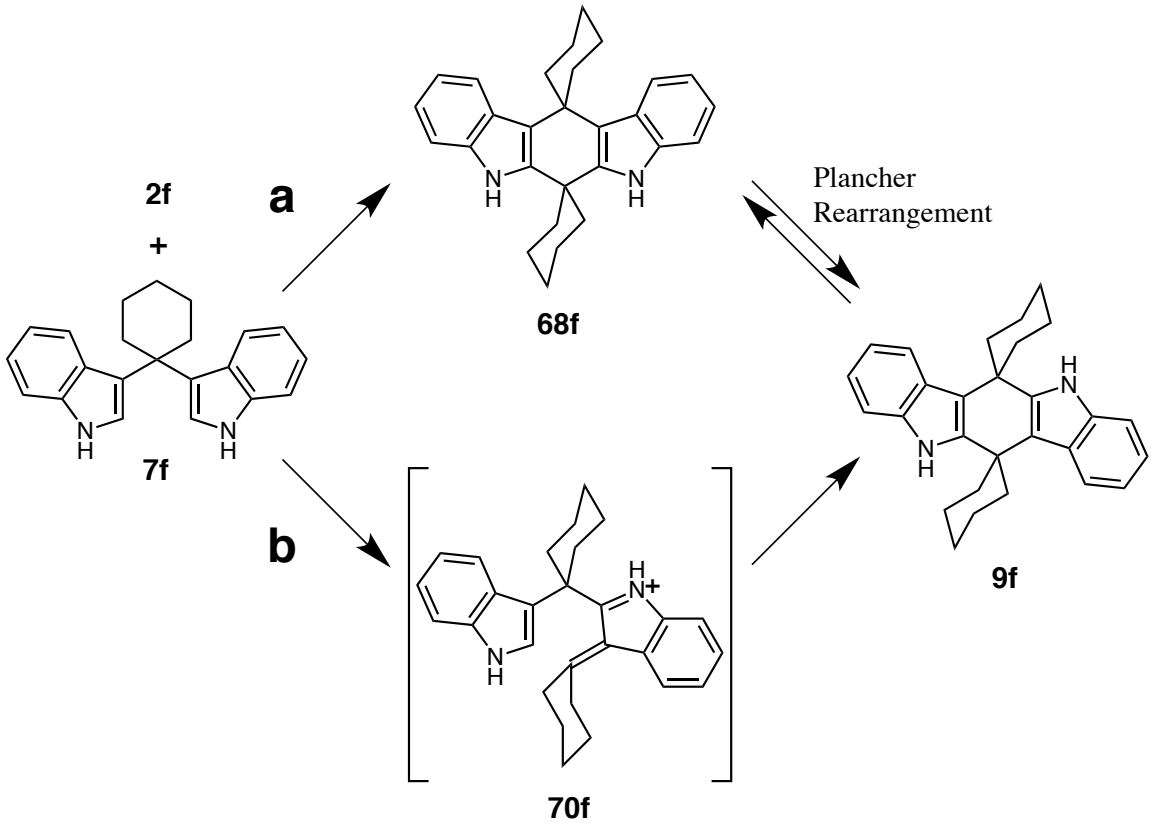

Because many indole-ketone condensation experiments of the type described in §§ 1.4–1.5 are carried out over the course of several days or longer, it was assumed that any Plancher arrangements approximately reach thermodynamic equilibrium. Early in the course of research for this dissertation, a computational study was performed to estimate the free energy difference between hypothetical compounds **9e** and **68e**. The computational model [67a] found that **9e** is approximately 19.2 kJ/mol lower in free energy than **68e** (Scheme 48). At equilibrium, a mixture of the two components would contain roughly 0.04 mol% **68e**, which would be difficult to characterize by NMR analysis. Had this computational work been done at a later time, cyclohexanone-derived compounds **9f** and **68f** would have been compared, since **9f** was obtained. The findings would probably be similar.

Scheme 48. The computationally estimated free energy difference between compounds **9e** and **68e**. The estimated equilibrium mole percentages are shown.

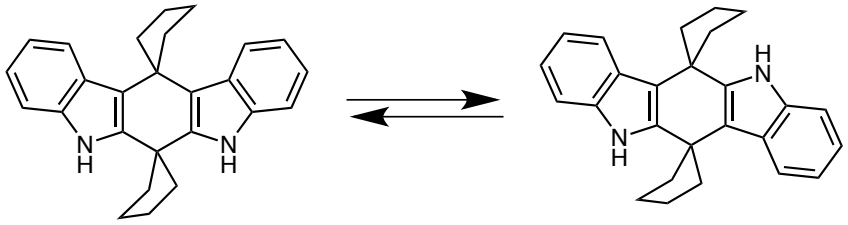

68e G_{rel} = 19.2 kJ/mol (0.04 mol%)

9e G_{rel} = 0 kJ/mol (99.96 mol%)

It was envisioned that if the substituents on the opposite corners of the central ring were asymmetrical, then the equilibrium concentration of one of the minor isomers would increase. Both of the benzene rings could orient away from the larger substituent, as in **19d** (Scheme 49). A second computational study was performed [67b]. Following the removal of one of the five-membered rings from **9e**, the equilibrium shifted as predicted. Although isomer **117** was still the major product, **19d** was estimated to reach 4.3 mol% at equilibrium. If **19d** were present in this amount during a synthetic experiment, it would probably be observable in NMR analysis.

Scheme 49. The computationally estimated free energy difference between compounds **19d**, **117**, and **118**. The estimated equilibrium mole percentages are shown.

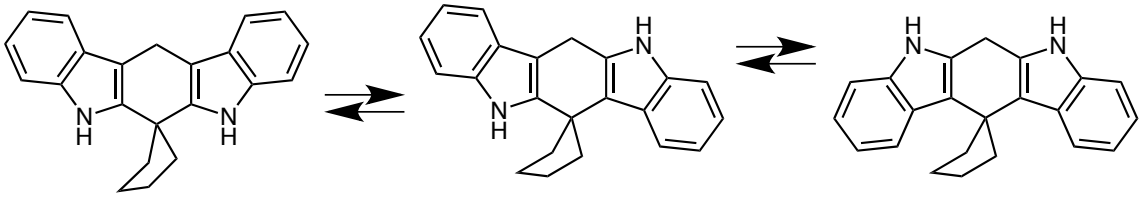

19d	**117**	**118**
G_{rel} = 7.57 kJ/mol	G_{rel} = 0 kJ/mol	G_{rel} = 15.48 kJ/mol
(4.3 mol%)	(95.5 mol%)	(0.2 mol%)

In addition to the mechanistic prospects, it was desirable to prepare several novel indolo[2,3-*b*]carbazoles (*i.e.*, products of types **19d**, **68**, and **118**) because precedent for this type of compound is very scarce. Plancher rearrangements can take place in the presence of acid, so any viable preparation of **19d** and its kin should take place in non-acidic conditions. Retrosynthetic analysis found that compound **19d** might be accessible *via* the two-step acid-free Fischer indole synthesis described by Miyata, *et al*. (Scheme 50) [8], which was introduced in Scheme 5 (p 4).

Scheme 50. The retrosynthesis of **19d** to diketone **17d** and phenylhydrazine (**23**).

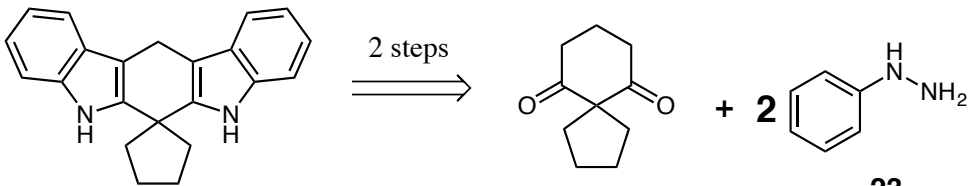

19d **17d** **23**

Accordingly, 1,3-diketone **17d** was prepared from cyclopentanone (**2e**) in a three-step sequence (Scheme 51). The self-aldol condensation of **2e** was carried out in the presence of lithium perchlorate and triethylamine. Aldol product **15** was converted into **17d** by epoxidation to **16**, followed by a Lewis-acid-catalyzed [1,2]-carbonyl shift, during which the keto ring of complex **120** expands [68].

Scheme 51. The preparation of diketone **17d** from cyclopentanone (**2e**).

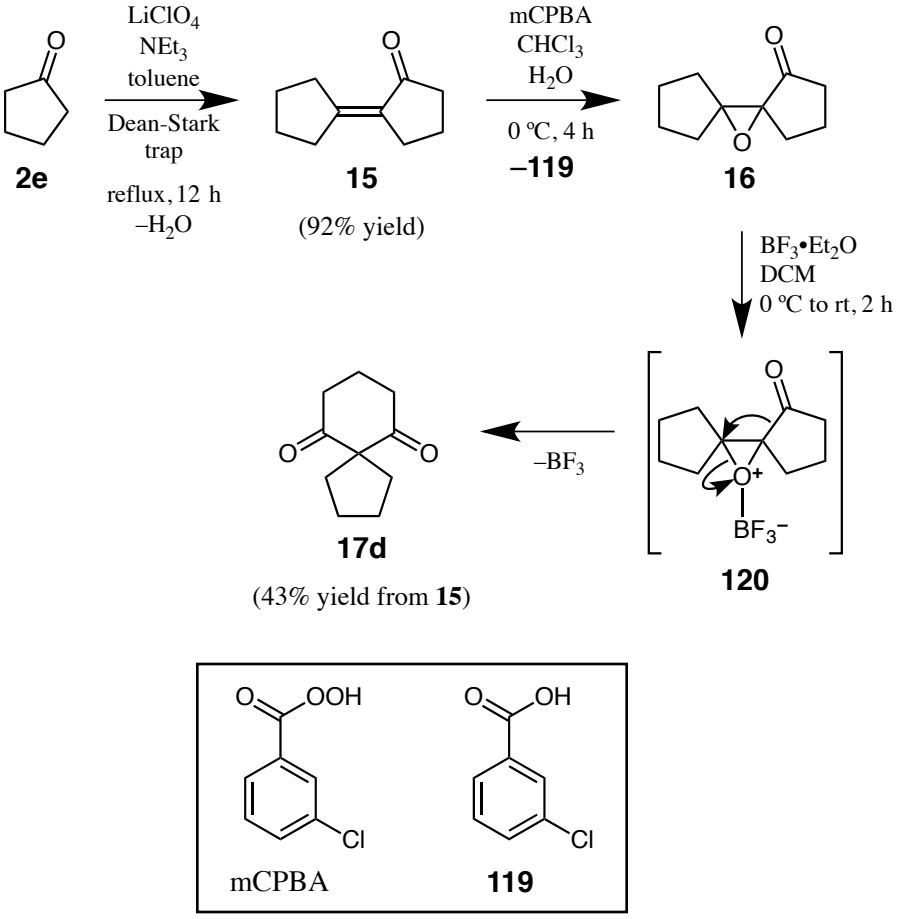

Before proceeding with the rest of the indolo[2,3-*b*]carbazole synthesis, 1,3-diketones **17b** and **17c** were added to the scope of the study (Scheme 52a), as was cyclohexanone (**2f**). Both of the diketones were prepared by methylation of the respective 2-unsubstituted ketones (**121b** and **121c**) [69]. Most of the remaining material was recovered in the form of *O*-alkylated products. Rings and larger alkyl substituents could not be added by this approach, because *O*-alkylation is strongly favored when alkyl halides other than methyl iodide are used (Scheme 52b) [70], even when conditions **a** are used. Thus, **17d** could not be prepared by alkylation of **121b** (Scheme 52c). Such attempts gave complex mixtures that were not separated. During the course of the present work, a new synthesis of **17d** was reported, *via* bis(allylation) of **121b**, followed by ring-closing metathesis, and then hydrogenation [71].

Scheme 52. (a) The preparation of diketones **17b** and **17c**; (b) the use of other alkyl halides favors *O*-alkylation; (c) **17d** could not be prepared by alkylation of **121b**.

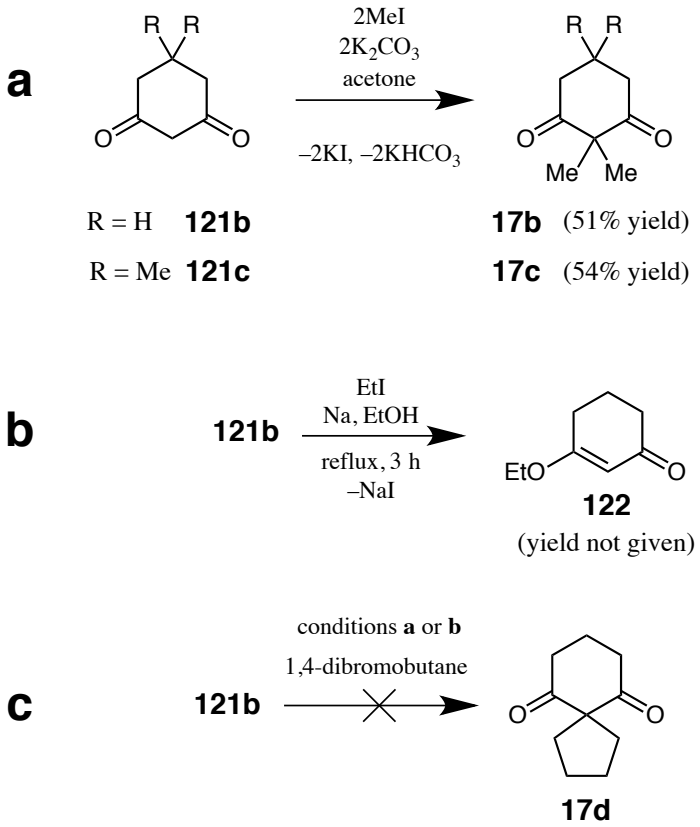

Ketones **2f** and **17b–d** were converted into the respective phenylhydrazones (**18a–d**, Table 9) [72]. A catalytic amount of $TsOH•H_2O$ was more efficient than using larger amounts of weaker acids. The performance of magnesium sulfate was superior to use of a Dean-Stark apparatus.

Table 9. The preparation of phenylhydrazones **18a–d**.

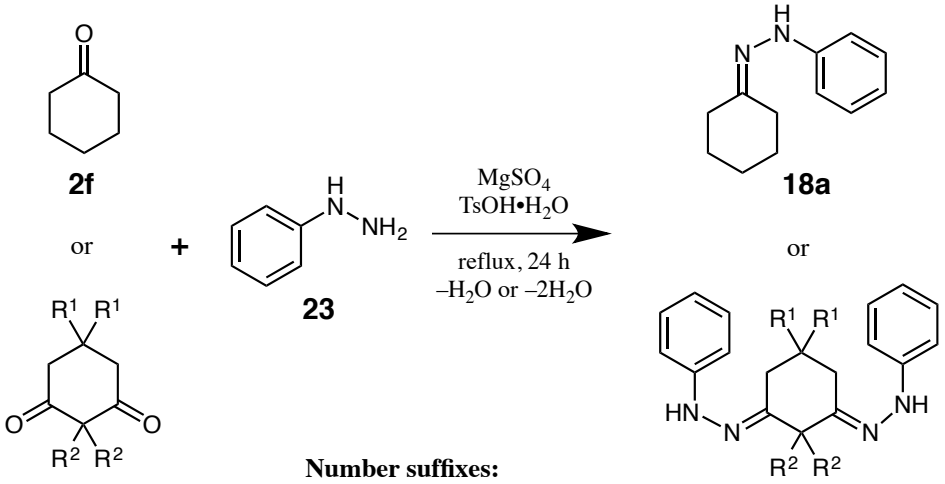

Number suffixes:

	b	**c**	**d**
R^1 =	H	Me	H
R^2 =	Me	Me	$–[CH_2]_4–$

product	ketone mmol	**23** mmol	$MgSO_4$ mmol	$TsOH•H_2O$ mmol	yield %
18a	78.2	77.3	37.3	3.86	88
18b	20.3	40.5	40.5	1.21	62
18c	10.1	20.2	24.4	0.62	66
18d	11.6	23.4	24.1	0.77	44

The acid-free Fischer indolizations were then attempted (Scheme 53) [8]. Although cyclohexanone-derived **18a** was a cooperative model substrate, no conditions were found by which **19b–d** would form. Because the characterization and mechanistic studies of indolo[2,3-*b*]carbazoles are secondary objectives, no further work was performed on this topic.

Scheme 53. (a) The preparation of 1,2,3,4-tetrahydrocarbazole (**19a**); (b) indolo[2,3-b]carbazoles **19b–d** were not observed.

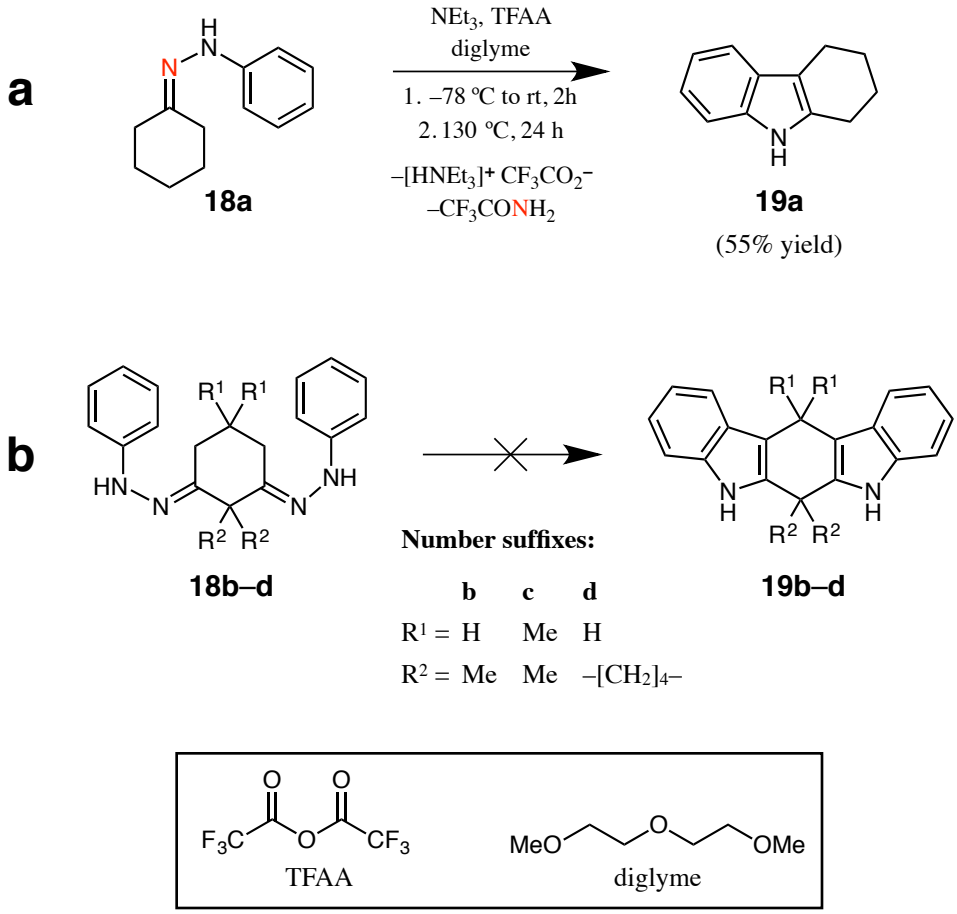

1.8. Conclusions

A series of condensation reactions was performed between indole (**1**) and cyclic ketones with ring sizes ranging from 4 to 12 (**2d–l**). Cyclononanone (**2i**, 18% yield) and cyclodecanone (**2j**, 31% yield) were prepared from cycloheptanone (**2g**) and cyclooctanone (**2h**), in four- and five-step ring-expansion sequences, respectively. The other ketones were used from inventory or as purchased. Paraformaldehyde (**2a**), acetone (**2b**), and acetophenone (**2c**) were used as benchmark ketones. Phosphoric, boric, acetic, trifluoroacetic, hydrochloric, and toluene-4-sulfonic acids were the catalysts that were used in this study.

Bisindoles **7a–l** were successfully obtained. The recommended conditions for preparing each of them are shown in Table 10. All of these bisindoles were solids. Bisindoles **7a**, **7d**, **7i**, and **7j** were air-sensitive.

Table 10. The recommended conditions for preparing bisindoles **7a–l**.

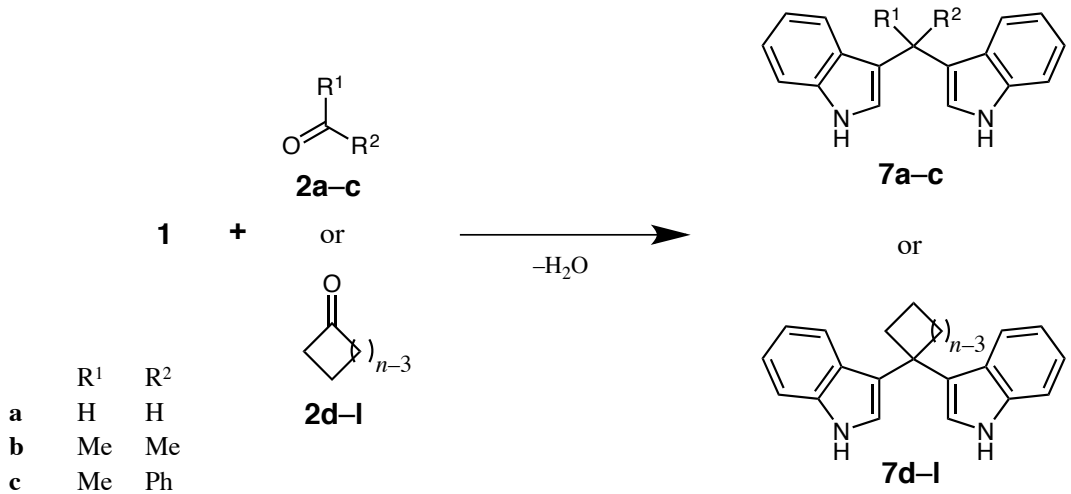

ketone	conditions	product	yield %
formaldehyde (**2a**)	AcOH, rt, 3 d	**7a**	96
acetone (**2b**)	excess **2b**, TFA, rt, 6 h	**7b**	76
acetophenone (**2c**)	TFA, EtOH, reflux, 3 d	**7c**	72
n = 4 (**2d**)	AcOH, 60 ºC, 24 h	**7d**	64
n = 5 (**2e**)	H_3BO_3, toluene, reflux, 5 d	**7e**	29
n = 6 (**2f**)	HCl, EtOH, 0 ºC, 10 min	**7f**	98
n = 7 (**2g**)	AcOH, reflux, 2 d	**7g**	70
n = 8 (**2h**)	AcOH, TsOH•H_2O, reflux, 2 d	**7h**	39
n = 9 (**2i**)	AcOH, TsOH•H_2O, reflux, 7 d	**7i**	6.5
n = 10 (**2j**)	TFA, 50 ºC, 17 d	**7j**	12
n = 11 (**2k**)	TFA, 50 ºC, 14 d	**7k**	11
n = 12 (**2l**)	TFA, 50 ºC, 3 d	**7l**	37

At least one additional product was obtained from each cyclic ketone (Table 11), except **2i** and **2j**, from which no promising NMR signals were observed. Biindolyl **6** was prepared by an alternate synthesis, and was used for the preparation of **11h** and **12h**. Overall, these findings point to 2:2 indole-ketone condensation being the dominant pathway for the smaller cyclic ketones (**2d–f**). The larger cyclic ketones (**2g–l**) react more slowly. Following 2:1 condensation, the dominant pathway is autoxidation of dimer **4** to biindolyl **6**, leading to products **10–13**. Diazepine derivative **12h** was also prepared in two steps from biindolyl (**6**) in 22% yield. Cyclododecanone (**2l**) gave the largest variety of products, including one which remains to be identified.

Table 11. A summary of the 2:2 and related condensation products that were obtained from one-pot reactions with indole and cyclic ketones.

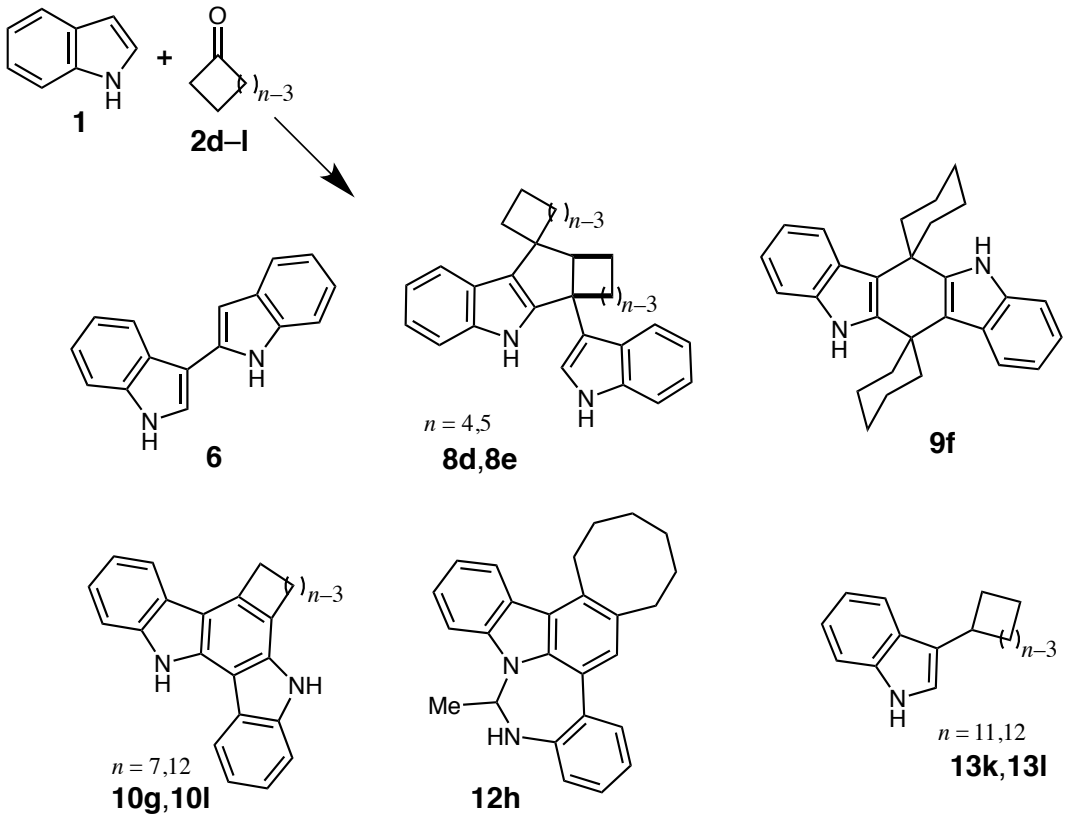

ketone	conditions	product	yield %
n = 4 (**2d**)	HCl, EtOH, rt, 5 d	**8d**	41
n = 5 (**2e**)	HCl, excess **2e**, 75 °C, 5 d	**8e**	48
n = 6 (**2f**)	HCl, MeCN, reflux, 24 h	**9f**	34
n = 7 (**2g**)	TFA, EtOH, 50 °C, 3 d	**10g**	4.4
n = 8 (**2h**)	TFA, EtOH, 50 °C, 8 d	**6**	4.5
		12h	2.1
n = 11 (**2k**)	TFA, 50 °C, 14 d	**6**	8.5
		13k	5.8
n = 12 (**2l**)	TFA, 50 °C, 7 d	**10l**	4.1
	AcOH, TsOH•H_2O, 50 °C, 15 d	**13l**	4.8

The major products that were obtained from reaction conditions of increasing harshness are summarized in Fig. 23. This is a qualitative guide, and the results will vary depending on concentration, acidity, and temperature. The ketones are arranged by increasing activation required to promote condensation with indole. Formaldehyde (**2a**) readily condenses with indole in the presence of mild acids, and tends to give complex mixtures in the presence of acids stronger than AcOH. The remaining small ketones (**2b–f**) have relatively wide windows within which 2:1 and 2:2 condensation products can be obtained. The exception is cyclopentanone (**2e**), which has an unusually low barrier to 2:2 product formation, and to the generation of tarry mixtures. Bisindole **7e** forms more slowly than the other small bisindoles (**7a–f**). Cyclobutanone (**2d**) also exhibits these behaviors to a smaller extent. In the order shown, cycloheptanone (**2g**) and larger ketones (**2h–l**) have a rapidly increasing barrier to 2:1 condensation, and also have a decreasing barrier to the formation of tarry mixtures. Thus, the latter entries in this sequence are challenging substrates. When performing NMR analysis of these reaction mixtures, the signals from indolyl C-2 and C-3 protons on monosubtituted indoles appear as low-*J*-value doublets (J = 1–2 Hz). These signals stand out, and their chemical shifts can be used to quickly identify some of the mixture components.

Fig. 23. A summary of the major products that can be obtained from the given conditions. Entries in parentheses are reported in the literature [37, 38, 39].

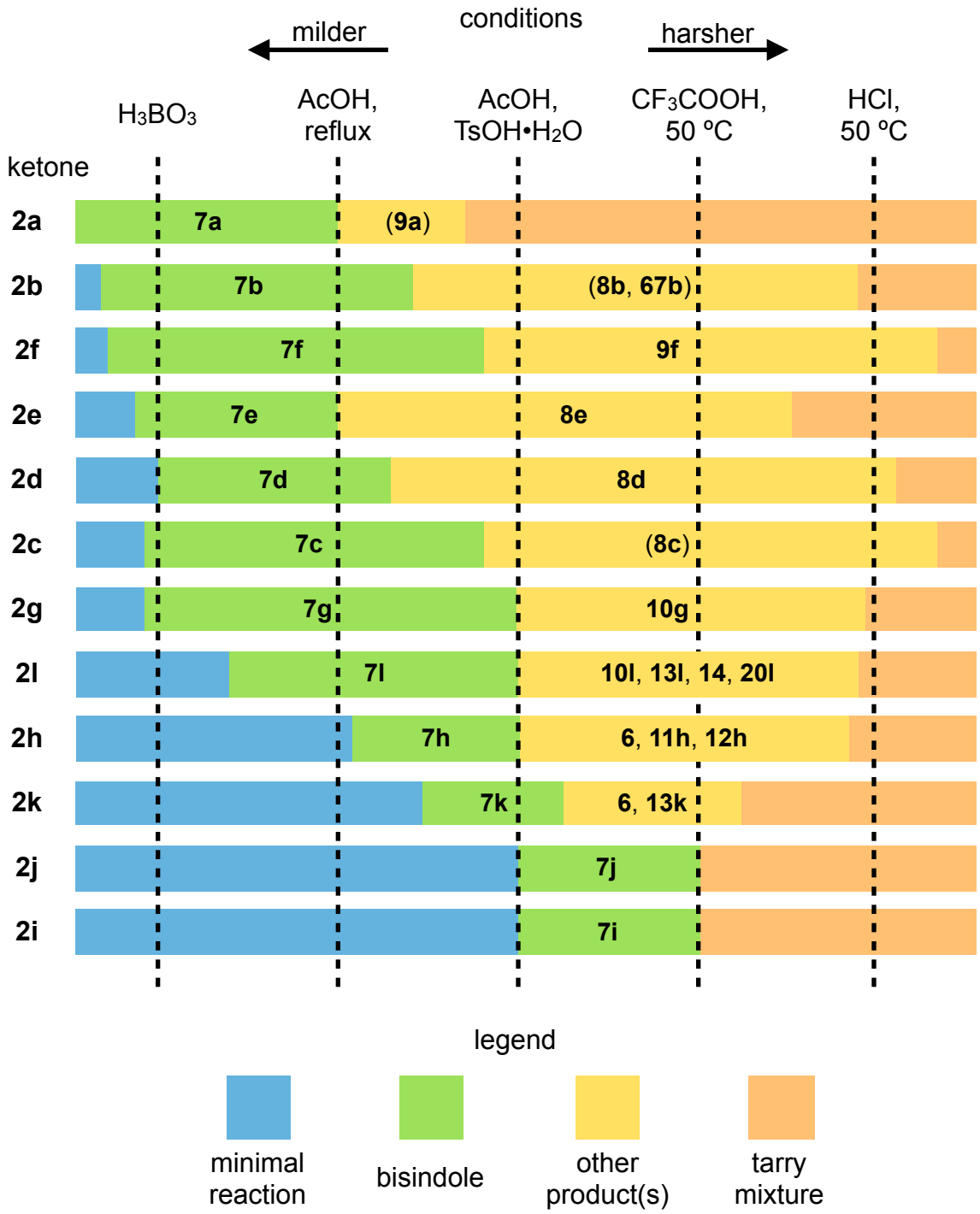

Attempts to prepare several analogs (**19b–d**) of postulated 2:2 product **68f** were unsuccessful (Fig. 24). Thus, the mechanism of the formation of 2:2 product **9f** was not explored.

Fig 24. Compounds **19b–d**, which were not obtained, were the main synthetic targets in the project described in § 1.7. One of the goals was to determine whether **68f** is a synthetic intermediate to **9f**.

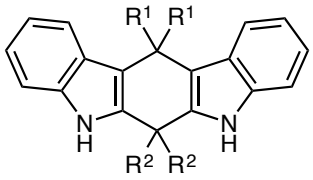

19b–d

not obtained

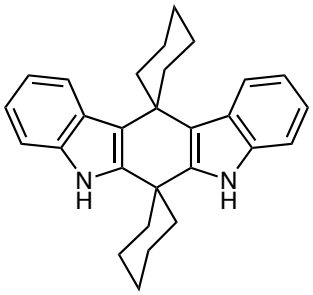

68f

postulated

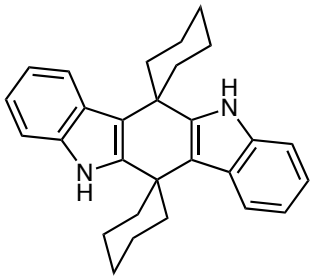

9f

Number suffixes:

	b	**c**	**d**
R^1 =	H	Me	H
R^2 =	Me	Me	$-[CH_2]_4-$

During the course of the research performed in §§ 1.1–1.7, eleven undergraduates made contributions in volunteer, fellowship-sponsored, and for-credit positions. All of the former undergraduates have co-authored an article, or are on track for co-authorship. The mentorship objective was successfully fulfilled.

1.9. Prospective Future Work

Based on the diversity of products that were obtained from indole (**1**) and cyclododecanone (**2l**), continued experimentation with **2l** may unlock additional clues to the underlying indole-ketone condensation chemistry. While this subject is promising, the most attractive extension to the present scope of research would be a series of condensation reactions between biindolyl (**6**) and various ketones (Scheme 54). Even though cyclooctanone (**2h**) was a

challenging substrate in indole-ketone reactions, **2h** performed well in condensations with **6**. Thus, a wider range of ketones may behave well in reactions with **6** than with indole.

Scheme 54. A proposed project that primarily explores cyclizative condensation reactions between ketones (**2a–n**) and biindolyl **6**.

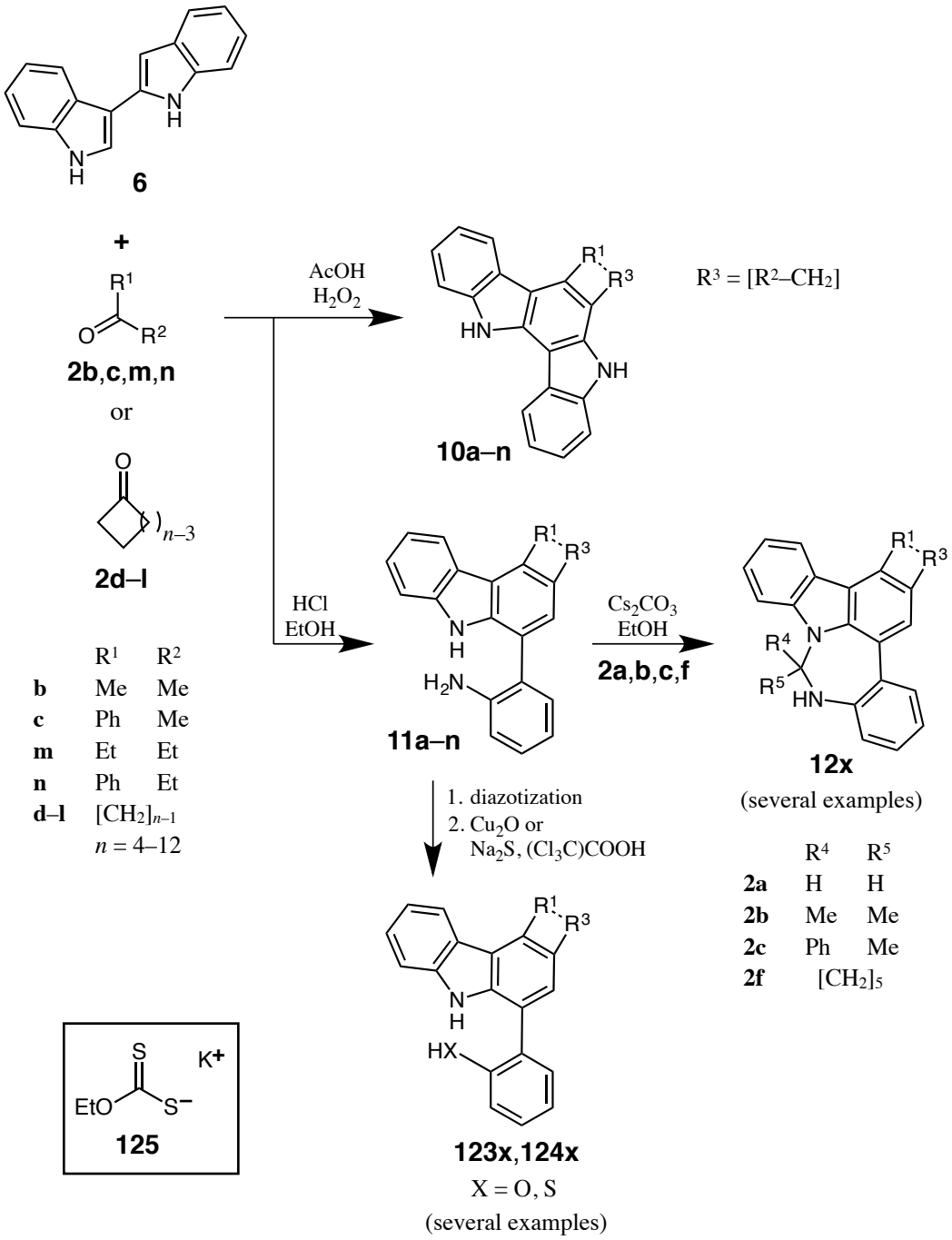

Although Bergman and coworkers performed several studies involving the preparation of indolocarbazole derivatives from **6** and similar substrates [35, 62, 66], they reported only one example of products of type **10**. Carbazolylaniline **11h** in the present work is the only known example of type **11**. The work described in Scheme 54 would allow for exploration of the ranges of substrates and conditions that can be used to prepare type **10** and type **11** products. Additionally, type **11** products could be subjected to a second condensation, potentially giving a range of type **12** products. Lastly, the amino group in carbazolylanilines (**11**) could be replaced *via* diazotization to give oxy- and thio-products of type **123** and **124**. Potassium ethyl xanthate (**125**) might be more suitable than sodium sulfide for substitutive thioation [73]. With a careful choice of ketones (**2a**–**n**), this entire project could be performed with no diastereomerism, simplifying separations.

Part II. Synthesis and Crystallographic Study of 2,6-Dihalobenzonitriles and Isocyanobenzenes

2.1. Background: Crystallography of 2,6-Dihalobenzonitriles and Isocyanobenzenes

2.1.1. Nitriles

Professor Emeritus Doyle Britton (1930–2015) [74] was interested in the crystallographic properties of substituted 2- and 4-halobenzonitriles. His goal was to expand foundational knowledge on the topic. During six decades of research, he published at least 31 articles on this subject [75]. Crystals composed of ribbons or sheets of hydrogen-bond-like interactions are generally of crystallographic interest [76b], including those obtained from halogenated nitriles [77]. Many crystalline 2-halobenzonitriles form short contacts [78] between the cyano N atom(s) and halo (F, Cl, Br, or I; a.k.a. X) atom(s). These contacts can be envisioned as weak pseudo-hydrogen bonds, where C–CN...X is analogous to O–H...O (Fig. 25). Pseudo-hydrogen-donor behavior is displayed by the *ipso* atom [79b, 80]. The X atom serves as the pseudo-hydrogen acceptor.

Fig. 25. (a) Hydrogen bonding between two molecules of methanol; (b) pseudo-hydrogen bonding between two molecules of a 2-halobenzonitrile. Dashed lines depict the hydrogen and pseudo-hydrogen bonds.

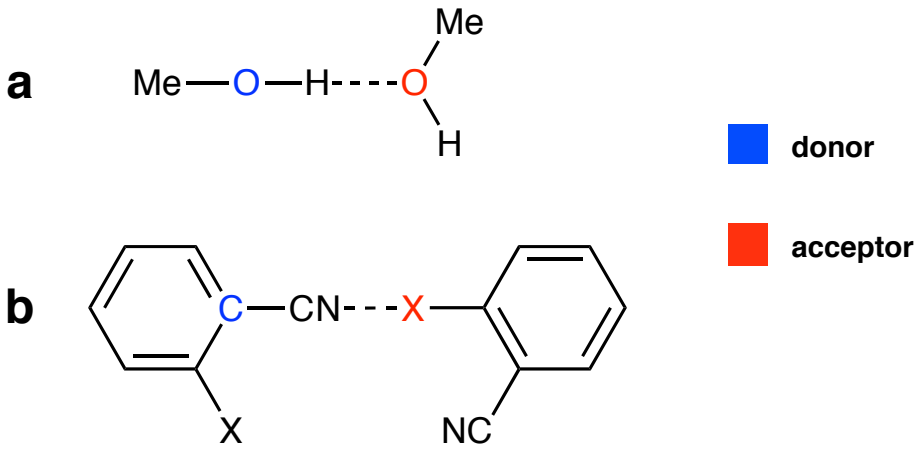

Short contacts of this type are often observed in pairs, forming inversion dimers [81], as was found in a crystal of 2,4,6-trichlorobenzonitrile (**204ba**, Fig. 26a) [82, 83]. For each dimer, bonds and contacts collectively form $R_2^2(10)$ rings [76] about an inversion or pseudoinversion center [84]. To simplify the discussion, rings of this type are herein called Type 1 rings (T1r).

Fig. 26. Examples of Type 1 crystallographic features: (a) A Type 1 ring formed by nitrile **204ba**, viewed along {4a, 0, c}; (b) a Type 1 ribbon formed by nitrile **214d**, viewed along {a, 0, –2c}; (c) a Type 1 sheet formed by dinitrile **210**, viewed along {4a, b, c}. CN...X contacts are shown as blue lines. In the sheet, ribbons are parallel to the purple arrow.

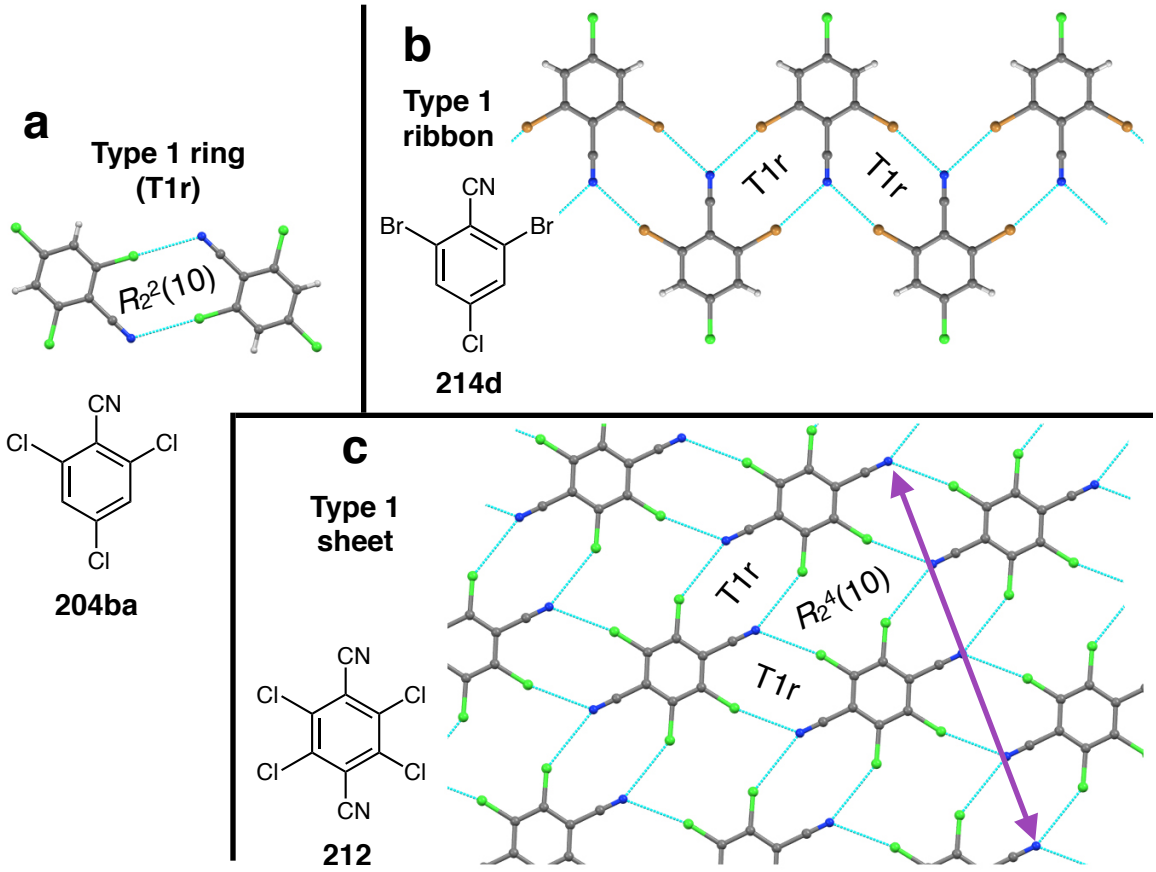

When a second *ortho* halogen atom is present, the cyano N atom may participate in two Type 1 rings. This was observed in **214d** (Fig. 26b) [85], and gives rise to Type 1 ribbons. Although **204ba** has 2 *ortho* Cl atoms, it did not form ribbons; adjacent inversion dimers were mutually rotated and inclined. Additional contact-forming groups allows the formation of sheet structures, as was demonstrated by 2,3,5,6-tetrachlorobenzene-1,4-dicarbonitrile (**212**, Fig. 26c) [86]. In this crystal of **212**, each molecule participated in two Type 1 ribbons, one passing

through each cyano N atom. This arrangement formed $R_2^4(10)$ rings between adjacent molecules of **210**, and thus each N atom participated in three rings.

Sheets can also form by other combinations of CN...X contacts. Two examples were of particular interest to Dr. Britton. First, in a crystal of 2,4,6-tribromobenzonitrile (**204ca**), sheets formed that were composed entirely of Type 1 ribbons (Fig. 27) [82]. In this sheet structure, adjacent ribbons are translated laterally (vertically as illustrated), and there are no short contacts between them. Sheets of this type are herein called Type 2 sheets.

Fig. 27. The Type 2 sheets that were observed in a crystal of **204ca**, viewed along {a, 0, –c}. CN...Br contacts are shown as blue lines.

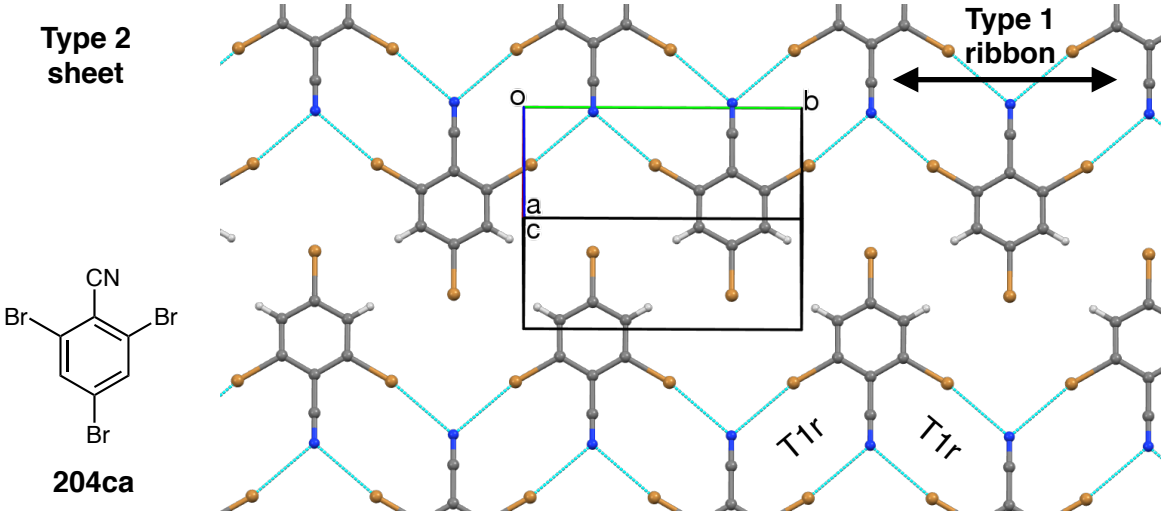

Dr. Britton wanted to find more examples of Type 2 sheets, and was also interested in searching for new polymorphs of compounds whose crystal structures were already reported. To assist with the process of selecting which nitriles would be synthesized and analyzed in the present work, a search of the current version of the Cambridge Structural Database (CSD) [87] was performed. A total of 4,799 entries were found that contained at least one benzonitrile moiety. Type 1 ribbons were only reported from 2,6-dihalobenzonitriles. When the halo atom in question is fluorine, Type 1 features were scarce. Many examples employed the benzonitrile unit as a metal ligand. Although this is a valuable application for substituted benzonitriles [88], metal coordination with the cyano N atom prevents the formation of Type 1 features. The original set of results was decreased to 54 entries that were 2,6-dihalogenated, had at least one non-fluorine *ortho* halo atom, and no metal coordination. These included four that were published from the present work during the preparation of this dissertation [79b].

The remaining 50 entries consisted of various solvates and polymorphs of 18 nitriles. The occurrence of Type 1 crystallographic features, polymorphism, and disorder is listed in Table 12. The relative frequency of disorder does not include rotamerism of simple functional groups (*e.g.*, methyl group rotation) or positioning of solvent molecules that does not appreciably affect the contact geometry between nitrile molecules.

Table 12. Type 1 CN...X contact features, polymorphism, and frequency of disorder reported in selected 2,6-dihalobenzonitriles in the Cambridge Structural Database.

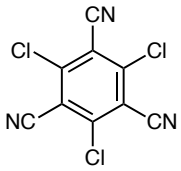

210

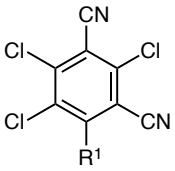

211a–c

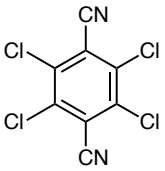

212

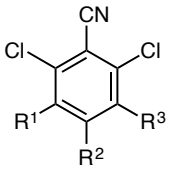

204ba,**bc** or **213a–d**

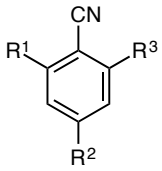

204ca,**cb** or **214a–e**

compd.	R^1	R^2	R^3	Type 1 rings	Type 1 ribbons	Type 1 sheets	disorder freq.	polym-orphism	ref.
210	-	-	-	Y	Y	Y	low	Y	89
211a	Cl	-	-	Y	Y	Y	high	Y	90
211b	I	-	-	Y	Y	Y	high	N	91
211c	SMe	-	-	N	N	N	none	N	92
212	-	-	-	Y	Y	Y	high	Y	86
213a	H	H	H	N	N	N	none	Y	93
204ba	H	Cl	H	Y	N	N	none	Y	94
213b	H	Br	H	N	N	N	none	N	95
204bc	H	CO_2H	H	N	N	N	none	Y	96
213c	H	OH	$CONH_2$	Y	N	N	none	N	97
213d	Cl	SMe	Cl	N	N	N	none	N	98
214a	F	H	I	N	N	N	none	N	95
214b	Br	H	Br	N	N	N	none	Y	93
214c	Br	F	Br	Y	N	N	none	N	100
214d	Br	Cl	Br	Y	Y	N	none	N	85
204ca	Br	Br	Br	Y	Y	N	none	N	83
214e	Br	I	Br	N	N	N	none	N	101
204cb	Br	Me	Br	N	N	N	none	N	102

Trends that are observed in these data include the following:

1. Examples with more than one cyano group (**210–212**) are likely to crystallize with Type 1 features, but they are also likely to give disorderly crystals. By contrast, no disorder was observed in any monocyano entry.
2. Non-planar polyatomic functional groups, including CH_3, are disruptive to Type 1 features. In all 3 examples listed (**211c**, **213d**, **204cb**), the vertical space occupied by the nonplanar group forces neighboring molecules into mutually inclined planes.
3. Some planar functional groups, including those that tend to form hydrogen bonds, are compatible with Type 1 features. Example **213c** displays networks of hydrogen-bond dimerization that support Type 1 rings. Carboxyl example **204bc** is discussed below.
4. 4-Hydro groups (**213a**, **214a**,**b**) are disruptive to Type 1 features. In all 3 examples, at least one polymorph is reported where the CN group sits in the void that would be occupied by a larger 4-substituent. Thus, the CN group is not able to contact more than 1 halo atom.
5. 2,4,6-Trihalomononitriles are very likely to give Type 1 rings and ribbons. However, they cannot form Type 1 sheets due to a lack of acceptors. 4-Iodo example **214e** is unique. It does not form Type 1 rings, even though it has no non-planar or hydro groups. However, **214e** forms sheets of another type, in spite of having a 3:1 acceptor:donor ratio.
6. Examples that feature iodine are scarce. All three examples (**211b**, **214a**, **214e**) incorporate CN...I contacts, including 4-hydro example **214a**. The larger contact radius and softer character of iodine probably facilitates the formation of short contacts in the presence of a wider range of substituent combinations.
7. Type 1 ribbons are only reported from molecules that have at least one vertical mirror plane.

The second area of Dr. Britton's interest was to expand upon his 2012 article on 3,5-dichloro-4-cyanobenzoic acid (**204bc**) [96]. In a 2:1 co-crystal of **204bc** with anthracene (**215a**), a honeycomb-like sheet structure was observed in which each molecule of **215a** was circumscribed by six molecules of **204bc** (Fig. 28a). Sheets with this general arrangement of cyano acid and anthracene molecules are herein called Type 3 sheets.

Fig. 28. (a) The Type 3 sheets observed in a 2:1 co-crystal of **204bc** with **215a**, viewed along {2a, 8b, –c}; (b) the envisioned Type 3 sheets with two Type 1 rings per N atom; (c) naphthalene (**39**), for comparison.

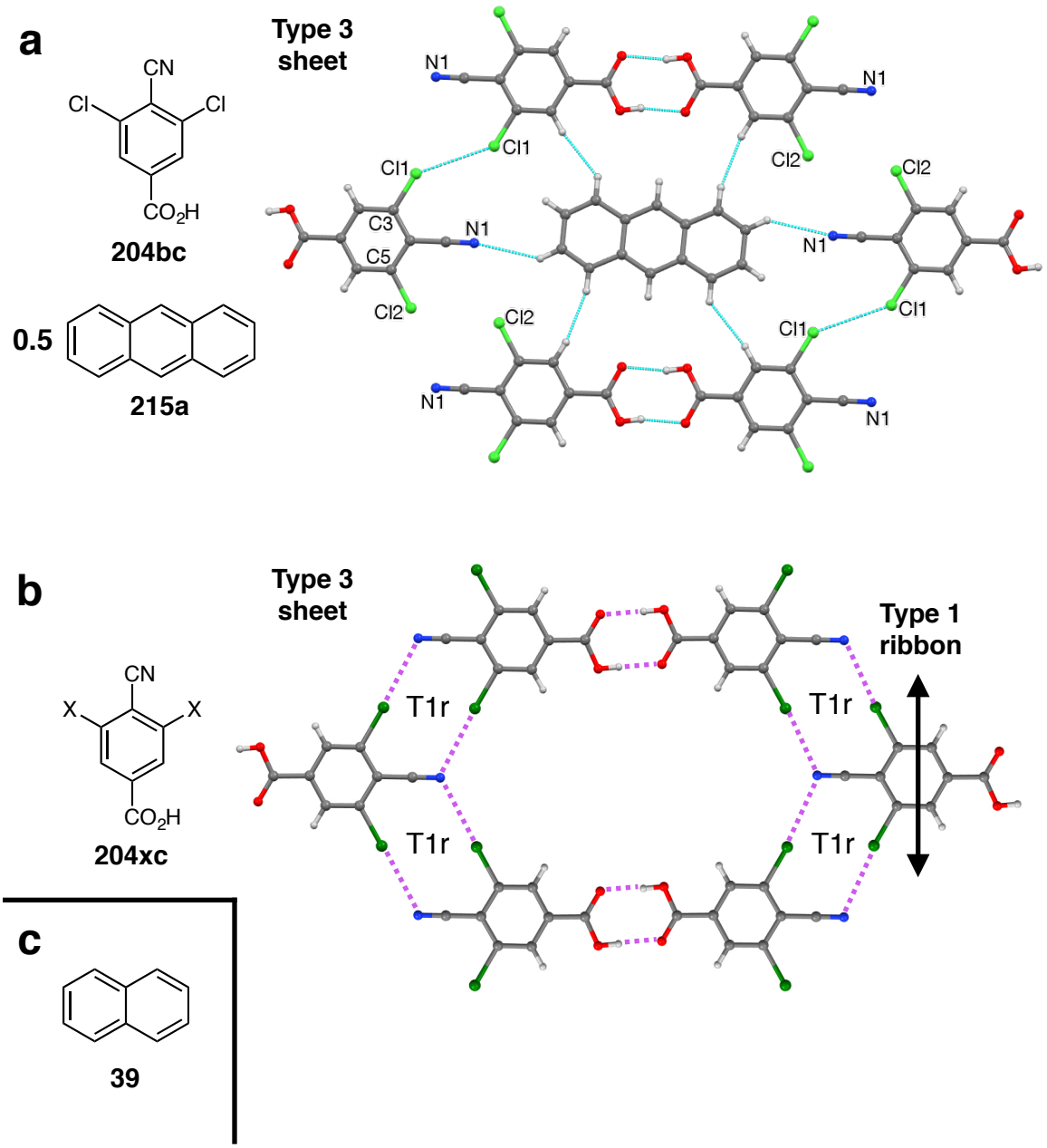

Dr. Britton envisioned that similar Type 3 sheets might be made, in which Type 1 rings form between all laterally adjacent nitrile molecules (Fig. 28b). In the second sheet structure, Type 1 ribbons are formed roughly orthogonal to the axes of the carboxyl hydrogen bonds. Essentially, this envisioned Type 3 sheet is a Type 2 sheet in which alternating ribbons have been flipped, and then the ribbons are connected with hydrogen bonds.

Two strategies for tuning the observed Type 3 sheets (Fig. 28a) are to find a substitute for anthracene (**215a**) that occupies a smaller area, or to find a substitute for nitrile **204bc** in which cyano-halo contacts can bridge a longer gap. The easier of the two options was to recrystallize **204cc** with naphthalene (**39**, Fig. 28c). In the resulting Type 3 sheets, no Type 1 rings formed [96]. Instead, an additional set of Cl...Cl contacts formed between pairs of atoms similar to Cl2 in Fig. 28a. Thus, it was the width of the anthracene molecule, not the length, that was preventing the envisioned Type 3 sheets from forming.

In the observed Type 3 sheet (Fig. 28a), the average gap between Cl and N atoms was 3.693 Å. If Br atoms were substituted for the Cl atoms in **204bc**, this gap should shrink. Based on the difference in atomic contact radii for Cl and Br, a simple predicted estimate of the resulting gap is 3.502 Å (Table 13) [103]. CN...Br short contacts can form across gaps smaller than 3.46 Å [78b]. If I atoms are used, the gap would shrink to roughly 3.243 Å by the same type of estimation [103], while CN...I short contacts can form across gaps of up to 3.61 Å. Therefore, diiodo cyano acid **204dc** is likely to form sheets of this type, if 2:1 co-crystals with **215a** can be obtained. Dibromo counterpart **204cc** is likely to be a borderline case, and might only form one half of the envisioned array of Type 1 rings.

Table 13. In Type 3 sheets, a comparison of the sum of N and X atomic contact radii with the observed (**204bc**) and predicted (**204cc**,**dc**) gaps between N and X atoms.

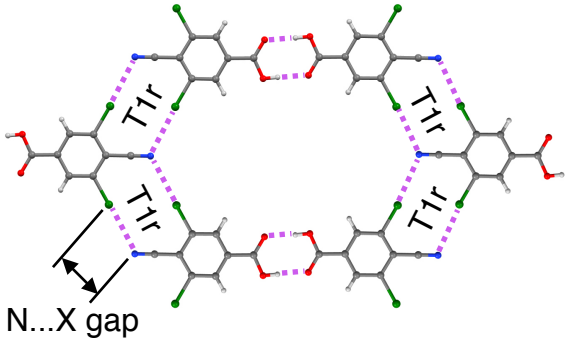

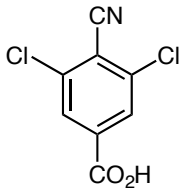

204bc

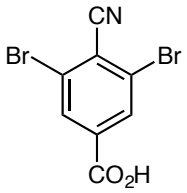

204cc

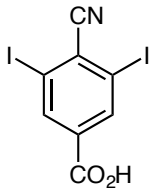

204dc

feature	observed	predicted	
	X = Cl	X = Br	X = I
N+X contact radius (Å)	3.35	3.46	3.61
N...X gap (Å)	3.693	3.502	3.243
difference (Å)	– 0.34 (gap)	– 0.04 (smaller gap)	+ 0.37 (contact)
Type 1 rings	none	possible	likely

2.1.2. Isocyanides

Halogenated nitriles and their corresponding isocyanides display nearly identical crystallographic properties. The isocyano C–NC unit acts as a slightly better pseudo-hydrogen-bond donor. Like their benzonitrile counterparts, 2,6-dihalo-1-isocyanobenzenes (non-systematic name) [104] have application as metal ligands [88], and those with at least one non-fluorine *ortho* halogen, and no metal coordination are of interest to the present work. Only two corresponding entries were found in the current version of the CSD [87] (Table 14). Neither polymorphism nor disorder was reported for either example.

Table 14. Type 1 NC...X contact features observed in selected 2,6-dihalo-1-isocyanobenzenes in the CSD.

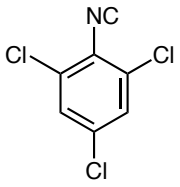

209ba

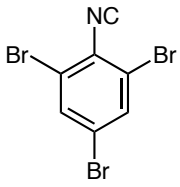

209ca

compd.	Type 1 rings	Type 1 ribbons	Type 1 sheets	ref.
209ba	Y	N	N	94
209ca	Y	Y	N	105

Although corresponding nitriles and isocyanides are almost perfectly isosteric and isoelectronic, small crystallographic differences can be expected. This outcome was reported for trichloro nitrile **204ba** and isocyanide **209ba**. Both formed $Z = 4$ monoclinic crystals in the $P2_1/c$ space group, with respective unit cell volumes of 794 and 819 Å^3. The molecules had nearly identical contacts (centric Type 1 ring dimers). The main difference was the shear angle (β = 90.1°, 97.2°, respectively), which is the main cause of isocyanide **209ba** occupying a slightly larger volume. Overall, the crystals were roughly isomorphous.

However, an unexpected result was reported for tribromo nitrile **204ca** and its isocyanide (**209ca**). Both formed Type 2 layers, so they would be expected to have nearly identical unit cells. Surprisingly, nitrile **204ca** formed $Z = 2$ monoclinic $P2_1/m$ crystals [82], and isocyanide **209ca** formed $Z = 8$ orthorhombic Pnma crystals [105]: a different space group and crystal system, and a unit cell larger by a factor of 4.

The cause of these major unit cell differences is the Type 2 layers stacking by two different patterns (Fig. 29). Each pair of adjacent layers in nitrile **204ca** stacked translationally (TT-stacking), whereas pairs of adjacent layers in isocyanide **209ca** stacked in an alternating pseudotranslational and pseudocentric array (TC-stacking).

Fig. 29. (Pseudo)translational and (pseudo)centric stacking of Type 2 layers. (T) Translational stacking between all adjacent layers of nitrile **204ca**, viewed along {2a, 0, –c}. (C) Pseudocentric stacking observed between alternating adjacent layer pairs of isocyanide **209ca**, viewed along {a, 0, 0}.

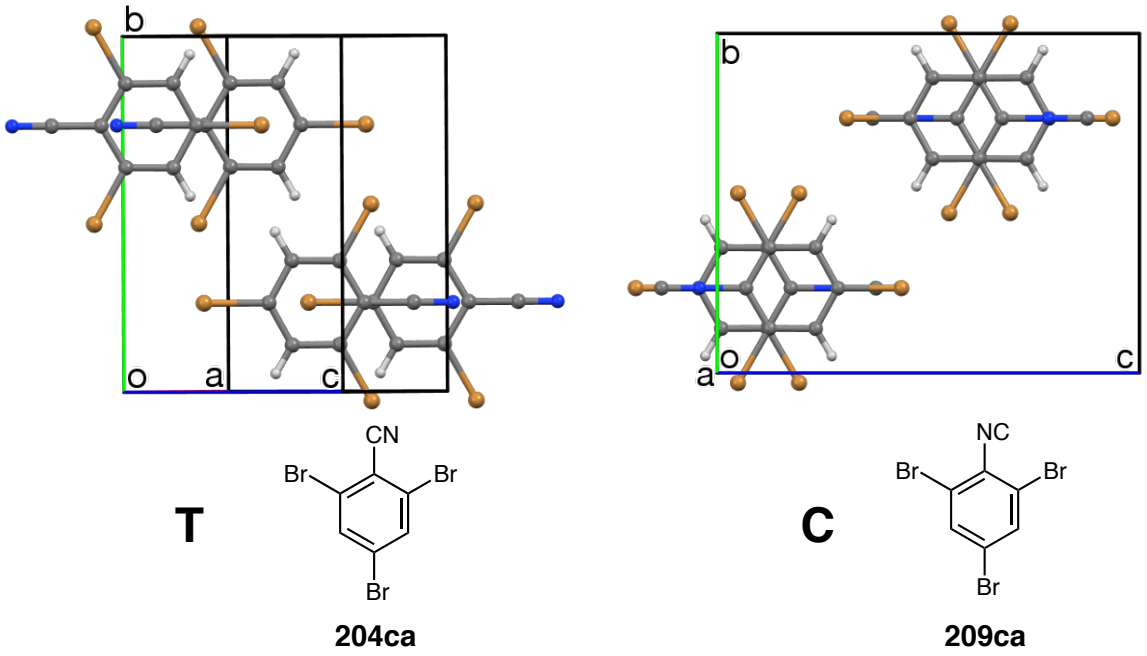

Polymorphs of this sort, composed of identical layers but different in layer stacking, are known as polytypes. Polytype organic crystals have historically been very scarce, but several examples have recently emerged [106]. It seemed plausible that growing crystals of **204ca** and **209ca** in varying conditions may give rise to previously unreported stacking patterns: TC crystals of nitrile **204ca**, TT crystals of isocyanide **209ca**, CC crystals, or other new polytypes. The prospects of finding new examples of organic polytypism arising from compounds that crystallize into Type 2 layers was the primary motivation for Dr. Britton's interest in finding more examples of this layer structure.

2.2. Background: Synthesis of 2,6-Dihalobenzonitriles and Isocyanobenzenes

2.2.1. Benzonitriles (General)

The Sandmeyer reaction (diazotization of aniline derivatives, followed by Cu(I)-catalyzed displacement of N_2, Scheme 55) is a widely used method of installing cyano, halo, hydroxyl, hydro, or similar functionality. This reaction sequence was reported by Traugott Sandmeyer [107] in 1884 [108]. Variations of the Sandmeyer reaction have been used for countless synthetic and material applications. The available synthetic transformations include nucleophilic substitution, cross-coupling, redox transformations, arylation, and the preparation of azo derivatives [109]. The intermediate diazonium salts (*e.g.*, **203aa**) can be unstable and are often prone to detonation, especially in the solid phase [110]. Thus, they are usually used *in situ* and in small batches. Some diazonium salts that have non-reducing and non-oxidizing sulfonate or perfluoride anions (*i.e.*, TsO^-, BF_4^-, or PF_6^-) are safe to isolate [111].

Scheme 55. The conversion of aniline (**201aa**) into benzonitrile (**204aa**) is an example of the Sandmeyer reaction.

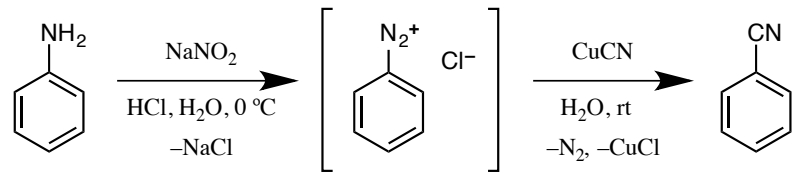

201aa **203aa** **204aa**

The mechanism of diazotization is thought to proceed *via* the *in situ* generation of nitrous acid (**216**) by protonation of aqueous sodium nitrite (Scheme 56). Attack by the aniline N atom at the N atom of **217**, and the subsequent elimination of two water molecules gives diazonium ion **203aa** [112].

Scheme 56. A proposed mechanism for the aqueous-phase diazotization of aniline.

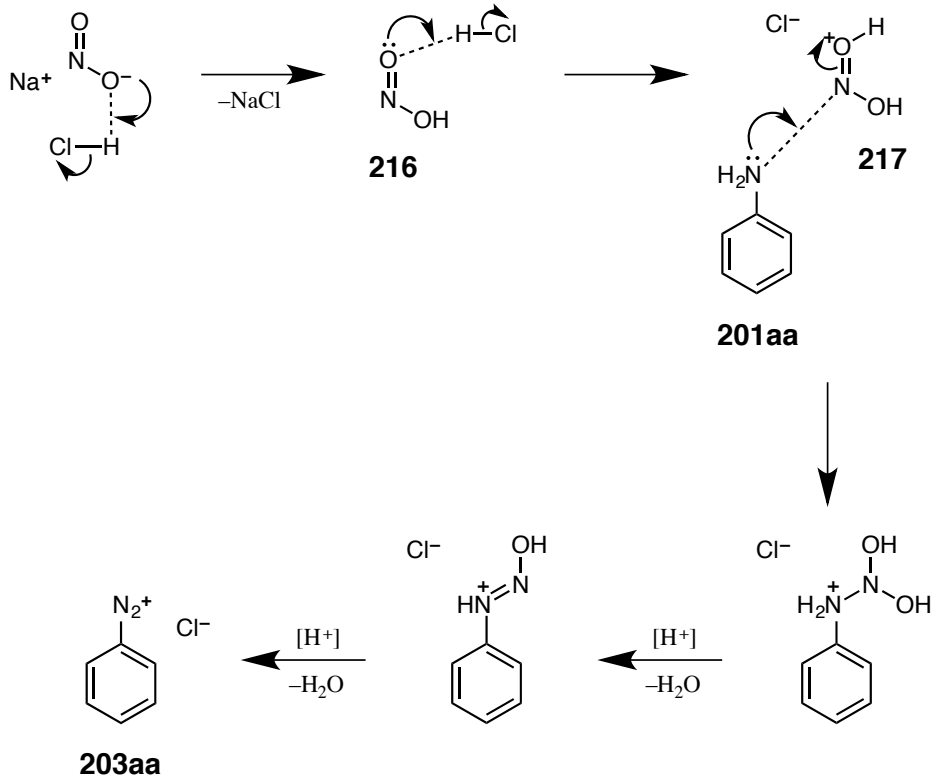

For substrates that have poor water solubility, including some macromolecules, diazotization can be performed in an organic solvent, with 3-methylbutyl nitrite (isoamyl nitrite, IAN) as the nitrous acid precursor [113]. The organic-phase diazotization mechanism is thought to be analogous to that of aqueous-phase diazotization, with nitrous acid generated by acid-catalyzed cleavage of the ester linkage. Diazotization has also been reported to take place with tertiary butyl nitrite in aprotic conditions [114], with diazotization probably mediated by a complex formed by the nitrite ester and Cu(I).

The mechanism of the cyanation stage was originally thought to proceed *via* even-electron intermediates. Studies performed by Waters [115] and Kochi [116] during the mid-twentieth century revealed that the kinetically major pathway is probably one in which the corresponding aryl radical (of type **219**) is formed by a single-electron reduction of the diazoium group in Cu(I) complexes of type **218** (Scheme 57). Loss of N_2 and intra-complex reductive radical abstraction of the CN ligand complete the transformation. It is also possible that the Cu(II) complex dissociates from the aryl radical in **219** and that cyanide abstraction in **220** occurs during a second bimolecular aryl-Cu(II) encounter.

Scheme 57. A proposed mechanism for the Sandmeyer cyanation of diazonium salt **203aa**.

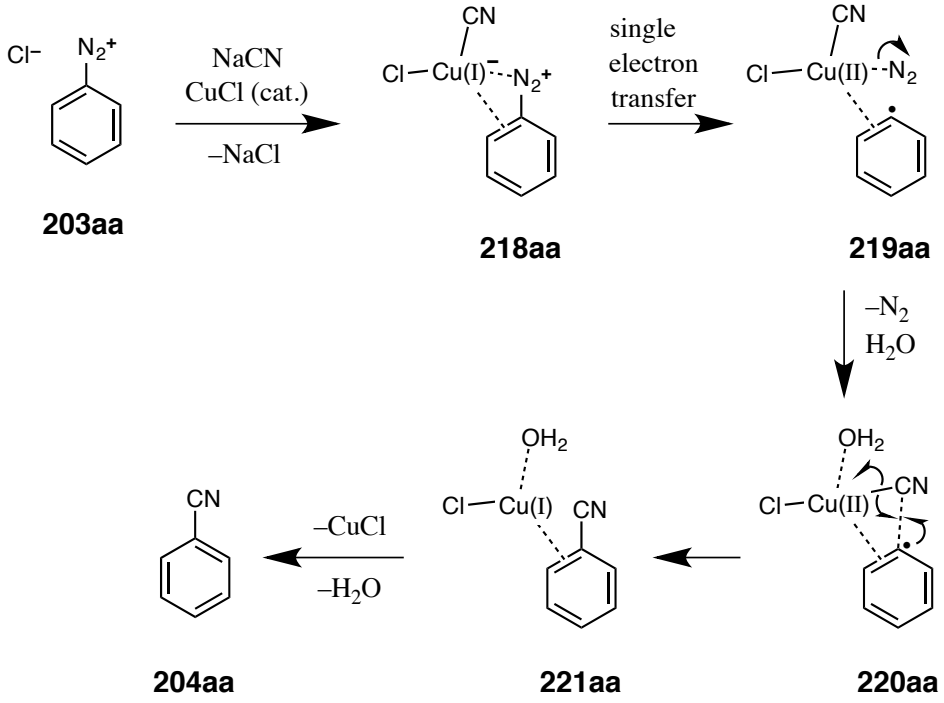

203aa **218aa** **219aa** **220aa** **221aa** **204aa**

Further study of the cyanation mechanism by Hanson, *et al*. [117] found that the CN^- ion has the fastest rate of insertion among nucleophiles commonly used in the Sandmeyer reaction. Thus, the cyanide ligand in radical Cu(II) complex **219** will insert preferentially over halide or aqua ligands. The regeneration of Cu(I) and preferential insertion of cyanide allows for the Cu(I) reagent to be used catalytically, with regeneration of cyanocuprate complexes promoted by other cyanide salts, such as NaCN.

2.2.2. Benzonitriles (2,6-Dihalo)

The majority of the reported preparations of 2,6-dihalobenzonitriles were for crystallographic purposes, and include minimal detail regarding synthetic procedures, characterization data, or yields. Because of the potent electrophilicity of protonated nitrous acid (**217**), 2,6-dihaloanilines were expected to diazotize readily, provided that they could be dissolved in an aqueous or organic nitrite mixture.

However, the cyanation stage was expected to be more challenging. Sterically hindered diazonium groups, such as those sandwiched between two halogen atoms, may tend to strongly favor dissociation of copper complex in **220ca** over radical abstraction of cyanide (Scheme 58). This would result in a buildup of free aryl radical **222ca**, in turn resulting in the increased formation of radical-derived byproducts. This was the case reported by Giumanini *et al*. [114], who obtained nitrile **204ca** in 20% yield, and a combined yield of 52% of radical-derived byproducts.

Scheme 58. A general mechanism for the formation of the radical-derived products reported by Giumanini, *et al.* [114], from their attempted cyanation of diazonium-derived complex **220ca**. Their yields are also shown.

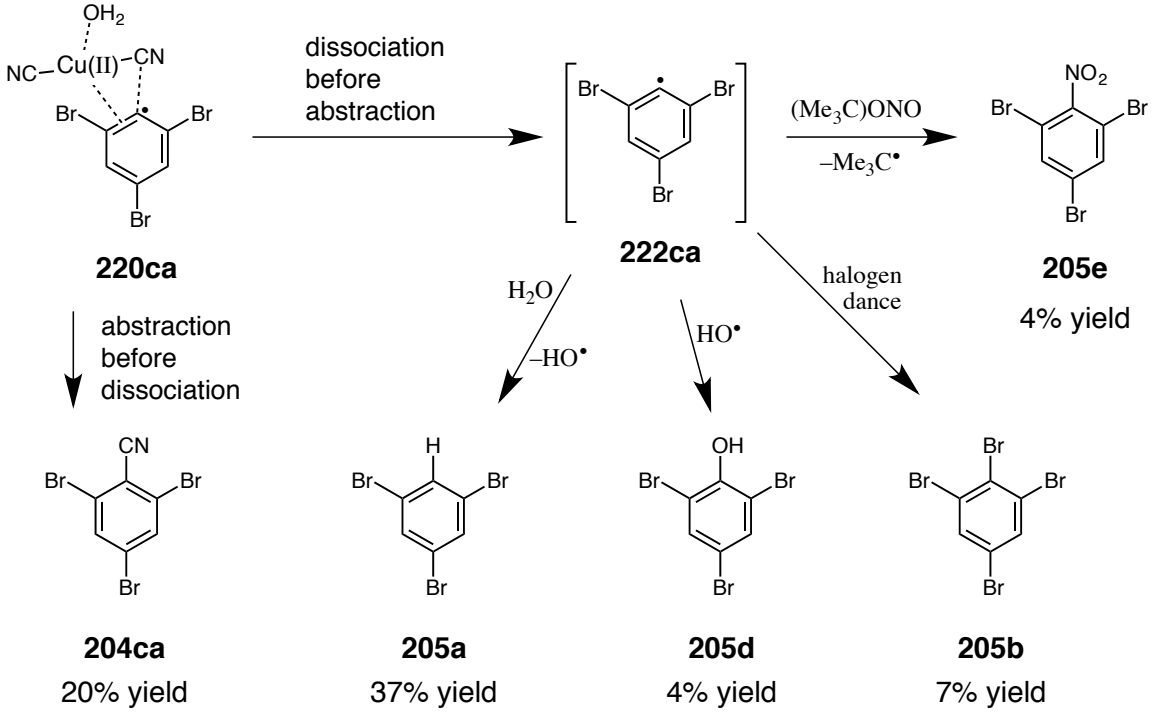

In this research by Giumanini, *et al*. [114], several points are worth noting. First, their study focused on anhydrous and aprotic conditions, so the principal source of hydrogen radicals was probably DMSO. Water is shown in Scheme 58 to depict the typical case, and is applicable to the present work. In an aqueous system, the radicals left over from byproduct formation are probably primarily terminated by the abstraction of hydrogen from water. The resulting hydroxyl radicals quickly oxidize Cu(I) to Cu(II) [117]. The resulting hydroxide ions react with one equivalent of the best available acid (commonly H_2SO_4, HCl, or AcOH). Biradical coupling probably occurs as a secondary termination pathway. This mechanism explains how the observed reduction product (**205a**) formed without a conventional source of hydride. Classically, primary alcohols (which get oxidized to aldehydes) [118] or hypophosphites (*e.g*., H_3PO_2) [119] are used for reductive dediazoniation of aryldiazonium species. Second, compound **205c** is not listed in Scheme 58. Compound **205c** was obtained in the present work, and is discussed in §§ 2.4.3 and 3.4.2, but it was not reported by Giumanini, *et al*.

Third, there is no chloride present in the conditions shown in Scheme 58. The classical conditions (Schemes 55–57) use CuCl. Because of the complexity of the product mixtures that were initially obtained, Giumanini and coworkers wanted to minimize the number of possible nucleophiles. Thus, they replaced CuCl with CuCN, and in some instances, added NaCN. Their plan was to generate sodium dicyanocuprate(I) (Na^+ $[Cu(CN)_2]^-$) *in situ*, increasing the effective nucleophilicity of the cyanide ligands by doubling the number of available CN ligands.

The dicyanocuprate modification to the Sandmeyer reaction was further modified by Toya, *et al*., who performed a Sandmeyer cyanation on 6-methoxybenzothiazol-2-ylamine (**223**, Scheme 59) [120]. Amine **223** was diazotized in an aqueous, mixed-acid system. In diazonium salt **224**, the diazonium group was conjugated with the methoxy group and the thiazole S atom, decreasing its electrophilicity and increasing the stability of the corresponding heteroaryl radical. 6-Methoxybenzothiazole-2-carbonitrile (**225**) was not observed when the cyanation mixture was aqueous CuCN or dicyanocuprate salts, probably a result of dissociation before cyano abstraction, although the products of these experiments were not described.

Scheme 59. The preparation of nitrile **225**, performed by Toya, *et al*. [120].

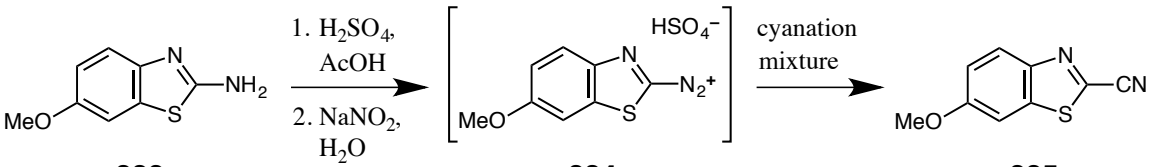

223 **224** **225**

In order to improve the effective nucleophilicity of cyanide in the cyanation mixture, Toya, *et al*. experimented with the addition of various bases. Their best reported results came from the addition of excess sodium bicarbonate to an aqueous solution of $K[Cu(CN)_2]$ (Scheme 60) [121]. To simplify the discussion, the resulting white suspension is treated as an aqueous mixture of sodium bicarbonate and disodium aqua(carboxyloxy)dicyanocuprate(I) (**227**, a.k.a. sodium bicarbonate dicyanocuprate, SBDC).

Scheme 60. (a) The postulated preparation of SBDC, performed by Toya, *et al.*; (b) A possible mechanism for the synthesis of nitrile **204ca**, with SBDC regenerated by the addition of NaCN.

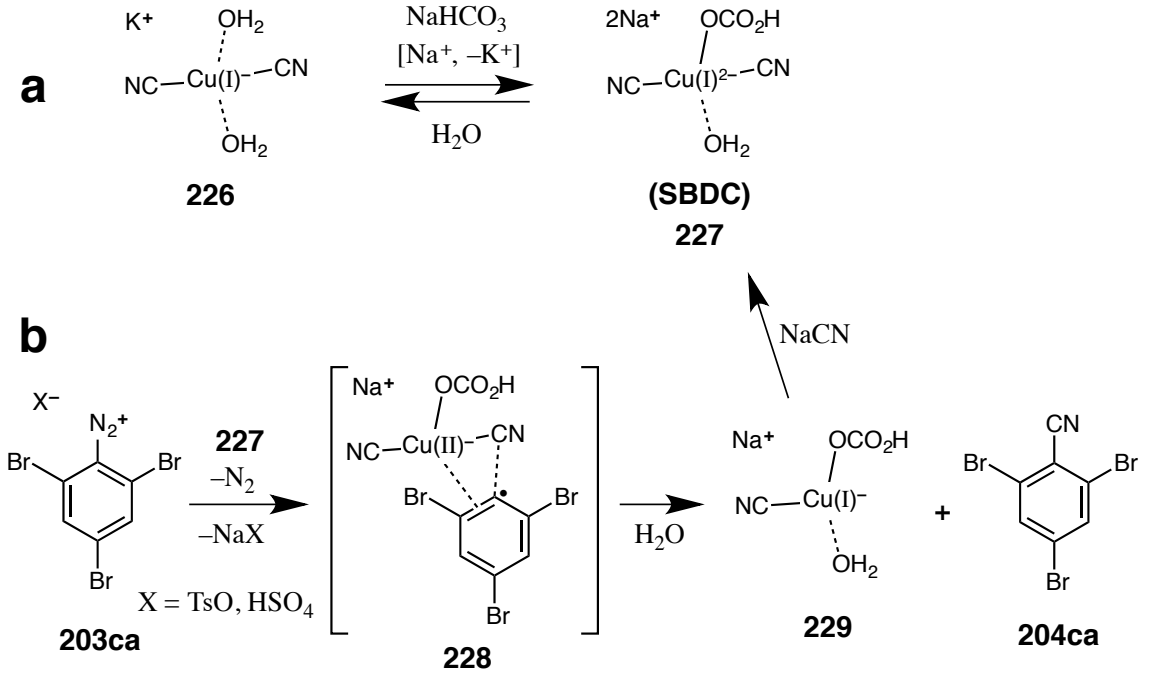

Although there is no direct evidence of SBDC presented in their article, the presence of **227** is a possibility inferred from the substantial increase in yield observed when a supersaturating excess of bicarbonate was used. Nitrile yields were also improved when the cyanation mixture was allowed to incubate in an ice bath for at least one hour prior to use [122]. Although the extent of coordination of bicarbonate with copper is not explored in this dissertation, the mixtures described herein as containing SBDC behave like they contain a cyanation catalyst that is distinctly superior to sodium or potassium dicyanocuprate.

Assuming that the 18-electron rule [123] is applicable, bicarbonate complex **227**, without the aqua ligand, is the postulated form of SBDC that is bound to the substrate during the cyanation portion of the Sandmeyer reaction. The Cu atom in complex **228** carries a charge of –1, enhancing the effective nucleophilicity of the cyanide ligands versus aqua analog **220aa**, which contains a neutral Cu atom. Furthermore, whether or not they are bound to Cu atoms, bicarbonate ions buffer the cyanation mixture pH such that the formation of HCN (a very poisonous gas) is suppressed. In addition to improving the safety of the cyanation reaction, bicarbonate buffering maintains a higher cyanide concentration for a longer interval.

The reported yields of **225** decreased when stronger bases were used instead of sodium bicarbonate. This is probably a result of the substitution of hydroxide for cyanide, giving the corresponding aryl alcohol instead of nitrile **225**.

2.2.3. Isocyanides

When preparing cyano derivatives, the Sandmeyer reaction is specific for the C atom of CN^- acting as the nucleophile. The corresponding isocyanides must be prepared by another route. The two most commonly reported approaches to organic isocyanides are the Hofmann carbylamine reaction and dehydration of primary formamides (Scheme 61) [124].

Scheme 61. The two common preparations of organic isocyanides (**209**) from the corresponding amines (**201**): (a) The Hofmann carbylamine reaction; (b) Synthesis and dehydration of the corresponding formamides. Aniline derivatives are shown; alkyl examples are also reported.

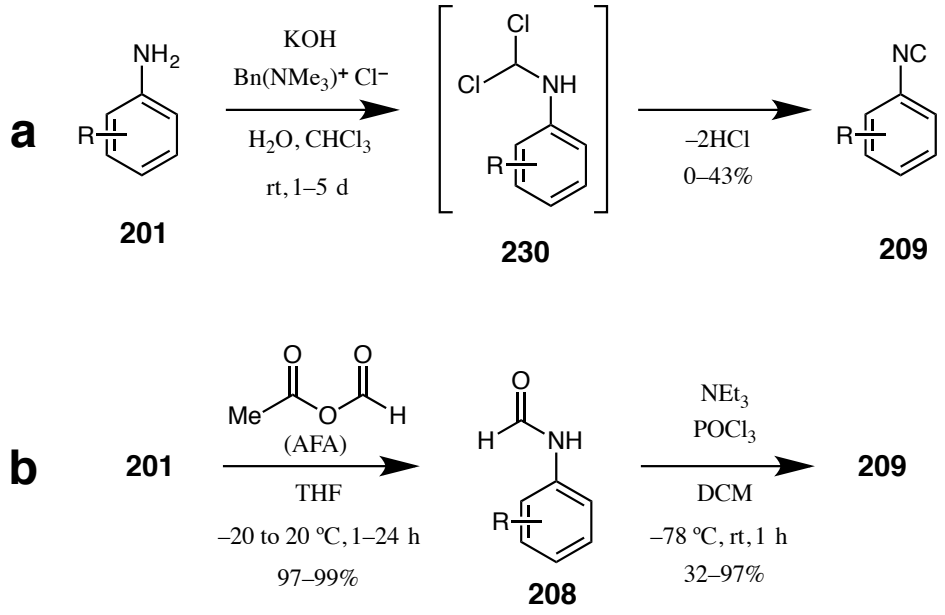

The Hofmann carbylamine reaction, reported in 1867, was used as a qualitative means of detecting primary amines. This was made possible by the one-pot nature of this transformation and the stunningly offensive odor of many organic isocyanides [125]. The reaction begins with the base-promoted conversion of $CHCl_3$ into dichlorocarbene (CCl_2). Addition of amine **201** to CCl_2, followed by a base-catalyzed 1,2-tautomerism gives intermediate **230**. Subsequent β- and α-eliminations of HCl give isocyanide **209**.

As crystallographic, organometallic, and material applications for isocyanides became more prevalent, the need arose for faster, higher-yielding preparations of isocyanides. Many primary amines are readily formylated by acetic formic anhydride (AFA) solution (Scheme 61b). Formic anhydride, $(HCO)_2O$, is too unstable to be synthetically useful. AFA solution has a shelf life of

several hours, and strongly favors formylation over acetylation, provided that the acylation is carried out at a sufficiently low temperature [126]. In cases where acetylation competes with formylation, a more hindered acyl component can be substituted for the acetyl group (*e.g.*, formic pivalic anhydride) [127].

Once suitable formylation conditions have been established for a given amine, the corresponding formamide is generally available at high yield and purity. Formamides generally have much lower solubility than their parent amines, and can usually be isolated by fractional crystallization.

Various acyl chlorides have been shown to efficiently dehydrate formamides to the corresponding isocyanides [124]. Phosgene ($COCl_2$) often gives the highest yields, however, phosphoryl chloride ($POCl_3$) is the most popular compromise between yield and safety, usually giving yields only slightly lower than phosgene. Although dehydration proceeds in the absence of base, most isocyanides are extremely sensitive to acid-catalyzed hydrolysis, and would revert back to the formamide during work-up. Triethylamine is the most commonly used base for this preparation.

The crystallographic samples of trichloro- and tribromoisocyanides **209ba**,**ca** that were reported in the literature (Table 14, p 107) were prepared by the Hofmann carbylamine reaction. The yields were not specified, however, they were probably less than 1%. Mironov & Mokrushin prepared both of these isocyanides by both synthetic methods described in Scheme 61 [128]. They obtained superior results from formylation-dehydration.

2.2.4 Halogenation of Anilines

Like many simple examples of electrophilic aromatic substitution, halogenation of anilines is a synthetic transformation that can be found among the oldest entries in organic chemistry literature [129]. Many moderately electrophilic halogen synthons can be used for this purpose, including molecular chlorine or bromine. *N*-Halogenated nitrogen heterocycles are also commonly used (*e.g.*, *N*-chlorosuccinimide) [130]. Because the amino group in aniline is electron-releasing, and halogen synthons are electrophilic, direct halogenation of anilines occurs at the 2, 4, and 6-positions. The easiest halogenations to perform on aniline or 4-substituted anilines are those in which excess halogenating agent may be used. This eliminates the problems of obtaining a mixture of dihalogenated and unreacted anilines when only one equivalent of halogenating agent is used and separating mixtures of regioisomers. Thus, 2,4,6-trihaloanilines are the easiest halogenated anilines to obtain from plain aniline, and 2,6-dihaloanilines from 4-substituted anilines. Conveniently, these have a vertical mirror plane, a desirable feature for Type 1, 2, and 3 ribbons and sheets in crystals of the corresponding nitriles and isocyanides, as discussed in § 2.1.

Because chlorine is a poisonous, corrosive gas, it is commonly generated as needed by the oxidation of chlorides, such as oxidation of HCl by $KMnO_4$ [131] or H_2O_2 [132]. Chlorine can be generated *in situ*, or in an external vessel and then delivered in a stream of nitrogen or argon. When the presence of sulfur dioxide is not problematic, sulfuryl chloride (SO_2Cl_2) [133] is a convenient option, because the byproducts are HCl and SO_2, and both can be easily removed (Scheme 62) [134]. Furthermore, SO_2Cl_2 is a stable, liquid source of chlorine, with electrophilicity comparable to that of bromine. Thus, handling is easy and chlorination with SO_2Cl_2 usually proceeds with high regioselectivity.

Scheme 62. The chlorination of aniline (**201aa**) with sulfuryl chloride.

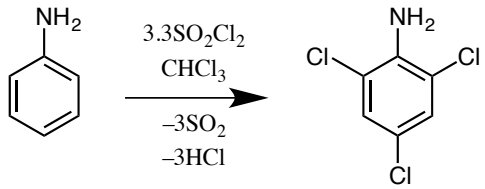

201aa **201ba**

Many anilines can be brominated in acidic bromine-containing suspensions (Scheme 63) [135]. As with chlorination, bromine could be present in the reaction vessel or delivered in vapor form in a stream of nitrogen or argon. Acetic acid is another common bromination solvent [136].

Scheme 63. The bromination of aniline (**201aa**) in hydrochloric acid.

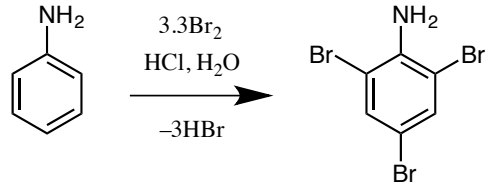

201aa **201ca**

Iodine is insufficiently electrophilic to iodinate most anilines directly. Iodine(I) monochloride, ICl, is an interhalogen compound that is slightly less reactive than bromine, and is electrophilic at the I atom. ICl is a solid in ambient conditions, but is close enough to its triple point to be messy to handle. ICl is commonly used in solution form with DCM, chloroform, or acetic acid as the solvent, or delivered in vapor form in a stream of nitrogen or argon [137]. Iodination conditions resemble the corresponding bromination conditions, with ICl in place of Br_2, and increased reaction times and temperatures. ICl can add to quaternary ammonium chloride salts to give the corresponding dichloroiodate(I) salts (NR_4^+ Cl_2I^-) [138], which are much less volatile than ICl and can have beneficial phase-transfer characteristics in multiphasic reaction mixtures [139], however, Cl_2I^- is less electrophilic than ICl.

Because of the scarcity of CN...F short contacts in crystalline fluorobenzonitriles, the preparation of fluoroanilines is not an objective of the present work. However, it is worth noting that many fluorine synthons are strong electrophiles, and give poor regioselectivity upon the attempted fluorination of anilines. Thus, fluoroanilines (**232**) are often prepared by manipulating fluorobenzenes, such as the reduction of fluoronitrobenzenes (**231**, Scheme 64) [140].

Scheme 64. The preparation of 4-fluoroaniline (**232**) by hydrogenation of 4-nitrofluorobenzene (**231**).

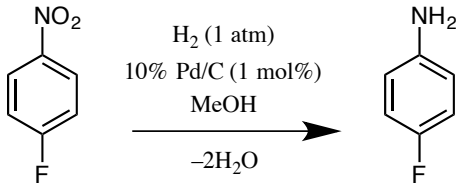

231 **232**

A similar strategy can be used for the preparation of 2- or 4-haloanilines, which is often easier to implement than partial halogenation of anilines. The reduction of 4-nitrobromobenzene (**234**) is a good method of preparing 4-bromoaniline (**235**, Scheme 65a) [141]. A related approach can also be used when the opposite regioselectivity is desired. 3-Halo or 3,5-dihalo anilines (**238**) can be prepared by halogenation of the corresponding 4-nitroanilines (**233**) [142]. Diazotization of **236** and reduction of the amino group, gives **237**. The nitro group is then reduced (Scheme 65b).

Scheme 65. (a) The preparation of 4-bromoaniline (**235**) by Sandmeyer bromination of 4-nitroaniline (**233**) and subsequent hydrogenation; (b) the preparation of 3,5-dibromoaniline (**238**) by bromination of **233**, followed by diazotization-reduction and then hydrogenation.

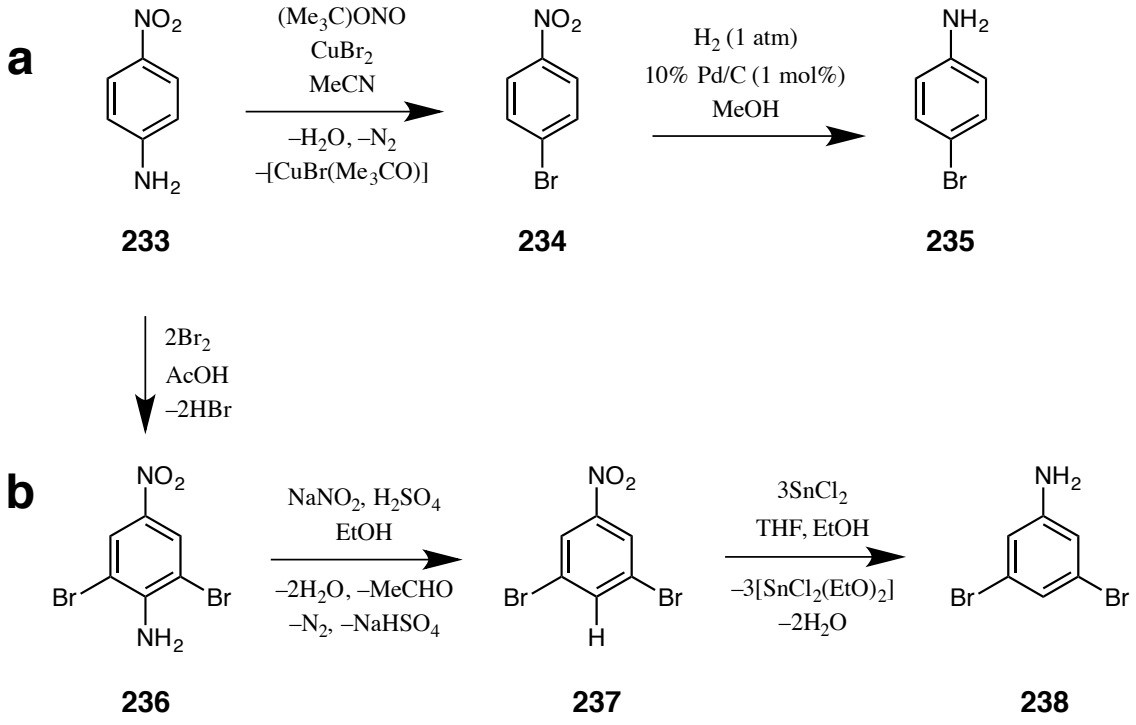

The suggested preparation of **234** is a modified Sandmeyer bromination of 4-nitroaniline (**233**) [143]. The primary author of this article is named Doyle. The introductory portion of Part II has pleasantly come full circle.

2.3. Scope of the Present Work

Based on the crystallographic and synthetic factors discussed in §§ 2.1–2.2, the original research objectives of the present work were:

1. Synthesize the 30 intermediates and products shown in Scheme 66. These are derived from aniline, 4-methylaniline, and 4-aminobenzoic acid (**201aa–ac**).

Scheme 66. The original scope of proposed synthetic work for Part II.

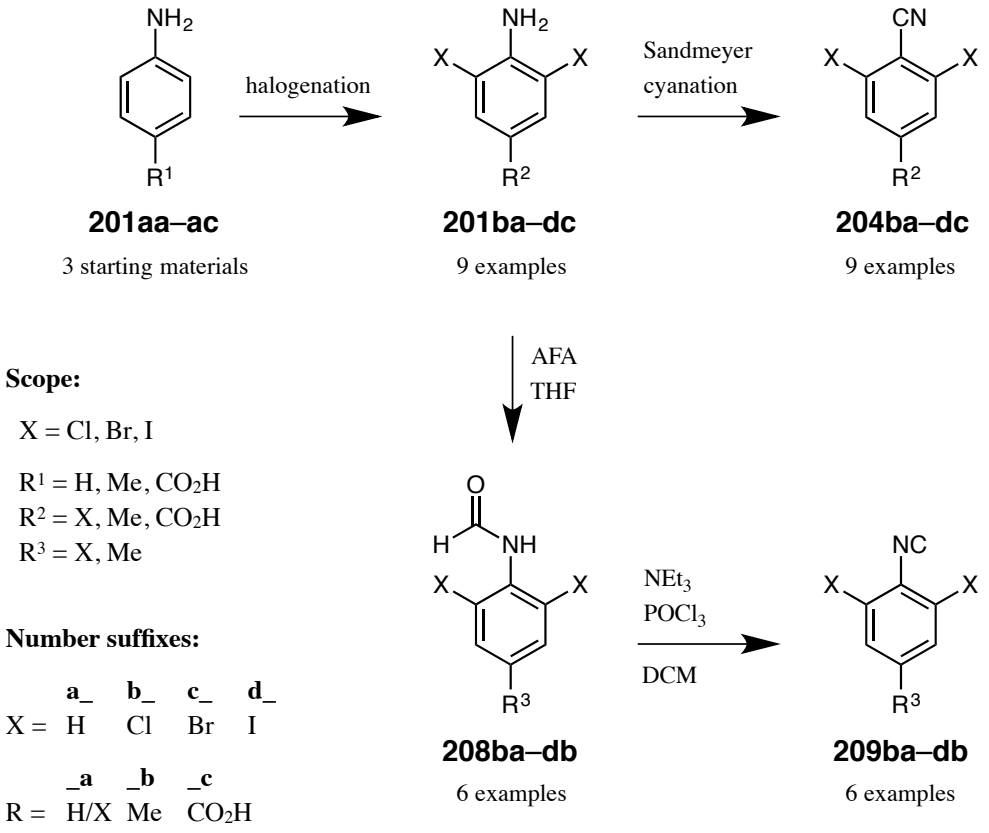

The scope of halogen substitution includes Cl, Br, and I (**201ba–dc**). Nitriles (**204ba–dc**) and isocyanides (**209ba–db**) have one halo contact donor, multiple halo atoms, and vertical mirror symmetry, maximizing the potential for Type 1–3 crystallographic features and orderly crystals. Because of the incompatibility of isocyano groups and acids [124], 4-carboxy analogs of formamides (**208**) and isocyanides (**209**) are not included.

2. Obtain yield, m.p., R_f, ^1H and ^{13}C NMR, IR, and HRMS data for these 30 compounds. Obtain elemental analysis data for novel products for which single-crystal determinations are not reported or obtained. There is a general lack of reported characterization data for these compounds, probably because the reported examples were first prepared before the widespread use of many spectroscopic techniques.

3. Obtain at least one publication-quality single-crystal determination for the 15 nitriles and isocyanides shown in Scheme 66.
   (a) Six already have entries in the CCDC:
      - **204cb** - A re-determination of the literature crystal structure would be of value [102a].
      - **204ba**,**ca** and **209ba**,**ca** - A search for polytypes and new polymorphs will be conducted.
      - **204bc** - A search for polytypes and new polymorphs will be conducted on the 2:1 co-crystal with anthracene.
   (b) The remaining nine do not have CCDC entries. Any single-crystal determination would be a novel structure. For 4-carboxynitriles **204cc**,**dc**, 2:1 co-crystals with anthracene will be sought.

4. Search for polymorphs of nitriles that have single-crystal determinations that are not isomorphous with the corresponding isocyanide, and vice-versa.

5. Serve as a research mentor to 10–15 undergraduates during the course of this work (roughly one per crystallographically analyzed compound). Elevate each of them, within this work and their personal goals, to the level where they earn co-authorship on a publication derived from the synthetic or crystallographic findings.

2.4. Synthetic Results

2.4.1. Initial Survey: Brominated PABA Derivatives

The 2,6-dibromo-4-carboxy series of compounds was the first to be explored. Bromination of 4-aminobenzoic acid (PABA, **201ac**) suspended in glacial acetic acid (AcOH) was attempted, according to the work of Elion (Scheme 67) [136]. The initial product mixture contained recovered PABA and monobrominated PABA (**201ce**), which were removed by selective acid-promoted precipitation from ammonium hydroxide solution. The poor solubility of **201ac** and **201ce** in AcOH was probably a limiting factor in the yield of **201cc**.

Scheme 67. Bromination of PABA (**201ac**) in (a) acidic and (b) alkaline conditions.

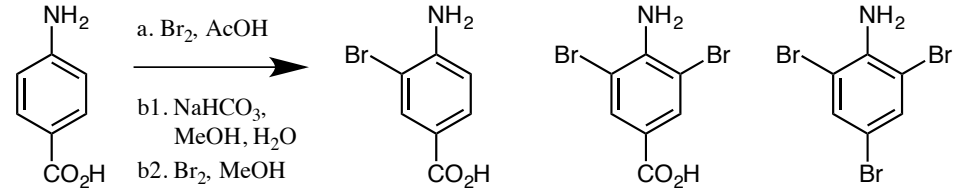

201ac		**201ce**	**201cc** (desired)	**201ca**
	Yields:			
(not calcd)	a	(not calcd)	58%	0%
6.7%	b	19%	32%	31%

Bromination was attempted under alkaline conditions, with the hope that the intermediate aminobenzoate anions would exhibit improved solubility and nucleophilicity, resulting in higher selectivity for dibromination. Instead, lower selectivity for **201cc** was observed. In spite of only using 2.05 stoichiometric equivalents of bromine, *ipso*-decarboxylative bromination occurred to a large extent, producing 2,4,6-tribromoaniline (**201ca**) at nearly identical yield to **201cc**. This mixture was not purified further.

Several Sandmeyer cyanations were attempted on batches of dibromo acid **201cc** (Scheme 68). The temperature (0–50 ºC), acid (HCl, AcOH, H_2SO_4, TsOH, HBF_4), and nitrite medium (aq. $NaNO_2$; IAN in DCM or $CHCl_3$) were varied. All attempted conditions gave complex mixtures with poor conversion of **201cc**. The desired cyano acid (**204cc**) may have formed at low yield, but the purification process would probably have been cumbersome.

Scheme 68. Attempted Sandmeyer cyanation of dibromo acid **201cc**.

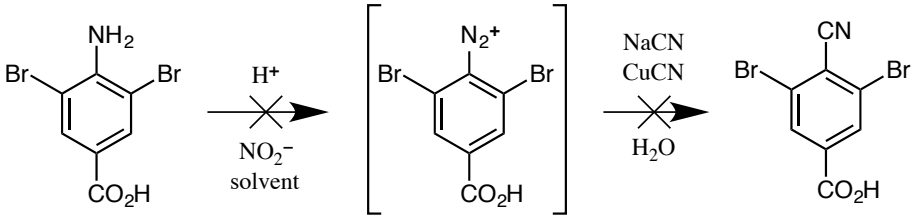

201cc **203cc** **204cc**

This negative result was somewhat surprising, given that the dichloro analog (**204bc**) was prepared by this method [144b], although many details, including the yield, were not given. The inability to access **204cc** by these conditions could be a result of diazonium intermediate **203cc** having lower solubility than its dichloro counterpart.

An alternate approach to dibromo nitrile **204cc** was planned, in which the carboxyl group would be protected as the methyl ester for bromination (Scheme 69) and cyanation (Schemes 70 & 71). The goal was to mitigate the solubility, stability, and purification challenges that were encountered with unprotected carboxylic acids.

Scheme 69. (a) Synthesis of dibromo ester **201cd** for subsequent cyanation; (b) The preparation of dibromo acid **201cc** by 1- and 3-step routes.

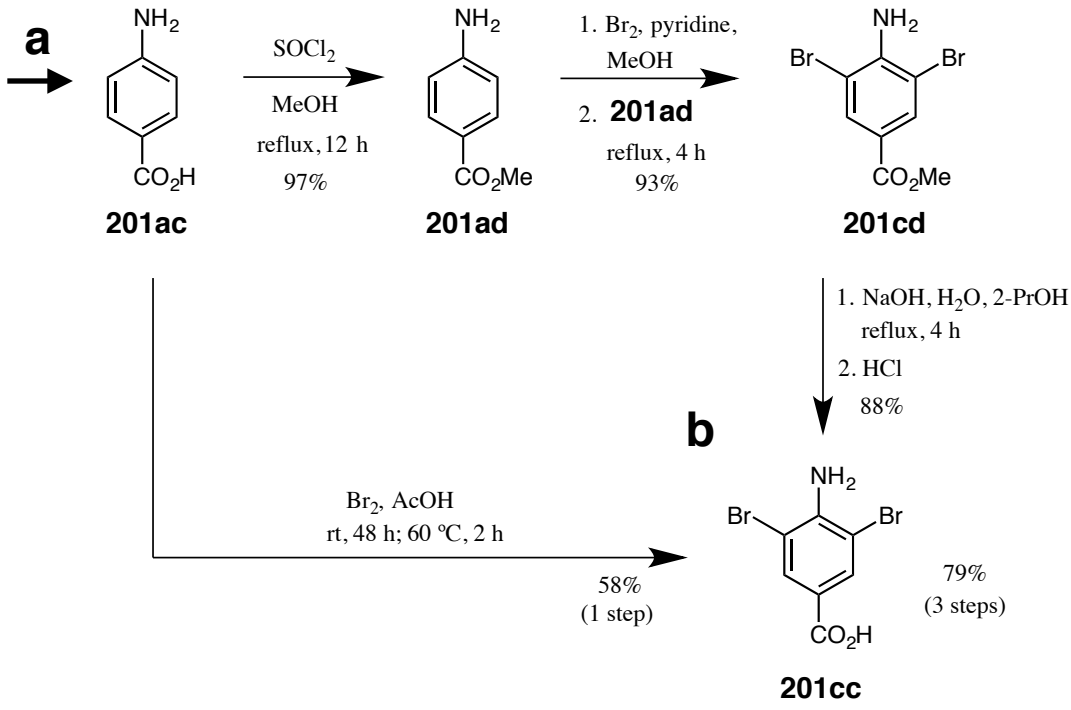

PABA (**201ac**) was esterified based on the work of Hinsberger *et al*. [145]. As planned, the dibromination of ester **201ad** proceeded smoothly. Several acidic, alkaline, aqueous, and organic bromination conditions were attempted. The best results were obtained by adding a methanolic mixture of pyridine and *N*-bromopyridinium bromide to a methanolic suspension of **201ad**, followed by 4 hours of reflux. The highest bromination yields usually come from acidic conditions. However, without the buffering effects of pyridine and use of an organic solvent, the esters in the reaction mixture were susceptible to hydrolysis.

The best results for the hydrolysis of **201cd** were obtained from a refluxing, alkaline, 1:1 (by volume) mixture of water and 2-PrOH. Aqueous hydrolysis of **201cd** did not proceed well, due to poor solubility. A moderate degree of transesterification was observed with primary alcohols, whereas heavier alcohols were difficult to remove from the product mixture. An alternate means of suppressing transesterification is *in situ* distillation of the alcohol. Acid-promoted hydrolysis of **201cd** proceeded slowly.

Cyano ester **204cd** was not observed in attempted Sandmeyer cyanations where simple aqueous cyanide solutions were used (Scheme 70). Instead, the major pathway was reduction of the corresponding diazonium intermediate to the hydro analog (**206**).

Scheme 70. The preparation of reduction product **206**, upon attempted Sandmeyer cyantion of **201cd** with NaCN and CuCN.

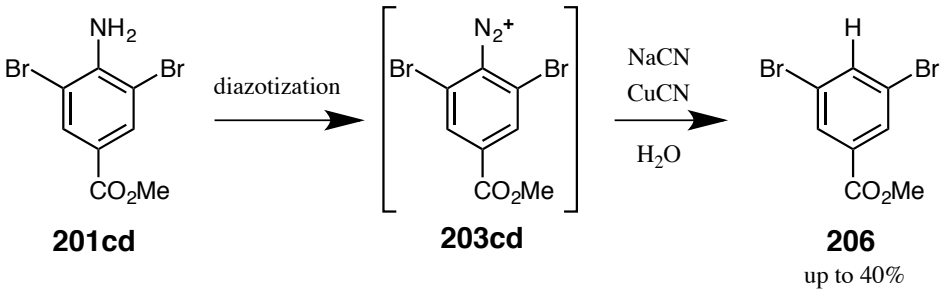

201cd **203cd** **206**
up to 40%

The use of SBDC suspensions gave Sandmeyer cyanation yields superior to any located in the literature for 2,6-dihaloanilines. Dibromo cyano ester **204cd** was obtained at 92% yield, a remarkable improvement considering that the only change was incubation of the cyanide solution with an excess of $NaHCO_3$ prior to use (Scheme 71).

Scheme 71. The preparation of dibromo cyano ester **204cd**, and subsequent hydrolysis transformations.

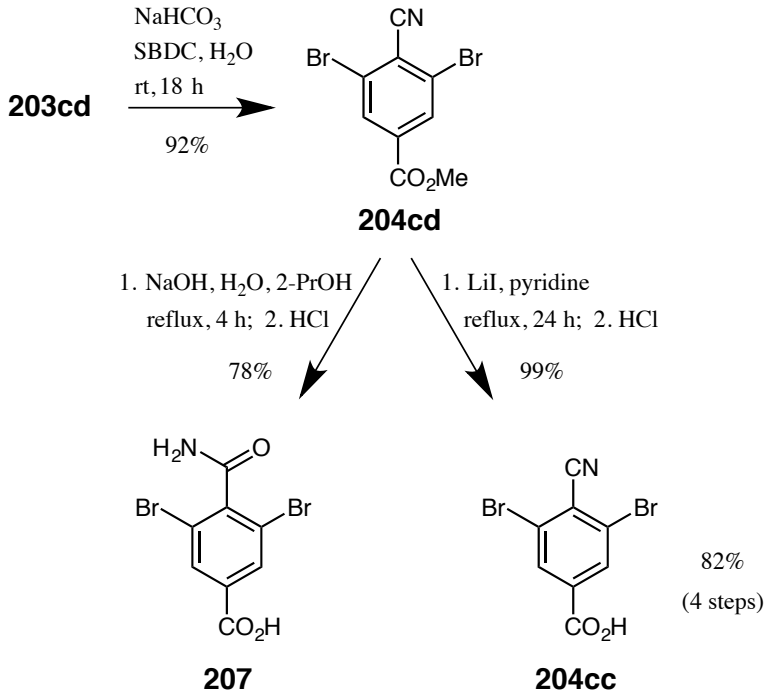

It was anticipated that the direct hydrolysis of cyano ester **204cd** would be troublesome, potentially producing mixtures that include carbamoyl acid **207**. Several acidic and alkaline hydrolysis conditions were attempted, in case one could be found by which ester hydrolysis outpaced destruction of the cyano group. No such condition was found. The highest yield of **207** was obtained from reflux in an alkaline mixture of water and 2-PrOH (Scheme 71).

With typical hydrolysis conditions ruled out as an approach to cyano acid **204cc**, an alternate means of de-esterification was required. Lithium iodide is moderately soluble in hot pyridine. The resulting solution has been shown to demethylate methyl esters while leaving more hindered esters unaltered [146]. The methoxy C atom is sufficiently unhindered to allow nucleophilic attack by iodide in refluxing pyridine. The resulting molecule of methyl iodide is quickly scavenged by pyridine, generating *N*-methylpyridinium, and regenerating LiI. It seemed likely

that LiI would not damage the cyano group in **204cd**. Yields of 88–94% of cyano acid **204cc** were obtained when 10 mol% LiI was used. Reproducibly, 99% yield was obtained when 1 stoichiometric equivalent of LiI was used. NaI or KI, both considerably less expensive than LiI, are not sufficiently soluble in refluxing pyridine to efficiently catalyze this transformation.

2.4.2. Halogenation Results

Having found good halogenation, cyanation, and de-esterification conditions for the 2,6-dibromo-4-carboxyl series, the focus shifted to the preparation of the remaining nitriles. For chlorination, the use of dilute chlorine vapor gave dark, sticky mixtures in which **201ba** and **201bd** were observed at moderate proportions. These mixtures were not separated. The use of SO_2Cl_2 gave better results (Table 15). No condition was found by which **201bb** was produced. Because of the low probability of observing the desired crystallographic features in crystals of the corresponding nitrile and isocyanide, no further work was performed in the 2,6-dichloro-4-methyl series.

Table 15. Halogenation yields. The highest-yielding conditions are listed.

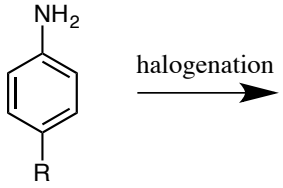

halogenation

201aa,ab,ad

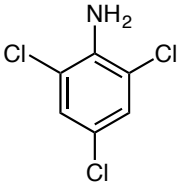

201ba
85%

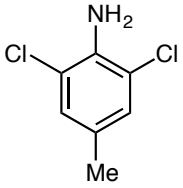

201bb
not obs.

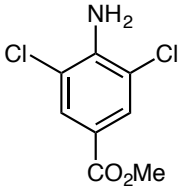

201bd
40%

Scope:

R = H, Me, CO_2Me

Number suffixes:

	a_	**b_**	**c_**	**d_**
X =	H	Cl	Br	I

	_a	**_b**	**_d**
R =	H/X	Me	CO_2Me

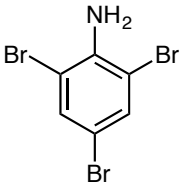

201ca
81%

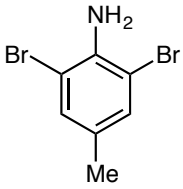

201cb
95%

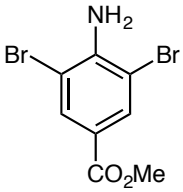

201cd
93%

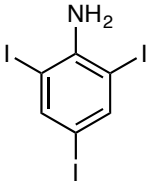

201da
89%

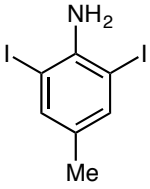

201db
95%

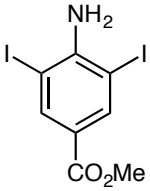

201dd
39%

product	X	R	condition	temp.	time	yield %
201ba	Cl	H	SO_2Cl_2, $CHCl_3$	rt	1 d	85
201bb	Cl	Me	SO_2Cl_2, $CHCl_3$	0 ºC	12 h	(not obs.)
201bd	Cl	CO_2Me	SO_2Cl_2, pyridine, $CHCl_3$	rt	1 d	40
201ca	Br	H	Br_2 vapor, HCl, H_2O	rt	1 d	81
201cb	Br	Me	Br_2, AcOH	50 ºC	2 d	95
201cd	Br	CO_2Me	Br_2, pyridine, MeOH	65 ºC	4 h	93
201da	I	H	ICl vapor, HCl, H_2O	rt	4 d	89
201db	I	Me	ICl vapor, HCl, H_2O	rt	2 d	95
201dd	I	CO_2Me	ICl, HCl, H_2O	rt	1 d	39

For bromination and iodination, **201ca**,**da**, and **db** were best obtained when the halogenating agent (Br_2 or ICl) was added slowly as a dilute vapor in a stream of nitrogen (Table 15). Addition of the halogenating agent directly to these reaction mixtures produced moderate amounts of dark sludge. However, the dilute vapor method required much longer production times for the remaining three products (**201cb**,**cd**, and **dd**). The brominations proceeded well when Br_2 was added directly to the reaction mixture, and then the resulting mixture was heated. For the iodination of ester **201ad**, heating the reaction mixture caused hydrolysis of the methyl ester outpacing iodination, giving an inconvenient mixture analogous to the products of PABA bromination. Ester hydrolysis had been suppressed in the chlorination and bromination of **201ad** by adding pyridine. However, the corresponding iodination proceeded at an impractically slow rate. The best compromise that was found, between promoting iodination and suppressing hydrolysis, was to add ICl directly to a hydrochloric acid suspension of **201ad** and then stirring the resulting mixture for one day. Diiodo ester **201dd** was easily separated from hydrolysis products by extraction, and it was fairly easy to separate from its monoiodo counterpart by column chromatography.

2.4.3. Sandmeyer Cyanation Results

For diazotization, the chlorinated and brominated anilines readily dissolved in EtOAc, DCM, or $CHCl_3$. However, the use of isoamyl nitrite (IAN) with AcOH or $TsOH•H_2O$ gave a very short lifetime to the desired diazonium intermediates. Mass spectrometry (HRMS-EI) signals were observed that were consistent with variously chlorinated and hydro analogs of starting materials, and the corresponding biaryls. Therefore, it is likely that a radical decomposition pathway was restricting yields of the desired benzonitriles.

For most substrates, the best diazotization results were obtained when the starting materials were finely ground in a mortar, and then suspended in a mixture of AcOH and H_2SO_4 (Table 16). Sodium nitrite, dissolved in a minimal amount of water, was then added in several aliquots. Triido (**201da**) and diiodo methyl (**201db**) anilines had particularly low aqueous solubilities, and the corresponding diazonium salts were more stable than their lighter counterparts. For these two substrates, organic phase diazotization was favorable.

Table 16. Sandmeyer cyanation yields. The highest-yielding conditions are listed.

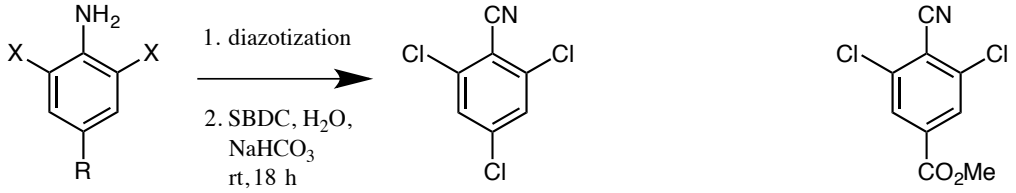

201ba–dd

204ba
93%

204bd
56%

Scope:

X = Cl, Br, I

R = X, Me, CO_2Me

Number suffixes:

	b_	**c_**	**d_**
X =	Cl	Br	I

	_a	**_b**	**_d**
R =	X	Me	CO_2Me

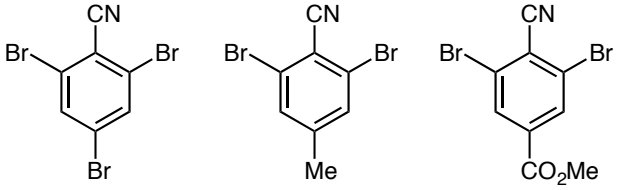

204ca
59%

204cb
88%

204cd
92%

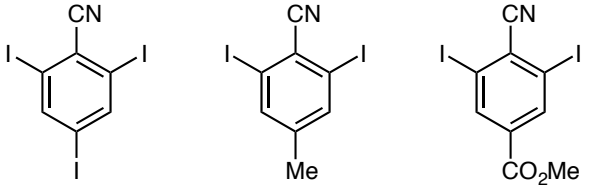

204da
65%

204db
83%

204dd
88%

product	X	R	diazotization conditions	yield %
204ba	Cl	Cl	$NaNO_2$ (aq.), H_2SO_4, AcOH; rt, 3 h	93
204bd	Cl	CO_2Me	$NaNO_2$ (aq.), H_2SO_4, AcOH; rt, 1 h	56
204ca	Br	Br	$NaNO_2$ (aq.), H_2SO_4, AcOH; 40 ºC, 1 h	59
204cb	Br	Me	$NaNO_2$ (aq.), H_2SO_4, AcOH; rt, 2 h	88
204cd	Br	CO_2Me	$NaNO_2$ (aq.), H_2SO_4, AcOH; rt, 3 h	92
204da	I	I	IAN, TsOH•H_2O, EtOAc; rt, 1 h	65
204db	I	Me	IAN, TsOH•H_2O, EtOAc; 0 ºC, 1 h, and then rt, 1 h	83
204dd	I	CO_2Me	$NaNO_2$ (aq.), H_2SO_4, AcOH; 40 ºC, 2 h	88

The incubation of the diazotization mixtures was a delicate balancing act between converting as much starting material as possible and minimizing the destruction of accumulated diazonium ions. Each batch was closely monitored by TLC analysis. The diazonium intermediates had a very low R_f value, appearing near the baseline of TLC plates. The decomposition products usually had R_f values slightly higher than the starting materials. Transfer of the diazonium mixture to an SBDC suspension was initiated as soon as decomposition signals began to intensify more rapidly than starting material was being consumed. The ideal diazotization interval varied between batches of the same substrate, but was usually between 0.5 and 2 h. Occasionally, rapid decomposition began earlier than expected. Therefore, it is recommended to split starting materials into several batches when performing Sandmeyer cyanations similar to those described herein. Substituting any amount of $TsOH•H_2O$ for H_2SO_4 gave worse results, apparently due to impeding the solubility of the starting materials. Substituting 2 molar equivalents of HBF_4 for H_2SO_4 marginally improved the stability of the diazonium species for the attempted substrates, and could potentially bear a significant improvement for some substrates related to the present work. However, H_2SO_4 was employed as the preferred diazotization acid as a compromise between yields, cost, and safety.

Whereas diazotization was a touchy process, SBDC suspensions consistently performed well for all attempted cyanations. The best yields were obtained from mixtures containing a 6:2 stoichiometric ratio of NaCN:CuCN, suspended with enough $NaHCO_3$ to neutralize all acids of the diazotization mixture, plus 3 to 5 additional equivalents of $NaHCO_3$. The use of less cyanide caused increased proportions of co-product formation. Additional cyanide did not observably improve yields. No improvements to nitrile yields were observed when KNO_2, KCN, and $KHCO_3$ were used in place of the corresponding sodium salts.

The main co-products of the preparation of tribromo nitrile **204ca** were identified by ^1H NMR and mass spectrometry analysis (Scheme 72). This reaction was chosen based on the favorable diazotization behavior of 2,4,6-tribromoaniline (**201ca**) and the convenient isotopomer abundances of each component of the product mixture [147].

Scheme 72. The products obtained from the Sandmeyer cyanation of **201ca**. The compounds shown inside of the box were obtained as a mixture.

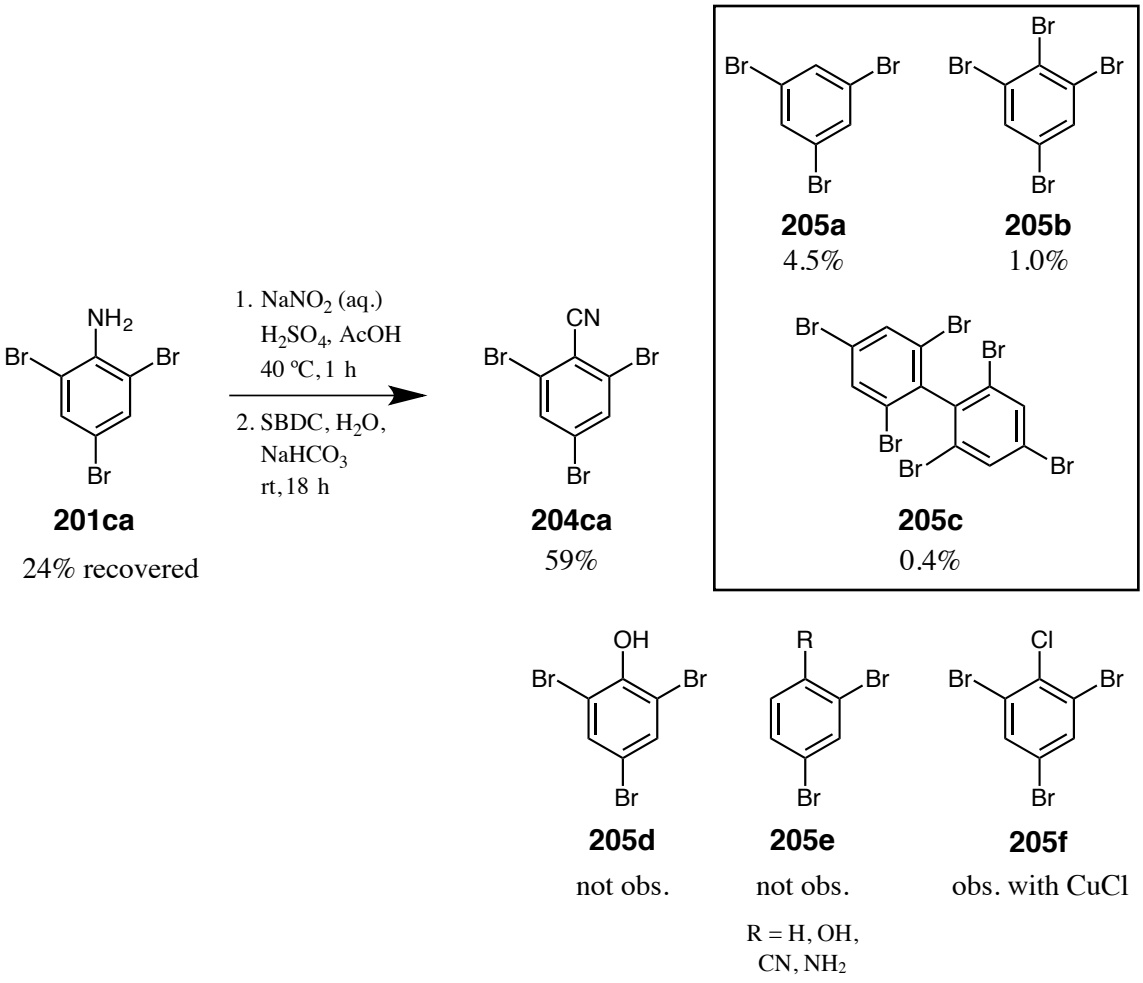

201ca
24% recovered

204ca
59%

205a
4.5%

205b
1.0%

205c
0.4%

205d
not obs.

205e
not obs.
R = H, OH, CN, NH_2

205f
obs. with CuCl

These results are consistent with reported investigations of the co-products formed by Sandmeyer cyanations [114, 117], although hydroxy analog **205d** was not observed during the present work. If tetrabromo product **205b** forms via radical halogen transfer, then the corresponding amount of a dihalo analog (**205e** or similar) was also generated, but none was observed. Some of the preliminary Sandmeyer cyanation trials used CuCl instead of CuCN. In these experiments, the chloro analog (**205f**) was observed by HRMS-EI. Therefore, it is recommended not to add anions other than cyanide or bicarbonate to the SDBC suspensions that are used for the cyanation of 2,6-dihaloanilines.

In order to confirm the identity of hydro product **206**, which was obtained during the initial synthetic survey (§ 2.4.1), several batches were prepared in the absence of copper salts. The best result was obtained when diazotization was performed in a cooled acetic acid suspension, followed by slow addition to a mixture of hypophosphorous acid (H_3PO_2) and sulfuric acid (Scheme 73). Based on HRMS-EI, HRMS-ESI, and ^1H NMR analysis, the main yield-limiting factors were incomplete diazotization and hydrolysis of the methyl ester.

Scheme 73. The preparation of methyl 3,5-dibromobenzoate (**206**).

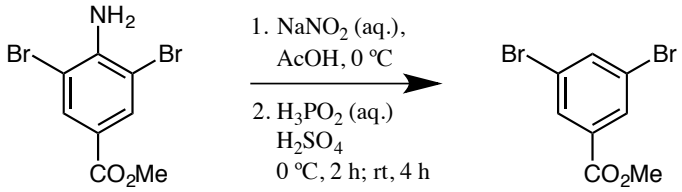

201cd **206**

67%

2.4.4. De-esterification Results

The LiI-promoted de-esterification of cyano esters **204bd** and **204cd**) proceeded well (Scheme 74). Dichloro ester **204bd** gave slightly lower yields than dibromo ester **204cd**, probably due to higher solubility, resulting in incomplete recovery during recrystallization. By TLC analysis, the demethylation of diiodo ester **204dd** seemed to proceed efficiently. However, **204dc** was very difficult to handle after protonation. Its solubility in all attempted solvents was significantly lower than **204bc** or **204cc**. The best samples obtained of **204dc** were contaminated with unidentified impurities. No combination of trituration, preparative TLC [148], or Soxhlet extraction [149] was found to improve the purity beyond roughly 73 mass%. This purity is estimated based on the assumption that the impurities identified in the ^{1}H NMR spectra have a similar molar mass to **204dc**. By this stage in the present work, 2:1 co-crystals of **204bc** and **204cc** had each been prepared with anthracene. It was hoped that a co-crystalline sample derived from **204dc** could be obtained by fractional crystallization. Attempts were made to grow such crystals using **204dc** and 0.5 stoichiometric equivalents of anthracene in methanol, DCM, $CHCl_3$, 1,4-dimethylbenzene, acetonitrile, and from a melt. No co-crystals were found. No further work was performed on the 4-carboxyl-2,6-diiodo series.

Scheme 74. De-esterification of cyano esters with lithium iodide.

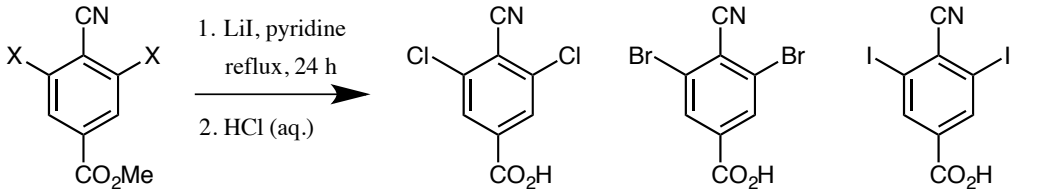

204bd–dd | **204bc** 93% | **204cc** 99% | **204dc** approx. 67% approx. 73 mass%

Scope:

X = Cl, Br, I

Number suffixes:

	b_	**c_**	**d_**
X =	Cl	Br	I

	_c	**_d**
	para-CO_2H	CO_2Me

2.4.5. *N*-Formylation Results

Six halogenated anilines *N*-formylated by acetic formic anhydride (AFA) solutions (Table 17). Chlorinated (**208ba**) and brominated (**208ca**,**cb**, and **cd**) formamides were best prepared at rt. Heating the reaction mixtures produced a small amount of acetylation products. The iodinated substrates are more sterically hindered, and exhibit very high selectivity for formylation, but they react more slowly. Heating these reaction mixtures to 40 ºC accelerated the formylation of iodinated anilines **208da** and **208db** to a similar rate as had been observed from the lighter substrates, with no observed acetylation. All of these experiments could probably be performed in THF or DCM, with similar results. Dibromo formamido ester **208cd** was not part of the initially proposed scope of this work. However, it was decided that a comparison of the single-crystal structures of the corresponding cyano ester (**204cd**, § 2.4.3) and isocyano ester (**209cd**, § 2.4.6) would be worth pursuing.

Table 17. *N*-Formylation of 2,6-dihaloanilines with acetic formic anhydride (AFA) solution. The highest-yielding conditions are listed.

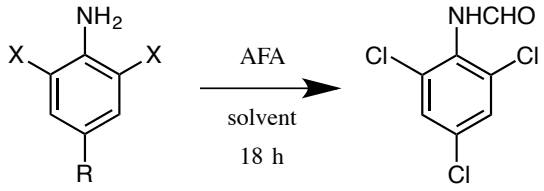

201ba–201db **208ba** 87%

Scope:

X = Cl, Br, I

R = X, Me, CO_2Me

Number suffixes:

	b_	**c_**	**d_**
X =	Cl	Br	I

	_a	**_b**	**_d**
R =	X	Me	CO_2Me

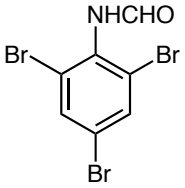

208ca 87%

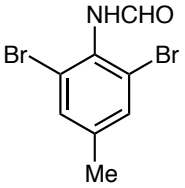

208cb 91%

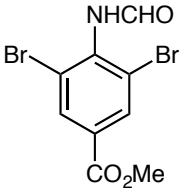

208cd 97%

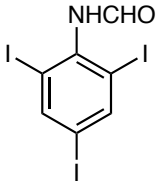

208da 90%

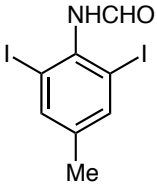

208db 88%

product	X	R	solvent	temp.	yield %
208ba	Cl	Cl	DCM	rt	87
208ca	Br	Br	THF	rt	87
208cb	Br	Me	DCM	rt	91
208cd	Br	CO_2Me	DCE	rt	97
208da	I	I	DCE	40 °C	90
208db	I	Me	DCE	40 °C	88

Early in the course of this work, the question arose as to whether formylation or halogenation should be first in the synthetic route to the desired isocyanides. The preparation and bromination of plain formanilide (**208aa**) was attempted (Scheme 75).

Scheme 75. *N*-Formylation of aniline with formic acid in a Dean-Stark trap. Subsequent bromination was not successful.

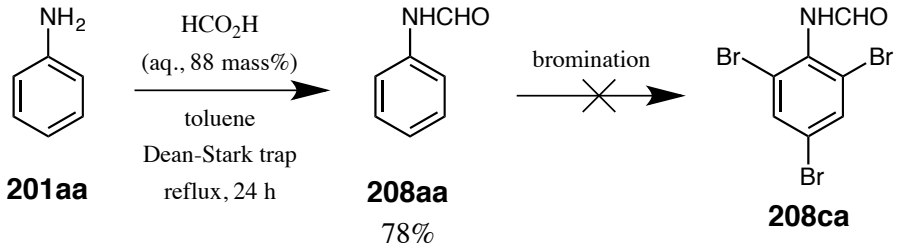

201aa **208aa** 78% **208ca**

The first batch of formanilide was prepared in AFA solution at 0 ºC, which gave an approximately 7:1 ratio of formylation:acetylation. The unhindered amino group in **201aa** had even lower selectivity for formylation than had been anticipated. The second batch was prepared in high purity by using a Dean-Stark trap [150] with **201aa** and formic acid solution in toluene. The bromination gave almost exclusively a mixture of 2- and 4-monobrominated formanilides. This experiment was carried out before most of the halogenation data (Table 15, p 131) had been acquired. Soon after this experiment (Scheme 75), it was clear that halogenation before formylation is the superior approach.

However, the simplified formylation technique that gave **208aa** had raised a new question: Could 2,6-dihaloanilines be formylated by refluxing them in toluene with formic acid? Trichloroaniline (**201ba**) was chosen as the first test substrate (Scheme 76). No reaction was observed in refluxing toluene or mixed xylenes, with or without the addition of $TsOH•H_2O$. The amino group in **201ba** is probably too hindered for the simplified formylation strategy to function. Thus, AFA was used for all remaining formylations of 2,6-dihaloanilines.

Scheme 76. The attempted formylation of 2,4,6-trichloroaniline (**201ba**) with formic acid and $TsOH•H_2O$ in refluxing mixed xylenes.

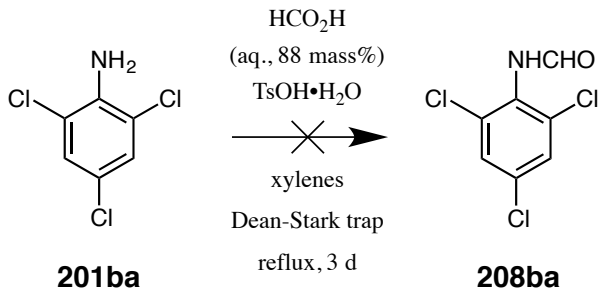

201ba **208ba**

2.4.6. Isocyanide Preparation Results

Dehydration of formanilides was attempted with phosphoryl chloride ($POCl_3$) and triethylamine (NEt_3) in DCM at low temperatures (–78 to –40 ºC), according to the literature [124]. The reaction was slow, often requiring eight hours or longer to run its course. This was probably a result of the very poor solubility of halogenated formanilides in these conditions, and possibly reactions between $POCl_3$ and NEt_3. Replacing NEt_3 with DIPEA (*N*,*N*-diisopropylethylamine) increased yields by approximately 2–5%. With many amides, this reaction proceeds vigorously if the mixture is not cooled before adding $POCl_3$. However, 2,6-dihaloformanilides are sufficiently hindered that no cooling was necessary (Scheme 77). This reaction was well-behaved if started at rt, and could be heated to reflux in DCE (approx. 85 ºC) once the $POCl_3$ had been added.

Scheme 77. Dehydration of formanilides with DIPEA and $POCl_3$ to give 2,6-dihaloisocyanobenzenes.

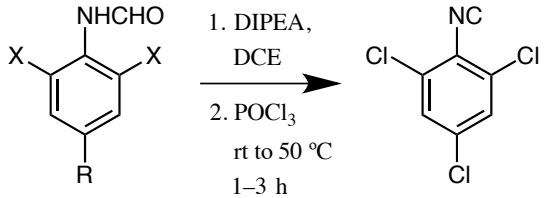

208ba–208db **209ba** 60%

Scope:

X = Cl, Br, I

R = X, Me, CO_2Me

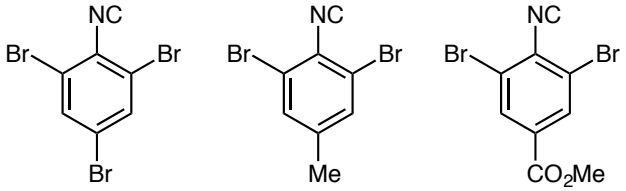

209ca 78% **209cb** 81% **209cd** 84%

Number suffixes:

	b_	**c_**	**d_**
X =	Cl	Br	I

	_a	**_b**	**_d**
R =	X	Me	CO_2Me

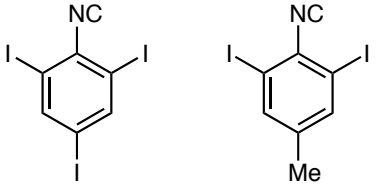

209da 86% **209db** 92%

Because of the low solubility of the starting materials (**208ba–208db**), these reactions can be monitored visually. By TLC analysis, every experiment attempted was found to be complete within 10 minutes of the disappearance of solids in the reaction mixture. Instead of warming the reaction mixture in DCE for several hours, these reactions can be performed overnight at rt in DCM.

The most convenient method found for isolating the products was to filter the reaction mixture through neutral alumina. The byproduct phosphate and ammonium salts remained in the alumina. The filtrate was found to consist of solvent, product, and unreacted DIPEA. The DIPEA was removed by washing the filtrate several times with dilute acetic acid solution, followed by several washes with $NaHCO_3$ solution and thorough drying. It is important to cool all liquid phases and the separatory funnel in ice baths during the DIPEA removal process. If this

is not done, some hydrolysis of the isocyano group was observed, especially with chlorinated isocyanide **209ba**. Although many isocyanides would be extensively hydrolyzed during the acetic acid washes, the steric hindrance of the *ortho* halo groups provided ample protection.

The brominated and iodinated isocyanides had mild or no detectable odors. By contrast, trichloro isocyanide **209ba** exhibited a potent isocyanide odor. Other 2,6-dichloro examples are likely to have offensive odors, and the logistics of handling them should be planned accordingly. Isocyanides **209ba**–**209db** were found to have shelf lives of at least 1 year, provided that the samples were carefully neutralized and stored in dry, tightly-sealed vials. Some iodinated examples that were prepared in our laboratories more than 10 years ago are still of crystallographic quality. Some trichloro or brominated samples degraded substantially during a 2-year interval, even with refrigerated, dark storage.

Even though a successful preparation of dibromo isocyano acid **209cc** seemed unlikely, an ample supply of **209cd** was on hand. Hydrolysis was attempted using lithium hydroxide in methanol (Scheme 78). Exposure of the resulting mixture to HCl, even at low temperature and concentration, gave hydrolysis of the isocyano group. This ruled out acid-catalyzed hydrolysis. This also ruled out the LiI de-esterification procedure, unless a work-up method could be developed that did not depend on the use of mineral acids for separating the desired product from pyridine and other product components. Developing such conditions could be tedious, and even if isocyano acid **209cc** were isolated, it would probably have a very short shelf life. Thus, no additional attempts to prepare **209cc** were made.

Scheme 78. The attempted selective hydrolysis of dibromo isocyano ester **209cd**.

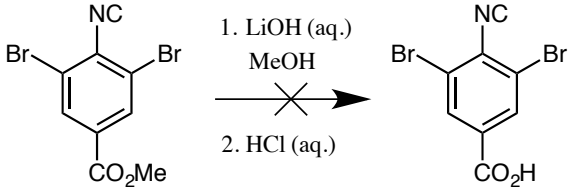

209cd **209cc**

2.4.7. Overall Multi-Step Yields

Table 18. The overall yields of nitriles **204ba–204dc**, prepared from anilines **201aa–201ac**.

Scope:

X = Cl, Br, I

R^1 = H, Me, CO_2H

R^2 = X, Me, CO_2H, CO_2Me

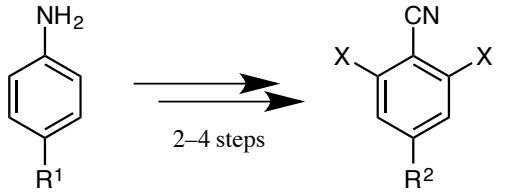

201aa–201ac **204ba–204dd**

product	X	R^2	steps	overall yield %
204ba	Cl	Cl	2	79
204bc	Cl	CO_2H	4	20
204bd	Cl	CO_2Me	3	22
204ca	Br	Br	2	48
204cb	Br	Me	2	84
204cc	Br	CO_2H	4	82
204cd	Br	CO_2Me	3	83
204da	I	I	2	58
204db	I	Me	2	79
204dc	I	CO_2H	4	22
204dd	I	CO_2Me	3	33

Table 19. The overall yields of isocyanides **209ba–209db**, prepared from anilines **201aa–201ac**.

Scope:

X = Cl, Br, I

R^1 = H, Me, CO_2H

R^2 = X, Me, CO_2Me

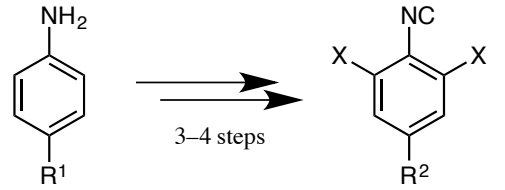

201aa–201ac **209ba–209db**

product	X	R^2	steps	overall yield %
209ba	Cl	Cl	3	44
209ca	Br	Br	3	55
209cb	Br	Me	3	70
209cd	Br	CO_2Me	4	76
209da	I	I	3	69
209db	I	Me	3	77

2.5. Crystallographic Results

2.5.1. Trihalo Nitriles and Isocyanides

Dr. Britton's focus was on brominated and iodinated derivatives. No crystallographic study was performed of the chlorinated compounds prepared in § 2.4. Samples of tribromo nitrile **204ca** and isocyanide **209ca** were recrystallized from several solvents (Table 20).

Table 20. The novelty and crystallization solvents for polytypes of tribromo nitrile **204ca** and isocyanide **209ca**.

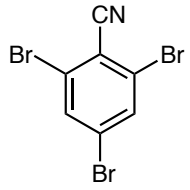

204ca

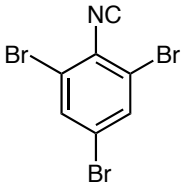

209ca

polytype	nitrile	isocyanide
***Z* = 2** (TT)	known [82]	not obs.
	MeCN, C_6H_6, $CHCl_3$, or DCM	
***Z* = 8** (TC)	novel	known [105]
	mesitylene	listed solvents or sublimation
***Z* = 12** (TCT)	novel	not obs.
	C_6H_6 or $CHCl_3$	

Unit cell determinations were performed on 23 crystals of **204ca** and 11 crystals of **209ca**. For nitrile **204ca**, three different unit cell volumes were found. Single-crystal determinations were performed on a sample with each unit cell. As desired, these crystals had Type 2 sheets and were polytypes. The Z = 2 polytype (Fig. 30) had translational (TT) layer stacking, and was identical to the literature structure of **204ca** [82]. The Z = 8 polytype of **204ca** was novel and isomorphous with the literature structure of **209ca** [105] (Fig. 31), with alternating pseudotranslational (T) and pseudocentric (C) layer stacking. The Z = 12 polytype was a novel structure (Fig. 32) with pseudocentric stacking between each third pair of layers (TCT stacking).

Fig 30. Translational (TT) stacking in the *Z* = 2 polytype of nitrile **204ca**, viewed along {a, b, 0}.

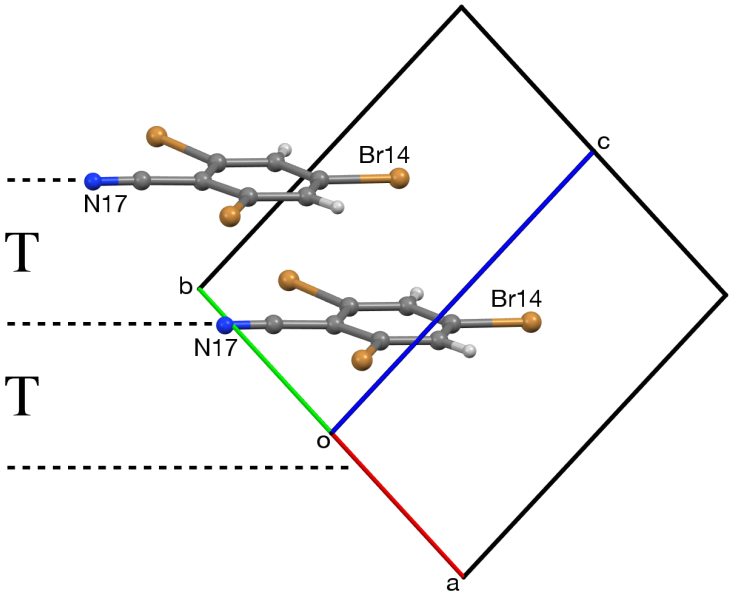

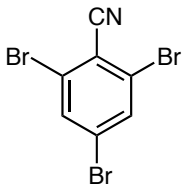

204ca

Fig 31. Pseudotranslational, pseudocentric (TC) stacking in the *Z* = 8 polytype of nitrile **204ca**, viewed along {a, 12b, 0}.

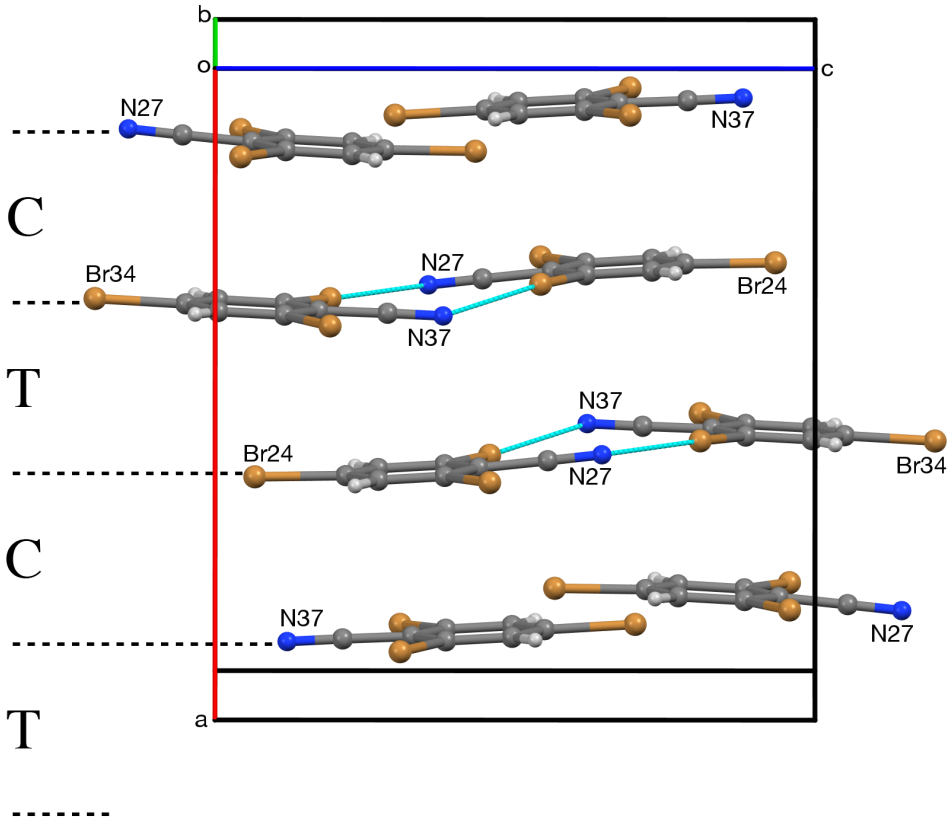

Fig 32. TCT stacking in the *Z* = 12 polytype of nitrile **204ca**, viewed along {a, 11b, 0}.

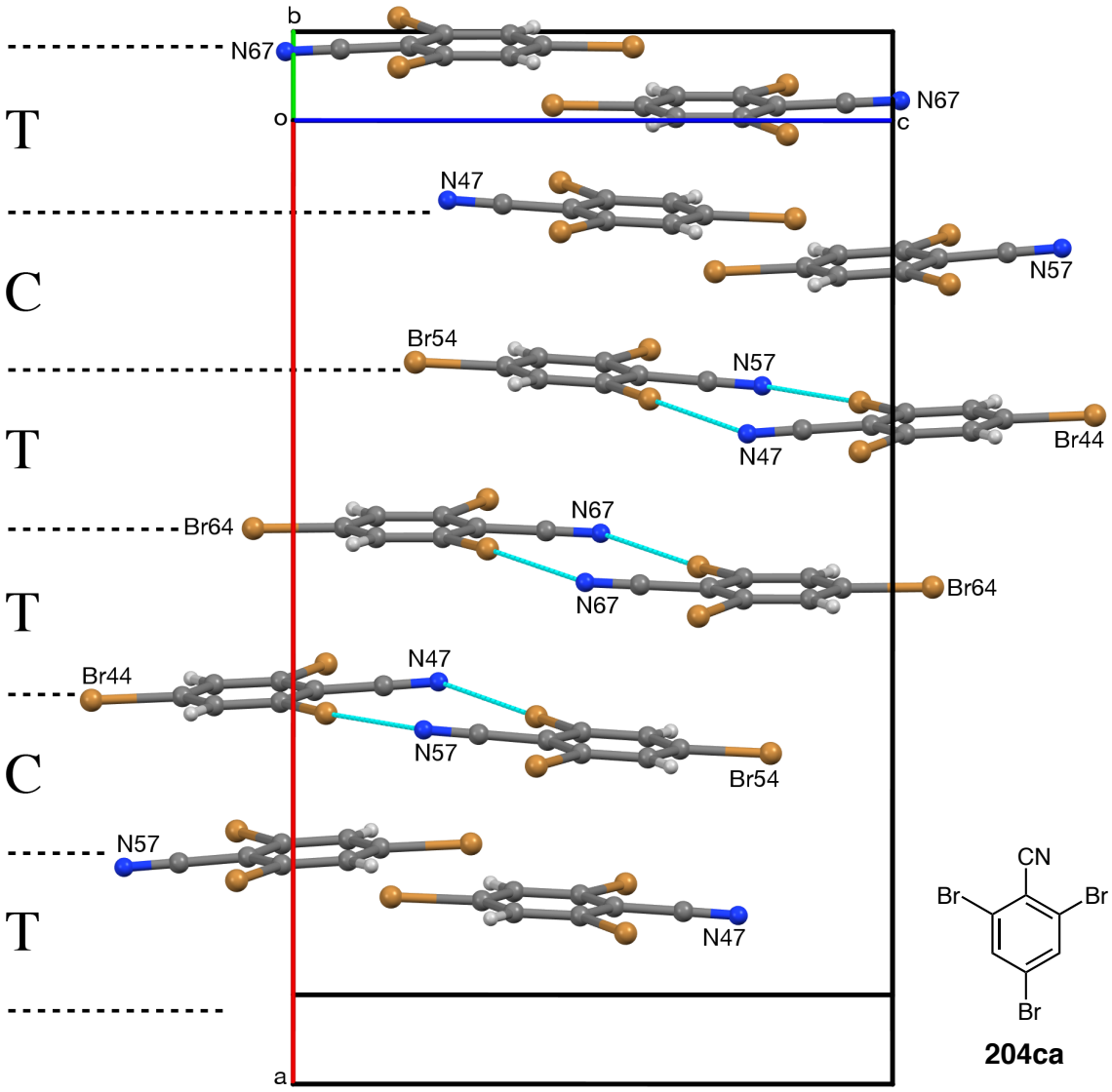

No new polymorphs of isocyanide **209ca** were located. The *Z* = 8 polytype was prepared by crystallization from any of the solvents that were used to recrystallize **204ca**, or sublimation. Swapping the cyano C and N atoms in Fig. 31 is a very close approximation to the crystal structure of **209ca**. These results were published in 2016 [79b].

It is possible that more polymorphs of either compound were produced, and were not among the 34 sampled crystals. As future work, the use of powder diffraction could be employed to provide a more thorough survey [151].

Single-crystal determinations were performed on a crystal of triiodo nitrile **204da** grown in acetonitrile, and a crystal of isocyanide **209da** grown in DCM. The crystals were isomorphous. Both had $Z = 4$ unit cells and were composed of Type 2 sheets with centric (CC) stacking (Fig. 33). Swapping the cyano C and N atoms gives a very close approximation to the structure of isocyanide **209da**. As with the TT polytype of tribromo nitrile **204ca**, adjacent intralayer molecules in the CC crystals were coplanar. By contrast, adjacent intralayer molecules in the mixed-stacking polytypes (TC and TCT) were mutually inclined by 6.5 to 7.5 degrees.

Fig 33. The $Z = 4$ unit cell of triiodo nitrile **204da**, with centric (CC) stacking, viewed along {a, 5b, 0}. The top and bottom layers are bisected by the *bc* face of the unit cell.

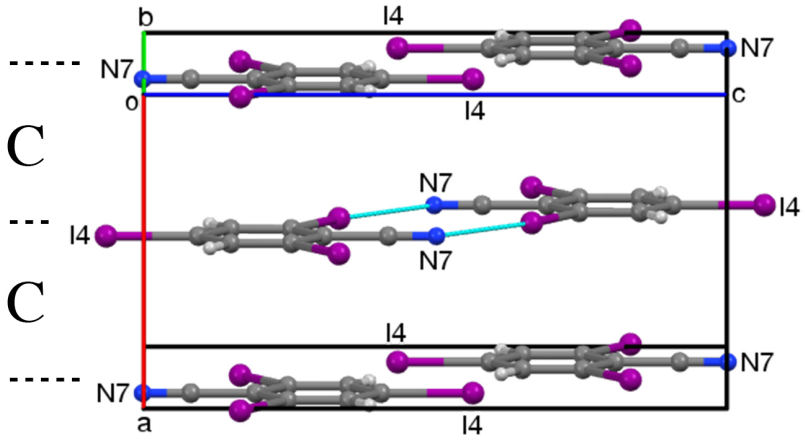

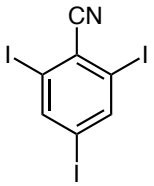

204da

2.5.2. 4-Methyl Nitriles and Isocyanides

Single-crystal determinations were performed on a crystal of dibromo 4-methyl nitrile **204cb**, and a crystal of isocyanide **209cb**, both grown in DCM. The crystals were isomorphous, and matched the previously reported structure of **204cb** [102] (Fig. 34).

Fig 34. The layer structure in dibromo 4-methyl nitrile **204cb**, viewed along {0, 0, c}. Two unit cells and two conformers of the methyl groups are shown. A, B, C, and D are the same cyano-methyl clusters shown in Fig. 35.

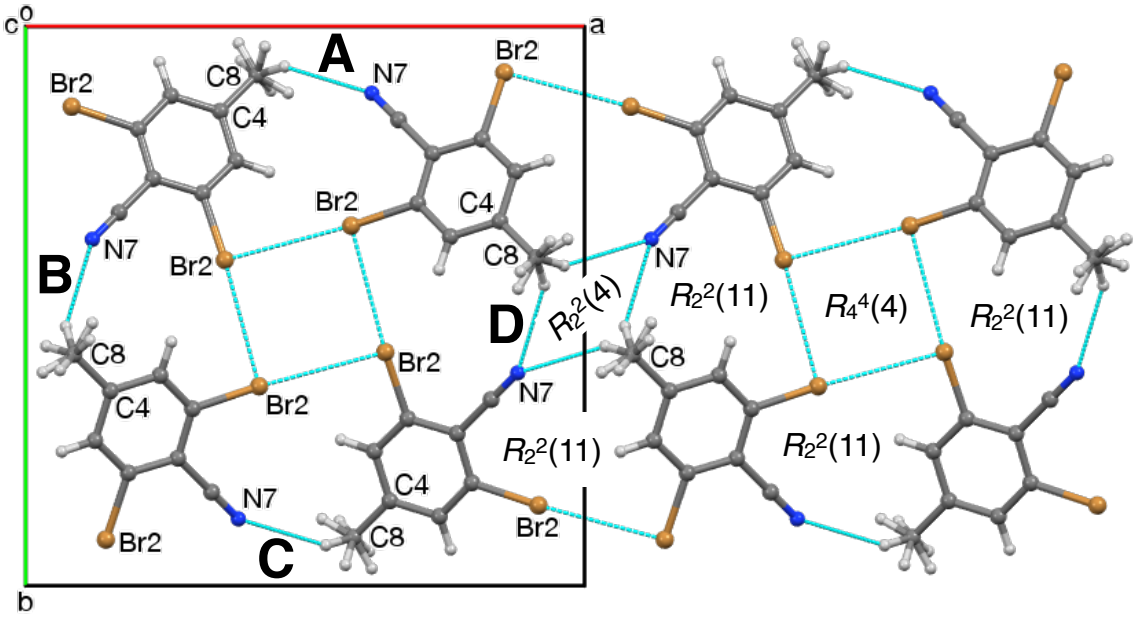

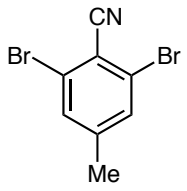

204cb

The thickness of the methyl groups prevented molecules of **204cb** and isocyanide **209cb** from arranging into Type 2 layers. Instead, the bulkiest and least bulky contacts (methyl groups, and cyano N atoms, respectively) clustered together (**A**, **B**, **C**, **D**), forming $R_2^2(4)$ rings [152, 153]. Each Br atom participated in one $R_4^4(4)$ ring [154] with three other symmetry-related Br atoms. Collectively, these contacts formed four symmetry-related $R_2^2(11)$ rings. There were two such sets of these six rings per unit cell; one set is labeled. Molecules on opposite sides of the bromine rings criss-crossed, allowing the methyl-cyano clusters to spread out along the *c*-axis

(Fig. 35). This packing motif resembles a composite photograph of a rear-propeller airplane making one lap (**A**, **B**, **C**, **D**) around a saddle-shaped track.

Fig 35. One unit cell of dibromo 4-methyl nitrile **204cb**, viewed along {a, b, 0}. Two conformers of the methyl groups are shown. A, B, C, and D are the same cyano-methyl clusters shown in Fig. 34.

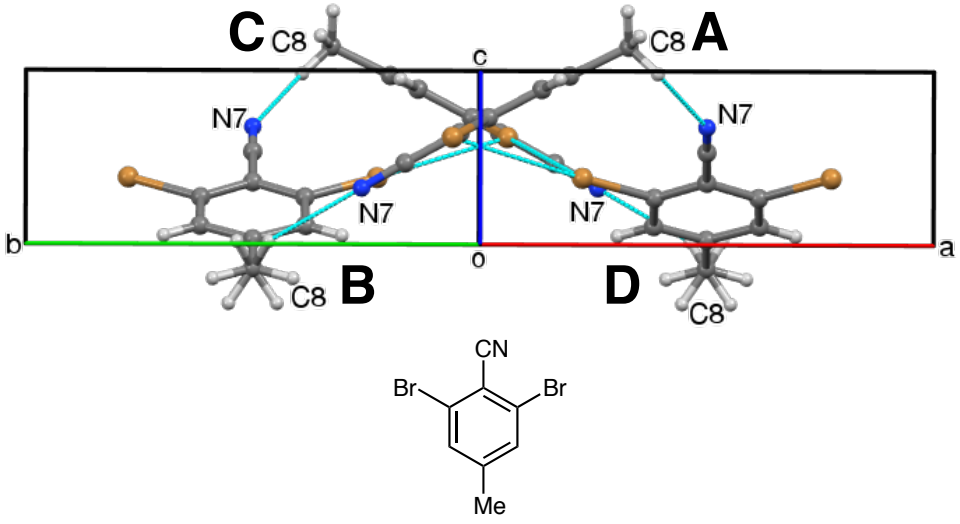

204cb

A single-crystal determination was performed on a crystal of diiodo 4-methyl nitrile **204db** that was grown in DCM. The sample was isomorphous with triiodo nitrile **204da**, forming Type 2 layers with $Z = 4$ and CC stacking (Fig 36). After applying an {0.5a, 0, 0} translation [155], the packing motifs in the unit cells of **204da** and **204bd** are identical. This is the first known example of Type 2 layers forming when the benzene ring has an alkyl substituent. The Type 2 sheets found in the crystals of trihalo nitriles and isocyanides (without methyl groups) have no interlayer short contacts. Because the methyl group has a larger radius than Br or I atoms, the layers in **204db** are connected along the *a*-axis by contacts between the methyl H atoms and the cyano N atom, forming $C_2^1(4)$ chains [153].

Fig 36. The *Z* = 4 unit cell of diiodo 4-methyl nitrile **204db**, with centric (CC) stacking, viewed along {a, 4b, 0}. The top and bottom layers are bisected by the *bc* face of the unit cell.

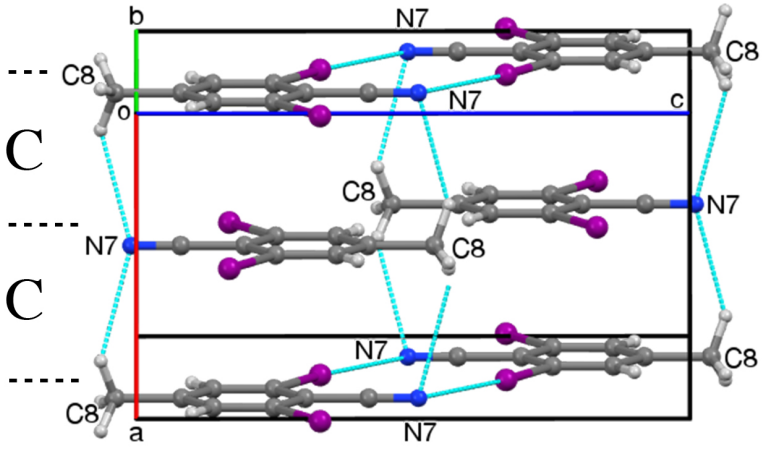

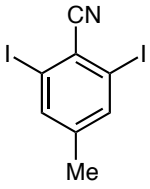

204db

A single-crystal determination was also performed for a crystal of diiodo 4-methyl isocyanide **209db** that was grown in DCM. The structure of **209db** was different than nitrile counterpart **204db**, and bromo counterpart **209cb**, but was an apparent hybrid of the two when comparing some of the main features (Table 21).

Table 21. A comparison of crystallographic features observed in **204db**, **209db**, and **209cb**.

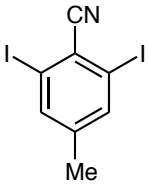

204db

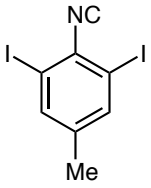

209db

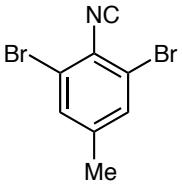

209cb

feature	diiodo nitrile	diiodo isocyanide	dibromo isocyanide
Z	4	4	4
X...X contacts	none	1 per I atom	2 per Br atom
Type 1 rings	2 contain each C≡*N* atom	1 contains each N≡*C* atom	none
$R_2^2(11)$ rings	none	4 per unit cell	8 per unit cell
sheet profile	flat	1-dimensional pleats	2-dimensional pleats

The sheet structure of **209db** had two Type 1 rings, and four $R_2^2(11)$ rings of nearly identical construction as those found in dibromo analog **209cb**, per unit cell. Collectively, these contacts formed two symmetry-related $R_6^6(16)$ rings [152, 153] per unit cell (Fig. 37). One half of this set of rings is labeled.

Fig 37. One layer of the sheet structure in **209db**, viewed along {a, 0, 0}.

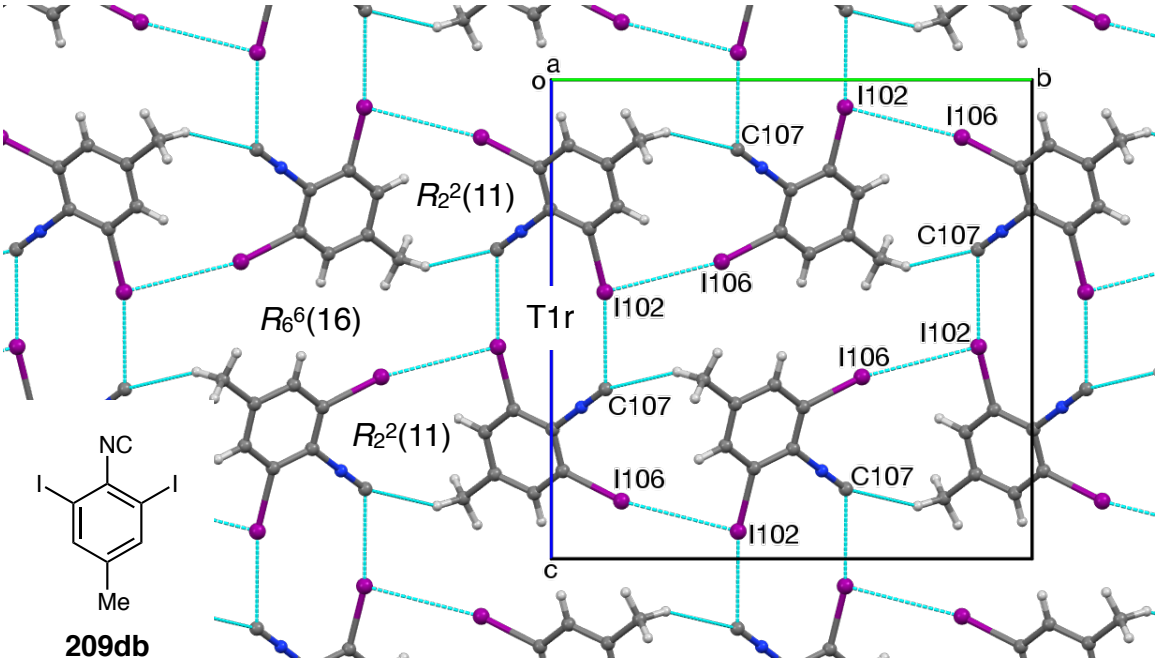

The sheet structure of **209db** was pleated along one dimension (Fig. 38). Each sheet was normal to {a, 0, –c} and the axes of the pleats were parallel to {a, 0, c}. A single layer had a sawtooth-shaped cross-section that is roughly 5.9 Å thick.

Fig 38. One layer of the sheet structure in **209db**, viewed along {a, 0, c}.

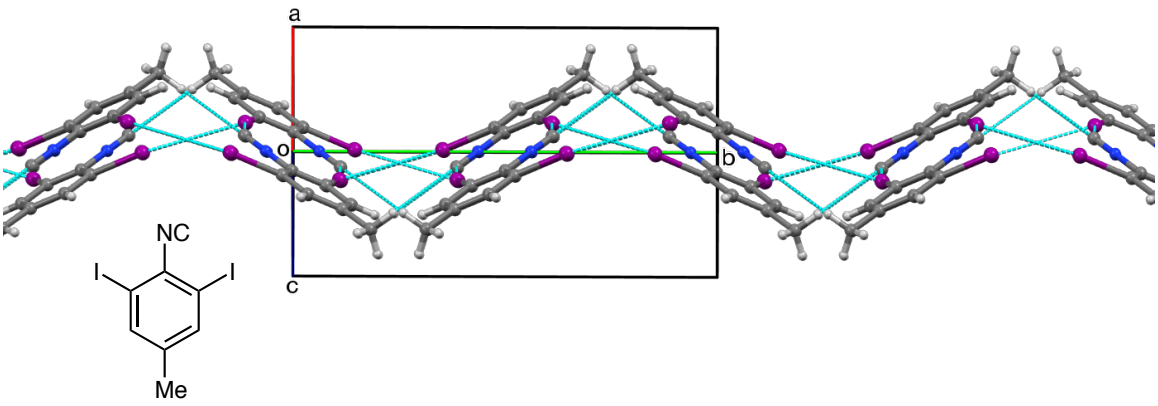

209db

The shaping of the layer profile in brominated analogs **204cb** and **209cb** appears to have been dominated by puckering to relieve steric strain brought into the crystal by the methyl groups. Conversely, it appears that in the crystal of diiodo nitrile **204db**, the larger and softer contact sphere of the I atoms allowed for the formation of strong CN...I contacts in flat sheet structures in the presence of methyl groups. The contact distances were 3.099 Å, which is comparable to those found in tribomo nitrile **204da** (3.114 Å; the standard uncertainties are roughly 0.008 Å). However, the result for isocyanide **209db** indicates that iodinated methyl benzonitriles and isocyanobenzenes of this type may be close to a tipping point between three modes of packing: Inclination to minimize steric congestion, planar packing to maximize CN...I and NC...I bonding, and a hybrid mode with decreased inclination and half as many cyano/isocyano-halo contacts.

2.5.3. 4-Carboxy Derivatives

Co-crystals of dibromo cyano acid **204cc** and anthracene (**215a**) were prepared by slow evaporation of a 2:1 stoichiometric mixture of these two components in DCM. A single-crystal determination was performed. Type 3 sheets were observed (Fig. 39a). The larger radius of Br atoms, versus Cl atoms, allowed the formation of one Type 1 ring per cyano N atom in **204cc**. This is half of the Type 1 ring set that Dr. Britton had envisioned when he analyzed the Type 3 sheets in **204bc** (Fig. 39b). This finding was in agreement with the prediction made in § 2.1.1.

Fig 39. (a) the Type 3 sheet structure observed in **209db**, viewed along {a, 0, c}; (b) The Type 3 sheet structure envisioned by Dr. Britton.

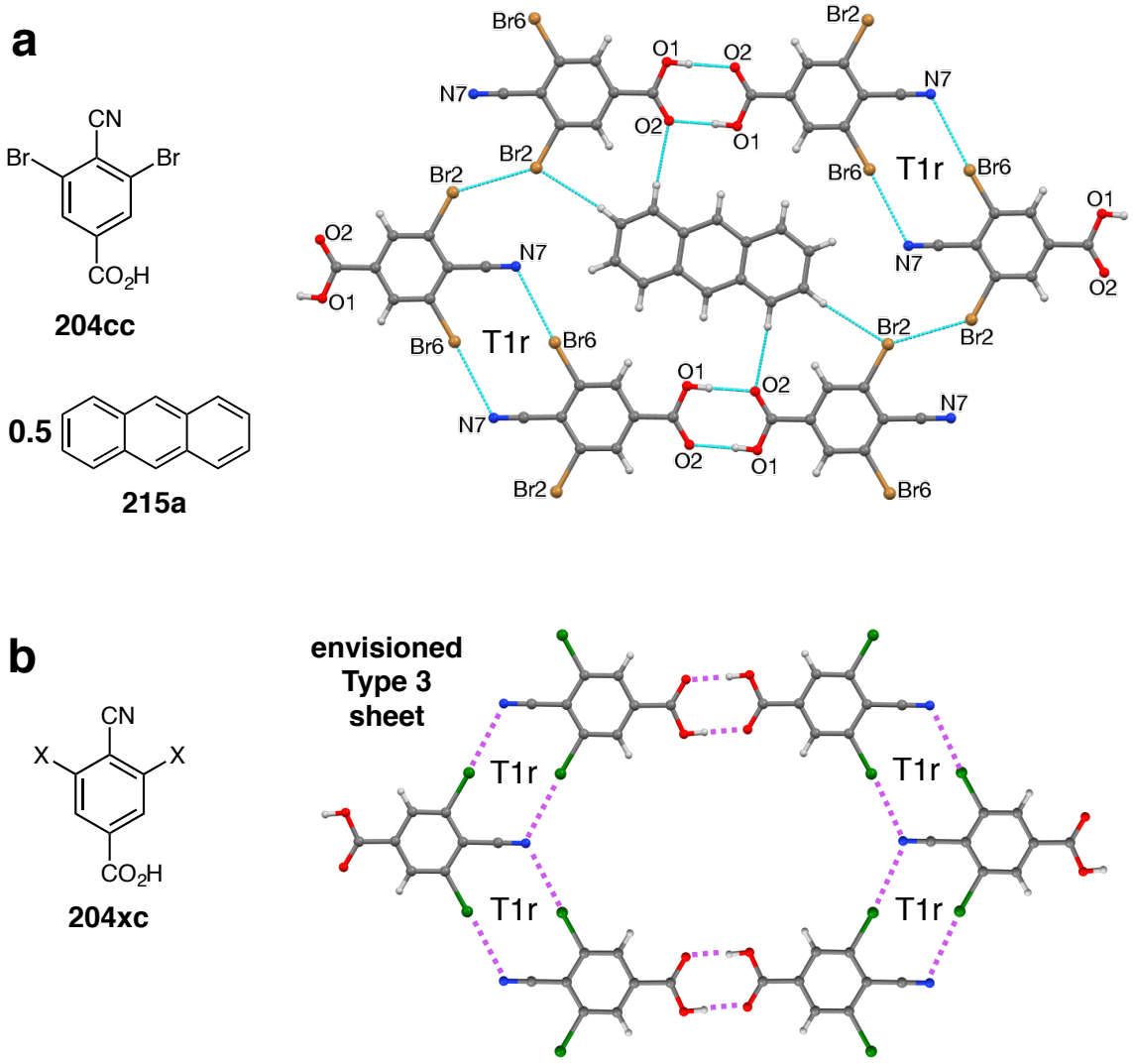

Although the qualitative result observed in the sheet structure of the dibromo co-crystals [**204cc**:**215a** (2:1)] matched predictions, the predicted mean N...Br distance was inaccurate (Table 22, boldface entries). Although the observed N...Br distance was shorter than the observed N...Cl distance, the change was roughly 57% smaller than predicted. There are apparently other factors that cause the molecules to pack less efficiently as the size of halo atoms increases, perhaps including increased interlayer spacing. If the observed rate of N...X gap closure (0.13 Å per 0.11 Å increase in atomic radius) is extrapolated to I atoms, the resulting prediction is that Type 3 sheets composed of **204dc** would have an 0.03 Å mean N...I contact gap. The revised prediction for Type 1 rings is that such crystals would form at least as many as were formed by **204cc**, with relatively even chances of forming additional Type 1 rings.

Table 22. A comparison of the N...X contact gaps in cyano acids **204bc–dc**.

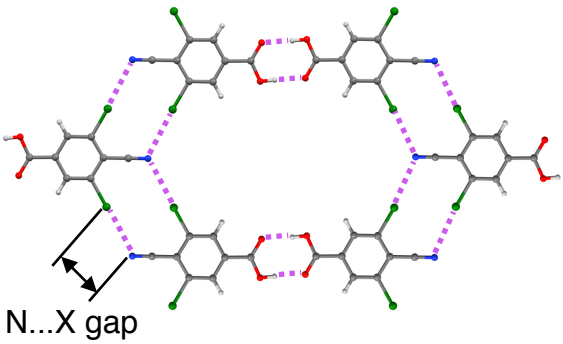

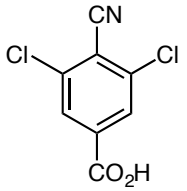

204bc

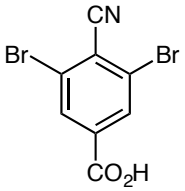

204cc

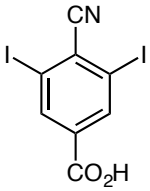

204dc

feature	X = Cl	X = Br		X = I
	observed	observed	predicted	new prediction
N+X radius (Å)	3.35	3.46	3.46	3.61
N...X gap (Å)	3.693	3.672	3.502	-
difference (Å)	– 0.34	**– 0.21**	**– 0.04**	– 0.03
Type 1 rings	none	1 contains each C≡*N* atom	possible	≥ **204cc**

Unfortunately, no conditions were found by which crystals of diiodo cyano acid **204dc** could be prepared neat, or as co-crystals with anthracene (**215a**). One idea was to find suitable substitutes for **215a**, and try to prepare the corresponding co-crystals. Based on the sheet structures observed for **204bc** and **204cc**, a good candidate would be roughly the same length as **215a**, but would be slightly narrower at the ends of the molecule. Thus, a 5:6:5-membered fused-ring structure would be desirable. Substitutes for **215a** should also be centrosymmetric (more specifically, a D_{3h} point group) and not contain basic functionality that would form salts with the cyano acid (*e.g.*, pyridine derivatives). If a prospective substitute has potential hydrogen bond donors and acceptors, their placement should be compatible with the locations of protons and heteroatoms in the Type 3 sheet structure. It should also be a solid. Among the short list of possibilities, pyromellitic diimide (**215b**) was the most attractive option (Fig. 40) [156].

Fig 40. The approximate contact dimensions of anthracene (**215a**) and pyromellitic diimide (**215b**).

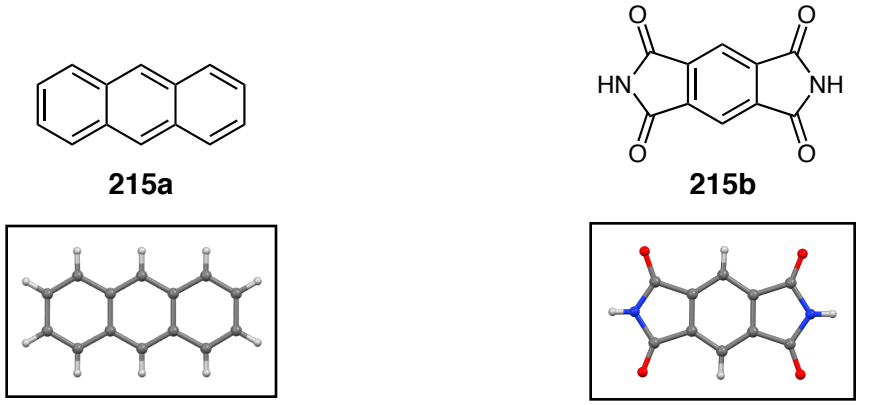

215a **215b**

contact size: 6.88 × 10.82 Å^2 contact size: 6.99 × 10.61 Å^2

Even though **215b** is 0.11 Å wider than **215a**, the added width is at the center of the molecule, which is where the opening in the Type 3 sheet is the widest (Fig. 41). The length of **215b** is roughly 0.21 Å less than that of **215a** and the ends are narrower. The peripheral H and O atoms appear to be compatibly placed. Overall, **215b** seemed like a reasonable fit inside of the Type 3 sheet.

Fig 41. The envisioned Type 3 sheet containing pyromellitic diimide (**215b**). Blue lines show the prospective alignment of donor and acceptor groups. Dioxa analog **215c** is shown for comparison.

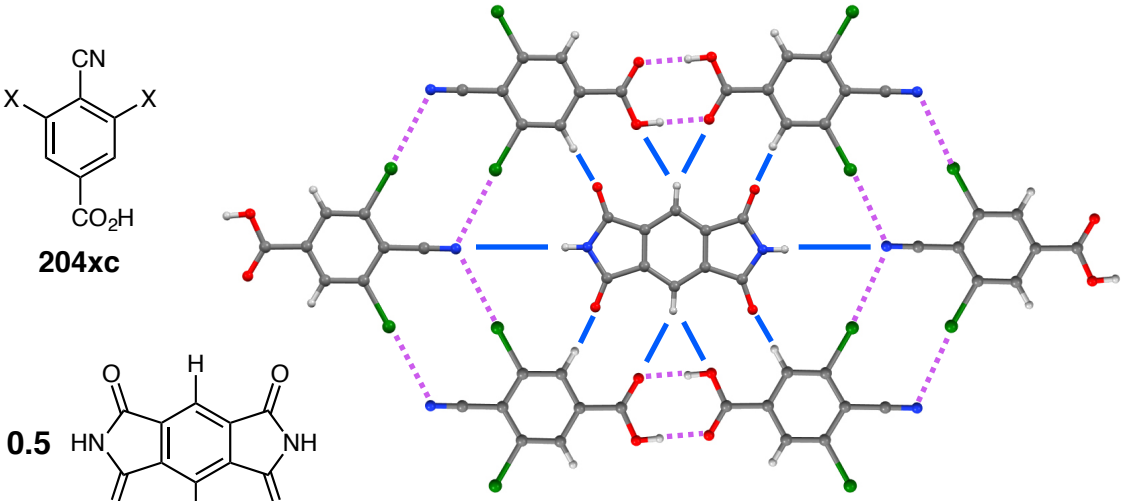

Unfortunately, all three cyano acids (**204bc**,**cc**, and **204dc**) were excluded from co-crystallization with **215b**. Instead, **215b** precipitated as neat crystals. The alignment of donors and acceptors (blue lines) would have required the central opening to distort into a taller but narrower area (as drawn) in order to get the best fit. This distortion combined with possible repulsion between **215b** and the carboxyl H atoms, the energy penalty was apparently too high for this sheet to form. Hypothetically, **215c** would be a better fit, replacing donor C–H atoms with acceptor O atoms, as neighbors to the carboxyl H atoms. However, **215c** is not reported in the literature, and it would probably be very challenging to prepare. No further research was done on Type 3 sheets.

Methyl esters were not part of the originally planned scope of crystallographic study. However, adequate amounts of cyano esters **204bc**,**cc**, and **204dc** were on-hand, since they were synthetic intermediates to the cyano acids. In methyl esters, carboxyl dimers cannot form, so Type 3 sheets were an unlikely outcome. However, the question arose as to whether Type 1 ribbons and/or a variant of Type 2 sheets would form. Brominated analogs were generally the best behaved, synthetically and crystallographically. Also, comparison of nitrile and isocyanide behavior was of interest, hence, isocyano ester **209cd** was prepared. Single crystal determinations were performed on crystals of **204cd** and **209cd** grown in DCM and pentane.

Dibromo cyano ester **204cd** formed sheets normal to {8a, 0, –c} that were pleated along two dimensions (Fig. 42). In each molecule, the Br2 and N7 atoms formed Type 1 rings with a neighboring molecule. The Br6 atom made a short contact with the carbonyl O atom of a third molecule. Sets of three Type 1 inversion dimers were connected by these Br6...O1 contacts, forming $R_6^6(34)$ rings, whose overall shape resembled a line drawing of cyclohexane in a chair conformation (purple lines). There were two Type 1 rings and two $R_6^6(34)$ rings per unit cell.

Fig 42. The sheet structure in a crystal of dibromo cyano ester **204cd**, viewed along {a, 0, –c}.

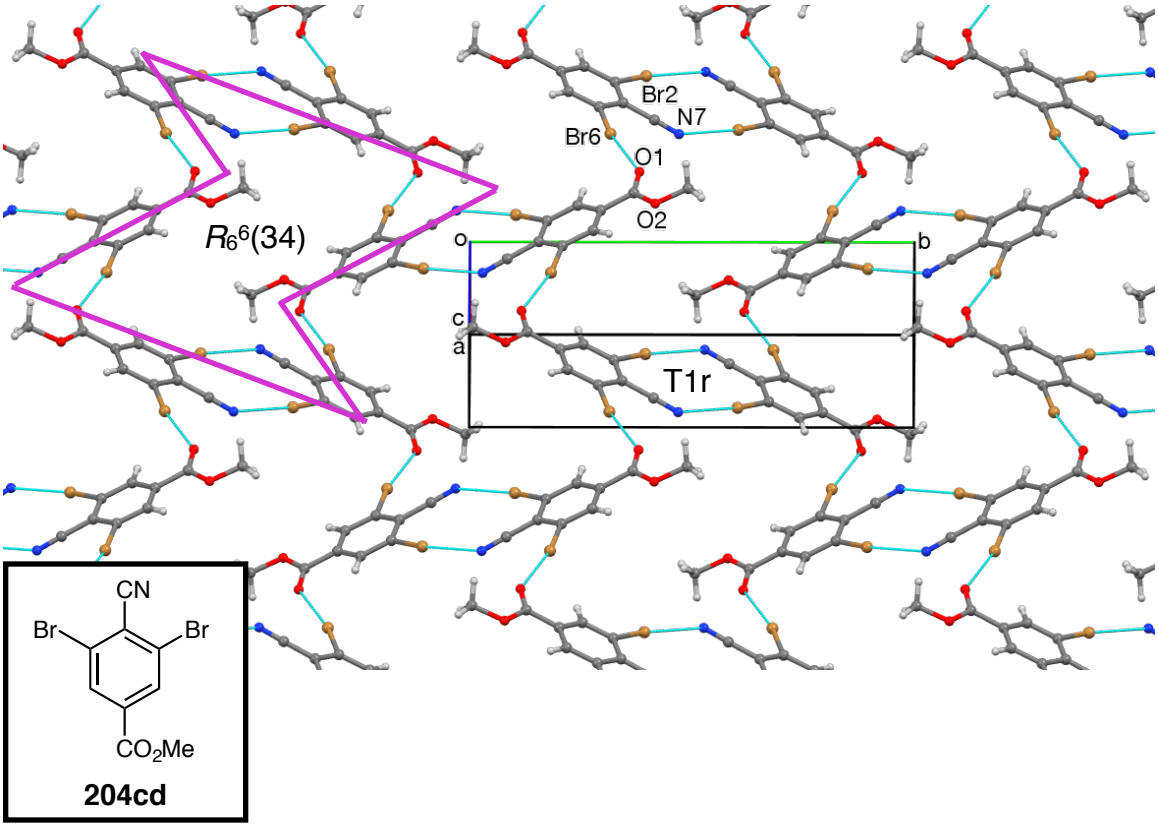

Although this sheet structure is different than all of those previously described in this study, the packing seems to be governed by a familiar theme. After rotating Fig. 42 about the *b*-axis to {2a, 0, c}, it appears as though molecules are packing in a fashion that allows Type 1 rings to form, while staggering to maximize the distance between methyl groups (Fig. 43).

Fig 43. The sheet structure in a crystal of dibromo cyano ester **204cd**, viewed along {2a, 0, c}.

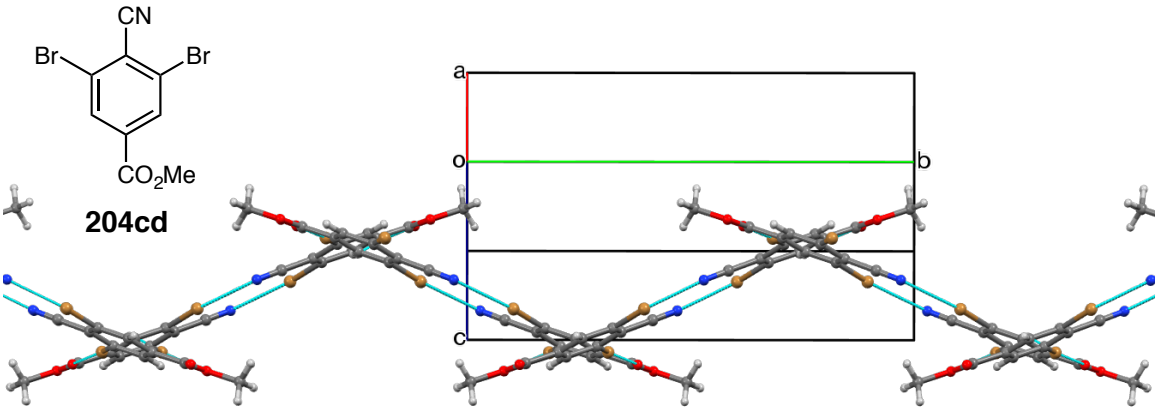

Although it seemed reasonable that isocyano counterpart **209cd** would also form sheets of this type, it was not surprising that a different structure was observed (Fig. 44). Type 1 rings did not form. A Br atom (Br2) and the carbonyl O atom (O1) formed inversion dimers, as $R_2^2(12)$ rings, with a neighboring molecule. There was not a sheet structure because of the mutual inclination of neighboring dimers. Carbonyl O1 also formed a short contact with the second Br atom (Br6) of a third molecule.

Fig 44. One unit cell of the observed crystal of dibromo isocyano ester **209cd**, translated by {–0.5a, 0, 0} and viewed along {a, 0, 0}.

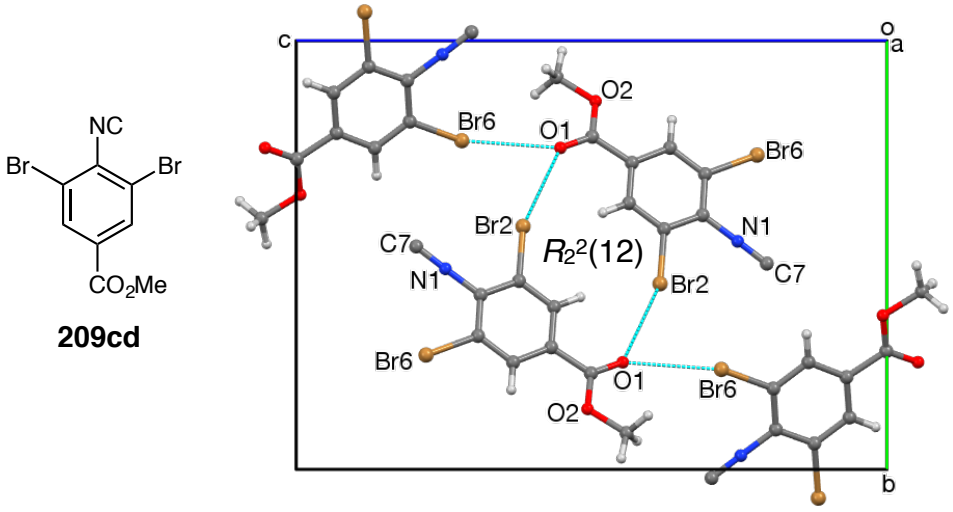

The isoycano C atom (C7) formed no halo or oxy contacts. Instead, it was capped by a methyl group from another unit cell, nearly collinear with the methoxy C–O bond (Table 23). The overall geometry of this contact was consistent with donation of isocyano π-electron density to the methoxy antibonding orbital, or π(N1≡C7)→σ*(C9–O2). Based on the ylide isocyano Lewis structure (R–N^{+}≡C^{-}, Table 26, p 168), one might assume that an n(C7)→σ*(C9–O2) interaction is more likely. However, that is less consistent with the observed bond angles, although it may be a minor contributor to the C7...C9 contact. From a pseudo-hydrogen bond standpoint, O2 was the donor, C9 was the hydrogen, and C7 was the acceptor. The isocyano group plays the opposite role here than it did in NC...X contacts.

Table 23. The geometry of the isocyano-methoxy (C7...C9) contacts observed in a crystal of **209cd**. The molecules are viewed along {a, 0, 0}.

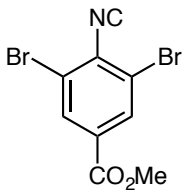

209cd

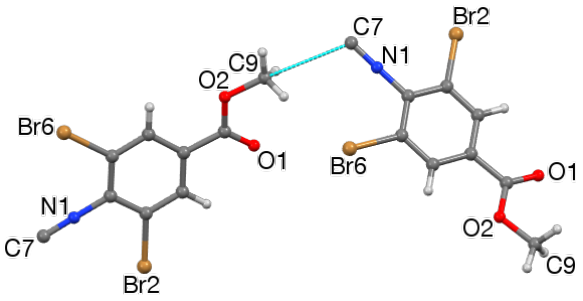

atoms A, B, C	bond length Å A–B or A≡B	contact radius Å B+C	distance Å B...C	bond angle ° ∠ABC
O2–C9...C7	1.453	3.50	3.242	164.5
N1≡C7...C9	1.161			112.9

Unlike the previously discussed structures, this is the only example in which different conformers could be expected a plausible explanation for the change of packing mode. However, the conformers in the two crystals are the same. Furthermore, most of the bond lengths and bond and torsion angles are nearly identical. The biggest differences (Table 24, boldface entries) are the bond and torsion angles of the methoxy group in **209cd**. Both of these angles are distorted toward the N1≡C7 π-cloud (not the C7 n-cloud) compared to the methoxy group in **204cd**, in support of the π(N1≡C7)→σ*(C9–O2) nature of the isocyano-methyl contact.

Table 24. A comparison of selected bond and torsion angles (°) in **204cd** and **209cd**.

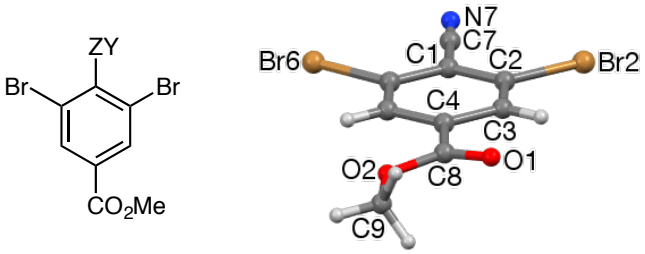

204cd **209cd**

bond or torsion angle	nitrile (**204cd**, ZY = CN)	isocyanide (**209cd**, ZY = NC)
C2–C1–(C7/N1)	120.8	120.8
C3–C4–C8	117.8	116.7
C3–C4–C8=O1	10.1	8.5
C8–O2–C9	117.1	**114.9**
C4–C8–O2–C9	180.0	**174.2**

These molecules are isoelectronic, have similar geometry, pack with emphasis on different contacts, and the crystals were grown in nearly identical conditions. Therefore, polymorphism and pressure- or temperature-induced crystalline phase changes are not unlikely to be found with these crystals. Only one specimen of **204cd** and **209cd** were analyzed in this study. For these reasons and the polytypism found for tribromo nitrile **204cc** and isocyanide **209cc**, it may be worthwhile to perform analysis on additional samples of **204cd** and **209cd**.

One final addition was made to the scope of crystallographic study. Dibromo carbamoyl acid **207** was an unplanned product of the hydrolysis of cyano ester **204cd** (Scheme 71, p 129). A search of the CSD revealed no examples of benzamides containing at least one *ortho*-Br atom, nor any 2-halogenated benzamides with a 4-carboxyl group [87]. Thus, it was deemed worthwhile to perform a single-crystal analysis of **207**. The only good crystals that were obtained were a 2-propanolate, which is consistent with the extreme difficulty with which 2-propanol was removed for IR and NMR analysis.

In the crystal (Fig. 45), the main packing feature was $R_2^2(18)$ head-to-tail hydrogen-bond dimerization between *endo* amido H1B and aprotic carboxyl O2 about the center of the unit cell. The head-to-tail dimers form $C_2^2(11)$ tail-to-tail chains along {0, b, –c} *via* hydrogen bonding between *exo* amino H1A and carbamoyl O1. These chains were connected along {a, 0, 0} into sheets normal to {0, b, c} via a $D_2^2(4)$ chain of 2 hydrogen bonds between carboxyl H3A, the alcohol O4–H4B group, and carbonyl O1. The Br atoms made no contacts, and were spectators to the hydrogen bond network. 2-Propanol was disordered into two components, roughly in a 3:2 ratio. Both disorder components showed similar hydrogen bond networks, in spite of a 54° change in the orientation of the alcohol OH group.

Fig. 45. Five molecules of carbamoyl acid **207** are shown, to illustrate the 3 main packing interactions, viewed along {–a, 3b, 0}. (a) Head-to-tail dimerization; (b) Tail-to-tail dimerization; (c) Carboxyl-hydroxyl-carbamoyl chains. The atoms in these interactions and one extra H3A atom are labeled. The major disorder component of 2-propanol is shown.

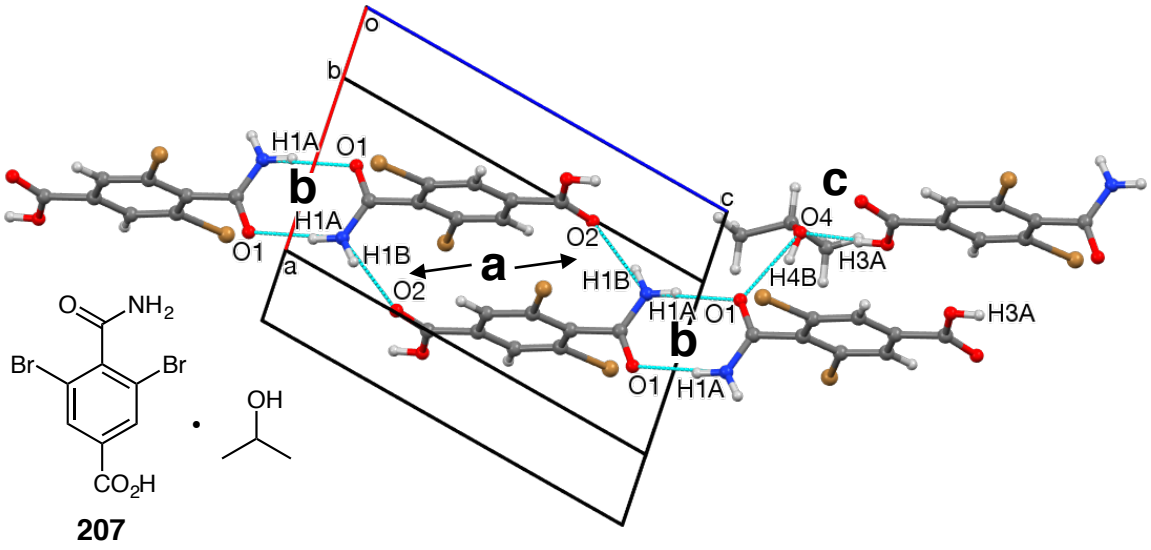

207

Regarding the inclination of the carbamoyl group to the phenyl ring, resonance stabilization would be maximized at zero inclincation, whereas relief from steric strain would be maximized at 90º. One would predict a trend where the torsion angle increases with increasing size of *ortho*-substituent. This trend is confirmed by the best available comparisons from the CSD (Fig. 46) [157]. Dibromo acid **207** makes a nice extension to this trend. No 2-iodo examples were found; the torsion angle would probably be nearly 90º.

Fig. 46. Substituted benzamides, in their crystals, viewed along the carbamoyl *ipso* bonds. The angles listed (ω) are torsions between the planes of the benzene rings and the axes of the carbamoyl C=O bonds.

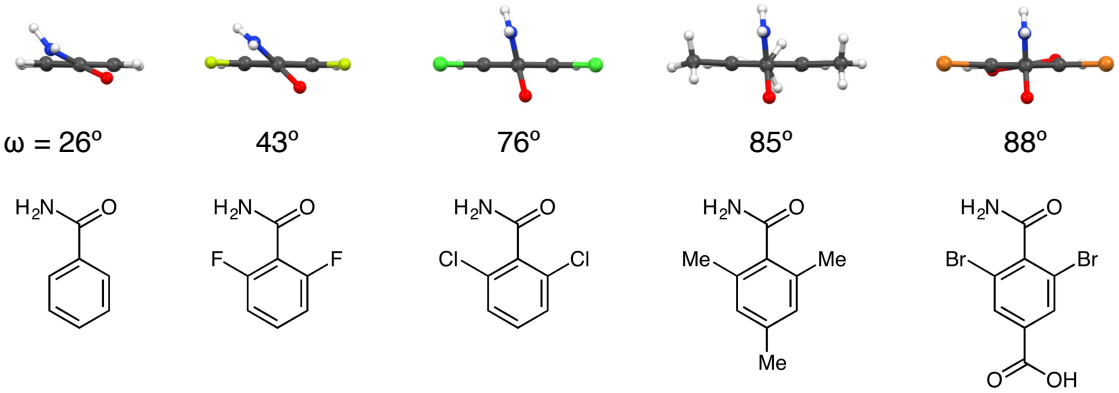

239a **239b** **239c** **239d** **207**

239a–d: reported structures novel

This finding explains the initially puzzling synthetic result that the cyano group in **204cd** would undergo the first stage of hydrolysis so readily, yet the resulting amide in **207** was so resistant to cleavage (Scheme 79). The disappearance of starting material (**204cd**) was nearly complete within the first 30 minutes of reflux. However, reflux times extended to 24 hours did not generate an observable amount of the corresponding dicarboxylic acid (**240**). Because the carbamoyl group in **207** is nearly perpendicular to the ring, hydrolysis would require a hydroxide ion to approach **207** equatorially, which is blocked by the Br atoms.

Scheme 79. The base-promoted hydrolysis of cyano ester **204cd** to **207**, which was not observed to continue to diacid **240**.

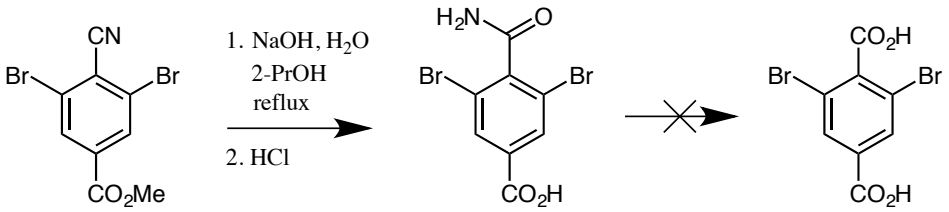

204cd **207** **240**

nearly complete after 30 min

not obs. after 24 h

2.5.4. Short Contact Geometry

The C≡N...X (cyano-halo), N≡C...X (isocyano-halo), and Z...Y...X (any-halo-halo) distances and bond angles found in the present study are given in Table 25. Corresponding nitriles and isocyanides are in consecutive crystal entries. Y+X distances are the sum of the contact radii of atoms Y and X [78b], and are included to illustrate the 'shortness' of each Y...X contact.

Table 25. Cyano-halo, isocyano-halo, and halo-halo short contact geometry in all applicable crystals surveyed in § 2.

crystal	atoms	distance Å			bond angle °
	Z, Y, X	C≡N	Y...X	Y+X	
204ca - TT	C17≡N17...Br12	1.144	3.053	3.46	131.45
204ca - TC	C27≡N27...Br32	1.132	3.059	3.46	131.76
	C37≡N37...Br22	1.156	3.077	3.46	130.68
209ca - TC	N127≡C127...Br132	1.147	3.141	3.60	134.01
	N137≡C137...Br122	1.164	3.161	3.60	133.23
204ca - TCT	C47≡N47...Br52	1.146	3.072	3.46	130.95
	C57≡N57...Br42	1.147	3.057	3.46	131.47
	C67≡N67...Br62	1.139	3.065	3.46	131.96
204cb	Br2...Br2...Br2	1.145[a]	3.557	3.70	86.10
209cb	Br102...Br102...Br102	1.160[a]	3.575	3.70	85.91
204cc : **215a** (2:1)	C7≡N7...Br6	1.143	3.307	3.46	115.90
	C2–Br2...Br2	-	3.553	3.70	133.43
204cd	C7≡N7...Br2	1.138	3.041	3.46	128.64
209cd	N107≡C107...(none)	1.161[a]	-	-	-
204da - CC	C7≡N7...I2	1.079	3.114	3.61	133.44
209da - CC	N107≡C107...I102	1.161	3.121	3.75	134.23
204db - CC	C7≡N7...I2	1.130	3.099	3.61	130.07
209db	N107≡C107...I102	1.154	3.183	3.75	131.34
	C102–I102...I106	-	3.787	4.00	93.45
	C106–I106...I102	-			167.54

[a]The cyano or isocyano group in this crystal has no halo contacts.

The mean C≡N bond lengths are shorter in cyanides than in isocyanides (Table 26). The standard uncertainties for these bond lengths are approximately 0.004–0.007 Å. The difference of cyano versus isocyano bond lengths is small, and both are nearly linear. Thus, the ylide resonance form of the isocyano group ($R–N^{+}\equiv C^{-}$) is a more accurate model than the carbene resonance form (R–N=C) for crystals in the CSD [158] and the present study. Based on the data from plain benzonitrile [159], the CSD (most have short contacts), and the present work, contacts of this type cause a shortening of the C≡N bond. However, the observed difference is close to the standard uncertainty.

Table 26. Mean C≡N bond lengths (Å).

compounds	CN	NC
plain benzonitrile [159]	1.167	not found
mean values in the CSD in 1985 [158]	1.138	1.144
the present work, no halo contacts	1.145	1.161
the present work, with halo contacts	1.135	1.157

When these changes in C≡N bond lengths are viewed in combination with the corresponding *ipso*–CN and *ipso*–NC distances, the findings are in agreement with the pseudo-hydrogen-bond behavior described in § 2.1.1 for cyano-halo and isocyano-halo short contacts (Table 27). The formation of these contacts causes the *ipso*-Z distance (distance a) to increase. This was roughly offset by a decrease in CN bond length (distance c), so that the ZY group was roughly stationary relative to the *ipso* atom (distance b). From a displacement perspective, the pseudo-hydrogen donor and acceptor are the *ipso* and X atoms, respectively. However, it is the Z atom that plays the role of the proton, rather than the whole ZY group. The values given are averages that include data from the crystals in the present work and benzonitrile [159]. The standard uncertainties for these distances are roughly 0.006–0.012 Å, so this analysis should be treated as tentative.

Table 27. Comparison of *ipso*-cyano/isocyano distances with and without halo contacts. The legend is not to scale.

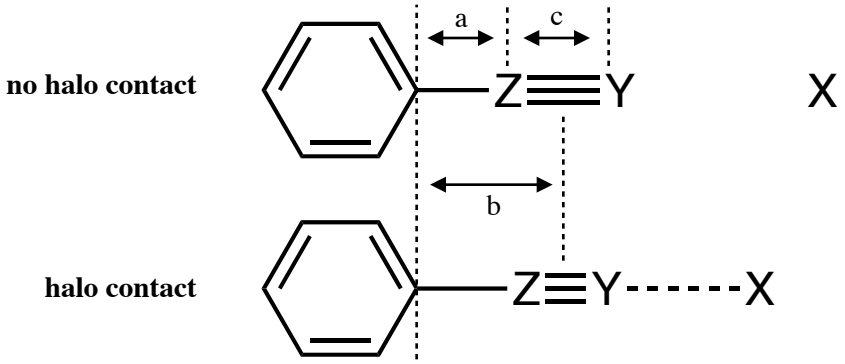

crystals	distances Å		
	a	b	c
nitriles, no halo contacts	1.437	2.016	1.156
nitriles, halo contacts	1.447	2.015	1.135
(change)	+ 0.010	– 0.001	– 0.021
isocyanides, no halo contacts	1.387	1.968	1.161
isocyanides, halo contacts	1.391	1.970	1.157
(change)	+ 0.004	+ 0.002	– 0.004

The crystals that formed Type 2 sheets are given entries in Table 25 with polytypes listed (*i.e.*, CC, TC). In these crystals, the mean bond angle in cyano-halo contacts was narrower than in isocyano-halo contacts (Table 28). The bromo and iodo contact angles are nearly identical, with iodo contacts being slightly wider. The standard uncertainties of these angles are approximately 0.08–0.15º. Although the sample size is small, the configuration of N and C atoms has a larger effect on contact angles than the type of halogen, for the available data.

Table 28. The mean cyano-halo and isocyano-halo contact angles (Z≡Y...X) in crystals that formed Type 2 sheets.

	CN...	NC...
Br	131.38º	133.62º
I	131.76º	134.23º

2.6. Conclusions

Progress toward the 5 objectives listed in § 2.3, deviations thereof, and key results are summarized here. Eight of the nine proposed 2,6-dihalobenzonitriles were prepared, as were five of the six corresponding isocyanobenzenes. The 2,6-dichloro-4-methyl analogs were not obtained. As additions to the proposed synthetic scope, the methyl esters of all three desired cyano acids were prepared, as was methyl 3,5-dibromo-4-isocyanobenzoate. The initially proposed synthetic route was largely used. The halogenations were best performed using SO_2Cl_2, Br_2, and ICl. Sandmeyer cyanations were best performed using SBDC suspensions. Removal of excess $NaHCO_3$ from the cyanation mixture gave very poor cyanation yields. Formylations were best performed using AFA solutions, and could not be carried out with halogenated anilines using formic acid and a Dean-Stark water separator. Halogenation prior to formylation was found to be the essential order of transformations. All six attempted formanilides were smoothly converted into the desired isocyanobenzenes using $POCl_3$ in a solution containing DIPEA. All synthetic transformations involving carboxy analogs were best carried out with the substrate protected as the corresponding methyl ester. Selective de- esterification of cyano esters could not be carried out using conventional acidic or alkaline mixtures. The use of LiI in pyridine for the demethylation of methyl esters was successful, although 3,5-diiodo-4-cyanobenzoic acid could not be isolated from the product mixture. Overall, 11 nitriles were prepared in 2 to 4 steps, with yields of 20 to 84%. Correspondingly, 6 isocyanides were prepared in 3 to 4 steps, with yields of 44 to 77%.

All of the desired characterization data were successfully obtained for the synthetic intermediates and desired products that were isolated. These data are reported in §3 and the corresponding appendices. For the bromination and cyanation mixtures that were discussed, a smaller set of characterization data were obtained. The minimum scope of characterization data for mixtures was ^{1}H NMR and HRMS spectra, and TLC data.

Because of time limitations, no crystallographic study was performed on chlorinated compounds. Polytypism with Type 2 sheets was observed in 2,4,6-tribromobenzonitrile and the corresponding isocyanide. Two new polytypes of the nitrile were observed (TC- and TCT-stacked) in addition to the reported TT-stacked polytype, whereas only the original TC- stacked polytype of the isocyanide was found. For 2,4,6-triiodobenzonitrile and the corresponding isocyanide, Type 2 sheets were observed with CC-stacking. With 2,6-diiodo-4-

methylbenzonitrile, Type 2 sheets with CC-stacking was also observed. This is the first known case of Type 2 sheets forming in a molecule with an alkyl substituent. The corresponding isocyanide had different packing in its crystal. The 2,6-dibromo-4-methyl nitrile and isocyanide were isomorphous and matched the reported structure for the nitrile, which is built from Br...Br contacts and contains no CN...Br contacts. Co-crystals of 3,5- dibromo-4-cyanobenzoic acid with anthracene (2:1) were successfully prepared. The analyzed crystal had Type 3 sheets with one half of the Type 1 rings that were envisioned by Dr. Britton. The corresponding diiodo co-crystals were not successfully obtained. As an extension to the proposed scope of study, crystals of methyl 3,5-dibromo-4-cyanobenzoate and the corresponding isocyanide were prepared and analyzed. These crystals were not isomorphous. A crystal of 3,5-dibromo-4-carbamoylbenzoic acid 2-propanolate was also analyzed. Two modes of hydrogen bond dimerization and a 3-hydrogen-bond chain were observed. Overall, brominated products demonstrated the best combination of simple synthetic preparation and interesting crystallography. The iodinated products demonstrated novel combinations of crystallographic features, as anticipated. Because of time constraints, no polymorphism searches were done, except with the tribromo nitrile and isocyanide.

As with Part I, 11 undergraduates made contributions in volunteer, fellowship-sponsored, and for-credit positions during the course of the work performed in §§ 2.4 and 2.5. Several manuscripts are in preparation, and all of the former undergraduates are on track for co-authorship. The mentorship objective was successfully fulfilled, and was mutually at least as significant as the research itself.

2.7. Prospective Future Work

Powder diffraction could be used to search for polymorphism in the two observed cases where crystals of the nitrile and the corresponding isocyanide had different packing motifs (Fig. 47). The present study has shown that all four of these compounds are easy to prepare. The crystallographic results could shed more light onto the nuances of nitrile versus isocyanide interactions in the solid state.

Fig. 47. The four compounds prepared in the present study for which a polymorph search is suggested as future work.

ZY = CN	**204cd**	**204db**
ZY = NC	**209cd**	**209db**

Given the favorable synthetic and crystallographic results obtained from brominated nitriles in the present work, the most attractive starting point for extensions to the synthetic scope is to prepare additional brominated nitriles. In 2002, Dr. Britton prepared a crystal of 3,5-difluorobenzonitrile (**241**, Fig. 48) [160].

Fig. 48. The ribbon structure reported in a crystal of **241**.

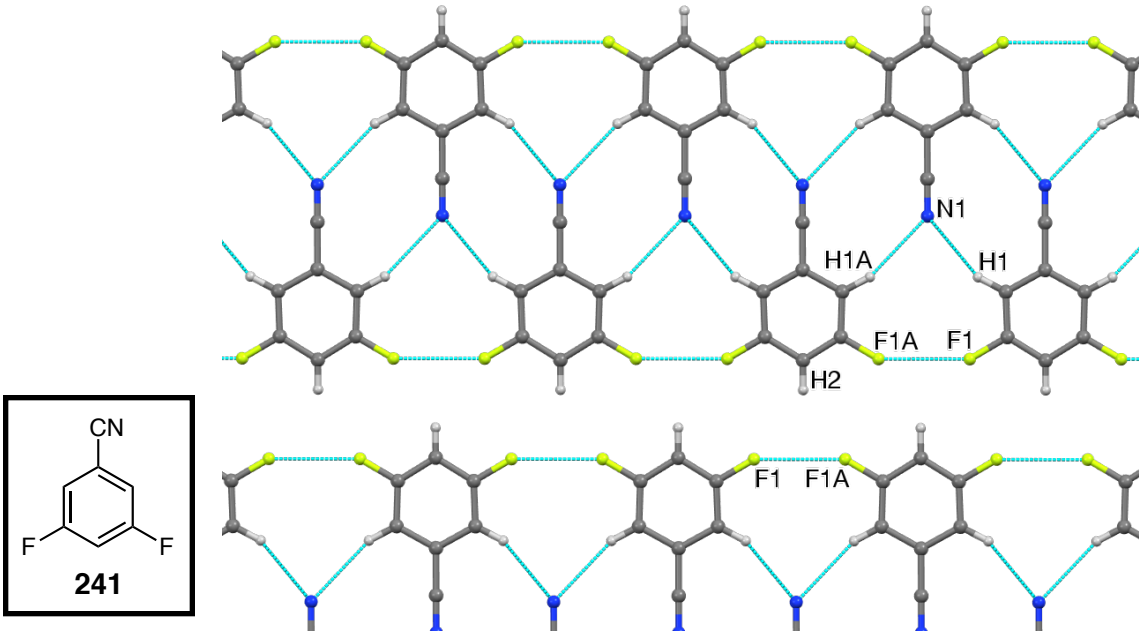

Dr. Britton reasoned that the crystal would probably contain either CN...F contacts or C–H...F hydrogen bonds, both of which are uncommon. Instead, the observed outcome was a ribbon structure constructed of CN...H and F...F contacts. Between ribbons, the H2 and F1/F1A atoms were spaced apart by almost exactly the sum of their atomic contact radii. This ribbon structure is a variation of a Type 1 ribbon, where the horizontal mirror plane of the molecules has been rotated 180° within the vertical mirror plane.

It would be interesting to see whether 3,5-dibromobenzonitrile (**242**, Scheme 80) packs in a similar fashion to **241**, or if the packing of **242** is governed by CN...Br contacts. Nitrile **242** could probably be prepared from 3,5-dibromoaniline (**238**), according to the same conditions that were used to prepare 2,4,6-tribromobenzonitrile (**204cc**). The preparation of **238** was described in Scheme 65 (p 122).

Scheme 80. The proposed synthesis of 3,5-dibromobenzonitrile (**242**).

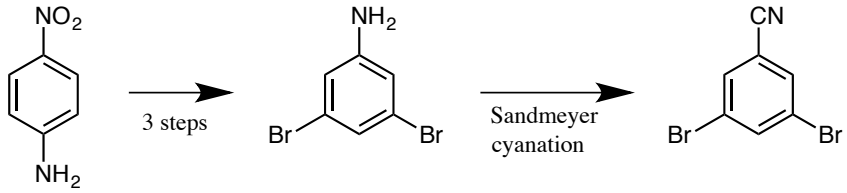

233 **238** **242**

The crystallographic study of biscarbonitrile **245** (Scheme 81) would be another interesting extension. Each benzene ring in **245** has the local symmetry that gave good results in the present study. The two benzene rings would probably be mutually inclined by 60º to 80º. The main crystallographic questions include whether a variant of Type 1 ribbons would form, and whether criss-crossing networks of ribbons would form. Numerous methods are reported in the literature for the preparation of benzidine (**244**) from nitrobenzene (**243**). An attractive option is the reductive coupling of nitrobenzene using aluminum foil in an alkaline suspension [161], followed by acid-catalyzed rearrangement [162]. The final two transformations could draw from the optimized conditions for the preparation of methyl 4-cyano-3,5-diiodobenzoate (**204dd**), since brominated benzidine derivatives are likely to have similar solubility-based limitations.

Scheme 81. The proposed synthesis of tetrabromo biscarbonitrile **245**. Iodinated nitrile **204dd** is shown for comparison.

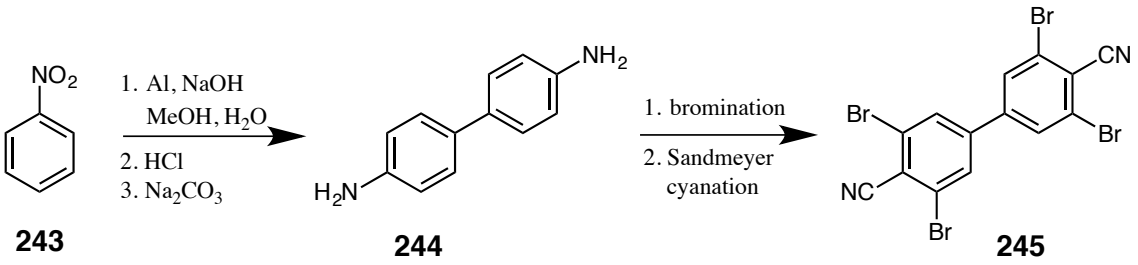

243 **244** **245**

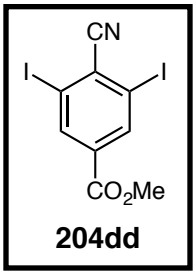

204dd

Part III. Experimental Procedures

3.1. General

3.1.1. Reagents, Packings, and Other Basics

Solvents and reagents were purchased and used as received. When phenylhydrazine had darkened beyond pale yellow in color, it was purified by vacuum distillation (114–117 ºC, 30 mmHg). Brine refers to saturated aqueous sodium chloride solution. Measurements of pH were taken using *Hydrion type B* pH-indicating paper test strips [163]. Packed-column reflux and distillation was performed using Pro-Pak 0.16" stainless steel protruded saddles [164]. Column chromatography was performed using 40–75 μm silica gel with 60 Å pores [165], 50–200 μm neutral alumina with 58 Å pores [166ab], or 44–250 μm basic alumina with 60 Å pores [167bc]. Qualitative TLC analyses (R_f) were performed on plastic-backed plates pre-coated with 0.2 mm of silica gel or basic alumina with UV_{254} indicator [168]. Chromatographic solvent ratios are reported by volume. All reaction mixtures were magnetically stirred. Rotary evaporation was performed at water aspirator pressure, typically at 20–60 mmHg and 20–50 ºC. Unless otherwise specified, recrystallized substances were dried for 2–4 h using an Abderhalden apparatus [169] at 0.01–0.1 mmHg and heated by the warmest of: refluxing acetone, EtOH, 1-PrOH, or toluene, such that the product tube was at least 30 ºC below the melting point of the product. N_2 or Ar-containing atmospheres were maintained close to 0 psig using a gas bubbler [170].

3.1.2. Instrumentation, Elemental Analyses, and Sample Purity

Melting points (M.p.) were obtained from samples in open 1.5 mm glass capillaries in a Mel-Temp apparatus [171] and are uncalibrated. Infrared spectra (IR) were collected on a Thermo Fisher Scientific Nicolet iS5 spectrophotometer [167bd]. High-resolution electron ionization mass spectra (HRMS-EI) were collected on a Finnigan *MAT 95* fitted with a solids probe [167bd], or an Agilent 7890B gas chromatograph using an Agilent *DB-5MS* 250 μm capillary column with an Agilent 7200 Q-TOF detector [172be]. Various column lengths were used as necessary to give reasonable retention times. HRMS-EI were calibrated using internal perfluorokerosene (Finnigan) or external perfluorotributylamine (Agilent) [166ac]. High-

resolution ESI mass spectra (HRMS-ESI) were collected on a Bruker *BioTOF II* reflectron ESI-TOF mass spectrometer [173bc]. In positive-polarity ESI experiments, 0.2% v/v formic acid in methanol was the solvent, and internal poly(ethylene oxide) [174] was the calibrant. In negative-polarity ESI experiments, methanol was the solvent, and internal 2,2'-[poly(ethylene oxide)-α,ω-diyl]bis(acetic acid) [175] or Agilent tuning mix [172bc] was the calibrant.

NMR spectra were collected on one of five instruments: A Bruker *Avance III* 400 MHz (AM400) or 500 MHz (AV500) spectrometer, a Bruker *Avance III HD* 500 MHz spectrometer (HD500) [173], or a Varian *Inova* 300 MHz (VI300) or 500 MHz (VI500) spectrometer [172bde]. Except where noted, ^{13}C NMR spectra were proton-decoupled.

X-ray crystallographic data were collected from Cu (1.542 Å) or Mo (0.711 Å) Kα radiation, by a Bruker ApexII CCD, Venture D8, or 1K area detector, or a Siemens (now Bruker) SMART area detector [177].

Elemental analyses (Anal.) were performed by M-H-W Laboratories (MHW) [178] or Atlantic Microlab (AML) [179]. Elemental analyses were performed on novel products, except most of those which were analyzed by X-ray crystallography. Additionally, elemental analyses were performed on several known products which lack elemental analysis data in the literature. Estimated purity, along with the masses of major impurities, are given for products where the combined mass fraction of identifiable impurities is at least 0.03 (by ^{1}H NMR analysis), and for novel products for which a matching elemental analysis could not be obtained, regardless of their NMR results.

3.1.3. Data Processing, Reporting, and Plotting

Infrared spectra were processed and plotted using *GRAMS/AI* version 7.02 with 4-point baseline correction [167ab]. All reported peaks are in cm^{-1}. Only the most intense or diagnostic peaks are reported. HRMS-EI were processed using *Mass Hunter Qualitative Analysis* version B. 07 build 7 [173ab]. HRMS-ESI were processed using *micrOTOF* version 3.4 [173ab].

All NMR spectral data were processed and plotted using *MestReNova* version 7 [180] using the default Fourier transform settings. All chemical shifts, δ, are reported in ppm. All coupling constants, *J*, are reported in Hz. Where NMR signals are assigned to specific atoms, C and N atoms are labeled with numbers, H atoms are labeled with lower-case letters, and are in order of decreasing chemical shift. For heteronuclear experiments, the lighter nucleus is listed first and is

the basis for the spectral frequency. ^{13}C and ^{1}H NMR chemical shifts were referenced to solvent peaks as follows [$\delta(^{13}C)$, $\delta(^{1}H)$]: $CDCl_3$ [77.160, 7.260),] CD_2Cl_2 [54.000, 5.320], $(CD_3)_2SO$ [39.520, 2.500], $(CD_3)_2CO$ [29.840 (CD_3), 2.050], CD_3CN [1.320 (CD_3), 1.940], and $(CD_3)_2NCDO$ [163.150 (*C*DO), 8.030 (C*H*O)]; the ^{1}H values are for residual monoprotiated solvent. Cubic spline baseline correction was applied to plots that include integration data. Where yields or ratios are reported as "calculated by ^{1}H NMR analysis," a mass balance was performed using resolved peaks of known components. Where this was not viable, naphthalene (25-100 mg) were added to the reaction mixture at the beginning of the experiment, or naphthalene or 1,4-dimethoxybenzene (5-25 mg) were added to samples following purification, and was used as an internal integration standard. Yield calculations used during Method F (§ 3.2.3) were after filtration, and before chromatography. Where chemical shifts were determined by HMBC analysis, the reported value is the mean of all resolved crosspeaks for the given signal.

X-ray crystallographic data were processed and refined using *SHELXS97* [181] or *SHELXL2014* [182]. Crystallographic drawings were generated from the corresponding CIF's [179] using *Mercury*, versions 3.5–3.8 [184].

3.2. Indole and Cyclic Ketones

3.2.1. Cyclic Ketones

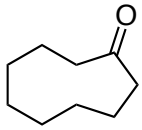

Cyclononanone (2i). Based on the work of Burpitt & Thweatt [56], including modifications described therein, by Brannock, *et al*. [57]: cycloheptanone (17.7 mL, 150 mmol), pyrrolidine (30 mL, 365 mmol), mixed xylenes (30 mL), and $TsOH•H_2O$ (20 mg, 105 μmol) were placed in a round-bottomed flask fitted with a packed column (2 cm × 10 cm, D × H) and a Dean-Stark trap (25 mL) that was filled with hexane. The reaction mixture was refluxed for 24 h and then allowed to cool to rt. The Dean-Stark trap was replaced with a distillation head, and then the reaction mixture was separated by fractional distillation. The desired fraction, *N*-cyclohepten-1-ylpyrrolidine (112–117 ºC, 8 mmHg; 13.9 g, 84.1 mmol), and ether (25 mL) were placed in a round-bottomed flask in a dry N_2 atmosphere. The reaction mixture was cooled in an ice bath. A solution of methyl propiolate (7.5 mL, 84.3 mmol) in ether (25 mL) was added dropwise over 30 min. Once the addition was complete, no more ice was added to the cooling bath, and the reaction mixture was stirred for 24

h, during which it had warmed to rt. The resulting mixture was cooled in an ice bath, and then AcOH (50 mL) was added dropwise over 10 min. The ether was removed on a rotary evaporator. The resulting mixture [185] was placed in a pressure flask [186]. AcOH (50 mL) and Pd on carbon (3.10 g, 5 mass%, 1.46 mmol Pd) were added.

Hydrogenation and hydrolysis: The oxygen content of the pressure flask was decreased via 10 iterations of reducing the pressure to 1 mmHg, and then filling the flask with argon to 760 mmHg. The resulting mixture was hydrogenated (rt, 40 psig, 24 h). The hydrogenated mixture was filtered through a column (SiO_2, 2 cm × 5 cm, D × H) packed with chloroform, and then the column was washed with additional chloroform (5 × 25 mL). The combined filtrate was concentrated on a rotary evaporator. The resulting brown oil, water (8 mL), 2-propanol (15 mL), and sodium hydroxide solution (aq., 50 mass%, 7 mL, 134 mmol NaOH) were placed in a round-bottomed flask. The resulting mixture was refluxed for 2 h. The reflux condenser was replaced with a packed column (2 cm × 10 cm, D × H) and a distillation head, and then the 2-propanol was removed by distillation. The resulting mixture was allowed to cool to rt, and then was extracted with ether (4 × 25 mL). The combined extract was washed with aliquots of hydrochloric acid (1.0 M, 20 mL) until the raffinate had a pH no higher than 2, and then aliquots of $NaHCO_3$ solution (aq., 50% sat., 20 mL) until the raffinate had a pH of 7.5. The resulting extract was washed with brine (20 mL), dried with Na_2SO_4, filtered, and then concentrated on a rotary evaporator. The resulting yellow oil was separated by fractional distillation through a packed column (2 cm × 10 cm, D × H), giving a clear oil (75–80 ºC, 1.9 mmHg; 3.74 g, 26.7 mmol, 18%). This product was found to be approximately 99 wt% pure by ^{1}H NMR spectroscopy, and was used without further purification. Acetic acid was the major contaminant (approx. 54 mg). ^{1}H NMR (AM400, 400 MHz, $CDCl_3$) δ 2.425–2.394 (m, 4H), 1.860–1.799 (m, 4H), 1.577–1.517 (m, 4H), 1.382–1.322 (m, 4H); ^{13}C NMR (AM400, 101 MHz, $CDCl_3$) δ 218.4 (1C), 43.7 (2C), 27.1 (2C), 25.1 (2C), 24.4 (2C); IR (KBr) 2926 (s), 2873 (m), 1700 (s), 1666 (w), 1471 (m), 1445 (m), 1344 (w), 1220 (w), 1151 (m), 784 (w); HRMS-EI $[M]^+$ calcd for $C_9H_{16}O$ 140.1196, found 140.1197.

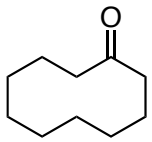

Cyclodecanone (2j). Based on the work of Burpitt & Thweatt [56]: cyclooctanone (13.4 g, 106 mmol), pyrrolidine (17 mL, 207 mmol), mixed xylenes (20 mL), and TsOH•H_2O (53 mg, 279 μmol) were placed in a round-bottomed flask fitted with a packed column (2 cm × 10 cm, D × H) and a Dean-Stark trap (25 mL) that was filled with hexane. The reaction mixture was refluxed for 24 h and then allowed to cool to rt. The Dean-Stark trap was replaced with a distillation head, and then solvents and the unreacted cyclooctanone and pyrrolidine were removed by fractional distillation (rt to 90 ºC, 7 mmHg). The brown oil that remained, mostly *N*-cycloocten-1-ylpyrrolidine (19.01 g, 106 mmol), and ether (50 mL) were placed in a round-bottomed flask, fitted with an internal thermometer, in a dry N_2 atmosphere. The temperature of the reaction mixture was maintained at 25–30 ºC by intermittent immersion in an ice bath, as a solution of methyl propiolate (9.5 mL, 107 mmol) in ether (25 mL) was added dropwise over 30 min. The temperature was maintained from 25 to 30 ºC as the resulting mixture was stirred for 1 h. The resulting mixture was cooled in an ice bath for 15 min. A beige solid [185] was collected by suction filtration, and then dissolved in hydrochloric acid (2 M, 100 mL). The resulting mixture was heated to 60 ºC for 4 h, and then allowed to cool to rt. The resulting mixture was extracted with ether (4 × 25 mL). The combined extract was washed with brine (20 mL), and then concentrated on a rotary evaporator. The resulting brown oil (8.61 g), methanol (30 mL), and Pd on Al_2O_3 (5 mass%, 500 mg, 235 μmol Pd) were placed in a pressure flask [186]. The resulting mixture was processed according to the hydrogenation and hydrolysis protocol described in the synthesis of cyclononanone (**2i**), with solvents and reagents used at 150% scale.

Cyclodecanone was obtained by fractional distillation (87–88 ºC, 2.8 mmHg) as a clear oil (5.03 g, 32.6 mmol, 31%). ^{1}H NMR (AV500, 500 MHz, $CDCl_3$) δ 2.525–2.500 (m, 4H), 1.872–1.823 (m, 4H), 1.503–1.479 (m, 4H), 1.368–1.337 (m, 6H); ^{13}C NMR (AV500, 126 MHz, $CDCl_3$) δ 215.0 (1C), 42.2 (2C), 25.2 (1C), 25.1 (2C), 24.9 (2C), 23.6 (2C); IR (NaCl) 2930 (s), 2874 (s), 1697 (s), 1474 (m), 1223 (s); HRMS-EI $[M]^+$ calcd for $C_{10}H_{18}O$ 154.1352, found 154.1355.

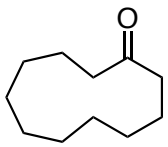

Cycloundecanone (2k) was taken from a bottle that was found to be approximately 95 wt% pure by ^{1}H NMR spectroscopy, and was used without further purification. Diacid **3** was the major contaminant (3.5 mol%). ^{1}H NMR (AV500, 500 MHz, $(CD_3)_2SO$) δ 2.500–2.457 (m, 4H), 1.675–1.626 (m, 4H), 1.377–1.327 (m, 4H), 1.306–1.193 (m, 8H); ^{13}C NMR (AV500, 126 MHz, CD_3CN) δ 214.7 (1C),

42.4 (2C), 26.8 (2C), 25.8 (2C), 25.1 (2C), 23.2 (2C); HRMS-EI $[M]^+$ calcd for $C_{11}H_{20}O$ 168.1509, found 168.1505.

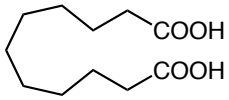

Undecane-1,11-dioic Acid (3) was obtained as a precipitate from the bottle of cycloundecanone (**2k**) used for this project, followed by trituration with pentane and then vacuum drying for 4 h. The NMR signals matched those of the impurity dissolved in **2k**. M.p. 106–107 °C (lit 107–109 °C) [187]; ^{1}H NMR (AV500, 500 MHz, $(CD_3)_2SO$) δ 11.943 (brs, 2H), 2.18 (t, J = 7.4, 4H), 1.45 (t, J = 7.1, 4H), 1.244–1.239 (m, 10H); ^{13}C NMR (AV500, 126 MHz, $(CD_3)_2SO$) δ 174.5 (2C), 33.7 (2C), 28.75 (1C), 28.66 (2C), 28.5 (2C), 24.5 (2C); IR (KBr) 3037 (s), 2919 (s), 2850 (s), 2688 (s), 1699 (s), 1436 (m), 1288 (m), 930 (m); HRMS-ESI $[M–H]^-$ calcd for $C_{11}H_{20}O_4$ 215.1289, found 215.1287.

3.2.2. Indole Dimer and Trimer, and Biindolyl

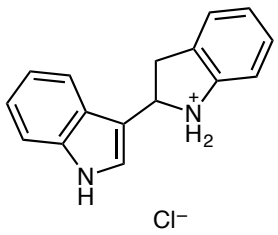

2-(Indol-3-yl)-indolinium Chloride (4H). Based on the work of Wahlström, *et al*. [62]: ether (250 mL) was cooled to –40 ºC in a reaction vessel in a dry N_2 atmosphere. Hydrogen chloride gas was sparged into the ether for 30 min. A solution of indole (29.8 g, 255 mmol) in ether (150 mL) was added dropwise over 30 min. The resulting mixture was allowed to warm to rt, and then was stirred for 18 h. The solid portion of the resulting mixture was collected by suction filtration, and then dried under vacuum (40 ºC, 250 mmHg, 4 h). The resulting pink powder was triturated twice with hexane and then dried under vacuum (60 ºC, 250 mmHg, 12 h), giving the hydrochloride salt as a white powder (31.4 g, 116 mmol, 91%). M.p. 167–171 °C (lit. 145–150 °C dec.) [188]; IR (KBr) 3336 (s), 3053 (w), 2813 (s), 2669 (m), 2584 (m), 2504 (m), 1571 (w), 1462 (s), 1354 (m), 740 (s); HRMS-ESI $[M+H]^+$ calcd for $C_{16}H_{14}N_2$ 235.1230, found 235.1234.

Free base: A sample of the hydrochloride salt (10 mg) was placed in a test tube with Na_2CO_3 (sat. aq., 1 mL) and CD_2Cl_2 (1 mL). The resulting mixture was agitated until nearly all solids had dissolved, and then for an additional 2 min. The proper volume of the organic portion was collected for NMR and TLC analysis. R_f = 0.37 (1:2 EtOAc:hexane on SiO_2); ^{1}H NMR (HD500, 500 MHz, CD_2Cl_2) δ 8.182 (s, 1H), 7.554 (dd, J = 8.0, 1.0, 1H), 7.375 (dt, J = 8.2, 0.9, 1H), 7.190–7.139 (m, 2H), 7.103–7.098 (m, 1H), 7.058–6.999 (m, 2H), 6.693 (td, J = 7.4, 1.0,

1H), 6.637 (d, *J* = 7.6, 1H), 5.236 (ddd, *J* = 9.1, 8.3, 0.7, 1H), 4.193 (s, 1H), 3.451 (dd, *J* = 15.5, 9.0, 1H), 3.152 (dd, *J* = 15.6, 8.3, 1H).

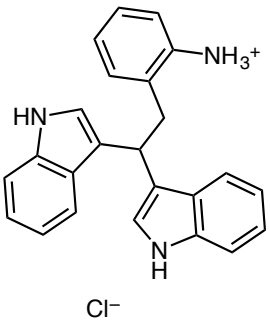

2-[2,2-Di(indol-3-yl)]ethylanilinium Chloride (5H) was prepared from indole according to Method E (p 185), in the absence of ketone (40 ºC, 36 h). After allowing the mixture to cool to rt, a beige powder was collected by filtration, triturated with hexane, and then vacuum dried for 12 h, giving the hydrochloride salt as a white powder (1.82 g, 4.69 mmol, 70%). M.p. 184–186 °C (lit. 175 °C) [63]; IR (KBr) 3443 (s), 3230 (s), 3061 (w), 2850 (s), 2552 (m), 1572 (m), 1453 (s), 1097 (m), 748 (s); HRMS-ESI $[M+H]^+$ calcd for $C_{24}H_{21}N_3$ 352.1808, found 352.1797.

Free base: A sample was prepared by the same procedure that was used for indole dimer hydrochloride **4H**. R_f = 0.14 (1:2 EtOAc:hexane on SiO_2); ^{1}H NMR (AV500, 500 MHz, CD_2Cl_2; N–*H*$_2$ not obs.) δ 8.131 (s, 2H), 7.444 (d, *J* = 7.9, 2H), 7.335 (d, *J* = 8.0, 2H), 7.108–7.080 (m, 4H), 6.957–6.909 (m, 4H), 6.567–6.545 (m, 2H), 4.857 (t, *J* = 7.0, 1H), 3.423 (d, *J* = 7.4, 2H).

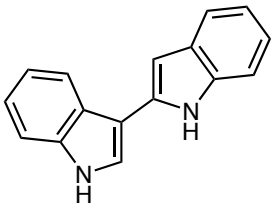

2,3'-Biindolyl (6) was obtained as a chromatographic fraction (R_f = 0.21 in 1:2 EtOAc:hexane on SiO_2) from the synthesis of bisindole **7h** *via* Method D [p 185; cyclooctanone (1.26 g), 8 d], which was processed according to Method F (p 185), giving a beige powder (104 mg, 448 μmol, 4.5%). The title compound was also obtained as a chromatographic fraction from the synthesis of bisindole **7k** (p 191), as a beige powder (198 mg, 852 μmol, 8.5%).

Preferred preparation: Based on the work of Wahlström, *et al*. [62]: EtOAc (150 mL), $NaHCO_3$ solution (aq., sat., 200 mL), and indole dimer hydrochloride (**4H**, 31.4 g, 116 mmol) were placed in a beaker. The resulting mixture was stirred for 2 h at rt, during which time the solid portion had dissolved. The aqueous portion was extracted with EtOAc (2 × 50 mL). The combined organic portions were washed with brine (50 mL) and then dried with $MgSO_4$. The resulting mixture was separated by filtration, and then the liquid portion was concentrated on a rotary evaporator. The resulting residue, toluene (250 mL), and Pd on C (10 mass%, 2.50 g, 2.34 mmol Pd) were placed in a round-bottomed flask in an N_2 atmosphere. The resulting mixture was

refluxed for 36 h. While still hot, the resulting mixture was separated by suction filtration through celite (3 cm × 3 cm, H × D). The filter cake was washed with hot methanol (3 × 100 mL) [189]. The combined filtrate was concentrated on a rotary evaporator. The resulting brown residue was triturated twice with DCM and then dried under vacuum (80 ºC, 250 mmHg, 24 h), giving a beige powder (18.9 g, 81.5 mmol, 70%). M.p. 200–204 °C (lit. 204–206 ºC) [190]; ^{1}H NMR (AV500, 500 MHz, CD_3CN) δ 9.510 (s, br, 2H), 8.019 (d, *J* = 7.7, 1H), 7.657 (d, *J* = 2.7, 1H), 7.64 (d, *J* = 7.8, 1H), 7.522 (d, *J* = 7.5, 1H), 7.417 (dd, *J* = 8.0, 0.5, 1H), 7.276–7.193 (m, 2H), 7.112 (ddd, *J* = 8.1, 7.1, 1.3, 1H), 7.046 (ddd, *J* = 8.1, 7.1, 1.1, 1H), 6.784 (d, *J* = 1.3, 1H); ^{13}C NMR (AV500, 126 MHz, CD_3CN) δ 137.9 (1C), 137.3 (1C), 134.9 (1C), 130.6 (1C), 126.0 (1C), 123.6 (1C), 123.3 (1C), 121.9 (1C), 121.2 (1C), 120.7 (1C), 120.4 (2C), 112.9 (1C), 111.4 (1C), 110.0 (1C), 98.8 (1C); IR (KBr) 3396 (s), 3049 (w), 3026 (w), 1593 (s), 1456 (s), 1432 (s), 1309 (s), 1020 (m), 777 (s), 746 (s), 672 (m); HRMS-EI $[M]^+$ calcd for $C_{16}H_{12}N_2$ 232.0995, found 232.1001.

3.2.3. Indole-Ketone Condensation Methodology

Method A or B: Indole with Substrates and Phosphoric Acid or Boric Acid

Indole (2.34 g, 20 mmol), substrate (12 mmol), and the solvent indicated in Table 4 (1 mL) were placed in a round-bottomed flask fitted with a reflux condenser. [Method A] Phosphoric acid (aq., 85% w/w, 460 mg, 4.0 mmol), or [Method B] boric acid (247 mg, 4.0 mmol), was added to the reaction mixture. The resulting mixture was refluxed for the indicated duration.

Method C: Indole with Substrates in Acetic Acid

Indole (2.34 g, 20 mmol), substrate (12 mmol), and AcOH (10 mL) were placed in a round-bottomed flask fitted with a reflux condenser. The temperature and duration of each experiment are indicated in Table 5. Where indicated, $TsOH•H_2O$ was added to the reaction mixture at the onset of the experiment.

Method D: Indole with Substrates in Trifluoroacetic Acid

Indole (2.34 g, 20 mmol), substrate (10 mmol), and trifluoroacetic acid (5 mL) were placed in a round-bottomed flask fitted with a reflux condenser. The resulting mixture was heated to 50 ºC for the duration indicated in Table 6.

Method E: Indole with Substrates in Ethanolic HCl

Indole (2.34 g, 20 mmol), substrate, and ethanol were placed in a round-bottomed flask fitted with a reflux condenser. Once the resulting mixture had been brought to the temperature indicated in Table 7, hydrochloric acid (7.5 M) was added dropwise. The reaction was allowed to continue for the indicated duration.

Method F: Work-Up Procedure for Reactions using Indole and Brønsted Acids

Neutralization: Once the reaction was complete as indicated by TLC, it was brought to rt. DCM (100 mL) was added to the reaction mixture. The resulting mixture was washed with water (2 × 25 mL), and then sodium bicarbonate solution (aq., sat., 50 mL), and then brine (25 mL).

Filtration: The organic portion was filtered through silica gel (3 cm × 4 cm, H × D). The filter was washed with additional DCM until the filtrate no longer contained the desired product, as indicated by TLC. The filtrate was concentrated using a rotary evaporator.

Chromatography: The resulting residue was purified by column chromatography on silica gel. For products with $R_f \geq 0.41$ (in 1:2 EtOAc:hexane, on SiO_2), the mobile phase was a gradient, from 1:3 to 1:1 toluene:hexane (v/v). For products with $R_f < 0.41$, or if additional eluting power was required following a toluene:hexane gradient, the mobile phase was a gradient, from 1:19 to 1:1 EtOAc:hexane. A typical column was 60 cm long and 3 cm in diameter. The elution rate was roughly 25–40 mL/min and the total elution time was roughly 2–4 hours, although some of the more challenging separations required an 8-hour gradient. The desired fraction was concentrated using a rotary evaporator.

3.2.4. Bisindoles (2:1 Condensation Products)

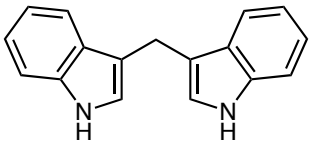

3,3'-Methylenebisindole (7a) was prepared according to Method C, with paraformaldehyde (380 mg), at rt. After 72 h, the reaction mixture was processed according to Method F. The resulting pink solid (R_f = 0.33, 1:2 EtOAc:hexane on SiO_2) was recrystallized from ethanol-water, giving a white powder (2.36 g, 9.58 mmol, 96%). M.p. 162–165 °C (lit. 167–169 °C) [191]; ^{1}H NMR (VI300, 300 MHz, CD_2Cl_2) δ 8.054 (s, br, 2H), 7.582 (dd, *J* = 7.9, 0.9, 2H), 7.365 (dt, *J* = 8.1, 1.0, 2H), 7.152 (ddd, *J* = 8.1, 7.0, 1.2, 2H), 7.044 (ddd, *J* = 8.0, 7.0, 1.1, 2H), 7.000 (dt, *J* = 2.2, 1.0, 2H), 4.236 (t, *J* = 1.0, 2H); ^{13}C NMR (HD500, 126 MHz, CD_2Cl_2) δ 137.0 (2C), 128.1 (2C), 122.7 (2C), 122.3 (2C), 119.6 (4C), 116.1 (2C), 111.6 (2C), 21.7 (1C); IR (KBr) 3397 (s), 3059 (w), 2890 (w), 2855 (w), 2832 (w), 1619 (w), 1488 (w), 1455 (m), 1427 (m), 1340 (m), 1220 (m), 1090 (m), 1034 (m), 1007 (m), 741 (s); HRMS-EI $[M]^+$ calcd for $C_{17}H_{14}N_2$ 246.1152, found 246.1144.

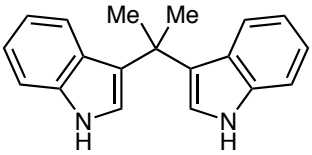

3,3'-Propane-2,2-diylbisindole (7b) was prepared according to Method A, with acetone (900 μL, 12.1 mmol). After 4 h, the reaction mixture was processed according to Method F. The resulting brown solid (R_f = 0.38, 1:2 EtOAc:hexane on SiO_2) was recrystallized from ethanol-water, giving a tan powder (2.16 g, 7.87 mmol, 79%). *Note:* Preparation of **7b** by Method D gave 76% yield, but was easier to perform. M.p. 156–157 °C (lit. 160–162 °C) [192]; ^{1}H NMR (HD500, 500 MHz, CD_2Cl_2) δ 8.054 (s, br, 2H), 7.331 (dd, *J* = 8.1, 1.0, 2H), 7.289 (dt, *J* = 8.1, 0.9, 2H), 7.187 (d, *J* = 2.6, 2H), 7.052 (ddd, *J* = 7.2, 7.1, 0.9, 2H), 6.825 (ddd, *J* = 8.0, 7.2, 1.0, 2H), 1.911 (s, 6H); ^{13}C NMR (HD500, 126 MHz, CD_2Cl_2) δ 137.6 (2C), 126.8 (2C), 125.8 (2C), 121.8 (2C), 121.2 (2C), 120.9 (2C), 119.0 (2C), 111.6 (2C), 35.1 (1C), 30.3 (2C); IR (KBr) 3408 (s), 3392 (s), 3047 (w), 2961, 2931 (w), 2866 (w), 1622 (w), 1486 (m), 1456 (m), 1415 (m), 1333 (m), 1242 (w), 1100 (m), 1010 (m), 744 (s); HRMS-EI $[M]^+$ calcd for $C_{19}H_{18}N_2$ 274.1465, found 274.1475.

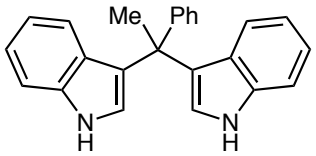

3,3'-(1-Phenylethane-1,1-diyl)bisindole (7c) was prepared according to Method D, with acetophenone (1.20 mL) and EtOH (5 mL), for 72 h. The reaction mixture was processed according to Method F. The resulting brown solid (R_f = 0.37, 1:2 EtOAc:hexane on SiO_2) was recrystallized from ethanol-water, giving a beige powder (2.43 g, 7.23 mmol, 72%). M.p. 153–156 °C (lit. 165–166 ºC) [192]; ^{1}H NMR (HD500, 500 MHz, CD_2Cl_2) δ 8.014 (s, br, 2H), 7.408 (m, 2H), 7.362 (d, *J* = 8.2, 2H), 7.263 (m, 4H), 7.208 (tdd, *J* = 7.2, 2.2, 1.4, 1H), 7.109 (ddd, *J* = 8.2, 7.0, 1.1, 2H), 6.892 (ddd, *J* = 8.1, 7.0, 1.0, 2H), 6.704 (d, *J* = 2.6, 2H), 2.347 (s, 3H); ^{13}C NMR (HD500, 126 MHz, CD_2Cl_2) δ 148.7 (1C), 137.7 (2C), 128.6 (2C), 128.2 (2C), 127.0 (2C), 126.4 (1C), 124.9 (2C), 123.8 (2C), 122.3 (2C), 122.0 (2C), 119.3 (2C), 111.7 (2C), 44.2 (1C), 29.3 (1C); IR (KBr) 3420 (s), 3366 (m), 3122 (w), 3052 (w), 2974 (w), 2936 (w), 1617 (w), 1490, 1456 (s), 1415 (m), 1338 (m), 1246 (w), 1101 (m), 1010 (m), 744 (s); HRMS-EI $[M]^+$ calcd for $C_{24}H_{20}N_2$ 336.1621, found 336.1646.

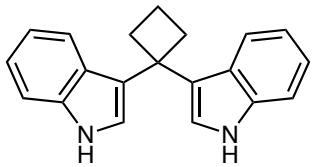

3,3'-Cyclobutylidenebisindole (7d) was prepared according to Method C, with cyclobutanone (0.76 mL). After 24 h at 60 ºC, the reaction mixture was processed according to Method F. The resulting brown solid (R_f = 0.37, 1:2 EtOAc:hexane on SiO_2) was dissolved in DCM (25 mL), and then filtered through neutral alumina (3 cm × 4 cm, H × D). The filter cake was washed with DCM (5 × 10 mL). The filtrate was concentrated on a rotary evaporator, and then dried under vacuum (78 ºC, 0.05 mmHg, 24 h), giving a beige, amorphous, air-sensitive solid (1.83 g), which was primarily composed of the title compound (99 mass%: 1.81 g, 6.38 mmol, 64%; calculated by elemental analysis). The major impurity was DCM (approx. 26 mg). M.p. 101–107 ºC; ^{1}H NMR (HD500, 500 MHz, CD_2Cl_2) δ 7.975 (s, br, 2H), 7.518 (dd, *J* = 8.0, 1.0, 2H), 7.330 (d, *J* = 8.1, 2H), 7.201 (d, *J* = 2.6, 2H), 7.128 (ddd, *J* = 8.2, 7.0, 1.2, 2H), 6.971 (ddd, *J* = 8.1, 7.0, 1.1, 2H), 2.885 (t, *J* = 7.6, 4H), 2.208 (p, *J* = 7.6, 2H); ^{13}C NMR (HD500, 126 MHz, CD_2Cl_2) δ 137.7 (2C), 126.8 (2C), 124.3 (2C), 122.1 (2C), 121.5 (2C), 120.9 (2C), 119.1 (2C), 111.7 (2C), 41.4 (1C), 34.8 (2C), 18.0 (1C); IR (KBr) 3411 (s), 3053 (w), 2978 (m), 2940 (m), 2861 (w), 1617 (w), 1484 (w), 1455 (s), 1416 (m), 1334 (m), 1242 (m), 1098 (m), 1012 (m), 741 (s); HRMS-EI $[M]^+$ calcd for $C_{20}H_{18}N_2$ 286.1465, found 286.1460. Anal. (AML) Calcd for $C_{20}H_{18}N_2$ C 83.88, H 6.34, N 9.78; Calcd for $[C_{20}H_{18}N_2 \bullet 0.050\ CH_2Cl_2]$ C 82.86, H 6.28, N 9.64; Found C 82.91, H 6.28, N 9.63.

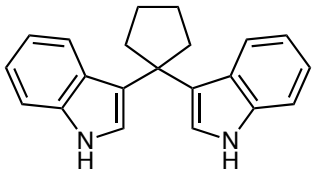

3,3'-Cyclopentylidenebisindole (7e) was prepared according to Method B, with cyclopentanone (0.90 mL) and toluene (1 mL). After 5 d at reflux, the reaction mixture was processed according to Method F. The resulting brown solid (R_f = 0.38, 1:2 EtOAc:hexane on SiO_2) was recrystallized from ethanol-water, giving a white powder (867 mg, 2.89 mmol, 29%). M.p. 164–167 °C (lit. 116–119 °C) [23]; ^{1}H NMR (VI300, 300 MHz, CD_2Cl_2) δ 8.058 (s, br, 2H), 7.401 (d, *J* = 8.1, 2H), 7.298 (dd, *J* = 8.2, 1.0, 2H), 7.220 (d, *J* = 2.5, 2H), 7.022 (ddd, *J* = 8.1, 7.6, 1.1, 2H), 6.830 (ddt, *J* = 8.1, 7.9, 1.0, 2H), 2.466 (m, 4H), 1.825 (m, 4H); ^{13}C NMR (HD500, 126 MHz, CD_2Cl_2) δ 137.7 (2C), 127.1 (2C), 123.7 (2C), 121.9 (2C), 121.4 (2C), 121.2 (2C), 119.0 (2C), 111.6 (2C), 46.5 (1C), 39.1 (2C), 24.2 (2C); IR (KBr) 3440 (s), 3419 (s), 3060 (w), 2960 (m), 2872 (w), 1622 (w), 1474 (w), 1453 (s), 1417 (m), 1342 (m), 1242 (m), 1106 (m), 1012 (m), 740 (s); HRMS-EI $[M]^+$ calcd for $C_{21}H_{20}N_2$ 300.1621, found 300.1614. Anal. (AML) Calcd for $C_{21}H_{20}N_2$ C 83.96, H 6.71, N 9.33; Found C 83.79, H 6.60, N 9.29.

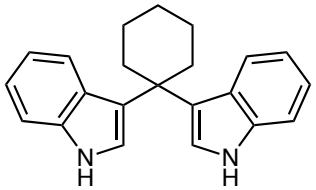

3,3'-Cyclohexylidenebisindole (7f) was prepared according to Method E, with cyclohexanone (1.5 mL, 15 mmol), EtOH (25 mL), and hydrochloric acid (7.5 M, 5 mL, 38 mmol), at 0 ºC. After 10 min, the reaction mixture was processed according to Method F. The resulting tan solid (R_f = 0.39, 1:2 EtOAc:hexane on SiO_2) was recrystallized from ethanol-water, giving colorless block-shaped crystals (3.06 g, 9.73 mmol, 98%). M.p. 164–168 °C, (lit. 119–120 °C) [24]; ^{1}H NMR (HD500, 500 MHz, CD_2Cl_2; NMR sample prepared via Method C) δ 8.078 (s, br, 2H), 7.429 (dd, *J* = 8.2, 1.0, 2H), 7.303 (d, *J* = 8.2, 2H), 7.242 (d, *J* = 2.5, 2H), 7.023 (ddd, *J* = 8.1, 7.0, 1.1, 2H), 6.826 (ddd, *J* = 8.1, 7.0, 1.0, 2H), 2.521 (m, 4H), 1.687 (p, *J* = 5.9, 4H), 1.598 (m, 2H); ^{13}C NMR (HD500, 126 MHz, CD_2Cl_2) δ 137.5 (2C), 126.8 (2C), 124.1 (2C), 122.4 (2C), 121.7 (2C), 121.5 (2C), 118.9 (2C), 111.6 (2C), 39.7 (1C), 37.6 (2C), 27.4 (1C), 23.6 (2C); IR (KBr) 3452 (m), 3408 (s), 3139 (w), 3051 (m), 2932 (s), 2854 (m), 1615 (w), 1484 (w), 1455 (s), 1414 (s), 1336 (m), 1243 (m), 1101 (s), 1014 (m), 992 (m), 817 (s), 742 (s); HRMS-EI $[M]^+$ calcd for $C_{22}H_{22}N_2$ 314.1778, found 314.1783. Anal. (AML) Calcd for $C_{22}H_{22}N_2$ C 84.04, H 7.05, N 8.91; Found C 84.05, H 7.05, N 8.81.

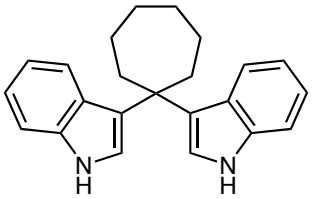

3,3'-Cycloheptylidenebisindole (7g) was prepared according to Method C, with cycloheptanone (1.4 mL). After 48 h, the reaction mixture was processed according to Method F. The resulting tan solid (R_f = 0.40, 1:2 EtOAc:hexane on SiO_2) was recrystallized from DCM-hexane, giving a white powder (2.30 g, 7.00 mmol, 70%). M.p. 176–178 °C; ^{1}H NMR (HD500, 500 MHz, CD_2Cl_2) δ 8.100 (s, br, 2H), 7.328 (d, *J* = 2.5, 2H), 7.291 (d, *J* = 8.2, 2H), 7.167 (d, *J* = 8.1, 2H), 6.984 (ddd, *J* = 8.1, 7.1, 1.1, 2H), 6.720 (dd, *J* = 8.1, 7.1, 2H), 2.518 (m, 4H), 1.654 (m, 8H); ^{13}C NMR (HD500, 126 MHz, CD_2Cl_2) δ 137.7 (2C), 127.1 (2C), 125.5 (2C), 121.8 (2C), 121.5 (2C), 121.3 (2C), 118.9 (2C), 111.5 (2C), 42.5 (1C), 39.5 (2C), 31.2 (2C), 23.6 (2C); IR (KBr) 3414 (s), 3054 (w), 2924 (s), 2853 (m), 1616 (w), 1484 (w), 1456 (s), 1415 (m), 1338 (m), 1243 (m), 1101 (m), 1013 (m), 952 (m), 742 (s); HRMS-EI $[M]^+$ calcd for $C_{23}H_{24}N_2$ 328.1934, found 328.1931. Anal. (AML) Calcd for $C_{23}H_{24}N_2$ C 84.11, H 7.37, N 8.53; Found C 84.02, H 7.39, N 8.58.

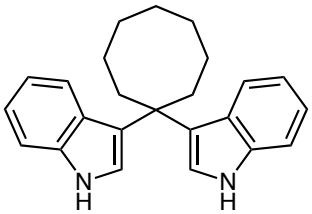

3,3'-Cyclooctylidenebisindole (7h) was prepared according to Method C, with cyclooctanone (1.51 g) and TsOH•H_2O (4 mg, 20 μmol). After 48 h at reflux, the reaction mixture was processed according to Method F. The resulting brown solid (R_f = 0.42, 1:2 EtOAc:hexane on SiO_2) was recrystallized from methanol-water, giving a tan powder (1.33 g, 3.88 mmol, 39%). M.p. 190–192 °C; ^{1}H NMR (HD500, 500 MHz, CD_2Cl_2) δ 8.138 (s, br, 2H), 7.382 (d, *J* = 2.5, 2H), 7.295 (d, *J* = 8.2, 2H), 7.067 (dd, *J* = 8.1, 1.0, 2H), 6.968 (ddd, *J* = 8.2, 7.0, 1.1, 2H), 6.674 (ddd, *J* = 8.0, 7.0, 1.0, 2H), 2.501 (m, 4H), 1.652 (m, 6H), 1.396 (pd, *J* = 5.7, 1.9, 4H); ^{13}C NMR (HD500, 126 MHz, CD_2Cl_2) δ 137.6 (2C), 126.9 (2C), 124.2 (2C), 122.0 (2C), 121.8 (2C), 121.0 (2C), 118.8 (2C), 111.5 (2C), 42.4 (1C), 33.2 (2C), 29.4 (2C), 26.0 (1C), 23.0 (2C); IR (KBr) 3404 (s), 3383 (s), 3311 (w), 3083 (w), 3054 (w), 2920 (s), 2849 (m), 1616 (w), 1475 (w), 1456 (s), 1416 (m), 1338 (m), 1243 (m), 1101 (m), 1013 (m), 804 (m), 744 (s); HRMS-EI $[M]^+$ calcd for $C_{24}H_{26}N_2$ 342.2091, found 342.2094. Anal. (AML) Calcd for $C_{24}H_{26}N_2$ C 84.17, H 7.65, N 8.18; Found C 84.19, H 7.67, N 8.19.

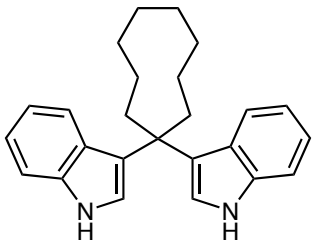

3,3'-Cyclononylidenebisindole (7i) was prepared according to Method C, with cyclononanone (1.68 g) and TsOH•H_2O (4 mg, 20 μmol). After 7 d at reflux, the reaction mixture was processed according to Method F. The resulting brown solid (R_f = 0.42, 1:2 EtOAc:hexane on SiO_2) was filtered through neutral alumina (3 cm × 4 cm, H × D) using DCM. The filtrate was concentrated on a rotary evaporator, and then dried under vacuum (56 ºC, 0.05 mmHg, 24 h), giving a yellow, amorphous, air-sensitive solid (151 mg), which was primarily composed of the title compound (77 mass%: 116 mg, 325 μmol, 6.5%; calculated by ^{1}H NMR analysis). The major impurities were indole (approx. 13 mg) and EtOAc (approx. 13 mg); the composition of the remaining 9 mg is uncertain. M.p. 82–83 °C; ^{1}H NMR (AV500, 500 MHz, CD_2Cl_2) δ 8.121 (s, br, 2H), 7.362 (d, *J* = 2.4, 2H), 7.293 (d, *J* = 8.1, 2H), 7.113 (d, *J* = 8.3, 2H), 6.979 (ddd, *J* = 8.2, 7.0, 1.2, 2H), 6.693 (ddd, *J* = 8.1, 6.9, 1.0, 2H), 2.415 (t, *J* = 6.2, 4H), 1.624–1.605 (m, 4H), 1.495–1.471 (m, 4H), 1.313–1.251 (m, 4H); ^{13}C NMR (AV500, 126 MHz, CD_2Cl_2) δ 137.6 (2C), 127.0 (2C), 123.9 (2C), 121.9 (2C), 121.8 (2C), 120.9 (2C), 118.8 (2C), 111.5 (2C), 42.1 (1C), 30.3 (2C), 28.2 (2C), 21.9 (2C), 19.4 (2C); IR (KBr) 3416 (s), 3053 (w), 2924 (s), 2848 (m), 1719 (w), 1456 (s), 1257 (m), 1099 (w), 741 (s); HRMS-EI $[M]^+$ calcd for $C_{25}H_{28}N_2$ 356.2247, found 356.2257.

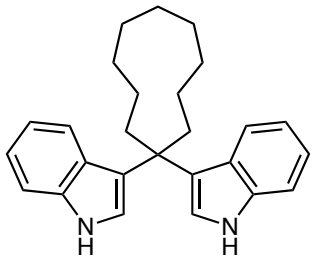

3,3'-Cyclodecylidenebisindole (7j) was prepared according to Method D, with cyclodecanone (1.54 g). After 17 d, the reaction mixture was processed according to Method F. The resulting yellow solid (R_f = 0.42, 1:2 EtOAc:hexane on SiO_2) was recrystallized from DCM-pentane giving white powder (215 mg, 580 μmol, 12%). M.p. 190–191 °C; ^{1}H NMR (AV500, 500 MHz, CD_2Cl_2) δ 8.125 (s, br, 2H), 7.335 (d, *J* = 2.5, 2H), 7.299 (d, *J* = 8.1, 2H), 7.120 (dd, *J* = 8.1, 1.0, 2H), 6.978 (ddd, *J* = 8.1, 6.9, 1.1, 2H), 6.691 (ddd, *J* = 8.0, 7.0, 1.0, 2H), 2.475 (t, *J* = 7.1, 4H), 1.679–1.642 (m, 4H), 1.607–1.570 (m, 2H), 1.538–1.488 (m, 4H), 1.277–1.223 (m, 4H); ^{13}C NMR (AV500, 126 MHz, CD_2Cl_2) δ 137.5 (2C), 127.0 (2C), 124.1 (2C), 121.8 (2C), 121.7 (2C), 121.0 (2C), 118.8 (2C), 111.4 (2C), 42.2 (1C), 32.1 (2C), 27.2 (2C), 26.7 (1C), 25.4 (2C), 21.7 (2C); IR (KBr) 3417 (s), 3054 (w), 2922 (s), 2849 (m), 1617 (w), 1456 (s), 1336 (m), 1100 (m), 740 (s); HRMS-EI $[M]^+$ calcd for $C_{26}H_{30}N_2$ 370.2404, found 370.2420. Anal. (AML) Calcd for $C_{26}H_{30}N_2$ C 84.28, H 8.16, N 7.56; Found C 84.00, H 8.16, N 7.56.

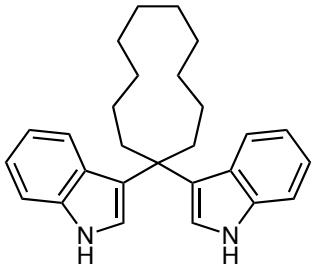

3,3'-Cycloundecylidenebisindole (7k) was prepared according to Method D, with cycloundecanone (1.76 g, 95 wt%). After 14 d, the reaction mixture was processed according to Method F. The resulting beige solid (R_f = 0.45, 1:2 EtOAc:hexane on SiO_2) was recrystallized from methanol, giving white powder (403 mg, 1.05 mmol, 11%). M.p. 197–198 °C; ^{1}H NMR (HD500, 500 MHz, CD_2Cl_2) δ 8.123 (s, br, 2H), 7.315 (d, *J* = 2.5, 2H), 7.294 (d, *J* = 8.1, 2H), 7.129 (dd, *J* = 8.1, 1.0, 2H), 6.973 (ddd, *J* = 8.1, 6.9, 1.1, 2H), 6.690 (ddd, *J* = 8.1, 7.0, 1.0, 2H), 2.410 (t, *J* = 7.6, 4H), 1.575 (m, 4H), 1.476 (m, 4H), 1.390 (t, *J* = 6.1, 4H), 1.128 (m, 4H); ^{13}C NMR (HD500, 126 MHz, CD_2Cl_2) δ 137.5 (2C), 127.0 (2C), 123.9 (2C), 121.8 (2C), 121.7 (2C), 120.9 (2C), 118.8 (2C), 111.4 (2C), 41.9 (1C), 33.4 (2C), 27.7 (2C), 27.1 (2C), 26.5 (2C), 22.2 (2C); IR (KBr) 3417 (s), 3051 (w), 2928 (s), 2858 (m), 1617 (w), 1475 (m), 1456 (s), 1415 (m), 1337 (m), 1243 (m), 1100 (m), 1013 (m), 741 (s); HRMS-EI $[M]^+$ calcd for $C_{27}H_{32}N_2$ 384.2560, found 384.2561. Anal. (AML) Calcd for $C_{27}H_{32}N_2$ C 84.33, H 8.39, N 7.28; Found C 84.27, H 8.39, N 7.22.

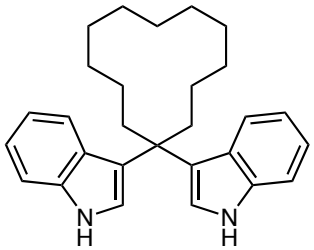

3,3'-Cyclododecylidenebisindole (7l) was prepared according to Method D, with cyclododecanone (2.19 g). After 72 h, the reaction mixture was processed according to Method F. The resulting beige solid (R_f = 0.46, 1:2 EtOAc:hexane on SiO_2) was recrystallized from DCM-hexane, giving colorless block-shaped crystals (1.46 g, 3.68 mmol, 37%). M.p. 210–213 °C; ^{1}H NMR (HD500, 500 MHz, CD_2Cl_2) δ 8.121 (s, br, 2H), 7.304 (d, *J* = 6.9, 2H), 7.295 (d, *J* = 2.2, 2H), 7.164 (d, *J* = 8.1, 2H), 6.987 (ddd, *J* = 8.1, 6.9, 1.1, 2H), 6.708 (ddd, *J* = 8.1, 6.9, 1.0, 2H), 2.311 (dd, *J* = 9.1, 7.2, 4H), 1.411 (m, 10H), 1.306 (m, 4H), 1.010 (m, 4H); ^{13}C NMR (HD500, 126 MHz, CD_2Cl_2) δ 137.5 (2C), 127.1 (2C), 124.0 (2C), 121.8 (2C), 121.6 (2C), 120.9 (2C), 118.8 (2C), 111.4 (2C), 40.9 (1C), 32.4 (2C), 27.1 (2C), 26.9 (1C), 23.0 (2C), 22.8 (2C), 20.1 (2C); IR (KBr) 3438 (s), 3395 (s), 3045 (m), 2934 (s), 2859 (m), 1617 (w), 1482 (s), 1470 (m), 1338 (m), 1101 (m), 1009 (w), 746 (s); HRMS-EI $[M]^+$ calcd for $C_{28}H_{34}N_2$ 398.2717, found 398.2722. Anal. (AML) Calcd for $C_{28}H_{34}N_2$ C 84.37, H 8.60, N 7.03; Found C 84.38, H 8.54, N 7.02.

3.2.5. Other Condensation-Derived Products

***rac*-(2a'*R*,8a'*R*)-2a'-(Indol-3-yl)-1',2',2a',8',8a'-pentahydrospiro[cyclobutane-1,8'-cyclobuta[4,5]cyclopenta[1,2-*b*]indole] (8d)** was prepared according to Method E, with cyclobutanone (1.40 g, 20.0 mmol) and hydrochloric acid (7.5 M, 2 mL, 15 mmol), at rt. After 5 d, the reaction mixture was processed according to Method F. The resulting yellow solid (R_f = 0.32, 1:2 EtOAc:hexane on SiO_2) was filtered through neutral alumina (3 cm × 4 cm, H × D) using DCM. The filter was washed with DCM until the filtrate no longer contained the desired product, as indicated by TLC. The filtrate was concentrated on a rotary evaporator, and then dried under vacuum (78 ºC, 0.05 mmHg, 24 h), giving a yellow, amorphous, air-sensitive solid (1.40 g), which was primarily composed of the title compound (98 mass%: 1.38 g, 4.08 mmol, 41%; calculated by elemental analysis). The major impurity was DCM (approx. 23 mg). M.p. 114–122 °C; ^{1}H NMR (AV500, 500 MHz, $(CD_3)_2SO$) δ 10.898 (s, 1H), 10.681 (s, 1H), 7.721–7.704 (m, 1H), 7.327 (d, *J* = 8.1, 1H), 7.265–7.239 (m, 2H), 7.031–6.976 (m, 3H), 6.955 (d, *J* = 8.0, 1H), 6.758 (t, *J* = 7.5, 1H), 3.383 (t, *J* = 8.2, 1H), 2.873 (q, *J* = 9.7, 1H), 2.605 (dd, *J* = 8.8, 8.4, 1H), 2.426 (q, *J* = 8.8, 1H), 2.297–2.129 (m, 4H), 2.061–2.015 (m, 1H), 1.953–1.885 (m, 1H), 1.872–1.797 (m, 1H); ^{13}C NMR (AV500, 126 MHz, $(CD_3)_2SO$) δ 147.1 (1C), 141.4 (1C), 136.7 (1C), 125.6 (1C), 124.4 (1C), 123.3 (1C), 122.0 (1C), 120.8 (1C), 119.9 (1C), 119.3 (1C), 118.7 (1C), 118.5 (1C), 118.1 (1C), 117.1 (1C), 112.1 (1C), 111.4 (1C), 63.1 (1C), 48.4 (1C), 35.8 (1C), 27.65 (1C), 27.59 (1C), 19.9 (1C), 16.1 (1C); IR (KBr) 3457 (m), 3407 (s), 3053 (w), 2970 (m), 2935 (s), 2849 (m), 1618 (w), 1458 (m), 1240 (m), 1096 (m), 742 (s); HRMS-EI $[M]^+$ calcd for $C_{24}H_{22}N_2$ 338.1778, found 338.1778. Anal. (AML) Calcd for $C_{24}H_{22}N_2$ C 85.17, H 6.55, N 8.28; Calcd for $[C_{20}H_{18}N_2 \bullet 0.069\ CH_2Cl_2]$ C 83.96, H 6.48, N 8.14; Found C 84.00, H 6.66, N 8.01.

***rac*-(3a'*R*,9a'*R*)-3a'-(Indol-3-yl)-1',2',3',3a',4',9a'-hexahydrospiro[cyclopentane-1,9'-pentaleno[1,2-*b*]indole] (8e)** was prepared according to Method E, performed at 50% scale, with

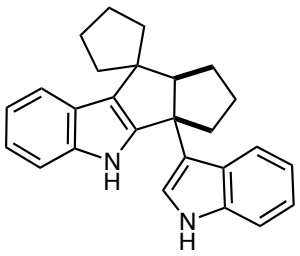

cyclopentanone (10 mL) in place of ethanol, hydrochloric acid (12 M, 0.1 mL), at 75 ºC, for 5 d. After allowing the mixture to cool to rt, DCM (20 mL), water (20 mL), $NaHCO_3$ (500 mg), and $NaHSO_3$ solution (sat., aq., 30 mL) were added. The resulting mixture was stirred for 2 h. The organic portion was filtered through neutral alumina (3 cm × 4 cm, H × D) using DCM. The filter was washed with DCM until the filtrate no longer contained the desired product, as indicated by TLC. The filtrate was concentrated on a rotary evaporator. The resulting yellow solid was separated by column chromatography, according to Method F. The desired fraction (R_f = 0.43, 1:2 EtOAc:hexane on SiO_2) was concentrated on a rotary evaporator, and then dried under vacuum (110 ºC, 0.05 mmHg, 12 h), giving a white powder (877 mg, 2.39 mmol, 48%). M.p. 193–195 °C; ^{1}H NMR (AV500, 500 MHz, CD_2Cl_2) δ 8.005 (s, 1H), 7.920 (s, 1H), 7.518 (d, *J* = 7.0, 1H), 7.480 (d, *J* = 7.9, 1H), 7.354 (d, *J* = 7.9, 1H), 7.320 (d, *J* = 7.1, 1H), 7.146 (ddd, *J* = 8.1, 7.0, 1.1, 1H), 7.081 (td, *J* = 7.1, 1.6, 1H), 7.049 (td, *J* = 7.0, 1.6, 1H), 7.018 (dd, *J* = 7.9, 7.7, 1H), 6.805 (d, *J* = 2.6, 1H), 3.090 (dd, *J* = 8.3, 5.6, 1H), 2.499 (dt, *J* = 13.0, 7.3, 1H), 2.235 (dt, *J* = 13.0, 6.6, 1H), 2.165 (dt, *J* = 13.0, 8.7, 1H), 2.085–1.820 (m, 6H), 1.793–1.693 (m, 3H), 1.612–1.547 (m, 1H), 1.499 (ddd, *J* = 11.9, 7.3, 4.0, 1H); ^{13}C NMR (AV500, 126 MHz, CD_2Cl_2) δ 147.0 (1C), 141.7 (1C), 137.8 (1C), 126.3 (1C), 125.1 (1C), 124.4 (1C), 123.7 (1C), 122.3 (1C), 121.9 (1C), 121.0 (1C), 120.6 (1C), 119.8 (1C), 119.7 (1C), 119.0 (1C), 112.3 (1C), 111.9 (1C), 68.5 (1C), 54.3 (1C), 53.4 (1C), 42.3 (1C), 39.0 (1C), 33.7 (1C), 31.4 (1C), 28.1 (1C), 25.2 (2C); IR (KBr) 3413 (s), 3044 (w), 2953 (s), 2868 (m), 1446 (s), 1250 (m), 1101 (m), 1015 (m), 749 (s); HRMS-EI $[M]^+$ calcd for $C_{26}H_{26}N_2$ 366.2091, found 366.2118. Anal. (AML) Calcd for $C_{26}H_{26}N_2$ C 85.21, H 7.15, N 7.64; Found C 85.30, H 7.18, N 7.62. X-ray crystallographic data of the hemi-1,4-dimethylbenzenate were obtained [64].

5',11'-Dihydrodispiro[cyclohexane-1,6'-indolo[3,2-*b*]carbazole-12',1"-cyclohexane] (9f).

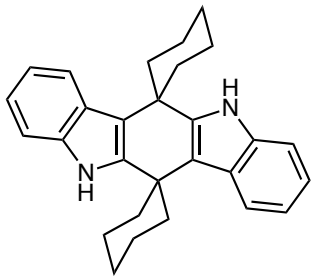

Based on the work of Guzei, *et al*. [41]: indole (3.00 g, 25.6 mmol), cyclohexanone (2.65 mL, 25.6 mmol), hydrochloric acid (aq., 7.5 M, 150 μL, 6 mmol), and acetonitrile (25 mL) were placed in a round-bottomed flask. The resulting mixture was refluxed for 24 h, and then allowed to cool to rt. The solid portion of the resulting mixture was collected by suction filtration, triturated three times with acetonitrile, and then dried under vacuum (110 ºC, 0.05 mmHg, 4 h), giving a white powder (1.72 g, 4.36 mmol, 34%). M.p. 382–383 °C (lit. not given) [41]; R_f = 0.55 (in 1:2 EtOAc:hexane on SiO_2); ^{1}H NMR (AV500, 500 MHz, $(CD_3)_2NCDO$) δ 10.457 (s, 2H), 7.914 (d, *J* = 7.7, 2H), 7.662 (d, *J* = 7.6, 2H), 7.117–7.055 (m, 4H), 2.796–2.750 (m, 4H), 2.293–2.205 (m, 4H), 2.016–1.989 (m, 2H), 1.864–1.710 (m, 10H); ^{13}C NMR (AV500, 126 MHz, $(CD_3)_2NCDO$) δ 142.3 (2C), 138.8 (2C), 125.2 (2C), 121.12 (2C), 121.10 (2C), 119.2 (2C), 115.7 (2C), 113.3 (2C), 38.1 (4C), 37.4 (2C), 26.1 (2C), 24.1 (4C); IR (KBr) 3497 (m), 3457 (s), 3051 (w), 2936 (s), 2915 (s), 2864 (m), 1615 (w), 1463 (s), 1310 (s), 900 (m), 741 (s), 709 (m); HRMS-EI $[M]^+$ calcd for $C_{28}H_{30}N_2$ 394.2404, found 394.2415.

6,7,8,9,10,15-Hexahydro-5*H*-cyclohepta[*a*]indolo[3,2-*c*]carbazole (10g) was obtained as a

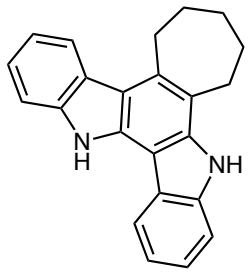

chromatographic fraction (R_f = 0.47, 1:2 EtOAc:hexane on SiO_2) from the synthesis of bisindole **7g** by Method D [cycloheptanone (1.2 mL), EtOH (5 mL), 72 h], which was processed according to Method F. The resulting yellow solid was iteratively triturated with DCM and then collected by decanting, until the triturate no longer contained indole or bisindole, as indicated by TLC. The resulting white solid was recrystallized from methanol-water, and then dried under vacuum (110 ºC, 0.05 mmHg, 12 h), and then additionally dried in a vacuum vessel containing P_2O_5 (120 ºC, 250 mmHg, 72 h), giving a white powder (146 mg), which was primarily composed of the title compound (99 mass%: 144 mg, 444 μmol, 4.4%; calculated by elemental analysis). The major impurity was water (approx. 2 mg). M.p. 301 °C dec.; ^{1}H NMR (AV500, 500 MHz, $(CD_3)_2SO$) δ 11.560 (s, 1H), 11.250 (s, 1H), 8.592 (d, *J* = 7.7, 1H), 8.245 (d, *J* = 7.9, 1H), 7.630 (d, *J* = 7.9, 1H), 7.547 (d, *J* = 8.0, 1H), 7.365 (t, *J* = 7.5, 1H), 7.309 (t, *J* = 7.5, 1H), 7.248 (t, *J* = 7.4, 1H), 7.155 (t, *J* = 7.5, 1H), 6.617–3.598 (m, 2H), 3.257–3.236 (m, 2H), 1.986–1.939 (m, 2H), 1.826–

1.783 (m, 2H), 1.741–1.698 (2H); ^{13}C NMR (AV500, 126 MHz, $(CD_3)_2SO$) δ 139.6 (1C), 138.8 (1C), 138.2 (1C), 136.3 (1C), 132.3 (1C), 123.7 (1C), 123.6 (1C), 122.7 (1C), 122.0 (1C), 120.71 (1C), 120.67 (1C), 118.6 (1C), 118.4 (1C), 118.0 (1C), 112.9 (1C), 111.0 (1C), 110.6 (1C), 104.2 (1C), 32.0 (1C), 30.1 (1C), 27.7 (1C), 27.5 (1C), 26.7 (1C); IR (KBr) 3436 (s), 3418 (s), 3049 (w), 2909 (s), 2845 (m), 1639 (s), 1463 (s), 1258 (s), 737 (s); HRMS-EI $[M]^+$ calcd for $C_{23}H_{20}N_2$ 324.1621, found 324.1630. Anal. (AML) Calcd for $C_{23}H_{20}N_2$ C 85.15, H 6.21, N 8.63; Calcd for $[C_{23}H_{20}N_2 \bullet 0.252\ H_2O]$ C 83.96, H 6.28, N 8.51; Found C 83.95, H 6.28, N 8.42.

5,6,7,8,9,10,11,12,13,14,15,20-Dodecahydrocyclododeca[*a*]indolo[3,2-*c*]carbazole (10l) was

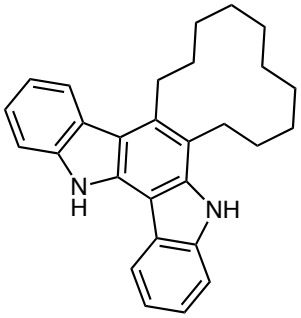

obtained as a chromatographic fraction (R_f = 0.47, 1:2 EtOAc:hexane on SiO_2) from the synthesis of bisindole **7l** by Method D [cyclododecanone (1.82 g), 7 d], which was processed according to Method F. The resulting yellow solid was purified and dried by the method described for carbazole **10g**, except that the triturations used hexane, giving a white powder (162 mg), which was primarily composed of the title compound (99 mass%: 160 mg, 406 μmol, 4.1%; calculated by elemental analysis). The major impurity was water (approx. 2 mg). M.p. 270–271 °C; ^{1}H NMR (AV500, 500 MHz, CD_2Cl_2) δ 8.741 (s, 1H), 8.401 (s, 1H), 8.162–8.132 (m, 2H), 7.624 (dt, *J* = 8.0, 0.9, 1H), 7.589 (dt, *J* = 8.1, 0.9, 1H), 7.435 (ddd, *J* = 8.1, 7.2, 1.1, 1H), 7.401–7.334 (m, 2H), 7.283 (ddd, *J* = 8.1, 7.2, 1.1, 1H), 3.475–3.443 (m, 2H), 3.177–3.146 (m, 2H), 2.043–2.011 (m, 2H), 1.979–1.923 (m, 2H), 1.779–1.706 (m, 4H), 1.686–1.608 (m, 4H), 1.539–1.527 (m, 4H); ^{13}C NMR (AV500, 126 MHz, CD_2Cl_2) δ 139.7 (1C), 139.6 (1C), 136.2 (1C), 135.3 (1C), 133.4 (1C), 124.69 (1C), 124.66 (1C), 123.8 (1C), 123.0 (1C), 122.1 (1C), 120.7 (1C), 120.3 (1C), 120.2 (1C), 116.3 (1C), 115.4 (1C), 111.3 (1C), 111.2 (1C), 105.3 (1C), 28.6 (1C), 28.5 (1C), 28.2 (1C), 28.1 (1C), 28.0 (1C), 27.2 (1C), 27.1 (1C), 26.0 (1C), 23.0 (1C), 22.8 (1C); IR (KBr) 3443 (s), 3053 (w), 2922 (m), 2851 (m), 1636 (m), 1372 (m), 1255 (s), 736 (s); HRMS-EI $[M]^+$ calcd for $C_{28}H_{30}N_2$ 394.2404, found 394.2390. Anal. (AML) Calcd for $C_{28}H_{30}N_2$ C 85.24, H 7.66, N 7.10; Calcd for $[C_{28}H_{30}N_2 \bullet 0.290\ H_2O]$ C 84.13, H 7.71, N 7.01; Found C 84.15, H 7.64, N 6.92.

2-(2,3,4,5,6,9-Hexahydro-1*H*-cycloocta[*c*]carbazol-8-yl)aniline (11h). *Hydrochloride:* 2,3'-Biindolyl (**6**; 3.07 g, 13.2 mmol), cyclooctanone (1.66 g, 13.2 mmol), and ethanol (100 mL) were combined in a round-bottomed flask fitted with a reflux condenser. The system was flushed with argon, and then hydrochloric acid (12 M, 15 mL, 180 mmol) was added via a syringe. The resulting mixture was refluxed under argon for 10 d, and then allowed to cool to rt. The ethanol was removed on a rotary evaporator. The resulting solid was triturated with hexane to remove most of the remaining cyclooctanone, and then was collected by suction filtration.

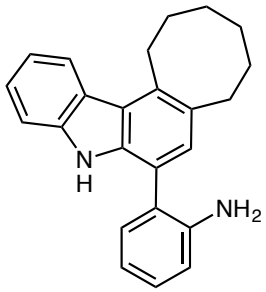

Free base: The triturated solids were placed in a conical flask with EtOAc (75 mL) and Na_2CO_3 solution (sat., aq., 75 mL). The resulting mixture was stirred at 50 ºC for 1.5 h, during which the solids dissolved. The aqueous portion was extracted with EtOAc (2 × 50 mL), and then the combined organic portions were washed with brine (50 mL), and then dried with $MgSO_4$. The liquid portion was concentrated on a rotary evaporator, and then the resulting brown solid was purified by column chromatography (1:19 to 1:9 EtOAc:hexane on SiO_2). Concentration of the desired fraction (R_f = 0.48, 1:2 EtOAc:hexane on SiO_2) on a rotary evaporator gave a white powder (1.90 g, 5.58 mmol, 42%). M.p. 157–158 ºC; ^{1}H NMR (AV500, 500 MHz, $(CD_3)_2SO$) δ 10.530 (s, 1H); 8.122 (d, *J* = 8.0, 1H), 7.517 (d, *J* = 8.0, 1H), 7.319 (t, *J* = 7.5, 1H), 7.163–7.126 (m, 3H), 7.080 (s, 1H), 6.868 (d, *J* = 7.7, 1H), 6.722 (td, *J* = 7.5, 0.9, 1H), 4.584 (s, 2H), 3.396–3.372 (m, 2H), 2.940–2.915 (m, 2H), 1.913–1.877 (m, 2H), 1.711–1.665 (m, 2H), 1.462–1.423 (m, 2H), 1.350–1.308 (m, 2H); ^{13}C NMR (AV500, 126 MHz, $(CD_3)_2SO$) δ 145.5 (1C), 140.5 (1C); 136.5 (1C); 133.5 (1C); 131.6 (1C); 130.5 (1C); 128.2 (1C); 127.8 (1C); 124.5 (1C); 123.0 (1C); 122.5 (1C); 121.7 (1C); 120.6 (1C); 120.0 (1C); 118.5 (1C); 116.6 (1C); 115.1 (1C); 111.4 (1C); 32.7 (1C); 31.9 (1C); 28.7 (1C); 27.1 (1C); 26.0 (1C); 25.7 (1C); IR (KBr) 3412 (m), 3052 (w), 3025 (w), 2918 (s), 2488 (m), 1613 (m), 1453 (s), 1259 (m), 1072 (w), 1024 (w), 738 (s), 618 (m); HRMS-EI $[M]^+$ calcd for $C_{24}H_{24}N_2$ 340.1934, found 340.1932. X-ray crystallographic data were obtained.

***rac*-1,2,3,4,5,6,11,12-Octahydro-12-methylbenzo[4,5][1,3]diazepino[1,7,6-*lm*]cycloocta[*c*]carbazole (12h)** was obtained as a chromatographic fraction (R_f = 0.47, 1:2 EtOAc:hexane on SiO_2) from the synthesis of bisindole **7h** by Method D [cyclooctanone (1.26 g), EtOH (5 mL), 8 d], which was processed according to Method F, giving a white powder (144 mg, 207 μmol, 2.1%). M.p. 218–220 °C

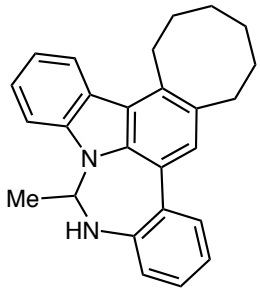

Acidic condensation with acetaldehyde: Carbazolylaniline **11h** (123 mg, 361 μmol), (1,1)-diethoxyethane (acetaldehyde diethyl acetal; 52 μL, 370 μmol), and ethanol (10 mL) were placed in a round-bottomed flask. After the resulting mixture had homogenized, TFA (28 μL, 350 μmol) was added. The resulting mixture was refluxed for 3 d, and then was allowed to cool to rt. Most of the ethanol was removed on a rotary evaporator. The resulting brown residue was transferred to a separatory funnel with DCM (25 mL). The resulting solution was washed with $NaHCO_3$ solution (aq., sat., 20 mL), and then brine (20 mL), dried with $MgSO_4$, and then filtered. The filtrate was concentrated on a rotary evaporator, giving a brown powder (169 mg). The title compound was observed as the principal molar component (40 mass%: 68 mg, 185 μmol, 51%; calculated by ^{1}H NMR analysis with internal 1,4-dimethoxybenzene). There appeared to be 2 impurities present in substantial abundance; these were not identified. Further purification of this mixture was not attempted. M.p. 102–134 ºC; R_f = 0.47 (1:2 EtOAc:hexane on SiO_2).

Alkaline condensation with acetaldehyde (preferred preparation): Carbazolylaniline **11h** (200 mg, 587 μmol), (1,1)-diethoxyethane (acetaldehyde diethyl acetal; 500 μL, 3.51 mmol), and ethanol (10 mL) were placed in a round-bottomed flask. The resulting mixture was refluxed for 2 h, and then allowed to cool to rt. Cesium carbonate (595 mg, 1.83 mmol) was added. The resulting mixture was refluxed for 3 d, and then allowed to cool to rt. Most of the ethanol was removed on a rotary evaporator. DCM (25 mL) was added. The resulting mixture was agitated for 5 min, and then filtered through celite (2 cm × 3 cm, H × D). The filtrate was concentrated on a rotary evaporator, and then separated by column chromatography. The desired fraction (R_f = 0.47 in 1:2 EtOAc:hexane on SiO_2) was concentrated on a rotary evaporator, giving a beige powder (115 mg, 314 μmol, 53%). M.p. 212–215 ºC. ^{1}H NMR (AV500, 500 MHz, CD_2Cl_2) δ 8.261 (d, *J* = 8.0, 1H), 7.891 (d, *J* = 8.9, 1H), 7.602 (s, 1H), 7.466 (t, *J* = 7.7, 1H), 7.334 (d, *J* = 8.2, 1H), 7.264–7.204 (m, 3H), 6.952 (dd, *J* = 6.9, 2.1, 1H), 5.999 (p, *J* = 6.3, 1H), 4.624 (d, *J* =

5.5, 1H), 3.510 (dt, *J* = 12.2, 5.9, 1H), 3.437 (dt, *J* = 13.4, 6.2, 1H), 3.048 (t, *J* = 5.7, 2H), 1.990 (q, *J* = 5.7, 2H), 1.859–1.795 (m, 1H), 1.761–1.695 (m, 1H), 1.552–1.475 (m, 2H), 1.448 (d, *J* = 6.5, 3H), 1.408–1.359 (m, 2H); ^{13}C NMR (AV500, 126 MHz, CD_2Cl_2) δ 144.2 (1C), 139.4 (1C), 136.3 (1C), 135.9 (1C), 133.7 (1C), 132.0 (1C), 129.0 (1C), 128.1 (1C), 127.8 (1C), 125.5 (1C), 124.2 (1C), 123.7 (1C), 123.3 (1C), 123.2 (1C), 122.1 (1C), 119.8 (1C), 119.4 (1C), 108.1 (1C), 66.7 (1C), 33.7 (1C), 33.3 (1C), 29.5 (1C), 28.0 (1C), 27.1 (1C), 26.7 (1C), 22.2 (1C); ^{15}N NMR (AV500, 50.7 MHz, CD_2Cl_2) [193] δ 136.7 (1N, tertiary), 78.5 (1N, *N*–H); IR (KBr) 3423 (m), 3356 (m), 3052 (w), 2920 (s), 2849 (m), 1610 (w), 1570 (m), 1457 (s), 1164 (m), 754 (s), 733 (s); HRMS-EI $[M]^+$ calcd for $C_{26}H_{26}N_2$ 366.2091, found 366.2101. X-ray crystallographic data were obtained.

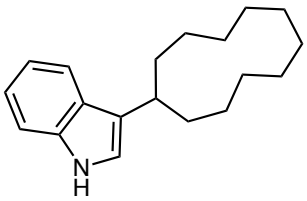

3-Cycloundecylindole (13k) was obtained as a chromatographic fraction (R_f = 0.58, 1:2 EtOAc:hexane on SiO_2) from the synthesis of bisindole **7k** by Method D (p 191), giving a white powder (157 mg, 583 μmol, 5.8%). M.p. 98–99 °C; ^{1}H NMR (HD500, 500 MHz, $(CD_3)_2SO$) δ 10.699 (s, 1H), 7.497 (d, *J* = 7.3, 1H), 7.311 (d, *J* = 8.1, 1H), 7.080 (d, *J* = 2.4, 1H), 7.033 (ddd, *J* = 8.2, 6.9, 1.2, 1H), 6.941 (ddd, *J* = 8.0, 6.9, 1.1, 1H), 3.066 (p, *J* = 6.4, 1H), 1.855–1.790 (m, 2H), 1.760–1.696 (m, 2H), 1.539–1.463 (m, 14H), 1.401–1.344 (m, 2H); ^{13}C NMR (HD500, 126 MHz, $(CD_3)_2SO$) δ 122.7 (1C), 113.1 (1C), 108.8 (1C), 107.7 (1C), 106.3 (1C), 105.4 (1C), 104.8 (1C), 97.1 (1C), 20.2 (1C), 19.1 (2C), 12.5 (2C), 12.3 (2C), 12.2 (2C), 11.1 (2C); IR (KBr) 3399 (s), 3051 (w), 2924 (s), 2858 (s), 1615 (w), 1457 (m), 1222 (m), 1095 (m), 741 (s); HRMS-EI $[M]^+$ calcd for $C_{19}H_{27}N$ 269.2138, found 269.2142. Anal. (AML) Calcd for $C_{19}H_{27}N$ C 84.70, H 10.10, N 5.20; Found C 84.99, H 10.32, N 5.12.

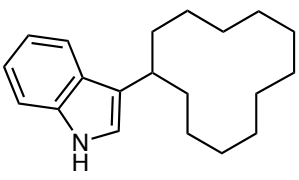

3-Cyclododecylindole (13l) was prepared based on Method C, with indole (2.92 g, 24.9 mmol), cyclododecanone (4.55 g, 25.0 mmol), $TsOH•H_2O$ (242 mg, 1.27 mmol), and AcOH (25 mL), at 50 ºC, for 15 d. The resulting mixture was processed according to Method F, giving white block-shaped crystals (2.36 g). The principal component was cyclododecanone (approx. 84 mass%, 1.99 g, 10.9 mmol, 44%; by ^{1}H NMR analysis). The title compound was the secondary component (approx. 14 mass%, 342 mg, 1.21

mmol, 4.8%). M.p. 42–49 ºC; R_f = 0.52 (1:2 EtOAc:hexane on SiO_2); ^{1}H NMR (AV500, 500 MHz, $(CD_3)_2SO$) δ 10.622 (s, 1H), 7.501 (d, *J* = 7.9, 1H), 7.321 (d, *J* = 8.1, 1H), 7.052 (d, *J* = 2.3, 1H), 7.028 (t, *J* = 7.8, 1H), 6.933 (t, *J* = 7.5, 1H), 3.044 (p, *J* = 5.8, 1H), 1.829 (ddt, *J* = 6.3, 6.2, 6.1, 2H), 1.664–1.356 (m, 18H), 1.291–1.183 (m, 2H); ^{13}C NMR (AV500, 126 MHz, $(CD_3)_2SO$) δ 136.3 (1C), 126.5 (1C), 120.8 (1C), 120.3 (1C), 119.5 (1C), 118.1 (1C), 117.6 (1C), 111.1 (1C), 30.4 (1C), 30.3 (2C), 23.31 (2C), 23.28 (2C), 23.25 (2C), 22.9 (1C), 22.3 (2C); IR (KBr) 3376, 1458, 741; HRMS-EI $[M]^+$ calcd for $C_{20}H_{29}N$ 283.2295, found 283.2297. Any additional IR spectral signals were obstructed by those of cyclododecanone. ^{1}H NMR signals were observed that were consistent with the corresponding 3-vinylindole (approx. 1.2 mass%, 27 mg, 97 μmol, 0.39%).

An unidentified cyclododecanone-derived product (14) was obtained as a chromatographic fraction (R_f = 0.57 in 1:2 EtOAc:hexane on SiO_2) from the preceding entry. The resulting white powder (470 mg) was triturated twice with pentane, giving a white powder (117 mg). The component of interest was present at approx. 26 mol%, with cyclododecanone as the principal component; calculated by ^{1}H NMR analysis. M.p. 52–57 ºC; ^{1}H NMR (AM400, 400 MHz, CD_2Cl_2; relative integrations) δ 7.759 (s, 1H), 7.599–7.577 (m, 1H), 7.246–7.224 (m, 1H), 7.072–7.017 (m, 2H), 2.766 (d, *J* = 13.0, 1H), 2.569 (d, *J* = 13.1, 1H), 2.281–2.222 (m, 1H), 1.935–1.882 (m, 1H), 1.763–1.719 (m, 2H); ^{13}C NMR (AM400, 101 MHz, CD_3CN) 146.8, 142.2, 127.4, 125.8, 121.3, 120.5, 119.8, 112.7, 60.6, 49.1, 47.3, 37.4, 36.4, 30.3, 27.7, 27.0, 23.5, 23.4, 23.1, 23.0, 22.2, 21.2; IR (KBr) 3286. Any additional NMR or IR spectral signals were obstructed by those of cyclododecanone.

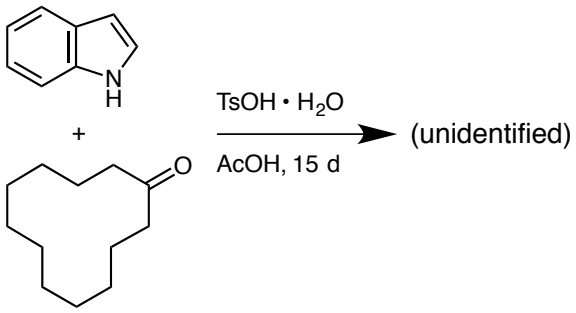

3.3. Progress Toward Indolo[2,3-*b*]carbazoles

3.3.1. Synthesis and Alkylations of Cyclohexane-1,3-diones

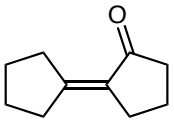

Bi(cyclopentylidene)-2-one (15). Based on the work of Arnold, *et al*. [194]: cyclopentanone (8.9 mL, 101 mmol), triethylamine (1.4 mL, 100 mmol), and toluene (80 mL) were placed in a round-bottomed flask fitted with a Dean-Stark trap. Lithium perchlorate (2.80 g, 26.3 mmol) was added. The resulting mixture was refluxed for 12 h, and then was allowed to cool to rt. The resulting mixture was washed with NH_4Cl solution (aq., sat., 200 mL). The organic portion was dried with Na_2SO_4, filtered, and then concentrated on a rotary evaporator. The resulting brown oil was purified by vacuum distillation through a packed column (8 cm × 2 cm, H × D; 102–125 ºC, 18 mmHg), giving a colorless oil (6.91 g, 46.0 mmol, 92%). The product was transferred to storage vials with DCM prior to NMR analysis, and was carried forward as an 86 mass% solution in DCM, as indicated by the ^{1}H NMR spectrum. Several batches were produced by this method, and then combined into a 77 mass% stock solution in DCM. R_f = 0.35 (1:5 EtOAc:hexane on SiO_2); ^{1}H NMR (VI500, 500 MHz, $CDCl_3$) δ 2.787–2.782 m, 2H), 2.555–2.517 (m, 2H), 2.322–2.273 (m, 4H), 1.915 (p, *J* = 7.6, 2H), 1.704 (qd, *J* = 14.7, 7.2, 4H); ^{13}C NMR (VI500, 126 MHz, $CDCl_3$) δ 207.5 (1C), 158.8 (1C), 128.0 (1C), 39.9 (1C), 34.4 (1C), 32.7 (1C), 29.7 (1C), 27.1 (1C), 25.4 (1C), 20.2 (1C) IR (NaCl) 2958 (s), 2873 (m), 1708 (s), 1640 (s), 1417 (w), 1252 (m), 1169 (m), 825 (w); HRMS-ESI $[M+Na]^+$ calcd for $C_{10}H_{14}O$ 173.0937, found 173.0930.

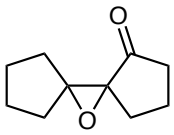

***rac*-11-Oxadispiro[4.0.4^6.1^5]undecan-1-one (16)**. Based on the work of Miah & Snieckus [68]: enone **115** (77 mass%, 14.2 g, 65.9 mmol), chloroform (80 mL), and water (50 mL) were placed in a round-bottomed flask. The resulting mixture was cooled in an ice bath. 3-Chloroperoxybenzoic acid (70 mass%, 18.0 g, 73.1 mmol) was added. The resulting mixture was stirred in an ice bath for 4 h. The resulting mixture was separated by suction filtration, and then the filter cake was washed with chloroform (3 × 10 mL). The aqueous portion of the filtrate was extracted with chloroform (2 × 20 mL). The extracts were combined with the organic portion of the filtrate.

Neutralization and chromatography: The combined organic portions were washed with $NaHCO_3$ solution (aq., sat., 3 × 25 mL), brine (40 mL), and then dried with Na_2SO_4. The resulting mixture was separated by filtration. The filtrate was concentrated on a rotary evaporator,

giving a pale yellow oil (9.31 g), which was primarily composed of the title compound (93 mass %: 8.64 g, 52.0 mmol, 79%; calculated by ^{1}H NMR analysis) [195]. R_f = 0.44 (1:4 EtOAc:hexane on Al_2O_3); ^{1}H NMR (VI500, 500 MHz, $CDCl_3$) δ 2.423–2.312 (m, 2H), 2.195–2.059 (m, 3H), 1.962–1.745 (m, 6H), 1.726–1.652 (m, 1H), 1.627–1.559 (m, 2H); ^{13}C NMR (VI300, 75 MHz, $CDCl_3$) δ 214.4 (1C), 76.7 (1C), 67.9 (1C), 37.2 (1C), 31.9 (1C), 29.5 (1C), 27.3 (1C), 25.4 (1C), 24.8 (1C), 17.9 (1C); IR (NaCl) 2963 (s), 2872 (m), 1746 (s), 1574 (w), 1406 (m), 1207 (m), 960 (m), 824 (m); HRMS-ESI $[M+Na]^+$ calcd for $C_{10}H_{14}O_2$ 189.0886, found 189.0882.

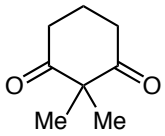

2,2-Dimethylcyclohexane-1,3-dione (17b). Based on the work of Shibuya & Isobe [69]: cyclohexane-1,3-dione (5.00 g, 44.6 mmol) was dissolved in acetone (100 mL) in a round-bottomed flask. Potassium carbonate (13.6 g, 98.4 mmol) was added, the resulting mixture was placed in an ice bath and then stirred for 15 min. Methyl iodide (6.1 mL, 98.0 mmol) was added. The resulting mixture was gradually warmed from 0 ºC to reflux over 2 h, and then was refluxed for 18 h. The resulting mixture was allowed to cool to rt, and then was separated by suction filtration. The filter cake was washed with DCM (25 mL). The filtrate was concentrated on a rotary evaporator, taken up in water (50 mL) and DCM (10 mL), and then extracted with DCM(2 × 25 mL). The filter cake was placed in a conical flask with water (100 mL) and ethyl acetate (50 mL). The resulting mixture was stirred for 10 min. The combined DCM portions were washed with brine (25 mL), dried with sodium sulfate, filtered, and then concentrated on a rotary evaporator. The resulting yellow residue (6.08 g) was separated by column chromatography (1:8–1:1 ethyl acetate:hexane on SiO_2). The desired fraction (R_f = 0.31 in 1:1 EtOAc:hexane on SiO_2, visualized with DNPH) [196] was concentrated on a rotary evaporator, and then dried under vacuum (rt, 0.1 mmHg, 2 h), giving a white powder (3.17 g, 22.6 mmol, 51%). M.p. 32–35 ºC (lit. 35–36 ºC) [197]; ^{1}H NMR (AM400, 400 MHz, $CDCl_3$) δ 2.687 (t, J = 6.8, 4H), 1.950 (p, J = 6.9, 2H), 1.311 (s, 6H); ^{13}C NMR (AM400, 101 MHz, $CDCl_3$) δ 210.5 (2C), 61.8 (1C), 37.4 (2C), 22.3 (2C), 18.1 (1C); IR (KBr) 2969 (m), 2944 (m), 2874 (w), 1728 (s), 1697 (s), 1607 (s), 1226 (m), 1029 (m), 844 (w); HRMS-ESI $[M+Na]^+$ calcd for $C_8H_{12}O_2$ 163.0730, found 163.0730.

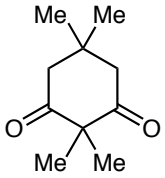

2,2,5,5-Tetramethylcyclohexane-1,3-dione (17c) was prepared according to the same procedure as dione **17a**, with dimedone (4.10 g, 29.2 mmol), K_2CO_3 (8.89 g, 64.3 mmol), acetone (100 mL), and methyl iodide (4.0 mL, 64.3 mmol), giving a white powder (2.68 g, 15.9 mmol, 54%). M.p. 97–98 ºC (lit. 95 ºC) [70]; R_f = 0.56 (1:1 EtOAc:hexane on SiO_2, visualized with DNPH) [196]; ^{1}H NMR (VI300, 300 MHz, $CDCl_3$) δ 2.604 (s, 4H), 1.290 (s, 6H), 0.979 (m, 6H); ^{13}C NMR (VI300, 75 MHz, $CDCl_3$) δ 210.6 (2C), 60.5 (1C), 51.2 (2C), 30.8 (1C), 28.6 (2C), 22.3 (2C); IR (KBr) 2936 (m), 2874 (m), 1722 (s), 1686 (s), 1321 (m), 802 (w); HRMS-ESI $[M+Na]^+$ calcd for $C_{10}H_{16}O_2$ 191.1043, found 191.1042.

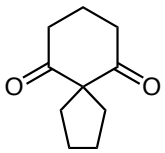

Spiro[4.5]decane-6,10-dione (17d). Based on the work of Miah & Snieckus [68]: epoxide **116** (93 mass%, 9.31 g, 52.0 mmol) and DCM were placed in a round-bottomed flask in a dry N_2 atmosphere. The resulting mixture was cooled to –78 ºC, and then boron trifluoride etherate (650 μL, 5.28 mmol) was added dropwise. The reaction mixture was warmed to rt in a water bath. After 10 min, the resulting mixture was placed in a separatory funnel, was washed with $NaHCO_3$ solution (2 × 50 mL), and then brine (50 mL). The organic portion was dried with Na_2SO_4, filtered, and then separated by column chromatography. The desired fraction (R_f = 0.53 in 1:5 EtOAc:hexane on Al_2O_3, visualized with DNPH) [196] was concentrated on a rotary evaporator, giving a pale yellow oil (4.52 g, 27.2 mmol, 52%).

Preferred preparation: Epoxide **16** was synthesized according to the previously described procedure, with enone **15** (77 mass%, 26.1 g, 121 mmol), chloroform (350 mL), water (200 mL), and 3-chloroperoxybenzoic acid (70 mass%, 38.91 g, 157 mmol). Instead of performing the neutralization and chromatography protocol, the combined extracts were washed with $Na_2S_2O_3$ solution (aq., 50% sat., 100 mL), and then brine (2 × 75 mL). The organic portion was placed in a round-bottomed flask, and then cooled to –78 ºC. Boron trifluoride etherate (1.25 mL, 10.2 mmol) was added, and then the resulting mixture was allowed to warm to rt. After 2 h, the reaction mixture was processed according to the preceding paragraph, giving a pale yellow oil (8.63 g, 51.9 mmol, 43 %). ^{1}H NMR (VI500, 500 MHz, CD_2Cl_2) δ 2.634 (t, J = 6.7, 4H), 2.018 (ddd, J = 7.1, 4.6, 2.8, 4H), 1.942 (p, J = 6.8, 2H), 1.648–1.620 (m, 4H); ^{13}C NMR (VI500, 126 MHz, CD_2Cl_2) δ 209.1 (2C), 73.1 (1C), 38.5 (2C), 33.6 (2C), 26.9 (2C), 18.4 (1C); IR (NaCl)

2956 (s), 2870 (m), 1724 (s), 1694 (s), 1449 (m), 1032 (m), 842 (w); HRMS-ESI $[M+Na]^+$ calcd for $C_{10}H_{14}O_2$ 189.0886, found 189.0885.

3.3.2. Syntheses and Indolization of Phenylhydrazones

Method G: Condensation of Ketones with Phenylhydrazine

Adapted from the work of Oppolzer, *et al*. [72]: the indicated amounts of ketone, phenylhydrazine, $MgSO_4$, and DCM were placed in a round-bottomed flask. After the resulting mixture had been stirred for 5 min, the indicated amount of $TsOH•H_2O$ was added. The resulting mixture was refluxed for 24 h in an N_2 atmosphere, allowed to cool to rt, and then filtered. The filter cake was washed with DCM (4 × 10 mL). The combined filtrates were washed with $NaHCO_3$ solution (aq., sat., 30 mL), and then brine (30 mL). The organic portion was dried with Na_2SO_4, filtered, and then concentrated on a rotary evaporator.

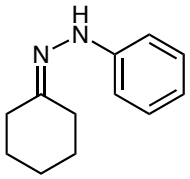

Cyclohexylidene-2-phenylhydrazine (18a) was prepared according to Method G, with cyclohexanone (8.1 mL, 78.2 mmol), phenylhydrazine (7.6 mL, 77.3 mmol), $MgSO_4$ (4.49 g, 37.3 mmol), DCM (150 mL), and $TsOH•H_2O$ (736 mg, 3.86 mmol). The resulting brown residue was washed with ice-cold hexane, and then dried under vacuum (rt, 0.05 mmHg, 12 h), giving a yellow powder (12.8 g, 68.0 mmol, 88%). M.p. 65–70 °C (lit. 71–75 ºC) [198]; R_f = 0.64 (1:1 EtOAc:hexane on SiO_2); ^{1}H NMR (AV500, 500 MHz, CD_2Cl_2) δ 7.206 (t, J = 7.8, 2H), 7.046–7.000 (m, 3H), 6.781 (t, J = 7.3, 1H), 2.333 (dt, J = 16.3, 6.2, 4H), 1.736–1.645 (m, 6H); ^{13}C NMR (AV500, 126 MHz, CD_2Cl_2) δ 150.1 (1C), 146.9 (1C), 129.6 (2C), 119.7 (1C), 113.1 (2C), 35.9 (1C), 27.7 (1C), 26.4 (1C), 26.3 (1C), 25.8 (1C); IR (KBr) 3280 (m), 3050 (w), 3027 (w), 2935 (s), 2861 (m), 1601 (s), 1499 (s), 1226 (s), 1052 (s), 887 (w), 749 (s), 693 (s), 668 (w); HRMS-EI $[M]^+$ calcd for $C_{12}H_{16}N_2$ 188.1308, found 188.1314.

1*E*,1'*E*-(2,2-Dimethylcyclohexane-1,3-diylidene)bis(2-phenylhydrazine) (18b) was prepared

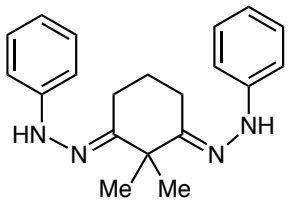

according to Method G, with 2,2-dimethylcyclohexane-1,3-dione (**17b**; 96 mass%, 2.96 g, 20.3 mmol), phenylhydrazine (4.0 mL, 40.5 mmol), $MgSO_4$ (4.88 g, 40.5 mmol), DCM (90 mL), and TsOH•H_2O (231 mg, 1.21 mmol). The resulting brown residue was recrystallized from toluene, and then washed with pentane, giving yellow flakes (4.00 g, 12.5 mmol, 62%). M.p. 134–136 °C; R_f = 0.66 (1:2 EtOAc:hexane on Al_2O_3); ^{1}H NMR (VI300, 300 MHz, CD_2Cl_2) [199] δ 7.276–7.210 (m, 4H), 7.114–7.058 (m, 6H), 6.824 (tt, J = 7.3, 1.2, 2H), 2.472 (t, *J* = 6.8, 4H), 2.097 (p, *J* = 7.0, 2H), 1.525 (s, 6H); ^{13}C NMR (VI300, 75 MHz, CD_2Cl_2) δ 151.4 (2C), 146.7 (2C), 129.6 (4C), 120.0 (2C), 113.4 (4C), 46.2 (1C), 27.4 (2C), 24.1 (2C), 18.7 (1C); IR (KBr) 3348 (m), 3051 (w), 2981 (m), 1706 (w), 1601 (s), 1502 (s), 1249 (s), 751 (s), 690 (s); HRMS-ESI $[M–H]^-$ calcd for $C_{20}H_{24}N_4$ 319.1928, found 319.1930. Anal. (MHW) Calcd for $C_{20}H_{24}N_4$ C 74.97, H 7.55, N 17.48; Found C 74.81, H 7.50, N 17.28.

1*E*,1'*E*-(2,2,5,5-Tetramethylcyclohexane-1,3-diylidene)bis(2-phenylhydrazine) (18c) was

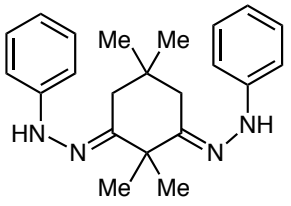

prepared according to Method G, with dimethyldimedone (**17c**; 1.70 g, 10.1 mmol), $MgSO_4$ (2.43 g, 20.2 mmol), phenylhydrazine (2.4 mL, 24.4 mmol), and DCM (25 mL), and TsOH•H_2O (118 mg, 620 μmol), giving an orange powder (2.81 g), which was primarily composed of the title compound (83 mass%: 2.32 g, 6.67 mmol, 66%; calculated by ^{1}H NMR analysis). The major impurity was DCM (approx. 487 mg). M.p. 150–158 °C dec. (lit. 163 ºC) [35]; R_f = 0.63 (1:2 EtOAc:hexane on Al_2O_3); ^{1}H NMR (AV500, 500 MHz, CD_2Cl_2) δ 7.226 (dd, *J* = 7.3, 7.2, 4H), 7.066 (d, *J* = 7.2, 4H), 6.804 (t, *J* = 7.3, 2H), 2.357 (s, 4H), 1.485 (s 6H), 1.020 (s, 6H); ^{13}C NMR (AV500, 126 MHz, CD_2Cl_2) δ 151.9 (2C), 146.9 (2C), 129.6 (4C), 120.0 (2C), 113.4 (4C), 47.2 (1C), 35.7 (2C), 34.0 (1C), 28.9 (2C), 26.4 (2C); IR (KBr) 3353 (m), 3049 (w), 2985 (m), 2960 (m), 2868 (w), 1601 (s), 1500 (s), 1248 (m), 1047 (m), 750 (s), 694 (m); HRMS-ESI $[M–H]^-$ calcd for $C_{22}H_{28}N_4$ 347.2241, found 347.2265.

1*E*,1'*E*-(Spiro[4.5]decane-6,10-diylidene)bis(2-phenylhydrazine) (18d) was prepared according to Method G, with spiro[4.5]decane-6,10-dione (**17d**; 2.01 g, 11.6 mmol), phenylhydrazine (2.3 mL, 23.4 mmol), $MgSO_4$ (2.90 g, 24.1 mmol), DCM (80 mL), and $TsOH•H_2O$ (147 mg, 770 μmol). The resulting brown residue was recrystallized from toluene, and then washed with pentane, giving orange blocks (1.76 g, 5.08 mmol, 44%). M.p. 121–124 °C; R_f = 0.76 (1:2 EtOAc:hexane on SiO_2); ^{1}H NMR (VI300, 300 MHz, CD_2Cl_2) [199] δ 7.268–7.202 (m, 4H), 7.105–7.059 (m, 4H), 7.019 (s, 2H), 6.816 (tt, *J* = 7.3, 1.1, 2H), 2.439 (t, *J* = 6.7, 4H), 2.263–2.215 (m, 4H), 2.091 (p, *J* = 6.6, 2H), 1.868–1.787 (m, 4H); ^{13}C NMR (VI300, 75 MHz, CD_2Cl_2) δ 150.3 (2C), 140.8 (2C), 129.6 (4C), 120.0 (2C), 113.4 (4C), 57.2 (1C), 35.9 (2C), 26.2 (2C), 24.9 (2C), 18.3 (1C); IR (KBr) 3347 (m), 3051 (m), 2952 (s), 2865 (m), 1701 (w), 1601 (s), 1502 (s), 1250 (s), 1096 (m), 728 (m), 711 (m), 693 (s); HRMS-ESI $[M+Na]^+$ calcd for $C_{22}H_{26}N_4$ 369.2050, found 369.2048. Anal. (AML) Calcd for $C_{22}H_{26}N_4$ C 76.27, H 7.56, N 16.17; Found C 76.00, H 7.57, N 15.92.

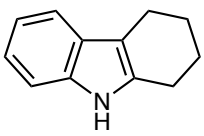

1,2,3,4-Tetrahydrocarbazole (19a). Based on the work of Miyata, *et al*. [8]: cyclohexylidene-2-phenylhydrazine (**18a**; 408 mg, 2.17 mmol), triethylamine (930 μL, 6.64 mmol), and diglyme (8 mL) were placed in a round-bottomed flask. The resulting mixture was cooled to –78 ºC, and then TFAA (340 μL, 2.41 mmol) was added dropwise. The resulting mixture was allowed to warm to rt, was stirred for 2 h, and then was heated to 130 ºC for 24 h. After cooling to rt, the reaction mixture was added to a separatory funnel that contained ether (100 mL). The resulting mixture was washed with water (5 × 25 mL), and then brine (25 mL). The organic portion was filtered through basic alumina (5 cm × 2 cm, H × D). The filter was washed with DCM until the filtrate no longer contained the desired product, as indicated by TLC. The filtrate was concentrated on a rotary evaporator, and then dried under vacuum (rt, 0.05 mmHg, 12 h), giving an orange oil (272 mg), which was primarily composed of the title compound (75 mass%: 205 mg, 1.20 mmol, 55%; calculated by ^{1}H NMR analysis). The major impurities were DCM (approx. 29 mg), diglyme (approx. 24 mg), and cyclohexanone (approx. 14 mg). R_f = 0.42 (1:4 EtOAc:hexane on SiO_2); ^{1}H NMR (HD500, 500 MHz, CD_2Cl_2) δ 7.805 (s, 1H), 7.417 (d, *J* = 7.8, 1H), 7.270 (d, *J* = 7.8, 1H), 7.069 (ddd, *J* = 8.0, 7.1, 1.4, 1H), 7.021 (ddd, *J* = 8.1, 7.0, 1.1, 1H), 2.749–2.718 (m, 2H), 2.704–2.674 (m, 2H), 1.942–1.842 (m, 4H); ^{13}C NMR (HD500, 126 MHz, CD_2Cl_2) δ 136.2 (1C), 134.8

(1C), 128.4 (1C), 121.2 (1C), 119.4 (1C), 118.0 (1C), 110.8 (1C), 110.4 (1C), 23.9 (1C), 23.8 (1C), 23.7 (1C), 21.4 (1C); IR (KBr) 3399 (s), 3050 (w), 2927 (s), 2848 (m), 1450 (m), 1304 (m), 1143 (w), 978 (m), 743 (s), 636 (m); HRMS-EI $[M]^+$ calcd for $C_{12}H_{13}N$ 171.1043, found 171.1044.

3.4. Syntheses of Nitriles and Isocyanides

3.4.1. Esterification and Halogenations of Anilines

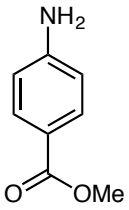

Methyl 4-Aminobenzoate (201ad). Based on the work of Hinsberger, *et al*. [145]: PABA (30.3 g, 221 mmol) and methanol (250 mL) were placed in a round-bottomed flask. The resulting mixture was cooled to –78 ºC. Thionyl chloride (19 mL, 262 mmol) was added dropwise. The resulting mixture was refluxed for 12 h, and then cooled in an ice bath. Sodium hydroxide solution (aq., 3.0 M, 158 mL, 475 mmol) was added over 10 min, followed by 25 mL aliquots of sodium bicarbonate solution (aq., 1.0 M) until the pH of the reaction mixture reached 7.5. The majority of the remaining methanol was then removed using a rotary evaporator. The resulting suspension was extracted with DCM (4 × 40 mL). The combined extracts were washed with water (50 mL), brine (50 mL), and then dried with magnesium sulfate. The resulting mixture was filtered and then concentrated using a rotary evaporator, giving beige flakes (32.6 g, 215 mmol, 97%). M.p. 112–113 ºC (lit. 112–113 ºC) [200]; R_f = 0.46 (1:1 EtOAc:hexane on SiO_2); ^{1}H NMR (VI300, 300 MHz, CD_2Cl_2) δ 7.818 (d, *J* = 8.8, 2H), 6.649 (d, *J* = 8.8, 2H), 4.250 (s, br, 2H), 3.825 (s, 3H); ^{13}C NMR (VI300, 75 MHz, CD_2Cl_2) δ 167.5 (1C), 151.9 (1C), 131.9 (2C), 119.8 (1C), 114.1 (2C), 51.9 (1C); IR (KBr) 3341 (m), 3231 (m), 2944 (w), 2845 (w), 1685 (s), 1599 (s), 1288 (s), 1176 (m), 1120 (m), 772 (w); HRMS-ESI $[M+Na]^+$ calcd for $C_8H_9NO_2$ 174.0525, found 174.0533.

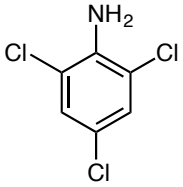

2,4,6-Trichloroaniline (201ba). Aniline (2.5 mL, 27.4 mmol) and chloroform (50 mL) were placed in a round-bottomed flask. The resulting mixture was cooled in an ice bath. Sulfuryl chloride (8.0 mL, 98.6 mmol) was added dropwise. The ice bath was removed, and then the reaction mixture was stirred for 24 h.

Neutralization and chromatography: The resulting mixture was washed with water (4 × 25 mL), and then aliquots of $NaHCO_3$ solution (aq., sat., n × 25 mL), until the raffinate had a pH of at least 7. The organic portion was washed with brine (25 mL), dried with $MgSO_4$, filtered, and then concentrated on a rotary evaporator. The resulting brown residue was separated by column chromatography. The desired fraction (R_f = 0.49 in 1:4 EtOAc:hexane on SiO_2) was concentrated on a rotary evaporator, and then recrystallized from toluene, giving yellow needles (4.56 g, 23.2 mmol, 85%). M.p. 75–76 ºC (lit. 77–78 ºC) [201]; ^{1}H NMR (HD500, 500 MHz, CD_2Cl_2) δ 7.206 (s, 2H), 4.497 (s, 2H); ^{13}C NMR (HD500, 126 MHz, CD_2Cl_2) δ 139.8 (1C), 128.1 (2C), 122.0 (1C), 120.1 (2C); IR (KBr) 3460 (m), 3426 (m), 3370 (m), 3328 (s), 3081 (w), 1725 (w), 1619 (s), 1471 (s), 1074 (m), 855 (s); HRMS-EI $[M]^+$ calcd for $C_6H_4{}^{35}Cl_3N$ 194.9404, found 194.9402.

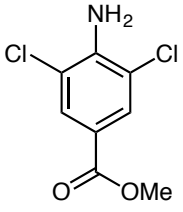

Methyl 4-Amino-3,5-dichlorobenzoate (201bd). Pyridine (6.6 mL, 81.9 mmol), methyl 4-aminobenzoate (**201ad**; 4.95 g, 32.6 mmol), and chloroform (50 mL) were placed in a round-bottomed flask. The resulting mixture was cooled in an ice bath. A solution of sulfuryl chloride (5.9 mL, 72.4 mmol) in chloroform (25 mL) was added dropwise during 30 min, and then the ice bath was removed. The reaction mixture was stirred for 24 h, and then processed according to the neutralization and chromatography protocol of the preceding entry, giving a tan powder (2.87 g, 13.0 mmol, 40%). M.p. 84–85 ºC (lit. 83–84 ºC) [202]; R_f = 0.49 (1:2 EtOAc:hexane on SiO_2); ^{1}H NMR (HD500, 500 MHz, CD_2Cl_2) δ 7.870 (s, 2H), 4.939 (s, 2H), 3.842 (s, 3H); ^{13}C NMR (HD500, 126 MHz, CD_2Cl_2; ^{1}H-coupled) δ 165.6 (q, J = 4.0, 1C), 144.7 (t, J = 6.7, 1C), 129.9 (dd, J = 168.1, 6.8, 2C), 120.5 (t, J = 1.1, 1C), 119.0 (td, J = 5.6, 2.7, 2C), 52.5 (q, J = 147.2, 1C); IR (KBr) 3325 (s), 3080 (w), 2957 (w), 1731 (s), 1617 (s), 1432 (s), 1305 (s), 1263 (s), 980 (m), 761 (s), 634 (m); HRMS-EI $[M]^+$ calcd for $C_8H_7{}^{35}Cl_2NO_2$ 218.9848, found 218.9855.

Method H: Halogenation by Bromine or Iodine Monochloride Vapor

Adapted from the bromine vapor generator reported by Robison & Robison [119], with a positive flow of N_2 applied to the vaporization flask, rather than applying suction at the trap (Fig. 49). The necks of a 3-necked round-bottomed flask (a) were fitted with a 2-barbed argon adapter connected to a source of N_2, a rubber septum, and a glass bridge (1) whose inlet was at the top of flask (a). The outlet of bridge 1 was set slightly above a magnetic stir bar in a second 3-necked round-bottomed flask (b). The other two necks of flask (b) were fitted with a glass stopper, and a second glass bridge (2) whose inlet was at the top of flask (b). The outlet of the second bridge 2 was set 4 cm from the bottom of a 2 L conical flask (c). A line was connected from the second barb of the argon adapter on flask (a), to the bottom of flask (c). The (a–c) line is a safety feature that provides a pathway for halogen vapor in case either of the bridges becomes clogged during the experiment. To trap and neutralize effluent halogen vapor, flask (c) was charged with $Na_2S_2O_3$ solution (aq., sat., 25 mL) and Na_2CO_3 solution (aq., sat., 25 mL), and then filled to within 1 cm of the rim with water [203]. Flasks (a) and (b) were then charged as indicated in each entry. A stream of N_2 (approx. 25 mL/min) was passed into flask (a) for the indicated duration. Flask (b) was stirred such that all solids were gradually turning over, but the central vortex was shallow enough that the outlet of bridge 1 was submerged.

Fig. 49. Vapor-fed halogenation apparatus.

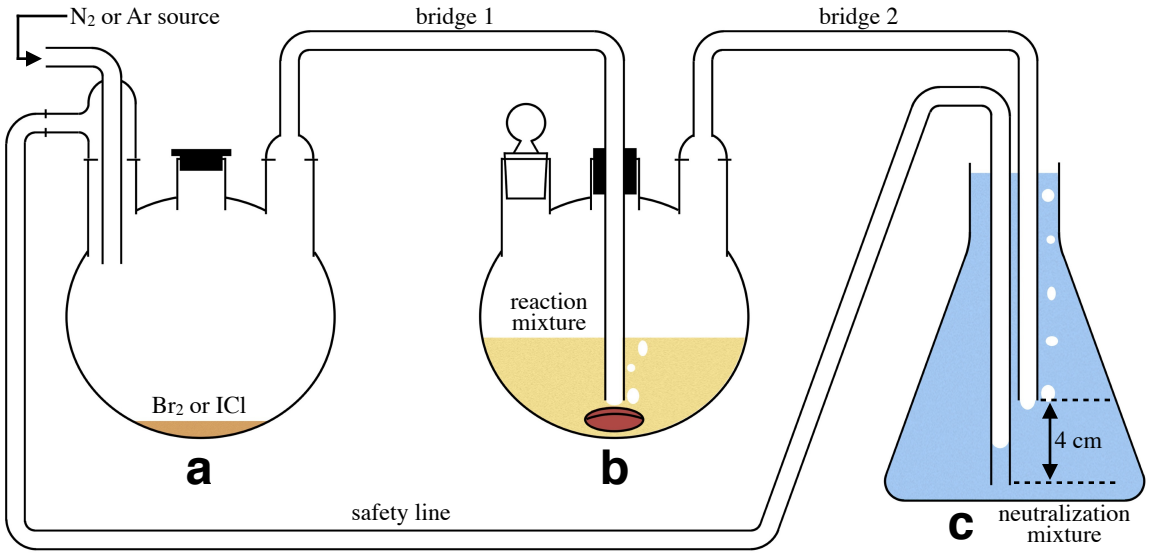

Method I: Neutralization of Bromination or Iodination Mixtures

The resulting mixture was cooled in an ice bath for 30 min, and then separated by suction filtration. The filter cake was washed with water (2 × 20 mL), and then transferred to a beaker with DCM (50 mL) and water (25 mL). The resulting mixture was stirred vigorously. Aliquots of Na_2CO_3 solution (aq., sat., n × 5–10 mL) were added every 2 min, until the aqueous portion retained a pH of at least 7. The aqueous portion, but not any solids, was removed by use of a separatory funnel and/or suction filtration. The combined organic and solid portions were washed with $Na_2S_2O_3$ solution (aq., 50% sat., 25 mL), water (25 mL), and then brine (25 mL).

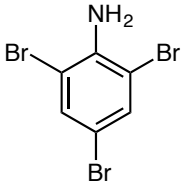

2,4,6-Tribromoaniline (201ca) was prepared according to Method H. Flask (b) was charged with aniline (3.25 mL, 35.6 mmol), water (200 mL), and hydrochloric acid (7.5 M, 5 mL, 37.5 mmol). Flask (a) was then charged with bromine (6.0 mL, 116 mmol). After 24 h of N_2 flow, the reaction mixture was neutralized according to Method I. The resulting mixture was concentrated on a rotary evaporator. The resulting yellow residue was recrystallized from toluene, giving white needles (9.56 g, 28.9 mmol, 81%). M.p. 120–121 ºC (lit. 119–120 ºC) [204]; R_f = 0.72 (1:1 EtOAc:hexane on SiO_2); ^{1}H NMR (VI300, 300 MHz, CD_2Cl_2) δ 7.524 (s, 2H), 4.624 (s, 2H); ^{13}C NMR (AV500, 126 MHz, CD_2Cl_2) δ 142.1 (1C), 134.3 (2C), 109.2 (2C), 109.0 (1C); IR (KBr) 3280 (m), 3073 (w), 1615 (s), 1455 (s), 1066 (w), 860 (m), 706 (m), 674 (m); HRMS-EI $[M]^+$ calcd for $C_6H_4{}^{79}Br^{81}Br_2N$ 330.7849, found 330.7888.

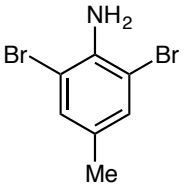

2,6-Dibromo-4-methylaniline (201cb). 4-Methylaniline (2.00 g, 18.7 mmol) and AcOH (100 mL) were placed in a round-bottomed flask. A solution of bromine (2.3 mL, 44.9 mmol) in AcOH (25 mL) was prepared in a separate vessel, and then added dropwise over 30 min. The resulting mixture was heated to 50 ºC for 48 h, and then allowed to cool to rt. The resulting mixture was neutralized according to Method I, and then concentrated on a rotary evaporator. The resulting brown residue was recrystallized from toluene, giving a white powder (4.71 g, 17.8 mmol, 95%). M.p. 74–75 ºC (lit. 74–75 ºC) [205]; R_f = 0.68 (1:3 EtOAc:hexane on SiO_2); ^{1}H NMR (AM400, 400 MHz, $CDCl_3$) δ 7.200 (s, 2H), 4.308 (s, 2H), 2.209 (s, 3H); ^{13}C NMR (AM400, 101 MHz, $CDCl_3$) δ 139.7 (1C), 132.3 (2C), 129.5 (1C), 108.9 (2C), 20.0 (1C); IR

(NaCl) 3308 (m), 2916 (w), 1619 (s), 1580 (m), 1479 (s), 1285 (w), 1058 (w), 855 (m), 735 (w), 707 (w); HRMS-EI $[M]^+$ calcd for $C_7H_7{}^{79}Br^{81}BrN$ 264.8919, found 264.8919.

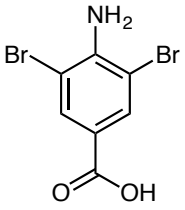

3,5-Dibromo-4-aminobenzoic Acid (201cc) was observed in 3 different experiments. For the preparation of **201cc**, as a mixture component, by bromination of PABA in an alkaline suspension, refer to the entry for **201ce** (p 211). For the preparation of **201cc** by hydrolysis of **201cd**, refer to the entry on p 222.

Bromination of PABA, acidic suspension: Based on the work of Elion [136]: PABA (3.00 g, 21.9 mmol) and AcOH (40 mL) were placed in a round-bottomed flask. A solution of bromine (2.3 mL, 45.0 mmol) in AcOH (35 mL) was added dropwise. The resulting mixture was stirred for 48 h, and then heated to 60 ºC for 2 h. Approximately 50% of the acetic acid was removed by distillation through a packed column (2 cm × 10 cm, D × H; rt to 38 ºC, 9 mmHg). The resulting mixture was separated by suction filtration. The filtrate was poured through the filter cake, and then the filter cake was washed with water (2 × 20 mL). The filter cake was dissolved in boiling ammonium hydroxide solution (aq., 28 mass%, 150 mL). While the ammonia solution was still hot, it was filtered, and then hydrochloric acid (12 M, 20 mL) was added dropwise over 15 min. The resulting mixture was removed from the heat source, and allowed to stand for 1 h. The resulting suspension was separated by suction filtration. The filter cake was washed with water (2 × 10 mL), and then dried under vacuum (80 ºC, 80 mmHg, 24 h), giving a white powder (3.73 g, 12.6 mmol, 58%). M.p. 314–317 ºC dec. (lit. 325 ºC dec.) [206]. All other characterization data matched those given in the entry on p 222.

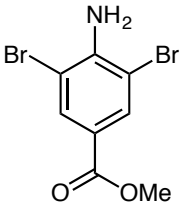

Methyl 4-Amino-3,5-dibromobenzoate (201cd). Pyridine (5.7 mL, 70.3 mmol) was dissolved in methanol (25 mL) in a round-bottomed flask. The resulting solution was cooled in an ice bath. Bromine (3.85 mL, 76.2 mmol) was dissolved in ice-cold methanol (10 mL) in a conical flask. The bromine solution was added to the pyridine solution dropwise over 10 min. The resulting *N*-bromopyridinium solution was transferred to a dropping funnel. Methyl 4-aminobenzoate (**201ad**; 5.06 g, 33.5 mmol) and methanol (50 mL) were placed in a 2-necked round-bottomed flask, that was then fitted with the dropping funnel and a reflux condenser. The *N*-bromopyridinium solution was added dropwise over 15 min. The resulting mixture was

refluxed for 4 h, allowed to cool to rt, neutralized according to Method I, and then concentrated on a rotary evaporator. The resulting brown residue was recrystallized from EtOAc, giving white needles (18.1 g, 58.7 mmol, 93%). M.p. 133–135 ºC (lit. 131–132.5 ºC, partially ^{3}H-labeled) [207]; R_f = 0.53 (1:3 EtOAc:hexane on SiO_2); ^{1}H NMR (VI300, 300 MHz, $CDCl_3$) δ 8.063 (s, 2H), 4.996 (s, 2H), 3.866 (s, 3H); ^{13}C NMR (VI300, 75 MHz, $CDCl_3$) δ 165.1 (1C), 145.9 (1C), 133.5 (2C), 121.0 (1C), 107.5 (2C), 52.3 (1C); IR (NaCl) 3321 (m), 3076 (w), 2958 (w), 1723 (s), 1713 (s), 1610 (s). 1432 (m), 1303 (s), 1268 (s), 975 (m), 855 (m), 761 (s); HRMS-ESI $[M+Na]^+$ calcd for $C_8H_7{}^{79}Br{}^{81}BrNO_2$ 331.8715, found 331.8709. Anal. (MHW) Calcd for $C_8H_7Br_2NO_2$ C 31.10, H 2.28, Br 51.73, N 4.53; Found C 31.35, H 2.32, Br 51.64, N 4.37.

4-Amino-3-bromobenzoic Acid (201ce), **4-Amino-3,5-dibromobenzoic Acid (201cc)**, and **2,4,6-Tribromoaniline (201ca)** were obtained as a mixture when brominating PABA in an alkaline suspension. For the preparation of **201ca** by bromination of aniline, or the preparation of **201cc** by bromination of PABA in an acidic suspension, refer to the earlier entries in this section. For the preparation of **201cc** by hydrolysis of **201cd**, refer to the entry on p 222.

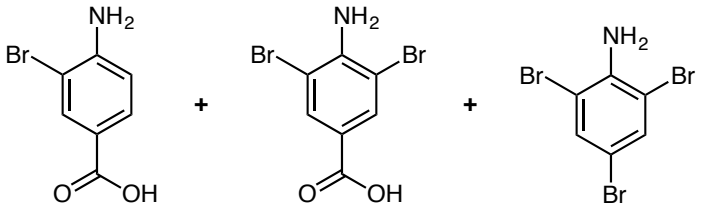

201ce **201cc** **201ca**

PABA (3.00 g, 21.9 mmol), methanol (40 mL), and water (75 mL) were placed in a round-bottomed flask. Sodium bicarbonate (6.00 g, 71.4 mmol) was added. After the release of CO_2 had subsided, a solution of bromine (2.3 mL, 45.0 mmol) in methanol (35 mL) was added dropwise. The resulting mixture was stirred for 48 h. Approximately 60% of the solvent was removed by distillation through a packed column (2 cm × 10 cm, D × H; rt to 55 ºC, 260 mmHg). The system was allowed to cool to rt, and then hydrochloric acid (1.0 M, 26.5 mL, 26.5 mmol) was added. The resulting mixture was separated by suction filtration. The filtrate was poured through the filter cake twice. The filter cake and benzene (60 mL) were placed in a round-bottomed flask. The resulting mixture was refluxed with a Dean-Stark trap until no more water droplets were observed in the reflux stream. After allowing the system to cool to rt, the benzene

was removed on a rotary evaporator, and the resulting dark purple residue was dried under vacuum (60 ºC, 20 mmHg, 24 h), giving a purple powder (5.43 g). M.p. 201–288 ºC.

Recovered PABA: (201 mg, 1.47 mmol, 6.7%; calculated by ^{1}H NMR analysis). R_f = 0.26 (1:1 EtOAc:hexane on SiO_2); ^{1}H NMR (VI300, 300 MHz, $(CD_3)_2SO$) δ 12.485 (s, 1H), 7.635–7.616 (overlapping with other components, 2H), 6.547 (d, *J* = 8.6, 2H), 5.960 (s, 2H); HRMS-ESI $[M–H]^-$ calcd for $C_7H_6NO_2$ 136.0404, found 136.0426.

4-Amino-3-bromobenzoic acid: (917 mg, 4.24 mmol, 19%; calculated by ^{1}H NMR analysis). R_f = 0.37 (1:1 EtOAc:hexane on SiO_2); ^{1}H NMR (VI300, 300 MHz, $(CD_3)_2SO$) δ 12.485 (s, 1H), 7.900–7.869 (overlapping with other components, 1H), 7.635–7.616 (overlapping with other components, 1H), 6.795 (d, *J* = 8.6, 1H), 6.043 (s, 2H); HRMS-ESI $[M–H]^-$ calcd for $C_7H_5{}^{81}BrNO_2$ 215.9489, found 215.9488.

4-Amino-3,5-dibromobenzoic acid: (2.09 g, 7.09 mmol, 32%; calculated by ^{1}H NMR analysis). R_f = 0.47 (1:1 EtOAc:hexane on SiO_2); ^{1}H NMR (VI300, 300 MHz, $(CD_3)_2SO$) δ 12.485 (s, 1H), 7.900 (s, 2H), 5.960 (s, 2H); HRMS-ESI $[M–H]^-$ calcd for $C_7H_4{}^{79}Br{}^{81}BrNO_2$ 293.8594, found 293.8570.

2,4,6-Tribromoaniline: (2.22 g, 6.73 mmol, 31%; calculated by ^{1}H NMR analysis). R_f = 0.72 (1:1 EtOAc:hexane on SiO_2); ^{1}H NMR (VI300, 300 MHz, $(CD_3)_2SO$) δ 12.485 (s, 1H), 7.616 (s, 2H), 5.495 (s, 2H); HRMS-EI $[M]^+$ calcd for $C_6H_4{}^{79}Br_2{}^{81}BrN$ 328.7868, found 328.7863.

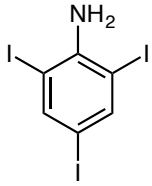

2,4,6-Triiodoaniline (201da) was prepared according to Method H. Flask (b) was charged with aniline (1.00 mL, 11.0 mmol), water (800 mL), and hydrochloric acid (12 M, 50 mL, 600 mmol). Flask (a) was then charged with iodine monochloride (8.16 g, 50.3 mmol), and then heated to 40 ºC during the halogenation process. After 4 d of N_2 flow, the reaction mixture was neutralized according to Method I.

Filtration: Additional DCM was added to the resulting mixture (up to 50 mL) such that nearly all solids dissolved. The resulting mixture was filtered through silica gel (3 cm × 4 cm, H × D). The filter was washed with DCM until the filtrate no longer contained the desired product, as indicated by TLC.

The filtrate was then placed in a loosely-covered beaker. Most of the DCM was allowed to evaporate during several days. The resulting mixture was separated by suction filtration. The

filter cake was dried under vacuum (110 ºC, 0.1 mmHg, 4 h), giving beige needles (4.48 g, 9.52 mmol, 89%). M.p. 186–187 ºC (lit. 185–187 ºC) [208]; R_f = 0.64 (1:4 EtOAc:hexane on Al_2O_3); ^{1}H NMR (VI300, 300 MHz, $CDCl_3$) δ 7.864 (s, 2H), 4.658 (s, 2H); ^{13}C NMR (VI300, 75 MHz, $(CD_3)_2SO$) δ 147.0 (1C), 145.4 (2C), 83.0 (2C), 78.8 (1C); IR (KBr) 3417 (s), 3056 (w), 2987 (w), 1632 (m), 1422 (w), 1265 (m). 741 (s), 704 (m); HRMS-EI $[M]^+$ calcd for $C_6H_4I_3N$ 470.7472, found 470.7470.

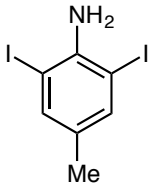

2,6-Diiodo-4-methylaniline (201db) was prepared according to Method H. Flask (b) was charged with 4-methylaniline (1.99 g, 18.6 mmol), water (900 mL), and hydrochloric acid (12 M, 50 mL, 600 mmol). Flask (a) was then charged with iodine monochloride (8.5 g, 44.8 mmol), and then heated to 40 ºC during the halogenation process. After 2 d of N_2 flow, the reaction mixture was neutralized according to Method I, and then filtered according to the preceding entry. The filtrate was concentrated on a rotary evaporator. The resulting brown residue was recrystallized from toluene, giving beige needles (6.33 g, 17.6 mmol, 95%). M.p. 122–125 ºC (lit. 123.5–125 ºC) [139]; R_f = 0.64 (1:3 EtOAc:hexane on SiO_2); ^{1}H NMR (AV500, 500 MHz, CD_2Cl_2) δ 7.481 (s, 2H), 4.465 (s, 2H), 2.158 (s, 3H); ^{13}C NMR (AV500, 126 MHz, CD_2Cl_2) δ 144.5 (1C), 140.3 (2C), 131.5 (1C), 81.6 (2C), 19.5 (1C); IR (NaCl) 3439 (s), 3054 (m), 2987 (m), 1613 (m), 1464 (w), 1265 (s), 896 (w), 749 (s), 705 (m); HRMS-ESI $[M+H]^+$ calcd for $C_7H_7I_2N$ 359.8741, found 359.8726.

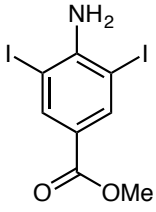

Methyl 4-Amino-3,5-diiodobenzoate (201dd). Methyl 4-aminobenzoate (**201ad**; 3.00 g, 19.8 mmol), water (300 mL), and hydrochloric acid (7.5 M, 50 mL) were placed in a round-bottomed flask. Water (100 mL) and ICl (7.63 g, 47.6 mmol) were placed in a conical flask. The iodine monochloride was crushed into small pieces with a glass rod. The resulting suspension was transferred into the hydrochloric acid mixture with water (100 mL). The resulting mixture was stirred for 24 h, and then neutralized according to Method I. The resulting mixture was concentrated on a rotary evaporator, and then separated by column chromatography. The desired fraction (R_f = 0.27 in 1:10 EtOAc:hexane on SiO_2) was concentrated on a rotary evaporator, and then recrystallized from toluene, giving a pale yellow powder (3.15 g, 7.83 mmol, 39%). M.p. 168–169 ºC (lit. 163–164 ºC) [137]; ^{1}H NMR (AM400, 400 MHz, $CDCl_3$) δ 8.300 (s, 2H), 5.056 (s, 2H), 3.857 (s, 3H); ^{13}C NMR (AM400, 101 MHz, $CDCl_3$) δ 164.5 (1C), 149.8 (1C), 141.1 (2C), 122.6 (1C),

79.5 (2C), 52.2 (1C); IR (KBr) 3408 (w), 3309 (m), 3062 (w), 2951 (w), 1717 (s), 1611 (s), 1430 (m), 1258 (s), 973 (m), 761 (s), 705 (m), 664 (w); HRMS-ES $[M]^+$ calcd for $C_8H_7I_2NO_2$ 402.8561, found 402.8566.

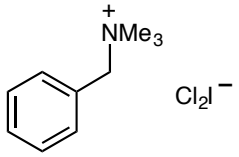

***N*-Benzyltrimethylammonium Dichloroiodate(I) (202)**. Based on the work of Kajigaeshi, *et al*. [139]: iodine monochloride (16.53 g, 101.8 mmol) was dissolved in DCM (200 mL) in a 500 mL round-bottomed flask. A solution of benzyltrimethylammonium chloride (18.76 g, 101.0 mmol) in water (100 mL) was prepared in a beaker, and then added portion-wise over 10 min to the reaction vessel. The resulting mixture was stirred at rt for 1 h. A yellow precipitate was collected by suction filtration. The organic portion of the filtrate was concentrated using a rotary evaporator, giving brown solids. The combined solids were recrystallized from 3:1 DCM:ether, and then dried under vacuum (120 mmHg, rt, 4 h), giving yellow needles (29.0 g, 83.4 mmol, 82%): Mp 124–126 ºC (lit. 125 ºC) [139]; ^{1}H NMR (HD500, 500 MHz, CD_2Cl_2) δ 7.553 (m, 5H), 4.568 (s, 2H), 3.196 (s, 9H); ^{13}C NMR (HD500, 126 MHz, $(CD_3)_2SO$) δ 132.7 (2C), 130.3 (1C), 128.9 (2C), 128.2 (1C), 67.9 (t, $^1J_{CN}$ = 2.6, 1C), 51.8 (t, $^1J_{CN}$ = 4.0, 3C); IR (KBr) 3021 (m), 2981 (w), 2958 (w), 1472 (s), 1456 (s), 1406 (m), 971 (m), 915 (m), 776 (s), 723 (s), 701 (s); HRMS-ESI $[M]^+$ calcd for $C_{10}H_{16}N$ 150.1277, found 150.1288; $[M]^-$ calcd for $^{35}Cl_2I$ 196.8427, found 196.8428.

3.4.2. Sandmeyer Cyanations

Method J: Diazotization of Anilines in Acetic Acid Suspensions

Based on the work of Toya, *et al*. [120]: the amounts of reagents and solvents are indicated in each entry. Substrate was pulverized in a mortar, and then transferred to a round-bottomed flask with AcOH. The reaction vessel was placed in an ice bath [209]. Sulfuric acid (98 mass%) was added dropwise. In a separate vessel, sodium nitrite was dissolved in water. After the reaction vessel had been in the ice bath for 5 min, the nitrite solution was added to the acetic acid suspension, dropwise, during 30 min. The resulting mixture was then stirred as indicated, and was ready to be used for the next step when as much starting material as possible had been converted into the diazonium salt (R_f = 0.00–0.05 in EtOAc on Al_2O_3), while minimizing the accumulation of other products.

Method K: Cyanation of Diazonium Salts with SBDC

SBDC suspension: Based on the work of Toya, *et al*. [120]: the indicated amounts of sodium cyanide, copper(I) cyanide, and water were placed in a properly-sized conical flask [210]. After the cyanide salts had completely dissolved, sodium bicarbonate was added. The resulting suspension was cooled in an ice bath, with vigorous stirring, for 2–4 h prior to use.

Cyanation: When the diazotization mixture was ready, as indicated by TLC, it was added dropwise to the center of the SBDC suspension, in 500 μL aliquots. The addition of each aliquot resulted in a dark orange or brown streak, followed the the formation of foam. Each subsequent aliquot was not added until the dark color had vanished, and the volume of the foam had begun to decrease. If necessary, after each 3–5 aliquots, a small amount of cold water (1–5 mL) was rinsed along the wall of the cyanation vessel to control the foam and to assist with mixing. After the addition of diazotization material was complete, the resulting suspension was removed from the ice bath. If poor mixing was observed, EtOAc or DCM (2 mL) was added [211]. The resulting mixture was stirred for 18 h.

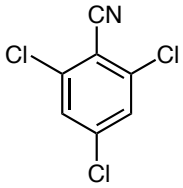

2,4,6-Trichlorobenzonitrile (204ba). Trichloroaniline (**201ba**; 2.10 g, 10.7 mmol) was diazotized according to Method J, with AcOH (11.6 mL, 203 mmol), H_2SO_4 (2.7 mL, 50.7 mmol), $NaNO_2$ (1.41 g, 20.4 mmol), and water (5 mL); stirred at rt for 3 h. The resulting mixture was processed according to Method K, with NaCN (2.99 g, 61.0 mmol), CuCN (1.82 g, 20.3 mmol), water (150 mL), and $NaHCO_3$ (29.1 g, 346 mmol). The resulting mixture was extracted with DCM (4 × 40 mL). The organic portion was washed with water (50 mL), brine (50 mL), dried with Na_2SO_4, filtered, and then concentrated on a rotary evaporator. The resulting brown residue was separated by column chromatography. The desired fraction (R_f = 0.58 in 1:3 EtOAc:hexane on SiO_2) was concentrated on a rotary evaporator, giving a beige powder (1.95 g, 9.44 mmol, 93%). M.p. 74–75 ºC (lit. 80–81 ºC) [94]; ^{1}H NMR (AM400, 400 MHz, CD_2Cl_2) δ 7.492 (s, 2H); ^{13}C NMR (HD500, 126 MHz, $CDCl_3$) δ 140.1 (1C), 139.2 (2C), 128.7 (2C), 113.2 (1C), 112.9 (1C); IR (KBr) 3079 (s), 2236 (s), 1561 (s), 1543 (s), 1377 (m), 1076 (m), 862 (s), 826 (m), 655 (m); HRMS-ESI $[M+Na]^+$ calcd for $C_7H_2{}^{35}Cl_2{}^{37}ClN$ 229.9116, found 229.9108.

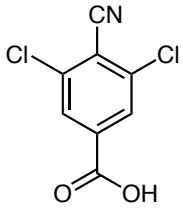

3,5-Dichloro-4-cyanobenzoic Acid (204bc) was prepared by selective hydrolysis of **204bd**; refer to the entry on p 223.

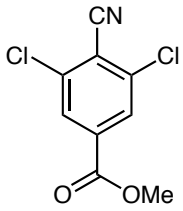

Methyl 3,5-Dichloro-4-cyanobenzoate (204bd). Dichloro ester **201bd** (515 mg, 2.34 mmol) was diazotized according to Method J, with AcOH (2.6 mL, 45.5 mmol), H_2SO_4 (650 μL, 12.2 mmol), $NaNO_2$ (314 mg, 4.55 mmol), and water (2 mL); stirred at rt for 1 h. The resulting mixture was processed according to Method K, with NaCN (668 mg, 13.6 mmol), CuCN (407 mg, 4.54 mmol), water (50 mL), and $NaHCO_3$ (6.49 g, 77.3 mmol). The resulting mixture was extracted with DCM (3 × 25 mL). The organic portion was washed with water (25 mL), brine (25 mL), dried with Na_2SO_4, filtered, and then concentrated on a rotary evaporator. The resulting brown residue was separated by column chromatography. The desired fraction (R_f = 0.29 in 1:4 EtOAc:hexane on SiO_2) was concentrated on a rotary evaporator, giving a beige powder (301 mg, 1.31 mmol, 56%). M.p. 104–105 ºC (lit. not given) [212]; ^{1}H NMR (AV500, 500 MHz, $CDCl_3$) δ

8.074 (s, 2H), 3.950 (s, 3H); ^{13}C NMR (AV500, 126 MHz, $CDCl_3$) δ 163.6 (1C), 139.0 (2C), 135.5 (1C), 129.0 (2C), 118.1 (1C), 113.0 (1C), 53.5 (1C); IR (KBr) 3076 (s), 2967 (w), 2238 (w), 1725 (s), 1548 (m), 1385 (s), 1299 (s), 970 (m), 821 (s), 767 (s); HRMS-EI $[M]^+$ calcd for $C_9H_5{}^{35}Cl_2NO_2$ 228.9692, found 228.9703.

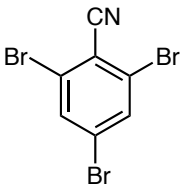

2,4,6-Tribromobenzonitrile (204ca). Tribromoaniline (**201ca**; 1.25 g, 3.79 mmol) was diazotized according to Method J, with AcOH (4.4 mL, 77.0 mmol), H_2SO_4 (1.0 mL, 18.8 mmol), $NaNO_2$ (520 mg, 7.54 mmol), and water (7 mL); stirred at 40 ºC for 1 h. The resulting mixture was processed according to Method K, with NaCN (1.12 g, 22.9 mmol), CuCN (680 mg, 7.59 mmol), water (20 mL), and $NaHCO_3$ (10.9 g, 130 mmol); EtOAc (10 mL) was added to the SBDC suspension before the diazonium suspension was added. The organic phase was set aside. The aqueous phase was extracted with EtOAc (3 × 10 mL). The combined organic portions were washed with brine (10 ml), dried with Na_2SO_4, and then concentrated on a rotary evaporator. The resulting brown powder was separated by column chromatography. The desired fraction (R_f = 0.61 in 1:8 EtOAc:hexane on SiO_2) was concentrated on a rotary evaporator, giving beige needles (760 mg, 2.24 mmol, 59%). M.p. 127–128 ºC (lit. 129 ºC) [114]; ^{1}H NMR (VI500, 500 MHz, CD_2Cl_2) δ 7.853 (s, 2H); ^{13}C NMR (VI500, 126 MHz, CD_2Cl_2) δ 135.3 (2C), 128.6 (1C), 127.4 (2C), 118.3 (1C), 116.0 (1C); IR (KBr) 3095 (w), 3068 (w), 2921 (w), 2853 (w), 2233 (m), 1563 (s), 1527 (s), 1370 (s), 854 (s), 810 (s), 747 (s); HRMS-EI $[M]^+$ calcd for $C_7H_2{}^{79}Br_2{}^{81}BrN$ 338.7711, found 338.7703. X-ray crystallographic data were obtained [79b].

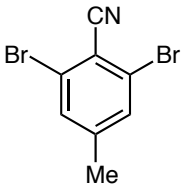

2,6-Dibromo-4-methylbenzonitrile (204cb). 2,6-Dibromo-4-methylaniline (**201cb**; 980 mg, 3.70 mmol) was diazotized according to Method J, with AcOH (4.3 mL, 75.2 mmol), H_2SO_4 (1.0 mL, 18.8 mmol), $NaNO_2$ (523 mg, 7.58 mmol), and water (2 mL); stirred at rt for 2 h. The resulting mixture was processed according to Method K, with NaCN (1.11 g, 22.6 mmol), CuCN (673 mg, 7.51 mmol), water (50 mL), and $NaHCO_3$ (10.8 g, 129 mmol). The resulting mixture was extracted with DCM (3 × 20 mL). The organic portion was washed with water (20 mL), brine (20 mL), dried with Na_2SO_4, filtered, and then concentrated on a rotary evaporator. The resulting brown residue was separated by column chromatography. The desired fraction (R_f = 0.49 in 1:2 EtOAc:hexane on SiO_2) was concentrated on a rotary evaporator, giving a tan powder

(898 mg, 3.27 mmol, 88%). M.p. 161–162 ºC (lit. 156–158 ºC [102a]; 155–157 ºC [102b]); ^{1}H NMR (HD500, 500 MHz, CD_2Cl_2) δ 7.490 (s, 2H), 2.380 (s, 3H); ^{13}C NMR (HD500, 126 MHz, CD_2Cl_2) δ 147.1 (1C), 133.2 (2C), 126.6 (2C), 116.6 (1C), 116.1 (1C), 21.7 (1C); IR (KBr) 3062 (w), 2231 (m), 1582 (s), 1451 (m), 1197 (m), 857 (s), 747 (s); HRMS-EI $[M]^+$ calcd for $C_8H_5{}^{79}Br^{81}BrN$ 274.8763, found 274.8766. X-ray crystallographic data were obtained.

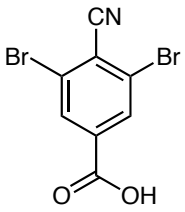

3,5-Dibromo-4-cyanobenzoic Acid (204cc) was prepared by selective hydrolysis of **204cd**; refer to the entry on p 223.

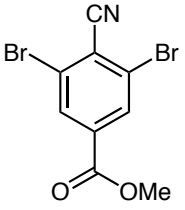

Methyl 3,5-Dibromo-4-cyanobenzoate (204cd). Dibromo ester **201cd** (720 mg, 2.33 mmol) was diazotized according to Method J, with AcOH (2.6 mL, 45.5 mmol), H_2SO_4 (600 μL, 11.3 mmol), $NaNO_2$ (313 mg, 4.54 mmol), and water (1.5 mL); stirred at rt for 3 h. The resulting mixture was processed according to Method K, with NaCN (680 mg, 13.9 mmol), CuCN (482 mg, 5.38 mmol), water (40 mL), and $NaHCO_3$ (6.47 g, 77 mmol). The resulting mixture was extracted with DCM (3 × 20 mL). The organic portion was washed with water (20 mL), brine (20 mL), dried with Na_2SO_4, filtered, and then concentrated on a rotary evaporator. The resulting brown residue was separated by column chromatography. The desired fraction (R_f = 0.34 in 1:3 EtOAc:hexane on SiO_2) was concentrated on a rotary evaporator, giving a tan powder (681 mg, 2.13 mmol, 92%). M.p. 137–138 ºC; ^{1}H NMR (AV500, 500 MHz, $CDCl_3$) δ 8.264 (s, 2H), 3.974 (s, 3H); ^{13}C NMR (AV500, 126 MHz, $CDCl_3$) δ 163.4 (1C), 135.5 (1C), 132.6 (2C), 127.1 (2C), 122.5 (1C), 115.5 (1C), 53.5 (1C); IR (KBr) 3076 (m), 2955 (w), 2229 (w), 1732 (s), 1429 (m), 1263 (s), 1124 (s), 971 (m), 748 (s); HRMS-ESI $[M+Na]^+$ calcd for $C_9H_5{}^{79}Br^{81}BrNO_2$ 341.8559, found 341.8547. X-ray crystallographic data were obtained.

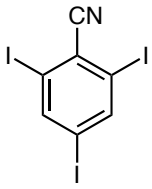

2,4,6-Triiodobenzonitrile (204da). Triiodoaniline (**201da**; 101 mg, 215 μmol), EtOAc (20 mL), and TsOH•H_2O (77 mg, 405 μmol) were placed in a round-bottomed flask [209b]. The resulting mixture was stirred for 15 min, and then 3-methylbutyl nitrite (60 μL, 446 μmol) was added dropwise. The resulting mixture was stirred for 1 h, and then processed according to Method K, with NaCN (60 mg, 1.22 mmol), CuCN (44 mg, 491 μmol), water (10 mL), and $NaHCO_3$ (155 mg, 1.85 mmol). The organic phase was set aside. The aqueous phase was extracted with EtOAc (3 × 10 mL). The combined organic portions were washed with brine (10 ml), dried with Na_2SO_4, and then concentrated on a rotary evaporator. The resulting brown powder was separated by column chromatography. The desired fraction (R_f = 0.44 in 1:4 EtOAc:hexane on SiO_2) was concentrated on a rotary evaporator, giving a beige powder (67 mg, 140 μmol, 65%). M.p. 244–245 ºC; ^{1}H NMR (HD500, 500 MHz, $(CD_3)_2SO$) δ 8.431 (s, 2H); ^{13}C NMR (HD500, 126 MHz, CD_2Cl_2) δ 147.5 (2C), 127.3 (1C), 120.7 (1C), 101.1 (1C), 99.6 (2C); IR (NaCl) 3070 (m), 2227 (m), 1532 (s), 1359 (m), 1206 (m), 1081 (m), 861 (m), 787 (w), 706 (w); HRMS-ESI $[M+Na]^+$ calcd for $C_7H_2I_3N$ 503.7213, found 503.7216. X-ray crystallographic data were obtained.

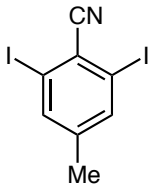

2,6-Diiodo-4-methylbenzonitrile (204db). 2,6-Diiodo-4-methylaniline (**201db**; 502 mg, 1.40 mmol), EtOAc (50 mL), and TsOH•H_2O (538 mg, 2.83 mmol) were placed in a round-bottomed flask [209b]. The resulting mixture was stirred for 15 min, cooled in an ice bath, and then 3-methylbutyl nitrite (370 μL, 2.75 mmol) was added dropwise. The resulting mixture was stirred for 1 h in an ice bath, and then the ice bath was removed. After stirring for 1 h at rt, the resulting mixture was processed according to Method K, with NaCN (412 mg, 8.41 mmol), CuCN (252 mg, 2.81 mmol), water (25 mL), and $NaHCO_3$ (950 mg, 11.3 mmol). The organic phase was set aside. The aqueous phase was extracted with EtOAc (3 × 20 mL). The combined organic portions were washed with brine (20 ml), dried with Na_2SO_4, and then concentrated on a rotary evaporator. The resulting brown residue was separated by column chromatography. The desired fraction (R_f = 0.41 in 1:4 EtOAc:hexane on SiO_2) was concentrated on a rotary evaporator, giving a tan powder (429 mg, 1.16 mmol, 83%). M.p. 188–189 ºC; ^{1}H NMR (HD500, 500 MHz, $CDCl_3$) δ 7.715 (s, 2H), 2.319 (s, 3H); ^{13}C NMR (HD500, 126 MHz, $CDCl_3$) δ 146.0 (1C), 139.8 (2C), 124.4 (1C), 120.7 (1C), 98.9 (2C), 21.0 (1C); IR (KBr) 3154 (w), 2984 (w), 2253 (w), 1580 (m), 1381 (m), 913 (s), 743

(s), 651 (s); HRMS-EI $[M]^+$ calcd for $C_8H_5I_2N$ 386.8506, found 386.8522. X-ray crystallographic data were obtained.

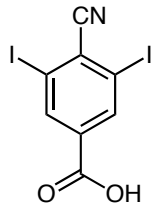

3,5-Diiodo-4-cyanobenzoic Acid (204dc) was prepared by selective hydrolysis of **204dd**; refer to the entry on p 224.

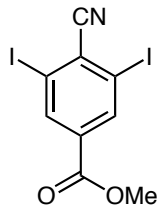

Methyl 4-Cyano-3,5-diiodobenzoate (204dd). Diiodo ester **201dd** (2.62 g, 6.50 mmol) was diazotized according to Method J, with AcOH (7.4 mL, 129 mmol), H_2SO_4 (1.7 mL, 31.9 mmol), $NaNO_2$ (898 mg, 13.0 mmol), and water (5 mL); stirred at 40 ºC for 2 h. The resulting mixture was processed according to Method K, with NaCN (1.91 g, 39.0 mmol), CuCN (1.17 g, 13.1 mmol), water (150 mL), and $NaHCO_3$ (18.6 g, 221 mmol). The resulting mixture was extracted with EtOAc (4 × 50 mL). The organic portion was washed with water (50 mL), brine (50 mL), dried with Na_2SO_4, filtered, and then concentrated on a rotary evaporator. The resulting brown residue was separated by column chromatography. The desired fraction (R_f = 0.40 in 1:3 EtOAc:hexane on SiO_2) was concentrated on a rotary evaporator, giving a beige powder (2.38 g, 5.77 mmol, 88%). M.p. 182–183 ºC; ^{1}H NMR (AV500, 500 MHz, CD_2Cl_2) δ 8.521 (s, 2H), 3.930 (s, 3H); ^{13}C NMR (AV500, 126 MHz, CD_2Cl_2) δ 163.5 (1C), 140.1 (2C), 135.5 (1C), 131.4 (1C), 120.6 (1C), 99.2 (2C), 53.6 (1C); IR (KBr) 3070 (m), 2956 (w), 2226 (w), 1730 (s), 1524 (m), 1277 (s), 960 (m), 765 (w); HRMS-EI $[M]^+$ calcd for $C_9H_5I_2NO_2$ 412.8404, found 412.8417. Anal. (AML) Calcd for $C_9H_5I_2NO_2$ C 26.18, H 1.22, I 61.46, N 3.39; Found C 26.43, H 1.24, I 61.66, N 3.38.

1,3,5-Tribromobenzene (205a), **1,2,3,5-Tetrabromobenzene (205b)**, and **2,2',4,4',6,6'-Hexabromobiphenyl (205c)** were obtained as a mixture, as a chromatographic fraction (R_f = 0.69 in 1:8 EtOAc:hexane on SiO_2) from the synthesis of tribromo nitrile **204ca**, as a white powder (82 mg). M.p. 96–121 ºC.

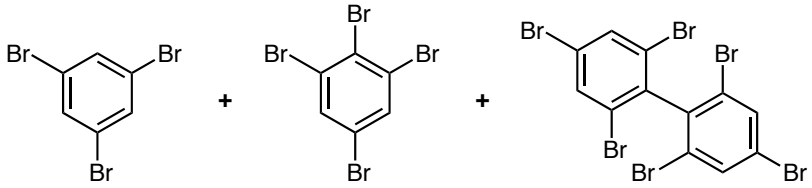

205a **205b** **205c**

1,3,5-Tribromobenzene: (54 mg, 172 μmol, 4.5%; calculated by ^{1}H NMR analysis). ^{1}H NMR (VI300, 300 MHz, CD_2Cl_2) δ 7.654 (s, 3H); HRMS-EI $[M]^+$ calcd for $C_6H_3{}^{79}Br^{81}Br_2$ 315.7738, found 315.7745, with the isotope and fragmentation patterns expected for a tribromo compound [213].

1,2,3,5-Tetrabromobenzene: (14 mg, 36 μmol, 1.0%; calculated by ^{1}H NMR analysis). ^{1}H NMR (VI300, 300 MHz, CD_2Cl_2) δ 7.771 (s, 2H); HRMS-EI $[M]^+$ calcd for $C_6H_3{}^{79}Br_4$ 389.6885, found 389.6895, with the isotope and fragmentation patterns expected for a tetrabromo compound [213].

2,4,6,2',4',6'-Hexabromobiphenyl: (5 mg, 8 μmol, 0.4%; calculated by ^{1}H NMR analysis). ^{1}H NMR (VI300, 300 MHz, CD_2Cl_2) δ 7.873 (s, 4H); HRMS-EI $[M]^+$ calcd for $C_{12}H_4{}^{79}Br_4{}^{81}Br_2$ 625.5367, found 625.5377, with the isotope and fragmentation patterns expected for a hexabromo compound [213].

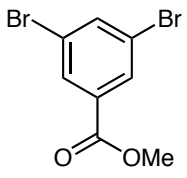

Methyl 3,5-Dibromobenzoate (206) was obtained as a chromatographic fraction from the synthesis of dibromo cyano ester **204cd** (R_f = 0.54 in 1:4 EtOAc:hexane on SiO_2), in yields ranging from trace to 40%, depending on conditions.

Preferred preparation: Based on the work of Robison & Robison [119]: sodium nitrite (1.24 g, 17.8 mmol), water (8 mL), and AcOH (6.2 mL) were placed in a round-bottomed flask. The resulting mixture was cooled in an ice bath. Sulfuric acid (3.4 mL), and then H_3PO_2 (50 mass%, aq., 6.5 mL, 62.6 mmol) were added dropwise. Dibromo ester **201cd** (2.08 g, 6.73 mmol) was pulverized in a mortar, and then transferred to a beaker with AcOH (12 mL). The

resulting suspension was added to the H_3PO_2 solution dropwise over 1 h. The resulting suspension was stirred for 1 h in an ice bath, and then the ice bath was removed. The reaction mixture was stirred at rt for 4 h. Water (50 mL) was added. The resulting mixture was cooled in an ice bath for 2 h, and then separated by suction filtration. The filter cake and $NaHCO_3$ solution (aq., 50% sat., 50 mL) were placed in a beaker and then stirred at rt for 30 min. The resulting mixture was separated by suction filtration. The filter cake was washed with water (2 × 10 mL), and then recrystallized from DCM-hexane [214], giving a white powder (380 mg, 1.29 mmol, 67%). M.p. 66–67 ºC (lit. 62–63 ºC) [215]; ^{1}H NMR (HD500, 500 MHz, CD_2Cl_2) δ 8.105 (s, 2H), 7.874 (s, 1H), 3.905 (s, 3H); ^{13}C NMR (HD500, 126 MHz, CD_2Cl_2) δ 164.9 (1C), 138.7 (1C), 134.0 (1C), 131.8 (2C), 123.4 (2C), 53.2 (1C); IR (NaCl) 3070 (m), 2951 (w), 2849 (w), 1730 (s), 1559 (s), 1440 (m), 1276 (s), 972 (m), 763 (s), 739 (s), 723 (m), 658 (w); HRMS-EI [M]$^+$ calcd for $C_8H_6{}^{79}Br^{81}BrO_2$ 293.8709, found 293.8698.

3.4.3. Hydrolyses of Esters

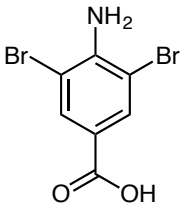

3,5-Dibromo-4-aminobenzoic Acid (201cc) was observed in 3 different experiments. For the preparation of **201cc** by bromination of PABA in an acidic suspension, refer to the entry on p210. For the preparation of **201cc**, as a mixture component, by bromination of PABA in an alkaline suspension, refer to the entry for **201ce** on p 211.

*Hydrolysis of methyl ester **201cd**:* Dibromo ester (**201cd**; 2.13 g, 6.89 mmol), 2-propanol (15 mL), and water (15 mL) were placed in a round-bottomed flask. Sodium hydroxide (97 mass%, 343 mg, 8.32 mmol) was added. The resulting mixture was refluxed for 1 h, and then was allowed to cool to rt. Hydrochloric acid (6 M) was added dropwise until the mixture had a pH of 4. The reaction mixture was allowed to stand for 1 h, and then it was separated by suction filtration. The filter cake was washed with water (2 × 5 mL), and then was dried under vacuum (97 ºC, 0.1 mmHg, 12 h), giving a white powder (1.96 g, 6.65 mmol, 88%). M.p. 286–293 ºC; R_f = 0.47 (1:1 EtOAc:hexane on SiO_2); ^{1}H NMR (AV500, 500 MHz, $(CD_3)_2SO$) δ 12.791 (s, 1H), 7.896 (s, 2H), 6.091 (s, 2H); ^{13}C NMR (VI300, 75 MHz, $(CD_3)_2SO$) δ 165.2 (1C), 146.7 (1C), 133.1 (2C), 120.0 (1C), 106.3 (2C); IR (KBr) 3486 (m), 3380 (m), 2922 (m), 2850 (w), 1684 (m), 1606 (m), 1253 (s), 1106 (m), 899 (m), 764 (m), 729 (m), 672 (m); HRMS-ESI [M–H]$^-$ calcd for $C_7H_5{}^{79}Br^{81}BrNO_2$ 293.8594, found 293.8600.

Method L: De-Esterification of Methyl Esters with Lithium Iodide

Adapted from the work of Lepage, *et al*. [146]: pyridine (10 mL) and the indicated amounts of ester and lithium iodide were placed in a round-bottomed flask. The resulting mixture was refluxed for 24 h, and then allowed to cool to rt. Chloroform (25 mL), water (25 mL), and hydrochloric acid (12 M, 25 mL, 300 mmol) were added. The resulting mixture was stirred for 15 min, and then separated by suction filtration.

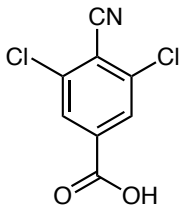

3,5-Dichloro-4-cyanobenzoic Acid (204bc) was prepared according to Method L, with dichloro cyano ester **204bd** (270 mg, 1.17 mmol) and lithium iodide (157 mg, 1.17 mmol). The resulting tan powder was recrystallized from chloroform, giving a beige powder (236 mg, 1.09 mmol, 93%). M.p. 181–183 ºC (lit. not given) [144a]; R_f = 0.44 (EtOAc on SiO_2); ^{1}H NMR (AV500, 500 MHz, $CDCl_3$) δ 9.672 (s, 1H), 8.135 (s, 2H); ^{13}C NMR (AM400, 101 MHz, $CDCl_3$) δ 168.1 (1C), 139.2 (2C), 134.3 (1C), 129.5 (2C), 119.0 (1C), 112.8 (1C); IR (KBr) 3080 (s), 2661 (m), 2536 (m), 2236 (m), 1731 (s), 1711 (s), 1459 (m), 1384 (s), 1285 (s), 908 (m), 740 (w), 629 (m); HRMS-ESI $[M–H]^-$ calcd for $C_8H_3{}^{35}Cl_2NO_2$ 213.9468, found 213.9464.

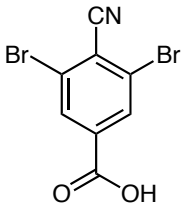

3,5-Dibromo-4-cyanobenzoic Acid (204cc) was prepared according to Method L, with dibromo cyano ester **204cd** (231 mg, 720 μmol) and lithium iodide (128 mg, 800 μmol). The resulting biphasic mixture was processed according to dichloro cyano acid **204bc**, giving a white powder (217 mg, 712 μmol, 99%). M.p. 150–152 ºC; R_f = 0.09 (1:1 EtOAc:hexane on SiO_2); ^{1}H NMR (AV500, 500 MHz, $(CD_3)_2SO$) δ 14.120 (s, 1H), 8.232 (s, 2H); ^{13}C NMR (AV500, 126 MHz, $(CD_3)_2SO$) δ 163.9 (1C), 137.0 (1C), 132.1 (2C), 126.7 (2C), 120.6 (1C), 115.9 (1C); IR (KBr) 3421 (s), 3077 (m), 2128 (w), 1811 (w), 1662 (m), 1537 (s), 1371 (s), 1296 (s), 1025 (s), 825 (m), 770 (s), 748 (m); HRMS-ESI $[M–H]^-$ calcd for $C_8H_3{}^{79}Br^{81}BrNO_2$ 303.8437, found 303.8443. X-ray crystallographic data of the hemianthracenate were obtained.

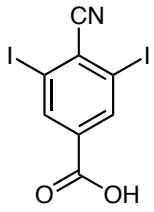

4-Cyano-3,5-diiodobenzoic Acid (204dc) was prepared based on Method L, with diiodo cyano ester **204dd** (1.83 g, 4.43 mmol), lithium iodide (600 mg, 4.48 mmol), and pyridine (50 mL). Increased amounts of chloroform (200 mL) and water (100 mL) were used. A Soxhlet extraction (chloroform, 150 mL, 18 h) was performed on the resulting brown residue. The extract was concentrated on a rotary evaporator, and then triturated with DCM, giving a tan powder (1.62 g), which was primarily composed of the title compound (73 mass%: 1.19 g, 2.97 mmol, 67%; estimated by ^{1}H NMR analysis). The major impurities were DCM (approx. 98 mg), and unidentified components with multiple aromatic ^{1}H NMR signals (approx. 335 mg) [216]. M.p. 204–215 ºC dec.; R_f = 0.16 (1:1 EtOAc:hexane on SiO_2); ^{1}H NMR (AV500, 500 MHz, $(CD_3)_2SO$) δ 13.924 (s, 1H), 8.380 (s, 2H); ^{13}C NMR (AM400, 101 MHz, $(CD_3)_2SO$) δ 163.8 (1C), 138.6 (2C), 136.0 (1C), 129.1 (1C), 120.4 (1C), 101.9 (2C); IR (KBr) 3447 (m), 3071 (m), 2920 (s), 2850 (w), 2639 (m), 2529 (m), 2226 (m), 1524 (s), 1368 (s), 1280 (s), 907 (m), 767 (s), 712 (m), 610 (m); HRMS-ESI $[M–H]^-$ calcd for $C_8H_3I_2NO_2$ 397.8180, found 397.8185.

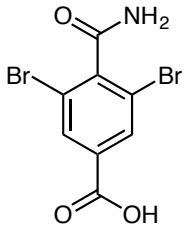

3,5-Dibromo-4-carbamoylbenzoic Acid (207). Was prepared according to the method described in this section for the preparation of amino acid **201cc**, with dibromo cyano ester **204cd** (589 mg, 1.85 mmol), 2-propanol (5 mL), water (5 mL), and NaOH (97 mass%, 186 mg, 4.50 mmol). The filter cake was triturated with ethanol, and then dried under vacuum (97 ºC, 0.05 mmHg, 12 h), giving a white powder (476 mg, 1.45 mmol, 78%). M.p. 255–256 ºC; R_f = 0.06 (1:1 EtOAc:hexane on SiO_2); ^{1}H NMR (AV500, 500 MHz, $(CD_3)_2SO$) δ 13.705 (s, 1H), 8.124 (s, 1H), 8.069 (s, 2H), 7.887 (s, 1H); ^{13}C NMR (AV500, 126 MHz, $(CD_3)_2SO$) δ 166.8 (1C), 164.5 (1C), 144.3 (1C), 133.4 (1C), 132.0 (2C), 119.7 (2C); IR (KBr) 3442 (s), 3314 (m), 3185 (m), 3088 (w), 2921 (w), 2487 (m), 1719 (s), 1648 (s), 1542 (m), 1465 (m), 1371 (s), 1270 (s), 901 (w), 769 (m), 743 (s); HRMS-ESI $[M–H]^-$ calcd for $C_8H_5{}^{79}Br^{81}BrNO_3$ 321.8543, found 321.8549. X-ray crystallographic data of the 2-propanolate were obtained.

3.4.4. *N*-Formylations of Anilines

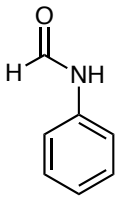

Formanilide (208aa). Based on the work of Jung, *et al*. [217]. Aniline (15.2 mL, 164 mmol) and formic acid (88 mass%, 10.6 mL, 247 mmol) were added to toluene (100 mL) in a round-bottomed flask fitted with a Dean-Stark trap. The resulting mixture was refluxed for 24 h, and then allowed to cool to rt. The toluene was removed using a rotary evaporator, giving a brown solid that was recrystallized from ether, giving white needles (15.1 g, 125 mmol, 78%). M.p. 46–49 ºC (lit. 46–48 ºC) [126]; R_f = 0.14 (1:2 EtOAc:hexane on SiO_2); ^{1}H NMR (HD500, 500 MHz, CD_2Cl_2; 2 conformers obs.) δ 8.721 (s, 1H), 8.348 (d, *J* = 2.0, 1H; major), 7.991 (s, 1H; minor), 7.570 (d, *J* = 8.2, 2H), 7.350 (m, 2H), 7.191 (t, *J* = 7.5, 1H; major), 7.138 (m, 1H; major & 2H; minor); ^{13}C NMR (HD500, 126 MHz, CD_2Cl_2; 2 conformers obs.) δ 163.3 (1C; minor), 159.9 (1C; major), 137.8 (1C; major), 137.6 (1C; minor), 130.2 (2C; minor), 129.5 (2C; major), 125.5 (1C; minor), 125.1 (1C; major), 120.4 (2C; major), 119.0 (2C; minor); IR (NaCl) 3627 (m), 3135 (m), 3056 (m), 2875 (w), 1683 (s), 1601 (s), 1546 (m), 1443 (s), 1315 (m), 752 (s), 691 (m), 656 (w); HRMS-EI $[M]^+$ calcd for C_7H_7NO 121.0522, found 121.0527.

Method M: *N*-Formylation of Anilines with Acetic Formic Anhydride

Adapted from the work of Krishnamurthy [126]. *Acetic formic anhydride solution:* The indicated amounts of acetic anhydride and solvent were placed in a flame-dried round-bottomed flask, in a dry N_2 atmosphere. The indicated amount of formic acid (88 mass%, aq.) was added dropwise. The resulting mixture was stirred at rt for 1 h.

Formylation: The indicated amount of substrate was dissolved in the indicated solvent in a round-bottomed flask. The resulting mixture was added dropwise to the acetic formic anhydride solution. The resulting mixture was stirred for 18 h at the indicated temperature.

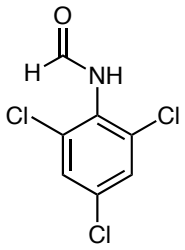

2,4,6-Trichloroformanilide (208ba) was prepared according to Method M, with acetic anhydride (8.7 mL, 92.0 mmol), DCM (25 mL), formic acid solution (4.4 mL, 101 mmol); trichloroaniline (**201ba**; 4.00 g, 20.4 mmol), and DCM (25 mL), at rt. The resulting mixture was washed with water (2 × 25 mL). The organic portion was cooled in a freezer (–5 ºC, 24 h), and then separated by suction filtration. The filter cake was recrystallized from toluene, giving white needles (3.97 g, 17.7 mmol, 87%). M.p. 165–167 ºC (lit. 180 ºC) [218]; R_f = 0.26 (1:2 EtOAc:hexane on SiO_2); ^{1}H NMR (VI500, 500 MHz, $(CD_3)_2SO$; 2 conformers obs.) δ 10.120 (s, 1H; major), 9.888 (s, 1H; minor), 8.309 (s, 1H; major), 8.133 (s, 1H; minor), 7.815 (s, 2H; minor), 7.779 (s, 2H; major); ^{13}C NMR (VI300, 75 MHz, $(CD_3)_2SO$; 2 conformers obs.) δ 159.8 (1C), 134.0 (2C), 132.6 (1C), 131.3 (1C), 128.7 (2C; minor), 128.3 (2C; major); IR (KBr) 3174 (m), 3071 (m), 2997 (w), 2894 (w), 1700 (m), 1667 (s), 1522 (m), 1278 (m), 1156 (m), 843 (s), 800 (m), 699 (m); HRMS-ESI $[M–H]^-$ calcd for $C_7H_4{}^{35}Cl_3NO$ 221.9286, found 221.9292.

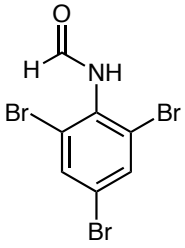

2,4,6-Tribromoformanilide (208ca) was prepared according to Method M, with acetic anhydride (3.2 mL, 33.9 mmol), THF (5 mL), formic acid solution (1.7 mL, 39.1 mmol); tribromoaniline (**201ca**; 1.82 g, 5.52 mmol), and THF (25 mL), at rt. The resulting mixture was filtered through neutral alumina (5 cm × 3 cm, H × D). The filter was washed with sufficient THF to elute all product, as indicated by TLC. The filtrate was concentrated on a rotary evaporator. The resulting residue was washed with $NaHCO_3$ solution, and then separated by suction filtration. The filter cake was recrystallized from acetone, giving white needles (1.72 g, 4.81 mmol, 87%). M.p. 220–221 ºC (lit. 222 ºC) [218]; R_f = 0.48 (1:1 EtOAc:hexane on SiO_2); ^{1}H NMR (VI300, 300 MHz, $(CD_3)_2SO$; 2 conformers obs.) δ 10.192 (s, 1H; major), 8.522 (s, 1H; minor), 8.260 (s, 1H), 8.018 (s, 2H); ^{13}C NMR (VI300, 75 MHz, $(CD_3)_2SO$; 2 conformers obs.) δ 165.9 (1C; minor), 159.8 (1C; major), 134.6 (1C), 134.4 (2C), 124.5 (2C), 121.1 (1C); IR (neat) 3201 (m), 3166 (m), 1661 (s), 1558 (m), 1441 (m), 1154 (s), 859 (s), 811 (s); HRMS-ESI $[M–H]^-$ calcd for $C_7H_4{}^{79}Br_2{}^{81}BrNO$ 355.7750, found 355.7758. Anal. (MHW) Calcd for $C_7H_4Br_3NO$ C 23.50, H 1.13, Br 66.99, N 3.91; Found C 23.42, H 1.15, Br 66.71, N 3.57.

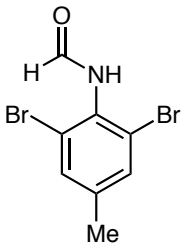

2,6-Dibromo-4-methylformanilide (208cb) was prepared according to Method M, with acetic anhydride (1.9 mL, 20.1 mmol), DCM (10 mL), formic acid solution (1.0 mL, 23.0 mmol); 2,6-dibromo-4-methylaniline (**201cb**; 997 mg, 3.76 mmol), and DCM (10 mL), at rt.

Filtration and extraction: Water (10 mL) was added, and then the resulting mixture was stirred for 30 min. The resulting mixture was separated by suction filtration, and then the filter cake and the organic portion of the filtrate were set aside. The aqueous portion was extracted with DCM (10 mL). The filter cake and the combined organic portions were concentrated on a rotary evaporator.

The resulting residue was recrystallized from toluene, giving white needles (1.00 g, 3.42 mmol, 91%). M.p. 232–233 ºC (lit. not given) [219]; R_f = 0.27 (1:2 EtOAc:hexane on SiO_2); ^{1}H NMR (AV500, 500 MHz, $(CD_3)_2SO$; 2 conformers obs.) δ 9.993 (s, 1H; major), 9.743 (d, J = 10.9, 1H; minor), 8.270 (s, 1H; major), 8.021 (d, J = 11.1, 1H; minor), 7.623 (s, 2H; minor), 7.571 (s, 2H; major), 2.303 (s, 3H); ^{13}C NMR (AV500, 126 MHz, $(CD_3)_2SO$; 2 conformers obs.) δ 164.5 (1C; minor), 159.6 (1C; major), 140.9 (1C; minor), 140.7 (1C; major), 133.0 (2C; minor), 132.6 (2C; major), 131.9 (1C; minor), 131.8 (1C; major), 123.3 (2C; minor), 123.2 (2C; major), 19.8 (1C); IR (KBr) 3247 (s), 2927 (w), 1656 (s), 1511 (s), 1152 (m), 1060 (w), 840 (m), 747 (s), 684 (m); HRMS-ESI $[M–H]^-$ calcd for $C_8H_7{}^{79}Br_2NO$ 289.8822, found 289.8814.

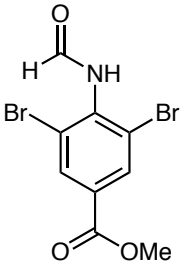

Methyl 3,5-Dibromo-4-formamidobenzoate (208cd) was prepared according to Method M, with acetic anhydride (5.1 mL, 54.0 mmol), DCE (10 mL), formic acid solution (2.7 mL, 62.1 mmol); dibromo ester **201cd** (1.24 g, 4.01 mmol), and DCE (50 mL), at rt. The resulting mixture was processed according to the filtration and extraction protocol of the preceding entry, with water and DCM (25 mL, each). The resulting residue was recrystallized from EtOAc, giving white needles (1.31 g, 3.89 mmol, 97%). M.p. 216–217 ºC; R_f = 0.19 (1:2 EtOAc:hexane on SiO_2); ^{1}H NMR (VI300, 300 MHz, $(CD_3)_2CO$) δ 9.203 (s, 1H), 8.441 (s, 1H), 8.226 (s, 2H), 3.928 (s, 3H); ^{13}C NMR (VI500, 126 MHz, $(CD_3)_2SO$) δ 163.5 (1C), 160.2 (1C), 139.5 (1C), 132.5 (2C), 130.7 (1C), 123.5 (2C), 52.9 (1C); IR (KBr) 3153 (s), 1727 (s), 1664 (s), 1524 (m), 1282 (s), 1154 (m), 966 (m), 765 (s), 749 (s); HRMS-ESI $[M+Na]^+$ calcd

for $C_9H_7{}^{79}Br^{81}BrNO_3$ 359.8664, found 359.8662. Anal. (MHW) Calcd for $C_9H_7Br_2NO_3$ C 32.08, H 2.09, Br 47.43, N 4.16; Found C 32.31, H 2.11, Br 47.17, N 4.17.

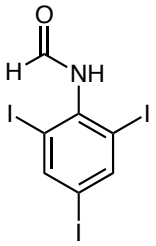

2,4,6-Triiodoformanilide (208da) was prepared according to Method M, with acetic anhydride (4.2 mL, 44.4 mmol), DCE (10 mL), formic acid solution (2.2 mL, 50.6 mmol); triiodoaniline (**201da**; 1.01 g, 2.15 mmol), and DCE (100 mL), at 40 ºC. Approximately 50% of the solvent was removed on a rotary evaporator, and then the resulting mixture was cooled in a freezer (–5 ºC, 24 h). The resulting mixture was separated by suction filtration. The filter cake was triturated with toluene, giving white needles (962 mg, 1.93 mmol, 90%). M.p. 284–285 ºC; R_f = 0.19 (1:2 EtOAc:hexane on SiO_2); ^{1}H NMR (VI300, 300 MHz, $(CD_3)_2SO$; 2 conformers obs.) δ 10.089 (s, 1H; major), 9.655 (s, 1H; minor), 8.303 (s, 1H; major), 8.278 (s, 2H; minor), 8.233 (s, 2H; major), 7.978 (s, 1H; minor); ^{13}C NMR (AV500, 126 MHz, $(CD_3)_2SO$; 2 conformers obs.) δ 164.4 (1C; minor), 159.4 (1C; major), 146.4 (2C; minor), 146.1 (2C; major), 141.0 (1C; major), 140.4 (1C; minor), 102.4 (2C; minor), 101.9 (2C; major), 95.9 (1C; minor), 95.6 (1C; major); IR (NaCl) 3221 (s), 3076 (m), 2919 (w), 1637 (s), 1490 (s), 1380 (s), 1232 (m), 1143 (s), 857 (s), 794 (s), 703 (s), 682 (m); HRMS-ESI $[M–H]^-$ calcd for $C_7H_4I_3NO$ 497.7354, found 497.7365. Anal. (AML) Calcd for $C_7H_4I_3NO$ C 16.85, H 0.81, I 76.32, N 2.81; Found C 17.08, H 0.89, I 76.42, N 2.75.

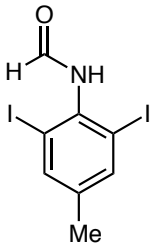

2,6-Diiodo-4-methylformanilide (208db) was prepared according to Method M, with acetic anhydride (5.6 mL, 60.8 mmol), DCE (10 mL), formic acid solution (2.85 mL, 65.6 mmol); 2,6-diiodo-4-methylaniline (**201db**; 1.00 g, 2.79 mmol), and DCE (50 mL), at 40 ºC. The resulting mixture was processed by the same method as the preceding entry, with recrystallization from toluene, giving white needles (948 mg, 2.45 mmol, 88%). M.p. 280–281 ºC; R_f = 0.27 (1:2 EtOAc:hexane on SiO_2); ^{1}H NMR (AV500, 500 MHz, $(CD_3)_2SO$; 2 conformers obs.) δ 9.983 (s, 1H; major), 9.686 (s, 1H; minor), 8.287 (s, 1H; major), 7.940 (s, 1H; minor), 7.810 (s, 2H; minor), 7.760 (s, 2H; major), 2.235 (s, 3H); ^{13}C NMR (AV500, 126 MHz, $(CD_3)_2SO$; 2 conformers obs.) δ 164.5 (1C; minor), 159.4 (1C; major), 141.4 (1C; minor), 141.0 (1C; major), 139.8 (2C; minor), 139.4 (2C; major), 138.2 (1C; major), 137.7 (1C; minor), 100.5 (2C; minor), 99.7 (2C; major), 19.2 (1C); IR (KBr) 3263 (s), 2919 (m), 1645 (s), 1502 (s), 1377 (s), 1150 (s),

1049 (m), 842 (s), 713 (s), 681 (s), 622 (m); HRMS-ESI [M–H]$^-$ calcd for $C_8H_7I_2NO$ 385.8544, found 385.8534. Anal. (AML) Calcd for $C_8H_7I_2NO$ C 24.83, H 1.82, I 65.59, N 3.62; Found C 24.98, H 1.83, I 65.45, N 3.55.

3.4.5. Isocyanide Syntheses

Method N: Dehydration of Formanilides with DIPEA and $POCl_3$

Adapted from the work of Ugi, *et al*. [124]: the indicated amounts of formanilide, DIPEA, and DCE were placed in a round-bottomed flask. The resulting mixture was refluxed for 10 min, and then was allowed to cool to rt. The indicated amount of $POCl_3$ was added dropwise, and then the reaction mixture was stirred at rt. The reaction was found to be complete by TLC analysis within 30 min after the disappearance of solid material, typically after 1–2 h. If solids remained after 2 h at rt, the reaction mixture was heated to 50 ºC, until all solids had dissolved, typically within 1 h. Once the reaction was complete and had cooled to rt, the mixture was filtered through neutral alumina (5 cm × 2 cm, H × D). The filter was washed with DCM until the filtrate no longer contained the desired product, as indicated by TLC. The filtrate was concentrated to approx. 100 mL on a rotary evaporator (if necessary), cooled in an ice bath, and then placed in a separatory funnel. The filtrate was then washed with ice-cold acetic acid solution (aq., 50 mM, 4 × 25 mL), and then ice-cold $NaHCO_3$ solution (aq., sat., 2 × 20 mL), and then ice-cold brine (25 mL). The organic portion was dried with Na_2SO_4, and then concentrated on a rotary evaporator.

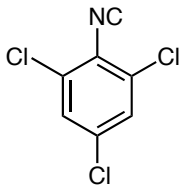

1,3,5-Trichloro-2-isocyanobenzene (209ba) was prepared according to Method N, with 2,4,6-trichloroformanilide (**208ba**, 500 mg, 2.23 mmol), DIPEA (1.35 mL, 7.66 mmol), DCE (20 mL), and $POCl_3$ (230 μL, 2.47 mmol). The resulting yellow solid (550 mg) was purified by sublimation (50 ºC, 0.05 mmHg), giving white needles (273 mg, 1.33 mmol, 60%). M.p. 49–50 ºC (lit. 52–53 ºC) [94]; R_f = 0.78 (1:4 EtOAc:hexane on SiO_2); ^{1}H NMR (AM400, 400 MHz, $(CD_3)_2SO$) δ 7.953 (s, 2H); ^{13}C NMR (AM400, 101 MHz, $(CD_3)_2SO$) δ 174.3 (1C), 135.3 (1C), 131.9 (2C), 128.8 (2C), 122.6 (1C); IR (KBr) 3071 (s), 2127 (s), 1563 (m), 1552 (m), 1377 (s), 1076 (m), 861 (s), 825 (s), 674 (s) HRMS-EI [M]$^+$ calcd for $C_7H_2{}^{35}Cl_3N$ 204.9247, found 204.9247.

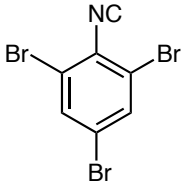

1,3,5-Tribromo-2-isocyanobenzene (209ca) was prepared according to Method N, with 2,4,6-tribromoformanilide (**208ca**, 417 mg, 1.17 mmol), DIPEA (700 μL, 3.97 mmol), DCE (25 mL), and $POCl_3$ (115 μL, 1.25 mmol), giving a white powder (309 mg, 691 μmol, 78%) [79abc]. M.p. 117 ºC dec. (lit. 121 ºC) [128]; R_f = 0.75 (1:2 EtOAc:hexane on Al_2O_3); ^{1}H NMR (VI300, 300 MHz, CD_2Cl_2) δ 7.827 (s, 2H); ^{13}C NMR (VI300, 75 MHz, $(CD_3)_2CO$) δ 159.7 (1C), 135.8 (2C), 135.4 (1C), 124.5 (1C), 122.0 (2C); IR (KBr) 3162 (m), 3068 (m), 2921 (w), 2128 (s), 1660 (s), 1555 (m), 1370 (m), 856 (s), 689 (m); HRMS-EI $[M]^+$ calcd for $C_7H_2{}^{79}Br_2{}^{81}BrN$ 338.7711, found 338.7708. X-ray crystallographic data were obtained [79b].

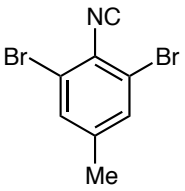

1,3-Dibromo-2-isocyano-4-methylbenzene (209cb) was prepared according to Method N, with 2,6-dibromo-4-methylformanilide (**208cb**, 254 mg, 856 μmol), DIPEA (530 μL, 3.01 mmol), DCE (10 mL), and $POCl_3$ (90 μL, 980 μmol), giving a beige powder (190 mg, 691 μmol, 81%). M.p. 128–129 ºC; R_f = 0.53 (1:3 EtOAc:hexane on SiO_2); ^{1}H NMR (AM400, 400 MHz, CD_2Cl_2) δ 7.456 (s, 2H), 2.346 (s, 3H); ^{13}C NMR (AM400, 101 MHz, CD_2Cl_2) δ 172.7 (1C), 142.9 (1C), 133.2 (2C), 126.0 (1C; by HMBC analysis),120.8 (2C), 21.2 (1C); IR (KBr) 3061 (w), 2922 (m), 2850 (w), 2118 (s), 1654 (m), 1586 (m), 1451 (s), 1384 (m), 1064 (w), 857 (s), 748 (s), 701 (m); HRMS-EI $[M]^+$ calcd for $C_8H_5{}^{79}Br{}^{81}BrN$ 274.8783, found 274.8784. X-ray crystallographic data were obtained.

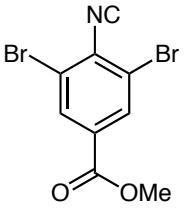

Methyl 3,5-Dibromo-4-isocyanobenzoate (209cd) was prepared according to Method N, with methyl 3,5-dibromo-4-formamidobenzoate (**208cd**, 594 mg, 1.69 mmol), DIPEA (1.00 mL, 5.68 mmol), DCE (20 mL), and $POCl_3$ (170 μL, 1.82 mmol). The resulting beige powder (490 mg) was recrystallized from DCM-pentane, washed with pentane, and then dried under vacuum (rt, 0.05 mmHg, 4 h), giving colorless blocks (453 mg, 1.42 mmol, 84%). M.p. 118–119 ºC; R_f = 0.49 (1:3 EtOAc:hexane on SiO_2); ^{1}H NMR (AV500, 500 MHz, CD_2Cl_2) [220] δ 8.278 (s, 2H), 3.930 (s, 3H); ^{13}C NMR (AV500, 126 MHz, $(CD_3)_2SO$) δ 174.1 (1C), 163.0 (1C), 132.5 (2C), 132.3 (1C), 130.1 (1C), 121.0 (2C), 53.2 (1C); IR (KBr) 3073 (m), 2961 (m), 2853 (w), 2122 (s), 1722 (s), 1426 (s), 1275 (s), 971 (m), 764 (s), 753 (s); HRMS-EI $[M]^+$ calcd for $C_9H_5{}^{79}Br_2NO_2$ 316.8682, found 316.8699. X-ray crystallographic data were obtained.

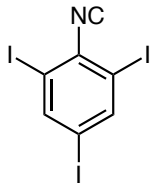

1,3,5-Triiodo-2-isocyanobenzene (209da) was prepared according to Method N, with 2,4,6-triiodoformanilide (**208da**, 397 mg, 802 μmol), DIPEA (500 μL, 2.81 mmol), DCE (75 mL), and $POCl_3$ (850 μL, 880 μmol), giving a white powder (330 mg, 686 μmol, 86%). M.p. 194–195 ºC; R_f = 0.54 (1:4 EtOAc:hexane on Al_2O_3); ^{1}H NMR (VI300, 300 MHz, $CDCl_3$) δ 8.198 (s, 2H); ^{13}C NMR (HD500, 126 MHz, $(CD_3)_2SO$) δ 170.0 (1C), 146.2 (2C), 133.8 (1C), 98.8 (1C), 97.7 (2C); IR (KBr) 3073 (m), 3037 (s), 2920 (w), 2126 (s), 1529 (s)1079 (m), 861 (s), 704 (s); HRMS-ESI $[M–H]^-$ calcd for $C_7H_2I_3N$ 479.7249, found 479.7226. X-ray crystallographic data were obtained.

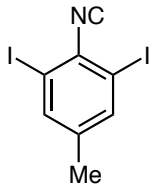

1,3-Diiodo-2-isocyano-4-methylbenzene (209db) was prepared according to Method N, with 2,6-diiodo-4-methylformanilide (**208db**, 509 mg, 1.32 mmol), DIPEA (800 μL, 4.54 mmol), DCE (50 mL), and $POCl_3$ (150 μL, 1.61 mmol), giving a white powder (447 mg, 1.21 mmol, 92%). M.p. 165–167 ºC; R_f = 0.56 (1:4 EtOAc:hexane on Al_2O_3); ^{1}H NMR (AV500, 500 MHz, $(CD_3)_2SO$) δ 7.842 (s, 2H); ^{13}C NMR (AV500, 126 MHz, $(CD_3)_2SO$) δ 168.3 (1C), 143.0 (1C), 139.5 (2C), 131.5 (1C), 95.6 (2C); IR (KBr) 3049 (w), 2919 (w), 2123 (s), 1576 (s), 1430 (s) 850 (s). 713 (s); HRMS-ESI $[M+Na]^+$ calcd for $C_8H_5I_2N$ 391.8404, found 391.8413. X-ray crystallographic data were obtained.

3.5. Preparation and Analyses of Crystallographic Samples

A sample of each compound listed in Table 29 was taken from the corresponding preparation described in §§ 3.2–3.4, and then dissolved in a refluxing mixture of the indicated solvent(s). The resulting mixture was separated by syringe filtration (0.45 μm pore diameter). The filtrate was cooled to rt during 2–4 h. If a large number of fine crystals was observed, the resulting mixture was iteratively dissolved in additional solvent and then allowed to cool to rt, until minimal or no precipitate was observed. The resulting mixture was allowed to partially evaporate in a loosely-capped vial for 2–10 d, until crystals suitable for X-ray diffraction (50–500 μm minor dimensions, generally flat faces, generally high clarity) were observed. Approximately 5–25 crystals were collected with a spatula or by decanting. The crystals were washed twice with pentane, dried under a stream of N_2 gas at ambient pressure [221], and then stored in a capped vial in an N_2 atmosphere until they were analyzed by Dr. Britton [74] or the University of Minnesota Department of Chemistry X-ray Crystallography Laboratory (XCL) [222].

Table 29. The solvents that were used to prepare crystallographic samples, and the person that performed each analysis.

compound	nickname	solvent(s)	analyzed by
8d	cyclopentanone 2:2 product	*p*-xylene	XCL
11h	cyclooctanone carbazolylaniline	2-propanol	XCL
12h	cyclooctanone diazepine	*p*-xylene	XCL
204ca	tribromo nitrile, polytype 1 (TT)	acetonitrile	Dr. Britton
204ca	tribromo nitrile, polytype 2 (TC)	mesitylene	Dr. Britton
204ca	tribromo nitrile, polytype 3 (TCT)	chloroform	Dr. Britton
204cb	dibromo 4-methyl nitrile	DCM	XCL
204cc:**215a** (2:1)	dibromo PABA nitrile, anthracene co-crystal	DCM, 0.5 molar equivalents of anthracene	XCL
204cd	dibromo PABA methyl ester nitrile	DCM, pentane	XCL
204da	triiodo nitrile (CC)	acetonitrile	Dr. Britton[a]
204db	diiodo 4-methyl nitrile (CC)	DCM	XCL
207	dibromo carbamoyl acid	2-propanol	XCL
209ca	tribromo isocyanide, polytype 2 (TC)	chloroform	XCL
209cb	dibromo 4-methyl isocyanide	DCM	XCL
209cd	dibromo PABA methyl ester isocyanide	DCM, pentane	XCL
209da	triiodo isocyanide (CC)	acetonitrile	Dr. Britton[a]
209db	diiodo 4-methyl isocyanide	DCM	XCL

[a]The X-ray data for these compounds were obtained from previously prepared samples [223].

For all crystal structures, the CIF content and additional information about data collection, structure solutions and refinements, are given in Appendices III–IV. The crystallographic data have also been published or deposited with the CCDC (Table 30). Copies of the data can be obtained, free of charge, on application to the CCDC via www.ccdc.cam.ac.uk/data_request/cif, by emailing data_request@ccdc.cam.ac.uk, or by contacting The Cambridge Crystallographic Data Centre, 12, Union Road, Cambridge CB2 1EZ, UK; fax: +44 1223 336033.

Table 30. The CCDC deposition number or literature reference for each crystal structure.

compound	nickname	CCDC number
8d	cyclopentanone 2:2 product	1059822 [64]
11h	cyclooctanone carbazolylaniline	1525807
12h	cyclooctanone diazepine	1525808
204ca	tribromo nitrile, polytype 1 (TT)	1445496 [79b]
204ca	tribromo nitrile, polytype 2 (TC)	1445497 [79b]
204ca	tribromo nitrile, polytype 3 (TCT)	1445498 [79b]
204cb	dibromo 4-methyl nitrile	1525810
204cc:**215a** (2:1)	dibromo PABA nitrile, anthracene co-crystal	1525811
204cd	dibromo PABA methyl ester nitrile	1525813
204da	triiodo nitrile (CC)	n/a [224]
204db	diiodo 4-methyl nitrile (CC)	1526007
207	dibromo carbamoyl acid	1525812
209ca	tribromo isocyanide, polytype 2 (TC)	1445499 [79b]
209cb	dibromo 4-methyl isocyanide	1525809
209cd	dibromo PABA methyl ester isocyanide	1525814
209da	triiodo isocyanide (CC)	n/a [224]
209db	diiodo 4-methyl isocyanide	1526008

Part IV. References and Notes

1. Alves, F. R. D.; Barreiro, E. J.; Fraga, C. A. M. *Mini-Rev. Med. Chem.* **2009**, *9*, 782–793.

2. Estimated based on searches performed in the Chemical Abstracts Service, Thomson Reuters ISI, and Beilstein databases.

3. Michalczuk, L.; Ribnicky, D. M.; Cooke, T. J.; Cohen, J. D. *Plant Physiol.* **1992**, *100*, 1346–1353.

4. Ucar, S.; Ozcan, A. R. *Bioresour. Technol.* **2008**, *99*, 8771–8776.

5. Yamamoto, Y.; Sato, Y.; Ebina, T.; Yokoyama, C.; Takahasi, S.; Mito, Y.; Tanabe, H.; Nishiguchi, N.; Nagaoka, K. *Fuel* **1991**, *70*, 565–566.

6. Taber, D. F.; Tirunahari, P. K. *Tetrahedron* **2011**, *67*, 7195–7210.

7. Hughes, D. L. *Org. Prep. Proced. Int.* **1993**, *25*, 607–632.

8. Miyata, O.; Kimura, Y.; Muroya, K.; Hiramatsu, H.; Naitu, T. *Tetrahedron Lett.* **1999**, *40*, 3601–3604.

9. Houlihan, W. J.; Parrino, V. A.; Uike, Y. *J. Org. Chem.* **1981**, *46*, 4511–4515.

10. Hayakawa, K.; Yasukouchi, T.; Kanematsu, K. *Tetrahedron Lett.* **1986**, *27*, 1837–1840.

11. Nickisch, K.; Klose, W.; Bohlmann, F. *Chem. Ber.* **1980**, *113*, 2036–2037.

12. Saxton, J. E. *J. Chem. Soc.* **1952**, *1952*, 3592–3594.

13. Pal, M.; Dakarapu, R.; Padakanti, S. *J. Org. Chem.* **2004**, *69*, 2913–2916.

14. Teranishi, K.; Hayashi, S.; Nakatsuka, S.-i.; Goto, T. *Synthesis*, **1995**, *1995*, 506–508.

15. Joule, J. A.; Mills, K. *Heterocyclic Chemistry, 4th Ed*; Blackwell Science, Inc.: Malden, MA, USA, **2000**; ISBN 9780632054534; esp. Alkylation [of Indoles], p 330.

16. Kanaoka, Y.; Miyashita, K.; Yonemitsu, O. *J. Chem. Soc. Chem. Commun.* **1969**, *1969*, 1365.

17. Nakazaki, M. *Bull. Chem. Soc. Jpn.* **1960**, *33*, 461–465.

18. Marx, I. E.; Dineen, T. A.; Able, J.; Bode, C.; Bregman, H.; Chu-Moyer, M.; DiMauro, E. F.; Du, B.; Foti, R. S.; Fremeau, R. T., Jr.; Gao, H.; Gunaydin, H.; Hall, B. E.; Huang, L.; Kornecook, T.; Kreiman, C. R.; La, D. S.; Ligutti, J.; Lin, M.-H. J.; Liu, D.; McDermott, J.; Moyer, B. D.; Peterson, E. A.; Roberts, J. T.; Rose, P.; Wang, J.; Youngblood, B. D.; Yu, V.; Weiss, M. M. *ACS Med. Chem. Lett.* **2016**, *7*, 1062–1067.

19. To simplify the discussion, aldehydes and their derivatives are included in "ketones" when discussing the scope of electrophiles that condense with indole in this dissertation. The exception is when ketones and aldehydes are explicitly contrasted.

20. Condensation reactions and products that are represented by *A*:*B* ratios involve the loss of *B* molecules of water.

21. Noland, W. E.; Venkiteswaran, M. R. *J. Org. Chem.* **1961**, *26*, 4263–4269.

22. Fischer, E. *Justus Liebigs Ann. Chem.* **1887**, *242*, 372–383.

23. Tayebee, R.; Nehzat, F.; Rezaei-Seresht, E.; Mohammadi, F. Z.; Rafiee, E. *J. Mol. Catal. A: Chem.* **2011**, *351*, 154–164.

24. Kamble, V. T.; Bandgar, B. P.; Suryawanshi, S. B. Bavikar, S. N. *Aust. J. Chem.* **2006**, *59*, 837–840.

25. Soliman, H. A.; Mubarak, A. Y.; Elmorsy, S. S. *Chin. Chem. Lett.* **2016**, *27*, 353–356.

26. Prasana, T. S. R.; Raju, K. M. *J. Korean Chem. Soc.* **2012**, *56*, 74–77.

27. Shiri, M.; Zolfigol, M. A.; Kruger, H. G.; Tanbakouchian, Z. *Chem. Rev.* **2010**, *110*, 2250–2293.

28. Dittmann, K.; Pindur, U. *Arch. Pharm.* **1985**, *318*, 340–350.

29. Gu, D.-G.; Ji, S.-J. *Chin. J. Chem.* **2008**, *26*, 578–582.

30. Mahboobi, S.; Uecker, A.; Sellmer, A.; Cénac, C.; Höcher, H.; Pongratz, H.; Eichhorn, E.; Hufsky, H.; Trümpler, A.; Sicker, M.; Heidel, F.; Fischer, T.; Stocking, C.; Elz, S.; Böhmer, F.-D.; Dove, S. *J. Med. Chem.* **2006**, *49*, 3101–3115.

31. (a) Jackson, A. H.; Smith, A. E. *Tetrahedron* **1965**, *21*, 989–1000; (b) Dittmann, K.; Pindur, U. *Heterocycles* **1986**, *24*, 1079–1093.

32. Cherioux, F.; Guyard, L.; Audebert, P. *Adv. Mater.* **1998**, *10*, 1013–1018.

33. (a) Muthyala, R. *Dyes Pigm.* **1994**, *25*, 303–324; (b) Noack, A.; Schröder, A.; Hartmann, H. *Dyes Pigm.* **2002**, *57*, 131–147.

34. Lavrenov, S. N.; Luzikov, Y. N.; Bykov, E. E.; Reznikova, M. I.; Stepanova, E. V.; Glazunova, V. A.; Volodina, Y. L.; Tatarsky, Jr., V. V. Shtil, A. A.; Preobrazhenskaya, M. N. *Bioorg. Med. Chem.* **2010**, *18*, 6905–6913.

35. Bergman, J.; Norrby, P. O.; Tilstam, U.; Venemalm, L. *Tetrahedron* **1989**, *45*, 5549–5564.

36. Scholtz, M. *Ber. Dtsch. Chem. Ges.* **1913**, *46*, 1082–1089.

37. Noland, W. E.; Venkiteswaran, M. R.; Lovald, R. A. *J. Org. Chem.* **1961**, *26*, 4249–4254.

38. Rodney D. DeKruif, "Condensation Reactions of Indole with Acetophenones: Substituent Effects and Reaction Conditions" *M.S. Dissertation*, **Dec. 1982**, University of Minnesota, Minneapolis, Minnesota.

39. Ingeborg Maas, "Über Neue Indolderivate" *Ph.D. Dissertation* **Feb. 1954**, Munich, Germany.

40. Bergman, J. *Tetrahedron* **1970**, *26*, 3353–3355.

41. Guzei, I. A.; Spencer, L. C.; Codner, E.; Boehm, J. M. *Acta Crystallogr. Sect. E.* **2012**, *68*, o1–o2.

42. Banerji, J.; Chatterjee, A.; Manna, S. *Heterocycles* **1981**, *15*, 325–336.

43. Banerji, J.; Dhara, K. P.; Saha, M.; Chatterjee, A.; Shoolery, J. N. *Ind. J. Chem.* **1984**, *23B*, 1223–1225.

44. Nayak, A.; Dutta, U.; Prangé, T.; Banerji, J. *J. Heterocycl. Chem.* **2011**, *48*, 608–612.

45. Noland, W. E.; Xia, G. M.; Gee, K. R.; Konkel, M. J.; Wahlstrom, M. J.; Condoluci, J. J.; Rieger, D. L. *Tetrahedron*, **1996**, *52*, 4555–4572.

46. Noland, W. E.; Lanzatella, N. P.; Sizova, E. P.; Venkatraman, L.; Afanasyev, O. V. *J. Heterocycl. Chem.* **2009**, *46*, 503–534.

47. Noland, W. E.; Walhstrom, M. J.; Konkel, M. J.; Brigham, M. E.; Trowbridge, A. G.; Konkel, L. M. C.; Gourneau, R. P.; Scholten, C. A.; Lee, N. H.; Condoluci, J. J.; Gac, T. S.; Pour, M. M.; Radford, P. M. *J. Heterocycl. Chem.* **1993**, *30*, 81–91.

48. The conclusions drawn in this paragraph, and the previous paragraph, are based on patterns found in the data presented in the references that are cited in §§ 1.1.3–1.1.5.

49. Musser, M. T. *Ullmann's Encycl. Ind. Chem. 7th Ed.* **2011** (11), Wiley-VCH Verlag GmbH & Co. KGaA, Weinheim, Germany, ISBN 978-3-527-32943-4, pp 49–60, DOI 10.1002/14356007.a08_217.pub2.

50. DeLuca, R. J.; Edwards, J. L.; Steffens, L. D.; Michel, B. W.; Qiao, X.; Zhu, C.; Cook, S. P.; Sigman, M. S. *J. Org. Chem.* **2013**, *78*, 1682–1686.

51. Barton, D. H. R.; Chavasiri, W. *Tetrahedron* **1994**, *50*, 19–30.

52. Dieckmann, W. *Ber. Dtsch. Chem. Ges.* **1894**, *27*, 102–103.

53. Kohler, E. P.; Tishler, M.; Potter, H.; Thompson, H. T. *J. Am. Chem. Soc.* **1939**, *61*, 1057–1061.

54. Lipp, P.; Köster, R. *Ber. Dtsch. Chem. Ges.* **1931**, *64*, 2823–2825.

55. Andreades, S.; Carlson, H. D. *Org. Synth.* **1965**, *45*, 50–54.

56. Burpitt, R. D.; Thweatt, J. G. *Org. Synth.*, **1968**, *48*, 56 (or **1973**, *Coll. Vol. 5*, 277).

57. Brannock, K. C.; Burpitt, R. D.; Goodlett, V. W.; Thweatt, J. G. *J. Org. Chem.* **1964**, *29*, 818–823.

58. Garbisch, E. W., Jr.; Wohllebe, J. *J. Org. Chem.* **1968**, *33*, 2157–2158.

59. Akhrem, A. A.; Ustynyuk, T. K.; Titov, Yu. A. *Russ. Chem. Rev.* **1970**, *39*, 732–746.

60. Aubé, J.; Milligan, G. L. *J. Am. Chem. Soc.* **1991**, *113*, 8965–8966.

61. Rao, D. V.; Stuber, F. A.; Ulrich, H. *J. Org. Chem.* **1979**, *44*, 456–458.

62. Wahlström, N.; Slätt, J.; Stensland, B.; Ertan, A.; Bergman, J.; Janosik, T. *J. Org. Chem.* **2007**, *72*, 5886–5889.

63. Ishi, H.; Murakami, K.; Sakurada, E. (née Kawanabe); Hosoya, K.; Murakami, Y. *J. Chem. Soc. Perkin Trans. 1* **1988**, *1988*, 2377–2386.

64. Noland, W. E.; Worth, M. A.; Schneerer, A. K.; Paal, C. L.; Tritch, K. J. *Acta Crystallogr. Sect. E* **2015**, *71*, 516–519.

65. Ning, Y.-C. *Interpretation of Organic Spectra* **2011**, Wiley-Blackwell, Hoboken, New Jersey, USA; ISBN 9780470825167.

66. Janosik, T.; Bergman, J. *Tetrahedron* **1999**, *55*, 2371–2380.

67. Computations were performed using *Gaussian 09* (Carnegie Mellon University, Pittsburgh, PA, USA), with the M06 density functional, and a 6-311 + G(*d*,*p*) basis set. These computations were performed by Dr. Hannah Leverentz in (a) September 2011; (b) March 2012.

68. Miah, M. A. J.; Snieckus, V. *J. Org. Chem.* **1985**, *50*, 5438–5440.

69. Shibuya, S.; Isobe, M. *Tetrahedron* **1998**, *54*, 6677–6698.

70. Desai, R. D. *J. Chem. Soc.* **1932**, 1079–1088.

71. Soni, R.; Collinson, J.-M.; Clarkson, G. C.; Wills, M. *Org. Lett.* **2011**, *13*, 4304–4307.

72. Oppolzer, W.; Zutterman, F.; Bättig, K. *Helv. Chim. Acta* **1983**, *66*, 522–533, esp. compound 24.

73. Hansch, C.; Carpenter, W.; Todd, J. *J. Org. Chem.* **1958**, *23*, 1924–1926.

74. Professor Emeritus, University of Minnesota. Deceased July 7, 2015, during the course of collecting the crystallographic data for this dissertation.

75. A search was performed in the CSD and SciFinder databases for pertinent articles co-authored by Doyle Britton between 1960 and 2016. Three articles were located in *J. Chem. Crystallogr.* and twenty-eight articles were located in various International Union of Crystallography journals. It is possible that Dr. Britton published additional articles. It should also be noted that Dr. Britton published approximately 12 additional articles on the crystallography of other substituted benzonitriles.

76. (a) The following notation is used to describe repeating contacts in crystals: $X_d^a(n)$, where *X* is C (chains), D (finite patterns), or R (rings); *d* is the number of donors, *a* is the number of acceptors, and *n* is the total number of atoms involved. (b) *See:* Bernstein, J.; Davis, R. E.; Shimono, L.; Chang, N.-L. *Angew. Chem. Int. Ed. Engl.* **1995**, *34*, 1555–1573.

77. Desiraju, G. R.; Harlow, R. L. *J. Am. Chem. Soc.* **1989**, *111*, 6757–6764.

78. (a) The interatomic distance is shorter than the sum of the atomic contact radii. Throughout this dissertation, contact radii are taken from: (b) Rowland, R. S.; Taylor, R. *J. Phys. Chem.* **1996**, *100*, 7384–7391, Table 3, entries in the R^d column.

79. (a) The 78% yield reported here is an improvement over the 34% yield reported in our crystallographic article, (b) Britton, D.; Noland, W. E.; Tritch, K. J. *Acta Crystallogr. Sect. E* **2016**, *72*, 178–183; (c) as a result of more precise experimental technique, especially during the extractive procedures.

80. One system of naming the positions of substituted benzenes is based on the minimum number of bonds between a given substituent and the ring position in question, as follows: *ipso* (1 bond), *ortho* (2 bonds), *meta* (3 bonds), *para* (4 bonds). Thus, the *ipso*-position is the point of attachment of a given substituent to the ring.

81. Two molecules that are connected by one or more short contacts or ionic bonds, and are centered on a crystallographic inversion center. When the two molecules in question are absolutely or conformationally chiral, they must be enantiomers. Molecules that are related in this way can be described as "centric."

82. Carter, V. B.; Britton, D. *Acta Crystallogr. Sect. B* **1972**, *28*, 945–950.

83. Herein, crystallographic vectors are formatted as {*x*a, *y*b, *z*c}, where *xyz* are scalar coefficients and abc are the unit cell unit vectors. Crystallographic vectors are commonly formatted as [*xyz*], but that convention would conflict with the format used herein for references and notes. In figures, the view is along the given vector, and the projected plane is orthogonal to the given vector.

84. Pseudoinversion centers are also known as local inversions or local centers. They resemble true inversion centers, but they are asymmetric due to slight atomic displacements. In large unit cells, pseudoinversion centers are sometimes located between several otherwise symmetry-equivalent molecules that differ in the conformation of a chain or ring, without affecting the overall packing motif.

85. Britton, D. *Acta Crystallogr. Sect E* **2005**, *61*, o1726–o1727.

86. Britton, D. *Acta Crystallogr. Sect. B* **2002**, *58*, 553–563.

87. Cambridge Structural Database (CSD), version 5.37, May 2016.

88. Michelin, R. A.; Mozzon, M.; Bertani, R. *Coord. Chem. Rev.* **1996**, *147*, 299–338.

89. Britton, D. *Cryst. Struct. Commun.* **1981**, *10*, 1061–1064.

90. Hu, X.; Yuan, Z.; Lu, G. *Powder Diffr.* **2004**, *19*, 325–328.

91. Britton, D. *Acta Crystallogr. Sect. E* **2004**, *60*, o184–o186.

92. Carter, D. R.; Turley, J. W.; Boer, F. P. *Acta Crystallogr. Sect. B* **1972**, *28*, 3430–3434.

93. Britton, D.; Noland, W. E.; Pinnow, M. J. *Acta Crystallogr. Sect. B* **2000**, *56*, 822–827.

94. Pink, M.; Britton, D.; Noland, W. E.; Pinnow, M. J. *Acta Crystallogr. Sect. C* **2000**, *56*, 1271–1273.

95. Britton, D. *Acta Crystallogr. Sect. C* **1997**, *53*, 225–227.

96. Britton, D. *J. Chem. Crystallogr.* **2012**, *42*, 851–855.

97. Britton, D. *Acta Crystallogr. Sect. C* **2008**, *64*, o109–o110.

98. Carter, D. R.; Boer, F. P. *J. Chem. Soc. Perkin Trans. 2* **1972**, *1972*, 2104–2107.

99. Britton, D. *Acta Crystallogr. Sect. E* **2001**, *57*, o702–o704.

100. Britton, D.; Noland, W. E.; Henke, T. K. *Acta Crystallogr. Sect. E* **2002**, *58*, o185–o187.

101. Gleason, W. B.; Britton, D. *Cryst. Struct. Commun.* **1978**, *7*, 365–370.

102. (a) Gleason, W. B.; Britton, D. *Cryst. Struct. Commun.* **1976**, *5*, 229–232; (b) Paek, K.; Knobler, C. B.; Maverick, E. F.; Cram, D. J. *J. Am. Chem. Soc.* **1989**, *111*, 8662–8671.

103. (a) The existing average N1...Cl1 gap is 3.693 Å. The difference in contact radii for Br and Cl atoms is 0.11 Å. There are two X atoms positioned across each end of the anthracene gap in the sheet, and they are roughly at a 60º angle to the longitudinal axis of the anthracene molecule. Thus, the estimated average gap between Br1...N1 and Br2...N1 is [3.693 – (2 sin 60º) × 0.11] = 3.502 Å, in the hypothetical case that Br atoms are substituted for Cl atoms and the resulting crystal is isomorphous; (b) Substituting the contact radius for I atoms gives [3.693 – (2 sin 60º) × 0.26] = 3.243 Å. This estimate ignores the difference in C–Br or C–I versus C–Cl bond length (≈ 0.15 or 0.34 Å, respectively). It was postulated that an increase in bond length would spread out cyano acid molecules along the longitudinal axis of anthracene, roughly canceling out the bond-length-increased reach across the N...X gaps.

104. According to systematic nomenclature, halogens have priority over isocyano groups. Also, carboxyl groups have priority over cyano and isocyano groups. Systematic names are given throughout § 1 and § 3. However, cyano and isocyano groups are assigned to the 1-position throughout § 2, and drawn at the top of Lewis structures. This was done to clarify the discussion.

105. Carter, V. B.; Britton, D.; Gleason, W. B. *Cryst. Struct. Commun.* **1977**, *6*, 543–548.

106. (a) Parrish, D. A.; Deschamps, J. R.; Gilardi, R. D.; Butcher, R. J. *Cryst. Growth Des.* **2008**, *8*, 57–62; (b) Britton, D.; Young, V. G.; Noland, W. E.; Pinnow, M. J.; Clark, C. M. *Acta Crystallogr. Sect. B* **2012**, *68*, 536–542.

107. Hagenbach, H. *Helv. Chim. Acta* **1923**, *6*, 134–186.

108. Sandmeyer, T. *Ber. Dtsch. Chem. Ges.* **1884**, *17*, 1633–1635.

109. Mo, F.; Dong, G.; Zhang, Y.; Wang, J. *Org. Biomol. Chem.* **2013**, *11*, 1582–1593.

110. Nielsen, M. A.; Nielsen, M. K.; Pittelkow, T. *Org. Proc. Res. Dev.* **2004**, *8*, 1059–1064.

111. Filimonov, V. D.; Trusova, M.; Postnikov, P.; Krasnokutskaya, E. A.; Lee, Y. M.; Hwang, H. Y.; Kim, H.; Chi, K.-W. *Org. Lett.* **2008**, *10*, 3961–3964.

112. Hughes, E. D.; Ingold, C. K.; Ridd, J. H. *Nature*, **1950**, *166*, 642–643.

113. Bahr, J. L.; Tour, J. M. *Chem. Mater.* **2001**, *13*, 3823–3824.

114. Giumanini, A. G.; Verardo, G.; Geatti, P.; Strazzolini, P. *Tetrahedron* **1996**, *52*, 7137–7148.

115. Waters, W. A. *J. Chem. Soc.* **1942**, *1942*, 266–270.

116. Kochi, J. K. *J. Am. Chem. Soc.* **1957**, *79*, 2942–2948.

117. Hanson, P.; Rowell, S. C.; Taylor, A. B.; Walton, P. H.; Timms, A. W. *J. Chem. Soc. Perkin Trans. 2* **2002**, *2002*, 1126–1134; other articles in this series investigate various mechanistic aspects of Sandmeyer reactions.

118. Zollinger, H. *Angew. Chem. Int. Ed. Engl.* **1978**, *17*, 141–150.

119. Robison, M. M.; Robison, B. L. *Org. Synth. Coll. Vol. 4* **1963**, 947–950, esp. step B.

120. Toya, Y.; Takagi, M.; Nakata, H.; Suzuki, N.; Isobe, M.; Goto, T. *Bull. Chem. Soc. Jpn.* **1992**, *65*, 392–395.

121. Because of the excess of dissolved sodium cations, complexes **224** and **225** are modeled as being sodium salts. It is assumed that the potassium cations have exchanged for sodium. In the present work, no difference in cyanation yields was observed when NaCN was substituted for KCN during the optimization of the cyanation conditions.

122. The effect of incubation time was observed in the present work, and is evidence for aqua-bicarbonate ligand exchange, or the formation of a heterogeneous substance that has performance similar to that expected from SBDC.

123. Tolman, C. A. *Chem. Soc. Rev.* **1972**, *1*, 337–353.

124. Ugi, I.; Fetzer, U.; Eholzer, U.; Knupfer, H.; Offerman, K. *Angew. Chem. Int. Ed. Engl.* **1965**, *4*, 472–484.

125. Hofmann, A. W. *Justus Liebigs Ann. Chem.* **1867**, *144*, 114–120.

126. Krishnamurthy, S. *Tetrahedron Lett.* **1982**, *23*, 3315–3318.

127. Vlietstra, E. J.; Zwikker, J. W.; Nolte, R. J. M.; Drenth, W. *Recl. Trav. Chim. Pays-Bas* **1982**, *101*, 460–462.

128. Mironov, M. A.; Mokrushin, V. S. *Russ. J. Org. Chem.* **1999**, *35*, 693–697.

129. De La Mare, P. B. D.; Ridd, J. H. *Aromatic Substitution: Nitration and Halogenation* **1959**, Butterworths Scientific Publications, London, England; ASIN: B0000CKCBU.

130. Buu-Hoï, Ng. Ph. *Recl. Trav. Chim. Pays-Bas* **1954**, *73*, 197–202.

131. Schlesinger, H. I. *General Chemistry* (3rd Ed.) **1938**, Longmans, Green & Co., New York, New York, USA; pp 379–380. The relevant section is titled "Preparation of Halogens."

132. Vyas, P. V.; Bhatt, A. K.; Ramachandraiah, G.; Bedekar, A. V. *Tetrahedron Lett.* **2003**, *44*, 4085–4088.

133. Not to be confused with thionyl chloride ($SOCl_2$), which is a source of chloride, and not a source of chlorine.

134. Bonesi, S. M.; Erra-Balsells, R. *J. Heterocycl. Chem.* **1997**, *34*, 877–889. In this article, the byproducts were removed by chromatography. Washing the reaction mixture with an alkaline, aqueous solution is an alternative.

135. Coleman, G. H.; Talbot, W. F. *Org. Synth. Coll. Vol. 2*, **1943**, 592–595.

136. Elion, L. *Recl. Trav. Chim. Pays-Bas* **1923**, *42*, 145–183.

137. Hill, M. L.; Raphael, R. A. *Tetrahedron* **1990**, *46*, 4587–4594.

138. R = Saturated or aromatic hydrocarbon.

139. Kajigaeshi, S.; Kakinami, T.; Yamasaki, H.; Fujisaki, S.; Okamoto, T. *Bull. Chem. Soc. Jpn.*, **1988**, *61*, 600–602.

140. Teo, T.; Yang, Y.; Yu, M.; Basnet, S. K. C.; Gilham, T.; Hou, J.; Schmid, R. M.; Kumarasiri, M.; Diab, S.; Albrecht, H.; Sykes, M. J.; Wang, S. *Eur. J. Med. Chem.* **2015**, *103*, 539–550.

141. There are numerous examples in the literature where complicated hydrogenation catalysts are used for this transformation, *e.g.*, Xie, M.; Zhang, F.; Long, Y.; Ma, J. *RSC Adv.* **2013**, *3*, 10329–10334. Although these catalysts probably have merit in niche or industrial applications, there are no reports that use palladium on carbon. This transformation would probably work very well using conditions otherwise identical to the preparation of **232** described in reference [140] (Teo *et al.*, numbered as compound **4a** therein).

142. Chanteau, S. H.; Tour, J. M. *J. Org. Chem.* **2003**, *68*, 8750–8766.

143. Doyle, M. P.; Siegfried, B.; Dellaria Jr., J. F. *J. Org. Chem.* **1977**, *42*, 2426–2431.

144. (a) Britton, D. *Acta Crystallogr. Sect. C.* **2006**, *62*, o510–o514; (b) In a verbal communication with Dr. Britton, he recalled that **204bc** had been prepared by a former colleague of his, by a Sandmeyer cyanation.

145. Hinsberger, S.; de Jong, J. C.; Groh, M.; Haupenthal, J.; Hartmann, R. W. *Eur. J. Med. Chem.* **2014**, *76*, 343–351.

146. Lepage, O.; Kattnig, E.; Fürstner, A. *J. Am. Chem. Soc.* **2004**, *126*, 15970–15971.

147. Crews, P.; Rodríguez, J.; Jaspars, M. *Organic Structure Analysis* **1998**, Oxford University Press, New York, New York, USA; ISBN 0-19-510102-2; p 257.

148. The TLC plates that were used were a product of Analtech, Inc., Newark, DE, USA; P/N 02013. Silica gel, 20 × 20 cm, 1 mm thick; developed with combinations of hexane, EtOAc, $CHCl_3$, and MeOH.

149. Harwood, L. M.; Moody, C. J. *Experimental Organic Chemistry: Principles and Practice* **1989**, Wiley-Blackwell, Hoboken, New Jersey, USA; ISBN 0-632-02017-2; pp 122–125.

150. Pavia, D. L.; Lampman, G. M.; Kritz, G. S.; Engel, R. G. *Introduction to Organic Laboratory Techniques: A Small-Scale Approach* **1998**, Harcourt Brace & Co., Orlando, Florida, USA; ISBN 0-03-024519-2; pp 749–751.

151. (a) Schreyer, M.; Guo, L.; Thirunahari, S.; Gao, F.; Garland, M. *J. Appl. Crystallogr.* **2014**, *47*, 659–667; (b) Fiala, J. *J. Appl. Crystallogr.* **1976**, *9*, 429–432; (c) Yun, Y.; Wan, W.; Rabbani, F.; Su, J.; Xu, H.; Hovmöller, S.; Johnsson, M.; Zou, X. *J. Appl. Crystallogr.* **2014**, *47*, 2048–2054.

152. If the methyl groups are assumed to rapidly rotate about the C4–C8 bond, then each methyl group can be approximated as having one donor H atom. This approximation results in $R_2^2(4)$ ring geometry.

153. Herein, CN and NC groups are treated as donors to contacts with X atoms. They are treated as acceptors to R–H...NC and R–H...CN contacts, where R is C or any electronegative atom.

154. The convention used herein is: If ∠(C–Br*...Br) ≈ 90°, then Br* is considered to be a donor for that contact; If ∠(C–Br*...Br) ≈ 180°, then Br* is considered to be an acceptor for that contact. In **204cb** and **209db**, each Br atom is a donor to one contact, and an acceptor to another.

155. This translation arises from a formality in establishing the position of the origin for the unit cell, which in this case changes when the C4-substituent changes from an I atom to a C atom.

156. Bulgarovskaya, I. V.; Novakovskaya, L. A.; Federov, Yu. G.; Zvonkova, Z. V. *Kristallografiya* **1976**, *21*, 515–519.

157. (**239a**) Blake, C. C. F.; Small, R. W. H. *Acta Crystallogr. Sect. B* **1972**, *28*, 2201–2206; (**239b**) Rauf, M. K.; Badshah, A.; Bolte, M.; Saeed, A. *Acta Crystallogr. Sect. E.* **2006**, *62*, o1070–o1071; (**239c**) Mukherjee, A.; Tothadi, S.; Chakraborty, S.; Ganguly, S.; Desiraju, G. R. *CrystEngComm* **2013**, *15*, 4640–4654; (**239d**) Gdaniec, M.; Olszewska, T.; Polonski, T. *Acta Crystallogr. Sect. C* **2004**, *60*, o41–o43.

158. Allen, F. H.; Kennard, O.; Watson, D. G. *J. Chem. Soc. Perkin Trans. 2* **1987**, *1987*, S1–S19.

159. Portalone, G.; Domenicano, A. *J. Mol. Struct.* **1987**, *160*, 97–107.

160. Britton, D. *Acta Crystallogr. Sect. E* **2002**, *58*, o840–o841.

161. Khurana, J. M.; Singh, S. *J. Chem. Soc. Perkin Trans. 1* **1999**, *1999*, 1893–1895.

162. Shine, H. J.; Zmuda, H.; Park, K. H.; Kwart, H.; Horgan, A. G.; Brechbiel, M. *J. Am. Chem. Soc.* **1982**, *104*, 2501–2509.

163. Micro Essential Laboratory, Inc., 4224 Avenue H, Brooklyn, NY, 11210, USA. P/N 165-B.

164. Cannon Instrument Co., 2139 High Tech Road, State College, PA, 16803, USA. P/N 3947-A20. This material was formerly known as "Cannon Protruded Packing."

165. Sorbent Technologies, Inc., 5955 Peachtree Corners East Suite A, Norcross, GA, 30071, USA. P/N 52500. This company is also known as SorbTech.

166. (a) Sigma-Aldrich Co. LLC, 3050 Spruce Street, Saint Louis, MO, 63103, USA. (b) P/N 199974. (c) Perfluorokerosene P/N 77275; perfluorotributylamine P/N 442747.

167. (a) A software product of (b) Thermo Fisher Scientific, Inc., 81 Wyman Street, Waltham, MA, 02451, USA. (c) Basic alumina used for chromatography is P/N A941. (d) This instrument is in the LeClaire-Dow Instrumentation Facility.

168. Macherey-Nagel GmbH & Co. KG, Postfach 10 13 52, D-52313 Düren Straße 6-8, Germany; silica plates are P/N 805021, alumina plates are P/N 802021.

169. ChemGlass, 3800 North Mill Road, Vineland, NJ, 08360, USA. P/N CG-1289.

170. *E.g.*, Chemglass Life Sciences, LLC, Vineland, NJ, USA; P/N AF-0513.

171. A discontinued product of Laboratory Devices, Inc., PO Box 68, Cambridge, MA, 02139, USA. The current form of the Mel-Temp apparatus can be found *via* Barnstead-Thermolyne Corp., 2555 Kerper Boulevard, Dubuque, IA, 52004, USA.

172. (a) A software product of (b) Agilent Technologies, Inc., 5301 Stevens Creek Boulevard, Santa Clara, CA, 95051, USA. (c) Tuning mix is P/N G2421. (d) Varian,

Inc. was purchased by Agilent Technologies, Inc. in 2010. (e) This instrument is in the LeClaire-Dow Instrumentation Facility.

173. (a) A software product of (b) Bruker Daltonics, Inc., 40 Manning Road, Billerica, MA, 01821, USA. (c) This instrument is in the LeClaire-Dow Instrumentation Facility.

174. $HO(C_2H_4O)_nH$, commonly known as polyethylene glycol, PEG, or polyglycol.

175. $HO_2CCH_2O(C_2H_4O)_nCH_2CO_2H$, commonly known as polyethylene glycol bis(carboxymethyl ether) or polyglycol diacid.

176. (a) Bruker BioSpin Corp., 2700 Technology Forest, The Woodlands, TX, 77381, USA. (b) This instrument is in the LeClaire-Dow Instrumentation Facility.

177. *APEX2*, *SADABS*, *SAINT*, and *SMART*. Bruker AXS Inc., Madison, Wisconsin, USA. Some products were formerly owned by or licensed to Siemens.

178. M-H-W Laboratories, PO Box 15149, Phoenix, AZ, 85060, USA.

179. Atlantic Microlab, Inc., 6180 Atlantic Boulevard Suite M, Norcross, GA, 30071, USA.

180. A software product of MestReLab Research, S. L., Feliciano Barrera 9B, Bajo, 15706, Santiago de Compostela, Spain.

181. (a) Sheldrick, G. M. *Acta Crystallogr., Sect. A: Found. Crystallogr.* **2008**, *64*, 112–122; (b) Versions of *SHELXS97* or *SHELXTL97* are older releases of software described in part (a) or references cited therein.

182. (a) Sheldrick, G. M. *Acta Crystallogr., Sect. C: Struct. Chem.* **2015**, *71*, 3–8; (b) Various versions of *SADABS 2012* or *2014*, or *SHELXL* or *SHELXT 2014*, are older releases of software described in part (a) or references cited therein.

183. The Cambridge Crystallographic Data Centre, Cambridge, CB2 1EZ, United Kingdom. CIF's are the commonly used medium for communicating crystallographic data.

184. Macrae, C. F., Bruno, I. J., Chisholm, J. A., Edgington, P. R., McCabe, P., Pidcock, E., Rodriguez-Monge, L., Taylor, R., van de Streek, J. & Wood, P. A. *J. Appl. Cryst.* **2008**, *41*, 466–470.

185. Where the quantities of intermediates are not specified, it is because they are prone to degradation. These intermediates were carried forward as quickly as possible, as was done in the literature [56, 57] (Burpitt & Thweatt; Brannock *et al.*), in order to maximize the yield of the title product.

186. Ace Glass, Inc., Vineland, NJ, USA; P/N 8415-21 (250 mL, round-bottomed, 60 psig); P/N 5808-45 (PTFE purge adapter). The line was fitted with a relief valve (stainless steel, 50 psig).

187. Smith, C. R., Jr.; Wilson, T. L.; Miwa, T. K.; Zobel, H.; Lohmar, R. L.; Wolff, I. A. *J. Org. Chem.* **1961**, *26*, 2903–2905.

188. Schmitz-Dumont, O.; Nicolojannis, B. *Ber. Dtsch. Chem. Ges.* **1930**, *63*, 323–326.

189. If a large portion of the desired product precipitates during filtration, it can be recovered by performing an overnight Soxhlet extraction on the filter cake, with chloroform (100 mL). A small funnel can be placed on the extraction thimble, to prevent the recovered catalyst from splashing into the extract.

190. Schmitz-Dumont, O.; Hamann, K.; Geller, K. H. *Justus Liebigs Ann. Chem.* **1933**, *504*, 1–9.

191. Abe, T.; Nakamura, S.; Yanada, R.; Choshi, T.; Hibino, S.; Ishikura, M. *Org. Lett.,* **2013**, *15*, 3622–3625.

192. Rani, V. J.; Vani, K. V.; Rao, C. V. *Synth. Commun.,* **2012**, *42*, 2048–2057.

193. Chemical shifts were determined by $^{1}H/^{15}N$ HMBC experiments, and are referenced to an external sample of nitromethane [$\delta(^{15}N)$ = 380.2 ppm] in a sealed 1.5 mm glass capillary. *See:* Wishart, D. S.; Bigam, C. G.; Yao, J.; Abildgaard, F.; Dyson, H. J.; Oldfield, E.; Markley, J. L.; Sykes, B. D. *J. Biomol. NMR* **1995**, *6*, 135-140, esp. Table 3, entry 6, column 3.

194. Arnold, A.; Markert, M.; Mahrwald, R. *Synthesis* **2006**, *38*, 1099–1102.

195. The specific nature of the impurities is not known with certainty, but likely they included 3-chlorobenzoic acid and closely related species. When estimating the mass fraction of the title epoxide, the combined integration of the aromatic signals in the ^{1}H NMR spectrum was divided by 4, and then weighted by the molar mass of 3-chlorobenzoic acid (156.565 g/mol). No convenient means was found by which this epoxide could be purified further without reaction of the epoxide group, as indicated by NMR and MS analyses. Because the next synthetic step successfully uses an acid catalyst, the attained purity was deemed acceptable.

196. Acidic 2,4-dinitrophenylhydrazine solution, which attaches a UV chromophore to most ketones and aldehydes. *E.g.,* Leonard, J.; Lygo, B.; Procter, G. *Advanced Practical Organic Chemistry, 2nd Ed.*; Chapman & Hall: Glasgow, G64 2NZ, UK, **1995**, esp. pp 148–149.

197. De Jongh, H. A. P.; Wynberg, H. *Tetrahedron* **1965**, *21*, 515–533.

198. Bellamy, A. J.; Guthrie, R. D. *J. Chem. Soc.* **1965**, *1965*, 3528–3533.

199. The signal at 3.42 ppm in the ^{1}H NMR spectrum is derived from an attempted recrystalization from methanol.

200. Xiao, Z.-P.; Wang, Y.-C.; Du, G.-Y.; Wu, J.; Luo, T.; Yi, S.-F. *Synth. Commun.* **2010**, *40*, 661–665.

201. Ottmann, G.; Hooks, Jr.; H. *J. Org. Chem.* **1965**, *30*, 952–954.

202. Horrom, B. W.; Lynes, T. E. *J. Med. Chem.* **1963**, *6*, 528–532.

203. Once flask (c) has been filled, it is important not to cool either of the other flasks without N_2 flow, or create any other condition by which the contents of flask (c) may siphon into flasks (a) or (b). It is also advisable to leak-test the apparatus with N_2 gas prior to placing any reagents in flasks (a) or (b).

204. Fittig, R.; Büchner, E. *Justus Liebigs Ann. Chem.* **1877**, *188*, 23–30.

205. Suzuki, H.; Mishina, T.; Hanafusa, T. *Bull. Chem. Soc. Jpn.* **1978**, *51*, 3099–3100.

206. Meisenheimer, J.; Schmidt, W.; Schäfer, G. *Justus Liebigs Ann. Chem.* **1933**, *501*, 131–150.

207. Otto, P. Ph. H. L.; Juppe, G. *J. Labelled Cmpd.* **1965**, *1*, 115–127.

208. Olaru, M.; Beckmann, J.; Rat, C. I. *Organometallics* **2014**, *33*, 3012–3020.

209. (a) The acetic acid suspension may begin to freeze if it is left in the ice bath for too long before adding the nitrite solution; (b) Where both diazotization and cyanation are to be performed, it is advisable to prepare the SBDC suspension (Method K) prior to beginning diazotization, in case the latter proceeds more rapidly than planned.

210. Generally, a flask with a nominal volume of 4–5 times the total volume of the dicyanocuprate suspension should be used. This often corresponds to a 500 mL flask for a 1-gram-scale reaction. This allows ample headspace to contain the large amount of foam that is generated during the cyanation process.

211. Organic solvent in the cyanation vessel should be kept to a minimal volume. Wait 10 min before adding more solvent, and see if the remaining foam disappears or decreases in volume such that it is being gradually turned over by the stir bar. The choice of solvent should match the first of (a) solvent used during diazotization; (b) solvent used during extraction; (c) EtOAc, which is used during chromatography.

212. Edward, C. J.; Palmer, C. J.; Larkin, J. P.; Smith, I. H. *Pesticidal Compounds*. Eur. Pat. Appl. EP0279698 A2, **1990**.

213. Pretsch, E.; Bühlmann, P.; Affolter, C. *Structure Determination of Organic Compounds*; Springer-Verlag: Berlin-Heidelberg-New York, **2000**, esp. § 2.5.6, p 30.

214. It is important to filter out insoluble material when recrystallizing, to minimize contamination of the product with the corresponding benzoic acid derivative.

215. Bachman, G. B.; Finholt, R. W. *J. Am. Chem. Soc.* **1948**, *70*, 622–624.

216. Except for DCM, the identity of the major impurities cannot be ascertained from the available data; the purity of this sample has been estimated based on the following assumptions: The aromatic signals in the ^{1}H NMR spectrum are assumed to be from components with the same molar mass as the desired product. The observed integrals

are approximately linear combinations of 0.17 and 0.11; the combined impurities have been assumed to have a 28 mole% abundance compared to the title compound. An internal NMR standard was not added because all of the available sample was used up trying to grow crystals and co-crystals suitable for X-ray diffraction, and for several attempted chromatographic separations.

217. Jung, S. H.; Ahn, J. H.; Park, S. K.; Choi, J.-K. *Bull. Korean Chem. Soc.* **2002**, *23*, 149–150.

218. Chattaway, F. D.; Orton, K. J. P.; Hurtley, W. H. *Ber. Dtsch. Chem. Ges.* **1899**, *32*, 3635–3638.

219. Nair, R. N.; Lee, P. J.; Rheingold, A. L.; Grotjahn, D. B. *Chem. Eur. J.* **2010**, *16*, 7992–7995.

220. The supplied NMR spectra are from the beige powder, which contained approximately 35 mg of DCM. The colorless blocks obtained from recrystallization were found to be of good quality by the X-ray crystallography lab; no additional NMR spectra were obtained.

221. It is important not to expose the crystals to reduced pressure.

222. 192C Kolthoff Hall, Le Claire-Dow Instrumentation Facility, Univeristy of Minnesota, Minneapolis, MN, USA. The XCL is directed by Victor G. Young, Jr.

223. The crystallographic samples were synthesized by Gregory Kent Sutton, an undergraduate researcher in the Noland Group from 2003–2004. Recrystallization and crystallographic analyses were performed by Dr. Britton some time between 2004 and 2009. These compounds were synthesized again in the present study in order to obtain additional characterization and yield data. By this time, Dr. Britton was no longer able to perform additional crystallographic work.

224. Structure factor files are required for CCDC deposition. Structure factor files for these samples were missing from Dr. Britton's computer at the time this dissertation was completed.

225. Allen, F. H.; Johnson, O.; Shields, G. P.; Smith, B. R.; Towler, M. *J. Appl. Crystallogr.* **2004**, *37*, 335–338.

226. Blessing, R. H. *Acta Crystallogr. Sect. A* **1995**, *51*, 33–38.

227. Sheldrick, G. M. *Acta Crystallogr. Sect. A* **2015**, *71*, 3–8.

Appendix I. NMR Data for Products in Part I and §§ 3.2–3.3

Table 31 (1 of 2). The contents of Appendix I.

compound	page	nickname
2i	251	cyclononanone
2j	254	cyclodecanone
2k	257	cycloundecanone
3	260	undecanedioic acid
4	263	indole dimer
5	266	indole trimer
6	268	biindolyl
7a	273	formaldehyde bisindole
7b	276	acetone bisindole
7c	279	acetophenone bisindole
7d	282	cyclobutanone bisindole
7e	285	cyclopentanone bisindole
7f	288	cyclohexanone bisindole
7g	292	cycloheptanone bisindole
7h	296	cyclooctanone bisindole
7i	300	cyclononanone bisindole
7j	305	cyclodecanone bisindole
7k	309	cycloundecanone bisindole
7l	313	cyclododecanone bisindole
8d	317	cyclobutanone 2:2 product
8e	339	cyclopentanone 2:2 product

Table 30 (2 of 2). The contents of Appendix I.

compound	page	nickname
9f	363	cyclohexanone 2:2 product
10g	370	cycloheptanone indolocarbazole
10l	390	cyclododecanone indolocarbazole
11h	398	cyclooctanone carbazolylaniline
12h	401	cyclooctanone diazepine
13k	424	cycloundecylindole
13l	428	cyclododecylindole
14	435	unidentified cyclododecanone product
15	442	cyclopentanone aldol
16	445	cyclopentanone epoxide
17b	448	dimethylcyclohexanedione
17c	450	dimethyldimedone
17d	452	spiro cyclopentane diketone
18a	454	cyclohexanone hydrazone
18b	456	cyclohexanedione hydrazone
18c	459	dimedone hydrazone
18d	461	spiro cyclopentane hydrazone
19a	464	tetrahydrocarbazole

^{1}H NMR 400 MHz in $CDCl_3$

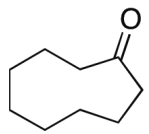

2i

^{1}H NMR 400 MHz in $CDCl_3$
2i
O
2.425
2.417
2.410
2.402
2.394
2.259
1.860
1.855
1.851
1.845
1.838
1.829
1.820
1.814
1.807
1.804
1.799
1.577
1.556
1.547
1.532
1.517
1.382
1.367
1.361
1.352
1.343
1.337
1.322
acetic acid (3H)
0.10
3.96
3.99
4.07
3.98
2.6
2.5
2.4
2.3
2.2
2.1
2.0
1.9
1.8
1.7
1.6
1.5
1.4
1.3
1.2
(ppm)

^{13}C NMR 101 MHz in $CDCl_3$

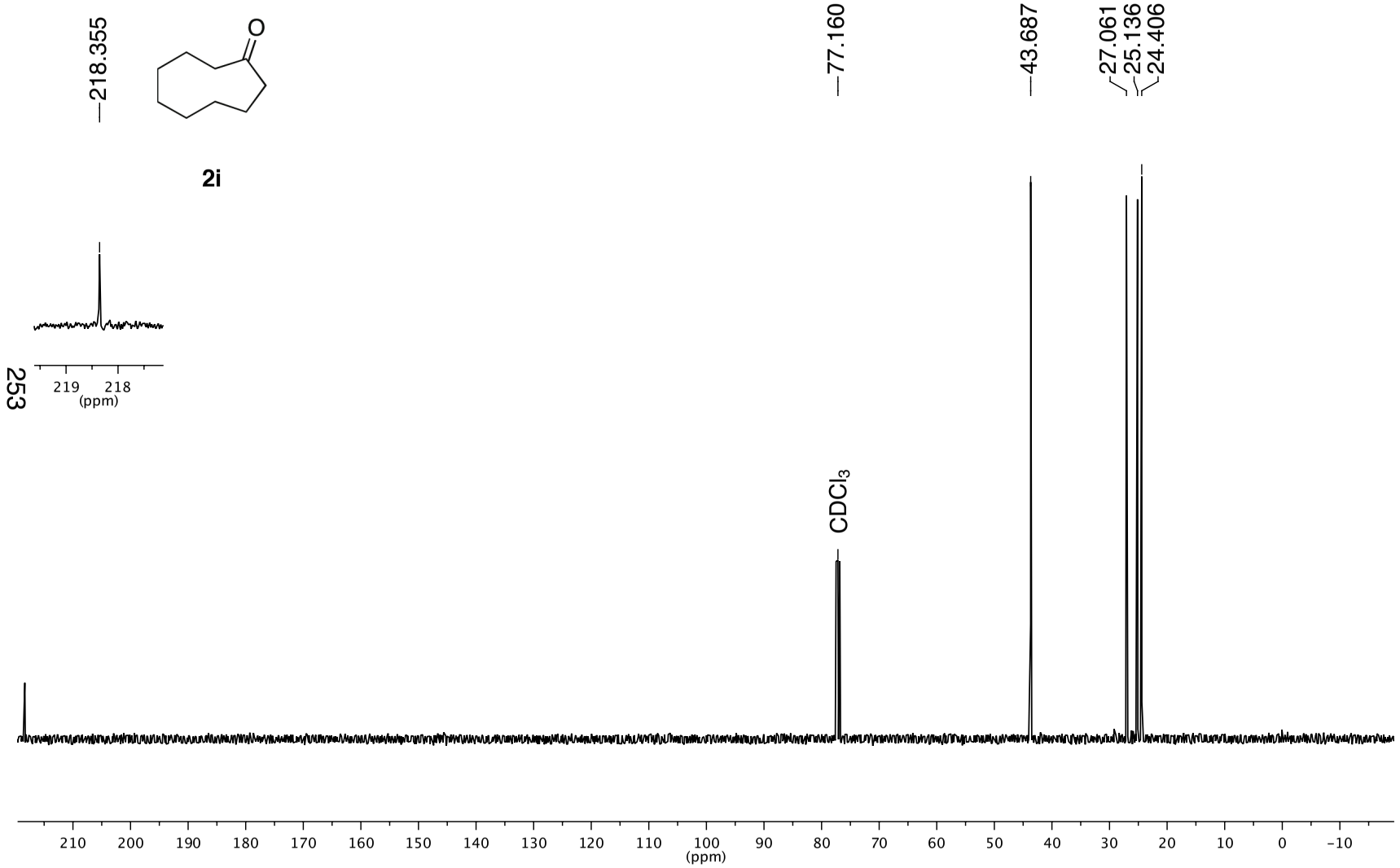

2i

^{1}H NMR 500 MHz in $CDCl_3$

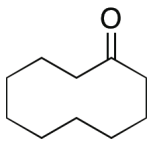

2j

^{1}H NMR 500 MHz in $CDCl_3$

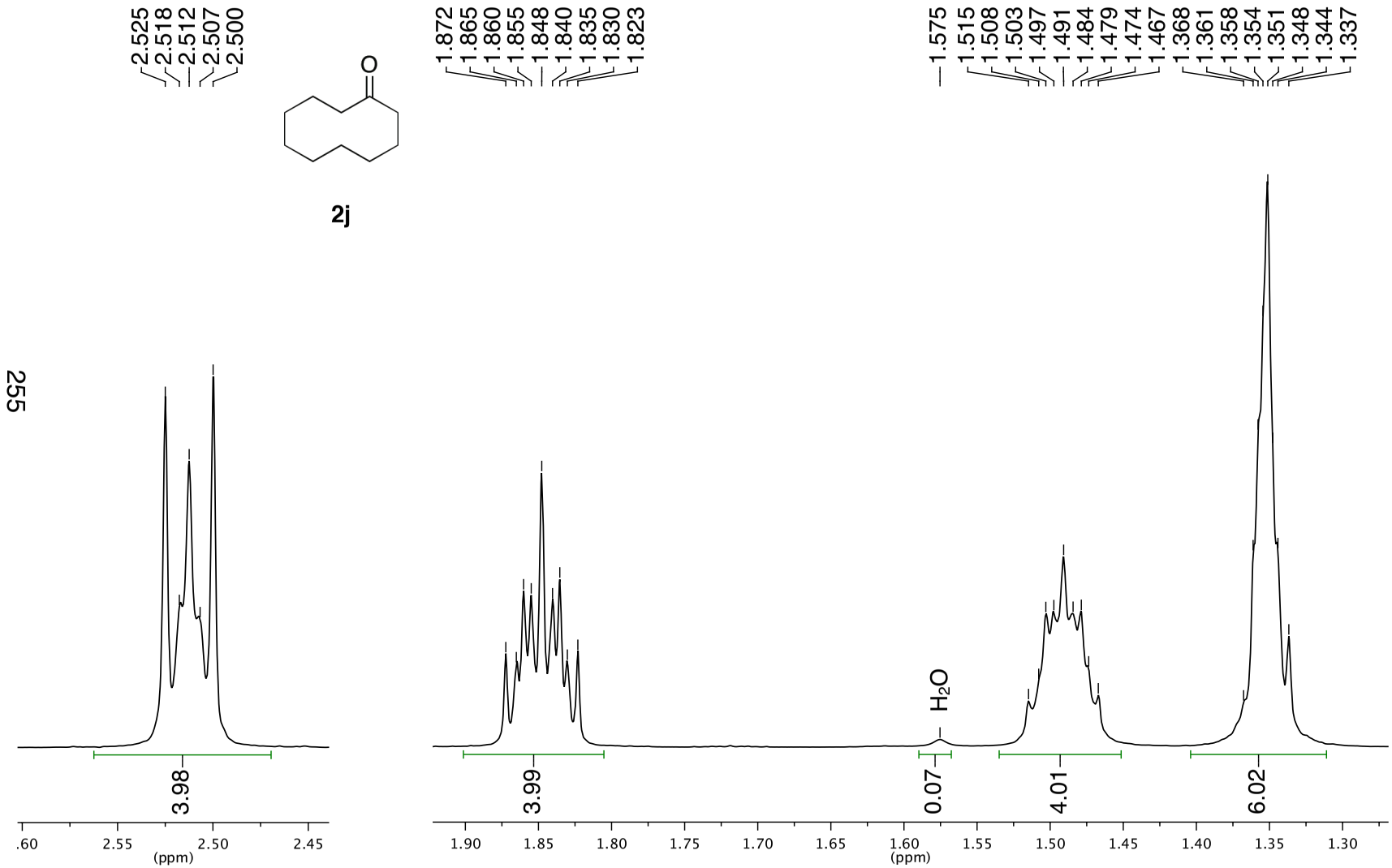

^{13}C NMR 126 MHz in $CDCl_3$

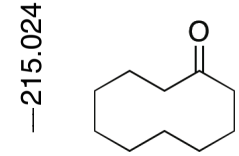

2j

^{1}H NMR 500 MHz in $(CD_3)_2SO$

^{1}H NMR 500 MHz in $(CD_3)_2SO$

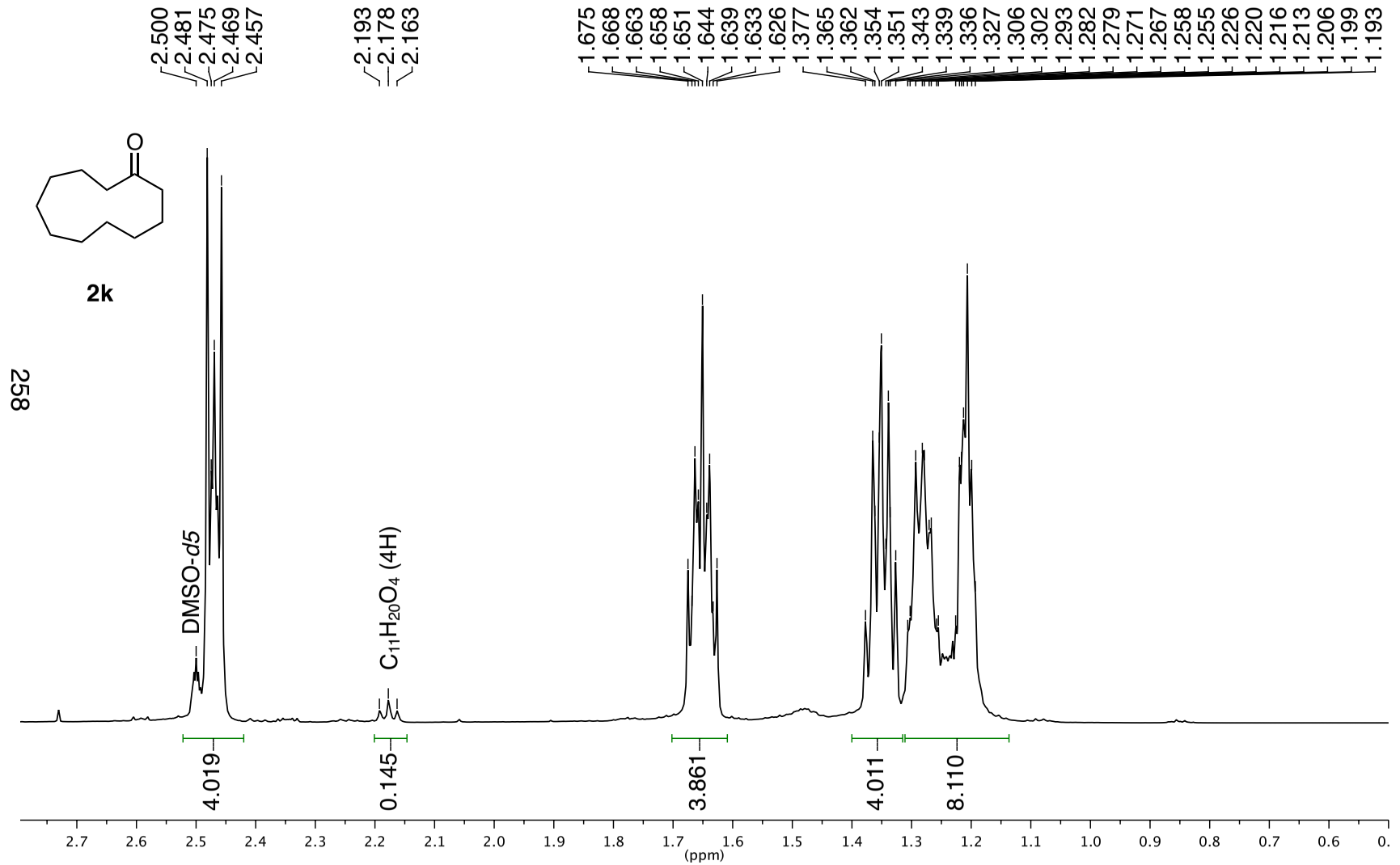

^{13}C NMR 126 MHz in CD_3CN

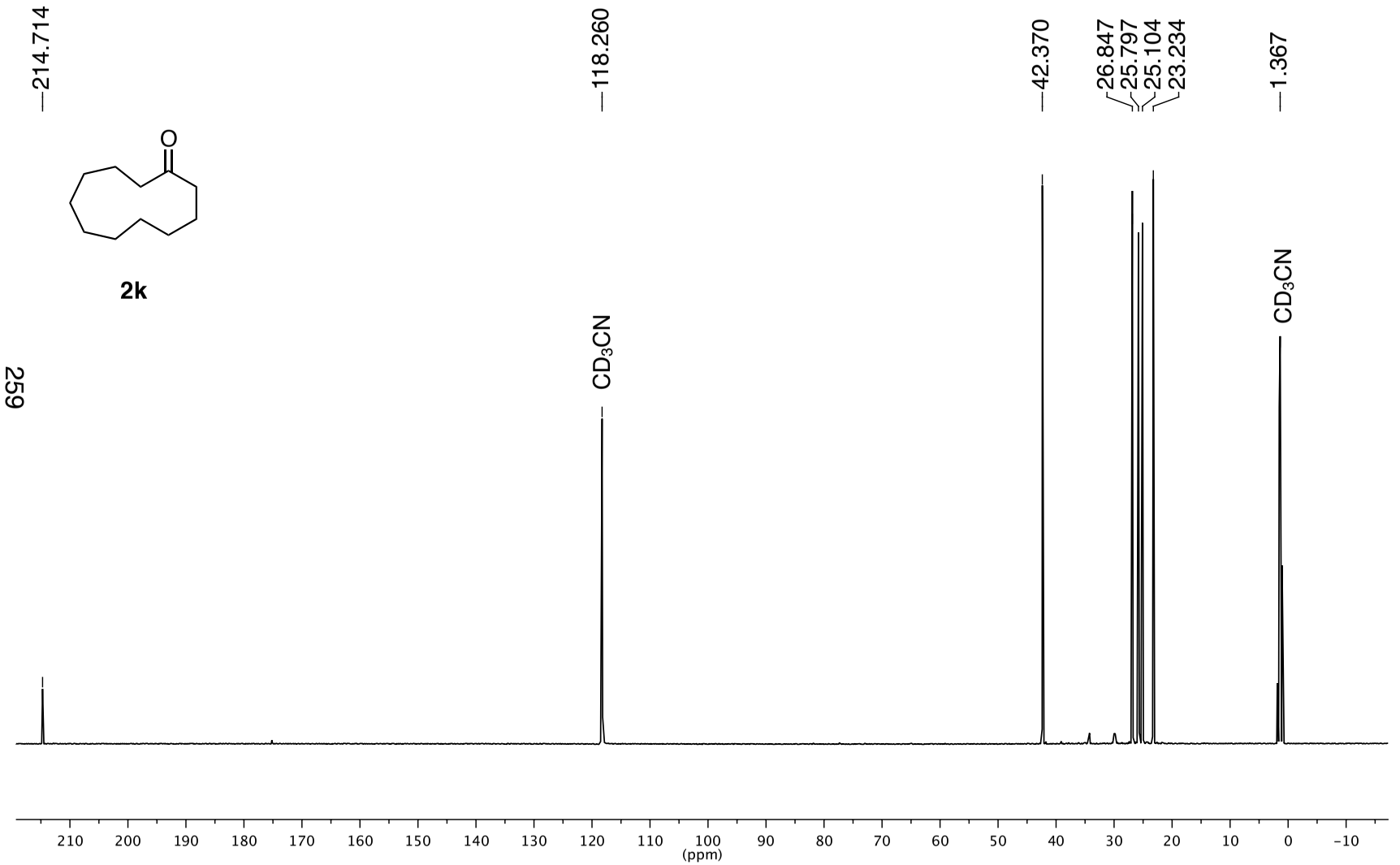

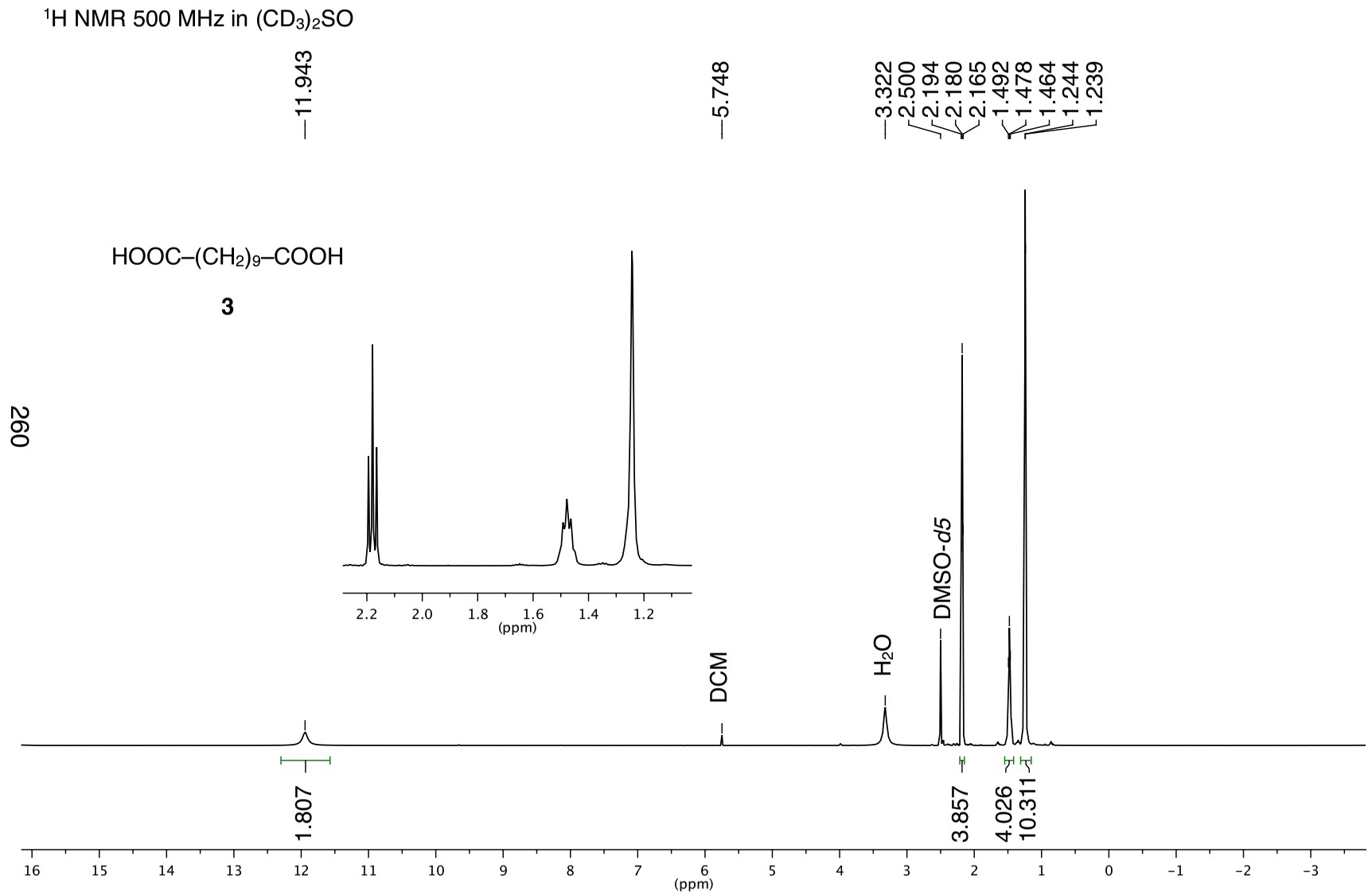
^{1}H NMR 500 MHz in $(CD_3)_2SO$
11.943
5.748
3.322
2.500
2.194
2.180
2.165
1.492
1.478
1.464
1.244
1.239
HOOC–$(CH_2)_9$–COOH
3
260
DCM
H_2O
DMSO-*d5*
1.807
3.857
4.026
10.311
(ppm)

^{13}C NMR 126 MHz in $(CD_3)_2SO$

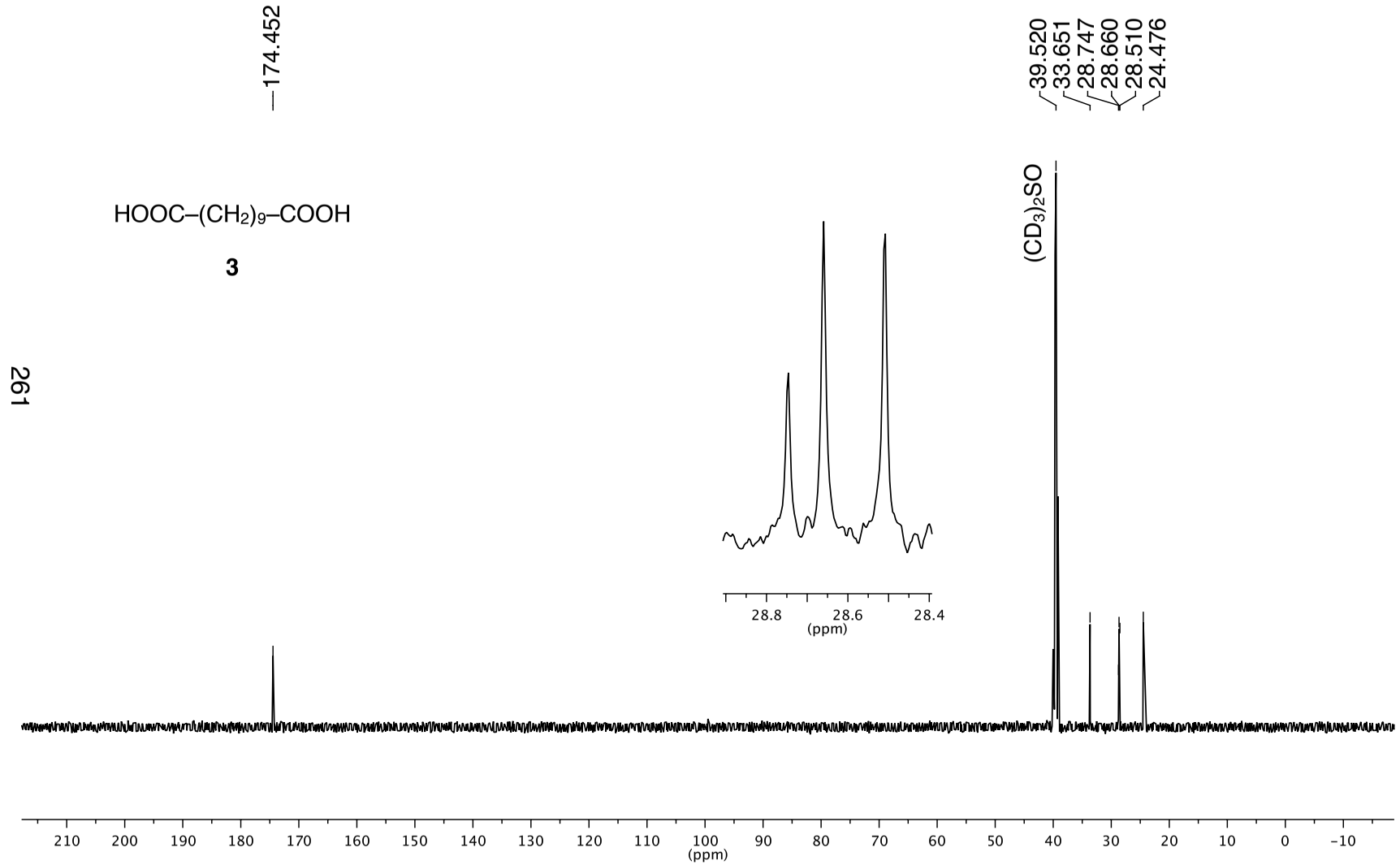

$HOOC–(CH_2)_9–COOH$

3

261

$^{1}H/^{13}C$ DEPT135 500 MHz in $(CD_3)_2SO$

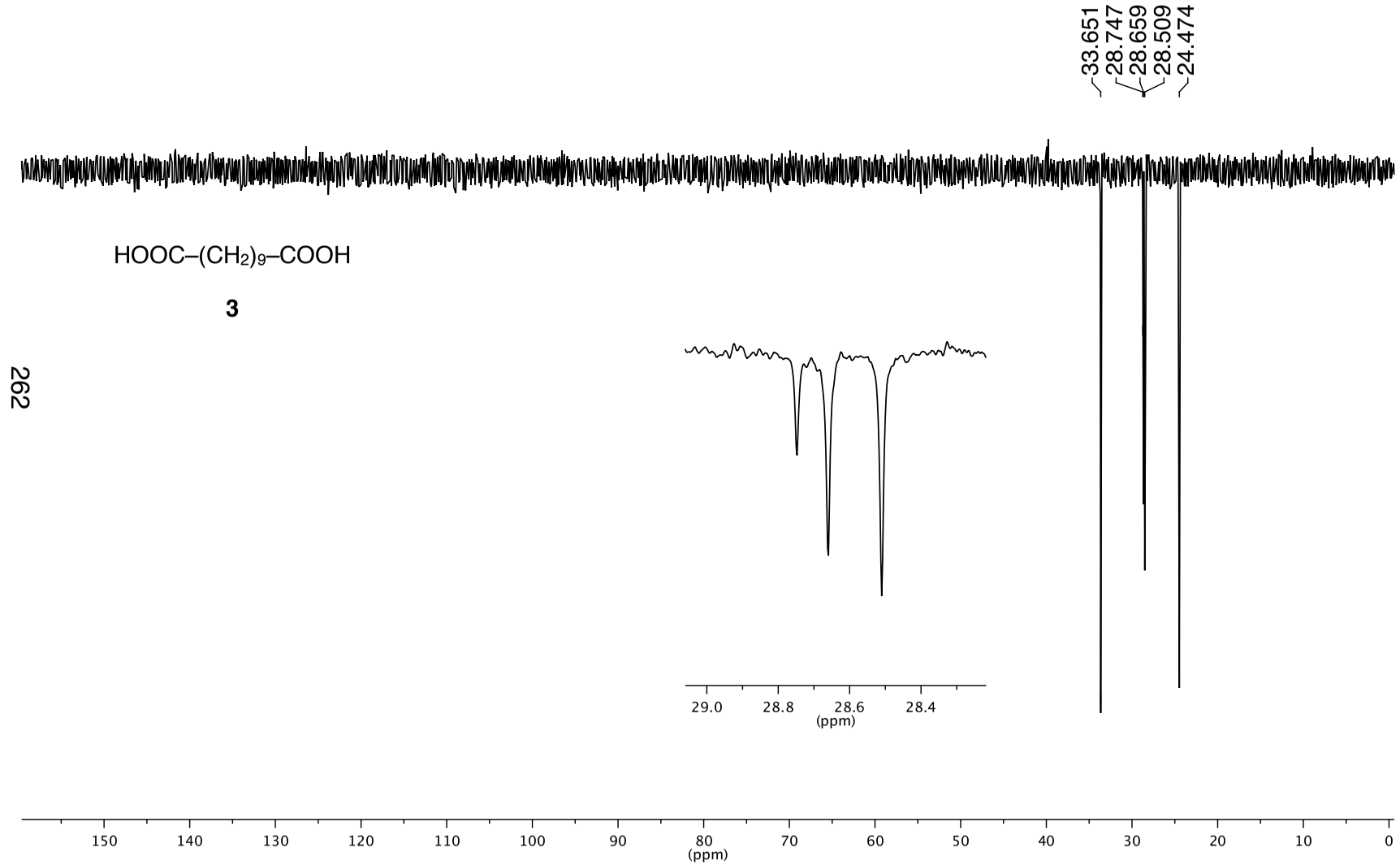

^{1}H NMR 500 MHz in CD_2Cl_2
4
8.182
5.259
5.257
5.238
5.236
5.234
5.234
5.215
5.213
3.481
3.458
3.442
3.420
3.182
3.161
3.143
3.122
CDHCl$_2$ 5.320
4.193
4.095
4.077
4.060
4.042
EtOAc
H$_2$O 1.583
EtOAc & hexanes
1.992
1.02
1.01
0.97
2.02
0.99
1.99
1.00
0.97
1.00
0.69
1.13
1.06
1.00
1.13
1.06
(ppm)

^{1}H NMR 500 MHz in CD_2Cl_2

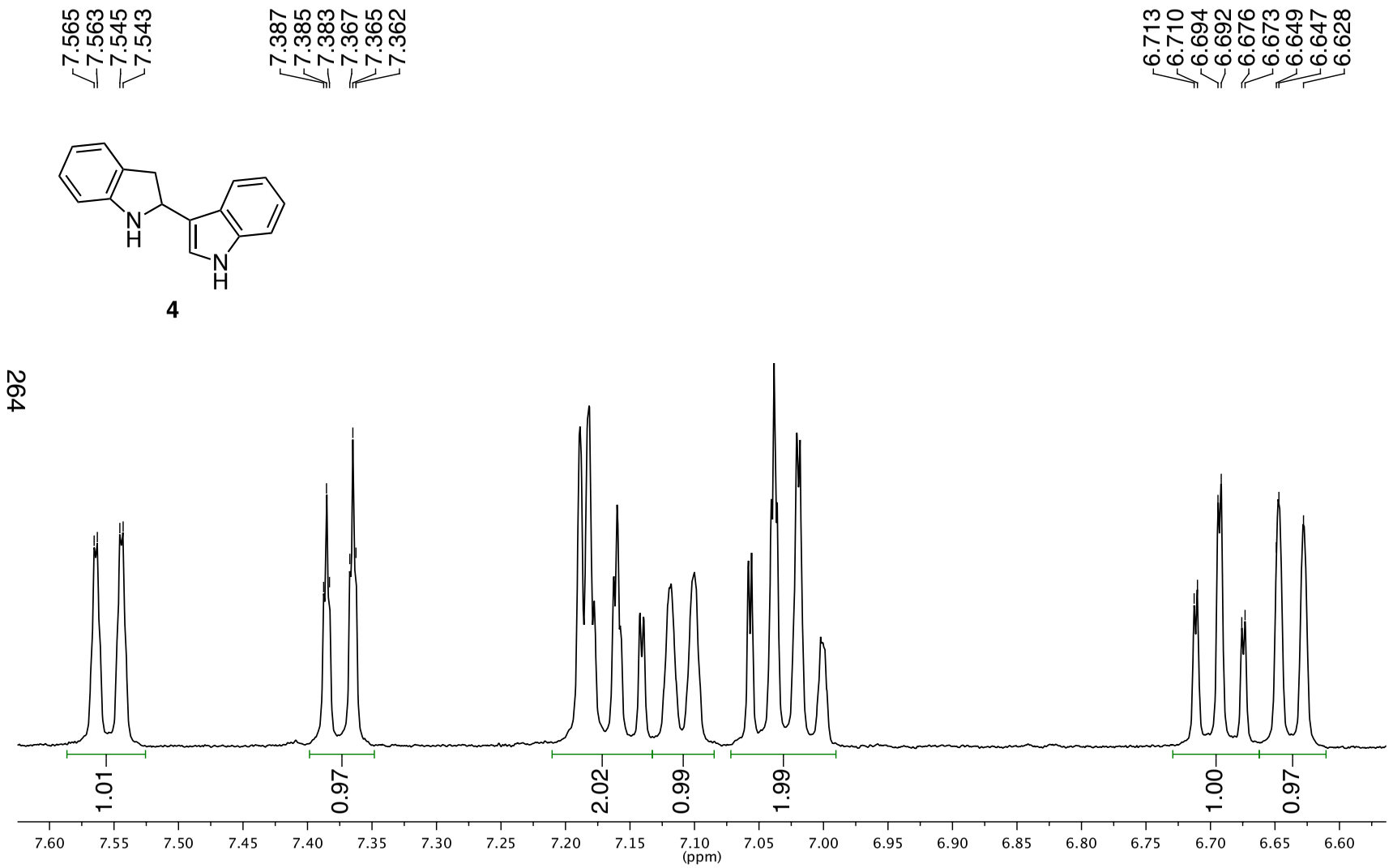

^{1}H NMR 500 MHz in CD_2Cl_2

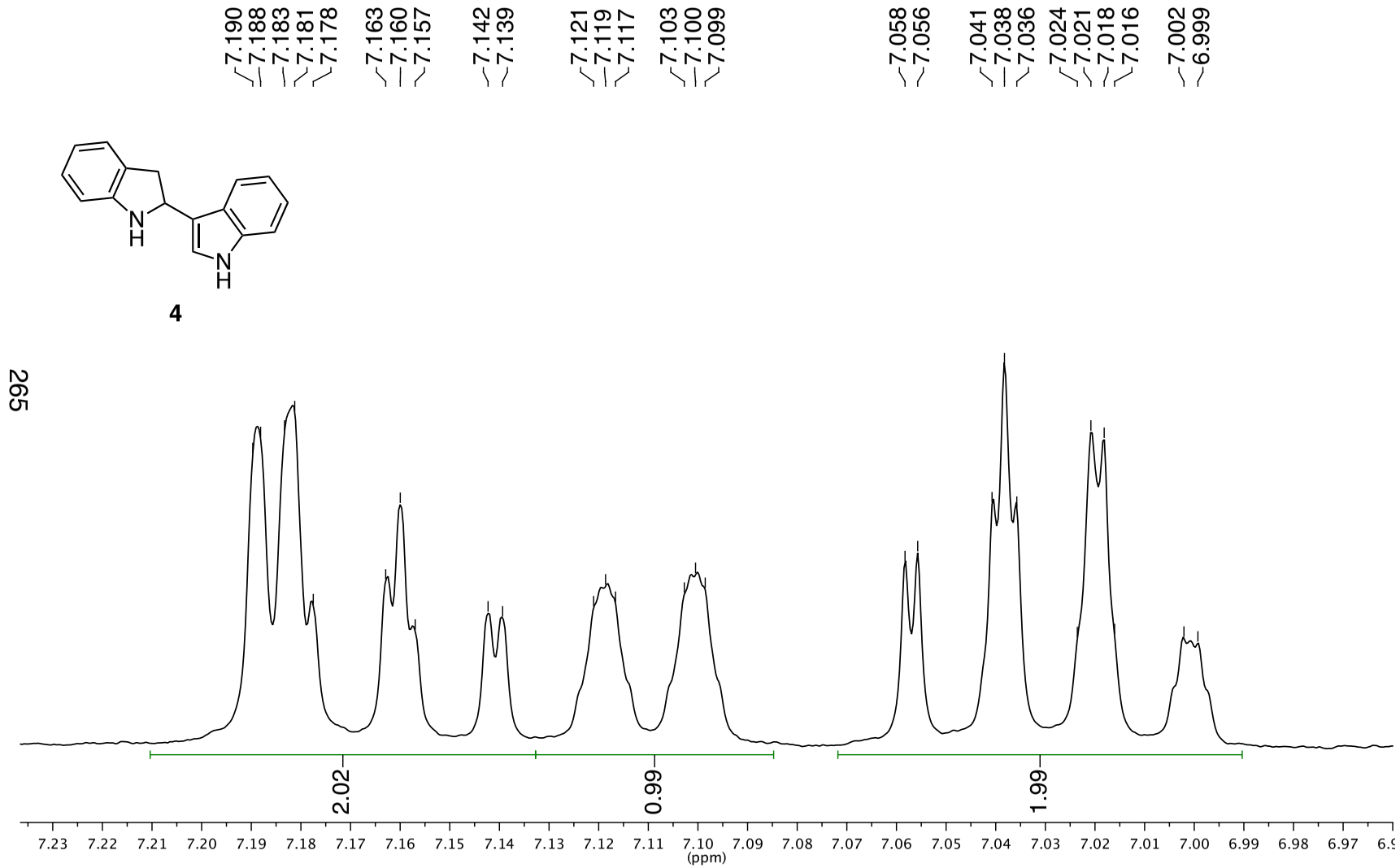

^{1}H NMR 500 MHz in CD_2Cl_2

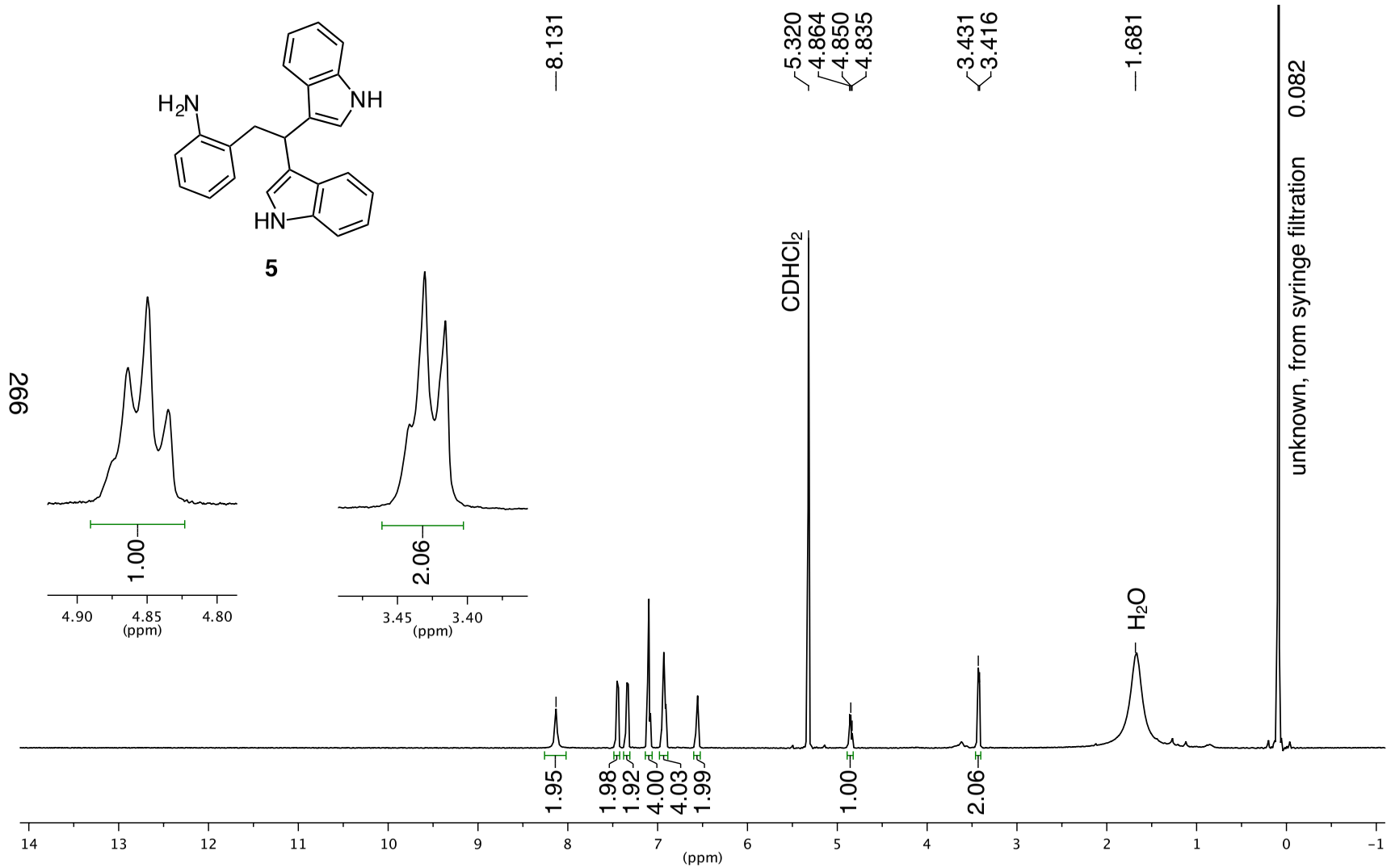

^{1}H NMR 500 MHz in CD_2Cl_2

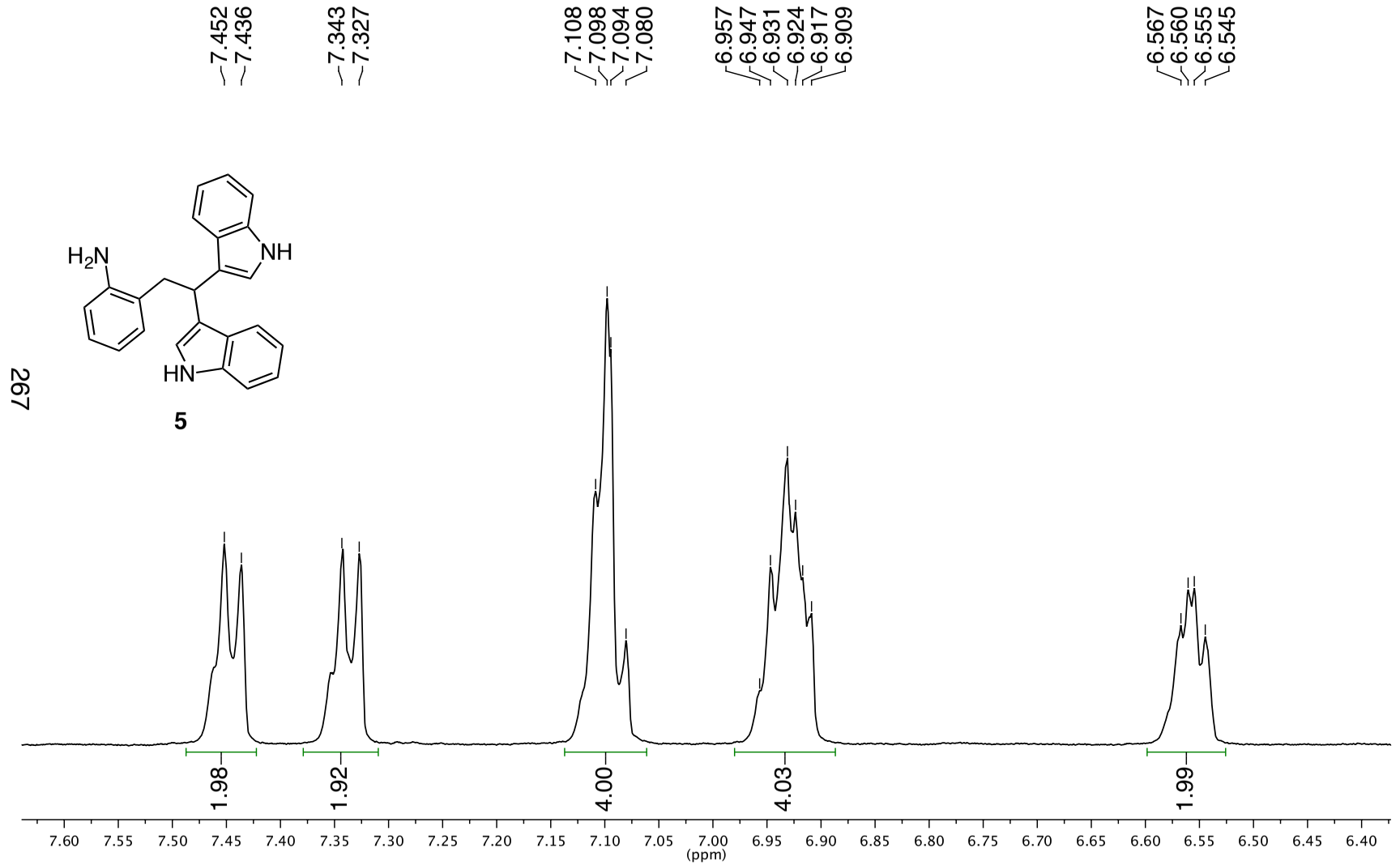

^{1}H NMR 500 MHz in CD_3CN

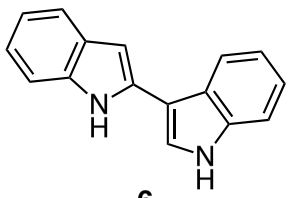

6

^{1}H NMR 500 MHz in CD_3CN

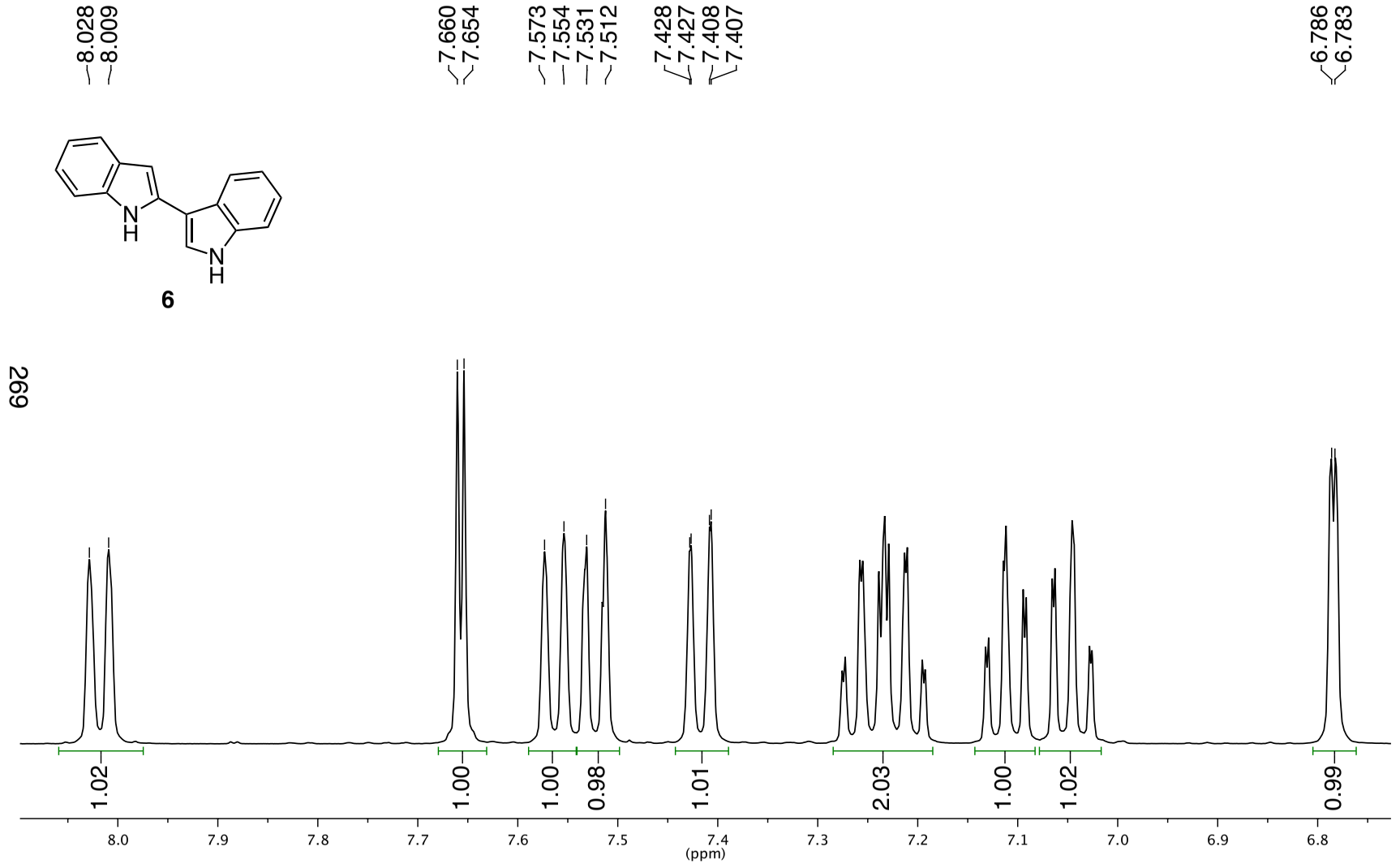

^{1}H NMR 500 MHz in CD_3CN

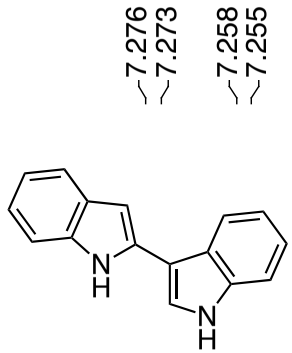

6

^{13}C NMR 126 MHz in CD_3CN

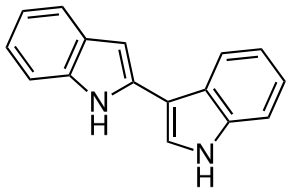

6

^{13}C NMR 126 MHz in CD_3CN

137.859
137.271
134.936
130.560
125.996
123.575
123.323
121.925
121.214
120.671
120.416

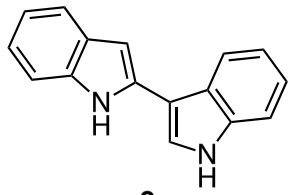

6

(2C)

272

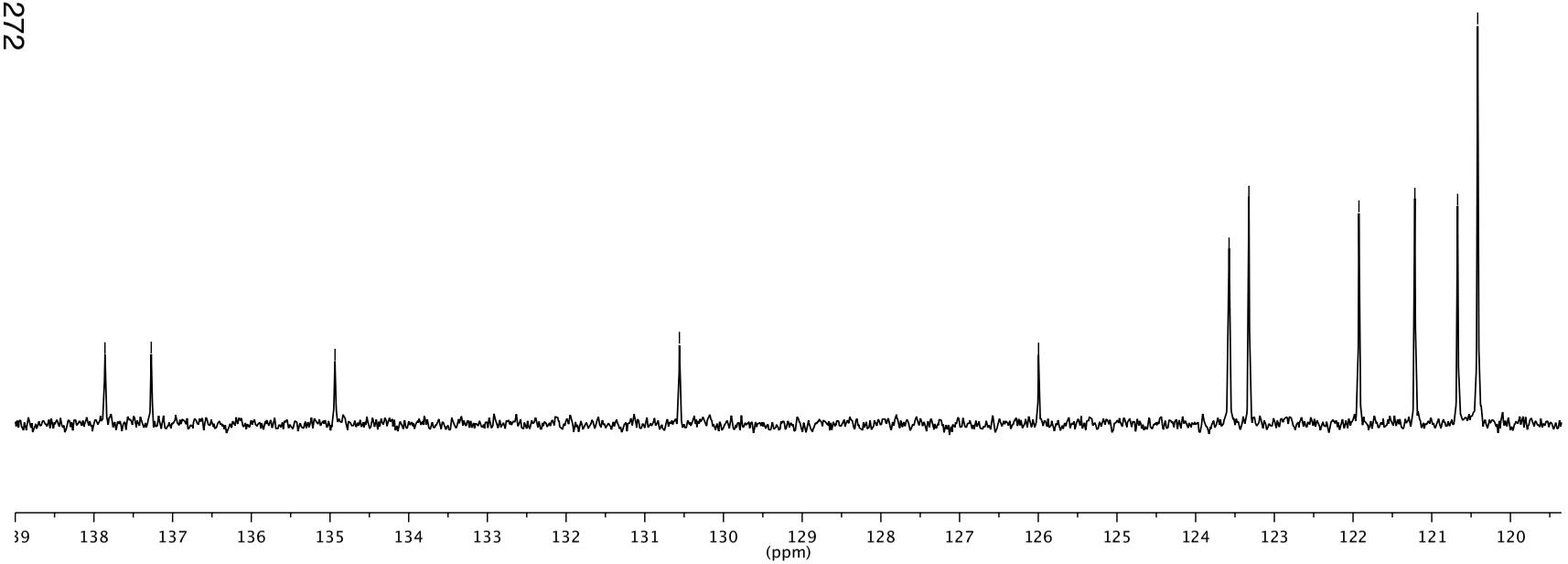

^{1}H NMR 300 MHz in CD_2Cl_2

7a

^{1}H NMR 300 MHz in CD_2Cl_2

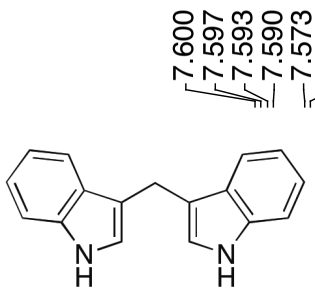

7a

^{13}C NMR 126 MHz in CD_2Cl_2

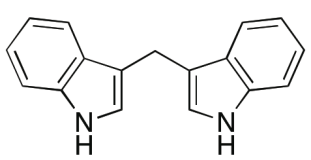

7a

^{1}H NMR 500 MHz in CD_2Cl_2

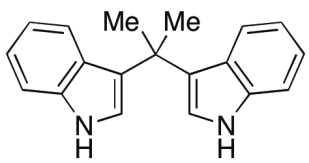

7b

^{1}H NMR 500 MHz in CD_2Cl_2

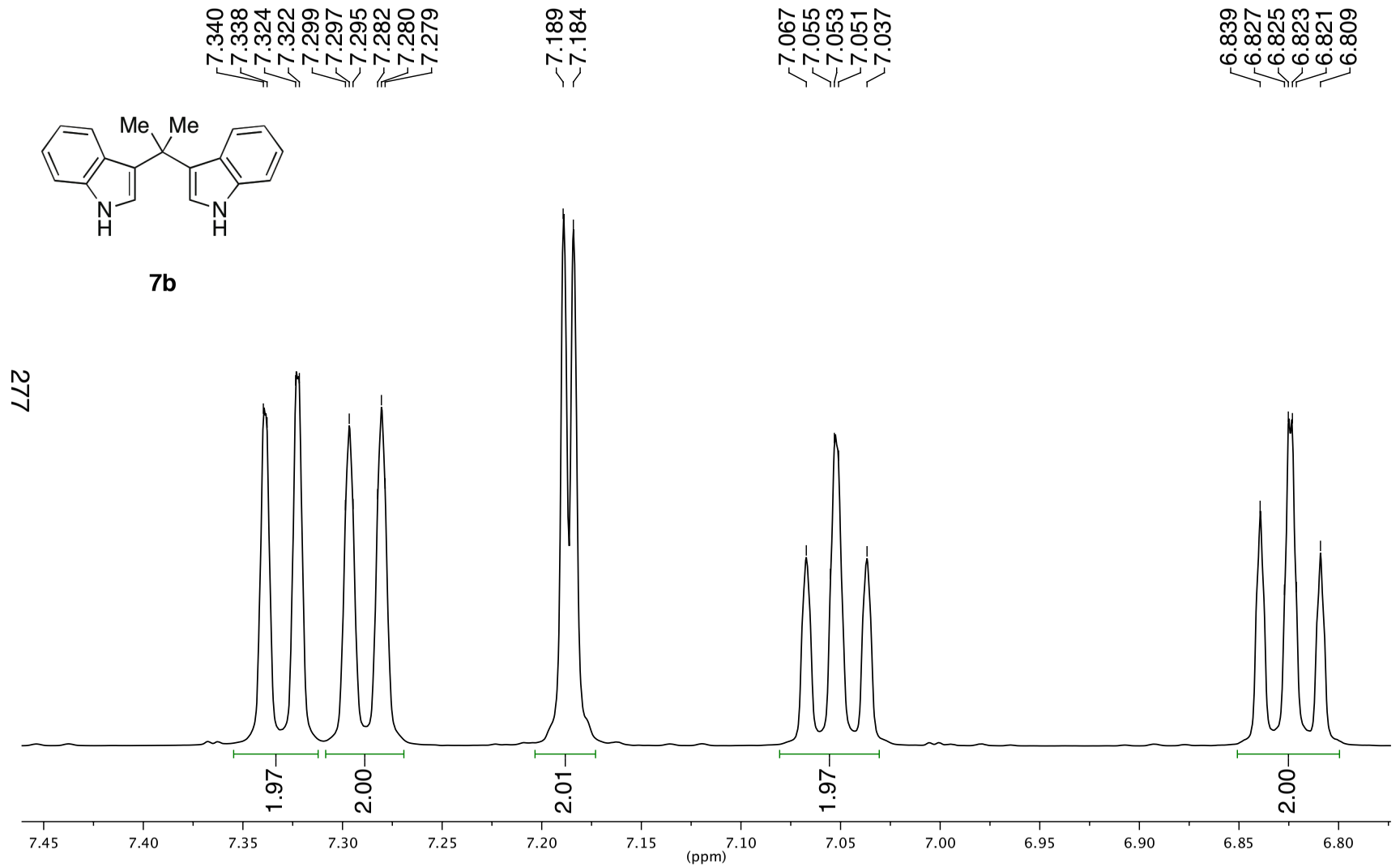

^{13}C NMR 126 MHz in CD_2Cl_2

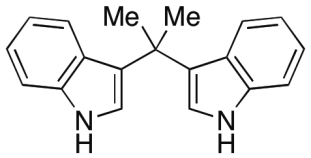

7b

^{1}H NMR 500 MHz in CD_2Cl_2

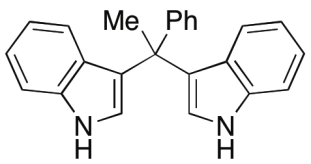

7c

279

^{1}H NMR 500 MHz in CD_2Cl_2

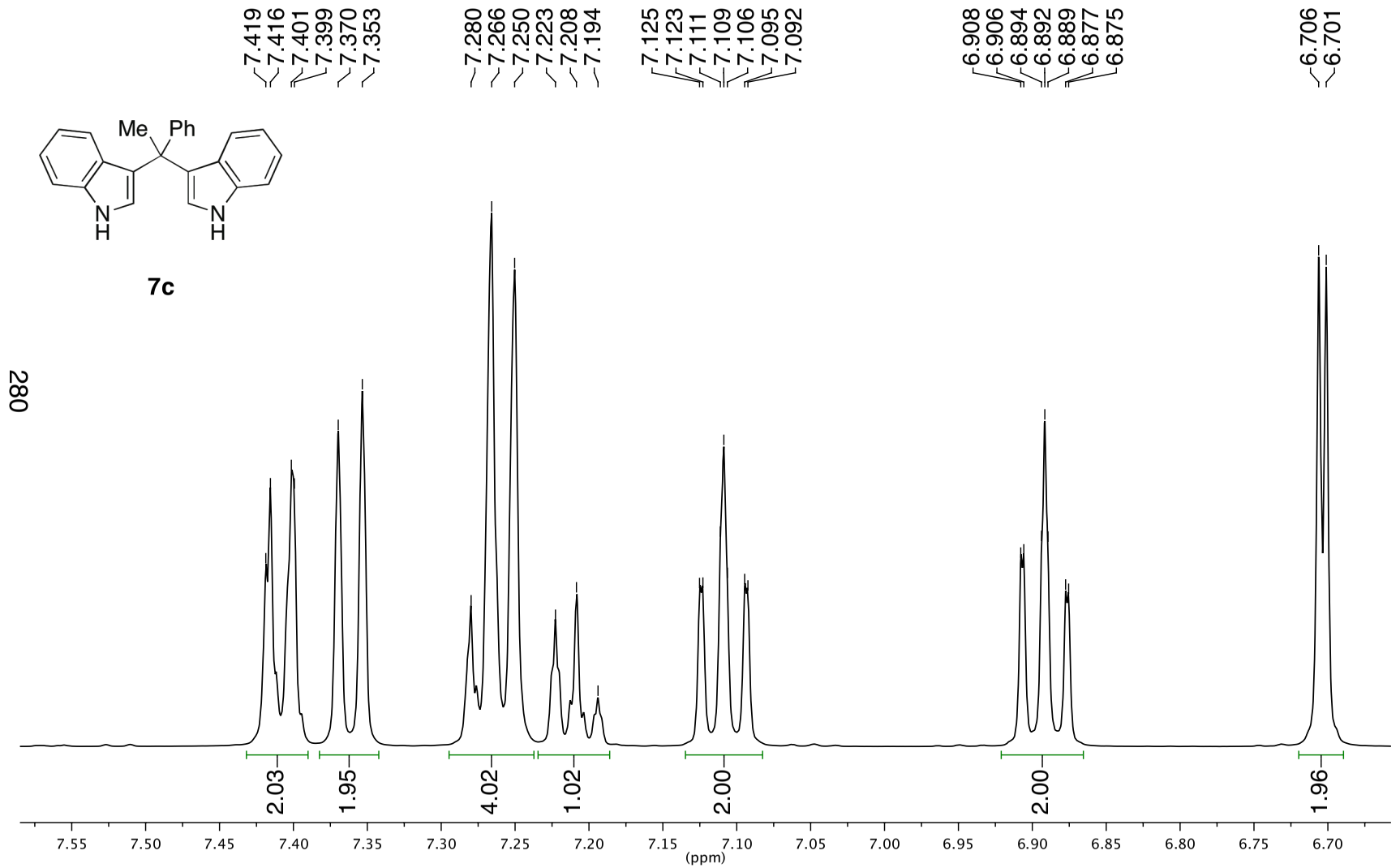

^{13}C NMR 126 MHz in CD_2Cl_2

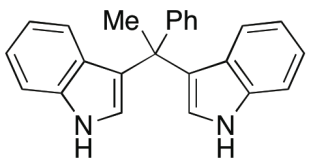

7c

148.686
137.699
128.550
128.246
127.004
126.350
124.910
123.837
122.259
122.006
119.321
111.748
54.000
44.183
29.252
CD_2Cl_2
281
129 128 127 126 125 124 123 122
(ppm)
210 200 190 180 170 160 150 140 130 120 110 100 90 80 70 60 50 40 30 20 10 0 -10
(ppm)

^{1}H NMR 500 MHz in CD_2Cl_2

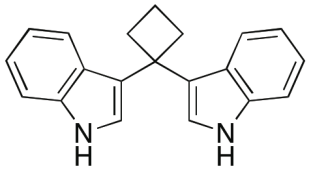

7d

^{1}H NMR 500 MHz in CD_2Cl_2

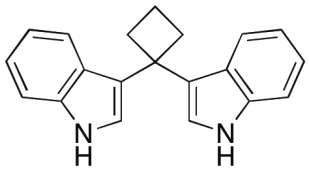

7d

^{13}C NMR 126 MHz in CD_2Cl_2

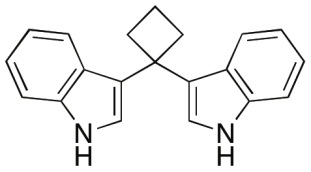

7d

^{1}H NMR 300 MHz in CD_2Cl_2

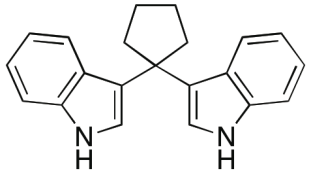

7e

^{1}H NMR 300 MHz in CD_2Cl_2

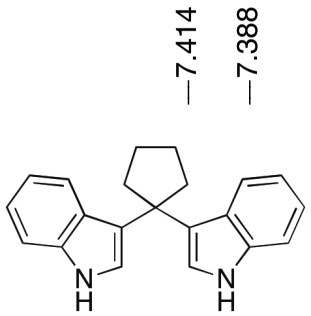

7e

^{13}C NMR 126 MHz in CD_2Cl_2

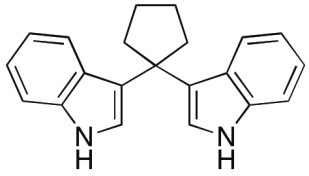

7e

^{1}H NMR 500 MHz in CD_2Cl_2

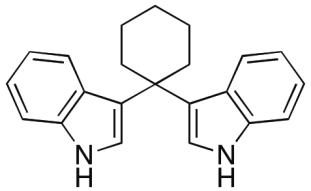

7f

^{1}H NMR 500 MHz in CD_2Cl_2

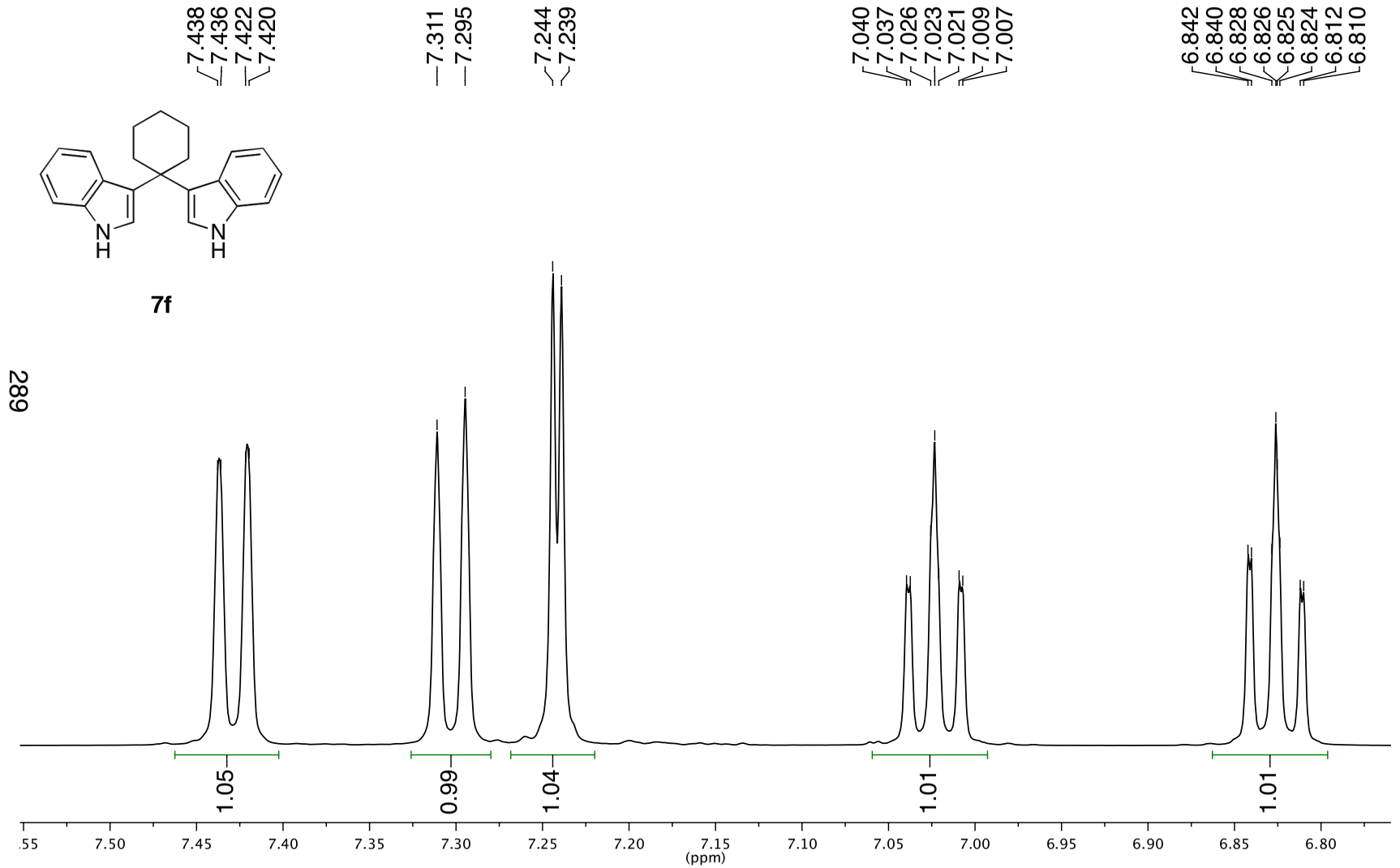

7f

^{1}H NMR 500 MHz in CD_2Cl_2

2.533
2.521
2.509

2.359

7f

1.710
1.699
1.687
1.676
1.664
1.618
1.606
1.596
1.584
1.574
1.539

^{13}C NMR 126 MHz in CD_2Cl_2

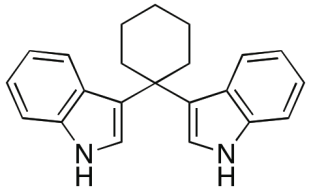

7f

137.546
126.826
124.115
122.351
121.720
121.503
118.918
111.611
54.000
39.692
37.578
27.393
23.564
CD_2Cl_2
291
127 126 125 124 123 122 121 120 119
(ppm)
210 200 190 180 170 160 150 140 130 120 110 100 90 80 70 60 50 40 30 20 10 0 -10
(ppm)

^{1}H NMR 500 MHz in CD_2Cl_2

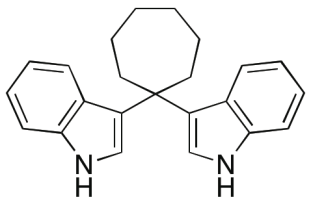

7g

^{1}H NMR 500 MHz in CD_2Cl_2

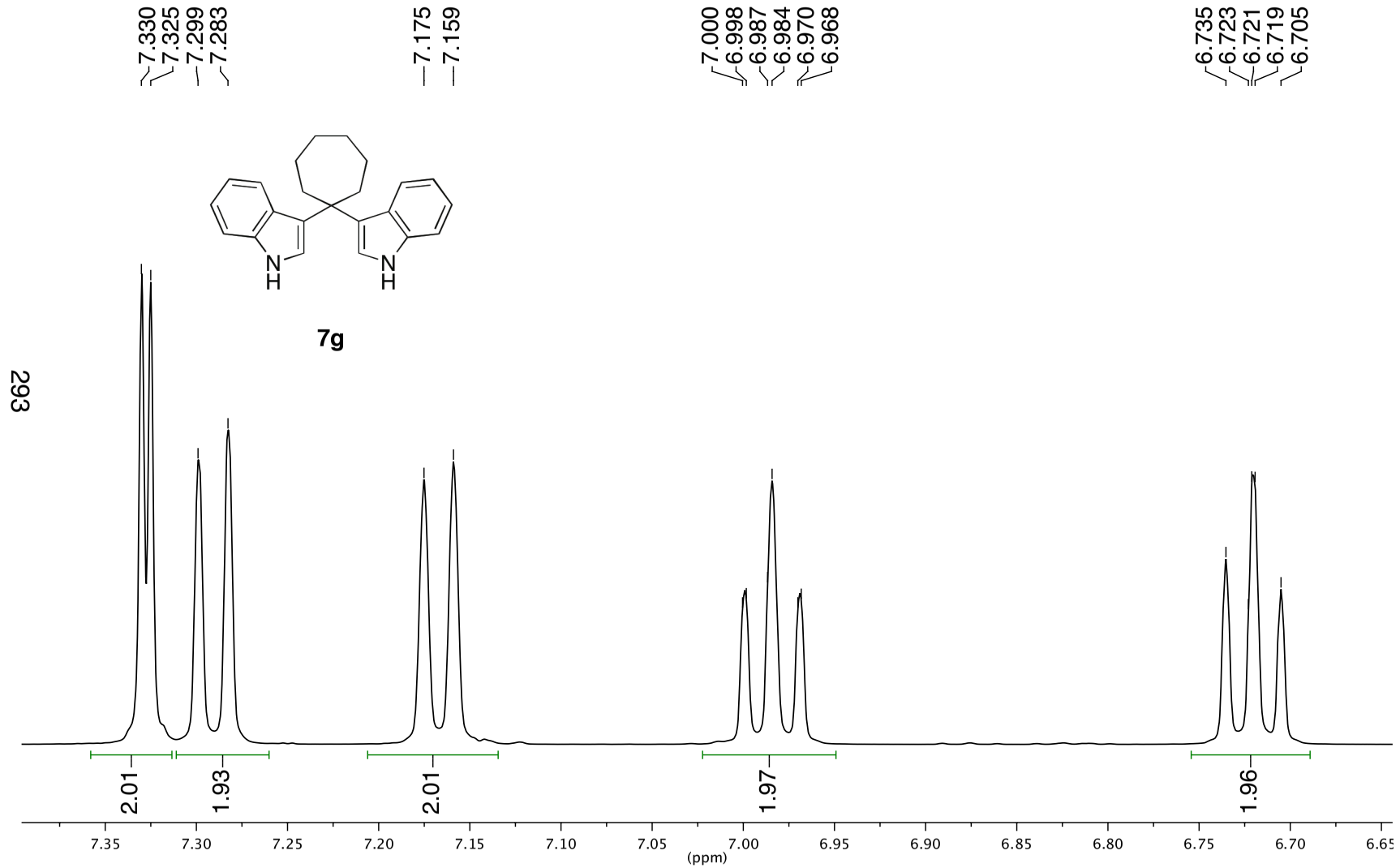

^{1}H NMR 500 MHz in CD_2Cl_2

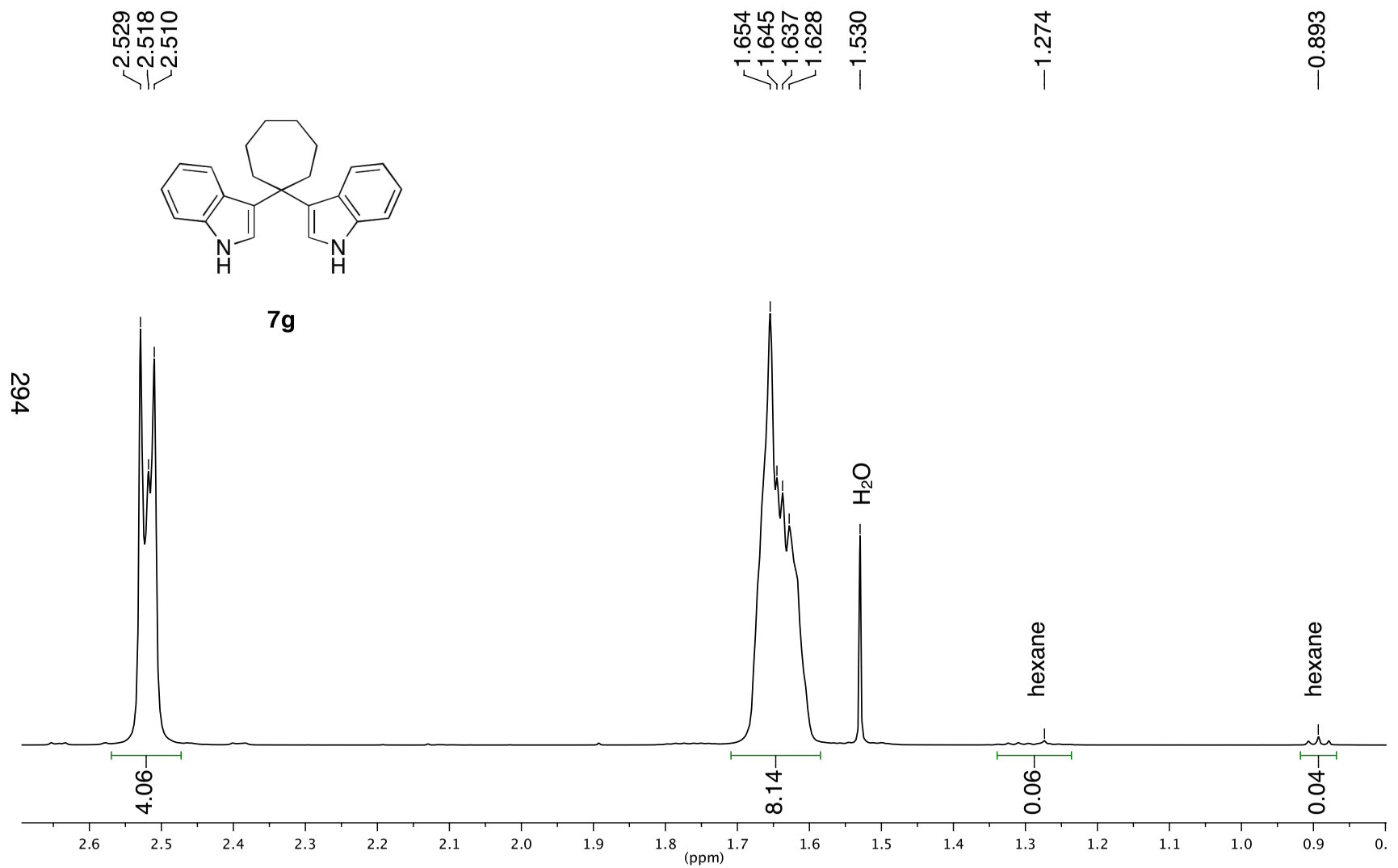

^{13}C NMR 126 MHz in CD_2Cl_2

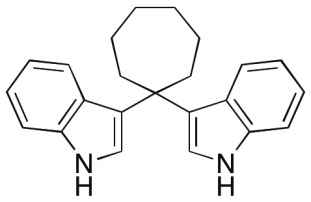

7g

^{1}H NMR 500 MHz in CD_2Cl_2

7h

^{1}H NMR 500 MHz in CD_2Cl_2

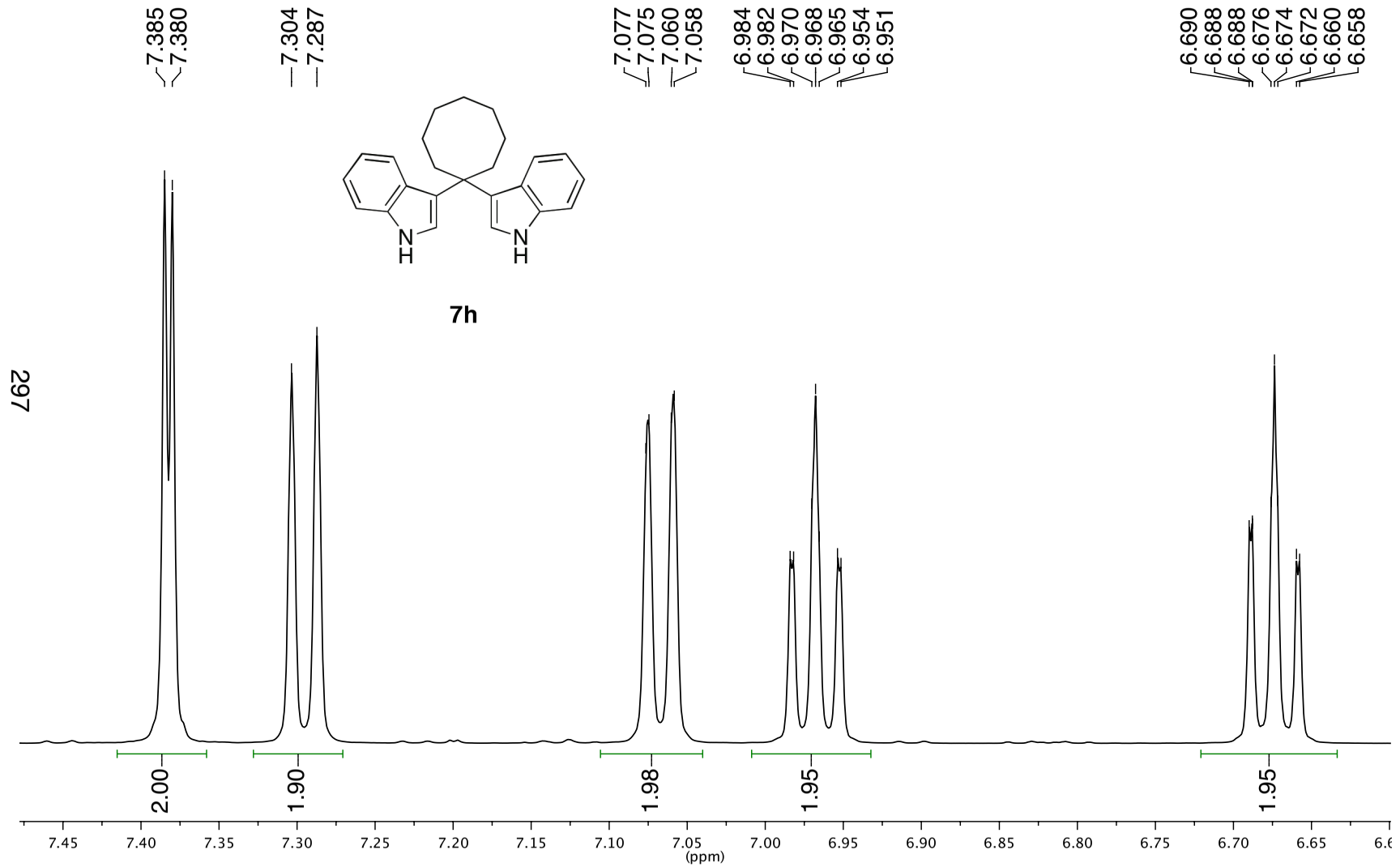

7h

^{1}H NMR 500 MHz in CD_2Cl_2

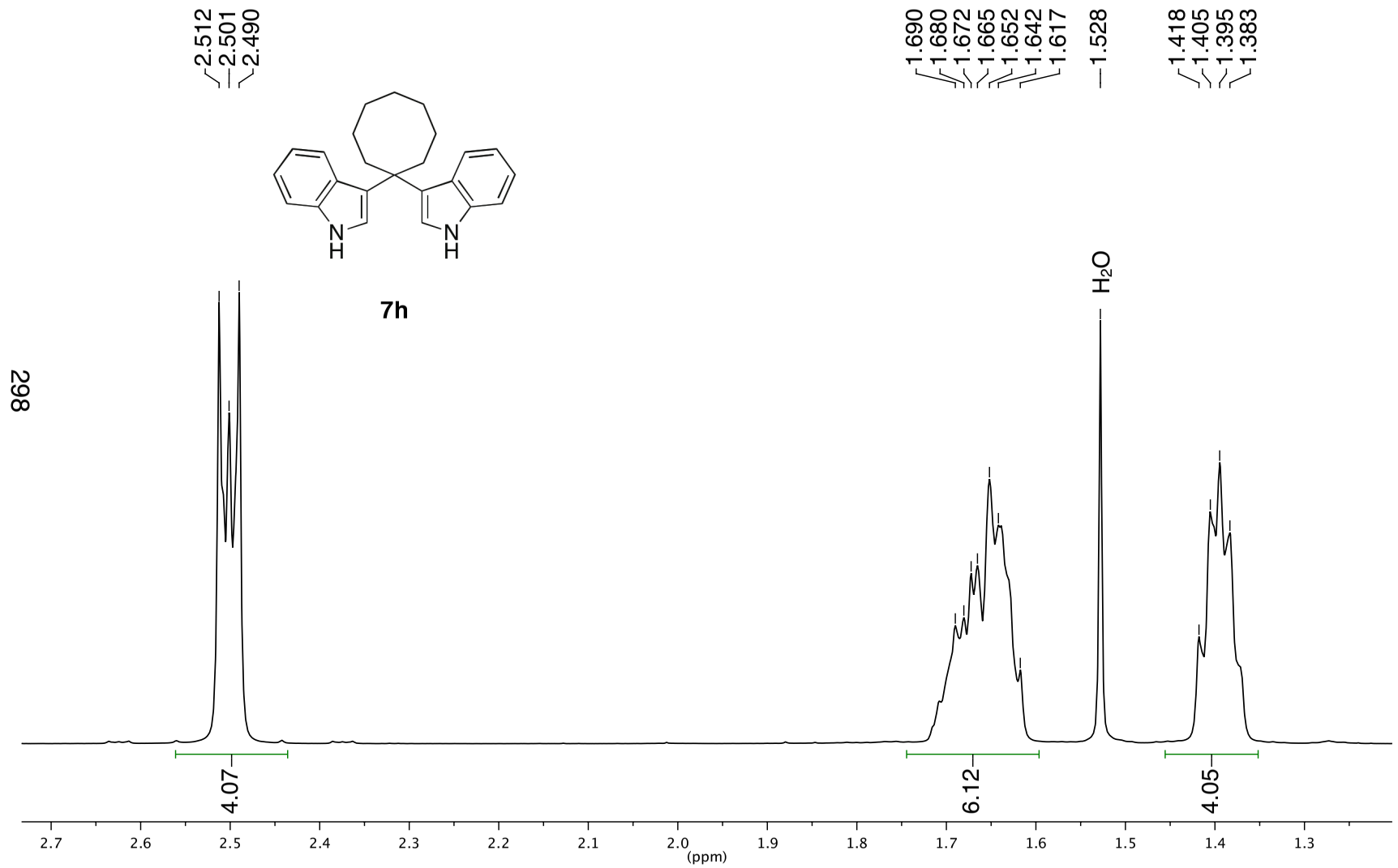

^{13}C NMR 126 MHz in CD_2Cl_2

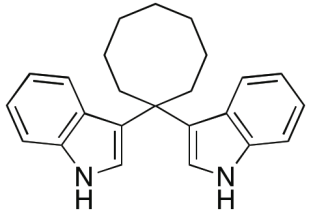

7h

^{1}H NMR 500 MHz in CD_2Cl_2

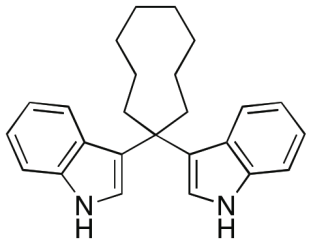

7i

mixture includes:
0.34 equiv. indole
0.47 equiv. EtOAc

Some signals are from **7i** and some are from EtOAc.

^{1}H NMR 500 MHz in CD_2Cl_2

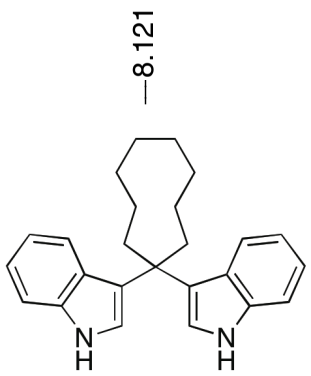

7i

mixture includes:
0.34 equiv. indole
0.47 equiv. EtOAc

^{1}H NMR 500 MHz in CD_2Cl_2
4.126
4.112
4.097
4.083
2.427
2.415
2.402
2.024
1.624
1.617
1.610
1.605
1.543
1.495
1.483
1.471
1.313
1.300
1.287
1.275
1.273
1.265
1.251
1.236
7i
mixture includes:
0.34 equiv. indole
0.47 equiv. EtOAc
EtOAc (2H)
7i (4H)
EtOAc (3H)
7i (4H)
H2O
7i (4H)
overlapping:
7i (4H) and EtOAc (3H)
0.89
4.00
1.44
5.19
4.89
5.87
(ppm)

^{13}C NMR 126 MHz in CD_2Cl_2

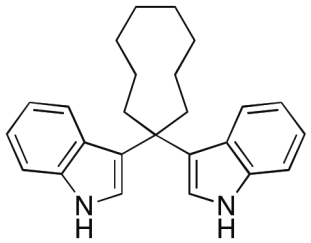

7i

mixture includes:
0.34 equiv. indole
0.47 equiv. EtOAc

303

^{13}C NMR 126 MHz in CD_2Cl_2

123.864
121.882
121.793
120.927
118.806

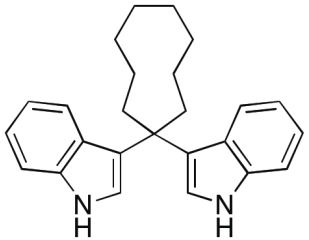

30.267
28.210
21.948
21.369
19.442

7i

mixture includes:
0.34 equiv. indole
0.47 equiv. EtOAc

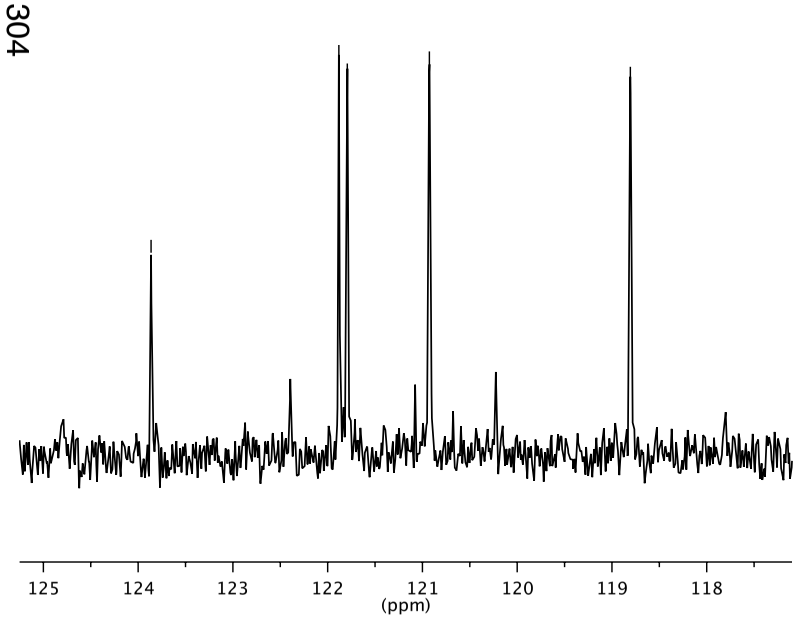

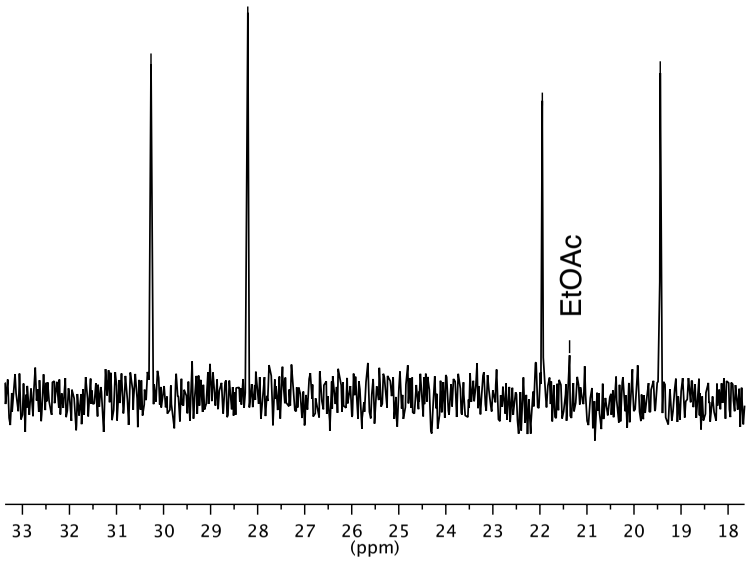

^{1}H NMR 500 MHz in CD_2Cl_2

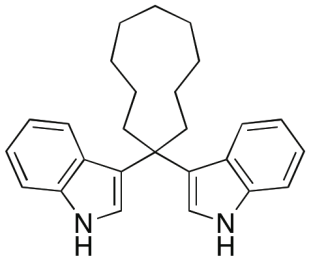

7j

^{1}H NMR 500 MHz in CD_2Cl_2

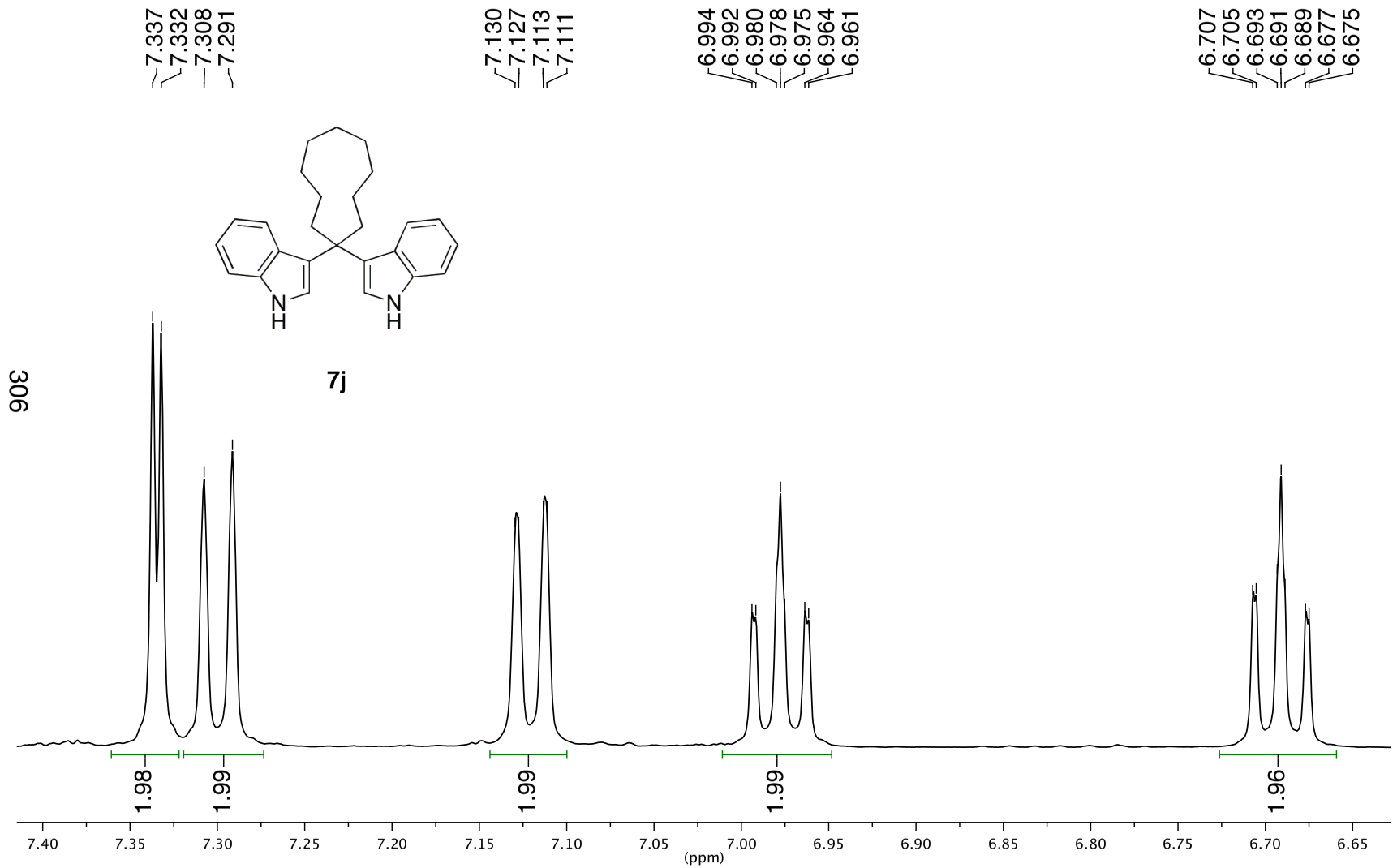

^{1}H NMR 500 MHz in CD_2Cl_2

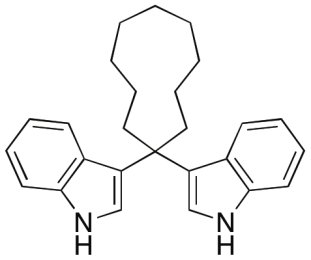

7j

^{13}C NMR 126 MHz in CD_2Cl_2

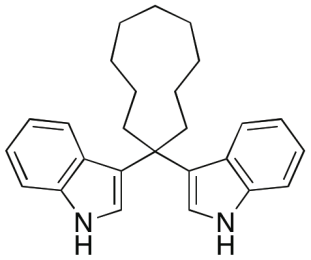

7j

^{1}H NMR 500 MHz in CD_2Cl_2

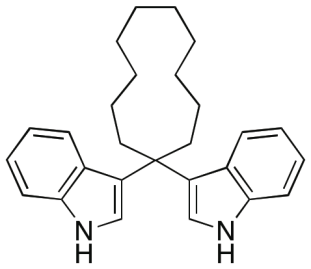

7k

^{1}H NMR 500 MHz in CD_2Cl_2

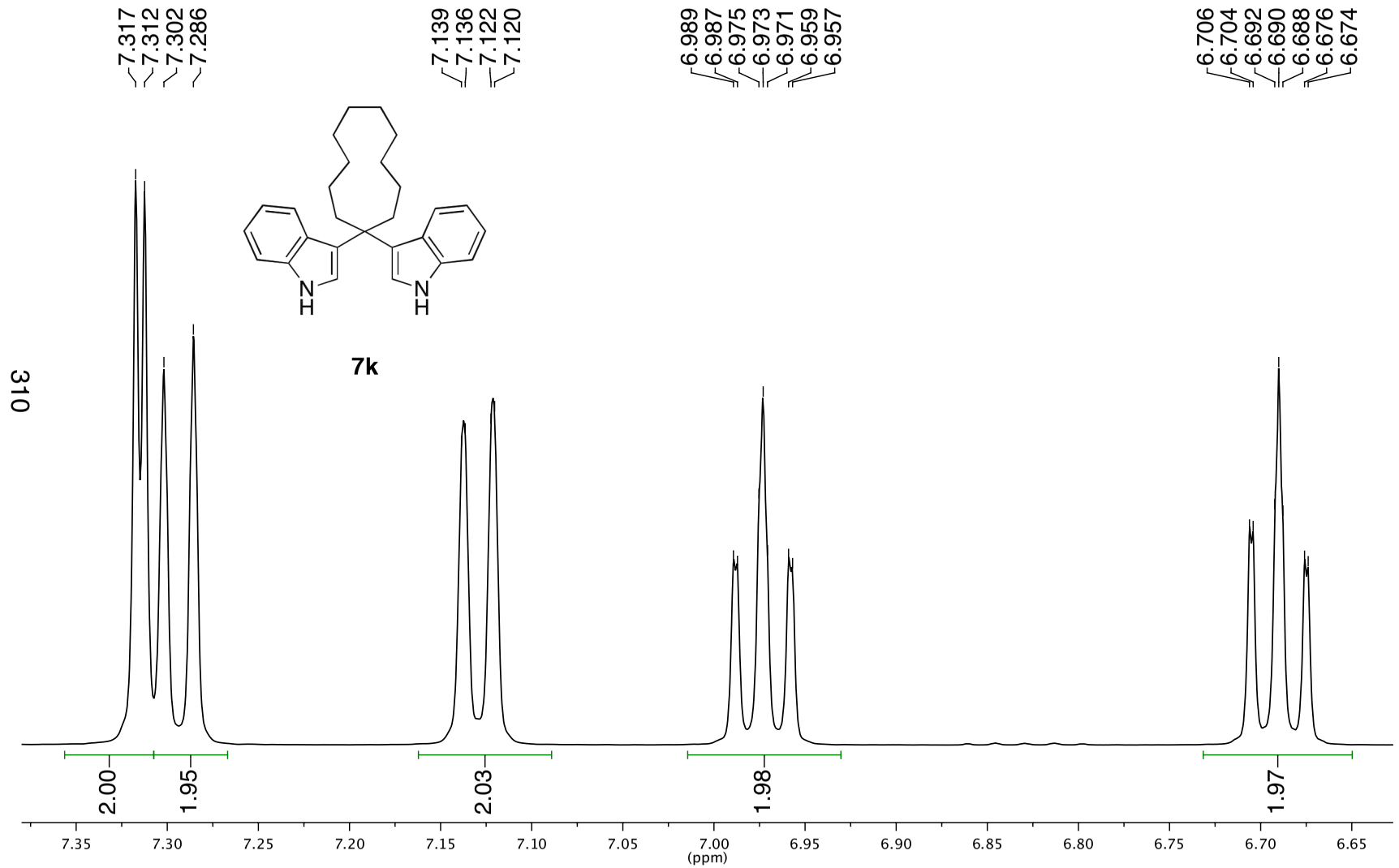

^{1}H NMR 500 MHz in CD_2Cl_2

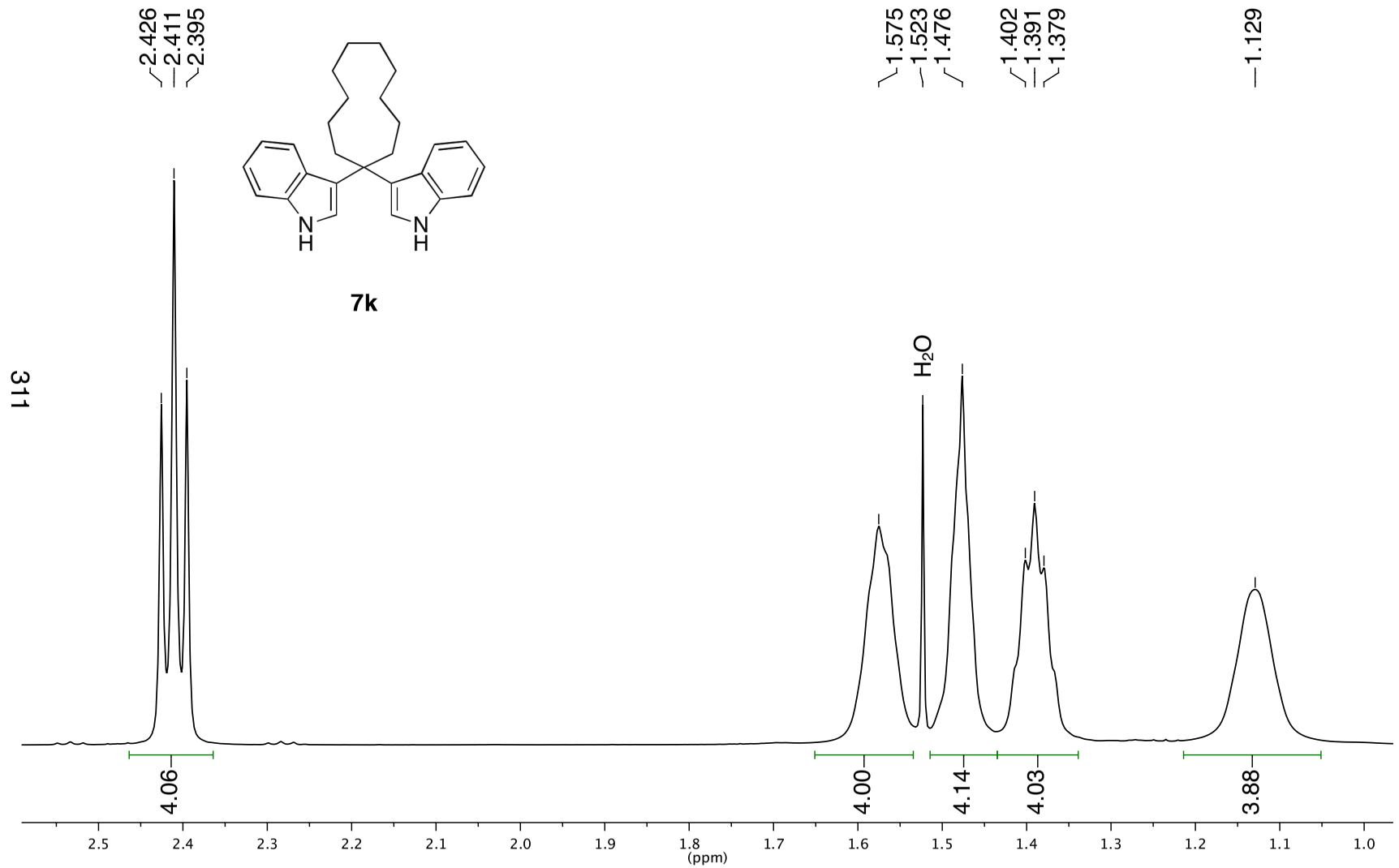

7k

^{13}C NMR 126 MHz in CD_2Cl_2

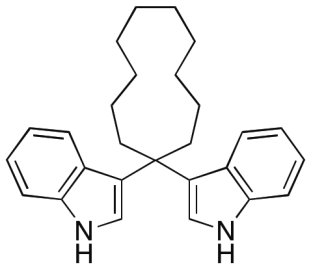

7k

^{1}H NMR 500 MHz in CD_2Cl_2

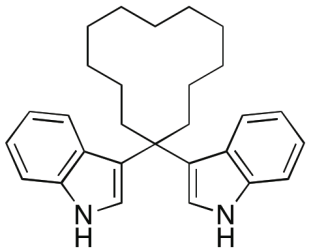

7l

^{1}H NMR 500 MHz in CD_2Cl_2

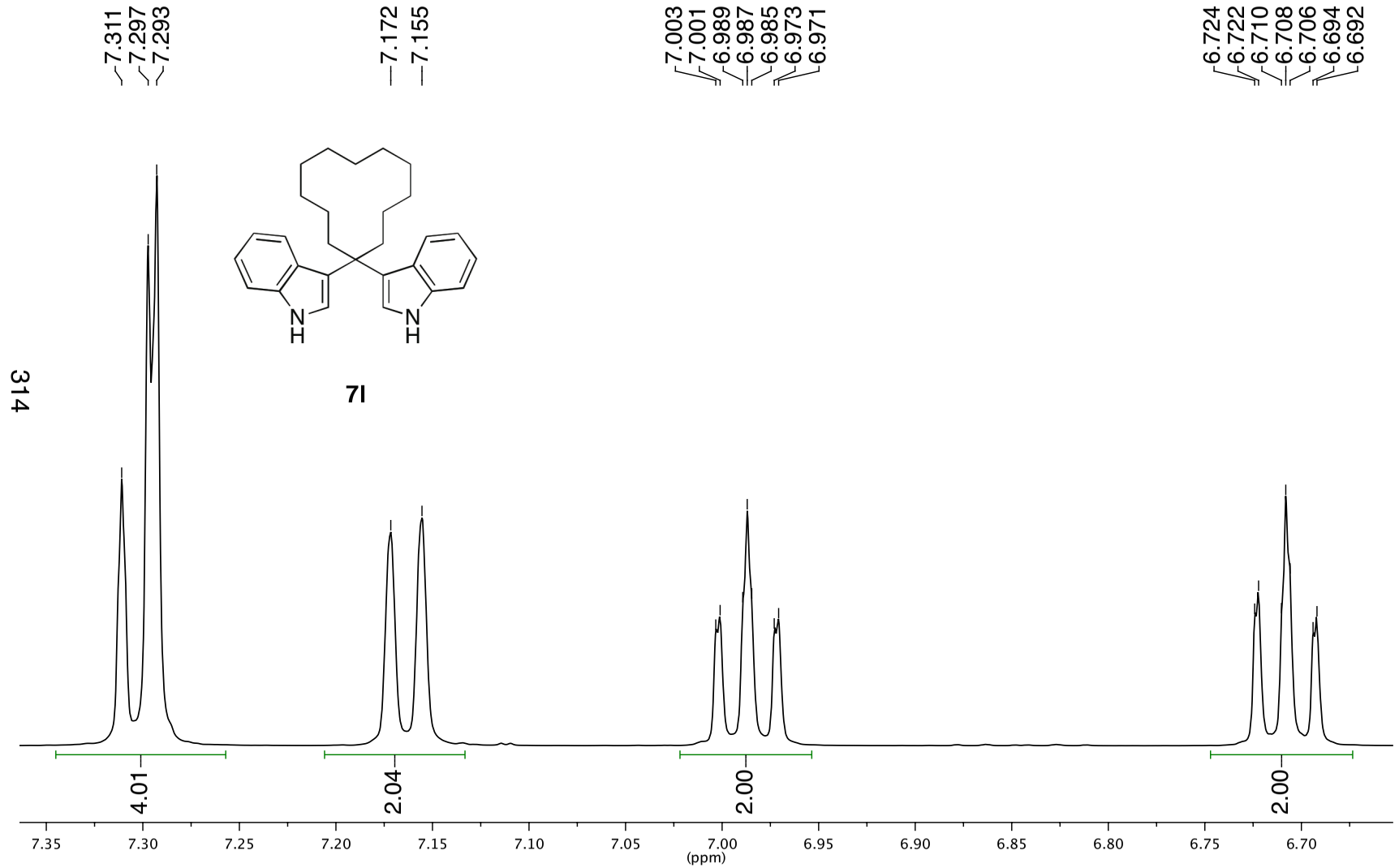

^{1}H NMR 500 MHz in CD_2Cl_2

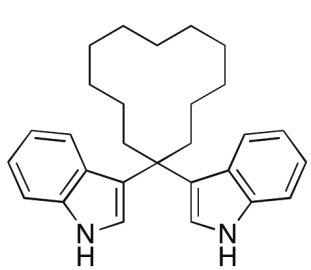

7l

^{13}C NMR 126 MHz in CD_2Cl_2

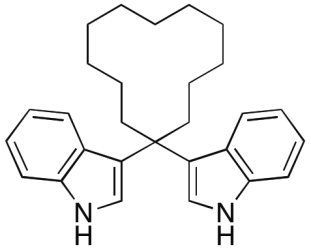

7l

^{1}H NMR 500 MHz in $(CD_3)_2SO$

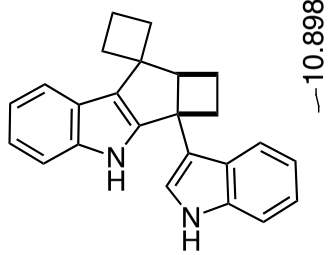

8d

^{1}H NMR 500 MHz in $(CD_3)_2SO$

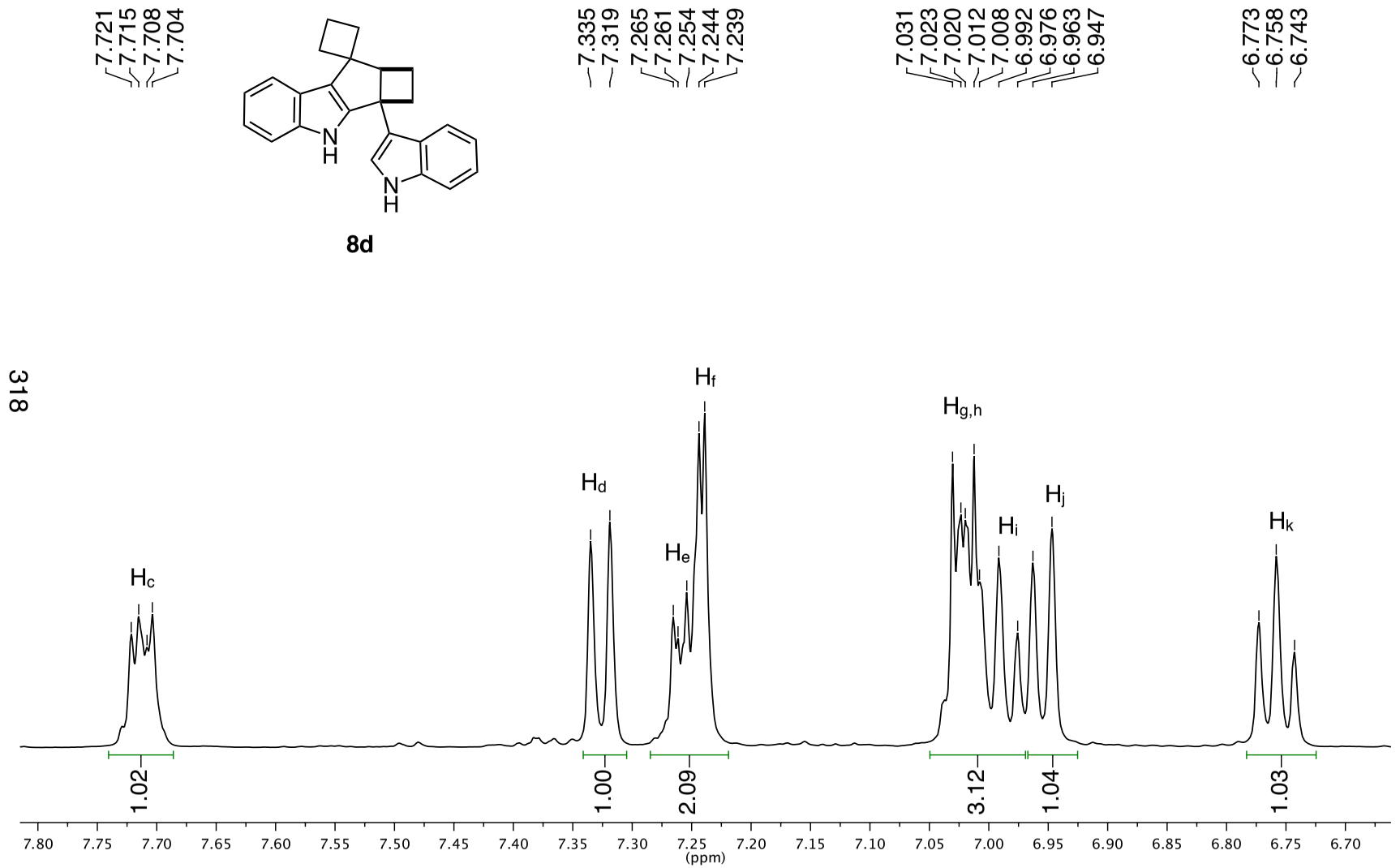

8d

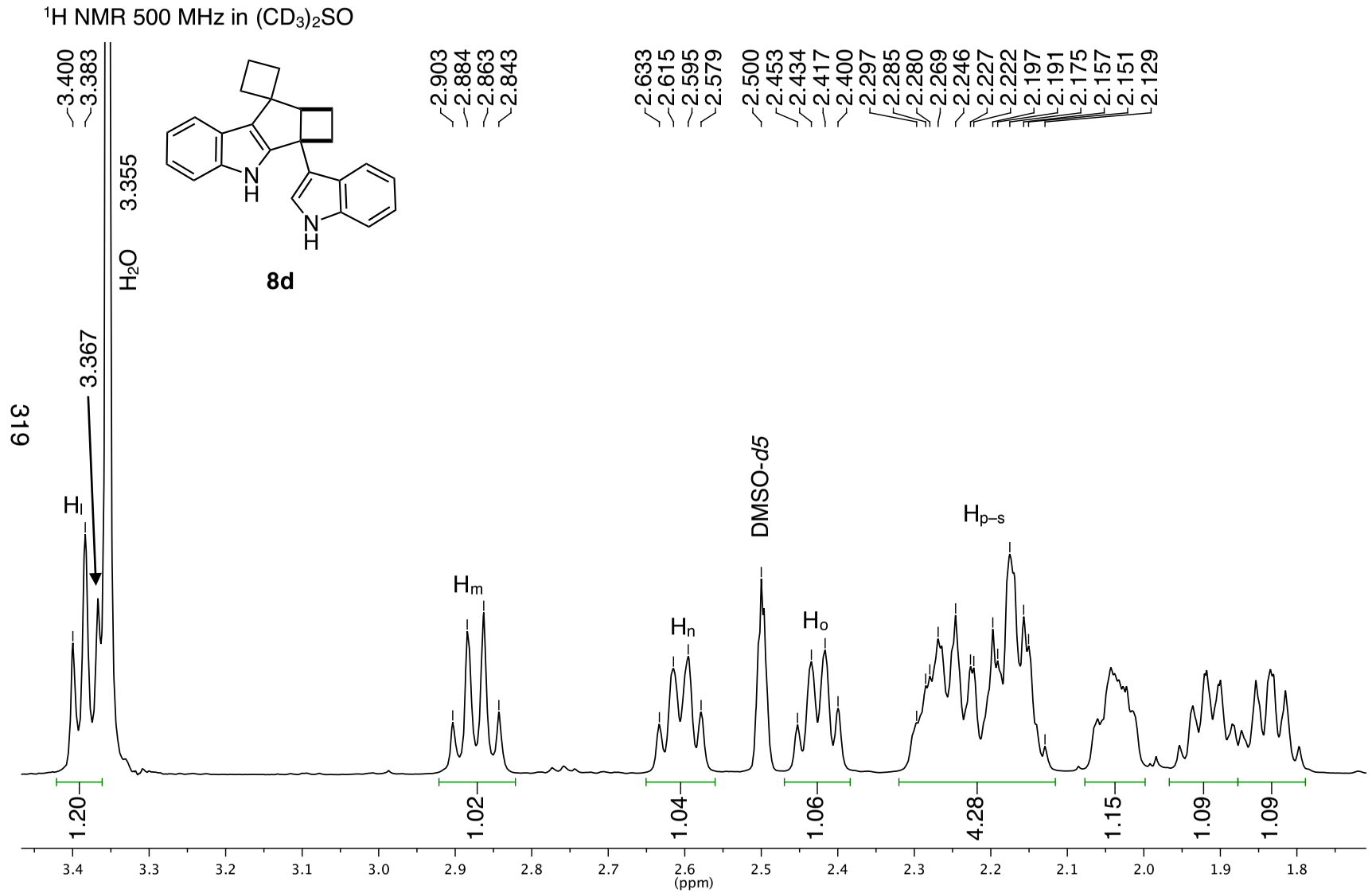
1H NMR 500 MHz in (CD3)2SO
3.400
3.383
3.355
H2O
3.367
3.19
2.903
2.884
2.863
2.843
2.633
2.615
2.595
2.579
2.500
2.453
2.434
2.417
2.400
2.297
2.285
2.280
2.269
2.246
2.227
2.222
2.197
2.191
2.175
2.157
2.151
2.129
8d
Hl
Hm
Hn
DMSO-d5
Ho
Hp–s
1.20
1.02
1.04
1.06
4.28
1.15
1.09
1.09
3.4
3.3
3.2
3.1
3.0
2.9
2.8
2.7
2.6
2.5
2.4
2.3
2.2
2.1
2.0
1.9
1.8
(ppm)

^{1}H NMR 500 MHz in $(CD_3)_2SO$

2.061 2.043 2.038 2.033 2.027 2.023 2.015 1.953 1.936 1.921 1.918 1.903 1.900 1.885 1.872 1.854 1.835 1.831 1.815 1.797

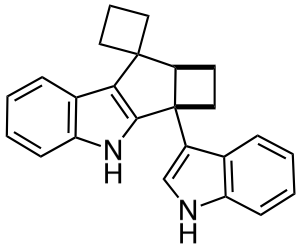

8d

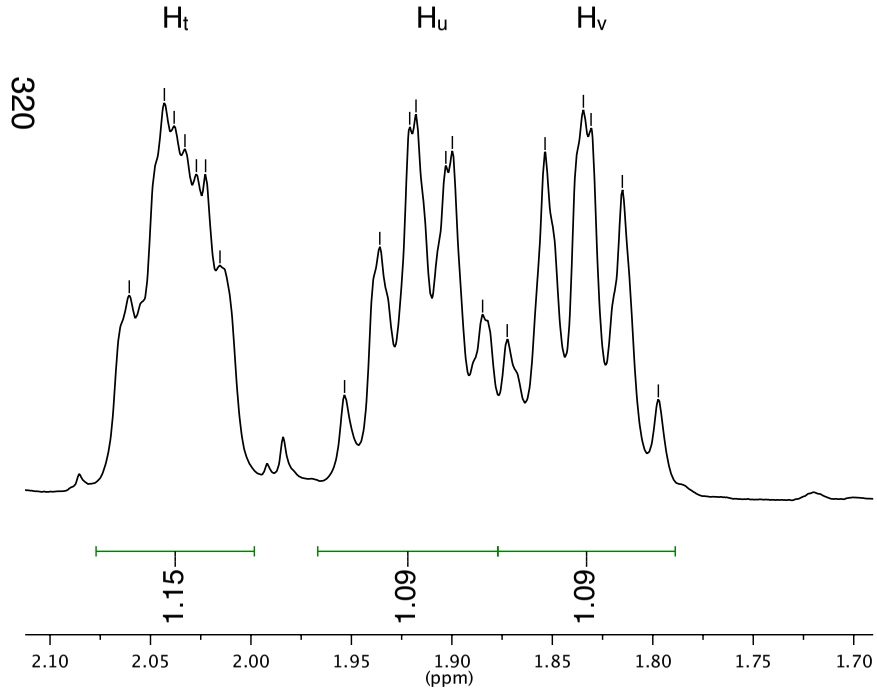

^{13}C NMR 126 MHz in $(CD_3)_2SO$

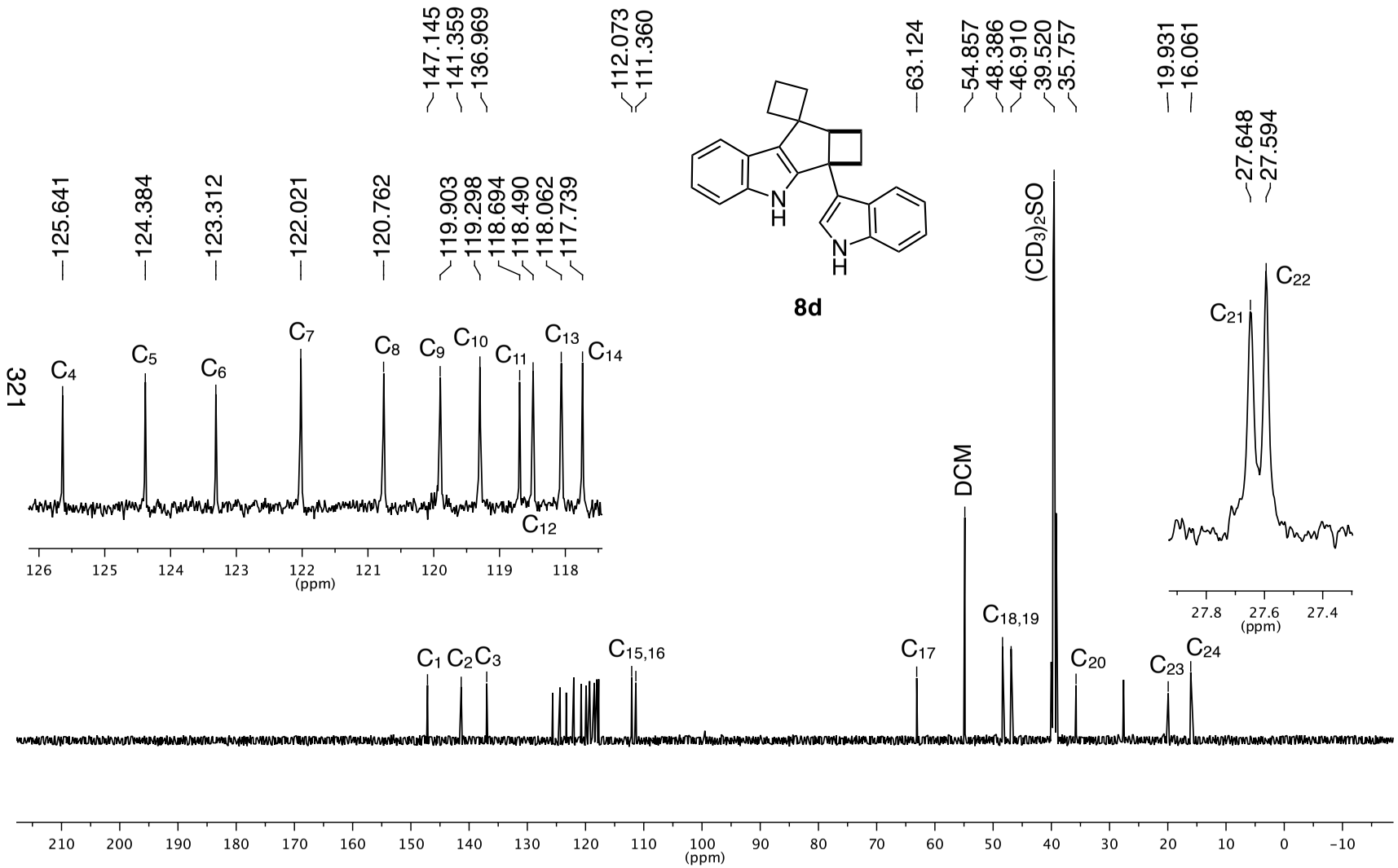

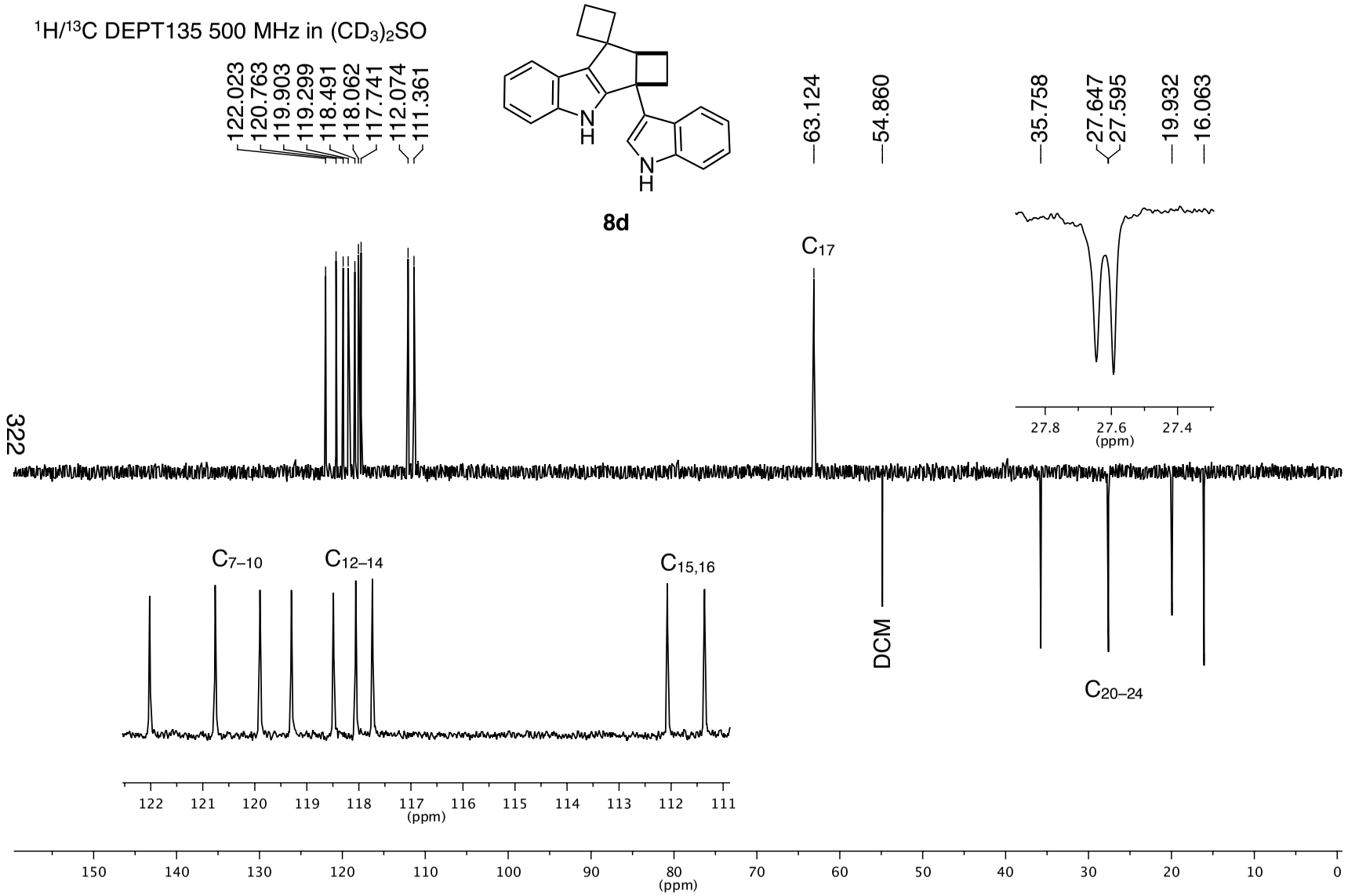
$^{1}H/^{13}C$ DEPT135 500 MHz in $(CD_3)_2SO$
122.023
120.763
119.903
119.299
118.491
118.062
117.741
112.074
111.361
63.124
54.860
35.758
27.647
27.595
19.932
16.063
8d
C_{17}
$C_{7–10}$
$C_{12–14}$
$C_{15,16}$
DCM
$C_{20–24}$
322
27.8
27.6
27.4
(ppm)
122
121
120
119
118
117
116
115
114
113
112
111
(ppm)
150
140
130
120
110
100
90
80
70
60
50
40
30
20
10
0
(ppm)

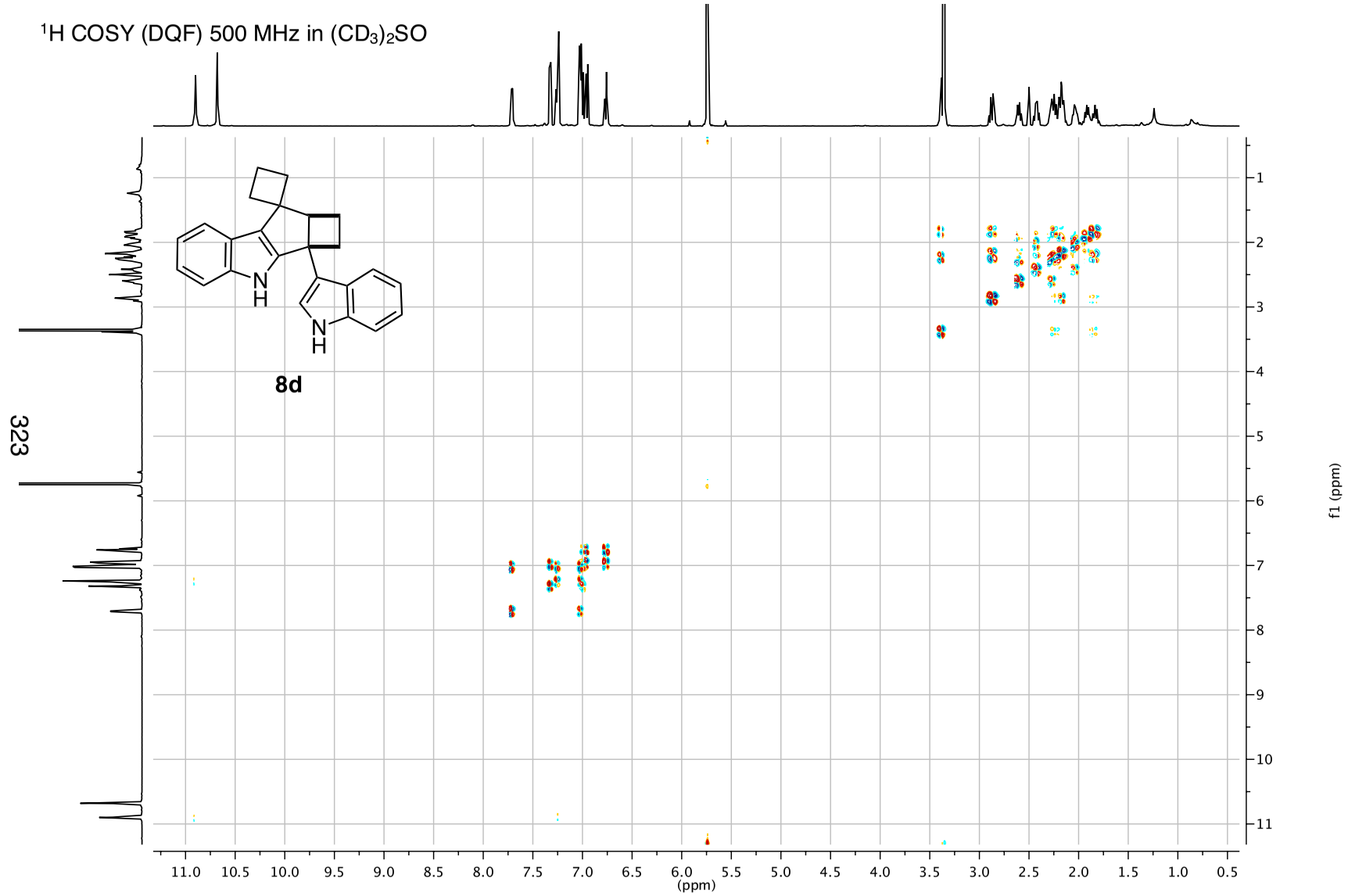
^{1}H COSY (DQF) 500 MHz in $(CD_3)_2SO$
8d
323
(ppm)
f1 (ppm)

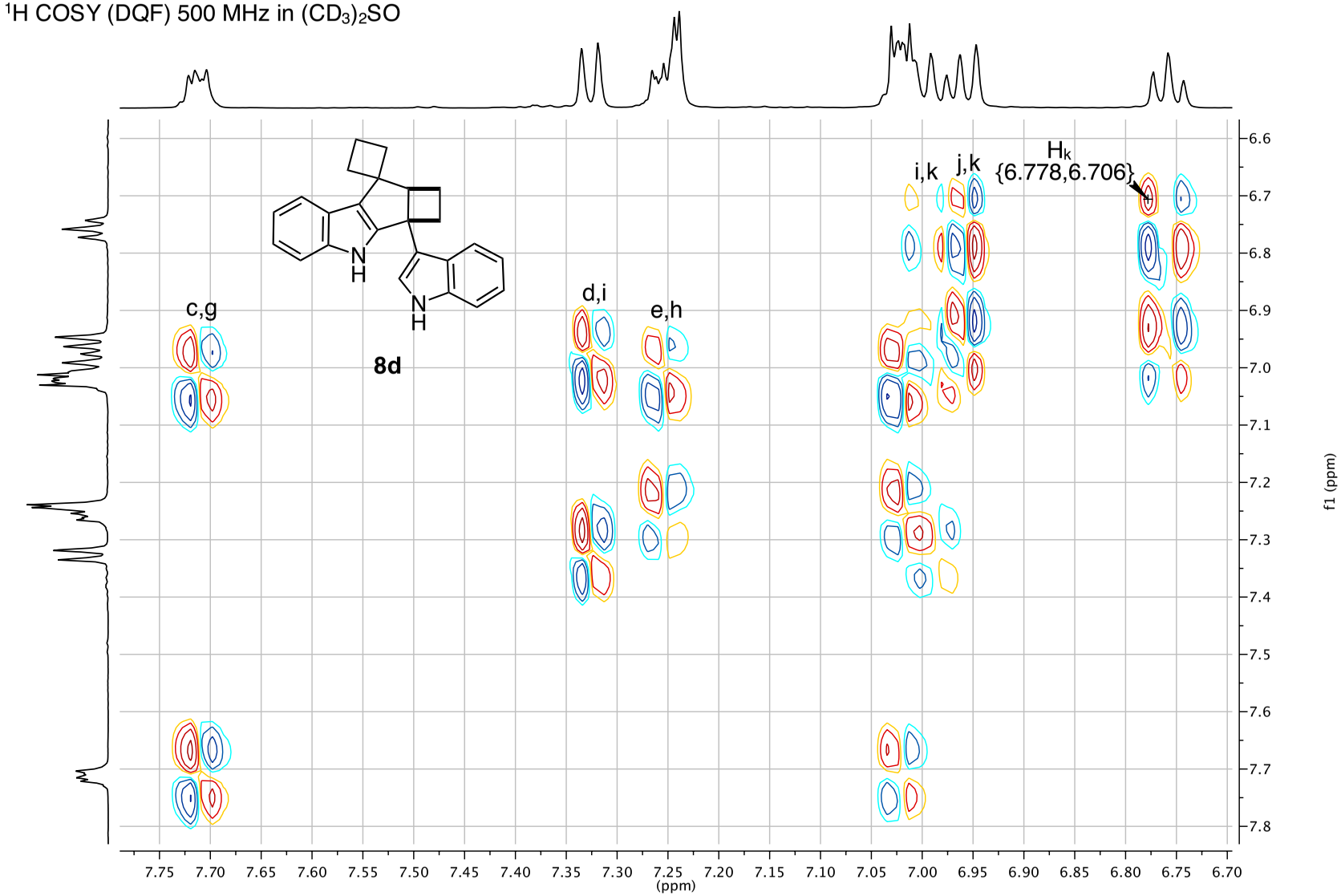
^{1}H COSY (DQF) 500 MHz in $(CD_3)_2SO$
c,g
d,i
e,h
i,k
j,k
H_k
{6.778,6.706}
8d
N
H
N
H
7.75 7.70 7.65 7.60 7.55 7.50 7.45 7.40 7.35 7.30 7.25 7.20 7.15 7.10 7.05 7.00 6.95 6.90 6.85 6.80 6.75 6.70
(ppm)
6.6 6.7 6.8 6.9 7.0 7.1 7.2 7.3 7.4 7.5 7.6 7.7 7.8
f1 (ppm)

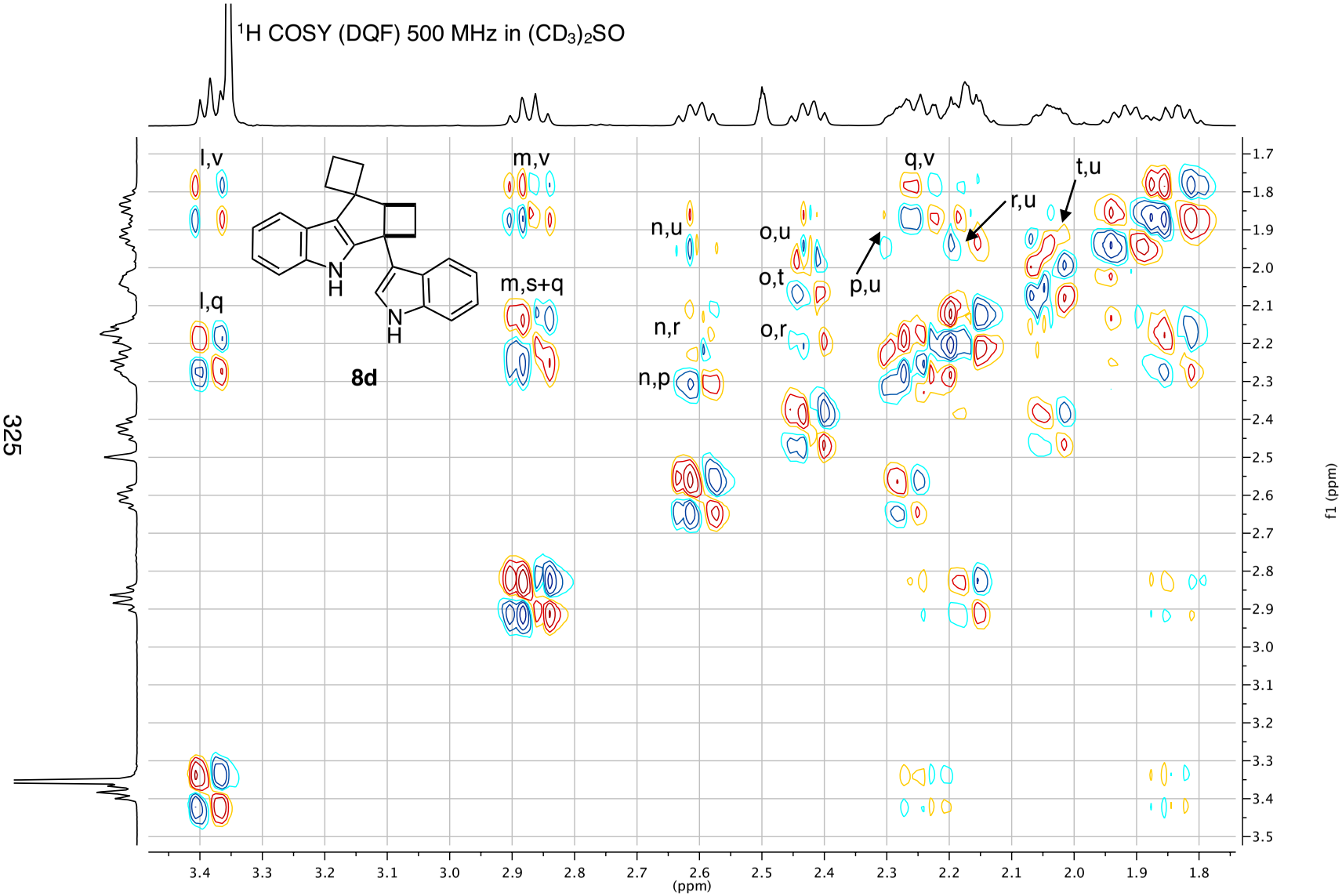
^{1}H COSY (DQF) 500 MHz in $(CD_3)_2SO$
l,v
l,q
m,v
m,s+q
n,u
n,r
n,p
o,u
o,t
o,r
p,u
q,v
r,u
t,u
8d
N
H
N
H
3.4
3.3
3.2
3.1
3.0
2.9
2.8
2.7
2.6
2.5
2.4
2.3
2.2
2.1
2.0
1.9
1.8
(ppm)
1.7
1.8
1.9
2.0
2.1
2.2
2.3
2.4
2.5
2.6
2.7
2.8
2.9
3.0
3.1
3.2
3.3
3.4
3.5
f1 (ppm)

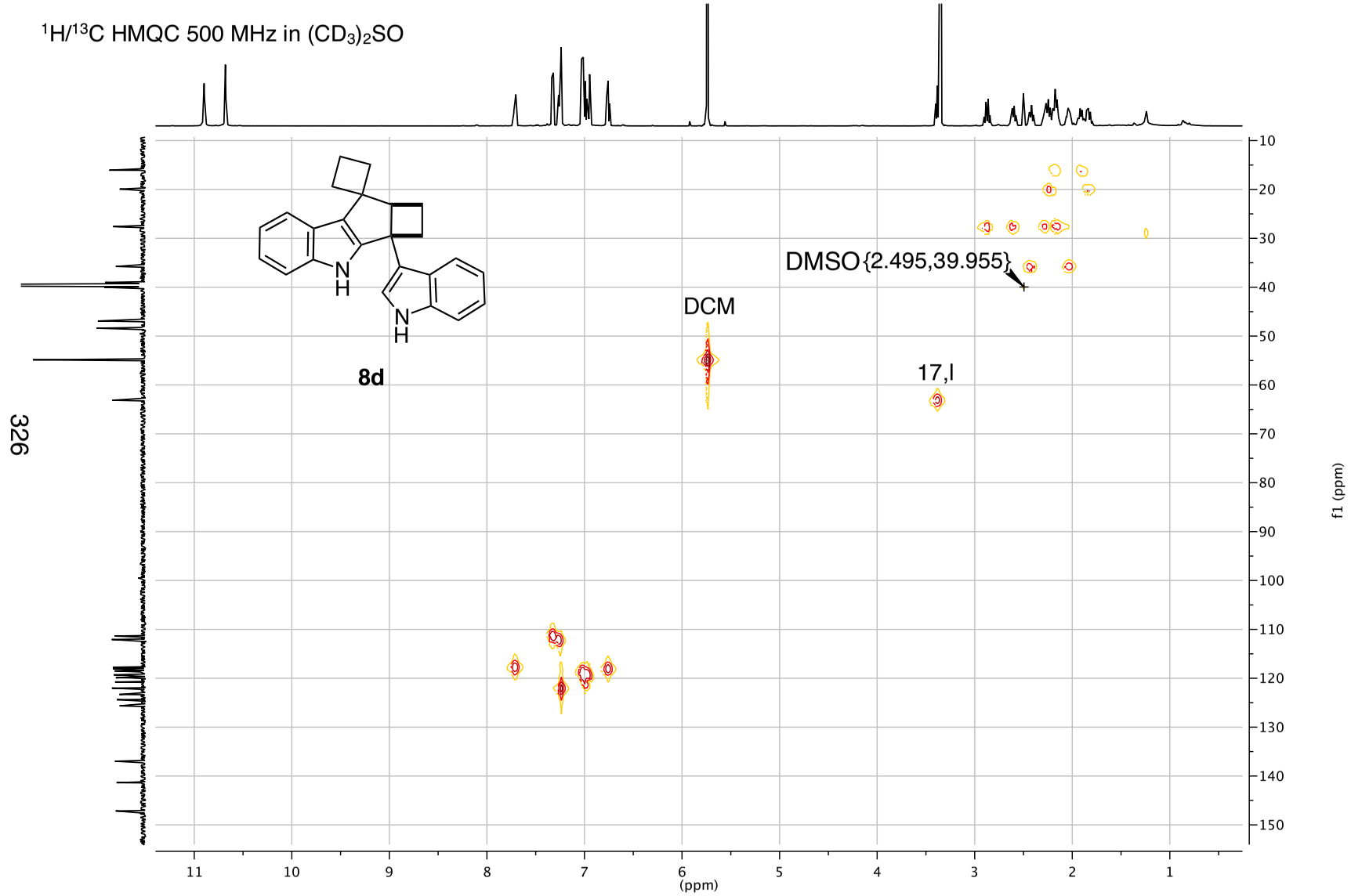
$^{1}H/^{13}C$ HMQC 500 MHz in $(CD_3)_2SO$
8d
DCM
DMSO{2.495,39.955}
17,l
326
(ppm)
f1 (ppm)

$^{1}H/^{13}C$ HMQC 500 MHz in $(CD_3)_2SO$

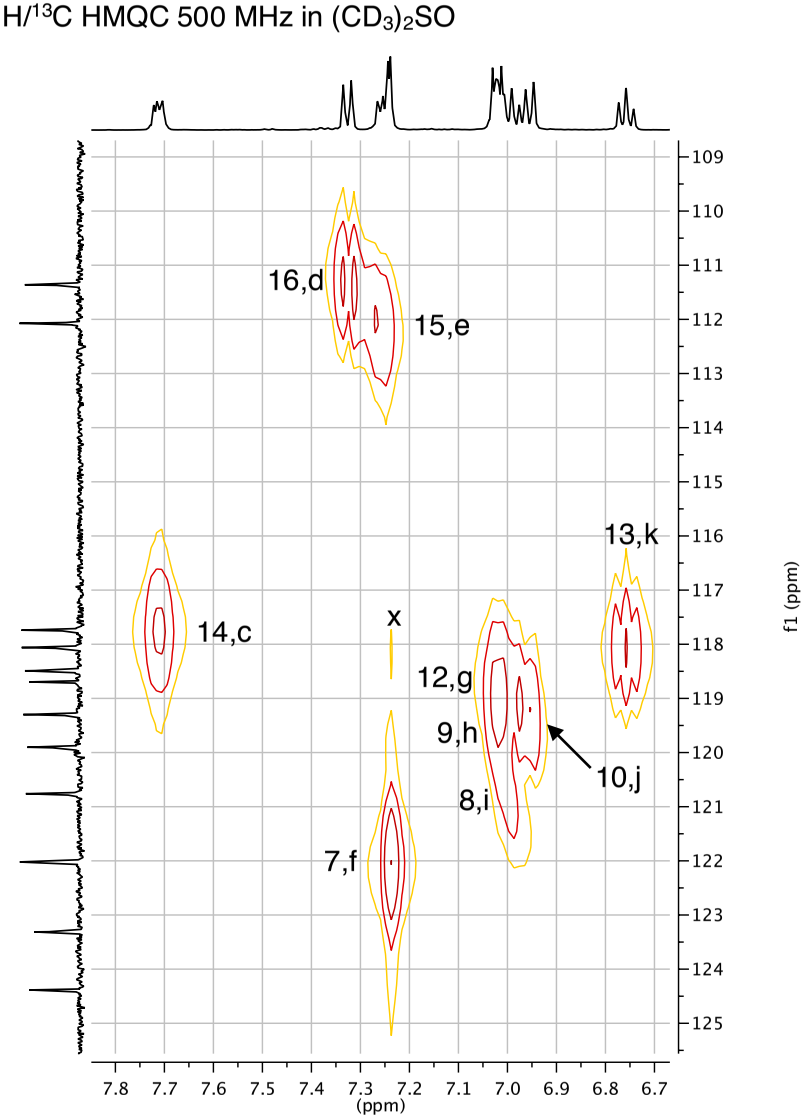

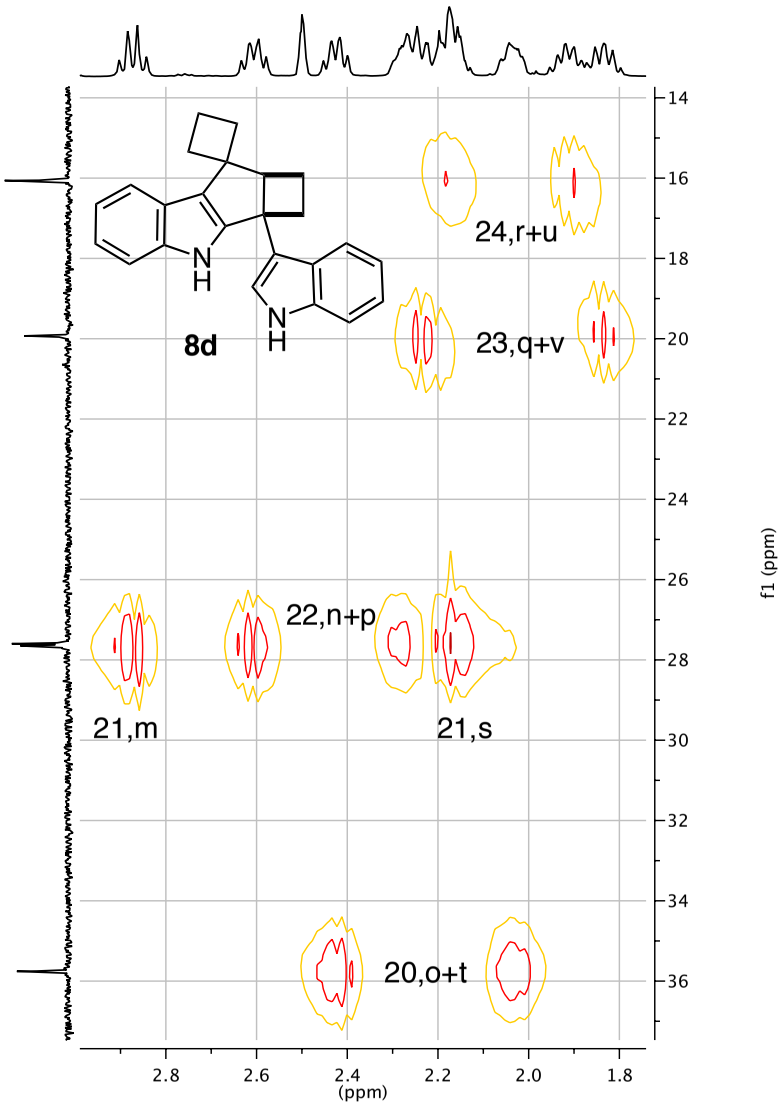

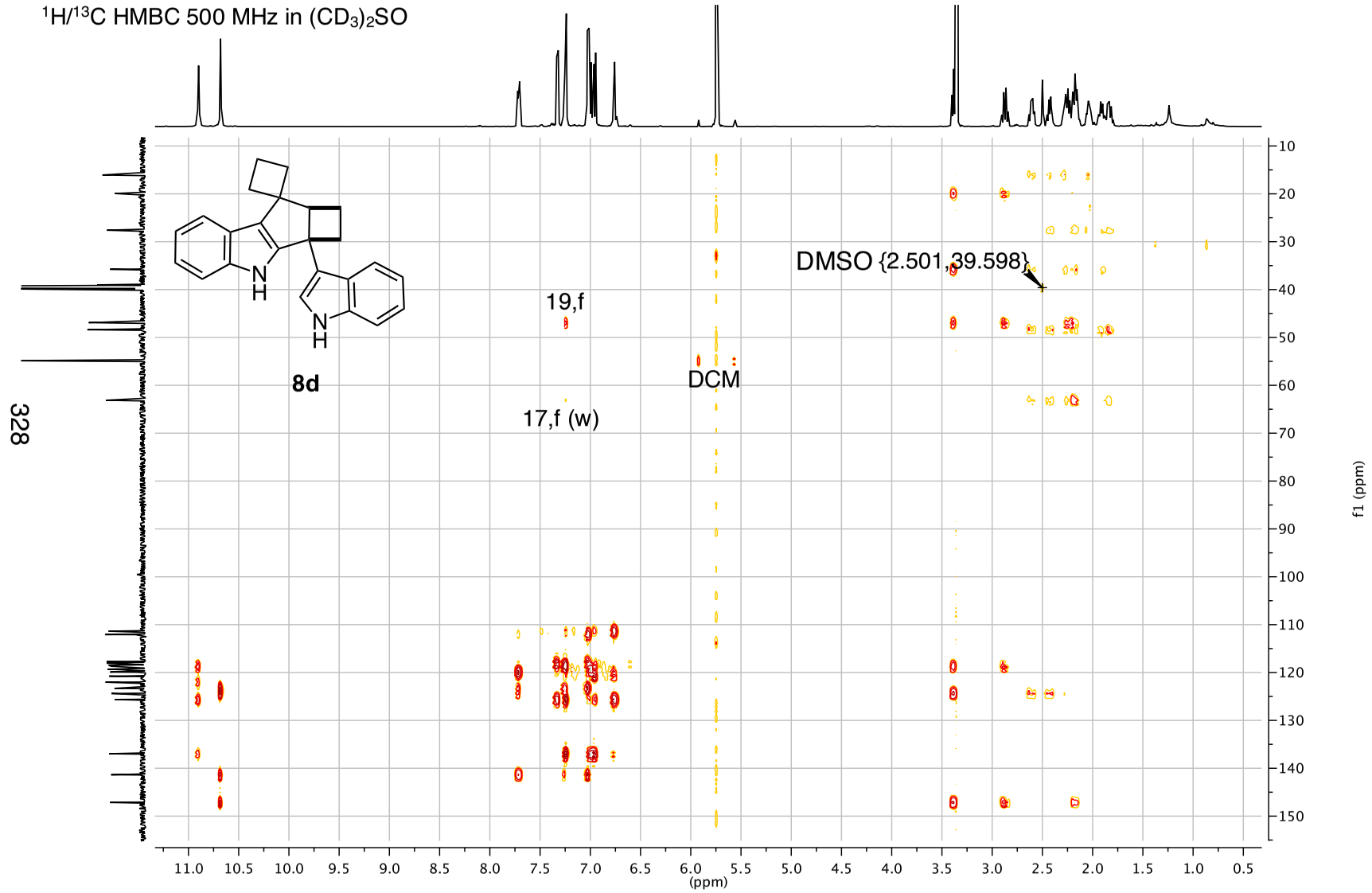
$^{1}H/^{13}C$ HMBC 500 MHz in $(CD_3)_2SO$
328
8d
19,f
17,f (w)
DCM
DMSO {2.501,39.598}
(ppm)
f1 (ppm)

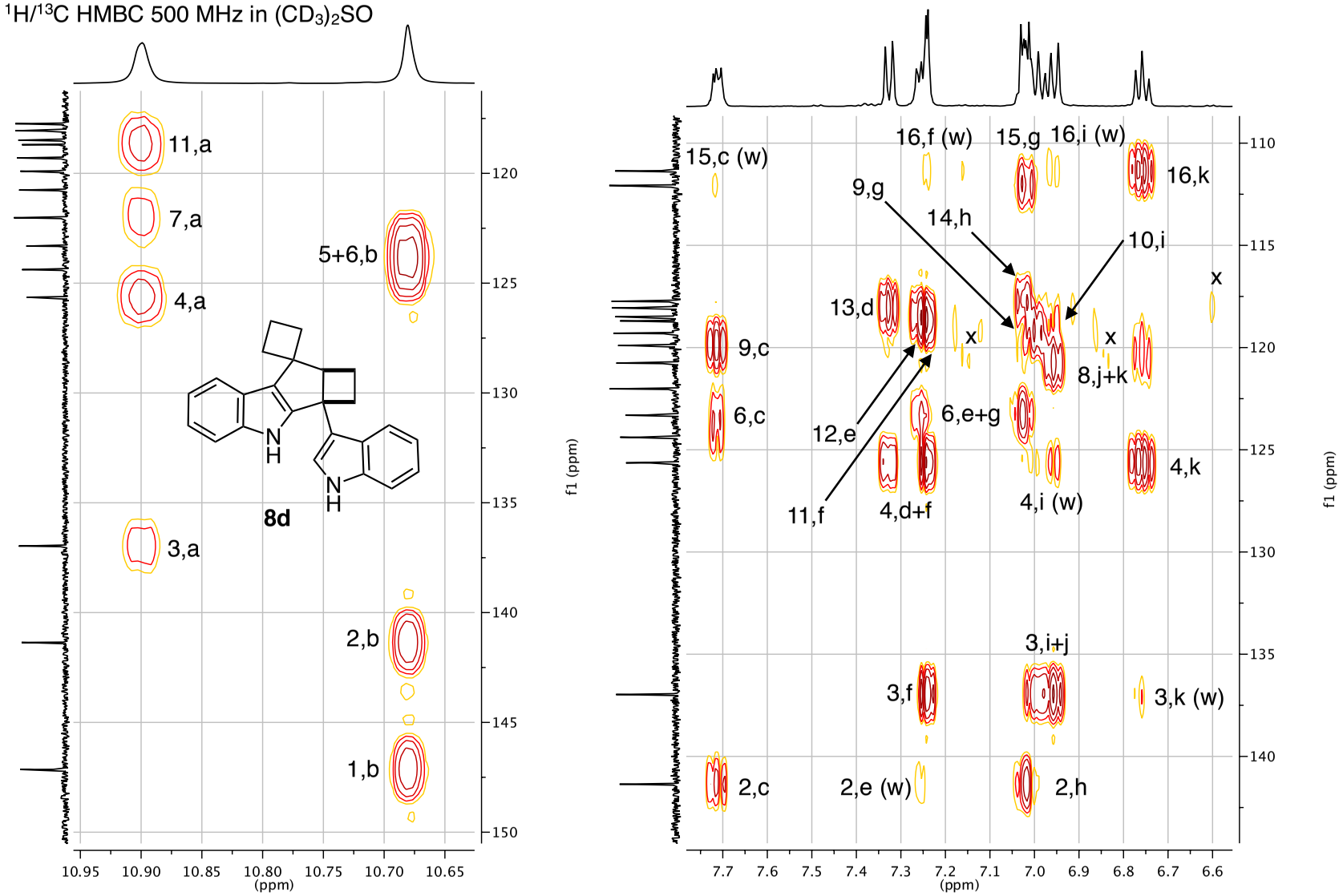
^{1}H/^{13}C HMBC 500 MHz in $(CD_3)_2SO$
11,a
7,a
4,a
5+6,b
3,a
2,b
1,b
8d
N
H
N
H
10.95
10.90
10.85
10.80
10.75
10.70
10.65
(ppm)
120
125
130
135
140
145
150
f1 (ppm)
15,c (w)
16,f (w)
15,g
16,i (w)
16,k
9,g
14,h
10,i
x
13,d
x
x
9,c
8,j+k
6,c
12,e
6,e+g
4,k
11,f
4,d+f
4,i (w)
3,i+j
3,f
3,k (w)
2,c
2,e (w)
2,h
7.7
7.6
7.5
7.4
7.3
7.2
7.1
7.0
6.9
6.8
6.7
6.6
(ppm)
110
115
120
125
130
135
140
f1 (ppm)

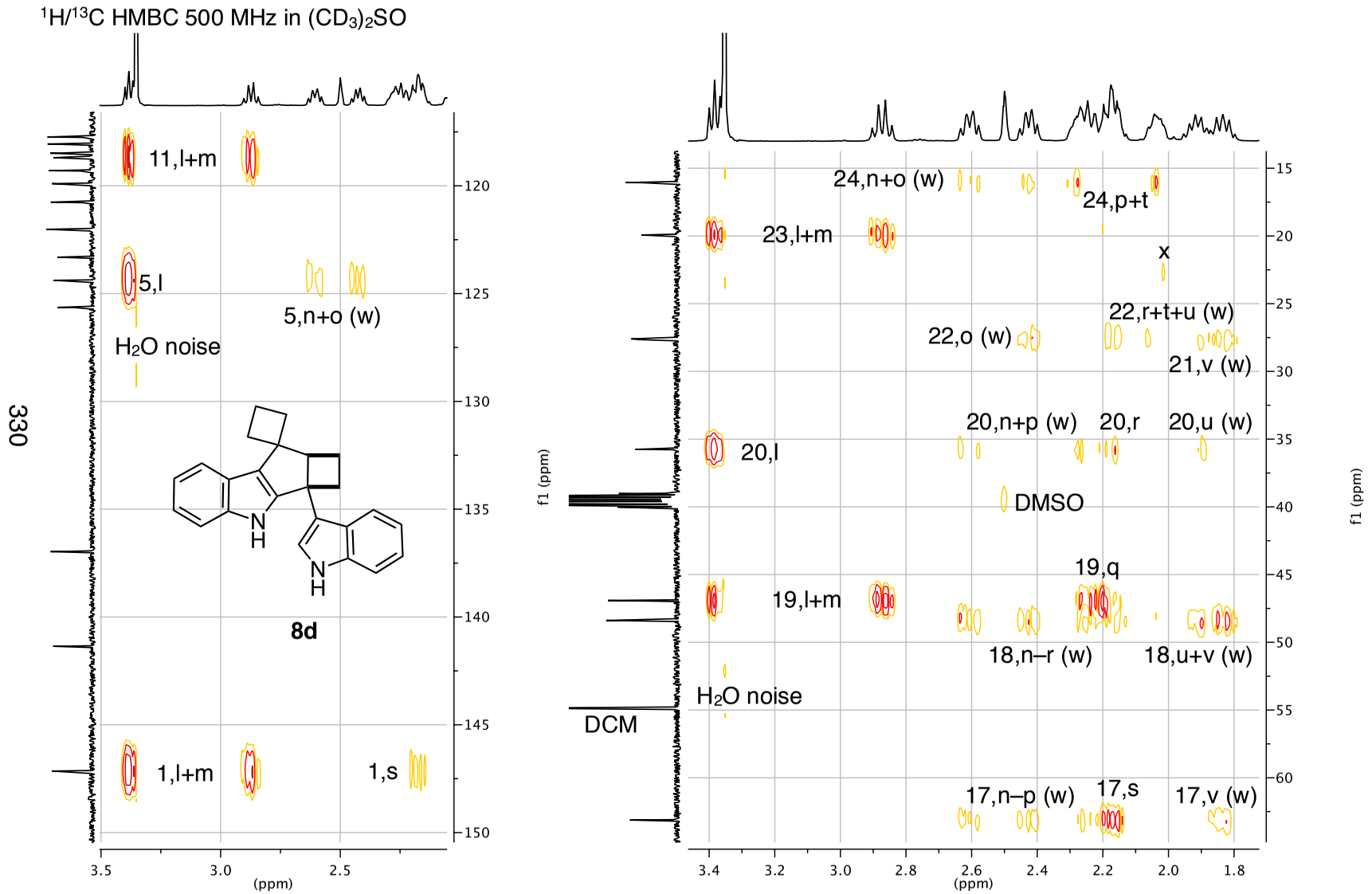
$^{1}H/^{13}C$ HMBC 500 MHz in $(CD_3)_2SO$
11,l+m
5,l
5,n+o (w)
H_2O noise
8d
1,l+m
1,s
(ppm)
24,n+o (w)
24,p+t
23,l+m
x
22,r+t+u (w)
22,o (w)
21,v (w)
20,n+p (w)
20,r
20,u (w)
20,l
DMSO
19,q
19,l+m
18,n–r (w)
18,u+v (w)
H_2O noise
DCM
17,n–p (w)
17,s
17,v (w)
f1 (ppm)

^{1}H GOESY 500 MHz in $(CD_3)_2SO$

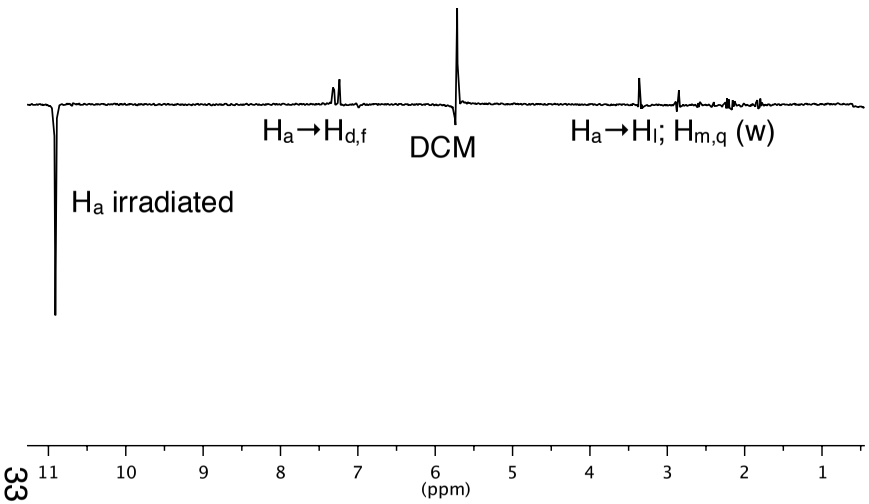

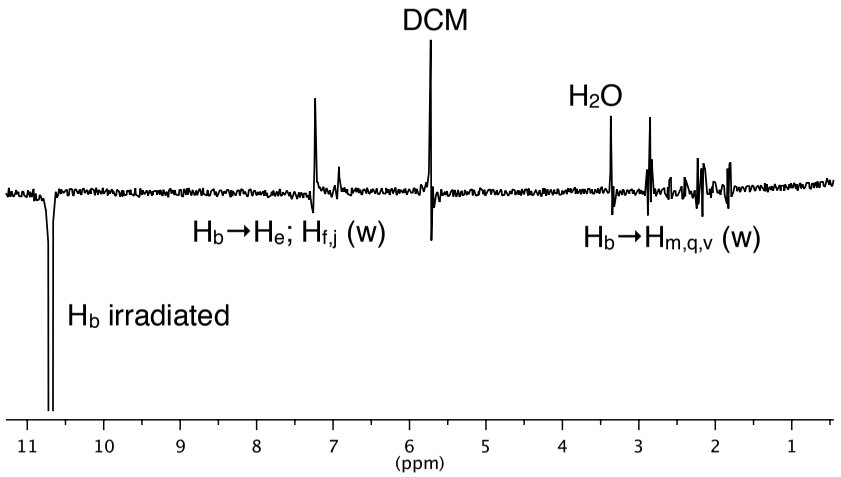

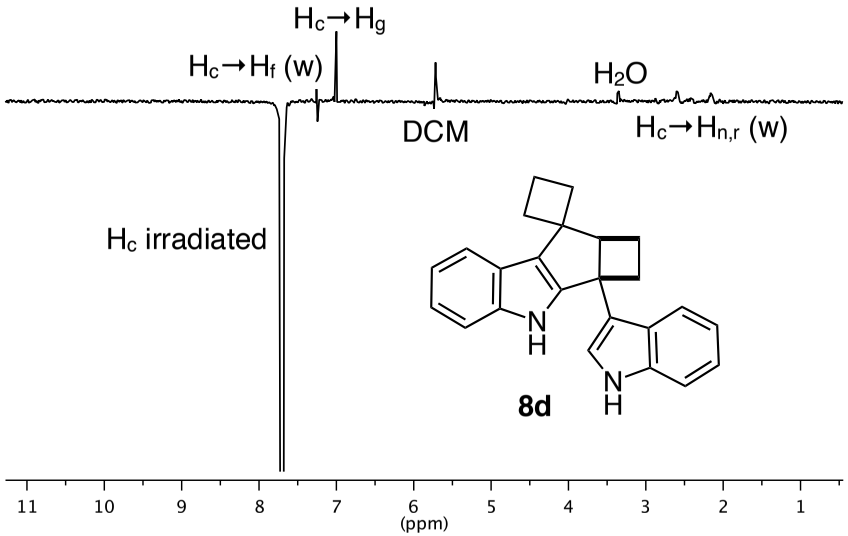

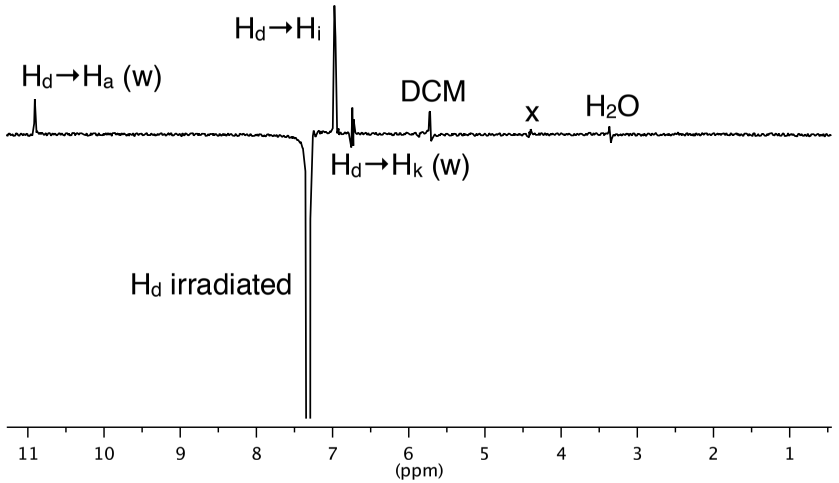

^{1}H GOESY 500 MHz in $(CD_3)_2SO$

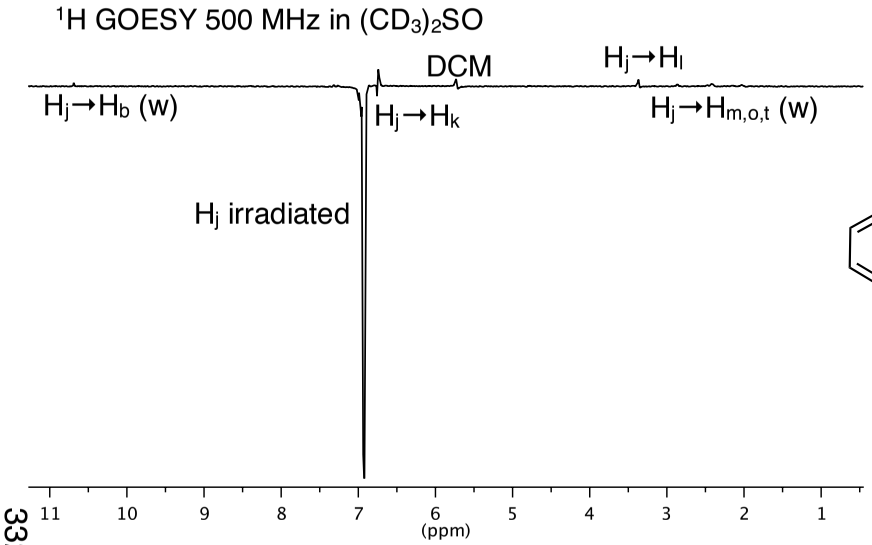

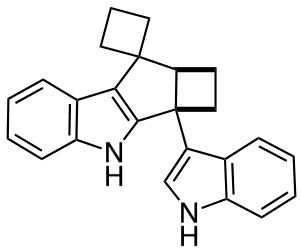

8d

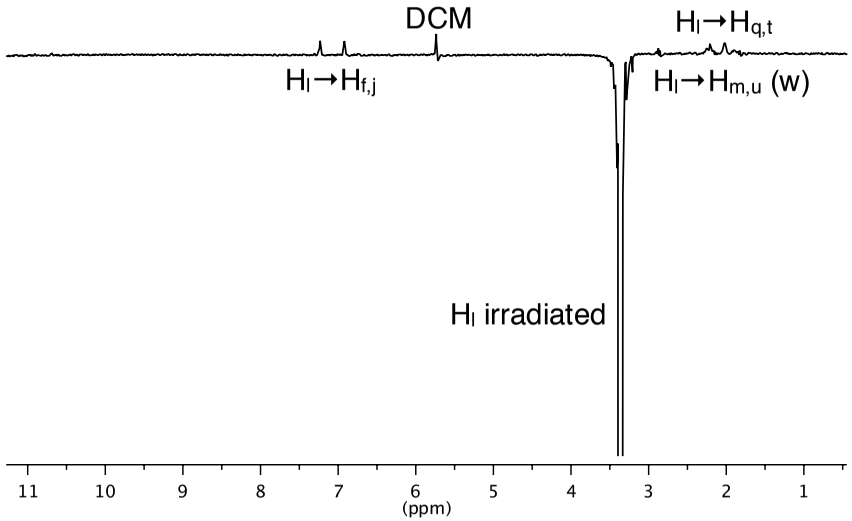

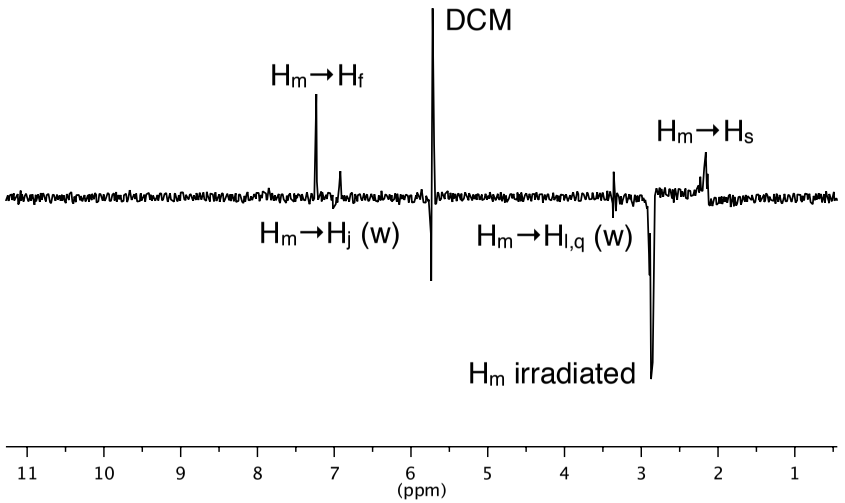

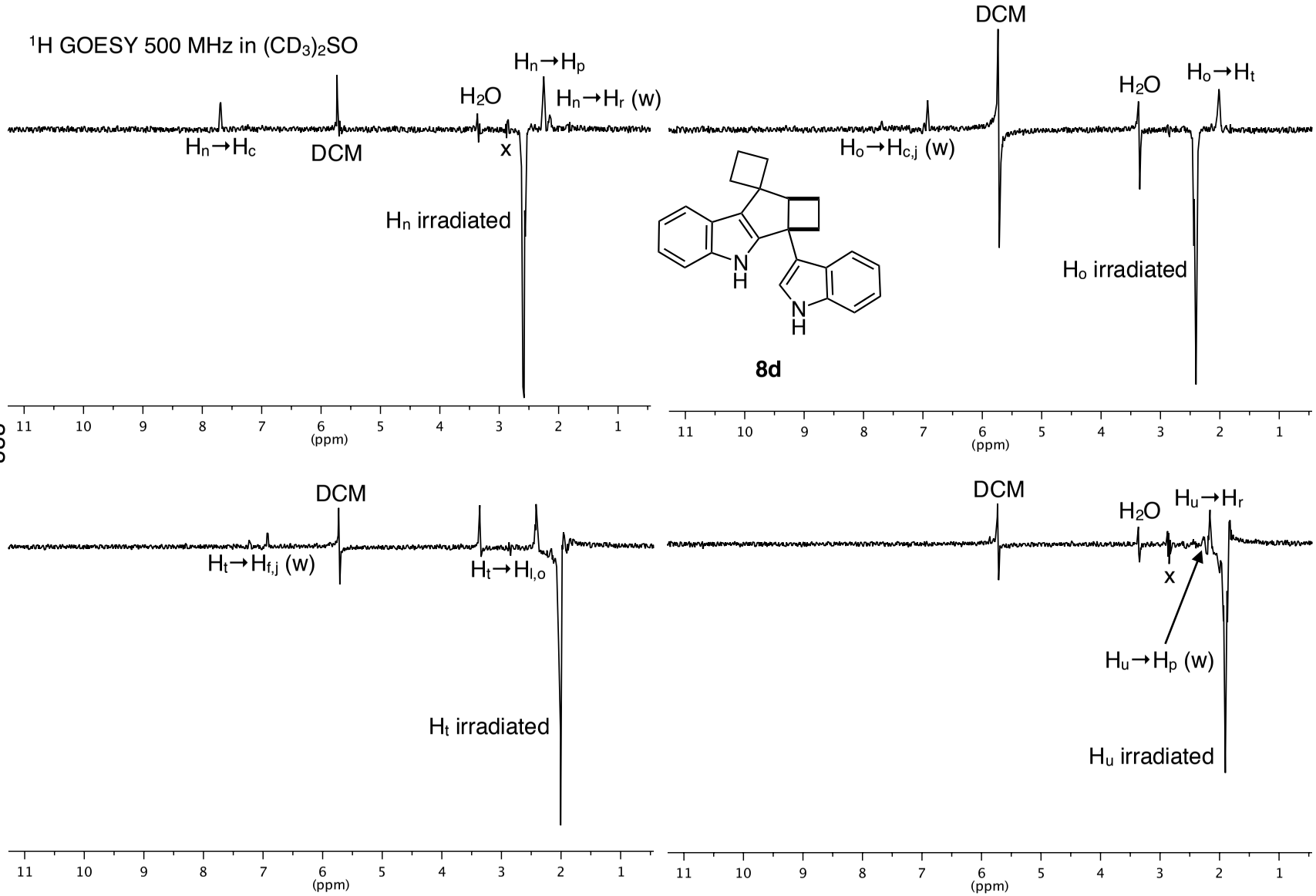
^{1}H GOESY 500 MHz in $(CD_3)_2SO$
$H_n \rightarrow H_p$
H_2O
$H_n \rightarrow H_r$ (w)
$H_n \rightarrow H_c$
DCM
x
H_n irradiated
DCM
H_2O
$H_o \rightarrow H_t$
$H_o \rightarrow H_{c,j}$ (w)
H_o irradiated
8d
DCM
$H_t \rightarrow H_{f,j}$ (w)
$H_t \rightarrow H_{l,o}$
H_t irradiated
DCM
H_2O
$H_u \rightarrow H_r$
x
$H_u \rightarrow H_p$ (w)
H_u irradiated
11 10 9 8 7 6 5 4 3 2 1
(ppm)

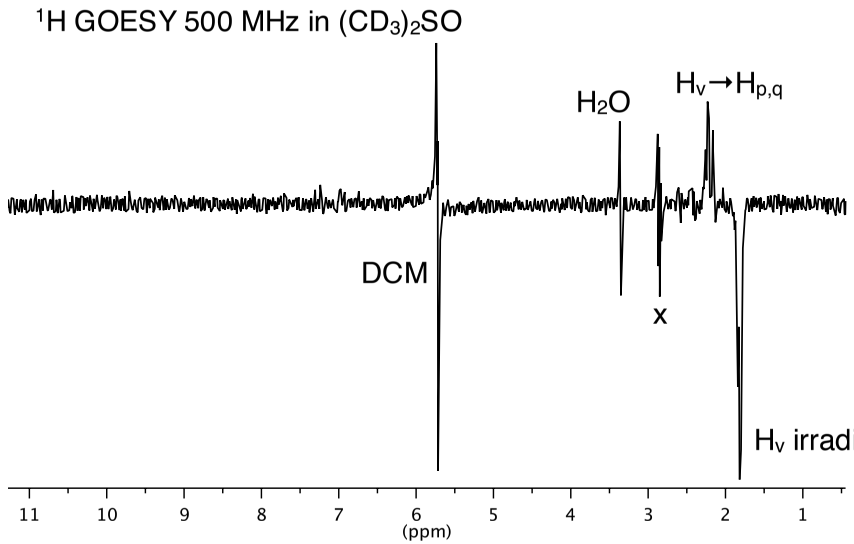
^{1}H GOESY 500 MHz in $(CD_3)_2SO$
H_2O
$H_v \rightarrow H_{p,q}$
DCM
x
H_v irradiated
11
10
9
8
7
6
5
4
3
2
1
(ppm)

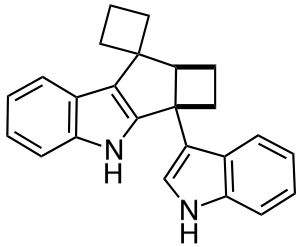
N
H
N
H

8d

Table 32 (1 of 2). Proton NMR summary for **8d**.

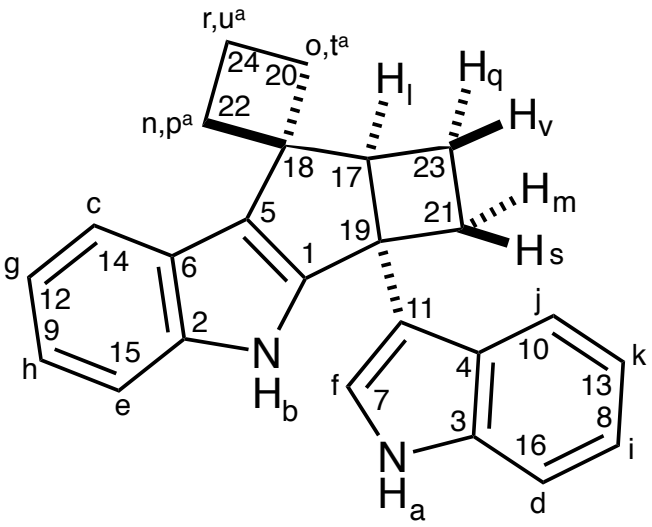

H label	δ	COSY	NOE
a	10.90	-	D,F,L,m,q
b	10.68	-	E,f,j,m,q,v
c	7.71	G	f,G,n,r
d	7.33	I	a,I,k
e	7.25	H	not done
f	7.24	-	not done
g[b]	7.03	C	not done
h[b]	7.02	E	not done
i	6.99	D,k	not done
j	6.96	K	b,K,L,m,o,t
k	6.76	i,J	I
l	3.38	Q,v	F,J,m,Q,T,u
m	2.87	Q,S,V	F,j,l,q,s

[a]$H_{n,o,r}$ are facing H_c; $H_{p,t,u}$ are facing H_l.

[b]$H_{g/h}$ are indistinguishable by the performed experiments and are arbitrarily assigned.

Table 32 (2 of 2). Proton NMR summary for **8d**.

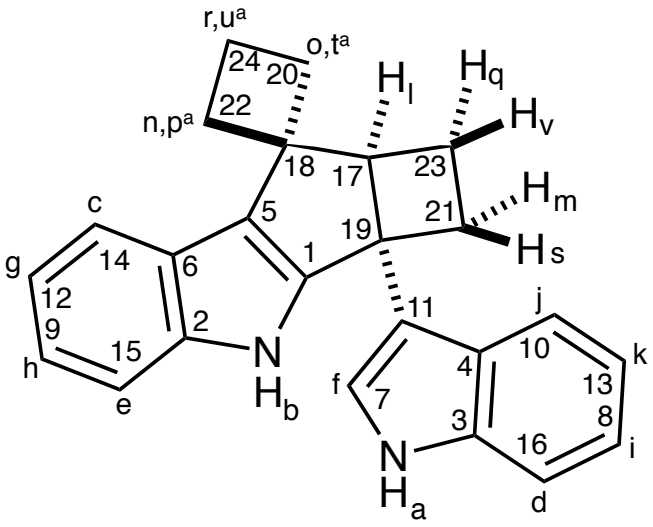

H label	δ	COSY	NOE
n	2.61	P,r,u	C,P,r
o	2.43	T	c,j,T
p	2.27	N,u	not done
q	2.22	L,M,V	not done
r	2.18	n,o,u	not done
s	2.16	M	not done
t	2.04	O,u	f,j,L,O
u	1.92	n,o,p,r,t	p,R
v	1.84	l,M,Q	P,Q

[a]$H_{n,o,r}$ are facing H_c; $H_{p,t,u}$ are facing H_l.

Table 33 (1 of 2). Carbon NMR summary for **8d**.

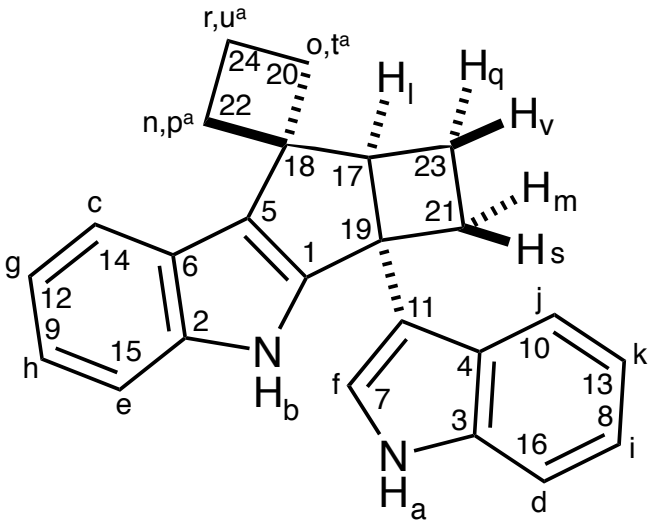

C label	δ	type	HMQC	HMBC
1	147.2	q	-	B,L,M,s
2	141.4	q	-	B,C,e,H
3	137.0	q	-	a,F,I,J,k
4	125.6	q	-	A,D,F,i,K
5	124.4	q	-	B,L,n,o
6	123.3	q	-	B,C,E,G
7	122.0	CH	f	a
8	120.8	CH	i	J,K
9	119.9	CH	h	C,G
10	119.3	CH	j	I
11	118.7	q	-	A,F,L,M
12	118.5	CH	g	E
13	118.1	CH	k	D
14	117.7	CH	c	H
15	112.1	CH	e	G,c

[a]$H_{n,o,r}$ are facing H_c; $H_{p,t,u}$ are facing H_l.

Table 33 (2 of 2). Carbon NMR summary for **8d**.

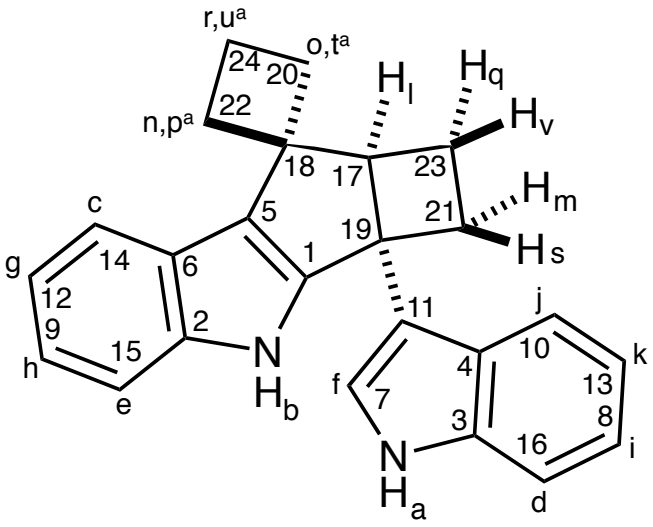

C label	δ	type	HMQC	HMBC
16	111.4	CH	d	f,i,K
17	63.1	CH	l	f,n,o,p,S,v
18	48.4	q	-	n,o,p,q,r,u,v
19	46.9	q	-	F,L,M,Q
20	35.8	CH_2	o,t	L,n,p,R,u
21[b]	27.65	CH_2	m,s	v
22[b]	27.59	CH_2	n,p	o,r,t,u
23	19.9	CH_2	q,v	L,M
24	16.1	CH_2	r,u	n,o,P,T

[a]$H_{n,o,r}$ are facing H_c; $H_{p,t,u}$ are facing H_l.

[b]$C_{21/22}$ are indistinguishable by the performed experiments and are arbitrarily assigned.

^{1}H NMR 500 MHz in CD_2Cl_2

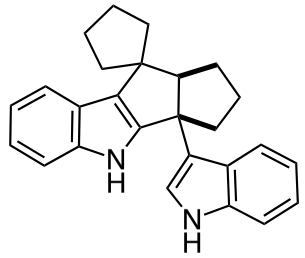

8e

^{1}H NMR 500 MHz in CD_2Cl_2

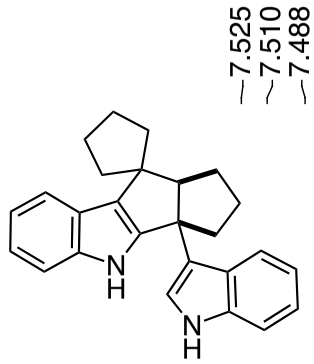

8e

^{1}H NMR 500 MHz in CD_2Cl_2

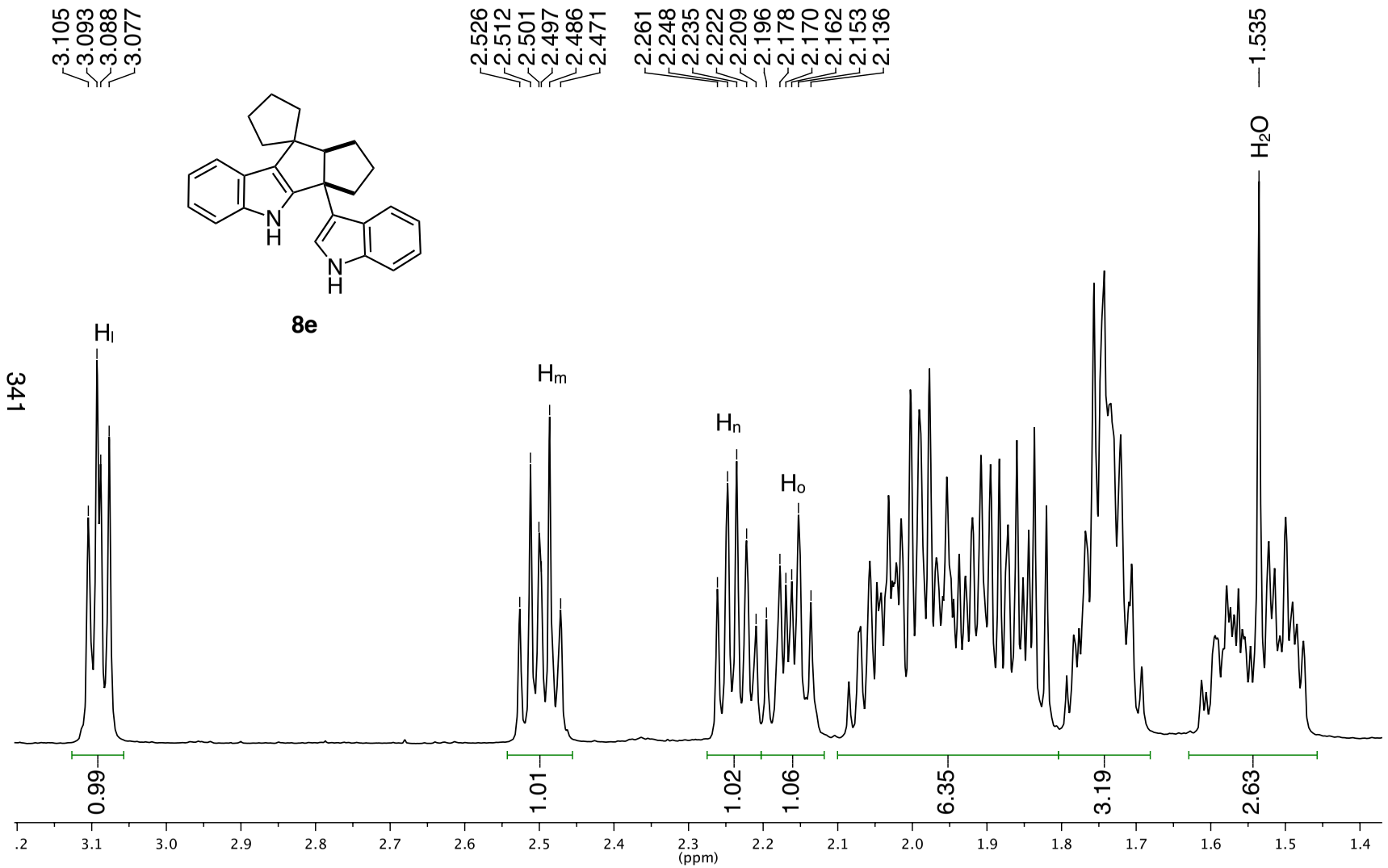

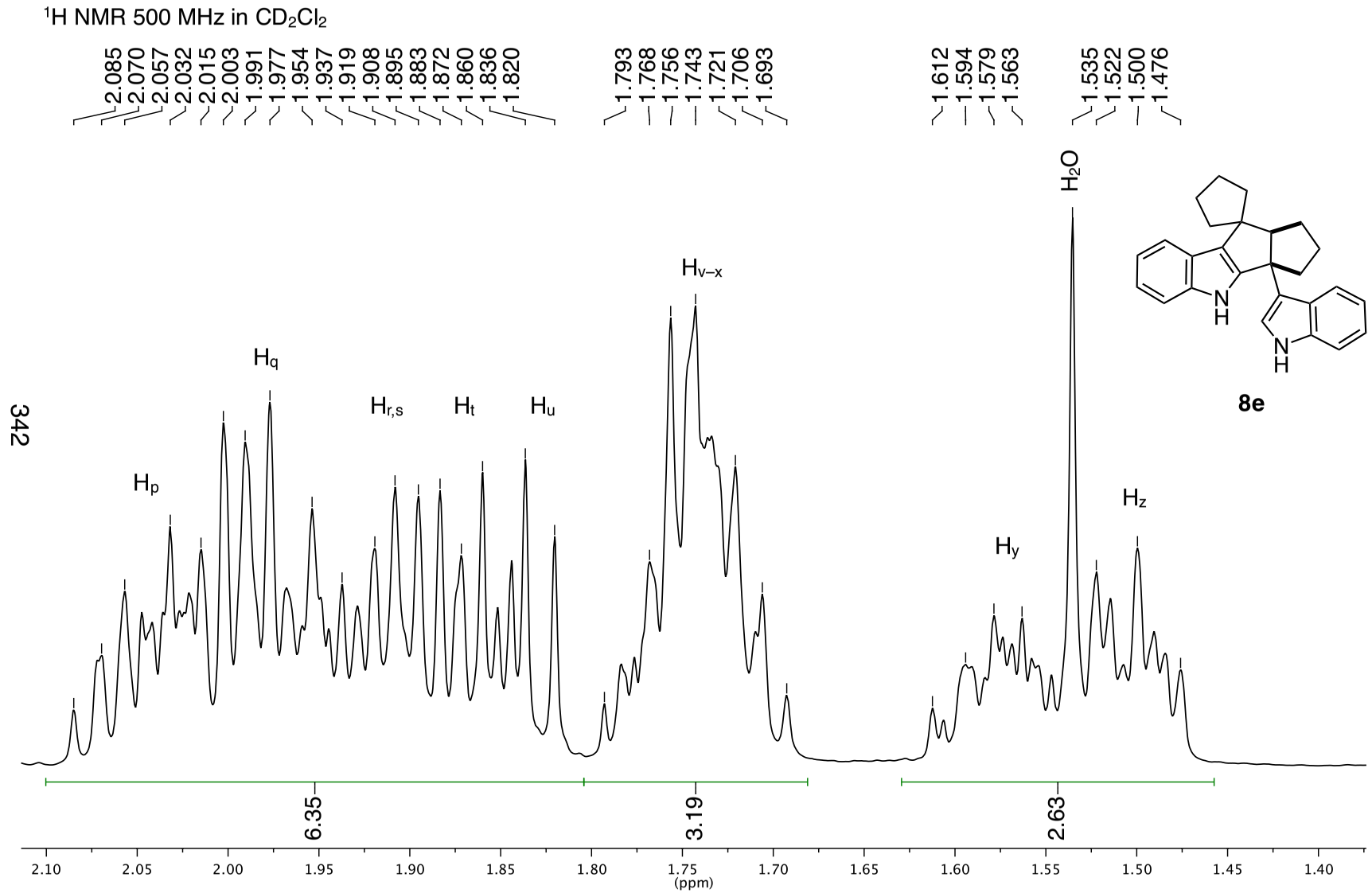
1H NMR 500 MHz in CD2Cl2
2.085
2.070
2.057
2.032
2.015
2.003
1.991
1.977
1.954
1.937
1.919
1.908
1.895
1.883
1.872
1.860
1.836
1.820
1.793
1.768
1.756
1.743
1.721
1.706
1.693
1.612
1.594
1.579
1.563
1.535
1.522
1.500
1.476
H2O
Hv–x
Hq
Hr,s
Ht
Hu
Hp
Hy
Hz
342
8e
6.35
3.19
2.63
2.10
2.05
2.00
1.95
1.90
1.85
1.80
1.75
1.70
1.65
1.60
1.55
1.50
1.45
1.40
(ppm)

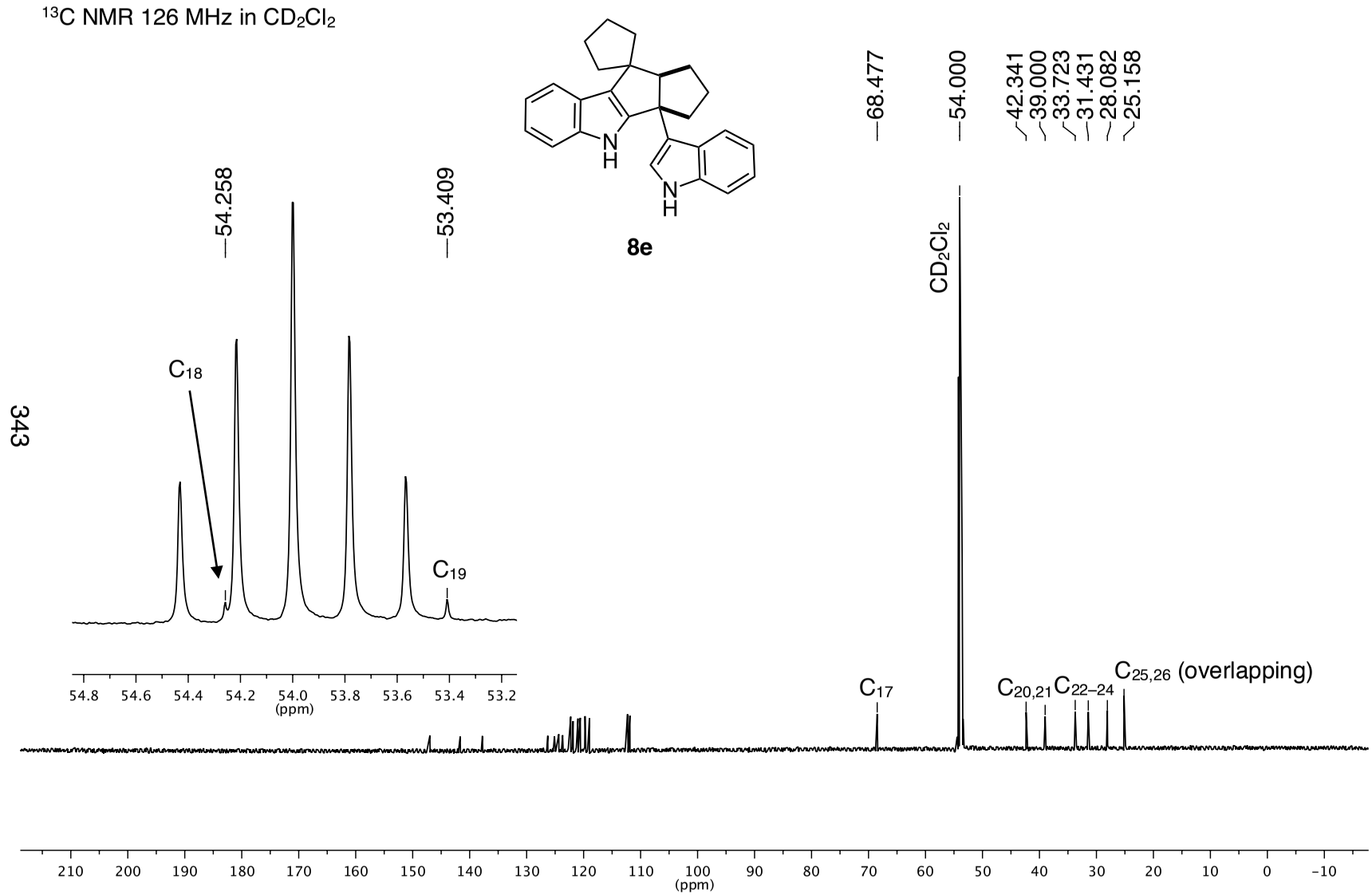
^{13}C NMR 126 MHz in CD_2Cl_2
8e
—68.477
—54.000
—42.341
—39.000
—33.723
—31.431
—28.082
—25.158
—54.258
—53.409
CD_2Cl_2
C_{18}
C_{19}
C_{17}
$C_{20,21}$
$C_{22–24}$
$C_{25,26}$ (overlapping)
343
54.8 54.6 54.4 54.2 54.0 53.8 53.6 53.4 53.2
(ppm)
210 200 190 180 170 160 150 140 130 120 110 100 90 80 70 60 50 40 30 20 10 0 -10
(ppm)

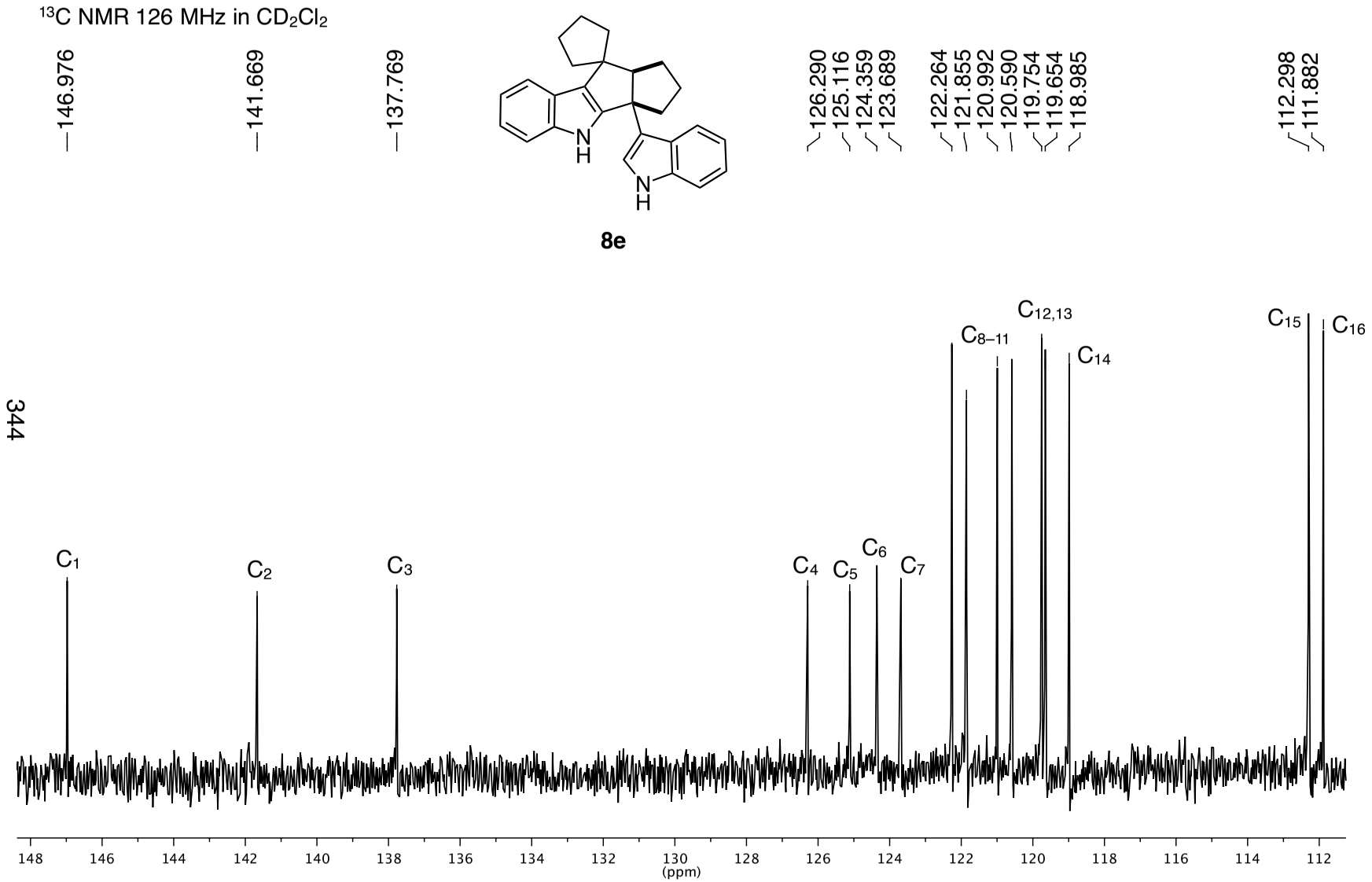
^{13}C NMR 126 MHz in CD_2Cl_2
146.976
141.669
137.769
126.290
125.116
124.359
123.689
122.264
121.855
120.992
120.590
119.754
119.654
118.985
112.298
111.882
8e
344
C1
C2
C3
C4
C5
C6
C7
C8–11
C12,13
C14
C15
C16
148
146
144
142
140
138
136
134
132
130
128
126
124
122
120
118
116
114
112
(ppm)

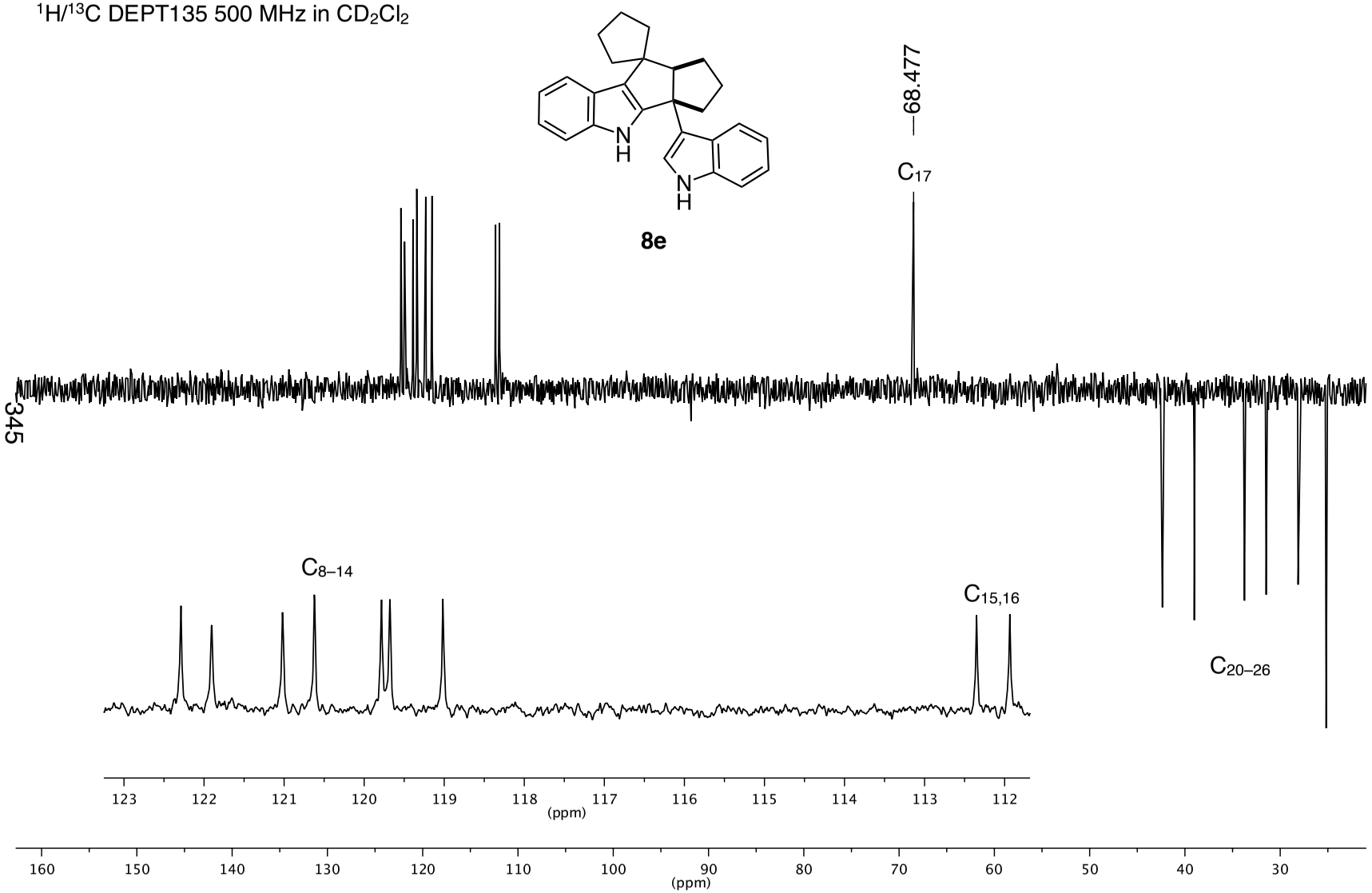
$^{1}H/^{13}C$ DEPT135 500 MHz in CD_2Cl_2
8e
68.477
C_{17}
$C_{8–14}$
$C_{15,16}$
$C_{20–26}$
345
123 122 121 120 119 118 117 116 115 114 113 112
(ppm)
160 150 140 130 120 110 100 90 80 70 60 50 40 30
(ppm)

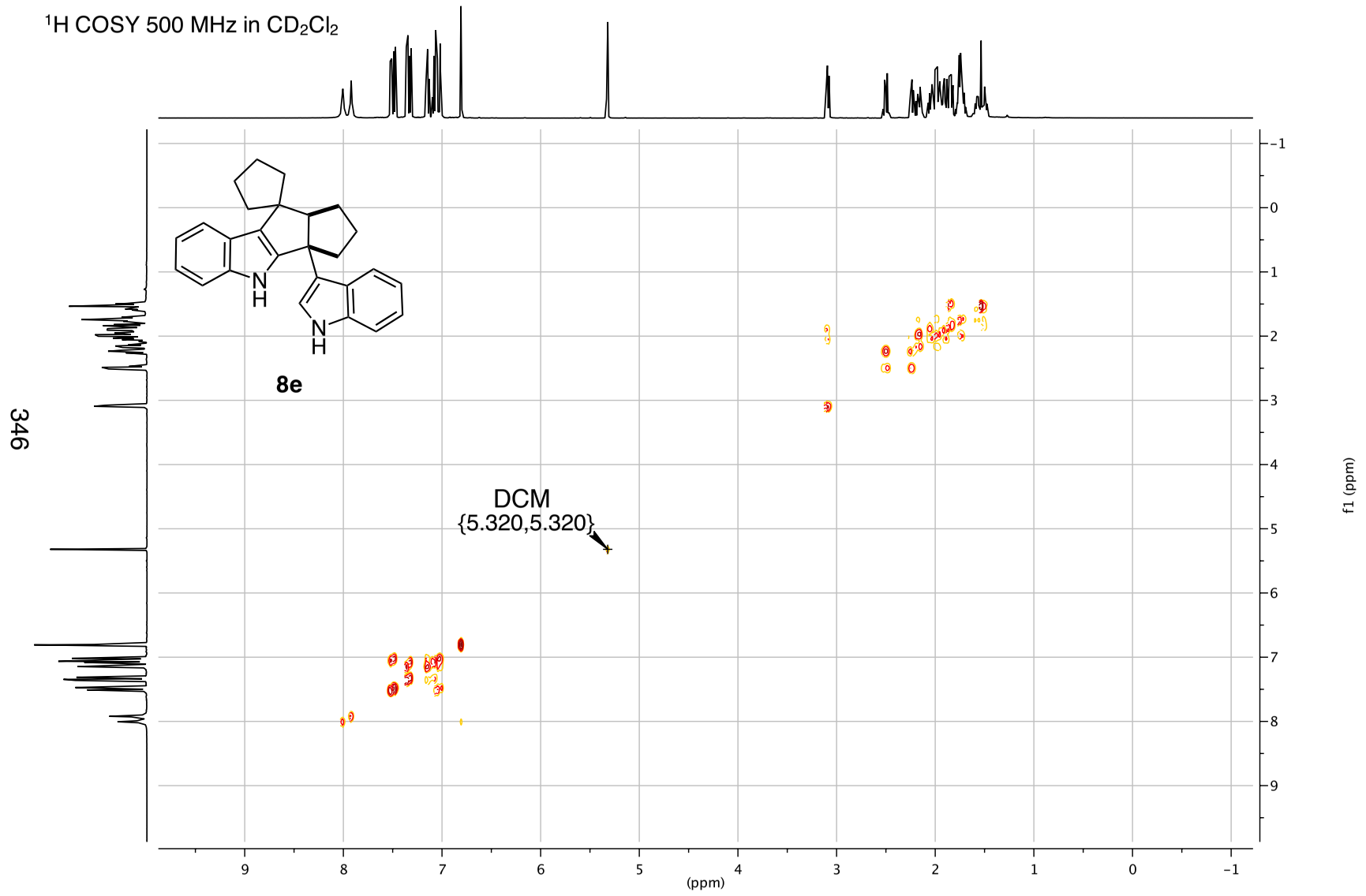
^{1}H COSY 500 MHz in CD_2Cl_2
8e
DCM
{5.320,5.320}
(ppm)
f1 (ppm)

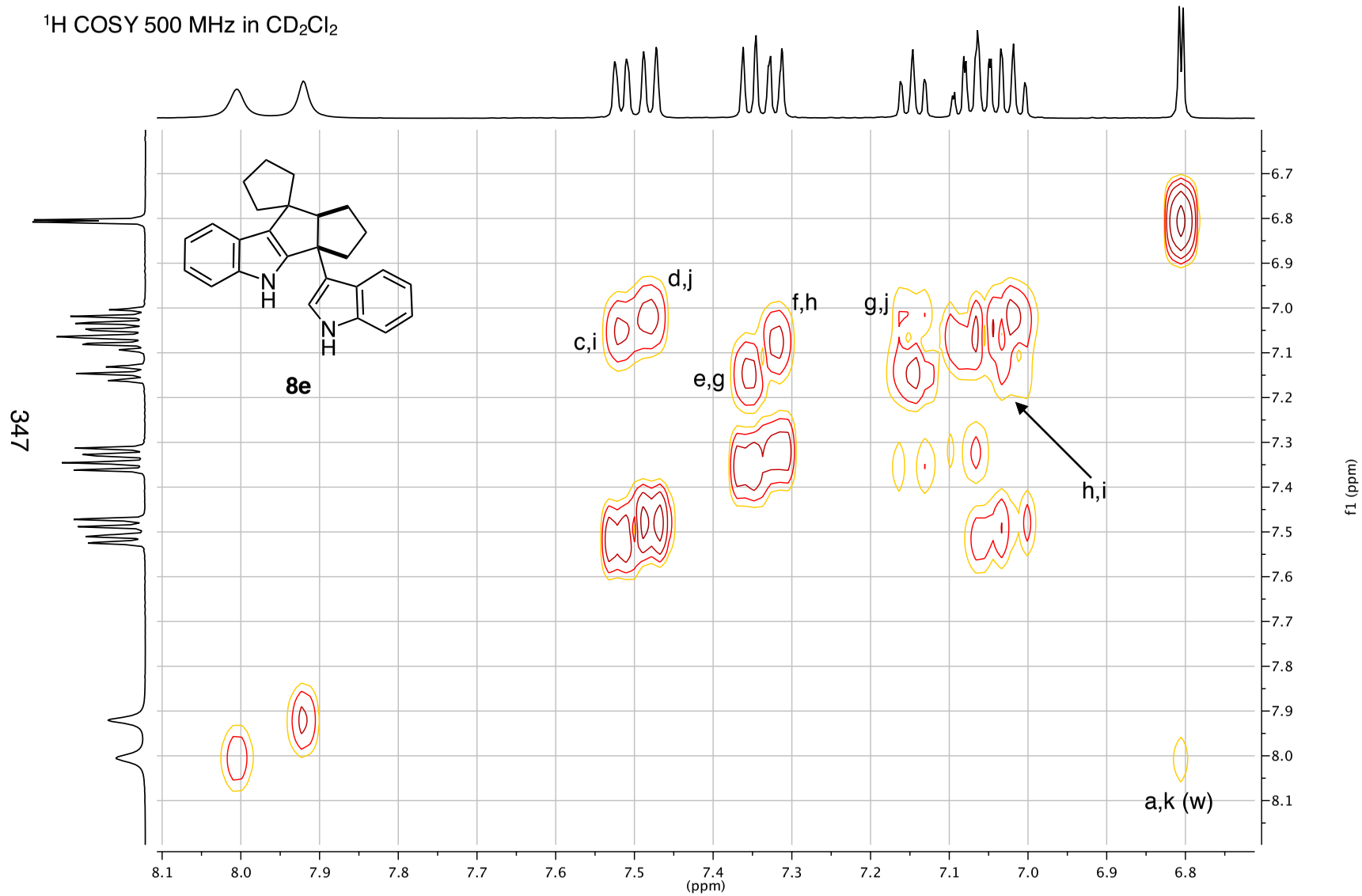
^{1}H COSY 500 MHz in CD_2Cl_2
347
8e
c,i
d,j
e,g
f,h
g,j
h,i
a,k (w)
8.1
8.0
7.9
7.8
7.7
7.6
7.5
7.4
7.3
7.2
7.1
7.0
6.9
6.8
(ppm)
f1 (ppm)

^{1}H COSY (Symmetrized) 500 MHz in CD_2Cl_2

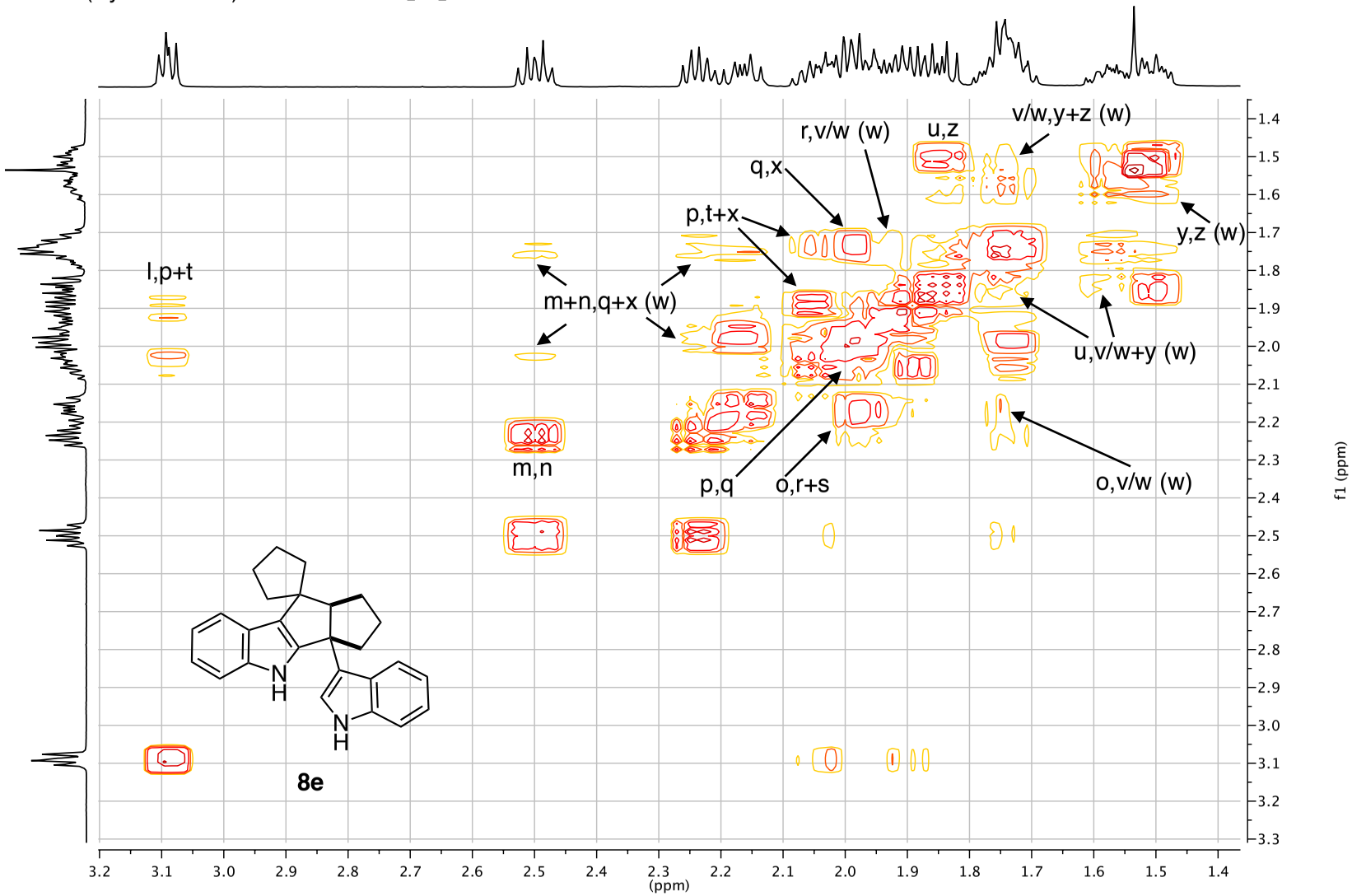

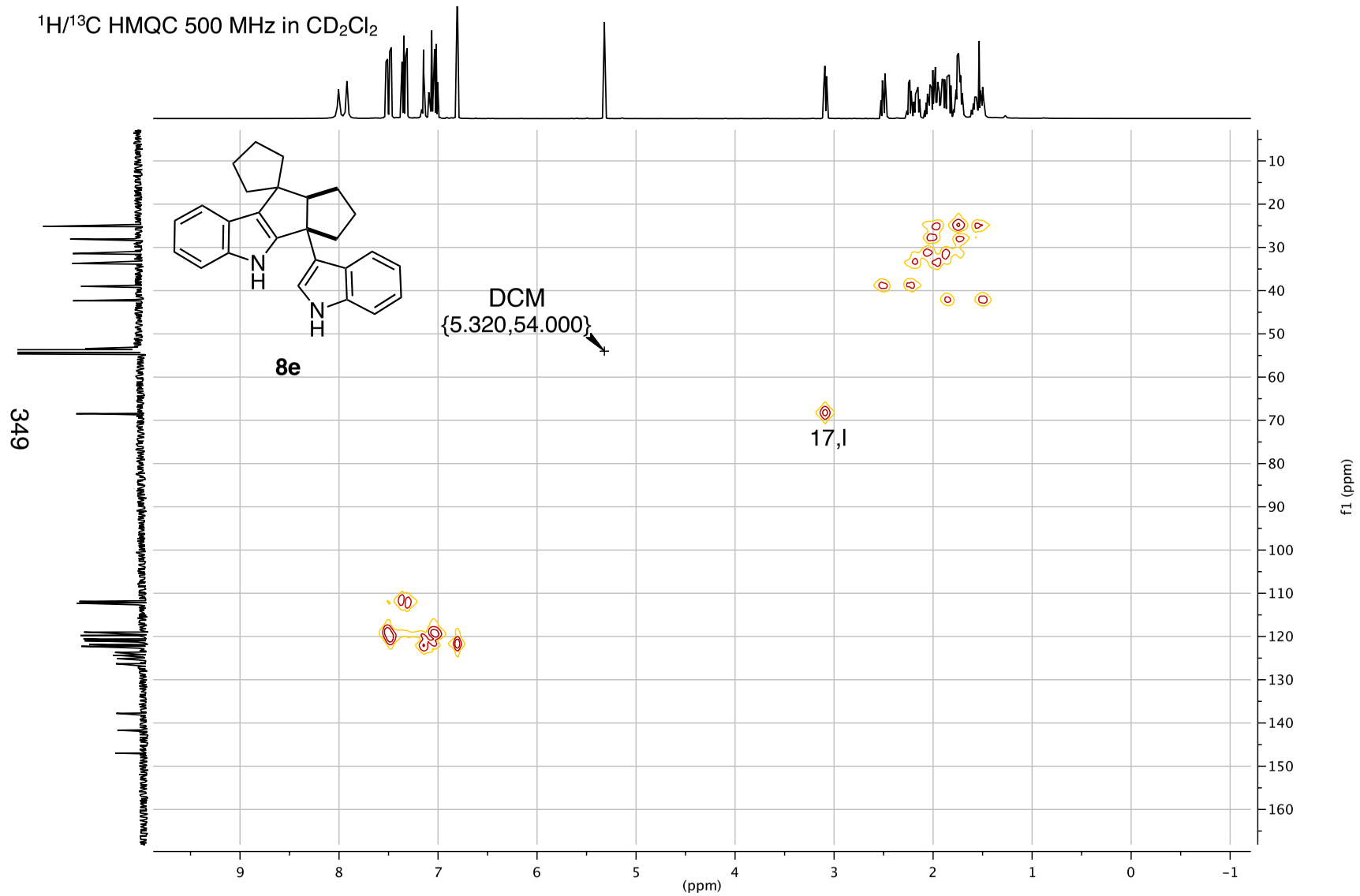
$^{1}H/^{13}C$ HMQC 500 MHz in CD_2Cl_2
8e
DCM
{5.320,54.000}
17,l
349
(ppm)
f1 (ppm)

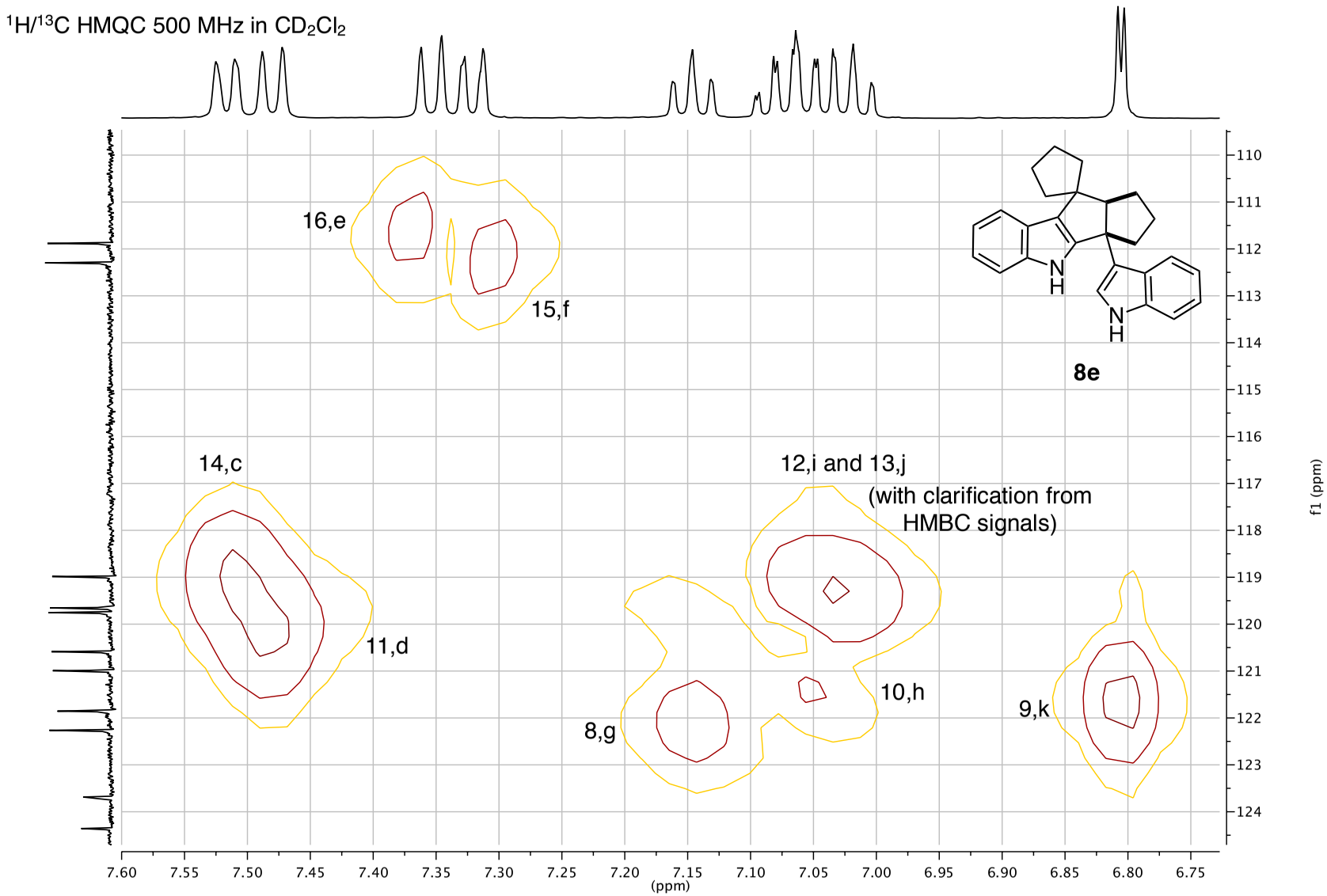
$^{1}H/^{13}C$ HMQC 500 MHz in CD_2Cl_2
16,e
15,f
14,c
11,d
12,i and 13,j
(with clarification from
HMBC signals)
10,h
8,g
9,k
N
H
N
H
8e
7.60 7.55 7.50 7.45 7.40 7.35 7.30 7.25 7.20 7.15 7.10 7.05 7.00 6.95 6.90 6.85 6.80 6.75
(ppm)
110 111 112 113 114 115 116 117 118 119 120 121 122 123 124
f1 (ppm)

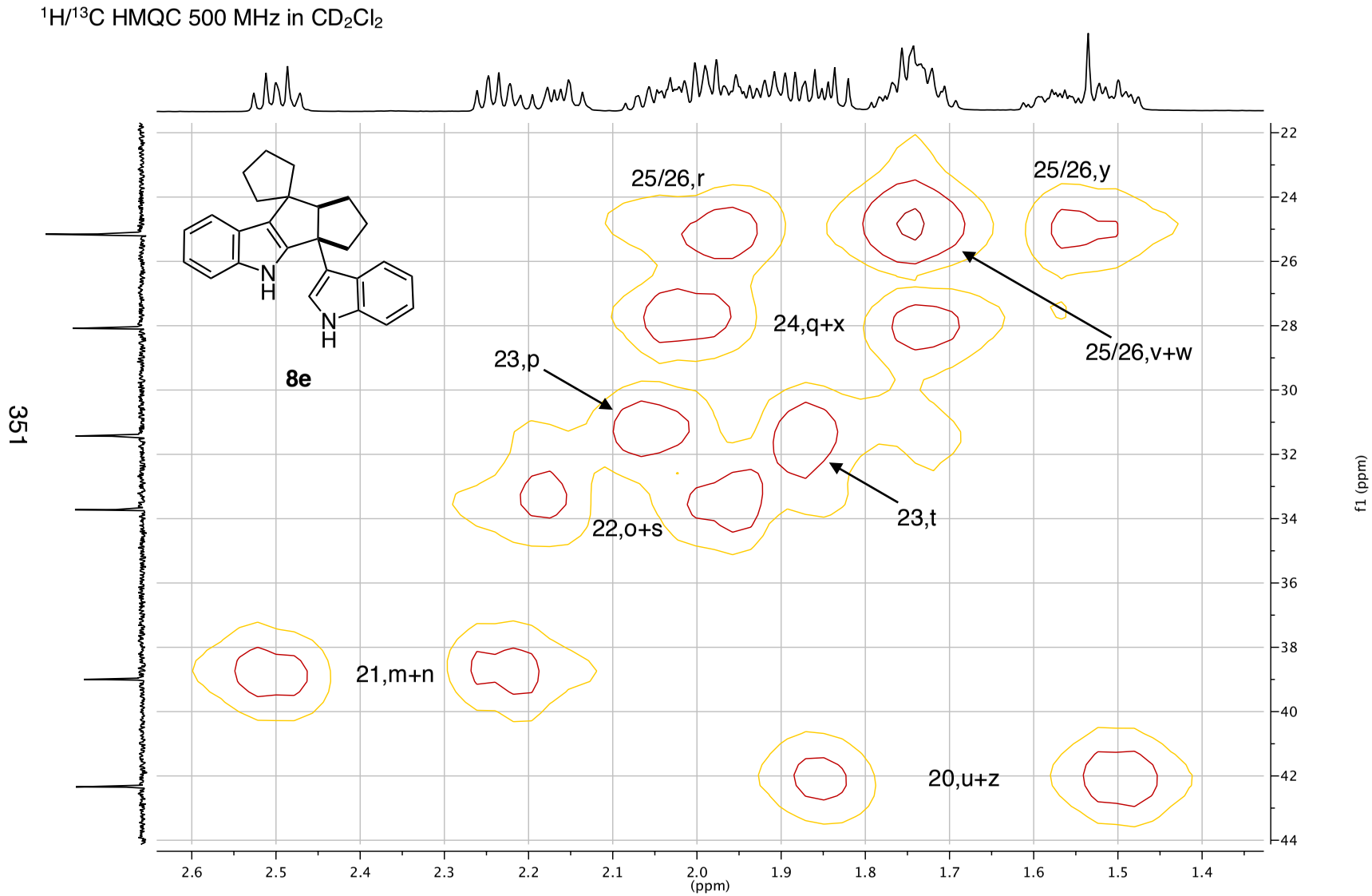
$^{1}H/^{13}C$ HMQC 500 MHz in CD_2Cl_2
351
8e
25/26,r
25/26,y
24,q+x
25/26,v+w
23,p
23,t
22,o+s
21,m+n
20,u+z
(ppm)
f1 (ppm)

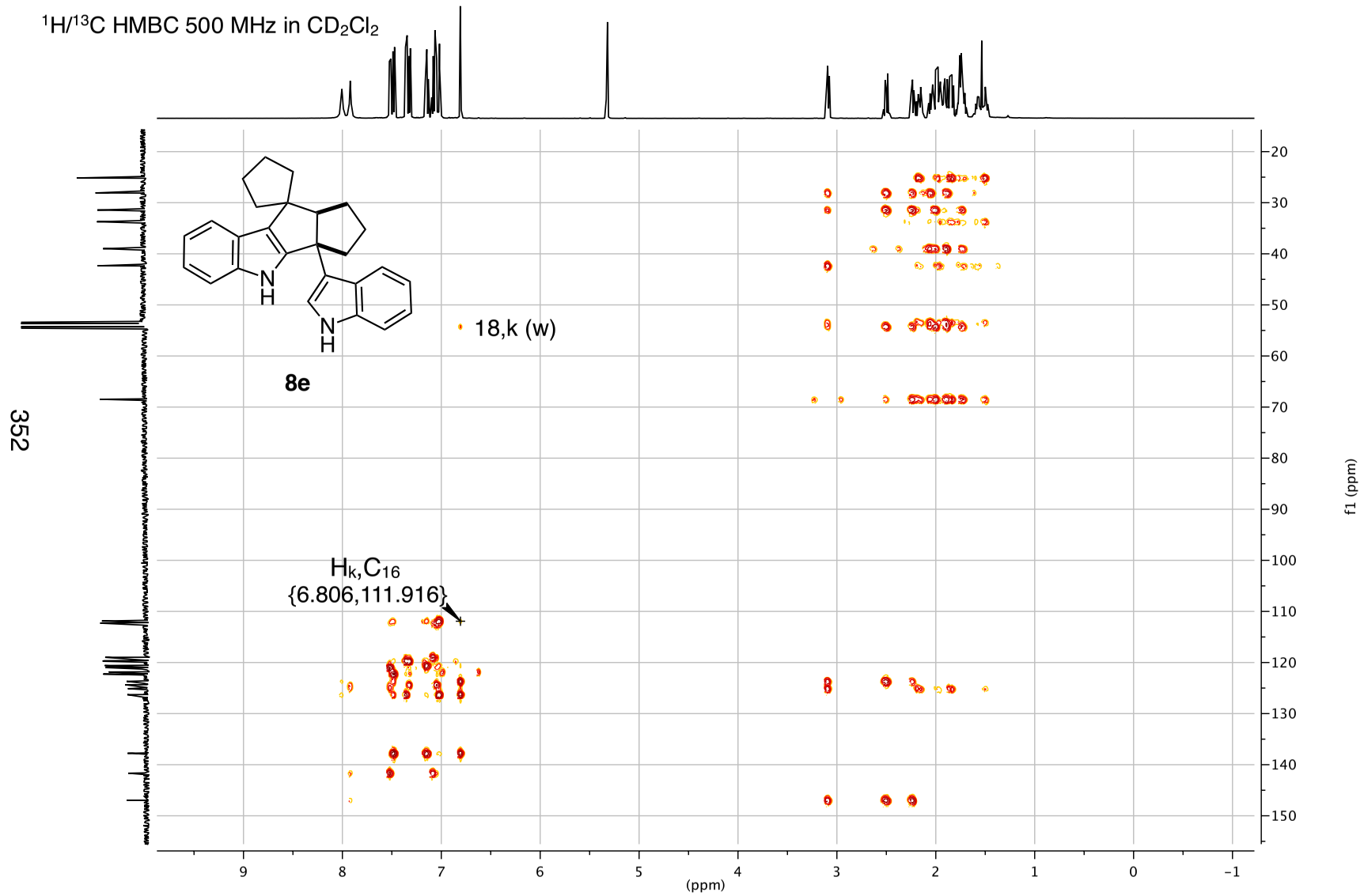
$^{1}H/^{13}C$ HMBC 500 MHz in CD_2Cl_2
352
N
H
N
H
8e
18,k (w)
H_k,C_{16}
{6.806,111.916}
(ppm)
f1 (ppm)

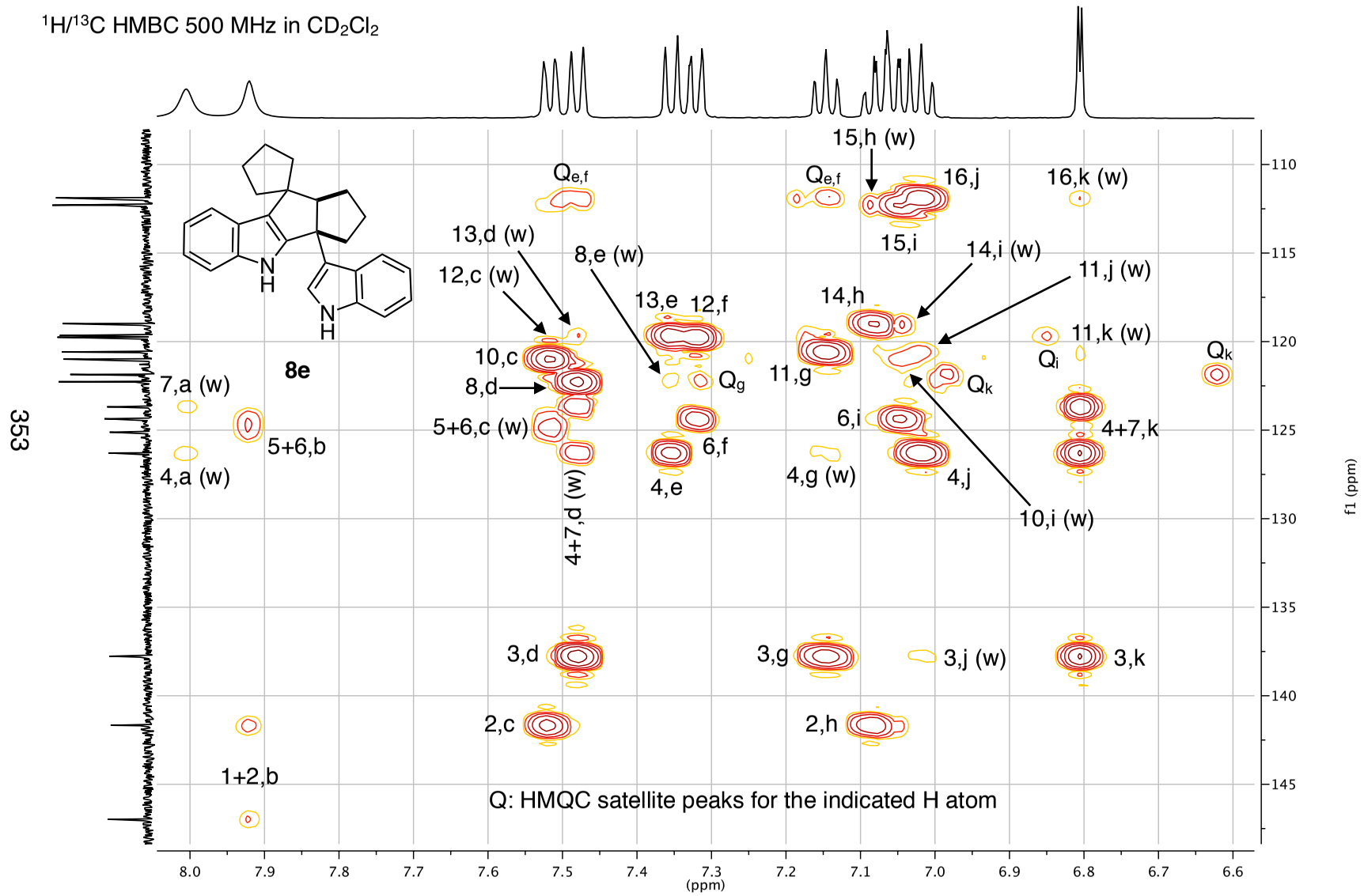
$^{1}H/^{13}C$ HMBC 500 MHz in CD_2Cl_2
353
8e
Q: HMQC satellite peaks for the indicated H atom
(ppm)
f1 (ppm)

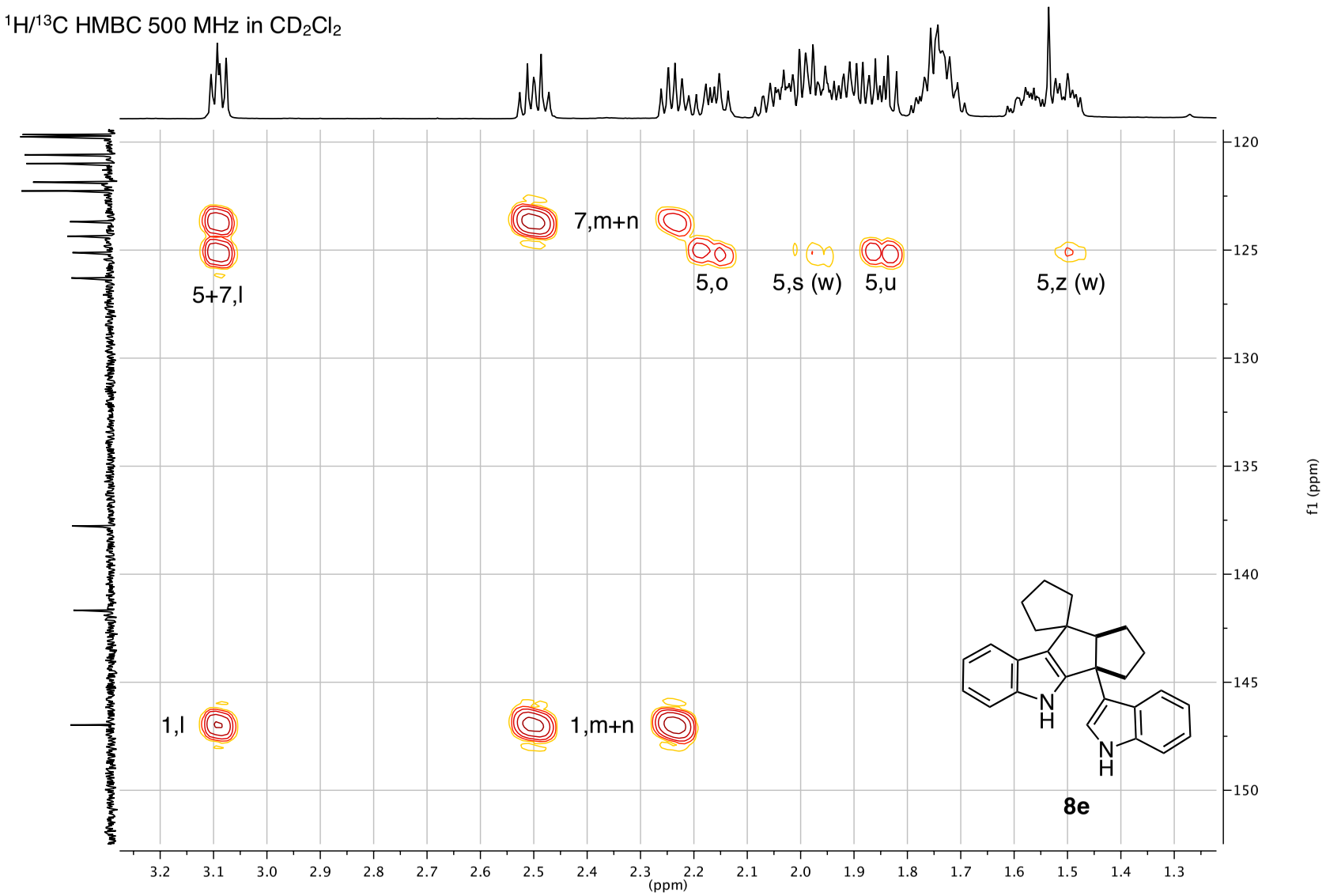
$^{1}H/^{13}C$ HMBC 500 MHz in CD_2Cl_2
5+7,l
7,m+n
5,o
5,s (w)
5,u
5,z (w)
1,l
1,m+n
8e
(ppm)
f1 (ppm)

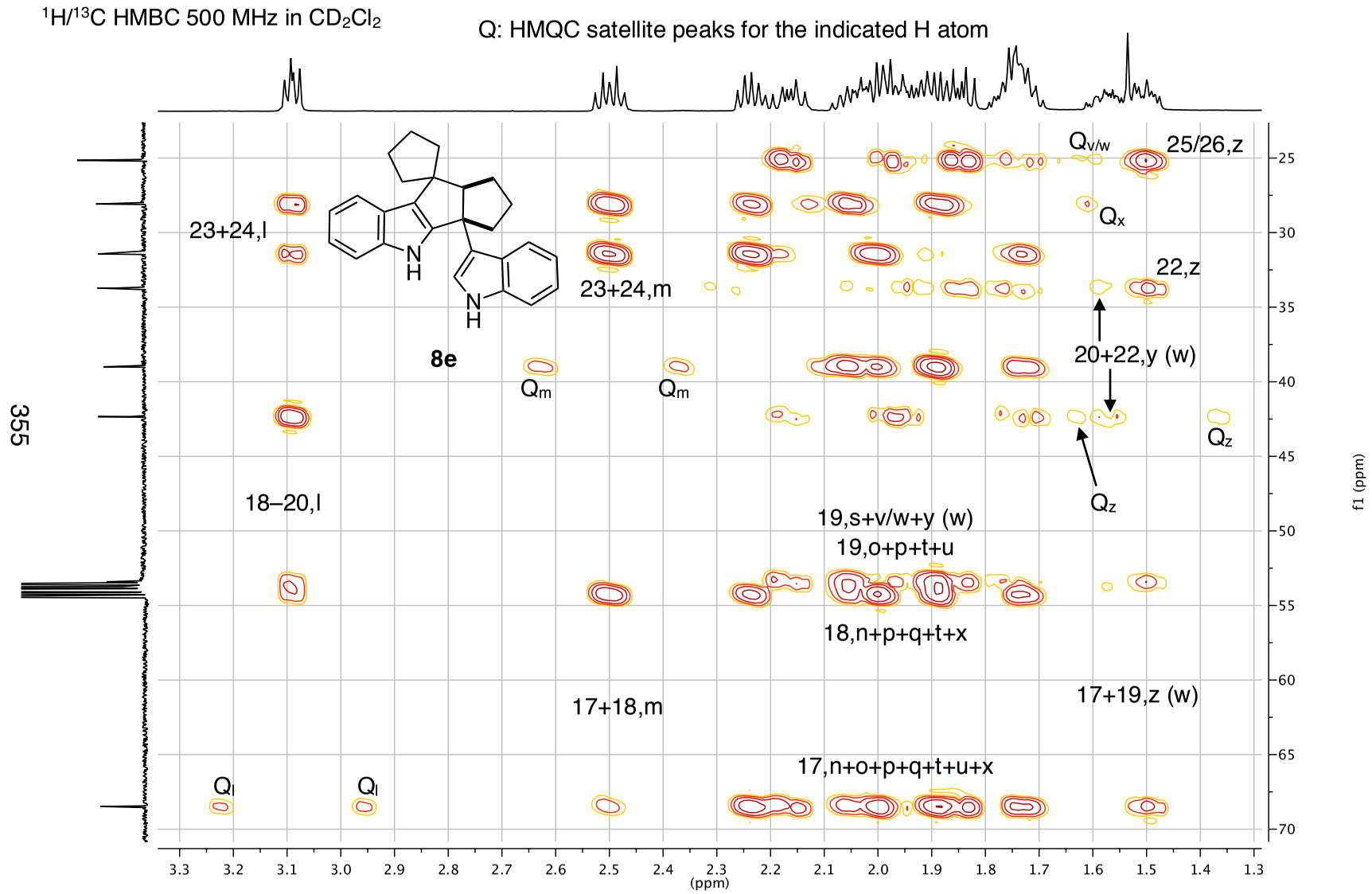
$^{1}H/^{13}C$ HMBC 500 MHz in CD_2Cl_2
Q: HMQC satellite peaks for the indicated H atom
355
8e
23+24,l
23+24,m
Q_m
Q_m
$Q_{v/w}$
25/26,z
Q_x
22,z
20+22,y (w)
Q_z
Q_z
18–20,l
19,s+v/w+y (w)
19,o+p+t+u
18,n+p+q+t+x
17+18,m
17+19,z (w)
17,n+o+p+q+t+u+x
Q_l
Q_l
(ppm)
f1 (ppm)

$^{1}H/^{13}C$ HMBC 500 MHz in CD_2Cl_2

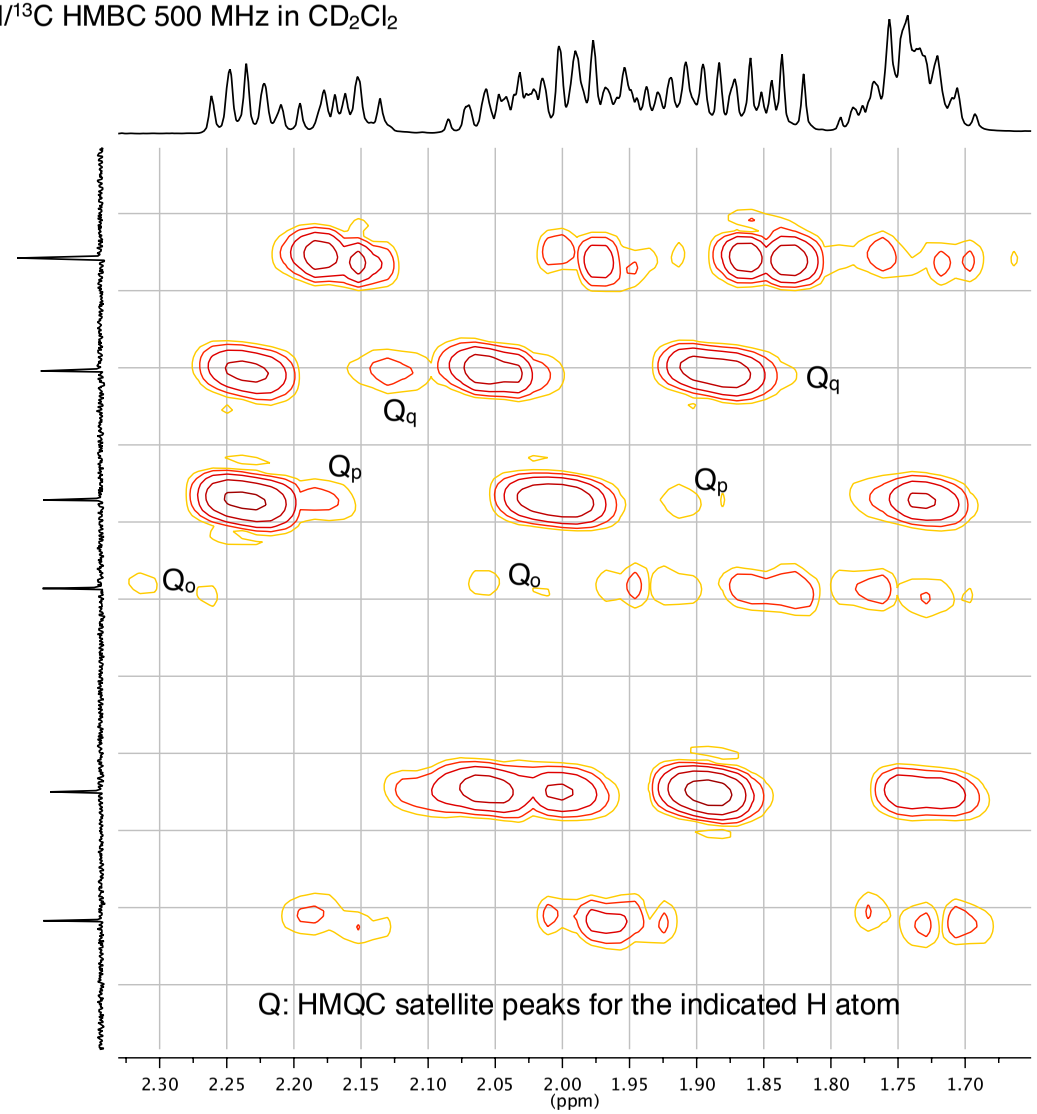

25/26,o+r/s+u+v/w

24,n+p+t

23,n+q+x

22,r+u+v/w

21,p+q+t+x

20,o+s+v/w

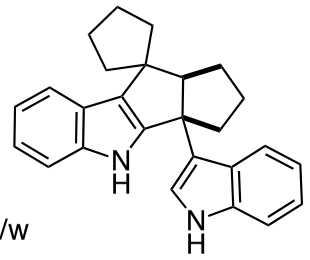

8e

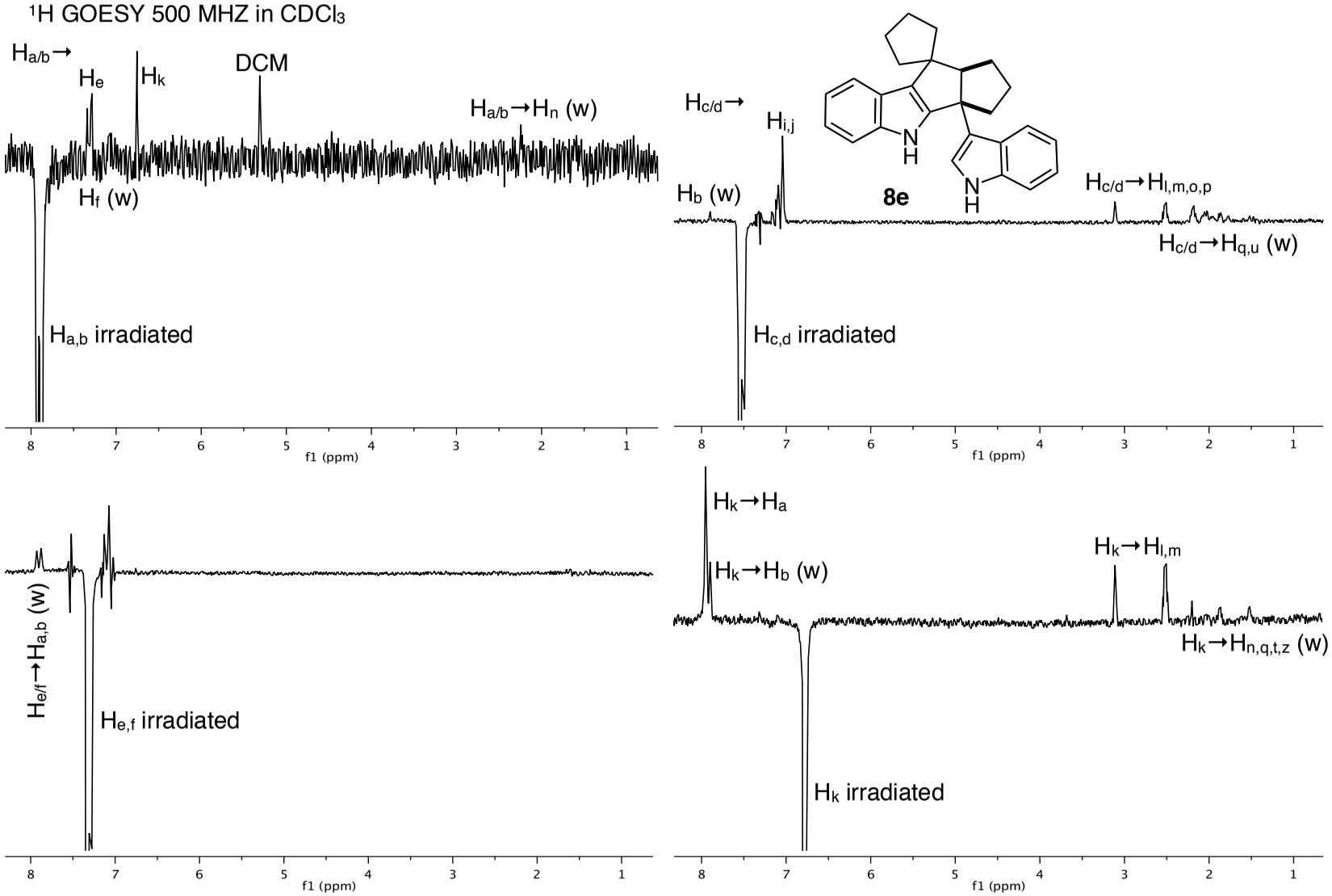
^{1}H GOESY 500 MHZ in $CDCl_3$
$H_{a/b}$→
H_e
H_k
DCM
$H_{a/b}$→H_n (w)
H_f (w)
$H_{a,b}$ irradiated
$H_{c/d}$→
$H_{i,j}$
H_b (w)
8e
$H_{c/d}$→$H_{l,m,o,p}$
$H_{c/d}$→$H_{q,u}$ (w)
$H_{c,d}$ irradiated
$H_{e/f}$→$H_{a,b}$ (w)
$H_{e,f}$ irradiated
H_k→H_a
H_k→H_b (w)
H_k→$H_{l,m}$
H_k→$H_{n,q,t,z}$ (w)
H_k irradiated
f1 (ppm)

^{1}H GOESY 500 MHZ in $CDCl_3$

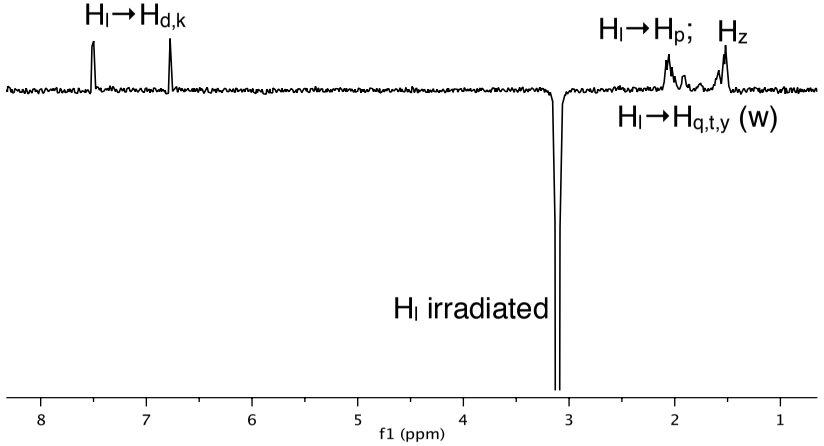

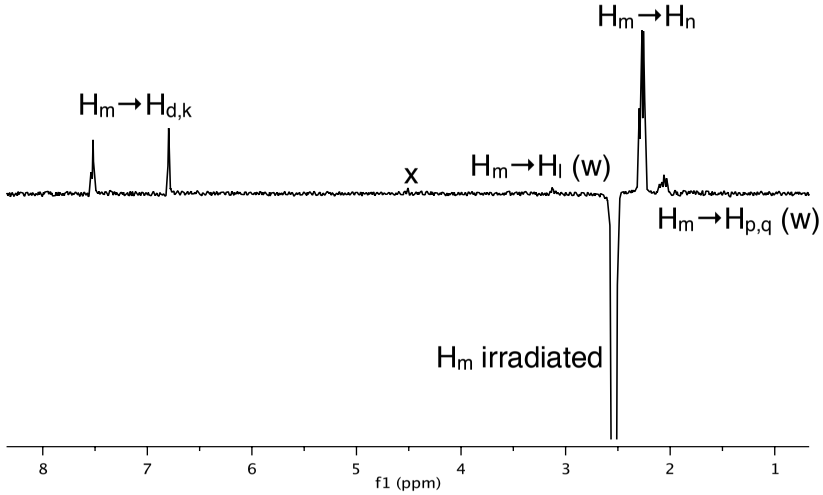

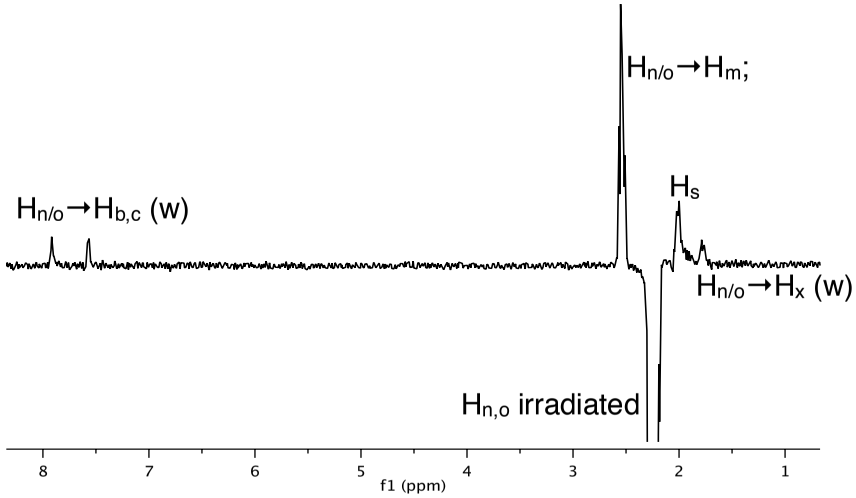

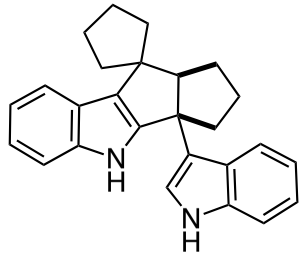

8e

Table 34 (1 of 2). Proton NMR summary for **8e**.

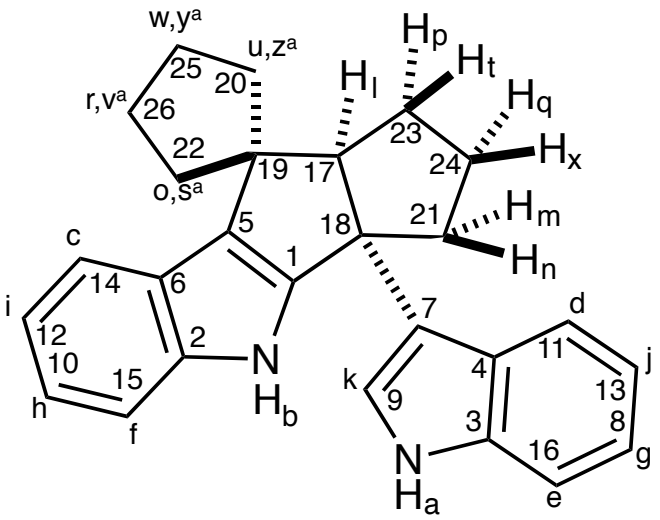

H label	δ	COSY	NOE[b]
a	8.01	k	E,f,K,n
b	7.92	-	
c	7.52	I	b,I,J,L,M,O,P,q,u
d	7.48	J	
e	7.35	G	a,b
f	7.32	H	
g	7.15	J	not done
h	7.08	I	not done
i	7.05	C,H	not done
j	7.02	D,G	not done
k	6.81	a	A,b,L,M,n,t,q,z
l	3.09	P,T	D,K,P,q,t,y,Z
m	2.50	N,q,x	D,K,l,N,p,q

[a]$H_{o,r,u,w}$ face H_c; $H_{s,v,y,z}$ face H_l.

[b]Merged entries were co-irradiated due to similar chemical shift.

Table 34 (2 of 2). Proton NMR summary for **8e**.

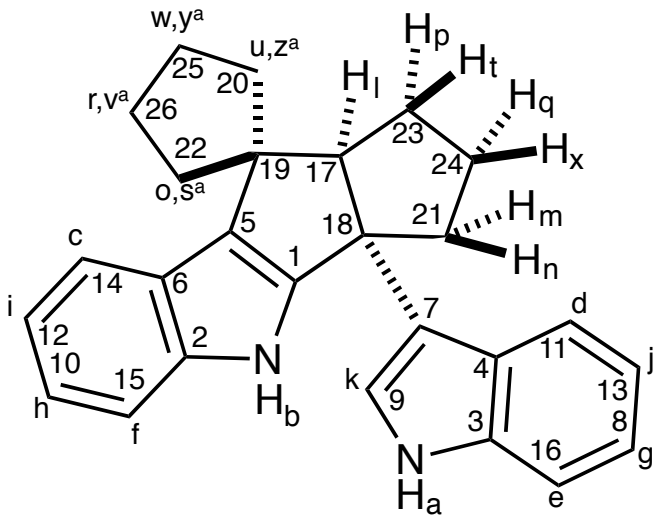

H label	δ	COSY	NOE[b]
n	2.24	M,q,x	b,c,M,S,x
o	2.17	r,S,v/w	
p	2.06	L,Q,T,X	not done
q	2.01	m,n,P,T,X	not done
r	1.97	o,v/w	not done
s	1.96	O	not done
t	1.87	L,P	not done
u	1.85	v/w,y,Z	not done
v[c]	1.75	o,r,u,y,z	not done
w[c]	1.75		not done
x	1.73	m,n,P,Q	not done
y	1.55	u,v/w,z	not done
z	1.50	U,v/w,y	not done

[a]$H_{o,r,u,w}$ face H_c; $H_{s,v,y,z}$ face H_l.

[b]Merged entries were co-irradiated due to similar chemical shift.

[c]$H_{v/w}$ are indistinguishable by the performed experiments and are arbitrarily assigned.

Table 35 (1 of 2). Carbon NMR summary for **8e**.

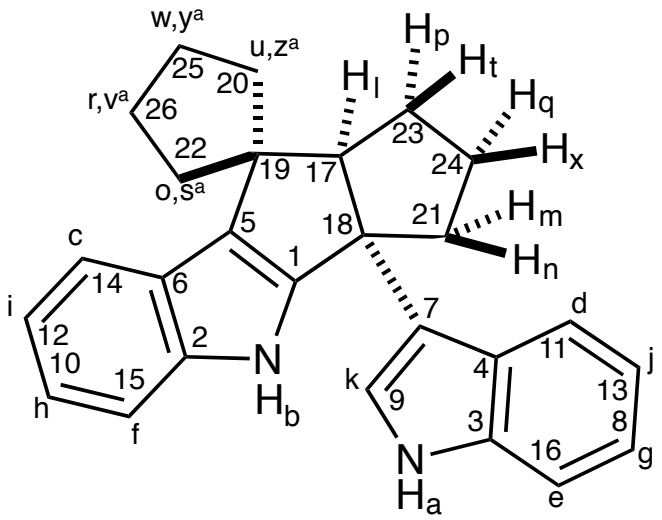

C label	δ	type	HMQC	HMBC
1	147.0	q	-	B,L,M,N
2	141.7	q	-	B,C,H
3	137.8	q	-	D,G,j,K
4	126.3	q	-	a,d,E,g,J,K
5	125.1	q	-	B,c,L,O,s,U,z
6	124.4	q	-	B,c,F,I
7	123.7	q	-	a,d,K,L,M,N
8	122.3	CH	g	D,e
9	121.9	CH	k	-
10	121.0	CH	h	C,i
11	120.6	CH	d	G,j,k
12	119.75	CH	i	c,F
13	119.65	CH	j	d,E
14	119.0	CH	c	H,i

[a]$H_{o,r,u,w}$ face H_c; $H_{s,v,y,z}$ face H_l.

Table 35 (2 of 2). Carbon NMR summary for **8e**.

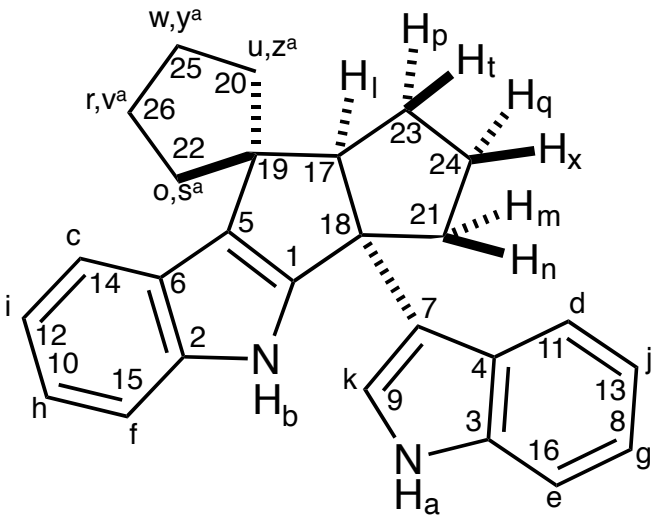

C label	δ	type	HMQC	HMBC
15	112.3	CH	f	h,I
16	111.9	CH	e	J,k
17	68.5	CH	l	M,N,O,P,Q,T,U,X,z
18	54.3	q	-	k,L,M,N,P,Q,T,X
19	53.4	q	-	L,O,P,s,T,U,V/W
20	42.3	CH_2	u,z	L,O,S,V/W,y
21	39.0	CH_2	m,n	P,Q,T,X
22	33.7	CH_2	o,s	R,U,V,y,Z
23	31.4	CH_2	p,t	L,M,N,Q,X
24	28.1	CH_2	q,x	L,M,N,P,T
25[b]	25.2	CH_2	r,v	O,R/S,U,V/W,Z
26[b]	25.2	CH_2	w,y	

[a]$H_{o,r,u,w}$ face H_c; $H_{s,v,y,z}$ face H_l.

[b]$C_{25/26}$ are indistinguishable by the performed experiments and are arbitrarily assigned.

^{1}H NMR 500 MHz in $(CD_3)_2NCDO$

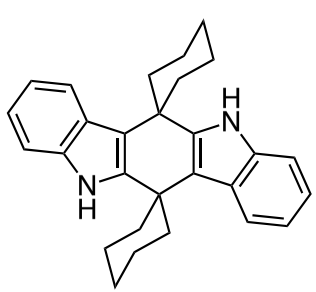

9f

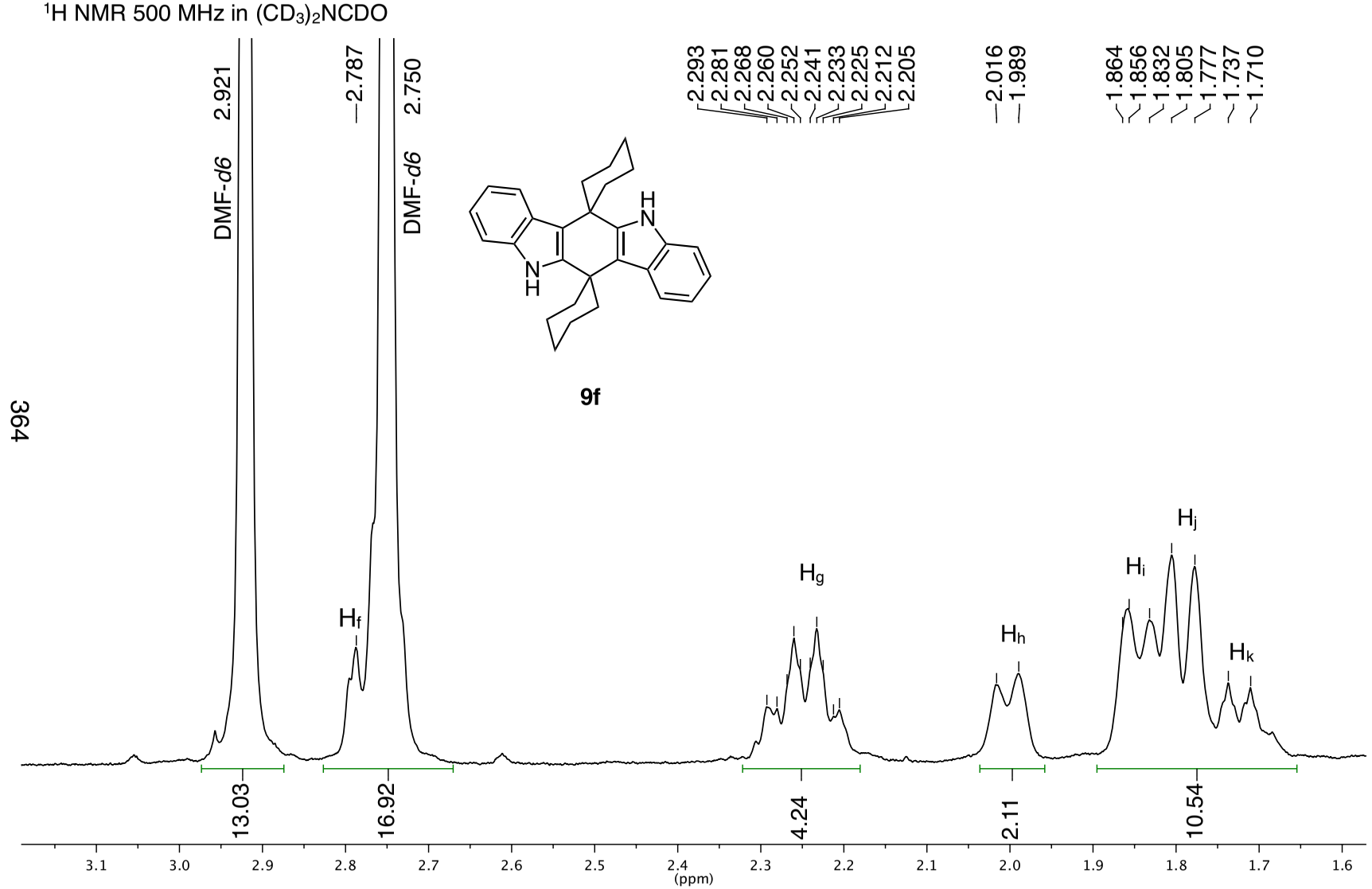
^{1}H NMR 500 MHz in $(CD_3)_2NCDO$
364
DMF-*d6* 2.921
2.787
2.750
DMF-*d6*
2.293
2.281
2.268
2.260
2.252
2.241
2.233
2.225
2.212
2.205
2.016
1.989
1.864
1.856
1.832
1.805
1.777
1.737
1.710
9f
H_f
H_g
H_h
H_i
H_j
H_k
13.03
16.92
4.24
2.11
10.54
3.1
3.0
2.9
2.8
2.7
2.6
2.5
2.4
2.3
2.2
2.1
2.0
1.9
1.8
1.7
1.6
(ppm)

^{13}C NMR 126 MHz in $(CD_3)_2NCDO$

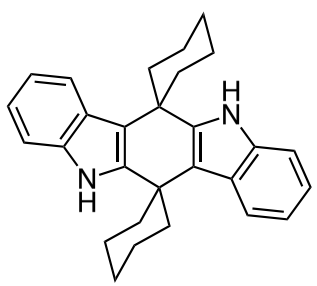

9f

365

^{13}C NMR 126 MHz in $(CD_3)_2NCDO$

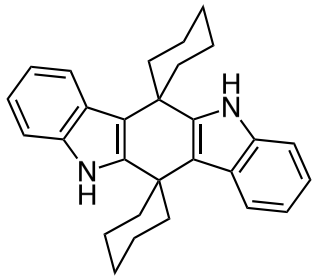

9f

^{1}H/^{13}C DEPT135 500 MHz in $(CD_3)_2NCDO$

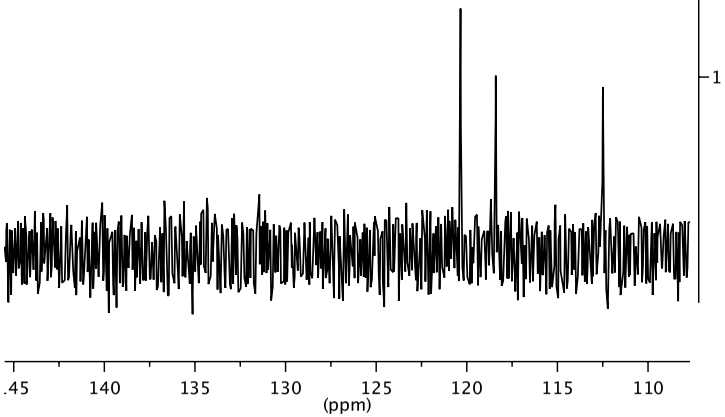

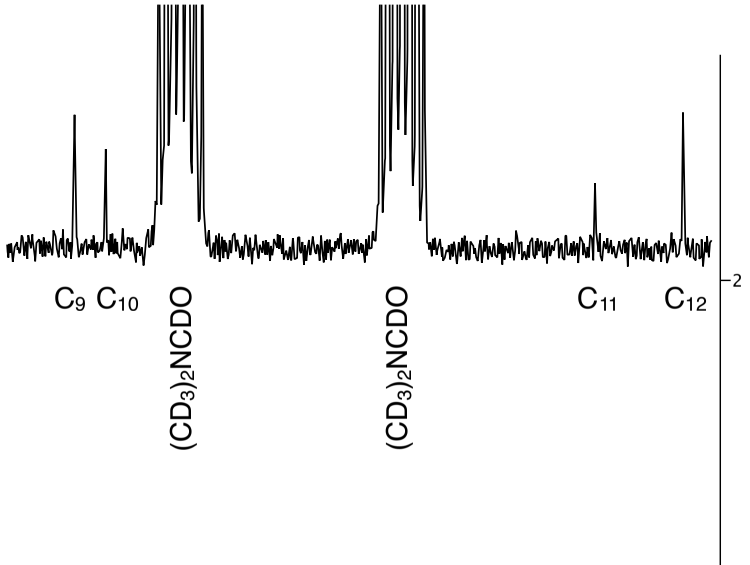

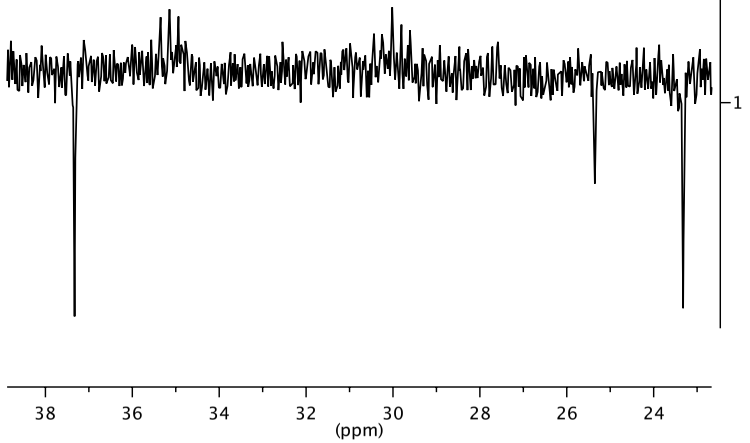

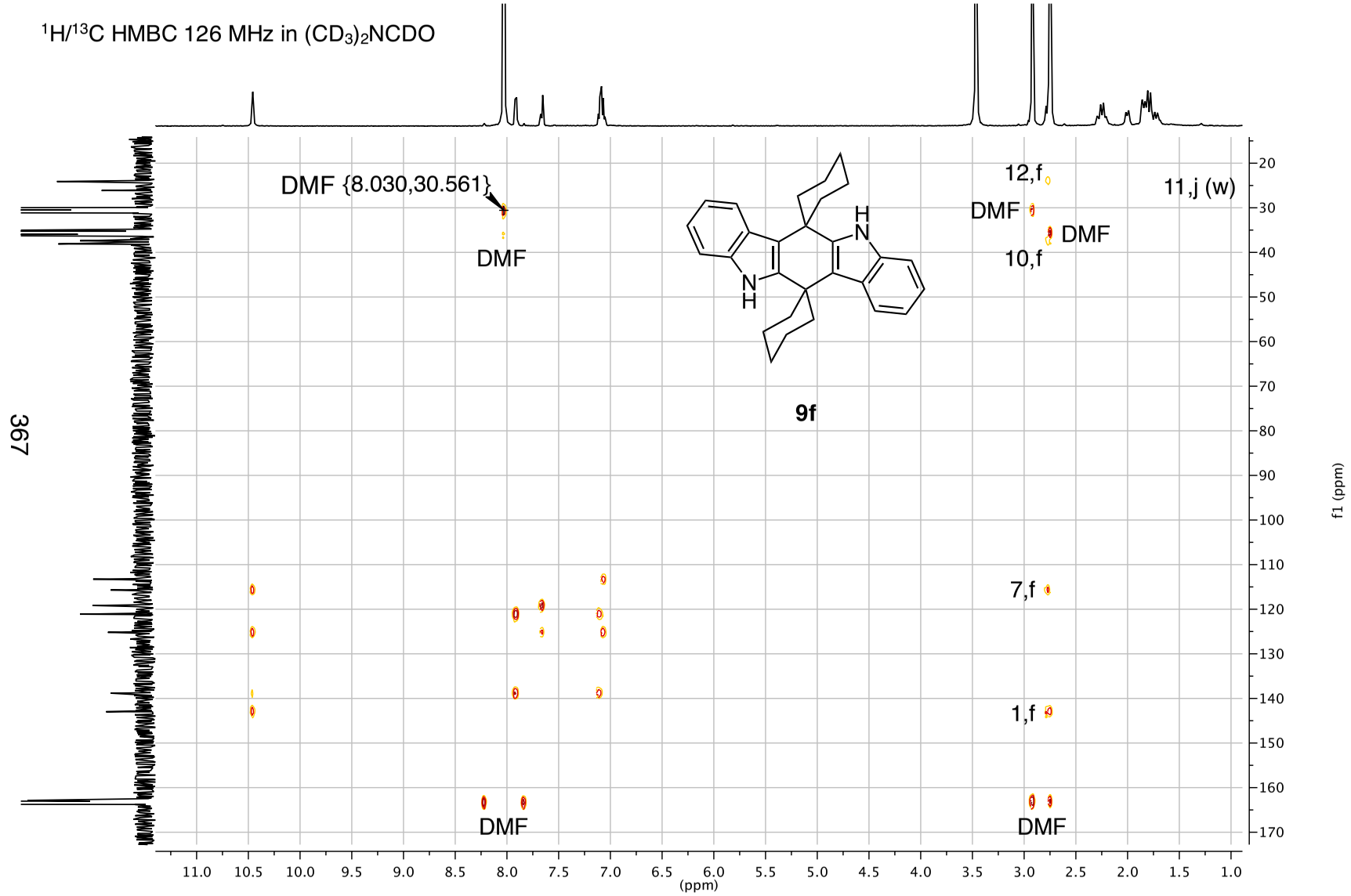
$^{1}H/^{13}C$ HMBC 126 MHz in $(CD_3)_2NCDO$
DMF {8.030,30.561}
DMF
12,f
DMF
DMF
10,f
11,j (w)
9f
7,f
1,f
DMF
DMF
367
(ppm)
f1 (ppm)

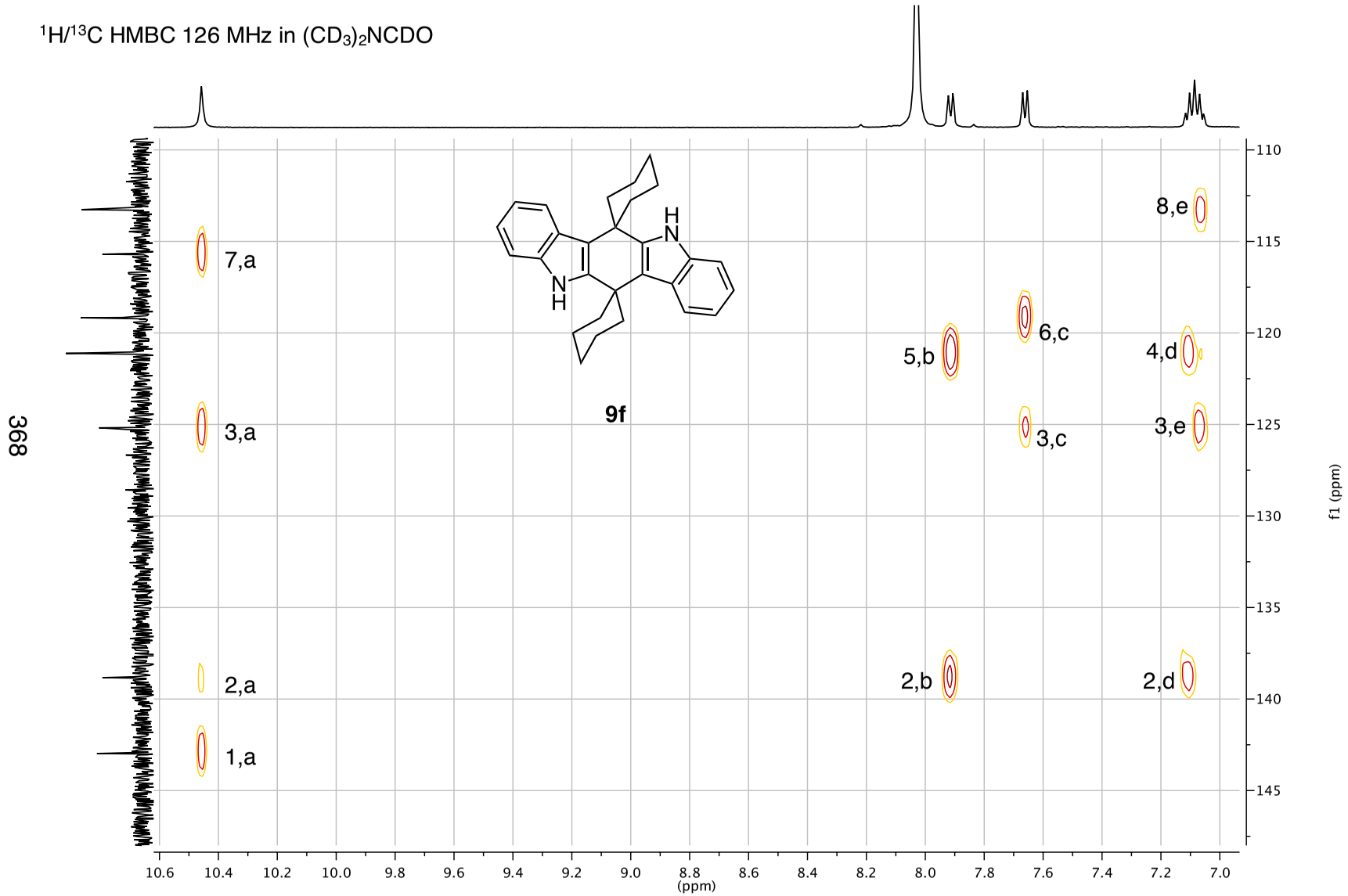
$^{1}H/^{13}C$ HMBC 126 MHz in $(CD_3)_2NCDO$
368
7,a
3,a
2,a
1,a
8,e
6,c
5,b
4,d
3,c
3,e
2,b
2,d
9f
H
N
N
H
10.6
10.4
10.2
10.0
9.8
9.6
9.4
9.2
9.0
8.8
8.6
8.4
8.2
8.0
7.8
7.6
7.4
7.2
7.0
(ppm)
110
115
120
125
130
135
140
145
f1 (ppm)

Table 36. Carbon NMR summary for **9f**.

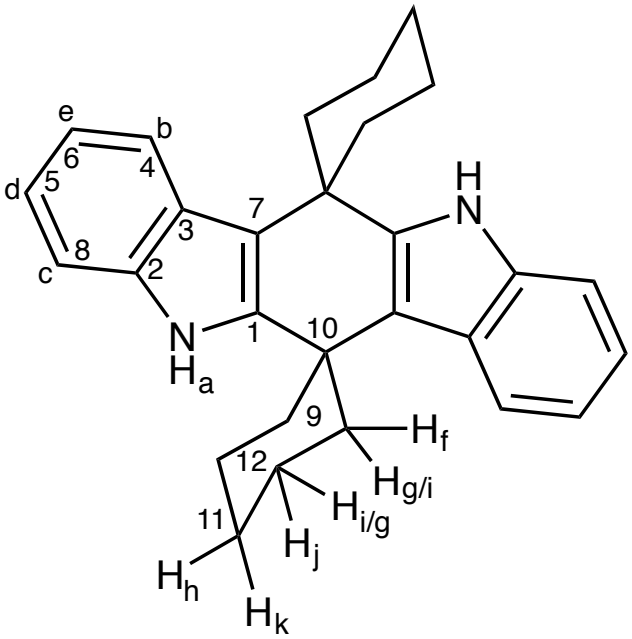

C label	δ	count	type	HMBC[a]
1	143.0	2	q	A,F
2	138.8	2	q	a,B,D
3	125.2	2	q	A,C,E
4[b]	121.12	2	CH	D
5[b]	121.10	2	CH	B
6	119.2	2	CH	C
7	115.7	2	q	A,F
8	113.3	2	CH	E
9	38.1	4	CH_2	-
10	37.4	2	q	F
11	26.1	2	CH_2	j
12	24.1	4	CH_2	f

[a]No crosspeaks are observed for $H_{g,h,i,k}$. $H_{h,k}$ are assigned to C_{11} based on their integrations of 2H.

[b]$C_{4/5}$ are indistinguishable by the performed experiments and are arbitrarily assigned.

^{1}H NMR 500 MHz in $(CD_3)_2SO$

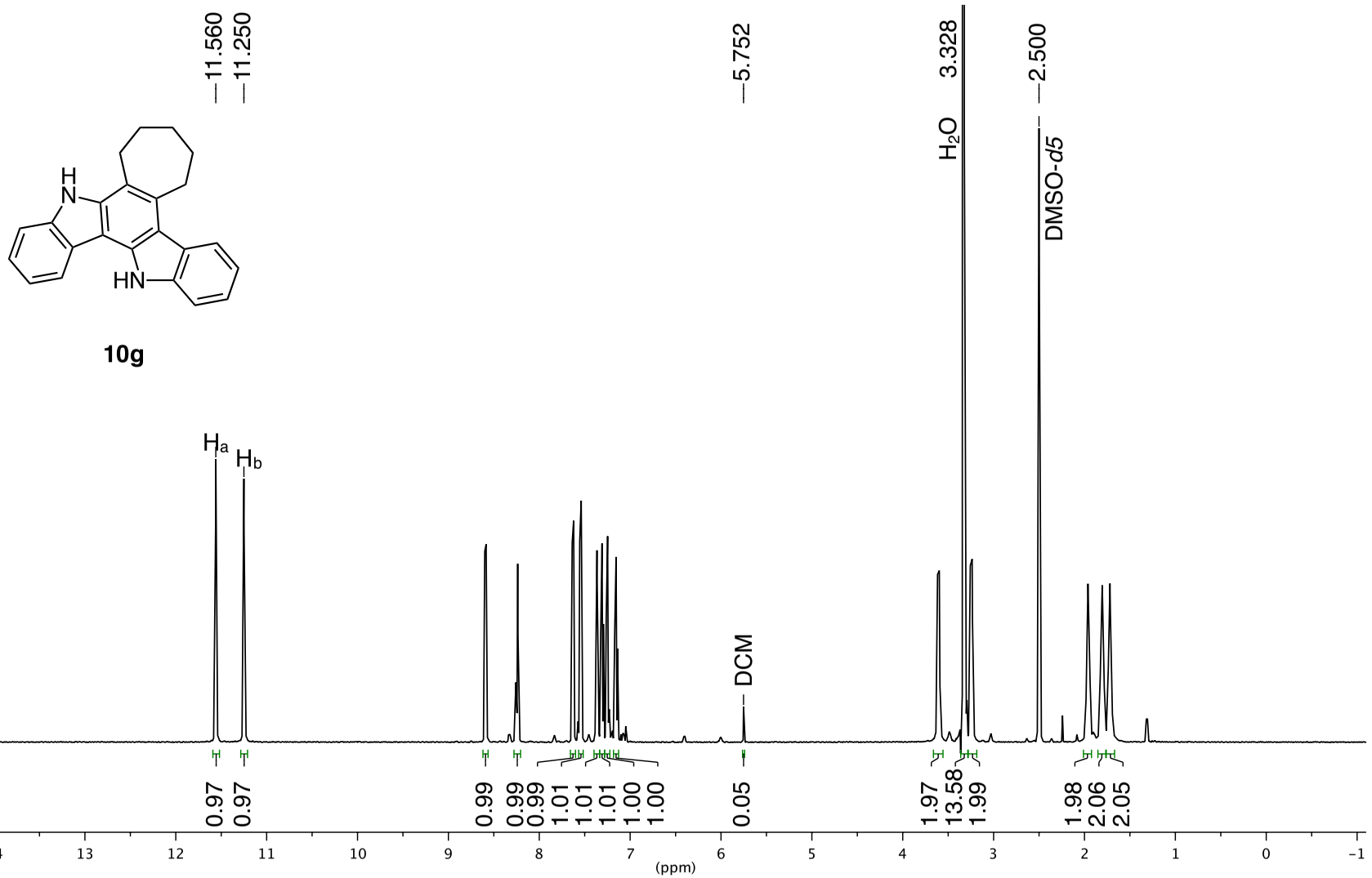

10g

^{1}H NMR 500 MHz in $(CD_3)_2SO$

8.600
8.585
8.253
8.237

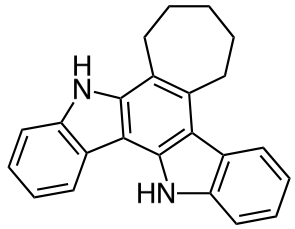

7.638
7.622
7.555
7.539
7.380
7.365
7.350
7.324
7.309
7.294
7.263
7.248
7.233
7.170
7.154
7.140

10g

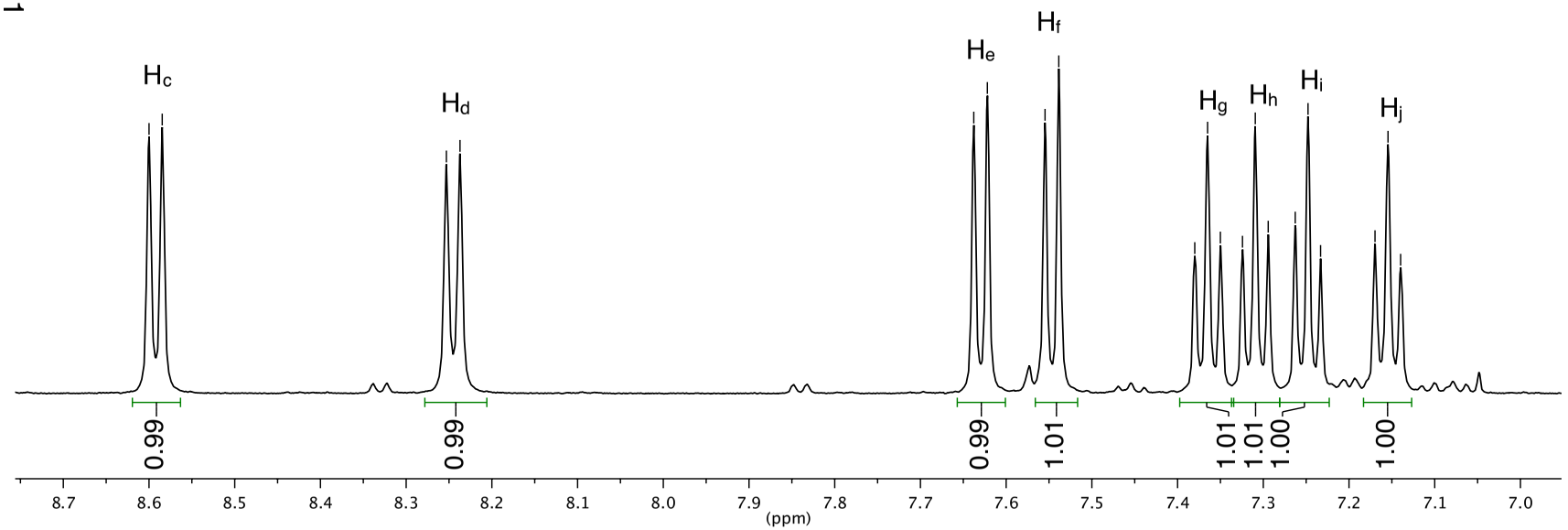

^{1}H NMR 500 MHz in $(CD_3)_2SO$

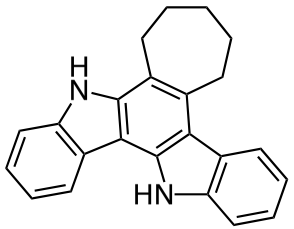

10g

^{13}C NMR 126 MHz in $(CD_3)_2SO$

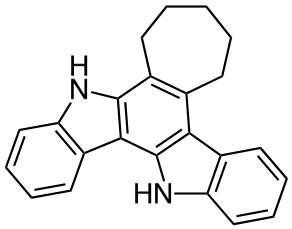

10g

^{13}C NMR 126 MHz in $(CD_3)_2SO$

139.626
138.811
138.207
136.252
132.318
123.694
123.570
122.651
122.013
120.712
120.672
118.593
118.410
117.963
112.852
110.971
110.571
104.175

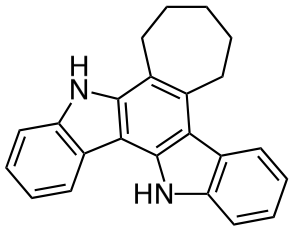

10g

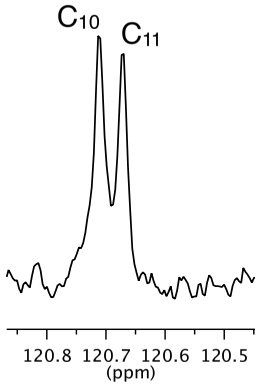

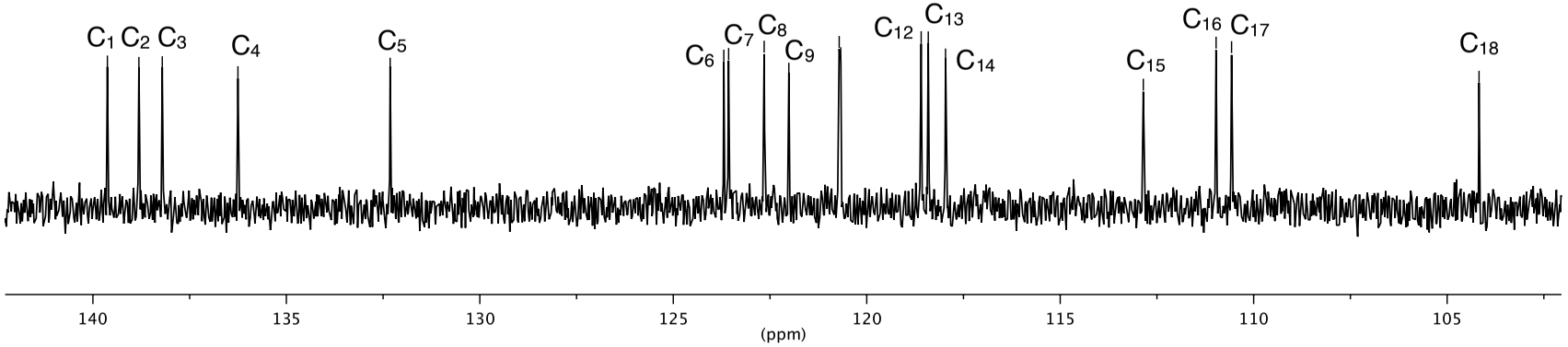

$^{1}H/^{13}C$ DEPT135 500 MHz in $(CD_3)_2SO$

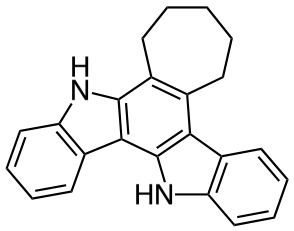

10g

123.568
122.650
120.709
120.669
118.590
118.408
110.967
110.567

32.017
30.104
27.721
27.496
26.729

$C_{7,8}$
$C_{10–13}$
$C_{16,17}$
$(CD_3)_2SO$
$C_{19–23}$

375

150 140 130 120 110 100 90 80 70 60 50 40 30 20 10 0
(ppm)

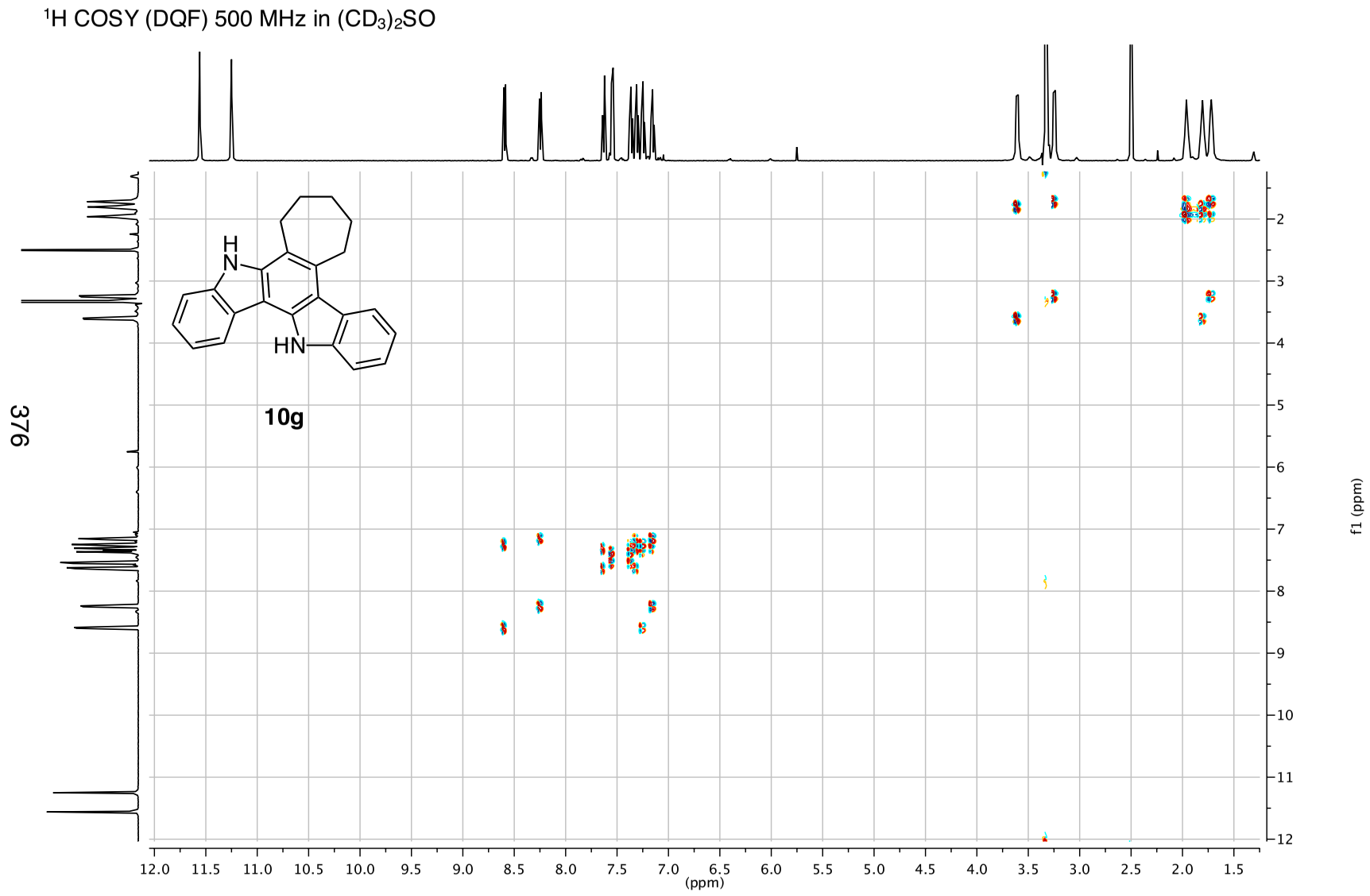
^{1}H COSY (DQF) 500 MHz in $(CD_3)_2SO$
376
H
N
HN
10g
12.0 11.5 11.0 10.5 10.0 9.5 9.0 8.5 8.0 7.5 7.0 6.5 6.0 5.5 5.0 4.5 4.0 3.5 3.0 2.5 2.0 1.5
(ppm)
2 3 4 5 6 7 8 9 10 11 12
f1 (ppm)

^{1}H COSY (DQF) 500 MHz in $(CD_3)_2SO$

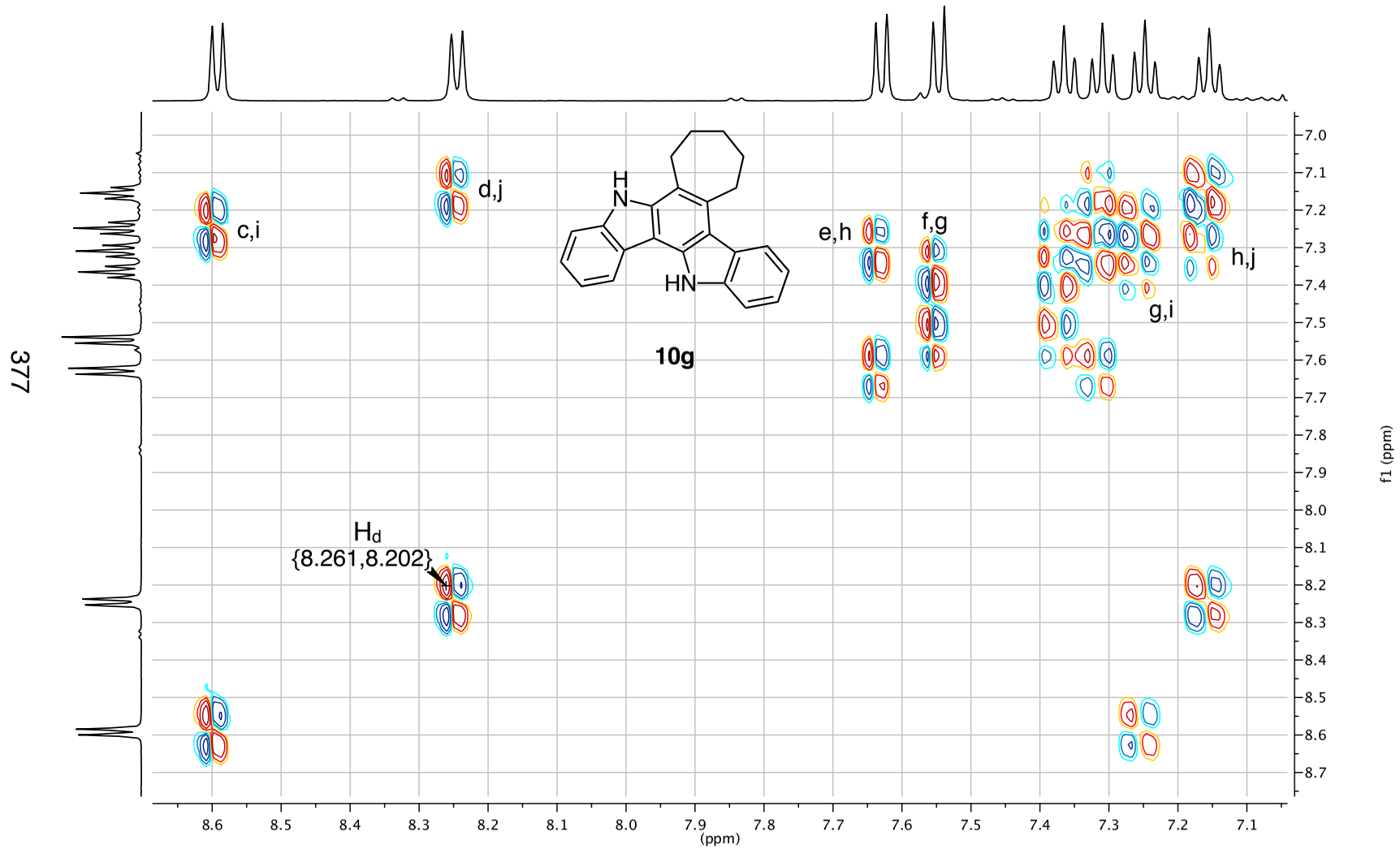

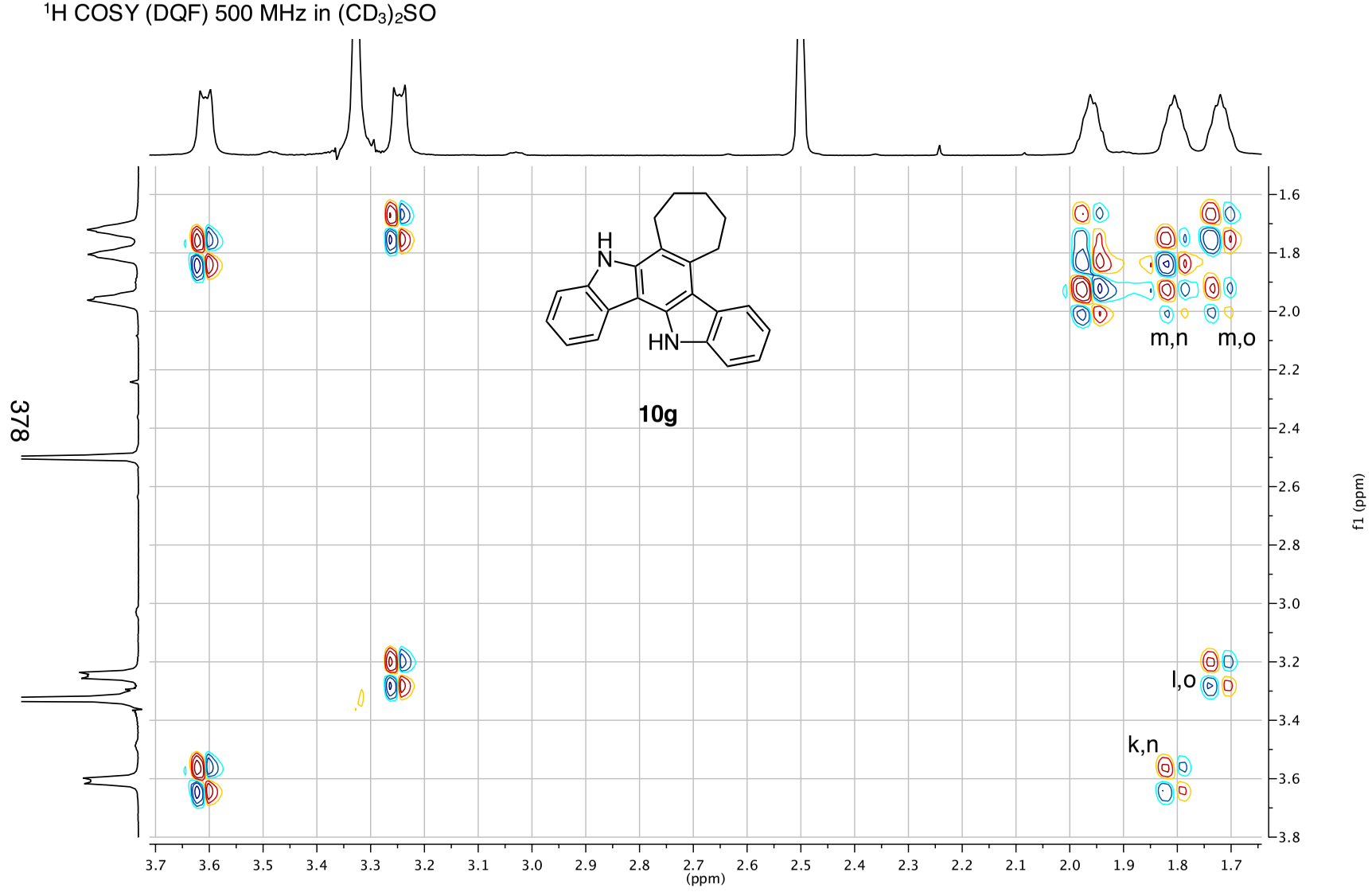
^{1}H COSY (DQF) 500 MHz in $(CD_3)_2SO$
378
H
N
HN
10g
m,n
m,o
l,o
k,n
3.7 3.6 3.5 3.4 3.3 3.2 3.1 3.0 2.9 2.8 2.7 2.6 2.5 2.4 2.3 2.2 2.1 2.0 1.9 1.8 1.7
(ppm)
1.6 1.8 2.0 2.2 2.4 2.6 2.8 3.0 3.2 3.4 3.6 3.8
f1 (ppm)

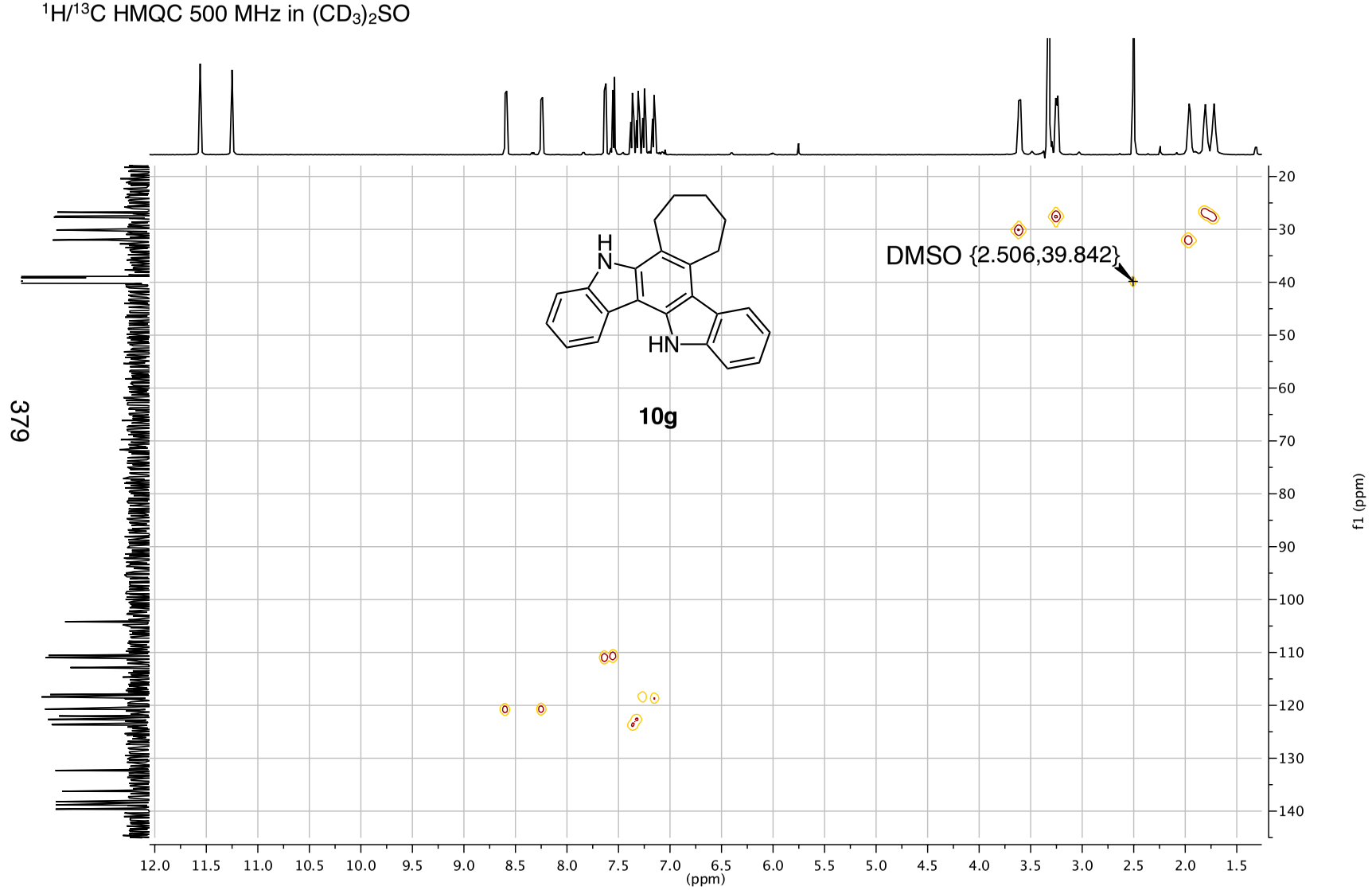
$^{1}H/^{13}C$ HMQC 500 MHz in $(CD_3)_2SO$
DMSO {2.506,39.842}
10g
379
(ppm)
f1 (ppm)

$^{1}H/^{13}C$ HMQC 500 MHz in $(CD_3)_2SO$

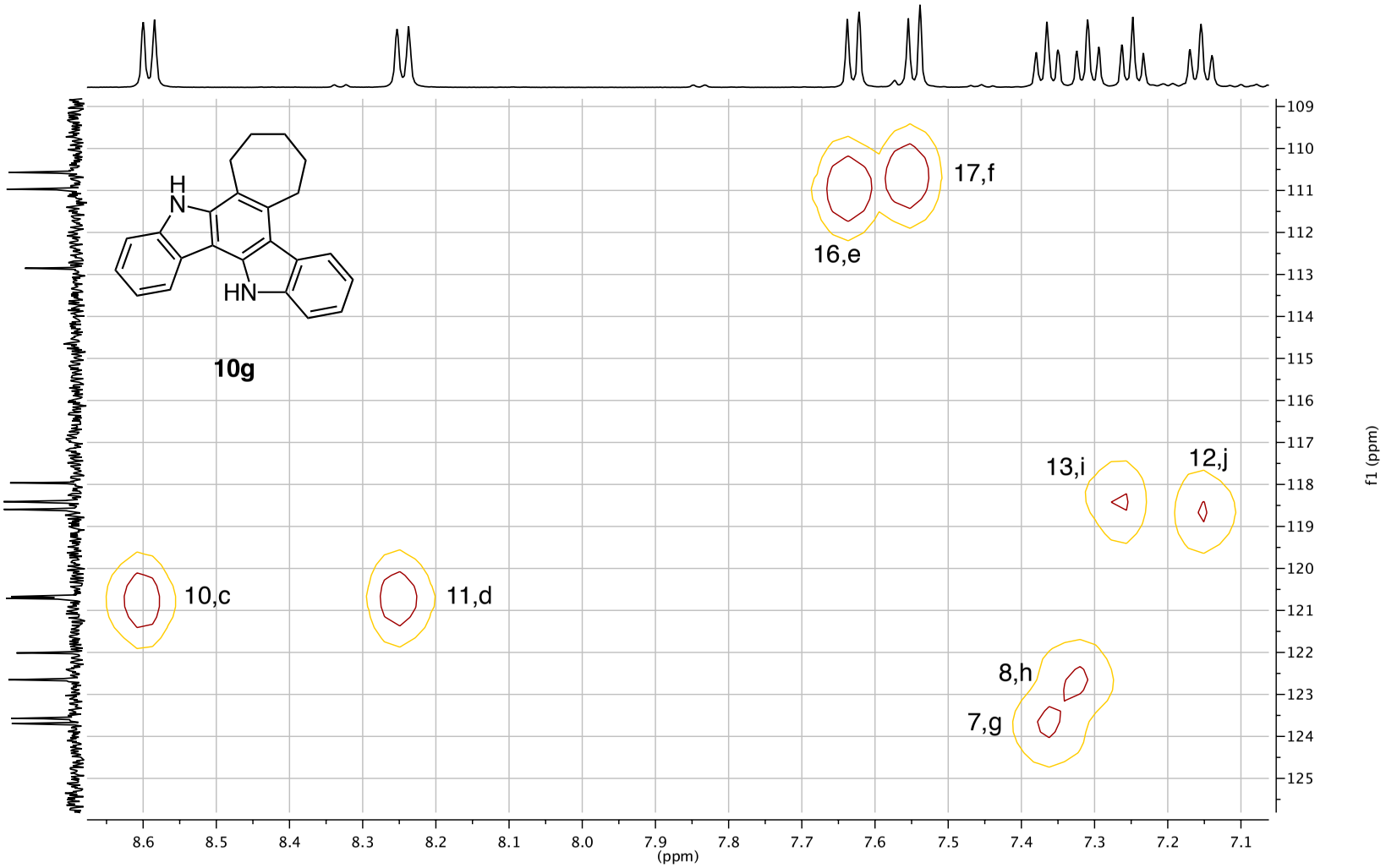

380

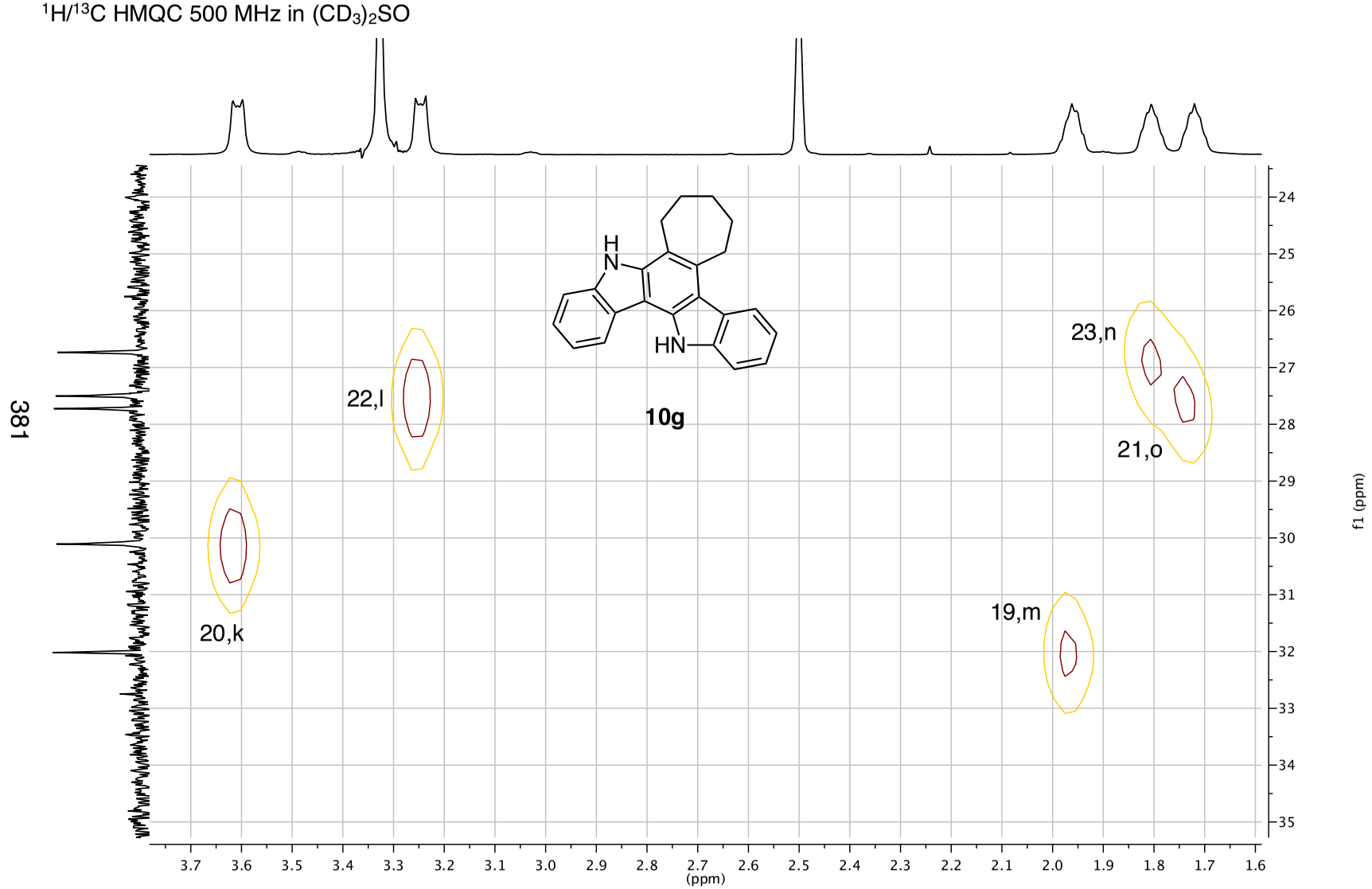
$^{1}H/^{13}C$ HMQC 500 MHz in $(CD_3)_2SO$
381
H
N
HN
10g
22,l
20,k
23,n
21,o
19,m
3.7 3.6 3.5 3.4 3.3 3.2 3.1 3.0 2.9 2.8 2.7 2.6 2.5 2.4 2.3 2.2 2.1 2.0 1.9 1.8 1.7 1.6
(ppm)
24 25 26 27 28 29 30 31 32 33 34 35
f1 (ppm)

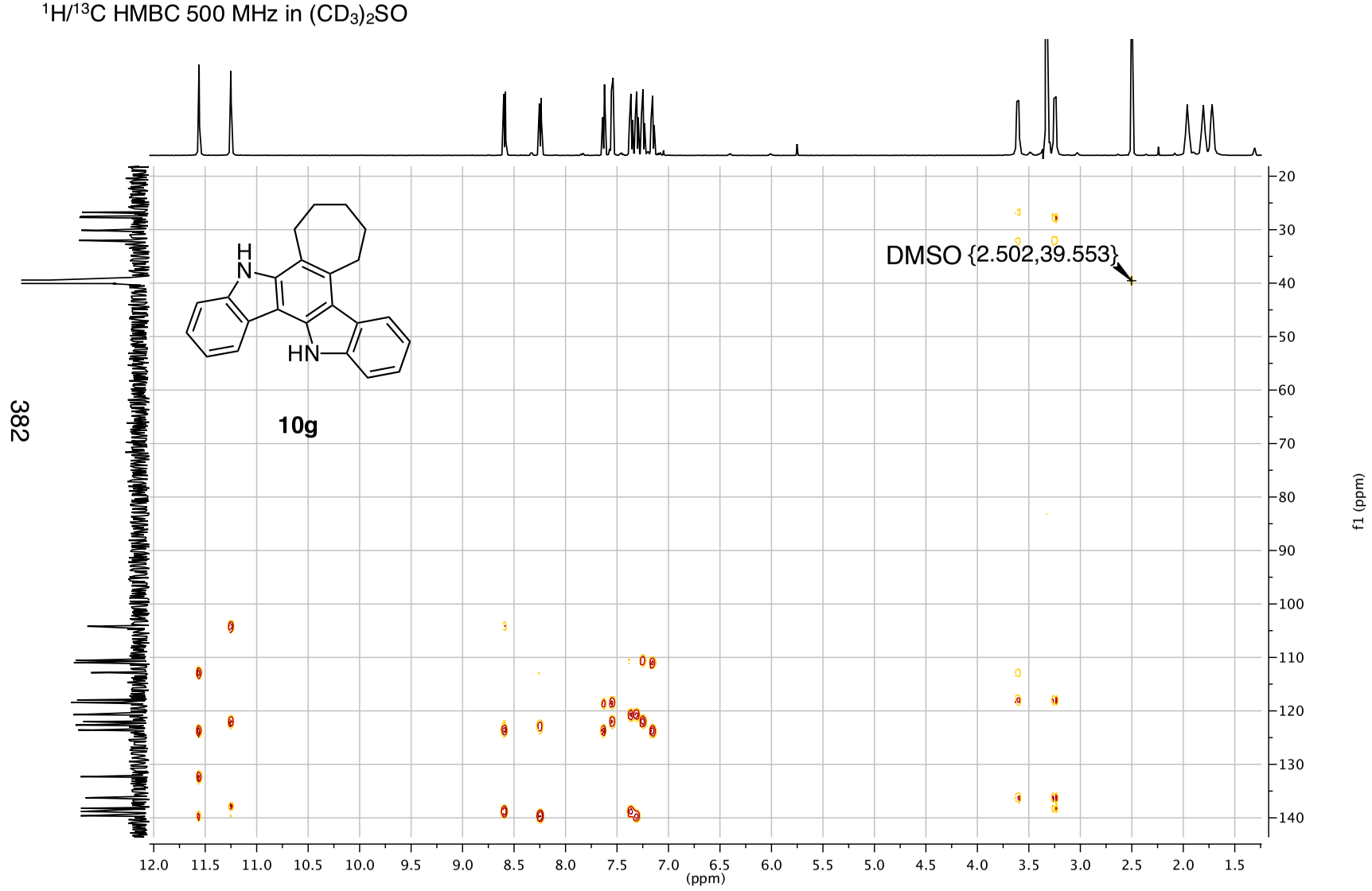
$^{1}H/^{13}C$ HMBC 500 MHz in $(CD_3)_2SO$
382
10g
DMSO {2.502,39.553}
(ppm)
f1 (ppm)

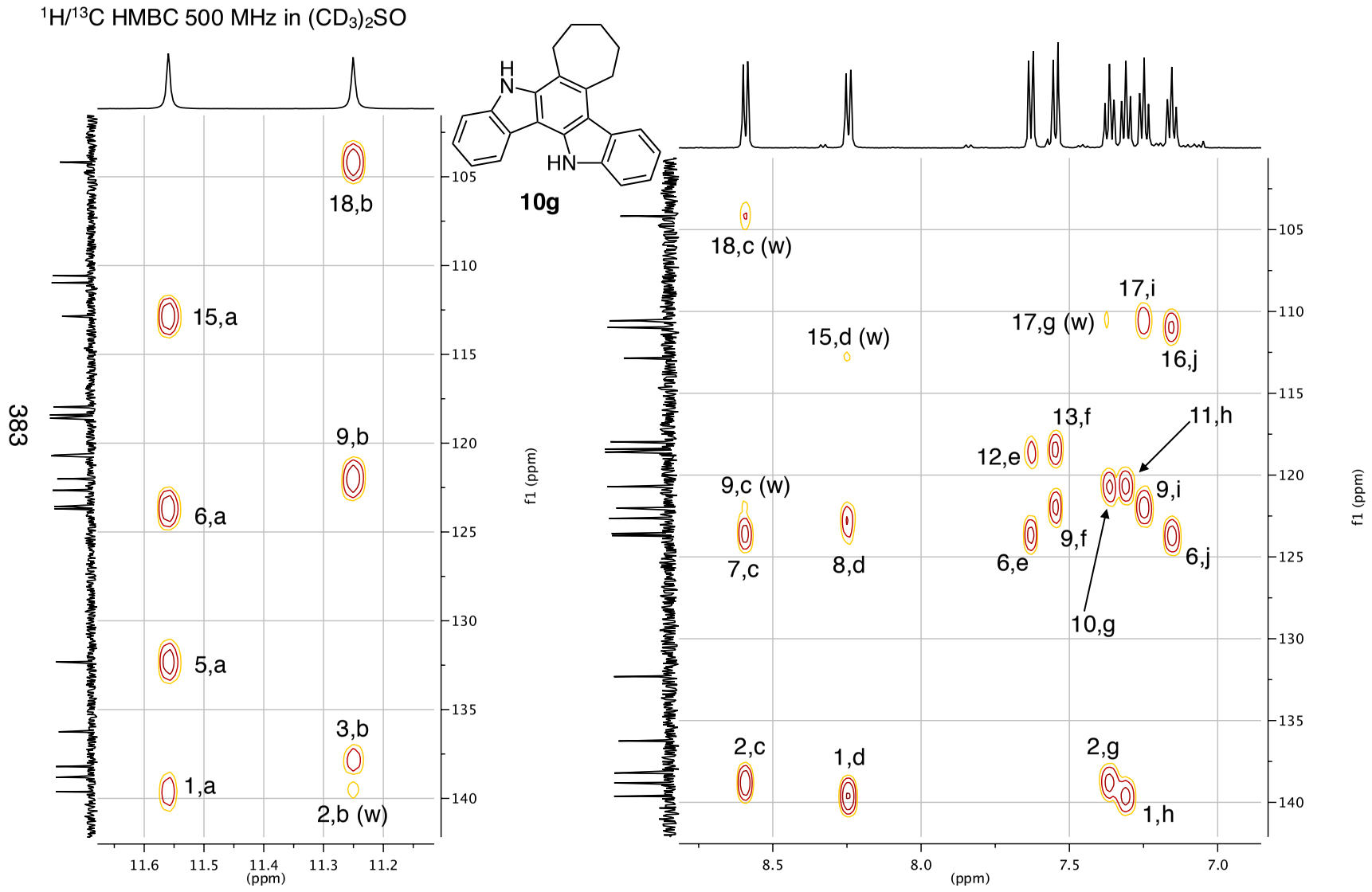
$^{1}H/^{13}C$ HMBC 500 MHz in $(CD_3)_2SO$
383
H
N
HN
10g
18,b
15,a
9,b
6,a
5,a
3,b
1,a
2,b (w)
18,c (w)
15,d (w)
17,i
17,g (w)
16,j
13,f
11,h
12,e
9,c (w)
9,i
9,f
6,e
6,j
7,c
8,d
10,g
2,c
1,d
2,g
1,h
f1 (ppm)
(ppm)

$^{1}H/^{13}C$ HMBC 500 MHz in $(CD_3)_2SO$

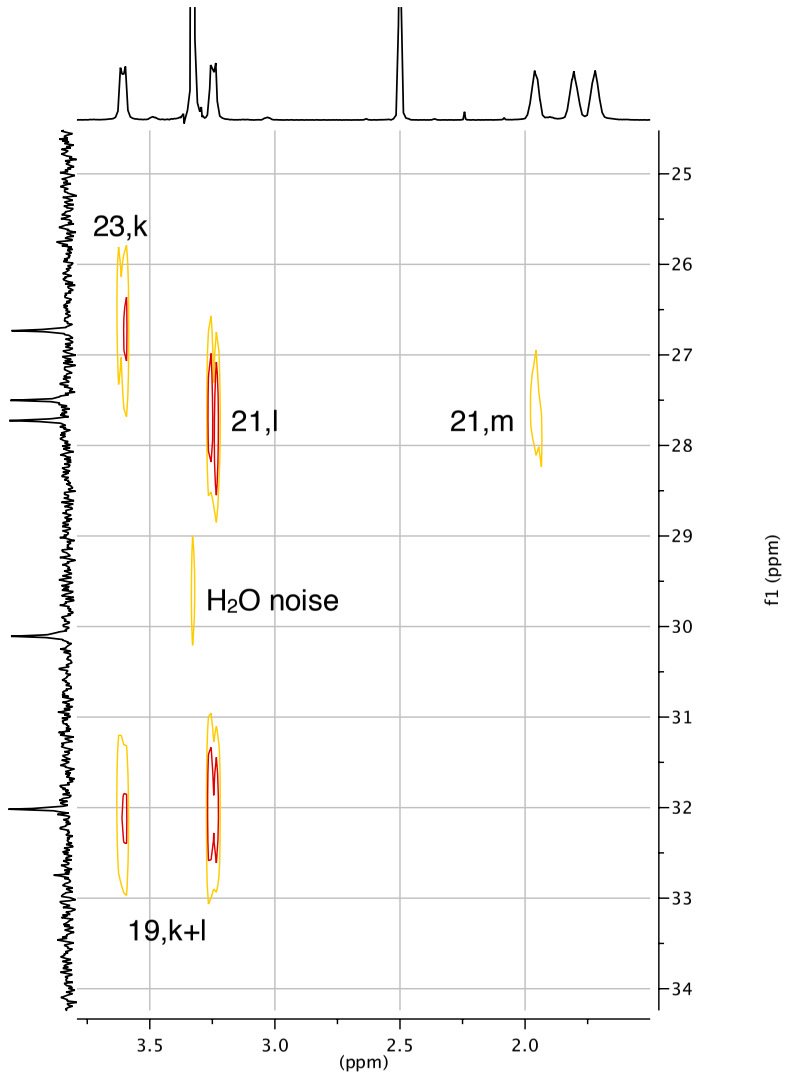

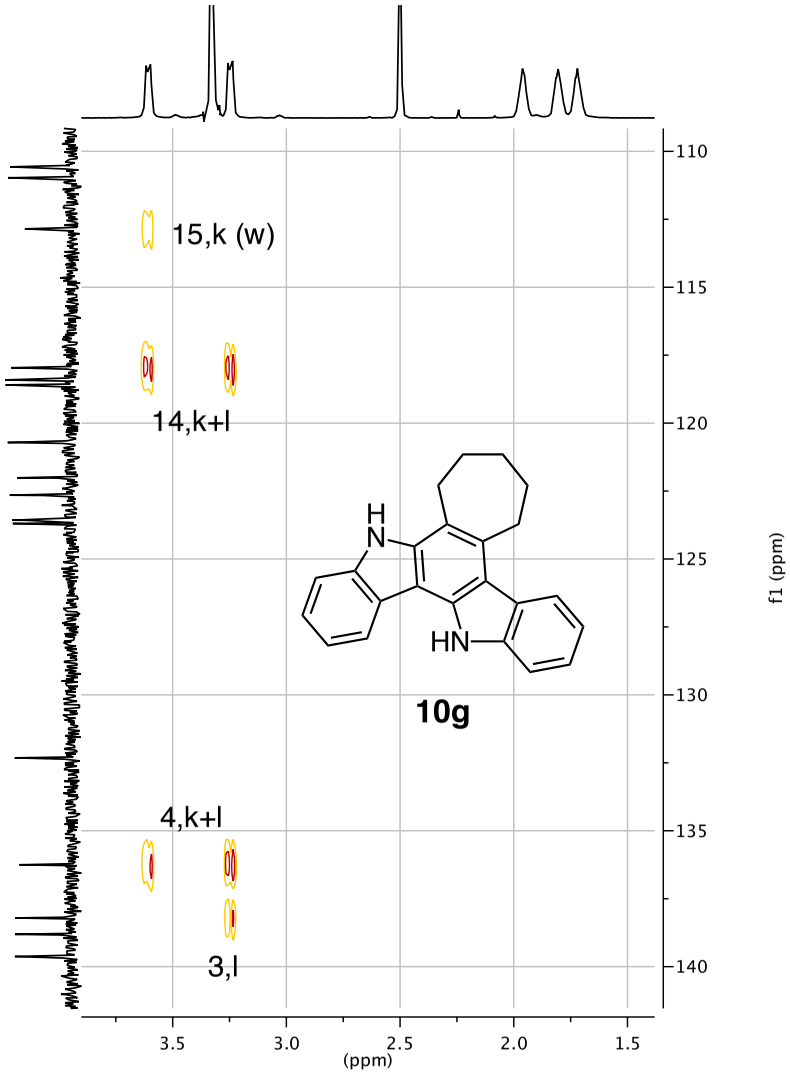

^{1}H GOESY 500 MHz in $(CD_3)_2SO$

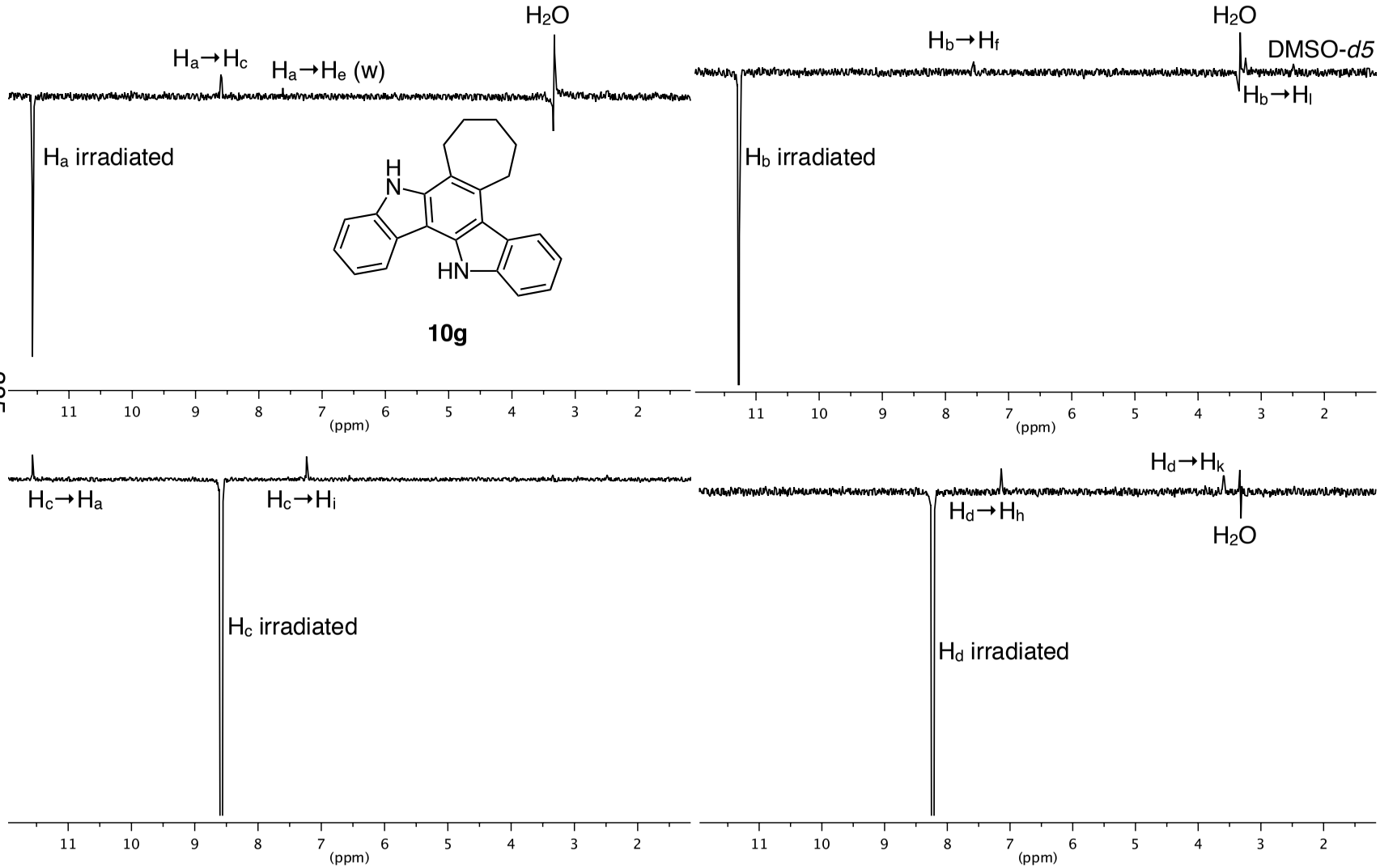

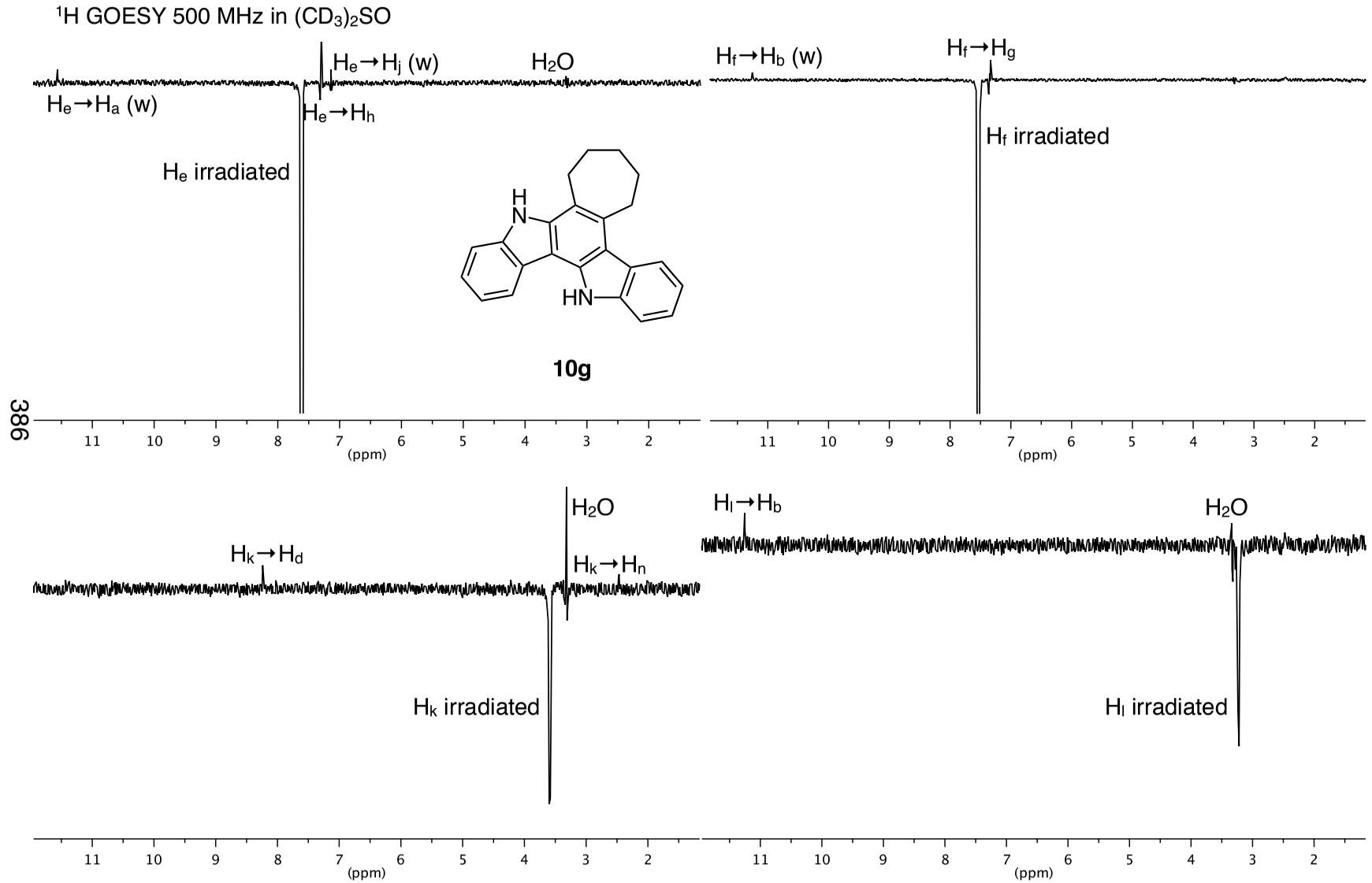
^{1}H GOESY 500 MHz in $(CD_3)_2SO$
$H_e \rightarrow H_j$ (w)
H_2O
$H_e \rightarrow H_a$ (w)
$H_e \rightarrow H_h$
H_e irradiated
H
N
HN
10g
386
11 10 9 8 7 6 5 4 3 2
(ppm)
$H_f \rightarrow H_b$ (w)
$H_f \rightarrow H_g$
H_f irradiated
H_2O
$H_k \rightarrow H_d$
$H_k \rightarrow H_n$
H_k irradiated
$H_l \rightarrow H_b$
H_2O
H_l irradiated

Table 37. Proton NMR summary for **10g**.

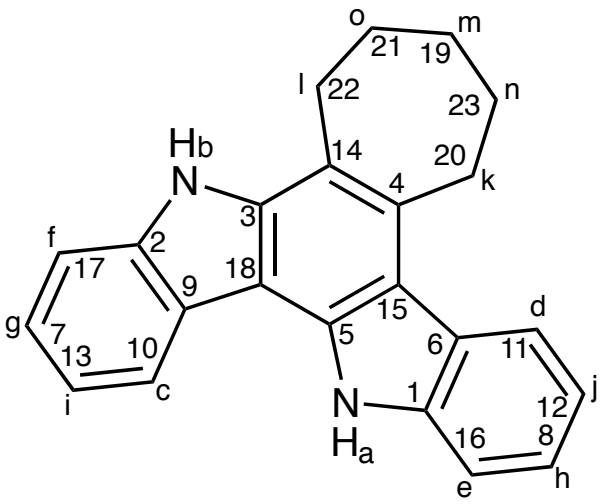

H label	δ	count	COSY	NOE
a	11.56	1	-	C,e
b	11.25	1	-	F,L
c	8.59	1	I	A,I
d	8.25	1	J	H,K
e	7.63	1	H	a,H,j
f	7.55	1	G	b,G
g	7.37	1	F,I	not done
h	7.31	1	J,E	not done
i	7.25	1	G,C	not done
j	7.16	1	H,D	not done
k	3.61	2	N	D,N
l	3.25	2	O	B
m	1.96	2	N,O	not done
n	1.81	2	K,M	not done
o	1.72	2	N,L	not done

Table 38 (1 of 2). Carbon NMR summary for **10g**.

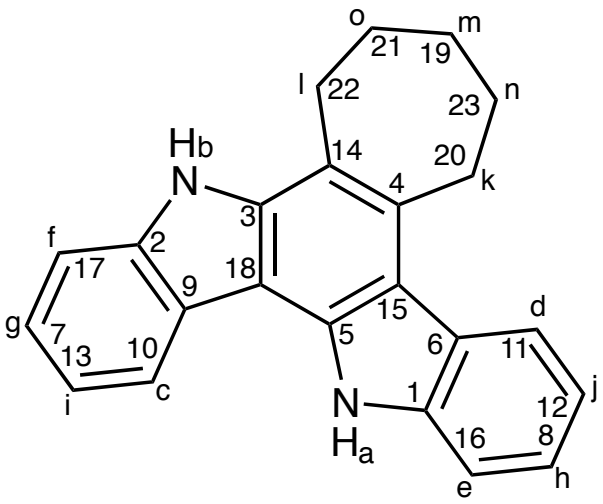

C label	δ	type	HMQC	HMBC
1	139.6	q	-	A,D
2	138.8	q	-	b,C,G
3	138.2	q	-	B,L
4	136.3	q	-	K,L
5	132.3	q	-	A
6	123.7	q	-	A,E,J
7	123.6	CH	g	C
8	122.7	CH	h	D
9	122.0	q	-	B,c,F,I
10	120.71	CH	c	G
11	120.67	CH	d	H
12	118.6	CH	j	E
13	118.4	CH	i	F
14	118.0	q	-	K,L
15	112.9	q	-	A,d,k

Table 38 (2 of 2). Carbon NMR summary for **10g**.

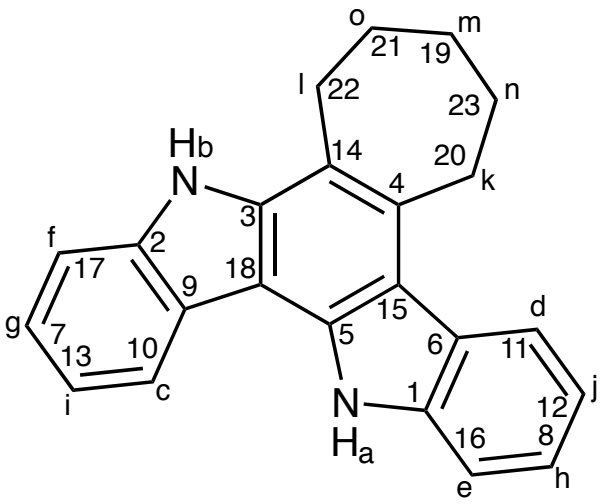

C label	δ	type	HMQC	HMBC
16	111.0	CH	e	J
17	110.6	CH	f	g,I
18	104.2	q	-	B,c
19	32.0	CH_2	m	K,L
20	30.1	CH_2	k	-
21	27.7	CH_2	o	L,m
22	27.5	CH_2	l	-
23	26.7	CH_2	n	K

^{1}H NMR 500 MHz in CD_2Cl_2

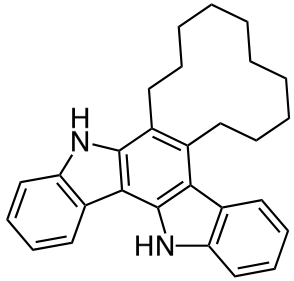

10l

^{1}H NMR 500 MHz in CD_2Cl_2

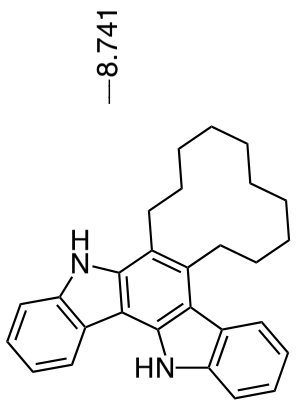

10l

391

^{1}H NMR 500 MHz in CD_2Cl_2

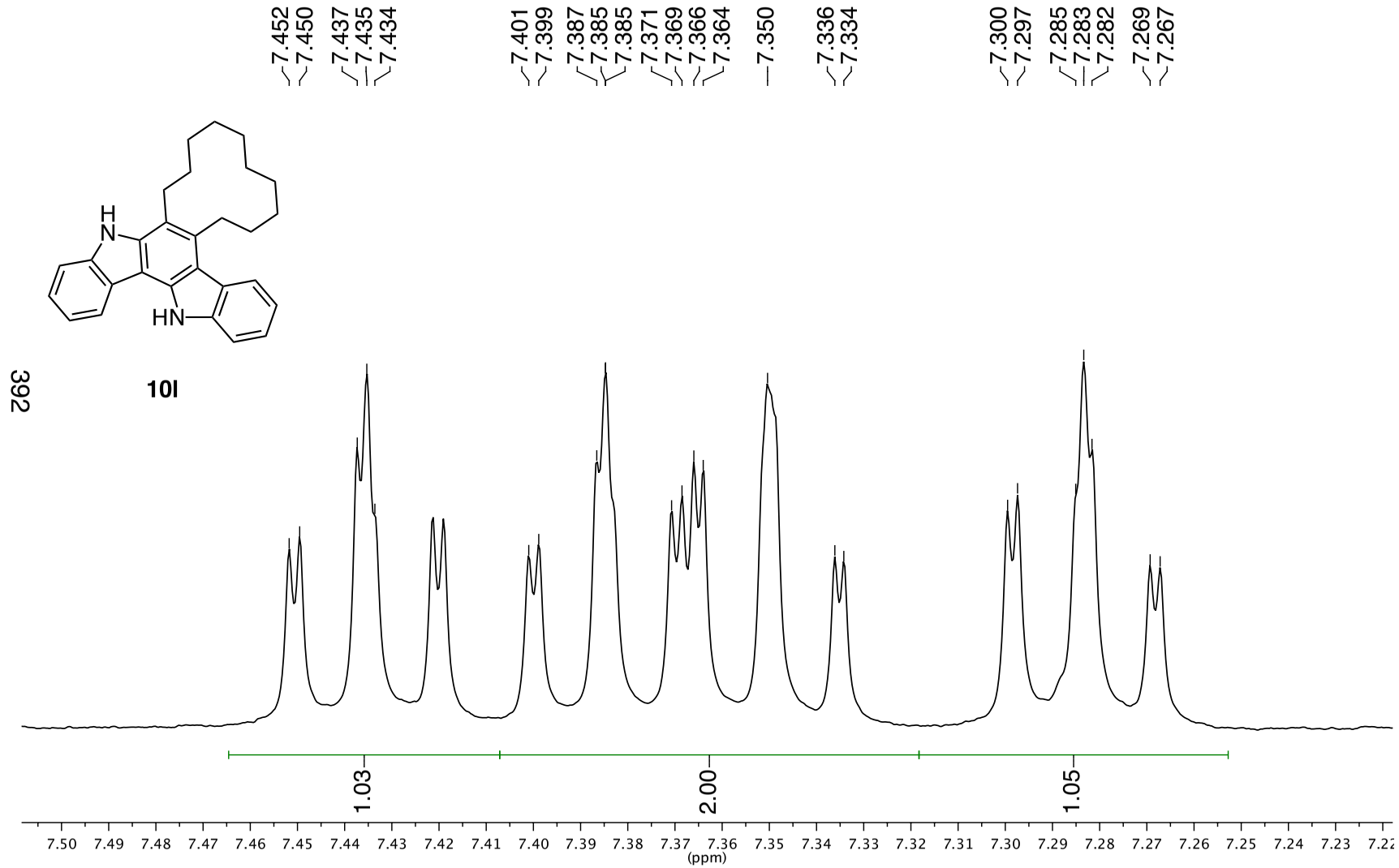

^{1}H NMR 500 MHz in CD_2Cl_2

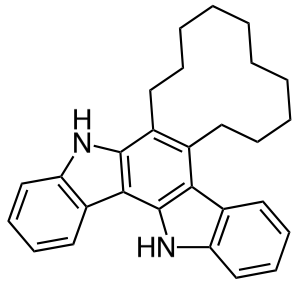

10l

^{13}C NMR 126 MHz in CD_2Cl_2

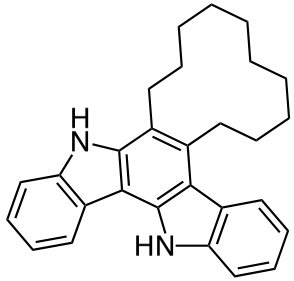

10l

^{13}C NMR 126 MHz in CD_2Cl_2

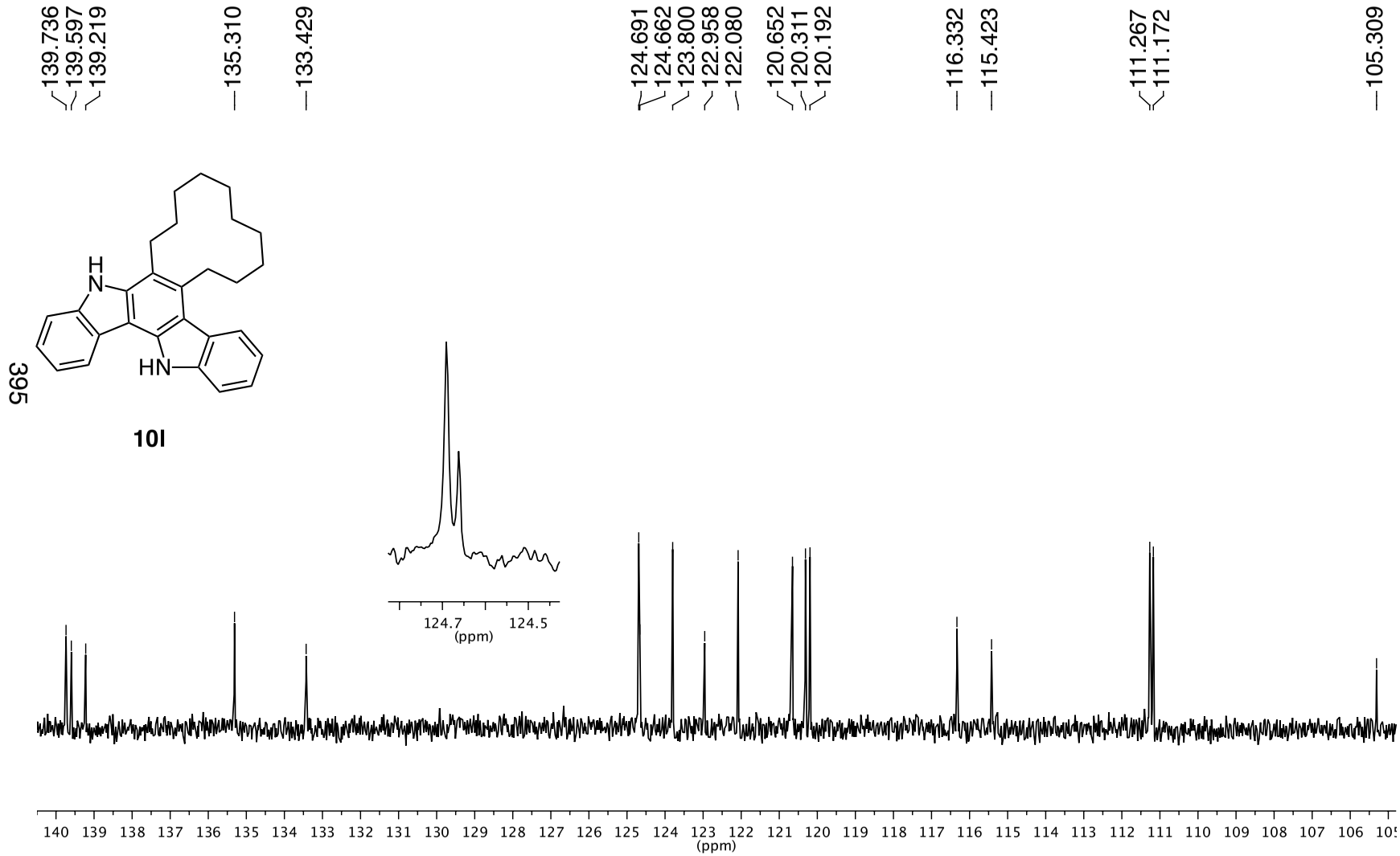

^{13}C NMR 126 MHz in CD_2Cl_2

28.568
28.483
28.214
28.137
28.045
27.185
27.127
25.960
22.985
22.766

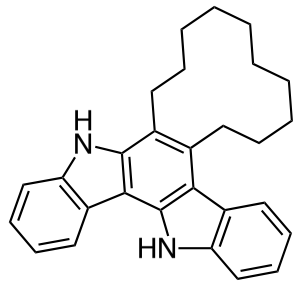

10l

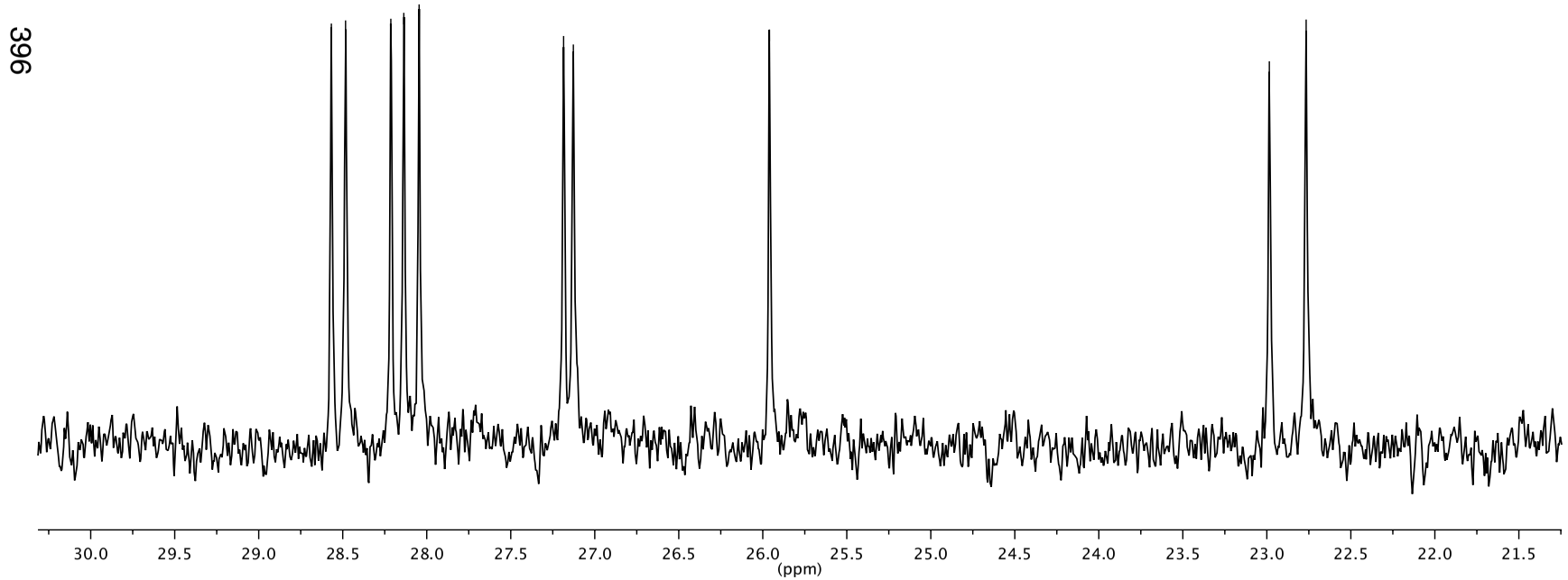

$^{1}H/^{13}C$ DEPT135 500 MHz in CD_2Cl_2

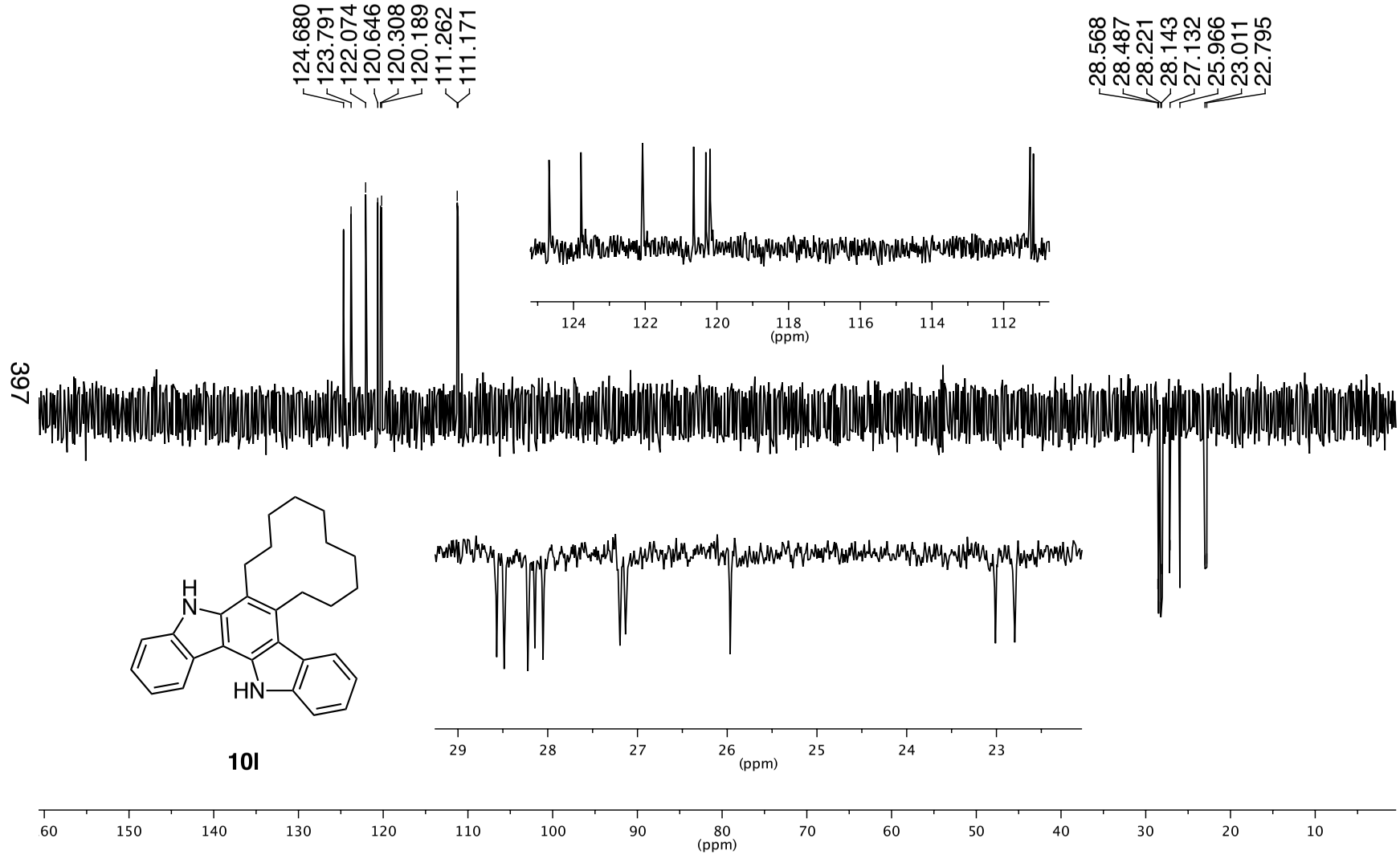

^{1}H NMR 500 MHz in $(CD_3)_2SO$

11h

^{1}H NMR 500 MHz in $(CD_3)_2SO$

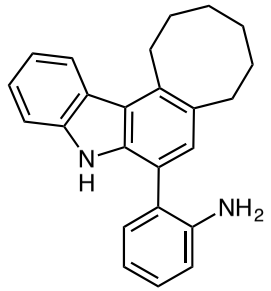

11h

8.130
8.114
7.526
7.509
7.334
7.319
7.304
7.163
7.148
7.140
7.133
7.126
7.080
6.876
6.860
6.738
6.735
6.723
6.721
6.708
6.706
1.925
1.913
1.901
1.889
1.888
1.877
1.688
1.445
1.332

399

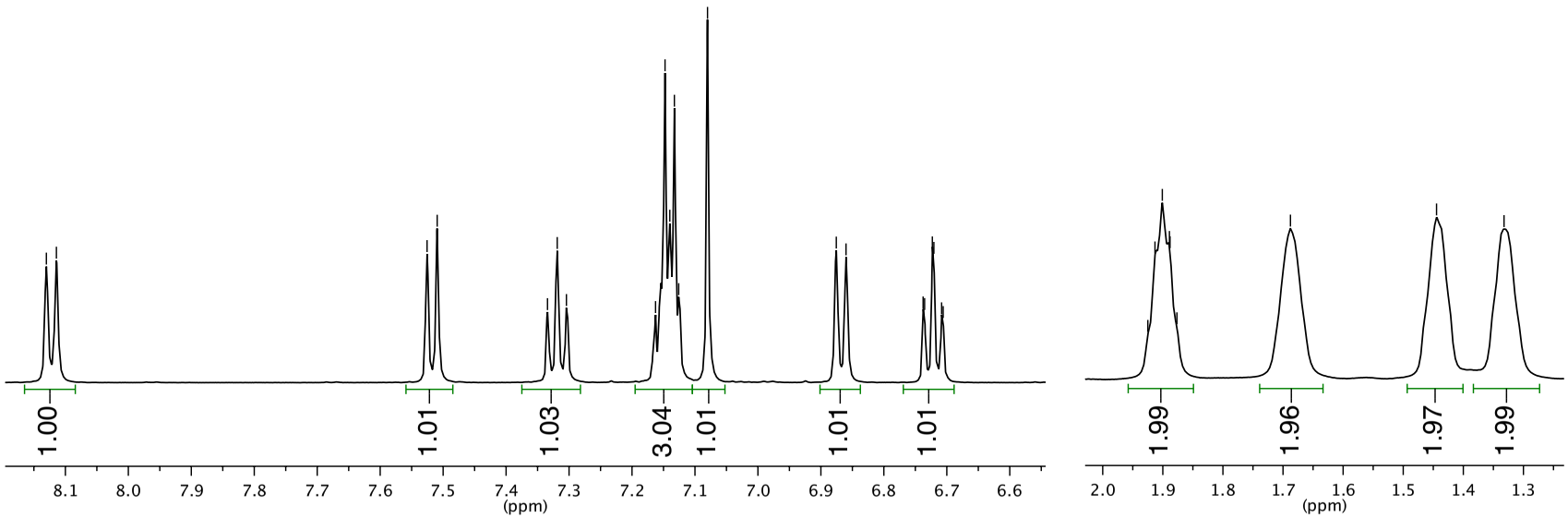

^{13}C NMR 126 MHz in $(CD_3)_2SO$

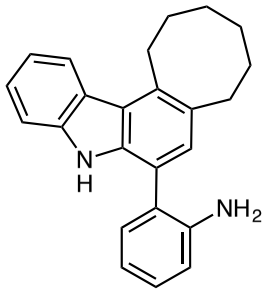

11h

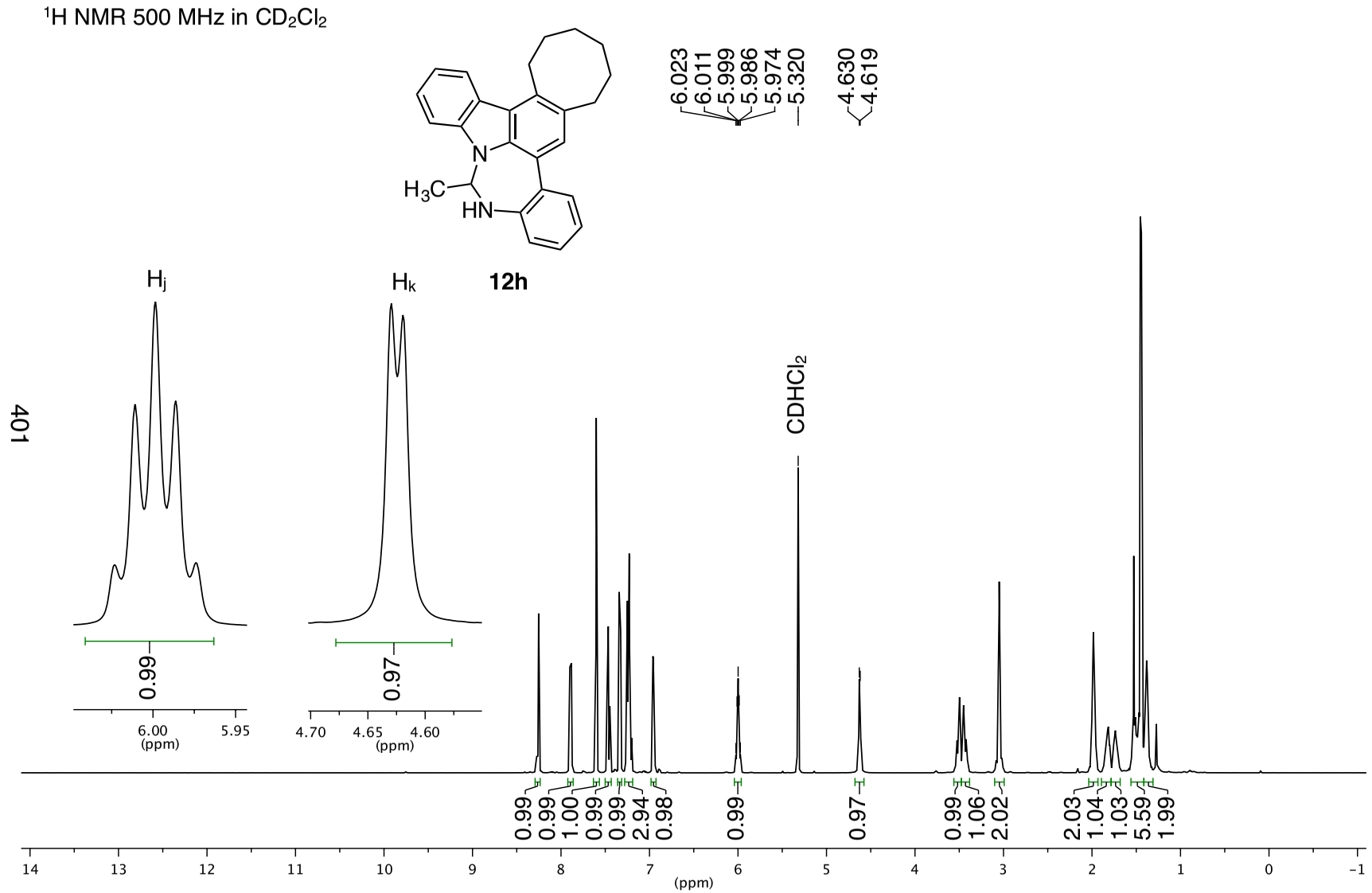
^{1}H NMR 500 MHz in CD_2Cl_2
6.023
6.011
5.999
5.986
5.974
5.320
4.630
4.619
N
H_3C
HN
12h
H_j
H_k
0.99
0.97
6.00
5.95
4.70
4.65
4.60
(ppm)
401
$CDHCl_2$
0.99
0.99
1.00
0.99
0.99
2.94
0.98
0.99
0.97
0.99
1.06
2.02
2.03
1.04
1.03
5.59
1.99
14
13
12
11
10
9
8
7
6
5
4
3
2
1
0
−1
(ppm)

^{1}H NMR 500 MHz in CD_2Cl_2

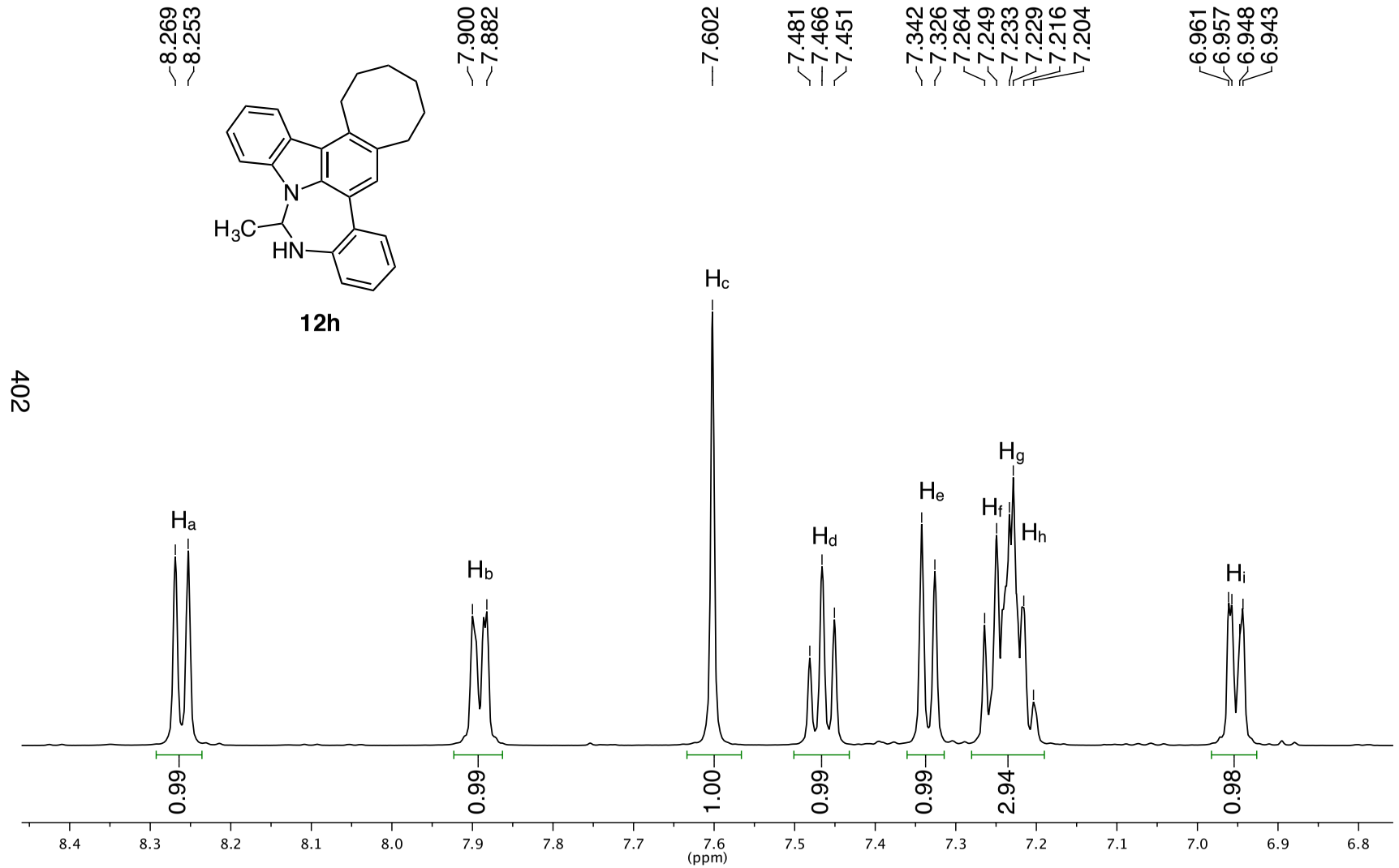

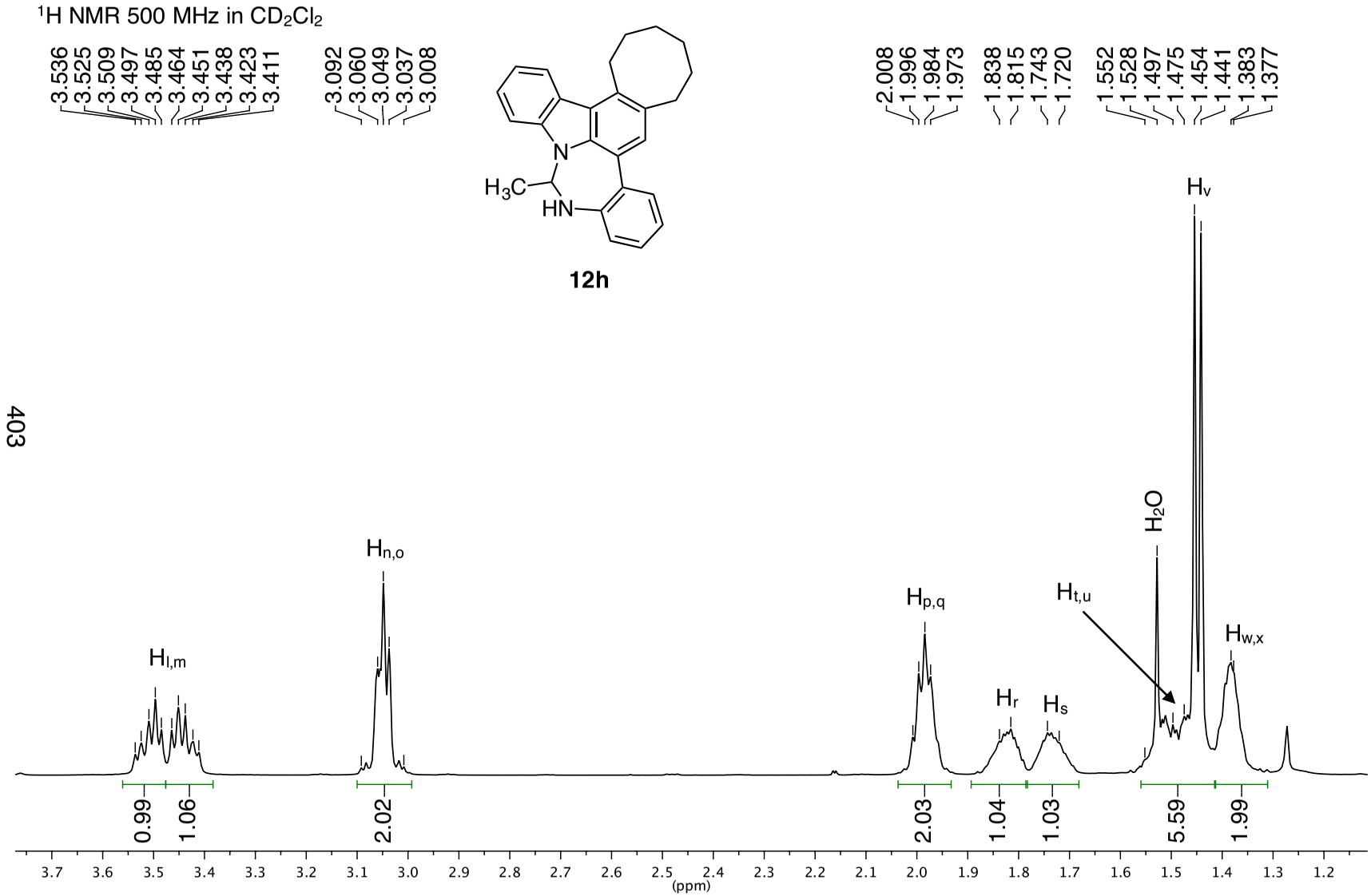
^{1}H NMR 500 MHz in CD_2Cl_2
3.536
3.525
3.509
3.497
3.485
3.464
3.451
3.438
3.423
3.411
3.092
3.060
3.049
3.037
3.008
2.008
1.996
1.984
1.973
1.838
1.815
1.743
1.720
1.552
1.528
1.497
1.475
1.454
1.441
1.383
1.377
N
H_3C
HN
12h
403
$H_{l,m}$
$H_{n,o}$
$H_{p,q}$
H_r
H_s
$H_{t,u}$
H_2O
H_v
$H_{w,x}$
0.99
1.06
2.02
2.03
1.04
1.03
5.59
1.99
3.7 3.6 3.5 3.4 3.3 3.2 3.1 3.0 2.9 2.8 2.7 2.6 2.5 2.4 2.3 2.2 2.1 2.0 1.9 1.8 1.7 1.6 1.5 1.4 1.3 1.2
(ppm)

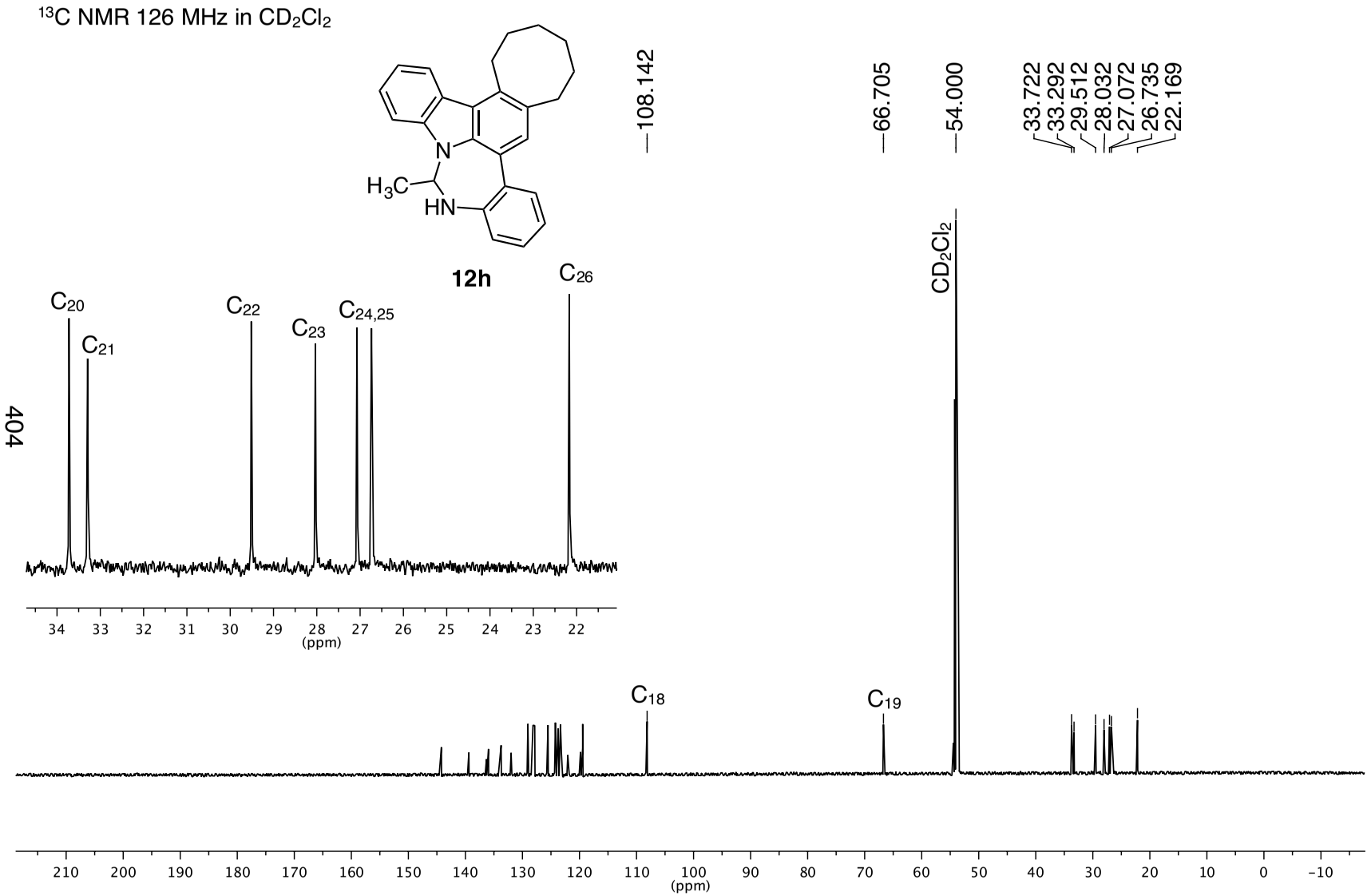
^{13}C NMR 126 MHz in CD_2Cl_2
12h
H_3C
N
HN
108.142
66.705
54.000
33.722
33.292
29.512
28.032
27.072
26.735
22.169
CD_2Cl_2
C_{18}
C_{19}
C_{20}
C_{21}
C_{22}
C_{23}
$C_{24,25}$
C_{26}
404
(ppm)
(ppm)

^{13}C NMR 126 MHz in CD_2Cl_2

144.207
139.393
136.310
135.948
133.738
131.991
129.048
128.149
127.843
125.518
124.228
123.748
123.339
123.164
122.051
119.822
119.440

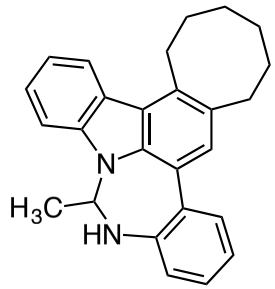

12h

405

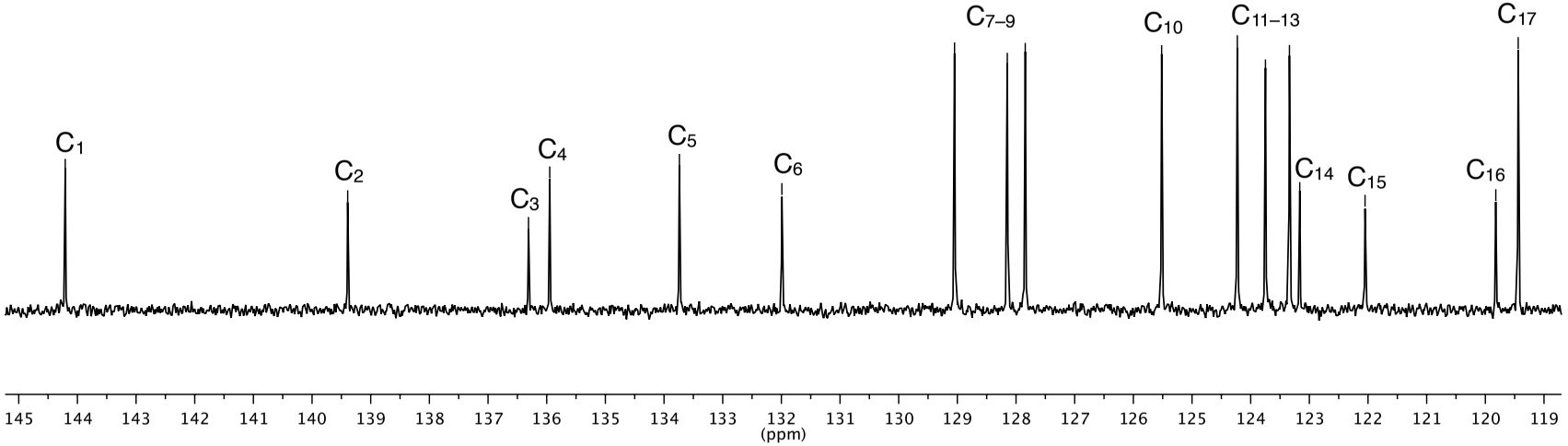

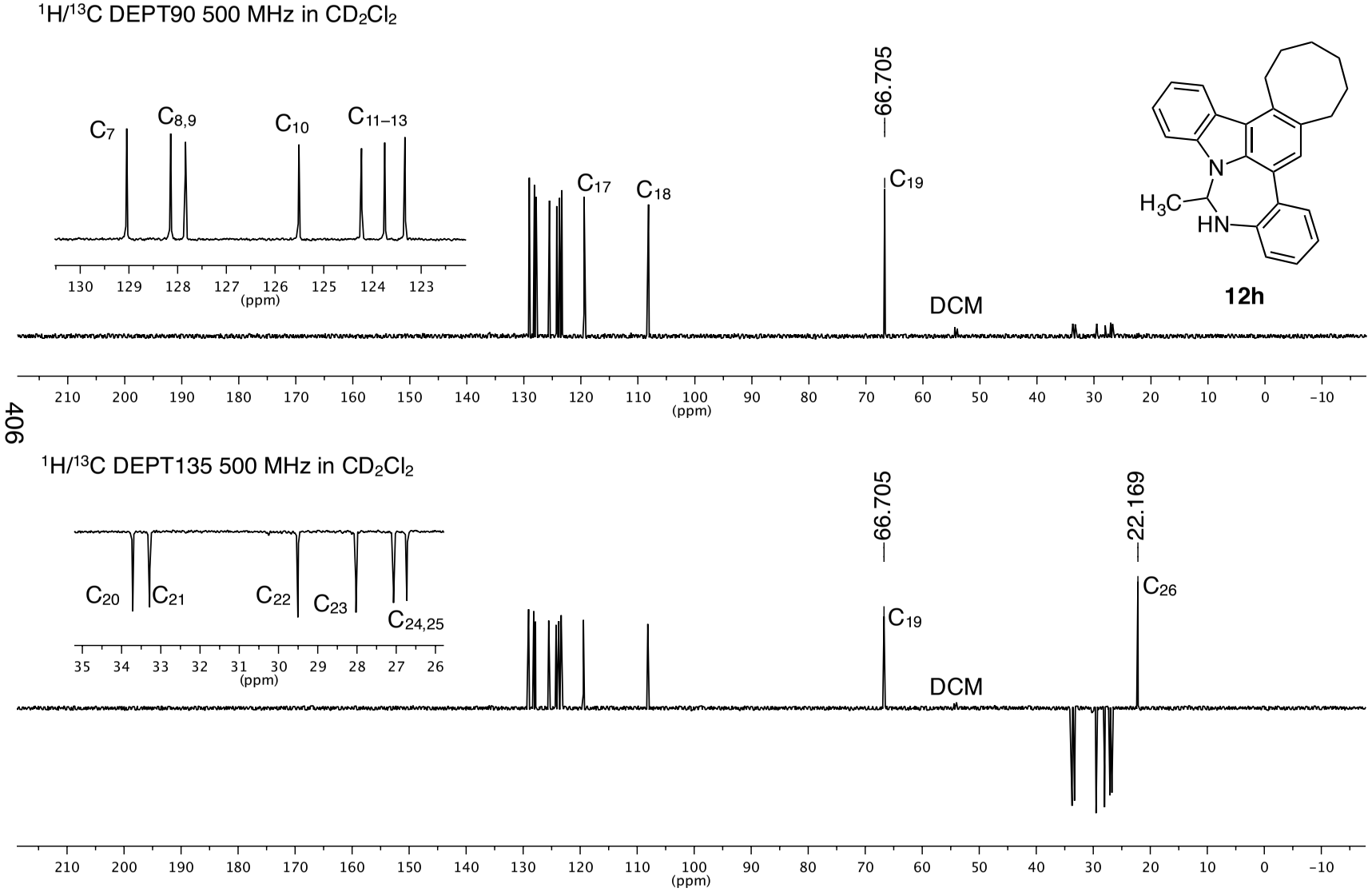
^{1}H/^{13}C DEPT90 500 MHz in CD_2Cl_2
C7
C8,9
C10
C11–13
C17
C18
66.705
C19
DCM
12h
(ppm)
406
^{1}H/^{13}C DEPT135 500 MHz in CD_2Cl_2
C20
C21
C22
C23
C24,25
66.705
22.169
C26
C19
DCM
(ppm)

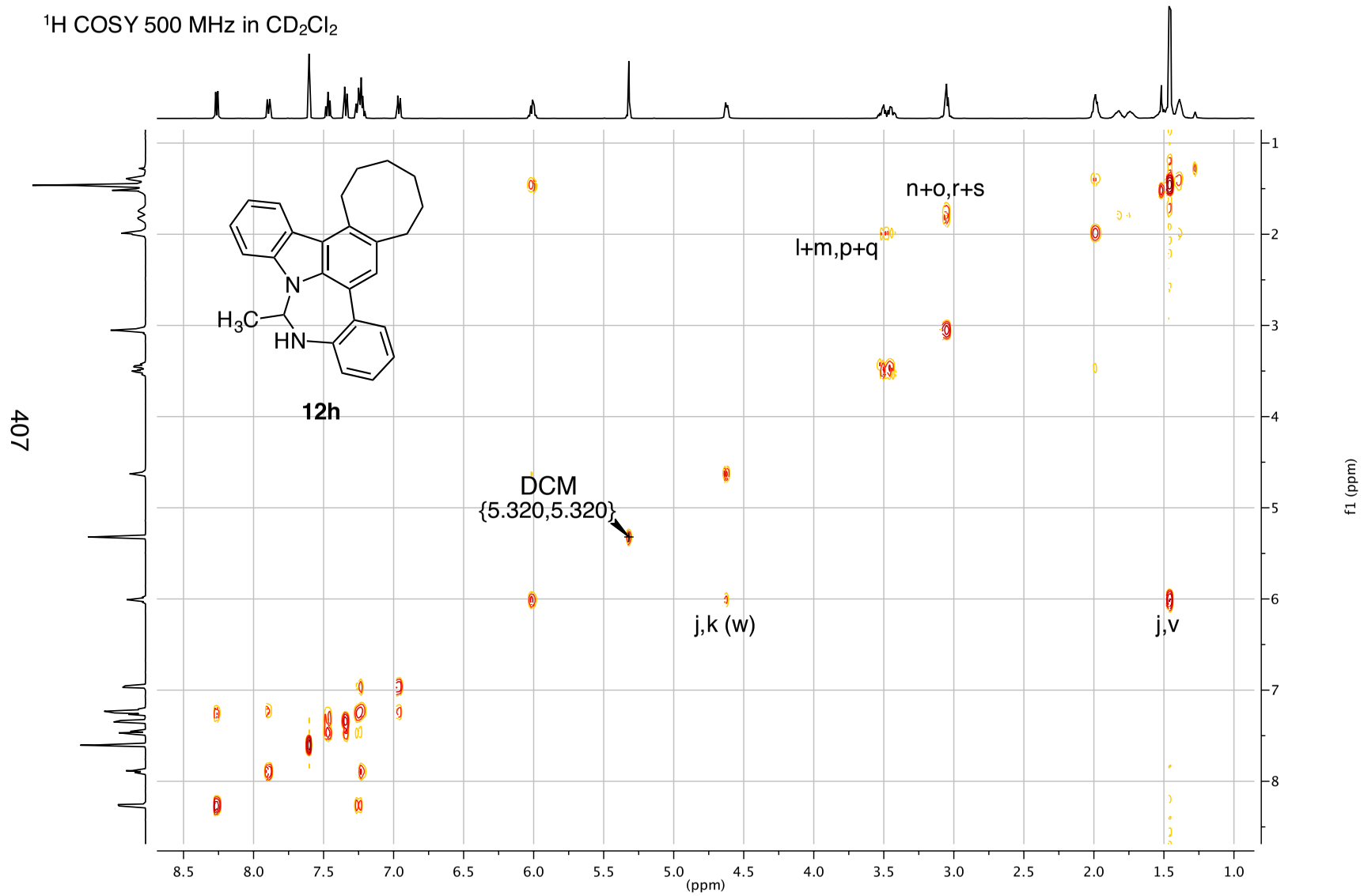
^{1}H COSY 500 MHz in CD_2Cl_2
407
N
H_3C
HN
12h
DCM
{5.320,5.320}
n+o,r+s
l+m,p+q
j,k (w)
j,v
8.5
8.0
7.5
7.0
6.5
6.0
5.5
5.0
4.5
4.0
3.5
3.0
2.5
2.0
1.5
1.0
(ppm)
f1 (ppm)

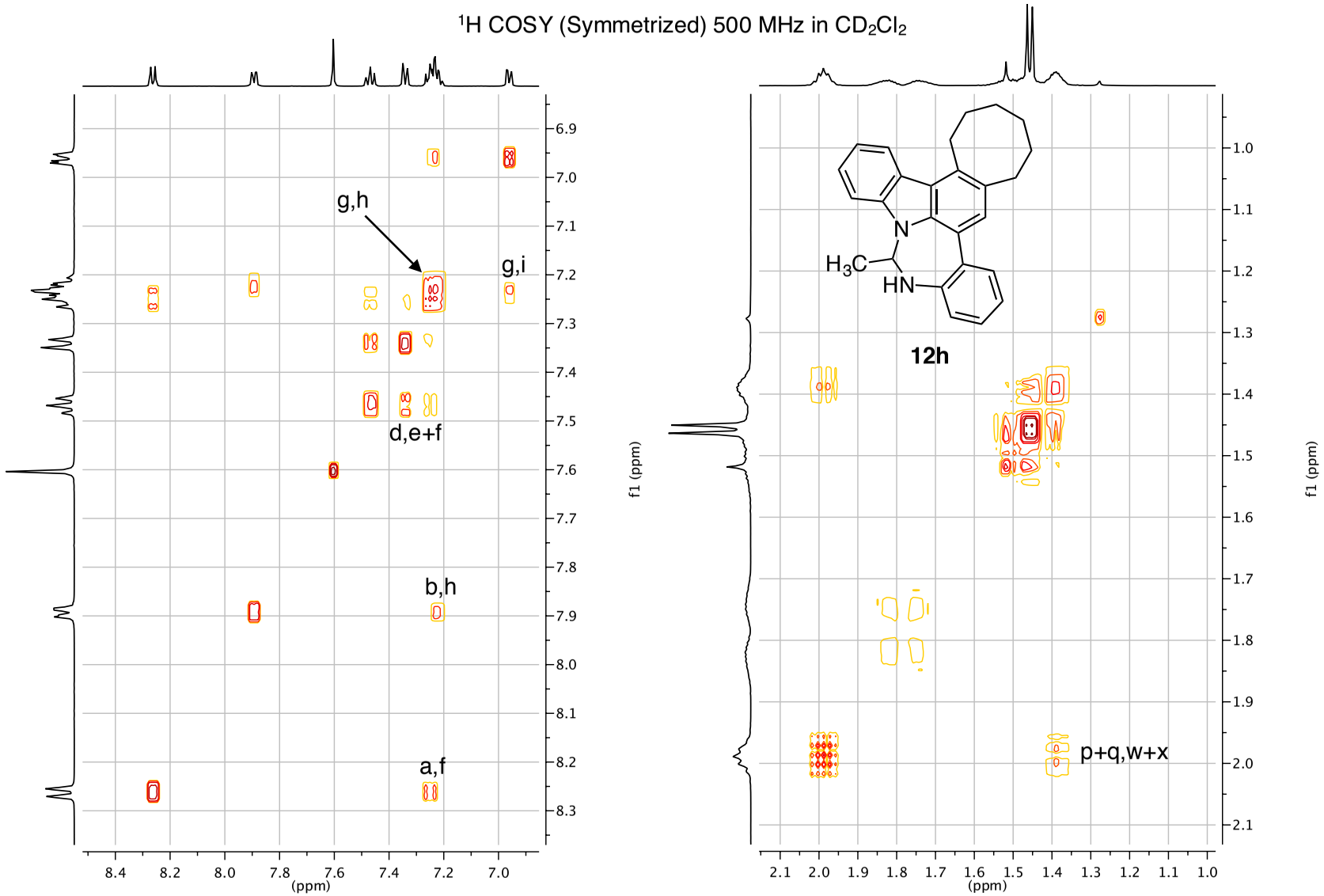
^{1}H COSY (Symmetrized) 500 MHz in CD_2Cl_2
g,h
g,i
d,e+f
b,h
a,f
12h
N
H_3C
HN
p+q,w+x
f1 (ppm)
(ppm)

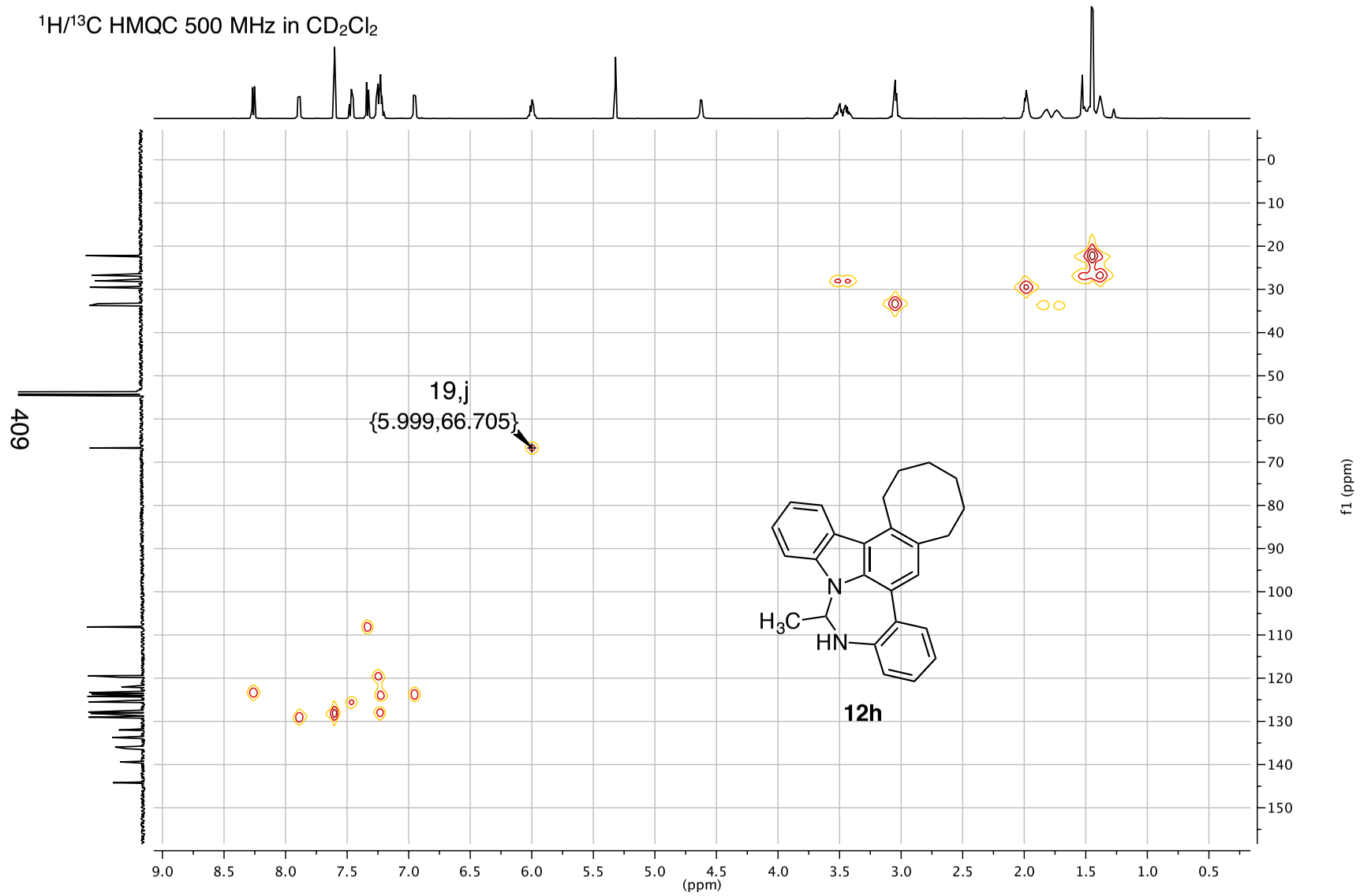
$^{1}H/^{13}C$ HMQC 500 MHz in CD_2Cl_2
19,j
{5.999,66.705}
409
N
H_3C
HN
12h
(ppm)
f1 (ppm)

$^{1}H/^{13}C$ HMQC 500 MHz in CD_2Cl_2

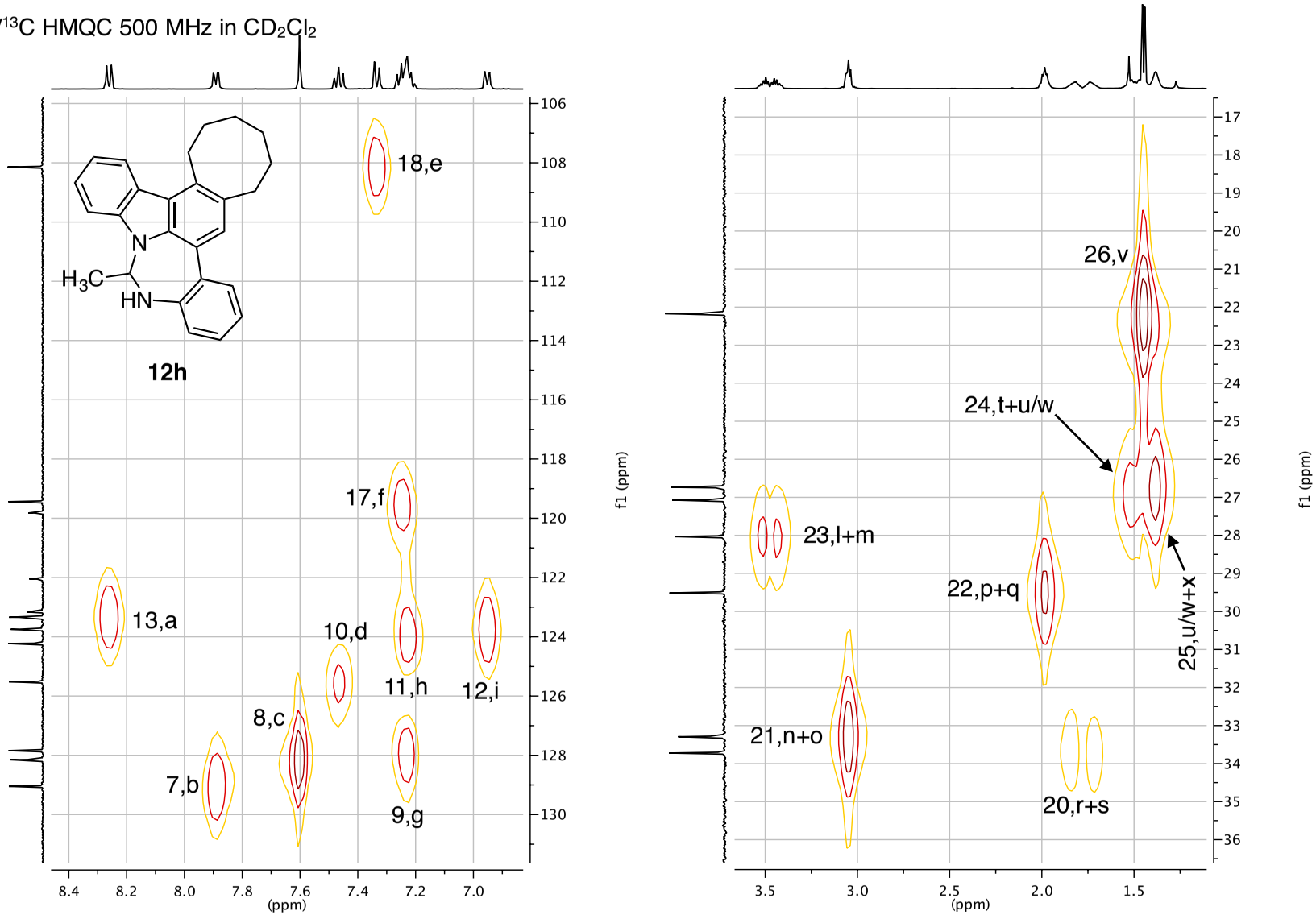

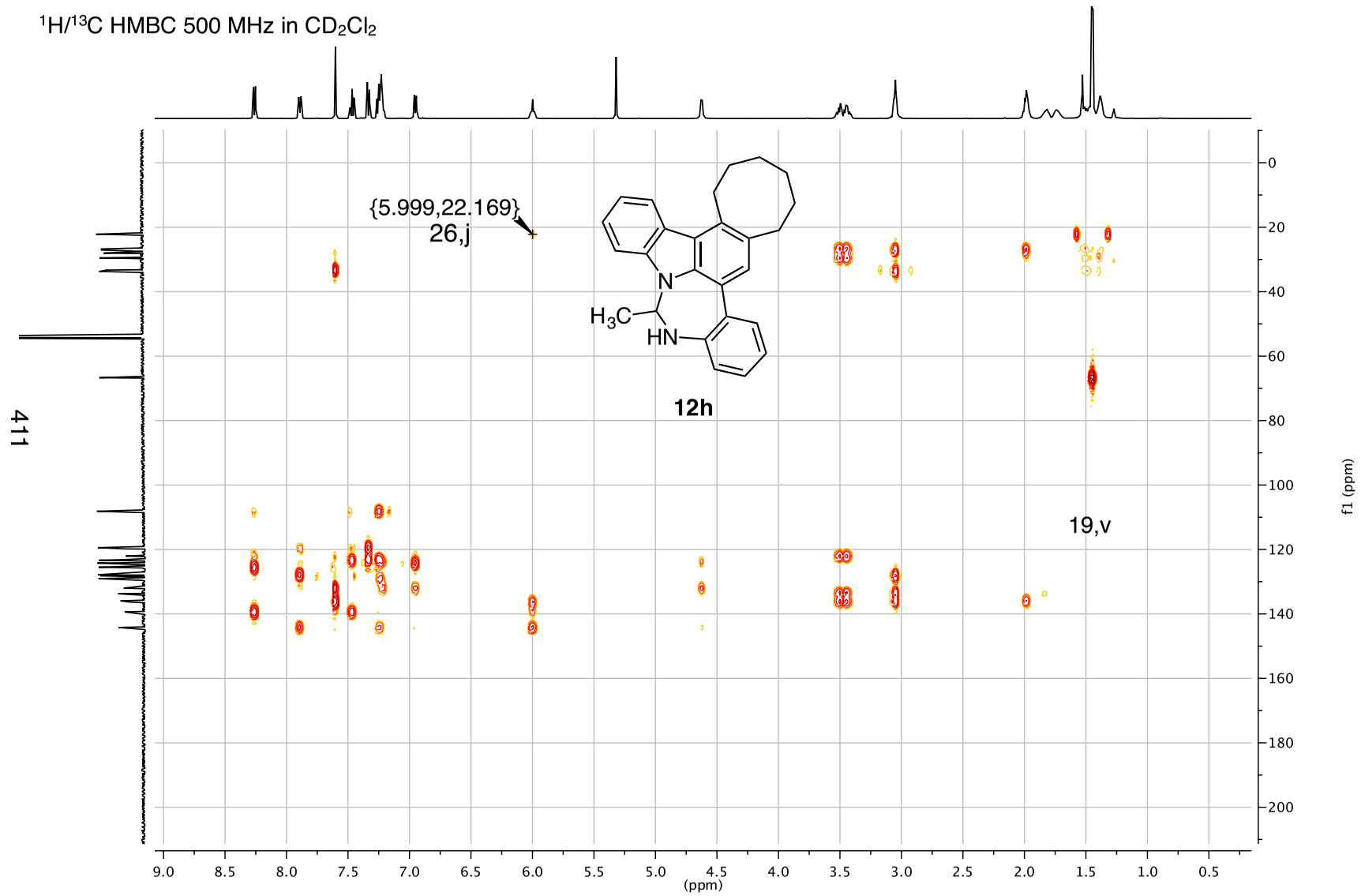
$^{1}H/^{13}C$ HMBC 500 MHz in CD_2Cl_2
{5.999,22.169}
26,j
N
H_3C
HN
12h
19,v
411
f1 (ppm)
(ppm)

$^{1}H/^{13}C$ HMBC 500 MHz in CD_2Cl_2

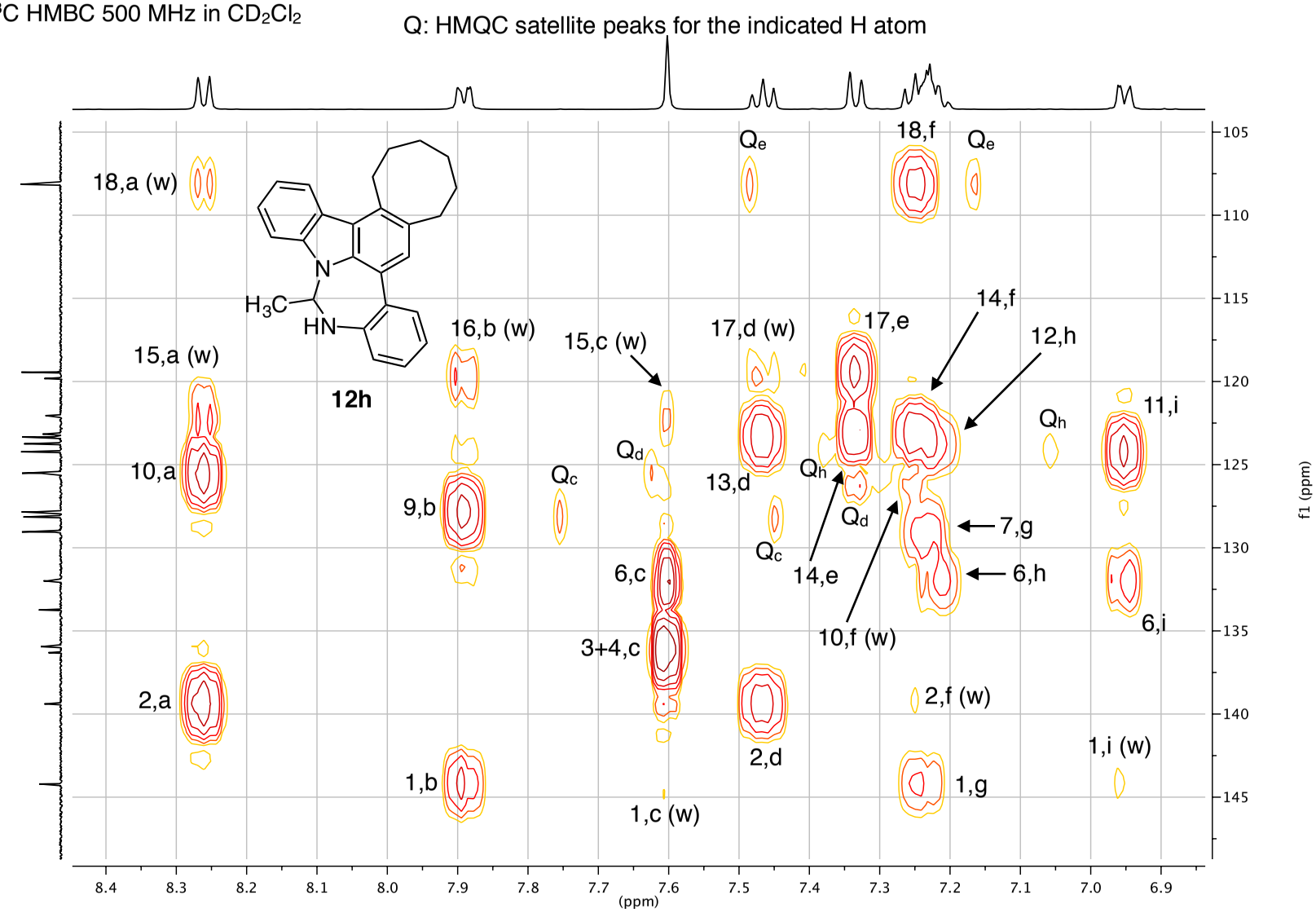

$^{1}H/^{13}C$ HMBC 500 MHz in CD_2Cl_2

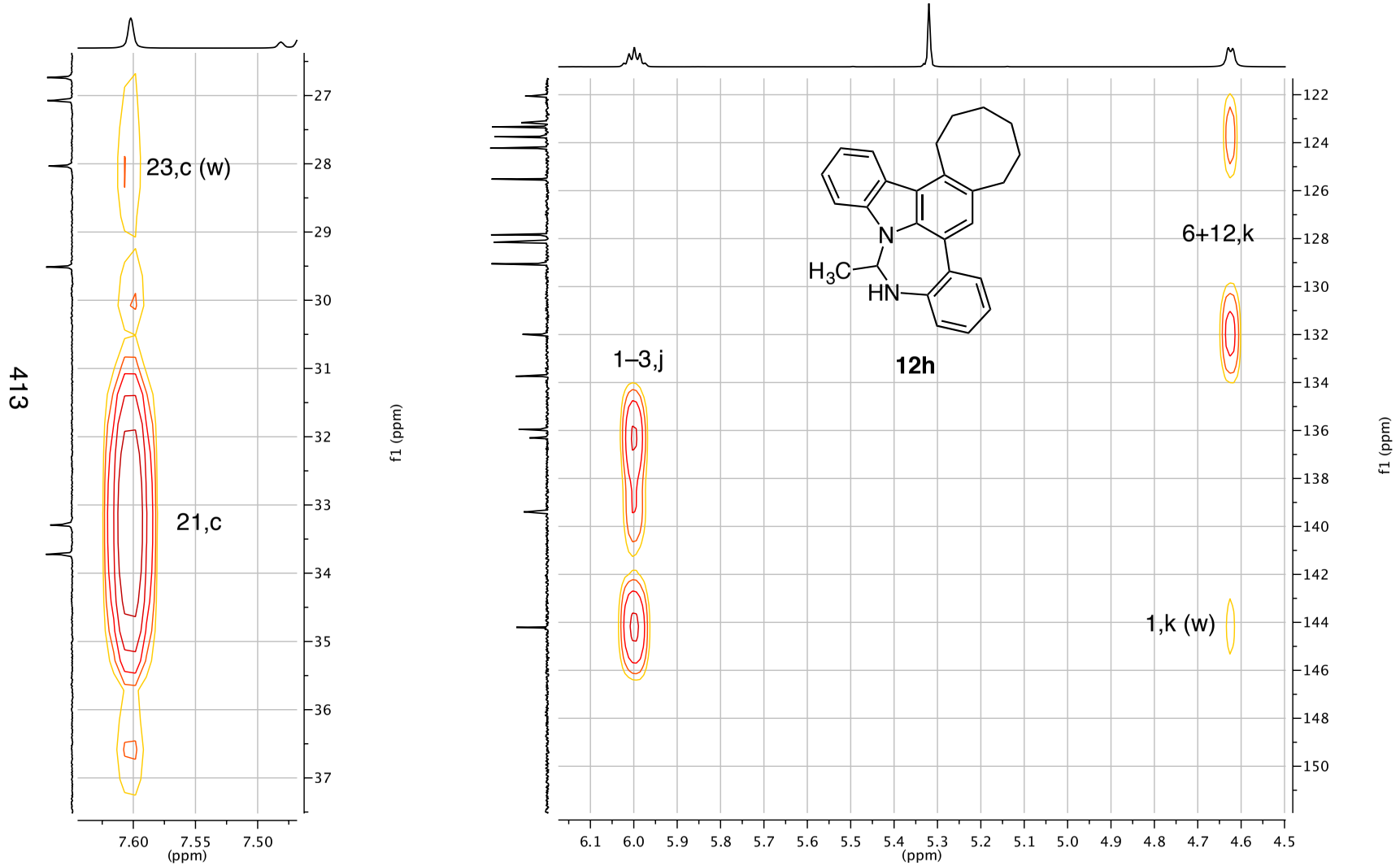

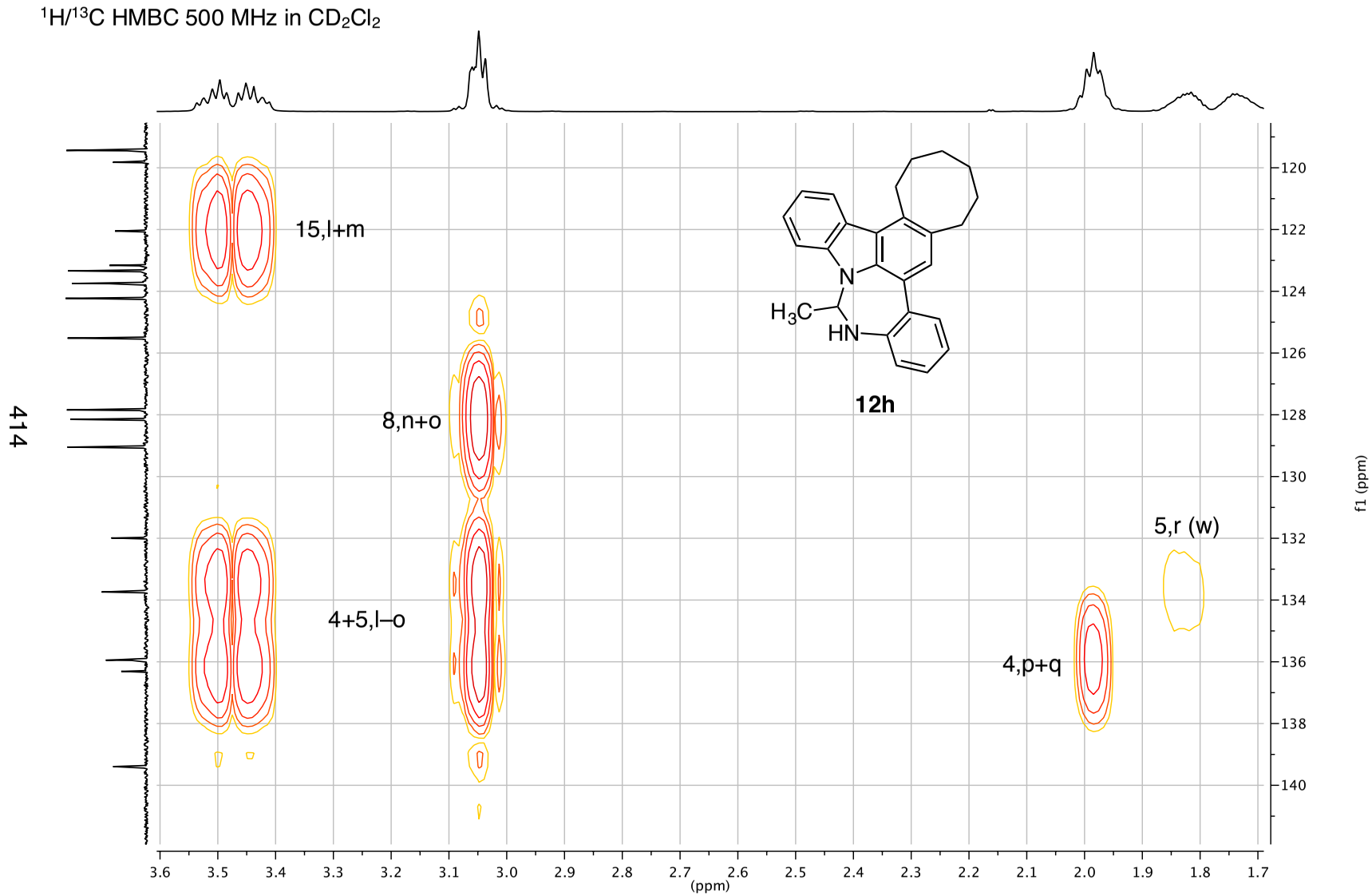
$^{1}H/^{13}C$ HMBC 500 MHz in CD_2Cl_2
414
15,l+m
8,n+o
4+5,l–o
4,p+q
5,r (w)
N
H_3C
HN
12h
3.6 3.5 3.4 3.3 3.2 3.1 3.0 2.9 2.8 2.7 2.6 2.5 2.4 2.3 2.2 2.1 2.0 1.9 1.8 1.7
(ppm)
120 122 124 126 128 130 132 134 136 138 140
f1 (ppm)

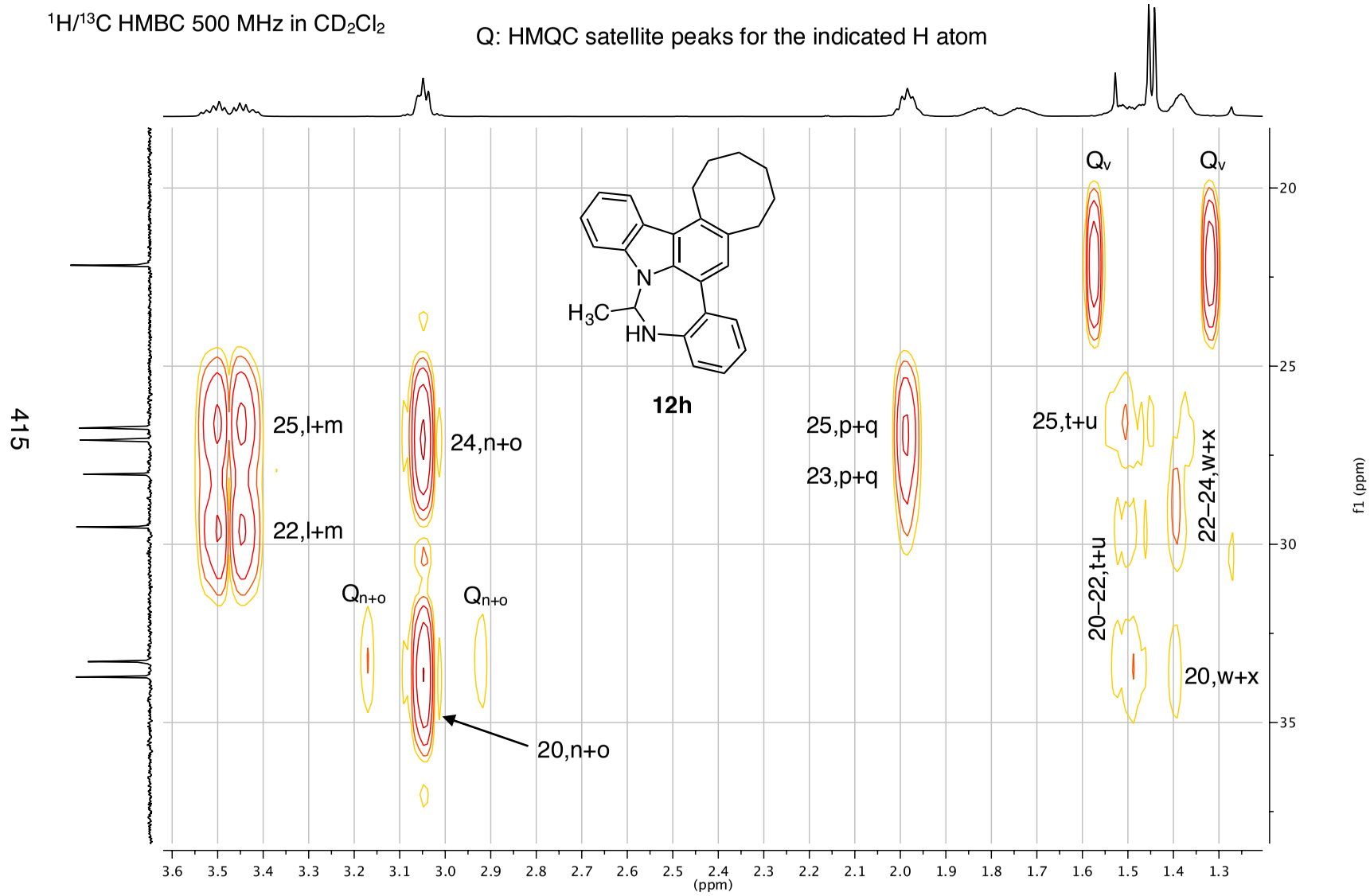
$^{1}H/^{13}C$ HMBC 500 MHz in CD_2Cl_2
Q: HMQC satellite peaks for the indicated H atom
415
12h
H_3C
N
HN
Q_v
Q_v
25,l+m
22,l+m
24,n+o
Q_{n+o}
Q_{n+o}
20,n+o
25,p+q
23,p+q
25,t+u
20–22,t+u
22–24,w+x
20,w+x
20
25
30
35
f1 (ppm)
3.6 3.5 3.4 3.3 3.2 3.1 3.0 2.9 2.8 2.7 2.6 2.5 2.4 2.3 2.2 2.1 2.0 1.9 1.8 1.7 1.6 1.5 1.4 1.3
(ppm)

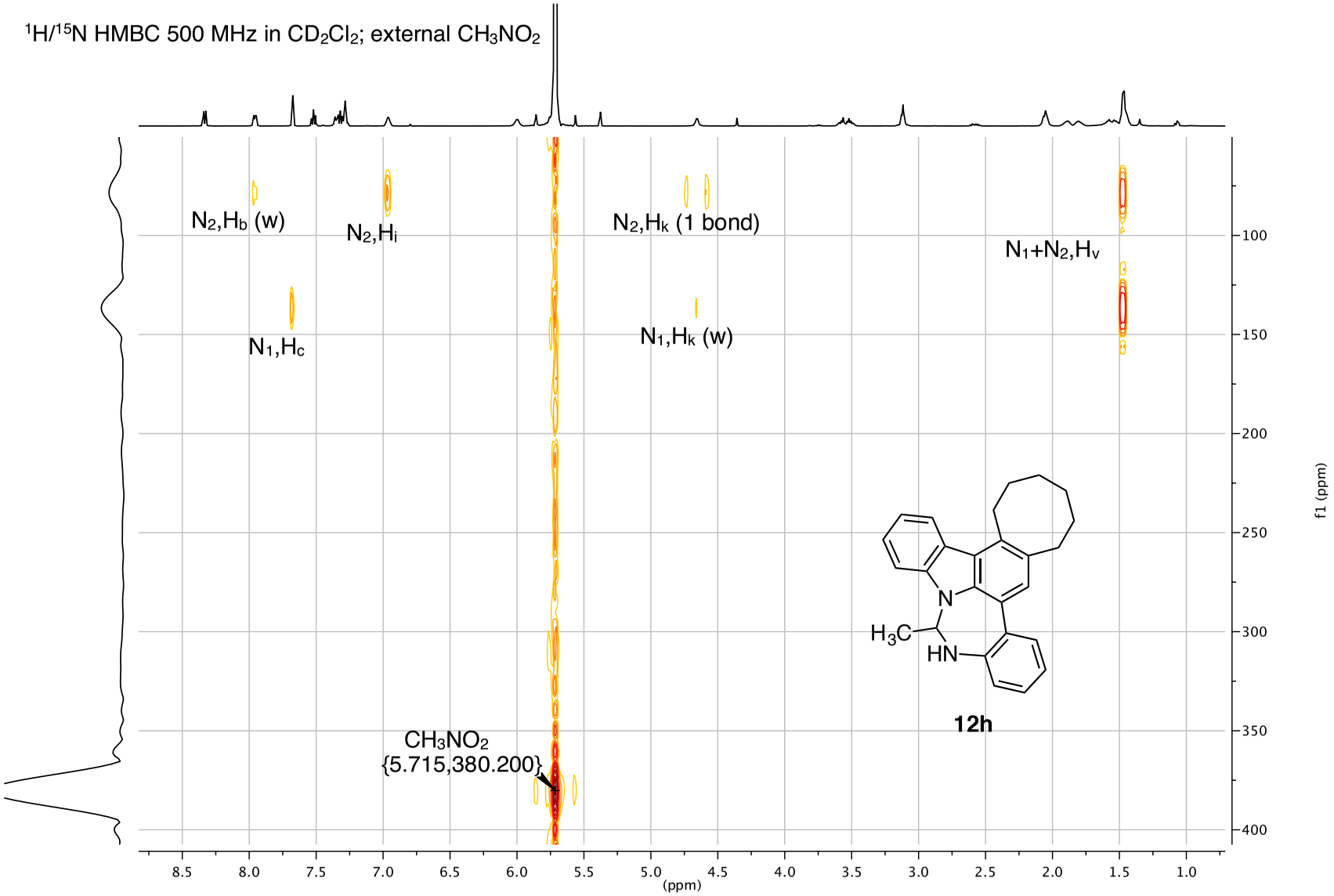
$^{1}H/^{15}N$ HMBC 500 MHz in CD_2Cl_2; external CH_3NO_2
N_2,H_b (w)
N_2,H_i
N_2,H_k (1 bond)
N_1+N_2,H_v
N_1,H_c
N_1,H_k (w)
CH_3NO_2
{5.715,380.200}
N
H_3C
HN
12h
8.5
8.0
7.5
7.0
6.5
6.0
5.5
5.0
4.5
4.0
3.5
3.0
2.5
2.0
1.5
1.0
(ppm)
100
150
200
250
300
350
400
f1 (ppm)

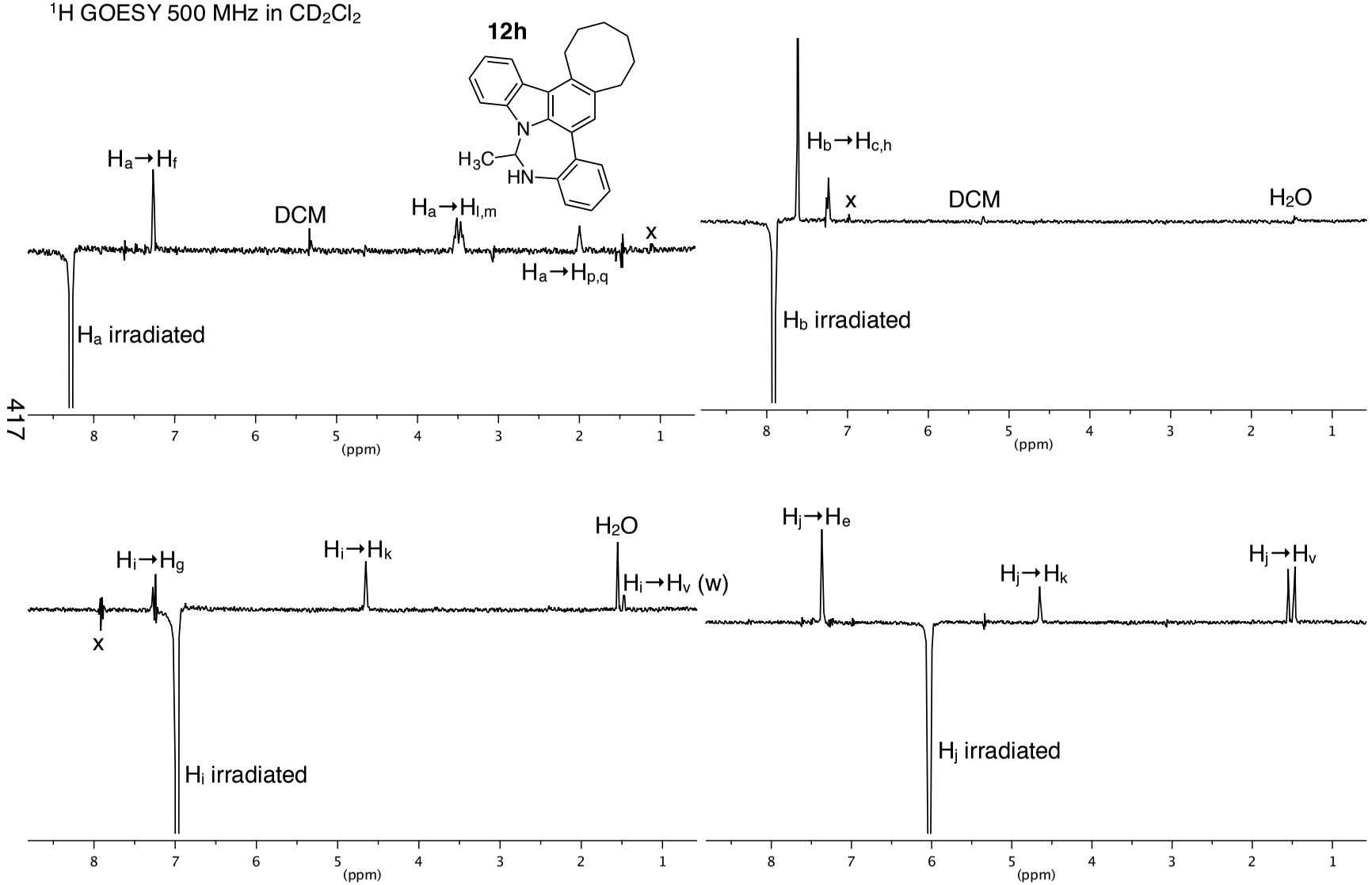
^{1}H GOESY 500 MHz in CD_2Cl_2
12h
N
H_3C
HN
$H_a \rightarrow H_f$
DCM
$H_a \rightarrow H_{l,m}$
x
$H_a \rightarrow H_{p,q}$
H_a irradiated
417
8 7 6 5 (ppm) 4 3 2 1
$H_b \rightarrow H_{c,h}$
x
DCM
H_2O
H_b irradiated
8 7 6 5 (ppm) 4 3 2 1
$H_i \rightarrow H_g$
$H_i \rightarrow H_k$
H_2O
$H_i \rightarrow H_v$ (w)
x
H_i irradiated
8 7 6 5 (ppm) 4 3 2 1
$H_j \rightarrow H_e$
$H_j \rightarrow H_k$
$H_j \rightarrow H_v$
H_j irradiated
8 7 6 5 (ppm) 4 3 2 1

^{1}H GOESY 500 MHz in CD_2Cl_2

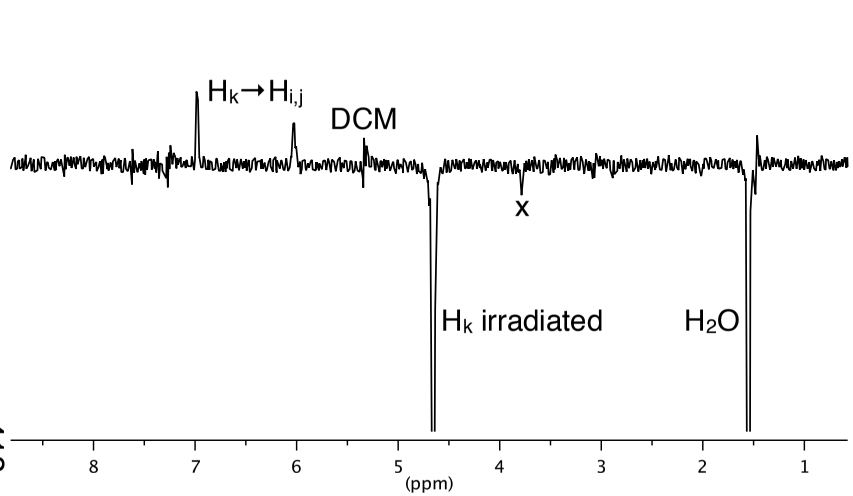

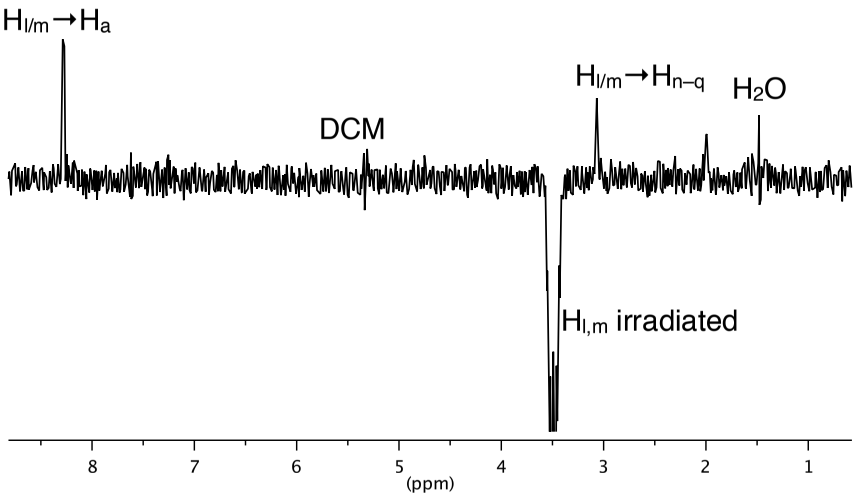

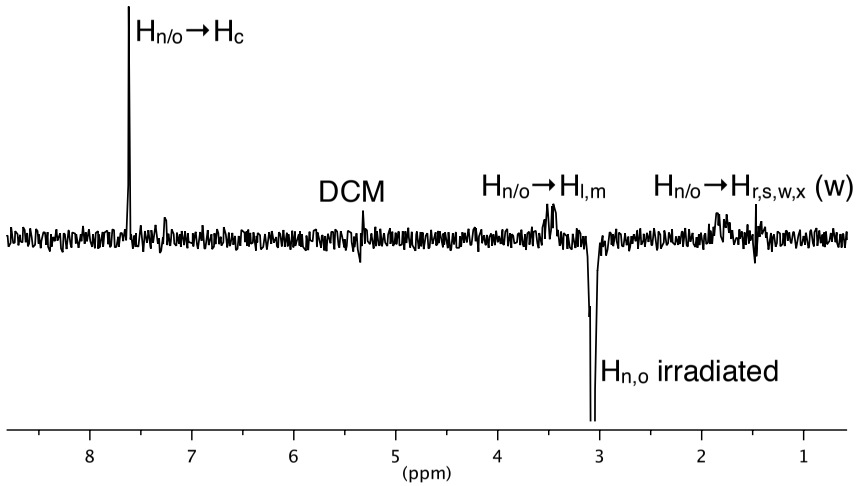

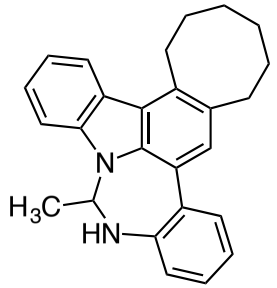

12h

Table 39 (1 of 2). Proton NMR summary for **12h**.

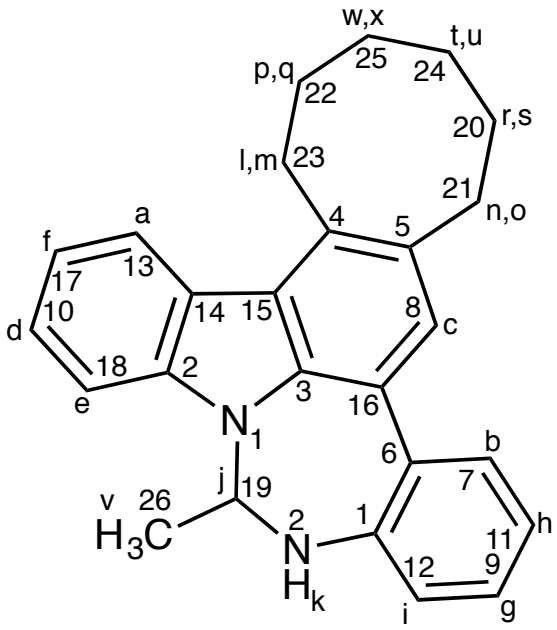

H label	δ	COSY	NOE[a]
a	8.26	F	F,L,M,P,Q
b	7.89	H	C,H
c	7.60	-	not done
d	7.47	E,F	not done
e	7.33	D	not done
f	7.26	A,D	not done
g	7.23	H,I	not done
h	7.22	B,G	not done
i	6.95	G	G,K,v
j	6.00	k,V	E,K,V
k	4.62	j	I,J
l	3.51	P,Q	A,N,O,P,Q
m	3.44	P,Q	

[a]Merged entries were co-irradiated due to similar chemical shift.

Table 39 (2 of 2). Proton NMR summary for **12h**.

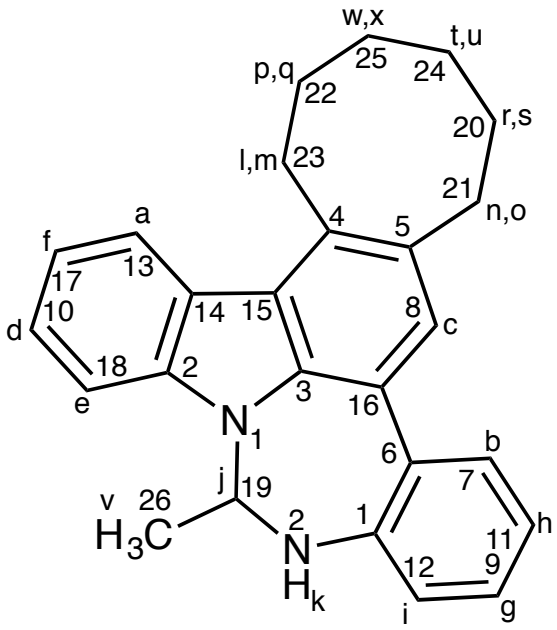

H label	δ	COSY	NOE[a]
n	3.05	R,S	C,L,M,r,s,w,x
o	3.05	R,S	
p	1.99	L,M,W,X	not done
q	1.99	L,M,W,X	not done
r	1.83	N,O	not done
s	1.73	N,O	not done
t	1.51	-	not done
u[b]	1.47	-	not done
v	1.45	J	not done
w[b]	1.38	P,Q	not done
x	1.38	P,Q	not done

[a]Merged entries were co-irradiated due to similar chemical shift.

[b]H_u and H_w are indistinguishable by COSY and HMQC and are arbitrarily assigned.

Table 40 (1 of 2). Carbon NMR summary for **12h**.

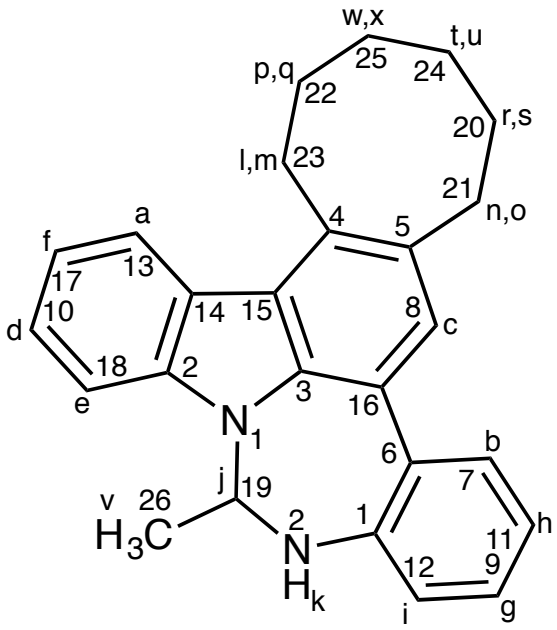

C label	δ	type	HMQC	HMBC
1	144.2	q	-	B,c,G,i,J,k
2	139.4	q	-	A,D,f,J
3	136.3	q	-	C,J
4	135.9	q	-	C,L,M,N,O,P,Q
5	133.7	q	-	L,M,N,O,r
6	132.0	q	-	C,H,I,K
7	129.0	CH	b	G
8	128.1	CH	c	N,O
9	127.8	CH	g	B
10	125.5	CH	d	A,f
11	124.2	CH	h	I
12	123.7	CH	i	H,K
13	123.3	CH	a	D
14	123.2	q	-	E,F

Table 40 (2 of 2). Carbon NMR summary for **12h**.

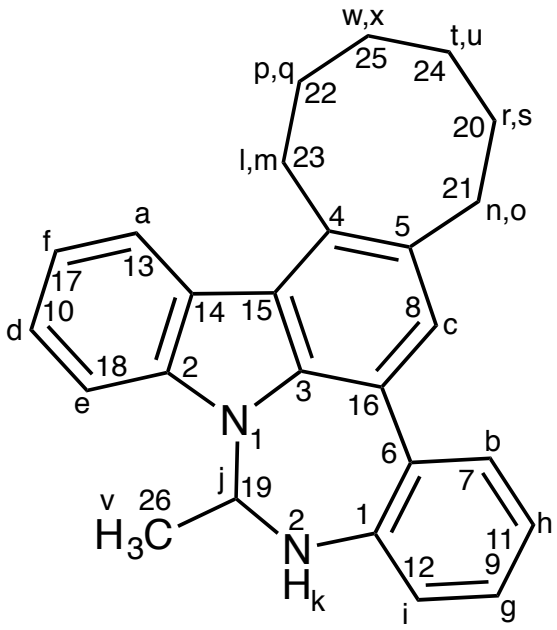

C label	δ	type	HMQC	HMBC
15	122.1	q	-	a,c,L,M
16	119.8	q	-	b
17	119.4	CH	f	d,E
18	108.1	CH	e	a,F
19	66.7	CH	j	V
20	33.7	CH_2	r,s	N,O,T,U,W,X
21	33.3	CH_2	n,o	C,T,U
22	29.5	CH_2	p,q	L,M,T,U,W,X
23	28.0	CH_2	l,m	c,P,Q,W,X
24	27.1	CH_2	t,u	N,O,W,X
25	26.7	CH_2	w,x	L,M,P,Q,T,U
26	22.2	CH_3	v	J

Table 41. Nitrogen NMR summary for **12h**.

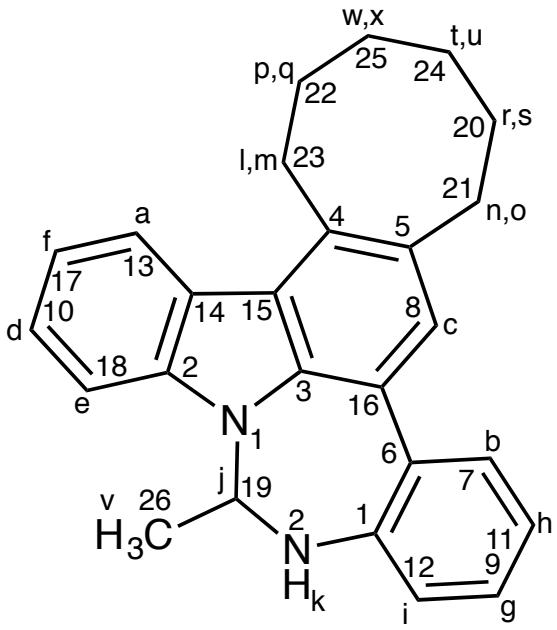

N label	δ[a]	type	HMBC
1	136.70	t	C,k,V
2	78.50	NH	b,I,K[b],V

[a]The mean value of ^{1}H HMBC crosspeaks relative to external nitromethane (δ = 380.2 ppm) [193].

[b]This is a 1-bond interaction, based on split crosspeaks.

^{1}H NMR 500 MHz in $(CD_3)_2SO$

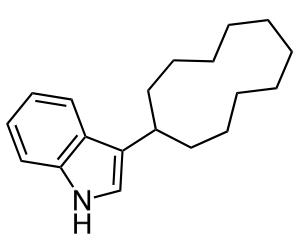

13k

^{1}H NMR 500 MHz in $(CD_3)_2SO$

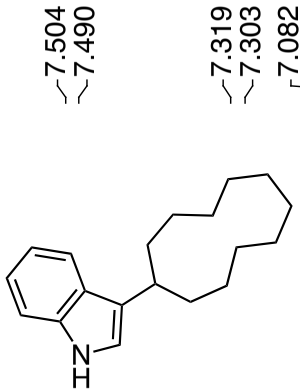

13k

425

^{13}C NMR 126 MHz in $(CD_3)_2SO$

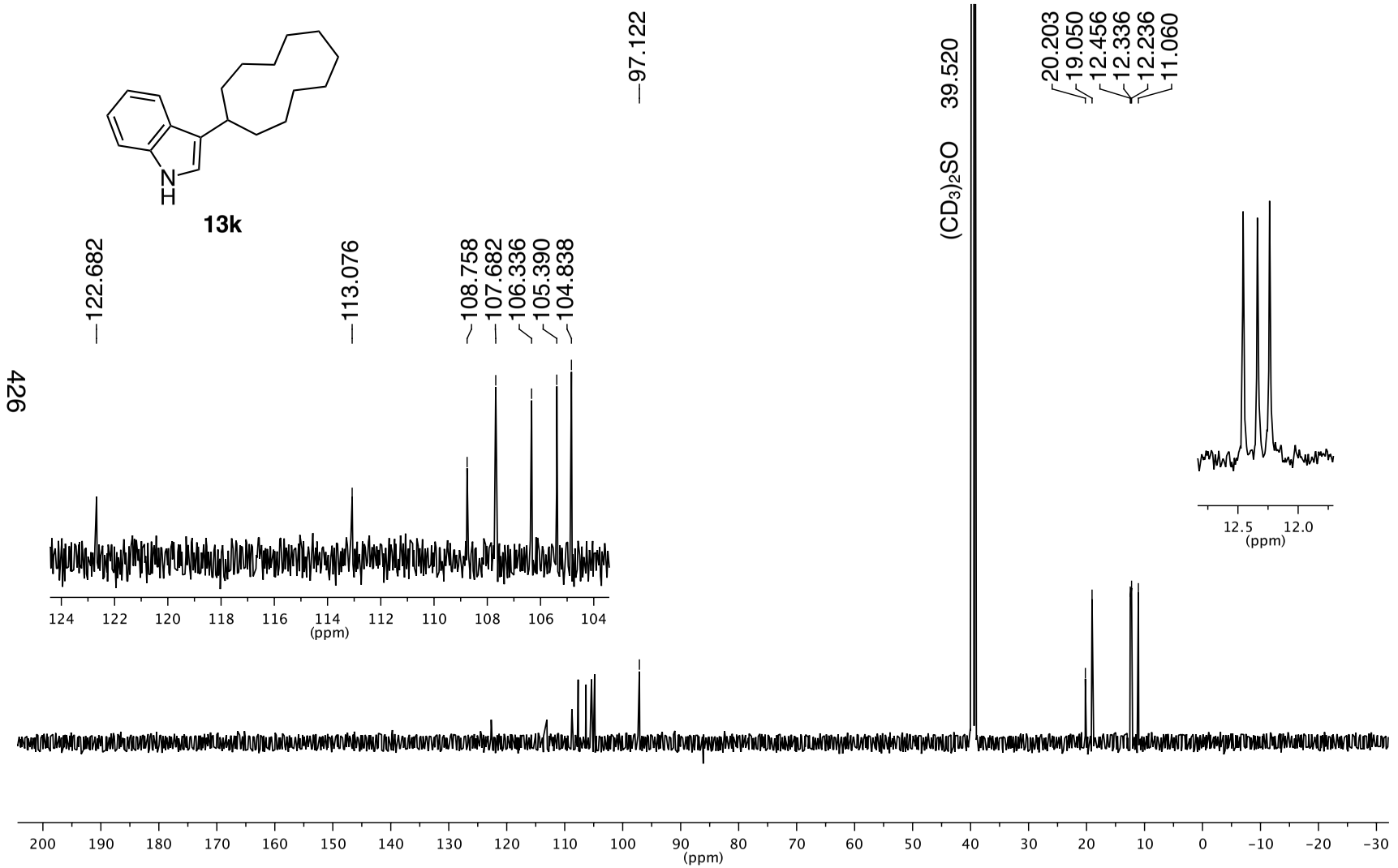

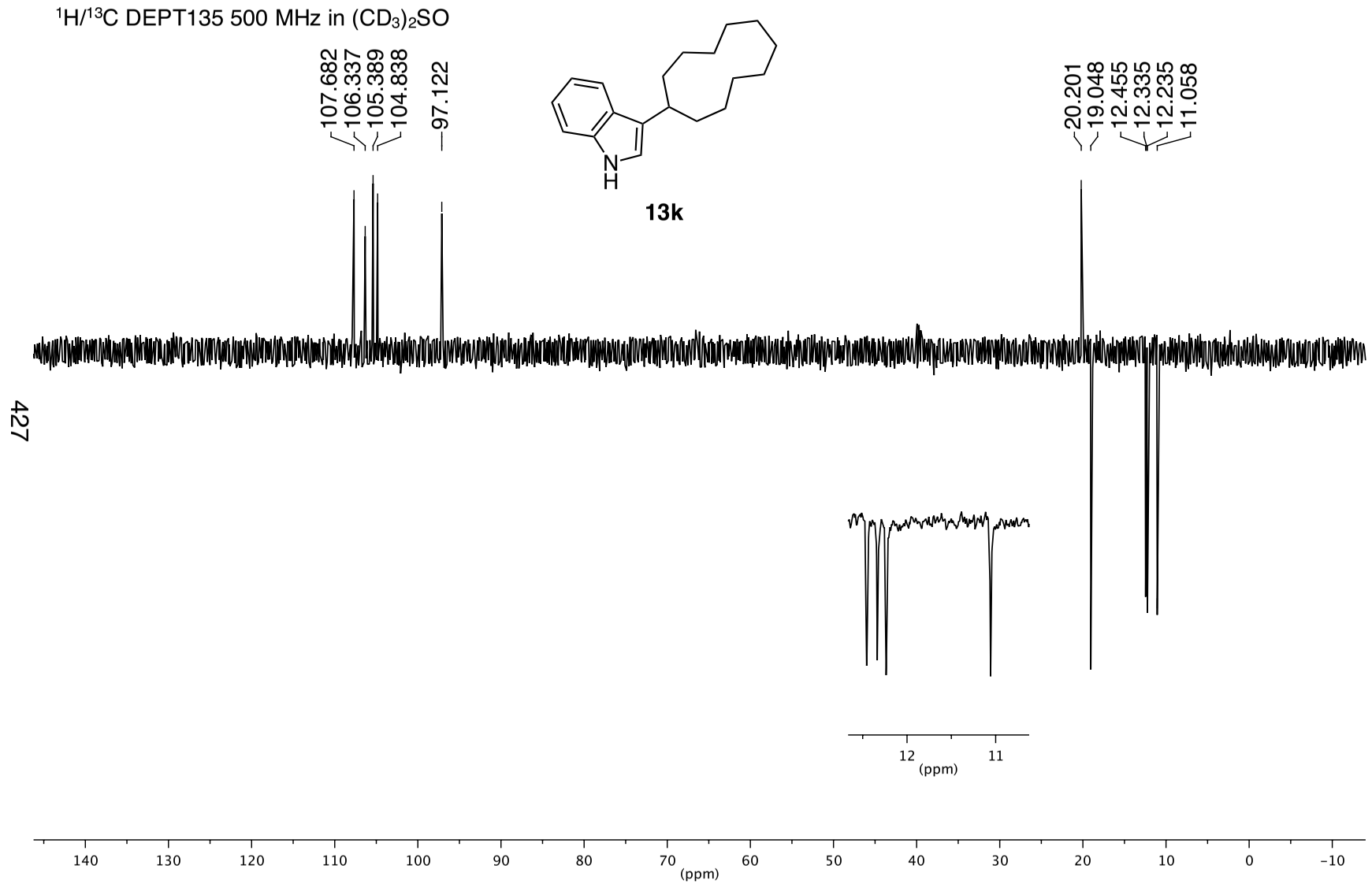
$^{1}H/^{13}C$ DEPT135 500 MHz in $(CD_3)_2SO$
107.682
106.337
105.389
104.838
97.122
20.201
19.048
12.455
12.335
12.235
11.058
13k
427
12
11
(ppm)
140
130
120
110
100
90
80
70
60
50
40
30
20
10
0
-10
(ppm)

^{1}H NMR 500 MHz in $(CD_3)_2SO$

^{1}H NMR 500 MHz in $(CD_3)_2SO$

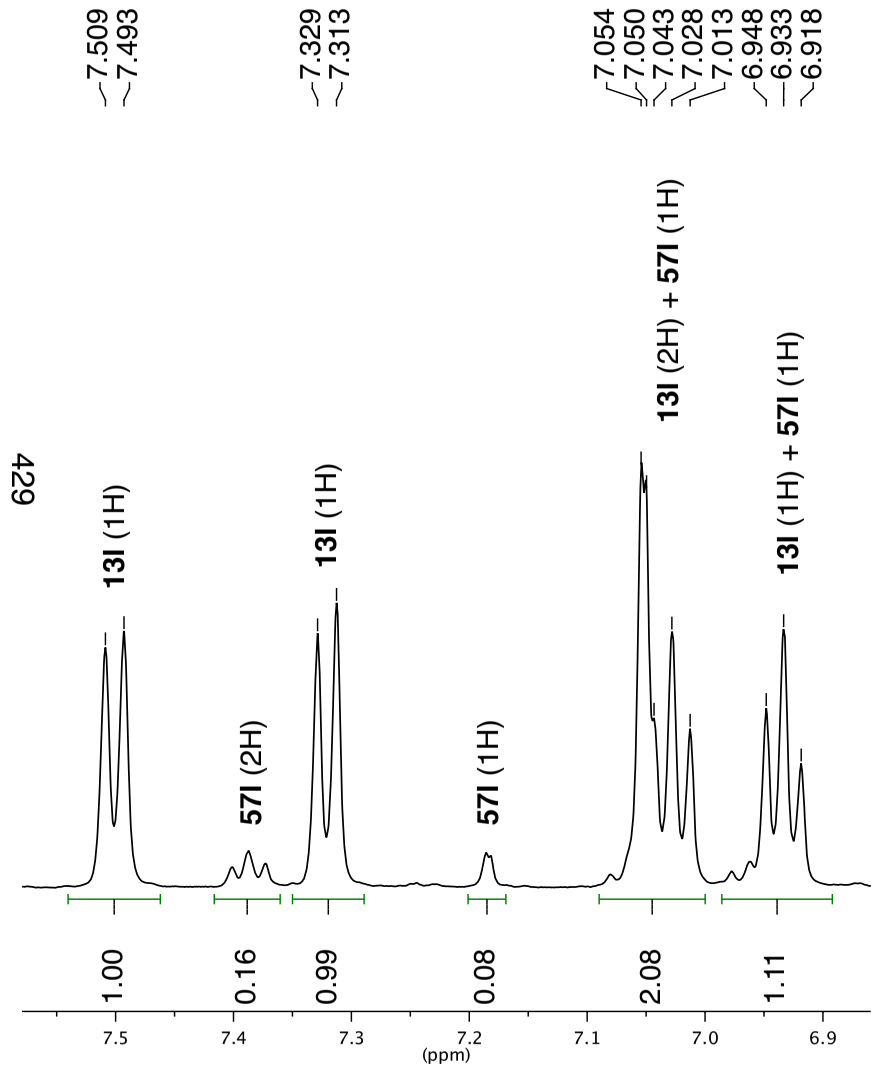

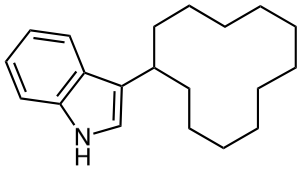

13I

Mixture includes
9.04 equiv. cyclododecanone.

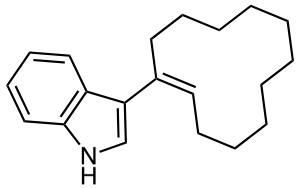

57I

0.07 equiv;
E or *Z* isomer

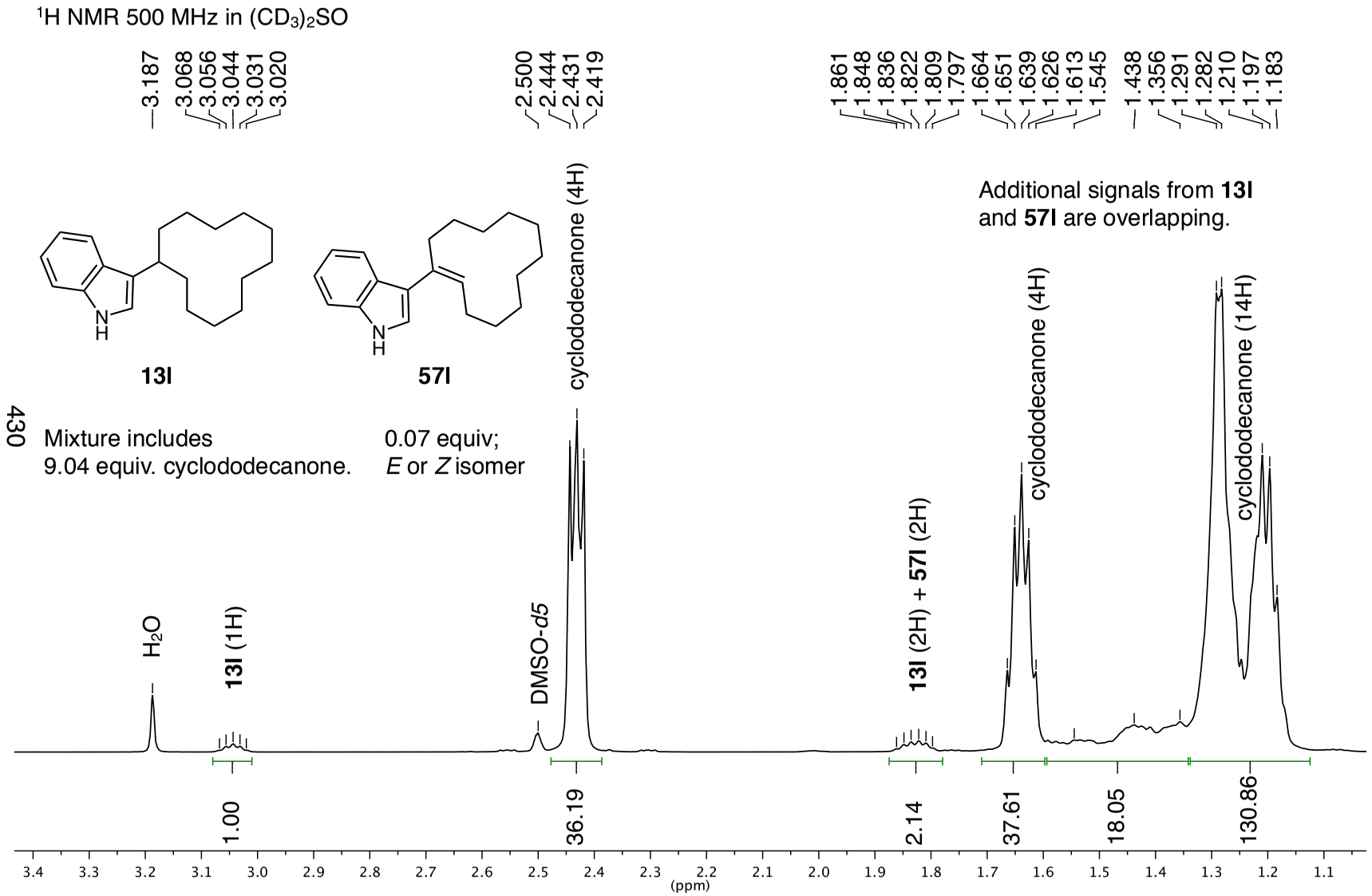
1H NMR 500 MHz in (CD3)2SO
3.187
3.068
3.056
3.044
3.031
3.020
2.500
2.444
2.431
2.419
1.861
1.848
1.836
1.822
1.809
1.797
1.664
1.651
1.639
1.626
1.613
1.545
1.438
1.356
1.291
1.282
1.210
1.197
1.183
13I
57I
Mixture includes
9.04 equiv. cyclododecanone.
0.07 equiv;
E or Z isomer
Additional signals from 13I
and 57I are overlapping.
cyclododecanone (4H)
cyclododecanone (4H)
cyclododecanone (14H)
H2O
13I (1H)
DMSO-d5
13I (2H) + 57I (2H)
1.00
36.19
2.14
37.61
18.05
130.86
(ppm)

^{13}C NMR 126 MHz in $(CD_3)_2SO$

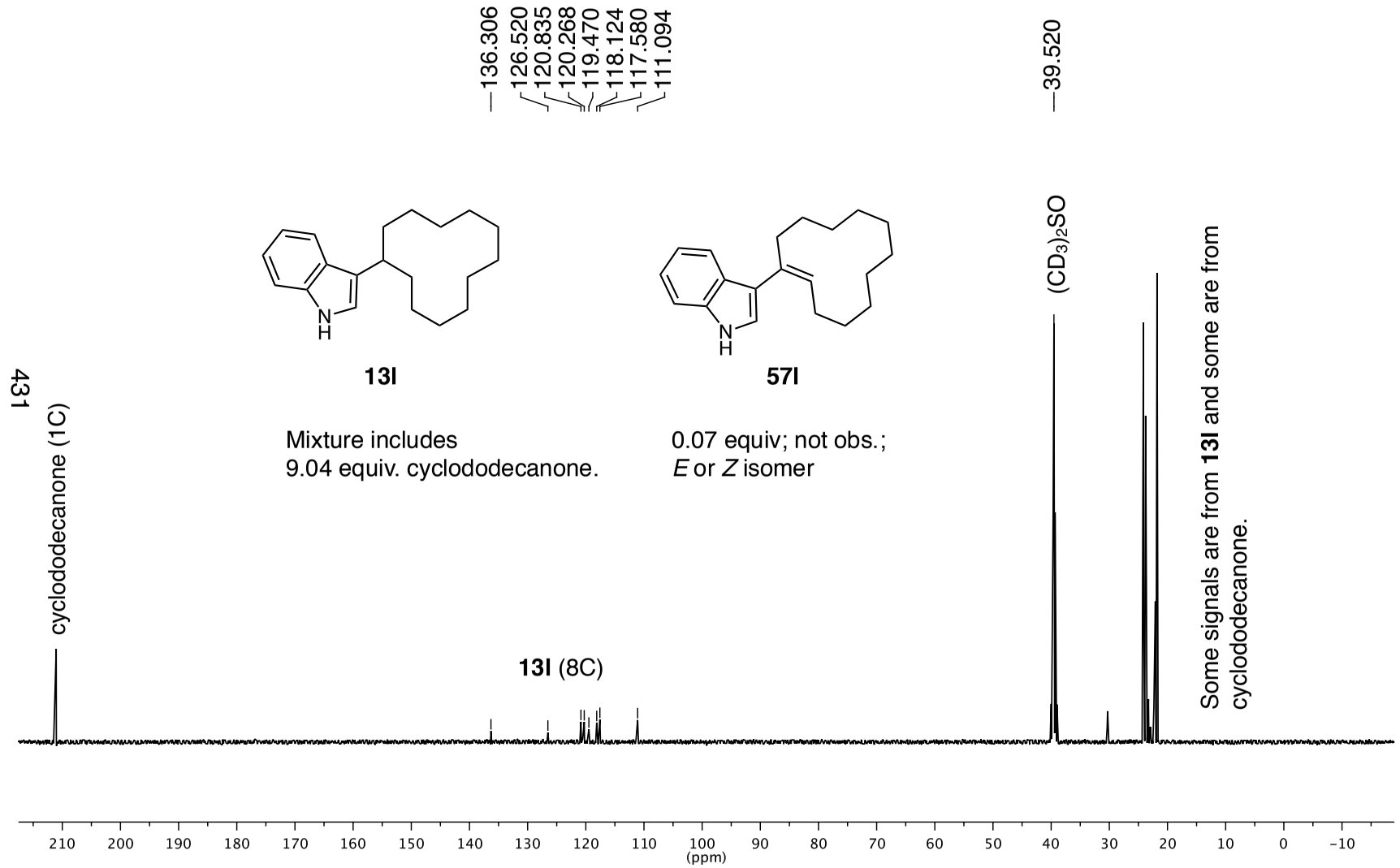

13l

Mixture includes
9.04 equiv. cyclododecanone.

57l

0.07 equiv; not obs.;
E or *Z* isomer

^{13}C NMR 126 MHz in $(CD_3)_2SO$

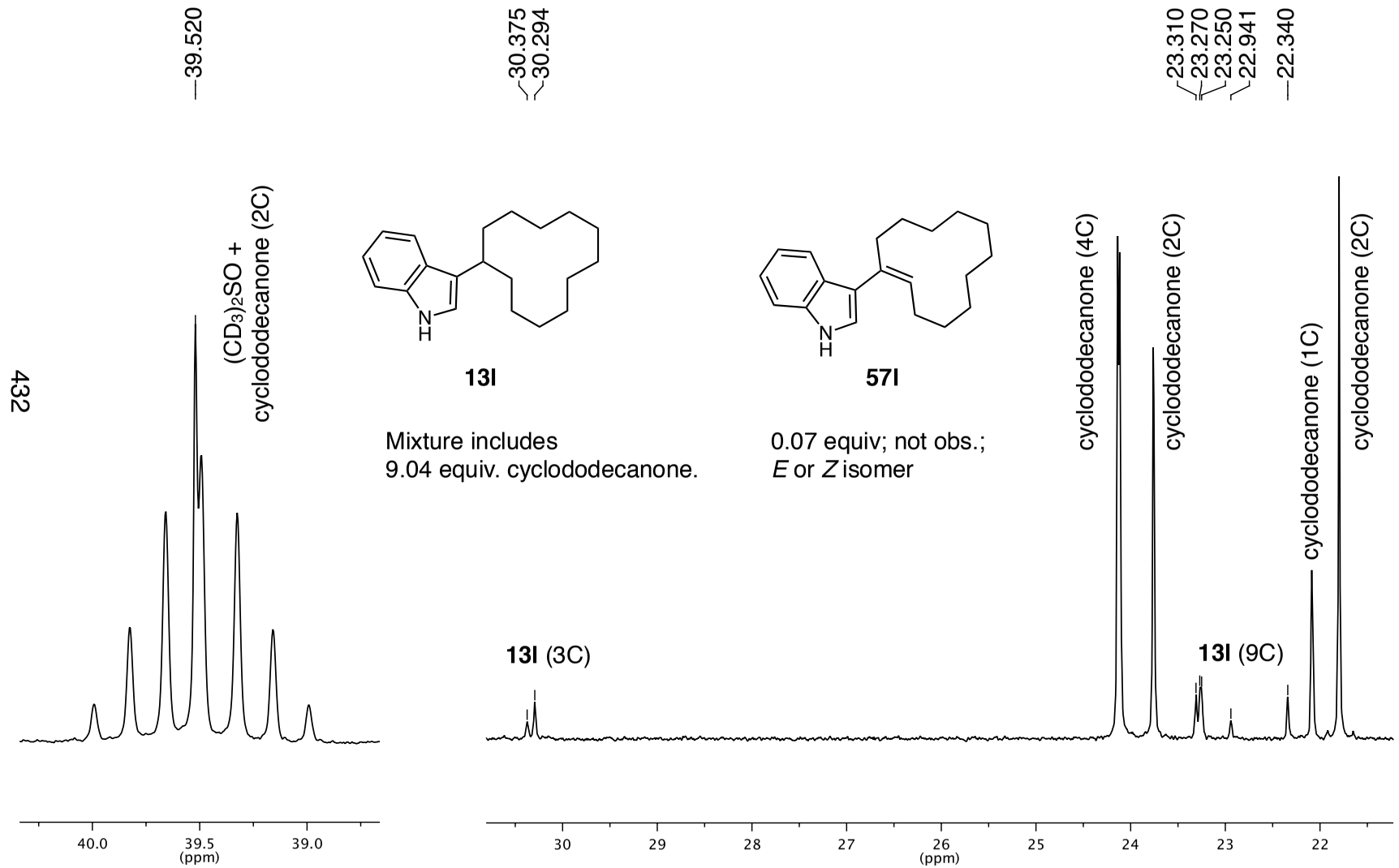

$^{1}H/^{13}C$ DEPT135 500 MHz in $(CD_3)_2SO$

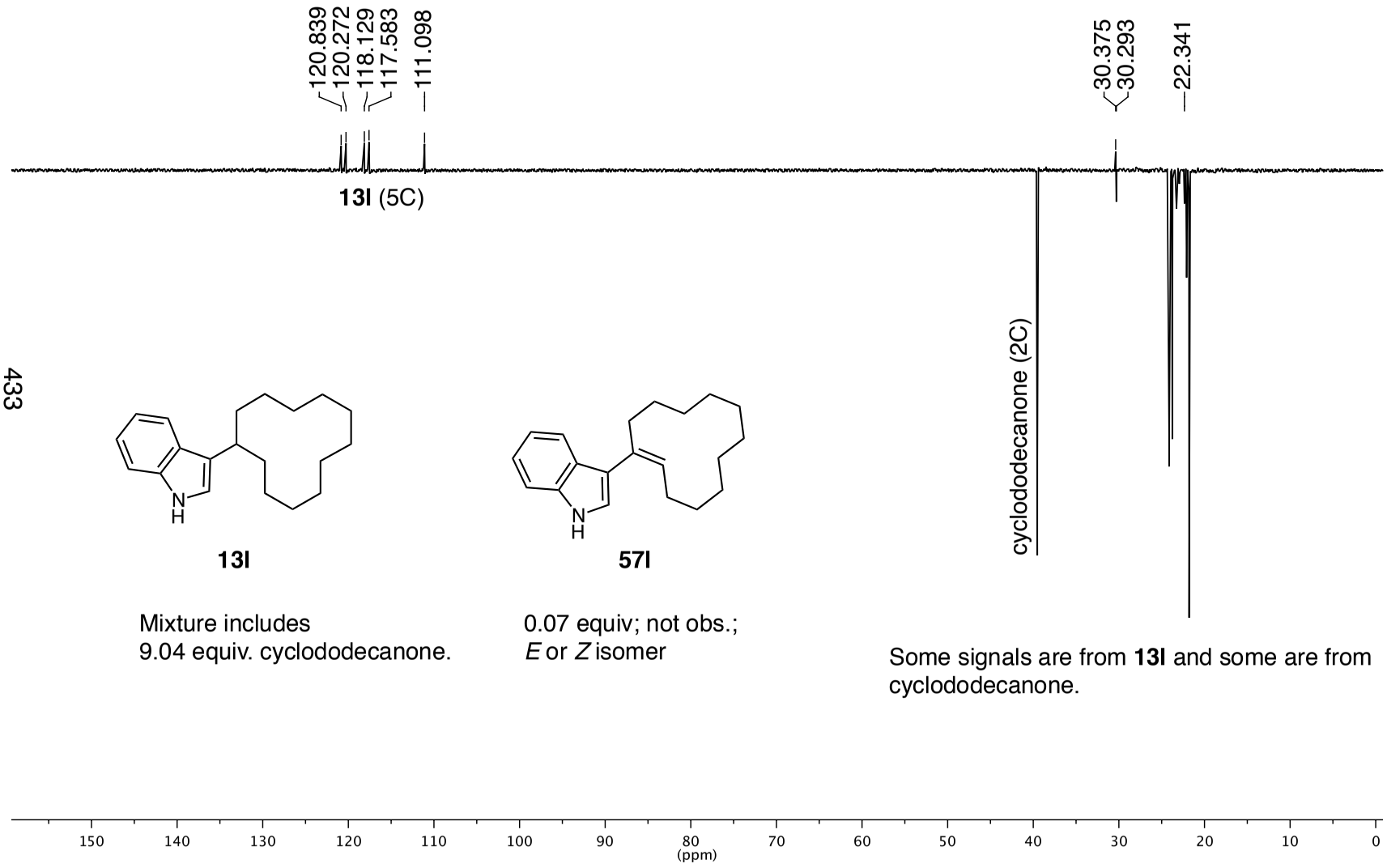

13l (5C)

13l

Mixture includes
9.04 equiv. cyclododecanone.

57l

0.07 equiv; not obs.;
E or *Z* isomer

Some signals are from **13l** and some are from cyclododecanone.

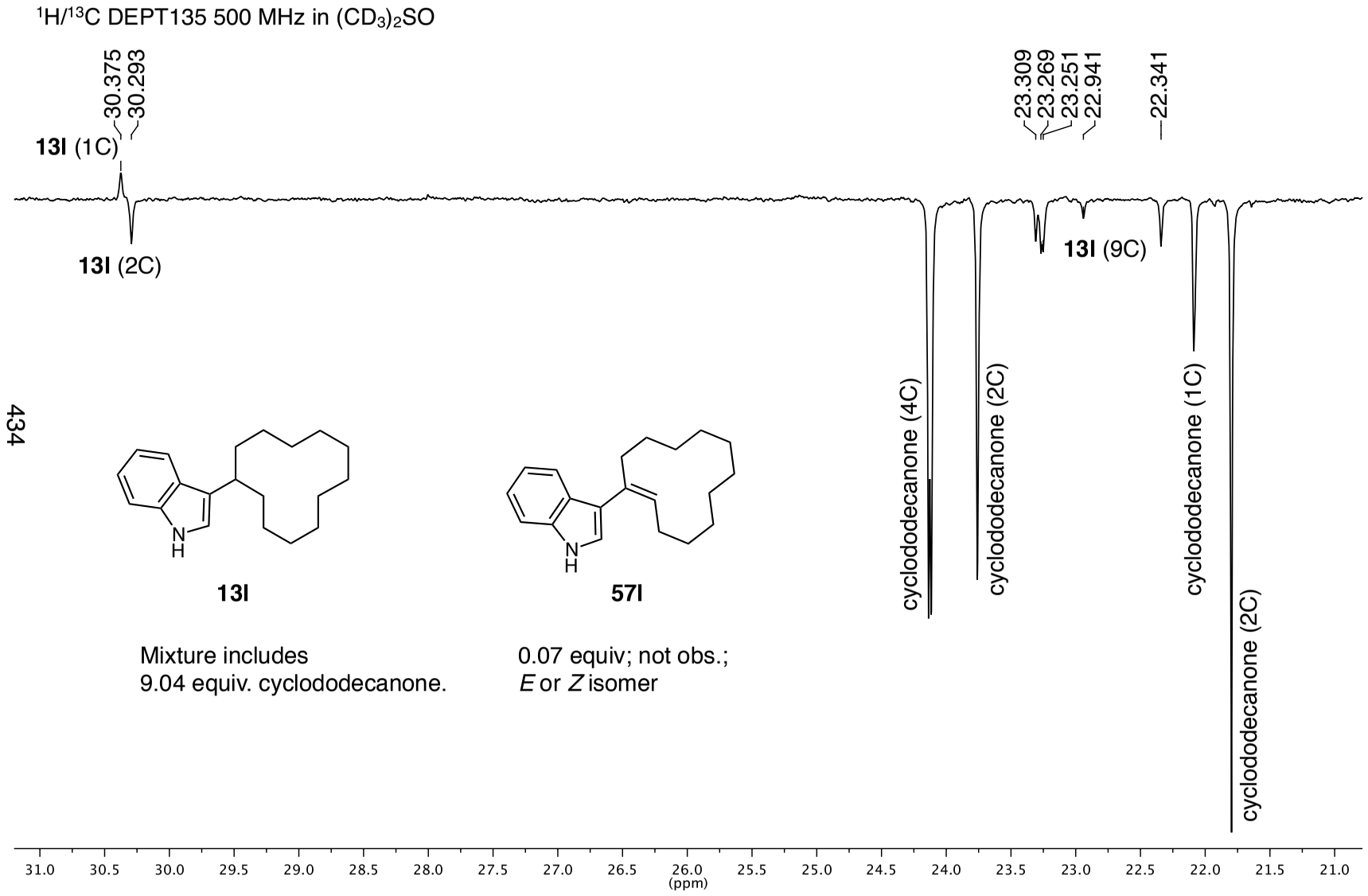
$^{1}H/^{13}C$ DEPT135 500 MHz in $(CD_3)_2SO$
30.375
30.293
23.309
23.269
23.251
22.941
22.341
13l (1C)
13l (2C)
13l (9C)
cyclododecanone (4C)
cyclododecanone (2C)
cyclododecanone (1C)
cyclododecanone (2C)
434
13l
57l
Mixture includes
9.04 equiv. cyclododecanone.
0.07 equiv; not obs.;
E or Z isomer
31.0
30.5
30.0
29.5
29.0
28.5
28.0
27.5
27.0
26.5
26.0
25.5
25.0
24.5
24.0
23.5
23.0
22.5
22.0
21.5
21.0
(ppm)

^{1}H NMR 400 MHz in CD_2Cl_2

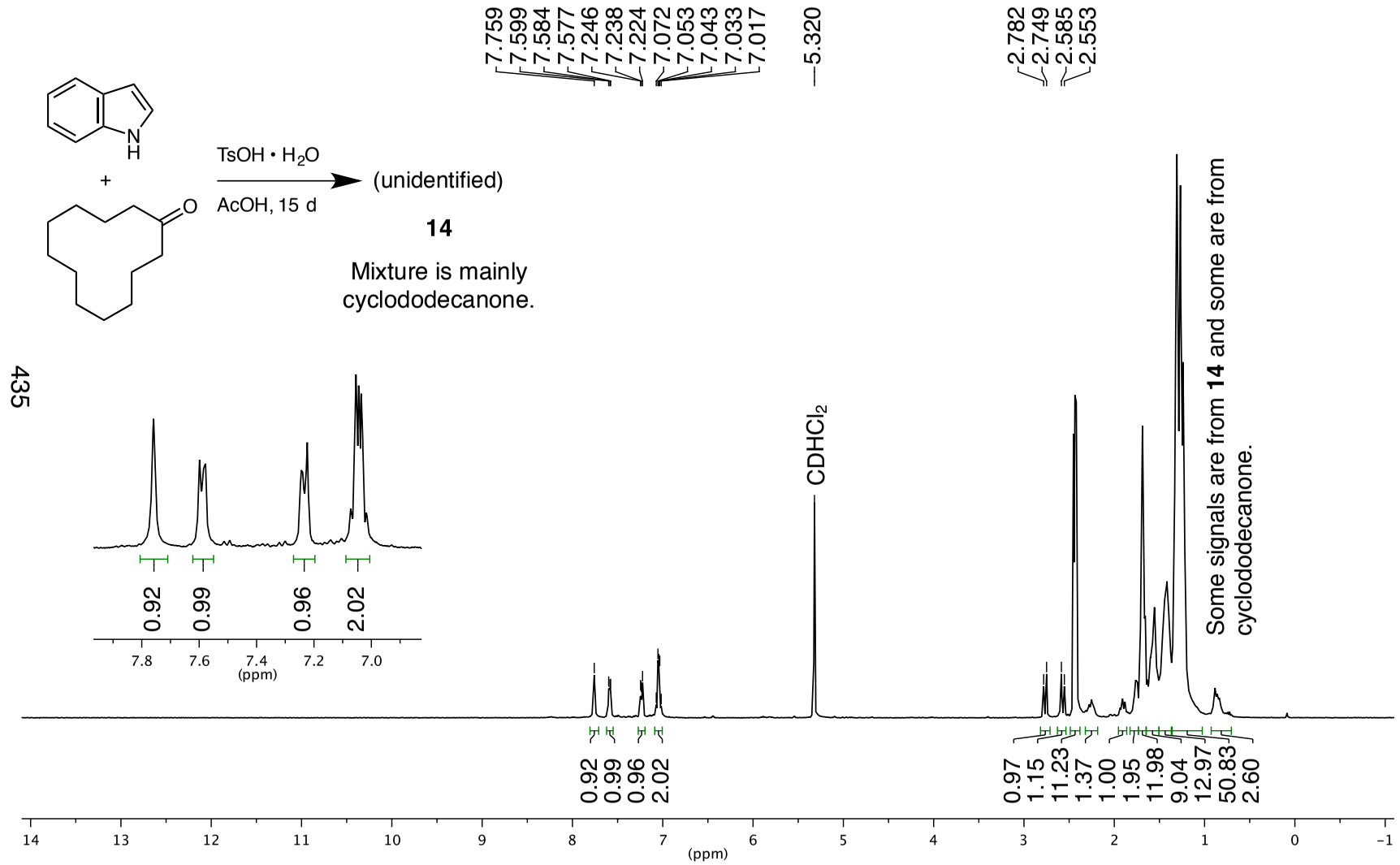

^{1}H NMR 400 MHz in CD_2Cl_2
2.782
2.749
2.585
2.553
2.451
2.436
2.421
2.281
2.251
2.222
1.935
1.908
1.882
1.763
1.743
1.719
1.703
1.688
1.672
1.656
1.555
1.417
1.307
1.268
1.255
1.239
1.223
0.896
0.884
0.859
0.837
cyclododecanone (4H)
cyclododecanone (14H)
14
0.97
1.15
11.23
1.37
1.00
1.95
11.98
9.04
12.97
50.83
2.60
(ppm)

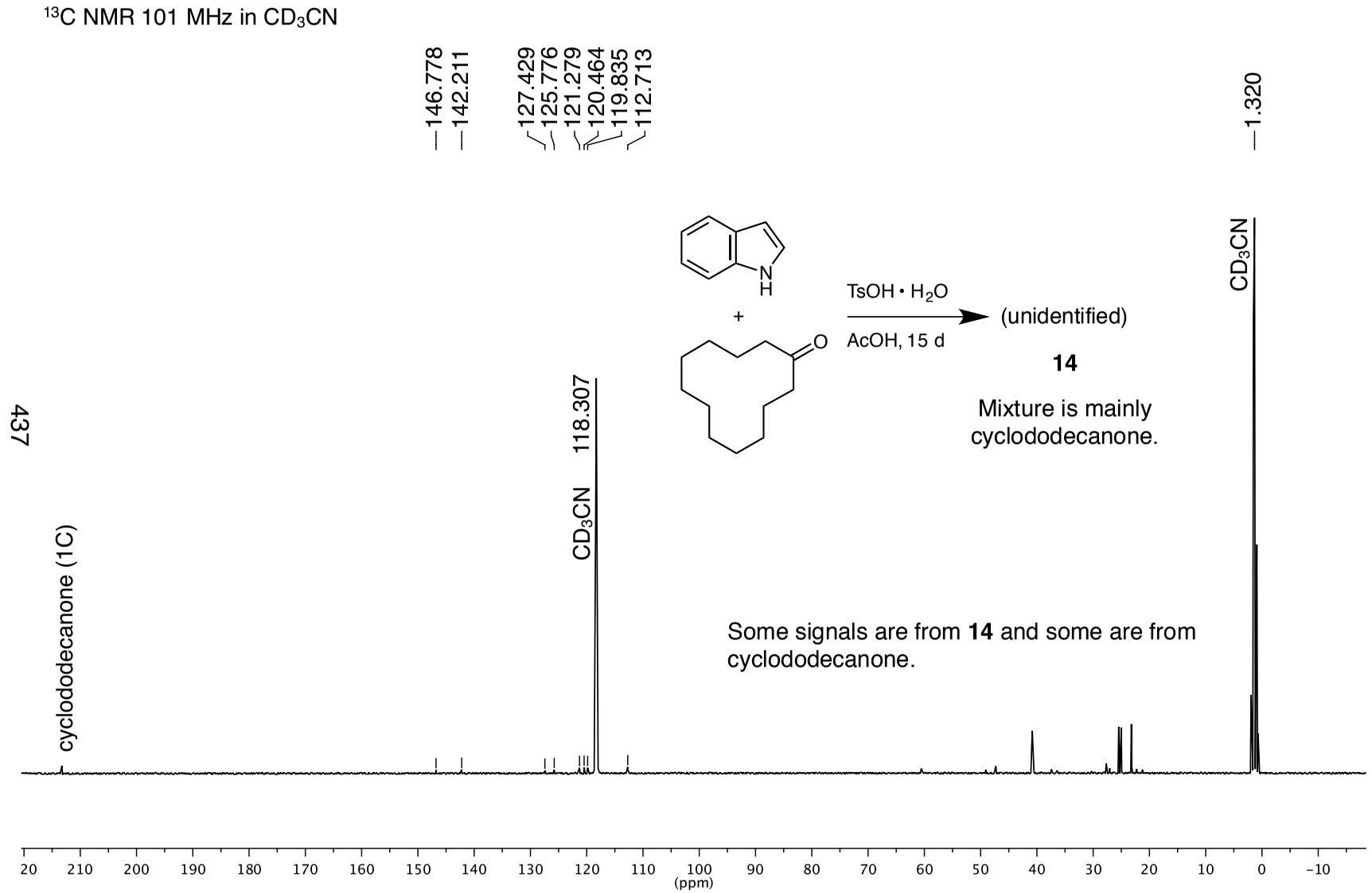
^{13}C NMR 101 MHz in CD_3CN
146.778
142.211
127.429
125.776
121.279
120.464
119.835
112.713
1.320
CD_3CN
118.307
CD_3CN
cyclododecanone (1C)
437
TsOH • H_2O
AcOH, 15 d
(unidentified)
14
Mixture is mainly cyclododecanone.
Some signals are from 14 and some are from cyclododecanone.
(ppm)

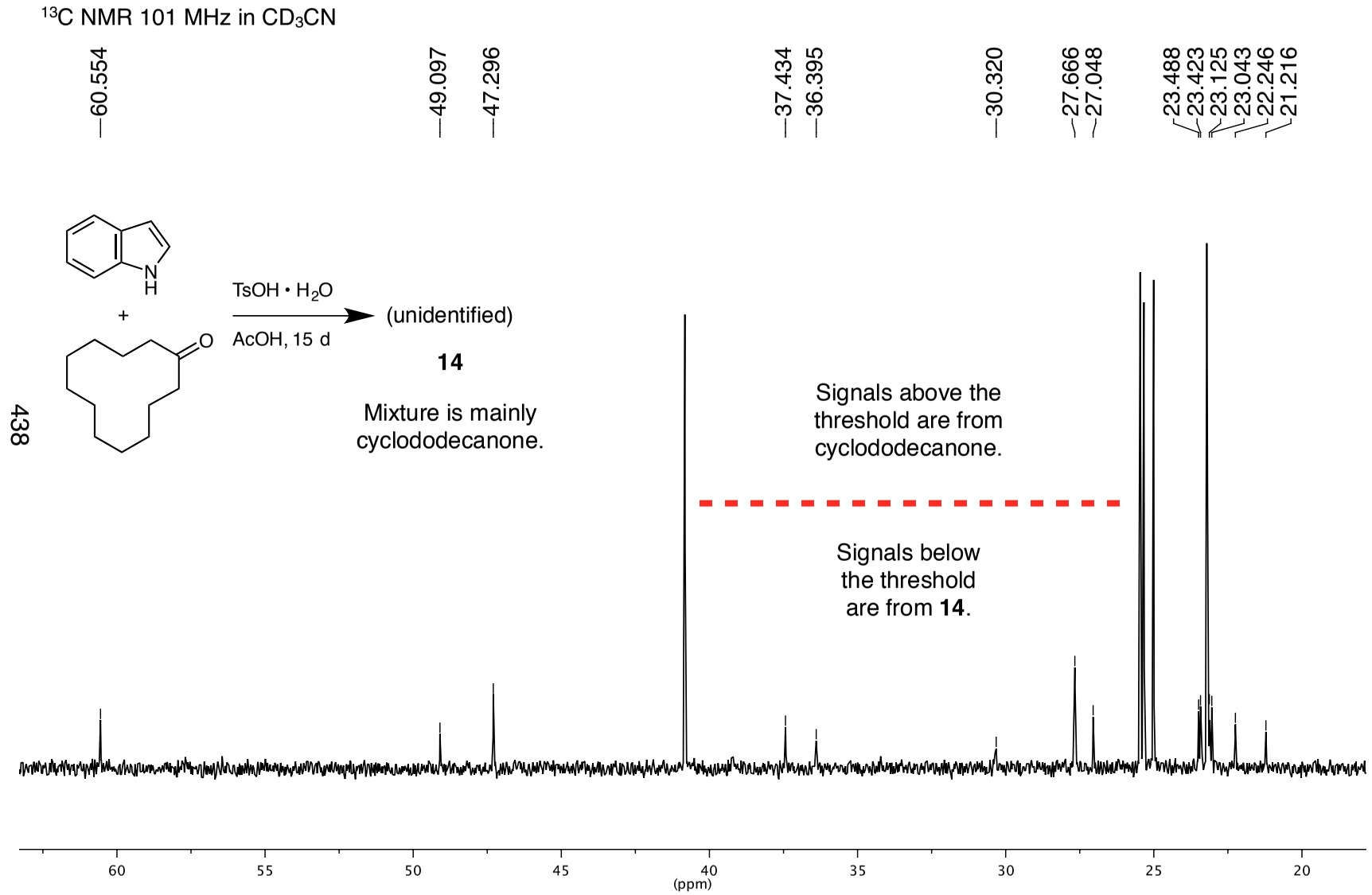
^{13}C NMR 101 MHz in CD_3CN
60.554
49.097
47.296
37.434
36.395
30.320
27.666
27.048
23.488
23.423
23.125
23.043
22.246
21.216
TsOH • H_2O
AcOH, 15 d
(unidentified)
14
Mixture is mainly cyclododecanone.
Signals above the threshold are from cyclododecanone.
Signals below the threshold are from 14.
438
60
55
50
45
40
35
30
25
20
(ppm)

$^{1}H/^{13}C$ DEPT135 400 MHz in CD_2Cl_2

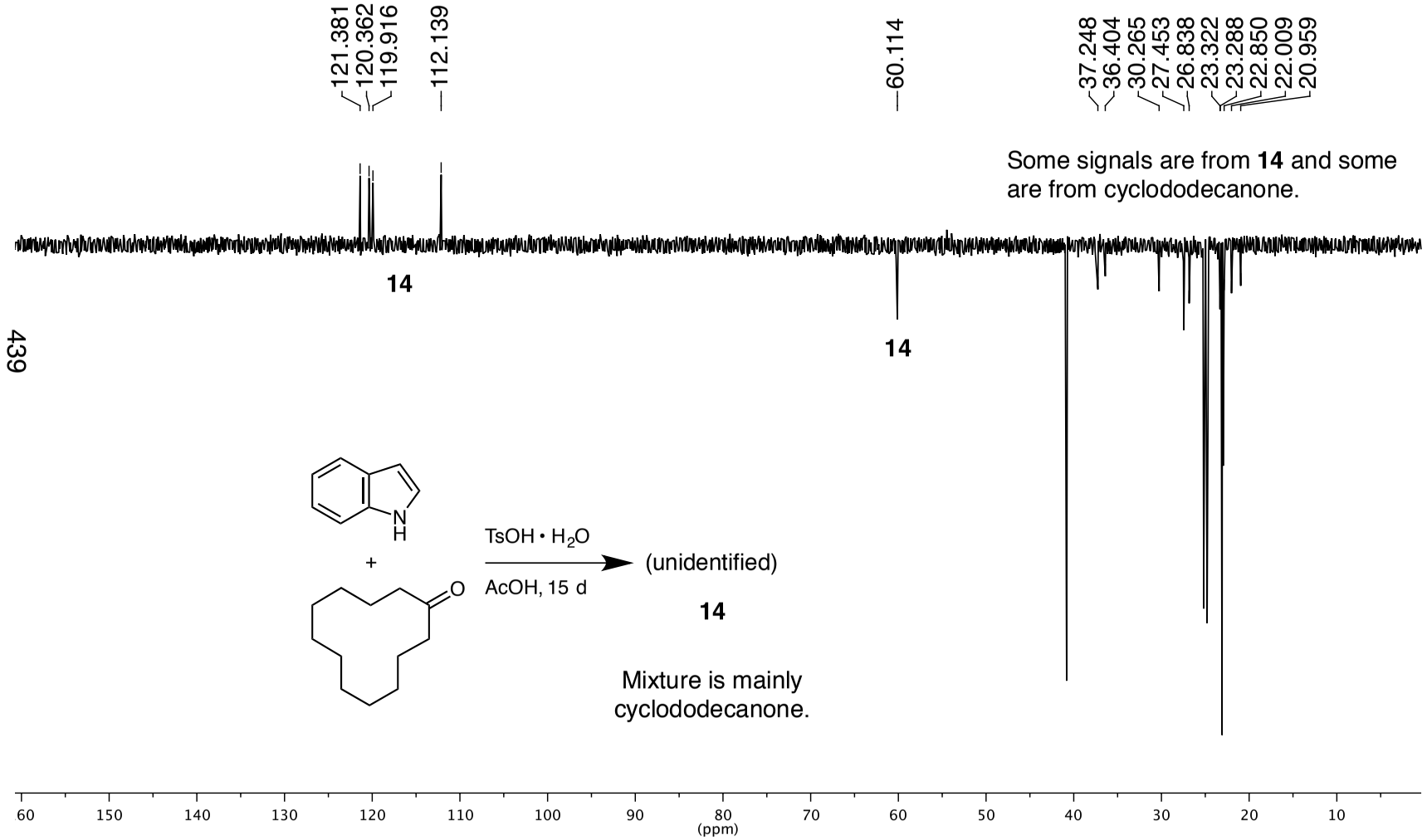

$^{1}H/^{13}C$ DEPT135 400 MHz in CD_2Cl_2

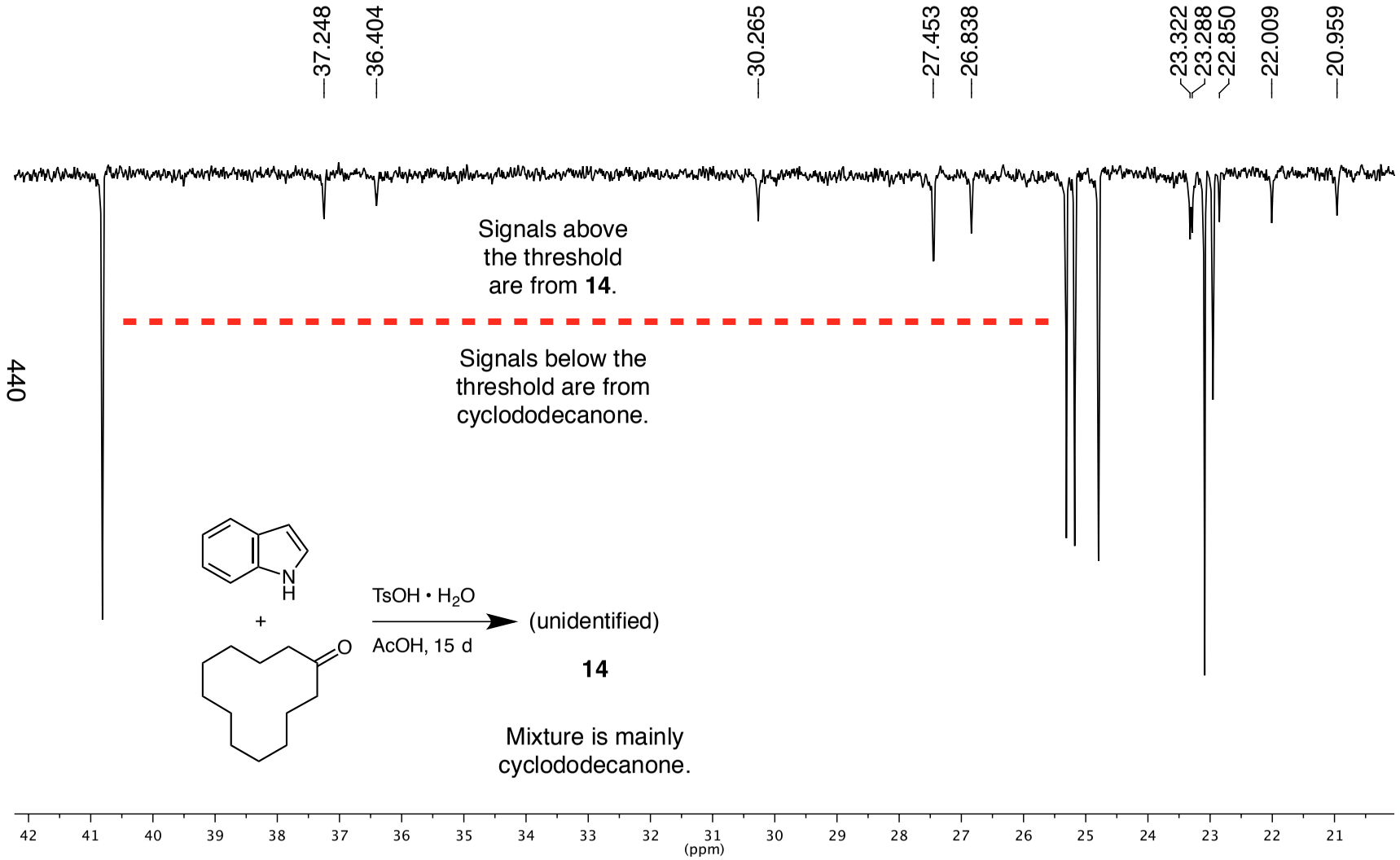

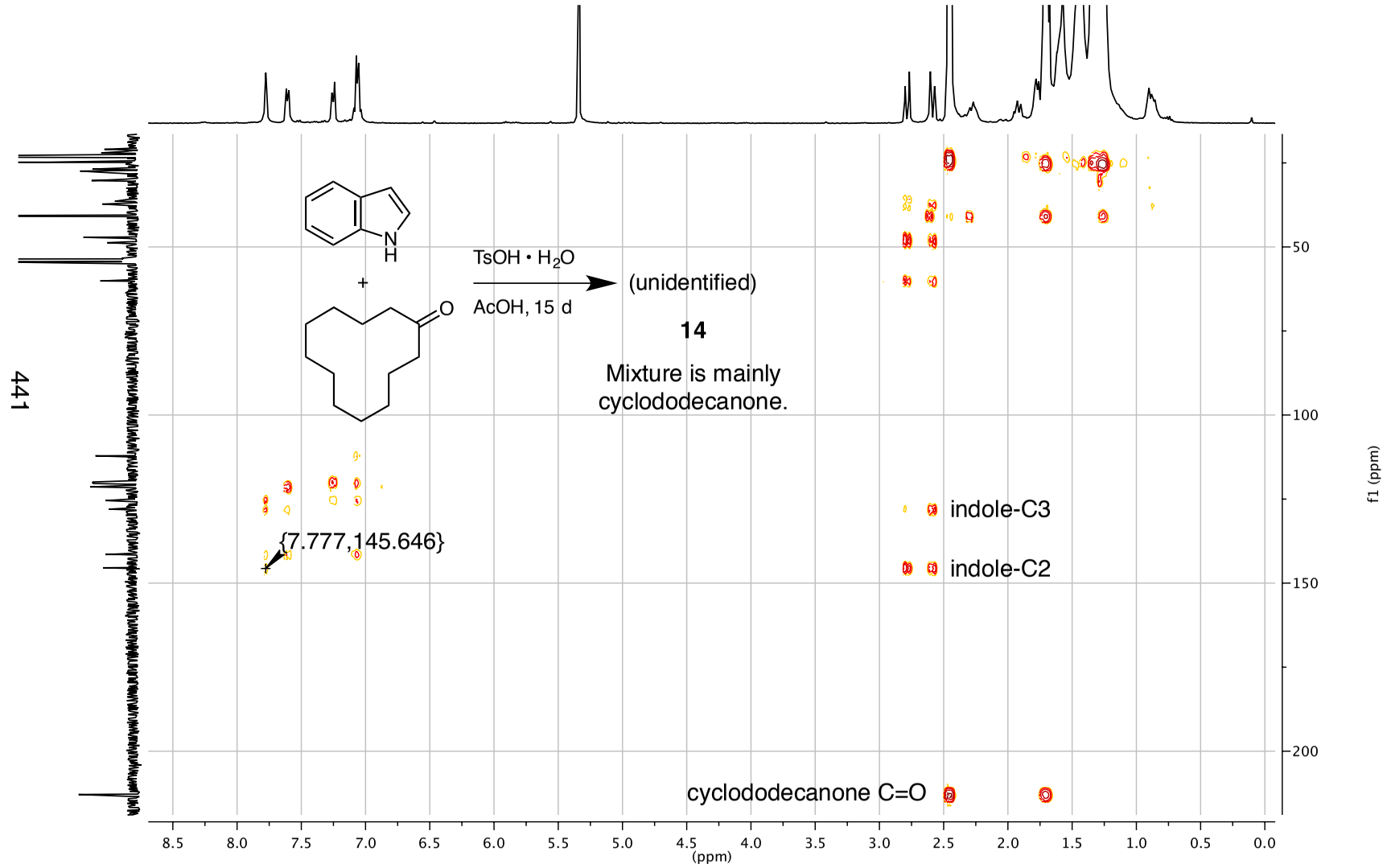
$^{1}H/^{13}C$ HMBC 400 MHz in CD_2Cl_2
441
TsOH • H_2O
AcOH, 15 d
(unidentified)
14
Mixture is mainly cyclododecanone.
{7.777,145.646}
indole-C3
indole-C2
cyclododecanone C=O
(ppm)
f1 (ppm)

^{1}H NMR 500 MHz in $CDCl_3$

15

^{1}H NMR 500 MHz in $CDCl_3$

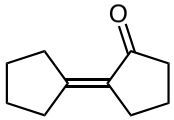

15

2.787
2.782
2.555
2.550
2.540
2.536
2.531
2.521
2.517
2.322
2.306
2.291
2.273
1.945
1.930
1.915
1.900
1.884
1.753
1.740
1.726
1.714
1.695
1.683
1.669
1.654

443

1.91
2.01
3.94
2.08
4.06

3.2 3.1 3.0 2.9 2.8 2.7 2.6 2.5 2.4 2.3 2.2 2.1 2.0 1.9 1.8 1.7 1.6 1.5 1.4 1.3
(ppm)

^{13}C NMR 126 MHz in $CDCl_3$

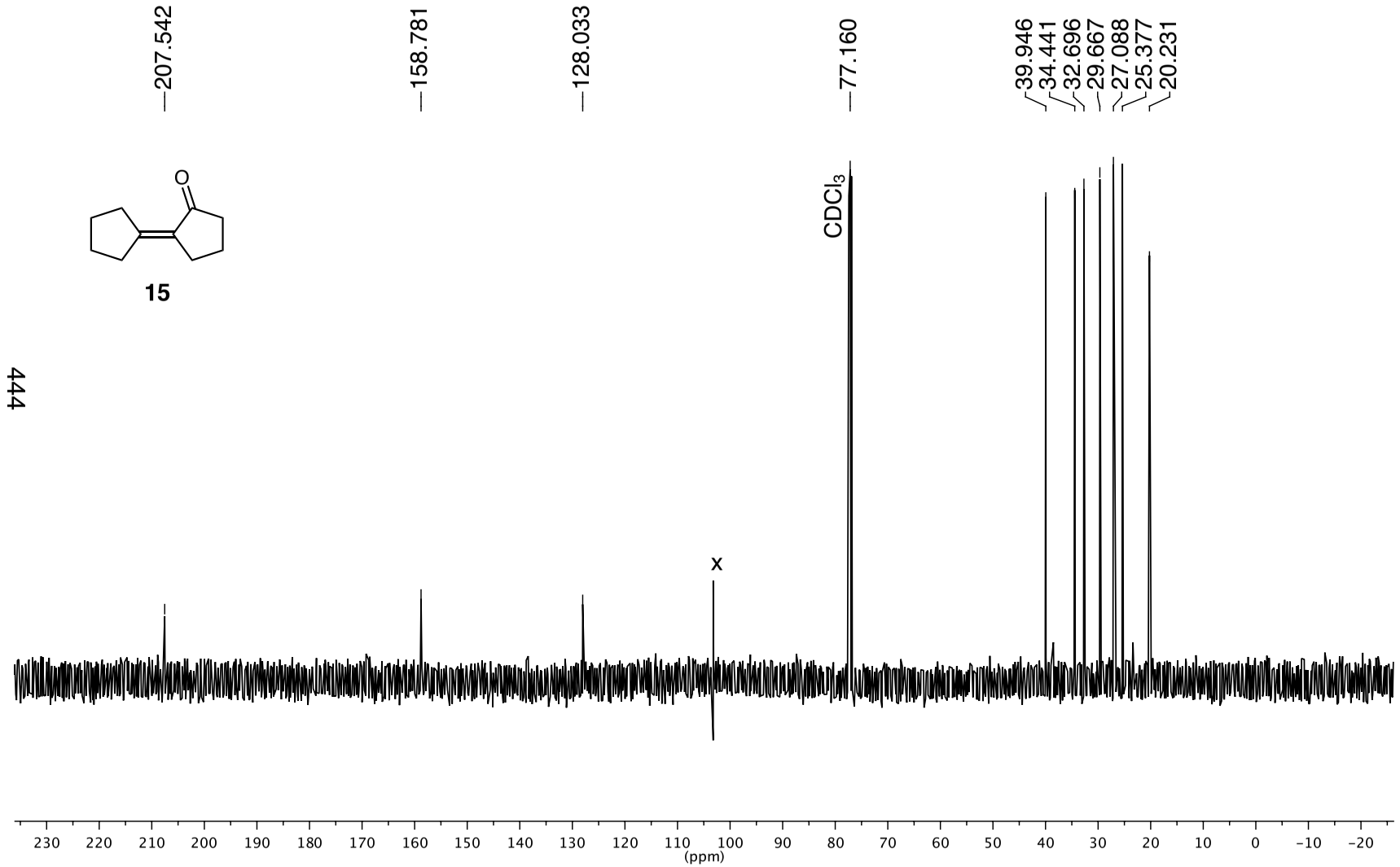

^{1}H NMR 500 MHz in $CDCl_3$

16

^{1}H NMR 500 MHz in $CDCl_3$

2.423 2.394 2.385 2.366 2.350 2.331 2.312 2.195 2.173 2.148 2.129 2.110 2.095 2.087 2.066 2.059 1.962 1.942 1.923 1.910 1.894 1.878 1.841 1.800 1.772 1.755 1.745 1.726 1.702 1.686 1.676 1.652 1.627 1.610 1.586 1.573 1.559

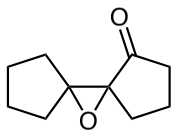

16

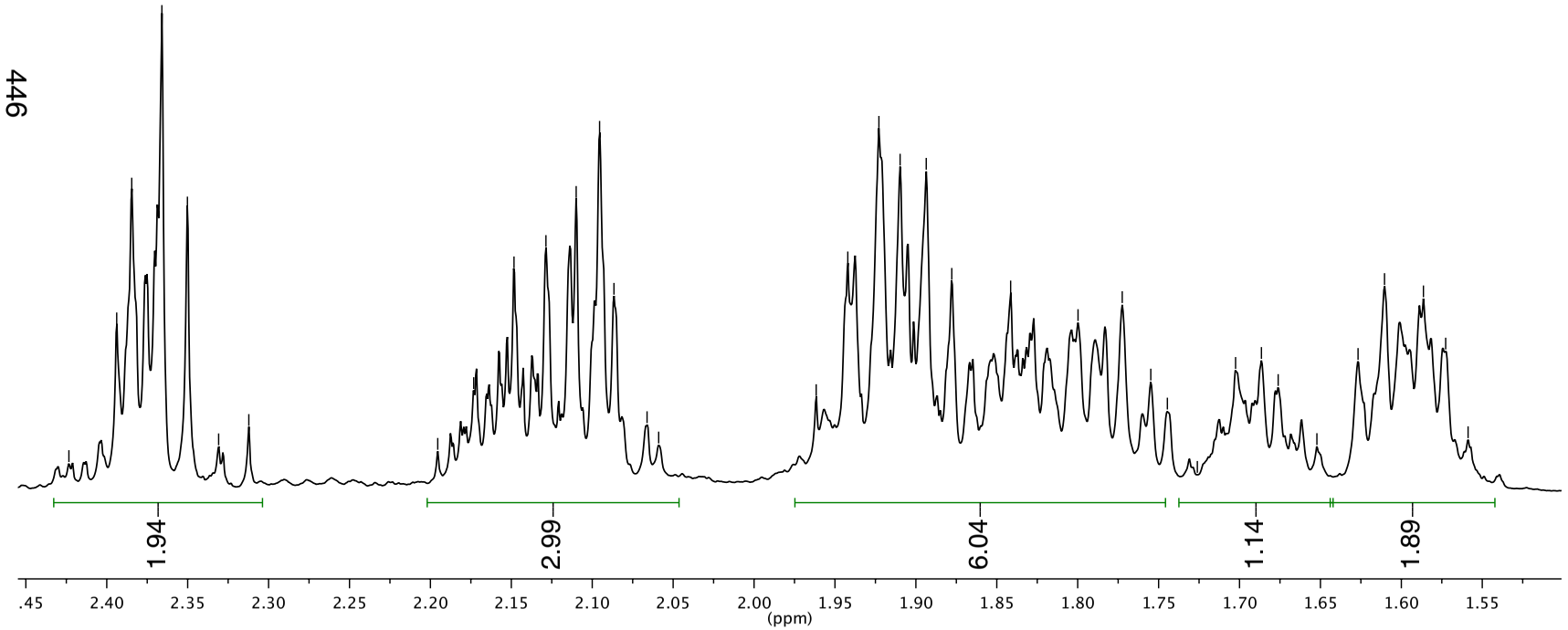

^{13}C NMR 75 MHz in $CDCl_3$

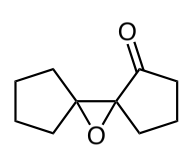

16

^{1}H NMR 400 MHz in $CDCl_3$

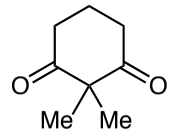

17b

448

^{13}C NMR 101 MHz in $CDCl_3$

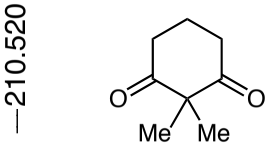

17b

^{1}H NMR 300 MHz in $CDCl_3$

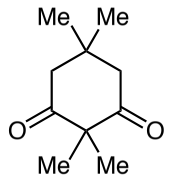

17c

^{13}C NMR 75 MHz in $CDCl_3$

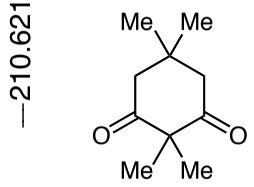

17c

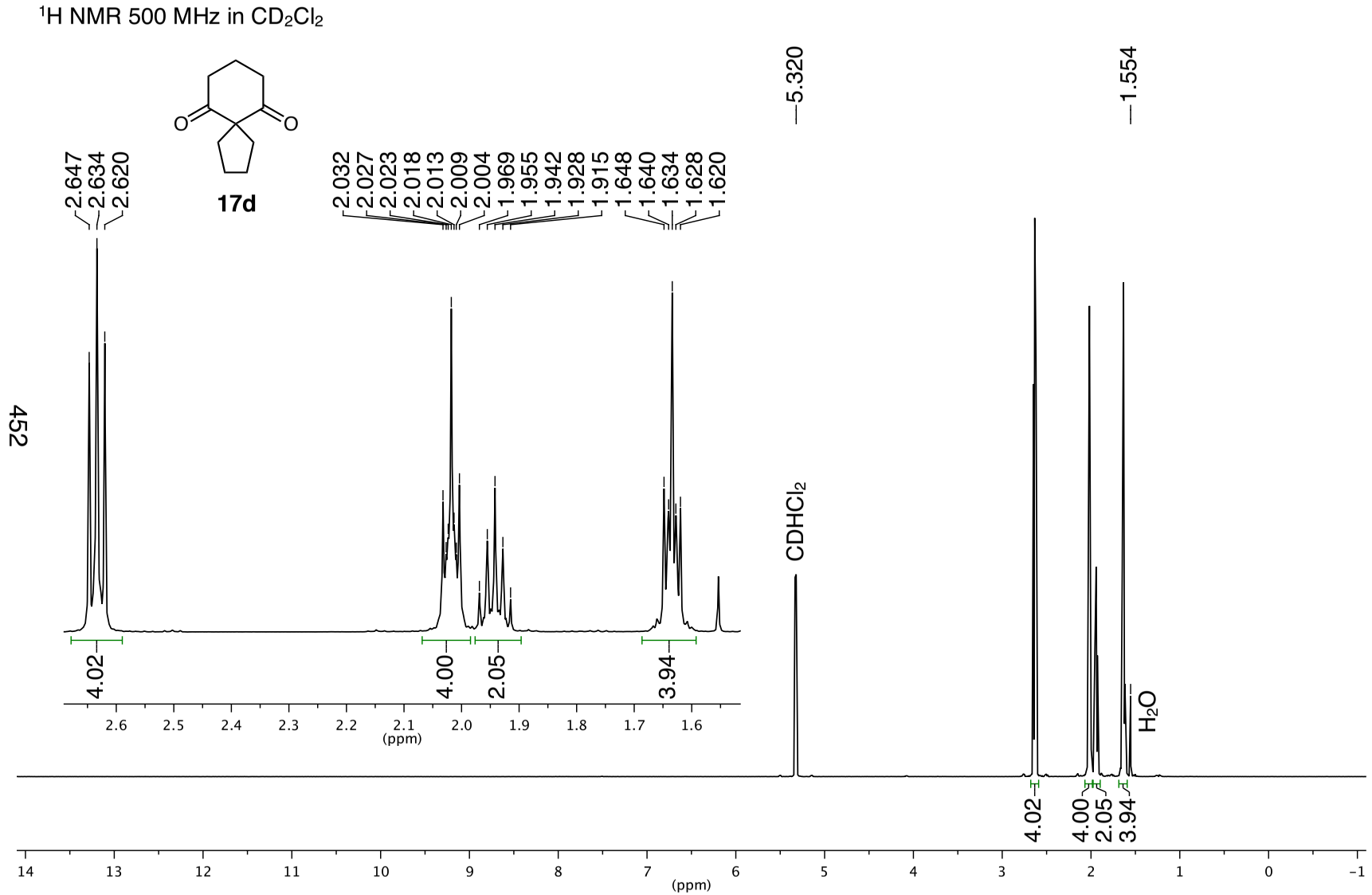
^{1}H NMR 500 MHz in CD_2Cl_2
17d
2.647
2.634
2.620
2.032
2.027
2.023
2.018
2.013
2.009
2.004
1.969
1.955
1.942
1.928
1.915
1.648
1.640
1.634
1.628
1.620
4.02
4.00
2.05
3.94
(ppm)
452
5.320
1.554
$CDHCl_2$
H_2O
4.02
4.00
2.05
3.94
(ppm)

^{13}C NMR 126 MHz in CD_2Cl_2

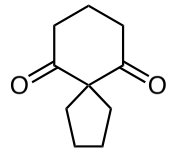

17d

^{1}H NMR 500 MHz in CD_2Cl_2

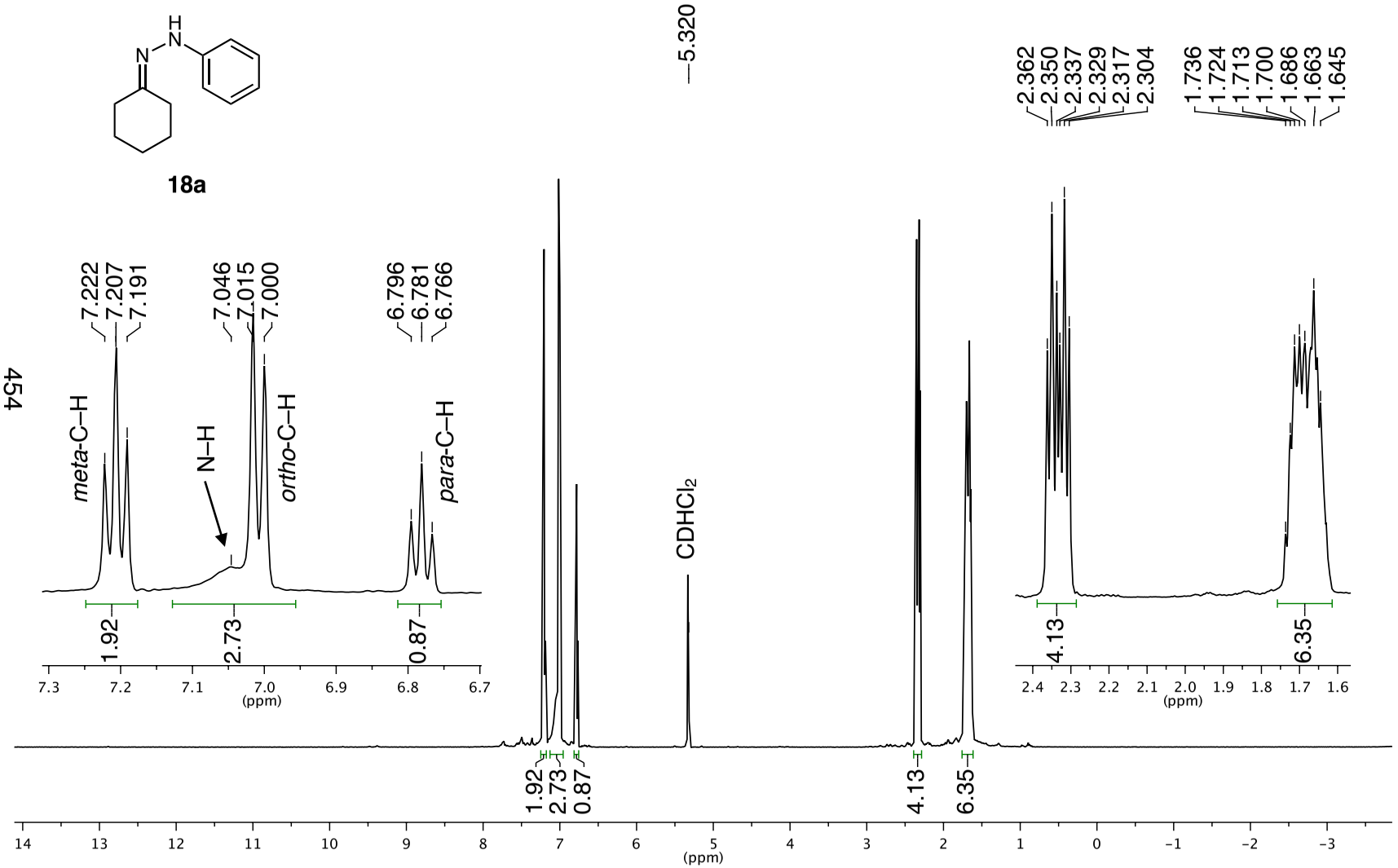

^{13}C NMR 126 MHz in CD_2Cl_2

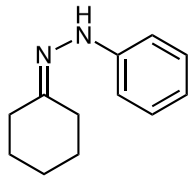

18a

150.965
146.887
129.625
119.683
113.139
54.000
35.881
27.680
26.408
26.266
25.820
CD_2Cl_2

455

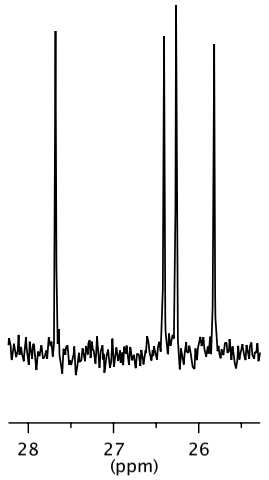

210 200 190 180 170 160 150 140 130 120 110 100 90 80 70 60 50 40 30 20 10 0 -10
(ppm)

^{1}H NMR 300 MHz in CD_2Cl_2

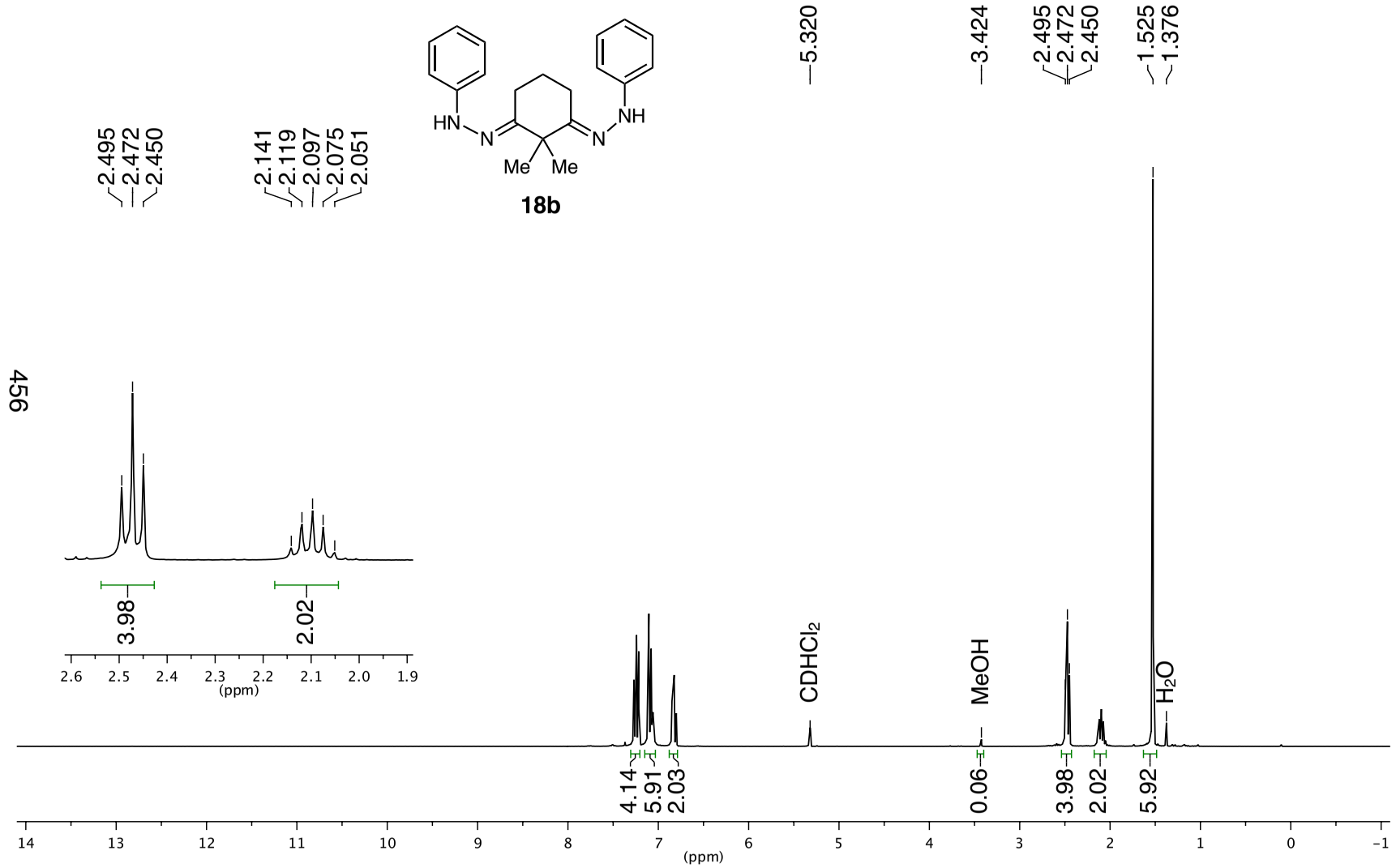

^{1}H NMR 500 MHz in CD_2Cl_2

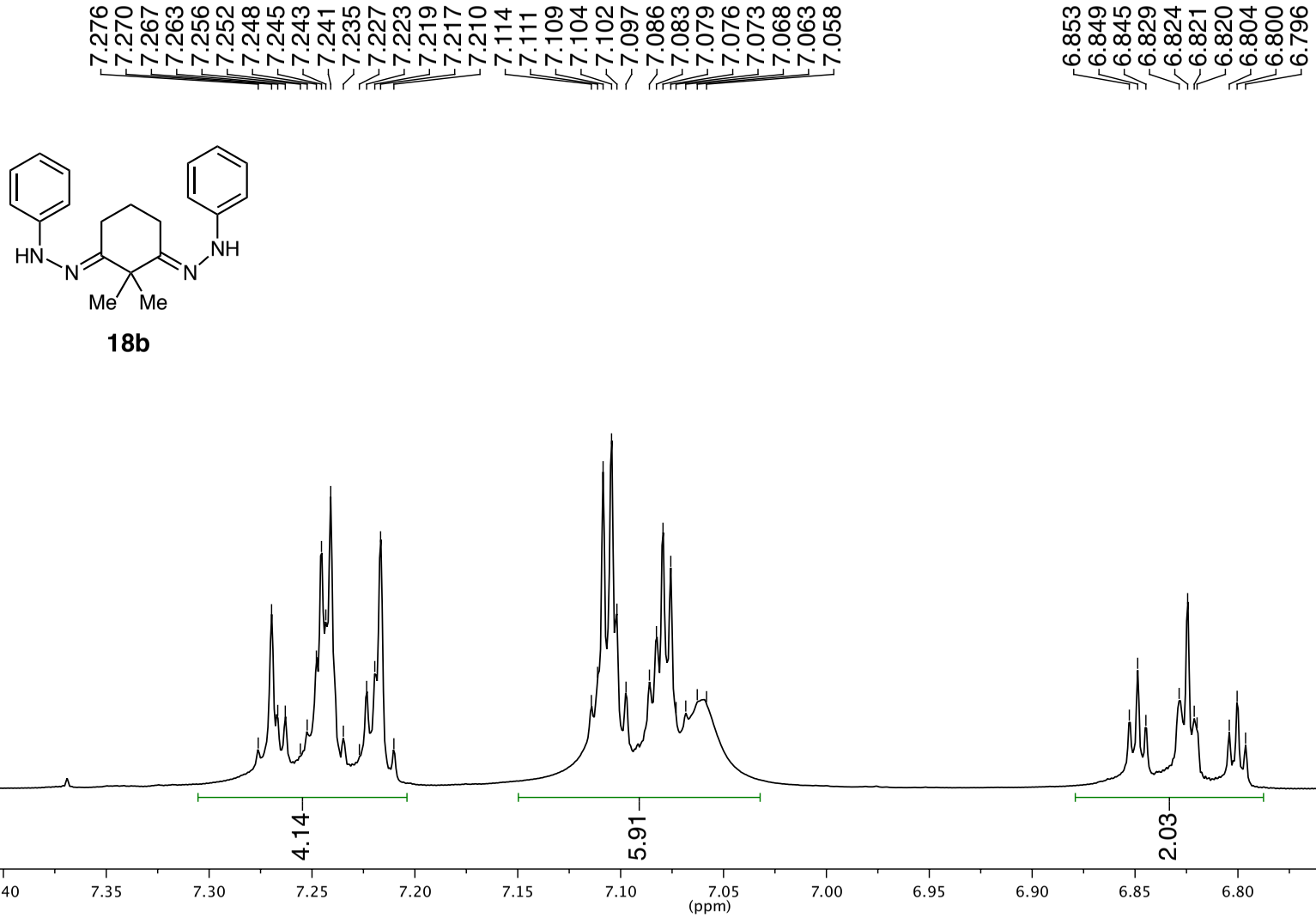

^{13}C NMR 75 MHz in CD_2Cl_2

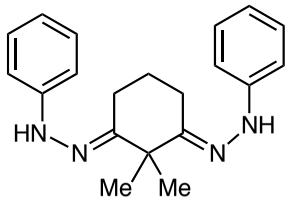

18b

^{1}H NMR 500 MHz in CD_2Cl_2
7.242
7.227
7.224
7.210
7.073
7.058
6.818
6.804
6.789
5.332
5.320
2.357
1.485
1.020
18c
Me
Me
Me
Me
NH
N
N
NH
CH_2Cl_2
$CDHCl_2$
1.72
3.94
6.11
5.95
4.06
4.02
1.91
(ppm)

^{13}C NMR 126 MHz in CD_2Cl_2

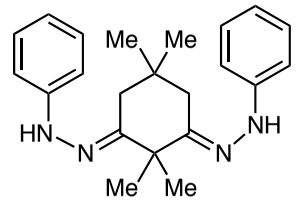

18c

^{1}H NMR 300 MHz in CD_2Cl_2

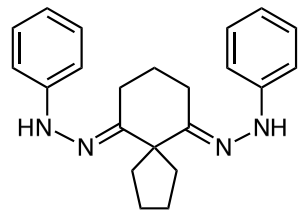

18d

^{1}H NMR 500 MHz in CD_2Cl_2

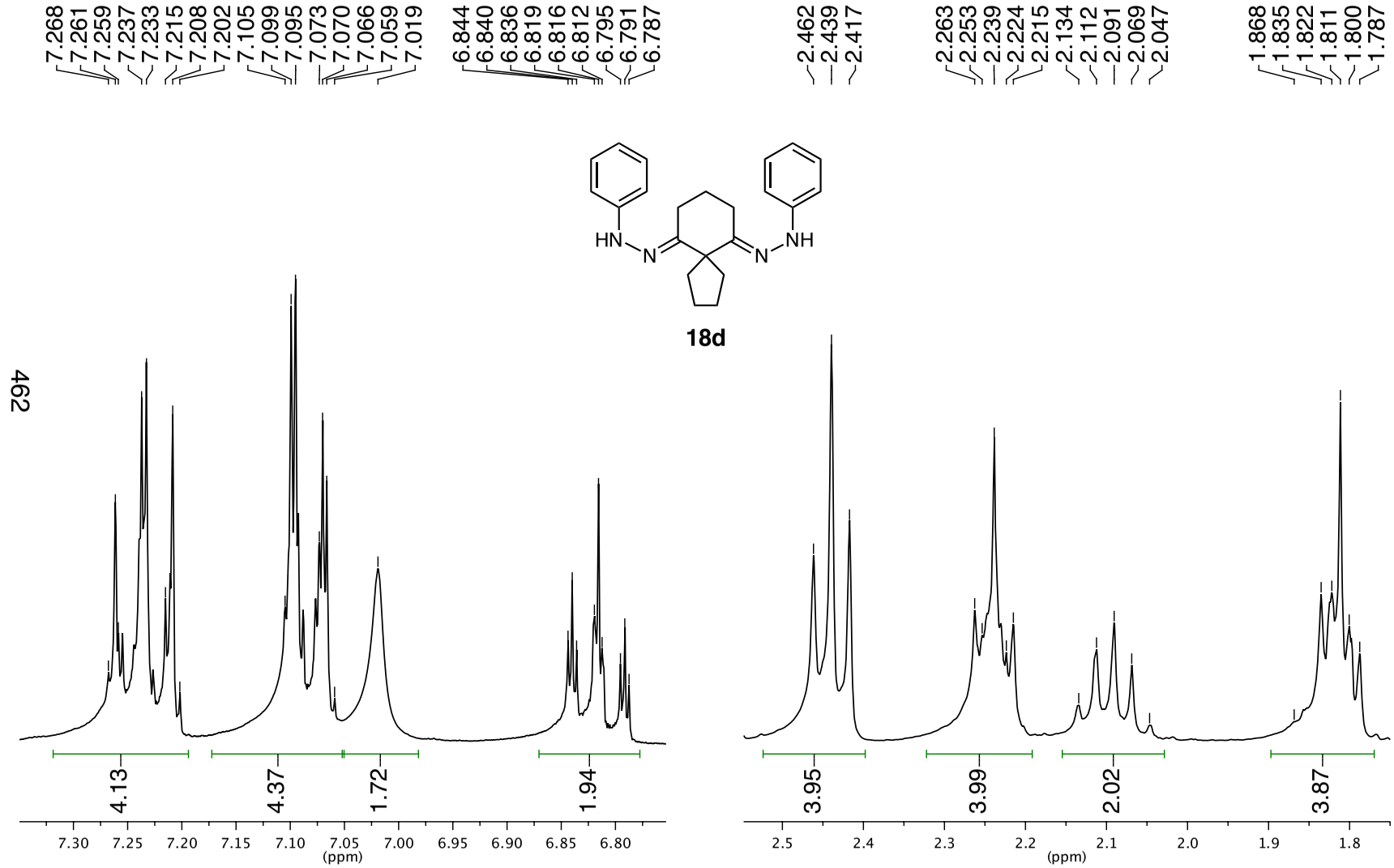

^{13}C NMR 75 MHz in CD_2Cl_2

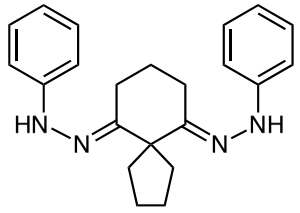

18d

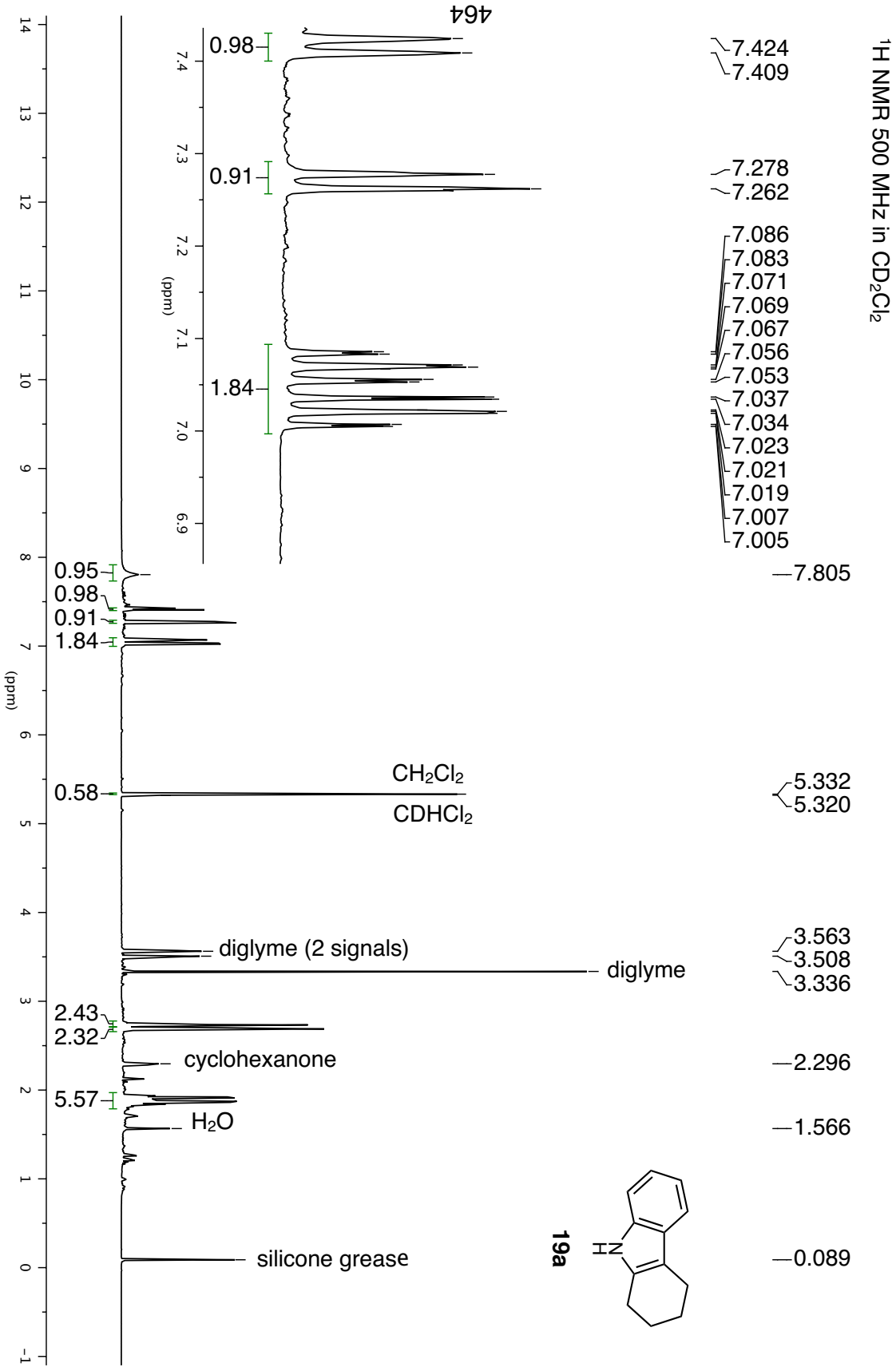
464
^{1}H NMR 500 MHz in CD_2Cl_2
7.424
7.409
7.278
7.262
7.086
7.083
7.071
7.069
7.067
7.056
7.053
7.037
7.034
7.023
7.021
7.019
7.007
7.005
7.805
5.332
5.320
3.563
3.508
3.336
2.296
1.566
0.089
0.98
0.91
1.84
0.95
0.98
0.91
1.84
0.58
5.57
2.43
2.32
CH_2Cl_2
$CDHCl_2$
diglyme (2 signals)
diglyme
cyclohexanone
H_2O
silicone grease
19a
(ppm)

^{1}H NMR 500 MHz in CD_2Cl_2
3.563
3.508
3.336
2.749
2.746
2.743
2.737
2.734
2.731
2.725
2.722
2.718
2.704
2.701
2.697
2.692
2.688
2.686
2.680
2.677
2.674
2.296
1.942
1.930
1.923
1.911
1.874
1.861
1.856
1.842
1.566
19a
0.61
0.60
diglyme (8H)
0.85
diglyme (6H)
2.43
2.32
cyclohexanone (4H)
0.47
5.57
H_2O
(ppm)

^{13}C NMR 126 MHz in CD_2Cl_2
19a
136.220
134.779
128.417
121.243
119.361
118.043
110.753
110.421
72.445
70.902
59.155
54.000
42.466
27.604
25.542
23.874
23.773
23.694
21.414
CD_2Cl_2
diglyme (2 signals)
diglyme
cyclohexanone
cyclohexanone (2 signals)
111.0
110.5
110.0
24.0
23.8
23.6
(ppm)
(ppm)

Appendix II. NMR Data for Products in Part II and § 3.4

Table 42 (1 of 2). The contents of Appendix II.

compound(s)	page	nickname or reaction condition
201ac, 201ca, 201cc, 201ce	469	alkaline bromination of PABA
201ad	471	PABA methyl ester
201ba	473	trichloroaniline
201bd	475	dichloro PABA methyl ester
201ca	477	tribromoaniline
201cb	479	dibromo 4-methylaniline
201cc	481	dibromo PABA
201cd	483	dibromo PABA methyl ester
201ce	469	monobromo PABA (in alkaline bromination mixture)
201da	485	triiodoaniline
201db	487	diiodotoluidine
201dd	489	diiodo PABA methyl ester
202	491	benzyltrimethylammonium dichloroiodate
204ba	493	trichloro nitrile
204bc	495	dichloro PABA nitrile
204bd	497	dichloro PABA methyl ester nitrile
204ca	499	tribromo nitrile
204cb	501	dibromo 4-methyl nitrile
204cc	503	dibromo PABA nitrile
204cd	505	dibromo PABA methyl ester nitrile
204da	507	triiodo nitrile
204db	509	diiodo 4-methyl nitrile

Table 42 (2 of 2). The contents of Appendix II

compound	page	nickname or reaction condition
204dc	511	diiodo PABA nitrile
204dd	514	diiodo PABA methyl ester nitrile
205a, 205b, 205c	516	tribromo Sandmeyer coproducts
206	517	dibromo ester Sandmeyer reduction product
207	519	dibromo carbamoyl acid
208aa	521	formanilide
208ba	524	trichloroformanilide
208ca	526	tribromoformanilide
208cb	528	dibromo 4-methyl formanilide
208cd	532	dibromo PABA methyl ester formanilide
208da	534	triiodoformanilide
208db	537	diiodo 4-methyl formanilide
209ba	540	trichloro isocyanide
209ca	543	tribromo isocyanide
209cb	545	dibromo 4-methyl isocyanide
209cd	548	dibromo PABA methyl ester isocyanide
209da	550	triiodo isocyanide
209db	552	diiodo 4-methyl isocyanide

^{1}H NMR 300 MHz in $(CD_3)_2SO$

Bromination of PABA, alkaline condition

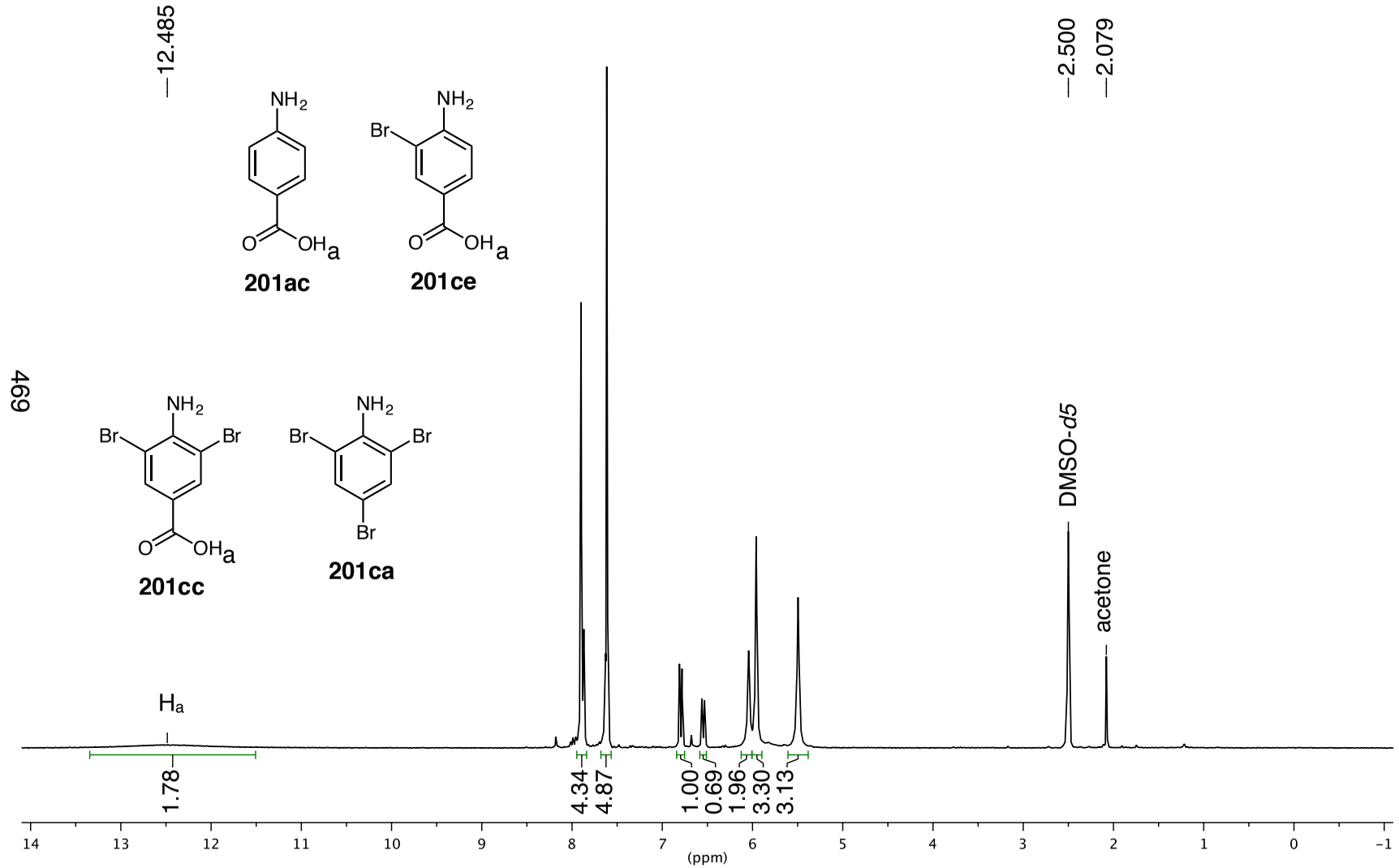

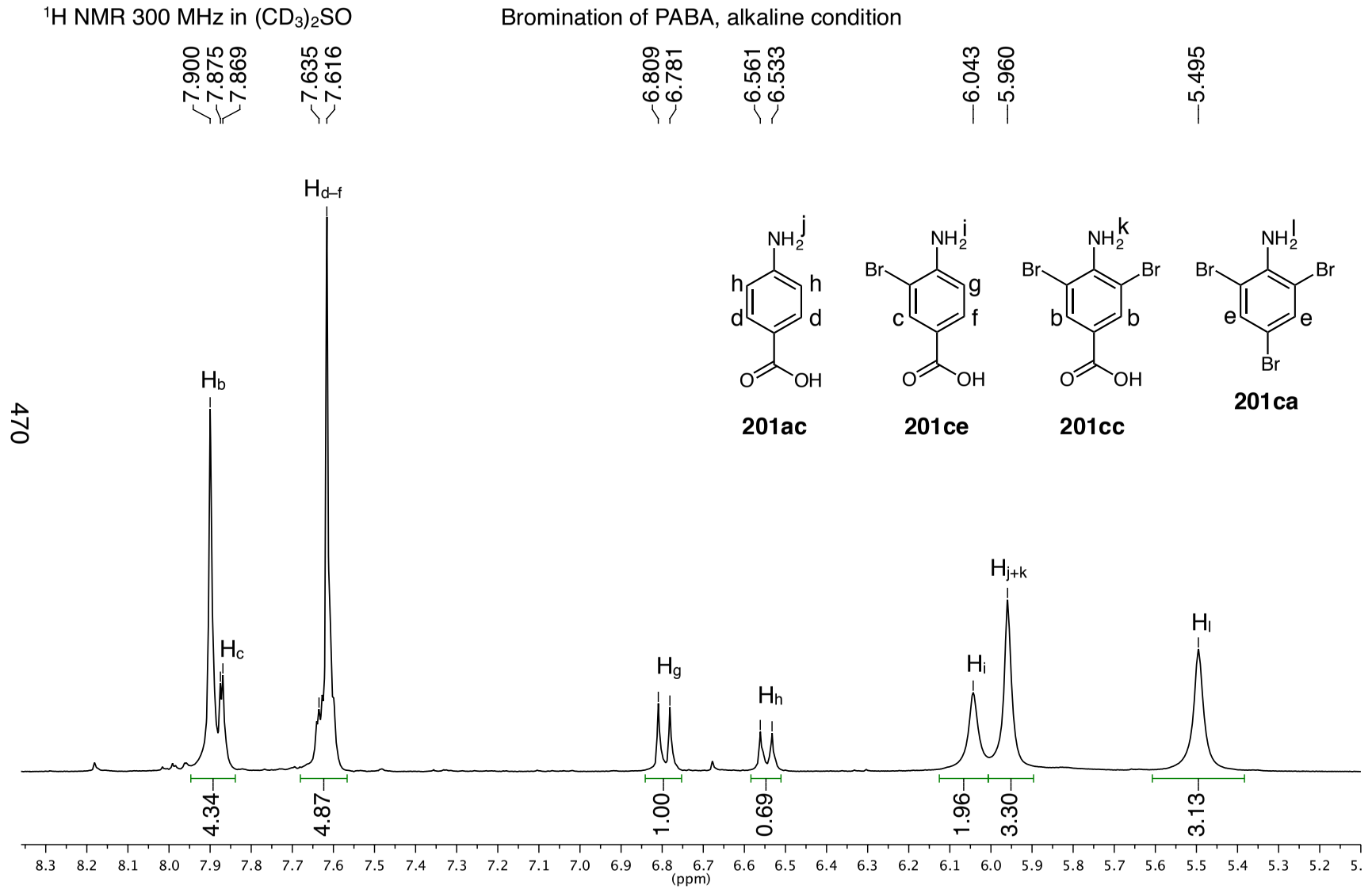
^{1}H NMR 300 MHz in $(CD_3)_2SO$
Bromination of PABA, alkaline condition
7.900
7.875
7.869
7.635
7.616
6.809
6.781
6.561
6.533
6.043
5.960
5.495
$H_{d–f}$
H_b
H_c
H_g
H_h
H_i
H_{j+k}
H_l
4.34
4.87
1.00
0.69
1.96
3.30
3.13
201ac
201ce
201cc
201ca
(ppm)

^{1}H NMR 300 MHz in CD_2Cl_2

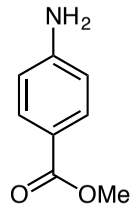

201ad

^{13}C NMR 75 MHz in CD_2Cl_2

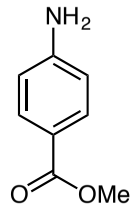

201ad

^{1}H NMR 500 MHz in CD_2Cl_2

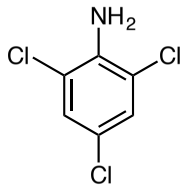

201ba

^{13}C NMR 126 MHz in CD_2Cl_2

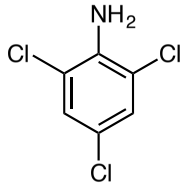

201ba

^{1}H NMR 500 MHz in CD_2Cl_2

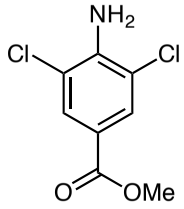

201bd

^{13}C NMR 126 MHz in CD_2Cl_2; ^{1}H-coupled

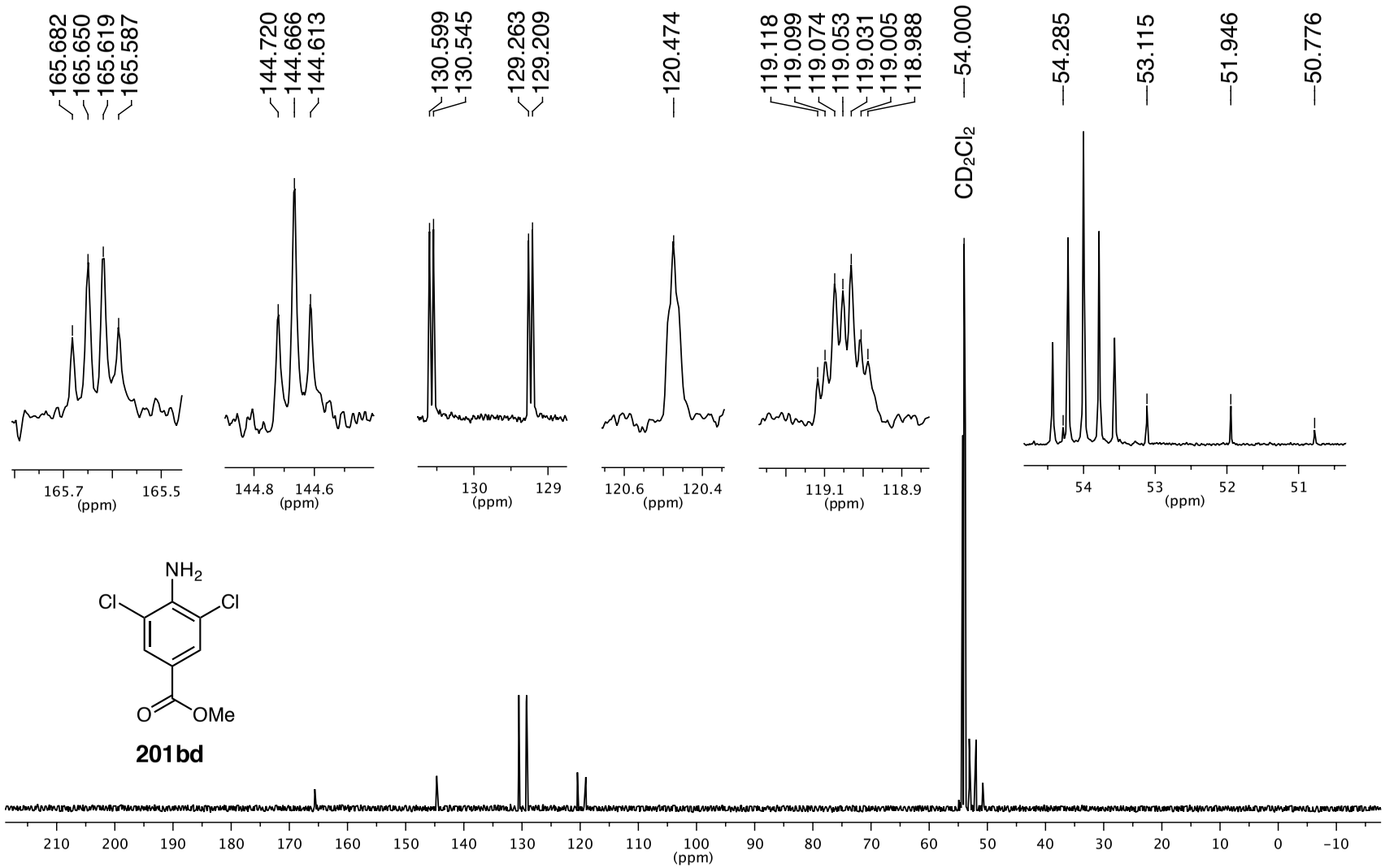

^{1}H NMR 300 MHz in CD_2Cl_2

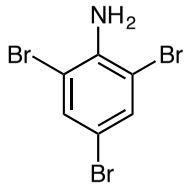

201ca

^{13}C NMR 126 MHz in CD_2Cl_2

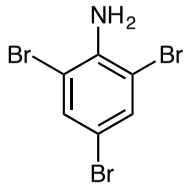

201ca

^{1}H NMR 400 MHz in $CDCl_3$

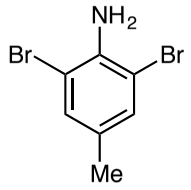

201cb

^{13}C NMR 101 MHz in $CDCl_3$

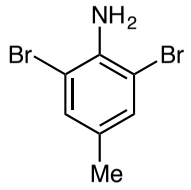

201cb

^{1}H NMR 500 MHz in $(CD_3)_2SO$

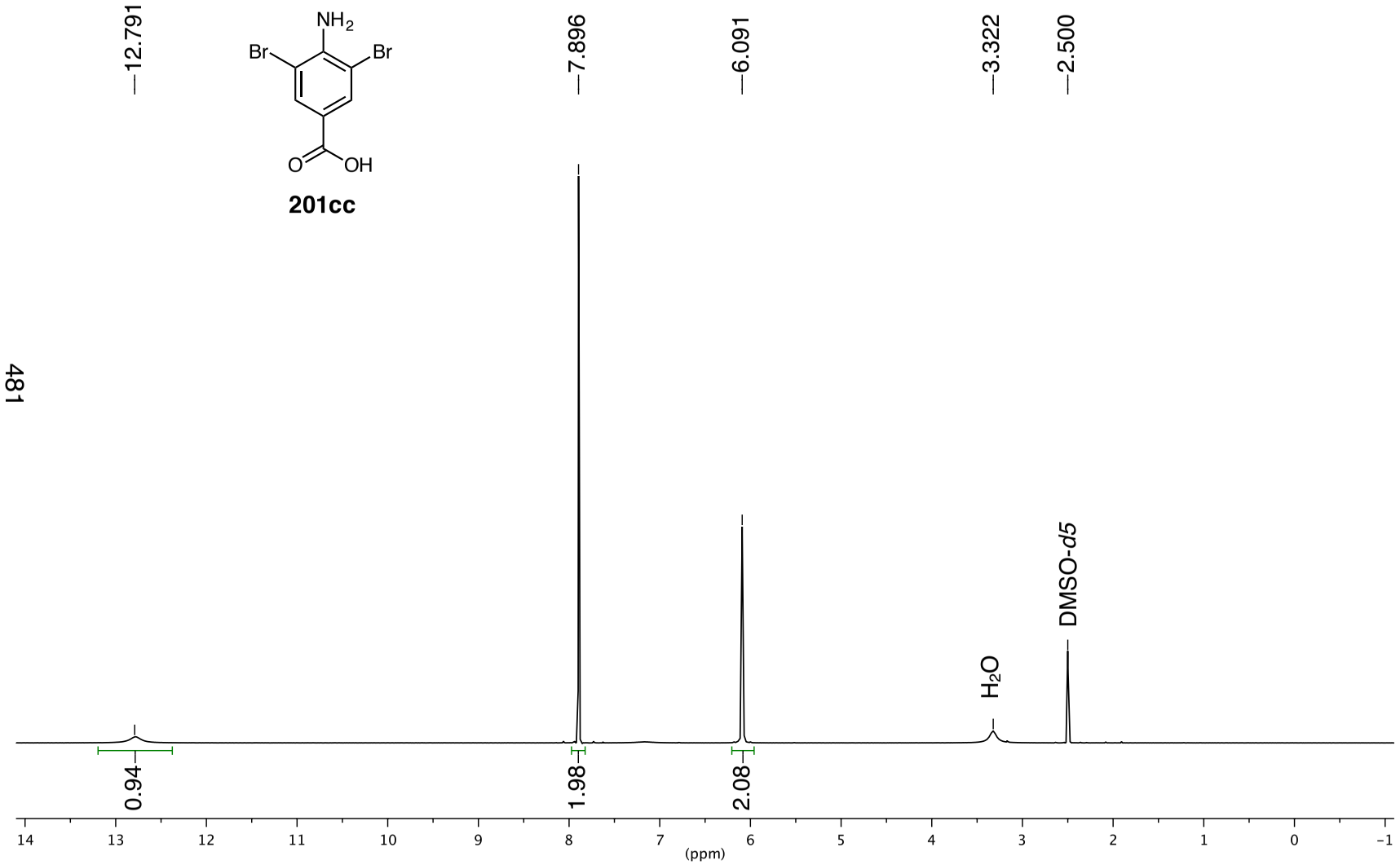

^{13}C NMR 75 MHz in $(CD_3)_2SO$

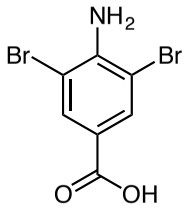

201cc

^{1}H NMR 300 MHz in $CDCl_3$

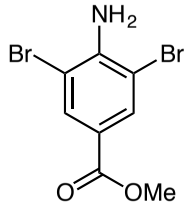

201cd

^{13}C NMR 75 MHz in $CDCl_3$

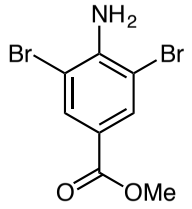

201cd

^{1}H NMR 300 MHz in $CDCl_3$

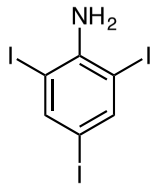

201da

^{13}C NMR 75 MHz in $(CD_3)_2SO$

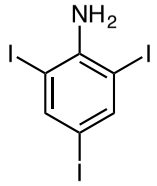

201da

^{1}H NMR 500 MHz in CD_2Cl_2

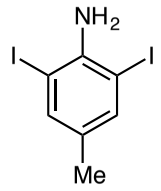

201db

^{13}C NMR 126 MHz in CD_2Cl_2

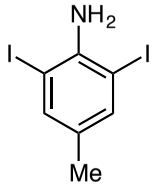

201db

^{1}H NMR 400 MHz in $CDCl_3$

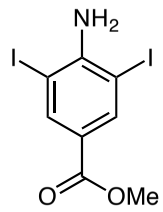

201dd

^{13}C NMR 101 MHz in $CDCl_3$

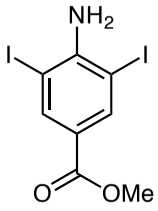

201dd

^{1}H NMR 500 MHz in CD_2Cl_2

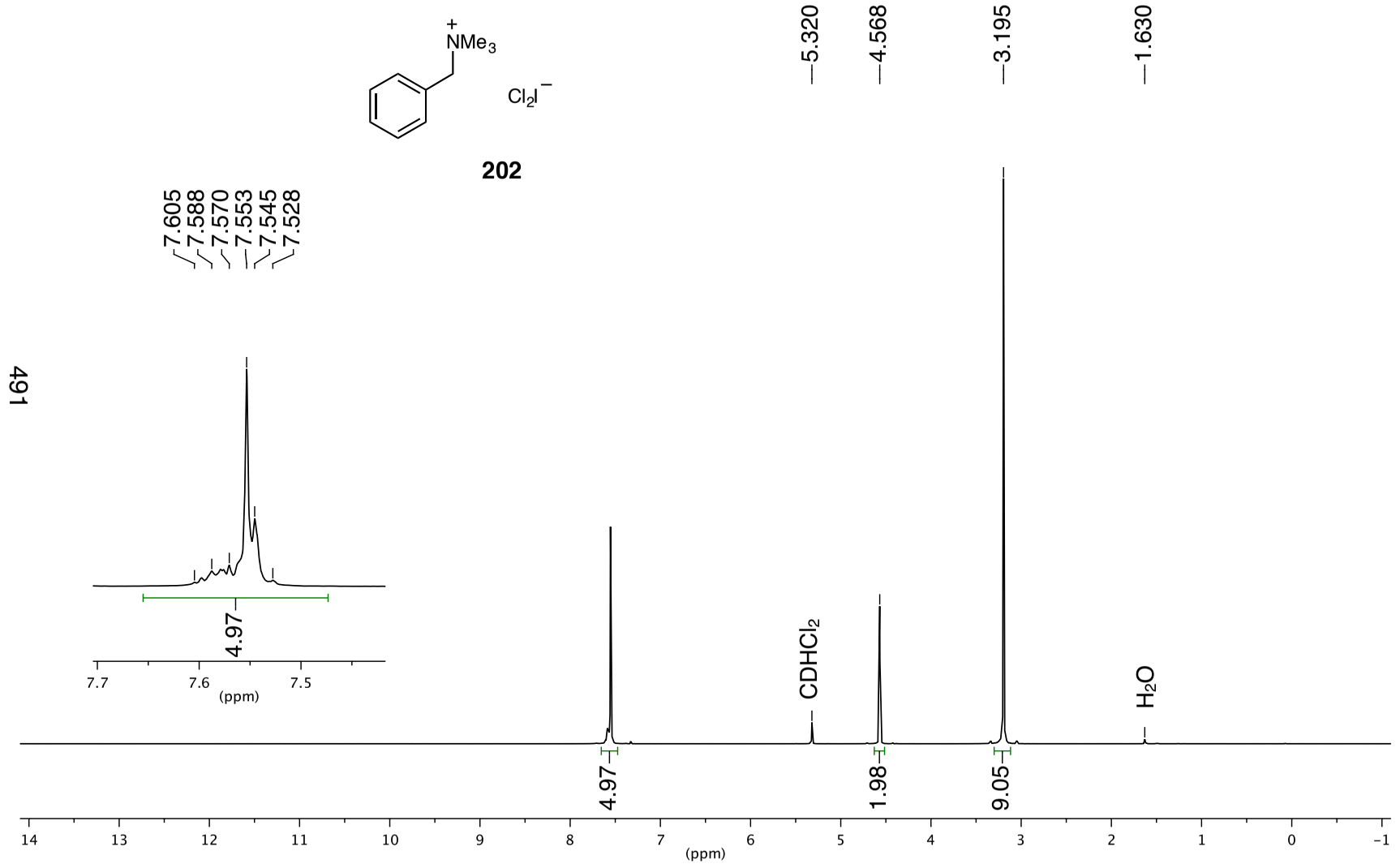

^{13}C NMR 126 MHz in $(CD_3)_2SO$

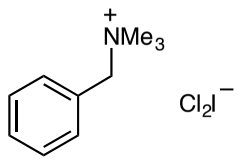

202

^{1}H NMR 400 MHz in CD_2Cl_2

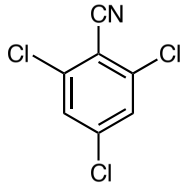

204ba

^{13}C NMR 126 MHz in $CDCl_3$

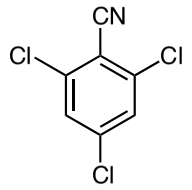

204ba

^{1}H NMR 500 MHz in $CDCl_3$

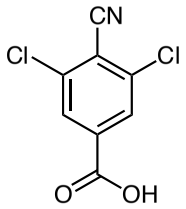

204bc

^{13}C NMR 101 MHz in $CDCl_3$

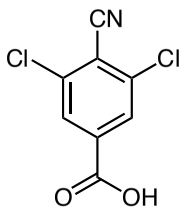

204bc

^{1}H NMR 500 MHz in CD_2Cl_2

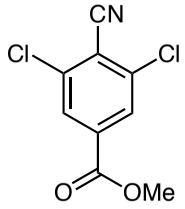

204bd

^{13}C NMR 126 MHz in $CDCl_3$

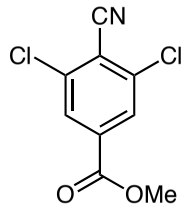

204bd

^{1}H NMR 500 MHz in CD_2Cl_2

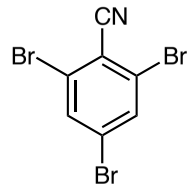

204ca

^{13}C NMR 126 MHz in CD_2Cl_2

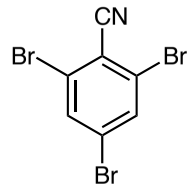

204ca

^{1}H NMR 500 MHz in CD_2Cl_2

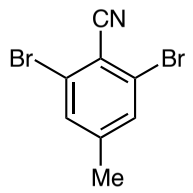

204cb

^{13}C NMR 126 MHz in CD_2Cl_2

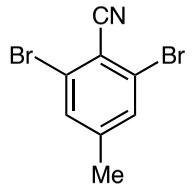

204cb

^{1}H NMR 500 MHz in $(CD_3)_2SO$

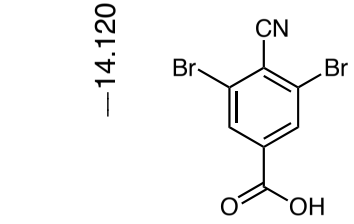

204cc

^{13}C NMR 126 MHz in $(CD_3)_2SO$

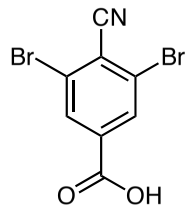

204cc

163.924
137.020
132.118
126.655
120.645
115.893
39.520
$(CD_3)_2SO$

504

210 200 190 180 170 160 150 140 130 120 110 100 90 80 70 60 50 40 30 20 10 0 -10
(ppm)

^{1}H NMR 500 MHz in $CDCl_3$

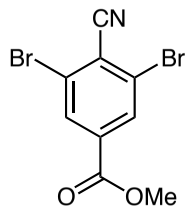

204cd

^{13}C NMR 126 MHz in $CDCl_3$

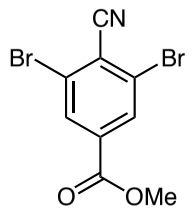

204cd

^{1}H NMR 500 MHz in $(CD_3)_2SO$

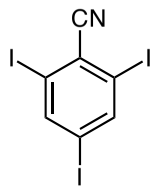

204da

^{13}C NMR 126 MHz in CD_2Cl_2

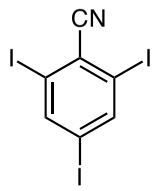

204da

^{1}H NMR 500 MHz in $CDCl_3$

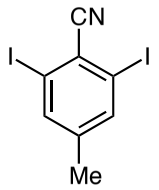

204db

^{13}C NMR 126 MHz in $CDCl_3$

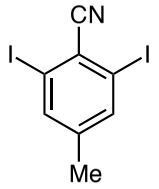

204db

^{1}H NMR 500 MHz in $(CD_3)_2SO$

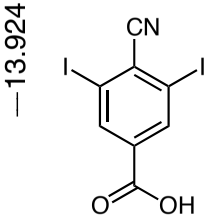

204dc

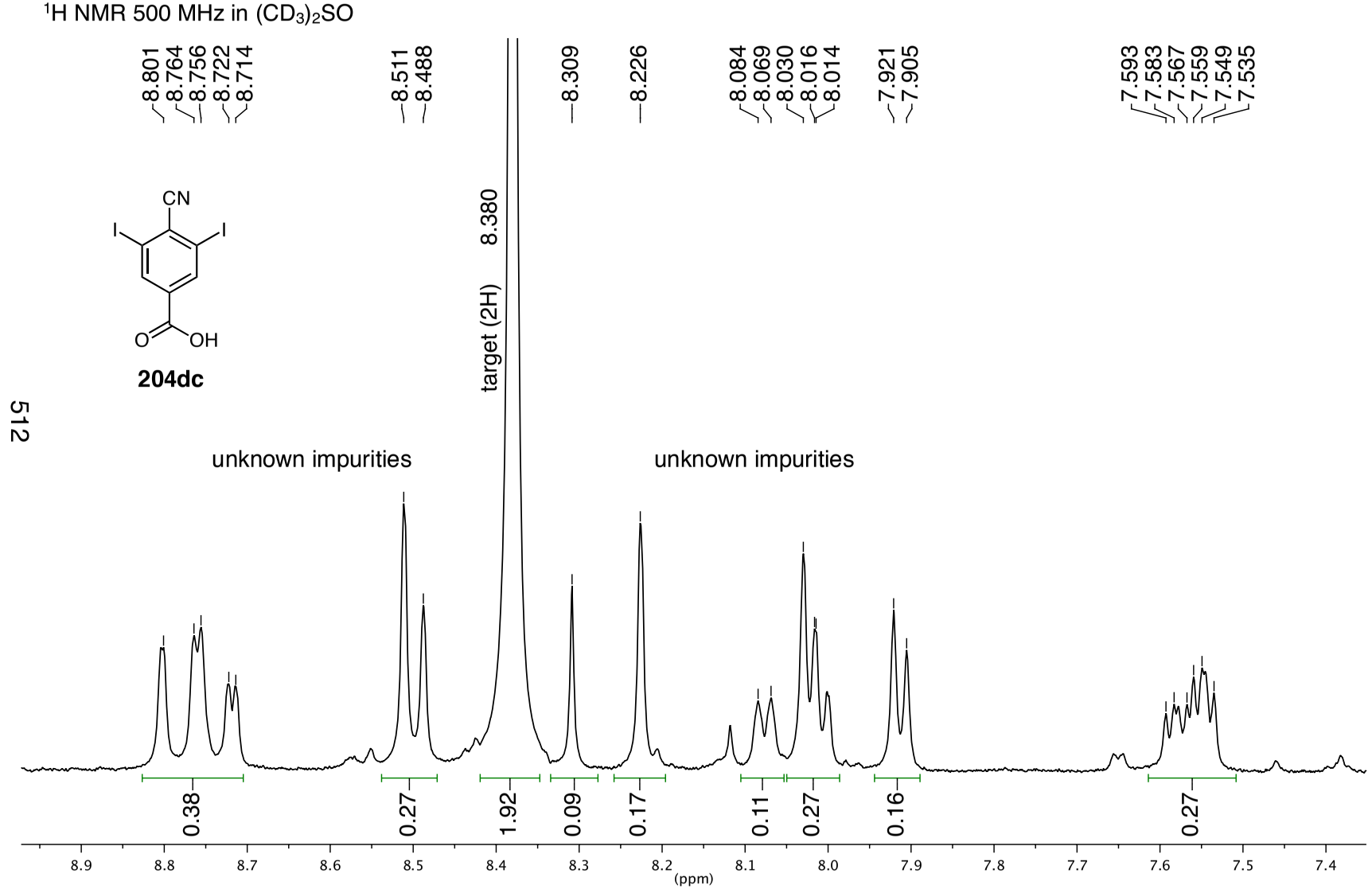
1H NMR 500 MHz in (CD3)2SO
8.801
8.764
8.756
8.722
8.714
8.511
8.488
8.380
8.309
8.226
8.084
8.069
8.030
8.016
8.014
7.921
7.905
7.593
7.583
7.567
7.559
7.549
7.535
CN
I
I
O
OH
204dc
target (2H)
512
unknown impurities
unknown impurities
0.38
0.27
1.92
0.09
0.17
0.11
0.27
0.16
0.27
8.9
8.8
8.7
8.6
8.5
8.4
8.3
8.2
8.1
8.0
7.9
7.8
7.7
7.6
7.5
7.4
(ppm)

^{13}C NMR 101 MHz in $(CD_3)_2SO$

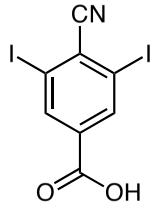

204dc

163.832
138.563
136.014
129.063
120.420
101.865
79.162
54.898
39.520
$(CD_3)_2SO$
$CHCl_3$
DCM

210 200 190 180 170 160 150 140 130 120 110 100 90 80 70 60 50 40 30 20 10 0 −10 −2
(ppm)

^{1}H NMR 500 MHz in CD_2Cl_2

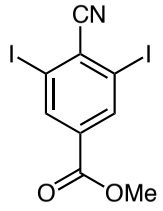

204dd

^{13}C NMR 101 MHz in CD_2Cl_2

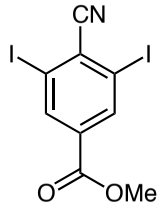

204dd

^{1}H NMR 300 MHz in CD_2Cl_2
205a
205b
205c
205a (3H)
205b (2H)
205c (4H)
1,4-dimethoxybenzene (4H)
1,4-dimethoxybenzene (6H)
$CDHCl_2$
H_2O
unknown
silicone grease
7.873
7.771
7.654
6.827
5.320
3.746
1.557
1.267
0.089
0.030
0.078
0.584
3.843
6.157
0.370
0.150
(ppm)

^{1}H NMR 500 MHz in CD_2Cl_2

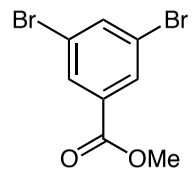

206

$^{1}H/^{13}C$ DEPT135 500 MHz in CD_2Cl_2

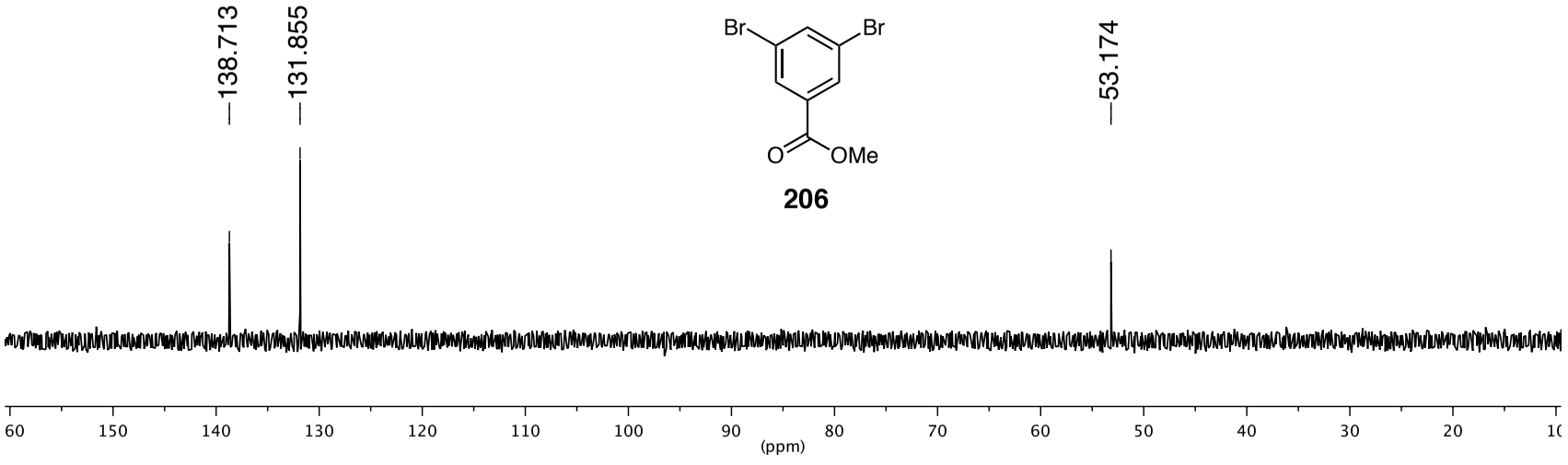

^{13}C NMR 126 MHz in CD_2Cl_2

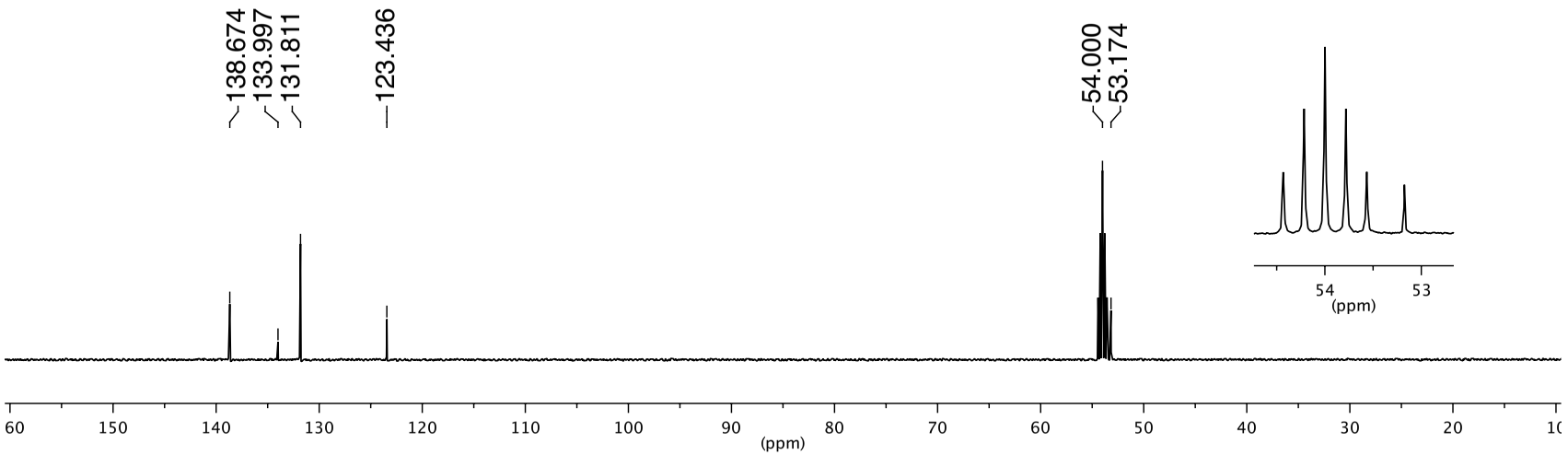

^{1}H NMR 500 MHz in $(CD_3)_2SO$

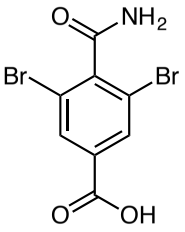

207

519

^{13}C NMR 126 MHz in $(CD_3)_2SO$

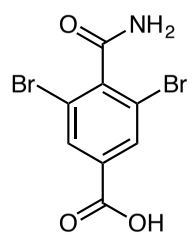

207

166.810
164.544
144.325
133.394
132.023
119.690
39.520
$(CD_3)_2SO$
x
520
210 200 190 180 170 160 150 140 130 120 110 100 90 80 70 60 50 40 30 20 10 0 -10
(ppm)

^{1}H NMR 500 MHz in CD_2Cl_2

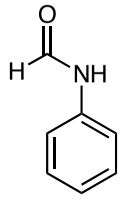

208aa

^{1}H NMR 500 MHz in CD_2Cl_2

208aa

8.721
8.350
8.346
7.991
7.579
7.563
7.381
7.366
7.350
7.335
7.319
7.206
7.191
7.176
7.153
7.137
7.120

major (1H)
minor (1H)
major (1H)
both (1H) + minor (1H)

0.92
0.55
0.52
1.10
2.01
0.45
1.44

9.0 8.9 8.8 8.7 8.6 8.5 8.4 8.3 8.2 8.1 8.0 (ppm) 7.9 7.8 7.7 7.6 7.5 7.4 7.3 7.2 7.1 7.0

^{13}C NMR 126 MHz in CD_2Cl_2

208aa

163.250
159.869
137.757
137.570
130.165
129.493
125.496
125.066
120.437
119.041
54.000
CD_2Cl_2
minor (1C)
major (1C)
minor (2C)
major (2C)
major (2C)
minor (2C)
major (1C)
minor (1C)
major (1C)
minor (1C)
(ppm)
(ppm)

^{1}H NMR 500 MHz in $(CD_3)_2SO$

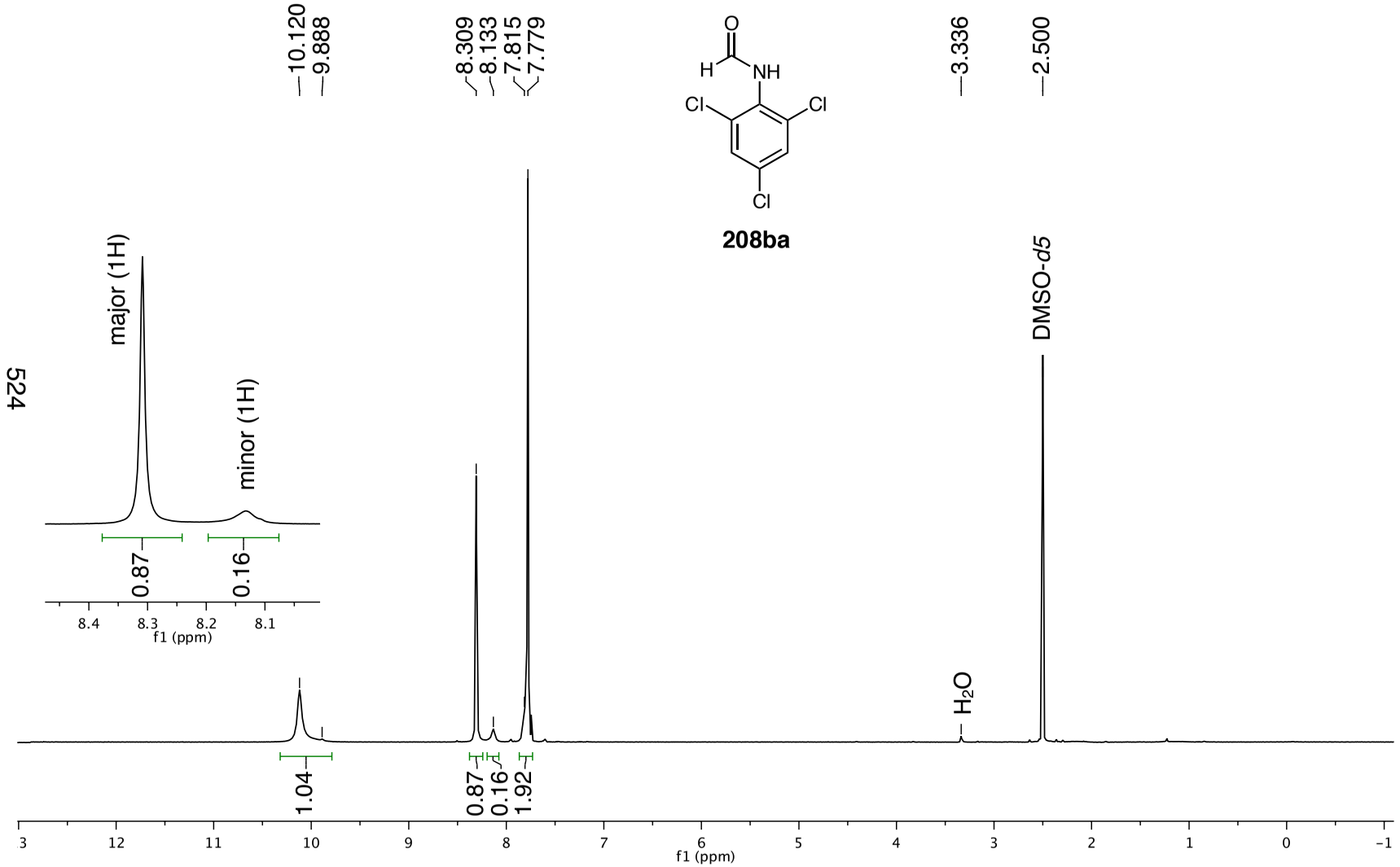

^{13}C NMR 75 MHz in $(CD_3)_2SO$

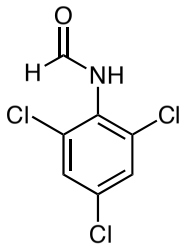

208ba

159.774
133.990
132.554
131.263
128.719
128.344
39.520
$(CD_3)_2SO$
major (1C)
minor (1C)
525
135 134 133 132 131 130 129 128
(ppm)
220 210 200 190 180 170 160 150 140 130 120 110 100 90 80 70 60 50 40 30 20 10 0 -10
(ppm)

^{1}H NMR 300 MHz in $(CD_3)_2SO$

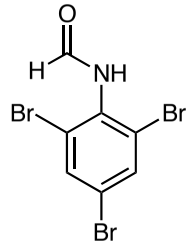

208ca

526

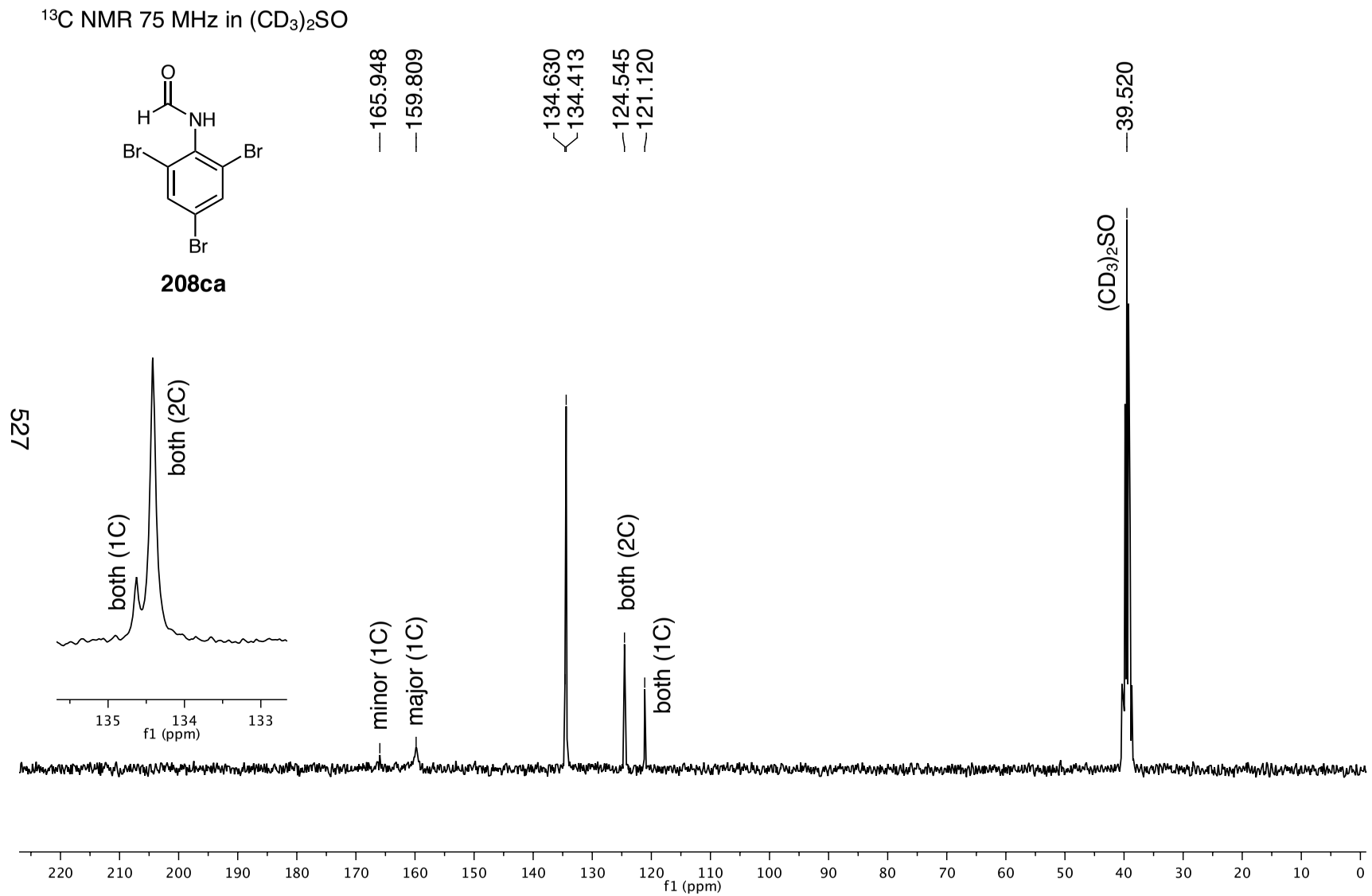
^{13}C NMR 75 MHz in $(CD_3)_2SO$
O
H
NH
Br
Br
Br
208ca
165.948
159.809
134.630
134.413
124.545
121.120
39.520
$(CD_3)_2SO$
both (2C)
both (1C)
minor (1C)
major (1C)
both (2C)
both (1C)
527
135
134
133
f1 (ppm)
220
210
200
190
180
170
160
150
140
130
120
110
100
90
80
70
60
50
40
30
20
10
0
f1 (ppm)

^{1}H NMR 500 MHz in $(CD_3)_2SO$

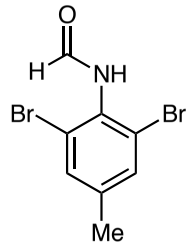

208cb

^{1}H NMR 500 MHz in $(CD_3)_2SO$
9.993
9.754
9.732
8.270
8.032
8.010
7.623
7.571
major (1H)
minor (1H)
major (1H)
minor (1H)
minor (2H)
major (2H)
0.78
0.20
0.79
0.20
0.40
1.55
Br
NH
O
H
Br
Me
208cb
(ppm)

^{13}C NMR 126 MHz in $(CD_3)_2SO$

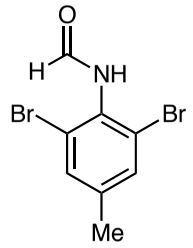

208cb

^{13}C NMR 126 MHz in $(CD_3)_2SO$
164.477
159.599
140.879
140.702
132.997
132.581
131.940
131.836
123.280
123.248
major (1C)
minor (1C)
major (1C)
minor (1C)
major (2C)
minor (2C)
major (1C)
minor (1C)
major (2C)
minor (2C)
123.3 123.2
(ppm)
132.5
(ppm)
133.0
132.0
144
(ppm)
166 164 162 160 158 156 154 152 150 148 146 142 140 138 136 134 132 130 128 126 124 122
208cb
Br
NH
O
H
Br
Me

^{1}H NMR 300 MHz in $(CD_3)_2CO$

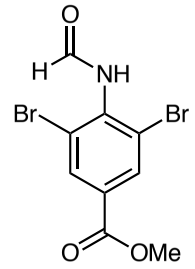

208cd

532

^{13}C NMR 126 MHz in $(CD_3)_2SO$

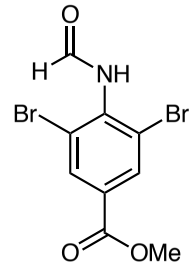

208cd

163.513
160.236
139.489
132.515
130.697
123.519
52.860
39.520
$(CD_3)_2SO$

533

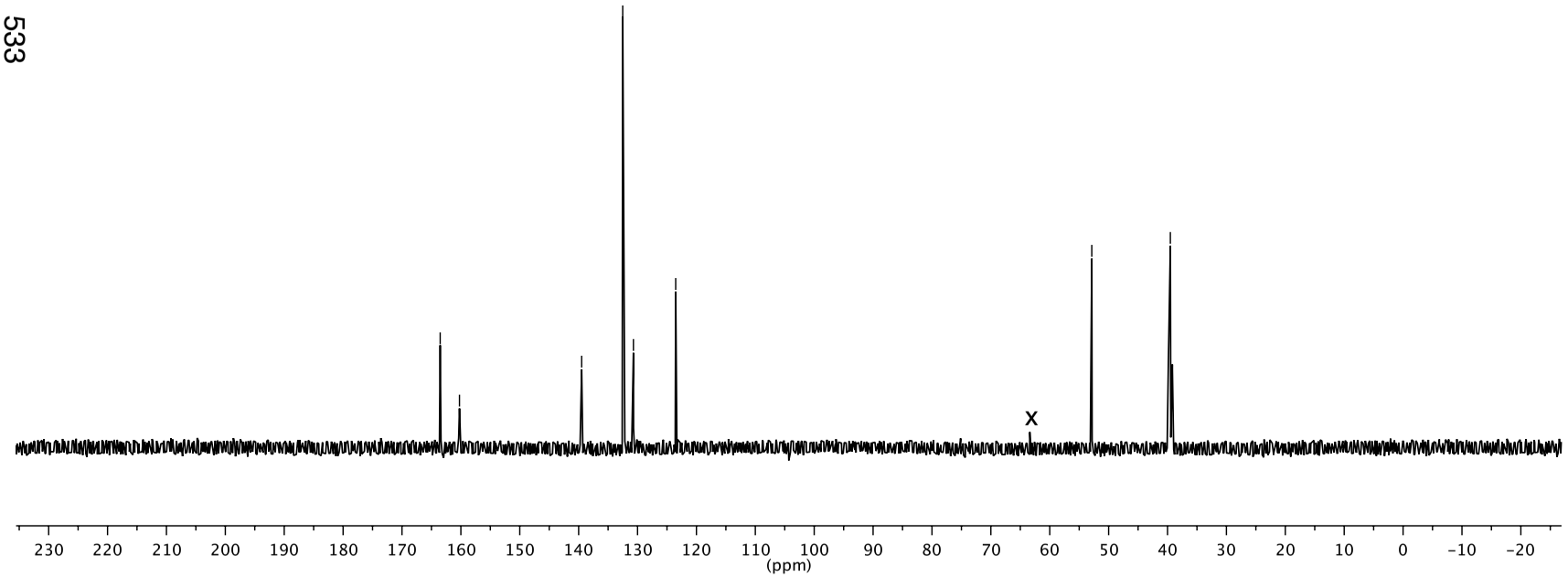

^{1}H NMR 300 MHz in $(CD_3)_2SO$
major (1H)
10.089
minor (1H)
9.655
0.93
0.19
10.0
(ppm)
0.92
0.99
0.40
1.71
0.22
8.303
8.278
8.233
7.978
major (1H)
minor (2H)
major (2H)
minor (1H)
0.99
0.40
1.71
0.22
8.3
8.2
8.1
8.0
(ppm)
7.978
3.344
H_2O
DMSO-*d5*
acetone
2.500
2.296
208da
(ppm)

^{13}C NMR 126 MHz in $(CD_3)_2SO$

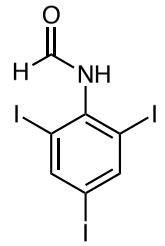

208da

^{13}C NMR 126 MHz in $(CD_3)_2SO$
164.369
159.360
146.435
146.117
141.035
140.396
102.384
101.857
95.914
95.574
minor (1C)
major (1C)
minor (2C)
major (2C)
major (1C)
minor (1C)
minor (2C)
major (2C)
minor (1C)
major (1C)
165
160
155
150
145
140
135
130
125
120
115
110
105
100
95
(ppm)
208da

^{1}H NMR 500 MHz in $(CD_3)_2SO$

208db

^{13}C NMR 126 MHz in $(CD_3)_2SO$

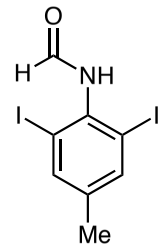

208db

^{13}C NMR 126 MHz in $(CD_3)_2SO$

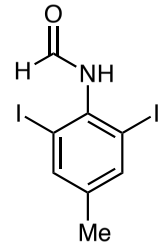

208db

^{1}H NMR 400 MHz in $(CD_3)_2SO$

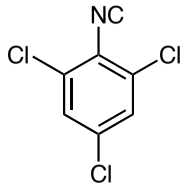

209ba

^{13}C NMR 101 MHz in $(CD_3)_2SO$

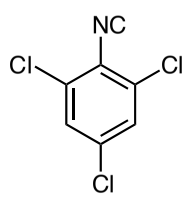

209ba

542

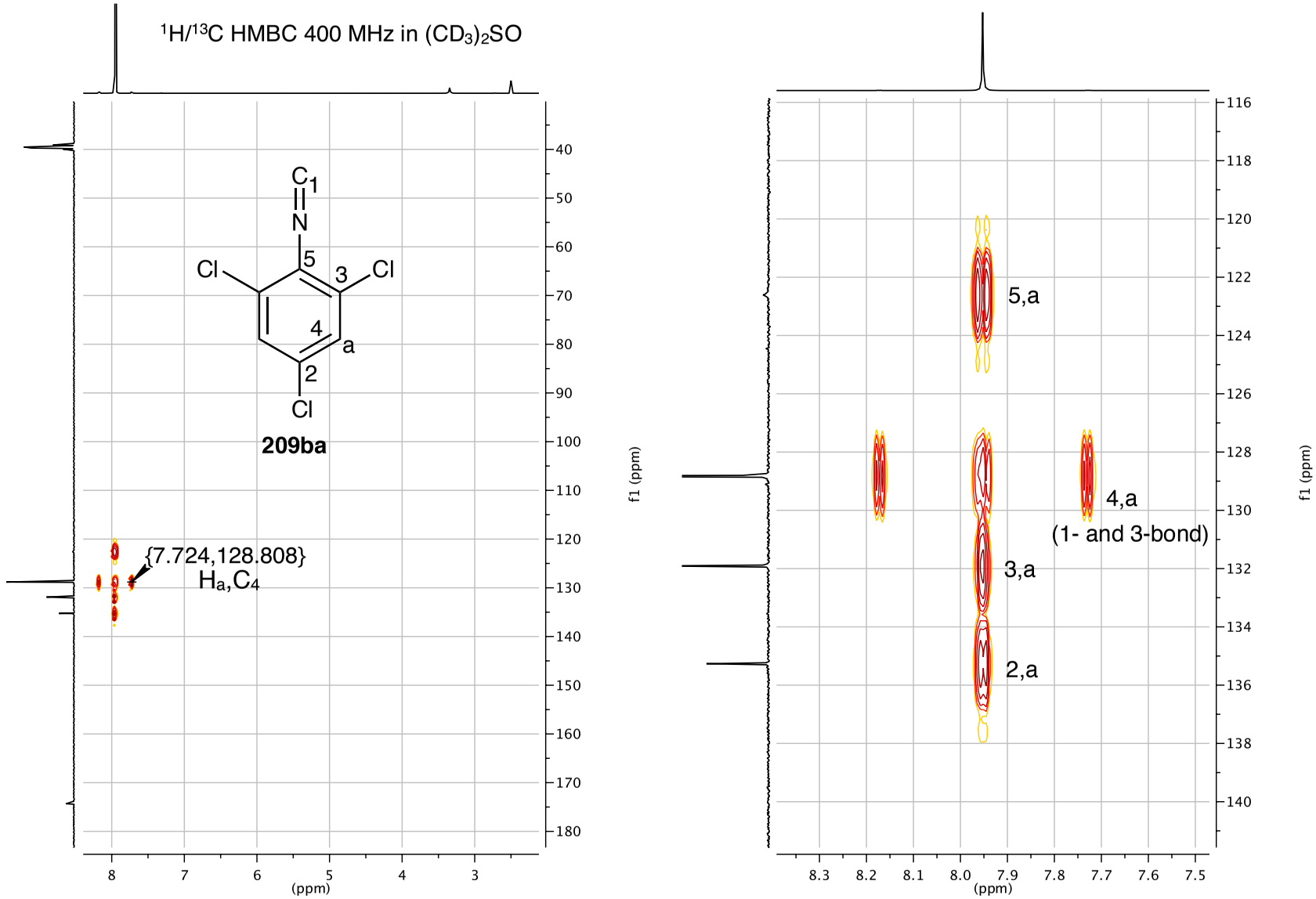
$^{1}H/^{13}C$ HMBC 400 MHz in $(CD_3)_2SO$
C1
N
5
3
Cl
Cl
4
a
2
Cl
209ba
{7.724,128.808}
H_a,C_4
f1 (ppm)
(ppm)
5,a
4,a
(1- and 3-bond)
3,a
2,a
f1 (ppm)
(ppm)

^{1}H NMR 300 MHz in CD_2Cl_2

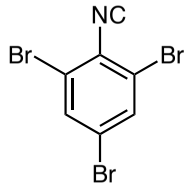

209ca

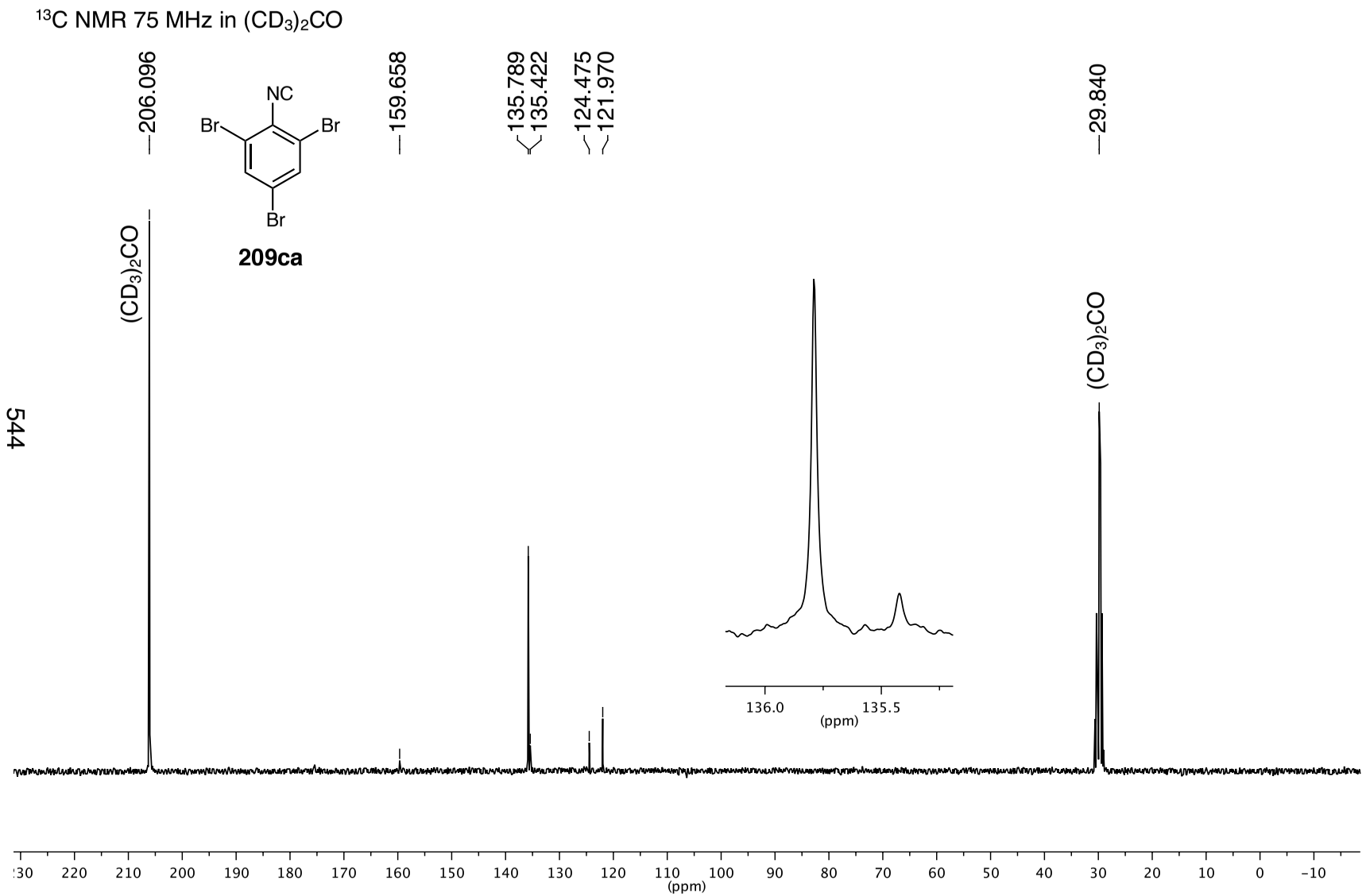
^{13}C NMR 75 MHz in $(CD_3)_2CO$
206.096
159.658
135.789
135.422
124.475
121.970
29.840
NC
Br
Br
Br
209ca
$(CD_3)_2CO$
$(CD_3)_2CO$
544
136.0
135.5
(ppm)
(ppm)

^{1}H NMR 400 MHz in CD_2Cl_2

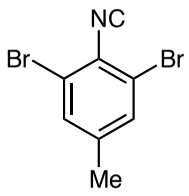

209cb

^{13}C NMR 101 MHz in CD_2Cl_2

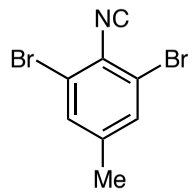

209cb

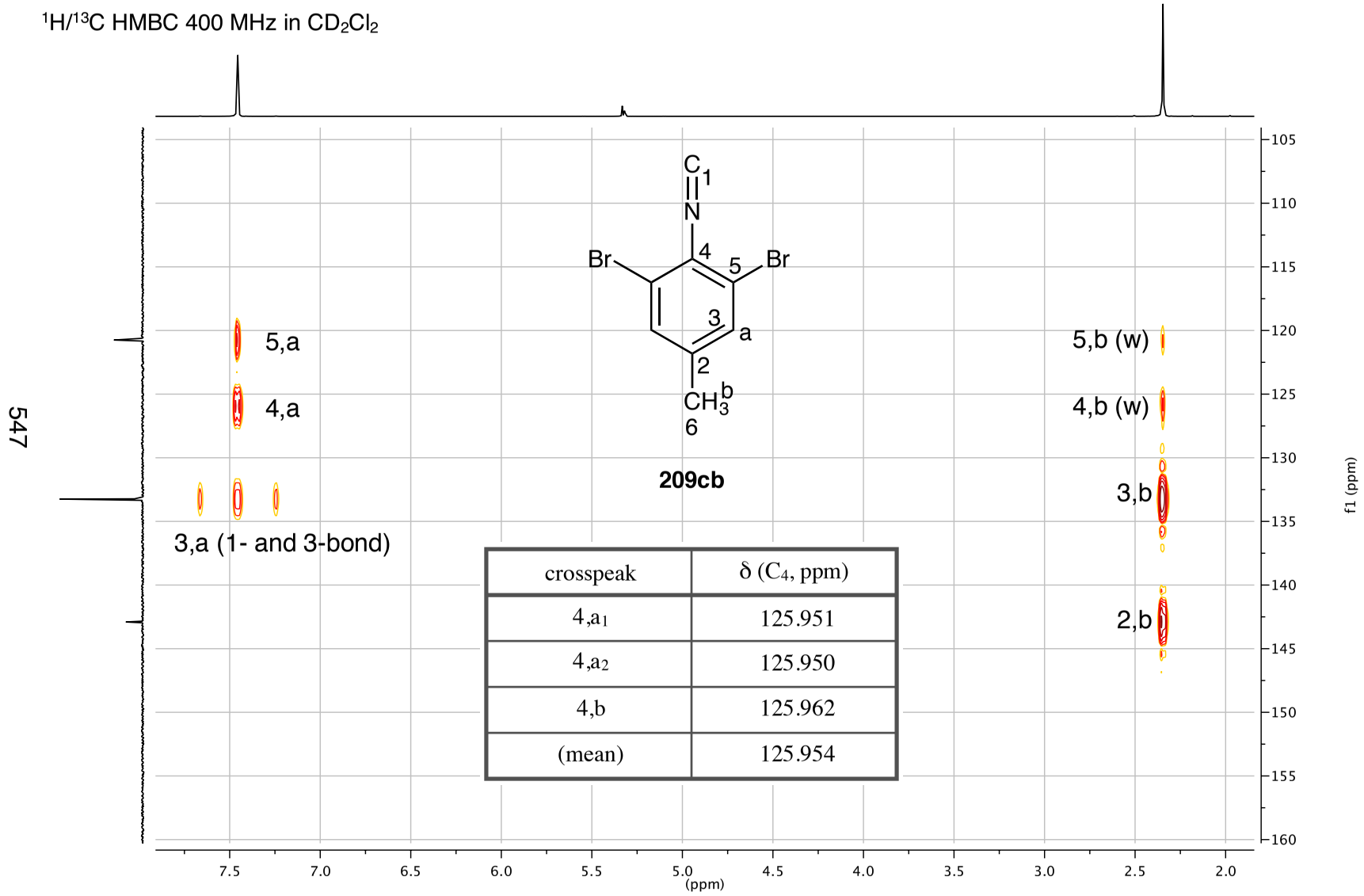

crosspeak	δ (C_4, ppm)
4,a_1	125.951
4,a_2	125.950
4,b	125.962
(mean)	125.954

^{1}H NMR 500 MHz in CD_2Cl_2

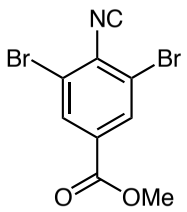

209cd

^{13}C NMR 126 MHz in $(CD_3)_2SO$

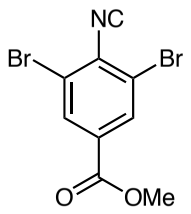

209cd

^{1}H NMR 300 MHz in $CDCl_3$

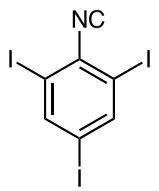

209da

^{13}C NMR 126 MHz in $(CD_3)_2SO$

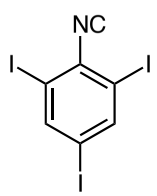

209da

169.971
146.209
133.812
98.769
97.670
39.520
$(CD_3)_2SO$

551

210 200 190 180 170 160 150 140 130 120 110 100 90 80 70 60 50 40 30 20 10 0 -10
(ppm)

^{1}H NMR 500 MHz in $(CD_3)_2SO$

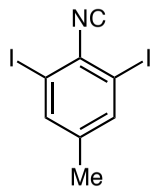

209db

^{13}C NMR 126 MHz in $(CD_3)_2SO$

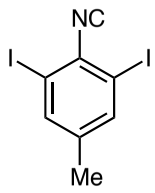

209db

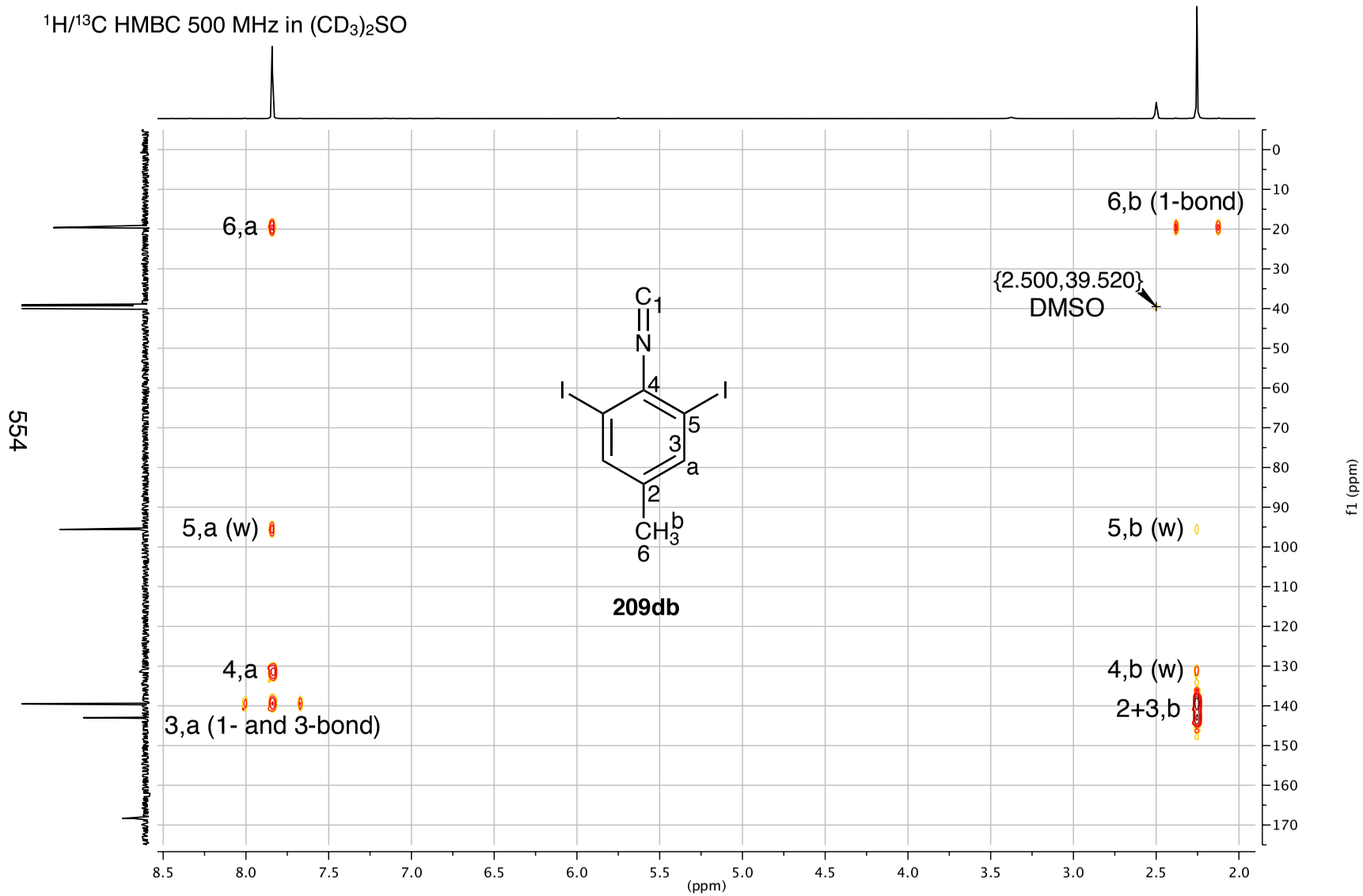
$^{1}H/^{13}C$ HMBC 500 MHz in $(CD_3)_2SO$
554
6,a
6,b (1-bond)
{2.500,39.520}
DMSO
5,a (w)
5,b (w)
4,a
4,b (w)
2+3,b
3,a (1- and 3-bond)
209db
(ppm)
f1 (ppm)

Appendix III. Crystallographic Data for Compounds 8d, 11h, and 12h.

Each entry contains a summary of how the crystallographic data for each sample were obtained and refined, along with the content of the resulting CIF file. CIF file content is presented verbatim, except for lines at the end of the file that begin with a number sign (#). These are comments that explain why some atom numbers were changed after refinement.

In the CIF files, melting point data are not given in the "_chemical_melting_point" fields. These fields are intended to reflect the melting point of the specific crystal that was examined, which was not obtained. For melting point data on the mixtures from which crystals described in this section were derived, refer to the respective entries in § 3.2.

Citations in CIF files are indicated by a name(s) and a year in parenthesis. Refer to Appendix V to find the corresponding reference number in § 4.

Table 43. The contents of Appendix III.

compound	page	nickname
8d	556	cyclopentanone 2:2 product (*p*-xylene 2:1)
11h	570	cyclooctanone carbazolylaniline
12h	584	cyclooctanone diazepine

***rac*-(3a'*R*,9a'*R*)-3a'-(Indol-3-yl)-1',2',3',3a',4',9a'-hexahydrospiro[cyclopentane-1,9'-pentaleno[1,2-*b*]indole] hemi-1,4-dimethylbenzenate (8ds)**.

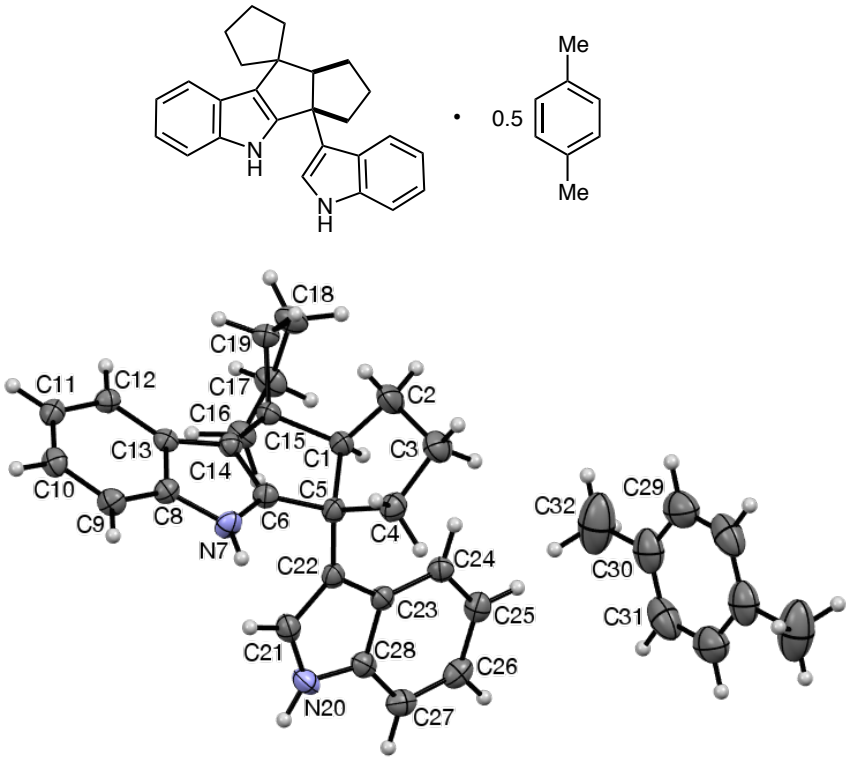

Data collection (by the XCL): A crystal (approx. 0.350 × 0.210 × 0.130 mm^3) was placed onto the tip of a 0.1 mm diameter glass capillary and mounted on a Bruker APEX-II CCD diffractometer for a data collection at 173 K. A preliminary set of cell constants was calculated from reflections harvested from three sets of 20 frames. These initial sets of frames were oriented such that orthogonal wedges of reciprocal space were surveyed. This produced initial orientation matrices determined from 124 reflections. The data collection was carried out using MoKα radiation (graphite monochromator) with a frame time of 60 sec and a detector distance of 60 mm. A randomly oriented region of reciprocal space was surveyed to the extent of one sphere and to a resolution of 0.77 Å. Four major sections of frames were collected with 0.30° steps in ω at four different ϕ settings and a detector position of –28° in 2θ. The intensity data were corrected for absorption and decay. Final cell constants were calculated from 2,946 strong reflections from the actual data collection after integration.

Structure solution and refinement (by the XCL): The space group $P2_1/c$ was determined based on systematic absences and intensity statistics. A direct-methods solution was calculated that provided most non-hydrogen atoms from the E-map. Full-matrix least squares / difference Fourier cycles were performed that located the remaining non-hydrogen atoms. All non-hydrogen atoms were refined with anisotropic displacement parameters. All hydrogen atoms were placed in ideal positions and refined as riding atoms with relative isotropic displacement parameters. The final full matrix least squares refinement converged to $R1 = 0.0478$ and $wR2 = 0.1261$ (F^2, all data).

CIF content:

```
data_8ds
_audit_creation_method     SHELXL-2014/6
_chemical_name_systematic
;
<i>rac</i>-(3a'<i>R</i>,9a'<i>R</i>)-3a'-(Indol-3-yl)-1',2',3',3a',4',9a'-\
hexahydrospiro[cyclopentane-1,9'-pentaleno[1,2-<i>b</i>]indole]
hemi-1,4-dimethylbenzenate
;
_chemical_name_common     ‘cyclopentanone 2:2 product’
_chemical_formula_moiety      'C26 H26 N2, 0.5(C8 H10)'
_chemical_formula_sum     'C30 H31 N2'
_chemical_formula_iupac      'C26 H26 N2, 0.5C8 H10'
_chemical_formula_weight      419.57
_chemical_melting_point     ?
_shelx_space_group_comment
;
The symmetry employed for this shelxl refinement is uniquely defined
by the following loop, which should always be used as a source of
symmetry information in preference to the above space-group names.
They are only intended as comments.
;
_space_group_crystal_system     monoclinic
_space_group_name_H-M_alt     'P 21/c'
_space_group_name_Hall     '-P 2ybc'
loop_
    _space_group_symop_operation_xyz
    'x, y, z'
    '-x, y+1/2, -z+1/2'
    '-x, -y, -z'
    'x, -y-1/2, z-1/2'
_cell_length_a     8.7618(7)
_cell_length_b     29.450(2)
_cell_length_c     9.6569(8)
_cell_angle_alpha     90
_cell_angle_beta     114.7320(10)
_cell_angle_gamma     90
_cell_volume     2263.2(3)
_cell_formula_units_Z     4
_cell_measurement_reflns_used     2946
_cell_measurement_theta_min     2.42
```

```
_cell_measurement_theta_max     27.28
_cell_measurement_temperature     173(2)
_exptl_crystal_description     'Block'
_exptl_crystal_colour     'colourless'
_exptl_crystal_size_max     0.350
_exptl_crystal_size_mid     0.210
_exptl_crystal_size_min     0.130
_exptl_crystal_density_diffrn     1.231
_exptl_crystal_density_meas     ?
_exptl_crystal_density_method     ?
_exptl_crystal_F_000     900
_exptl_absorpt_coefficient_mu     0.071
_exptl_absorpt_correction_type     multi-scan
_exptl_absorpt_process_details
;
(SADABS; Sheldrick, 1996)
;
_shelx_estimated_absorpt_T_min     0.975
_shelx_estimated_absorpt_T_max     0.991
_exptl_absorpt_correction_T_min     0.7000
_exptl_absorpt_correction_T_max     0.7456
_diffrn_ambient_temperature     173(2)
_diffrn_radiation_type     MoK\a
_diffrn_radiation_wavelength     0.71073
_diffrn_measurement_device_type     'Bruker APEXII CCD'
_diffrn_measurement_method     '\f and \w scans'
_diffrn_detector_area_resol_mean     ?
_diffrn_reflns_number     25883
_diffrn_reflns_av_R_equivalents     0.0323
_diffrn_reflns_theta_min     2.423
_diffrn_reflns_theta_max     27.483
_diffrn_reflns_theta_full     25.242
_diffrn_measured_fraction_theta_max     0.997
_diffrn_measured_fraction_theta_full     1.000
_diffrn_reflns_limit_h_min     -11
_diffrn_reflns_limit_h_max     11
_diffrn_reflns_limit_k_min     -38
_diffrn_reflns_limit_k_max     38
_diffrn_reflns_limit_l_min     -12
_diffrn_reflns_limit_l_max     12
_refine_special_details     ?
_reflns_number_total     5184
_reflns_number_gt     4102
_reflns_threshold_expression     I>2\s(I)
_refine_ls_structure_factor_coef     Fsqd
_refine_ls_matrix_type     full
_refine_ls_R_factor_all     0.0621
_refine_ls_R_factor_gt     0.0478
_refine_ls_wR_factor_gt     0.1164
_refine_ls_wR_factor_ref     0.1261
_refine_ls_goodness_of_fit_ref     1.058
_refine_ls_restrained_S_all     1.040
_refine_ls_number_reflns     5184
_refine_ls_number_parameters     294
_refine_ls_number_restraints     321
_refine_ls_hydrogen_treatment     constr
```

```
_refine_ls_weighting_scheme     calc
_refine_ls_weighting_details
            'w=1/[\s^2^(Fo^2^)+(0.0542P)^2^+0.8656P] where P=(Fo^2^+2Fc^2^)/3'
_atom_sites_solution_hydrogens     geom
_atom_sites_solution_primary     ?
_atom_sites_solution_secondary     ?
_refine_ls_shift/su_max     0.000
_refine_ls_shift/su_mean     0.000
_refine_diff_density_max     0.508
_refine_diff_density_min     -0.371
_refine_ls_extinction_method     none
_refine_ls_extinction_coef     .
loop_
    _atom_type_symbol
    _atom_type_description
    _atom_type_scat_dispersion_real
    _atom_type_scat_dispersion_imag
    _atom_type_scat_source
    'C' 'C' 0.0033 0.0016
                        'International Tables Vol C Tables 4.2.6.8 and 6.1.1.4'
    'H' 'H' 0.0000 0.0000
                        'International Tables Vol C Tables 4.2.6.8 and 6.1.1.4'
    'N' 'N' 0.0061 0.0033
                        'International Tables Vol C Tables 4.2.6.8 and 6.1.1.4'
_computing_data_collection
;
APEX2 (Bruker, 2007)
;
_computing_cell_refinement
;
SAINT (Bruker, 2007)
;
_computing_data_reduction
;
SAINT (Bruker, 2007)
;
_computing_structure_solution
;
SHELXS97 (Sheldrick, 2008)
;
_computing_structure_refinement
;
SHELXL2014 (Sheldrick, 2015)
;
_computing_molecular_graphics
;
Mercury (Macrae <i>et al.</i>, 2008)
;
_computing_publication_material
;
SHELXL2014 (Sheldrick, 2015), enCIFer (Allen <i>et al.</i>,
2004), and publCIF (Westrip, 2010)
;
loop_
    _atom_site_type_symbol
    _atom_site_label
```

```
_atom_site_fract_x
_atom_site_fract_y
_atom_site_fract_z
_atom_site_U_iso_or_equiv
_atom_site_adp_type
_atom_site_calc_flag
_atom_site_occupancy
_atom_site_disorder_assembly
_atom_site_disorder_group
C C1 0.44662(19) 0.09927(5) 0.06623(16) 0.0282(3) Uani d 1 . .
H H1 0.3383 0.1017 0.0771 0.034 Uiso calc 1 A 1
C C2 0.5227(3) 0.05186(5) 0.1165(2) 0.0462(4) Uani d 0.819(4) B 1
H H2A 0.5987 0.0441 0.0678 0.055 Uiso calc 0.819(4) B 1
H H2B 0.4328 0.0287 0.0876 0.055 Uiso calc 0.819(4) B 1
C C2' 0.5227(3) 0.05186(5) 0.1165(2) 0.0462(4) Uani d 0.181(4) B 2
H H2C 0.5252 0.0353 0.0284 0.055 Uiso calc 0.181(4) B 2
H H2D 0.4529 0.0343 0.1561 0.055 Uiso calc 0.181(4) B 2
C C3 0.6179(3) 0.05373(7) 0.2856(2) 0.0428(5) Uani d 0.819(4) B 1
H H3A 0.7056 0.0299 0.3217 0.051 Uiso calc 0.819(4) B 1
H H3B 0.5417 0.0496 0.3367 0.051 Uiso calc 0.819(4) B 1
C C3' 0.6949(6) 0.0567(2) 0.2367(9) 0.0428(5) Uani d 0.181(4) B 2
H H3C 0.7774 0.0576 0.1913 0.051 Uiso calc 0.181(4) B 2
H H3D 0.7229 0.0309 0.3089 0.051 Uiso calc 0.181(4) B 2
C C4 0.6968(2) 0.10088(5) 0.31725(17) 0.0335(3) Uani d 0.819(4) B 1
H H4A 0.8117 0.0998 0.3215 0.040 Uiso calc 0.819(4) B 1
H H4B 0.7039 0.1125 0.4160 0.040 Uiso calc 0.819(4) B 1
C C4' 0.6968(2) 0.10088(5) 0.31725(17) 0.0335(3) Uani d 0.181(4) B 2
H H4C 0.8122 0.1133 0.3680 0.040 Uiso calc 0.181(4) B 2
H H4D 0.6504 0.0968 0.3939 0.040 Uiso calc 0.181(4) B 2
C C5 0.58207(17) 0.13233(5) 0.18429(15) 0.0261(3) Uani d 1 . .
C C6 0.66437(17) 0.14891(5) 0.08495(16) 0.0262(3) Uani d 1 . .
N N7 0.80742(15) 0.17360(4) 0.11129(13) 0.0292(3) Uani d 1 . .
H H7 0.8814 0.1831 0.2005 0.035 Uiso calc 1 . .
C C8 0.81381(17) 0.18073(5) -0.02801(16) 0.0260(3) Uani d 1 . .
C C9 0.93197(17) 0.20408(5) -0.06175(17) 0.0292(3) Uani d 1 . .
H H9 1.0285 0.2173 0.0165 0.035 Uiso calc 1 . .
C C10 0.90408(18) 0.20741(5) -0.21329(17) 0.0299(3) Uani d 1 . .
H H10 0.9825 0.2234 -0.2395 0.036 Uiso calc 1 . .
C C11 0.76282(18) 0.18777(5) -0.32891(16) 0.0284(3) Uani d 1 . .
H H11 0.7467 0.1908 -0.4321 0.034 Uiso calc 1 . .
C C12 0.64618(17) 0.16398(5) -0.29538(16) 0.0253(3) Uani d 1 . .
H H12 0.5512 0.1505 -0.3746 0.030 Uiso calc 1 . .
C C13 0.67016(16) 0.16009(4) -0.14320(15) 0.0230(3) Uani d 1 . .
C C14 0.57911(17) 0.13989(5) -0.06520(15) 0.0240(3) Uani d 1 . .
C C15 0.41925(17) 0.11434(4) -0.09859(15) 0.0241(3) Uani d 1 . .
C C16 0.26029(17) 0.14373(5) -0.17142(17) 0.0297(3) Uani d 1 . .
H H16A 0.2674 0.1639 -0.2506 0.036 Uiso calc 1 . .
H H16B 0.2454 0.1627 -0.0934 0.036 Uiso calc 1 . .
C C17 0.11381(19) 0.11002(5) -0.2425(2) 0.0371(4) Uani d 1 . .
H H17A 0.0327 0.1209 -0.3435 0.044 Uiso calc 1 . .
H H17B 0.0542 0.1062 -0.1759 0.044 Uiso calc 1 . .
C C18 0.1935(2) 0.06478(5) -0.2582(2) 0.0382(4) Uani d 1 . .
H H18A 0.1389 0.0533 -0.3642 0.046 Uiso calc 1 . .
H H18B 0.1822 0.0416 -0.1889 0.046 Uiso calc 1 . .
C C19 0.37848(18) 0.07557(5) -0.21480(16) 0.0282(3) Uani d 1 . .
H H19A 0.3959 0.0853 -0.3053 0.034 Uiso calc 1 . .
```

```
    H H19B 0.4499 0.0487 -0.1689 0.034 Uiso calc 1 . .
    N N20 0.46954(16) 0.24080(4) 0.31417(15) 0.0329(3) Uani d 1 . .
    H H20 0.4794 0.2703 0.3303 0.039 Uiso calc 1 . .
    C C21 0.55349(19) 0.21573(5) 0.24806(17) 0.0308(3) Uani d 1 . .
    H H21 0.6315 0.2278 0.2129 0.037 Uiso calc 1 . .
    C C22 0.50921(17) 0.17099(5) 0.23994(15) 0.0250(3) Uani d 1 . .
    C C23 0.38834(17) 0.16807(5) 0.30492(15) 0.0245(3) Uani d 1 . .
    C C24 0.29604(18) 0.13280(5) 0.33118(16) 0.0281(3) Uani d 1 . .
    H H24 0.3062 0.1026 0.3015 0.034 Uiso calc 1 . .
    C C25 0.19025(18) 0.14242(5) 0.40062(17) 0.0320(3) Uani d 1 . .
    H H25 0.1275 0.1186 0.4183 0.038 Uiso calc 1 . .
    C C26 0.17390(19) 0.18680(6) 0.44541(17) 0.0335(3) Uani d 1 . .
    H H26 0.0999 0.1925 0.4925 0.040 Uiso calc 1 . .
    C C27 0.26304(18) 0.22218(5) 0.42229(17) 0.0321(3) Uani d 1 . .
    H H27 0.2531 0.2522 0.4540 0.039 Uiso calc 1 . .
    C C28 0.36823(18) 0.21257(5) 0.35091(16) 0.0277(3) Uani d 1 . .
    C C29 0.9782(3) -0.02919(8) 0.8839(3) 0.0599(5) Uani d 1 . .
    H H29 0.9643 -0.0498 0.8039 0.072 Uiso calc 1 . .
    C C30 0.8857(3) 0.01069(8) 0.8504(3) 0.0570(5) Uani d 1 . .
    C C31 0.9101(3) 0.03952(7) 0.9693(3) 0.0593(6) Uani d 1 . .
    H H31 0.8488 0.0672 0.9502 0.071 Uiso calc 1 . .
    C C32 0.7658(3) 0.02275(12) 0.6900(3) 0.0962(10) Uani d 1 . .
    H H32A 0.7930 0.0530 0.6647 0.144 Uiso calc 1 . .
    H H32B 0.6505 0.0226 0.6819 0.144 Uiso calc 1 . .
    H H32C 0.7760 0.0004 0.6190 0.144 Uiso calc 1 . .
loop_
    _atom_site_aniso_label
    _atom_site_aniso_U_11
    _atom_site_aniso_U_22
    _atom_site_aniso_U_33
    _atom_site_aniso_U_12
    _atom_site_aniso_U_13
    _atom_site_aniso_U_23
    C1 0.0335(8) 0.0263(7) 0.0256(7) -0.0062(6) 0.0131(6) -0.0011(5)
    C2 0.0684(12) 0.0257(8) 0.0365(9) -0.0030(8) 0.0141(8) 0.0047(7)
    C3 0.0532(13) 0.0311(10) 0.0395(11) 0.0073(9) 0.0150(9) 0.0062(8)
    C4 0.0364(8) 0.0354(8) 0.0275(7) 0.0046(6) 0.0121(6) 0.0042(6)
    C2' 0.0684(12) 0.0257(8) 0.0365(9) -0.0030(8) 0.0141(8) 0.0047(7)
    C3' 0.0532(13) 0.0311(10) 0.0395(11) 0.0073(9) 0.0150(9) 0.0062(8)
    C4' 0.0364(8) 0.0354(8) 0.0275(7) 0.0046(6) 0.0121(6) 0.0042(6)
    C5 0.0276(7) 0.0277(7) 0.0219(6) -0.0033(5) 0.0092(5) 0.0003(5)
    C6 0.0244(7) 0.0276(7) 0.0253(7) -0.0020(5) 0.0090(5) -0.0002(5)
    N7 0.0248(6) 0.0383(7) 0.0209(6) -0.0074(5) 0.0061(5) -0.0033(5)
    C8 0.0235(7) 0.0280(7) 0.0244(7) 0.0007(5) 0.0081(5) 0.0002(5)
    C9 0.0217(7) 0.0335(8) 0.0307(7) -0.0033(6) 0.0091(6) -0.0021(6)
    C10 0.0257(7) 0.0316(7) 0.0353(8) 0.0004(6) 0.0157(6) 0.0027(6)
    C11 0.0299(7) 0.0309(7) 0.0257(7) 0.0032(6) 0.0128(6) 0.0024(6)
    C12 0.0239(7) 0.0261(7) 0.0241(7) 0.0009(5) 0.0083(5) -0.0008(5)
    C13 0.0208(6) 0.0216(6) 0.0255(7) 0.0018(5) 0.0086(5) 0.0001(5)
    C14 0.0243(7) 0.0229(6) 0.0238(7) 0.0006(5) 0.0089(5) 0.0003(5)
    C15 0.0254(7) 0.0220(6) 0.0242(6) -0.0022(5) 0.0097(5) -0.0013(5)
    C16 0.0270(7) 0.0252(7) 0.0352(8) -0.0001(5) 0.0114(6) 0.0004(6)
    C17 0.0257(8) 0.0368(8) 0.0448(9) -0.0045(6) 0.0110(7) -0.0022(7)
    C18 0.0337(8) 0.0326(8) 0.0446(9) -0.0087(6) 0.0127(7) -0.0072(7)
    C19 0.0308(7) 0.0252(7) 0.0276(7) -0.0037(6) 0.0111(6) -0.0037(5)
    N20 0.0377(7) 0.0210(6) 0.0374(7) -0.0013(5) 0.0132(6) 0.0010(5)
```

```
    C21 0.0318(8) 0.0288(7) 0.0303(7) -0.0030(6) 0.0115(6) 0.0036(6)
    C22 0.0263(7) 0.0263(7) 0.0200(6) -0.0027(5) 0.0073(5) 0.0017(5)
    C23 0.0245(7) 0.0257(7) 0.0192(6) -0.0004(5) 0.0050(5) 0.0011(5)
    C24 0.0282(7) 0.0281(7) 0.0259(7) -0.0031(6) 0.0092(6) -0.0014(5)
    C25 0.0270(7) 0.0387(8) 0.0289(7) -0.0028(6) 0.0104(6) 0.0026(6)
    C26 0.0261(7) 0.0452(9) 0.0266(7) 0.0063(6) 0.0086(6) 0.0002(6)
    C27 0.0298(7) 0.0322(8) 0.0280(7) 0.0076(6) 0.0058(6) -0.0014(6)
    C28 0.0269(7) 0.0259(7) 0.0243(7) 0.0014(5) 0.0046(6) 0.0018(5)
    C29 0.0650(13) 0.0548(12) 0.0731(15) -0.0183(10) 0.0420(12) -0.0085(10)
    C30 0.0449(11) 0.0646(13) 0.0655(13) -0.0117(9) 0.0270(10) 0.0147(10)
    C31 0.0563(12) 0.0447(11) 0.0901(16) 0.0027(9) 0.0436(12) 0.0157(11)
    C32 0.0633(15) 0.139(3) 0.0742(17) -0.0256(16) 0.0172(13) 0.0335(17)
_geom_special_details
;
All e.s.d.'s (except the e.s.d. in the dihedral angle between two l.s. planes)
are estimated using the full covariance matrix. The cell e.s.d.'s are taken
into account individually in the estimation of e.s.d.'s in distances, angles
and torsion angles; correlations between e.s.d.'s in cell parameters are only
used when they are defined by crystal symmetry. An approximate (isotropic)
treatment of cell e.s.d.'s is used for estimating e.s.d.'s involving l.s.
planes.
;
loop_
    _geom_bond_atom_site_label_1
    _geom_bond_atom_site_label_2
    _geom_bond_site_symmetry_2
    _geom_bond_distance
    _geom_bond_publ_flag
    C1 C2' . 1.536(2) ?
    C1 C2 . 1.536(2) ?
    C1 C5 . 1.5886(19) ?
    C1 C15 . 1.5711(19) ?
    C1 H1 . 1.0000 ?
    C2 C3 . 1.492(3) ?
    C2 H2A . 0.9900 ?
    C2 H2B . 0.9900 ?
    C2' C3' . 1.476(4) ?
    C2' H2C . 0.9900 ?
    C2' H2D . 0.9900 ?
    C3 C4 . 1.524(2) ?
    C3 H3A . 0.9900 ?
    C3 H3B . 0.9900 ?
    C3' C4' . 1.513(4) ?
    C3' H3C . 0.9900 ?
    C3' H3D . 0.9900 ?
    C4 C5 . 1.561(2) ?
    C4 H4A . 0.9900 ?
    C4 H4B . 0.9900 ?
    C4' C5 . 1.561(2) ?
    C4' H4C . 0.9900 ?
    C4' H4D . 0.9900 ?
    C5 C6 . 1.5025(19) ?
    C5 C22 . 1.510(2) ?
    C6 N7 . 1.3775(18) ?
    C6 C14 . 1.3509(19) ?
    N7 C8 . 1.3856(18) ?
```

```
    N7 H7 . 0.8800 ?
    C8 C9 . 1.390(2) ?
    C8 C13 . 1.4211(19) ?
    C9 C10 . 1.383(2) ?
    C9 H9 . 0.9500 ?
    C10 C11 . 1.399(2) ?
    C10 H10 . 0.9500 ?
    C11 C12 . 1.385(2) ?
    C11 H11 . 0.9500 ?
    C12 C13 . 1.3995(19) ?
    C12 H12 . 0.9500 ?
    C13 C14 . 1.4356(19) ?
    C14 C15 . 1.5013(18) ?
    C15 C16 . 1.5376(19) ?
    C15 C19 . 1.5347(19) ?
    C16 C17 . 1.539(2) ?
    C16 H16A . 0.9900 ?
    C16 H16B . 0.9900 ?
    C17 C18 . 1.541(2) ?
    C17 H17A . 0.9900 ?
    C17 H17B . 0.9900 ?
    C18 C19 . 1.528(2) ?
    C18 H18A . 0.9900 ?
    C18 H18B . 0.9900 ?
    C19 H19A . 0.9900 ?
    C19 H19B . 0.9900 ?
    N20 C21 . 1.374(2) ?
    N20 C28 . 1.3670(19) ?
    N20 H20 . 0.8800 ?
    C21 C22 . 1.366(2) ?
    C21 H21 . 0.9500 ?
    C22 C23 . 1.4418(19) ?
    C23 C24 . 1.4032(19) ?
    C23 C28 . 1.4182(19) ?
    C24 C25 . 1.382(2) ?
    C24 H24 . 0.9500 ?
    C25 C26 . 1.403(2) ?
    C25 H25 . 0.9500 ?
    C26 C27 . 1.375(2) ?
    C26 H26 . 0.9500 ?
    C27 C28 . 1.392(2) ?
    C27 H27 . 0.9500 ?
    C29 C30 . 1.386(3) ?
    C29 C31 3_757 1.378(3) ?
    C29 H29 . 0.9500 ?
    C30 C31 . 1.372(3) ?
    C30 C32 . 1.505(3) ?
    C31 C29 3_757 1.378(3) ?
    C31 H31 . 0.9500 ?
    C32 H32A . 0.9800 ?
    C32 H32B . 0.9800 ?
    C32 H32C . 0.9800 ?
loop_
    _geom_angle_atom_site_label_1
    _geom_angle_atom_site_label_2
    _geom_angle_atom_site_label_3
```

```
_geom_angle_site_symmetry_1
_geom_angle_site_symmetry_3
_geom_angle
_geom_angle_publ_flag
C2 C1 C15 . . 116.07(12) ?
C2 C1 C5 . . 103.60(12) ?
C2' C1 C5 . . 103.60(12) ?
C2' C1 C15 . . 116.07(12) ?
C5 C1 C15 . . 107.79(11) ?
C2 C1 H1 . . 109.7 ?
C5 C1 H1 . . 109.7 ?
C15 C1 H1 . . 109.7 ?
C1 C2 C3 . . 106.41(14) ?
C1 C2 H2A . . 110.4 ?
C1 C2 H2B . . 110.4 ?
C3 C2 H2A . . 110.4 ?
C3 C2 H2B . . 110.4 ?
H2A C2 H2B . . 108.6 ?
C1 C2' C3' . . 109.1(3) ?
C1 C2' H2C . . 109.9 ?
C1 C2' H2D . . 109.9 ?
C3' C2' H2C . . 109.9 ?
C3' C2' H2D . . 109.9 ?
H2C C2' H2D . . 108.3 ?
C2 C3 C4 . . 104.62(15) ?
C2 C3 H3A . . 110.8 ?
C2 C3 H3B . . 110.8 ?
C4 C3 H3A . . 110.8 ?
C4 C3 H3B . . 110.8 ?
H3A C3 H3B . . 108.9 ?
C2' C3' C4' . . 105.9(2) ?
C2' C3' H3C . . 110.5 ?
C2' C3' H3D . . 110.5 ?
C4' C3' H3C . . 110.5 ?
C4' C3' H3D . . 110.5 ?
H3C C3' H3D . . 108.7 ?
C3 C4 C5 . . 107.06(13) ?
C3 C4 H4A . . 110.3 ?
C3 C4 H4B . . 110.3 ?
C5 C4 H4A . . 110.3 ?
C5 C4 H4B . . 110.3 ?
H4A C4 H4B . . 108.6 ?
C3' C4' C5 . . 102.9(3) ?
C3' C4' H4C . . 111.2 ?
C3' C4' H4D . . 111.2 ?
C5 C4' H4C . . 111.2 ?
C5 C4' H4D . . 111.2 ?
H4C C4' H4D . . 109.1 ?
C1 C5 C4 . . 104.92(11) ?
C1 C5 C4' . . 104.92(11) ?
C1 C5 C6 . . 98.91(11) ?
C1 C5 C22 . . 114.67(11) ?
C4 C5 C6 . . 113.69(12) ?
C4' C5 C6 . . 113.69(12) ?
C4 C5 C22 . . 112.17(11) ?
C4' C5 C22 . . 112.17(11) ?
```

```
C6 C5 C22 . . 111.68(11) ?
C5 C6 N7 . . 134.14(12) ?
C5 C6 C14 . . 115.07(12) ?
N7 C6 C14 . . 110.72(12) ?
C6 N7 C8 . . 107.70(11) ?
C6 N7 H7 . . 126.2 ?
C8 N7 H7 . . 126.2 ?
N7 C8 C9 . . 129.71(13) ?
N7 C8 C13 . . 108.23(12) ?
C9 C8 C13 . . 122.05(13) ?
C8 C9 C10 . . 117.64(13) ?
C8 C9 H9 . . 121.2 ?
C10 C9 H9 . . 121.2 ?
C9 C10 C11 . . 121.40(13) ?
C9 C10 H10 . . 119.3 ?
C11 C10 H10 . . 119.3 ?
C10 C11 C12 . . 121.05(13) ?
C10 C11 H11 . . 119.5 ?
C12 C11 H11 . . 119.5 ?
C11 C12 C13 . . 119.06(13) ?
C11 C12 H12 . . 120.5 ?
C13 C12 H12 . . 120.5 ?
C8 C13 C12 . . 118.80(12) ?
C8 C13 C14 . . 105.74(12) ?
C12 C13 C14 . . 135.45(13) ?
C6 C14 C13 . . 107.61(12) ?
C6 C14 C15 . . 112.11(12) ?
C13 C14 C15 . . 140.21(12) ?
C1 C15 C14 . . 100.99(11) ?
C1 C15 C16 . . 110.34(11) ?
C1 C15 C19 . . 114.89(11) ?
C14 C15 C16 . . 113.66(11) ?
C14 C15 C19 . . 116.15(11) ?
C16 C15 C19 . . 101.26(11) ?
C15 C16 C17 . . 105.53(11) ?
C15 C16 H16A . . 110.6 ?
C17 C16 H16A . . 110.6 ?
C15 C16 H16B . . 110.6 ?
C17 C16 H16B . . 110.6 ?
H16A C16 H16B . . 108.8 ?
C16 C17 C18 . . 105.90(12) ?
C16 C17 H17A . . 110.6 ?
C16 C17 H17B . . 110.6 ?
C18 C17 H17A . . 110.6 ?
C18 C17 H17B . . 110.6 ?
H17A C17 H17B . . 108.7 ?
C17 C18 C19 . . 105.40(12) ?
C17 C18 H18A . . 110.7 ?
C17 C18 H18B . . 110.7 ?
C19 C18 H18A . . 110.7 ?
C19 C18 H18B . . 110.7 ?
H18A C18 H18B . . 108.8 ?
C15 C19 C18 . . 104.54(12) ?
C15 C19 H19A . . 110.8 ?
C15 C19 H19B . . 110.8 ?
C18 C19 H19A . . 110.8 ?
```

```
    C18 C19 H19B . . 110.8 ?
    H19A C19 H19B . . 108.9 ?
    C21 N20 C28 . . 109.01(12) ?
    C21 N20 H20 . . 125.5 ?
    C28 N20 H20 . . 125.5 ?
    N20 C21 C22 . . 110.53(13) ?
    N20 C21 H21 . . 124.7 ?
    C22 C21 H21 . . 124.7 ?
    C5 C22 C21 . . 126.53(13) ?
    C5 C22 C23 . . 127.37(12) ?
    C21 C22 C23 . . 105.97(13) ?
    C22 C23 C24 . . 134.96(13) ?
    C22 C23 C28 . . 106.94(12) ?
    C24 C23 C28 . . 118.10(13) ?
    C23 C24 C25 . . 119.36(14) ?
    C23 C24 H24 . . 120.3 ?
    C25 C24 H24 . . 120.3 ?
    C24 C25 C26 . . 121.09(14) ?
    C24 C25 H25 . . 119.5 ?
    C26 C25 H25 . . 119.5 ?
    C25 C26 C27 . . 121.17(14) ?
    C25 C26 H26 . . 119.4 ?
    C27 C26 H26 . . 119.4 ?
    C26 C27 C28 . . 117.73(14) ?
    C26 C27 H27 . . 121.1 ?
    C28 C27 H27 . . 121.1 ?
    N20 C28 C23 . . 107.55(12) ?
    N20 C28 C27 . . 129.90(14) ?
    C23 C28 C27 . . 122.54(13) ?
    C30 C29 C31 3_757 . 121.5(2) ?
    C30 C29 H29 . . 119.3 ?
    C31 C29 H29 3_757 . 119.3 ?
    C29 C30 C31 . . 117.2(2) ?
    C29 C30 C32 . . 121.9(2) ?
    C31 C30 C32 . . 120.9(2) ?
    C29 C31 C30 . 3_757 121.3(2) ?
    C29 C31 H31 3_757 . 119.3 ?
    C30 C31 H31 . . 119.3 ?
    C30 C32 H32A . . 109.5 ?
    C30 C32 H32B . . 109.5 ?
    C30 C32 H32C . . 109.5 ?
    H32A C32 H32B . . 109.5 ?
    H32A C32 H32C . . 109.5 ?
    H32B C32 H32C . . 109.5 ?
loop_
    _geom_torsion_atom_site_label_1
    _geom_torsion_atom_site_label_2
    _geom_torsion_atom_site_label_3
    _geom_torsion_atom_site_label_4
    _geom_torsion_site_symmetry_1
    _geom_torsion_site_symmetry_2
    _geom_torsion_site_symmetry_3
    _geom_torsion_site_symmetry_4
    _geom_torsion
    _geom_torsion_publ_flag
    C5 C1 C2 C3 . . . . 32.92(18) ?
```

```
C15 C1 C2 C3 . . . . 150.85(15) ?
C5 C1 C2' C3' . . . . -7.4(4) ?
C15 C1 C2' C3' . . . . 110.5(4) ?
C2 C1 C5 C4 . . . . -15.51(15) ?
C2 C1 C5 C6 . . . . 102.06(13) ?
C2 C1 C5 C22 . . . . -139.03(13) ?
C2' C1 C5 C4' . . . . -15.51(15) ?
C2' C1 C5 C6 . . . . 102.06(13) ?
C2' C1 C5 C22 . . . . -139.03(13) ?
C15 C1 C5 C4 . . . . -139.04(12) ?
C15 C1 C5 C4' . . . . -139.04(12) ?
C15 C1 C5 C6 . . . . -21.48(14) ?
C15 C1 C5 C22 . . . . 97.44(13) ?
C2 C1 C15 C14 . . . . -94.01(15) ?
C2 C1 C15 C16 . . . . 145.46(14) ?
C2 C1 C15 C19 . . . . 31.79(18) ?
C2' C1 C15 C14 . . . . -94.01(15) ?
C2' C1 C15 C16 . . . . 145.46(14) ?
C2' C1 C15 C19 . . . . 31.79(18) ?
C5 C1 C15 C14 . . . . 21.58(14) ?
C5 C1 C15 C16 . . . . -98.95(13) ?
C5 C1 C15 C19 . . . . 147.39(12) ?
C1 C2 C3 C4 . . . . -37.5(2) ?
C1 C2' C3' C4' . . . . 28.4(7) ?
C2 C3 C4 C5 . . . . 26.9(2) ?
C2' C3' C4' C5 . . . . -37.3(6) ?
C3 C4 C5 C1 . . . . -6.50(17) ?
C3 C4 C5 C6 . . . . -113.49(15) ?
C3 C4 C5 C22 . . . . 118.60(15) ?
C3' C4' C5 C1 . . . . 32.1(4) ?
C3' C4' C5 C6 . . . . -74.9(4) ?
C3' C4' C5 C22 . . . . 157.2(4) ?
C1 C5 C6 N7 . . . . -169.36(16) ?
C1 C5 C6 C14 . . . . 14.02(15) ?
C4 C5 C6 N7 . . . . -58.7(2) ?
C4 C5 C6 C14 . . . . 124.72(14) ?
C4' C5 C6 N7 . . . . -58.7(2) ?
C4' C5 C6 C14 . . . . 124.72(14) ?
C22 C5 C6 N7 . . . . 69.5(2) ?
C22 C5 C6 C14 . . . . -107.11(14) ?
C1 C5 C22 C21 . . . . -132.41(15) ?
C1 C5 C22 C23 . . . . 52.30(18) ?
C4 C5 C22 C21 . . . . 108.04(16) ?
C4 C5 C22 C23 . . . . -67.25(18) ?
C4' C5 C22 C21 . . . . 108.04(16) ?
C4' C5 C22 C23 . . . . -67.25(18) ?
C6 C5 C22 C21 . . . . -20.9(2) ?
C6 C5 C22 C23 . . . . 163.78(13) ?
C5 C6 N7 C8 . . . . -176.63(15) ?
C14 C6 N7 C8 . . . . 0.10(16) ?
C5 C6 C14 C13 . . . . 176.90(11) ?
C5 C6 C14 C15 . . . . -0.66(17) ?
N7 C6 C14 C13 . . . . -0.51(16) ?
N7 C6 C14 C15 . . . . -178.07(12) ?
C6 N7 C8 C9 . . . . 179.23(15) ?
C6 N7 C8 C13 . . . . 0.36(16) ?
```

```
    N7 C8 C9 C10 . . . . -177.64(14) ?
    C13 C8 C9 C10 . . . . 1.1(2) ?
    N7 C8 C13 C12 . . . . 178.11(12) ?
    N7 C8 C13 C14 . . . . -0.65(15) ?
    C9 C8 C13 C12 . . . . -0.9(2) ?
    C9 C8 C13 C14 . . . . -179.63(13) ?
    C8 C9 C10 C11 . . . . -0.5(2) ?
    C9 C10 C11 C12 . . . . -0.4(2) ?
    C10 C11 C12 C13 . . . . 0.6(2) ?
    C11 C12 C13 C8 . . . . 0.0(2) ?
    C11 C12 C13 C14 . . . . 178.27(14) ?
    C8 C13 C14 C6 . . . . 0.70(15) ?
    C8 C13 C14 C15 . . . . 177.17(16) ?
    C12 C13 C14 C6 . . . . -177.75(15) ?
    C12 C13 C14 C15 . . . . -1.3(3) ?
    C6 C14 C15 C1 . . . . -13.29(15) ?
    C6 C14 C15 C16 . . . . 104.85(14) ?
    C6 C14 C15 C19 . . . . -138.25(13) ?
    C13 C14 C15 C1 . . . . 170.34(16) ?
    C13 C14 C15 C16 . . . . -71.5(2) ?
    C13 C14 C15 C19 . . . . 45.4(2) ?
    C1 C15 C16 C17 . . . . -85.04(14) ?
    C14 C15 C16 C17 . . . . 162.36(12) ?
    C19 C15 C16 C17 . . . . 37.06(14) ?
    C1 C15 C19 C18 . . . . 77.39(15) ?
    C14 C15 C19 C18 . . . . -165.10(12) ?
    C16 C15 C19 C18 . . . . -41.49(14) ?
    C15 C16 C17 C18 . . . . -18.99(16) ?
    C16 C17 C18 C19 . . . . -6.91(17) ?
    C17 C18 C19 C15 . . . . 30.33(16) ?
    C28 N20 C21 C22 . . . . 0.09(17) ?
    C21 N20 C28 C23 . . . . -0.48(16) ?
    C21 N20 C28 C27 . . . . 178.45(15) ?
    N20 C21 C22 C5 . . . . -175.78(13) ?
    N20 C21 C22 C23 . . . . 0.33(16) ?
    C5 C22 C23 C24 . . . . -3.6(3) ?
    C5 C22 C23 C28 . . . . 175.45(13) ?
    C21 C22 C23 C24 . . . . -179.71(15) ?
    C21 C22 C23 C28 . . . . -0.61(15) ?
    C22 C23 C24 C25 . . . . 178.81(15) ?
    C28 C23 C24 C25 . . . . -0.2(2) ?
    C22 C23 C28 N20 . . . . 0.67(15) ?
    C22 C23 C28 C27 . . . . -178.36(13) ?
    C24 C23 C28 N20 . . . . 179.96(12) ?
    C24 C23 C28 C27 . . . . 0.9(2) ?
    C23 C24 C25 C26 . . . . -0.1(2) ?
    C24 C25 C26 C27 . . . . -0.3(2) ?
    C25 C26 C27 C28 . . . . 0.9(2) ?
    C26 C27 C28 N20 . . . . 179.94(14) ?
    C26 C27 C28 C23 . . . . -1.3(2) ?
    C31 C29 C30 C31 3_757 . . . 0.1(3) ?
    C31 C29 C30 C32 3_757 . . . 178.78(19) ?
    C29 C30 C31 C29 . . . 3_757 -0.1(3) ?
    C32 C30 C31 C29 . . . 3_757 -178.80(19) ?
loop_
    _geom_hbond_atom_site_label_d
```

```
    _geom_hbond_atom_site_label_h
    _geom_hbond_atom_site_label_a
    _geom_hbond_site_symmetry_a
    _geom_hbond_distance_dh
    _geom_hbond_distance_ha
    _geom_hbond_distance_da
    _geom_hbond_angle_dha
    _geom_hbond_publ_flag
    N7 H7 C26 1_655 0.880 2.66 3.493(2) 157 y
    C11 H11 '<i>Cg</i>1' 1_554 0.950 2.82 3.5419(16) 133 y
    C12 H12 '<i>Cg</i>2' 1_554 0.950 2.70 3.4652(16) 138 y
    N20 H20 '<i>Cg</i>3' 4_555 0.880 2.82 3.5654(14) 144 y
    C21 H21 '<i>Cg</i>4' 4_555 0.950 2.92 3.4970(17) 120 y

# Some H atom labels have been edited after refinement
# so that A and B labels are grouped on the same faces
# of rings. - KJT
```

2-(2,3,4,5,6,9-Hexahydro-1*H*-cycloocta[*c*]carbazol-8-yl)aniline (11h).

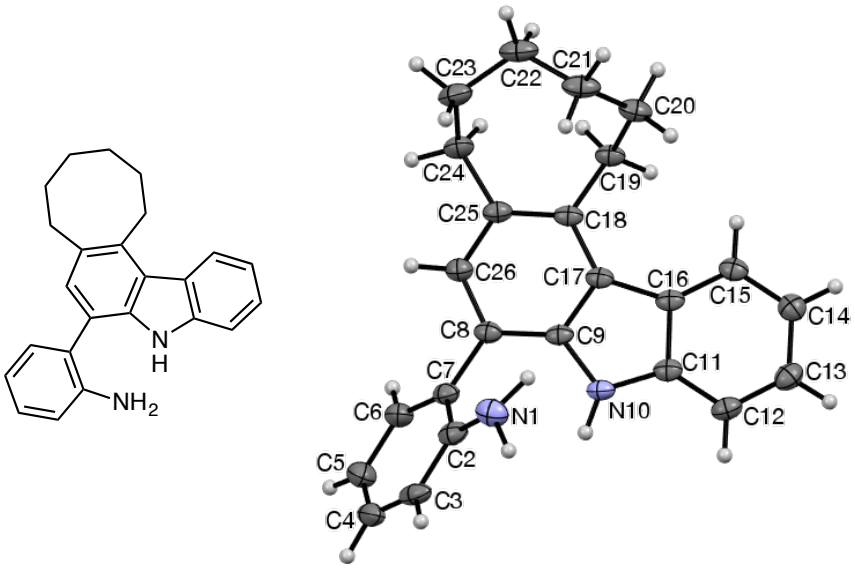

Data collection (by the XCL): A crystal (approx. 0.240 × 0.120 × 0.040 mm^3) was placed onto the tip of an 0.1 mm Mitegen mount and mounted on a Bruker VENTURE PHOTON-II diffractometer for a data collection at 123 K. A preliminary set of cell constants was calculated from reflections harvested from three sets of frames. These initial sets of frames were oriented such that orthogonal wedges of reciprocal space were surveyed. This produced an initial orientation matrix determined from 241 reflections. The data collection was carried out using CuKα radiation (parabolic mirrors) with a frame time of 10 sec and a detector distance of 40 mm. A strategy program was used to assure complete coverage of all unique data to a resolution of 0.80 Å. All major sections of frames were collected with 1.20º steps in ω or ϕ at different detector positions in 2θ. The intensity data were corrected for absorption and decay. Final cell constants were calculated from 2,991 strong reflections from the actual data collection after integration.

Structure solution and refinement (by the XCL): The space group C2/c was determined based on systematic absences and intensity statistics. A direct-methods solution was calculated that provided most non-hydrogen atoms from the E-map. Full-matrix least squares / difference Fourier cycles were performed that located the remaining non-hydrogen atoms. All non-hydrogen atoms were refined with anisotropic displacement parameters. All hydrogen atoms were placed in ideal positions and refined as riding atoms with relative isotropic displacement

parameters. The final full matrix least squares refinement converged to $R1 = 0.0469$ and $wR2 = 0.1219$ (F^2, obs. data).

CIF content:

```
data_11h

_audit_creation_method            SHELXL-2014/6
_chemical_name_systematic
;
2-(2,3,4,6,9-Hexahydro-1<i>H</i>-cycloocta[<i>c</i>]carbazol-
8-yl)aniline
;
_chemical_name_common             'cyclooctanone carbazolylaniline'
_chemical_melting_point           ?
_chemical_formula_moiety          'C24 H24 N2'
_chemical_formula_sum             'C24 H24 N2'
_chemical_formula_weight          340.45

loop_
 _atom_type_symbol
 _atom_type_description
 _atom_type_scat_dispersion_real
 _atom_type_scat_dispersion_imag
 _atom_type_scat_source
 'C'  'C'   0.0181   0.0091
 'International Tables Vol C Tables 4.2.6.8 and 6.1.1.4'
 'H'  'H'   0.0000   0.0000
 'International Tables Vol C Tables 4.2.6.8 and 6.1.1.4'
 'N'  'N'   0.0311   0.0180
 'International Tables Vol C Tables 4.2.6.8 and 6.1.1.4'

_space_group_crystal_system       monoclinic
_space_group_IT_number            15
_space_group_name_H-M_alt         'C 2/c'
_space_group_name_Hall            '-C 2yc'

_shelx_space_group_comment
;
The symmetry employed for this shelxl refinement is uniquely defined
by the following loop, which should always be used as a source of
symmetry information in preference to the above space-group names.
They are only intended as comments.
;

loop_
 _space_group_symop_operation_xyz
 'x, y, z'
 '-x, y, -z+1/2'
 'x+1/2, y+1/2, z'
 '-x+1/2, y+1/2, -z+1/2'
 '-x, -y, -z'
 'x, -y, z-1/2'
 '-x+1/2, -y+1/2, -z'
 'x+1/2, -y+1/2, z-1/2'
```

```
_cell_length_a                    30.190(3)
_cell_length_b                    7.6795(8)
_cell_length_c                    16.8507(19)
_cell_angle_alpha                 90
_cell_angle_beta                  111.120(6)
_cell_angle_gamma                 90
_cell_volume                      3644.3(7)
_cell_formula_units_Z             8
_cell_measurement_temperature     123(2)
_cell_measurement_reflns_used     2991
_cell_measurement_theta_min       3.14
_cell_measurement_theta_max       74.51

_exptl_crystal_description       'Needle'
_exptl_crystal_colour            'colourless'
_exptl_crystal_density_meas       ?
_exptl_crystal_density_method     ?
_exptl_crystal_density_diffrn     1.241
_exptl_crystal_F_000              1456
_exptl_transmission_factor_min    0.6404
_exptl_transmission_factor_max    0.7538
_exptl_crystal_size_max           0.240
_exptl_crystal_size_mid           0.120
_exptl_crystal_size_min           0.040
_exptl_absorpt_coefficient_mu     0.553
_shelx_estimated_absorpt_T_min    0.879
_shelx_estimated_absorpt_T_max    0.978
_exptl_absorpt_correction_type    multi-scan
_exptl_absorpt_correction_T_min   0.6404
_exptl_absorpt_correction_T_max   0.7538
_exptl_absorpt_process_details    'SADABS-2014/5 (Sheldrick, 2014)'
_exptl_absorpt_special_details    ?
_exptl_special_details            'K. Tritch / Prof. W. Noland'
_diffrn_ambient_temperature       123(2)
_diffrn_radiation_wavelength      1.54178
_diffrn_radiation_type            CuK\a
_diffrn_source                    'ImuS microfocus'
_diffrn_measurement_device_type   'Bruker VENTURE PHOTON-II'
_diffrn_measurement_method        '\f and \w scans'
_diffrn_detector_area_resol_mean  ?
_diffrn_reflns_number             20433
_diffrn_reflns_av_unetI/netI      0.0239
_diffrn_reflns_av_R_equivalents   0.0361
_diffrn_reflns_limit_h_min        -37
_diffrn_reflns_limit_h_max        37
_diffrn_reflns_limit_k_min        -9
_diffrn_reflns_limit_k_max        9
_diffrn_reflns_limit_l_min        -21
_diffrn_reflns_limit_l_max        21
_diffrn_reflns_theta_min          3.138
_diffrn_reflns_theta_max          74.773
_diffrn_reflns_theta_full         67.679
_diffrn_measured_fraction_theta_max   0.995
_diffrn_measured_fraction_theta_full  1.000
_diffrn_reflns_Laue_measured_fraction_max    0.995
_diffrn_reflns_Laue_measured_fraction_full   1.000
```

```
_diffrn_reflns_point_group_measured_fraction_max   0.995
_diffrn_reflns_point_group_measured_fraction_full  1.000
_reflns_number_total              3729
_reflns_number_gt                 3183
_reflns_threshold_expression      'I > 2\s(I)'
_reflns_Friedel_coverage          0.000
_reflns_Friedel_fraction_max      .
_reflns_Friedel_fraction_full     .

_reflns_special_details
;
 Reflections were merged by SHELXL according to the crystal
 class for the calculation of statistics and refinement.

 _reflns_Friedel_fraction is defined as the number of unique
 Friedel pairs measured divided by the number that would be
 possible theoretically, ignoring centric projections and
 systematic absences.
;

_computing_data_collection       'Bruker APEX3'
_computing_cell_refinement       'Bruker SAINT'
_computing_data_reduction        'Bruker SAINT'
_computing_structure_solution    'SHELXT-2014/6 (Sheldrick, 2014)'
_computing_structure_refinement  'SHELXL-2014/6 (Sheldrick, 2014)'
_computing_molecular_graphics    'Bruker SHELXTL'
_computing_publication_material  'Bruker SHELXTL'
_refine_special_details           ?
_refine_ls_structure_factor_coef  Fsqd
_refine_ls_matrix_type            full
_refine_ls_weighting_scheme       calc
_refine_ls_weighting_details
'w=1/[\s^2^(Fo^2^)+(0.0654P)^2^+3.4235P] where P=(Fo^2^+2Fc^2^)/3'
_atom_sites_solution_primary      ?
_atom_sites_solution_secondary    ?
_atom_sites_solution_hydrogens    mixed
_refine_ls_hydrogen_treatment     mixed
_refine_ls_extinction_method      none
_refine_ls_extinction_coef        .
_refine_ls_number_reflns          3729
_refine_ls_number_parameters      244
_refine_ls_number_restraints      0
_refine_ls_R_factor_all           0.0544
_refine_ls_R_factor_gt            0.0469
_refine_ls_wR_factor_ref          0.1307
_refine_ls_wR_factor_gt           0.1219
_refine_ls_goodness_of_fit_ref    1.052
_refine_ls_restrained_S_all       1.052
_refine_ls_shift/su_max           0.000
_refine_ls_shift/su_mean          0.000

loop_
 _atom_site_label
 _atom_site_type_symbol
 _atom_site_fract_x
 _atom_site_fract_y
```

```
 _atom_site_fract_z
 _atom_site_U_iso_or_equiv
 _atom_site_adp_type
 _atom_site_occupancy
 _atom_site_site_symmetry_order
 _atom_site_calc_flag
 _atom_site_refinement_flags_posn
 _atom_site_refinement_flags_adp
 _atom_site_refinement_flags_occupancy
 _atom_site_disorder_assembly
 _atom_site_disorder_group
N1 N 0.26883(5) 0.18738(19) 0.24866(10) 0.0350(3) Uani 1 1 d . . . . .
H1A H 0.2364(8) 0.223(3) 0.2095(13) 0.042 Uiso 1 1 d . U . . .
H1B H 0.2895(8) 0.141(3) 0.2192(13) 0.042 Uiso 1 1 d . U . . .
C2 C 0.26981(5) 0.08876(19) 0.31774(10) 0.0288(3) Uani 1 1 d . . . . .
C3 C 0.31151(5) -0.0063(2) 0.36270(12) 0.0342(4) Uani 1 1 d . . . . .
H3 H 0.3367 -0.0090 0.3415 0.041 Uiso 1 1 calc R U . . .
C4 C 0.31639(6) -0.0943(2) 0.43588(11) 0.0378(4) Uani 1 1 d . . . . .
H4 H 0.3444 -0.1594 0.4642 0.045 Uiso 1 1 calc R U . . .
C5 C 0.28049(7) -0.0884(2) 0.46854(11) 0.0403(4) Uani 1 1 d . . . . .
H5 H 0.2841 -0.1457 0.5205 0.048 Uiso 1 1 calc R U . . .
C6 C 0.23886(6) 0.0025(2) 0.42452(10) 0.0325(4) Uani 1 1 d . . . . .
H6 H 0.2143 0.0056 0.4472 0.039 Uiso 1 1 calc R U . . .
C7 C 0.23211(5) 0.08906(19) 0.34820(9) 0.0261(3) Uani 1 1 d . . . . .
C8 C 0.18550(5) 0.17288(18) 0.30115(9) 0.0235(3) Uani 1 1 d . . . . .
C9 C 0.15742(5) 0.12361(17) 0.21805(9) 0.0222(3) Uani 1 1 d . . . . .
N10 N 0.16837(4) 0.00535(16) 0.16601(8) 0.0243(3) Uani 1 1 d . . . . .
H10 H 0.1913(7) -0.074(3) 0.1865(11) 0.029 Uiso 1 1 d . U . . .
C11 C 0.13085(5) -0.00233(18) 0.08892(9) 0.0238(3) Uani 1 1 d . . . . .
C12 C 0.12643(5) -0.10303(19) 0.01769(10) 0.0280(3) Uani 1 1 d . . . . .
H12 H 0.1508 -0.1811 0.0177 0.034 Uiso 1 1 calc R U . . .
C13 C 0.08532(6) -0.0856(2) -0.05318(10) 0.0313(3) Uani 1 1 d . . . . .
H13 H 0.0815 -0.1529 -0.1025 0.038 Uiso 1 1 calc R U . . .
C14 C 0.04927(5) 0.0298(2) -0.05333(10) 0.0296(3) Uani 1 1 d . . . . .
H14 H 0.0214 0.0396 -0.1028 0.036 Uiso 1 1 calc R U . . .
C15 C 0.05372(5) 0.12948(18) 0.01746(9) 0.0257(3) Uani 1 1 d . . . . .
H15 H 0.0291 0.2074 0.0167 0.031 Uiso 1 1 calc R U . . .
C16 C 0.09483(5) 0.11461(17) 0.09038(9) 0.0224(3) Uani 1 1 d . . . . .
C17 C 0.11179(5) 0.19447(17) 0.17452(9) 0.0215(3) Uani 1 1 d . . . . .
C18 C 0.09205(5) 0.31434(17) 0.21582(9) 0.0224(3) Uani 1 1 d . . . . .
C19 C 0.04215(5) 0.38205(19) 0.17286(10) 0.0254(3) Uani 1 1 d . . . . .
H19A H 0.0288 0.4100 0.2171 0.030 Uiso 1 1 calc R U . . .
H19B H 0.0224 0.2884 0.1368 0.030 Uiso 1 1 calc R U . . .
C20 C 0.03843(6) 0.5439(2) 0.11768(11) 0.0322(3) Uani 1 1 d . . . . .
H20B H 0.0454 0.5091 0.0668 0.039 Uiso 1 1 calc R U . . .
H20A H 0.0052 0.5859 0.0977 0.039 Uiso 1 1 calc R U . . .
C21 C 0.07095(6) 0.6953(2) 0.16039(12) 0.0357(4) Uani 1 1 d . . . . .
H21A H 0.0633 0.7941 0.1200 0.043 Uiso 1 1 calc R U . . .
H21B H 0.1040 0.6598 0.1702 0.043 Uiso 1 1 calc R U . . .
C22 C 0.06898(6) 0.7609(2) 0.24485(12) 0.0377(4) Uani 1 1 d . . . . .
H22A H 0.0373 0.7320 0.2463 0.045 Uiso 1 1 calc R U . . .
H22B H 0.0717 0.8894 0.2457 0.045 Uiso 1 1 calc R U . . .
C23 C 0.10683(6) 0.6898(2) 0.32645(12) 0.0365(4) Uani 1 1 d . . . . .
H23B H 0.1383 0.7066 0.3219 0.044 Uiso 1 1 calc R U . . .
H23A H 0.1061 0.7615 0.3748 0.044 Uiso 1 1 calc R U . . .
C24 C 0.10251(6) 0.4979(2) 0.34808(10) 0.0304(3) Uani 1 1 d . . . . .
```

```
H24B H 0.1207 0.4805 0.4095 0.036 Uiso 1 1 calc R U . . .
H24A H 0.0688 0.4730 0.3381 0.036 Uiso 1 1 calc R U . . .
C25 C 0.11979(5) 0.36661(19) 0.29834(9) 0.0247(3) Uani 1 1 d . . . . .
C26 C 0.16558(5) 0.29564(19) 0.33877(10) 0.0256(3) Uani 1 1 d . . . . .
H26 H 0.1837 0.3339 0.3947 0.031 Uiso 1 1 calc R U . . .

loop_
 _atom_site_aniso_label
 _atom_site_aniso_U_11
 _atom_site_aniso_U_22
 _atom_site_aniso_U_33
 _atom_site_aniso_U_23
 _atom_site_aniso_U_13
 _atom_site_aniso_U_12
N1 0.0275(7) 0.0315(8) 0.0466(8) 0.0025(6) 0.0139(6) -0.0011(5)
C2 0.0243(7) 0.0202(7) 0.0425(8) -0.0079(6) 0.0129(6) -0.0045(6)
C3 0.0206(7) 0.0235(8) 0.0574(10) -0.0151(7) 0.0129(7) -0.0021(6)
C4 0.0286(8) 0.0289(8) 0.0446(9) -0.0091(7) -0.0007(7) 0.0072(6)
C5 0.0419(9) 0.0335(9) 0.0372(9) 0.0003(7) 0.0042(7) 0.0114(7)
C6 0.0318(8) 0.0310(8) 0.0333(8) -0.0010(6) 0.0100(6) 0.0084(6)
C7 0.0220(7) 0.0198(7) 0.0351(8) -0.0051(6) 0.0086(6) 0.0009(5)
C8 0.0217(6) 0.0187(6) 0.0314(7) 0.0028(5) 0.0113(5) 0.0006(5)
C9 0.0226(6) 0.0144(6) 0.0329(7) 0.0020(5) 0.0140(6) -0.0002(5)
N10 0.0224(6) 0.0173(6) 0.0350(7) -0.0002(5) 0.0125(5) 0.0027(5)
C11 0.0238(7) 0.0166(6) 0.0341(7) 0.0023(5) 0.0142(6) -0.0019(5)
C12 0.0308(7) 0.0209(7) 0.0373(8) -0.0013(6) 0.0183(6) 0.0000(6)
C13 0.0389(8) 0.0245(7) 0.0338(8) -0.0025(6) 0.0173(7) -0.0035(6)
C14 0.0295(7) 0.0267(7) 0.0318(7) 0.0020(6) 0.0101(6) -0.0025(6)
C15 0.0256(7) 0.0195(7) 0.0335(7) 0.0050(6) 0.0124(6) 0.0001(5)
C16 0.0232(7) 0.0145(6) 0.0332(7) 0.0031(5) 0.0148(6) -0.0014(5)
C17 0.0205(6) 0.0149(6) 0.0315(7) 0.0037(5) 0.0121(5) -0.0009(5)
C18 0.0219(6) 0.0162(6) 0.0333(7) 0.0048(5) 0.0148(6) 0.0008(5)
C19 0.0220(7) 0.0214(7) 0.0356(8) 0.0030(6) 0.0138(6) 0.0023(5)
C20 0.0316(8) 0.0259(8) 0.0412(8) 0.0090(6) 0.0156(7) 0.0080(6)
C21 0.0357(8) 0.0223(8) 0.0571(10) 0.0102(7) 0.0261(8) 0.0061(6)
C22 0.0362(8) 0.0214(8) 0.0626(11) 0.0019(7) 0.0263(8) 0.0059(6)
C23 0.0329(8) 0.0253(8) 0.0547(10) -0.0085(7) 0.0197(7) 0.0030(6)
C24 0.0290(7) 0.0287(8) 0.0364(8) -0.0015(6) 0.0154(6) 0.0060(6)
C25 0.0256(7) 0.0195(7) 0.0332(7) 0.0024(6) 0.0155(6) 0.0018(5)
C26 0.0259(7) 0.0220(7) 0.0303(7) 0.0003(6) 0.0117(6) 0.0011(5)

_geom_special_details
;
 All esds (except the esd in the dihedral angle between two l.s. planes)
 are estimated using the full covariance matrix.  The cell esds are taken
 into account individually in the estimation of esds in distances, angles
 and torsion angles; correlations between esds in cell parameters are only
 used when they are defined by crystal symmetry.  An approximate (isotropic)
 treatment of cell esds is used for estimating esds involving l.s. planes.
;

loop_
 _geom_bond_atom_site_label_1
 _geom_bond_atom_site_label_2
 _geom_bond_distance
 _geom_bond_site_symmetry_2
```

```
 _geom_bond_publ_flag
N1 C2 1.380(2) . ?
N1 H1A 1.00(2) . ?
N1 H1B 0.99(2) . ?
C2 C7 1.407(2) . ?
C2 C3 1.416(2) . ?
C3 C4 1.367(3) . ?
C3 H3 0.9500 . ?
C4 C5 1.382(3) . ?
C4 H4 0.9500 . ?
C5 C6 1.395(2) . ?
C5 H5 0.9500 . ?
C6 C7 1.396(2) . ?
C6 H6 0.9500 . ?
C7 C8 1.4896(19) . ?
C8 C26 1.388(2) . ?
C8 C9 1.403(2) . ?
C9 N10 1.3827(18) . ?
C9 C17 1.4156(19) . ?
N10 C11 1.3834(19) . ?
N10 H10 0.89(2) . ?
C11 C12 1.393(2) . ?
C11 C16 1.4172(19) . ?
C12 C13 1.384(2) . ?
C12 H12 0.9500 . ?
C13 C14 1.403(2) . ?
C13 H13 0.9500 . ?
C14 C15 1.382(2) . ?
C14 H14 0.9500 . ?
C15 C16 1.402(2) . ?
C15 H15 0.9500 . ?
C16 C17 1.458(2) . ?
C17 C18 1.4093(19) . ?
C18 C25 1.399(2) . ?
C18 C19 1.5092(19) . ?
C19 C20 1.532(2) . ?
C19 H19A 0.9900 . ?
C19 H19B 0.9900 . ?
C20 C21 1.524(2) . ?
C20 H20B 0.9900 . ?
C20 H20A 0.9900 . ?
C21 C22 1.531(3) . ?
C21 H21A 0.9900 . ?
C21 H21B 0.9900 . ?
C22 C23 1.537(3) . ?
C22 H22A 0.9900 . ?
C22 H22B 0.9900 . ?
C23 C24 1.535(2) . ?
C23 H23B 0.9900 . ?
C23 H23A 0.9900 . ?
C24 C25 1.519(2) . ?
C24 H24B 0.9900 . ?
C24 H24A 0.9900 . ?
C25 C26 1.412(2) . ?
C26 H26 0.9500 . ?
```

```
loop_
 _geom_angle_atom_site_label_1
 _geom_angle_atom_site_label_2
 _geom_angle_atom_site_label_3
 _geom_angle
 _geom_angle_site_symmetry_1
 _geom_angle_site_symmetry_3
 _geom_angle_publ_flag
C2 N1 H1A 115.1(12) . . ?
C2 N1 H1B 113.5(12) . . ?
H1A N1 H1B 114.1(17) . . ?
N1 C2 C7 122.17(14) . . ?
N1 C2 C3 118.61(14) . . ?
C7 C2 C3 119.07(15) . . ?
C4 C3 C2 121.57(15) . . ?
C4 C3 H3 119.2 . . ?
C2 C3 H3 119.2 . . ?
C3 C4 C5 119.88(15) . . ?
C3 C4 H4 120.1 . . ?
C5 C4 H4 120.1 . . ?
C4 C5 C6 119.37(17) . . ?
C4 C5 H5 120.3 . . ?
C6 C5 H5 120.3 . . ?
C5 C6 C7 122.19(16) . . ?
C5 C6 H6 118.9 . . ?
C7 C6 H6 118.9 . . ?
C6 C7 C2 117.81(14) . . ?
C6 C7 C8 119.50(13) . . ?
C2 C7 C8 122.66(14) . . ?
C26 C8 C9 115.70(13) . . ?
C26 C8 C7 122.14(13) . . ?
C9 C8 C7 122.00(13) . . ?
N10 C9 C8 127.86(13) . . ?
N10 C9 C17 109.52(12) . . ?
C8 C9 C17 122.61(13) . . ?
C9 N10 C11 108.76(12) . . ?
C9 N10 H10 122.2(12) . . ?
C11 N10 H10 126.3(12) . . ?
N10 C11 C12 128.64(13) . . ?
N10 C11 C16 109.29(12) . . ?
C12 C11 C16 122.06(14) . . ?
C13 C12 C11 117.84(14) . . ?
C13 C12 H12 121.1 . . ?
C11 C12 H12 121.1 . . ?
C12 C13 C14 121.11(14) . . ?
C12 C13 H13 119.4 . . ?
C14 C13 H13 119.4 . . ?
C15 C14 C13 120.94(14) . . ?
C15 C14 H14 119.5 . . ?
C13 C14 H14 119.5 . . ?
C14 C15 C16 119.43(13) . . ?
C14 C15 H15 120.3 . . ?
C16 C15 H15 120.3 . . ?
C15 C16 C11 118.62(13) . . ?
C15 C16 C17 135.07(13) . . ?
C11 C16 C17 106.31(12) . . ?
```

```
C18 C17 C9 120.06(13) . . ?
C18 C17 C16 133.82(13) . . ?
C9 C17 C16 106.10(12) . . ?
C25 C18 C17 118.03(13) . . ?
C25 C18 C19 120.98(13) . . ?
C17 C18 C19 120.98(13) . . ?
C18 C19 C20 114.39(12) . . ?
C18 C19 H19A 108.7 . . ?
C20 C19 H19A 108.7 . . ?
C18 C19 H19B 108.7 . . ?
C20 C19 H19B 108.7 . . ?
H19A C19 H19B 107.6 . . ?
C21 C20 C19 115.99(13) . . ?
C21 C20 H20B 108.3 . . ?
C19 C20 H20B 108.3 . . ?
C21 C20 H20A 108.3 . . ?
C19 C20 H20A 108.3 . . ?
H20B C20 H20A 107.4 . . ?
C20 C21 C22 117.11(14) . . ?
C20 C21 H21A 108.0 . . ?
C22 C21 H21A 108.0 . . ?
C20 C21 H21B 108.0 . . ?
C22 C21 H21B 108.0 . . ?
H21A C21 H21B 107.3 . . ?
C21 C22 C23 116.69(13) . . ?
C21 C22 H22A 108.1 . . ?
C23 C22 H22A 108.1 . . ?
C21 C22 H22B 108.1 . . ?
C23 C22 H22B 108.1 . . ?
H22A C22 H22B 107.3 . . ?
C24 C23 C22 117.01(14) . . ?
C24 C23 H23B 108.0 . . ?
C22 C23 H23B 108.0 . . ?
C24 C23 H23A 108.0 . . ?
C22 C23 H23A 108.0 . . ?
H23B C23 H23A 107.3 . . ?
C25 C24 C23 115.53(13) . . ?
C25 C24 H24B 108.4 . . ?
C23 C24 H24B 108.4 . . ?
C25 C24 H24A 108.4 . . ?
C23 C24 H24A 108.4 . . ?
H24B C24 H24A 107.5 . . ?
C18 C25 C26 120.03(13) . . ?
C18 C25 C24 122.50(13) . . ?
C26 C25 C24 117.47(13) . . ?
C8 C26 C25 123.49(14) . . ?
C8 C26 H26 118.3 . . ?
C25 C26 H26 118.3 . . ?

loop_
 _geom_torsion_atom_site_label_1
 _geom_torsion_atom_site_label_2
 _geom_torsion_atom_site_label_3
 _geom_torsion_atom_site_label_4
 _geom_torsion
 _geom_torsion_site_symmetry_1
```

```
 _geom_torsion_site_symmetry_2
 _geom_torsion_site_symmetry_3
 _geom_torsion_site_symmetry_4
 _geom_torsion_publ_flag
N1 C2 C3 C4 174.24(14) . . . . ?
C7 C2 C3 C4 -1.5(2) . . . . ?
C2 C3 C4 C5 -1.4(2) . . . . ?
C3 C4 C5 C6 2.3(3) . . . . ?
C4 C5 C6 C7 -0.2(3) . . . . ?
C5 C6 C7 C2 -2.6(2) . . . . ?
C5 C6 C7 C8 175.60(15) . . . . ?
N1 C2 C7 C6 -172.14(14) . . . . ?
C3 C2 C7 C6 3.5(2) . . . . ?
N1 C2 C7 C8 9.7(2) . . . . ?
C3 C2 C7 C8 -174.73(13) . . . . ?
C6 C7 C8 C26 55.6(2) . . . . ?
C2 C7 C8 C26 -126.21(16) . . . . ?
C6 C7 C8 C9 -119.68(16) . . . . ?
C2 C7 C8 C9 58.5(2) . . . . ?
C26 C8 C9 N10 179.88(13) . . . . ?
C7 C8 C9 N10 -4.5(2) . . . . ?
C26 C8 C9 C17 0.4(2) . . . . ?
C7 C8 C9 C17 176.01(13) . . . . ?
C8 C9 N10 C11 -179.29(13) . . . . ?
C17 C9 N10 C11 0.24(15) . . . . ?
C9 N10 C11 C12 179.79(14) . . . . ?
C9 N10 C11 C16 0.56(15) . . . . ?
N10 C11 C12 C13 -178.94(14) . . . . ?
C16 C11 C12 C13 0.2(2) . . . . ?
C11 C12 C13 C14 0.0(2) . . . . ?
C12 C13 C14 C15 -0.1(2) . . . . ?
C13 C14 C15 C16 -0.1(2) . . . . ?
C14 C15 C16 C11 0.3(2) . . . . ?
C14 C15 C16 C17 -179.66(14) . . . . ?
N10 C11 C16 C15 178.89(12) . . . . ?
C12 C11 C16 C15 -0.4(2) . . . . ?
N10 C11 C16 C17 -1.11(15) . . . . ?
C12 C11 C16 C17 179.60(13) . . . . ?
N10 C9 C17 C18 177.82(12) . . . . ?
C8 C9 C17 C18 -2.6(2) . . . . ?
N10 C9 C17 C16 -0.91(15) . . . . ?
C8 C9 C17 C16 178.65(12) . . . . ?
C15 C16 C17 C18 2.7(3) . . . . ?
C11 C16 C17 C18 -177.26(14) . . . . ?
C15 C16 C17 C9 -178.79(15) . . . . ?
C11 C16 C17 C9 1.21(14) . . . . ?
C9 C17 C18 C25 3.29(19) . . . . ?
C16 C17 C18 C25 -178.41(14) . . . . ?
C9 C17 C18 C19 -175.72(12) . . . . ?
C16 C17 C18 C19 2.6(2) . . . . ?
C25 C18 C19 C20 93.27(17) . . . . ?
C17 C18 C19 C20 -87.75(16) . . . . ?
C18 C19 C20 C21 -51.77(18) . . . . ?
C19 C20 C21 C22 -53.34(19) . . . . ?
C20 C21 C22 C23 96.62(18) . . . . ?
C21 C22 C23 C24 -70.60(19) . . . . ?
```

```
C22 C23 C24 C25 78.43(18) . . . . ?
C17 C18 C25 C26 -1.9(2) . . . . ?
C19 C18 C25 C26 177.13(13) . . . . ?
C17 C18 C25 C24 178.69(13) . . . . ?
C19 C18 C25 C24 -2.3(2) . . . . ?
C23 C24 C25 C18 -80.89(18) . . . . ?
C23 C24 C25 C26 99.66(17) . . . . ?
C9 C8 C26 C25 1.1(2) . . . . ?
C7 C8 C26 C25 -174.52(14) . . . . ?
C18 C25 C26 C8 -0.3(2) . . . . ?
C24 C25 C26 C8 179.12(13) . . . . ?

loop_
 _geom_hbond_atom_site_label_D
 _geom_hbond_atom_site_label_H
 _geom_hbond_atom_site_label_A
 _geom_hbond_distance_DH
 _geom_hbond_distance_HA
 _geom_hbond_distance_DA
 _geom_hbond_angle_DHA
 _geom_hbond_site_symmetry_A
N10 H10 N1  0.89(2) 2.25(2) 3.1081(19) 161.7(16) 4_545

_refine_diff_density_max    0.822
_refine_diff_density_min   -0.270
_refine_diff_density_rms    0.047

_shelxl_version_number 2014/6

_shelx_res_file
;

TITL 16225a in C2/c
CELL  1.54178  30.1901   7.6795  16.8507   90.000  111.120   90.000
ZERR    8.000   0.0031   0.0008   0.0019    0.000    0.006    0.000
LATT  7
SYMM -X, Y, 1/2-Z
SFAC C   H   N
UNIT 192 192 16
TEMP -150.130
SIZE 0.04 0.12 0.24

L.S. 10
ACTA
CONF
BOND $H
LIST 4
FMAP 2
PLAN 20
EQIV $1 -x+1/2, y-1/2, -z+1/2
HTAB N10 N1_$1

WGHT    0.065400    3.423500
FVAR       0.07699
N1    3    0.268827    0.187381    0.248663    11.00000    0.02749    0.03147 =
         0.04656    0.00247    0.01392   -0.00115
```

```
REM  AFIX  93
H1A   2    0.236391    0.222728    0.209485    11.00000   -1.20000
H1B   2    0.289481    0.141133    0.219233    11.00000   -1.20000
REM  AFIX   0
C2    1    0.269806    0.088758    0.317744    11.00000    0.02430    0.02023 =
         0.04249   -0.00785    0.01286   -0.00447
C3    1    0.311512   -0.006318    0.362705    11.00000    0.02062    0.02351 =
         0.05738   -0.01511    0.01287   -0.00205
AFIX  43
H3    2    0.336704   -0.009025    0.341493    11.00000   -1.20000
AFIX   0
C4    1    0.316391   -0.094276    0.435882    11.00000    0.02856    0.02891 =
         0.04455   -0.00905   -0.00067    0.00716
AFIX  43
H4    2    0.344412   -0.159354    0.464248    11.00000   -1.20000
AFIX   0
C5    1    0.280491   -0.088378    0.468538    11.00000    0.04194    0.03352 =
         0.03720    0.00031    0.00416    0.01139
AFIX  43
H5    2    0.284132   -0.145689    0.520478    11.00000   -1.20000
AFIX   0
C6    1    0.238862    0.002508    0.424523    11.00000    0.03185    0.03100 =
         0.03326   -0.00099    0.01002    0.00844
AFIX  43
H6    2    0.214282    0.005614    0.447239    11.00000   -1.20000
AFIX   0
C7    1    0.232112    0.089062    0.348202    11.00000    0.02203    0.01984 =
         0.03513   -0.00512    0.00859    0.00091
C8    1    0.185504    0.172882    0.301155    11.00000    0.02173    0.01874 =
         0.03136    0.00281    0.01126    0.00055
C9    1    0.157424    0.123610    0.218052    11.00000    0.02261    0.01438 =
         0.03294    0.00196    0.01396   -0.00018
N10   3    0.168370    0.005349    0.166011    11.00000    0.02239    0.01728 =
         0.03501   -0.00023    0.01250    0.00275
REM  AFIX  43
H10   2    0.191252   -0.073981    0.186470    11.00000   -1.20000
REM  AFIX   0
C11   1    0.130846   -0.002332    0.088918    11.00000    0.02385    0.01660 =
         0.03411    0.00229    0.01420   -0.00193
C12   1    0.126432   -0.103035    0.017687    11.00000    0.03083    0.02092 =
         0.03728   -0.00128    0.01832   -0.00004
AFIX  43
H12   2    0.150846   -0.181144    0.017746    11.00000   -1.20000
AFIX   0
C13   1    0.085315   -0.085577   -0.053183    11.00000    0.03891    0.02454 =
         0.03376   -0.00248    0.01726   -0.00349
AFIX  43
H13   2    0.081450   -0.152863   -0.102543    11.00000   -1.20000
AFIX   0
C14   1    0.049266    0.029798   -0.053325    11.00000    0.02954    0.02672 =
         0.03176    0.00197    0.01006   -0.00248
AFIX  43
H14   2    0.021395    0.039576   -0.102765    11.00000   -1.20000
AFIX   0
C15   1    0.053719    0.129479    0.017458    11.00000    0.02563    0.01954 =
         0.03354    0.00497    0.01243    0.00011
```

```
AFIX  43
H15  2    0.029123    0.207387    0.016681    11.00000   -1.20000
AFIX   0
C16   1    0.094834    0.114606    0.090379    11.00000    0.02318    0.01453 =
         0.03323    0.00310    0.01479   -0.00143
C17   1    0.111789    0.194469    0.174516    11.00000    0.02049    0.01487 =
         0.03148    0.00365    0.01215   -0.00091
C18   1    0.092046    0.314340    0.215823    11.00000    0.02190    0.01622 =
         0.03325    0.00482    0.01484    0.00079
C19   1    0.042148    0.382047    0.172859    11.00000    0.02200    0.02142 =
         0.03563    0.00298    0.01380    0.00228
AFIX  23
H19A  2    0.028813    0.410030    0.217095    11.00000   -1.20000
H19B  2    0.022424    0.288450    0.136769    11.00000   -1.20000
AFIX   0
C20   1    0.038428    0.543942    0.117679    11.00000    0.03157    0.02593 =
         0.04117    0.00898    0.01556    0.00798
AFIX  23
H20B  2    0.045370    0.509052    0.066805    11.00000   -1.20000
H20A  2    0.005200    0.585897    0.097741    11.00000   -1.20000
AFIX   0
C21   1    0.070955    0.695256    0.160387    11.00000    0.03566    0.02229 =
         0.05707    0.01017    0.02610    0.00605
AFIX  23
H21A  2    0.063327    0.794130    0.119984    11.00000   -1.20000
H21B  2    0.104048    0.659849    0.170245    11.00000   -1.20000
AFIX   0
C22   1    0.068982    0.760908    0.244852    11.00000    0.03618    0.02138 =
         0.06264    0.00190    0.02627    0.00591
AFIX  23
H22A  2    0.037331    0.732047    0.246340    11.00000   -1.20000
H22B  2    0.071659    0.889433    0.245678    11.00000   -1.20000
AFIX   0
C23   1    0.106829    0.689806    0.326451    11.00000    0.03288    0.02529 =
         0.05470   -0.00847    0.01974    0.00297
AFIX  23
H23B  2    0.138340    0.706619    0.321901    11.00000   -1.20000
H23A  2    0.106148    0.761502    0.374826    11.00000   -1.20000
AFIX   0
C24   1    0.102515    0.497907    0.348082    11.00000    0.02904    0.02872 =
         0.03639   -0.00148    0.01536    0.00597
AFIX  23
H24B  2    0.120689    0.480460    0.409472    11.00000   -1.20000
H24A  2    0.068759    0.472996    0.338132    11.00000   -1.20000
AFIX   0
C25   1    0.119795    0.366609    0.298340    11.00000    0.02556    0.01950 =
         0.03318    0.00242    0.01549    0.00177
C26   1    0.165583    0.295640    0.338774    11.00000    0.02590    0.02205 =
         0.03030    0.00031    0.01169    0.00114
AFIX  43
H26  2    0.183722    0.333931    0.394698    11.00000   -1.20000

AFIX   0
HKLF 4

REM  16225a in C2/c
```

```
REM R1 =  0.0469 for    3183 Fo > 4sig(Fo)  and  0.0544 for all    3729 data
REM    244 parameters refined using      0 restraints

END

WGHT      0.0654      3.4325

REM Highest difference peak  0.822,  deepest hole -0.270,  1-sigma level  0.047
Q1    1   0.2926 -0.0311  0.4399  11.00000  0.05    0.38
Q2    1   0.3030  0.0720  0.3175  11.00000  0.05    0.34
Q3    1   0.2516  0.1039  0.3388  11.00000  0.05    0.23
Q4    1   0.3238 -0.0004  0.4111  11.00000  0.05    0.22
Q5    1   0.1458  0.3569  0.3103  11.00000  0.05    0.22
Q6    1   0.1135  0.0613  0.0871  11.00000  0.05    0.22
Q7    1   0.0427  0.4640  0.1503  11.00000  0.05    0.21
Q8    1   0.0698  0.3528  0.1950  11.00000  0.05    0.21
Q9    1   0.1022  0.3136  0.2667  11.00000  0.05    0.21
Q10   1   0.1711  0.1463  0.2602  11.00000  0.05    0.20
Q11   1   0.0713  0.1053  0.0694  11.00000  0.05    0.20
Q12   1   0.1113  0.4356  0.3216  11.00000  0.05    0.19
Q13   1   0.1341  0.1678  0.2046  11.00000  0.05    0.19
Q14   1   0.2435  0.0852  0.3980  11.00000  0.05    0.19
Q15   1   0.2085  0.1328  0.3206  11.00000  0.05    0.18
Q16   1   0.3305  0.0044  0.3007  11.00000  0.05    0.18
Q17   1   0.2580  0.1218  0.2763  11.00000  0.05    0.17
Q18   1   0.0981  0.1618  0.1326  11.00000  0.05    0.17
Q19   1   0.1069  0.2841  0.1872  11.00000  0.05    0.17
Q20   1   0.1670  0.2005  0.3222  11.00000  0.05    0.16
;
_shelx_res_checksum   48549

# Some H atom labels have been edited after refinement
# so that A and B labels are grouped on the same faces
# of rings. - KJT
```

***rac*-1,2,3,4,5,6,11,12-Octahydro-12-methylbenzo[4,5][1,3]diazepino[1,7,6-*lm*]cycloocta[*c*]carbazole (12h)**.

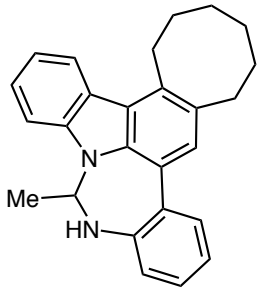

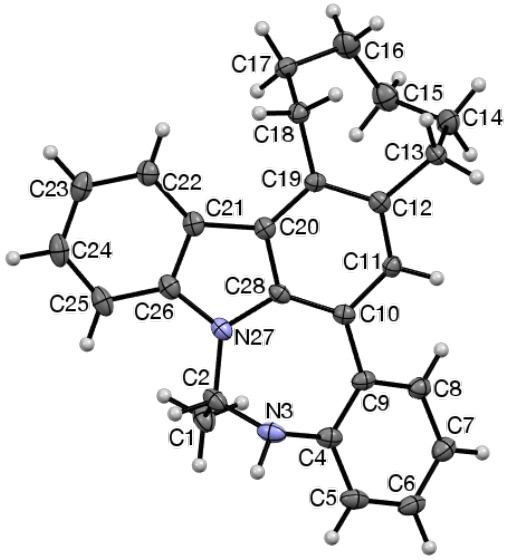

Data collection (by the XCL): A crystal (approx. 0.175 × 0.110 × 0.070 mm^3) was placed onto the tip of an 0.05 mm Mitegen loop and mounted on a Bruker-AXS Venture D8 diffractometer for a data collection at 123 K. A preliminary set of cell constants was calculated from reflections harvested from three sets of frames. These initial sets of frames were oriented such that orthogonal wedges of reciprocal space were surveyed. This produced an initial orientation matrix determined from 316 reflections. The data collection was carried out using CuKα radiation (parabolic mirrors) with a frame time of 5 or 10 sec and a detector distance of 40 mm. A strategy program was used to assure complete coverage of all unique data to a resolution of 0.80 Å. All major sections of frames were collected with 0.80° steps in ω or ϕ at different detector positions in 2θ. The intensity data were corrected for absorption and decay. Final cell constants were calculated from 2,977 strong reflections from the actual data collection after integration.

Structure solution and refinement (by the XCL): The space group $P2_12_12_1$ was determined based on systematic absences and intensity statistics. A direct-methods solution was calculated that provided most non-hydrogen atoms from the E-map. Full-matrix least squares / difference Fourier cycles were performed that located the remaining non-hydrogen atoms. All non-hydrogen atoms were refined with anisotropic displacement parameters. All hydrogen atoms were placed in ideal positions and refined as riding atoms with relative isotropic displacement

parameters. The final full matrix least squares refinement converged to $R1 = 0.0398$ and $wR2 = 0.0966$ (F^2, obs. data).

CIF content:

```
data_12h

_audit_creation_method            SHELXL-2014/6
_chemical_name_systematic
;
<i>rac</i>-1,2,3,4,5,6,11,12-Octahydro-12-methylbenzo[4,5][1,3]diazepino
[1,7,6-<i>lm</i>]cycloocta[<i>c</i>]carbazole
;
_chemical_name_common             'cyclooctanone diazepine'
_chemical_melting_point           ?
_chemical_formula_moiety          'C26 H26 N2'
_chemical_formula_sum             'C26 H26 N2'
_chemical_formula_weight          366.49

loop_
 _atom_type_symbol
 _atom_type_description
 _atom_type_scat_dispersion_real
 _atom_type_scat_dispersion_imag
 _atom_type_scat_source
 'C'  'C'   0.0181   0.0091
 'International Tables Vol C Tables 4.2.6.8 and 6.1.1.4'
 'H'  'H'   0.0000   0.0000
 'International Tables Vol C Tables 4.2.6.8 and 6.1.1.4'
 'N'  'N'   0.0311   0.0180
 'International Tables Vol C Tables 4.2.6.8 and 6.1.1.4'

_space_group_crystal_system       orthorhombic
_space_group_IT_number            19
_space_group_name_H-M_alt         'P 21 21 21'
_space_group_name_Hall            'P 2ac 2ab'

_shelx_space_group_comment
;
The symmetry employed for this shelxl refinement is uniquely defined
by the following loop, which should always be used as a source of
symmetry information in preference to the above space-group names.
They are only intended as comments.
;

loop_
 _space_group_symop_operation_xyz
 'x, y, z'
 '-x+1/2, -y, z+1/2'
 '-x, y+1/2, -z+1/2'
 'x+1/2, -y+1/2, -z'

_cell_length_a                    8.8186(4)
_cell_length_b                    13.5847(6)
_cell_length_c                    15.8483(7)
_cell_angle_alpha                 90
```

```
_cell_angle_beta                   90
_cell_angle_gamma                  90
_cell_volume                       1898.60(15)
_cell_formula_units_Z              4
_cell_measurement_temperature      123(2)
_cell_measurement_reflns_used      2977
_cell_measurement_theta_min        5.74
_cell_measurement_theta_max        74.41

_exptl_crystal_description        'block'
_exptl_crystal_colour             'colourless'
_exptl_crystal_density_meas        ?
_exptl_crystal_density_method      ?
_exptl_crystal_density_diffrn      1.282
_exptl_crystal_F_000               784
_exptl_transmission_factor_min     0.7073
_exptl_transmission_factor_max     0.7538
_exptl_crystal_size_max            0.175
_exptl_crystal_size_mid            0.110
_exptl_crystal_size_min            0.070
_exptl_absorpt_coefficient_mu      0.569
_shelx_estimated_absorpt_T_min     0.907
_shelx_estimated_absorpt_T_max     0.961
_exptl_absorpt_correction_type     multi-scan
_exptl_absorpt_correction_T_min    0.7073
_exptl_absorpt_correction_T_max    0.7538
_exptl_absorpt_process_details     'SADABS-2014/5 (Sheldrick, 2014)'
_exptl_absorpt_special_details     ?
_exptl_special_details             'K. Tritch / Prof. W. Noland'
_diffrn_ambient_temperature        123(2)
_diffrn_radiation_wavelength       1.54178
_diffrn_radiation_type             CuK\a
_diffrn_source                     'ImuS microfucus'
_diffrn_measurement_device_type    'Bruker-AXS Venture D8'
_diffrn_measurement_method         '\f and \w scans'
_diffrn_detector_area_resol_mean   ?
_diffrn_reflns_number              22976
_diffrn_reflns_av_unetI/netI       0.0216
_diffrn_reflns_av_R_equivalents    0.0340
_diffrn_reflns_limit_h_min         -11
_diffrn_reflns_limit_h_max         10
_diffrn_reflns_limit_k_min         -16
_diffrn_reflns_limit_k_max         16
_diffrn_reflns_limit_l_min         -19
_diffrn_reflns_limit_l_max         19
_diffrn_reflns_theta_min           4.286
_diffrn_reflns_theta_max           74.641
_diffrn_reflns_theta_full          67.679
_diffrn_measured_fraction_theta_max   0.997
_diffrn_measured_fraction_theta_full  0.999
_diffrn_reflns_Laue_measured_fraction_max    0.997
_diffrn_reflns_Laue_measured_fraction_full   0.999
_diffrn_reflns_point_group_measured_fraction_max   0.995
_diffrn_reflns_point_group_measured_fraction_full  0.999
_reflns_number_total               3861
_reflns_number_gt                  3700
```

```
_reflns_threshold_expression      'I > 2\s(I)'
_reflns_Friedel_coverage          0.745
_reflns_Friedel_fraction_max      0.992
_reflns_Friedel_fraction_full     0.998

_reflns_special_details
;
 Reflections were merged by SHELXL according to the crystal
 class for the calculation of statistics and refinement.

 _reflns_Friedel_fraction is defined as the number of unique
 Friedel pairs measured divided by the number that would be
 possible theoretically, ignoring centric projections and
 systematic absences.
;

_computing_data_collection       'Bruker APEX3'
_computing_cell_refinement       'Bruker SAINT'
_computing_data_reduction        'Bruker SAINT'
_computing_structure_solution    'SHELXT-2014/5 (Sheldrick, 2014)'
_computing_structure_refinement  'SHELXL-2014/6 (Sheldrick, 2014)'
_computing_molecular_graphics    'Bruker SHELXTL'
_computing_publication_material  'Bruker SHELXTL'
_refine_special_details           ?
_refine_ls_structure_factor_coef  Fsqd
_refine_ls_matrix_type            full
_refine_ls_weighting_scheme       calc
_refine_ls_weighting_details
'w=1/[\s^2^(Fo^2^)+(0.0425P)^2^+0.8498P] where P=(Fo^2^+2Fc^2^)/3'
_atom_sites_solution_primary      ?
_atom_sites_solution_secondary    ?
_atom_sites_solution_hydrogens    mixed
_refine_ls_hydrogen_treatment     mixed
_refine_ls_extinction_method      none
_refine_ls_extinction_coef        .
_refine_ls_abs_structure_details
;
 Flack x determined using 1560 quotients [(I+)-(I-)]/[(I+)+(I-)]
 (Parsons, Flack and Wagner, Acta Cryst. B69 (2013) 249-259).
;
_refine_ls_abs_structure_Flack    -0.05(17)
_chemical_absolute_configuration  unk
_refine_ls_number_reflns          3861
_refine_ls_number_parameters      257
_refine_ls_number_restraints      1
_refine_ls_R_factor_all           0.0427
_refine_ls_R_factor_gt            0.0398
_refine_ls_wR_factor_ref          0.1005
_refine_ls_wR_factor_gt           0.0966
_refine_ls_goodness_of_fit_ref    1.107
_refine_ls_restrained_S_all       1.107
_refine_ls_shift/su_max           0.000
_refine_ls_shift/su_mean          0.000

loop_
 _atom_site_label
```

```
 _atom_site_type_symbol
 _atom_site_fract_x
 _atom_site_fract_y
 _atom_site_fract_z
 _atom_site_U_iso_or_equiv
 _atom_site_adp_type
 _atom_site_occupancy
 _atom_site_site_symmetry_order
 _atom_site_calc_flag
 _atom_site_refinement_flags_posn
 _atom_site_refinement_flags_adp
 _atom_site_refinement_flags_occupancy
 _atom_site_disorder_assembly
 _atom_site_disorder_group
C1 C 0.2687(3) 0.69668(19) 0.40927(18) 0.0291(6) Uani 1 1 d . . . . .
H1A H 0.2104 0.7533 0.3888 0.044 Uiso 1 1 calc R U . . .
H1B H 0.2037 0.6552 0.4447 0.044 Uiso 1 1 calc R U . . .
H1C H 0.3054 0.6583 0.3611 0.044 Uiso 1 1 calc R U . . .
C2 C 0.4030(3) 0.73280(18) 0.46088(14) 0.0231(5) Uani 1 1 d . . . . .
H2 H 0.3620 0.7739 0.5080 0.028 Uiso 1 1 calc R U . . .
N3 N 0.4939(2) 0.65401(15) 0.49880(12) 0.0250(4) Uani 1 1 d D . . . .
H3 H 0.450(3) 0.639(2) 0.5490(15) 0.030 Uiso 1 1 d D U . . .
C4 C 0.5229(3) 0.57005(17) 0.44894(14) 0.0212(5) Uani 1 1 d . . . . .
C5 C 0.4704(3) 0.47755(19) 0.47442(15) 0.0254(5) Uani 1 1 d . . . . .
H5 H 0.4129 0.4720 0.5249 0.030 Uiso 1 1 calc R U . . .
C6 C 0.5006(3) 0.39422(18) 0.42754(15) 0.0267(5) Uani 1 1 d . . . . .
H6 H 0.4675 0.3315 0.4467 0.032 Uiso 1 1 calc R U . . .
C7 C 0.5799(3) 0.40266(19) 0.35203(16) 0.0260(5) Uani 1 1 d . . . . .
H7 H 0.5976 0.3462 0.3180 0.031 Uiso 1 1 calc R U . . .
C8 C 0.6331(3) 0.49412(17) 0.32676(15) 0.0219(5) Uani 1 1 d . . . . .
H8 H 0.6859 0.4993 0.2747 0.026 Uiso 1 1 calc R U . . .
C9 C 0.6115(3) 0.57896(17) 0.37538(13) 0.0192(5) Uani 1 1 d . . . . .
C10 C 0.6863(3) 0.67255(16) 0.35090(13) 0.0181(4) Uani 1 1 d . . . . .
C11 C 0.8235(3) 0.66954(17) 0.30680(13) 0.0185(4) Uani 1 1 d . . . . .
H11 H 0.8658 0.6067 0.2949 0.022 Uiso 1 1 calc R U . . .
C12 C 0.9029(3) 0.75260(16) 0.27899(13) 0.0184(4) Uani 1 1 d . . . . .
C13 C 1.0437(3) 0.73772(18) 0.22606(15) 0.0225(5) Uani 1 1 d . . . . .
H13A H 1.0985 0.6785 0.2460 0.027 Uiso 1 1 calc R U . . .
H13B H 1.1118 0.7951 0.2329 0.027 Uiso 1 1 calc R U . . .
C14 C 1.0036(4) 0.72521(19) 0.13168(15) 0.0306(6) Uani 1 1 d . . . . .
H14A H 0.9619 0.6583 0.1232 0.037 Uiso 1 1 calc R U . . .
H14B H 1.0982 0.7300 0.0983 0.037 Uiso 1 1 calc R U . . .
C15 C 0.8879(3) 0.8010(2) 0.09610(16) 0.0321(6) Uani 1 1 d . . . . .
H15B H 0.8682 0.7849 0.0362 0.039 Uiso 1 1 calc R U . . .
H15A H 0.7911 0.7933 0.1271 0.039 Uiso 1 1 calc R U . . .
C16 C 0.9363(3) 0.9079(2) 0.10146(16) 0.0334(6) Uani 1 1 d . . . . .
H16A H 0.9081 0.9405 0.0478 0.040 Uiso 1 1 calc R U . . .
H16B H 1.0482 0.9098 0.1057 0.040 Uiso 1 1 calc R U . . .
C17 C 0.8715(3) 0.96844(17) 0.17369(15) 0.0233(5) Uani 1 1 d . . . . .
H17A H 0.7595 0.9642 0.1713 0.028 Uiso 1 1 calc R U . . .
H17B H 0.8994 1.0382 0.1646 0.028 Uiso 1 1 calc R U . . .
C18 C 0.9229(3) 0.93845(16) 0.26277(15) 0.0209(5) Uani 1 1 d . . . . .
H18B H 1.0338 0.9272 0.2624 0.025 Uiso 1 1 calc R U . . .
H18A H 0.9018 0.9932 0.3023 0.025 Uiso 1 1 calc R U . . .
C19 C 0.8447(2) 0.84672(17) 0.29415(13) 0.0175(4) Uani 1 1 d . . . . .
C20 C 0.7057(3) 0.85355(17) 0.33729(13) 0.0182(4) Uani 1 1 d . . . . .
```

```
C21 C 0.6088(3) 0.93657(17) 0.35882(13) 0.0197(5) Uani 1 1 d . . . . .
C22 C 0.6094(3) 1.03837(17) 0.34197(14) 0.0236(5) Uani 1 1 d . . . . .
H22 H 0.6913 1.0673 0.3119 0.028 Uiso 1 1 calc R U . . .
C23 C 0.4898(3) 1.09593(19) 0.36958(15) 0.0282(5) Uani 1 1 d . . . . .
H23 H 0.4899 1.1646 0.3580 0.034 Uiso 1 1 calc R U . . .
C24 C 0.3686(3) 1.05450(19) 0.41427(16) 0.0295(6) Uani 1 1 d . . . . .
H24 H 0.2884 1.0957 0.4331 0.035 Uiso 1 1 calc R U . . .
C25 C 0.3633(3) 0.95504(19) 0.43154(15) 0.0270(5) Uani 1 1 d . . . . .
H25 H 0.2807 0.9269 0.4616 0.032 Uiso 1 1 calc R U . . .
C26 C 0.4841(3) 0.89712(17) 0.40314(14) 0.0215(5) Uani 1 1 d . . . . .
N27 N 0.5012(2) 0.79599(14) 0.40981(12) 0.0205(4) Uani 1 1 d . . . . .
C28 C 0.6315(3) 0.76799(17) 0.36757(13) 0.0179(4) Uani 1 1 d . . . . .

loop_
 _atom_site_aniso_label
 _atom_site_aniso_U_11
 _atom_site_aniso_U_22
 _atom_site_aniso_U_33
 _atom_site_aniso_U_23
 _atom_site_aniso_U_13
 _atom_site_aniso_U_12
C1 0.0195(12) 0.0305(13) 0.0373(14) -0.0110(11) 0.0019(11) -0.0015(10)
C2 0.0207(12) 0.0274(12) 0.0213(11) -0.0072(9) 0.0054(9) -0.0044(10)
N3 0.0295(11) 0.0304(10) 0.0151(8) -0.0008(8) 0.0026(9) -0.0084(9)
C4 0.0205(11) 0.0261(11) 0.0172(10) 0.0033(9) -0.0033(9) -0.0035(9)
C5 0.0225(12) 0.0320(13) 0.0217(11) 0.0090(9) -0.0024(9) -0.0054(10)
C6 0.0240(12) 0.0243(11) 0.0319(12) 0.0125(10) -0.0048(10) -0.0038(10)
C7 0.0243(12) 0.0218(11) 0.0319(12) 0.0028(10) -0.0035(10) -0.0012(9)
C8 0.0206(11) 0.0227(11) 0.0225(10) 0.0036(9) -0.0015(9) -0.0001(9)
C9 0.0179(11) 0.0210(11) 0.0189(10) 0.0044(8) -0.0037(8) -0.0028(9)
C10 0.0193(11) 0.0204(11) 0.0145(9) -0.0002(8) -0.0013(8) -0.0017(9)
C11 0.0188(11) 0.0179(10) 0.0189(10) 0.0011(8) -0.0013(9) 0.0020(9)
C12 0.0167(10) 0.0230(11) 0.0154(9) 0.0000(8) -0.0025(8) 0.0003(9)
C13 0.0203(11) 0.0225(11) 0.0247(11) -0.0009(9) 0.0051(9) 0.0007(9)
C14 0.0425(15) 0.0256(12) 0.0237(11) -0.0025(9) 0.0079(11) 0.0055(12)
C15 0.0331(14) 0.0400(15) 0.0232(11) -0.0034(11) 0.0005(11) 0.0028(11)
C16 0.0363(15) 0.0416(15) 0.0223(12) 0.0049(11) 0.0020(11) 0.0080(12)
C17 0.0228(11) 0.0213(11) 0.0258(11) 0.0057(9) 0.0011(10) 0.0004(9)
C18 0.0197(11) 0.0196(10) 0.0234(11) 0.0010(9) -0.0003(9) -0.0008(9)
C19 0.0174(11) 0.0193(10) 0.0159(9) 0.0012(8) -0.0013(8) -0.0008(9)
C20 0.0179(11) 0.0204(10) 0.0163(10) -0.0021(8) -0.0021(8) -0.0007(8)
C21 0.0196(11) 0.0223(11) 0.0173(10) -0.0048(8) -0.0031(9) 0.0004(9)
C22 0.0252(12) 0.0239(11) 0.0216(11) -0.0036(9) -0.0017(10) 0.0009(9)
C23 0.0334(14) 0.0233(11) 0.0277(12) -0.0059(9) -0.0065(11) 0.0069(11)
C24 0.0276(13) 0.0340(13) 0.0269(12) -0.0118(10) -0.0035(10) 0.0105(11)
C25 0.0213(12) 0.0357(13) 0.0240(11) -0.0103(10) 0.0005(10) 0.0037(10)
C26 0.0210(11) 0.0252(11) 0.0183(10) -0.0055(9) -0.0006(9) -0.0005(9)
N27 0.0168(9) 0.0243(9) 0.0203(8) -0.0034(7) 0.0028(8) -0.0014(8)
C28 0.0161(10) 0.0238(11) 0.0137(9) -0.0005(8) 0.0003(8) -0.0013(9)

_geom_special_details
;
 All esds (except the esd in the dihedral angle between two l.s. planes)
 are estimated using the full covariance matrix.  The cell esds are taken
 into account individually in the estimation of esds in distances, angles
 and torsion angles; correlations between esds in cell parameters are only
```

```
 used when they are defined by crystal symmetry.  An approximate (isotropic)
 treatment of cell esds is used for estimating esds involving l.s. planes.
;

loop_
 _geom_bond_atom_site_label_1
 _geom_bond_atom_site_label_2
 _geom_bond_distance
 _geom_bond_site_symmetry_2
 _geom_bond_publ_flag
C1 C2 1.521(3) . ?
C1 H1A 0.9800 . ?
C1 H1B 0.9800 . ?
C1 H1C 0.9800 . ?
C2 N27 1.463(3) . ?
C2 N3 1.466(3) . ?
C2 H2 1.0000 . ?
N3 C4 1.411(3) . ?
N3 H3 0.91(2) . ?
C4 C5 1.399(3) . ?
C4 C9 1.408(3) . ?
C5 C6 1.380(4) . ?
C5 H5 0.9500 . ?
C6 C7 1.391(4) . ?
C6 H6 0.9500 . ?
C7 C8 1.387(3) . ?
C7 H7 0.9500 . ?
C8 C9 1.399(3) . ?
C8 H8 0.9500 . ?
C9 C10 1.484(3) . ?
C10 C11 1.398(3) . ?
C10 C28 1.409(3) . ?
C11 C12 1.399(3) . ?
C11 H11 0.9500 . ?
C12 C19 1.399(3) . ?
C12 C13 1.512(3) . ?
C13 C14 1.546(3) . ?
C13 H13A 0.9900 . ?
C13 H13B 0.9900 . ?
C14 C15 1.555(4) . ?
C14 H14A 0.9900 . ?
C14 H14B 0.9900 . ?
C15 C16 1.516(4) . ?
C15 H15B 0.9900 . ?
C15 H15A 0.9900 . ?
C16 C17 1.521(3) . ?
C16 H16A 0.9900 . ?
C16 H16B 0.9900 . ?
C17 C18 1.538(3) . ?
C17 H17A 0.9900 . ?
C17 H17B 0.9900 . ?
C18 C19 1.508(3) . ?
C18 H18B 0.9900 . ?
C18 H18A 0.9900 . ?
C19 C20 1.407(3) . ?
C20 C28 1.418(3) . ?
```

```
C20 C21 1.455(3) . ?
C21 C22 1.409(3) . ?
C21 C26 1.411(3) . ?
C22 C23 1.384(4) . ?
C22 H22 0.9500 . ?
C23 C24 1.400(4) . ?
C23 H23 0.9500 . ?
C24 C25 1.379(4) . ?
C24 H24 0.9500 . ?
C25 C26 1.399(3) . ?
C25 H25 0.9500 . ?
C26 N27 1.386(3) . ?
N27 C28 1.383(3) . ?

loop_
 _geom_angle_atom_site_label_1
 _geom_angle_atom_site_label_2
 _geom_angle_atom_site_label_3
 _geom_angle
 _geom_angle_site_symmetry_1
 _geom_angle_site_symmetry_3
 _geom_angle_publ_flag
C2 C1 H1A 109.5 . . ?
C2 C1 H1B 109.5 . . ?
H1A C1 H1B 109.5 . . ?
C2 C1 H1C 109.5 . . ?
H1A C1 H1C 109.5 . . ?
H1B C1 H1C 109.5 . . ?
N27 C2 N3 109.38(19) . . ?
N27 C2 C1 110.6(2) . . ?
N3 C2 C1 114.2(2) . . ?
N27 C2 H2 107.4 . . ?
N3 C2 H2 107.4 . . ?
C1 C2 H2 107.4 . . ?
C4 N3 C2 117.38(18) . . ?
C4 N3 H3 112.6(19) . . ?
C2 N3 H3 107(2) . . ?
C5 C4 C9 120.0(2) . . ?
C5 C4 N3 120.3(2) . . ?
C9 C4 N3 119.6(2) . . ?
C6 C5 C4 121.2(2) . . ?
C6 C5 H5 119.4 . . ?
C4 C5 H5 119.4 . . ?
C5 C6 C7 119.5(2) . . ?
C5 C6 H6 120.2 . . ?
C7 C6 H6 120.2 . . ?
C8 C7 C6 119.5(2) . . ?
C8 C7 H7 120.3 . . ?
C6 C7 H7 120.3 . . ?
C7 C8 C9 122.2(2) . . ?
C7 C8 H8 118.9 . . ?
C9 C8 H8 118.9 . . ?
C8 C9 C4 117.4(2) . . ?
C8 C9 C10 120.1(2) . . ?
C4 C9 C10 122.4(2) . . ?
C11 C10 C28 114.7(2) . . ?
```

```
C11 C10 C9 119.4(2) . . ?
C28 C10 C9 125.9(2) . . ?
C10 C11 C12 124.5(2) . . ?
C10 C11 H11 117.7 . . ?
C12 C11 H11 117.7 . . ?
C19 C12 C11 120.0(2) . . ?
C19 C12 C13 121.2(2) . . ?
C11 C12 C13 118.5(2) . . ?
C12 C13 C14 111.3(2) . . ?
C12 C13 H13A 109.4 . . ?
C14 C13 H13A 109.4 . . ?
C12 C13 H13B 109.4 . . ?
C14 C13 H13B 109.4 . . ?
H13A C13 H13B 108.0 . . ?
C13 C14 C15 115.3(2) . . ?
C13 C14 H14A 108.4 . . ?
C15 C14 H14A 108.4 . . ?
C13 C14 H14B 108.4 . . ?
C15 C14 H14B 108.4 . . ?
H14A C14 H14B 107.5 . . ?
C16 C15 C14 115.4(2) . . ?
C16 C15 H15B 108.4 . . ?
C14 C15 H15B 108.4 . . ?
C16 C15 H15A 108.4 . . ?
C14 C15 H15A 108.4 . . ?
H15B C15 H15A 107.5 . . ?
C15 C16 C17 117.0(2) . . ?
C15 C16 H16A 108.0 . . ?
C17 C16 H16A 108.0 . . ?
C15 C16 H16B 108.0 . . ?
C17 C16 H16B 108.0 . . ?
H16A C16 H16B 107.3 . . ?
C16 C17 C18 115.9(2) . . ?
C16 C17 H17A 108.3 . . ?
C18 C17 H17A 108.3 . . ?
C16 C17 H17B 108.3 . . ?
C18 C17 H17B 108.3 . . ?
H17A C17 H17B 107.4 . . ?
C19 C18 C17 112.75(19) . . ?
C19 C18 H18B 109.0 . . ?
C17 C18 H18B 109.0 . . ?
C19 C18 H18A 109.0 . . ?
C17 C18 H18A 109.0 . . ?
H18B C18 H18A 107.8 . . ?
C12 C19 C20 117.6(2) . . ?
C12 C19 C18 122.1(2) . . ?
C20 C19 C18 120.3(2) . . ?
C19 C20 C28 120.9(2) . . ?
C19 C20 C21 132.6(2) . . ?
C28 C20 C21 106.57(19) . . ?
C22 C21 C26 118.0(2) . . ?
C22 C21 C20 135.6(2) . . ?
C26 C21 C20 106.2(2) . . ?
C23 C22 C21 119.5(2) . . ?
C23 C22 H22 120.3 . . ?
C21 C22 H22 120.3 . . ?
```

```
C22 C23 C24 121.0(2) . . ?
C22 C23 H23 119.5 . . ?
C24 C23 H23 119.5 . . ?
C25 C24 C23 121.3(2) . . ?
C25 C24 H24 119.3 . . ?
C23 C24 H24 119.3 . . ?
C24 C25 C26 117.5(3) . . ?
C24 C25 H25 121.3 . . ?
C26 C25 H25 121.3 . . ?
N27 C26 C25 128.0(2) . . ?
N27 C26 C21 109.3(2) . . ?
C25 C26 C21 122.7(2) . . ?
C28 N27 C26 109.02(19) . . ?
C28 N27 C2 126.71(19) . . ?
C26 N27 C2 124.0(2) . . ?
N27 C28 C10 129.0(2) . . ?
N27 C28 C20 108.78(19) . . ?
C10 C28 C20 122.2(2) . . ?

loop_
 _geom_torsion_atom_site_label_1
 _geom_torsion_atom_site_label_2
 _geom_torsion_atom_site_label_3
 _geom_torsion_atom_site_label_4
 _geom_torsion
 _geom_torsion_site_symmetry_1
 _geom_torsion_site_symmetry_2
 _geom_torsion_site_symmetry_3
 _geom_torsion_site_symmetry_4
 _geom_torsion_publ_flag
N27 C2 N3 C4 -83.5(2) . . . . ?
C1 C2 N3 C4 41.2(3) . . . . ?
C2 N3 C4 C5 -118.1(2) . . . . ?
C2 N3 C4 C9 65.0(3) . . . . ?
C9 C4 C5 C6 -1.6(4) . . . . ?
N3 C4 C5 C6 -178.5(2) . . . . ?
C4 C5 C6 C7 -2.4(4) . . . . ?
C5 C6 C7 C8 2.7(4) . . . . ?
C6 C7 C8 C9 0.9(4) . . . . ?
C7 C8 C9 C4 -4.7(3) . . . . ?
C7 C8 C9 C10 172.6(2) . . . . ?
C5 C4 C9 C8 5.0(3) . . . . ?
N3 C4 C9 C8 -178.1(2) . . . . ?
C5 C4 C9 C10 -172.2(2) . . . . ?
N3 C4 C9 C10 4.7(3) . . . . ?
C8 C9 C10 C11 -28.5(3) . . . . ?
C4 C9 C10 C11 148.7(2) . . . . ?
C8 C9 C10 C28 151.2(2) . . . . ?
C4 C9 C10 C28 -31.7(3) . . . . ?
C28 C10 C11 C12 -1.0(3) . . . . ?
C9 C10 C11 C12 178.7(2) . . . . ?
C10 C11 C12 C19 -0.7(3) . . . . ?
C10 C11 C12 C13 -175.3(2) . . . . ?
C19 C12 C13 C14 -89.6(3) . . . . ?
C11 C12 C13 C14 85.0(3) . . . . ?
C12 C13 C14 C15 46.3(3) . . . . ?
```

```
C13 C14 C15 C16 60.0(3) . . . . ?
C14 C15 C16 C17 -99.8(3) . . . . ?
C15 C16 C17 C18 66.6(3) . . . . ?
C16 C17 C18 C19 -76.3(3) . . . . ?
C11 C12 C19 C20 -0.3(3) . . . . ?
C13 C12 C19 C20 174.2(2) . . . . ?
C11 C12 C19 C18 -177.7(2) . . . . ?
C13 C12 C19 C18 -3.3(3) . . . . ?
C17 C18 C19 C12 89.1(3) . . . . ?
C17 C18 C19 C20 -88.3(3) . . . . ?
C12 C19 C20 C28 2.9(3) . . . . ?
C18 C19 C20 C28 -179.6(2) . . . . ?
C12 C19 C20 C21 -175.5(2) . . . . ?
C18 C19 C20 C21 2.0(4) . . . . ?
C19 C20 C21 C22 4.5(5) . . . . ?
C28 C20 C21 C22 -174.1(3) . . . . ?
C19 C20 C21 C26 -179.6(2) . . . . ?
C28 C20 C21 C26 1.8(2) . . . . ?
C26 C21 C22 C23 0.5(3) . . . . ?
C20 C21 C22 C23 176.0(2) . . . . ?
C21 C22 C23 C24 0.2(4) . . . . ?
C22 C23 C24 C25 -0.7(4) . . . . ?
C23 C24 C25 C26 0.4(4) . . . . ?
C24 C25 C26 N27 -177.2(2) . . . . ?
C24 C25 C26 C21 0.4(3) . . . . ?
C22 C21 C26 N27 177.2(2) . . . . ?
C20 C21 C26 N27 0.4(2) . . . . ?
C22 C21 C26 C25 -0.8(3) . . . . ?
C20 C21 C26 C25 -177.6(2) . . . . ?
C25 C26 N27 C28 175.3(2) . . . . ?
C21 C26 N27 C28 -2.5(2) . . . . ?
C25 C26 N27 C2 -10.2(4) . . . . ?
C21 C26 N27 C2 172.0(2) . . . . ?
N3 C2 N27 C28 30.0(3) . . . . ?
C1 C2 N27 C28 -96.7(3) . . . . ?
N3 C2 N27 C26 -143.5(2) . . . . ?
C1 C2 N27 C26 89.8(3) . . . . ?
C26 N27 C28 C10 -173.5(2) . . . . ?
C2 N27 C28 C10 12.2(4) . . . . ?
C26 N27 C28 C20 3.7(2) . . . . ?
C2 N27 C28 C20 -170.6(2) . . . . ?
C11 C10 C28 N27 -179.5(2) . . . . ?
C9 C10 C28 N27 0.8(4) . . . . ?
C11 C10 C28 C20 3.6(3) . . . . ?
C9 C10 C28 C20 -176.0(2) . . . . ?
C19 C20 C28 N27 177.84(19) . . . . ?
C21 C20 C28 N27 -3.4(2) . . . . ?
C19 C20 C28 C10 -4.8(3) . . . . ?
C21 C20 C28 C10 174.0(2) . . . . ?

_refine_diff_density_max    0.621
_refine_diff_density_min   -0.283
_refine_diff_density_rms    0.048

_shelxl_version_number 2014/6
```

```
_shelx_res_file
;
TITL 16182a in P2(1)2(1)2(1)
CELL  1.54178   8.8186  13.5847  15.8483   90.000   90.000   90.000
ZERR    4.000   0.0004   0.0006   0.0007    0.000    0.000    0.000
LATT -1
SYMM 1/2-X, -Y, 1/2+Z
SYMM -X, 1/2+Y, 1/2-Z
SYMM 1/2+X, 1/2-Y, -Z
SFAC C   H   N
UNIT 104 104 8
TEMP -150.120
SIZE 0.07 0.11 0.175
HTAB

L.S. 10
ACTA
CONF
BOND $H
LIST 4
FMAP 2
PLAN 5
WGHT    0.042500    0.849800
FVAR       0.21686
C1    1    0.268695    0.696677    0.409275    11.00000    0.01946    0.03052 =
         0.03731   -0.01099    0.00190   -0.00152
AFIX 137
H1A   2    0.210403    0.753271    0.388822    11.00000   -1.50000
H1B   2    0.203690    0.655216    0.444663    11.00000   -1.50000
H1C   2    0.305432    0.658268    0.361088    11.00000   -1.50000
AFIX   0
C2    1    0.403039    0.732801    0.460883    11.00000    0.02072    0.02740 =
         0.02133   -0.00720    0.00544   -0.00444
AFIX  13
H2    2    0.361985    0.773897    0.507986    11.00000   -1.20000
AFIX   0
DFIX  0.91 N3 H3A
N3    3    0.493913    0.654013    0.498796    11.00000    0.02945    0.03036 =
         0.01512   -0.00084    0.00258   -0.00842
H3    2    0.450416    0.638845    0.548984    11.00000   -1.20000
C4    1    0.522934    0.570052    0.448939    11.00000    0.02045    0.02606 =
         0.01719    0.00333   -0.00335   -0.00352
C5    1    0.470378    0.477547    0.474422    11.00000    0.02248    0.03198 =
         0.02174    0.00899   -0.00241   -0.00538
AFIX  43
H5    2    0.412872    0.471994    0.524887    11.00000   -1.20000
AFIX   0
C6    1    0.500601    0.394219    0.427541    11.00000    0.02399    0.02431 =
         0.03187    0.01253   -0.00477   -0.00379
AFIX  43
H6    2    0.467462    0.331545    0.446700    11.00000   -1.20000
AFIX   0
C7    1    0.579940    0.402663    0.352029    11.00000    0.02431    0.02180 =
         0.03186    0.00275   -0.00354   -0.00123
AFIX  43
H7    2    0.597591    0.346222    0.318027    11.00000   -1.20000
```

```
AFIX   0
C8    1    0.633082    0.494123    0.326759    11.00000    0.02056    0.02270 =
         0.02247    0.00364   -0.00153   -0.00012
AFIX  43
H8    2    0.685891    0.499348    0.274705    11.00000   -1.20000
AFIX   0
C9    1    0.611505    0.578961    0.375384    11.00000    0.01790    0.02097 =
         0.01888    0.00444   -0.00368   -0.00282
C10   1    0.686313    0.672554    0.350902    11.00000    0.01932    0.02036 =
         0.01448   -0.00016   -0.00127   -0.00174
C11   1    0.823500    0.669537    0.306797    11.00000    0.01878    0.01785 =
         0.01886    0.00111   -0.00126    0.00200
AFIX  43
H11   2    0.865766    0.606733    0.294879    11.00000   -1.20000
AFIX   0
C12   1    0.902879    0.752595    0.278987    11.00000    0.01674    0.02300 =
         0.01537    0.00001   -0.00247    0.00028
C13   1    1.043710    0.737716    0.226060    11.00000    0.02028    0.02254 =
         0.02472   -0.00093    0.00507    0.00066
AFIX  23
H13A  2    1.098451    0.678513    0.246036    11.00000   -1.20000
H13B  2    1.111779    0.795110    0.232933    11.00000   -1.20000
AFIX   0
C14   1    1.003581    0.725213    0.131677    11.00000    0.04245    0.02563 =
         0.02372   -0.00250    0.00792    0.00547
AFIX  23
H14A  2    0.961950    0.658252    0.123246    11.00000   -1.20000
H14B  2    1.098225    0.729954    0.098327    11.00000   -1.20000
AFIX   0
C15   1    0.887905    0.801033    0.096101    11.00000    0.03314    0.03996 =
         0.02320   -0.00345    0.00053    0.00277
AFIX  23
H15B  2    0.868163    0.784853    0.036192    11.00000   -1.20000
H15A  2    0.791114    0.793341    0.127053    11.00000   -1.20000
AFIX   0
C16   1    0.936270    0.907909    0.101464    11.00000    0.03632    0.04155 =
         0.02227    0.00487    0.00204    0.00800
AFIX  23
H16A  2    0.908063    0.940511    0.047846    11.00000   -1.20000
H16B  2    1.048237    0.909829    0.105687    11.00000   -1.20000
AFIX   0
C17   1    0.871459    0.968435    0.173686    11.00000    0.02282    0.02128 =
         0.02582    0.00569    0.00111    0.00043
AFIX  23
H17A  2    0.759473    0.964165    0.171269    11.00000   -1.20000
H17B  2    0.899447    1.038204    0.164571    11.00000   -1.20000
AFIX   0
C18   1    0.922870    0.938446    0.262771    11.00000    0.01966    0.01964 =
         0.02336    0.00105   -0.00034   -0.00077
AFIX  23
H18B  2    1.033787    0.927206    0.262368    11.00000   -1.20000
H18A  2    0.901752    0.993201    0.302284    11.00000   -1.20000
AFIX   0
C19   1    0.844709    0.846722    0.294145    11.00000    0.01737    0.01928 =
         0.01587    0.00124   -0.00131   -0.00077
C20   1    0.705658    0.853548    0.337286    11.00000    0.01789    0.02041 =
```

```
         0.01631   -0.00211   -0.00210   -0.00065
C21   1    0.608850    0.936570    0.358816    11.00000    0.01960    0.02229 =
         0.01731   -0.00476   -0.00308    0.00039
C22   1    0.609432    1.038374    0.341968    11.00000    0.02520    0.02394 =
         0.02156   -0.00360   -0.00174    0.00094
AFIX  43
H22  2    0.691272    1.067301    0.311891    11.00000   -1.20000
AFIX   0
C23   1    0.489807    1.095929    0.369584    11.00000    0.03340    0.02335 =
         0.02772   -0.00594   -0.00655    0.00687
AFIX  43
H23  2    0.489926    1.164553    0.358049    11.00000   -1.20000
AFIX   0
C24   1    0.368620    1.054499    0.414273    11.00000    0.02757    0.03399 =
         0.02694   -0.01177   -0.00349    0.01052
AFIX  43
H24  2    0.288432    1.095722    0.433079    11.00000   -1.20000
AFIX   0
C25   1    0.363312    0.955039    0.431542    11.00000    0.02127    0.03569 =
         0.02403   -0.01033    0.00047    0.00370
AFIX  43
H25  2    0.280745    0.926943    0.461582    11.00000   -1.20000
AFIX   0
C26   1    0.484116    0.897116    0.403144    11.00000    0.02101    0.02516 =
         0.01829   -0.00547   -0.00057   -0.00054
N27   3    0.501171    0.795992    0.409809    11.00000    0.01682    0.02431 =
         0.02034   -0.00344    0.00285   -0.00138
C28   1    0.631451    0.767993    0.367567    11.00000    0.01613    0.02377 =
         0.01368   -0.00049    0.00030   -0.00129

HKLF 4

REM  16182a in P2(1)2(1)2(1)
REM R1 =  0.0398 for    3700 Fo > 4sig(Fo)  and  0.0427 for all    3861 data
REM    257 parameters refined using      1 restraints

END

WGHT      0.0425      0.8485

REM No hydrogen bonds found for HTAB generation

REM Highest difference peak  0.621,  deepest hole -0.283,  1-sigma level  0.048
Q1    1   1.0287  0.8243  0.0925  11.00000  0.05    0.62
Q2    1   0.8658  0.8630  0.1013  11.00000  0.05    0.47
Q3    1   1.1006  0.7257  0.1496  11.00000  0.05    0.19
Q4    1   0.5508  0.5752  0.4033  11.00000  0.05    0.17
Q5    1   1.1350  0.8592  0.1078  11.00000  0.05    0.16
;
_shelx_res_checksum   33450
# Some H atom labels have been edited after refinement
# so that A and B labels are grouped on the same faces
# of rings. - KJT
```

Appendix IV. Crystallographic Data for Selected Products from Part II

Each entry contains a summary of how the crystallographic data for each sample were obtained and refined, along with the content of the resulting CIF file. CIF file content is presented verbatim, except for lines at the end of the file that begin with a number sign (#). These are comments that explain why some atom numbers were changed after refinement, or to note information or data that are missing from the current version of the CIF file.

In the CIF files, melting point data are not given in the "_chemical_melting_point" fields. These fields are intended to reflect the melting point of the specific crystal that was examined, which was not obtained. For melting point data on the mixtures from which crystals described in this section were derived, refer to the respective entries in § 3.4.

Citations in CIF files are indicated by a name(s) and a year in parenthesis. Refer to Appendix V to find the corresponding reference number in § 4.

Table 44. The contents of Appendix IV.

compound	page	nickname
204ca	600	tribromo nitrile, polytype 1 (TT)
204ca	606	tribromo nitrile, polytype 2 (TC)
204ca	613	tribromo nitrile, polytype 3 (TTC)
204cb	622	dibromo 4-methyl nitrile
204cc	630	dibromo PABA nitrile, anthracene co-crystal
204cd	640	dibromo PABA methyl ester nitrile
204da	649	triiodo nitrile (CC)
204db	654	diiodo 4-methyl nitrile (CC)
207	662	dibromo carbamoyl acid (2-propanolate)
209ca	673	tribromo isocyanide, polytype 2 (TC)
209cb	682	dibromo 4-methyl isocyanide
209cd	690	dibromo PABA methyl ester isocyanide
209da	699	triiodo isocyanide (CC)
209db	704	diiodo 4-methyl isocyanide

2,4,6-Tribromobenzonitrile (204ca), $Z = 2$ TT polytype.

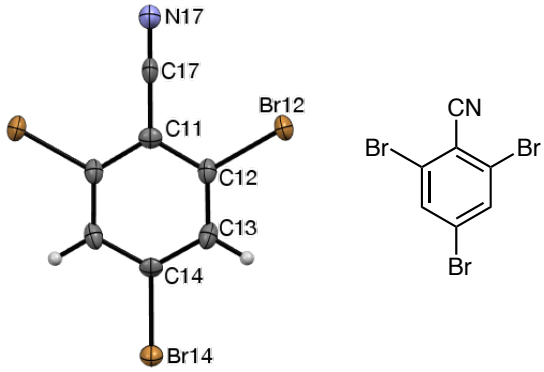

CIF content:

```
data_204ca1
_audit_creation_method     <i>SHELXTL</i>
_chemical_name_systematic
;
 2,4,6-Tribromobenzonitrile
;
_chemical_name_common     ‘tribromo nitrile, polytype 1’
_chemical_formula_moiety     'C7 H2 Br3 N'
_chemical_formula_sum     'C7 H2 Br3 N'
_chemical_formula_iupac     'C7 H2 Br3 N'
_chemical_formula_weight     339.83
_chemical_melting_point     ?
_symmetry_cell_setting     monoclinic
_symmetry_space_group_name_H-M     'P 21/m'
_symmetry_space_group_name_Hall     '-P 2yb'
loop_
    _symmetry_equiv_pos_as_xyz
    'x, y, z'
    '-x, y+1/2, -z'
    '-x, -y, -z'
    'x, -y-1/2, z'
_cell_length_a     4.8742(15)
_cell_length_b     10.247(3)
_cell_length_c     8.683(3)
_cell_angle_alpha     90.00
_cell_angle_beta     94.970(10)
_cell_angle_gamma     90.00
_cell_volume     432.0(2)
_cell_formula_units_Z     2
_cell_measurement_reflns_used     2049
_cell_measurement_theta_min     2.35
_cell_measurement_theta_max     27.4
_cell_measurement_temperature     173(2)
_exptl_crystal_description     needle
_exptl_crystal_colour     colorless
_exptl_crystal_size_max     0.50
_exptl_crystal_size_mid     0.15
_exptl_crystal_size_min     0.10
_exptl_crystal_density_diffrn     2.612
```

```
_exptl_crystal_density_meas     ?
_exptl_crystal_density_method     'not measured'
_exptl_crystal_F_000     312
_exptl_absorpt_coefficient_mu     13.934
_exptl_absorpt_correction_type     multi-scan
_exptl_absorpt_process_details
;
(SADABS; Bruker, 2002)
;
_exptl_absorpt_correction_T_min     0.080
_exptl_absorpt_correction_T_max     0.248
_diffrn_ambient_temperature     173(2)
_diffrn_radiation_type     MoK\a
_diffrn_radiation_wavelength     0.71073
_diffrn_radiation_source     'fine-focus sealed tube'
_diffrn_radiation_monochromator     graphite
_diffrn_measurement_device_type
;
Bruker 1K area-detector diffractometer
;
_diffrn_measurement_method     '\w scans'
_diffrn_detector_area_resol_mean     ?
_diffrn_reflns_number     4093
_diffrn_reflns_av_R_equivalents     0.1270
_diffrn_reflns_av_sigmaI/netI     0.0745
_diffrn_reflns_theta_min     2.35
_diffrn_reflns_theta_max     27.47
_diffrn_reflns_theta_full     27.00
_diffrn_measured_fraction_theta_max     0.993
_diffrn_measured_fraction_theta_full     0.993
_diffrn_reflns_limit_h_min     -6
_diffrn_reflns_limit_h_max     6
_diffrn_reflns_limit_k_min     -13
_diffrn_reflns_limit_k_max     13
_diffrn_reflns_limit_l_min     -11
_diffrn_reflns_limit_l_max     11
_diffrn_standards_number     0
_diffrn_standards_interval_count     ?
_diffrn_standards_interval_time     ?
_diffrn_standards_decay_%     '< 1'
_reflns_number_total     1024
_reflns_number_gt     856
_reflns_threshold_expression     '>2\s(I) '
_refine_ls_structure_factor_coef     Fsqd
_refine_ls_matrix_type     full
_refine_ls_R_factor_all     0.0563
_refine_ls_R_factor_gt     0.0462
_refine_ls_wR_factor_gt     0.1106
_refine_ls_wR_factor_ref     0.1158
_refine_ls_goodness_of_fit_ref     1.012
_refine_ls_restrained_S_all     1.012
_refine_ls_number_reflns     1024
_refine_ls_number_parameters     58
_refine_ls_number_restraints     0
_refine_ls_hydrogen_treatment     constr
_refine_ls_weighting_scheme     calc
```

```
_refine_ls_weighting_details
        'calc w=1/[\s^2^(Fo^2^)+(0.0690P)^2^+0.0000P] where P=(Fo^2^+2Fc^2^)/3'
_atom_sites_solution_hydrogens     geom
_atom_sites_solution_primary     direct
_atom_sites_solution_secondary     difmap
_refine_ls_shift/su_max     0.001
_refine_ls_shift/su_mean     0.000
_refine_diff_density_max     1.356
_refine_diff_density_min     -1.284
_refine_ls_extinction_method     none
_refine_ls_extinction_coef     ?
loop_
    _atom_type_symbol
    _atom_type_description
    _atom_type_scat_dispersion_real
    _atom_type_scat_dispersion_imag
    _atom_type_scat_source
    'C' 'C' 0.0033 0.0016
                        'International Tables Vol C Tables 4.2.6.8 and 6.1.1.4'
    'H' 'H' 0.0000 0.0000
                        'International Tables Vol C Tables 4.2.6.8 and 6.1.1.4'
    'N' 'N' 0.0061 0.0033
                        'International Tables Vol C Tables 4.2.6.8 and 6.1.1.4'
    'Br' 'Br' -0.2901 2.4595
                        'International Tables Vol C Tables 4.2.6.8 and 6.1.1.4'
_computing_data_collection
;
SMART (Bruker, 2002)
;
_computing_cell_refinement
;
SAINT (Bruker, 2002)
;
_computing_data_reduction
;
SAINT (Bruker, 2002)
;
_computing_structure_solution
;
<i>SHELXTL</i> (Sheldrick, 2008)
;
_computing_structure_refinement
;
<i>SHELXTL</i> (Sheldrick, 2008)
;
_computing_molecular_graphics
;
Mercury (Macrae <i>et al.</i>, 2008)
;
_computing_publication_material
;
<i>SHELXTL</i> (Sheldrick, 2008), enCIFer (Allen <i>et al.</i>,
2004),
and publCIF (Westrip, 2010)
;
loop_
```

```
    _atom_site_type_symbol
    _atom_site_label
    _atom_site_fract_x
    _atom_site_fract_y
    _atom_site_fract_z
    _atom_site_U_iso_or_equiv
    _atom_site_adp_type
    _atom_site_calc_flag
    _atom_site_refinement_flags
    _atom_site_occupancy
    _atom_site_symmetry_multiplicity
    _atom_site_disorder_assembly
    _atom_site_disorder_group
    Br Br12 0.33356(11) 0.47324(5) 0.18676(7) 0.0280(2) Uani d . 1 1 . .
    Br Br14 1.11323(14) 0.7500 0.57820(9) 0.0256(3) Uani d S 1 2 . .
    N N17 -0.0263(14) 0.7500 -0.0147(8) 0.0313(16) Uani d S 1 2 . .
    C C11 0.3828(14) 0.7500 0.1960(8) 0.0204(15) Uani d S 1 2 . .
    C C12 0.4932(10) 0.6324(5) 0.2559(6) 0.0224(11) Uani d . 1 1 . .
    C C13 0.7107(10) 0.6313(5) 0.3688(6) 0.0244(11) Uani d . 1 1 . .
    H H13 0.7842 0.5512 0.4091 0.029 Uiso calc R 1 1 . .
    C C14 0.8200(14) 0.7500 0.4224(8) 0.0197(15) Uani d S 1 2 . .
    C C17 0.1523(16) 0.7500 0.0799(9) 0.0241(16) Uani d S 1 2 . .
loop_
    _atom_site_aniso_label
    _atom_site_aniso_U_11
    _atom_site_aniso_U_22
    _atom_site_aniso_U_33
    _atom_site_aniso_U_12
    _atom_site_aniso_U_13
    _atom_site_aniso_U_23
    Br12 0.0334(4) 0.0160(3) 0.0337(4) -0.0043(2) -0.0015(2) -0.0016(2)
    Br14 0.0229(4) 0.0239(4) 0.0295(5) 0.000 -0.0018(3) 0.000
    N17 0.041(4) 0.021(3) 0.031(4) 0.000 -0.006(3) 0.000
    C11 0.022(3) 0.025(4) 0.015(4) 0.000 0.005(3) 0.000
    C12 0.023(2) 0.016(2) 0.029(3) -0.0012(19) 0.006(2) 0.001(2)
    C13 0.024(2) 0.017(3) 0.033(3) 0.004(2) 0.007(2) 0.004(2)
    C14 0.024(3) 0.025(4) 0.011(3) 0.000 0.003(3) 0.000
    C17 0.030(4) 0.011(3) 0.032(4) 0.000 0.004(3) 0.000
loop_
    _geom_bond_atom_site_label_1
    _geom_bond_atom_site_label_2
    _geom_bond_site_symmetry_2
    _geom_bond_distance
    _geom_bond_publ_flag
    Br12 C12 . 1.883(5) ?
    Br14 C14 . 1.881(7) ?
    C11 C12 . 1.401(6) ?
    C11 C17 . 1.443(10) ?
    C12 C13 . 1.380(8) ?
    C13 C14 . 1.391(6) ?
    C13 H13 . 0.9500 ?
    N17 C17 . 1.144(10) ?
loop_
    _geom_angle_atom_site_label_1
    _geom_angle_atom_site_label_2
    _geom_angle_atom_site_label_3
```

```
    _geom_angle_site_symmetry_1
    _geom_angle_site_symmetry_3
    _geom_angle
    _geom_angle_publ_flag
    C12 C11 C12 . 4_575 118.6(6) ?
    C12 C11 C17 . . 120.7(3) ?
    C13 C12 C11 . . 121.2(5) ?
    C13 C12 Br12 . . 119.3(4) ?
    C11 C12 Br12 . . 119.4(4) ?
    C12 C13 C14 . . 118.6(5) ?
    C12 C13 H13 . . 120.7 ?
    C14 C13 H13 . . 120.7 ?
    C13 C14 C13 . 4_575 121.9(6) ?
    C13 C14 Br14 . . 119.0(3) ?
    N17 C17 C11 . . 178.4(9) ?
loop_
    _geom_torsion_atom_site_label_1
    _geom_torsion_atom_site_label_2
    _geom_torsion_atom_site_label_3
    _geom_torsion_atom_site_label_4
    _geom_torsion_site_symmetry_1
    _geom_torsion_site_symmetry_2
    _geom_torsion_site_symmetry_3
    _geom_torsion_site_symmetry_4
    _geom_torsion
    _geom_torsion_publ_flag
    C12 C11 C12 C13 4_575 . . . -1.6(11) ?
    C17 C11 C12 C13 . . . . -178.9(7) ?
    C12 C11 C12 Br12 4_575 . . . 176.0(3) ?
    C17 C11 C12 Br12 . . . . -1.3(9) ?
    C11 C12 C13 C14 . . . . -0.2(10) ?
    Br12 C12 C13 C14 . . . . -177.8(5) ?
    C12 C13 C14 C13 . . . 4_575 2.0(12) ?
    C12 C13 C14 Br14 . . . . 179.2(5) ?
_iucr_refine_instructions_details
;
TITL RCN-I in P2(1)/m
CELL 0.71073   4.8742  10.247   8.683  90.000  94.97  90.000
ZERR    2.00   0.0015   0.003   0.003   0.000   0.01   0.000
LATT  1
SYMM -X, 0.5+Y, -Z
SFAC C H N BR
UNIT 14 4 2 6
TEMP -100
L.S.10
BOND $h
FMAP 2
PLAN 5
acta
WGHT    0.069000
FVAR       0.43013
BR12    4    0.333556    0.473244    0.186758    11.00000    0.03343    0.01596
=
         0.03370   -0.00162   -0.00154   -0.00427
BR14    4    1.113227    0.750000    0.578201    10.50000    0.02285    0.02388
=
```

```
         0.02946    0.00000   -0.00178    0.00000
N17     3   -0.026313     0.750000    -0.014738     10.50000     0.04076     0.02098
=
         0.03072    0.00000   -0.00582    0.00000
C11     1     0.382769     0.750000     0.196030     10.50000     0.02250     0.02451
=
         0.01474    0.00000    0.00455    0.00000
C12     1     0.493243     0.632445     0.255884     11.00000     0.02338     0.01572
=
         0.02874    0.00146    0.00614   -0.00116
C13     1     0.710709     0.631326     0.368818     11.00000     0.02438     0.01705
=
         0.03276    0.00416    0.00732    0.00368
AFIX  43
H13     2    0.784217    0.551239    0.409105    11.00000   -1.20000
AFIX   0
C14     1     0.819959     0.750000     0.422392     10.50000     0.02362     0.02473
=
         0.01088    0.00000    0.00274    0.00000
C17     1     0.152257     0.750000     0.079888     10.50000     0.02952     0.01089
=
         0.03220    0.00000    0.00406    0.00000
HKLF 4
REM  new in P2(1)/m
REM R1 =  0.0462 for    856 Fo > 4sig(Fo)  and  0.0563 for all   1024 data
REM     58 parameters refined using      0 restraints
END
WGHT      0.0693      0.0000
REM Highest difference peak  1.356,  deepest hole -1.284,  1-sigma level  0.256
Q1    1   0.3194  0.5008  0.0803  11.00000  0.05    1.36
Q2    1   0.3055  0.4481  0.0816  11.00000  0.05    1.30
Q3    1   1.1380  0.7035  0.6615  11.00000  0.05    1.18
Q4    1   0.3424  0.5165  0.2638  11.00000  0.05    1.12
Q5    1   1.1261  0.7500  0.7037  10.50000  0.05    1.11
;
# Data collection and refinement data were not provided by Dr. Britton.
# Some atom labels have been edited after refinement
# to be consistent with other compounds. - KJT
```

2,4,6-Tribromobenzonitrile (204ca), $Z = 8$ TC polytype.

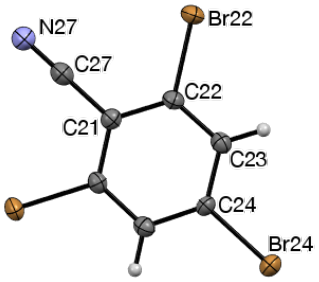

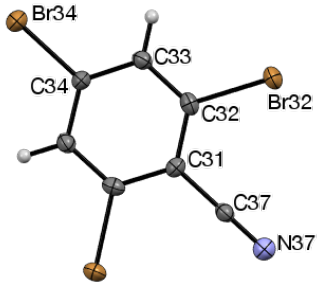

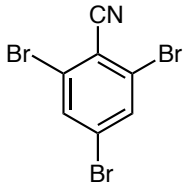

CIF content:

```
data_204ca2
_audit_creation_method     <i>SHELXTL</i>
_chemical_name_systematic
;
 2,4,6-Tribromobenzonitrile
;
_chemical_name_common     ‘tribromo nitrile, polytype 2’
_chemical_formula_moiety      'C7 H2 Br3 N'
_chemical_formula_sum     'C7 H2 Br3 N'
_chemical_formula_iupac      'C7 H2 Br3 N'
_chemical_formula_weight      339.83
_chemical_melting_point     ?
_symmetry_cell_setting     orthorhombic
_symmetry_space_group_name_H-M     'P n m a'
_symmetry_space_group_name_Hall     '-P 2ac 2n'
loop_
    _symmetry_equiv_pos_as_xyz
    'x, y, z'
    '-x+1/2, -y, z+1/2'
    '-x, y+1/2, -z'
    'x+1/2, -y+1/2, -z+1/2'
    '-x, -y, -z'
    'x-1/2, y, -z-1/2'
    'x, -y-1/2, z'
    '-x-1/2, y-1/2, z-1/2'
_cell_length_a     13.6183(13)
_cell_length_b     10.2147(10)
_cell_length_c     12.4754(12)
_cell_angle_alpha     90.00
_cell_angle_beta     90.00
_cell_angle_gamma     90.00
_cell_volume     1735.4(3)
_cell_formula_units_Z     8
_cell_measurement_reflns_used     3180
_cell_measurement_theta_min     2.9
_cell_measurement_theta_max     27.2
_cell_measurement_temperature     173(2)
_exptl_crystal_description     plate
_exptl_crystal_colour     colorless
_exptl_crystal_size_max     0.25
```

```
_exptl_crystal_size_mid     0.20
_exptl_crystal_size_min     0.07
_exptl_crystal_density_diffrn     2.601
_exptl_crystal_density_meas     ?
_exptl_crystal_density_method     'not measured'
_exptl_crystal_F_000     1248
_exptl_absorpt_coefficient_mu     13.876
_exptl_absorpt_correction_type     multi-scan
_exptl_absorpt_process_details
;
(SADABS; Bruker, 2002)
;
_exptl_absorpt_correction_T_min     0.06
_exptl_absorpt_correction_T_max     0.37
_diffrn_ambient_temperature     173(2)
_diffrn_radiation_type     MoK\a
_diffrn_radiation_wavelength     0.71073
_diffrn_radiation_source     'fine-focus sealed tube'
_diffrn_radiation_monochromator     graphite
_diffrn_measurement_device_type
;
Bruker 1K area-detector diffractometer
;
_diffrn_measurement_method     '\w scans'
_diffrn_detector_area_resol_mean     ?
_diffrn_reflns_number     16607
_diffrn_reflns_av_R_equivalents     0.0516
_diffrn_reflns_av_sigmaI/netI     0.0297
_diffrn_reflns_theta_min     2.21
_diffrn_reflns_theta_max     27.50
_diffrn_reflns_theta_full     27.50
_diffrn_measured_fraction_theta_max     0.997
_diffrn_measured_fraction_theta_full     0.997
_diffrn_reflns_limit_h_min     -17
_diffrn_reflns_limit_h_max     17
_diffrn_reflns_limit_k_min     -13
_diffrn_reflns_limit_k_max     13
_diffrn_reflns_limit_l_min     -16
_diffrn_reflns_limit_l_max     16
_diffrn_standards_number     0
_diffrn_standards_interval_count     ?
_diffrn_standards_interval_time     ?
_diffrn_standards_decay_%     '< 1'
_reflns_number_total     2093
_reflns_number_gt     1692
_reflns_threshold_expression     '>2\s(I)'
_refine_ls_structure_factor_coef     Fsqd
_refine_ls_matrix_type     full
_refine_ls_R_factor_all     0.0421
_refine_ls_R_factor_gt     0.0283
_refine_ls_wR_factor_gt     0.0589
_refine_ls_wR_factor_ref     0.0628
_refine_ls_goodness_of_fit_ref     1.020
_refine_ls_restrained_S_all     1.020
_refine_ls_number_reflns     2093
_refine_ls_number_parameters     115
```

```
_refine_ls_number_restraints     0
_refine_ls_hydrogen_treatment     constr
_refine_ls_weighting_scheme     calc
_refine_ls_weighting_details
        'calc w=1/[\s^2^(Fo^2^)+(0.0300P)^2^+1.5600P] where P=(Fo^2^+2Fc^2^)/3'
_atom_sites_solution_hydrogens     geom
_atom_sites_solution_primary     direct
_atom_sites_solution_secondary     difmap
_refine_ls_shift/su_max     0.001
_refine_ls_shift/su_mean     0.000
_refine_diff_density_max     0.438
_refine_diff_density_min     -0.687
_refine_ls_extinction_method     none
_refine_ls_extinction_coef     ?
loop_
    _atom_type_symbol
    _atom_type_description
    _atom_type_scat_dispersion_real
    _atom_type_scat_dispersion_imag
    _atom_type_scat_source
    'C' 'C' 0.0033 0.0016
                        'International Tables Vol C Tables 4.2.6.8 and 6.1.1.4'
    'H' 'H' 0.0000 0.0000
                        'International Tables Vol C Tables 4.2.6.8 and 6.1.1.4'
    'N' 'N' 0.0061 0.0033
                        'International Tables Vol C Tables 4.2.6.8 and 6.1.1.4'
    'Br' 'Br' -0.2901 2.4595
                        'International Tables Vol C Tables 4.2.6.8 and 6.1.1.4'
_computing_data_collection
;
SMART (Bruker, 2002)
;
_computing_cell_refinement
;
SAINT (Bruker, 2002)
;
_computing_data_reduction
;
SAINT (Bruker, 2002)
;
_computing_structure_solution
;
<i>SHELXTL</i> (Sheldrick, 2008)
;
_computing_structure_refinement
;
<i>SHELXTL</i> (Sheldrick, 2008)
;
_computing_molecular_graphics
;
Mercury (Macrae <i>et al.</i>, 2008)
;
_computing_publication_material
;
<i>SHELXTL</i> (Sheldrick, 2008), enCIFer (Allen <i>et al.</i>,
2004),
```

```
and publCIF (Westrip, 2010)
;
loop_
    _atom_site_type_symbol
    _atom_site_label
    _atom_site_fract_x
    _atom_site_fract_y
    _atom_site_fract_z
    _atom_site_U_iso_or_equiv
    _atom_site_adp_type
    _atom_site_calc_flag
    _atom_site_refinement_flags
    _atom_site_occupancy
    _atom_site_symmetry_multiplicity
    _atom_site_disorder_assembly
    _atom_site_disorder_group
    Br Br22 0.13341(3) 0.52761(3) 0.04244(3) 0.02658(11) Uani d . 1 1 . .
    Br Br24 0.14558(4) 0.2500 0.43375(4) 0.02477(13) Uani d S 1 2 . .
    C C21 0.1318(3) 0.2500 0.0608(4) 0.0197(10) Uani d S 1 2 . .
    C C22 0.1359(2) 0.3683(3) 0.1174(3) 0.0206(7) Uani d . 1 1 . .
    C C23 0.1418(2) 0.3697(3) 0.2282(3) 0.0217(7) Uani d . 1 1 . .
    H H23 0.1444 0.4500 0.2666 0.026 Uiso calc R 1 1 . .
    C C24 0.1437(3) 0.2500 0.2821(4) 0.0190(10) Uani d S 1 2 . .
    C C27 0.1207(4) 0.2500 -0.0545(4) 0.0257(11) Uani d S 1 2 . .
    N N27 0.1115(3) 0.2500 -0.1447(4) 0.0332(11) Uani d S 1 2 . .
    Br Br32 0.10699(3) 0.47273(3) 0.69146(3) 0.02650(11) Uani d . 1 1 . .
    Br Br34 0.12804(4) 0.7500 0.29979(4) 0.02786(13) Uani d S 1 2 . .
    C C31 0.1095(3) 0.7500 0.6720(3) 0.0175(9) Uani d S 1 2 . .
    C C32 0.1116(2) 0.6320(3) 0.6155(3) 0.0195(7) Uani d . 1 1 . .
    C C33 0.1171(2) 0.6315(3) 0.5049(3) 0.0201(7) Uani d . 1 1 . .
    H H33 0.1189 0.5511 0.4666 0.024 Uiso calc R 1 1 . .
    C C34 0.1199(3) 0.7500 0.4508(4) 0.0196(10) Uani d S 1 2 . .
    C C37 0.1056(3) 0.7500 0.7873(4) 0.0200(10) Uani d S 1 2 . .
    N N37 0.1015(3) 0.7500 0.8798(3) 0.0255(9) Uani d S 1 2 . .
loop_
    _atom_site_aniso_label
    _atom_site_aniso_U_11
    _atom_site_aniso_U_22
    _atom_site_aniso_U_33
    _atom_site_aniso_U_12
    _atom_site_aniso_U_13
    _atom_site_aniso_U_23
    Br22 0.0364(2) 0.01742(19) 0.0259(2) -0.00058(15) -0.00196(15) 0.00451(14)
    Br24 0.0303(3) 0.0261(3) 0.0179(2) 0.000 0.00098(19) 0.000
    C21 0.018(2) 0.021(3) 0.021(2) 0.000 0.0017(19) 0.000
    C22 0.0208(16) 0.0182(16) 0.0227(17) 0.0016(14) -0.0003(13) 0.0017(14)
    C23 0.0225(16) 0.0186(18) 0.0240(17) -0.0012(14) -0.0012(14) -0.0017(14)
    C24 0.021(2) 0.021(3) 0.015(2) 0.000 0.0022(18) 0.000
    C27 0.028(3) 0.020(3) 0.029(3) 0.000 0.000(2) 0.000
    N27 0.048(3) 0.026(2) 0.026(3) 0.000 -0.002(2) 0.000
    Br32 0.0386(2) 0.01618(19) 0.02475(19) -0.00117(15) 0.00205(14) 0.00374(14)
    Br34 0.0418(3) 0.0243(3) 0.0174(2) 0.000 -0.0003(2) 0.000
    C31 0.017(2) 0.021(2) 0.015(2) 0.000 -0.0003(17) 0.000
    C32 0.0182(15) 0.0163(16) 0.0241(17) 0.0004(13) -0.0006(13) 0.0044(14)
    C33 0.0229(17) 0.0157(18) 0.0216(17) 0.0015(14) -0.0009(13) -0.0018(14)
    C34 0.025(2) 0.018(2) 0.015(2) 0.000 -0.0001(18) 0.000
```

```
    C37 0.023(2) 0.014(2) 0.023(3) 0.000 -0.0009(19) 0.000
    N37 0.030(2) 0.024(2) 0.023(2) 0.000 -0.0002(17) 0.000
loop_
    _geom_bond_atom_site_label_1
    _geom_bond_atom_site_label_2
    _geom_bond_site_symmetry_2
    _geom_bond_distance
    _geom_bond_publ_flag
    Br22 C22 . 1.877(3) ?
    Br24 C24 . 1.892(5) ?
    C21 C22 . 1.400(4) ?
    C21 C27 . 1.446(7) ?
    C22 C23 . 1.385(5) ?
    C23 C24 . 1.395(4) ?
    C23 H23 . 0.9500 ?
    C27 N27 . 1.132(7) ?
    Br32 C32 . 1.884(3) ?
    Br34 C34 . 1.887(4) ?
    C31 C32 . 1.396(4) ?
    C31 C37 . 1.439(6) ?
    C32 C33 . 1.382(5) ?
    C33 C34 . 1.387(4) ?
    C33 H33 . 0.9500 ?
    C37 N37 . 1.156(6) ?
loop_
    _geom_angle_atom_site_label_1
    _geom_angle_atom_site_label_2
    _geom_angle_atom_site_label_3
    _geom_angle_site_symmetry_1
    _geom_angle_site_symmetry_3
    _geom_angle
    _geom_angle_publ_flag
    C22 C21 C22 7_565 . 119.3(4) ?
    C22 C21 C27 . . 120.3(2) ?
    C23 C22 C21 . . 120.9(3) ?
    C23 C22 Br22 . . 119.3(3) ?
    C21 C22 Br22 . . 119.8(3) ?
    C22 C23 C24 . . 118.2(3) ?
    C22 C23 H23 . . 120.9 ?
    C24 C23 H23 . . 120.9 ?
    C23 C24 C23 7_565 . 122.4(4) ?
    C23 C24 Br24 . . 118.8(2) ?
    N27 C27 C21 . . 179.7(5) ?
    C32 C31 C32 7_575 . 119.3(4) ?
    C32 C31 C37 . . 120.3(2) ?
    C33 C32 C31 . . 120.6(3) ?
    C33 C32 Br32 . . 120.0(3) ?
    C31 C32 Br32 . . 119.4(2) ?
    C32 C33 C34 . . 118.9(3) ?
    C32 C33 H33 . . 120.5 ?
    C34 C33 H33 . . 120.5 ?
    C33 C34 C33 7_575 . 121.6(4) ?
    C33 C34 Br34 . . 119.2(2) ?
    N37 C37 C31 . . 179.3(5) ?
loop_
    _geom_torsion_atom_site_label_1
```

```
    _geom_torsion_atom_site_label_2
    _geom_torsion_atom_site_label_3
    _geom_torsion_atom_site_label_4
    _geom_torsion_site_symmetry_1
    _geom_torsion_site_symmetry_2
    _geom_torsion_site_symmetry_3
    _geom_torsion_site_symmetry_4
    _geom_torsion
    _geom_torsion_publ_flag
    C22 C21 C22 C23 7_565 . . . -1.4(6) ?
    C27 C21 C22 C23 . . . . 176.8(4) ?
    C22 C21 C22 Br22 7_565 . . . 178.6(2) ?
    C27 C21 C22 Br22 . . . . -3.2(5) ?
    C21 C22 C23 C24 . . . . 0.1(5) ?
    Br22 C22 C23 C24 . . . . -179.9(3) ?
    C22 C23 C24 C23 . . . 7_565 1.3(7) ?
    C22 C23 C24 Br24 . . . . -177.1(2) ?
    C32 C31 C32 C33 7_575 . . . 0.8(6) ?
    C37 C31 C32 C33 . . . . -178.9(4) ?
    C32 C31 C32 Br32 7_575 . . . -179.2(2) ?
    C37 C31 C32 Br32 . . . . 1.1(5) ?
    C31 C32 C33 C34 . . . . -0.3(5) ?
    Br32 C32 C33 C34 . . . . 179.7(3) ?
    C32 C33 C34 C33 . . . 7_575 -0.2(7) ?
    C32 C33 C34 Br34 . . . . 179.7(2) ?
_iucr_refine_instructions_details
;
TITL RCN-II in Pnma
CELL 0.71073  13.6183  10.2147  12.4754  90.000  90.000  90.000
ZERR    8.00   0.0013   0.0010   0.0012   0.000   0.000   0.000
LATT  1
SYMM 0.5-X, -Y, 0.5+Z
SYMM -X, 0.5+Y, -Z
SYMM 0.5+X, 0.5-Y, 0.5-Z
SFAC C H N BR
UNIT 56 16 8 24
TEMP -100
L.S. 6
BOND $h
FMAP 2
PLAN 10
acta
conf
WGHT    0.030000    1.560000
FVAR       0.11811
BR22  4    0.133411    0.527611    0.042435    11.00000    0.03638    0.01742 =
         0.02593    0.00451   -0.00196   -0.00058
BR24  4    0.145575    0.250000    0.433753    10.50000    0.03027    0.02615 =
         0.01790    0.00000    0.00098    0.00000
C21   1    0.131848    0.250000    0.060832    10.50000    0.01801    0.02059 =
         0.02065    0.00000    0.00170    0.00000
C22   1    0.135935    0.368286    0.117379    11.00000    0.02077    0.01816 =
         0.02275    0.00172   -0.00032    0.00164
C23   1    0.141785    0.369699    0.228241    11.00000    0.02246    0.01859 =
         0.02403   -0.00169   -0.00121   -0.00123
AFIX  43
```

```
H23   2    0.144441    0.449992    0.266558    11.00000   -1.20000
AFIX   0
C24   1    0.143669    0.250000    0.282100    10.50000    0.02098    0.02106 =
        0.01507    0.00000    0.00217    0.00000
C27   1    0.120663    0.250000   -0.054469    10.50000    0.02752    0.02022 =
        0.02942    0.00000   -0.00017    0.00000
N27   3    0.111499    0.250000   -0.144689    10.50000    0.04771    0.02595 =
        0.02601    0.00000   -0.00211    0.00000
BR32  4    0.106987    0.472731    0.691461    11.00000    0.03857    0.01618 =
        0.02475    0.00374    0.00205   -0.00117
BR34  4    0.128037    0.750000    0.299795    10.50000    0.04184    0.02431 =
        0.01741    0.00000   -0.00029    0.00000
C31   1    0.109512    0.750000    0.671997    10.50000    0.01668    0.02069 =
        0.01509    0.00000   -0.00030    0.00000
C32   1    0.111640    0.632049    0.615502    11.00000    0.01818    0.01628 =
        0.02409    0.00439   -0.00056    0.00038
C33   1    0.117087    0.631451    0.504912    11.00000    0.02289    0.01571 =
        0.02159   -0.00181   -0.00089    0.00150
AFIX  43
H33   2    0.118862    0.551133    0.466568    11.00000   -1.20000
AFIX   0
C34   1    0.119922    0.750000    0.450764    10.50000    0.02533    0.01826 =
        0.01533    0.00000   -0.00010    0.00000
C37   1    0.105635    0.750000    0.787296    10.50000    0.02283    0.01403 =
        0.02322    0.00000   -0.00092    0.00000
N37   3    0.101486    0.750000    0.879809    10.50000    0.02962    0.02369 =
        0.02309    0.00000   -0.00019    0.00000
HKLF 4
REM  RCN-II in Pnma
REM R1 =  0.0283 for   1692 Fo > 4sig(Fo)  and  0.0421 for all   2093 data
REM    115 parameters refined using      0 restraints
END
WGHT      0.0178      2.2158
REM Highest difference peak  0.438,  deepest hole -0.687,  1-sigma level  0.132
Q1    1   0.0126  0.1227 -0.1446  11.00000  0.05    0.44
Q2    1   0.1288  0.8732  0.3011  11.00000  0.05    0.40
Q3    1   0.0169  0.6178  0.0202  11.00000  0.05    0.38
Q4    1   0.2751  0.4623  0.3201  11.00000  0.05    0.37
Q5    1   0.2527  0.5481  0.4448  11.00000  0.05    0.37
Q6    1   0.0481  0.4222  0.6437  11.00000  0.05    0.36
Q7    1   0.2639  0.5419  0.0200  11.00000  0.05    0.36
Q8    1   0.0478  0.2500  0.2381  10.50000  0.05    0.36
Q9    1   0.1871  0.4624 -0.0809  11.00000  0.05    0.35
Q10   1   0.2008  0.6304  0.0991  11.00000  0.05    0.35
;
# Data collection and refinement data were not provided by Dr. Britton.
# Some atom labels have been edited after refinement
# to be consistent with other compounds. - KJT
```

2,4,6-Tribromobenzonitrile (204ca), $Z = 12$ TCT polytype.

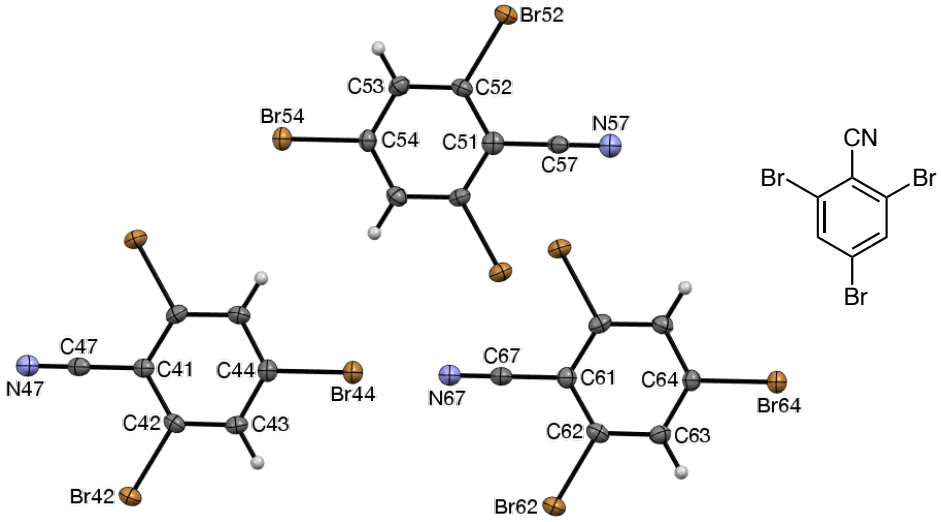

CIF content:

```
data_204ca3
_audit_creation_method     <i>SHELXTL</i>
_chemical_name_systematic
;
 2,4,6-Tribromobenzonitrile
;
_chemical_name_common     ‘tribromo nitrile, polytype 3’
_chemical_formula_moiety     'C7 H2 Br3 N'
_chemical_formula_sum     'C7 H2 Br3 N'
_chemical_formula_iupac     'C7 H2 Br3 N'
_chemical_formula_weight     339.83
_chemical_melting_point     ?
_symmetry_cell_setting     orthorhombic
_symmetry_space_group_name_H-M     'P n m a'
_symmetry_space_group_name_Hall     '-P 2ac 2n'
loop_
    _symmetry_equiv_pos_as_xyz
    'x, y, z'
    '-x+1/2, -y, z+1/2'
    '-x, y+1/2, -z'
    'x+1/2, -y+1/2, -z+1/2'
    '-x, -y, -z'
    'x-1/2, y, -z-1/2'
    'x, -y-1/2, z'
    '-x-1/2, y-1/2, z-1/2'
_cell_length_a     20.399(4)
_cell_length_b     10.2167(18)
_cell_length_c     12.493(2)
_cell_angle_alpha     90.00
_cell_angle_beta     90.00
_cell_angle_gamma     90.00
_cell_volume     2603.7(8)
_cell_formula_units_Z     12
```

```
_cell_measurement_reflns_used     2928
_cell_measurement_theta_min     2.58
_cell_measurement_theta_max     26.7
_cell_measurement_temperature     173(2)
_exptl_crystal_description     needle
_exptl_crystal_colour     colorless
_exptl_crystal_size_max     0.50
_exptl_crystal_size_mid     0.15
_exptl_crystal_size_min     0.10
_exptl_crystal_density_diffrn     2.601
_exptl_crystal_density_meas     ?
_exptl_crystal_density_method     'not measured'
_exptl_crystal_F_000     1872
_exptl_absorpt_coefficient_mu     13.873
_exptl_absorpt_correction_type     multi-scan
_exptl_absorpt_process_details
;
(SADABS; Bruker, 2002)
;
_exptl_absorpt_correction_T_min     0.054
_exptl_absorpt_correction_T_max     0.337
_diffrn_ambient_temperature     173(2)
_diffrn_radiation_type     MoK\a
_diffrn_radiation_wavelength     0.71073
_diffrn_radiation_source     'fine-focus sealed tube'
_diffrn_radiation_monochromator     graphite
_diffrn_measurement_device_type
;
Bruker 1K area-detector diffractometer
;
_diffrn_measurement_method     '\w scans'
_diffrn_detector_area_resol_mean     ?
_diffrn_reflns_number     22804
_diffrn_reflns_av_R_equivalents     0.0548
_diffrn_reflns_av_sigmaI/netI     0.0285
_diffrn_reflns_theta_min     2.58
_diffrn_reflns_theta_max     25.97
_diffrn_reflns_theta_full     25.97
_diffrn_measured_fraction_theta_max     0.994
_diffrn_measured_fraction_theta_full     0.994
_diffrn_reflns_limit_h_min     -24
_diffrn_reflns_limit_h_max     24
_diffrn_reflns_limit_k_min     -12
_diffrn_reflns_limit_k_max     12
_diffrn_reflns_limit_l_min     -15
_diffrn_reflns_limit_l_max     15
_diffrn_standards_number     0
_diffrn_standards_interval_count     ?
_diffrn_standards_interval_time     ?
_diffrn_standards_decay_%     '< 1'
_reflns_number_total     2691
_reflns_number_gt     2165
_reflns_threshold_expression     '>2\s(I)'
_refine_ls_structure_factor_coef     Fsqd
_refine_ls_matrix_type     full
_refine_ls_R_factor_all     0.0362
```

```
_refine_ls_R_factor_gt     0.0230
_refine_ls_wR_factor_gt     0.0428
_refine_ls_wR_factor_ref     0.0460
_refine_ls_goodness_of_fit_ref     1.066
_refine_ls_restrained_S_all     1.066
_refine_ls_number_reflns     2691
_refine_ls_number_parameters     173
_refine_ls_number_restraints     0
_refine_ls_hydrogen_treatment     constr
_refine_ls_weighting_scheme     calc
_refine_ls_weighting_details
        'calc w=1/[\s^2^(Fo^2^)+(0.0096P)^2^+3.3900P] where P=(Fo^2^+2Fc^2^)/3'
_atom_sites_solution_hydrogens     geom
_atom_sites_solution_primary     direct
_atom_sites_solution_secondary     difmap
_refine_ls_shift/su_max     0.001
_refine_ls_shift/su_mean     0.000
_refine_diff_density_max     0.557
_refine_diff_density_min     -0.494
_refine_ls_extinction_method     SHELXL
_refine_ls_extinction_coef     0.00028(3)
_refine_ls_extinction_expression
                               'Fc^*^=kFc[1+0.001xFc^2^\l^3^/sin(2\q)]^-1/4^'
loop_
    _atom_type_symbol
    _atom_type_description
    _atom_type_scat_dispersion_real
    _atom_type_scat_dispersion_imag
    _atom_type_scat_source
    'C' 'C' 0.0033 0.0016
                        'International Tables Vol C Tables 4.2.6.8 and 6.1.1.4'
    'H' 'H' 0.0000 0.0000
                        'International Tables Vol C Tables 4.2.6.8 and 6.1.1.4'
    'N' 'N' 0.0061 0.0033
                        'International Tables Vol C Tables 4.2.6.8 and 6.1.1.4'
    'Br' 'Br' -0.2901 2.4595
                        'International Tables Vol C Tables 4.2.6.8 and 6.1.1.4'
_computing_data_collection
;
SMART (Bruker, 2002)
;
_computing_cell_refinement
;
SAINT (Bruker, 2002)
;
_computing_data_reduction
;
SAINT (Bruker, 2002)
;
_computing_structure_solution
;
<i>SHELXTL</i> (Sheldrick, 2008)
;
_computing_structure_refinement
;
<i>SHELXTL</i> (Sheldrick, 2008)
```

```
;
_computing_molecular_graphics
;
Mercury (Macrae <i>et al.</i>, 2008)
;
_computing_publication_material
;
<i>SHELXTL</i> (Sheldrick, 2008), enCIFer (Allen <i>et al.</i>,
2004),
and publCIF (Westrip, 2010)
;
loop_
    _atom_site_type_symbol
    _atom_site_label
    _atom_site_fract_x
    _atom_site_fract_y
    _atom_site_fract_z
    _atom_site_U_iso_or_equiv
    _atom_site_adp_type
    _atom_site_calc_flag
    _atom_site_refinement_flags
    _atom_site_occupancy
    _atom_site_symmetry_multiplicity
    _atom_site_disorder_assembly
    _atom_site_disorder_group
    Br Br42 0.340999(16) 0.52705(3) -0.05464(3) 0.02707(10) Uani d . 1 1 . .
    Br Br44 0.32895(2) 0.2500 0.33679(4) 0.02913(13) Uani d S 1 2 . .
    Br Br52 0.332551(16) 0.47245(3) 0.59427(3) 0.02775(9) Uani d . 1 1 . .
    Br Br54 0.32011(2) 0.7500 0.20370(3) 0.02542(12) Uani d S 1 2 . .
    Br Br62 0.511839(16) 0.52774(3) 0.67598(3) 0.02743(10) Uani d . 1 1 . .
    Br Br64 0.50730(2) 0.2500 1.06666(4) 0.02435(12) Uani d S 1 2 . .
    C C41 0.33919(19) 0.2500 -0.0353(3) 0.0182(9) Uani d S 1 2 . .
    C C42 0.33772(14) 0.3675(3) 0.0214(2) 0.0207(7) Uani d . 1 1 . .
    C C43 0.33432(14) 0.3686(3) 0.1321(2) 0.0226(7) Uani d . 1 1 . .
    H H43 0.3331 0.4487 0.1706 0.027 Uiso calc R 1 1 . .
    C C44 0.3328(2) 0.2500 0.1851(4) 0.0219(10) Uani d S 1 2 . .
    C C47 0.3440(2) 0.2500 -0.1508(4) 0.0218(10) Uani d S 1 2 . .
    N N47 0.34814(18) 0.2500 -0.2423(3) 0.0272(9) Uani d S 1 2 . .
    C C51 0.3338(2) 0.7500 0.5758(4) 0.0221(10) Uani d S 1 2 . .
    C C52 0.33096(14) 0.6320(3) 0.5193(2) 0.0211(7) Uani d . 1 1 . .
    C C53 0.32641(14) 0.6314(3) 0.4085(2) 0.0228(7) Uani d . 1 1 . .
    H H53 0.3246 0.5512 0.3701 0.027 Uiso calc R 1 1 . .
    C C54 0.3245(2) 0.7500 0.3549(3) 0.0204(10) Uani d S 1 2 . .
    C C57 0.3399(2) 0.7500 0.6908(4) 0.0225(10) Uani d S 1 2 . .
    N N57 0.3445(2) 0.7500 0.7823(3) 0.0329(10) Uani d S 1 2 . .
    C C61 0.5080(2) 0.2500 0.6942(4) 0.0204(10) Uani d S 1 2 . .
    C C62 0.50889(14) 0.3676(3) 0.7509(2) 0.0216(7) Uani d . 1 1 . .
    C C63 0.50886(14) 0.3686(3) 0.8618(2) 0.0218(7) Uani d . 1 1 . .
    H H63 0.5092 0.4488 0.9002 0.026 Uiso calc R 1 1 . .
    C C64 0.5083(2) 0.2500 0.9155(4) 0.0200(10) Uani d S 1 2 . .
    C C67 0.5049(2) 0.2500 0.5783(4) 0.0225(10) Uani d S 1 2 . .
    N N67 0.5024(2) 0.2500 0.4872(3) 0.0329(10) Uani d S 1 2 . .
loop_
    _atom_site_aniso_label
    _atom_site_aniso_U_11
    _atom_site_aniso_U_22
```

```
    _atom_site_aniso_U_33
    _atom_site_aniso_U_12
    _atom_site_aniso_U_13
    _atom_site_aniso_U_23
    Br42 0.03864(19) 0.01711(17) 0.02545(18) -0.00178(14) 0.00143(15)

0.00391(15)
    Br44 0.0432(3) 0.0252(3) 0.0190(3) 0.000 0.0007(2) 0.000
    Br52 0.03826(19) 0.01818(17) 0.02682(18) -0.00040(15) -0.00267(15)

0.00467(15)
    Br54 0.0309(3) 0.0270(3) 0.0184(2) 0.000 0.0017(2) 0.000
    Br62 0.03877(19) 0.01736(17) 0.02617(18) -0.00080(15) -0.00036(15)

0.00376(15)
    Br64 0.0300(2) 0.0243(3) 0.0188(2) 0.000 -0.00018(19) 0.000
    C41 0.016(2) 0.017(2) 0.022(2) 0.000 -0.0010(18) 0.000
    C42 0.0214(15) 0.0175(17) 0.0233(17) -0.0001(14) -0.0011(13) 0.0052(14)
    C43 0.0269(16) 0.0160(17) 0.0248(17) -0.0016(14) -0.0003(14) -0.0016(15)
    C44 0.023(2) 0.024(3) 0.019(2) 0.000 0.0000(19) 0.000
    C47 0.020(2) 0.016(2) 0.029(3) 0.000 -0.004(2) 0.000
    N47 0.033(2) 0.022(2) 0.026(2) 0.000 -0.0017(19) 0.000
    C51 0.016(2) 0.026(3) 0.024(2) 0.000 0.001(2) 0.000
    C52 0.0244(15) 0.0154(17) 0.0234(16) 0.0002(14) -0.0002(13) 0.0037(14)
    C53 0.0255(16) 0.0198(18) 0.0232(17) 0.0025(14) 0.0024(14) -0.0031(15)
    C54 0.020(2) 0.024(3) 0.017(2) 0.000 0.0021(18) 0.000
    C57 0.025(2) 0.015(2) 0.027(3) 0.000 -0.003(2) 0.000
    N57 0.048(3) 0.027(2) 0.024(2) 0.000 -0.001(2) 0.000
    C61 0.020(2) 0.022(2) 0.020(2) 0.000 0.0041(19) 0.000
    C62 0.0199(15) 0.0188(17) 0.0261(17) 0.0017(13) 0.0011(13) 0.0047(15)
    C63 0.0236(16) 0.0178(18) 0.0239(16) 0.0007(14) 0.0018(13) -0.0028(15)
    C64 0.020(2) 0.022(2) 0.018(2) 0.000 0.0017(19) 0.000
    C67 0.028(2) 0.016(2) 0.024(3) 0.000 0.000(2) 0.000
    N67 0.055(3) 0.021(2) 0.024(2) 0.000 -0.002(2) 0.000
loop_
    _geom_bond_atom_site_label_1
    _geom_bond_atom_site_label_2
    _geom_bond_site_symmetry_2
    _geom_bond_distance
    _geom_bond_publ_flag
    Br42 C42 . 1.888(3) ?
    Br44 C44 . 1.897(5) ?
    Br52 C52 . 1.880(3) ?
    Br54 C54 . 1.892(4) ?
    Br62 C62 . 1.885(3) ?
    Br64 C64 . 1.889(4) ?
    C41 C42 . 1.394(4) ?
    C41 C47 . 1.447(6) ?
    C42 C43 . 1.384(4) ?
    C43 C44 . 1.381(4) ?
    C43 H43 . 0.9500 ?
    C47 N47 . 1.146(6) ?
    C51 C52 . 1.399(4) ?
    C51 C57 . 1.443(6) ?
    C52 C53 . 1.387(4) ?
    C53 C54 . 1.384(4) ?
```

```
    C53 H53 . 0.9500 ?
    C57 N57 . 1.147(6) ?
    C61 C62 . 1.395(4) ?
    C61 C67 . 1.450(6) ?
    C62 C63 . 1.386(4) ?
    C63 C64 . 1.385(4) ?
    C63 H63 . 0.9500 ?
    C67 N67 . 1.139(6) ?
loop_
    _geom_angle_atom_site_label_1
    _geom_angle_atom_site_label_2
    _geom_angle_atom_site_label_3
    _geom_angle_site_symmetry_1
    _geom_angle_site_symmetry_3
    _geom_angle
    _geom_angle_publ_flag
    C42 C41 C42 . 7_565 118.9(4) ?
    C42 C41 C47 . . 120.5(2) ?
    C43 C42 C41 . . 121.0(3) ?
    C43 C42 Br42 . . 119.9(2) ?
    C41 C42 Br42 . . 119.2(2) ?
    C44 C43 C42 . . 118.3(3) ?
    C44 C43 H43 . . 120.9 ?
    C42 C43 H43 . . 120.9 ?
    C43 C44 C43 7_565 . 122.6(4) ?
    C43 C44 Br44 . . 118.7(2) ?
    N47 C47 C41 . . 179.7(5) ?
    C52 C51 C52 7_575 . 119.1(4) ?
    C52 C51 C57 . . 120.4(2) ?
    C53 C52 C51 . . 120.7(3) ?
    C53 C52 Br52 . . 119.7(2) ?
    C51 C52 Br52 . . 119.7(2) ?
    C54 C53 C52 . . 118.7(3) ?
    C54 C53 H53 . . 120.6 ?
    C52 C53 H53 . . 120.6 ?
    C53 C54 C53 7_575 . 122.1(4) ?
    C53 C54 Br54 . . 119.0(2) ?
    N57 C57 C51 . . 179.8(5) ?
    C62 C61 C62 7_565 . 119.0(4) ?
    C62 C61 C67 . . 120.5(2) ?
    C63 C62 C61 . . 120.9(3) ?
    C63 C62 Br62 . . 119.4(3) ?
    C61 C62 Br62 . . 119.8(2) ?
    C64 C63 C62 . . 118.6(3) ?
    C64 C63 H63 . . 120.7 ?
    C62 C63 H63 . . 120.7 ?
    C63 C64 C63 7_565 . 122.0(4) ?
    C63 C64 Br64 . . 119.0(2) ?
    N67 C67 C61 . . 180.0(5) ?
loop_
    _geom_torsion_atom_site_label_1
    _geom_torsion_atom_site_label_2
    _geom_torsion_atom_site_label_3
    _geom_torsion_atom_site_label_4
    _geom_torsion_site_symmetry_1
    _geom_torsion_site_symmetry_2
```

```
    _geom_torsion_site_symmetry_3
    _geom_torsion_site_symmetry_4
    _geom_torsion
    _geom_torsion_publ_flag
    C42 C41 C42 C43 7_565 . . . -0.5(6) ?
    C47 C41 C42 C43 . . . . -178.8(3) ?
    C42 C41 C42 Br42 7_565 . . . 179.07(19) ?
    C47 C41 C42 Br42 . . . . 0.8(5) ?
    C41 C42 C43 C44 . . . . 0.4(5) ?
    Br42 C42 C43 C44 . . . . -179.2(3) ?
    C42 C43 C44 C43 . . . 7_565 -0.2(6) ?
    C42 C43 C44 Br44 . . . . 179.4(2) ?
    C52 C51 C52 C53 7_575 . . . 0.9(6) ?
    C57 C51 C52 C53 . . . . -178.7(3) ?
    C52 C51 C52 Br52 7_575 . . . -178.48(19) ?
    C57 C51 C52 Br52 . . . . 1.9(5) ?
    C51 C52 C53 C54 . . . . -0.2(5) ?
    Br52 C52 C53 C54 . . . . 179.2(3) ?
    C52 C53 C54 C53 . . . 7_575 -0.6(6) ?
    C52 C53 C54 Br54 . . . . 178.7(2) ?
    C62 C61 C62 C63 7_565 . . . -1.7(6) ?
    C67 C61 C62 C63 . . . . 177.0(3) ?
    C62 C61 C62 Br62 7_565 . . . 177.1(2) ?
    C67 C61 C62 Br62 . . . . -4.2(5) ?
    C61 C62 C63 C64 . . . . 0.4(5) ?
    Br62 C62 C63 C64 . . . . -178.4(3) ?
    C62 C63 C64 C63 . . . 7_565 1.0(6) ?
    C62 C63 C64 Br64 . . . . -179.3(2) ?
_iucr_refine_instructions_details
;
TITL RCN-III in Pnma
CELL 0.71073  20.3990  10.2167  12.4930  90.000  90.000  90.000
ZERR   12.00   0.0036   0.0018   0.0022   0.000   0.000   0.000
LATT  1
SYMM 0.5-X, -Y, 0.5+Z
SYMM -X, 0.5+Y, -Z
SYMM 0.5+X, 0.5-Y, 0.5-Z
SFAC C H N BR
UNIT 84 24 12 36
TEMP -100
L.S. 10
BOND $h
FMAP 2
PLAN 10
conf
acta
size 0.50 0.15 0.10
omit -3 52
WGHT    0.009600    3.390000
EXTI    0.000276
FVAR       0.08043
BR42  4    0.340999    0.527049   -0.054642    11.00000    0.03864    0.01711 =
         0.02545    0.00391    0.00143   -0.00178
BR44  4    0.328952    0.250000    0.336790    10.50000    0.04320    0.02518 =
         0.01901    0.00000    0.00065    0.00000
BR52  4    0.332551    0.472449    0.594265    11.00000    0.03826    0.01818 =
```

```
         0.02682    0.00467   -0.00267   -0.00040
BR54  4    0.320108    0.750000    0.203697    10.50000    0.03088    0.02697 =
         0.01842    0.00000    0.00175    0.00000
BR62  4    0.511839    0.527742    0.675978    11.00000    0.03877    0.01736 =
         0.02617    0.00376   -0.00036   -0.00080
BR64  4    0.507299    0.250000    1.066658    10.50000    0.02997    0.02430 =
         0.01878    0.00000   -0.00018    0.00000
C41   1    0.339189    0.250000   -0.035271    10.50000    0.01568    0.01721 =
         0.02174    0.00000   -0.00105    0.00000
C42   1    0.337720    0.367531    0.021412    11.00000    0.02137    0.01749 =
         0.02329    0.00521   -0.00112   -0.00006
C43   1    0.334321    0.368562    0.132086    11.00000    0.02693    0.01604 =
         0.02481   -0.00161   -0.00028   -0.00158
AFIX  43
H43   2    0.333055    0.448734    0.170551    11.00000   -1.20000
AFIX   0
C44   1    0.332818    0.250000    0.185098    10.50000    0.02274    0.02382 =
         0.01923    0.00000    0.00005    0.00000
C47   1    0.344047    0.250000   -0.150845    10.50000    0.01999    0.01592 =
         0.02936    0.00000   -0.00371    0.00000
N47   3    0.348142    0.250000   -0.242299    10.50000    0.03316    0.02209 =
         0.02645    0.00000   -0.00174    0.00000
C51   1    0.333772    0.750000    0.575798    10.50000    0.01631    0.02630 =
         0.02379    0.00000    0.00121    0.00000
C52   1    0.330958    0.631987    0.519256    11.00000    0.02442    0.01545 =
         0.02341    0.00372   -0.00023    0.00021
C53   1    0.326408    0.631443    0.408502    11.00000    0.02546    0.01984 =
         0.02322   -0.00308    0.00240    0.00253
AFIX  43
H53   2    0.324616    0.551248    0.370124    11.00000   -1.20000
AFIX   0
C54   1    0.324527    0.750000    0.354939    10.50000    0.01972    0.02435 =
         0.01726    0.00000    0.00215    0.00000
C57   1    0.339893    0.750000    0.690841    10.50000    0.02534    0.01480 =
         0.02728    0.00000   -0.00297    0.00000
N57   3    0.344526    0.750000    0.782315    10.50000    0.04776    0.02708 =
         0.02387    0.00000   -0.00145    0.00000
C61   1    0.508004    0.250000    0.694229    10.50000    0.01952    0.02164 =
         0.02008    0.00000    0.00413    0.00000
C62   1    0.508888    0.367625    0.750855    11.00000    0.01995    0.01882 =
         0.02607    0.00473    0.00105    0.00173
C63   1    0.508857    0.368556    0.861775    11.00000    0.02365    0.01776 =
         0.02388   -0.00279    0.00176    0.00072
AFIX  43
H63   2    0.509178    0.448823    0.900159    11.00000   -1.20000
AFIX   0
C64   1    0.508349    0.250000    0.915464    10.50000    0.02019    0.02164 =
         0.01825    0.00000    0.00167    0.00000
C67   1    0.504881    0.250000    0.578257    10.50000    0.02795    0.01571 =
         0.02383    0.00000    0.00023    0.00000
N67   3    0.502382    0.250000    0.487180    10.50000    0.05457    0.02058 =
         0.02369    0.00000   -0.00218    0.00000
HKLF 4
REM  RCN-III in Pnma
REM R1 =  0.0230 for   2165 Fo > 4sig(Fo)  and  0.0362 for all   2691 data
REM    173 parameters refined using      0 restraints
```

```
END
WGHT      0.0081      3.4272
REM Highest difference peak  0.557,  deepest hole -0.494,  1-sigma level  0.099
Q1    1   0.5114  0.6011  0.7358  11.00000  0.05    0.56
Q2    1   0.3357  0.5987  0.0008  11.00000  0.05    0.51
Q3    1   0.3475  0.4587  0.0092  11.00000  0.05    0.47
Q4    1   0.5085  0.4656  0.6200  11.00000  0.05    0.46
Q5    1   0.3403  0.4033  0.5407  11.00000  0.05    0.45
;
# Data collection and refinement data were not provided by Dr. Britton.
# Some atom labels have been edited after refinement
# to be consistent with other compounds. - KJT
```

2,6-Dibromo-4-methylbenzonitrile (204cb).

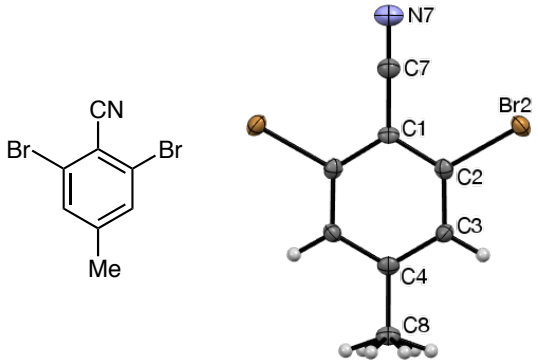

Data collection (by the XCL): A crystal (approx. 0.500 × 0.070 × 0.035 mm^3) was placed onto the tip of an 0.1 mm diameter glass capillary and mounted on a Bruker-AXS D8 Venture PHOTON-II diffractometer for a data collection at 123 K. A preliminary set of cell constants was calculated from reflections harvested from three sets of frames. These initial sets of frames were oriented such that orthogonal wedges of reciprocal space were surveyed. This produced an initial orientation matrix determined from 219 reflections. The data collection was carried out using CuKα radiation (parabolic mirrors) with a frame time of 5, 10, or 15 sec with a detector distance of 40 mm. A strategy program was used to assure complete coverage of all unique data to a resolution of 0.80 Å. All major sections of frames were collected with 2.0° steps in ω or ϕ at different detector positions in 2θ. The intensity data were corrected for absorption and decay. Final cell constants were calculated from 2,980 strong reflections from the actual data collection after integration.

Structure solution and refinement (by the XCL): The space group P-42_1m was determined based on systematic absences and intensity statistics. A direct-methods solution was calculated τηατ provided most non-hydrogen atoms from the E-map. Full-matrix least squares / difference Fourier cycles were performed τηατ located the remaining non-hydrogen atoms. All non-hydrogen atoms were refined with anisotropic displacement parameters. All hydrogen atoms were placed in ideal positions and refined as riding atoms with relative isotropic displacement parameters. The final full matrix least squares refinement converged to $R1$ = 0.0201 and $wR2$ = 0.0571 (F^2, obs. data).

CIF content:

data_204cb

```
_audit_creation_method            'SHELXL-2014/7'
_shelx_SHELXL_version_number      '2014/7'
_chemical_name_systematic
;
2,6-Dibromo-4-methylbenzonitrile
;
_chemical_name_common             ‘dibromo methyl nitrile'
_chemical_melting_point           ?
_chemical_formula_moiety          'C8 H5 Br2 N'
_chemical_formula_sum             'C8 H5 Br2 N'
_chemical_formula_weight          274.95

loop_
 _atom_type_symbol
 _atom_type_description
 _atom_type_scat_dispersion_real
 _atom_type_scat_dispersion_imag
 _atom_type_scat_source
 'C'  'C'   0.0181   0.0091
 'International Tables Vol C Tables 4.2.6.8 and 6.1.1.4'
 'H'  'H'   0.0000   0.0000
 'International Tables Vol C Tables 4.2.6.8 and 6.1.1.4'
 'N'  'N'   0.0311   0.0180
 'International Tables Vol C Tables 4.2.6.8 and 6.1.1.4'
 'Br'  'Br'  -0.6763   1.2805
 'International Tables Vol C Tables 4.2.6.8 and 6.1.1.4'

_space_group_crystal_system       tetragonal
_space_group_IT_number            113
_space_group_name_H-M_alt         'P -4 21 m'
_space_group_name_Hall            'P -4 2ab'

_shelx_space_group_comment
;
The symmetry employed for this shelxl refinement is uniquely defined
by the following loop, which should always be used as a source of
symmetry information in preference to the above space-group names.
They are only intended as comments.
;

loop_
 _space_group_symop_operation_xyz
 'x, y, z'
 '-x, -y, z'
 'y, -x, -z'
 '-y, x, -z'
 '-x+1/2, y+1/2, -z'
 'x+1/2, -y+1/2, -z'
 '-y+1/2, -x+1/2, z'
 'y+1/2, x+1/2, z'

_cell_length_a                    14.6731(5)
```

```
_cell_length_b                    14.6731(5)
_cell_length_c                    3.9727(1)
_cell_angle_alpha                 90
_cell_angle_beta                  90
_cell_angle_gamma                 90
_cell_volume                      855.32(6)
_cell_formula_units_Z             4
_cell_measurement_temperature     123(2)
_cell_measurement_reflns_used     2980
_cell_measurement_theta_min       4.26
_cell_measurement_theta_max       74.01

_exptl_crystal_description       'Needle'
_exptl_crystal_colour            'colourless'
_exptl_crystal_density_meas       ?
_exptl_crystal_density_method     ?
_exptl_crystal_density_diffrn     2.135
_exptl_crystal_F_000              520
_exptl_transmission_factor_min    0.3135
_exptl_transmission_factor_max    0.7538
_exptl_crystal_size_max           0.500
_exptl_crystal_size_mid           0.070
_exptl_crystal_size_min           0.035
_exptl_absorpt_coefficient_mu     11.456
_shelx_estimated_absorpt_T_min    0.069
_shelx_estimated_absorpt_T_max    0.690
_exptl_absorpt_correction_type    multi-scan
_exptl_absorpt_correction_T_min   0.3135
_exptl_absorpt_correction_T_max   0.7538
_exptl_absorpt_process_details    'SADABS-2014 (Sheldrick, 2014)'
_exptl_absorpt_special_details
;
 Equivalent reflections defined by point group -42m
;
_exptl_special_details            'K. Tritch / Prof. W. Noland'
_diffrn_ambient_temperature       123(2)
_diffrn_radiation_wavelength      1.54178
_diffrn_radiation_type            CuK\a
_diffrn_source                    'ImuS micro-focus'
_diffrn_measurement_device_type   'Bruker-AXS D8 Venture PHOTON-II'
_diffrn_measurement_method        '\f and \w scans'
_diffrn_detector_area_resol_mean  ?
_diffrn_reflns_number             8444
_diffrn_reflns_av_unetI/netI      0.0234
_diffrn_reflns_av_R_equivalents   0.0387
_diffrn_reflns_limit_h_min        -18
_diffrn_reflns_limit_h_max        18
_diffrn_reflns_limit_k_min        -17
_diffrn_reflns_limit_k_max        17
_diffrn_reflns_limit_l_min        -4
_diffrn_reflns_limit_l_max        4
_diffrn_reflns_theta_min          6.032
_diffrn_reflns_theta_max          74.241
_diffrn_reflns_theta_full         67.679
_diffrn_measured_fraction_theta_max   0.996
_diffrn_measured_fraction_theta_full  0.998
```

```
_diffrn_reflns_Laue_measured_fraction_max    0.996
_diffrn_reflns_Laue_measured_fraction_full   0.998
_diffrn_reflns_point_group_measured_fraction_max   0.989
_diffrn_reflns_point_group_measured_fraction_full  0.996
_reflns_number_total              904
_reflns_number_gt                 902
_reflns_threshold_expression      'I > 2\s(I)'
_reflns_Friedel_coverage          0.632
_reflns_Friedel_fraction_max      0.978
_reflns_Friedel_fraction_full     0.994

_reflns_special_details
;
 Reflections were merged by SHELXL according to the crystal
 class for the calculation of statistics and refinement.

 _reflns_Friedel_fraction is defined as the number of unique
 Friedel pairs measured divided by the number that would be
 possible theoretically, ignoring centric projections and
 systematic absences.
;

_computing_data_collection       'Bruker APEX2'
_computing_cell_refinement       'Bruker SAINT'
_computing_data_reduction        'Bruker SAINT'
_computing_structure_solution    'SHELXT-2014/5 (Sheldrick, 2014)'
_computing_structure_refinement  'SHELXL-2014/7 (Sheldrick, 2014)'
_computing_molecular_graphics    'Bruker SHELXTL'
_computing_publication_material  'Bruker SHELXTL'
_refine_special_details           ?
_refine_ls_structure_factor_coef  Fsqd
_refine_ls_matrix_type            full
_refine_ls_weighting_scheme       calc
_refine_ls_weighting_details
'w=1/[\s^2^(Fo^2^)+2.1952P] where P=(Fo^2^+2Fc^2^)/3'
_atom_sites_solution_primary      ?
_atom_sites_solution_secondary    ?
_atom_sites_solution_hydrogens    geom
_refine_ls_hydrogen_treatment     constr
_refine_ls_extinction_method      'SHELXL-2014/7 (Sheldrick 2014)'
_refine_ls_extinction_coef        0.0055(4)
_refine_ls_extinction_expression
 'Fc^*^=kFc[1+0.001xFc^2^\l^3^/sin(2\q)]^-1/4^'
_refine_ls_abs_structure_details
;
 Flack x determined using 348 quotients [(I+)-(I-)]/[(I+)+(I-)]
 (Parsons, Flack and Wagner, Acta Cryst. B69 (2013) 249-259).
;
_refine_ls_abs_structure_Flack    -0.02(3)
_chemical_absolute_configuration  ad
_refine_ls_number_reflns          904
_refine_ls_number_parameters      60
_refine_ls_number_restraints      0
_refine_ls_R_factor_all           0.0201
_refine_ls_R_factor_gt            0.0201
_refine_ls_wR_factor_ref          0.0571
```

```
_refine_ls_wR_factor_gt           0.0571
_refine_ls_goodness_of_fit_ref    1.270
_refine_ls_restrained_S_all       1.270
_refine_ls_shift/su_max           0.001
_refine_ls_shift/su_mean          0.000

loop_
 _atom_site_label
 _atom_site_type_symbol
 _atom_site_fract_x
 _atom_site_fract_y
 _atom_site_fract_z
 _atom_site_U_iso_or_equiv
 _atom_site_adp_type
 _atom_site_occupancy
 _atom_site_site_symmetry_order
 _atom_site_calc_flag
 _atom_site_refinement_flags_posn
 _atom_site_refinement_flags_adp
 _atom_site_refinement_flags_occupancy
 _atom_site_disorder_assembly
 _atom_site_disorder_group
C1 C 0.2722(3) 0.7722(3) 0.357(2) 0.0156(13) Uani 1 2 d S T P . .
C2 C 0.2985(3) 0.6837(4) 0.2695(13) 0.0177(10) Uani 1 1 d . . . . .
Br2 Br 0.41762(3) 0.64354(3) 0.38319(19) 0.0222(2) Uani 1 1 d . . . . .
C3 C 0.2404(3) 0.6240(3) 0.1067(15) 0.0185(9) Uani 1 1 d . . . . .
H3 H 0.2605 0.5645 0.0486 0.022 Uiso 1 1 calc R U . . .
C4 C 0.1517(3) 0.6517(3) 0.0283(18) 0.0189(15) Uani 1 2 d S T P . .
C7 C 0.3328(4) 0.8328(4) 0.532(2) 0.0223(17) Uani 1 2 d S T P . .
N7 N 0.3806(3) 0.8806(3) 0.676(2) 0.0309(17) Uani 1 2 d S T P . .
C8 C 0.0866(3) 0.5866(3) -0.138(2) 0.0212(13) Uani 1 2 d S T P . .
H8A H 0.0306 0.6190 -0.1991 0.032 Uiso 0.5 1 calc R U P . .
H8B H 0.0720 0.5369 0.0175 0.032 Uiso 0.5 1 calc R U P . .
H8C H 0.1148 0.5615 -0.3417 0.032 Uiso 0.5 1 calc R U P . .

loop_
 _atom_site_aniso_label
 _atom_site_aniso_U_11
 _atom_site_aniso_U_22
 _atom_site_aniso_U_33
 _atom_site_aniso_U_23
 _atom_site_aniso_U_13
 _atom_site_aniso_U_12
C1 0.0183(18) 0.0183(18) 0.010(3) 0.000(2) 0.000(2) -0.003(2)
C2 0.015(2) 0.019(2) 0.019(3) 0.0025(19) 0.0034(19) 0.0001(19)
Br2 0.0147(3) 0.0236(3) 0.0282(3) 0.0042(3) -0.0017(2) 0.00002(17)
C3 0.018(2) 0.015(2) 0.022(2) -0.003(2) 0.002(3) -0.0001(17)
C4 0.018(2) 0.018(2) 0.020(4) 0.0031(18) 0.0031(18) -0.005(3)
C7 0.022(2) 0.022(2) 0.024(4) 0.000(2) 0.000(2) -0.002(3)
N7 0.031(2) 0.031(2) 0.030(4) -0.003(2) -0.003(2) -0.009(3)
C8 0.023(2) 0.023(2) 0.017(3) 0.000(2) 0.000(2) -0.005(3)

_geom_special_details
;
 All esds (except the esd in the dihedral angle between two l.s. planes)
 are estimated using the full covariance matrix.  The cell esds are taken
```

```
 into account individually in the estimation of esds in distances, angles
 and torsion angles; correlations between esds in cell parameters are only
 used when they are defined by crystal symmetry.  An approximate (isotropic)
 treatment of cell esds is used for estimating esds involving l.s. planes.
;

loop_
 _geom_bond_atom_site_label_1
 _geom_bond_atom_site_label_2
 _geom_bond_distance
 _geom_bond_site_symmetry_2
 _geom_bond_publ_flag
C1 C2 1.399(6) 8_455 ?
C1 C2 1.399(6) . ?
C1 C5 1.437(10) . ?
C2 C3 1.383(8) . ?
C2 Br2 1.899(5) . ?
C3 C4 1.398(6) . ?
C3 H3 0.9500 . ?
C4 C3 1.398(6) 8_455 ?
C4 C6 1.505(10) . ?
C7 N7 1.145(11) . ?
C8 H8A 0.9800 . ?
C8 H8B 0.9800 . ?
C8 H8C 0.9800 . ?

loop_
 _geom_angle_atom_site_label_1
 _geom_angle_atom_site_label_2
 _geom_angle_atom_site_label_3
 _geom_angle
 _geom_angle_site_symmetry_1
 _geom_angle_site_symmetry_3
 _geom_angle_publ_flag
C2 C1 C2 116.8(7) 8_455 . ?
C2 C1 C7 121.6(3) 8_455 . ?
C2 C1 C7 121.6(3) . . ?
C3 C2 C1 122.3(5) . . ?
C3 C2 Br2 118.8(4) . . ?
C1 C2 Br2 118.9(4) . . ?
C2 C3 C4 119.6(5) . . ?
C2 C3 H3 120.2 . . ?
C4 C3 H3 120.2 . . ?
C3 C4 C3 119.5(6) 8_455 . ?
C3 C4 C8 120.3(3) 8_455 . ?
C3 C4 C8 120.3(3) . . ?
N7 C7 C1 179.0(9) . . ?
C4 C8 H8A 109.5 . . ?
C4 C8 H8B 109.5 . . ?
H8A C8 H8B 109.5 . . ?
C4 C8 H8C 109.5 . . ?
H8A C8 H8C 109.5 . . ?
H8B C8 H8C 109.5 . . ?

loop_
 _geom_torsion_atom_site_label_1
```

```
 _geom_torsion_atom_site_label_2
 _geom_torsion_atom_site_label_3
 _geom_torsion_atom_site_label_4
 _geom_torsion
 _geom_torsion_site_symmetry_1
 _geom_torsion_site_symmetry_2
 _geom_torsion_site_symmetry_3
 _geom_torsion_site_symmetry_4
 _geom_torsion_publ_flag
C2 C1 C2 C3 -0.5(10) 8_455 . . . ?
C7 C1 C2 C3 178.7(7) . . . . ?
C2 C1 C2 Br2 -179.7(4) 8_455 . . . ?
C5 C1 C2 Br2 -0.5(9) . . . . ?
C1 C2 C3 C4 -0.7(9) . . . . ?
Br2 C2 C3 C4 178.5(5) . . . . ?
C2 C3 C4 C3 1.9(11) . . . 8_455 ?
C2 C3 C4 C8 -178.0(6) . . . . ?

_refine_diff_density_max    0.371
_refine_diff_density_min   -0.316
_refine_diff_density_rms    0.092

_shelx_res_file
;
    16098a.res created by SHELXL-2014/7

TITL 16098a_a.res in P-42(1)m
REM Old TITL 16098a in P4(2)2(1)2

REM SHELXT solution in P-42(1)m
REM R1 0.067,  Rweak 0.029,  Alpha 0.011,  Orientation as input
REM Flack x =  0.012 ( 0.035 ) from Parsons' quotients
REM Formula found by SHELXT:  C8 N Br2

CELL  1.54178  14.6731  14.6731   3.9727   90.000   90.000   90.000
ZERR    4.000   0.0005   0.0005   0.0001    0.000    0.000    0.000
LATT -1
SYMM -X, -Y, Z
SYMM Y, -X, -Z
SYMM -Y, X, -Z
SYMM 1/2-X, 1/2+Y, -Z
SYMM 1/2+X, 1/2-Y, -Z
SYMM 1/2-Y, 1/2-X, Z
SYMM 1/2+Y, 1/2+X, Z
SFAC C  H  N BR
UNIT 32 20 4 8
TEMP -150.130
SIZE 0.035 0.07 0.50

L.S. 10
ACTA
BOND $H
LIST 4
CONF
FMAP 2
PLAN 5
```

```
WGHT    0.000000    2.195200
EXTI    0.005499
FVAR       0.20382
C1    1    0.272227    0.772227    0.356998    10.50000    0.01834    0.01834 =
         0.01000    0.00028    0.00028   -0.00333
C2    1    0.298499    0.683713    0.269530    11.00000    0.01542    0.01901 =
         0.01874    0.00246    0.00339    0.00014
BR2   4    0.417618    0.643540    0.383195    11.00000    0.01473    0.02361 =
         0.02818    0.00423   -0.00167    0.00002
C3    1    0.240366    0.623981    0.106741    11.00000    0.01818    0.01517 =
         0.02226   -0.00282    0.00206   -0.00007
AFIX  43
H3   2    0.260543    0.564506    0.048645    11.00000   -1.20000
AFIX   0
C4    1    0.151734    0.651734    0.028319    10.50000    0.01841    0.01841 =
         0.01984    0.00314    0.00314   -0.00519
C7    1    0.332822    0.832822    0.532176    10.50000    0.02158    0.02158 =
         0.02385    0.00004    0.00004   -0.00167
N7    3    0.380626    0.880626    0.676329    10.50000    0.03146    0.03146 =
         0.02986   -0.00276   -0.00276   -0.00885
C8    1    0.086605    0.586605   -0.138290    10.50000    0.02328    0.02328 =
         0.01719   -0.00026   -0.00026   -0.00470
AFIX 137
H8A   2    0.030565    0.618994   -0.199116    10.50000   -1.50000
H8B   2    0.072024    0.536915    0.017496    10.50000   -1.50000
H8C   2    0.114812    0.561493   -0.341749    10.50000   -1.50000

AFIX   0
HKLF 4

REM  16098a_a.res in P-42(1)m
REM R1 =  0.0201 for     902 Fo > 4sig(Fo)  and  0.0201 for all     904 data
REM     60 parameters refined using      0 restraints

END

WGHT      0.0000      2.2079

REM Highest difference peak  0.371,  deepest hole -0.316,  1-sigma level  0.092
Q1    1   0.4022  0.6409  0.0016  11.00000  0.05    0.37
Q2    1   0.0000  0.5000 -0.1172  10.25000  0.05    0.31
Q3    1   0.0826  0.5826 -0.6104  10.50000  0.05    0.31
Q4    1   0.3567  0.8566  0.1109  10.50000  0.05    0.30
Q5    1   0.3577  0.8577  0.8455  10.50000  0.05    0.30
;
_shelx_res_checksum   13414
# start Validation Reply Form
_vrf_PLAT934_16098a
;
PROBLEM: Number of (Iobs-Icalc)/SigmaW > 10 Outliers ....          2 Check
RESPONSE: ... These reflections were likely behind the beamstop - VGY
;
# end Validation Reply Form
# Some atom labels have been edited after refinement
# to be consistent with other compounds. - KJT
```

3,5-Dibromo-4-cyanobenzoic acid hemianthracenate [204cc : 215a (2:1)**]**.

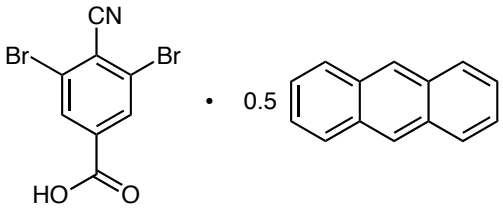

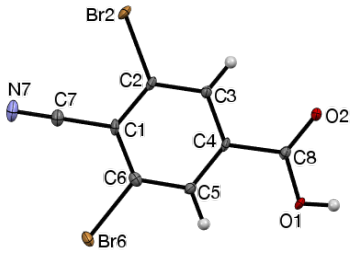

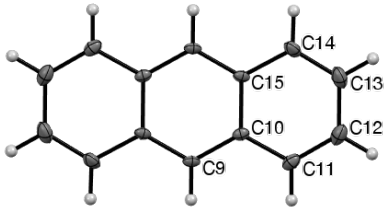

Data collection (by the XCL): A crystal (approx. 0.180 × 0.090 × 0.030 mm^3) was placed onto the tip of am 0.1 mm diameter glass capillary and mounted on a Bruker VENTURE PHOTON-100 diffractometer for data collection at 123 K. A preliminary set of cell constants was calculated from reflections harvested from three sets of frames. These initial sets of frames were oriented such that orthogonal wedges of reciprocal space were surveyed. This produced an initial orientation matrix determined from 95 reflections. The data collection was carried out using CuKα radiation (parabolic mirrors) with a frame time of 20 or 40 sec, depending on detector 2θ, with a detector distance of 40 mm. A strategy program was used to assure complete coverage of all unique data to a resolution of 0.80 Å. All major sections of frames were collected with 1.20º steps in ω or ϕ at different detector positions in 2θ. The intensity data were corrected for absorption and decay. Final cell constants were calculated from 2,967 strong reflections from the actual data collection after integration.

Structure solution and refinement (by the XCL): The space group P-1 was determined based on systematic absences and intensity statistics. A direct-methods solution was calculated that provided most non-hydrogen atoms from the E-map. Full-matrix least squares / difference Fourier cycles were performed that located the remaining non-hydrogen atoms. All non-hydrogen atoms were refined with anisotropic displacement parameters. All hydrogen atoms were placed in ideal positions and refined as riding atoms with relative isotropic displacement parameters. The final full matrix least squares refinement converged to $R1$ = 0.0264 and $wR2$ = 0.0668 (F^2, obs. data).

CIF content:

```
data_204cc

_audit_creation_method            SHELXL-2014/6
_chemical_name_systematic
;
3,5-Dibromo-4-cyanobenzoic acid hemianthracenate
;
_chemical_name_common
;
dibromo nitrile acid, anthracene co-crystal
;
_chemical_melting_point           ?
_chemical_formula_moiety          'C8 H3 Br2 N O2, 0.5(C14 H10)'
_chemical_formula_sum             'C15 H8 Br2 N O2'
_chemical_formula_weight          394.04

loop_
 _atom_type_symbol
 _atom_type_description
 _atom_type_scat_dispersion_real
 _atom_type_scat_dispersion_imag
 _atom_type_scat_source
 'C'  'C'   0.0181   0.0091
 'International Tables Vol C Tables 4.2.6.8 and 6.1.1.4'
 'H'  'H'   0.0000   0.0000
 'International Tables Vol C Tables 4.2.6.8 and 6.1.1.4'
 'N'  'N'   0.0311   0.0180
 'International Tables Vol C Tables 4.2.6.8 and 6.1.1.4'
 'O'  'O'   0.0492   0.0322
 'International Tables Vol C Tables 4.2.6.8 and 6.1.1.4'
 'Br'  'Br'  -0.6763   1.2805
 'International Tables Vol C Tables 4.2.6.8 and 6.1.1.4'

_space_group_crystal_system       triclinic
_space_group_IT_number            2
_space_group_name_H-M_alt         'P -1'
_space_group_name_Hall            '-P 1'

_shelx_space_group_comment
;
The symmetry employed for this shelxl refinement is uniquely defined
by the following loop, which should always be used as a source of
symmetry information in preference to the above space-group names.
They are only intended as comments.
;

loop_
 _space_group_symop_operation_xyz
 'x, y, z'
 '-x, -y, -z'

_cell_length_a                    8.8963(8)
_cell_length_b                    9.4701(9)
_cell_length_c                    9.5839(9)
_cell_angle_alpha                 115.356(3)
```

```
_cell_angle_beta                    106.876(3)
_cell_angle_gamma                   94.119(3)
_cell_volume                        680.03(11)
_cell_formula_units_Z               2
_cell_measurement_temperature       123(2)
_cell_measurement_reflns_used       2967
_cell_measurement_theta_min         5.31

_cell_measurement_theta_max         74.60
_exptl_crystal_description         'Plate'
_exptl_crystal_colour              'yellow'
_exptl_crystal_density_meas         ?
_exptl_crystal_density_method       ?
_exptl_crystal_density_diffrn       1.924
_exptl_crystal_F_000                382
_exptl_transmission_factor_min      0.5094
_exptl_transmission_factor_max      0.7538
_exptl_crystal_size_max             0.180
_exptl_crystal_size_mid             0.090
_exptl_crystal_size_min             0.030
_exptl_absorpt_coefficient_mu       7.569
_shelx_estimated_absorpt_T_min      0.343
_shelx_estimated_absorpt_T_max      0.805
_exptl_absorpt_correction_type      multi-scan
_exptl_absorpt_correction_T_min     0.5094
_exptl_absorpt_correction_T_max     0.7538
_exptl_absorpt_process_details      ‘SADABS 2014/3 (Sheldrick, 2014)'
_exptl_absorpt_special_details      ?
_exptl_special_details              ?
_diffrn_ambient_temperature         123(2)
_diffrn_radiation_wavelength        1.54178
_diffrn_radiation_type              CuK\a
_diffrn_source                      ?
_diffrn_measurement_device_type     'Bruker VENTURE PHOTON-1000'
_diffrn_measurement_method          '\f and \w scans'
_diffrn_detector_area_resol_mean    ?
_diffrn_reflns_number               9139
_diffrn_reflns_av_unetI/netI        0.0339
_diffrn_reflns_av_R_equivalents     0.0349
_diffrn_reflns_limit_h_min          -11
_diffrn_reflns_limit_h_max          11
_diffrn_reflns_limit_k_min          -11
_diffrn_reflns_limit_k_max          11
_diffrn_reflns_limit_l_min          -11
_diffrn_reflns_limit_l_max          11
_diffrn_reflns_theta_min            5.307
_diffrn_reflns_theta_max            74.590
_diffrn_reflns_theta_full           67.679
_diffrn_measured_fraction_theta_max   0.988
_diffrn_measured_fraction_theta_full  0.992
_diffrn_reflns_Laue_measured_fraction_max    0.988
_diffrn_reflns_Laue_measured_fraction_full   0.992
_diffrn_reflns_point_group_measured_fraction_max   0.988
_diffrn_reflns_point_group_measured_fraction_full  0.992
_reflns_number_total                2745
_reflns_number_gt                   2607
```

```
_reflns_threshold_expression      'I > 2\s(I)'
_reflns_Friedel_coverage          0.000
_reflns_Friedel_fraction_max      .
_reflns_Friedel_fraction_full     .

_reflns_special_details
;
 Reflections were merged by SHELXL according to the crystal
 class for the calculation of statistics and refinement.

 _reflns_Friedel_fraction is defined as the number of unique
 Friedel pairs measured divided by the number that would be
 possible theoretically, ignoring centric projections and
 systematic absences.
;

_computing_data_collection       'Bruker APEX2'
_computing_cell_refinement       'Bruker SAINT'
_computing_data_reduction        'Bruker SAINT'
_computing_structure_solution    'SHELXS-97 (Sheldrick 2008)'
_computing_structure_refinement  'SHELXL-2014/6 (Sheldrick, 2014)'
_computing_molecular_graphics    'Bruker SHELXTL'
_computing_publication_material  'Bruker SHELXTL'
_refine_special_details           ?
_refine_ls_structure_factor_coef  Fsqd
_refine_ls_matrix_type            full
_refine_ls_weighting_scheme       calc
_refine_ls_weighting_details
'w=1/[\s^2^(Fo^2^)+(0.0369P)^2^+0.5603P] where P=(Fo^2^+2Fc^2^)/3'
_atom_sites_solution_primary      ?
_atom_sites_solution_secondary    ?
_atom_sites_solution_hydrogens    geom
_refine_ls_hydrogen_treatment     constr
_refine_ls_extinction_method      none
_refine_ls_extinction_coef        .
_refine_ls_number_reflns          2745
_refine_ls_number_parameters      182
_refine_ls_number_restraints      0
_refine_ls_R_factor_all           0.0277
_refine_ls_R_factor_gt            0.0264
_refine_ls_wR_factor_ref          0.0681
_refine_ls_wR_factor_gt           0.0668
_refine_ls_goodness_of_fit_ref    1.055
_refine_ls_restrained_S_all       1.055
_refine_ls_shift/su_max           0.001
_refine_ls_shift/su_mean          0.000

loop_
 _atom_site_label
 _atom_site_type_symbol
 _atom_site_fract_x
 _atom_site_fract_y
 _atom_site_fract_z
 _atom_site_U_iso_or_equiv
 _atom_site_adp_type
 _atom_site_occupancy
```

```
 _atom_site_site_symmetry_order
 _atom_site_calc_flag
 _atom_site_refinement_flags_posn
 _atom_site_refinement_flags_adp
 _atom_site_refinement_flags_occupancy
 _atom_site_disorder_assembly
 _atom_site_disorder_group
Br2 Br 0.38562(3) 0.12356(3) 0.93908(3) 0.01483(9) Uani 1 1 d . . . . .
Br6 Br 0.81803(2) 0.51847(3) 0.84679(3) 0.01686(9) Uani 1 1 d . . . . .
O1 O 0.21809(18) 0.54610(19) 0.5615(2) 0.0154(3) Uani 1 1 d . . . . .
H1 H 0.1338 0.5671 0.5146 0.023 Uiso 1 1 calc R U . . .
O2 O 0.04198(18) 0.38413(18) 0.5858(2) 0.0139(3) Uani 1 1 d . . . . .
N7 N 0.8230(2) 0.2641(3) 1.0526(3) 0.0211(4) Uani 1 1 d . . . . .
C8 C 0.1800(3) 0.4429(2) 0.6097(3) 0.0102(4) Uani 1 1 d . . . . .
C4 C 0.3217(2) 0.4018(2) 0.7011(2) 0.0092(4) Uani 1 1 d . . . . .
C3 C 0.2929(2) 0.2999(2) 0.7650(2) 0.0096(4) Uani 1 1 d . . . . .
H3 H 0.1859 0.2573 0.7495 0.011 Uiso 1 1 calc R U . . .
C2 C 0.4229(3) 0.2615(2) 0.8516(2) 0.0100(4) Uani 1 1 d . . . . .
C1 C 0.5815(2) 0.3249(2) 0.8767(2) 0.0102(4) Uani 1 1 d . . . . .
C7 C 0.7162(3) 0.2888(3) 0.9728(3) 0.0135(4) Uani 1 1 d . . . . .
C6 C 0.6057(3) 0.4265(3) 0.8107(3) 0.0116(4) Uani 1 1 d . . . . .
C5 C 0.4777(3) 0.4647(2) 0.7223(2) 0.0103(4) Uani 1 1 d . . . . .
H5 H 0.4958 0.5328 0.6766 0.012 Uiso 1 1 calc R U . . .
C9 C 0.4142(3) 0.8993(2) 0.5372(3) 0.0131(4) Uani 1 1 d . . . . .
H9 H 0.3562 0.8307 0.5622 0.016 Uiso 1 1 calc R U . . .
C10 C 0.5827(3) 0.9268(2) 0.5908(3) 0.0126(4) Uani 1 1 d . . . . .
C11 C 0.6714(3) 0.8552(3) 0.6831(3) 0.0179(5) Uani 1 1 d . . . . .
H11 H 0.6149 0.7875 0.7102 0.022 Uiso 1 1 calc R U . . .
C12 C 0.8344(3) 0.8823(3) 0.7326(3) 0.0230(5) Uani 1 1 d . . . . .
H12 H 0.8912 0.8345 0.7947 0.028 Uiso 1 1 calc R U . . .
C13 C 0.9206(3) 0.9822(3) 0.6915(3) 0.0247(5) Uani 1 1 d . . . . .
H13 H 1.0347 0.9989 0.7249 0.030 Uiso 1 1 calc R U . . .
C14 C 0.8420(3) 1.0540(3) 0.6055(3) 0.0198(5) Uani 1 1 d . . . . .
H14 H 0.9019 1.1211 0.5803 0.024 Uiso 1 1 calc R U . . .
C15 C 0.6700(3) 1.0296(2) 0.5522(3) 0.0121(4) Uani 1 1 d . . . . .

loop_
 _atom_site_aniso_label
 _atom_site_aniso_U_11
 _atom_site_aniso_U_22
 _atom_site_aniso_U_33
 _atom_site_aniso_U_23
 _atom_site_aniso_U_13
 _atom_site_aniso_U_12
Br2 0.01625(14) 0.01597(13) 0.01776(14) 0.01426(10) 0.00336(10) 0.00482(9)
Br6 0.00653(13) 0.02493(15) 0.02190(14) 0.01464(11) 0.00341(10) 0.00266(9)
O1 0.0098(7) 0.0197(8) 0.0244(8) 0.0196(7) 0.0021(6) 0.0037(6)
O2 0.0079(7) 0.0163(7) 0.0211(8) 0.0141(6) 0.0017(6) 0.0027(6)
N7 0.0163(10) 0.0255(10) 0.0221(10) 0.0136(9) 0.0021(8) 0.0110(8)
C8 0.0104(10) 0.0099(9) 0.0095(9) 0.0053(7) 0.0010(7) 0.0028(7)
C4 0.0092(9) 0.0086(9) 0.0081(9) 0.0046(7) -0.0007(7) 0.0037(7)
C3 0.0084(9) 0.0091(9) 0.0107(9) 0.0054(7) 0.0014(7) 0.0020(7)
C2 0.0115(10) 0.0100(9) 0.0090(9) 0.0062(8) 0.0011(8) 0.0045(7)
C1 0.0080(9) 0.0111(9) 0.0082(9) 0.0035(8) -0.0005(7) 0.0045(7)
C7 0.0117(10) 0.0140(10) 0.0131(10) 0.0059(8) 0.0025(8) 0.0048(8)
C6 0.0088(9) 0.0128(9) 0.0112(9) 0.0044(8) 0.0028(8) 0.0016(7)
```

```
C5 0.0113(9) 0.0095(9) 0.0108(9) 0.0063(8) 0.0025(8) 0.0021(7)
C9 0.0162(10) 0.0082(9) 0.0148(10) 0.0047(8) 0.0070(8) 0.0001(8)
C10 0.0172(11) 0.0081(9) 0.0113(9) 0.0033(8) 0.0056(8) 0.0016(8)
C11 0.0245(12) 0.0125(10) 0.0156(10) 0.0069(9) 0.0049(9) 0.0033(9)
C12 0.0257(13) 0.0167(11) 0.0196(11) 0.0082(9) -0.0010(10) 0.0055(9)
C13 0.0135(11) 0.0222(12) 0.0276(13) 0.0071(10) 0.0007(9) 0.0018(9)
C14 0.0131(11) 0.0152(11) 0.0261(12) 0.0072(9) 0.0052(9) -0.0012(8)
C15 0.0138(10) 0.0073(9) 0.0131(9) 0.0027(8) 0.0057(8) 0.0000(7)

_geom_special_details
;
 All esds (except the esd in the dihedral angle between two l.s. planes)
 are estimated using the full covariance matrix.  The cell esds are taken
 into account individually in the estimation of esds in distances, angles
 and torsion angles; correlations between esds in cell parameters are only
 used when they are defined by crystal symmetry.  An approximate (isotropic)
 treatment of cell esds is used for estimating esds involving l.s. planes.
;

loop_
 _geom_bond_atom_site_label_1
 _geom_bond_atom_site_label_2
 _geom_bond_distance
 _geom_bond_site_symmetry_2
 _geom_bond_publ_flag
Br2 C2 1.886(2) . ?
Br6 C6 1.890(2) . ?
O1 C8 1.309(3) . ?
O1 H1 0.8400 . ?
O2 C8 1.224(3) . ?
N7 C7 1.142(3) . ?
C8 C4 1.493(3) . ?
C4 C3 1.390(3) . ?
C4 C5 1.391(3) . ?
C3 C2 1.386(3) . ?
C3 H3 0.9500 . ?
C2 C1 1.402(3) . ?
C1 C6 1.394(3) . ?
C1 C7 1.446(3) . ?
C6 C5 1.381(3) . ?
C5 H5 0.9500 . ?
C9 C15 1.394(3) 2_676 ?
C9 C10 1.400(3) . ?
C9 H9 0.9500 . ?
C10 C11 1.432(3) . ?
C10 C15 1.432(3) . ?
C11 C12 1.356(4) . ?
C11 H11 0.9500 . ?
C12 C13 1.423(4) . ?
C12 H12 0.9500 . ?
C13 C14 1.359(4) . ?
C13 H13 0.9500 . ?
C14 C15 1.433(3) . ?
C14 H14 0.9500 . ?
C15 C9 1.394(3) 2_676 ?
```

```
loop_
 _geom_angle_atom_site_label_1
 _geom_angle_atom_site_label_2
 _geom_angle_atom_site_label_3
 _geom_angle
 _geom_angle_site_symmetry_1
 _geom_angle_site_symmetry_3
 _geom_angle_publ_flag
C8 O1 H1 109.5 . . ?
O2 C8 O1 124.6(2) . . ?
O2 C8 C4 121.29(19) . . ?
O1 C8 C4 114.08(18) . . ?
C3 C4 C5 121.22(19) . . ?
C3 C4 C8 117.98(18) . . ?
C5 C4 C8 120.80(19) . . ?
C2 C3 C4 118.88(19) . . ?
C2 C3 H3 120.6 . . ?
C4 C3 H3 120.6 . . ?
C3 C2 C1 121.09(19) . . ?
C3 C2 Br2 119.34(16) . . ?
C1 C2 Br2 119.57(15) . . ?
C6 C1 C2 118.42(19) . . ?
C6 C1 C7 121.09(19) . . ?
C2 C1 C7 120.47(19) . . ?
N7 C7 C1 178.1(2) . . ?
C5 C6 C1 121.37(19) . . ?
C5 C6 Br6 119.04(16) . . ?
C1 C6 Br6 119.57(16) . . ?
C6 C5 C4 119.02(19) . . ?
C6 C5 H5 120.5 . . ?
C4 C5 H5 120.5 . . ?
C15 C9 C10 121.3(2) 2_676 . ?
C15 C9 H9 119.4 2_676 . ?
C10 C9 H9 119.4 . . ?
C9 C10 C11 122.1(2) . . ?
C9 C10 C15 119.3(2) . . ?
C11 C10 C15 118.6(2) . . ?
C12 C11 C10 121.2(2) . . ?
C12 C11 H11 119.4 . . ?
C10 C11 H11 119.4 . . ?
C11 C12 C13 120.0(2) . . ?
C11 C12 H12 120.0 . . ?
C13 C12 H12 120.0 . . ?
C14 C13 C12 121.0(2) . . ?
C14 C13 H13 119.5 . . ?
C12 C13 H13 119.5 . . ?
C13 C14 C15 120.7(2) . . ?
C13 C14 H14 119.7 . . ?
C15 C14 H14 119.7 . . ?
C9 C15 C10 119.5(2) 2_676 . ?
C9 C15 C14 122.1(2) 2_676 . ?
C10 C15 C14 118.5(2) . . ?

loop_
 _geom_torsion_atom_site_label_1
 _geom_torsion_atom_site_label_2
```

```
 _geom_torsion_atom_site_label_3
 _geom_torsion_atom_site_label_4
 _geom_torsion
 _geom_torsion_site_symmetry_1
 _geom_torsion_site_symmetry_2
 _geom_torsion_site_symmetry_3
 _geom_torsion_site_symmetry_4
 _geom_torsion_publ_flag
O2 C8 C4 C3 -2.9(3) . . . . ?
O1 C8 C4 C3 176.48(18) . . . . ?
O2 C8 C4 C5 177.60(19) . . . . ?
O1 C8 C4 C5 -3.1(3) . . . . ?
C5 C4 C3 C2 0.2(3) . . . . ?
C8 C4 C3 C2 -179.35(18) . . . . ?
C4 C3 C2 C1 0.6(3) . . . . ?
C4 C3 C2 Br2 179.97(14) . . . . ?
C3 C2 C1 C6 -0.7(3) . . . . ?
Br2 C2 C1 C6 180.00(14) . . . . ?
C3 C2 C1 C7 177.55(18) . . . . ?
Br2 C2 C1 C7 -1.8(3) . . . . ?
C2 C1 C6 C5 -0.1(3) . . . . ?
C7 C1 C6 C5 -178.35(19) . . . . ?
C2 C1 C6 Br6 178.40(14) . . . . ?
C7 C1 C6 Br6 0.2(3) . . . . ?
C1 C6 C5 C4 1.0(3) . . . . ?
Br6 C6 C5 C4 -177.60(15) . . . . ?
C3 C4 C5 C6 -1.0(3) . . . . ?
C8 C4 C5 C6 178.55(18) . . . . ?
C15 C9 C10 C11 179.81(19) 2_676 . . . ?
C15 C9 C10 C15 -0.3(3) 2_676 . . . ?
C9 C10 C11 C12 179.4(2) . . . . ?
C15 C10 C11 C12 -0.5(3) . . . . ?
C10 C11 C12 C13 -0.6(4) . . . . ?
C11 C12 C13 C14 1.2(4) . . . . ?
C12 C13 C14 C15 -0.7(4) . . . . ?
C9 C10 C15 C9 0.3(3) . . . 2_676 ?
C11 C10 C15 C9 -179.81(19) . . . 2_676 ?
C9 C10 C15 C14 -178.88(19) . . . . ?
C11 C10 C15 C14 1.0(3) . . . . ?
C13 C14 C15 C9 -179.6(2) . . . 2_676 ?
C13 C14 C15 C10 -0.4(3) . . . . ?

loop_
 _geom_hbond_atom_site_label_D
 _geom_hbond_atom_site_label_H
 _geom_hbond_atom_site_label_A
 _geom_hbond_distance_DH
 _geom_hbond_distance_HA
 _geom_hbond_distance_DA
 _geom_hbond_angle_DHA
 _geom_hbond_site_symmetry_A
O1 H1 O2  0.84 1.79 2.627(2) 178.4 2_566

_refine_diff_density_max    0.397
_refine_diff_density_min   -0.531
_refine_diff_density_rms    0.125
```

```
_shelxl_version_number 2014/6

_shelx_res_file
;
TITL 15185a in P-1
CELL 1.54178 8.8963 9.4701 9.5839 115.356 106.876 94.119
ZERR 2.00    0.0008 0.0009 0.0009   0.003   0.003  0.003
LATT 1
SFAC C H N O BR
UNIT 30 16 2 4 4
TEMP -150.140
SIZE 0.030 0.090 0.180

L.S. 10
ACTA
LIST 4
CONF
BOND $H
FMAP 2
PLAN 5

EQIV $1 -x, -y+1, -z+1
HTAB O1 O2_$1

WGHT    0.036900    0.560300
FVAR       0.14636
BR2   5    0.385615    0.123558    0.939082    11.00000    0.01625    0.01597 =
         0.01776    0.01426    0.00336    0.00482
BR6   5    0.818035    0.518473    0.846794    11.00000    0.00653    0.02493 =
         0.02190    0.01464    0.00341    0.00266
O1    4    0.218089    0.546101    0.561480    11.00000    0.00976    0.01974 =
         0.02438    0.01958    0.00207    0.00369
AFIX 147
H1    2    0.133831    0.567110    0.514627    11.00000   -1.50000
AFIX   0
O2    4    0.041977    0.384134    0.585756    11.00000    0.00794    0.01631 =
         0.02110    0.01414    0.00168    0.00275
N7    3    0.823015    0.264058    1.052564    11.00000    0.01629    0.02547 =
         0.02206    0.01360    0.00215    0.01096
C8    1    0.179986    0.442923    0.609722    11.00000    0.01035    0.00985 =
         0.00951    0.00533    0.00099    0.00279
C4    1    0.321696    0.401765    0.701063    11.00000    0.00923    0.00859 =
         0.00811    0.00464   -0.00067    0.00371
C3    1    0.292877    0.299905    0.764962    11.00000    0.00837    0.00905 =
         0.01066    0.00538    0.00137    0.00199
AFIX  43
H3    2    0.185872    0.257332    0.749499    11.00000   -1.20000
AFIX   0
C2    1    0.422906    0.261518    0.851607    11.00000    0.01155    0.00999 =
         0.00898    0.00624    0.00112    0.00445
C1    1    0.581456    0.324856    0.876656    11.00000    0.00799    0.01108 =
         0.00819    0.00352   -0.00047    0.00454
C7    1    0.716219    0.288789    0.972841    11.00000    0.01165    0.01401 =
         0.01310    0.00586    0.00247    0.00483
C6    1    0.605693    0.426549    0.810689    11.00000    0.00883    0.01276 =
```

```
         0.01116    0.00445    0.00278    0.00161
C5    1    0.477671    0.464654    0.722266    11.00000    0.01129    0.00950 =
         0.01082    0.00634    0.00245    0.00212
AFIX  43
H5   2    0.495823    0.532808    0.676578    11.00000   -1.20000
AFIX   0
C9    1    0.414221    0.899275    0.537162    11.00000    0.01616    0.00815 =
         0.01477    0.00466    0.00701    0.00011
AFIX  43
H9   2    0.356154    0.830747    0.562178    11.00000   -1.20000
AFIX   0
C10   1    0.582699    0.926825    0.590757    11.00000    0.01716    0.00814 =
         0.01133    0.00333    0.00560    0.00161
C11   1    0.671399    0.855239    0.683093    11.00000    0.02445    0.01246 =
         0.01555    0.00692    0.00495    0.00333
AFIX  43
H11  2    0.614941    0.787547    0.710174    11.00000   -1.20000
AFIX   0
C12   1    0.834443    0.882283    0.732573    11.00000    0.02574    0.01671 =
         0.01957    0.00818   -0.00099    0.00553
AFIX  43
H12  2    0.891247    0.834539    0.794658    11.00000   -1.20000
AFIX   0
C13   1    0.920574    0.982184    0.691549    11.00000    0.01354    0.02223 =
         0.02764    0.00711    0.00073    0.00179
AFIX  43
H13  2    1.034653    0.998881    0.724861    11.00000   -1.20000
AFIX   0
C14   1    0.842046    1.054009    0.605458    11.00000    0.01313    0.01518 =
         0.02615    0.00722    0.00520   -0.00116
AFIX  43
H14  2    0.901876    1.121144    0.580327    11.00000   -1.20000
AFIX   0
C15   1    0.669952    1.029552    0.552187    11.00000    0.01385    0.00726 =
         0.01311    0.00273    0.00566    0.00000

HKLF 4 1 1 0 0 0 1 0 0 0 1

REM  15185a in P-1
REM R1 =  0.0264 for    2607 Fo > 4sig(Fo)  and  0.0277 for all    2745 data
REM    182 parameters refined using      0 restraints

END

WGHT      0.0369      0.5606

REM Highest difference peak  0.397,  deepest hole -0.531,  1-sigma level  0.125
Q1    1   0.0046  0.4583  0.7382  11.00000  0.05    0.40
Q2    1   0.6412  0.2812  0.7068  11.00000  0.05    0.39
Q3    1   0.7997  0.7624  0.9549  11.00000  0.05    0.38
Q4    1   0.7496  0.7603  0.8884  11.00000  0.05    0.37
Q5    1   0.4093  0.8909  0.7472  11.00000  0.05    0.36
;
_shelx_res_checksum   69439
# Some atom labels have been edited after refinement
# to be consistent with other compounds. - KJT
```

Methyl 3,5-dibromo-4-cyanobenzoate (204cd).

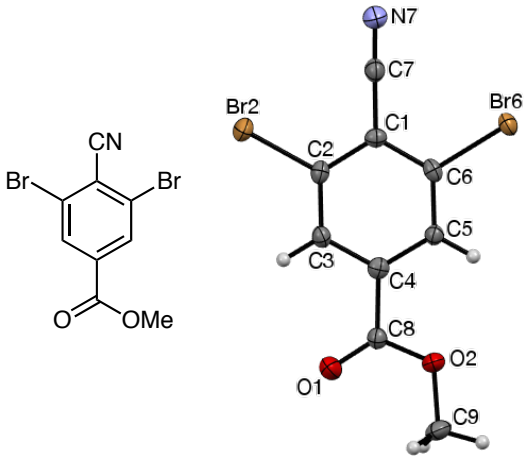

Data collection (by the XCL): A crystal (approx. 0.320 × 0.270 × 0.250 mm^3) was placed onto the tip of a Mitegen mount and mounted on a Bruker APEX-II CCD diffractometer for a data collection at 173 K. A preliminary set of cell constants was calculated from reflections harvested from three sets of 20 frames. These initial sets of frames were oriented such that orthogonal wedges of reciprocal space were surveyed. This produced initial orientation matrices determined from 72 reflections. The data collection was carried out using MoKα radiation (graphite monochromator) with a frame time of 5 sec and a detector distance of 60 mm. A randomly oriented region of reciprocal space was surveyed to the extent of one sphere and to a resolution of 0.77 Å. Four major sections of frames were collected with 0.30° steps in ω at four different ϕ settings and a detector position of –28° in 2θ. The intensity data were corrected for absorption and decay. Final cell constants were calculated from 2,977 strong reflections from the actual data collection after integration.

Structure solution and refinement (by the XCL): The space group P2$_1$/c was determined based on systematic absences and intensity statistics. A direct-methods solution was calculated that provided most non-hydrogen atoms from the E-map. Full-matrix least squares / difference Fourier cycles were performed that located the remaining non-hydrogen atoms. All non-hydrogen atoms were refined with anisotropic displacement parameters. All hydrogen atoms were placed in ideal positions and refined as riding atoms with relative isotropic displacement parameters. The final full matrix least squares refinement converged to $R1$ = 0.0263 and $wR2$ = 0.0593 (F^2, all data).

CIF content:

```
 data_204cd

_audit_creation_method            SHELXL-2014/6
_chemical_name_systematic
;
Methyl 3,5-dibromo-4-cyanobenzoate
;
_chemical_name_common             'dibromo nitrile ester'
_chemical_melting_point           ?
_chemical_formula_moiety          'C9 H5 Br2 N O2'
_chemical_formula_sum             'C9 H5 Br2 N O2'
_chemical_formula_weight          318.96

loop_
 _atom_type_symbol
 _atom_type_description
 _atom_type_scat_dispersion_real
 _atom_type_scat_dispersion_imag
 _atom_type_scat_source
 'C'  'C'   0.0033   0.0016
 'International Tables Vol C Tables 4.2.6.8 and 6.1.1.4'
 'H'  'H'   0.0000   0.0000
 'International Tables Vol C Tables 4.2.6.8 and 6.1.1.4'
 'N'  'N'   0.0061   0.0033
 'International Tables Vol C Tables 4.2.6.8 and 6.1.1.4'
 'O'  'O'   0.0106   0.0060
 'International Tables Vol C Tables 4.2.6.8 and 6.1.1.4'
 'Br'  'Br'  -0.2901   2.4595
 'International Tables Vol C Tables 4.2.6.8 and 6.1.1.4'

_space_group_crystal_system       monoclinic
_space_group_IT_number            14
_space_group_name_H-M_alt         'P 21/c'
_space_group_name_Hall            '-P 2ybc'

_shelx_space_group_comment
;
The symmetry employed for this shelxl refinement is uniquely defined
by the following loop, which should always be used as a source of
symmetry information in preference to the above space-group names.
They are only intended as comments.
;

loop_
 _space_group_symop_operation_xyz
 'x, y, z'
 '-x, y+1/2, -z+1/2'
 '-x, -y, -z'
 'x, -y-1/2, z-1/2'

_cell_length_a                    3.9273(18)
_cell_length_b                    17.881(8)
_cell_length_c                    14.739(7)
_cell_angle_alpha                 90
_cell_angle_beta                  93.757(7)
```

```
_cell_angle_gamma                  90
_cell_volume                       1032.9(8)
_cell_formula_units_Z              4
_cell_measurement_temperature      173(2)
_cell_measurement_reflns_used      2977
_cell_measurement_theta_min        2.67
_cell_measurement_theta_max        27.59

_exptl_crystal_description        'Block'
_exptl_crystal_colour             'colourless'
_exptl_crystal_density_meas        ?
_exptl_crystal_density_method      ?
_exptl_crystal_density_diffrn      2.051
_exptl_crystal_F_000               608
_exptl_transmission_factor_min     0.4139
_exptl_transmission_factor_max     0.7456
_exptl_crystal_size_max            0.320
_exptl_crystal_size_mid            0.270
_exptl_crystal_size_min            0.250
_exptl_absorpt_coefficient_mu      7.820
_shelx_estimated_absorpt_T_min     0.189
_shelx_estimated_absorpt_T_max     0.245
_exptl_absorpt_correction_type     multi-scan
_exptl_absorpt_correction_T_min    0.4139
_exptl_absorpt_correction_T_max    0.7456
_exptl_absorpt_process_details     'SADABS 2012/1 (Sheldrick, 2012)'
_exptl_absorpt_special_details     ?
_exptl_special_details             'K. Tritch / Prof. W. Noland'
_diffrn_ambient_temperature        173(2)
_diffrn_radiation_wavelength       0.71073
_diffrn_radiation_type             MoK\a
_diffrn_source                     'sealed tube'
_diffrn_measurement_device_type    'Bruker APEX-II CCD'
_diffrn_measurement_method         '\f and \w scans'
_diffrn_detector_area_resol_mean   ?
_diffrn_reflns_number              11889
_diffrn_reflns_av_unetI/netI       0.0338
_diffrn_reflns_av_R_equivalents    0.0430
_diffrn_reflns_limit_h_min         -5
_diffrn_reflns_limit_h_max         5
_diffrn_reflns_limit_k_min         -23
_diffrn_reflns_limit_k_max         23
_diffrn_reflns_limit_l_min         -19
_diffrn_reflns_limit_l_max         19
_diffrn_reflns_theta_min           1.793
_diffrn_reflns_theta_max           27.814
_diffrn_reflns_theta_full          25.242
_diffrn_measured_fraction_theta_max   0.991
_diffrn_measured_fraction_theta_full  1.000
_diffrn_reflns_Laue_measured_fraction_max    0.991
_diffrn_reflns_Laue_measured_fraction_full   1.000
_diffrn_reflns_point_group_measured_fraction_max   0.991
_diffrn_reflns_point_group_measured_fraction_full  1.000
_reflns_number_total               2426
_reflns_number_gt                  2013
_reflns_threshold_expression       'I > 2\s(I)'
```

```
_reflns_Friedel_coverage          0.000
_reflns_Friedel_fraction_max      .
_reflns_Friedel_fraction_full     .

_reflns_special_details
;
 Reflections were merged by SHELXL according to the crystal
 class for the calculation of statistics and refinement.

 _reflns_Friedel_fraction is defined as the number of unique
 Friedel pairs measured divided by the number that would be
 possible theoretically, ignoring centric projections and
 systematic absences.
;

_computing_data_collection       'Bruker APEX2'
_computing_cell_refinement       'Bruker SAINT'
_computing_data_reduction        'Bruker SAINT'
_computing_structure_solution    'SHELXT-2014 (Sheldrick, 2014)'
_computing_structure_refinement  'SHELXL-2014/6 (Sheldrick, 2014)'
_computing_molecular_graphics    'Bruker SHELXTL'
_computing_publication_material  'Bruker SHELXTL'
_refine_special_details           ?
_refine_ls_structure_factor_coef  Fsqd
_refine_ls_matrix_type            full
_refine_ls_weighting_scheme       calc
_refine_ls_weighting_details
'w=1/[\s^2^(Fo^2^)+(0.0274P)^2^+0.0295P] where P=(Fo^2^+2Fc^2^)/3'
_atom_sites_solution_primary      ?
_atom_sites_solution_secondary    ?
_atom_sites_solution_hydrogens    geom
_refine_ls_hydrogen_treatment     constr
_refine_ls_extinction_method      none
_refine_ls_extinction_coef        .
_refine_ls_number_reflns          2426
_refine_ls_number_parameters      128
_refine_ls_number_restraints      0
_refine_ls_R_factor_all           0.0373
_refine_ls_R_factor_gt            0.0263
_refine_ls_wR_factor_ref          0.0593
_refine_ls_wR_factor_gt           0.0564
_refine_ls_goodness_of_fit_ref    1.069
_refine_ls_restrained_S_all       1.069
_refine_ls_shift/su_max           0.001
_refine_ls_shift/su_mean          0.000

loop_
 _atom_site_label
 _atom_site_type_symbol
 _atom_site_fract_x
 _atom_site_fract_y
 _atom_site_fract_z
 _atom_site_U_iso_or_equiv
 _atom_site_adp_type
 _atom_site_occupancy
 _atom_site_site_symmetry_order
```

```
 _atom_site_calc_flag
 _atom_site_refinement_flags_posn
 _atom_site_refinement_flags_adp
 _atom_site_refinement_flags_occupancy
 _atom_site_disorder_assembly
 _atom_site_disorder_group
C1 C 0.6370(6) 0.65590(14) 0.86321(17) 0.0196(5) Uani 1 1 d . . . . .
C2 C 0.7731(6) 0.67398(14) 0.95078(16) 0.0199(5) Uani 1 1 d . . . . .
Br2 Br 0.74408(8) 0.60384(2) 1.04534(2) 0.02954(9) Uani 1 1 d . . . . .
C3 C 0.9245(6) 0.74304(14) 0.96807(17) 0.0204(5) Uani 1 1 d . . . . .
H3 H 1.0169 0.7548 1.0275 0.024 Uiso 1 1 calc R U . . .
C4 C 0.9412(6) 0.79516(14) 0.89815(17) 0.0197(5) Uani 1 1 d . . . . .
C5 C 0.8100(6) 0.77825(14) 0.81049(16) 0.0193(5) Uani 1 1 d . . . . .
H5 H 0.8216 0.8138 0.7629 0.023 Uiso 1 1 calc R U . . .
C6 C 0.6624(6) 0.70889(15) 0.79351(16) 0.0193(5) Uani 1 1 d . . . . .
Br6 Br 0.49149(7) 0.68383(2) 0.67451(2) 0.02395(9) Uani 1 1 d . . . . .
C7 C 0.4695(7) 0.58481(16) 0.84529(18) 0.0251(6) Uani 1 1 d . . . . .
N7 N 0.3333(6) 0.52966(14) 0.82991(16) 0.0359(6) Uani 1 1 d . . . . .
C8 C 1.1066(6) 0.86917(14) 0.92064(17) 0.0203(5) Uani 1 1 d . . . . .
O1 O 1.2632(5) 0.88220(11) 0.99159(14) 0.0357(5) Uani 1 1 d . . . . .
O2 O 1.0590(5) 0.91760(10) 0.85308(13) 0.0292(5) Uani 1 1 d . . . . .
C9 C 1.2078(8) 0.99150(15) 0.8667(2) 0.0326(7) Uani 1 1 d . . . . .
H9A H 1.1628 1.0215 0.8115 0.049 Uiso 1 1 calc R U . . .
H9B H 1.4548 0.9868 0.8798 0.049 Uiso 1 1 calc R U . . .
H9C H 1.1063 1.0161 0.9179 0.049 Uiso 1 1 calc R U . . .

loop_
 _atom_site_aniso_label
 _atom_site_aniso_U_11
 _atom_site_aniso_U_22
 _atom_site_aniso_U_33
 _atom_site_aniso_U_23
 _atom_site_aniso_U_13
 _atom_site_aniso_U_12
C1 0.0183(13) 0.0179(13) 0.0226(13) -0.0010(11) 0.0018(10) 0.0008(11)
C2 0.0187(13) 0.0237(14) 0.0174(12) 0.0039(10) 0.0022(10) 0.0018(11)
Br2 0.03760(18) 0.02881(17) 0.02189(15) 0.00724(11) -0.00044(12) -0.00681(12)
C3 0.0225(13) 0.0220(14) 0.0164(12) -0.0013(10) -0.0001(10) 0.0024(11)
C4 0.0174(13) 0.0198(13) 0.0219(13) -0.0002(10) 0.0021(10) 0.0036(10)
C5 0.0213(14) 0.0189(14) 0.0177(13) 0.0011(10) 0.0011(10) 0.0009(10)
C6 0.0164(13) 0.0256(14) 0.0158(12) -0.0029(10) 0.0002(10) 0.0028(10)
Br6 0.02657(15) 0.02717(16) 0.01735(14) -0.00197(10) -0.00436(10) -0.00102(11)
C7 0.0273(15) 0.0289(16) 0.0189(13) 0.0023(11) 0.0009(11) -0.0006(12)
N7 0.0486(17) 0.0303(15) 0.0282(13) 0.0024(11) -0.0021(11) -0.0132(12)
C8 0.0214(13) 0.0207(14) 0.0187(13) 0.0007(10) 0.0014(10) 0.0020(11)
O1 0.0487(13) 0.0283(11) 0.0283(11) 0.0008(9) -0.0112(10) -0.0060(10)
O2 0.0403(12) 0.0195(10) 0.0270(10) 0.0025(8) -0.0036(9) -0.0074(9)
C9 0.0387(17) 0.0196(15) 0.0388(17) 0.0053(12) -0.0018(13) -0.0077(12)

_geom_special_details
;
 All esds (except the esd in the dihedral angle between two l.s. planes)
 are estimated using the full covariance matrix.  The cell esds are taken
 into account individually in the estimation of esds in distances, angles
 and torsion angles; correlations between esds in cell parameters are only
 used when they are defined by crystal symmetry.  An approximate (isotropic)
```

```
 treatment of cell esds is used for estimating esds involving l.s. planes.
;

loop_
 _geom_bond_atom_site_label_1
 _geom_bond_atom_site_label_2
 _geom_bond_distance
 _geom_bond_site_symmetry_2
 _geom_bond_publ_flag
C1 C2 1.402(4) . ?
C1 C6 1.406(4) . ?
C1 C7 1.448(4) . ?
C2 C3 1.387(3) . ?
C2 Br2 1.884(3) . ?
C3 C4 1.394(3) . ?
C3 H3 0.9500 . ?
C4 C5 1.393(3) . ?
C4 C8 1.502(4) . ?
C5 C6 1.385(4) . ?
C5 H5 0.9500 . ?
C6 Br6 1.890(2) . ?
C7 N7 1.138(3) . ?
C8 O1 1.201(3) . ?
C8 O2 1.324(3) . ?
O2 C9 1.454(3) . ?
C9 H9A 0.9800 . ?
C9 H9B 0.9800 . ?
C9 H9C 0.9800 . ?

loop_
 _geom_angle_atom_site_label_1
 _geom_angle_atom_site_label_2
 _geom_angle_atom_site_label_3
 _geom_angle
 _geom_angle_site_symmetry_1
 _geom_angle_site_symmetry_3
 _geom_angle_publ_flag
C2 C1 C6 118.4(2) . . ?
C2 C1 C7 120.8(2) . . ?
C6 C1 C7 120.8(2) . . ?
C3 C2 C1 120.5(2) . . ?
C3 C2 Br2 120.19(19) . . ?
C1 C2 Br2 119.32(19) . . ?
C2 C3 C4 120.0(2) . . ?
C2 C3 H3 120.0 . . ?
C4 C3 H3 120.0 . . ?
C5 C4 C3 120.5(2) . . ?
C5 C4 C8 121.6(2) . . ?
C3 C4 C8 117.8(2) . . ?
C6 C5 C4 119.2(2) . . ?
C6 C5 H5 120.4 . . ?
C4 C5 H5 120.4 . . ?
C5 C6 C1 121.4(2) . . ?
C5 C6 Br6 119.93(19) . . ?
C1 C6 Br6 118.71(19) . . ?
N7 C7 C1 178.6(3) . . ?
```

```
O1 C8 O2 124.6(2) . . ?
O1 C8 C4 123.6(2) . . ?
O2 C8 C4 111.9(2) . . ?
C8 O2 C9 117.1(2) . . ?
O2 C9 H9A 109.5 . . ?
O2 C9 H9B 109.5 . . ?
H9A C9 H9B 109.5 . . ?
O2 C9 H9C 109.5 . . ?
H9A C9 H9C 109.5 . . ?
H9B C9 H9C 109.5 . . ?

loop_
 _geom_torsion_atom_site_label_1
 _geom_torsion_atom_site_label_2
 _geom_torsion_atom_site_label_3
 _geom_torsion_atom_site_label_4
 _geom_torsion
 _geom_torsion_site_symmetry_1
 _geom_torsion_site_symmetry_2
 _geom_torsion_site_symmetry_3
 _geom_torsion_site_symmetry_4
 _geom_torsion_publ_flag
C6 C1 C2 C3 0.9(4) . . . . ?
C7 C1 C2 C3 -178.1(2) . . . . ?
C6 C1 C2 Br2 -179.76(18) . . . . ?
C7 C1 C2 Br2 1.2(3) . . . . ?
C1 C2 C3 C4 0.2(4) . . . . ?
Br2 C2 C3 C4 -179.11(18) . . . . ?
C2 C3 C4 C5 -0.7(4) . . . . ?
C2 C3 C4 C8 179.8(2) . . . . ?
C3 C4 C5 C6 0.0(4) . . . . ?
C8 C4 C5 C6 179.5(2) . . . . ?
C4 C5 C6 C1 1.2(4) . . . . ?
C4 C5 C6 Br6 -178.62(18) . . . . ?
C2 C1 C6 C5 -1.6(4) . . . . ?
C7 C1 C6 C5 177.4(2) . . . . ?
C2 C1 C6 Br6 178.18(18) . . . . ?
C7 C1 C6 Br6 -2.8(3) . . . . ?
C5 C4 C8 O1 -169.5(3) . . . . ?
C3 C4 C8 O1 10.1(4) . . . . ?
C5 C4 C8 O2 10.4(3) . . . . ?
C3 C4 C8 O2 -170.0(2) . . . . ?
O1 C8 O2 C9 0.0(4) . . . . ?
C4 C8 O2 C9 -179.9(2) . . . . ?

loop_
 _geom_hbond_atom_site_label_D
 _geom_hbond_atom_site_label_H
 _geom_hbond_atom_site_label_A
 _geom_hbond_distance_DH
 _geom_hbond_distance_HA
 _geom_hbond_distance_DA
 _geom_hbond_angle_DHA
 _geom_hbond_site_symmetry_A
C3 H3 Br6  0.95 2.97 3.878(3) 159.6 4_676
```

```
_refine_diff_density_max    0.371
_refine_diff_density_min   -0.518
_refine_diff_density_rms    0.099

_shelxl_version_number 2014/6

_shelx_res_file
;
TITL 16081a in P2(1)/c
CELL 0.71073   3.9273  17.8815  14.7394  90.000  93.757  90.000
ZERR    4.00   0.0018   0.0081   0.0068   0.000   0.007   0.000
LATT  1
SYMM -X, 0.5+Y, 0.5-Z
SFAC C  H  N O BR
UNIT 36 20 4 8 8
TEMP -100
SIZE 0.25 0.27 0.32

L.S. 12
ACTA
BOND $H
CONF
FMAP 2
PLAN 5
EQIV $1 x+1, -y+3/2, z+1/2
HTAB C3 Br6_$1

WGHT    0.027400    0.029500
FVAR       0.11376
C1    1    0.637005    0.655902    0.863207    11.00000    0.01829    0.01792 =
         0.02261   -0.00097    0.00181    0.00082
C2    1    0.773073    0.673985    0.950785    11.00000    0.01875    0.02365 =
         0.01739    0.00386    0.00216    0.00183
BR2   5    0.744076    0.603836    1.045339    11.00000    0.03760    0.02881 =
         0.02189    0.00724   -0.00044   -0.00681
C3    1    0.924520    0.743038    0.968069    11.00000    0.02248    0.02203 =
         0.01641   -0.00126   -0.00009    0.00235
AFIX  43
H3    2    1.016901    0.754817    1.027533    11.00000   -1.20000
AFIX   0
C4    1    0.941154    0.795163    0.898154    11.00000    0.01743    0.01984 =
         0.02193   -0.00016    0.00207    0.00363
C5    1    0.809967    0.778252    0.810494    11.00000    0.02126    0.01887 =
         0.01773    0.00113    0.00112    0.00093
AFIX  43
H5    2    0.821573    0.813843    0.762944    11.00000   -1.20000
AFIX   0
C6    1    0.662362    0.708892    0.793507    11.00000    0.01641    0.02559 =
         0.01584   -0.00292    0.00021    0.00283
BR6   5    0.491489    0.683828    0.674506    11.00000    0.02657    0.02717 =
         0.01735   -0.00197   -0.00436   -0.00102
C7    1    0.469486    0.584814    0.845292    11.00000    0.02732    0.02889 =
         0.01888    0.00228    0.00085   -0.00058
N7    3    0.333274    0.529664    0.829913    11.00000    0.04857    0.03029 =
         0.02816    0.00243   -0.00207   -0.01323
C8    1    1.106608    0.869165    0.920644    11.00000    0.02140    0.02072 =
```

```
         0.01874    0.00065    0.00137    0.00203
O1    4    1.263235    0.882200    0.991591    11.00000    0.04870    0.02829 =
         0.02832    0.00076   -0.01121   -0.00605
O2    4    1.058984    0.917598    0.853082    11.00000    0.04031    0.01949 =
         0.02696    0.00251   -0.00361   -0.00743
C9    1    1.207833    0.991504    0.866680    11.00000    0.03874    0.01960 =
         0.03875    0.00532   -0.00183   -0.00768
AFIX 137
H9A   2    1.162772    1.021456    0.811517    11.00000   -1.50000
H9B   2    1.454764    0.986818    0.879827    11.00000   -1.50000
H9C   2    1.106312    1.016064    0.917864    11.00000   -1.50000

AFIX   0
HKLF 4

REM  16081a in P2(1)/c
REM R1 =  0.0263 for    2013 Fo > 4sig(Fo)  and  0.0373 for all    2426 data
REM    128 parameters refined using      0 restraints

END

WGHT      0.0260      0.1151

REM Highest difference peak  0.371,  deepest hole -0.518,  1-sigma level  0.099
Q1    1   0.3686  0.6099  1.1398  11.00000  0.05    0.37
Q2    1   1.5051  0.9798  0.8419  11.00000  0.05    0.36
Q3    1   0.5595  0.7322  0.6552  11.00000  0.05    0.34
Q4    1   1.0573  1.0287  0.8461  11.00000  0.05    0.33
Q5    1   0.6816  0.4389  0.8583  11.00000  0.05    0.33
;
_shelx_res_checksum   82408

# Some atom labels have been edited after refinement
# to be consistent with other compounds. - KJT
```

2,4,6-Triiodobenzonitrile (204da), $Z = 4$ CC polytype.

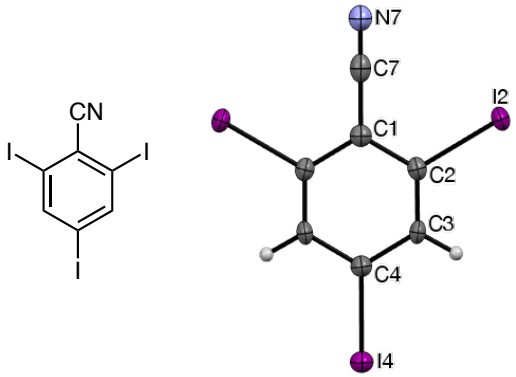

CIF content:

```
data_204da

_audit_creation_method            'SHELXTL'
_chemical_name_systematic
;
 2,4,6-Triiodobenzonitrile
;
_chemical_name_common         'triiodo nitrile'
_chemical_melting_point           ?
_chemical_formula_moiety         'C7 H2 I3 N'
_chemical_formula_sum            'C7 H2 I3 N'
_chemical_formula_weight          480.80

loop_
 _atom_type_symbol
 _atom_type_description
 _atom_type_scat_dispersion_real
 _atom_type_scat_dispersion_imag
 _atom_type_scat_source
 'C'  'C'   0.0033   0.0016
 'International Tables Vol C Tables 4.2.6.8 and 6.1.1.4'
 'H'  'H'   0.0000   0.0000
 'International Tables Vol C Tables 4.2.6.8 and 6.1.1.4'
 'N'  'N'   0.0061   0.0033
 'International Tables Vol C Tables 4.2.6.8 and 6.1.1.4'
 'I'  'I'  -0.4742   1.8119
 'International Tables Vol C Tables 4.2.6.8 and 6.1.1.4'

_symmetry_cell_setting            orthorhombic
_symmetry_space_group_name_H-M  'I m m a'
_symmetry_space_group_name_Hall   '-I 2b 2'

loop_
 _symmetry_equiv_pos_as_xyz
 'x, y, z'
 '-x, -y+1/2, z'
 '-x, y+1/2, -z'
 'x, -y, -z'
 'x+1/2, y+1/2, z+1/2'
```

```
 '-x+1/2, -y+1, z+1/2'
 '-x+1/2, y+1, -z+1/2'
 'x+1/2, -y+1/2, -z+1/2'
 '-x, -y, -z'
 'x, y-1/2, -z'
 'x, -y-1/2, z'
 '-x, y, z'
 '-x+1/2, -y+1/2, -z+1/2'
 'x+1/2, y, -z+1/2'
 'x+1/2, -y, z+1/2'
 '-x+1/2, y+1/2, z+1/2'

_cell_length_a                    7.111(2)
_cell_length_b                    10.546(3)
_cell_length_c                    13.094(4)
_cell_angle_alpha                 90.00
_cell_angle_beta                  90.00
_cell_angle_gamma                 90.00
_cell_volume                      982.0(5)
_cell_formula_units_Z             4
_cell_measurement_temperature     173(2)
_cell_measurement_reflns_used     2037
_cell_measurement_theta_min       2.5
_cell_measurement_theta_max       27.2

_exptl_crystal_description        needle
_exptl_crystal_colour             colorless
_exptl_crystal_size_max           0.30
_exptl_crystal_size_mid           0.15
_exptl_crystal_size_min           0.10
_exptl_crystal_density_meas       'not measured'
_exptl_crystal_density_diffrn     3.252
_exptl_crystal_density_method     'not measured'
_exptl_crystal_F_000              840
_exptl_absorpt_coefficient_mu     9.488
_exptl_absorpt_correction_type    'multi-scan'
_exptl_absorpt_correction_T_min   0.18
_exptl_absorpt_correction_T_max   0.39
_exptl_absorpt_process_details
;
SADABS; Sheldrick, 1996; Blessing, 1995
;


_diffrn_ambient_temperature       173(2)
_diffrn_radiation_wavelength      0.71073
_diffrn_radiation_type            MoK\a
_diffrn_radiation_source          'fine-focus sealed tube'
_diffrn_radiation_monochromator   graphite
_diffrn_measurement_device_type
;
Siemens SMART area detector diffractometer
;
_diffrn_measurement_method        '\w scans'
_diffrn_detector_area_resol_mean  ?
_diffrn_standards_number          0
```

```
_diffrn_standards_interval_count  ?
_diffrn_standards_interval_time   ?
_diffrn_standards_decay_%         'less than 1'
_diffrn_reflns_number             2887
_diffrn_reflns_av_R_equivalents   0.045
_diffrn_reflns_av_sigmaI/netI     0.039
_diffrn_reflns_limit_h_min        -7
_diffrn_reflns_limit_h_max        9
_diffrn_reflns_limit_k_min        -11
_diffrn_reflns_limit_k_max        13
_diffrn_reflns_limit_l_min        -16
_diffrn_reflns_limit_l_max        16
_diffrn_reflns_theta_min          2.48
_diffrn_reflns_theta_max          27.52
_reflns_number_total              643
_reflns_number_gt                 578
_reflns_threshold_expression      '>2\s(I) '

_computing_data_collection        'SMART (Siemens, 1995)'
_computing_cell_refinement        'SAINT (Siemens, 1995)'
_computing_data_reduction         'SAINT'
_computing_structure_solution     'SHELXTL (Sheldrick, 1997)'
_computing_structure_refinement   'SHELXTL'
_computing_molecular_graphics     'SHELXTL'
_computing_publication_material   'SHELXTL'

_refine_ls_structure_factor_coef  Fsqd
_refine_ls_matrix_type            full
_refine_ls_weighting_scheme       calc
_refine_ls_weighting_details
 'calc w=1/[\s^2^(Fo^2^)+(0.053P)^2^] where P=(Fo^2^+2Fc^2^)/3'
_atom_sites_solution_primary      direct
_atom_sites_solution_secondary    difmap
_atom_sites_solution_hydrogens    geom
_refine_ls_hydrogen_treatment     riding
_refine_ls_extinction_method      none
_refine_ls_extinction_coef        ?
_refine_ls_number_reflns          643
_refine_ls_number_parameters      39
_refine_ls_number_restraints      0
_refine_ls_R_factor_all           0.038
_refine_ls_R_factor_gt            0.034
_refine_ls_wR_factor_ref          0.079
_refine_ls_wR_factor_gt           0.078
_refine_ls_goodness_of_fit_ref    1.05
_refine_ls_restrained_S_all       1.05
_refine_ls_shift/su_max           0.013
_refine_ls_shift/su_mean          0.002

loop_
 _atom_site_label
 _atom_site_type_symbol
 _atom_site_fract_x
 _atom_site_fract_y
 _atom_site_fract_z
 _atom_site_U_iso_or_equiv
```

```
 _atom_site_adp_type
 _atom_site_occupancy
 _atom_site_symmetry_multiplicity
 _atom_site_calc_flag
 _atom_site_refinement_flags
 _atom_site_disorder_assembly
 _atom_site_disorder_group
I2 I 0.0000 0.53558(4) 0.16534(3) 0.0267(2) Uani 1 2 d S . .
I4 I 0.0000 0.2500 0.56449(4) 0.0279(2) Uani 1 4 d S . .
N7 N 0.0000 0.2500 -0.0018(7) 0.0332(19) Uani 1 4 d S . .
C1 C 0.0000 0.2500 0.1919(7) 0.0223(18) Uani 1 4 d S . .
C2 C 0.0000 0.3646(6) 0.2467(5) 0.0215(13) Uani 1 2 d S . .
C3 C 0.0000 0.3652(6) 0.3511(5) 0.0232(13) Uani 1 2 d S . .
H3 H 0.0000 0.4437 0.3867 0.028 Uiso 1 2 calc SR . .
C4 C 0.0000 0.2500 0.4067(7) 0.0255(19) Uani 1 4 d S . .
C7 C 0.0000 0.2500 0.0806(8) 0.026(2) Uani 1 4 d S . .

loop_
 _atom_site_aniso_label
 _atom_site_aniso_U_11
 _atom_site_aniso_U_22
 _atom_site_aniso_U_33
 _atom_site_aniso_U_23
 _atom_site_aniso_U_13
 _atom_site_aniso_U_12
I2 0.0375(3) 0.0161(3) 0.0264(3) 0.00414(16) 0.000 0.000
I4 0.0372(4) 0.0254(4) 0.0210(3) 0.000 0.000 0.000
N7 0.044(5) 0.025(5) 0.031(5) 0.000 0.000 0.000
C1 0.021(4) 0.022(5) 0.023(4) 0.000 0.000 0.000
C2 0.023(3) 0.017(3) 0.025(3) 0.002(3) 0.000 0.000
C3 0.032(3) 0.012(3) 0.026(3) -0.002(3) 0.000 0.000
C4 0.034(5) 0.021(5) 0.021(4) 0.000 0.000 0.000
C7 0.019(4) 0.020(5) 0.039(6) 0.000 0.000 0.000


loop_
 _geom_bond_atom_site_label_1
 _geom_bond_atom_site_label_2
 _geom_bond_distance
 _geom_bond_site_symmetry_2
 _geom_bond_publ_flag
I2 C2 2.094(6) . ?
I4 C4 2.066(9) . ?
N7 C7 1.079(13) . ?
C1 C2 1.405(8) . ?
C1 C2 1.405(8) 2 ?
C1 C7 1.458(13) . ?
C2 C3 1.367(10) . ?
C3 C4 1.417(8) . ?
C3 H3 0.9500 . ?
C4 C3 1.417(8) 2 ?

loop_
 _geom_angle_atom_site_label_1
 _geom_angle_atom_site_label_2
 _geom_angle_atom_site_label_3
```

```
 _geom_angle
 _geom_angle_site_symmetry_1
 _geom_angle_site_symmetry_3
 _geom_angle_publ_flag
C2 C1 C2 118.6(8) . 2 ?
C2 C1 C7 120.7(4) . . ?
C2 C1 C7 120.7(4) 2 . ?
C3 C2 C1 120.9(6) . . ?
C3 C2 I2 120.3(5) . . ?
C1 C2 I2 118.8(5) . . ?
C2 C3 C4 120.7(6) . . ?
C2 C3 H3 119.6 . . ?
C4 C3 H3 119.6 . . ?
C3 C4 C3 118.1(8) 2 . ?
C3 C4 I4 121.0(4) 2 . ?
C3 C4 I4 121.0(4) . . ?
N7 C7 C1 180.000(1) . . ?

_diffrn_measured_fraction_theta_max    0.998
_diffrn_reflns_theta_full              27.52
_diffrn_measured_fraction_theta_full   0.998
_refine_diff_density_max    1.96
_refine_diff_density_min   -1.39
_refine_diff_density_rms    0.289

# Data collection, refinement, and
# torsion data were not provided by Dr. Britton. - KJT
```

2,6-Diiodo-4-methylbenzonitrile (204db), $Z = 4$ CC polytype.

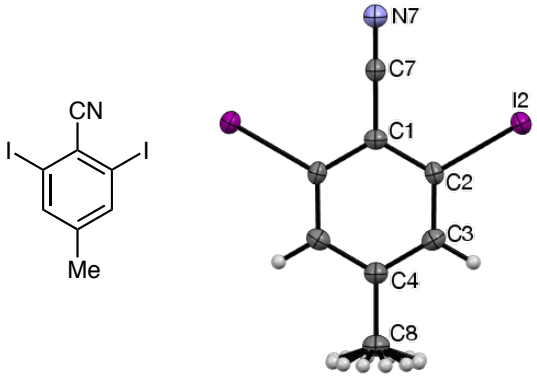

Data collection (by the XCL): A crystal (approx. 0.250 × 0.250 × 0.130 mm^3) was placed onto the tip of a Mitegen mount and mounted on a Bruker APEX-II CCD diffractometer for a data collection at 173 K. A preliminary set of cell constants was calculated from reflections harvested from three sets of 20 frames. These initial sets of frames were oriented such that orthogonal wedges of reciprocal space were surveyed. This produced initial orientation matrices determined from 85 reflections. The data collection was carried out using MoKα radiation (graphite monochromator) with a frame time of 5 sec and a detector distance of 60 mm. A randomly oriented region of reciprocal space was surveyed to the extent of one sphere and to a resolution of 0.77 Å. Four major sections of frames were collected with 0.50° steps in ω at four different ϕ settings and a detector position of –28° in 2θ. The intensity data were corrected for absorption and decay. Final cell constants were calculated from 2,977 strong reflections from the actual data collection after integration.

Structure solution and refinement (by the XCL): The space group Imma was determined based on systematic absences and intensity statistics. A direct-methods solution was calculated that provided most non-hydrogen atoms from the E-map. Full-matrix least squares / difference Fourier cycles were performed that located the remaining non-hydrogen atoms. All non-hydrogen atoms were refined with anisotropic displacement parameters. All hydrogen atoms were placed in ideal positions and refined as riding atoms with relative isotropic displacement parameters. The final full matrix least squares refinement converged to $R1 = 0.0138$ and $wR2 = 0.0315$ (F^2, all data).

CIF content:

```
data_204db

_audit_creation_method            SHELXL-2014/6
_chemical_name_systematic
;
2,6-Diiodo-4-methylbenzonitrile
;
_chemical_name_common             'diiodo methyl nitrile'
_chemical_melting_point           ?
_chemical_formula_moiety          'C8 H5 I2 N'
_chemical_formula_sum             'C8 H5 I2 N'
_chemical_formula_weight          368.93

loop_
 _atom_type_symbol
 _atom_type_description
 _atom_type_scat_dispersion_real
 _atom_type_scat_dispersion_imag
 _atom_type_scat_source
 'C'  'C'   0.0033   0.0016
 'International Tables Vol C Tables 4.2.6.8 and 6.1.1.4'
 'H'  'H'   0.0000   0.0000
 'International Tables Vol C Tables 4.2.6.8 and 6.1.1.4'
 'N'  'N'   0.0061   0.0033
 'International Tables Vol C Tables 4.2.6.8 and 6.1.1.4'
 'I'  'I'  -0.4742   1.8119
 'International Tables Vol C Tables 4.2.6.8 and 6.1.1.4'

_space_group_crystal_system       orthorhombic
_space_group_IT_number            74
_space_group_name_H-M_alt         'I m m a'
_space_group_name_Hall            '-I 2b 2'

_shelx_space_group_comment
;
The symmetry employed for this shelxl refinement is uniquely defined
by the following loop, which should always be used as a source of
symmetry information in preference to the above space-group names.
They are only intended as comments.
;

loop_
 _space_group_symop_operation_xyz
 'x, y, z'
 '-x, -y+1/2, z'
 '-x, y+1/2, -z'
 'x, -y, -z'
 'x+1/2, y+1/2, z+1/2'
 '-x+1/2, -y+1, z+1/2'
 '-x+1/2, y+1, -z+1/2'
 'x+1/2, -y+1/2, -z+1/2'
 '-x, -y, -z'
 'x, y-1/2, -z'
 'x, -y-1/2, z'
 '-x, y, z'
```

```
 '-x+1/2, -y+1/2, -z+1/2'
 'x+1/2, y, -z+1/2'
 'x+1/2, -y, z+1/2'
 '-x+1/2, y+1/2, z+1/2'

_cell_length_a                    7.047(2)
_cell_length_b                    10.783(4)
_cell_length_c                    12.584(4)
_cell_angle_alpha                 90
_cell_angle_beta                  90
_cell_angle_gamma                 90
_cell_volume                      956.2(5)
_cell_formula_units_Z             4
_cell_measurement_temperature     173(2)
_cell_measurement_reflns_used     2977
_cell_measurement_theta_min       2.49
_cell_measurement_theta_max       27.50

_exptl_crystal_description       'Block'
_exptl_crystal_colour            'colourless'
_exptl_crystal_density_meas       ?
_exptl_crystal_density_method     ?
_exptl_crystal_density_diffrn     2.563
_exptl_crystal_F_000              664
_exptl_transmission_factor_min    0.5419
_exptl_transmission_factor_max    0.7456
_exptl_crystal_size_max           0.250
_exptl_crystal_size_mid           0.250
_exptl_crystal_size_min           0.130
_exptl_absorpt_coefficient_mu     6.515
_shelx_estimated_absorpt_T_min    0.293
_shelx_estimated_absorpt_T_max    0.485
_exptl_absorpt_correction_type    multi-scan
_exptl_absorpt_correction_T_min   0.5419
_exptl_absorpt_correction_T_max   0.7456
_exptl_absorpt_process_details    'SADABS-2014/4 (Sheldrick, 2014)'
_exptl_absorpt_special_details    ?
_exptl_special_details            'K. Tritch / Prof. W. Noland'
_diffrn_ambient_temperature       173(2)
_diffrn_radiation_wavelength      0.71073
_diffrn_radiation_type            MoK\a
_diffrn_source                    'sealed tube'
_diffrn_measurement_device_type   'Bruker APEX-II CCD'
_diffrn_measurement_method        '\f and \w scans'
_diffrn_detector_area_resol_mean  ?
_diffrn_reflns_number             5311
_diffrn_reflns_av_unetI/netI      0.0137
_diffrn_reflns_av_R_equivalents   0.0243
_diffrn_reflns_limit_h_min        -9
_diffrn_reflns_limit_h_max        9
_diffrn_reflns_limit_k_min        -13
_diffrn_reflns_limit_k_max        13
_diffrn_reflns_limit_l_min        -16
_diffrn_reflns_limit_l_max        16
_diffrn_reflns_theta_min          2.487
_diffrn_reflns_theta_max          27.497
```

```
_diffrn_reflns_theta_full         25.242
_diffrn_measured_fraction_theta_max   0.995
_diffrn_measured_fraction_theta_full  0.998
_diffrn_reflns_Laue_measured_fraction_max    0.995
_diffrn_reflns_Laue_measured_fraction_full   0.998
_diffrn_reflns_point_group_measured_fraction_max   0.995
_diffrn_reflns_point_group_measured_fraction_full  0.998
_reflns_number_total              625
_reflns_number_gt                 560
_reflns_threshold_expression      'I > 2\s(I)'
_reflns_Friedel_coverage          0.000
_reflns_Friedel_fraction_max      .
_reflns_Friedel_fraction_full     .

_reflns_special_details
;
 Reflections were merged by SHELXL according to the crystal
 class for the calculation of statistics and refinement.

 _reflns_Friedel_fraction is defined as the number of unique
 Friedel pairs measured divided by the number that would be
 possible theoretically, ignoring centric projections and
 systematic absences.
;

_computing_data_collection       'Bruker APEX2'
_computing_cell_refinement       'Bruker SAINT'
_computing_data_reduction        'Bruker SAINT'
_computing_structure_solution    'SHELXT-2014 (Sheldrick 2014)'
_computing_structure_refinement  'SHELXL-2014/6 (Sheldrick, 2014)'
_computing_molecular_graphics    'Bruker SHELXTL'
_computing_publication_material  'Bruker SHELXTL'
_refine_special_details           ?
_refine_ls_structure_factor_coef  Fsqd
_refine_ls_matrix_type            full
_refine_ls_weighting_scheme       calc
_refine_ls_weighting_details
'w=1/[\s^2^(Fo^2^)+(0.0146P)^2^+1.5446P] where P=(Fo^2^+2Fc^2^)/3'
_atom_sites_solution_primary      ?
_atom_sites_solution_secondary    ?
_atom_sites_solution_hydrogens    geom
_refine_ls_hydrogen_treatment     constr
_refine_ls_extinction_method      none
_refine_ls_extinction_coef        .
_refine_ls_number_reflns          625
_refine_ls_number_parameters      40
_refine_ls_number_restraints      0
_refine_ls_R_factor_all           0.0163
_refine_ls_R_factor_gt            0.0138
_refine_ls_wR_factor_ref          0.0315
_refine_ls_wR_factor_gt           0.0306
_refine_ls_goodness_of_fit_ref    1.052
_refine_ls_restrained_S_all       1.052
_refine_ls_shift/su_max           0.001
_refine_ls_shift/su_mean          0.000
```

```
loop_
 _atom_site_label
 _atom_site_type_symbol
 _atom_site_fract_x
 _atom_site_fract_y
 _atom_site_fract_z
 _atom_site_U_iso_or_equiv
 _atom_site_adp_type
 _atom_site_occupancy
 _atom_site_site_symmetry_order
 _atom_site_calc_flag
 _atom_site_refinement_flags_posn
 _atom_site_refinement_flags_adp
 _atom_site_refinement_flags_occupancy
 _atom_site_disorder_assembly
 _atom_site_disorder_group
N7 N 0.5000 0.7500 1.0095(3) 0.0286(8) Uani 1 4 d S T P . .
C1 C 0.5000 0.7500 0.8044(3) 0.0205(8) Uani 1 4 d S T P . .
C2 C 0.5000 0.6375(3) 0.7484(2) 0.0202(6) Uani 1 2 d S T P . .
I2 I 0.5000 0.46990(2) 0.83198(2) 0.02402(8) Uani 1 2 d S T P . .
C3 C 0.5000 0.6389(3) 0.6381(2) 0.0241(6) Uani 1 2 d S T P . .
H3 H 0.5000 0.5627 0.6003 0.029 Uiso 1 2 calc R U P . .
C4 C 0.5000 0.7500 0.5821(3) 0.0244(9) Uani 1 4 d S T P . .
C7 C 0.5000 0.7500 0.9197(3) 0.0222(9) Uani 1 4 d S T P . .
C8 C 0.5000 0.7500 0.4617(4) 0.0314(11) Uani 1 4 d S T P . .
H8A H 0.6268 0.7283 0.4357 0.047 Uiso 0.25 1 calc R U P . .
H8B H 0.4654 0.8326 0.4357 0.047 Uiso 0.25 1 calc R U P . .
H8C H 0.4078 0.6891 0.4357 0.047 Uiso 0.25 1 calc R U P . .

loop_
 _atom_site_aniso_label
 _atom_site_aniso_U_11
 _atom_site_aniso_U_22
 _atom_site_aniso_U_33
 _atom_site_aniso_U_23
 _atom_site_aniso_U_13
 _atom_site_aniso_U_12
N7 0.039(2) 0.0244(19) 0.023(2) 0.000 0.000 0.000
C1 0.021(2) 0.023(2) 0.0177(18) 0.000 0.000 0.000
C2 0.0224(14) 0.0154(15) 0.0227(14) 0.0021(11) 0.000 0.000
I2 0.03082(13) 0.01862(12) 0.02262(11) 0.00243(7) 0.000 0.000
C3 0.0278(16) 0.0240(17) 0.0205(14) -0.0031(12) 0.000 0.000
C4 0.029(2) 0.024(2) 0.020(2) 0.000 0.000 0.000
C7 0.026(2) 0.017(2) 0.023(2) 0.000 0.000 0.000
C8 0.042(3) 0.032(3) 0.020(2) 0.000 0.000 0.000

_geom_special_details
;
 All esds (except the esd in the dihedral angle between two l.s. planes)
 are estimated using the full covariance matrix.  The cell esds are taken
 into account individually in the estimation of esds in distances, angles
 and torsion angles; correlations between esds in cell parameters are only
 used when they are defined by crystal symmetry.  An approximate (isotropic)
 treatment of cell esds is used for estimating esds involving l.s. planes.
;
```

```
loop_
 _geom_bond_atom_site_label_1
 _geom_bond_atom_site_label_2
 _geom_bond_distance
 _geom_bond_site_symmetry_2
 _geom_bond_publ_flag
N7 C7 1.131(5) . ?
C1 C2 1.403(3) 2_665 ?
C1 C2 1.403(3) . ?
C1 C5 1.451(6) . ?
C2 C3 1.387(4) . ?
C2 I2 2.091(3) . ?
C3 C4 1.390(4) . ?
C3 H3 0.9500 . ?
C4 C3 1.390(4) 2_665 ?
C4 C6 1.515(6) . ?
C8 H8A 0.9800 . ?
C8 H8B 0.9800 . ?
C8 H8C 0.9800 . ?

loop_
 _geom_angle_atom_site_label_1
 _geom_angle_atom_site_label_2
 _geom_angle_atom_site_label_3
 _geom_angle
 _geom_angle_site_symmetry_1
 _geom_angle_site_symmetry_3
 _geom_angle_publ_flag
C2 C1 C2 119.7(4) 2_665 . ?
C2 C1 C7 120.18(19) 2_665 . ?
C2 C1 C7 120.17(19) . . ?
C3 C2 C1 119.5(3) . . ?
C3 C2 I2 120.8(2) . . ?
C1 C2 I2 119.6(2) . . ?
C4 C3 C2 121.1(3) . . ?
C4 C3 H3 119.4 . . ?
C2 C3 H3 119.4 . . ?
C3 C4 C3 119.0(4) 2_665 . ?
C3 C4 C8 120.5(2) 2_665 . ?
C3 C4 C8 120.5(2) . . ?
N7 C7 C1 180.0 . . ?
C4 C8 H8A 109.5 . . ?
C4 C8 H8B 109.5 . . ?
H8A C8 H8B 109.5 . . ?
C4 C8 H8C 109.5 . . ?
H8A C8 H8C 109.5 . . ?
H8B C8 H8C 109.5 . . ?

loop_
 _geom_torsion_atom_site_label_1
 _geom_torsion_atom_site_label_2
 _geom_torsion_atom_site_label_3
 _geom_torsion_atom_site_label_4
 _geom_torsion
 _geom_torsion_site_symmetry_1
 _geom_torsion_site_symmetry_2
```

```
 _geom_torsion_site_symmetry_3
 _geom_torsion_site_symmetry_4
 _geom_torsion_publ_flag
C2 C1 C2 C3 0.000(2) 2_665 . . . ?
C7 C1 C2 C3 180.000(1) . . . . ?
C2 C1 C2 I2 180.000(1) 2_665 . . . ?
C7 C1 C2 I2 0.000(1) . . . . ?
C1 C2 C3 C4 0.000(2) . . . . ?
I2 C2 C3 C4 180.000(1) . . . . ?
C2 C3 C4 C3 0.000(2) . . . 2_665 ?
C2 C3 C4 C8 180.000(1) . . . . ?

_refine_diff_density_max    0.345
_refine_diff_density_min   -0.622
_refine_diff_density_rms    0.105

_shelxl_version_number 2014/6

_shelx_res_file
;
TITL 16078a in Imma
CELL 0.71073   7.0469  10.7834  12.5838  90.000  90.000  90.000
ZERR    4.00   0.0023   0.0035   0.0040   0.000   0.000   0.000
LATT  2
SYMM -X, 0.5-Y, Z
SYMM -X, 0.5+Y, -Z
SYMM X, -Y, -Z
SFAC C  H  N I
UNIT 32 20 4 8
TEMP -100
SIZE 0.130 0.250 0.250

L.S. 10
ACTA
LIST 4
CONF
BOND $H
HTAB
FMAP 2
PLAN 5

WGHT    0.014600    1.544600
FVAR       0.06275
N7    3    0.500000    0.750000    1.009539    10.25000    0.03896    0.02438 =
         0.02252    0.00000    0.00000    0.00000
C1    1    0.500000    0.750000    0.804419    10.25000    0.02074    0.02297 =
         0.01775    0.00000    0.00000    0.00000
C2    1    0.500000    0.637509    0.748373    10.50000    0.02241    0.01540 =
         0.02273    0.00213    0.00000    0.00000
I2    4    0.500000    0.469901    0.831981    10.50000    0.03082    0.01862 =
         0.02262    0.00243    0.00000    0.00000
C3    1    0.500000    0.638941    0.638132    10.50000    0.02777    0.02396 =
         0.02054   -0.00308    0.00000    0.00000
AFIX  43
H3   2    0.500000    0.562696    0.600309    10.50000   -1.20000
AFIX   0
```

```
C4    1    0.500000    0.750000    0.582061    10.25000    0.02851    0.02444 =
         0.02020    0.00000    0.00000    0.00000
C7    1    0.500000    0.750000    0.919688    10.25000    0.02642    0.01699 =
         0.02320    0.00000    0.00000    0.00000
C8    1    0.500000    0.750000    0.461691    10.25000    0.04179    0.03241 =
         0.02001    0.00000    0.00000    0.00000
AFIX 137
H8A   2    0.626823    0.728256    0.435732    10.25000   -1.50000
H8B   2    0.465404    0.832646    0.435732    10.25000   -1.50000
H8C   2    0.407773    0.689097    0.435732    10.25000   -1.50000

AFIX   0
HKLF 4

REM  16078a in Imma
REM R1 =  0.0138 for     560 Fo > 4sig(Fo)  and  0.0163 for all     625 data
REM     40 parameters refined using      0 restraints

END

WGHT      0.0096      1.5534

REM No hydrogen bonds found for HTAB generation

REM Highest difference peak  0.345,  deepest hole -0.622,  1-sigma level  0.105
Q1    1   0.7520  0.7500  0.8200  10.50000  0.05    0.35
Q2    1   0.6138  0.7500  0.8083  10.50000  0.05    0.32
Q3    1   0.5000  0.6363  0.6944  10.50000  0.05    0.29
Q4    1   0.5000  0.7500  0.5396  10.25000  0.05    0.29
Q5    1   0.5000  0.7500  0.8496  10.25000  0.05    0.27
;
_shelx_res_checksum   33321

# Some atom labels have been edited after refinement
# to be consistent with other compounds. - KJT
```

3,5-Dibromo-4-carbamoylbenzoic acid 2-propanolate (207s).

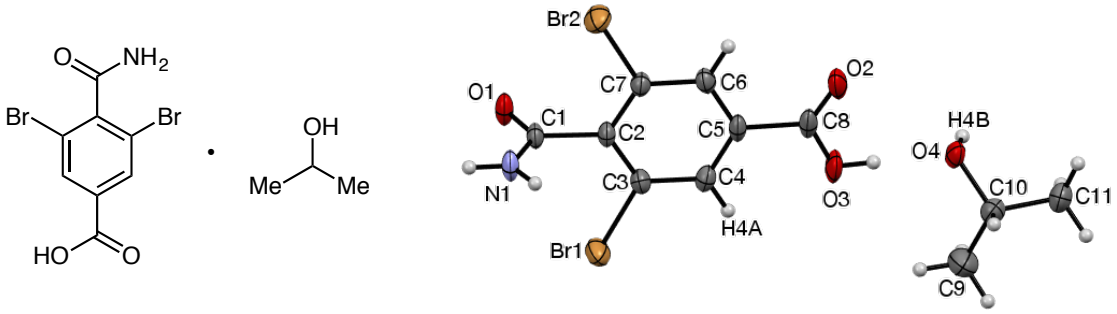

Data collection (by the XCL): A crystal (approx. 0.40 × 0.38 × 0.16 mm^3) was placed onto the tip of an 0.1 mm diameter glass capillary and mounted on a Bruker APEX-II CCD diffractometer for a data collection at 173 K. A preliminary set of cell constants was calculated from reflections harvested from three sets of 20 frames. These initial sets of frames were oriented such that orthogonal wedges of reciprocal space were surveyed. This produced initial orientation matrices determined from 82 reflections. The data collection was carried out using MoKα radiation (graphite monochromator) with a frame time of 20 sec and a detector distance of 60 mm. A randomly oriented region of reciprocal space was surveyed to the extent of one sphere and to a resolution of 0.77 Å. Four major sections of frames were collected with 0.30° steps in ω at four different ϕ settings and a detector position of –28° in 2θ. The intensity data were corrected for absorption and decay. Final cell constants were calculated from the xyz centroids of 2,971 strong reflections from the actual data collection after integration.

Structure solution and refinement (by the XCL): The space group P-1 was determined based on systematic absences and intensity statistics. A direct-methods solution was calculated that provided most non-hydrogen atoms from the E-map. Full-matrix least squares / difference Fourier cycles were performed that located the remaining non-hydrogen atoms. All non-hydrogen atoms were refined with anisotropic displacement parameters. All hydrogen atoms were placed in ideal positions and refined as riding atoms with relative isotropic displacement parameters. The final full matrix least squares refinement converged to $R1$ = 0.0262 and $wR2$ = 0.0650 (F^2, all data).

CIF content:

```
data_207

_audit_creation_method            SHELXL-2014/6
_chemical_name_systematic
```

```
;
3,5-Dibromo-4-carbamoylbenzoic acid 2-propanolate
;
_chemical_name_common              ‘dibromo carbamoyl acid'
_chemical_melting_point            ?
_chemical_formula_moiety           'C8 H5 Br2 N O3, C3 H8 O'
_chemical_formula_sum              'C11 H13 Br2 N O4'
_chemical_formula_weight           383.04

loop_
 _atom_type_symbol
 _atom_type_description
 _atom_type_scat_dispersion_real
 _atom_type_scat_dispersion_imag
 _atom_type_scat_source
 'C'  'C'   0.0033   0.0016
 'International Tables Vol C Tables 4.2.6.8 and 6.1.1.4'
 'H'  'H'   0.0000   0.0000
 'International Tables Vol C Tables 4.2.6.8 and 6.1.1.4'
 'N'  'N'   0.0061   0.0033
 'International Tables Vol C Tables 4.2.6.8 and 6.1.1.4'
 'O'  'O'   0.0106   0.0060
 'International Tables Vol C Tables 4.2.6.8 and 6.1.1.4'
 'Br'  'Br'  -0.2901   2.4595
 'International Tables Vol C Tables 4.2.6.8 and 6.1.1.4'

_space_group_crystal_system        triclinic
_space_group_IT_number             2
_space_group_name_H-M_alt          'P -1'
_space_group_name_Hall             '-P 1'

_shelx_space_group_comment
;
The symmetry employed for this shelxl refinement is uniquely defined
by the following loop, which should always be used as a source of
symmetry information in preference to the above space-group names.
They are only intended as comments.
;

loop_
 _space_group_symop_operation_xyz
 'x, y, z'
 '-x, -y, -z'

_cell_length_a                     7.2866(5)
_cell_length_b                     8.5212(6)
_cell_length_c                     12.1832(8)
_cell_angle_alpha                  71.376(1)
_cell_angle_beta                   81.745(1)
_cell_angle_gamma                  83.682(1)
_cell_volume                       707.76(8)
_cell_formula_units_Z              2
_cell_measurement_temperature      173(2)
_cell_measurement_reflns_used      2971
_cell_measurement_theta_min        2.60
_cell_measurement_theta_max        27.28
```

```
_exptl_crystal_description        'block'
_exptl_crystal_colour             'colourless'
_exptl_crystal_density_meas       ?
_exptl_crystal_density_method     ?
_exptl_crystal_density_diffrn     1.797
_exptl_crystal_F_000              376
_exptl_transmission_factor_min    0.4855
_exptl_transmission_factor_max    0.7455
_exptl_crystal_size_max           0.400
_exptl_crystal_size_mid           0.380
_exptl_crystal_size_min           0.160
_exptl_absorpt_coefficient_mu     5.732
_shelx_estimated_absorpt_T_min    0.208
_shelx_estimated_absorpt_T_max    0.461
_exptl_absorpt_correction_type    multi-scan
_exptl_absorpt_correction_T_min   0.4855
_exptl_absorpt_correction_T_max   0.7455
_exptl_absorpt_process_details    'SADABS-2012/1 (Sheldrick, 2012)'
_exptl_absorpt_special_details    ?
_exptl_special_details            'K. Tritch and Prof. W. Noland'
_diffrn_ambient_temperature       173(2)
_diffrn_radiation_wavelength      0.71073
_diffrn_radiation_type            MoK\a
_diffrn_source                    'sealed tube'
_diffrn_measurement_device_type   'Bruker APEX-II CCD'
_diffrn_measurement_method        '\f and \w scans'
_diffrn_detector_area_resol_mean  ?
_diffrn_reflns_number             8139
_diffrn_reflns_av_unetI/netI      0.0231
_diffrn_reflns_av_R_equivalents   0.0213
_diffrn_reflns_limit_h_min        -9
_diffrn_reflns_limit_h_max        9
_diffrn_reflns_limit_k_min        -11
_diffrn_reflns_limit_k_max        10
_diffrn_reflns_limit_l_min        -15
_diffrn_reflns_limit_l_max        15
_diffrn_reflns_theta_min          1.776
_diffrn_reflns_theta_max          27.306
_diffrn_reflns_theta_full         25.242
_diffrn_measured_fraction_theta_max   0.981
_diffrn_measured_fraction_theta_full  0.997
_diffrn_reflns_Laue_measured_fraction_max    0.981
_diffrn_reflns_Laue_measured_fraction_full   0.997
_diffrn_reflns_point_group_measured_fraction_max   0.981
_diffrn_reflns_point_group_measured_fraction_full  0.997
_reflns_number_total              3128
_reflns_number_gt                 2683
_reflns_threshold_expression      'I > 2\s(I)'
_reflns_Friedel_coverage          0.000
_reflns_Friedel_fraction_max      .
_reflns_Friedel_fraction_full     .

_reflns_special_details
;
 Reflections were merged by SHELXL according to the crystal
```

```
 class for the calculation of statistics and refinement.

 _reflns_Friedel_fraction is defined as the number of unique
 Friedel pairs measured divided by the number that would be
 possible theoretically, ignoring centric projections and
 systematic absences.
;

_computing_data_collection      'Bruker APEX2'
_computing_cell_refinement      'Bruker SAINT'
_computing_data_reduction       'Bruker SAINT'
_computing_structure_solution   'SHELXT-2014 (Sheldrick, 2014)'
_computing_structure_refinement 'SHELXL-2014/6 (Sheldrick, 2014)'
_computing_molecular_graphics   'Bruker SHELXTL'
_computing_publication_material 'Bruker SHELXTL'
_refine_special_details           ?
_refine_ls_structure_factor_coef  Fsqd
_refine_ls_matrix_type            full
_refine_ls_weighting_scheme       calc
_refine_ls_weighting_details
'w=1/[\s^2^(Fo^2^)+(0.0296P)^2^+0.5063P] where P=(Fo^2^+2Fc^2^)/3'
_atom_sites_solution_primary      ?
_atom_sites_solution_secondary    ?
_atom_sites_solution_hydrogens    geom
_refine_ls_hydrogen_treatment     constr
_refine_ls_extinction_method      none
_refine_ls_extinction_coef        .
_refine_ls_number_reflns          3128
_refine_ls_number_parameters      189
_refine_ls_number_restraints      152
_refine_ls_R_factor_all           0.0326
_refine_ls_R_factor_gt            0.0262
_refine_ls_wR_factor_ref          0.0650
_refine_ls_wR_factor_gt           0.0623
_refine_ls_goodness_of_fit_ref    1.037
_refine_ls_restrained_S_all       1.018
_refine_ls_shift/su_max           0.001
_refine_ls_shift/su_mean          0.000

loop_
 _atom_site_label
 _atom_site_type_symbol
 _atom_site_fract_x
 _atom_site_fract_y
 _atom_site_fract_z
 _atom_site_U_iso_or_equiv
 _atom_site_adp_type
 _atom_site_occupancy
 _atom_site_site_symmetry_order
 _atom_site_calc_flag
 _atom_site_refinement_flags_posn
 _atom_site_refinement_flags_adp
 _atom_site_refinement_flags_occupancy
 _atom_site_disorder_assembly
 _atom_site_disorder_group
Br1 Br 0.61784(4) 0.53550(3) 0.84990(2) 0.04349(9) Uani 1 1 d . U . . .
```

```
Br2 Br 0.61751(4) 0.03664(3) 0.63196(2) 0.04169(9) Uani 1 1 d . U . . .
O1 O 0.6947(2) 0.0875(2) 0.90020(14) 0.0332(4) Uani 1 1 d . U . . .
O2 O 0.8164(3) 0.6055(2) 0.30554(14) 0.0404(4) Uani 1 1 d . U . . .
O3 O 0.8603(3) 0.7832(2) 0.39911(15) 0.0416(4) Uani 1 1 d . U . . .
H3A H 0.8912 0.8450 0.3313 0.050 Uiso 1 1 calc R U . . .
N1 N 0.3941(3) 0.1687(2) 0.87687(16) 0.0327(4) Uani 1 1 d . U . . .
H1A H 0.3539 0.0977 0.9440 0.039 Uiso 1 1 calc R U . . .
H1B H 0.3143 0.2349 0.8323 0.039 Uiso 1 1 calc R U . . .
C1 C 0.5730(3) 0.1757(3) 0.84327(18) 0.0252(4) Uani 1 1 d . U . . .
C2 C 0.6308(3) 0.3004(3) 0.72638(17) 0.0241(4) Uani 1 1 d . U . . .
C3 C 0.6625(3) 0.4624(3) 0.71657(19) 0.0264(4) Uani 1 1 d . U . . .
C4 C 0.7250(3) 0.5743(3) 0.61079(19) 0.0278(5) Uani 1 1 d . U . . .
H4A H 0.7484 0.6838 0.6061 0.033 Uiso 1 1 calc R U . . .
C5 C 0.7527(3) 0.5239(3) 0.51214(18) 0.0264(5) Uani 1 1 d . U . . .
C6 C 0.7196(3) 0.3647(3) 0.51799(19) 0.0276(5) Uani 1 1 d . U . . .
H6A H 0.7373 0.3314 0.4497 0.033 Uiso 1 1 calc R U . . .
C7 C 0.6603(3) 0.2545(3) 0.62525(19) 0.0256(4) Uani 1 1 d . U . . .
C8 C 0.8134(3) 0.6414(3) 0.3944(2) 0.0308(5) Uani 1 1 d . U . . .
O4 O 0.9369(13) 0.9719(8) 0.1873(10) 0.0309(14) Uani 0.598(8) 1 d D U P A 1
H4B H 1.0535 0.9638 0.1830 0.046 Uiso 0.598(8) 1 calc R U P A 1
C9 C 0.871(3) 1.205(2) 0.2601(10) 0.059(2) Uani 0.598(8) 1 d D U P A 1
H9A H 0.8187 1.3205 0.2410 0.089 Uiso 0.598(8) 1 calc R U P A 1
H9B H 0.9983 1.1994 0.2787 0.089 Uiso 0.598(8) 1 calc R U P A 1
H9C H 0.7949 1.1360 0.3275 0.089 Uiso 0.598(8) 1 calc R U P A 1
C10 C 0.8715(7) 1.1440(5) 0.1583(4) 0.0345(13) Uani 0.598(8) 1 d D U P A 1
H10A H 0.7402 1.1527 0.1408 0.041 Uiso 0.598(8) 1 calc R U P A 1
C11 C 0.9847(11) 1.2461(12) 0.0493(6) 0.0421(16) Uani 0.598(8) 1 d D U P A 1
H11A H 0.9794 1.2013 -0.0148 0.063 Uiso 0.598(8) 1 calc R U P A 1
H11B H 1.1142 1.2410 0.0643 0.063 Uiso 0.598(8) 1 calc R U P A 1
H11C H 0.9336 1.3617 0.0282 0.063 Uiso 0.598(8) 1 calc R U P A 1
O4' O 0.978(2) 0.9792(13) 0.2007(16) 0.0309(14) Uani 0.402(8) 1 d D U P A 2
H4C H 1.0454 0.9485 0.1484 0.046 Uiso 0.402(8) 1 calc R U P A 2
C9' C 0.886(4) 1.202(3) 0.2795(16) 0.059(2) Uani 0.402(8) 1 d D U P A 2
H9D H 0.8908 1.3208 0.2657 0.089 Uiso 0.402(8) 1 calc R U P A 2
H9E H 0.9418 1.1393 0.3506 0.089 Uiso 0.402(8) 1 calc R U P A 2
H9F H 0.7558 1.1749 0.2884 0.089 Uiso 0.402(8) 1 calc R U P A 2
C10' C 0.9901(10) 1.1550(7) 0.1784(5) 0.0305(17) Uani 0.402(8) 1 d D U P A 2
H10B H 1.1238 1.1761 0.1739 0.037 Uiso 0.402(8) 1 calc R U P A 2
C11' C 0.9222(17) 1.2500(19) 0.0640(10) 0.0421(16) Uani 0.402(8) 1 d D U P A 2
H11D H 0.7927 1.2274 0.0656 0.063 Uiso 0.402(8) 1 calc R U P A 2
H11E H 0.9991 1.2158 0.0016 0.063 Uiso 0.402(8) 1 calc R U P A 2
H11F H 0.9304 1.3690 0.0497 0.063 Uiso 0.402(8) 1 calc R U P A 2

loop_
 _atom_site_aniso_label
 _atom_site_aniso_U_11
 _atom_site_aniso_U_22
 _atom_site_aniso_U_33
 _atom_site_aniso_U_23
 _atom_site_aniso_U_13
 _atom_site_aniso_U_12
Br1 0.0693(2) 0.03621(15) 0.02540(13) -0.01126(10) 0.00169(12) -0.00969(12)
Br2 0.05996(18) 0.02836(13) 0.03767(15) -0.00992(11) -0.00301(12) -0.01118(11)
O1 0.0279(8) 0.0364(9) 0.0226(8) 0.0086(7) -0.0010(6) -0.0049(7)
O2 0.0472(10) 0.0394(10) 0.0202(8) 0.0058(7) 0.0023(7) 0.0043(8)
O3 0.0467(10) 0.0324(9) 0.0293(9) 0.0100(7) 0.0080(8) -0.0094(8)
```

```
N1 0.0296(10) 0.0354(11) 0.0201(9) 0.0081(8) 0.0010(8) -0.0036(8)
C1 0.0313(11) 0.0240(10) 0.0156(10) 0.0007(8) 0.0000(8) -0.0062(9)
C2 0.0260(10) 0.0236(10) 0.0171(10) 0.0014(8) -0.0003(8) -0.0044(8)
C3 0.0308(11) 0.0269(11) 0.0187(10) -0.0038(8) -0.0007(8) -0.0024(9)
C4 0.0283(11) 0.0239(10) 0.0256(11) 0.0005(9) -0.0023(9) -0.0044(9)
C5 0.0221(10) 0.0275(11) 0.0196(10) 0.0052(8) 0.0003(8) -0.0012(8)
C6 0.0294(11) 0.0298(11) 0.0185(10) -0.0021(8) -0.0010(8) 0.0002(9)
C7 0.0281(11) 0.0232(10) 0.0216(10) -0.0019(8) -0.0011(8) -0.0032(8)
C8 0.0223(10) 0.0311(12) 0.0246(11) 0.0080(9) 0.0017(9) 0.0026(9)
O4 0.027(4) 0.0233(10) 0.032(3) 0.0021(10) 0.007(2) -0.0050(15)
C9 0.089(4) 0.0449(19) 0.041(4) -0.016(3) 0.007(3) -0.002(2)
C10 0.037(3) 0.027(2) 0.035(2) -0.0047(16) -0.0002(18) 0.0007(17)
C11 0.056(5) 0.0294(14) 0.032(2) 0.0006(16) 0.000(3) -0.001(3)
O4' 0.027(4) 0.0233(10) 0.032(3) 0.0021(10) 0.007(2) -0.0050(15)
C9' 0.089(4) 0.0449(19) 0.041(4) -0.016(3) 0.007(3) -0.002(2)
C10' 0.040(4) 0.019(2) 0.030(3) -0.001(2) -0.008(2) -0.007(2)
C11' 0.056(5) 0.0294(14) 0.032(2) 0.0006(16) 0.000(3) -0.001(3)

_geom_special_details
;
 All esds (except the esd in the dihedral angle between two l.s. planes)
 are estimated using the full covariance matrix.  The cell esds are taken
 into account individually in the estimation of esds in distances, angles
 and torsion angles; correlations between esds in cell parameters are only
 used when they are defined by crystal symmetry.  An approximate (isotropic)
 treatment of cell esds is used for estimating esds involving l.s. planes.
;

loop_
 _geom_bond_atom_site_label_1
 _geom_bond_atom_site_label_2
 _geom_bond_distance
 _geom_bond_site_symmetry_2
 _geom_bond_publ_flag
Br1 C3 1.893(2) . ?
Br2 C7 1.890(2) . ?
O1 C1 1.236(3) . ?
O2 C8 1.213(3) . ?
O3 C8 1.311(3) . ?
N1 C1 1.311(3) . ?
C1 C2 1.515(3) . ?
C2 C3 1.389(3) . ?
C2 C7 1.390(3) . ?
C3 C4 1.385(3) . ?
C4 C5 1.382(3) . ?
C5 C6 1.381(3) . ?
C5 C8 1.501(3) . ?
C6 C7 1.386(3) . ?
O4 C10 1.438(7) . ?
C9 C10 1.490(9) . ?
C10 C11 1.518(7) . ?
O4' C10' 1.446(10) . ?
C9' C10' 1.493(13) . ?
C10' C11' 1.494(11) . ?

loop_
```

```
 _geom_angle_atom_site_label_1
 _geom_angle_atom_site_label_2
 _geom_angle_atom_site_label_3
 _geom_angle
 _geom_angle_site_symmetry_1
 _geom_angle_site_symmetry_3
 _geom_angle_publ_flag
O1 C1 N1 124.31(19) . . ?
O1 C1 C2 118.97(19) . . ?
N1 C1 C2 116.72(19) . . ?
C3 C2 C7 117.57(19) . . ?
C3 C2 C1 121.60(19) . . ?
C7 C2 C1 120.79(19) . . ?
C4 C3 C2 121.8(2) . . ?
C4 C3 Br1 118.38(17) . . ?
C2 C3 Br1 119.85(16) . . ?
C5 C4 C3 118.9(2) . . ?
C6 C5 C4 121.02(19) . . ?
C6 C5 C8 117.6(2) . . ?
C4 C5 C8 121.3(2) . . ?
C5 C6 C7 118.9(2) . . ?
C6 C7 C2 121.8(2) . . ?
C6 C7 Br2 118.33(17) . . ?
C2 C7 Br2 119.83(15) . . ?
O2 C8 O3 124.9(2) . . ?
O2 C8 C5 122.0(2) . . ?
O3 C8 C5 113.2(2) . . ?
O4 C10 C9 110.2(8) . . ?
O4 C10 C11 110.6(6) . . ?
C9 C10 C11 112.9(9) . . ?
O4' C10' C9' 108.0(12) . . ?
O4' C10' C11' 110.0(10) . . ?
C9' C10' C11' 113.9(13) . . ?

loop_
 _geom_torsion_atom_site_label_1
 _geom_torsion_atom_site_label_2
 _geom_torsion_atom_site_label_3
 _geom_torsion_atom_site_label_4
 _geom_torsion
 _geom_torsion_site_symmetry_1
 _geom_torsion_site_symmetry_2
 _geom_torsion_site_symmetry_3
 _geom_torsion_site_symmetry_4
 _geom_torsion_publ_flag
O1 C1 C2 C3 -91.0(3) . . . . ?
N1 C1 C2 C3 89.4(3) . . . . ?
O1 C1 C2 C7 86.7(3) . . . . ?
N1 C1 C2 C7 -92.9(3) . . . . ?
C7 C2 C3 C4 -1.3(3) . . . . ?
C1 C2 C3 C4 176.4(2) . . . . ?
C7 C2 C3 Br1 178.08(16) . . . . ?
C1 C2 C3 Br1 -4.2(3) . . . . ?
C2 C3 C4 C5 1.3(3) . . . . ?
Br1 C3 C4 C5 -178.05(16) . . . . ?
C3 C4 C5 C6 -0.2(3) . . . . ?
```

```
C3 C4 C5 C8 177.7(2) . . . . ?
C4 C5 C6 C7 -0.9(3) . . . . ?
C8 C5 C6 C7 -178.9(2) . . . . ?
C5 C6 C7 C2 0.9(3) . . . . ?
C5 C6 C7 Br2 -179.53(16) . . . . ?
C3 C2 C7 C6 0.1(3) . . . . ?
C1 C2 C7 C6 -177.6(2) . . . . ?
C3 C2 C7 Br2 -179.39(16) . . . . ?
C1 C2 C7 Br2 2.8(3) . . . . ?
C6 C5 C8 O2 7.2(3) . . . . ?
C4 C5 C8 O2 -170.8(2) . . . . ?
C6 C5 C8 O3 -173.2(2) . . . . ?
C4 C5 C8 O3 8.9(3) . . . . ?

loop_
 _geom_hbond_atom_site_label_D
 _geom_hbond_atom_site_label_H
 _geom_hbond_atom_site_label_A
 _geom_hbond_distance_DH
 _geom_hbond_distance_HA
 _geom_hbond_distance_DA
 _geom_hbond_angle_DHA
 _geom_hbond_site_symmetry_A
O3 H3A O4  0.84 1.75 2.586(11) 175.2 .
O3 H3A O4'  0.84 1.72 2.550(18) 172.1 .
N1 H1A O1  0.88 2.06 2.929(2) 170.1 2_657
N1 H1B O2  0.88 2.07 2.931(3) 165.2 2_666
O4 H4B O1  0.84 2.04 2.797(11) 149.8 2_766
O4' H4C O1  0.84 1.92 2.615(18) 138.9 2_766
C9' H9D O2  0.98 2.61 3.53(2) 157.2 1_565

_refine_diff_density_max    0.632
_refine_diff_density_min   -0.902
_refine_diff_density_rms    0.090

_shelxl_version_number 2014/6

# start Validation Reply Form
_vrf_PLAT417_15162a
;
PROBLEM: Short Inter D-H..H-D H3A .. H4B .. 2.04 Ang.
RESPONSE: The isoprpoyl alcohol is disordered in 0.60:0.40 ratio. The acid
group O3 denates to disordered O4 and O4' of the isopropyl alcohol. The alcohol
function O4 and O4' then donates to an O1 acceptor on another molecule. The
short contact found here is due to the disorder of the isopropyl alcohol
within the chain of hydrogen bonds.
;
# end Validation Reply Form

_shelx_res_file
;
TITL 15162a
CELL 0.71073   7.2866   8.5212  12.1832  71.3760  81.7450  83.6820
ZERR       2   0.0005   0.0006   0.0008    0.001    0.001    0.001
LATT  1
SFAC  C  H  N O Br
```

```
UNIT  22 26 2 8 4
TEMP -100
SIZE 0.40 0.38 0.16

L.S. 16
ACTA
LIST 4
FMAP 2
PLAN 10
CONF

HTAB O3 O4
HTAB O3 O4'
EQIV $1 -x+1, -y, -z+2
HTAB N1 O1_$1
EQIV $2 -x+1, -y+1, -z+1
HTAB N1 O2_$2
EQIV $3 -x+2, -y+1, -z+1
HTAB O4 O1_$3
HTAB O4' O1_$3
EQIV $4 x, y+1, z
HTAB C9' O2_$4

RIGU

WGHT    0.029600    0.506300
FVAR       0.18678   0.59760
BR1   5    0.617835    0.535501    0.849899    11.00000    0.06934    0.03621 =
         0.02540   -0.01126    0.00169   -0.00969
BR2   5    0.617513    0.036639    0.631962    11.00000    0.05996    0.02836 =
         0.03767   -0.00992   -0.00301   -0.01118
O1    4    0.694671    0.087497    0.900202    11.00000    0.02791    0.03643 =
         0.02256    0.00858   -0.00101   -0.00491
O2    4    0.816358    0.605531    0.305539    11.00000    0.04724    0.03945 =
         0.02024    0.00581    0.00229    0.00431
O3    4    0.860289    0.783210    0.399109    11.00000    0.04675    0.03241 =
         0.02927    0.01003    0.00802   -0.00940
AFIX 147
H3A   2    0.891171    0.844962    0.331263    11.00000   -1.20000
AFIX   0
N1    3    0.394149    0.168666    0.876873    11.00000    0.02962    0.03544 =
         0.02015    0.00808    0.00103   -0.00361
AFIX  93
H1A   2    0.353918    0.097671    0.943963    11.00000   -1.20000
H1B   2    0.314297    0.234926    0.832340    11.00000   -1.20000
AFIX   0
C1    1    0.573039    0.175717    0.843270    11.00000    0.03133    0.02402 =
         0.01561    0.00073    0.00004   -0.00617
C2    1    0.630756    0.300441    0.726375    11.00000    0.02602    0.02363 =
         0.01707    0.00145   -0.00032   -0.00443
C3    1    0.662493    0.462403    0.716571    11.00000    0.03083    0.02688 =
         0.01873   -0.00379   -0.00069   -0.00237
C4    1    0.724977    0.574268    0.610788    11.00000    0.02832    0.02391 =
         0.02564    0.00046   -0.00231   -0.00436
AFIX  43
H4A   2    0.748408    0.683836    0.606125    11.00000   -1.20000
```

```
AFIX   0
C5    1    0.752674    0.523871    0.512136    11.00000    0.02211    0.02753 =
        0.01961    0.00515    0.00034   -0.00119
C6    1    0.719632    0.364693    0.517994    11.00000    0.02945    0.02981 =
        0.01848   -0.00206   -0.00104    0.00021
AFIX  43
H6A   2    0.737290    0.331356    0.449665    11.00000   -1.20000
AFIX   0
C7    1    0.660289    0.254481    0.625253    11.00000    0.02811    0.02316 =
        0.02162   -0.00186   -0.00107   -0.00325
C8    1    0.813374    0.641440    0.394438    11.00000    0.02229    0.03115 =
        0.02461    0.00805    0.00169    0.00257
PART 1
SAME O4 C11 C10 C9
EADP O4  O4'
EADP C9  C9'
EADP C11 C11'
O4    4    0.936876    0.971909    0.187326    21.00000    0.02698    0.02331 =
        0.03240    0.00214    0.00666   -0.00503
AFIX 147
H4B   2    1.053451    0.963834    0.182958    21.00000   -1.50000
AFIX   0
C9    1    0.870790    1.205212    0.260080    21.00000    0.08855    0.04485 =
        0.04138   -0.01562    0.00651   -0.00180
AFIX 137
H9A   2    0.818667    1.320475    0.241022    21.00000   -1.50000
H9B   2    0.998322    1.199419    0.278660    21.00000   -1.50000
H9C   2    0.794894    1.135988    0.327504    21.00000   -1.50000
AFIX   0
C10   1    0.871528    1.144037    0.158325    21.00000    0.03674    0.02659 =
        0.03491   -0.00467   -0.00015    0.00071
AFIX  13
H10A  2    0.740163    1.152703    0.140844    21.00000   -1.20000
AFIX   0
C11   1    0.984717    1.246066    0.049332    21.00000    0.05596    0.02938 =
        0.03176    0.00059    0.00029   -0.00130
AFIX 137
H11A  2    0.979409    1.201334   -0.014844    21.00000   -1.50000
H11B  2    1.114192    1.241033    0.064265    21.00000   -1.50000
H11C  2    0.933607    1.361686    0.028227    21.00000   -1.50000
AFIX   0
PART 2
SAME O4  C9   C10  C11
SAME O4' C11' C10' C9'
O4'   4    0.977716    0.979173    0.200724   -21.00000    0.02698    0.02331 =
        0.03240    0.00214    0.00666   -0.00503
AFIX 147
H4C   2    1.045404    0.948476    0.148418   -21.00000   -1.50000
AFIX   0
C9'   1    0.885669    1.201504    0.279480   -21.00000    0.08855    0.04485 =
        0.04138   -0.01562    0.00651   -0.00180
AFIX 137
H9D   2    0.890846    1.320778    0.265745   -21.00000   -1.50000
H9E   2    0.941801    1.139312    0.350639   -21.00000   -1.50000
H9F   2    0.755806    1.174922    0.288417   -21.00000   -1.50000
AFIX   0
```

```
C10'  1    0.990129    1.155030    0.178360   -21.00000    0.03999    0.01950 =
         0.02960   -0.00066   -0.00837   -0.00672
AFIX  13
H10B  2    1.123753    1.176063    0.173873   -21.00000   -1.20000
AFIX   0
C11'  1    0.922244    1.249963    0.063982   -21.00000    0.05596    0.02938 =
         0.03176    0.00059    0.00029   -0.00130
AFIX 137
H11D  2    0.792695    1.227409    0.065641   -21.00000   -1.50000
H11E  2    0.999109    1.215761    0.001556   -21.00000   -1.50000
H11F  2    0.930385    1.369011    0.049700   -21.00000   -1.50000
PART 0
AFIX   0
HKLF       4

REM  15162a
REM R1 =  0.0262 for    2683 Fo > 4sig(Fo)  and  0.0326 for all    3128 data
REM    189 parameters refined using    152 restraints

END

WGHT      0.0295      0.5048

REM Highest difference peak  0.632,  deepest hole -0.902,  1-sigma level  0.090
Q1    1   0.7252  0.4908  0.8379  11.00000  0.05    0.63
Q2    1   0.6019  0.2382  0.7785  11.00000  0.05    0.35
Q3    1   0.7309  0.0393  0.6079  11.00000  0.05    0.30
Q4    1   0.5361  0.4720  0.8515  11.00000  0.05    0.30
Q5    1   0.7804  0.5779  0.4568  11.00000  0.05    0.26
Q6    1   0.6691  0.2611  0.6836  11.00000  0.05    0.26
Q7    1   0.8163  1.2739 -0.0898  11.00000  0.05    0.24
Q8    1   0.7387  1.3940  0.0356  11.00000  0.05    0.23
Q9    1   0.6145  1.0562  0.2219  11.00000  0.05    0.23
Q10   1   0.6733  0.4518  0.5108  11.00000  0.05    0.23
;
_shelx_res_checksum   33130
```

1,3,5-Tribromoisocyanobenzene (209ca), $Z = 8$ TC polytype.

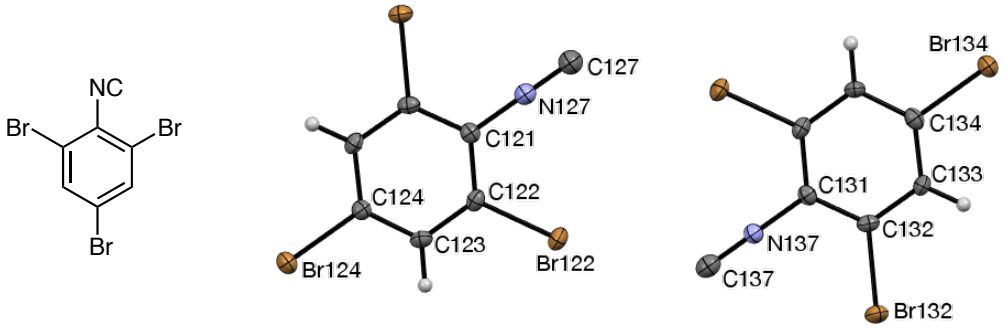

CIF content:

```
data_209ca2

_audit_creation_method            SHELXL-2014/6
_chemical_name_systematic
;
 1,3,5-Tribromo-2-isocyanobenzene
;
_chemical_name_common             'tribromo isocyanide, polytype 2'
_chemical_melting_point           ?
_chemical_formula_moiety          'C7 H2 Br3 N'
_chemical_formula_sum             'C7 H2 Br3 N'
_chemical_formula_weight          339.83

loop_
 _atom_type_symbol
 _atom_type_description
 _atom_type_scat_dispersion_real
 _atom_type_scat_dispersion_imag
 _atom_type_scat_source
 'C'  'C'   0.0033   0.0016
 'International Tables Vol C Tables 4.2.6.8 and 6.1.1.4'
 'H'  'H'   0.0000   0.0000
 'International Tables Vol C Tables 4.2.6.8 and 6.1.1.4'
 'N'  'N'   0.0061   0.0033
 'International Tables Vol C Tables 4.2.6.8 and 6.1.1.4'
 'Br'  'Br'  -0.2901   2.4595
 'International Tables Vol C Tables 4.2.6.8 and 6.1.1.4'

_space_group_crystal_system       orthorhombic
_space_group_IT_number            62
_space_group_name_H-M_alt         'P n m a'
_space_group_name_Hall            '-P 2ac 2n'

_shelx_space_group_comment
;
The symmetry employed for this shelxl refinement is uniquely defined
by the following loop, which should always be used as a source of
symmetry information in preference to the above space-group names.
They are only intended as comments.
```

```
;

loop_
 _space_group_symop_operation_xyz
 'x, y, z'
 '-x+1/2, -y, z+1/2'
 '-x, y+1/2, -z'
 'x+1/2, -y+1/2, -z+1/2'
 '-x, -y, -z'
 'x-1/2, y, -z-1/2'
 'x, -y-1/2, z'
 '-x-1/2, y-1/2, z-1/2'

_cell_length_a                    13.5916(18)
_cell_length_b                    10.1464(13)
_cell_length_c                    12.6158(16)
_cell_angle_alpha                 90
_cell_angle_beta                  90
_cell_angle_gamma                 90
_cell_volume                      1739.8(4)
_cell_formula_units_Z             8
_cell_measurement_temperature     173(2)
_cell_measurement_reflns_used     2721
_cell_measurement_theta_min       3.00
_cell_measurement_theta_max       27.37

_exptl_crystal_description       'Block'
_exptl_crystal_colour            'colourless'
_exptl_crystal_density_meas       ?
_exptl_crystal_density_method     ?
_exptl_crystal_density_diffrn     2.595
_exptl_crystal_F_000              1248
_exptl_transmission_factor_min    0.1704
_exptl_transmission_factor_max    0.3334
_exptl_crystal_size_max           0.400
_exptl_crystal_size_mid           0.350
_exptl_crystal_size_min           0.200
_exptl_absorpt_coefficient_mu     13.841
_shelx_estimated_absorpt_T_min    0.072
_shelx_estimated_absorpt_T_max    0.168
_exptl_absorpt_correction_type    multi-scan
_exptl_absorpt_correction_T_min   0.1704
_exptl_absorpt_correction_T_max   0.3334
_exptl_absorpt_process_details
;
SADABS (Bruker, 2002)
;
_diffrn_ambient_temperature       173(2)
_diffrn_radiation_wavelength      0.71073
_diffrn_radiation_type            MoK\a
_diffrn_source                    'sealed tube'
_diffrn_measurement_device_type
;
Bruker APEX-II CCD
;
_diffrn_measurement_method        '\f and \w scans'
```

```
_diffrn_detector_area_resol_mean  ?
_diffrn_reflns_number             19459
_diffrn_reflns_av_unetI/netI      0.0397
_diffrn_reflns_av_R_equivalents   0.0782
_diffrn_reflns_limit_h_min        -17
_diffrn_reflns_limit_h_max        17
_diffrn_reflns_limit_k_min        -13
_diffrn_reflns_limit_k_max        13
_diffrn_reflns_limit_l_min        -16
_diffrn_reflns_limit_l_max        16
_diffrn_reflns_theta_min          2.203
_diffrn_reflns_theta_max          27.505
_diffrn_reflns_theta_full         25.242
_diffrn_measured_fraction_theta_max   0.997
_diffrn_measured_fraction_theta_full  1.000
_diffrn_reflns_Laue_measured_fraction_max    0.997
_diffrn_reflns_Laue_measured_fraction_full   1.000
_diffrn_reflns_point_group_measured_fraction_max   0.997
_diffrn_reflns_point_group_measured_fraction_full  1.000
_reflns_number_total              2105
_reflns_number_gt                 1638
_reflns_threshold_expression      'I > 2\s(I)'
_reflns_Friedel_coverage          0.000
_reflns_Friedel_fraction_max      .
_reflns_Friedel_fraction_full     .

_reflns_special_details
;
 Reflections were merged by SHELXL according to the crystal
 class for the calculation of statistics and refinement.

 _reflns_Friedel_fraction is defined as the number of unique
 Friedel pairs measured divided by the number that would be
 possible theoretically, ignoring centric projections and
 systematic absences.
;


_computing_data_collection
;
APEX2 (Bruker, 2002)
;
_computing_cell_refinement
;
SAINT (Bruker, 2002)
;
_computing_data_reduction
;
SAINT (Bruker, 2002)
;
_computing_structure_solution
;
SHELXT (Sheldrick, 2015a)
;
_computing_structure_refinement
;
```

```
SHELXL2014 (Sheldrick, 2015b)
;
_computing_molecular_graphics
;
Mercury (Macrae <i>et al.</i>, 2008)
;
_computing_publication_material
;
SHELXTL (Sheldrick, 2008), enCIFer (Allen <i>et al.</i>, 2004),
and publCIF (Westrip, 2010)
;
_refine_ls_structure_factor_coef  Fsqd
_refine_ls_matrix_type            full
_refine_ls_weighting_scheme       calc
_refine_ls_weighting_details
'w=1/[\s^2^(Fo^2^)+(0.0121P)^2^+1.0004P] where P=(Fo^2^+2Fc^2^)/3'
_atom_sites_solution_primary      ?
_atom_sites_solution_secondary    ?
_atom_sites_solution_hydrogens    geom
_refine_ls_hydrogen_treatment     constr
_refine_ls_extinction_method      SHELXL
_refine_ls_extinction_coef        0.00269(12)
_refine_ls_extinction_expression
 'Fc^*^=kFc[1+0.001xFc^2^\l^3^/sin(2\q)]^-1/4^'
_refine_ls_number_reflns          2105
_refine_ls_number_parameters      116
_refine_ls_number_restraints      0
_refine_ls_R_factor_all           0.0423
_refine_ls_R_factor_gt            0.0254
_refine_ls_wR_factor_ref          0.0554
_refine_ls_wR_factor_gt           0.0507
_refine_ls_goodness_of_fit_ref    1.057
_refine_ls_restrained_S_all       1.057
_refine_ls_shift/su_max           0.001
_refine_ls_shift/su_mean          0.000

loop_
 _atom_site_label
 _atom_site_type_symbol
 _atom_site_fract_x
 _atom_site_fract_y
 _atom_site_fract_z
 _atom_site_U_iso_or_equiv
 _atom_site_adp_type
 _atom_site_occupancy
 _atom_site_site_symmetry_order
 _atom_site_calc_flag
 _atom_site_refinement_flags_posn
 _atom_site_refinement_flags_adp
 _atom_site_refinement_flags_occupancy
 _atom_site_disorder_assembly
 _atom_site_disorder_group
C121 C 0.3678(3) 0.7500 0.5680(3) 0.0162(9) Uani 1 2 d S T P . .
C122 C 0.3637(2) 0.6315(3) 0.6238(2) 0.0176(7) Uani 1 1 d . . . . .
C123 C 0.3573(2) 0.6306(3) 0.7332(2) 0.0182(7) Uani 1 1 d . . . . .
H123 H 0.3541 0.5499 0.7712 0.022 Uiso 1 1 calc R U . . .
```

```
C124 C 0.3559(3) 0.7500 0.7858(4) 0.0173(9) Uani 1 2 d S T P . .
N127 N 0.3793(3) 0.7500 0.4583(3) 0.0215(9) Uani 1 2 d S T P . .
C127 C 0.3909(4) 0.7500 0.3682(4) 0.0285(12) Uani 1 2 d S T P . .
Br122 Br 0.36763(3) 0.47074(3) 0.54952(3) 0.02456(11) Uani 1 1 d . . . . .
Br124 Br 0.35282(4) 0.7500 0.93610(4) 0.02254(13) Uani 1 2 d S T P . .
C131 C 0.3904(3) 0.2500 0.1747(3) 0.0161(10) Uani 1 2 d S T P . .
C132 C 0.3885(2) 0.3685(3) 0.1192(3) 0.0169(7) Uani 1 1 d . . . . .
C133 C 0.3821(2) 0.3691(3) 0.0100(2) 0.0179(7) Uani 1 1 d . . . . .
H133 H 0.3806 0.4499 -0.0281 0.021 Uiso 1 1 calc R U . . .
C134 C 0.3781(3) 0.2500 -0.0428(4) 0.0190(10) Uani 1 2 d S T P . .
N137 N 0.3955(3) 0.2500 0.2840(3) 0.0180(8) Uani 1 2 d S T P . .
C137 C 0.3995(3) 0.2500 0.3761(4) 0.0246(11) Uani 1 2 d S T P . .
Br132 Br 0.39399(3) 0.52885(3) 0.19404(3) 0.02480(11) Uani 1 1 d . . . . .
Br134 Br 0.36801(4) 0.2500 -0.19267(4) 0.02564(14) Uani 1 2 d S T P . .

loop_
 _atom_site_aniso_label
 _atom_site_aniso_U_11
 _atom_site_aniso_U_22
 _atom_site_aniso_U_33
 _atom_site_aniso_U_23
 _atom_site_aniso_U_13
 _atom_site_aniso_U_12
C121 0.013(2) 0.019(2) 0.016(2) 0.000 0.0002(19) 0.000
C122 0.0164(16) 0.0157(16) 0.0207(17) -0.0031(13) -0.0016(14) 0.0016(14)
C123 0.0191(17) 0.0152(17) 0.0202(17) 0.0039(13) -0.0017(14) 0.0013(14)
C124 0.017(2) 0.017(2) 0.018(2) 0.000 0.0003(19) 0.000
N127 0.026(2) 0.018(2) 0.021(2) 0.000 0.0008(17) 0.000
C127 0.035(3) 0.025(3) 0.026(3) 0.000 0.002(2) 0.000
Br122 0.0339(2) 0.01579(18) 0.0239(2) -0.00522(14) 0.00210(15) -0.00052(15)
Br124 0.0290(3) 0.0231(3) 0.0155(2) 0.000 -0.0005(2) 0.000
C131 0.014(2) 0.019(2) 0.015(2) 0.000 -0.0026(17) 0.000
C132 0.0158(16) 0.0138(16) 0.0210(17) -0.0042(13) 0.0003(13) 0.0001(13)
C133 0.0229(18) 0.0132(17) 0.0174(17) 0.0035(13) -0.0001(13) 0.0014(14)
C134 0.018(2) 0.024(3) 0.015(2) 0.000 -0.0016(18) 0.000
N137 0.019(2) 0.017(2) 0.018(2) 0.000 0.0008(16) 0.000
C137 0.024(3) 0.019(3) 0.030(3) 0.000 -0.001(2) 0.000
Br132 0.0360(2) 0.01500(19) 0.0234(2) -0.00427(14) -0.00260(14) -0.00111(15)
Br134 0.0393(3) 0.0222(3) 0.0154(3) 0.000 0.0003(2) 0.000

_geom_special_details
;
 All esds (except the esd in the dihedral angle between two l.s. planes)
 are estimated using the full covariance matrix.  The cell esds are taken
 into account individually in the estimation of esds in distances, angles
 and torsion angles; correlations between esds in cell parameters are only
 used when they are defined by crystal symmetry.  An approximate (isotropic)
 treatment of cell esds is used for estimating esds involving l.s. planes.
;

loop_
 _geom_bond_atom_site_label_1
 _geom_bond_atom_site_label_2
 _geom_bond_distance
 _geom_bond_site_symmetry_2
 _geom_bond_publ_flag
```

```
C121 N127 1.393(6) . ?
C121 C122 1.395(4) 7_575 ?
C122 C123 1.382(4) . ?
C122 Br122 1.882(3) . ?
C123 C124 1.381(4) 7_575 ?
C123 H123 0.9500 . ?
C124 Br124 1.897(5) . ?
N127 C127 1.147(6) . ?
C131 N137 1.380(6) . ?
C131 C132 1.392(4) 7_565 ?
C132 C133 1.380(4) . ?
C132 Br132 1.883(3) . ?
C133 C134 1.381(4) 7_565 ?
C133 H133 0.9500 . ?
C134 Br134 1.895(4) . ?
N137 C137 1.164(6) . ?

loop_
 _geom_angle_atom_site_label_1
 _geom_angle_atom_site_label_2
 _geom_angle_atom_site_label_3
 _geom_angle
 _geom_angle_site_symmetry_1
 _geom_angle_site_symmetry_3
 _geom_angle_publ_flag
N127 C121 C122 120.4(2) . 7_575 ?
C122 C121 C122 119.1(4) . 7_575 ?
C123 C122 C121 120.8(3) . . ?
C123 C122 Br122 119.6(2) . . ?
C121 C122 Br122 119.6(2) . . ?
C124 C123 C122 118.3(3) . . ?
C124 C123 H123 120.8 . . ?
C122 C123 H123 120.8 . . ?
C123 C124 C123 122.5(4) . 7_575 ?
C123 C124 Br124 118.7(2) 7_575 . ?
C127 N127 C121 178.5(5) . . ?
N137 C131 C132 120.3(2) . 7_565 ?
C132 C131 C132 119.5(4) 7_565 . ?
C133 C132 C131 120.5(3) . . ?
C133 C132 Br132 119.9(2) . . ?
C131 C132 Br132 119.5(2) . . ?
C132 C133 C134 118.7(3) . . ?
C132 C133 H133 120.7 . . ?
C134 C133 H133 120.7 . . ?
C133 C134 C133 122.1(4) 7_565 . ?
C133 C134 Br134 118.9(2) 7_565 . ?
C137 N137 C131 179.8(4) . . ?

loop_
 _geom_torsion_atom_site_label_1
 _geom_torsion_atom_site_label_2
 _geom_torsion_atom_site_label_3
 _geom_torsion_atom_site_label_4
 _geom_torsion
 _geom_torsion_site_symmetry_1
 _geom_torsion_site_symmetry_2
```

```
 _geom_torsion_site_symmetry_3
 _geom_torsion_site_symmetry_4
 _geom_torsion_publ_flag
N127 C121 C122 C123 176.7(3) . . . . ?
C122 C121 C122 C123 -1.0(6) 7_575 . . . ?
N127 C121 C122 Br122 -3.0(5) . . . . ?
C122 C121 C122 Br122 179.30(19) 7_575 . . . ?
C121 C122 C123 C124 -0.5(5) . . . . ?
Br122 C122 C123 C124 179.2(3) . . . . ?
C122 C123 C124 C123 2.1(7) . . . 7_575 ?
C122 C123 C124 Br124 -177.4(2) . . . . ?
N137 C131 C132 C133 -179.2(3) . . . . ?
C132 C131 C132 C133 1.6(6) 7_565 . . . ?
N137 C131 C132 Br132 0.6(5) . . . . ?
C132 C131 C132 Br132 -178.6(2) 7_565 . . . ?
C131 C132 C133 C134 -0.2(5) . . . . ?
Br132 C132 C133 C134 -179.9(3) . . . . ?
C132 C133 C134 C133 -1.3(7) . . . 7_565 ?
C132 C133 C134 Br134 179.3(3) . . . . ?

loop_
 _geom_hbond_atom_site_label_D
 _geom_hbond_atom_site_label_H
 _geom_hbond_atom_site_label_A
 _geom_hbond_distance_DH
 _geom_hbond_distance_HA
 _geom_hbond_distance_DA
 _geom_hbond_angle_DHA
 _geom_hbond_site_symmetry_A
 _geom_hbond_publ_flag
C123 H123 Br134  0.95 3.08 3.976(3) 157.3 1_556 n
C133 H133 Br124  0.95 3.10 3.995(3) 157.4 1_554 n

_refine_diff_density_max    0.436
_refine_diff_density_min   -0.480
_refine_diff_density_rms    0.120

_shelxl_version_number 2014/6

_shelx_res_file
;
TITL RNC-II in Pnma
CELL 0.71073  13.5916  10.1464  12.6158  90.000  90.000  90.000
ZERR    8.00   0.0018   0.0013   0.0016   0.000   0.000   0.000
LATT  1
SYMM 0.5-X, -Y, 0.5+Z
SYMM -X, 0.5+Y, -Z
SYMM 0.5+X, 0.5-Y, 0.5-Z
SFAC C  H  N BR
UNIT 56 16 8 24
TEMP -100
SIZE 0.20 0.35 0.40

EQIV $1 x, y, z+1
HTAB C123 Br134_$1
EQIV $2 x, y, z-1
```

```
HTAB C133 Br124_$2
RTAB CBR C127 Br132
RTAB CBR C137 Br122
RTAB NCBR N127 C127 Br132
RTAB NCBR N137 C137 Br122

L.S. 8
ACTA
LIST 4
CONF
BOND $H
FMAP 2
PLAN 5

WGHT    0.012100    1.000400
EXTI    0.002693
FVAR       0.04944
C121   1    0.367761    0.750000    0.567988    10.50000    0.01315    0.01918
=
         0.01617    0.00000    0.00017    0.00000
C122   1    0.363701    0.631496    0.623847    11.00000    0.01638    0.01570
=
         0.02073   -0.00312   -0.00156    0.00161
C123   1    0.357340    0.630636    0.733180    11.00000    0.01912    0.01524
=
         0.02022    0.00389   -0.00172    0.00128
AFIX  43
H123  2    0.354053    0.549946    0.771212    11.00000   -1.20000
AFIX   0
C124   1    0.355880    0.750000    0.785771    10.50000    0.01654    0.01687
=
         0.01836    0.00000    0.00027    0.00000
N127   3    0.379270    0.750000    0.458266    10.50000    0.02557    0.01844
=
         0.02056    0.00000    0.00081    0.00000
C127   1    0.390899    0.750000    0.368228    10.50000    0.03451    0.02503
=
         0.02600    0.00000    0.00184    0.00000
BR122  4    0.367627    0.470742    0.549523    11.00000    0.03393    0.01579
=
         0.02395   -0.00522    0.00210   -0.00052
BR124  4    0.352818    0.750000    0.936096    10.50000    0.02899    0.02308
=
         0.01555    0.00000   -0.00054    0.00000
C131   1    0.390417    0.250000    0.174723    10.50000    0.01402    0.01930
=
         0.01503    0.00000   -0.00255    0.00000
C132   1    0.388464    0.368473    0.119158    11.00000    0.01585    0.01381
=
         0.02104   -0.00418    0.00026    0.00012
C133   1    0.382141    0.369105    0.009977    11.00000    0.02293    0.01323
=
         0.01744    0.00347   -0.00011    0.00138
AFIX  43
H133  2    0.380601    0.449859   -0.028096    11.00000   -1.20000
AFIX   0
```

```
C134    1     0.378097     0.250000    -0.042825     10.50000     0.01802     0.02423
=
          0.01483    0.00000   -0.00165    0.00000
N137    3     0.395518     0.250000     0.283986     10.50000     0.01902     0.01704
=
          0.01807    0.00000    0.00076    0.00000
C137    1     0.399543     0.250000     0.376113     10.50000     0.02406     0.01941
=
          0.03020    0.00000   -0.00111    0.00000
BR132   4     0.393987     0.528853     0.194038     11.00000     0.03597     0.01500
=
          0.02344   -0.00427   -0.00260   -0.00111
BR134   4     0.368007     0.250000    -0.192669     10.50000     0.03928     0.02222
=
          0.01543    0.00000    0.00029    0.00000

HKLF 4

REM  RNC-II in Pnma
REM R1 =  0.0254 for    1638 Fo > 4sig(Fo)  and  0.0423 for all    2105 data
REM    116 parameters refined using      0 restraints

END

WGHT      0.0120      1.0141

REM Highest difference peak  0.436,  deepest hole -0.480,  1-sigma level  0.120
Q1    1   0.3423  0.7500  0.8622  10.50000  0.05    0.44
Q2    1   0.3037  0.4524  0.5813  11.00000  0.05    0.43
Q3    1   0.3726  0.4218  0.1464  11.00000  0.05    0.43
Q4    1   0.4052  0.1498 -0.2021  11.00000  0.05    0.43
Q5    1   0.3803  0.5595  0.1160  11.00000  0.05    0.41
;

_shelx_res_checksum   28925

# Data collection and refinement details were not given by
# Dr. Britton or the XCL.
# Some atom labels have been edited after refinement
# to be consistent with other compounds. - KJT
```

1,3-Dibromo-2-isocyano-5-methylbenzene (209cb).

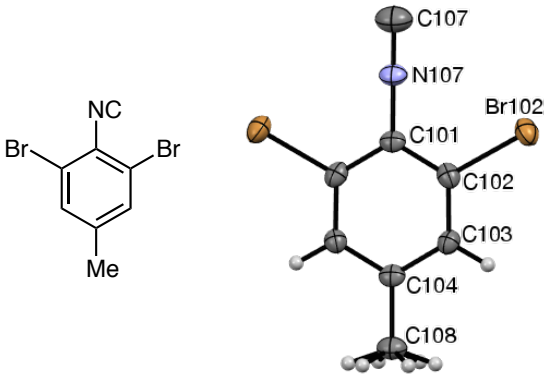

Data collection (by the XCL): A crystal (approx. 0.400 × 0.140 × 0.080 mm^3) was placed onto the tip of a Mitegen mount and mounted on a Bruker APEX-II CCD diffractometer for a data collection at 173 K. A preliminary set of cell constants was calculated from reflections harvested from three sets of 20 frames. These initial sets of frames were oriented such that orthogonal wedges of reciprocal space were surveyed. This produced initial orientation matrices determined from 81 reflections. The data collection was carried out using MoKα radiation (graphite monochromator) with a frame time of 6 sec and a detector distance of 60 mm. A randomly oriented region of reciprocal space was surveyed to the extent of one sphere and to a resolution of 0.77 Å. Four major sections of frames were collected with 0.50º steps in ω at four different ϕ settings and a detector position of –28º in 2θ. The intensity data were corrected for absorption and decay. Final cell constants were calculated from 2,995 strong reflections from the actual data collection after integration.

Structure solution and refinement (by the XCL): The space group P-42$_1$m was determined based on systematic absences and intensity statistics. A direct-methods solution was calculated that provided most non-hydrogen atoms from the E-map. Full-matrix least squares / difference Fourier cycles were performed that located the remaining non-hydrogen atoms. All non-hydrogen atoms were refined with anisotropic displacement parameters. All hydrogen atoms were placed in ideal positions and refined as riding atoms with relative isotropic displacement parameters. The final full matrix least squares refinement converged to $R1$ = 0.0232 and $wR2$ = 0.0508 (F^2, all data).

CIF content:

```
data_209cb

_audit_creation_method            SHELXL-2014/6
_chemical_name_systematic
;
1,3-Dibromo-2-isocyano-5-methylbenzene
;
_chemical_name_common             'dibromo methyl isocyanide'
_chemical_melting_point           ?
_chemical_formula_moiety          'C8 H5 Br2 N'
_chemical_formula_sum             'C8 H5 Br2 N'
_chemical_formula_weight          274.95

loop_
 _atom_type_symbol
 _atom_type_description
 _atom_type_scat_dispersion_real
 _atom_type_scat_dispersion_imag
 _atom_type_scat_source
 'C'  'C'   0.0033   0.0016
 'International Tables Vol C Tables 4.2.6.8 and 6.1.1.4'
 'H'  'H'   0.0000   0.0000
 'International Tables Vol C Tables 4.2.6.8 and 6.1.1.4'
 'N'  'N'   0.0061   0.0033
 'International Tables Vol C Tables 4.2.6.8 and 6.1.1.4'
 'Br'  'Br'  -0.2901   2.4595
 'International Tables Vol C Tables 4.2.6.8 and 6.1.1.4'

_space_group_crystal_system       tetragonal
_space_group_IT_number            113
_space_group_name_H-M_alt         'P -4 21 m'
_space_group_name_Hall            'P -4 2ab'

_shelx_space_group_comment
;
The symmetry employed for this shelxl refinement is uniquely defined
by the following loop, which should always be used as a source of
symmetry information in preference to the above space-group names.
They are only intended as comments.
;

loop_
 _space_group_symop_operation_xyz
 'x, y, z'
 '-x, -y, z'
 'y, -x, -z'
 '-y, x, -z'
 '-x+1/2, y+1/2, -z'
 'x+1/2, -y+1/2, -z'
 '-y+1/2, -x+1/2, z'
 'y+1/2, x+1/2, z'

_cell_length_a                    14.690(5)
_cell_length_b                    14.690(5)
_cell_length_c                    4.0703(15)
```

```
_cell_angle_alpha                 90
_cell_angle_beta                  90
_cell_angle_gamma                 90
_cell_volume                      878.3(7)
_cell_formula_units_Z             4
_cell_measurement_temperature     173(2)
_cell_measurement_reflns_used     2995
_cell_measurement_theta_min       2.77
_cell_measurement_theta_max       26.91

_exptl_crystal_description       'Needle'
_exptl_crystal_colour            'colourless'
_exptl_crystal_density_meas       ?
_exptl_crystal_density_method     ?
_exptl_crystal_density_diffrn     2.079
_exptl_crystal_F_000              520
_exptl_transmission_factor_min    0.2551
_exptl_transmission_factor_max    0.7456
_exptl_crystal_size_max           0.400
_exptl_crystal_size_mid           0.140
_exptl_crystal_size_min           0.080
_exptl_absorpt_coefficient_mu     9.160
_shelx_estimated_absorpt_T_min    0.121
_shelx_estimated_absorpt_T_max    0.528
_exptl_absorpt_correction_type    multi-scan
_exptl_absorpt_correction_T_min   0.2551
_exptl_absorpt_correction_T_max   0.7456
_exptl_absorpt_process_details    'SADABS 2012/1 (Sheldrick, 2012)'
_exptl_absorpt_special_details    ?
_exptl_special_details            'K. Tritch / Prof. W. Noland'
_diffrn_ambient_temperature       173(2)
_diffrn_radiation_wavelength      0.71073
_diffrn_radiation_type            MoK\a
_diffrn_source                    'sealed tube'
_diffrn_measurement_device_type   'Bruker APEX-II CCD'
_diffrn_measurement_method        '\f and \w scans'
_diffrn_detector_area_resol_mean  ?
_diffrn_reflns_number             10248
_diffrn_reflns_av_unetI/netI      0.0233
_diffrn_reflns_av_R_equivalents   0.0453
_diffrn_reflns_limit_h_min        -18
_diffrn_reflns_limit_h_max        19
_diffrn_reflns_limit_k_min        -19
_diffrn_reflns_limit_k_max        19
_diffrn_reflns_limit_l_min        -5
_diffrn_reflns_limit_l_max        5
_diffrn_reflns_theta_min          1.961
_diffrn_reflns_theta_max          27.594
_diffrn_reflns_theta_full         25.242
_diffrn_measured_fraction_theta_max   0.997
_diffrn_measured_fraction_theta_full  1.000
_diffrn_reflns_Laue_measured_fraction_max    0.997
_diffrn_reflns_Laue_measured_fraction_full   1.000
_diffrn_reflns_point_group_measured_fraction_max   0.995
_diffrn_reflns_point_group_measured_fraction_full  1.000
_reflns_number_total              1074
```

```
_reflns_number_gt                1001
_reflns_threshold_expression     'I > 2\s(I)'
_reflns_Friedel_coverage         0.655
_reflns_Friedel_fraction_max     0.993
_reflns_Friedel_fraction_full    1.000

_reflns_special_details
;
 Reflections were merged by SHELXL according to the crystal
 class for the calculation of statistics and refinement.

 _reflns_Friedel_fraction is defined as the number of unique
 Friedel pairs measured divided by the number that would be
 possible theoretically, ignoring centric projections and
 systematic absences.
;

_computing_data_collection      'Bruker APEX2'
_computing_cell_refinement      'Bruker SAINT'
_computing_data_reduction       'Bruker SAINT'
_computing_structure_solution   'SHELXT-2014/4 (Sheldrick, 2014)'
_computing_structure_refinement 'SHELXL-2014/6 (Sheldrick, 2014)'
_computing_molecular_graphics   'Bruker SHELXTL'
_computing_publication_material 'Bruker SHELXTL'
_refine_special_details          ?
_refine_ls_structure_factor_coef  Fsqd
_refine_ls_matrix_type           full
_refine_ls_weighting_scheme      calc
_refine_ls_weighting_details
'w=1/[\s^2^(Fo^2^)+(0.0267P)^2^+0.0073P] where P=(Fo^2^+2Fc^2^)/3'
_atom_sites_solution_primary     ?
_atom_sites_solution_secondary   ?
_atom_sites_solution_hydrogens   geom
_refine_ls_hydrogen_treatment    constr
_refine_ls_extinction_method     none
_refine_ls_extinction_coef       .
_refine_ls_abs_structure_details
;
 Flack x determined using 381 quotients [(I+)-(I-)]/[(I+)+(I-)]
 (Parsons, Flack and Wagner, Acta Cryst. B69 (2013) 249-259).
;
_refine_ls_abs_structure_Flack   -0.024(13)
_chemical_absolute_configuration  ad
_refine_ls_number_reflns         1074
_refine_ls_number_parameters     59
_refine_ls_number_restraints     0
_refine_ls_R_factor_all          0.0267
_refine_ls_R_factor_gt           0.0232
_refine_ls_wR_factor_ref         0.0508
_refine_ls_wR_factor_gt          0.0500
_refine_ls_goodness_of_fit_ref   1.141
_refine_ls_restrained_S_all      1.141
_refine_ls_shift/su_max          0.000
_refine_ls_shift/su_mean         0.000

loop_
```

```
 _atom_site_label
 _atom_site_type_symbol
 _atom_site_fract_x
 _atom_site_fract_y
 _atom_site_fract_z
 _atom_site_U_iso_or_equiv
 _atom_site_adp_type
 _atom_site_occupancy
 _atom_site_site_symmetry_order
 _atom_site_calc_flag
 _atom_site_refinement_flags_posn
 _atom_site_refinement_flags_adp
 _atom_site_refinement_flags_occupancy
 _atom_site_disorder_assembly
 _atom_site_disorder_group
Br102 Br 0.64344(3) 0.58324(2) 0.38265(14) 0.03268(14) Uani 1 1 d . . . . .
N107 N 0.8281(2) 0.6719(2) 0.5307(11) 0.0278(11) Uani 1 2 d S T P . .
C101 C 0.7708(2) 0.7292(2) 0.3538(15) 0.0228(11) Uani 1 2 d S T P . .
C103 C 0.6256(2) 0.7587(2) 0.0981(10) 0.0243(8) Uani 1 1 d . . . . .
H103 H 0.5664 0.7382 0.0402 0.029 Uiso 1 1 calc R U . . .
C104 C 0.6535(3) 0.8465(3) 0.0132(13) 0.0237(11) Uani 1 2 d S T P . .
C102 C 0.6845(3) 0.7013(3) 0.2671(9) 0.0245(8) Uani 1 1 d . . . . .
C108 C 0.5894(3) 0.9106(3) -0.1624(14) 0.0328(12) Uani 1 2 d S T P . .
H108A H 0.5318 0.8793 -0.2065 0.049 Uiso 0.5 1 calc R U P . .
H108B H 0.6169 0.9300 -0.3703 0.049 Uiso 0.5 1 calc R U P . .
H108C H 0.5781 0.9640 -0.0241 0.049 Uiso 0.5 1 calc R U P . .
C107 C 0.8753(3) 0.6247(3) 0.6829(18) 0.0474(18) Uani 1 2 d S T P . .

loop_
 _atom_site_aniso_label
 _atom_site_aniso_U_11
 _atom_site_aniso_U_22
 _atom_site_aniso_U_33
 _atom_site_aniso_U_23
 _atom_site_aniso_U_13
 _atom_site_aniso_U_12
Br102 0.0337(2) 0.02125(19) 0.0431(2) 0.0013(2) 0.0071(2) -0.00062(15)
N107 0.0268(15) 0.0268(15) 0.030(3) -0.0005(13) 0.0005(13) 0.009(2)
C101 0.0238(15) 0.0238(15) 0.021(3) -0.0031(16) 0.0031(16) 0.0067(19)
C103 0.0214(17) 0.0240(17) 0.0273(19) -0.0043(19) 0.0017(18) 0.0001(14)
C104 0.0245(16) 0.0245(16) 0.022(3) -0.0038(14) 0.0038(14) 0.007(2)
C102 0.0267(19) 0.0202(18) 0.027(2) -0.0028(15) 0.0080(16) 0.0008(16)
C108 0.0329(18) 0.0329(18) 0.033(3) 0.0013(18) -0.0013(18) 0.009(3)
C107 0.048(2) 0.048(2) 0.046(5) 0.002(2) -0.002(2) 0.016(3)

_geom_special_details
;
 All esds (except the esd in the dihedral angle between two l.s. planes)
 are estimated using the full covariance matrix.  The cell esds are taken
 into account individually in the estimation of esds in distances, angles
 and torsion angles; correlations between esds in cell parameters are only
 used when they are defined by crystal symmetry.  An approximate (isotropic)
 treatment of cell esds is used for estimating esds involving l.s. planes.
;

loop_
```

```
 _geom_bond_atom_site_label_1
 _geom_bond_atom_site_label_2
 _geom_bond_distance
 _geom_bond_site_symmetry_2
 _geom_bond_publ_flag
Br102 C102 1.896(4) . ?
N107 C107 1.161(8) . ?
N107 C101 1.391(7) . ?
C101 C102 1.379(5) . ?
C101 C102 1.379(5) 7_665 ?
C103 C102 1.389(6) . ?
C103 C104 1.396(4) . ?
C103 H103 0.9500 . ?
C104 C103 1.396(4) 7_665 ?
C104 C108 1.511(7) . ?
C108 H108A 0.9800 . ?
C108 H108B 0.9800 . ?
C108 H108C 0.9800 . ?

loop_
 _geom_angle_atom_site_label_1
 _geom_angle_atom_site_label_2
 _geom_angle_atom_site_label_3
 _geom_angle
 _geom_angle_site_symmetry_1
 _geom_angle_site_symmetry_3
 _geom_angle_publ_flag
C107 N107 C101 178.9(6) . . ?
C102 C101 C102 118.7(5) . 7_665 ?
C102 C101 N107 120.6(3) . . ?
C102 C101 N107 120.6(3) 7_665 . ?
C102 C103 C104 120.0(4) . . ?
C102 C103 H103 120.0 . . ?
C104 C103 H103 120.0 . . ?
C103 C104 C103 118.7(5) . 7_665 ?
C103 C104 C108 120.6(2) . . ?
C103 C104 C108 120.6(2) 7_665 . ?
C101 C102 C103 121.3(4) . . ?
C101 C102 Br102 120.0(3) . . ?
C103 C102 Br102 118.7(3) . . ?
C104 C108 H108A 109.5 . . ?
C104 C108 H108B 109.5 . . ?
H108A C108 H108B 109.5 . . ?
C104 C108 H108C 109.5 . . ?
H108A C108 H108C 109.5 . . ?
H108B C108 H108C 109.5 . . ?

loop_
 _geom_torsion_atom_site_label_1
 _geom_torsion_atom_site_label_2
 _geom_torsion_atom_site_label_3
 _geom_torsion_atom_site_label_4
 _geom_torsion
 _geom_torsion_site_symmetry_1
 _geom_torsion_site_symmetry_2
 _geom_torsion_site_symmetry_3
```

```
 _geom_torsion_site_symmetry_4
 _geom_torsion_publ_flag
C102 C103 C104 C103 0.7(7) . . . 7_665 ?
C102 C103 C104 C108 -178.3(4) . . . . ?
C102 C101 C102 C103 -0.5(8) 7_665 . . . ?
N107 C101 C102 C103 178.2(4) . . . . ?
C102 C101 C102 Br102 -179.8(3) 7_665 . . . ?
N107 C101 C102 Br102 -1.1(7) . . . . ?
C104 C103 C102 C101 -0.1(6) . . . . ?
C104 C103 C102 Br102 179.2(3) . . . . ?

_refine_diff_density_max    0.299
_refine_diff_density_min   -0.509
_refine_diff_density_rms    0.107

_shelxl_version_number 2014/6

_shelx_res_file
;
TITL 16124a in P-42(1)m
CELL  0.71073  14.6898  14.6898   4.0703   90.000   90.000   90.000
ZERR    4.000   0.0051   0.0051   0.0015    0.000    0.000    0.000
LATT -1
SYMM -X, -Y, Z
SYMM Y, -X, -Z
SYMM -Y, X, -Z
SYMM 1/2-X, 1/2+Y, -Z
SYMM 1/2+X, 1/2-Y, -Z
SYMM 1/2-Y, 1/2-X, Z
SYMM 1/2+Y, 1/2+X, Z
SFAC C  H  N BR
UNIT 32 20 4 8
TEMP -100
SIZE 0.08 0.14 0.40

L.S. 10
ACTA
BOND $H
LIST 4
CONF
FMAP 2
PLAN 5
WGHT    0.026700    0.007300
FVAR       0.17362
BR102   4    0.643438    0.583244    0.382655    11.00000    0.03368    0.02125
=
         0.04309    0.00126    0.00715   -0.00062
N107    3    0.828062    0.671938    0.530733    10.50000    0.02683    0.02683
=
         0.02984   -0.00052    0.00052    0.00921
C101    1    0.770791    0.729209    0.353762    10.50000    0.02381    0.02381
=
         0.02065   -0.00310    0.00310    0.00672
C103    1    0.625614    0.758709    0.098057    11.00000    0.02143    0.02402
=
         0.02733   -0.00427    0.00168    0.00009
```

```
AFIX  43
H103   2    0.566405    0.738216    0.040246    11.00000   -1.20000
AFIX   0
C104    1    0.653516    0.846484    0.013158    10.50000    0.02447    0.02447
=
         0.02209   -0.00376    0.00376    0.00722
C102    1    0.684458    0.701345    0.267097    11.00000    0.02666    0.02023
=
         0.02651   -0.00280    0.00798    0.00084
C108    1    0.589435    0.910565   -0.162371    10.50000    0.03294    0.03294
=
         0.03257    0.00128   -0.00128    0.00939
AFIX 137
H108A   2    0.531780    0.879312   -0.206546    10.50000   -1.50000
H108B   2    0.616883    0.929968   -0.370345    10.50000   -1.50000
H108C   2    0.578076    0.963981   -0.024078    10.50000   -1.50000
AFIX   0
C107    1    0.875329    0.624671    0.682928    10.50000    0.04801    0.04801
=
         0.04608    0.00227   -0.00227    0.01606

HKLF 4

REM  16124a in P-42(1)m
REM R1 =  0.0232 for    1001 Fo > 4sig(Fo)  and  0.0267 for all    1074 data
REM     59 parameters refined using      0 restraints

END

WGHT      0.0264      0.0145

REM Highest difference peak  0.299,  deepest hole -0.509,  1-sigma level  0.107
Q1    1   0.6420  0.5808  0.6261  11.00000  0.05    0.30
Q2    1   0.7456  0.7088 -0.1289  11.00000  0.05    0.29
Q3    1   0.5206  0.7055 -0.0362  11.00000  0.05    0.28
Q4    1   0.5329  0.5057  0.0929  11.00000  0.05    0.27
Q5    1   0.8037  0.7590  0.6807  11.00000  0.05    0.26
;



_shelx_res_checksum   83001

# Some atom labels have been edited after refinement
# to be consistent with other compounds. - KJT
```

Methyl 3,5-dibromo-4-isocyanobenzoate (209cd).

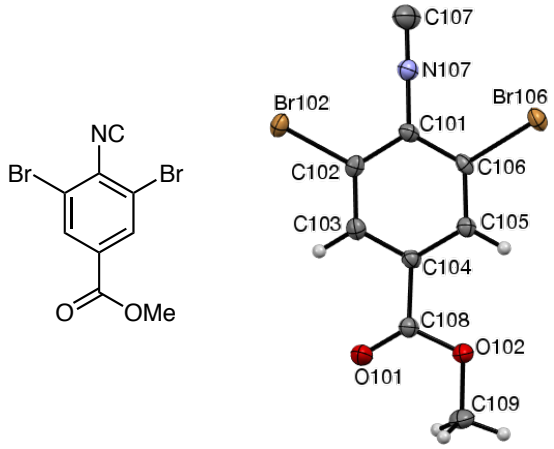

Data collection (by the XCL): A crystal (approx. 0.500 × 0.120 × 0.030 mm^3) was placed onto the tip of a Mitegen loop and mounted on a Bruker APEX-II CCD diffractometer for a data collection at 173 K. A preliminary set of cell constants was calculated from reflections harvested from three sets of 20 frames. These initial sets of frames were oriented such that orthogonal wedges of reciprocal space were surveyed. This produced initial orientation matrices determined from 133 reflections. The data collection was carried out using MoKα radiation (graphite monochromator) with a frame time of 20 sec and a detector distance of 60 mm. A randomly oriented region of reciprocal space was surveyed to the extent of one sphere and to a resolution of 0.77 Å. Four major sections of frames were collected with 0.50° steps in ω at four different ϕ settings and a detector position of –28° in 2θ. The intensity data were corrected for absorption and decay. Final cell constants were calculated from 2,953 strong reflections from the actual data collection after integration.

Structure solution and refinement (by the XCL): The space group $P2_1/n$ was determined based on systematic absences and intensity statistics. A direct-methods solution was calculated that provided most non-hydrogen atoms from the E-map. Full-matrix least squares / difference Fourier cycles were performed that located the remaining non-hydrogen atoms. All non-hydrogen atoms were refined with anisotropic displacement parameters. All hydrogen atoms were placed in ideal positions and refined as riding atoms with relative isotropic displacement parameters. The specimen was refined as a two-component pseudo-merohedral twin in a 0.67:0.33 ratio with the twin symmetry element being a 180° rotation of [001]. The final full matrix least squares refinement converged to $R1 = 0.0287$ and $wR2 = 0.0689$ (F^2, all data).

CIF content:

```
data_209cd

_audit_creation_method            SHELXL-2014/6
_chemical_name_systematic
;
Methyl 3,5-dibromo-4-isocyanobenzoate
;
_chemical_name_common             'dibromo isocyanide ester'
_chemical_melting_point           ?
_chemical_formula_moiety          'C9 H5 Br2 N O2'
_chemical_formula_sum             'C9 H5 Br2 N O2'
_chemical_formula_weight          318.96

loop_
 _atom_type_symbol
 _atom_type_description
 _atom_type_scat_dispersion_real
 _atom_type_scat_dispersion_imag
 _atom_type_scat_source
 'C'  'C'   0.0033   0.0016
 'International Tables Vol C Tables 4.2.6.8 and 6.1.1.4'
 'H'  'H'   0.0000   0.0000
 'International Tables Vol C Tables 4.2.6.8 and 6.1.1.4'
 'N'  'N'   0.0061   0.0033
 'International Tables Vol C Tables 4.2.6.8 and 6.1.1.4'
 'O'  'O'   0.0106   0.0060
 'International Tables Vol C Tables 4.2.6.8 and 6.1.1.4'
 'Br'  'Br'  -0.2901   2.4595
 'International Tables Vol C Tables 4.2.6.8 and 6.1.1.4'

_space_group_crystal_system       monoclinic
_space_group_IT_number            14
_space_group_name_H-M_alt         'P 21/n'
_space_group_name_Hall            '-P 2yn'

_shelx_space_group_comment
;
The symmetry employed for this shelxl refinement is uniquely defined
by the following loop, which should always be used as a source of
symmetry information in preference to the above space-group names.
They are only intended as comments.
;

loop_
 _space_group_symop_operation_xyz
 'x, y, z'
 '-x+1/2, y+1/2, -z+1/2'
 '-x, -y, -z'
 'x-1/2, -y-1/2, z-1/2'

_cell_length_a                    3.9233(9)
_cell_length_b                    13.554(3)
_cell_length_c                    18.672(4)
_cell_angle_alpha                 90
_cell_angle_beta                  90.002(3)
```

```
_cell_angle_gamma                  90
_cell_volume                       992.9(4)
_cell_formula_units_Z              4
_cell_measurement_temperature      173(2)
_cell_measurement_reflns_used      2953
_cell_measurement_theta_min        2.18
_cell_measurement_theta_max        27.39

_exptl_crystal_description         'Needle'
_exptl_crystal_colour              'colourless'
_exptl_crystal_density_meas        ?
_exptl_crystal_density_method      ?
_exptl_crystal_density_diffrn      2.134
_exptl_crystal_F_000               608
_exptl_transmission_factor_min     0.4176
_exptl_transmission_factor_max     0.7456
_exptl_crystal_size_max            0.500
_exptl_crystal_size_mid            0.120
_exptl_crystal_size_min            0.030
_exptl_absorpt_coefficient_mu      8.134
_shelx_estimated_absorpt_T_min     0.106
_shelx_estimated_absorpt_T_max     0.792
_exptl_absorpt_correction_type     multi-scan
_exptl_absorpt_correction_T_min    0.4176
_exptl_absorpt_correction_T_max    0.7456
_exptl_absorpt_process_details     'SADABS-2012/1 (Sheldrick, 2012)'
_exptl_absorpt_special_details     ?
_exptl_special_details             'K. Tritch / Prof. W. Noland'
_diffrn_ambient_temperature        173(2)
_diffrn_radiation_wavelength       0.71073
_diffrn_radiation_type             MoK\a
_diffrn_source                     'sealed tube'
_diffrn_measurement_device_type    'Bruker APEX-II CCD'
_diffrn_measurement_method         '\f and \w scans'
_diffrn_detector_area_resol_mean   ?
_diffrn_reflns_number              11400
_diffrn_reflns_av_unetI/netI       0.0420
_diffrn_reflns_av_R_equivalents    0.0526
_diffrn_reflns_limit_h_min         -5
_diffrn_reflns_limit_h_max         5
_diffrn_reflns_limit_k_min         -17
_diffrn_reflns_limit_k_max         17
_diffrn_reflns_limit_l_min         -24
_diffrn_reflns_limit_l_max         24
_diffrn_reflns_theta_min           1.090
_diffrn_reflns_theta_max           27.531
_diffrn_reflns_theta_full          25.242
_diffrn_measured_fraction_theta_max   0.998
_diffrn_measured_fraction_theta_full  1.000
_diffrn_reflns_Laue_measured_fraction_max    0.998
_diffrn_reflns_Laue_measured_fraction_full   1.000
_diffrn_reflns_point_group_measured_fraction_max   0.998
_diffrn_reflns_point_group_measured_fraction_full  1.000
_reflns_number_total               2277
_reflns_number_gt                  2132
_reflns_threshold_expression       'I > 2\s(I)'
```

```
_reflns_Friedel_coverage          0.000
_reflns_Friedel_fraction_max      .
_reflns_Friedel_fraction_full     .

_reflns_special_details
;
 Reflections were merged by SHELXL according to the crystal
 class for the calculation of statistics and refinement.

 _reflns_Friedel_fraction is defined as the number of unique
 Friedel pairs measured divided by the number that would be
 possible theoretically, ignoring centric projections and
 systematic absences.
;

_computing_data_collection      'Bruker APEX2'
_computing_cell_refinement      'Bruker SAINT'
_computing_data_reduction       'Bruker SAINT'
_computing_structure_solution   'SHELXT-2014 (Sheldrick, 2014)'
_computing_structure_refinement 'SHELXL-2014/6 (Sheldrick, 2014)'
_computing_molecular_graphics   'Bruker SHELXTL'
_computing_publication_material 'Bruker SHELXTL'
_refine_special_details
;
 Refined as a 2-component pseudo-merohedral twin in an ~0.67:0.33 ratio.
;
_refine_ls_structure_factor_coef  Fsqd
_refine_ls_matrix_type            full
_refine_ls_weighting_scheme       calc
_refine_ls_weighting_details
'w=1/[\s^2^(Fo^2^)+(0.0385P)^2^] where P=(Fo^2^+2Fc^2^)/3'
_atom_sites_solution_primary      ?
_atom_sites_solution_secondary    ?
_atom_sites_solution_hydrogens    geom
_refine_ls_hydrogen_treatment     constr
_refine_ls_extinction_method      none
_refine_ls_extinction_coef        .
_refine_ls_number_reflns          2277
_refine_ls_number_parameters      129
_refine_ls_number_restraints      0
_refine_ls_R_factor_all           0.0322
_refine_ls_R_factor_gt            0.0287
_refine_ls_wR_factor_ref          0.0689
_refine_ls_wR_factor_gt           0.0673
_refine_ls_goodness_of_fit_ref    1.025
_refine_ls_restrained_S_all       1.025
_refine_ls_shift/su_max           0.001
_refine_ls_shift/su_mean          0.000

loop_
 _atom_site_label
 _atom_site_type_symbol
 _atom_site_fract_x
 _atom_site_fract_y
 _atom_site_fract_z
 _atom_site_U_iso_or_equiv
```

```
 _atom_site_adp_type
 _atom_site_occupancy
 _atom_site_site_symmetry_order
 _atom_site_calc_flag
 _atom_site_refinement_flags_posn
 _atom_site_refinement_flags_adp
 _atom_site_refinement_flags_occupancy
 _atom_site_disorder_assembly
 _atom_site_disorder_group
C101 C 0.5312(10) 0.5930(3) 0.6880(2) 0.0187(7) Uani 1 1 d . . . . .
C102 C 0.6653(9) 0.5605(2) 0.6228(2) 0.0193(7) Uani 1 1 d . . . . .
Br102 Br 0.85319(11) 0.43306(2) 0.61597(2) 0.02497(11) Uani 1 1 d . . . . .
C103 C 0.6606(10) 0.6211(2) 0.5634(2) 0.0216(8) Uani 1 1 d . . . . .
H103 H 0.7504 0.5983 0.5192 0.026 Uiso 1 1 calc R U . . .
C104 C 0.5246(10) 0.7153(2) 0.56835(19) 0.0188(8) Uani 1 1 d . . . . .
C105 C 0.3900(9) 0.7501(2) 0.63284(19) 0.0185(8) Uani 1 1 d . . . . .
H105 H 0.2971 0.8147 0.6360 0.022 Uiso 1 1 calc R U . . .
C106 C 0.3944(9) 0.6887(3) 0.69219(18) 0.0181(7) Uani 1 1 d . . . . .
Br106 Br 0.21859(11) 0.73312(2) 0.78028(2) 0.02528(11) Uani 1 1 d . . . . .
N107 N 0.5307(9) 0.5321(2) 0.74742(17) 0.0240(7) Uani 1 1 d . . . . .
C107 C 0.5282(15) 0.4800(3) 0.7968(2) 0.0402(11) Uani 1 1 d . . . . .
C108 C 0.5255(11) 0.7760(2) 0.5011(2) 0.0210(8) Uani 1 1 d . . . . .
O101 O 0.6712(9) 0.75012(19) 0.44732(15) 0.0321(7) Uani 1 1 d . . . . .
O102 O 0.3467(8) 0.85902(17) 0.50681(14) 0.0270(6) Uani 1 1 d . . . . .
C109 C 0.3135(13) 0.9150(3) 0.4408(2) 0.0306(9) Uani 1 1 d . . . . .
H109A H 0.1794 0.9747 0.4498 0.046 Uiso 1 1 calc R U . . .
H109B H 0.1984 0.8745 0.4046 0.046 Uiso 1 1 calc R U . . .
H109C H 0.5404 0.9335 0.4234 0.046 Uiso 1 1 calc R U . . .

loop_
 _atom_site_aniso_label
 _atom_site_aniso_U_11
 _atom_site_aniso_U_22
 _atom_site_aniso_U_33
 _atom_site_aniso_U_23
 _atom_site_aniso_U_13
 _atom_site_aniso_U_12
C101 0.0214(19) 0.0192(16) 0.0153(18) -0.0001(14) -0.0002(15) -0.0050(15)
C102 0.0169(19) 0.0166(15) 0.0246(19) -0.0022(13) -0.0002(18) -0.0021(13)
Br102 0.0280(2) 0.01584(15) 0.0310(2) -0.00255(14) 0.0011(2) 0.00238(13)
C103 0.021(2) 0.0209(16) 0.0231(19) -0.0034(14) 0.0031(16) -0.0018(15)
C104 0.023(2) 0.0176(16) 0.0160(18) -0.0007(14) 0.0008(15) -0.0025(14)
C105 0.020(2) 0.0185(15) 0.0175(19) -0.0022(13) -0.0019(15) -0.0019(13)
C106 0.0196(19) 0.0210(16) 0.0138(16) -0.0060(13) 0.0001(14) -0.0049(14)
Br106 0.0296(2) 0.02670(18) 0.01950(19) -0.00694(13) 0.00484(19) -0.00182(15)
N107 0.0310(19) 0.0198(15) 0.0213(17) -0.0014(13) 0.0011(14) -0.0029(13)
C107 0.065(3) 0.028(2) 0.027(2) -0.0025(19) -0.003(2) -0.008(2)
C108 0.027(2) 0.0172(17) 0.0187(19) -0.0021(14) -0.0015(16) -0.0031(14)
O101 0.048(2) 0.0235(12) 0.0245(15) 0.0019(10) 0.0087(16) 0.0022(14)
O102 0.0391(17) 0.0219(12) 0.0201(13) 0.0016(10) 0.0001(13) 0.0055(12)
C109 0.039(3) 0.0269(18) 0.026(2) 0.0071(15) -0.003(2) 0.0042(19)

_geom_special_details
;
 All esds (except the esd in the dihedral angle between two l.s. planes)
 are estimated using the full covariance matrix.  The cell esds are taken
```

```
 into account individually in the estimation of esds in distances, angles
 and torsion angles; correlations between esds in cell parameters are only
 used when they are defined by crystal symmetry.  An approximate (isotropic)
 treatment of cell esds is used for estimating esds involving l.s. planes.
;

loop_
 _geom_bond_atom_site_label_1
 _geom_bond_atom_site_label_2
 _geom_bond_distance
 _geom_bond_site_symmetry_2
 _geom_bond_publ_flag
C101 N107 1.383(5) . ?
C101 C102 1.396(5) . ?
C101 C106 1.407(5) . ?
C102 C103 1.379(5) . ?
C102 Br102 1.883(3) . ?
C103 C104 1.387(5) . ?
C103 H103 0.9500 . ?
C104 C105 1.397(5) . ?
C104 C108 1.501(5) . ?
C105 C106 1.386(5) . ?
C105 H105 0.9500 . ?
C106 Br106 1.882(3) . ?
N107 C107 1.162(5) . ?
C108 O101 1.207(5) . ?
C108 O102 1.331(4) . ?
O102 C109 1.454(4) . ?
C109 H109A 0.9800 . ?
C109 H109B 0.9800 . ?
C109 H109C 0.9800 . ?

loop_
 _geom_angle_atom_site_label_1
 _geom_angle_atom_site_label_2
 _geom_angle_atom_site_label_3
 _geom_angle
 _geom_angle_site_symmetry_1
 _geom_angle_site_symmetry_3
 _geom_angle_publ_flag
N107 C101 C102 120.8(3) . . ?
N107 C101 C106 120.3(3) . . ?
C102 C101 C106 118.9(3) . . ?
C103 C102 C101 120.5(3) . . ?
C103 C102 Br102 119.8(3) . . ?
C101 C102 Br102 119.7(3) . . ?
C102 C103 C104 120.0(3) . . ?
C102 C103 H103 120.0 . . ?
C104 C103 H103 120.0 . . ?
C103 C104 C105 120.9(3) . . ?
C103 C104 C108 116.6(3) . . ?
C105 C104 C108 122.5(3) . . ?
C106 C105 C104 118.8(3) . . ?
C106 C105 H105 120.6 . . ?
C104 C105 H105 120.6 . . ?
C105 C106 C101 120.9(3) . . ?
```

```
C105 C106 Br106 120.2(3) . . ?
C101 C106 Br106 118.9(3) . . ?
C107 N107 C101 179.1(4) . . ?
O101 C108 O102 124.2(4) . . ?
O101 C108 C104 122.6(3) . . ?
O102 C108 C104 113.2(3) . . ?
C108 O102 C109 114.8(3) . . ?
O102 C109 H109A 109.5 . . ?
O102 C109 H109B 109.5 . . ?
H109A C109 H109B 109.5 . . ?
O102 C109 H109C 109.5 . . ?
H109A C109 H109C 109.5 . . ?
H109B C109 H109C 109.5 . . ?

loop_
 _geom_torsion_atom_site_label_1
 _geom_torsion_atom_site_label_2
 _geom_torsion_atom_site_label_3
 _geom_torsion_atom_site_label_4
 _geom_torsion
 _geom_torsion_site_symmetry_1
 _geom_torsion_site_symmetry_2
 _geom_torsion_site_symmetry_3
 _geom_torsion_site_symmetry_4
 _geom_torsion_publ_flag
N107 C101 C102 C103 179.1(3) . . . . ?
C106 C101 C012 C103 -0.6(6) . . . . ?
N107 C101 C102 Br102 -0.8(5) . . . . ?
C106 C101 C102 Br102 179.5(3) . . . . ?
C101 C102 C103 C104 0.6(6) . . . . ?
Br102 C102 C103 C104 -179.5(3) . . . . ?
C102 C103 C104 C105 -0.3(6) . . . . ?
C102 C103 C104 C108 -179.3(4) . . . . ?
C103 C104 C105 C106 0.0(6) . . . . ?
C108 C104 C105 C016 179.0(3) . . . . ?
C104 C105 C106 C101 -0.1(6) . . . . ?
C104 C105 C106 Br106 179.5(3) . . . . ?
N107 C101 C106 C105 -179.3(4) . . . . ?
C102 C101 C106 C105 0.4(5) . . . . ?
N107 C101 C106 Br106 1.1(5) . . . . ?
C102 C101 C106 Br106 -179.2(3) . . . . ?
C103 C104 C108 O101 -8.6(6) . . . . ?
C105 C104 C108 O101 172.4(4) . . . . ?
C103 C014 C108 O102 170.5(3) . . . . ?
C105 C104 C108 O102 -8.5(6) . . . . ?
O101 C108 O102 C109 4.8(6) . . . . ?
C104 C108 O102 C109 -174.2(4) . . . . ?

_refine_diff_density_max    0.849
_refine_diff_density_min   -0.653
_refine_diff_density_rms    0.109

_shelxl_version_number 2014/6

_shelx_res_file
;
```

```
TITL 16114z in P2(1)/n
CELL 0.71073   3.9233  13.5536  18.6723  90.000  90.002  90.000
ZERR    4.00   0.0009   0.0031   0.0042   0.000   0.003   0.000
LATT  1
SYMM -x+1/2, y+1/2, -z+1/2
SFAC C  H  N O BR
UNIT 36 20 4 8 8
TEMP -100
SIZE 0.030 0.120 0.500

L.S. 8
ACTA
LIST 4
CONF
BOND $H
FMAP 2
PLAN 5
TWIN -1 0 0 0 -1 0 0 0 1
WGHT    0.038500
BASF   0.32770
FVAR       0.13345
C101    1    0.531236    0.592957    0.687973    11.00000    0.02145    0.01921
=
         0.01532   -0.00012   -0.00021   -0.00497
C102    1    0.665285    0.560543    0.622819    11.00000    0.01687    0.01657
=
         0.02455   -0.00218   -0.00016   -0.00212
BR102   5    0.853191    0.433062    0.615970    11.00000    0.02804    0.01584
=
         0.03104   -0.00255    0.00115    0.00238
C103    1    0.660552    0.621089    0.563448    11.00000    0.02080    0.02087
=
         0.02313   -0.00341    0.00310   -0.00184
AFIX  43
H103   2    0.750409    0.598255    0.519207    11.00000   -1.20000
AFIX   0
C104    1    0.524562    0.715327    0.568350    11.00000    0.02292    0.01757
=
         0.01600   -0.00072    0.00078   -0.00253
C105    1    0.390007    0.750088    0.632838    11.00000    0.01955    0.01845
=
         0.01747   -0.00220   -0.00193   -0.00191
AFIX  43
H105   2    0.297102    0.814673    0.635954    11.00000   -1.20000
AFIX   0
C106    1    0.394368    0.688744    0.692189    11.00000    0.01955    0.02099
=
         0.01381   -0.00597    0.00013   -0.00486
BR106   5    0.218588    0.733124    0.780279    11.00000    0.02964    0.02670
=
         0.01950   -0.00694    0.00484   -0.00182
N107    3    0.530722    0.532089    0.747416    11.00000    0.03102    0.01975
=
         0.02129   -0.00136    0.00110   -0.00289
C107    1    0.528178    0.480029    0.796826    11.00000    0.06523    0.02816
=
```

```
         0.02717   -0.00248   -0.00350   -0.00782
C108    1    0.525467    0.775952    0.501064    11.00000    0.02721    0.01721
=
         0.01868   -0.00214   -0.00149   -0.00306
O101    4    0.671226    0.750120    0.447319    11.00000    0.04827    0.02346
=
         0.02450    0.00185    0.00867    0.00222
O102    4    0.346657    0.859022    0.506812    11.00000    0.03911    0.02187
=
         0.02010    0.00158    0.00008    0.00551
C109    1    0.313514    0.914989    0.440754    11.00000    0.03875    0.02694
=
         0.02601    0.00706   -0.00262    0.00423
AFIX 137
H109A   2    0.179401    0.974713    0.449764    11.00000   -1.50000
H109B   2    0.198430    0.874506    0.404610    11.00000   -1.50000
H109C   2    0.540369    0.933475    0.423362    11.00000   -1.50000

AFIX   0
HKLF 4 1 1 0 0 0 1 0 0 0 1

REM  16114z in P2(1)/n
REM R1 =  0.0287 for    2132 Fo > 4sig(Fo)  and  0.0322 for all    2277 data
REM    129 parameters refined using      0 restraints

END

WGHT      0.0385      0.0000

REM Highest difference peak  0.849,  deepest hole -0.653,  1-sigma level  0.109
Q1    1   0.8447  0.4358  0.6618  11.00000  0.05    0.85
Q2    1   0.1976  0.7335  0.8250  11.00000  0.05    0.75
Q3    1  -0.0152  0.7311  0.7805  11.00000  0.05    0.72
Q4    1   0.8480  0.4312  0.5605  11.00000  0.05    0.71
Q5    1   1.0874  0.4267  0.6202  11.00000  0.05    0.70
;
_shelx_res_checksum    7953

# Some atom labels have been edited after refinement
# to be consistent with other compounds. - KJT
```

1,3,5-Triiodo-2-isocyanobenzene (209da), *Z*=4 CC polytype.

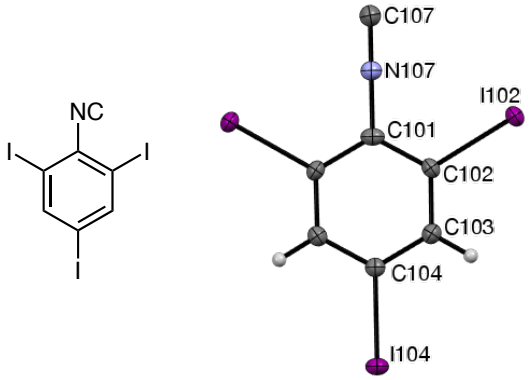

CIF content:

```
data_209da

_audit_creation_method          'SHELXTL'
_chemical_name_systematic
;
 1,3,5-Triiodo-2-isocyanobenzene
;
_chemical_name_common             'triiodo isocyanide'
_chemical_melting_point           ?
_chemical_formula_moiety          'C7 H2 I3 N'
_chemical_formula_sum
 'C7 H2 I3 N'
_chemical_formula_weight          480.80

loop_
 _atom_type_symbol
 _atom_type_description
 _atom_type_scat_dispersion_real
 _atom_type_scat_dispersion_imag
 _atom_type_scat_source
 'C'  'C'   0.0033   0.0016
 'International Tables Vol C Tables 4.2.6.8 and 6.1.1.4'
 'H'  'H'   0.0000   0.0000
 'International Tables Vol C Tables 4.2.6.8 and 6.1.1.4'
 'N'  'N'   0.0061   0.0033
 'International Tables Vol C Tables 4.2.6.8 and 6.1.1.4'
 'I'  'I'  -0.4742   1.8119
 'International Tables Vol C Tables 4.2.6.8 and 6.1.1.4'

_symmetry_cell_setting            orthorhombic
_symmetry_space_group_name_H-M    'I m m a'
_symmetry_space_group_name_Hall    '-I 2b 2'

loop_
 _symmetry_equiv_pos_as_xyz
 'x, y, z'
 '-x, -y+1/2, z'
 '-x, y+1/2, -z'
```

```
 'x, -y, -z'
 'x+1/2, y+1/2, z+1/2'
 '-x+1/2, -y+1, z+1/2'
 '-x+1/2, y+1, -z+1/2'
 'x+1/2, -y+1/2, -z+1/2'
 '-x, -y, -z'
 'x, y-1/2, -z'
 'x, -y-1/2, z'
 '-x, y, z'
 '-x+1/2, -y+1/2, -z+1/2'
 'x+1/2, y, -z+1/2'
 'x+1/2, -y, z+1/2'
 '-x+1/2, y+1/2, z+1/2'

_cell_length_a                    7.097(2)
_cell_length_b                    10.508(3)
_cell_length_c                    13.182(4)
_cell_angle_alpha                 90.00
_cell_angle_beta                  90.00
_cell_angle_gamma                 90.00
_cell_volume                      983.1(5)
_cell_formula_units_Z             4
_cell_measurement_temperature     173(2)
_cell_measurement_reflns_used     3022
_cell_measurement_theta_min       2.5
_cell_measurement_theta_max       27.3

_exptl_crystal_description        needle
_exptl_crystal_colour             colorless
_exptl_crystal_size_max           0.35
_exptl_crystal_size_mid           0.04
_exptl_crystal_size_min           0.02
_exptl_crystal_density_meas       'not measured'
_exptl_crystal_density_diffrn     3.249
_exptl_crystal_density_method     'not measured'
_exptl_crystal_F_000              840
_exptl_absorpt_coefficient_mu     9.477
_exptl_absorpt_correction_type    'multi-scan'
_exptl_absorpt_correction_T_min   0.66
_exptl_absorpt_correction_T_max   0.83
_exptl_absorpt_process_details
;
SADABS; Sheldrick, 1996; Blessing, 1995
;


_diffrn_ambient_temperature       173(2)
_diffrn_radiation_wavelength      0.71073
_diffrn_radiation_type            MoK\a
_diffrn_radiation_source          'fine-focus sealed tube'
_diffrn_radiation_monochromator   graphite
_diffrn_measurement_device_type
;
Siemens SMART area detector diffractometer
;
_diffrn_measurement_method        '\w scans'
```

```
_diffrn_detector_area_resol_mean  ?
_diffrn_standards_number          0
_diffrn_standards_interval_count  ?
_diffrn_standards_interval_time   ?
_diffrn_standards_decay_%         ?
_diffrn_reflns_number             5514
_diffrn_reflns_av_R_equivalents   0.047
_diffrn_reflns_av_sigmaI/netI     0.026
_diffrn_reflns_limit_h_min        -9
_diffrn_reflns_limit_h_max        9
_diffrn_reflns_limit_k_min        -13
_diffrn_reflns_limit_k_max        13
_diffrn_reflns_limit_l_min        -16
_diffrn_reflns_limit_l_max        17
_diffrn_reflns_theta_min          2.48
_diffrn_reflns_theta_max          27.50
_reflns_number_total              642
_reflns_number_gt                 603
_reflns_threshold_expression      '>2\s(I) '

_computing_data_collection        'SMART (Siemens, 1995)'
_computing_cell_refinement        'SAINT (Siemens, 1995)'
_computing_data_reduction         'SAINT'
_computing_structure_solution     'SHELXTL (Sheldrick, 1997)'
_computing_structure_refinement   'SHELXTL'
_computing_molecular_graphics     'SHELXTL'
_computing_publication_material   'SHELXTL'

_refine_ls_structure_factor_coef  Fsqd
_refine_ls_matrix_type            full
_refine_ls_weighting_scheme       calc
_refine_ls_weighting_details
 'calc w=1/[\s^2^(Fo^2^)+(0.022P)^2^+0.81P] where P=(Fo^2^+2Fc^2^)/3'
_atom_sites_solution_primary      direct
_atom_sites_solution_secondary    difmap
_atom_sites_solution_hydrogens    geom
_refine_ls_hydrogen_treatment     riding
_refine_ls_extinction_method      SHELXL
_refine_ls_extinction_coef        0.0056(2)
_refine_ls_extinction_expression
 'Fc^*^=kFc[1+0.001xFc^2^\l^3^/sin(2\q)]^-1/4^'
_refine_ls_number_reflns          642
_refine_ls_number_parameters      40
_refine_ls_number_restraints      0
_refine_ls_R_factor_all           0.021
_refine_ls_R_factor_gt            0.019
_refine_ls_wR_factor_ref          0.044
_refine_ls_wR_factor_gt           0.043
_refine_ls_goodness_of_fit_ref    1.08
_refine_ls_restrained_S_all       1.08
_refine_ls_shift/su_max           0.001
_refine_ls_shift/su_mean          0.000

loop_
 _atom_site_label
 _atom_site_type_symbol
```

```
 _atom_site_fract_x
 _atom_site_fract_y
 _atom_site_fract_z
 _atom_site_U_iso_or_equiv
 _atom_site_adp_type
 _atom_site_occupancy
 _atom_site_symmetry_multiplicity
 _atom_site_calc_flag
 _atom_site_refinement_flags
 _atom_site_disorder_assembly
 _atom_site_disorder_group
I104 I 0.0000 0.2500 0.56191(3) 0.02207(14) Uani 1 4 d S . .
N107 N 0.0000 0.2500 0.0878(4) 0.0183(10) Uani 1 4 d S . .
C101 C 0.0000 0.2500 0.1937(4) 0.0184(11) Uani 1 4 d S . .
C104 C 0.0000 0.2500 0.4030(4) 0.0171(11) Uani 1 4 d S . .
C107 C 0.0000 0.2500 -0.0003(5) 0.0229(12) Uani 1 4 d S . .
I102 I 0.0000 0.53717(2) 0.16543(2) 0.02110(13) Uani 1 2 d S . .
C102 C 0.0000 0.3659(4) 0.2458(3) 0.0170(8) Uani 1 2 d S . .
C103 C 0.0000 0.3650(4) 0.3510(3) 0.0185(8) Uani 1 2 d S . .
H103 H 0.0000 0.4429 0.3876 0.022 Uiso 1 2 calc SR . .

loop_
 _atom_site_aniso_label
 _atom_site_aniso_U_11
 _atom_site_aniso_U_22
 _atom_site_aniso_U_33
 _atom_site_aniso_U_23
 _atom_site_aniso_U_13
 _atom_site_aniso_U_12
I104 0.0288(2) 0.0245(2) 0.0129(2) 0.000 0.000 0.000
N107 0.019(2) 0.020(3) 0.016(2) 0.000 0.000 0.000
C101 0.016(2) 0.026(3) 0.013(3) 0.000 0.000 0.000
C104 0.017(2) 0.018(3) 0.016(3) 0.000 0.000 0.000
C107 0.029(3) 0.020(3) 0.020(3) 0.000 0.000 0.000
I102 0.02999(19) 0.01516(18) 0.01813(19) 0.00348(9) 0.000 0.000
C102 0.0194(17) 0.0147(18) 0.017(2) 0.0031(14) 0.000 0.000
C103 0.0211(19) 0.0166(19) 0.018(2) -0.0016(15) 0.000 0.000


loop_
 _geom_bond_atom_site_label_1
 _geom_bond_atom_site_label_2
 _geom_bond_distance
 _geom_bond_site_symmetry_2
 _geom_bond_publ_flag
I104 C104 2.095(6) . ?
N107 C107 1.162(8) . ?
N107 C101 1.396(7) . ?
C101 C102 1.399(5) . ?
C101 C102 1.399(5) 2 ?
C104 C103 1.389(5) 2 ?
C104 C103 1.389(5) . ?
I102 C102 2.088(4) . ?
C102 C103 1.387(6) . ?
C103 H103 0.9500 . ?
```

```
loop_
 _geom_angle_atom_site_label_1
 _geom_angle_atom_site_label_2
 _geom_angle_atom_site_label_3
 _geom_angle
 _geom_angle_site_symmetry_1
 _geom_angle_site_symmetry_3
 _geom_angle_publ_flag
C107 N107 C101 180.000(1) . . ?
N107 C101 C102 119.4(3) . . ?
N107 C101 C102 119.4(3) . 2 ?
C102 C101 C012 121.2(5) . 2 ?
C103 C104 C103 120.9(5) 2 . ?
C103 C104 I104 119.5(3) 2 . ?
C103 C104 I104 119.5(3) . . ?
C103 C102 C101 119.0(4) . . ?
C103 C102 I102 120.9(3) . . ?
C101 C102 I102 120.1(3) . . ?
C102 C103 C104 120.0(4) . . ?
C102 C103 H103 120.0 . . ?
C104 C103 H103 120.0 . . ?

_diffrn_measured_fraction_theta_max    0.997
_diffrn_reflns_theta_full              27.50
_diffrn_measured_fraction_theta_full   0.997
_refine_diff_density_max    0.96
_refine_diff_density_min   -0.73
_refine_diff_density_rms    0.194

# Data collection, refinement, and
# torsion data were not provided by Dr. Britton.
# Some atom labels have been edited after refinement
# to be consistent with other compounds. - KJT
```

1,3-Diiodo-2-isocyano-5-methylbenzene (209db).

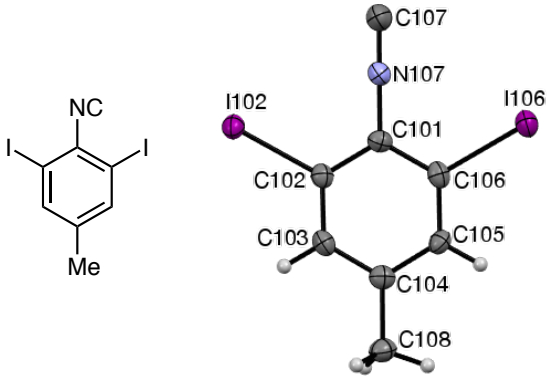

Data collection (by the XCL): A crystal (approx. 0.500 × 0.100 × 0.050 mm^3) was placed onto the tip of an 0.1 mm diameter glass capillary and mounted on a Bruker APEX-II CCD diffractometer for a data collection at 173 K. A preliminary set of cell constants was calculated from reflections harvested from three sets of 20 frames. These initial sets of frames were oriented such that orthogonal wedges of reciprocal space were surveyed. This produced initial orientation matrices determined from 185 reflections. The data collection was carried out using MoKα radiation (graphite monochromator) with a frame time of 5 sec and a detector distance of 60 mm. A randomly oriented region of reciprocal space was surveyed to the extent of one sphere and to a resolution of 0.77 Å. Four major sections of frames were collected with 0.30° steps in ω at four different ϕ settings and a detector position of –28° in 2θ. The intensity data were corrected for absorption and decay. Final cell constants were calculated from 2,977 strong reflections from the actual data collection after integration.

Structure solution and refinement (by the XCL): The structure was solved by Patterson methods. The space group $P2_1/n$ was determined based on systematic absences and intensity statistics. A direct-methods solution was calculated that provided most non-hydrogen atoms from the E-map. Full-matrix least squares / difference Fourier cycles were performed that located the remaining non-hydrogen atoms. All non-hydrogen atoms were refined with anisotropic displacement parameters. All hydrogen atoms were placed in ideal positions and refined as riding atoms with relative isotropic displacement parameters. Some secondary extinction was refined. The final full matrix least squares refinement converged to $R1 = 0.0224$ and $wR2 = 0.0465$ (F^2, all data).

CIF content:

```
data_209db

_audit_creation_method            SHELXL-2014/6
_chemical_name_systematic
;
1,3-Diiodo-2-isocyano-5-methylbenzene
;
_chemical_name_common             ‘diiodo methyl isocyanide'
_chemical_melting_point           ?
_chemical_formula_moiety          'C8 H5 I2 N'
_chemical_formula_sum             'C8 H5 I2 N'
_chemical_formula_weight          368.93

loop_
 _atom_type_symbol
 _atom_type_description
 _atom_type_scat_dispersion_real
 _atom_type_scat_dispersion_imag
 _atom_type_scat_source
 'C'  'C'   0.0033   0.0016
 'International Tables Vol C Tables 4.2.6.8 and 6.1.1.4'
 'H'  'H'   0.0000   0.0000
 'International Tables Vol C Tables 4.2.6.8 and 6.1.1.4'
 'N'  'N'   0.0061   0.0033
 'International Tables Vol C Tables 4.2.6.8 and 6.1.1.4'
 'I'  'I'  -0.4742   1.8119
 'International Tables Vol C Tables 4.2.6.8 and 6.1.1.4'

_space_group_crystal_system       monoclinic
_space_group_IT_number            14
_space_group_name_H-M_alt         'P 21/n'
_space_group_name_Hall            '-P 2yn'

_shelx_space_group_comment
;
The symmetry employed for this shelxl refinement is uniquely defined
by the following loop, which should always be used as a source of
symmetry information in preference to the above space-group names.
They are only intended as comments.
;

loop_
 _space_group_symop_operation_xyz
 'x, y, z'
 '-x+1/2, y+1/2, -z+1/2'
 '-x, -y, -z'
 'x-1/2, -y-1/2, z-1/2'

_cell_length_a                    4.4094(15)
_cell_length_b                    14.707(5)
_cell_length_c                    14.658(5)
_cell_angle_alpha                 90
_cell_angle_beta                  93.812(4)
_cell_angle_gamma                 90
_cell_volume                      948.5(6)
```

```
_cell_formula_units_Z             4
_cell_measurement_temperature     173(2)
_cell_measurement_reflns_used     2977
_cell_measurement_theta_min       2.77
_cell_measurement_theta_max       27.21

_exptl_crystal_description       'Needle'
_exptl_crystal_colour            'colourless'
_exptl_crystal_density_meas       ?
_exptl_crystal_density_method     ?
_exptl_crystal_density_diffrn     2.584
_exptl_crystal_F_000              664
_exptl_transmission_factor_min    0.1291
_exptl_transmission_factor_max    0.2616
_exptl_crystal_size_max           0.500
_exptl_crystal_size_mid           0.100
_exptl_crystal_size_min           0.050
_exptl_absorpt_coefficient_mu     6.568
_shelx_estimated_absorpt_T_min    0.138
_shelx_estimated_absorpt_T_max    0.735
_exptl_absorpt_correction_type    'multi-scan'
_exptl_absorpt_correction_T_min   0.1291
_exptl_absorpt_correction_T_max   0.2616
_exptl_absorpt_process_details    'SADABS-2012/1 (Sheldrick, 2014)'
_exptl_absorpt_special_details    ?
_exptl_special_details            'K. Tritch / Prof. W. Noland'
_diffrn_ambient_temperature       173(2)
_diffrn_radiation_wavelength      0.71073
_diffrn_radiation_type            MoK\a
_diffrn_source                    'normal-focus sealed tube'
_diffrn_measurement_device_type   'Bruker APEX-II CCD'
_diffrn_measurement_method        '\f and \w scans'
_diffrn_detector_area_resol_mean  ?
_diffrn_reflns_number             10946
_diffrn_reflns_av_unetI/netI      0.0313
_diffrn_reflns_av_R_equivalents   0.0421
_diffrn_reflns_limit_h_min        -5
_diffrn_reflns_limit_h_max        5
_diffrn_reflns_limit_k_min        -19
_diffrn_reflns_limit_k_max        19
_diffrn_reflns_limit_l_min        -18
_diffrn_reflns_limit_l_max        18
_diffrn_reflns_theta_min          1.964
_diffrn_reflns_theta_max          27.579
_diffrn_reflns_theta_full         25.242
_diffrn_measured_fraction_theta_max   0.998
_diffrn_measured_fraction_theta_full  1.000
_diffrn_reflns_Laue_measured_fraction_max    0.998
_diffrn_reflns_Laue_measured_fraction_full   1.000
_diffrn_reflns_point_group_measured_fraction_max   0.998
_diffrn_reflns_point_group_measured_fraction_full  1.000
_reflns_number_total              2192
_reflns_number_gt                 1844
_reflns_threshold_expression      'I > 2\s(I)'
_reflns_Friedel_coverage          0.000
_reflns_Friedel_fraction_max      .
```

```
_reflns_Friedel_fraction_full     .

_reflns_special_details
;
 Reflections were merged by SHELXL according to the crystal
 class for the calculation of statistics and refinement.

 _reflns_Friedel_fraction is defined as the number of unique
 Friedel pairs measured divided by the number that would be
 possible theoretically, ignoring centric projections and
 systematic absences.
;

_computing_data_collection       'Bruker APEX2'
_computing_cell_refinement       'Bruker SAINT'
_computing_data_reduction        'Bruker SAINT'
_computing_structure_solution    'SHELXS-97 (Sheldrick, 2008)'
_computing_structure_refinement  'SHELXL-2014/6 (Sheldrick, 2014)'
_computing_molecular_graphics    'Bruker SHELXTL'
_computing_publication_material  'Bruker SHELXTL'
_refine_special_details           ?
_refine_ls_structure_factor_coef  Fsqd
_refine_ls_matrix_type            full
_refine_ls_weighting_scheme       calc
_refine_ls_weighting_details
'w=1/[\s^2^(Fo^2^)+(0.0132P)^2^+0.5629P] where P=(Fo^2^+2Fc^2^)/3'
_atom_sites_solution_primary      ?
_atom_sites_solution_secondary    ?
_atom_sites_solution_hydrogens    geom
_refine_ls_hydrogen_treatment     constr
_refine_ls_extinction_method      SHELXL
_refine_ls_extinction_coef        0.0069(2)
_refine_ls_extinction_expression
 'Fc^*^=kFc[1+0.001xFc^2^\l^3^/sin(2\q)]^-1/4^'
_refine_ls_number_reflns          2192
_refine_ls_number_parameters      102
_refine_ls_number_restraints      0
_refine_ls_R_factor_all           0.0294
_refine_ls_R_factor_gt            0.0224
_refine_ls_wR_factor_ref          0.0465
_refine_ls_wR_factor_gt           0.0434
_refine_ls_goodness_of_fit_ref    1.069
_refine_ls_restrained_S_all       1.069
_refine_ls_shift/su_max           0.002
_refine_ls_shift/su_mean          0.000

loop_
 _atom_site_label
 _atom_site_type_symbol
 _atom_site_fract_x
 _atom_site_fract_y
 _atom_site_fract_z
 _atom_site_U_iso_or_equiv
 _atom_site_adp_type
 _atom_site_occupancy
 _atom_site_site_symmetry_order
```

```
 _atom_site_calc_flag
 _atom_site_refinement_flags_posn
 _atom_site_refinement_flags_adp
 _atom_site_refinement_flags_occupancy
 _atom_site_disorder_assembly
 _atom_site_disorder_group
C101 C 0.3859(7) 0.4975(2) 0.2296(2) 0.0230(8) Uani 1 1 d . . . . .
C102 C 0.4635(8) 0.5790(2) 0.1891(2) 0.0232(8) Uani 1 1 d . . . . .
I102 I 0.28653(6) 0.61134(2) 0.05716(2) 0.02662(9) Uani 1 1 d . . . . .
C103 C 0.6638(8) 0.6377(2) 0.2357(3) 0.0250(8) Uani 1 1 d . . . . .
H103 H 0.7179 0.6929 0.2073 0.030 Uiso 1 1 calc R U . . .
C104 C 0.7882(8) 0.6178(2) 0.3234(3) 0.0244(8) Uani 1 1 d . . . . .
C105 C 0.7093(8) 0.5358(2) 0.3632(2) 0.0241(8) Uani 1 1 d . . . . .
H105 H 0.7927 0.5206 0.4227 0.029 Uiso 1 1 calc R U . . .
C106 C 0.5101(8) 0.4764(2) 0.3167(2) 0.0242(8) Uani 1 1 d . . . . .
I106 I 0.39503(6) 0.35409(2) 0.37966(2) 0.03000(9) Uani 1 1 d . . . . .
N107 N 0.1846(7) 0.4375(2) 0.1836(2) 0.0257(7) Uani 1 1 d . . . . .
C107 C 0.0202(10) 0.3871(3) 0.1456(3) 0.0377(10) Uani 1 1 d . . . . .
C108 C 1.0001(8) 0.6834(3) 0.3736(3) 0.0307(9) Uani 1 1 d . . . . .
H108A H 1.1615 0.7009 0.3342 0.046 Uiso 1 1 calc R U . . .
H108B H 1.0902 0.6545 0.4292 0.046 Uiso 1 1 calc R U . . .
H108C H 0.8868 0.7377 0.3901 0.046 Uiso 1 1 calc R U . . .

loop_
 _atom_site_aniso_label
 _atom_site_aniso_U_11
 _atom_site_aniso_U_22
 _atom_site_aniso_U_33
 _atom_site_aniso_U_23
 _atom_site_aniso_U_13
 _atom_site_aniso_U_12
C101 0.0199(18) 0.0220(18) 0.027(2) -0.0021(15) 0.0022(15) 0.0002(14)
C102 0.0238(18) 0.0204(17) 0.0255(19) -0.0003(15) 0.0026(15) 0.0041(14)
I102 0.03372(15) 0.02294(14) 0.02294(14) 0.00065(9) -0.00015(10) 0.00248(10)
C103 0.0276(19) 0.0202(18) 0.028(2) 0.0025(15) 0.0060(16) 0.0006(15)
C104 0.0209(18) 0.0233(18) 0.029(2) -0.0039(15) 0.0025(15) 0.0035(14)
C105 0.0269(19) 0.0259(19) 0.0190(18) -0.0020(15) -0.0009(15) 0.0042(15)
C106 0.0246(18) 0.0213(18) 0.027(2) 0.0019(15) 0.0066(15) 0.0054(14)
I106 0.03460(16) 0.02573(15) 0.02977(16) 0.00619(10) 0.00290(11) -0.00013(10)
N107 0.0298(17) 0.0212(16) 0.0260(17) 0.0020(13) 0.0000(13) -0.0022(13)
C107 0.042(2) 0.031(2) 0.039(3) 0.0051(19) -0.007(2) -0.0047(19)
C108 0.031(2) 0.028(2) 0.032(2) -0.0050(17) -0.0038(17) 0.0005(16)

_geom_special_details
;
 All esds (except the esd in the dihedral angle between two l.s. planes)
 are estimated using the full covariance matrix.  The cell esds are taken
 into account individually in the estimation of esds in distances, angles
 and torsion angles; correlations between esds in cell parameters are only
 used when they are defined by crystal symmetry.  An approximate (isotropic)
 treatment of cell esds is used for estimating esds involving l.s. planes.
;

loop_
 _geom_bond_atom_site_label_1
 _geom_bond_atom_site_label_2
```

```
 _geom_bond_distance
 _geom_bond_site_symmetry_2
 _geom_bond_publ_flag
C101 C102 1.390(5) . ?
C101 C016 1.391(5) . ?
C101 N107 1.393(4) . ?
C102 C103 1.383(5) . ?
C102 I102 2.091(4) . ?
C103 C104 1.394(5) . ?
C103 H103 0.9500 . ?
C104 C105 1.395(5) . ?
C104 C108 1.501(5) . ?
C105 C106 1.386(5) . ?
C105 H105 0.9500 . ?
C106 I106 2.099(3) . ?
N107 C107 1.154(5) . ?
C108 H108A 0.9800 . ?
C108 H108B 0.9800 . ?
C108 H108C 0.9800 . ?

loop_
 _geom_angle_atom_site_label_1
 _geom_angle_atom_site_label_2
 _geom_angle_atom_site_label_3
 _geom_angle
 _geom_angle_site_symmetry_1
 _geom_angle_site_symmetry_3
 _geom_angle_publ_flag
C102 C101 C106 119.5(3) . . ?
C102 C101 N107 120.4(3) . . ?
C106 C011 N107 120.1(3) . . ?
C103 C102 C101 119.6(3) . . ?
C103 C102 I102 120.1(3) . . ?
C101 C012 I102 120.3(3) . . ?
C102 C103 C104 121.6(3) . . ?
C102 C103 H103 119.2 . . ?
C104 C103 H103 119.2 . . ?
C103 C104 C105 118.3(3) . . ?
C103 C104 C108 120.7(3) . . ?
C105 C104 C108 121.0(3) . . ?
C106 C105 C104 120.5(3) . . ?
C106 C105 H105 119.8 . . ?
C104 C105 H105 119.8 . . ?
C105 C106 C101 120.6(3) . . ?
C105 C106 I106 119.2(3) . . ?
C101 C106 I106 120.2(3) . . ?
C107 N107 C101 179.3(4) . . ?
C104 C108 H108A 109.5 . . ?
C104 C108 H108B 109.5 . . ?
H108A C108 H108B 109.5 . . ?
C104 C108 H108C 109.5 . . ?
H108A C108 H108C 109.5 . . ?
H108B C108 H108C 109.5 . . ?

loop_
 _geom_torsion_atom_site_label_1
```

```
 _geom_torsion_atom_site_label_2
 _geom_torsion_atom_site_label_3
 _geom_torsion_atom_site_label_4
 _geom_torsion
 _geom_torsion_site_symmetry_1
 _geom_torsion_site_symmetry_2
 _geom_torsion_site_symmetry_3
 _geom_torsion_site_symmetry_4
 _geom_torsion_publ_flag
C106 C101 C102 C103 0.2(5) . . . . ?
N107 C101 C102 C103 -180.0(3) . . . . ?
C106 C101 C102 I102 178.8(2) . . . . ?
N107 C101 C102 I102 -1.4(5) . . . . ?
C101 C102 C103 C104 -0.8(5) . . . . ?
I102 C102 C103 C104 -179.4(3) . . . . ?
C102 C103 C104 C105 1.0(5) . . . . ?
C102 C103 C104 C108 -178.7(3) . . . . ?
C103 C104 C105 C106 -0.6(5) . . . . ?
C108 C104 C105 C106 179.1(3) . . . . ?
C104 C105 C106 C101 0.1(5) . . . . ?
C104 C105 C106 I106 -179.5(3) . . . . ?
C102 C101 C106 C105 0.1(5) . . . . ?
N107 C101 C106 C105 -179.7(3) . . . . ?
C102 C101 C106 I106 179.7(2) . . . . ?
N107 C101 C106 I106 -0.1(4) . . . . ?

loop_
 _geom_hbond_atom_site_label_D
 _geom_hbond_atom_site_label_H
 _geom_hbond_atom_site_label_A
 _geom_hbond_distance_DH
 _geom_hbond_distance_HA
 _geom_hbond_distance_DA
 _geom_hbond_angle_DHA
 _geom_hbond_site_symmetry_A
C103 H103 I106  0.95 3.23 4.148(4) 162.6 2_655

_refine_diff_density_max    0.503
_refine_diff_density_min   -0.546
_refine_diff_density_rms    0.124

_shelxl_version_number 2014/6

_shelx_res_file
;
TITL 16058a in P2(1)/n
CELL 0.71073   4.4094  14.7073  14.6577  90.000  93.812  90.000
ZERR    4.00   0.0015   0.0051   0.0051   0.000   0.004   0.000
LATT  1
SYMM 0.5-X, 0.5+Y, 0.5-Z
SFAC C  H  N I
UNIT 32 20 4 8
TEMP -100
SIZE 0.05 0.10 0.50

L.S. 30
```

```
ACTA
LIST 4
BOND $H
CONF
FMAP 2
PLAN 6
EQIV $1 -x+3/2, y+1/2, -z+1/2
HTAB C3 I6_$1

WGHT    0.013200    0.562900
EXTI    0.006894
FVAR       0.10629
C1    1    0.385863    0.497509    0.229584    11.00000    0.01990    0.02205 =
         0.02724   -0.00206    0.00223    0.00024
C2    1    0.463493    0.578967    0.189059    11.00000    0.02375    0.02036 =
         0.02548   -0.00025    0.00265    0.00407
I2    4    0.286527    0.611343    0.057156    11.00000    0.03372    0.02294 =
         0.02294    0.00065   -0.00015    0.00248
C3    1    0.663820    0.637707    0.235712    11.00000    0.02758    0.02018 =
         0.02786    0.00247    0.00599    0.00061
AFIX  43
H3   2    0.717938    0.692912    0.207322    11.00000   -1.20000
AFIX   0
C4    1    0.788201    0.617847    0.323381    11.00000    0.02088    0.02329 =
         0.02913   -0.00391    0.00246    0.00351
C5    1    0.709313    0.535808    0.363236    11.00000    0.02694    0.02586 =
         0.01903   -0.00198   -0.00091    0.00418
AFIX  43
H5   2    0.792742    0.520555    0.422692    11.00000   -1.20000
AFIX   0
C6    1    0.510080    0.476372    0.316730    11.00000    0.02462    0.02134 =
         0.02726    0.00188    0.00664    0.00540
I6    4    0.395032    0.354093    0.379661    11.00000    0.03460    0.02573 =
         0.02977    0.00619    0.00290   -0.00013
N1    3    0.184554    0.437524    0.183609    11.00000    0.02978    0.02119 =
         0.02600    0.00197    0.00003   -0.00218
C7    1    0.020156    0.387107    0.145560    11.00000    0.04177    0.03078 =
         0.03930    0.00509   -0.00746   -0.00471
C8    1    1.000072    0.683429    0.373559    11.00000    0.03065    0.02812 =
         0.03241   -0.00498   -0.00385    0.00046
AFIX 137
H8A   2    1.161507    0.700947    0.334206    11.00000   -1.50000
H8B   2    1.090230    0.654491    0.429165    11.00000   -1.50000
H8C   2    0.886819    0.737670    0.390069    11.00000   -1.50000

AFIX   0
HKLF 4

REM  16058a in P2(1)/n
REM R1 =  0.0224 for    1844 Fo > 4sig(Fo)  and  0.0294 for all    2192 data
REM    102 parameters refined using      0 restraints

END

WGHT      0.0132      0.5692
```

```
REM Highest difference peak  0.503,  deepest hole -0.546,  1-sigma level  0.124
Q1    1   0.2155  0.6441 -0.0015  11.00000  0.05    0.50
Q2    1   0.5341  0.3831  0.4153  11.00000  0.05    0.50
Q3    1   0.3263  0.4601  0.1990  11.00000  0.05    0.48
Q4    1   0.2701  0.4021  0.3163  11.00000  0.05    0.46
Q5    1   0.4967  0.5760  0.1253  11.00000  0.05    0.44
Q6    1  -0.0658  0.3782  0.2804  11.00000  0.05    0.44
;
_shelx_res_checksum    8682

# Some atom labels have been edited after refinement
# to be consistent with other compounds. - KJT
```

Appendix V. Index of References Found Within CIFs

Citations within CIFs are in parentheses, and consist of a name(s), followed by a year. Herein, the entries are arranged alphanumerically by the content of the parentheses in each CIF. The second column gives the corresponding entry number in Part IV.

Table 45. The corresponding reference numbers for references found in CIFs.

CIF reference	reference # in Part IV
Allen, *et al*., 2004	225
Blessing, 1995	226
Bruker, 2002	177
Bruker, 2007	177
Macrae, *et al*., 2008	184
Sheldrick, 1996	182b
Sheldrick, 1997	181b
Sheldrick, 2008	181a
Sheldrick, 2012	182b
Sheldrick, 2014	182b
Sheldrick, 2015	182a
Sheldrick, 2015a	227
Sheldrick, 2015b	182a
Siemens, 1995	177